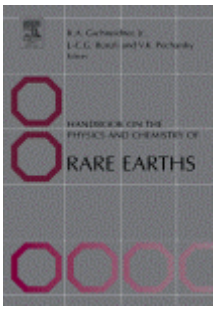

Handbook on the Physics and Chemistry of Rare Earths volume 11

Two-Hundred-Year Impact of Rare Earths on Science

Elsevier, 1988

Edited by: Karl A. Gschneidner, Jr. and LeRoy Eyring
ISBN: 978-0-444-87080-3

Handbook on the Physics and Chemistry of Rare Earths, Vol. 11
edited by K.A. Gschneidner, Jr. and L. Eyring

PREFACE

Karl A. GSCHNEIDNER, Jr., and LeRoy EYRING

These elements perplex us in our rearches [sic], *baffle us in our speculations, and haunt us in our very dreams. They stretch like an unknown sea before us – mocking, mystifying, and murmuring strange revelations and possibilities.*

Sir William Crookes (February 16, 1887)

With this volume we celebrate the contribution of rare earth research to the development of science since these elements' published discovery two centuries ago. These assessments inevitably suggest their probable future impact. The omens are propitious.

This tome has been referred to, during its preparation, as the 'cosmic' volume. This was intended to suggest the key role the rare earths play in science from the terrestrial to the celestial. For example, the periodic table of the elements is certainly one of the grandest of human intellectual generalizations and the placement of the rare earths in that scheme completed it. 'Cosmic' is not too grand a term.

This assessment of the contribution of the study of the rare earths to the structure of modern science is not an epitaph to a noble endeavor but an introduction to what some, anticipating the next hundred years, see as the century of the rare earths, so-called because of the expected largesse to science and technology of their unique physical and chemical properties. The chapters contained herein should allow the reader to assess the validity of this assertion.

The prologue by H.J. Svec is a biographical account of F.H. Spedding whose extensive contributions to rare earth science during one-fourth of the two centuries since the discovery of the rare earths is indeed prologue to the third. This intellectual warrior lead a host of rare earth scientists in pushing back the enemy – ignorance – across a wide front. The breadth of his interests and the intensity of his attacks puts him in the company of the dynamic Auer von Welsbach who developed uses for these materials and the great Berzelius who entered the battle at the very beginning.

The romance of the discovery and separation of the rare earths is narrated by F. Szabadváry. He has succeeded in lighting many dark corners of this confusing history and hence provides many new scenes in this lively yet serious saga. All in all, it is a tale of intrepid explorers and adventurers who opened up a vast, difficult terrain essential to the commonwealth of science.

The techniques of atomic spectroscopy were applied immediately upon this development to the identification of the new rare earths, dashing the claims of many and confirming those of others. B.R. Judd provides us with a definitive and perceptive account of the further success in the use of this science during the past sixty years to clarify the electronic configuration of the rare earths.

C.K. Jørgensen records his own special insights into the idiosyncratic chemical behavior of these seventeen elements. The scope of his treatment begins with their primordial formation in the stars and includes the chemical basis of their classification and integration into the fabric of science. His cosmic coverage provides unifying insights into topics dealt with in other chapters of this volume.

Magnetism in the lanthanides has been of interest at least since the observation of ferromagnetism in gadolinium by Urbain in 1935. Since that time these materials have been center-stage in the development of magnetic theory and advanced applications. Quantum mechanics brought in the modern theories of magnetism. Hund appears to be the first to have applied quantum theory to the rare earths in 1925. More than sixty years later it is still one of the most dynamic of scientific interests. Two chapters emphasize the unique role played by these elements in understanding magnetic interactions. The first chapter by J.J. Rhyne highlights certain exotic magnetic phenomena in the lanthanides and the second, by B. Bleaney, considers the general field of magnetic resonance spectroscopy and hyperfine interactions including a description of the modern techniques that evoke this information.

The rare earths did not play an important role in ancient metallurgy because of the difficulty of reducing their compounds, particularly their oxides. Even after the reduction of cerium by Mosander, in 1827, the metallurgy of rare earths advanced only sporadically during the next century or so. However, forty years ago with the more facile separation of rare earths, and hence their ready availability in pure form, the science has risen to impressive heights and now involves numerous laboratories around the world. Two of those most active in this area during its rapid ascension are the authors of chapter 78, K.A. Gschneidner, Jr. and A.H. Daane.

The very name 'rare earths' designates them as candidates of importance in geochemistry and cosmochemistry. S.R. Taylor and S.M. McLennan in closing this volume show how the progressive change of chemical and physical properties of the series, with the useful discontinuous exceptions, finds especial use in revealing the progress of geochemical and geophysical processes in the formation of many of earth's features and analogous ones of the heavenly bodies. The effective use of these fiducial elements began a scant quarter-century ago when very accurate analytical procedures became available.

The reader of any chapter of special interest in this volume could find sections of other chapters that give extended coverage of some aspects of the same topic. This underlines the breadth of the impact on science of the discovery, separation and study of the rare earths.

January 17, 1988

CONTENTS

CONTENTS OF VOLUMES 1–10

VOLUME 1: METALS

VOLUME 2: ALLOYS AND INTERMETALLICS

VOLUME 3: NON-METALLIC COMPOUNDS – I

VOLUME 4: NON-METALLIC COMPOUNDS – II

VOLUME 5

VOLUME 6

VOLUME 7

VOLUME 8

VOLUME 9

VOLUME 10: HIGH ENERGY SPECTROSCOPY

Handbook on the Physics and Chemistry of Rare Earths, Vol. 11
edited by K.A. Gschneidner, Jr. and L. Eyring

PROLOGUE

Harry J. SVEC
Ames Laboratory – DOE and Department of Chemistry, Iowa State University, Ames, IA 50011, USA

Contents

Prof. Frank H. Spedding

F.H. Spedding (Oct. 22, 1902–Dec. 15, 1984)

Frank Harold Spedding (FHS) was born on 22 October 1902 in Hamilton, Ontario to Howard Leslie Spedding and Mary Ann Elizabeth (Marshall) Spedding. The family moved to the United States soon after his birth (November 1902) and spent the early part of their tenure in this country in southeastern Michigan and then in the Chicago, Illinois area. Frank Harold attended grade schools in the Chicago area and attended Oak Park River Forest Township High School from 1916 to 1918. The family then moved to Ann Arbor, Michigan where FHS's father set up shop as a photographer, and FHS graduated from the Ann Arbor High School in the Spring of 1920. He matriculated at the University of Michigan in the fall of 1920 and received the B.S. degree in Chemical Engineering in 1925. The M.S. degree in Analytical Chemistry was earned the following year, also from the University of Michigan. From there he went to the University of California, Berkeley from which he obtained the Ph.D. in Physical Chemistry in 1929 under G.N. Lewis.

As an undergraduate at Michigan FHS displayed the curiosity and creativity that was to be the hallmark of his life as a first class researcher. As a sophomore in an elementary organic chemistry class he found the explanation then given for how the six carbon atoms in benzene were held together unconvincing and by the time he was a senior in 1925 he came up with a different scheme of his own. This was prior to the development and application of quantum mechanics to chemical problems and the prevailing bonding theory was mainly that of Kekulé. When he showed his idea to one of his rather pedantic organic chemistry teachers he was upbraided for the presumption of trying to improve on Kekulé. Undeterred, FHS took his model to Professor Moses Gomberg, famed for his work on free radicals in organic chemistry, in whose class FHS had spent part of his junior year. Gomberg was more sympathetic and immediately recognized Spedding's model as one proposed by Professor Landenburg (Ber. *2*, 140 (1869)) during the much heralded debate that took place between Victor Meyer, Kekulé and Landenburg in the early 1870's. Gomberg led FHS to the pertinent literature on the subject that recorded the controversy. Of course none of these early models is accepted today as a result of quantum-mechanical arguments concerning the bonding of carbon atoms in benzene.

It was due to this association with Gomberg, however, that FHS landed at the University of California at Berkeley. Gomberg not only recommended that he go to Berkeley but he also put in a good word with Professor Gilbert N. Lewis so that he was accepted as a graduate student. Thus, FHS with a B.S. in Chemical Engineering and an M.S. in Analytical Chemistry came to get a teaching fellowship in Physical Chemistry at Berkeley, G.N. Lewis (GNL) became his major professor and FHS felt he had arrived in a young chemist's heaven.

Research during graduate school years was spent learning about the vagaries of spectroscopy, especially absorption spectra. Spedding's first publication was with Simon Freed in 1929, the year he was awarded the Ph.D. degree, and had to do with line absorption of solids at low temperature in the visible and ultraviolet regions of

the spectra. Low temperature at this time meant boiling liquid air. It was also a time when his interest in the rare earth elements was whetted. More publications with Freed followed soon after the first one in which comparisons were made of the spectral properties of crystalline halogen compounds of samarium and gadolinium.

The Chemistry Department at Berkeley during the tenure of G.N. Lewis was the mecca for physical chemistry in this country. At one time a large proportion of the physical chemists in universities in the United States obtained their training at Berkeley. Lewis' interests ran the gamut of what we now categorize as physical chemistry and this was passed on to the graduates of the University of California. Indeed, when once asked for a definition of physical chemistry, Lewis is reported to have replied, "anything I'm interested in".

Early during graduate student days, FHS was put to work testing some of GNL's theories by complex experiments. FHS reported later in his career that the first three or four ideas turned out to be wild goose chases because they were wrong. The experiments, although unsuccessful, turned out however to give valuable experience. Thus was engendered in FHS the conviction that although a genius may have ten ideas and have only one success, a large part of the reason for success ordinarily attributed to genius is the result of sheer hard work and ability to overcome frustrations.

Spedding finished work required for the Ph.D. in 1929 and was greeted by the Great Depression. Jobs for chemists were virtually non-existent and so for the next seven years he lived on promises and a series of temporary fellowships. Although these carried prestige and honor they were financially meager and at best offered only a hand-to-mouth existence. The stress of the period probably produced the ulcer that plagued him much of his life.

For the years 1930–1932 FHS was awarded one of the scarce National Research Fellowships which enabled him to stay on at Berkeley doing fulltime research. After the fellowship ran out G.N. Lewis hired him as a temporary chemistry instructor whose main chores involved continuing the research on the absorption spectra of solids. The appointment was for two additional years, 1932–1934.

It was during this time that FHS was able to integrate ideas from the newly developing quantum mechanics into his chemical thinking. He was a spectroscopist and was able to use this powerful tool in his studies of atomic and molecular structure. It was already well established that gaseous elements gave sharp-line spectra corresponding to quantized energy levels which in turn provided a theoretical base for calculating important physical properties. Liquids and solids did not yield sharp absorption bands but it was already known that the rare-earth containing mineral xenotime did exhibit sharp lines when cooled to boiling liquid air temperatures. Spedding reasoned that this was due to the peculiar atomic structure of the rare earth constituents in the mineral. These elements usually occur together in nature and were then very difficult to separate. Hence *pure* rare earths were scarce and it was almost impossible to obtain even a small amount. The name rare earth is a misnomer because these elements are not really rare but are actually more abundant in the earth's crust than many of the elements we assume to be reasonably abundant, e.g., Ag, Au, Hg, Cd, Pt. Professor B. Smith Hopkins of the University of

Illinois had a small supply of some of the rare earths in relatively pure compounds so FHS appealed to him for a loan of a few tenths of a gram which would not be consumed in any way but which would only have some light shined on them. "I practically went down on my knees to Dr Hopkins" is the way Spedding tells the story but he did get the loan. Upon examination of the cooled pure rare earth compounds Spedding did observe sharp lines. He was able to show that the fine-structure of these lines depended on the symmetry of neighboring atoms in crystals of the compounds he had that contained rare earth elements, and the spectra enabled him to determine the symmetry of the crystals. It was for this work that in 1933 he was awarded the Langmuir Prize, then given to outstanding young chemists who had not yet reached 31 years of age. Oscar K. Rice and Linus Pauling preceded him in winning the award. After Spedding received the award its name was changed to the Award in Pure Chemistry of the American Chemical Society, its sponsorship taken over by the chemical fraternity Alpha Chi Sigma, and the age limit changed to 35.

Frank Harold Spedding and Ethel Annie MacFarlane were married on June 21, 1931 during the tenure of the National Research Fellowship and they took up housekeeping under spartan conditions during his stay at Berkeley. He related that their greatest source of pleasure and recreation was in the great outdoors, camping, hiking, mountain climbing, because it was what they could afford.

The Langmuir Prize was awarded in 1933 at the Chicago World's Fair. This exposition dramatized the progress in technology during the first 100 years of the city's existence; the award and the advances in chemistry it recognized were appropriate showpieces for the exposition. Spedding was to give a talk describing his work and so he borrowed money in order to travel to Chicago. When he arrived at the amphitheater, he had to fight his way through a large crowd to get to the platform. After he was introduced he relates that "I froze and could not remember how to get started". Tongue-tiedness afflicts many of us and FHS was no different. He goes on to say that he was struck dumb for an interminable time, actually perhaps only ~ 10 seconds, and then he called for the first slide. The talk went off without a hitch and was greeted at the end by a pleasant round of applause. After answering a question or two and the award presentation*, the crowd disbanded but an elderly gentleman made his way up to the platform. Spedding relates that the man's appearance reminded him of a then current comic strip character called "Foxy Grandpa". The man was short, had a long white beard and was bald. Getting Spedding's attention, the man blurted out "How would you like to have a pound of europium and two or three pounds of samarium?" (These were the scarcest of the rare earths and ordinarily obtainable only in milligram quantities.) Spedding related "I thought this guy's crazy" but "I was polite to him and agreed that it would be fine and would help to further my work". The trip back to California was uneventful but not long after arriving FHS received a box containing fruit jars of europium and samarium oxides. It was then that he busied himself to find out who his benefactor

*Of all the medals FHS received during his lifetime, the Langmuir Medal is the only one misplaced and never relocated.

was. The man turned out to be Dr Herbert M. McCoy, a professor of chemistry at the University of Chicago.

McCoy had always been interested in rare earth chemistry and had succeeded in separating some of them by fractional crystallization. He was also aware that the Lindsey Light and Chemical Company had a supply of residues containing rare earths that were left over after the thorium had been extracted from a feed stock*. He also knew that europium could be reduced to the divalent state and as such was easily separable from the other rare earths by coprecipitating it with barium sulfate.

When he was no longer active as a University of Chicago staff member McCoy arranged with Lindsay to work up some of the rare earth residues they had stored in a pond on their premises. Thus he produced kilogram quantities of one of the scarcest of the rare earths by starting with a residue containing only a small fraction of a percent of europium. He was also generous according to FHS and gave deserving people such quantities of europium compounds that many interested scientists considered this rare earth to be one of the most abundant.

Spedding's life was again to be influenced by Herbert M. McCoy but that was about nine years later in his career.

The Langmuir Award included not only a gold medal but also an honorarium of $1000, a lot of money in 1933. This augmented FHS's University of California stipend so he and Ethel looked forward to an easing of their lives in Berkeley. However, the Depression was becoming more severe and universities were then hardly able to pay their faculty. Thus G.N. Lewis was hard pressed to support other promising Ph.D. potential staff members each year. Spedding recounts being called into Lewis' office during the 1933/34 academic year to be greeted by, "'Now that you won your $1000, you won't need all the money we're paying you,' so my salary for 1933 was cut by $500". That was the last year FHS spent at Berkeley.

The country was still in the throes of the depression and there were no jobs to be had so Spedding applied for and received a then rare Guggenheim travel grant for the year 1934–1935. He planned to spend part of the time abroad in Germany working with Nobel Prize awardee James Franck who had made a brief visit to Berkeley and also part time with Professor Francis Simon, a leading low-temperature physicist. However, Germany had become under the heel of Adolf Hitler and Franck and Simon, both Jews, had fled from Germany to Denmark and England. Thus instead of travelling to Germany, Frank and Ethel planned to go to England where the major portion of his European stay was to be. He was warmly received at the Cavendish Laboratory in Cambridge by Ralph Fowler, professor of theoretical physics and authority on statistical mechanics. Fowler was the son-in-law of Ernest Rutherford, then chief of the Cavendish Laboratory. While at the

*Thorium nitrate was used in the production of Welsbach mantles, important components of gas light fixtures. Welsbach mantles are made by impregnating small cotton or rayon sacks with $Th(NO_3)_4$ containing small amounts of $Ce(NO_3)_2$ and $Mg(NO_3)_2$. When these are first burned after being attached to a gas jet, the nitrates decompose and leave a fine network mainly of thorium oxide which catalizes the burning of a hydrocarbon producing an intense incandescent light. Modern gasoline or propane camp lanterns still use Welsbach mantles.

Cavendish FHS had a chance to work with John E. Lennard-Jones in quantum mechanics, met Max Born who had also left Germany, and attended Born's seminars. He regretted that he was unable to work with Peter Kapitza who had been at Cambridge with Rutherford for fourteen years but was spending his annual vacation in 1934 visiting relatives in the Soviet Union. Kapitza did not return to England, clearly not by his choice but due to Stalin's decree.

Travel expenses were to be paid by the Guggenheim Foundation but the first lump sum payment given quarterly to the Speddings would have had Frank and Ethel arriving in Europe with little left over on which to live. After consulting a travel agent in Oakland Frank found that they could travel via a Japanese liner across the Pacific and then on other ship lines to England for less than half of the quoted fares across the United States and Atlantic Ocean. Spedding relates that their tourist class tickets on the Japanese liner only restricted their shipboard quarters until they were beyond land whenceforth they were allowed free access to all parts of the ship. "The captain was all too happy to have paying customers aboard" so the story went. There were leisurely stopovers in Japan, China, Malaya and Ceylon, they sailed up the Red Sea, through the Mediterranean and finally landed in Southampton, about four months after leaving the United States. The young couple profitted immensely by their round-about route to England; no charges for food or lodging all the way and immeasurable experiences to boot.

Abraham F. Joffe, a Soviet physicist who had met Spedding in Berkeley and knew he was in England, invited him to lecture in Leningrad, Moscow and Kharkov at the expense of the Russian government. With some reservations the Speddings accepted and did travel to the Soviet Union. Frank lectured at Leningrad but for unknown reasons never went to the other cities.

Being in Europe had other advantages for the young scientist. There were side trips to the Netherlands to visit Kamerlingh Onnes' low temperature laboratory, to research laboratories in France, Germany and Latvia, and to Copenhagen to visit Niels Bohr. Bohr was a kindly man and greeted the then unknown young scientist warmly. Spedding liked Bohr because not only did he treat Spedding as a friend but also because of his "brilliant mind". Bohr's English was difficult to understand. He had a tendency to run words together and drop them to an inaudible range at the ends of sentences. "One really had to listen to him twice" according to FHS, "but there was no doubt about his grasp of a subject". Spedding recounts an experience at an Atoms for Peace Conference in Geneva in 1955 where Bohr was addressing the assembly. As usual Bohr's English was incomprehensible so FHS started to flip through the list of simultaneous translations. Much to his astonishment he turned the knob to a point where "I heard a translator speaking understandable English, he was translating Bohr's English into Oxford English". Spedding spent a month in Bohr's institute but although he did some theoretical work, he was determined to be an experimentalist and so he left. The Guggenheim Fellowship was nearing its end and the Speddings felt they had to get back to the United States to look for a position that would pay a regular stipend. They returned to his parent's home in Michigan full of grand experiences but in dire need of a permanent job.

Canvassing the job market for a permanent position proved fruitless but the

George Fisher Baker assistant professor position at Cornell University was open so FHS took another temporary position, this time for the period 1935–1937. Spectroscopic studies of other crystalline compounds of samarium continued at Cornell and the studies were expanded to compounds of thulium, gadolinium, neodymium, erbium, and praseodymium. It was during this time, working with Hans Bethe, that FHS showed conclusively that the sharp lines observed in the absorption spectra of rare earth solid compounds arose from the inner shells of the rare earth ions and were due to 4f transitions.

The entire period between 1930 and 1937 was a fateful one for Spedding. In addition to other spectroscopic studies he had also studied the effect of magnetic fields on the sharp lines in crystals and how it affected energy levels. It was also during this time that FHS assisted G.N. Lewis in his efforts to concentrate deuterium, the heavy isotope of hydrogen discovered by Harold C. Urey. The cooperation between FHS, C.D. Shane (who was an astronomer and had a large grating) and N.S. Grace (who had a Fabry–Pérot etalon) made it possible to separate the H_α and D_α lines well enough to follow how rapidly D_2O was being enriched in Lewis' electrolysis cells. This work was described in the only publication bearing Spedding's and G.N. Lewis' name. It also made it possible to use spectroscopic techniques to add another significant figure or two to the then known value of e/m, the charge-to-mass ratio of the electron, and to determine a better value for α, the fine-structure constant. The broad scope of FHS's spectroscopic studies made him one of the premier spectroscopists in the country and also one of the country's experts in the chemistry of rarer elements. Thus the next period in his life was set.

As the position at Cornell was winding down, FHS was again on the job market. After following several unproductive leads he heard about a chance for a tenure track position at Ohio State University (OSU). He and Ethel thus got in their old Chevrolet car and drove to Columbus, Ohio. There an interview with Professor Evans, then head of Chemistry at OSU proved to be another frustration because Evans had just hired a new physical chemist. However, Evans knew that his friend Winfred F. (Buck) Coover at Iowa State College (ISC) had lost much of his physical chemistry staff due to resignations stimulated by greener pastures for the people involved and was looking for a replacement. Thus again the Spedding's trekked west. An interview with Coover was encouraging in that FHS was offered an assistant professorship on the spot. Although this was one step above the usual rank into which new staff members were hired at ISC, it still was no assurance of anything more than a three-year appointment, subject to review before possible promotion to associate professor with tenure. Spedding already had seven years of uncertain positions behind him so he opted for an associate professorship at ISC from the onset. This Coover could not offer him without consultation with college administrative officers and the Regents. The situation was left that way with Spedding continuing to head west (there was a chance that some kind of position could be had at Berkeley where at least they had good spectroscopic equipment) and the Spedding's hoped to stop at Yellowstone Park for several days on their way. Coover was to wire FHS in care of general delivery at the Yellowstone Lodge. After several days and no wire, another frustration loomed. On the day Frank and Ethel

were to leave the park a last minute check produced the wire from Coover. Spedding's name was garbled in the address on the wire but the Associate Professorship with tenure came through. The Spedding's travelled on to Berkeley where some old friends were met and some loose ends tied up. In the fall of 1937, Spedding and his wife checked into Ames, Iowa as the head of the physical chemistry section of the chemistry department at Iowa State College.

There was meager modern equipment at Iowa State when Spedding got there. Although Harley Wilhelm had earned his Ph.D. degree working with a Hilger–Watts spectrograph, it was an instrument designed more for analytical spectroscopy than the kind of research that FHS had been doing and wanted to continue. Funds were tight but some money was made available for a ruled rating to be mounted on a Rowland circle which was set up in the basement of the chemistry building. In the meantime Spedding changed his research program to a type of chemistry done with equipment available at ISC. He had always had great trouble getting even small amounts of pure rare earths, since the isolation of these elements involved enormous amounts of labor in the part of the *few people* that were even interested in the rare earths. These people were naturally loathe to part with a rare earth sample once they obtained any of these elements in reasonable purity because they wanted to explore the properties of the rare earth themselves. Spedding, therefore, started a program to separate individual adjacent rare earths one from the other. He knew he would have to develop a process which automatically would repeat the enrichment interaction thousands of times and do this rapidly. Some years earlier, Tswett had developed the Tswett Chromatographic Columns where a solution made up to several components would have the components pass through such columns at various rates and *when* the operation was successful, good separations were made of components in mixed solutions. Spedding thus had his students work on problems involving chromatographic columns with various absorbers using forms of aluminum oxide or silica gel, but they had little success in separating the adjacent rare earths. He explored paper chromatographic methods which were being developed at that time, but these also were not successful for rare earth separations. This work was interrupted by the onset of World War II, at which time Dr Spedding dropped all basic research underway and devoted his attention to the war effort. As a result, there are no publications describing this early chromatographic work.

During the late 1930s, physicists around the world had found that a slow moving neutron (thermal energies) could fission uranium (U^{235}) and they became convinced that if they could get a chain reaction going with the U^{235}, they could tap the enormous energies available in the nucleus of atoms. World War II had already started in Europe and United States involvement seemed very probable. Germany had been one of the leaders in basic nuclear research prior to that time and since a super bomb, millions of times more powerful than any existing chemical bombs, would be possible if the chain reaction problem could be solved, it was imperative that scientists in the United States should be working in this field. Accordingly, the government decided in what is a well-known story to get behind this research program and gathered workers who knew something about the subject in three great centers of research, Berkeley, Columbia University and Chicago, so that maximum

progress could be achieved. Professor A.H. Compton of the University of Chicago was put in charge of the Chicago Program. The object of the project was to see if a nuclear chain reaction could be started with *natural* uranium. In December 1941, Compton decided that the physicists needed chemists to help them with their program. He requested his chemist friends to give him a list of outstanding inorganic chemists in the country who also knew something about the rarer elements, particularly uranium and the rare earths. Consulting with H.M. McCoy he learned about FHS and gathered a list of other names. From this list, Compton selected Spedding to head the chemistry program at Chicago. After Spedding acquainted himself with the chemical problems, he informed Professor Compton that he had some space available at Iowa State College in Ames, and that he could enlist a number of his associates, among them being H.A. Wilhelm and some graduate students, to help with these programs. It was then decided that Spedding would spend half a week in Ames, working with his group there to solve some of the immediate chemical problems, and spend the other half of the week in Chicago organizing the chemical division. One of the most pressing problems was to get the materials used to build a nuclear reactor under the West Stands of Stagg Field pure enough so that the chain reaction would have a chance of going critical. The theorists had pointed out that ordinary uranium contained such a small amount of U^{235} that the reactor would have to be built to very exacting specifications for the spacing of the uranium metal in a graphite matrix and that further, both of these materials would have to be of exceptional purity, since many expected impurities were known to absorb neutrons and would close down the nuclear reaction.

Only a little uranium metal had ever been produced prior to the war. Westinghouse had made a few grams when exploring its possible use as a filament in light bulb manufacturing. (At that time uranium was considered to be part of the Group VIA elements in the Periodic Table and was placed below tungsten.) They used an elaborate photochemical process to form KUF_5 and then used an electrolytic process in fused salts to form the metal. Westinghouse agreed to step up their processes and to supply Chicago with uranium metal. Also, Metal Hydrides Inc. had a hydride process for making uranium metal powder, which was later compacted into various forms, and they also agreed to furnish metal. However, the metal from these sources was slow in coming to Chicago and was cast or compacted into small blocks, one inch cubes or smaller, and at the beginning was not very pure. In fact, there was so much oxide in the metal that all the handbooks published prior to 1942 reported the melting point of uranium to be $\sim$1800°C. (It was later shown that the pure metal melted at 1132°C.) Therefore, one of the great needs of the program was to find a process which could produce massive ultrapure uranium metal in large quantity.

The first chores at Chicago involved assembling a group of outstanding scientists to head the various chemical sections. Dr Glenn Seaborg, who led the group of scientists at California who had discovered plutonium, was asked to head the section on plutonium chemistry. Dr Charles Coryell of MIT was brought in to be in charge of fission product chemistry. More knowledge about the fission products was essential, since they contained most of the dangerous radiation produced by the

fissioning and many of them tended to destroy the chain reaction as their concentrations built up. Dr Milton Burton was asked to head the radiation and radiation damage chemistry section, as it was obvious at this time that this would be an important part of the program. Dr George Boyd was asked to lead the inorganic and analytical section. An entire new field of analytical chemistry had to be explored, since there were very few methods then available for analyzing quantitatively for the low level impurities demanded in the construction materials for the reactor. While it had been known for a long time that uranium could be purified by an ether extraction from an aqueous solution of uranyl salts, it was not known exactly how much of the various impurities would remain with the extracted uranium. Boyd's group at Chicago had as one of its first problems the determination of whether such uranium would be satisfactory with regard to purity. He reported that the method looked quite promising in this regard. Spedding reported to Compton that the suggestions of some people of building large pools of uranium salts in solution in Arizona, where there was plenty of sunshine in order to scale up Westinghouse's photochemical process, did not seem feasible, and that they ought to arrange for the ether separation instead. As a result, Compton and Spedding visited the Mallinckrodt Chemical plant in St. Louis to contract for the solvent extraction work. Since Mallinckrodt was a chief manufacturer of ether it was felt they could do the work. At that time, not many people were anxious to scale up this process since it was inherently *very* dangerous. Because of the fire hazard, unless the plant was carefully designed it was likely it would burn down before much pure uranium was produced. While Compton spent his time at St. Louis, discussing contract terms with Mr. Mallinckrodt, Spedding spent his time with Dr Ruhoff, superintendent of the Mallinckrodt plant, discussing a flow sheet for the chemical engineering operations which would be necessary to obtain the right grade of purified uranium. Mallinckrodt accepted the contract, and Ruhoff with his staff designed in detail the type of plant needed. They did a remarkable job in designing and then building a plant in an exceptionally short time which could turn out large quantities of highly purified uranium oxide with minimal hazard.

The groups at Chicago were crowded for space at first because only a few rooms were available in the chemistry laboratories, since other University of Chicago professor also had programs and important work in submarine detection, chemical warfare, etc. At that time the so-called "Compton's Folly" of trying to get energy from the atomic nucleus did not have too high a local priority. However, in a few months a one-story building (the Metallurgical Laboratory) was constructed on a vacant field and much of the chemistry work then was done in much better space. Spedding remained head of Chemistry at Chicago until the first chain reaction went critical and was present as the Director of Chemistry on that historic occasion.

In order to get some of the chemical work underway immediately, Spedding was given a 'letter of intent' to Iowa State College for a 3-month contract from the Office of Scientific Research and Development (OSRD) with the understanding that as soon as suitable space became available at the University of Chicago, he would move his group to Chicago. He was joined at Ames by Professors Harley Wilhelm and I.V. Johns, members of the Chemistry Department. They immediately enlisted their

graduate students and this was the nucleus of a group that started the work in Ames. They were soon joined by other graduate students and young scientists and professors in the Chemistry Department so the group grew rapidly. One of the first problems was to search for materials which could contain molten uranium. Until then, uranium was either cast in small beryllium oxide crucibles or was compacted into a dense metal briquet by pressing powder under high pressure. Graphite, another possible crucible material, was known to react with uranium metal to form various uranium carbides. The Ames team soon found that if the graphite was kept at a temperature only slightly lower than the molten uranium and was not kept there too long, most of the carbide forming reaction took place at the interface between the metal and the graphite and thereafter very little carbon entered the metal. This made it possible to make large castings of massive uranium, in which the carbon and oxygen content was less than 0.02% or 0.03% by weight. As the technique improved they were able to lower this considerably, so that the uranium now melted in the neighborhood of 1130°C instead of 1800°C.

Dr Wilhelm, Dr W.H. Keller (former graduate student of Spedding) and Spedding patented the process. Since they were working with government funds however the patent rights were turned over to the Manhattan District to be used for the public welfare.

The Ames team was trying initially to reduce uranium oxide to the pure metal using H_2 but did not have much success. (This was a reasonable ploy because at the time uranium was considered to be one of the Group VIA elements and was placed below tungsten in the Periodic Table.) At high temperatures, molten uranium metal dissolves much oxygen which forms uranium oxides and on cooling, the oxides form a honeycomb of films surrounding irregular "droplets" of uranium throughout the metal. These prevent the molten metal from flowing, so that it cannot be easily recast in a desirable shape.

While the other groups supplying uranium metal to Chicago greatly improved their processes during this period, they were slow in delivering the metal and by the late summer of 1942, less than half of the six tons of uranium needed for the Stagg Field reactor had been delivered. The lack of uranium metal was holding up the overall program and a number of alternatives were considered. One of these was to use briquets of pressed uranium tetrafluoride, which could be obtained commercially. Since UF_4 was being manufactured for the Y-12 isotope separation program at Oak Ridge via magnetic methods using calutrons, which were modified mass spectroscopes, it was available. One of these bright green briquets was brought to Chicago and passed around the table at the October Project Administrative Board Meeting, and it occurred to Spedding that this fluoride might work better in the reduction process than the oxide. He took a block back to Ames and asked Wilhelm and Keller to try using it in place of the oxide. By that time they were using a "thermite" type reduction process, that is, reacting a less active metal oxide or salt with a more active metal, such as calcium, magnesium, aluminum, etc. to produce the less active metal. This reaction had been tried with U_3O_8 50 years earlier by Moissan for the production of uranium, but his product was impure due to the equipment and the impure materials with which he had to work. The "metal" he

obtained did not even show the expected properties of a metal. This process was tried many times thereafter by various chemists, but in no case was uranium metal of the desired quality obtained.

At Ames, uranium tetrafluoride was first mixed with calcium, and later, magnesium as the reductant*. The reaction was done in a steel pipe welded closed at one end and provided with a steel cap on the other end. The reaction mixture had to be isolated from the steel pipe because molten uranium metal reacts with iron to form an alloy which has a melting point lower than the molten uranium. Therefore, a layer of hard fired, finely ground calcium oxide was tamped in place to be between the steel pipe and the reaction mixture. On the first attempt using Ca as the reductant, a small ingot of massive uranium metal was obtained. Thus started the inexpensive production of cylinders of massive uranium of good purity. During the next month (Nov. 1942) two tons of uranium metal as machined cylinders, 2″ in diameter and 2″ long, were sent to Chicago. This was one-third of the required six tons needed for the Stagg Field reactor and, as a result of this delivery, the Chicago group succeeded in making their exponential reactor go critical on December 2, 1942. Spedding was present on this occasion, as Director of the Chemistry Division of the Chicago Manhattan Project. Again, Spedding, Wilhelm and Keller took out patents, the rights of which were given to the government to benefit the public welfare.

The ingots of uranium furnished from Ames were so much purer and less expensive than the uranium metal being produced by others that the now "Manhattan District" asked three companies, Mallinckrodt, the Electrometallurgical Division of Union Carbide Co. and Dupont, to make the large amounts of metal available which would be needed for the Oak Ridge and Hanford reactors. These company scientists and technicians studied the Ames process and went back to their companies and started building facilities to produce the metal. In the meantime, the government asked Spedding and his coworkers to produce all the uranium metal that they could. Since it took time to design and build the commercial plants to make the metal, during the ensuing several months more than two million pounds of uranium metal were produced at Iowa State College in Ames in a scaled-up pilot plant set up in a temporary building the college inherited after World War I. A large amount of this metal was used in Oak Ridge to build the prototype plutonium production reactor. Another large amount of the metal went to various sites all over the Manhattan Project, since it was needed for research and development work on the properties of uranium metal. The remainder went to Hanford to help get the first Hanford plutonium production reactor started.

As soon as the companies started producing metal, Ames stopped its production. Again, Spedding and his coworkers took out patents on the processes they developed and again the rights were turned over to the government. It is interesting that, at the time the Ames process was developed, it was generally thought that

*Eugene-Melchior Peligot has first isolated uranium metal in 1841 by reacting anhydrous UCl_4 with potassium in a platinum crucible.

better and cheaper processes would be found for making metallic uranium. However, even today, the Ames Thermoreduction Process as modified by the companies when they scaled up their operation, is the method in general commercial use.

During the time uranium metal was being produced in Ames, each week it was made somewhat purer. As a result of this research, two analytical groups were built up in Ames to develop analytical methods so that improvements in the metal's quality could be certified. Thus groups in Ames were responsible for developing a large number of these analytical methods and many are still in general use.

When the large uranium billets (as they were called) were cast, there was always a thin, rather profuse layer of uranium carbide on the surface so that the billets had to be machined before shipping. The machining operation accumulated a large supply of turnings which were heavily contaminated with carbide so again, the ISC Manhattan Project laboratory developed a process for remelting the turnings in order to remove most of the carbide and make usable metal from them.

During the war, many tentative designs for constructing power reactors were conceived and patented throughout the Manhattan District. On the basis of then known reserves it was not certain that there would be enough uranium readily available to supply all the future needs, so many of the reactors were so-called breeders and were designed with thorium metal as an outer blanket to absorb stray neutrons. While natural thorium does not fission due to slow neutrons, it absorbs them and converts some of the Th^{232} atoms to U^{233} which is relatively long lived and fissions similarly to U^{235}. Therefore, a process for making metallic thorium was badly needed. However, thorium metal melts at $\sim$1800°C, 500° above the melting point of uranium, and the uranium process did not produce solid thorium metal. More heat was needed in the reduction vessel in order to melt the thorium to a palpable ingot, so "boosters" consisting of calculated amounts of potassium chlorate or other oxidizing agents were added to the reaction mixture to supply this extra heat. By co-reducing a mixture of ThF_4 and ZnF_2 a lower-melting alloy was produced. The zinc was then distilled from the alloy under vacuum to produce a thorium 'sponge' which was then cast in a desirable form. Sound thorium metal was produced by this method and so Spedding was asked to produce it in quantity. Again, the Manhattan District had commercial companies come to look at the Ames process for making thorium and a contract was let to one of the companies to produce it. In the interim period, 600 000 pounds of thorium metal were produced in Ames. Wilhelm, Keller and Spedding again took out a patent and turned the rights over to the government. That process for producing thorium metal, now modified, is still in use in industry today.

The first of the rare earths was discovered at the end of the eighteenth century. It was soon found that there were many rare earths and they had similar chemical properties, so it was extremely difficult to separate them from one another when all the rare earths were present in a mixture. By laborious processes, mainly fractional crystallizations, in some cases requiring more than 10 000 separations, chemists had succeeded in separating all the rare earths in what was considered fairly high purity,

but in *very small* amounts. It was relatively easy, requiring only four or five fractionations, to separate mixtures of cerium, lanthanum, and the so-called "light" lanthanides from yttrium and the heavy lanthanides, but to separate individual adjacent rare earths required several hundred fractionations for some pairs and even several thousand for others. While the resulting rare earth salts were thought to be pure, later work showed that they were not as pure as believed at the time, because their atomic weights changed appreciably as purer rare earths became available.

Intensely radioactive rare earth atoms are formed when U^{235} fissions. Some of these have extremely high neutron capture cross-sections, so they would stop the chain reaction after a certain amount of U^{235} had been consumed. Individual rare earths were needed for research so that chemical processes could be developed to separate them from the fissioned uranium and plutonium. Therefore, a program was started at Ames on the separation of rare earths. Spedding along with Drs J. Powell, A. Voigt and others developed an ion-exchange elution technique which was capable of separating adjacent rare earths in moderate quantities, particularly the light rare earths. Similar work was being done at Oak Ridge, to separate rare earth fission products using radioactive tracers, and their first report showed three peaks corresponding to the separation of yttrium, the "missing rare earth promethium" and cerium. Since secrecy requirements during the war made it impossible to publish results from either laboratory and notebooks were not exchanged, there was some controversy as to who developed the ion-exchange process first. However, after the war, when attorneys for the government took out patents in Spedding and Voigt's names, the Ames work was given precedence and the patent was awarded to Spedding and Voigt who turned them over to the government for the general welfare.

Spedding, Dr A. Newton and others also studied the properties of uranium hydride and found that purer uranium metal could be made from solid ingots by first going through a hydride stage. They also reported that this purer uranium was an excellent "getter" for purifying various gases from impurities, since the uranium metal reacted readily with these impurities.

Another development which should be mentioned was that in purifying the thorium salts, a process was developed at Ames using a liquid–liquid extraction with hexanone, where the thorium went into the hexanone and the impurities stayed in the water phase. While this process was successful and produced pure thorium, it had the disagreeable property that occasionally the apparatus would catch fire, so tributyl phosphate was substituted for the hexanone and this made the process completely satisfactory. It later also formed the basis, being used with uranium, for the Redox Process, which was used widely at Hanford and elsewhere for separating the radioactive fission product impurities from the uranium and plutonium.

After peace was declared in 1945, the Institute for Atomic Research was set up at Iowa State College and Spedding became its director. Support for this institute was provided on a modest scale by the college with state funds. However, there was a need to reorganize the laboratories all over the country that had accomplished so much during Manhattan Project days under federal auspices. This was accom-

plished by the creation of the Atomic Energy Commission (AEC) whose objective was to fill in the gaps that were left unfilled in research during the war years and to promote peaceful uses of atomic energy. In 1947 the Ames Laboratory of the AEC was set up on the campus of ISC and FHS became its first director. Administering the operation of this laboratory fell to officers of the Institute for Atomic Research. Thus Spedding and his administrative crew took care of the college obligations under the contract and Spedding directed and expanded the scientific program.

One of FHS's personal scientific interests, the rare earths, returned to the forefront after the war. The ion-exchange process was developed into displacement ion chromatography on larger columns where the individual rare earths could be separated in kilogram and even ton quantities from each other in a higher purity than almost any other element. In some cases, oxides containing only a few parts-per-million of all other elements, including other rare earths, were produced. Thus, the rare earths changed from being among the most impure elements in the Periodic Table to being listed among the purest that could be produced. During Atomic Energy Commission days, Spedding was asked to produce kilogram quantities of all the rare earths for general research purposes throughout the AEC laboratories and elsewhere. Hundreds of scientists all over the world were supplied with pure rare earth salt samples. A patent by Spedding and Dr E. Wheelwright was issued for this process, and again the rights were turned over to the government for the general welfare. More than 80 commercial companies sent their scientists to Iowa State to study this process and several of these companies set up plants to make rare earths generally available. Parallel with this work Spedding and Dr A. Daane developed processes for producing pure rare earth metals in quantity. Once the rare earths became generally available to the general scientific community, many practical applications were found and a considerable industry has developed which involves the use of rare earths. It was found by some companies once they had materials to work with, that for certain elements a liquid–liquid separation process would be successful, and europium and yttrium became available at relatively reasonable prices. One of the applications using the liquid–liquid extraction of these elements resulted in the bright colors we now see on color television screens.

Spedding's group at Ames also showed that the rare earths had interesting magnetic properties when the temperature was lowered. As a result, many scientists worked with these metals and learned a great deal about the nature of magnetism. Today the best permanent magnets are made with neodymium or samarium metals as one of the constituents in an alloy.

During the early 1950s much interest in yttrium developed due to the fact that it was a light metal ($d = 4.34$ g/ml), was high melting, was not corroded in air and water vapor, and its hydride had pronounced metallic properties. Such a material could conceivably be used not only as a construction material but also as a neutron energy modifier. There was considerable interest in developing a nuclear reactor that could be used in airplanes. Thus in 1954 and early 1955 Spedding's group at Iowa State (now Iowa State University) was asked to produce tons of yttrium metal. This meant scaling up the process already developed for producing metallic yttrium. It

turned out that a scheme similar to one used in producing thorium, namely co-reduction of the fluoride to form an alloy with a readily volatile metal, was successful. In this case yttrium fluoride was reduced by a mixture of calcium and magnesium in the presence of calcium chloride (to minimize oxide contamination) to produce a low-melting Y/Mg alloy. The magnesium was sublimed from this alloy under high vacuum and the resulting yttrium sponge then formed into acceptable billets by vacuum arc melting on a copper anvil. By 1957 20 000 lbs of cast metal was produced at Iowa State along with 65 000 lbs of YF_3 that was sent to commercial metal producers all over the country. Thus again, the research group at Ames under the direction of FHS was able to take a process developed on a laboratory scale and produce gross amounts of a needed commodity.

Spedding continued his research with various coworkers, both students and some professors, and in the long run, many basic researches which were done at Ames supplied vital information on the properties of the rare earth salts and metals.

In his later years, Spedding set up a program to study the thermodynamic properties of electrolytes using rare earth solutions. An extensive literature on the properties of solutions of the rare earth elements with various anions was accumulated as a result of this program.

Spedding's work was not solely restricted to the study of rare earth spectroscopy, the production of uranium, thorium, and yttrium in large quantities, and rare earth separations and characterization as implied in the foregoing narrative. The displacement ion chromatography he and Powell developed and whose theory they also developed was applied to the separation of the nitrogen isotopes. In the early/mid 1950s, Spedding, Powell and H.J. Svec, using the NH_4^+ ions as the isotopic carrier, produced both the ^{15}N and ^{14}N species in unprecedented isotopic purities (99.9+% ^{15}N, 99.98+% ^{14}N). Large amounts of highly enriched and depleted NH_4^+ salts were made available for research in chemistry, biology and agronomy as a result of this work. The method was simple and could be set up easily in the laboratory of any scientist who needed a pure nitrogen isotopic material for tracer work.

This narrative summarizes the work Professor F.H. Spedding and his many coworkers accomplished during his long and creative career. The breadth of the work is such that the coworkers were many but the inspiration and drive to do the work was largely due to Spedding's perception of what needed to be done, how it should be done and when it should be accomplished.

After Spedding retired as an active academician in 1972 at the age of 70 years, Iowa State University named him an Emeritus Professor in Chemistry, Physics, and Metallurgy. For several of his remaining years he carried on work with postdoctoral students and fulltime Ames Laboratory scientists in all three areas. An additional 60 or so publications were coauthored by him during this time. In the beginning he was in his office almost every day but finally his energies began to fail. His last scientific publication came out in the Physical Review in 1981. Early in the fall of 1984 he suffered a stroke which was to end his life on December 15, 1984. His remains are interred in the Iowa State University Cemetery. His wife Ethel now resides in California with their daughter Elizabeth Calciano.

Patents of F.H. Spedding

US Patent No.	Date	Title	Inventors
2 539 282	Jan. 23, 1951	Rare-earth Separation by Adsorption and Desorption	F.H. Spedding A.F. Voigt
2 714 554	Aug. 2, 1955	Method of Producing Gadolinium	F.H. Spedding A.H. Daane
2 778 730	Jan. 22, 1957	Plutonium Alloy and Method of Separating it from Uranium	F.H. Spedding T.A. Butler
2 782 116	Feb. 19, 1957	Method of Preparing Metals from Their Halides	F.H. Spedding H.A. Wilhelm W.H. Keller
2 785 065	Mar. 12, 1957	Method of Producing Metals from Their Halides	F.H. Spedding H.A. Wilhelm W.H. Keller
2 787 536	Apr. 2, 1957	Process for Melting and Refining Uranium	F.H. Spedding H.A. Wilhelm
2 787 538	Apr. 2, 1957	Production of Uranium	F.H. Spedding H.A. Wilhelm W.H. Keller
2 796 320	June 18, 1957	Solvent Extraction Process for Purification of Thorium	F.H. Spedding A. Kant
2 797 160	June 25, 1957	Production of Zirconium	F.H. Spedding H.A. Wilhelm W.H. Keller
2 798 789	July 9, 1957	Method of Separating Rare Earths	F.H. Spedding E.J. Wheelwright J.E. Powell
2 826 495	Mar. 11, 1958	Alloy for Use in Nuclear Fission	F.H. Spedding H.A. Wilhelm
2 830 894	Apr. 15, 1958	Production of Uranium	F.H. Spedding H.A. Wilhelm W.H. Keller
2 837 548	June 3, 1958	Separation Process Using Complexing and Adsorption	F.H. Spedding J.A. Ayres
2 852 364	Sep. 16, 1958	Melting and Purification of Uranium	F.H. Spedding C.F. Gray
2 877 109	Mar. 10, 1959	Process for Separating Uranium Fission Products	F.H. Spedding T.A. Butler I.B. Johns
2 882 125	Apr. 14, 1959	Volatile Fluoride Process for Separating Plutonium from Other Materials	F.H. Spedding A.S. Newton

Patents of F.H. Spedding (cont'd)

US Patent No.	Date		Title	Inventors
2 889 205	June 2,	1959	Method of Separating Nitrogen Isotopes by Ion-exchange	F.H. Spedding J.E. Powell
2 903 351	Sep. 8,	1959	Th–Be Alloys and Method of Producing Same	F.H. Spedding H.A. Wilhelm W.H. Keller
2 938 784	May 31,	1960	Nuclear Fuel Composition	F.H. Spedding H.A. Wilhelm
2 950 962	Aug. 30,	1960	Reduction of Fluoride to Metal	F.A. Schmidt O.N. Carlson F.H. Spedding
2 956 858	Oct. 18,	1960	Method of Separating Rare Earths by Ion Exchange	F.H. Spedding J.E. Powell
3 000 726	Sep. 19,	1961	Production of Metals	F.H. Spedding H.A. Wilhelm W.H. Keller
3 034 889	May 15,	1962	Decontamination of Uranium	F.H. Spedding T.A. Butler

F.H. Spedding's awards

Langmuir Award (American Chemical Society Award in Pure Chemistry for chemists under 31)	1933
Guggenheim Fellowship to Europe	1935
LL.D., Drake University	1946
Iowa Medal of the American Chemical Society	1948
D.Sc., University of Michigan	1949
Phi Lambda Upsilon Jubilee Plaque for Outstanding Work in Inorganic Chemistry	1949
Nichols Medal of the New York Section of the American Chemical Society	1952
Member National Academy of Sciences	1952
D.Sc., Case Institute of Technology (now Case/Western Reserve University)	1956
Distinguished Professor in Sciences and Humanities, Iowa State University	1957
Honorary Member, Verein Österreichischer Chemiker	1958
James Douglas Gold Medal of American Institute of Mining, Metallurgical and Petroleum Engineers	1961
Distinguished Citizen Award of the State of Iowa	1961
Faculty Citation presented by the Alumni Association of Iowa State University	1964
Honorary Member, Phi Lambda Upsilon	1966

Atomic Energy Commission Citation Award for meritorious contributions to the Nation's atomic energy program	1967
American Chemical Society Midwest Award	1967
Distinguished Service Award by Ames Chamber of Commerce	1968
Honorary Member, Applied Spectroscopy Society	1969
Francis J. Clamer Medal of the Franklin Institute	1969
Award of Merit, Iowa Academy of Science	1974
Spedding Symposium, Eleventh Rare Earth Research Conference	1974
Distinguished Fellow, Iowa Academy of Science	1975

Frank H. Spedding Prize – named after F.H. Spedding and awarded to scientists at the Rare Earth Research Conferences in recognition of distinguished contributions in the field of rare earth science and/or technology. First presented in 1979 at the 14th Conference.

Publications of F.H. Spedding

1929

with S. Freed, Line absorption spectra in solids at low temperatures in the visible and ultraviolet regions of the spectrum. Nature **123**, 525, 526.

with S. Freed, Line absorption spectra of solids at low temperatures in the visible and ultraviolet regions of the spectrum. Phys. Rev. **34**, 945–953.

1930

with S. Freed, A comparison of the reflection spectra of $SmCl_3 \cdot 6H_2O$ at room temperature and at that of liquid air with its absorption spectra at low temperatures. Phys. Rev. **35**, 212, 213.

with S. Freed, The line spectra of ions in the solid state in the visible and ultraviolet regions of the spectrum. The absorption spectra of $GdBr_3 \cdot 6H_2O$ at room temperature and at that of liquid air and their comparison with those of $GdCl_3 \cdot 6H_2O$. J. Am. Chem. Soc. **52**, 3747.

with S. Freed, Paschen-back effect on the line spectra of solids. Phys. Rev. **35**, 1408, 1409.

1931

with S. Freed, Diagram of some of the energy levels of gadolinium IV in the crystal lattice as obtained from the ultraviolet absorption spectra of $GdCl_3 \cdot 6H_2O$ and $GdBr_3 \cdot 6H_2O$. Phys. Rev. **38**, 670–678.

with G.C. Nutting, Effect of crystal symmetry on the energy levels of solids. Experimental evidence of definite orientation of coordinated water molecules about rare earth ions in solution. Phys. Rev. **38**, 2294, 2295.

Interpretation of the spectra of rare earth crystals. Phys. Rev. **37**, 777–779.

Zeeman effect in solids. Phys. Rev. **38**, 2080–2082.

1932

with R.S. Bear, Absorption spectra of the samarium ion in solids. I. Absorption by large crystals of $SmCl_3 \cdot 6H_2O$. Phys. Rev. **42**, 58–75.

with R.S. Bear, Absorption spectra of the samarium ion in solids. II. Conglomerate absorption of $SmCl_3 \cdot 6H_2O$ and a partial energy level diagram of the Sm^{+++} ion as it exists in crystalline $SmCl_3 \cdot 6H_2O$. Phys. Rev. **42**, 76–85.

with R.S. Bear, Line reflection spectra of solids. Phys. Rev. **39**, 948–952.

Magnetic susceptibility of samarium sulfate. J. Am. Chem. Soc. **54**, 2593–2597.

1933

with G.C. Nutting, The effect of crystal symmetry and chemical composition on the energy levels of solids. J. Am. Chem. Soc. **55**, 496–504.

Interpretation of line spectra in crystals. Phys. Rev. **43**, 143, 144.

Zeeman effect in solids. J. Chem. Phys. **1**, 144–154.

with G.N. Lewis, A spectroscopic search for H^3 in concentrated H^2. Phys. Rev. **43**, 964–966.

with C.D. Shane and N.S. Grace, Fine structure of H^2-α. Phys. Rev. **44**, 58.

with R.S. Bear, Absorption spectra of the samarium ion in solids. III. Absorption of $Sm(BrO_3)_3 \cdot 9H_2O$ and a partial energy-level diagram for the Sm^{+++} ion as it exists in crystalline $Sm(BrO_3)_3 \cdot 9H_2O$. Phys. Rev. **44**, (4), 287–295.

1934

with R.S. Bear, Absorption spectra of the samarium ion in solids. IV. Absorption of $Sm(C_2H_3SO_4)_3 \cdot 9H_2O$ and partial energy-level diagrams for the Sm^{+++} ion as it exists in hydrated crystalline samarium ethyl sulfate, samarium iodide and samarium perchlorate. Phys. Rev. **46**, 308–315.

with R.S. Bear, Absorption spectra of the samarium ion in solids. V. The absorption spectrum and energy levels of the Sm^{+++} ion as it exists in monoclinic crystals of $Sm_2(SO_4)_3 \cdot 8H_2O$. Phys. Rev. **46**, 975–983.

with G.C. Nutting, The line absorption spectrum of crystalline $KCr(SO_4)_2 \cdot 12H_2O$. J. Chem. Phys. **2**, 421–431.

1935

with C.D. Shane, A spectroscopic determination of *e/m*. Phys. Rev. **47**, 33.

with C.D. Shane and N.S. Grace, The fine structure of Hα. Phys. Rev. **47**, 38–44.

with G.C. Nutting, Zeeman effect of the absorption lines of crystalline $KCr(SO_4)_2 \cdot 12H_2O$. J. Chem. Phys. **3**, 369–375.

1936

The nature of energy states in solids. Phys. Rev. **50**, 574.

1937

with H.A. Bethe, The absorption spectrum of $Tm_2(SO_4)_3 \cdot 8H_2O$. Phys. Rev. **52**, 454, 455.

with G.C. Nutting, The line absorption spectrum of gadolinium ion in crystals. J. Chem. Phys. **5**, 33–45.

Further relationships between absorption spectra of rare earth solids and crystal structure. J. Chem. Phys. **5**, 160.

with H.F. Hamlin and G.C. Nutting, Energy states of solids with particular reference to the energy states of $Nd_2(SO_4)_3 \cdot 8H_2O$. J. Chem. Phys. **5**, 191–198.

The nature of the crystalline fields present in $Er_2(SO_4)_3 \cdot 8H_2O$. J. Chem. Phys. **5**, 316–320.

with J.P. Howe and W.H. Keller, The energy states of crystalline $Pr_2(SO_4)_3 \cdot 8H_2O$. J. Chem. Phys. **5**, 416–429.

with H.F. Hamlin, Energy states in solids with particular reference to $NdCl_3 \cdot 6H_2O$. J. Chem. Phys. **5**, 429–442.

Sharp absorption lines for use as a comparison spectrum in stellar photography. Phys. Rev. **52**, 137, 138.

1939

Luminescence in solids. Introductory paper. J. Chem. Soc. Faraday Trans. **35**, 65–69.

1940

The absorption of praseodymium ion in solutions and in the solid state. Phys. Rev. **58**, 255–257.

with C.C. Moss and R.C. Waller, The absorption spectra of europium ion in some hydrated salts. J. Chem. Phys. **8**, 908–918.

with R.M. Hixon, Raman spectra of sugars, dextrins and starches. Rep. Agr. Research, Part 2, Iowa Corn Research Inst., 5th Ann. Rep. 1940, pp. 62, 63.

1942

with R.F. Stamm, The Raman spectra of the sugars in the solid state and in solution. 1. The Raman spectra of α- and β-d-glucose. J. Chem. Phys. **10**, 176–183.

1947

with A.F. Voigt, E.M. Gladrow and N.R. Sleight, The separation of rare earths by ion exchange. I. Cerium and yttrium. J. Am. Chem. Soc. **69**, 2777–2781.

with A.F. Voigt, E.M. Gladrow, N.R. Sleight, J.E. Powell, J.M. Wright, T.A. Butler and P. Figard, The separation of rare earths by ion exchange. II. Neodymium and praseodymium. J. Am. Chem. Soc. **69**, 2786–2792.

with E.I. Fulmer, T.A. Butler, E.M. Gladrow, M. Gobush, P.E. Porter, J.E. Powell and J.M. Wright, The separation of rare earths by ion exchange. III. Pilot plant scale separations. J. Am. Chem. Soc. **69**, 2812–2818.

1948

with E.I. Fulmer, B. Ayers, T.A. Butler, J. Powell, A.D. Tevebaugh and R. Thompson, Improved ion-exchange method for separating rare earths in macro quantities. J. Am. Chem. Soc. **70**, 1671, 1672.

1949

A chemist views the atomic energy problem. J. Electrochem. Soc. **95**, 17c–24c.

with A.S. Newton, J.C. Warf, O. Johnson, R.W. Nottorf, I.B. Johns and A.H. Daane, Uranium hydride. I. Preparation, composition and physical properties. Nucleonics **4**(1), 4–15.

with A.S. Newton, J.C. Warf, O. Johnson, I.B. Johns, R.W. Nottorf, J.A. Ayers, R.W. Fisher and A. Kant, Uranium hydride. II. Radiochemical and chemical properties. Nucleonics **4**(2), 17–25.

with J.C. Warf, A.S. Newton and T.A. Butler, Uranium hydride. III. Dispersions in mercury. Nucleonics **4**(3), 43–47.

Large scale separation of rare earth salts and preparation of the pure metals. Discussions Faraday Soc. **7**, 214–231.

1950

with E.I. Fulmer, T.A. Butler and J.E. Powell, The separation of rare earths by ion exchange. IV. Further investigations concerning variables involved in the separation of samarium, neodymium and praseodymium. J. Am. Chem. Soc. **72**, 2349–2354.

with E.I. Fulmer, T.A. Butler and J.E. Powell, The separation of rare earths by ion exchange. V. Investigations with one-tenth per cent citric acid–ammonium citrate solutions. J. Am. Chem. Soc. **72**, 2354–2361.

1951

with E.I. Fulmer, J.E. Powell, T.A. Butler and I.S. Yaffe, The separation of rare earths by ion exchange. VI. Conditions for effecting separations with Nalcite–HCR and one-thenth per cent citric acid–ammonium citrate solutions. J. Am. Chem. Soc. **73**, 4840–4847.

The rare earths. Sci. Amer. **185**(5), 26–30.

with D.H. Parkinson and F.E. Simon, The atomic heats of the rare earth elements. Proc. R. Soc. (London) **207**, 137–155.

1952

with J.E. Powell, Quantitative calculations of the behavior of elution bands in the separation of rare earths by ion-exchange columns. J. Am. Chem. Soc. **74**, 856.

with J.E. Powell, Quantitative theory of rare earth separations on ion-exchange columns. J. Am. Chem. Soc. **74**, 857.

with P.E. Porter and J.M. Wright, Conductances of aqueous solutions of some rare earth chlorides at 25°C. J. Am. Chem. Soc. **74**, 2055–2058.

with P.E. Porter and J.M. Wright, Transference numbers of rare earth chlorides in aqueous solution at 25°C. J. Am. Chem. Soc. **74**, 2778–2781.

with P.E. Porter and J.M. Wright, Activity coefficients of rare earth chlorides in aqueous solutions at 25°C. J. Am. Chem. Soc. **74**, 2781–2783.

with A.H. Daane, The preparation of rare earth metals. J. Am. Chem. Soc. **74**, 2783–2785.

with C.F. Miller, The heat capacities and heat contents of solutions of cerium and neodymium chlorides at 25°C. J. Am. Chem. Soc. **74**, 3158–3162.

with C.F. Miller, Thermochemistry of the rare earths. I. Cerium and neodymium. J. Am. Chem. Soc. **74**, 4195–4198.

with I.S. Yaffe, Conductances, transference numbers, and activity coefficients of aqueous solutions of some rare earth halides at 25°C. J. Am. Chem. Soc. **74**, 4751–4755.

with H.A. Wilhelm, W.H. Keller, D.H. Ahmann, A.H. Daane, C.C. Hach and R.P. Ericson, The production of pure rare earth metals. Ind. & Eng. Chem. **44**, 553–556.

with N. James and S. Legvold, The resistivity of lanthanum, cerium, praseodymium, and neodymium at low temperatures. Phys. Rev. **88**, 1092–1098.

with B.A. Rogers, Progress in metallurgy. Ann. Rev. Nucl. Sci. **1**, 441–464.

1953

with A.F. Kip, C. Kittel, A.H. Portis and R. Barton, Microwave resonance absorption in gadolinium metal. Phys. Rev. **89**, 518.

with E.J. Wheelwright, A rapid method for fractionating crude rare earth ores into mixtures greatly enriched with regard to particular rare earths. J. Am. Chem. Soc. **75**, 2529.

with A.H. Daane and D.H. Dennison, The preparation of samarium and ytterbium metals. J. Am. Chem. Soc. **75**, 2272.

with E.J. Wheelwright and G. Schwarzenbach, The stability of the rare earth complexes with ethylene diamine tetraacetic acid. J. Am. Chem. Soc. **75**, 4196.

with J.F. Elliott and S. Legvold, Some magnetic properties of gadolinium metal. Phys. Rev. **91**, 28–30.

with A.H. Daane, Preparation of yttrium and some heavy rare earth metals. J. Electrochem. Soc. **100**, 442.

with C.J. Kevane and S. Legvold, The Hall effect in yttrium, lanthanum, cerium, praseodymium, neodymium, gadolinium, dysprosium and erbium. Phys. Rev. **91**, 1372–1379.

with S. Legvold, F. Barson and J. Elliott, Some magnetic and electrical properties of gadolinium, dysprosium and erbium metals. Rev. Mod. Phys. **25**, 129, 130.

1954

with J.E. Powell and E.J. Wheelwright, The separation of adjacent rare earths with ethylenediaminetetraacetic acid by elution from an ion-exchange resin. J. Am. Chem. Soc. **76**, 612, 613.

with J. Dye, Conductances, transference numbers and activity coefficients of aqueous solutions of some rare earth chlorides at 25°C. J. Am. Chem. Soc. **76**, 879–881.

with S. Jaffe, Conductances, solubilities and ionization constants of some rare earth sulfates in aqueous solutions at 25°C. J. Am. Chem. Soc. **76**, 882–884.

with S. Jaffe, Conductances, transference numbers and activity coefficients of some rare earth perchlorates and nitrates at 25°C. J. Am. Chem. Soc. **76**, 884–888.

with J. Dye, The application of Onsager's theory of conductance to the conductances and transference numbers of unsymmetrical electrolytes, J. Am. Chem. Soc. **76**, 888–892.

with J. Flynn, Integral heats of solution of some rare earth trichlorides. J. Am. Chem. Soc. **76**, 1477.

with J. Flynn, Thermochemistry of the rare earths. II. La, Pr, Sm, Gd, Er, Yb, Y. J. Am. Chem. Soc. **76**, 1474.

with M. Griffel and R. Skochdopole, The heat capacity of gadolinium from 15°K to 355°K. Phys. Rev. **93**, 657–661.

with J.E. Powell, A practical separation of yttrium group rare earths from gadolinite by ion-exchange. Chem. Eng. Prog. **50**(14), 7–15.

with J.E. Powell, The separation of rare earths by ion exchange. VII. Quantitative data for the elution of neodymium. J. Am. Chem. Soc. **76**, 2545.

with J.E. Powell, The separation of rare earths by ion exchange. VIII. Quantitative theory of the mechanism involved in elution by dilute citrate solution. J. Am. Chem. Soc. **76**, 2550.

with S. Legvold and J. Elliott, The magnetic susceptibility of neodymium metal. Phys. Rev. **94**, 50, 51.

with S. Legvold and J. Elliott, Some magnetic properties of dysprosium metal. Phys. Rev. **94**, 1143–1145.

with J.E. Powell and E. Wheelwright, The use of copper as the retaining ion in the elution of rare earths with ammonium ethylenediamine tetraacetate solutions. J. Am. Chem. Soc. **76**, 2557.

with A.H. Daane, R.E. Rundle and H.G. Smith, The crystal structure of samarium. Acta Crystallogr. **7**, 532–535.

with J.E. Powell, Methods for separating rare earth elements in quantity as developed at Iowa State College, J. Met. **6**, 1131–1135.

with A.H. Daane, Methods of producing pure rare earth metals as developed at Iowa State College, J. Met. **6**, 504–510.

with S. Legvold and J. Banister, The structure of Gd, Dy, and Er at low temperatures, Phys. Rev. **94**, 1140–1142.

with S. Untermyer, A.H. Daane, J.E. Powell and R.J. Hasterlik, Portable thulium X-ray unit. Nucleonics **12**(5), 35–37.

1955

with S. Legvold and J. Elliott, Some of the ferromagnetic properties of erbium metal. Phys. Rev. **100**, 1595, 1596.

with R.E. Skochdopole and M. Griffel, The heat capacity of erbium from 15 to 320°K. J. Chem. Phys. **23**, 2258–2263.

with J.E. Powell and H.J. Svec, A laboratory method for separating nitrogen isotopes by ion exchange. J. Am. Chem. Soc. **77**, 1393 (Letter to the Editor).

with J.L. Dye, The vapor pressure of mercury at 250–360°C. J. Phys. Chem. **59**, 581.

with J.E. Powell and H.J. Svec, A laboratory method for separating nitrogen isotopes by ion exchange. J. Am. Chem. Soc. **77**, 6125.

1956

with J.E. Powell and E.J. Wheelwright, The stability of the rare earth complexes with n-hydroxyethelethylene-diaminetriacetic acid. J. Am. Chem. Soc. **78**, 34.

with A.H. Daane and K.W Hermann, The crystal structures and lattice parameters of high-purity scandium, yttrium and the rare earth metals. Acta Crystallogr. **9**, 559.

with J.E. Powell, The isolation in quantity of individual rare earths of high purity by ion exchange, in: Ion Exchange Technology, eds F.C. Nachod and J. Schubert (Academic Press, New York) ch. 15, pp. 359–360.

with M. Griffel and R.E. Skochdopole, Heat capacity of dysprosium from 15 to 300°K. J. Chem. Phys. **25**, 75–79.

with A.H. Daane, The preparation and properties of rare earth metals, in: Series V of Progress in Nuclear Energy, Vol. 1 (Pergamon Press, New York) ch. 5.

with R.G. Johnson, D.F. Hudson, W.C. Caldwell and W.R. Savage, Mass spectrometric study of phase changes in aluminum, praseodymium, and neodymium, J. Chem. Phys. **25**, 917–925.

1957

with H. Frank, Atomic Fuels, in: Proc. 5th World Power Conference in Vienna, 1956; see also Metal Progress, October 1957, pp. 105–111.

with S. Legvold, A.H. Daane and L.D. Jennings, Some physical properties of the rare earth metals, in: Progress in Low Temperatures Physics, Vol. II, ed. C.J. Gorter (North-Holland, Amsterdam) ch. XII.

with F. Barson and S. Legvold, Thermal expansion of rare earth metals. Phys. Rev. **105**, 418–424.

with D.R. Behrendt and S. Legvold, Magnetic properties of neodymium single crystals. Phys. Rev. **106**, 723–725.

with A.H. Daane and K.W. Herrmann, Electrical resistivities and phase transformations of lanthanum, cerium, praseodymium and neodymium, J. Met. **9**, 895–897.

with B.C. Gerstein, M. Griffel, L.D. Jennings, R.E. Miller and R.E. Skochdopole, Heat capacity of holmium from 15 to 300°K. J. Chem. Phys. **27**, 394–399.

with J.F. Smith and C.E. Carlson, Elastic properties of yttrium and eleven of the rare earth elements, J. Met. **9**, 1212, 1213.

with R.J. Barton and A.H. Daane, The vapor pressure of thulium metal. J. Am. Chem. Soc. **79**, 5160.

with L.D. Jennings and R.M. Stanton, Heat capacity of terbium from 15 to 350°K. J. Chem. Phys. **27**, 909–913.

1958

with M. Smutz and J. Bochinski, Some of the ferromagnetic properties of erbium metal. Phys. Rev. **100**, 1595, 1596.

with J. Bochinski and M. Smutz, Separation of individual rare earths by liquid–liquid extraction from multicomponent monozite rare earth nitrates. Undiluted tributyl phosphate and concentrated aqueous rare earth nitrate systems at low acid concentrations. Chem. Eng. Prog. **50**(2), 157.

with G.S. Anderson and S. Legvold, Superconductivity of lanthanum and some lanthanum alloys. Phys. Rev. **109**, 243–247.

with D.R. Behrendt and S. Legvold, Magnetic properties of dysprosium single crystals. Phys. Rev. **109**, 1544–1547.

with B.L. Rhodes and S. Legvold, Magnetic properties of holmium and thulium metals. Phys. Rev. **109**, 1547–1550.

with Masao Atoji, K. Gschneidner Jr, A.H. Daane and R.E. Rundle, The structures of lanthanum dicarbide and sesquicarbide by X-ray and neutron diffration. J. Am. Chem. Soc. **80**, 1804.

with J.J. Hanak and A.H. Daane, The preparation and properties of europium. Trans. Met. Soc. AIME A **212**, 379.

with W.C. Thoburn and S. Legvold, Magnetic properties of the Gd–La and Gd–Y alloys. Phys. Rev. **110**, 1298–1301.

with K.A. Gschneidner Jr and A.H. Daane, The crystal structures of some of the rare-earth carbides. J. Am. Chem. Soc. **80**, 4499.

with J.E. Powell, A.H. Daane, M.A. Miller and W.H. Adams, Methods for preparing pure scandium oxide. J. Electrochem. Soc. **105**, 683–686.

with G.S. Anderson and S. Legvold, Hall effect in Lu, Yb, Tm, and Sm. Phys. Rev. **111**, 1257, 1258.

with W.C. Thoburn and S. Legvold, Magnetic properties of terbium metal. Phys. Rev. **112**, 56–58.

1959

with A.W. Naumann and R.E. Eberts, Heats of dilution and related thermodynamic properties of aqueous rare-earth salt solutions at 25°C; integral heats of solution of $NdCl_3 \cdot 6H_2O$. J. Am. Chem. Soc. **81**, 23.

with W.R. Savage and D.E. Hudson, Mass spectrometric study of heats of sublimation of dysprosium, samarium, thulium and ytterbium. J. Chem. Phys. **30**, 221–227.

with G. Atkinson, Properties of rare-earth salts in electrolytic solutions, in: The Structure of Electrolytic Solutions, ed. W.J. Hamer (Wiley, Inc., New York) pp. 319–339.

with J.E. Powell, Basic principles involved in the macroseparation of adjacent rare earths from each other by means of ion exchange. Chem. Eng. Prog. Symp. Ser. **55**(24), 101–113.

with K.A. Gschneidner Jr and A.H. Daane, The lanthanum–carbon system. Trans. Met. Soc. AIME **215**, 192–197.

with J.E. Powell, The separation of rare earths by ion exchange. Trans. Met. Soc. AIME **215**, 457–463.

with L.D. Jennings and E.D. Hill, Heat capacity of samarium from 13 to 350°K. J. Chem. Phys. **31**, 1240–1243.

with S. Legvold and P.M. Hall, Electrical resistivity of yttrium single crystals. Phys. Rev. **116**, 1446, 1447.

1960

with R.M. Stanton and L.D. Jennings, Heat capacity of terbium from 1.4 to 4.0°K. J. Chem. Phys. **32**, 630, 631.

with J.J McKeown and A.H. Daane, The high temperature thermodynamic functions of cerium, neodymium and samarium. J. Phys. Chem. **64**, 289.

with S. Legvold and M.A. Curry, Electrical resistivity of europium and ytterbium. Phys. Rev. **117**, 953, 954.

with S. Legvold and P.M. Hall, Electrical resistivity of dysprosium single crystals. Phys. Rev. **117**, 971–973.

with O.N. Carlson, J.A. Heafling and F.A. Schmidt, Preparation and refining of yttrium metal by Y–Mg alloy process. J. Electrochem. Soc. **107**, 540–545.

with A.H. Daane, G. Wakefield and D.H. Dennison, Preparation and properties of high purity scandium metal. Trans. Met. Soc. AIME **218**, 608–611.

with A.H. Daane, The rare-earth metals. Met. Rev. **5**, 297–348.

with R.V. Colvin and S. Legvold, Electrical resistivity of the heavy rare-earth metals. Phys. Rev. **120**, 741–745.

with J.E. Powell and D.B. James, The separation of rare earths. J. Chem. Educ. **37**, 629.

with L.D. Jennings and R.E. Miller, Lattice heat capacity of the rare earths. Heat capacities of yttrium and lutetium from 15–350°K. J. Chem. Phys. **33**, 1849–1852.

1961

with J.K. Alstad, R.V. Colvin and S. Legvold, Electrical resistivity of lanthanum, praseodymium, neodymium and samarium. Phys. Rev. **121**, 1637–1639.

with J.J. Hanak and A.H. Daane, High temperature allotropy and thermal expansion of the rare-earth metals. J. Less-Common Met. **3**, 110–124.

with R.W. Green and S. Legvold, Magnetization and electrical resistivity of erbium single crystals. Phys. Rev. **122**, 827–830.

with L.D. Jennings and E. Hill, Heat capacity of thulium from 15° to 360°K. J. Chem. Phys. **34**, 2082–2089.

with D.B. James and J.E. Powell, Cation-exchange elution sequences – Divalent and rare-earth cations with EDTA, HEDTA and citrate. J. Inorg. Nucl. Chem. **19**, 133–141.

with O.C. Trulson and D.E. Hudson, Cohesive energies of europium, gadolinium, holmium and erbium. J. Chem. Phys. **35**, 1018–1026.

with H.J. Born and S. Legvold, Low-temperature thermoelectric power of the rare earth metals. J. Appl. Phys. **32**, 2543–2549.

with A.H. Daane, eds, The Rare Earths (Wiley, Inc., New York).

1962

Rare Earths. Int. Science & Technology, April 1962, pp. 39–46.

with B.C. Gerstein and F.J. Jelinek, Correlation between heat capacity anomaly in Tb and magnetic transition in Tb_2O_3. Phys. Rev. Lett. **8**, 425.

with J.L. Mackey and J.E. Powell, A calorimetric study of the reaction of rare-earth ions with EDTA in aqueous solution. J. Am. Chem. Soc. **84**, 2047.

with R.M. Valletta and A.H. Daane, Some rare-earth alloy systems – La–Gd, La–Y, Gd–Y. Trans. Quarterly (ASM) **55**, 483–491.

with L. Strandburg and S. Legvold, Electrical and magnetic properties of holmium single crystals. Phys. Rev. **127**, 2046–2051.

with B.C. Gerstein and L.D. Jennings, Thermal and magnetic study of crystal field splittings in thulium ethylsulfate. J. Chem. Phys. **37**, 1496–1508.

with B.C. Gerstein and C.J. Penney, Thermal study of crystal field splittings in erbium ethylsulfate. J. Chem. Phys. **37**, 2610–2615.

1963

The macro separation of stable isotopes on ion exchange columns. J. Chim. Phys. (France) **60**, 89.

with D.E. Hegland and S. Legvold, Magnetization and electrical resistivity of terbium single crystals. Phys. Rev. **131**, 158–162.

with H.E. Nigh and S. Legvold, Magnetization and electrical resistivity of gadolinium single crystals. Phys. Rev. **132**, 1092–1097.

1964

with D.K. Finnemore, B.J. Beaudry, J.D. Leslie, R.L. Cappelletti and D.M. Ginsberg, Far-infrared absorption in superconducting lanthanum. Phys. Rev. **134**, A309–A311.

with B.C. Gerstein, J. Mullaly, E. Phillips and R.E. Miller, Heat capacity of Yb from 15°–350°K. J. Chem. Phys. **41**, 883–889.

with K.A. Gschneidner Jr, Rare earth oxides. Industrial Research, December 1964, pp. 60–65.

with H.E. Nigh, S. Legvold and B.J. Beaudry, Magnetic properties of Gd–Sc alloys. J. Chem. Phys. **41**, 3799–3801.

1965

with D.K. Finnemore, D.L. Johnson, J.E. Ostenson and B.J. Beaudry, Superconductivity in pure La and La–Gd. Phys. Rev. **137**, A550–A556.

with T. Murao and R.H. Good Jr, Theory of Zeeman effect for rare-earth ions in crystal field with C_{3h} symmetry. J. Chem. Phys. **42**, 993–1011.

with W.J. Haas, W.L. Sutherland and C.A. Eckroth, Anisotropic Zeeman effect in erbium ethylsulfate when the magnetic field is perpendicular to the C uniaxis of the crystal. J. Chem. Phys. **42**, 981–992.

with D.K. Finnemore, Specific heat evidence for gapless superconductivity, in: Proc. 9th Conf. on Low Temperature Physics – LT9, Part A (Plenum Press, New York) pp. 521–523.

with B.J. Beaudry, M. Michel and A.H. Daane, The Y–Nd and Sc–Nd phase systems, in: Rare Earth Research III, ed. L. Eyring (Gordon and Breach, New York) pp. 247–260.

1966

with D.A. Csejka and C.W. DeKock, Heats of dilution of aqueous rare earth chloride solutions at 25°. J. Chem. Phys. **70**, 2423.

with M.J. Pikal, Relative viscosities of some aqueous rare earth chloride solutions at 25°. J. Chem. Phys. **70**, 2430.

with M.J. Pikal and B.O. Ayers, Apparent molal volumes of some aqueous rare earth chloride and nitrate solutions at 25°. J. Phys. Chem. **70**, 2440.

with K.C. Jones, Heat capacities of aqueous rare earth chloride solutions at 25°. J. Phys. Chem. **70**, 2450.

with F.J. Jelinek, B.C. Gerstein, M. Griffel and R.E. Skochdopole, Re-evaluation of some thermodynamic properties of gadolinium metal. Phys. Rev. **149**, 489, 490.

1967

with T. Murao, W.J. Haas, R.W.G. Syme and R.H. Good Jr, Theory of Zeeman effect for rare-earth ions in crystal field with C_{3h} symmetry. II. J. Chem. Phys. **47**, 1572–1580.

with F.J. Jelinek, J.R. Mullaly, W.D. Shickell and B.C. Gerstein, Heat capacity of europium from 5°–300°K. J. Chem. Phys. **47**, 5194.

with G.F. Wakefield and A.H. Daane, Vapor pressure of holmium. J. Chem. Phys. **47**, 4994.

1968

with R.W.G. Syme, W.J. Haas and R.H. Good Jr, Theory of Zeeman effect for rare-earth ions in crystal field with C_{3h} symmetry. III. J. Chem. Phys. **48**, 2772–2785.

with M.T. Rothwell, W.J. Haas and W.L. Sutherland, Absorption spectrum and Zeeman effect of the transitions $^5I_8 \rightarrow {}^3K_8$ and $^5I_8 \rightarrow {}^5G_4$ in holmium ethylsulfate. J. Chem. Phys. **48**, 4843.

with R.W.G. Syme, W.J. Haas and R.H. Good Jr, Ratios of odd-parity crystal-field parameters for erbium ethylsulfate. Chem. Phys. Lett. **2**, 132–136.

with D.K. Finnemore, L.J. Williams and D.C. Hopkins, Neutron diffraction and susceptibility study of dilute La–rare-earth alloys. Phys. Rev. **176**, 712–717.

with B.J. Beaudry, J.J. Croat and P.E. Palmer, The properties, preparation and handling of 'pure' rare earth metals. Materials technology – An interamerican approach, in: Proc. Inter-American Conf. on Materials Technology, San Antonio, TX, May 20–24, 1968, p. 151.

1969

with R.G. Jordan and R.W. Williams, Magnetic properties of Tb–Ho single-crystal alloys, I. Magnetization measurements. J. Chem. Phys. **51**, 509–520.

with B.C. Gerstein, W.A. Taylor and W.D. Shickell, Heat capacity of lutetium from 6 to 300°K. J. Chem. Phys. **51**, 2924–2928.

with W.J. Gray, A technique for cutting and polishing small metal spheres. Rev. Sci. Instrum. **40**, 1427, 1428.

1970

with T.O. Brun, S.K. Sinha, N. Wakabayashi, G.H. Lander and L.R. Edwards, Temperature dependence of the periodicity of the magnetic structure of thulium metal. Phys. Rev. B **1**, 1251–1253.

with B.J. Beaudry, J.J. Croat and P.E. Palmer, The preparation and properties of ultra-pure metals. Research and Development Report, U.S.A.E.C. IS-2238, Vol. I, No. 180, pp. 25–45.

with Y. Ito and R.G. Jordan, Magnetic properties of Tb–Ho single-crystal alloys. II. Neutron diffraction studies. J. Chem. Phys. **53**, 1455–1465.

1971

with Y. Ito, R.G. Jordan and J. Croat, Magnetic properties of Tb–Ho single-crystal alloys. III. Neutron diffraction studies of Ho rich alloys. J. Chem. Phys. **54**, 1995–2003.

with D. Cress and B.J. Beaudry, The resistivity of scandium single crystals. J. Less-Common Met. **23**, 263–270.

with D.C. Henderson, High-temperature heat contents and related thermodynamic functions of seven trifluorides of the rare earths: Y, La, Pr, Nd, Gd, Ho and Lu. J. Chem. Phys. **54**, 2476–2483.

with B.C. Gerstein, W.A. Taylor and W.D. Shickell, Heat capacity of scandium from 6 to 350°K. J. Chem. Phys. **54**, 4723–4728.

with B.J. Beaudry, The effect of impurities, particularly hydrogen, on the lattice parameters of the ABAB rare earth metals. J. Less-Common Met. **25**, 61–73.

with J.J. Tonnies and K.A. Gschneidner Jr, Elastic moduli and thermal expansion of lutetium single crystals from 4.2 to 300°K. J. Appl. Phys. **42**, 3275–3283.

with N. Wakabayashi and S.K. Sinha, Phonon spectrum of scandium metal by inelastic scattering of neutrons. Phys. Rev. B **4**, 2398–2406.

1972

with D.C. Rulf and B.C. Gerstein, Thermal study of entropies and crystal field splittings in heavy rare earth trichloride hexahydrates. Heat capacities from 5–300°K. J. Chem. Phys. **56**, 1498–1506.

with W.A. Taylor, B.C. Gerstein and W.D. Shickell, On a thermal and magnetic study of the crystal field energy levels in dilute rare-earth alloys. I. $Lu_{0.9035}Er_{0.0965}$. J. Chem. Phys. **56**, 2722–2730.

with T. Kambara, W.J. Haas and R.H. Good Jr, Theory of Zeeman effect for rare-earth ions in crystal field with C_{3h} symmetry. IV. J. Chem. Phys. **56**, 4475–4480.

with C.F. Hale, Thermodynamics of the association of aqueous europium(III) and sulfate ions. J. Phys. Chem. **76**, 1887–1894.

with Koreyuki Shiba, Anisotropic self-diffusion in erbium single crystals. J. Chem. Phys. **57**, 612–617.

with C.F. Hale, Effect of high pressure on the formation of aqueous $EuSO_4^+$ at 25°. J. Phys. Chem. **76**, 2925–2929.

with W. Gildseth and A. Habenschuss, Precision measurements of densities and thermal dilation of water between 5° and 80°C. J. Chem. Eng. Data **17**, 402–409.

1973

with T. Kambara, W.J. Haas and R.H. Good Jr, Theory of Zeeman effect for rare earth ions in crystal field with D_2 symmetry and application to rare earths garnets. J. Chem. Phys. **58**, 672–686.

with B. Sanden and B.J. Beaudry, The Er–Y, Tb–Ho, Tb–Er, Dy–Ho, Dy–Er and Ho–Er phase systems. J. Less-Common Met. **31**, 1–13.

with T. Kambara, W.J. Haas and R.H. Good Jr, Theory of crystal distortion and Zeeman effects in rare earth compounds with zircon structure. Phys. Rev. B **7**, 3945–3953.

with T. Kambara and W.J. Haas, Paramagnetoelectric effect in rare-earth garnets. J. Chem. Phys. **58**, 3656–3660.

with J.J. Croat, Magnetic properties of high purity scandium and the effect of impurities on these properties. J. Chem. Phys. **58**, 5514.

with W.C. Mundy and L. Gutierrez, Raman intensities of the uncoupled OD oscillators in liquid water. J. Chem. Phys. **59**, 2173.

with W.C. Mundy, Raman spectra of water in rare earth chloride solutions. J. Chem. Phys. **59**, 2183–2190.

with J.J. Croat, Magnetic properties of high purity yttrium, lanthanum and lutetium and the effects of impurities on these properties. J. Chem. Phys. **59**, 2451.

with M. Habenschuss, C. Stassis and S.K. Sinha, Neutron diffraction study of the magnetic structure of $Er_{0.75}Lu_{0.25}$. Phys. Lett. A **45**, 281.

with J.D. Greiner, R.J. Schiltz Jr, J.J. Tonnies and J.F. Smith, Elastic constants of praseodymium single crystals in the temperature range 4.2–300°K. J. Appl. Phys. **44**, 3862–3867.

1974

with B.J. Beaudry, D.C. Henderson and J. Moorman, High temperature enthalpies and related thermodynamic functions of the trifluorides of Sc, Ce, Sm, Eu, Gd, Tb, Dy, Er, Tm and Yb. J. Chem. Phys. **60**, 1578, 1588.

with P.F. Cullen and A. Habenschuss, Apparent molal volumes of some dilute aqueous rare earth salt solutions at 25°. J. Phys. Chem. **78**, 1106–1110.

with J.A. Rard, Electrical conductances of some aqueous rare earth electrolyte solutions at 25°. I. The rare earth perchlorates. J. Phys. Chem. **78**, 1435.

with M. Habenschuss, C. Stassis, S.K. Sinha and H.W. Deckman, Neutron diffraction study of the magnetic structure of erbium. Phys. Rev. B **10**, 1020.

with B.J. Beaudry, The Gd–Yb and Lu–Yb phase systems. Metall. Trans. **5**, 1631.

with L. Gutierrez and W.C. Mundy, Raman spectrum of HDO in rare earth perchlorate solutions. J. Chem. Phys. **61**, 1953–1959.

Rare earth elements and their compounds, in: Encyclopedia Britannica, Vol. 15, pp. 515–527.

Some remarks on the rare earths by a Fifty-Year student of the subject, in: Proc. 11th Rare Earth Research Conference, Traverse City, MI, October 7–10, 1974, Vol. 1, pp. 266–277.

with A. Habenschuss, A survey of some properties of aqueous rare earth salt solutions. I. Volume, thermal expansion, Raman spectra and x-ray diffraction, in: Proc. 11th Rare Earth Research Conference, Traverse City, MI, October 7–10, 1974, Vol. 2, p. 909.

with J.A. Rard, A survey of some properties of aqueous rare earth salt solutions. II. Heats of dilution, heat capacities, activity coefficients, electrical conductances and relative viscosities, in: Proc. 11th Rare Earth Research Conference, Traverse City, MI, October 7–10, 1974, Vol. 2, p. 919.

with D.L. Witte, L.E. Shiers and A. Rard, Relative viscosities of some aqueous rare earth chloride solutions at 25°C. J. Chem. Eng. Data **19**, 369–373.

with J.A. Rard and V.W. Saeger, Electrical conductances of some aqueous rare earth electrolyte solutions at 25°C. II. Rare earth chlorides. J. Chem. Eng. Data **19**, 373–378.

with R.A. Nelson and J.A. Rard, Conductances, transference numbers and activity coefficients of some aqueous terbium halides at 25°C. J. Chem. Eng. Data **19**, 379–381.

1975

with L.E. Shiers and J.A. Rard, Relative viscosities of some aqueous rare earth perchlorate solutions at 25°C. J. Chem. Eng. Data **20**, 66–72.

with V.W. Saeger, K.A. Gray, P.K. Boneau, M.A. Brown, C.W. DeKock, J.L. Baker, L.E. Shiers, H.O. Weber and A. Habenschuss, Densities and apparent molal volumes of some aqueous rare earth solutions at 25°C. I. Rare earth chlorides. J. Chem. Eng. Data **20**, 72–81.

with L.E. Shiers, M.A. Brown, J.L. Derer, D.L. Swanson and A. Habenschuss, Densities and apparent molal volumes of some aqueous rare earth solutions at 25°C. II. Rare earth perchlorates. J. Chem. Eng. Data **20**, 81–88.

with L.E. Shiers and J.A. Rard, Relative viscosities of some aqueous rare earth nitrate solutions at 25°C. J. Chem. Eng. Data **20**, 88–93.

with J.A. Rard, Electrical conductances of some aqueous rare earth electrolyte solutions at 25°C. III. The rare earth nitrates. J. Phys. Chem. **79**, 257–262.

with J.L. Baker and J.P. Walters, Apparent and partial molal heat capacities of aqueous rare earth perchlorate solutions at 25°C. J. Chem. Eng. Data **20**, 189–195.

with L.E. Shiers, M.A. Brown, J.L. Baker, L. Guitierrez, L.S. McDowell and A. Habenschuss, Densities and apparent molal volumes of some aqueous rare earth solutions at 25°C. III. Rare earth nitrates. J. Phys. Chem. **79**, 1087–1096.

with W.M. Gildseth and A. Habenschuss, Densities and thermal expansion of some aqueous rare earth chloride solutions between 5° and 80°C. I. $LaCl_3$, $PrCl_3$ and $NdCl_3$. J. Chem. Eng. Data **20**, 292–309.

with B.J. Beaudry, The solubility of RH_{2-x} in Gd, Er, Tm, Lu and Y from ambient to 850°C. Metall. Trans. B **6**, 419–427.

with J.P. Walters and J.L. Baker, Apparent and partial molal heat capacities of some aqueous rare earth chloride solutions at 25°C. J. Chem. Eng. Data **20**, 438–443.

1976

with A. Habenschuss, Densities and thermal expansion of some aqueous rare earth chloride solutions between 5° and 80°C. II. $SmCl_3$, $GdCl_3$, $DyCl_3$, $ErCl_3$ and $YbCl_3$. J. Chem. Eng. Data **21**, 95–113.

with B.J. Beaudry and W.D. Cress, Single crystal resistivity of erbium and Er–Lu alloys between 2 and 300K. Rev. Chim. Miner. (France) **13**, 62–70.

with G.P. Felcher, G.H. Lander, T. Arai and S.K. Sinha, Asphericity in the magnetization distribution of holmium. Phys. Rev. B **13**, 3034–3045.

with H.O. Weber, V.W. Saeger, H.H. Petheram, J.A. Rard and A. Habenschuss, Isopiestic determination of the activity coefficients of some aqueous rare earth electrolyte solutions at 25°C. I. The rare earth chlorides. J. Chem. Eng. Data **21**, 341–360.

with J.A. Rard, A. Habenschuss, A review of the osmotic coefficients of aqueous H_2SO_4 at 25°C. J. Chem. Eng. Data **21**, 374–379.

with J.L. Derer, M.A. Mohs and J.A. Rard, Heats of dilution of some aqueous rare earth electrolyte solutions at 25°C. II. Rare earth nitrates. J. Chem. Eng. Data **21**, 474–488.

1977

with J.A. Rard, Isopiestic determination of the osmotic coefficients of aqueous $CaCl_2$ solutions at 25°C. J. Chem. Eng. Data **22**, 56–58.

with C.W. DeKock, G.W. Pepple and A. Habenschuss, Heats of dilution of some aqueous rare earth electrolyte solutions at 25°C. III. Rare earth chlorides. J. Chem. Eng. Data **22**, 58–70.

with M.A. Mohs, J.L. Derer and A. Habenschuss, Heats of dilution of some aqueous rare earth electrolyte solutions at 25°C. I. Rare Earth Perchlorates. J. Chem. Eng. Data **22**, 142–153.

with J.A. Rard and A. Habenschuss, A review of the osmotic coefficients of aqueous $CaCl_2$ at 25°C. J. Chem. Eng. Data **22**, 180–186.

with J.A. Rard and H.O. Weber, Isopiestic determination of the activity coefficients of some aqueous rare earth electrolyte solutions at 25°C. II. The rare earth perchlorates. J. Chem. Eng. Data **22**, 187–201.

with J.A. Rard and A. Habenschuss, Standard state entropies of the aqueous rare earth ions. J. Phys. Chem. **81**, 1069–1974.

with J.A. Rard, L.E. Shiers and D.J. Heiser, Isopiestic determination of the activity coefficients of some aqueous rare earth electrolyte solutions at 25°C. III. The rare earth nitrates. J. Chem. Eng. Data **22**, ~~56–58.~~ 337-347.

1978

with A. Habenschuss, Di-μ-chloro-bis[heptaaquapraseodymium(III)] tetrachloride $[(H_2O)_7PrCl_2$ $Pr(H_2O)_7]Cl_4$. J. Cryst. Struct. Commun. **7**, 535.

with W.A. Taylor and M.B. Levy, Specific heat of lutetium from 1.6 to 18K. J. Phys. F **8**, 2293–2299.

Prologue, in: Handbook on the Physics and Chemistry of Rare Earths, Vol. 1, eds K.A. Gschneidner Jr and L. Eyring (North-Holland, Amsterdam) pp. 15–25.

1979

with A. Habenschuss, The coordination (hydration) of rare earth ions in aqueous chloride solutions from x-ray diffraction. I. $TbCl_3$, $DyCl_3$, $ErCl_3$, $TmCl_3$ and $LuCl_3$. J. Chem. Phys. **70**, 2797–2806.

with A. Habenschuss, The coordination (hydration) of rare earth ions in aqueous chloride solutions from x-ray diffraction. II. $LaCl_3$, $PrCl_3$ and $NdCl_3$. J. Chem. Phys. **70**, ~~2797–2806.~~ 3758-5763

with A. Habenschuss, Di-μ-chloro-bis[heptaaqualanthanum(III)] tetrachloride $[(H_2O)_7LaCl_2La(H_2O)_7]Cl_4$. J. Cryst. Struct. Commun. **8**, 511.

with J.A. Rard and D.G. Miller, Isopiestic determination of the activity coefficients of some aqueous rare earth electrolyte solutions at 25°C. IV. $La(NO_3)_3$, $Pr(NO_3)_3$ and $Nd(NO_3)_3$. J. Chem. Eng. Data **24**, 348–354.

with J.L. Baker and J.P. Walters, Apparent and partial molal heat capacities of aqueous rare earth nitrate solutions at 25°C. J. Chem. Eng. Data **24**, 298–305.

1980

with A. Habenschuss, Dichlorohexaaquaneodymium (III) chloride $[NdCl_2(H_2O)_6]Cl$. J. Cryst. Struct. Commun. **9**, 71.

with A. Habenschuss, Dichlorohexaaqualutetium (III) chloride $[LuCl_2(H_2O)_6]Cl$. J. Cryst. Struct. Commun. **9**, 157.

with A. Habenschuss, Dichlorohexaaquasamarium chloride $[SmCl_2(H_2O)_6]Cl$. J. Cryst. Struct. Commun. **9**, 207.

with A. Habenschuss, Dichlorohexaaquagadolinium chloride $[GdCl_2(H_2O)_6]Cl$. J. Cryst. Struct. Commun. **9**, 213.

with A. Habenschuss, The coordination (hydration) of rare earth ions in aqueous chloride solutions from x-ray diffraction. III. $SmCl_3$, $EuCl_3$ and series behavior. J. Chem. Phys. **73**, 442–450.

1981[*]

with K.K. Sharma and D.R. Blinde, Optical and magnetic studies of HoF_3. Phys. Rev. B **24**, 82–89.

1982

with J.A. Rard, Isopiestic determination of the activity coefficients of some aqueous rare earth electrolyte solutions at 25°C. 6. $Eu(NO_3)_3$, $Y(NO_3)_3$ and YCl_3. J. Chem. Eng. Data **27**, 454–461.

* with J.A. Rard, Isopiestic determination of the activity coefficients of some aqueous rare earth electrolyte solutions at 25°C. 5. $Dy(NO_3)_3$, $Ho(NO_3)_3$ and $Lu(NO_3)_3$. J. Chem. Eng. Data, 26, 391-395.

Handbook on the Physics and Chemistry of Rare Earths, Vol. 11
edited by K.A. Gschneidner, Jr. and L. Eyring

Chapter 73

THE HISTORY OF THE DISCOVERY AND SEPARATION OF THE RARE EARTHS

F. SZABADVARY
Museum for Science and Technology, Kaposvár u. 13, Budapest POB 311, Hungary H 1502.

Contents

Introduction

The great age of discovering new elements, stimulated by the new definition conceived by Boyle, Lavoisier and Dalton that a chemical element is a substance that cannot be further decomposed by chemical means, occurred in the 18th and 19th century. During this period, sixty-eight of the ninety natural elements were discovered. To discover a new element meant great scientific fame; no wonder that new elements were being announced in large numbers, including many which – sooner or later – turned out to be errors. Overmore, the errors outnumbered the discoveries of true elements. For a long time no foothold existed as to how many chemical elements could possibly exist, and only practice gave some hints as where to look for new elements.

The path of discovery of the elements belonging to the group termed rare earth elements was particularly confused and chaotic. It started 200 years ago, in 1787, and it closed in 1947 with the discovery of promethium. The rare earth elements cannot be properly and decently arranged in any of the numerous periodic tables of chemical elements developed since Mendeleev and Meyer, and though the modern

picture of atomic structure provides an explanation for their unusual behaviour, there is no definite answer as yet to the question *why* these elements behave in such an unusual manner.

Literature on the history of chemistry deals with the history of rare earth elements only a sketchy manner; it is due for a thorough and detailed discussion. While I was working on this chapter, I fully understood the reasons of this perfunctory treatment, experiencing the vast confusion, the many contradictions, errors and mistakes accompanying the discovery of the rare earth elements. I certainly do not venture to claim that I succeeded – within the narrow scope of this chapter – to fill all gaps in the history of the rare earth elements. I do hope, however, that I may have offered more than was known up until now on all the admirable analytical efforts needed to discover these peculiar elements, which stubbornly resisted usual analytical separation techniques.

1. The beginnings: yttrium and cerium

In tables representing the periodic system the element lanthanum (La) having the atomic number 57 is followed in most cases immediately by element 72, hafnium (Hf). The elements in between, i.e. cerium (Ce, 58), praseodymium (Pr, 59), neodymium (Nd, 60), promethium (Pm, 61), samarium (Sm, 62), europium (Eu, 63), gadolinium (Gd, 64), terbium (Tb, 65), dysprosium (Dy, 66), holmium (Ho, 67), erbium (Er, 68), thulium (Tm, 69), ytterbium (Yb, 70) and lutetium (Lu, 71), are listed separately, usually somewhere at the bottom of the table, just as if these elements existed only to annoy the constructors of the various types of periodic tables with the problem of how to place them in some acceptable manner. The elements cited – together with yttrium and scandium located above them in the periodic table – are collectively termed rare earth elements, on the one hand because most of them were found, in their oxide form, in two minerals, and were considered 'earths' as was usual at the time, and on the other hand because apparently they were rare. The latter attribute, however, is not fully correct. The rare earth elements are actually not very rare; moreover, some of them, e.g., yttrium, are more abundant on our planet than cadmium or mercury. Whereas, however, the latter elements occur in rather high concentrations in their minerals, the former are found in numerous rocks, but in very low concentrations. This was one of the reasons why it was so difficult to identify them. Since they usually occur together and their chemical behaviour – owing to their particular atomic structure – is extremely similar, their separation is a very exacting analytical task. This is the other reason why their discovery took so long; it was in fact a process that lasted over 160 years. Rare earth elements are found mainly in two minerals: yttria and ceria, both of them contained in monazite sand. With much laborious work the chemists lured new element after element from these minerals, only to find out later that the new 'elements' were not homogeneous substances, but mixtures, which – after further wearisome separation operations – turned out to consist of two or more elements. Whenever some novel method appeared in analytical chemistry and was applied to these substances, new elements were discovered in most cases.

1.1. *Yttria*

The history of rare earth elements began in 1787. Carl Axel Arrhenius, a lieutenant of the Swedish Royal Army, was a gifted, though amateur, mineralogist. At an excursion in the vicinity of Ytterby, a small Swedish town three miles away from Stockholm, he found a curious black mineral that had never before been mentioned by anyone. He just called it 'black stone'. Ever since, many rare earth elements bear the name of the town Ytterby. As new elements again and again turned up from analyzing the black mineral, the discoverers gave them names by varying the name Ytterby: yttrium, ytterbium, terbium, erbium all stem from it.

The new mineral was first studied by an acquaintance of Arrhenius, Bengt Reinhold Geijer. He was the first to report on it in the literature. He assumed that the asphalt-like mineral contained tungsten, by reason of its high density (Geijer 1788).

The next scientist who took interest in the mineral was a Finnish chemist, Johan Gadolin. He analyzed it in 1794 and found a new 'earth' in it that was similar in many respects to alumina and also to lime. It amounted to 38% of the mineral; Gadolin also found iron and silicate as constituents (Gadolin 1794, 1796).

Gadolin's statement was confirmed by the investigation of Ekeberg in Stockholm during the following year. Ekeberg found that the mineral also contained beryllium; finally, it turned out to be iron–beryllium–yttrium silicate. Ekeberg's finding demonstrates the surprising rapidity of scientific information in those years: beryllium had only just been discovered by the French chemist Vauquelin. (Vauquelin's discovery attracted much attention in Sweden, presumably because he discovered beryllium in the precious stones beryl and emerald which had earlier been analyzed by one of the greatest figures in Swedish chemistry: Torbern Bergman. This scientist maintained that he found aluminium in them. It was Vauquelin's discovery that exposed Bergman's error. Let it be said in Bergman's excuse that the properties of beryllium and aluminium are largely similar, the only analytical difference detectable with the techniques available at the time is that aluminium hydroxide is soluble in excess alkali and beryllium hydroxide is not.) It was Ekeberg who gave the name yttria to the new earth discovered by Gadolin (Ekeberg 1797, 1799). At the time, 'earths' were universally considered elements. Although Antal Ruprecht, professor at the Mining Academy in Selmecbánya (Hungary) reported in 1790 that he obtained metals by reducing alkaline earths (i.e. alkaline-earth metal oxides) with carbon (Ruprecht 1790), Klaproth proved that Ruprecht's metal clumps were derived from impurities in the crucible used in the experiments (Klaproth 1791). The fact that 'earths' were not elements but compounds was conclusively demonstrated only from 1807 on, when Davy electrolyzed their melts and undisputably obtained metals from them.

Ekeberg again detected yttria in 1802 in another black mineral, yttrotantalite (found also close to Ytterby). However, in this mineral he also discovered another new metal: tantalum.

After Davy had separated numerous metals such as calcium, strontium and barium from alkaline earths in the first decade of the 19th century, chemists began to use the name yttrium for the metal instead of yttria, however, it still took a long

time until they were able to produce the element in the pure state.

When two well-known analytical chemists, Klaproth (1801) and Vauquelin (1801), confirmed the existence of Gadolin's and Ekeberg's new element, yttrium occupied its rightful place among the elements, or rather among the 'earths', still considered elements in those years. Klaproth then gave a new name to the 'black stone', the mineral found by Arrhenius: he called it gadolinite, after the discoverer of yttrium, who was still alive at that time. (To name minerals after persons became a fairly regular habit in mineralogy. Similar suggestions to name new elements after persons also came up in chemistry, but – mainly due to the opposition of Berzelius – were not realized. It is of interest that Gadolin's name was the only one later given to a natural element still bearing it.)

Carl Axel Arrhenius (1757–1824) did not care much for the military profession (he was an officer of the engineer corps), but was passionately interested in chemistry and mineralogy. He frequently visited the laboratory of the Mining Academy. During his stay in Paris he attended the lectures of Lavoisier and Fourcroy. He was one of the first champions in Sweden of the new antiphlogistic chemistry based on oxygen. When in Sweden, he attended the lectures of Berzelius and also worked in his laboratory. He terminated his military career as lieutenant-colonel, but parallelly he also made a remarkable scientific career: he was elected a member of the Swedish Academy of Science (Anonymous 1824).

Bengt Reinhold Geijer (1758–1815) was a member of the Swedish Royal Council of Mines, royal chief assayer, later director of the Royal Institute of Mining. He was a member of the Swedish Academy of Sciences (Anonymous 1816).

Johan Gadolin (1760–1822) was born in Åbo (today Turku), an old Finnish university town which at the time belonged to Sweden. His father was professor of physics at the university. (After a great fire in 1828 the university moved to Helsinki and is still run there.) Johan Gadolin studied at the University of Åbo and subsequently spent five years in Uppsala in Torbern Bergman's institute. It was there that he acquired extensive experience in mineral analysis. After Bergman's death he hoped to become his successor. Since, however, he was not appointed, he returned to the university of his birthplace. He travelled much all over Europe and became acquainted with the leading chemists of the age. It was he who published the first book in Swedish (*Inleding till chemien*, 1798) that was based on Lavoisier's new theory of chemistry. In 1797 he was appointed professor of chemistry and mineralogy to the University of Åbo and remained in this position until his death. Besides his activity in analytical chemistry, his papers dealing with specific heat are also noteworthy. Gadolin was active in politics too: he was one of the pioneers fighting for the independence of Finland. It took, however, another hundred years for independence to come true. Gadolin, anyhow, still lived to see Swedish rule over Finland change to Russian rule in 1809 (Ojala 1937).

Anders Gustaf Ekeberg (1767–1813) was born in Stockholm. He studied in Uppsala, Greifswald and Berlin. He began his career in the Swedish Mining Council and later became associate professor of chemistry at the University of Uppsala. In 1799, he was elected a member of the Swedish Academy of Science. Based on Lavoisier's chemical nomenclature he developed a Swedish chemical nomenclature (1795), he published it anonymously, however, because he feared his professor, who remained faithful to the phlogiston theory. Ekeberg is also significant as an analytical chemist. With the discovery of tantalum he acquired lasting merits (Boklund 1971).

Nicolas Louis Vauquelin (1763–1829) was born in the French village St. André. At the age of 14, he began to work as a pharmacist's apprentice in Rouen and, subsequently, as an assistant in Paris

Fig. 1. Johan Gadolin (Courtesy of the National Museum of Finland).

to a pharmacist who was, as it happens, the brother-in-law of Fourcroy, the famous chemist. Fourcroy then employed Vauquelin as an assistant in his own laboratory. In 1794 he became associate professor at the new École des Travaux Publiques (the later École Polytechnique).

In 1797 he became professor of analytical chemistry at the École des Mines, later professor of chemistry of the Collége de France. Later he also taught chemistry at the Musée d'Histoire Naturelle and at the medical faculty. His activity in mineral analysis is very significant. He discovered two new elements: beryllium as mentioned above, and chromium (Cuvier 1833).

1.2. *Ceria*

The other basic mineral of the rare earth elements is the mineral today called cerite. It was also first found in Sweden, earlier than gadolinite, and the chemists suspected as early as in the middle of the 18th century that it contains some unknown 'earth'. The mineral occurred in the Bastnäsgrube mine close to Rydderhyttan. Very many silicate-based related minerals and found there, most of

Fig. 2. Martin Heinrich Klaproth.

them containing rare earths and besides them other metals as well. Even their mineralogical systematization was rather a problem, no wonder that the chemists of that age were unable to cope with the task. Already Cronstedt, the famous discoverer of nickel (Cronstedt 1751), and thirty years later the greatest analyst of the age, Torbern Bergman (Bergman 1784) suspected something, but neither got farther than suspicion. Another twenty years had to pass until simultaneously Berzelius and Hisinger in Sweden and Klaproth in Berlin confirmed the suspicion, and separated the unknown 'earth' from the mineral. It proved to be the main component besides silicate. They achieved their results independently from one another and reported on them in one and the same year (Hisinger and Berzelius 1804, Klaproth 1804) in one and the same journal, namely in the *Neues Allgemeines Journal der Chemie*, cited after its editor, professor Gehlen, usually as Gehlen's Journal. They sent their papers so nearly simultaneously that Berzelius received a letter saying that Klaproth's paper on the same subject will appear in the current issue, his paper in the next. The fairness of the editor is characterized by

the fact that in the issue in which Klaproth's paper was published a note appeared announcing that a paper on a similar subject had already arrived at the journal simultaneously. Klaproth named the new earth ochroite earth, while Berzelius and Hisinger named it cerium after the small planet Ceres discovered at the time. (It is perhaps unfair to cite Berzelius's name first, since Hisinger's name stands first as author. However, at the time Berzelius was quite a novice as yet, while Hisinger was a well-known, rich factory owner who was much interested in scientific questions and recognized Berzelius's talent. The latter's career makes it seem probable that it was he who performed the bulk of analytical work. By the way, in that same year Berzelius – with Hisinger's material support – founded a journal '*Afhandlingar i Fysik, Kemi och Mineralogi*' which appeared for six years and involved a significant financial loss. However, Hisinger was on bad terms at the time with the journal of the Swedish Academy of Science. In the first issue of the new journal, Hisinger and Berzelius also published their paper on the discovery of ceria in Swedish.)

Klaproth believed that the new substance was an element, Berzelius, however, already assumed that it was the oxide of a new element.

Martin Heinrich Klaproth (1743–1817), the son of a country tailor, started his career, as so many great chemists, as a pharmacist's apprentice. He then worked as an assistant in Hannover, Danzig and Berlin in various pharmacies. While Klaproth worked in Berlin the owner of the pharmacy died unexpectedly and Klaproth led the pharmacy until the son came of age. Later Klaproth bought a pharmacy from the dowry of his wife. Meanwhile he was continually occupied with scientific problems, namely with the chemical analysis of minerals. In 1788, he was elected a member of the Scientific Academy in Berlin, and in 1800 he was charged with leading the chemical laboratory of the Academy. In 1809, he was appointed professor of chemistry at the University of Berlin then founded, and remained in this position until his death. Besides cerium he discovered the elements uranium and zirconium, and he was the first to study thoroughly the metals strontium, titanium and tellurium discovered by others. The name tellurium was given to the element by Klaproth (Szabadváry 1966, p. 117).

Jöns Jakob Berzelius (1779–1848) was the greatest and most important chemist of the first half of the past century. He was born in Väversunda, his father was a school teacher. He was orphaned early and studied unaided to graduate as a medical doctor. He became an assistant and, in 1807, professor of chemistry in the Collegium Medicum in Stockholm, at the time still a school to train army surgeons, it was transformed into a medical university during Berzelius's professorship. (Nowadays, it is called the Karolinska Institute, which up to the present day awards the Nobel Prizes in medicine and biology.) Berzelius was elected a member of the Swedish Academy of Sciences in 1808 and became its secretary in 1820. He also undertook several industrial ventures, most of which, however, were unsuccessful. In 1835, he was raised to the baronial rank in recognition of his merits in chemical science.

Berzelius was the first to determine the atomic mass of the elements with satisfactory accuracy. It was he who introduced the chemical symbols still in use. His dualistic electrochemical hypothesis concerning the structure of compounds was a fundamental and progressive chemical theory for a long period. He was one of the pioneers of elemental analysis of organic substances. Berzelius wrote numerous books. His manual of chemistry has been translated into several languages and was reprinted five times in Berzelius's lifetime. In his annual reports, entitled *Jahresbericht*, published from 1821 until his death he critically abstracted the scientific publications of the year. The *Jahresbericht* was the ancestor of the numerous present scientific abstracting publications, all of them can be traced back to it. Besides cerium Berzelius discovered

thorium and selenium, the latter in the mud of his own sulfuric acid factory. He was the first to produce elemental zirconium, silicon and thorium (Szabadváry 1966, p.125).

Wilhelm Hisinger (1766–1852) was born in Skinnskatteberg, where his father was proprietor of a thriving iron-works. Hisinger studied mining and subsequently took over the family enterprise. He occupied himself with many branches of science, with chemistry, mineralogy, zoology and cartography. In 1804, he was elected a member of the Swedish Academy of Science.

2. Mosander's activities: the first division

It appears that for two decades nobody was concerned particularly with the two new elements. They were not considered elemental earths any more, since by then it was established that 'earths' are metal oxides. Ceria was put down as cerium oxide, and yttria as yttrium oxide. Berzelius, with his complicated method, calculated the atomic masses of the elements from their compounds. It is known that huge errors were involved in this method: one could obtain half or twice, eventually three times the correct value, by reason of assuming the number of atoms in the compound incorrectly. It thus happened that Berzelius gave a value of 46.05 to the atomic mass of cerium relative to H = 1, that is, about one third of the true value (140.13), and 32.254 instead of 88.92 for yttrium (Szabadváry 1966, p. 144). The values demonstrate that in addition to the theoretical error, an analytical error was also included. The analytical error was imperative, since it later turned out that the compounds considered oxides of a single element were, in fact, mixtures of about a dozen oxides of different elements.

It was Carl Gustaf Mosander, assistant of Berzelius who, in the twenties of the 19th century, again took up the oxides of the two elements and continued his work imperturbably for over two decades, with the result that the two elements turned into six.

He first attempted to obtain cerium in the elemental metallic state. It was already known at that time that reduction with carbon is unsuited to produce the metal from these 'earths'. Davy, in the first decade of the century, obtained pure alkali metals and alkaline-earth metals by using melt electrolysis. Gay Lussac and Thénard applied metallic potassium as a new reducing agent in 1808: they mixed boric acid and potassium in a proportion of 1 : 1 and heated the mixture in a hydrogen flow. They succeeded in this manner to obtain elemental boron. The method was successful for decomposing other oxides too, and Mosander tried it for cerium. His first experiences were negative, potassium metal had no effect on cerium oxide. He therefore experimented with the chloride. He heated cerium sulfide in a glass tube with chlorine gas, left the chloride formed in the tube and passed potassium vapour in hydrogen through it, while heating the tube. Potassium chloride and elemental cerium were formed. He demonstrated the formation of the latter by dissolving it in water. The reaction proceeded with evolution of hydrogen, without, however, the solution turning alkaline, thereby excluding the possibility that it was potassium which was being dissolved. Mosander then treated the mixture with alcohol and dried it in vacuum. He obtained a chocolate brown powder, which

turned successively lighter as it became oxidized during storage in air. Mosander then studied the reactions of cerium with various substances: sulfur, selenium, phosphoric acid, organic acids, etc. This work was all carried out in 1826 (Berzelius 1828).

Certain phenomena, namely that the colour of cerium and its compounds varied in different experiments, and that slight differences were found in the densities of cerium oxides from different provenances, made Mosander assume that maybe the substance was not homogeneous after all, maybe something unknown was still hidden in it. He began to study the problem very thoroughly and for a very long time.

Mosander was a slow, conscientious and very reserved researcher. Wöhler, the well-known chemist, the first to perform the synthesis of an organic compound, worked for a longer period in Berzelius's laboratory, where he was the colleague of Mosander and knew about his research work. Wöhler, after his return to Germany, stood in correspondence with Berzelius until the death of the latter. Their correspondence appeared in bookform too, it is a very good and entertaining source for getting acquainted with the scientific background of the period (Wallach 1901). In this correspondence Wöhler inquired several times how Mosander stood with his investigations, all the more so, because he would have liked to get a paper from Mosander for the journal *Annalen der Chemie* (today generally termed *Liebig's Annalen*) whose editor he was.

> 'I can't tell you anything new about Father Moses, he never says anything about what he has found, not so much because he is so reserved, but perhaps because he has not found anything. He is so busy with his mineral water factory that he has no time for anything else. Write to him directly, you may then perhaps get a paper from him for the Annalen'

wrote Berzelius once, apparently with the discontent of the boss. However, Mosander did progress and found very interesting things. He reported in 1839 that his assumption proved correct. Cerium oxide considered homogeneous earlier did contain, in an amount of two fifths, another element which he named lanthanum (from the Greek work *lanthano* meaning *escape notice*) (Mosander 1839, Berzelius 1840). The name was suggested by Berzelius to his co-worker who by then was his successor in the professorial chair. (The human attitude of Berzelius is well characterized by a letter to Magnus, another of his former pupils: In the spring of this year I'll give up my post at the Karolinska Institute... I feel it my duty to make over this post to Mosander, since otherwise his hair could turn grey as my first assistant (Hjelt 1900).) Berzelius was presumably led in this suggestion by the fact that it had remained hidden before him, the discoverer of cerite, that the substance was not homogeneous, but contained another element besides cerium.

Mosander discovered the new element in the following manner: he transformed cerium (III) oxide into the carbonate, which he dissolved in nitric acid and evaporated to dryness. He pulverized the residue to a fine powder and treated it with cold dilute nitric acid, in which the more basic lanthanum oxide was dissolved, while cerium oxide remained undissolved. He then separated the lanthanum from

Fig. 3. Jöns Jakob Berzelius.

the solution with sodium oxalate, by igniting the precipitate, he obtained pale brick-coloured lanthanum oxide. The oxide could not be reduced with metallic potassium, similarly to cerium oxide, but from the chloride the metallic lanthanum could be obtained. After purification with alkohol he obtained soft scales with a metallic glimmer, which dissolved in water accompanied by hydrogen evolution. In the aqueous solution slimy lanthanum hydroxide was formed, the solution changed the colour of litmus to blue. By treating the oxide with hydrogen sulfide he obtained lanthanum sulfide. The atomic mass of lanthanum being smaller than the atomic mass of the mixture earlier assumed to be pure cerium, the true atomic mass of cerium must be higher than the earlier value.

It was high time for Mosander to publish his results, because meanwhile, also in 1839, Axel Erdmann, a former pupil of Berzelius and Mosander, also detected an unknown element in a Norwegian mineral, which – a strange coincidence – he

proposed to name mosandrite. From the mineral sample sent to Berzelius, Mosander stated that the element is identical with lanthanum. (Wöhler was informed of lanthanum already earlier through Berzelius, he inquired with astonishment why Mosander did not publish his results. Berzelius replied that he also had encouraged him many times to publish, but Mosander only shrugged his shoulders irritably, maintaining that he could not publish anything before he had finally finished the investigations, and that takes much time. In fact, Berzelius, in his *Jahresbericht*, which in the Swedish original appeared in 1839, was ahead of Mosander's own paper on the discovery of lanthanum. Berzelius recognized the importance of the discovery and therefore – departing from his custom, to the luck of Mosander – he reported the work of Mosander executed in Berzelius's former laboratory without referring to an already printed source.)

However, the lanthanum oxides obtained in different experiments were not identical in colour, differences in shade were observable. Nor were the cerium oxide residues fully identical. From these phenomena, based on his previous experiences, Mosander again began to suspect that the lanthanum separated was not a pure element, but may contain yet another new element. He continued his experiments and reported their success in 1842 (Mosander 1842). He detected a further new element, which he named didymium. This element figured under this name for 50 years in books on chemistry, until it was disclosed that didymium is not a homogeneous element, but the mixture of two elements. Today, when instrumental analysis presents innumerable high-performance techniques to the analyst, we can hardly imagine how difficult it was, how much skill and inventiveness was required to separate these elements by the traditional gravimetric processes. The analyst of our days would probably be unable to repeat it. By way of example I shall cite the process used in the discovery of didymium, as abstracted by Berzelius (Berzelius 1844a):

'Earlier studies made Mosander suspect that cerium oxide obtained from cerite contains a foreign substance. He attempted to separate it by shaking cerium oxide hydrate with water, introducing chlorine gas to transform cerium oxydul into cerium oxide and the unknown substance into chlorure. Insoluble yellow cerium oxide was precipitated in the operation. From the filtrate he again precipitated the solute with potassium hydrate, shook the suspension and again introduced chlorine gas. Further cerium oxide was precipitated and the rest was dissolved. He repeated this operation several times, in this manner he succeeded to separate the total amount of cerium oxide and obtain a chlorure from which potassium hydrate precipitated a hydrate that did not turn yellow in air and when treated with chlorine, was completely soluble in water. Thus the separation was terminated, and the oxide which is not further oxidized by chlorine gas was termed lanthanum oxide, as generally known.

When treating a mixture of lanthanum oxide and cerium oxide with 50–200 parts of nitric acid diluted with water, lanthanum oxide was dissolved, but the residual cerium oxide was not yellow, but brownish-red, and the lanthanum oxide also had a more or less similar reddish tint. From this phenomenon Mosander concluded that a third substance must be present, following in one experiment lanthanum oxide

completely, whereas in the other experiment it is distributed between cerium oxide and lanthanum oxide. Vast experimenting was needed to separate it with the certainty allowing Mosander to claim that the substance is the oxide of a previously unknown element. In no way did it appear possible to separate the substances in question completely, since all precipitating agents tested acted similarly on them. Finally Mosander succeeded to separate their sulfates be repeated crystallization. The sulfate of cerium oxidul is least soluble, that of lanthanum oxide somewhat more and that of the third metal oxide readiest. The salts of the third metal oxide have a fine amethyst purple colour with a pale violet tint. Their solutions are pink, with a blue tint. Mosander named the metal oxide separated in the above manner didymium oxide from the Greek word didymos, that is, twins, since it accompanies cerium and lanthanum as a twin in cerium minerals ...

The preparation of didymium oxide will give a good picture on the difficulties connected with the separation of these substances. The sulfates of the mixture of lanthanum oxide and didymium oxide are dissolved in small portions in 6 parts of cold water cooled from the outside, so that its temperature should remain below $+9^{\circ}C$. The solution is then heated to $+40^{\circ}C$, where a slightly amethyst-coloured powder separates. It is the sulfate of lanthanum oxide contaminated with some didymium oxide. This precipitation results from the property of the lanthanum salt that at a certain temperature it changes its chemically bonded water content. The pure reddish solution is decanted, the precipitate is dried, again dissolved in 6 parts of water at $+9^{\circ}C$, subsequently it is heated to $50^{\circ}C$ and kept at this temperature until a precipitate is formed. This is again the lanthanum salt, now contaminated with less didymium. By repeating this operation 10–12 times, one obtains almost pure lanthanum salt and a solution containing both salts. This solution is red. It is mixed with an equal weight of water, acidified with sulfuric acid and left standing to evaporate at a lukewarm place. When the volume of the solution has decreased to one sixth, the usually yellow liquid is decanted from the salt mass at the bottom. The latter consist of larger red crystals and smaller prismatic needles. A small amount of boiling water is poured on it and subsequently rapidly decanted. The remaining larger red crystals are then again dissolved in water, acidified with sulfuric acid and slightly evaporated. Again two types of crystals separate, long, narrow rhombic prisms and larger red ones. The former are meticulously singled out, the latter consist of the sulfate of didymium oxide.

They are again dissolved in water, and precipitated with potassium hydrate. The precipitate is didymium oxide hydrate. When filtered on paper it is bluish violet. During filtration and wash it rapidly takes up carbonic acid and thereby changes its colour to a slightly reddish violet. After ignition didymium oxide is obtained...' (Berzelius 1844a,b).

To be sure, this work did need lots of patience!

Wöhler, Berzelius's permanent correspondence partner, was not satisfied with the name didymium. He wrote that it sounds like childish babble, it is not worthy to specify an element. He urged Berzelius to persuade Mosander to choose a better name. We are informed from Berzelius's reply that in addition to 'twinship' Mosander had other points speaking for the name didymium.

Fig. 4. Carl Gustaf Mosander (Courtesy Library Karolinska Institutet Stockholm).

'No, dear friend, I don't like the name either, but can't ask him to change it, since he has already publicly announced it. You are surely unable to understand our friend Father Moses. He doesn't accept suggestions from anyone. He would be offended by a proposal to change a name given by him. He was led by the point of view that the name should begin with a D, since this letter is as yet free as a chemical symbol. You're right the repetition of the consonants and vowels is displeasant to the ear, but one can get accustomed to it ...'.

Well, Mosander invented the name didymium in vain in favour of the symbol D, it did not remain permanently in the list of the elements, as will be seen in what follows. Also, the name mosandrium was later introduced by others several times for elements, but no element by this name now exists.

Let us return, however, to Mosander, since he had not nearly finished his successful activities in the complex world of the rare earth elements. He hunted up two further elements. Encouraged by the success with cerite, he now started investigating gadolinite. Maybe yttrium is no homogeneous element either? And he proved to be correct.

His suspicion, of course, had antecedents. Heinrich Rose discovered earlier that yttrium chloride itself is not volatile, although it was thought to be so earlier. What appears volatile is the impurity beryllium chloride. This finding spoke in favour of yttrium not being a pure element as believed earlier. Rose was the first to prepare metallic yttrium by reducing yttrium chloride and yttrium fluoride with metallic sodium. It turned out later, however, that this yttrium metal was still largely contaminated.

Also, Berzelius observed that when working with yttrium oxide and adding ammonia to a solution of yttrium nitrate, precipitation takes place in the following sequence: first, beryllium hydroxide is separated, and, subsequently, a yellowish substance mixed with the whitish yttrium hydroxide (Berzelius 1844b).

Mosander reported in 1843 on his results connected with gadolinite. He found not only one, but two new elements in it. The yellowish substance precipitated first with ammonia he termed erbium. The residue again precipitates in two fractions. He retained the name yttrium for the first colourless substance, and gave the name terbium to the second, pale amethyst-coloured substance. This mode of separation, however, was very cumbersome and uncertain. He found a better method for separating the substances by fractioned precipitation of the oxalates: Erbium oxalate is the first to precipitate, subsequently the terbium salt contaminated with important amounts of yttrium, and finally the yttrium salt. By dissolving and repeatedly precipitating the substances obtained, the products will become purified successively (Mosander 1843).

In his not too ingenuous naming of the new elements (he only diversified the name of the place of discovery, Ytterby, from which the name yttrium also stemmed), Mosander was presumably again led by his intention to find free letters for the symbols of the new elements. Both E and T were free. However, his symbol concepts did not survive. I cannot see the reason why, since the letter T in itself is not used as a chemical symbol up to the present day, although we know ten elements whose names begin with a T. The reason was perhaps that the elements tellurium, tantalum, titanium and thorium all known earlier than terbium were given symbols in Berzelius's nomenclature consisting of two letters, and so terbium got the symbol Tb. Presumably per analogiam erbium was given the symbol Er, though no element whose name begins with E was known at the time, and only later was europium (Eu) discovered with the continuing division of rare earth elements.

Thus, Mosander's activities led to the originally two-element division into a six-element division. The cerium compounds are yellow at the higher oxidation level and colourless at the lower oxidation level, lanthanum compounds are white, didymium compounds are red, yttrium and erbium compounds are white, terbium compounds are pink. Chemists existed, of course, who disputed the existence of these elements. Unequivocal identification of elements was, however, possible in later times only. In the period in question, the main characteristics on the basis of which a substance could be qualified as a new element were separability, colour, crystal shape and reactivity. Even atomic mass determinations were largely uncertain, particularly in the group of the rare earth elements, it will be seen in the

following that several among the above six elements were later found to contain additional elements.

The first important aid in identification was spectral analysis introduced in the fifties of the 19th century. The method will be discussed later, let us, however, note here that the names given by Mosander were fatally and permanently mixed up in the course of spectro-analytical identification. Delafontaine who unequivocally proved and confirmed the existence of the elements yttrium, terbium and erbium in 1864, named the pink compound erbium and the white compound terbium, presumably out of pure absence of mind, anyhow, these names were then kept on for good (Delafontaine 1864).

Carl Gustaf Mosander (1797–1858) – like so many chemists of the age – started his career as a pharmacist's apprentice in Stockholm. Later he entered the school for army surgeons and served for some years in the army as surgeon. Meanwhile he studied at the University of Medicine, and after graduation became an assistant at its department of chemistry headed by Berzelius. In 1832, after Berzelius's retirement, Mosander was appointed professor as successor of Berzelius and held that post until his death. In general, he was reluctant to write papers, most of his results survived in the *Jahresberichte* of Berzelius or as printed notes of his lectures (Kopperl 1974).

Heinrich Rose (1795–1864) studied at the University of Berlin, and subsequently spent two years in Stockholm in Berzelius's laboratory as his private assistant. In 1823, he was appointed an associate professor and later regular professor at the University of Berlin, where he worked till his death. Rose discovered niobium. His manual *Handbuch der analytischen Chemie* (1829) was published several times, it was the first systematic comprehensive book on analytical chemistry in its entirety on the level of the age (Szabadváry 1966, p. 165).

Marc Delafontaine (1837–1911) was born in Switzerland. He probably studied at the University of Geneva and worked there for some time. Later he emigrated to the United States and continued his activities in chemistry and geology there. I was unable to find any further biographical facts concerning Delafontaine.

3. Rearrangement and further divisions: 1843–1886

In the three decades following Mosander's results from 1843 the matter of rare earth elements was fairly quiet. In fact, inorganic chemistry lost importance in that period. Berzelius, the leading personality of chemistry for close to 50 years, was dead, after living to see that his electrochemical dualistic theory was not applicable to organic chemistry, this new branch growing in importance. Actually, the elucidation of the structure of organic compounds stood in the center of interest. Most chemists, including the greatest chemists of the time, were occupied with the numerous theories related to this subject and with their discussion. It appeared that the great period of discovering new elements was over. It was increasingly difficult to progress along the classical pathway, i.e., the complex techniques of gravimetric separation, though some elements were still discovered by such methods. Novel potentials appeared by applying entirely new physical techniques, first of all by utilizing spectral analysis. In its useful form, spectral analysis was developed in 1859

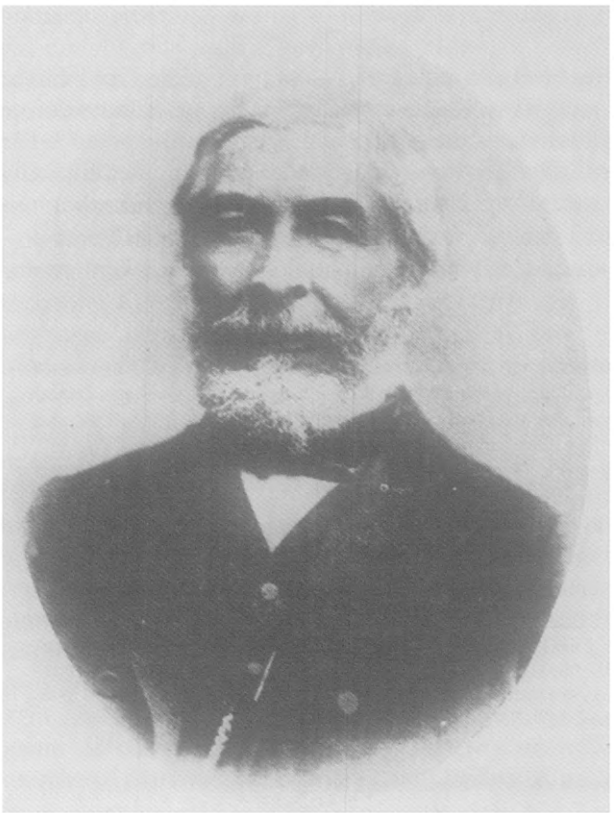

Fig. 5. Jean Charles Marignac.

by Bunsen and Kirchhoff. The periodic system (Mendeleev 1869, Meyer 1870), on the other hand, showed the direction, one might say put a map into the hands of the researchers, of where to look for new elements and how many unknown elements may as yet be discovered. However, it still took a long time, until the periodic system was found to be capable of serving this purpose, until it became accepted that the periodic system was not just a game of scientists having no better ideas.

None the less, studying rare earth elements did not stop altogether. Papers appeared about investigations of the rare earth elements known at the time, though a few papers only, and they were exclusively concerned with the cerium, lanthanum and didymium groups. Up to 1864, for instance, I did not find a single paper on yttrium. However, the new leading man in the field of rare earth elements, who later increased their number from the known six by three further elements by further division, Jean Charles Marignac from Switzerland, had already made his appearance. Marignac determined the atomic weights of several elements more exactly than earlier, including cerium, lanthanum and didymium. He improved the separation method developed by Mosander in order to obtain purer products. In 1848, he calculated the atomic weight of cerium from the reaction of Ce(III) sulfate with barium chloride, and found a value of 47.26 (Marignac 1848). In the same period

Rammelsberg found a value of 45.8, and Hermann of 46.0, while in 1853 Bunsen stated a value of 58.2 (Bunsen 1853). It may be seen that Marignac's value was closest to the true one. Let us keep in mind that all this happened before the congress in Karlsruhe and hence the concept of atomic weight was far from being defined unequivocally. It was frequently mixed up with equivalent weight, and its determination was based on an assumed atomic composition of compounds, easily leading to results that amounted to half or one third of the correct value, as in the above cases. At that time the researchers believed these elements to be 'bivalent'. I use the quotation marks, because the valence concept was unclear too, this statement can only be regarded as a conclusion from the calculation method used by the researchers. One year later (1849), Marignac published his results regarding the atomic weights of lanthanum and didymium: 47.04 and 49.6, respectively. The sequence of the values is correct again, the atomic mass of lanthanum is indeed somewhat less than that of cerium, while that of didymium is necessarily higher, since the atomic masses of its two constituting elements neodymium and praseodymium are both higher than that of cerium (Marignac 1849). In 1853, Marignac studied the chemical reactions of didymium in detail: the colour, crystal shape, solubility and mode of preparation of the halogenides, sulfides, phosphates, sulfates, arsenic compounds and oxalates (Marignac 1853a), two years later he carried out similar studies with lanthanum (Marignac 1855).

Delafontaine took up to work with gadolinite again in 1864 to study Mosander's yttrium elements. He studied erbium and its compounds in greatest detail, using various methods including the blowpipe. He unequivocally confirmed the existence of erbium, but was not unequivocal regarding the existence of terbium (Delafontaine 1864). In the same year another chemist, O. Popp, questioned the existence of both erbium and terbium. He had already made use of absorption spectrometry, and based on its results he asserted that erbium is didymium contaminated with cerium. In the same paper he reported the properties and preparation of yttrium and its compounds, he prepared metallic yttrium by reduction with sodium (Popp 1864). At the same time, Bahr and Bunsen also studied gadolinite. They asserted that erbium was a true element, but denied the existence of terbium. They dissolved the mineral in hydrochloric acid, filtered off silica and precipitated with oxalic acid. After dissolution of the precipitate in nitric acid, ceria earths were precipitated as sulfates, they precipitated the filtrate again with oxalic acid and repeated these operations until the didymium spectrum disappeared. The nitric acid solution then contained only yttria earths. It was evaporated to dryness, they took up the residue in water and let the solution crystallize. The pink erbium salt crystallized first, yttrium remained in the solution. This fractional crystallization they repeated several times. In what was earlier considered terbium they could only discover spectral lines of erbium, yttrium and cerium (Bahr and Bunsen 1866). Cleve also denied the existence of terbium (Cleve later became an important figure in the study of the rare earth elements). Delafontaine, however, continued to hold on to the opinion that terbium exists, though not identical with Mosander's terbium. He proposed a new name for it: mosandrium, while he considered Mosander's terbium identical with what Bahr and Bunsen separated as erbium (Delafontaine 1865). It may be seen that things

around yttrium and its companion elements became very tangled. Erbium was accepted, since Young demonstrated its existence in the solar spectrum too (Young 1872).

For some time everything was quiet around terbium, only Delafontaine returned to the issue, persisting and confirming his statement that the element mosandrium exists with new observations (Delafontaine 1874). Bunsen, in his famous spectroscopic investigations, found erbium, yttrium, cerium, lanthanum and didymium chloride spark spectra very characteristic, and also the flame spectrum of erbium and the absorption spectra of erbium and didymium salt solutions, but still did not find terbium (Bunsen 1875). Delafontaine, however, continued his search. In the mineral samarskite, discovered by G. Rose in 1839 and containing yttrium group elements, Delafontaine again detected the oxide discovered by Mosander, but denied by Bunsen and Cleve which he named mosandrium, but this time – following Marignac's suggestion – he proposed the name terbium for it, and suggested that what was originally terbium and separated by Bunsen shall remain erbium (Delafontaine 1877). In the next year he reported in detail about his terbium, which finally was what we call terbium up to the present time. In analyzing samarskite, his starting point was that the formates of the cerium group are slightly soluble, while the formates of the yttrium group can be separated by fractional crystallization. Terbium compounds are distinctly different from erbium compounds (Delafontaine 1878a). In his next paper he remarked that probably – in addition to terbium – another very similar unknown element was also present, he even gave it a name, he termed it philippium (symbol Pp) after a certain Philippe Plantamour. Following Mendeleev he predicted its atomic weight between 90 and 95 and outlined the characteristics of its compounds, with less success, however, than his great contemporary. Mendeleev also – as is well known – predicted new elements and their properties, but at least he did not name them. Anyhow, with time Mendeleev's elements were actually discovered, whereas Delafontaine's philippium turned out to be a mistake (Delafontaine 1878b).

Whenever something is started, it will get going easily. This was the case with mistaken element discoveries too. Delafontaine thought he discovered another new element in samarskite, and gave it a name: decipium, symbol Dp, expected atomic weight 122. He even predicted its absorption spectral line: $\lambda \approx 416$. This element persisted in books on chemistry for a rather long time, one even meets it here and there in the first years of our century (Delafontaine 1878c).

In the same year Marignac again studied gadolinite and confirmed the presence of terbium in it. He assigned an atomic weight of either 99 or 148.5 to the element, depending on whether its oxide has the composition TbO or Tb_2O_3 (Marignac 1878a). It is an interesting episode that in the same year a chemist called Smith also discovered terbium in samarskite, but termed it mosandrum (Smith 1878). A priority dispute began between Delafontaine and Smith, ending with Delafontaine's victory. In 1880, Soret reported the absorption spectrum of terbium together with other elements, including the non-existing philippium and decipium (Soret 1880). In 1882 Roscoe and Schuster reported the exact spectrum of terbium: 194 lines, and thereby the existence of terbium was definitively confirmed (Roscoe 1882).

Fig. 6. Marc Delafontaine.

Following the adventurous story of terbium it is actually impossible to decide by now who was the true discoverer, Mosander, Delafontaine or Smith? The element names, as indicated above were applied inconsistently, and we cannot know whether they referred to the same substance. Did Mosander find the same substance and called it erbium that finally became terbium with Delafontaine, or was Bunsen correct and consequently Mosander's fraction was a mixture only? No data were reported that would allow us to state now, at this late date, what substances were identical, no characteristic spectral lines, no exact atomic weight values are at our disposal as yet.

During that same period, progress was achieved also in the field of cerite. Delafontaine the indefatigable, a figure unfairly neglected in the history of chemistry, investigated the cerium group in the same mineral samarskite. He noted that in his opinion, didymium was not homogeneous, since didymium separated from samarskite had an absorption spectrum not fully identical with that separated from cerite: certain lines in the blue region were missing and lines in the violet also differed (Delafontaine 1878c). His assumption was confirmed in the following year by Lecoq de Boisbaudran, whose name became famous earlier, in 1875, by his spectrographic discovery of gallium, the first among the eka-prefix elements predicted by

Mendeleev, evidencing that Mendeleev's periodic table was not mere speculation, but a system reflecting reality based on some deeper law.

It is of interest that Lecoq de Boisbaudran found a new element in the didymium precipitate obtained from samarskite while simultaneously disproving Delafontaine's statement that the spectra of didymium obtained from cerite and samarskite differ. He reported simultaneously that he found in samarskite – in the stage before didymium separation – new lines by spark spectrography indicating the presence of a further hitherto unknown element. He gave approximate values for the corresponding wave lengths and stated that the double salt with potassium sulfate of the new element precipitates together with the corresponding didymium salt, while its sulfate is less soluble than didymium sulfate. Its oxalate separates before didymium oxalate and its hydroxide precipitated with ammonia behaves similarly (Lecoq de Boisbaudran 1879a). In a next paper he gave the exact wave length values for the characteristic lines of the new element ($\lambda = 480, 463.5$) and described a complicated fractional separation method, by means of which he succeeded in separating the new element in a relatively pure state from didymium and also from decipium. He gave it the name samarium, referring to the mineral in which he detected in (Lecoq de Boisbaudran 1879b).

The results around 1878–1880 made the family relations of rare earth elements rather puzzling. To facilitate finding one's bearings, it appears expedient now to trace a genealogical table to aid in following this tangled story. The various divisions, multiplications and propagations discussed and the ramifications to be discussed in the following taking place around 1880, and moreover, leaping ahead in time, the last events in the history of the discovery of the rare earth elements which took place in the years following the turn of the century shall all be included.

As can be seen in the genealogical table, many novelties came forth from gadolinite too. Marignac confirmed Delafontaine's statements that terbium is an existing element. He determined its atomic weight amounting to either 99 or 148.5, depending on its oxide corresponding to the formule TbO or Tb_2O_3. At that time many discussions went on as to the valence of rare earth elements, we shall come back on this issue. Terbium oxide is orange and turns white upon ignition in H_2, it is readily dissolved in dilute acids, its solutions are colourless and presumably have no absorption spectrum (Marignac 1878a). As to the erbium precipitate obtained in the separation, Marignac stated that it is not homogeneous, but the mixture of two elements. The oxide of one of them is pink, with a characteristic absorption spectrum. Marignac retained the name erbium for this element. The other oxide is colourless and so are the salts. According to Soret there are no characteristic lines in its visible and UV absorption spectra. Its neutral chloride does not give a precipitate with hyposulfurous acid, while erbium chloride does, based on this property it can be separated from erbium. Its atomic weight is high, 115, or 172.6 in case it is tetravalent. Marignac gave the name ytterbium to the new element, since it stands between yttrium and erbium in its properties (Marignac 1878b).

In 1877, Mallet discovered an yttrium niobate mineral called sipylite in Virginia (USA). Analyzing it he found that it contained niobium and cerium and yttrium group elements (Mallet 1877). In 1878, Delafontaine identified Marignac's ytterbium in this mineral too (Delafontaine 1878d).

TABLE I
Genealogical table of the rare earth elements.

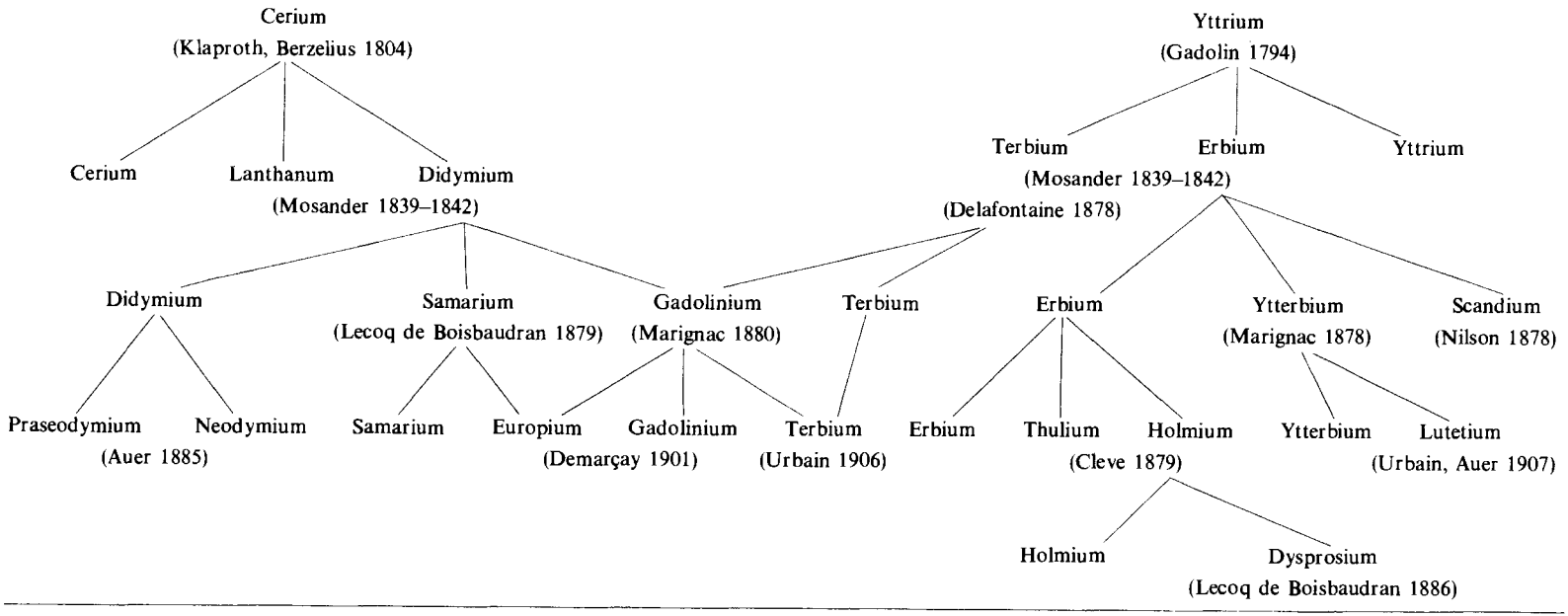

However, the division of erbium did not end here. After the Swiss results from 1878 it was again the Swedish school of rare earth elements that took a great step forward in 1879: erbium again multiplied into four elements. Nilson repeated the separation of erbium described by Marignac and confirmed the existence of ytterbium and the statements of the Geneva master regarding it, with the only difference that according to Nilson, the atomic weight is 116 instead of 115 as reported by Marignac. (Owing to a slip of the pen, Nilson's paper cites 132 and 131, respectively, obviously not the atomic weight data of the element, but the molecular weight data of the oxide). Nilson also thought tetravalence conceivable, in that case the atomic weight would amount to 174 (Nilson 1879).

By an exceedingly intricate fractioning method consisting of 13 steps and starting from the nitrates, Nilson finally obtained a 'basic' nitrate from gadolinite, dissolved in nitric acid it yielded a weak absorption line in the red and in the green. A precipitate was formed with oxalate. Nilson considered it a new element and termed it scandium after his wider homeland Scandinavia, following thereby the patriotic line of giving names to elements started with Lecoq de Boisbaudran's gallium and repeated many times in the following decades with new elements. Nilson studied the spectrum of scandium with Thalén's assistance very thoroughly and found several identifiable lines. The chemical properties of the new element: the oxide is white, sparingly soluble in nitric acid, more readily in hydrochloric acid; its nitrate decomposes at a relatively low temperature as compared to other rare earth elements. In the case of ScO the atomic weight is 80, however, by reason of the ready decomposition of the nitrate Nilson assumed that the element is tetravalent. He pointed out that by its properties and assumed valence scandium fits very well into the empty square in Mendeleev's periodic table between tin and thorium (?) (Nilson 1879).

In a somewhat later French version of that same paper Nilson discussed the properties of scandium in greater detail, he does not, however, mention tetravalence, but assumes that – similarly to the other rare earth elements – scandium is trivalent. On this basis its atomic weight amounts to 44, and this value, he writes, 'corresponds to the eka-boron predicted by Mendeleev'. Based on its atomic weight scandium is located between beryllium and yttrium. Nilson, though referring to Mendeleev's prediction, avoids the expression 'periodic system' (Nilson 1880), maybe because in another paper published in the same year with Peterson and dealing with the atomic weight determination of beryllium, he declared that 'in its present state the periodic system cannot be considered the adequate expression of the properties of elements'. The reason for his negative attitude was that in his atomic weight determinations of beryllium he found 13.65 and with this value he could not place beryllium in the periodic system. Therefore he preferred to believe in the incorrectness of the system rather than accept that his own determinations gave false results (Nilson and Peterson 1880).

The quality of the analytical performance cannot be demonstrated better than by the quantitative control investigation performed in the same year by Cleve: starting from 4 kg gadolinite mineral he obtained 0.8 g scandium oxide (Cleve 1879a).

In 1880, Nilson, by processing a larger amount of auxenite (after digestion with

Fig. 7. Per Teodor Cleve (Courtesy Library University of Uppsala).

potassium sulfate in a platinum vessel, precipitation with ammonia, dissolution of the precipitate in nitric acid, precipitation with oxalic acid, dissolution in nitric acid, evaporation to dryness, precipitation with hydroxide, evaporation of the filtrate and subsequent fractionation consisting of 30 operations to separate the individual rare earths) obtained pure ytterbium oxide and scandium oxide. From there he determined the atomic weights (Yb 173, Sc 44) and prepared numerous compounds (Nilson 1880). As the reader may have already noticed, it is astonishing how immediately the colleagues reacted to true or assumed discoveries by repeating, confirming or refuting.

Cleve studied the erbium remaining after the separation of ytterbium in 1879 and decided that the fraction is still not homogeneous. His starting point was the spectrum taken by Thalén. He separated the substance into three fractions, one close to yttrium, the second to ytterbium and the third to erbium. Among the assumed spectral lines of erbium, one was present only in the fraction close to ytterbium, but not in ytterbium itself, a second similarly only in the fraction close to yttrium, but not in yttrium itself, both lines were present very weakly in the spectrum of the erbium fraction. Based on this finding, Cleve assumed the existence of two further elements and immediately gave them names: thulium (originating from the legendary old name of Scandinavia), and holmium (from the medieval Latin name of

Stockholm, Holmia). He estimated their atomic weights to 113 and 108, respectively. He reported that holmium had a yellowish oxide. He acknowledged that the separation of these elements was not at all complete and fully successful (Cleve 1979b). Soret, a member of the Swiss school then referred to the fact that he, in an erbium sample given him by Marignac, already a year earlier stated from the results of absorption spectrometry that an unknown element is probably present in one of the chloride fractions, in that paper (Soret 1878) he denoted it by X. In his opinion this element corresponds to Cleve's holmium (Soret 1979). Cleve politely acknowledged the priority of Soret regarding this element (Cleve 1879c). It was the great spectroscopist Lecoq de Boisbaudran who confirmed the statements and discoveries of Cleve and Soret (Lecoq de Boisbaudran 1979c).

Let us now leap forward in time to be able to close the matter of the division of erbium. Lecoq de Boisbaudran developed a fantastically intricate and wearisome method for the separation of gadolinite rare earth elements, consisting of 32 precipitations with ammonia and 26 subsequent precipitations with oxalate, separation of the fractions and their spectroscopic and fluorescence studies. In 1886, he came to the conclusion that holmium is not homogeneous either, it contains another element which he named dysprosium. This element was apparently accepted by the chemists of the world without the usual unbelief and debate (Lecoq de Boisbaudran 1886).

Let us now return to 1880, when Marignac also started to investigate samarskite. With fractional precipitation using potassium sulfate he separated four groups, in one of the groups he followed Delafontaine's formate method and by finally applying separation with oxalate he obtained a substance that differed in many respects, above all in the behaviour of its nitrate from other rare earth elements. He assumed that it was a new element, however, with Swiss cautiousness he did not yet give it a name, but marked it Yα. In another group he found a substance which he termed Yβ (Marignac 1880).

In that same year, Delafontaine summarized the new results in the field of rare earth elements in a paper. He judged that the existence of decipium and philippium which he believed to have discovered was unquestionable. He considered Yα to be identical with decipium and holmium identical with philippium, but soon withdrew the latter statement in a following paper. In a further paper, still in the same year, he reported the preparation and properties of quite a number of the compounds of the would-be decipium (Delafontaine 1880). Soret, on the other hand, came to the conclusion by spectral analysis that Yβ was identical with samarium, while Yα did not correspond to decipium (Soret 1880). In 1881, Delafontaine again studied the decipium problem thoroughly. Based on the behaviour of its double sulfate with sodium he now stated that what he had earlier considered pure decipium was a mixture of two elements. One component is identical with samarium, and let the other remain decipium, which is presumably identical with Marignac's Yα (Delafontaine 1881). So by now decipium occurred both in the gadolinite and the cerite line. However, this is the last occurrence of decipium by this name in the literature. Marignac, in 1886, proposed the name gadolinium for his Yα and this actually remained the accepted name (Marignac 1886).

Fig. 8. Robert Wilhelm Bunsen.

The existence of philippium was refuted definitely by Roscoe in 1882: he wrote that the formates of erbium and terbium form mixed crystals which have the properties ascribed to philippium. Nor does the periodic table indicate the probability of the existence of this element (Roscoe 1882). Philippium still appeared in the following few years in lists of rare earth elements, but subsequently it completely disappeared, just like Philippe Plantamour to whose honour Delafontaine originally named it fell into oblivion. I at least could not find a trace on who he actually was.

Delafontaine was certainly unlucky. He had so many merits and results in the field of rare earth elements and not a single one of the names he gave to the new elements survived, although it is very probable that his decipium and gadolinium were identical. However, habent sua fata et nomina: decipium stemmed from the latin verb *decipior* meaning *be disappointed!*

Johan Fridrik Bahr (1815–1875) studied at the Uppsala university, and then worked in Bunsen's laboratory in Heidelberg. In their cited paper they introduced the concept of extinction coefficient so important in absorption photometry. Later Bahr worked as first assistant at the Uppsala university.

Robert Wilhelm Bunsen was born in 1811 in Göttingen, where his father was professor at the

university. The son studied science also at this university. He made his doctoral dissertation dealing with hygrometers (still written in Latin) with F. Stromeyer. In the years 1830–1833 he visited various German, French and Austrian universities with stipendia. He became a lecturer in Göttingen. In 1836 he was appointed professor of chemistry as the successor of Wöhler at the Polytechnical School of Kassel. He became professor of chemistry in 1838 at the Marburg university, in 1851 at the Breslau (today Wroclaw) University and finally in 1852 at the prestigious university of Heidelberg, he remained in this position until his retirement, refusing in the meantime an invitation to the Berlin University. He died in Heidelberg in 1899. Bunsen was one of the best-known chemical authorities of the past century. His name is still current in modern laboratories due to his numerous ingenious inventions (Bunsen burner, Bunsen valve, Bunsen pump). Above all, he was a master in analytical chemistry. His best-known achievement was the method of spectral analysis developed together with Kirchhoff, which proved so important in the study of rare earth elements. He was the first to apply emission spectral analyses to discover new elements: rubidium and cesium as early as 1860. Together with Bahr he developed absorption photometry in 1865. He improved the method of analyzing smoke gases. He introduced iodometry for determining oxidizing substances by iodine liberation from potassium iodine (Szabadváry 1966, p. 326).

Per Teodor Cleve was born in Stockholm in 1840. He studied science at the Uppsala university and started his career as an assistant at this university, in 1874 he was appointed professor of chemistry and held this post until his death. He was the first president, between 1900 and 1905, of the commission which awards the Nobel Prize in chemistry. He began with investigating complex platinum compounds and turned subsequently to rare earth elements. He opposed the ion theory of his contemporary Arrhenius and the novel physico-chemical views of Wilhelm Ostwald. In the last decade of his life his interest turned towards biology and he was occupied with plankton. He died in Uppsala in 1905 (Boklund 1971).

Hans Rudolf Hermann was born in Dresden in 1804. He studied pharmacy. In 1827 he went to Moscow, founded a soda water plant and continued to live and work there until his death. Besides his profession he was a gifted mineralogist, his merits in exploring the mineral riches of Russia are great. He published many papers on this topic.

Paul Émile Lecoq de Boisbaudran was born in 1838 in Cognac, the son of a wine merchant. He started to work in the family enterprise and remained a wine merchant until the end of his life, he was occupied with chemistry and within its frame above all with spectral analysis as a hobby in his own laboratory. He became an authority in this field, in his book *Spectres lumineux* (1874) he presented the results of analyzing 35 elements, giving their characteristic lines. In 1875, he discovered gallium in a zinc ore from the Pyrenees which proved to be the eka-aluminium predicted by Mendeleev and was the first proof of the reality of the periodic table and of the predictions of as yet unknown elements by Mendeleev. Lecoq de Boisbaudran died in 1912 in Paris (Ramsay 1913).

John William Mallet was born in 1832 in Dublin, Ireland. He studied in Germany under Wöhler. In 1853 he went to the USA and became professor of chemistry in Amherst College and later in Charlotteville. He participated in the Civil War on the side of the South. He determined the atomic weight of lithium more exactly and analyzed numerous minerals. He died in 1912 in Charlotteville.

Jean Charles Marignac was born in Geneva in 1817. After his studies at the Académie de Genève he studied chemistry at the École Polytechnique in Paris and subsequently mineralogy and mine engineering at the École des Mines. He carried on organic chemical research in Giessen in Liebig's laboratory and then took up work in the Sévres porcelain manufacture. He was invited to teach chemistry in 1841 at the chemical department of the Académie de Genève. In 1878 this institution was transformed into an university. Marignac retired in 1878 and died in 1894 in

Geneva. His major activity was the exact determination of atomic weights, he modified the atomic weights of some dozens of elements. In addition to his work on rare earth elements he was largely successful in solving intricate chemical issues of niobates, tantalates, tungstates (Ador 1894).

Lars Fredrik Nilson was born in 1840 in Skönberga. He studied in Uppsala and became an assistant and in 1878 professor of analytical chemistry there. In 1883 he was appointed professor of agricultural chemistry at the agricultural academy in Stockholm. He died in 1899 in Stockholm. In addition to rare earth elements he investigated inorganic complex compounds, later he published papers on agricultural chemical subjects.

Karl Friedrich Rammelsberg was born in Berlin in 1813. He studied pharmacy. He started his career at the Berlin university and became lecturer there. From 1850 on he was professor of chemistry at the Industry School in Berlin which later developed into the Technological University. In 1874 he became professor of inorganic chemistry at the Berlin university as successor of Henrich Rose. He died in 1899 in Gross-Lichterfelde. His activities were above all in mineralogy and in analytical chemistry. He published over 100 papers on the analysis of minerals.

Sir Henry Enfield Roscoe was born in London in 1833. He studied in London in Graham's and in Heidelberg in Bunsen's institute. He began his career in Manchester, in the Owens College, and remained there as professor of chemistry after it was organized into a university, until his retirement in 1885. He died in Leatherhead in 1915. He became famous by the photochemical work published together with Bunsen. He investigated vanadium and its compounds thoroughly. His other activities were also mainly in the field of inorganic chemistry (Thorpe 1916).

Gustav Rose, mineralogist, was born in Berlin in 1798. His father was a pharmacist, his brother Heinrich became a famous chemist, and a professor of the Berlin university. Gustav Rose studied in Berlin and in Kiel and subsequently worked in Berzelius's laboratory in Stockholm. After returning to his native town he became lecturer at the university and, in 1839, professor of mineralogy and remained in this post till his death in 1879 in Berlin. His famous book is entitled *Elemente der Krystallographie* (1833).

J. Lawrence Smith was born in 1818 in the United States. He was a mineralogist and analytical chemist. He died in 1883.

Tobias Robert Thalén was born in 1827 in Köping. He studied in Uppsala and remained at that university as co-worker of Angström and from 1874 as his successor heading the department of physics. He was a member of the Swedish Academy of Science. He died in 1905.

Charles Augustus Young was born in USA in the town of Hanover in 1834. He studied at the academy of his native town. Originally he studied theology, but later turned towards science. He became professor of mathematics and physics in 1857 at the Western Reserve College of Hudson. In 1866 he became professor of mathematics and philosophy of nature at Dartmouth College near his native town, this post had been formerly occupied by his father and his grandfather. He retired in 1905. His main interest was in astronomy, he was among the first who investigated stars by spectrometry. He wrote several scientific and popular books on astronomy which were great successes in his time. He died in his native town in 1908.

4. Final divisions: rare earth elements as industrial raw materials

Up to that stage the elucidation of the puzzling group of rare earth elements was the business of a small group of scientists who carried on to satisfy their own

scientific curiosity. Many scientific papers were written, the scientific positions of the authors was raised by them, and in some cases the author could consider himself the discoverer of a new element hitherto unknown. However, at that time so many announcements of new elements appeared in the literature that such notice was accepted with great doubts, and rightfully so, since very frequently it turned out that the discovery was a mistake. The field of rare earth elements was particularly difficult to follow, so many opinions and counter-opinions were announced by the researchers, who also rivalized with one another to a certain extent. The whole issue was of no importance for practice: the rare earth elements were not used for any purpose.

Around the turn of the century, however, the picture changed, insofar as it turned out that these elements do have industrial importance, rare earth elements turned into industrial raw materials and this fact had great impact on the research relating to them.

This chapter begins with 1885, with the discovery of a new division. The discoverer was a young man and his first paper was of pure scientific character. The young chemist was Austrian, his name was Carl Auer von Welsbach. The rest of his life was devoted to rare earth elements; they were turned into industrial raw materials by him, and he not only gathered fame but became a very rich man through them. For his scientific and industrial merits he was raised to the rank of baron, he became proprietor of castles and baronial estates in addition to his industrial enterprises. When he was granted the barony, the emperor Francis Joseph I received him in audience and told him that he had heard about the success of his discovery. Auer von Welsbach proudly answered:

'Yes Your Majesty, owing to my inventions 40 000 people have found a job by now all over the world'. As far as I know Auer was the only chemist in the world whose picture ever adorned a banknote. After World War II his portrait was on the 20-Schilling note of the Austrian Republic. Today it is no more in circulation:

Fig. 9. Carl Auer von Welsbach (Courtesy Austrian National Bank Vienna).

inflation led to the use of coins instead of banknotes for the Austrian 20-Schilling value.

In 1885, Auer ascertained that didymium, after separation from samarium, is still not homogeneous, but consists of two elements. Let us note that didymium was liable to suspicion to many researchers earlier. Marignac in his youth, as early as 1853, doubted that it was a homogeneous element and carried out many experiments to prove his suspicion, but did not succeed (Marignac 1853a). Delafontaine, as discussed in the previous chapter, thought he had discovered decipium in didymium, and Marignac also succeeded in discovering it, but named it gadolinium. Lecoq de Boisbaudran detected samarium in didymium and made the separation. But what remained was still doubtful, among others to our friend Delafontaine by reason of its absorption spectrum, since the didymium samples prepared from different minerals revealed differences. A new personage, Bohuslav Brauner a Czech chemist, whom we shall meet several times in what follows, was extremely conscientious in atomic weight determinations. He published a long paper, one might say a book, on the past and present of rare earth elements, including his own results, namely his atomic weight determinations in this field. His data for didymium samples prepared from different minerals did not agree either. On this basis, he decidedly pronounced in 1882 that didymium is a mixture of elements: it contains a component owing to which some preparations reveal a higher atomic weight. He termed this component Diγ (Brauner 1882). At about the same time Cleve from Sweden also came to the conclusion that an element must be hidden between lanthanum and didymium (Cleve 1882). Next year Brauner attempted the separation with the usual oxalate-formate method. By determining the atomic weights and absorption spectra of the different fractions he was able to identify several rare earth elements already known, namely samarium, erbium, holmium, terbium and yttrium as contaminations, but was unable to confirm the existence of a new element, i.e. of his assumed Diγ experimentally (Brauner 1883).

In that year Auer published a paper dealing with the separation of the elements of the gadolinite group. He followed the traditional method with the difference that in some cases he did not decompose the nitrates by ignition, but made suspensions of rare earths, i.e. the oxides in the nitrate solutions; as a result, the less basic nitrates were enriched in the precipitate (Auer von Welsbach 1883). The next year he further developed this method and separated lanthanum from didymium by means of the different solubility of their double nitrates, that is, by means of the fact that they did not crystallize simultaneously, but followed one another (Auer von Welsbach 1884). Auer's recognition, of decisive importance, was to apply fractional crystallization instead of fractional precipitation for the separation. Using this method he was able, in 1886, to obtain two separate crystallized fractions of didymium ammonium nitrate. He investigated the double salt fractions using absorption and spark spectrometry and proved that they were indeed different. Let us note that this work was extremely painstaking: it took more than hundred operations and one had to wait 24–48 hours at each individual crystallizations. The final two fractions differed in colour too: one was greenish both as a precipitate and in solution, this Auer termed praseodidymium owing to its colour. The other fraction was pink; this he

termed neodidymium (Auer von Welsbach 1885). Consequently Mosander's name for the element, *didymium* meaning *twins*, turned out to be fully justified. The two elements were twins indeed, and very difficult to separate. The reader will remember that Wöhler objected to the name didymium because it sounded like baby talk. His objection was removed. With time the original names praseodidymium and neodidymium were reduced to praseodymium and neodymium. Apparently this change was spontaneous. In the few papers dealing with the new elements, the names given by Auer were used in the beginning, and then the syllable 'di' was somehow or other omitted. I met the simplified names first in a paper dealing with molybdates and vanadates of rare earth elements (Hitchcock 1895).

However, in the years following 1885, one still frequently meets with didymium and its study. Apparently many researchers were unaware of Auer's results; one reason might have been that his papers appeared in the Viennese *Monatshefte für Chemie*, a young journal, which never belonged to the important and generally known chemical journals. The nature of absorption spectra was also unknown, so that the researchers of the time could readily imagine that they change with conditions. Becquerel (who in 1896 became worldfamous by the discovery of radioactivity in uranium) dealt with didymium too in a paper on absorption spectra. He acknowledged that the changes in the bands appear to indicate different components, but in his opinion this fact was no proof that the components termed praseodidymium and neodidymium were actually independent chemical elements (Becquerel 1887).

Becquerel at least knew about Auer's result. Krüss, one of the founders of photometry (Szabadváry 1966, p. 343), in a paper published together with Nilson, concluded from their absorption photometric studies that the rare earth elements known up to then include at least twenty as yet unknown elements (Krüss and Nilson 1887). Bettendorf repeated Auer's experiments in 1890 and by subjecting all mother liquors individually to spectrometry he confirmed the existence of praseodidymium and neodidymium (Bettendorf 1890).

Auer himself continued to use the name didymium, deliberately, however, when he spoke about the two non-separated substances, but applied them together in the form of the old didymium, since at the time Auer von Welsbach had already experimented with the technological application and utilization of an observation in which the accurate chemical separation of the rare earths was of no importance. A separate chapter in this volume deals with the industrial applications of rare earth elements; I shall not go into details. It is, however, necessary to emphasize this issue, since Auer's inventions largely contributed to the further scientific elucidation of the rare earth elements and had a great impact on this process.

During his student years Auer also worked in Heidelberg in Bunsen's laboratory. It was there that he acquainted himself with the method of spectral analysis, and also with the old observation studied more systematically by Bunsen that the light emitted by the flame of the Bunsen burner increases by the effect of various elements and oxides. This phenomenon was studied much by Bunsen's co-workers, and it is said that Bunsen once pronounced that the future of gas lighting will be ensured by a solid glowing in the gas burner's flame. This, at least, is what can be read in a

leaflet of the Welsbach Incandescent Company, an American daughter organization of Auer's later enterprise. In Auer's later experiments with rare earths he found that lanthanum oxide greatly increases light emission of the Bunsen flame. Maybe remembering what Bunsen had said, Auer attempted to fabricate a luminator from lanthanum oxide. He impregnated cotton yarn with lanthanum nitrate and ignited it, obtaining a net-like lanthanum oxide formation. This was the ancestor of Auer's later gas mantle; he surrounded the burner's flame with it and light emission improved greatly. The trouble was, however, that after some hours of incandescence, the mantle fell to pieces. None the less, Auer realized the potentials in the phenomenon. At that time he already worked in Vienna, at the institute of chemistry of the university. He began to combine lanthanum oxide with other oxides and attained the best effects with zirconium oxide combinations. In 1886 he invited the representatives of the Vienna press into his laboratory to introduce them to his novel gas lamp which he termed 'actinophor'. The presentation was highly successful and the press wrote enthusiastically about the new invention. This was quite obvious: at the time electric lighting was still undeveloped, and the main tools for lighting were candles and petroleum lamps. Auer immediately patented his invention and it sold under good conditions in various countries. He turned out to be not only an excellent chemist and inventor, but also a first-class businessman. He supplied the impregnating solution himself to the manufacturers. For this purpose he first hired a small basement and subsequently he moved to better and better places until, in 1887, he bought a bankrupt pharmaceutical plant in Atzgersdorf close to Vienna. There, using his fractional crystallization process, rare earth minerals were processed at an industrial scale to make the impregnating solution. He left the manufacture of the gas mantle to other companies. In a further patent he improved the effect by adding thorium oxide; the new composition was 30% thorium oxide, 30% zirconium oxide and 40% lanthanum oxide. In this patent he mentions that cerium oxide further improves the effect.

After success, decline followed. The light of the gas lamps was too greenish (presumably owing to the praseodymium content), their lifetime was too short, the raw material was too expensive and rare, and – on top of it – the great rival, electric light appeared. In 1889, Auer had to close down the factory in Atzgersdorf. However, Auer did not lose faith. He continued to experiment in the laboratory set up in his house.

He looked for a new raw material and found it in monazite sand. The mineral was mentioned first in 1826 under the name turnerite; it was Breithaupt who gave it the name monazite, stemming from the Greek word for solitary; it indicates that the mineral occurs mainly independently, without being mixed with other minerals (Breithaupt 1829). Chemically monazite is cerium orthophosphate containing other rare earth elements and in addition substantial amounts of thorium. It occurs in Russia along the Ural mountain range, in the United States and, above all, in Brazil, in the form of monazite sand, the eroded form of the mineral. This readily available material abundantly ensured the raw material source of the rare earth elements industry beginning to take shape. Auer developed a method to separate the components of monazite, based on his earlier fractional crystallization procedure

after digestion with sulfuric acid. The large amount of thorium, which he separated in the form of thorium ammonium nitrate from rare earth elements and other alkaline earths present in the mineral, was a new product. He found out that gas mantles impregnated with thorium oxide and cerium oxide are far better, both regarding light emission and lifetime, than those impregnated with lanthanum oxide and zirconium oxide. The best results were achieved with 1% cerium oxide. The 'public rehearsal' was held on November 4, 1891: the Opera Café in Vienna was illuminated with these new Auer lamps which had great success. At the time it was cheaper to use them than electric bulbs. The factory in Atzgersdorf again operated at full capacity. These lamps were mainly used inside buildings, because they were less resistant to outdoor conditions. None the less, public lighting using them was introduced in some cities, first in Bombay. During the first nine months of renewed large-scale production, 90 000 Auer lamps were sold in Vienna and Budapest alone. In 1913, production amounted to 300 million lamps requiring the processing of 3000 tons of monazite sand.

Auer lamps defied the competition of electric lighting for a long time, to the last in trains. The writer still remembers how in his childhood the conductor came into the compartments of the trains pulled by steam engines and lit the gas lamps: the white mantle surrounding the flame began to glow and the compartment was flooded with light.

It should be noted that similarly to most successful inventors Auer was exposed to many patent attacks and had to suffer the vexations of many patent suits in several countries of the world. He personally retired in the nineties from industry and business. He bought an estate in the south of Austria and built a castle on it, with a modern laboratory on the ground floor where he continued his research mainly concerned with light. He presented numerous new and important inventions, one of them again connected with rare earth elements. He observed the spark-inducing capability of a cerium–iron alloy and on this basis, using the alloy as synthetic flint material, he constructed the first pocket lighter that really worked. He patented the inventions, which brought him great incomes and many unpleasant lawsuits. And after all this, Auer still had the energy to return to the chemistry of the rare earth elements and to discover a final separation and by it a new element in this still mysterious group. Similarly to his inventions, this discovery was also accompanied by priority disputes, though not lawsuits. However, this is not yet the moment to anticipate events.

Because in the meantime other researchers were also busy. The reader will remember that Lecoq de Boisbaudran discovered samarium in 1879 in the original didymium, and as in each rare earth element discovery story, again it was questioned. Cleve who had so many merits in the field of rare earth elements occupied himself much with the element, so much that he finally wrote a monograph in 1885 entitled *Contributions to the Knowledge of Samarium*, in which – based on his experiments – he unquestionably confirmed that samarium is an independent and homogeneous new element. However, the homogeneity was questioned, already in the following year, by the French chemist Demarçay, who announced that he separated a presumably new rare earth element from samarium, at least so it

appears on the basis of its absorption spectral lines (Demarçay 1886). Some years later Bettendorf denied this statement and took up the position that samarium is homogeneous (Bettendorf 1891). Subsequently Lecoq de Boisbaudran gave his opinion in the samarium matter; also based on the absorption spectrum, he thought to have discovered not one, but several other new elements in samarium (Lecoq de Boisbaudran 1892, 1893). In 1893, Demarçay backed out of his earlier opinion that the variations of samarium spectra indicate the presence of two elements (Demarçay 1893). At that time chemists were extremely exacting, even more than as organic chemists in the present day.

They were not satisfied with a spectral line as proof of the existence of an unknown new element, or compound, they wanted palpable substance. On this issue they discussed during a decade, Demarçay finally produced the substance: from a large quantity of separated samarium he succeeded, by means of repeated re-crystallization of nitrates from nitric acid solution to produce a fraction with an individual spectrum. It was colourless, less soluble than samarium nitrate but more soluble than gadolinium nitrate. Having lost courage in the former debates, he termed it Σ for the time being (Demarçay 1896), since spectral lines were still his main proof. In 1901, he finally succeeded to prepare the pure substance in the form of the double nitrate of the new element with magnesium which he named europium (Demarçay 1901). In 1904 this element was also separated from gadolinium by the last great figure in the history of the discovery of the rare earth elements, Urbain. Together with his co-worker Lacombe, he had developed a new method; they applied a so-called 'separating element', usually bismuth, whose nitrate is isomorphous with the rare earth element nitrates. The solubility of bismuth nitrate is such that it frequently crystallizes between two rare earth element nitrates, and by this means the two rare earth element salts can readily be separated (Urbain and Lacombe 1903). Studying gadolinium by this method gave three fractions, one being europium, the second proved to be terbium, and for the third they retained the name gadolinium, so that no new name was required (Urbain and Lacombe 1904).

Ever since Marignac's ytterbium was 'matriculated' in 1878, not much was heard about it. And as it frequently happens, after a long pause two chemists simultaneously started to work on ytterbium. One of them was Auer von Welsbach. In the first years of this century he again developed a new method for the separation of rare earth elements: fractional crystallization of their double oxalates with ammonium. Working with this method, ytterbium became questionable to him. In 1905, he gave a report on his new method to the Academy of Vienna and mentioned that presumably ytterbium consists of two components (Auer von Welsbach 1905). In 1907, he published his experimental results, again in less current Austrian journals. Starting from half a ton of yttrium group oxalates he produced a material rich in ytterbium, which he separated into 100 fractions and finally stated that ytterbium consists of two elements, giving them the high-flown names aldebaranium and cassiopeium (Auer von Welsbach 1907).

Encouraged by his success with gadolinium, Urbain simultaneously started to try his method with ytterbium and came to the same result at almost the same time as Auer, namely that ytterbium consists of two elements. He also gave them names: one

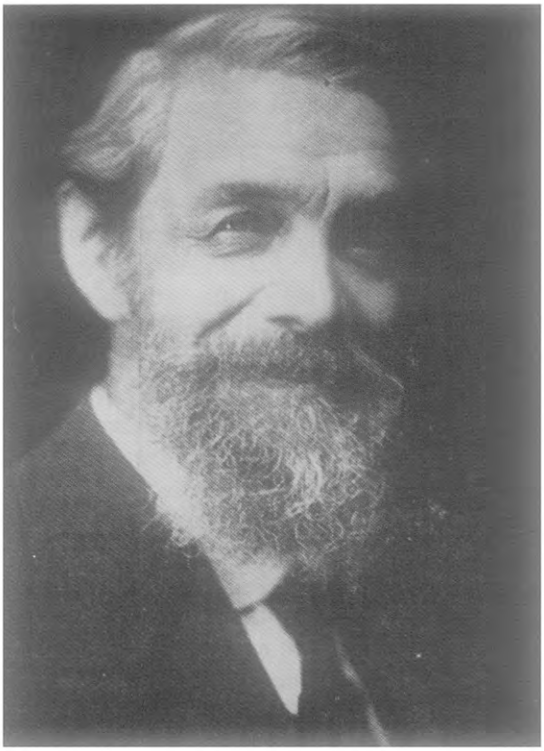

Fig. 10. Georges Urbain.

was neoytterbium, the other, derived from the ancien Roman name of Paris, lutetium (Urbain 1907, 1908). Urbain's first paper appeared somewhat later than Auer's, but he sent it to the editors somewhat earlier. A priority dispute started; both claimed the glory of the discovery. Urbain referred to the fact that he read a lecture on his discovery at the Academy of Paris 44 days earlier than Auer at the Vienna Academy, and sent his paper 40 days earlier, while Auer referred to his uncertain hints from 1905. Both insisted upon their own names for the new elements.

By reason of the sharpening antagonism between Germany and France, the official chemical Organizations stood by their fellow-countrymen. The Society of German Chemists suggested a compromise: let neoytterbium keep the old name ytterbium, and the other be cassiopeium. However, the International Commission of Atomic Weights decided for the names ytterbium and lutetium, to the great exasperation of Auer. The German Atomic Weight Commission did not accept the decision of the International Commission and kept to its own suggestion. Thus, in the German literature cassiopeium continued to be in use, and it needed the lost World War II for the name lutetium be accepted in the German literature.

The division of ytterbium into two elements was the last division, with it the story of the discovery of rare earth elements lasting for over a century came to an end. However, at the time the chemists did not yet know that this was in fact the end of

the story. They could not know, since the theoretical explanation of the great similarity of the properties of rare earth elements did not exist as yet. It is this theoretical explanation that simultaneously yields information on the number of rare earth elements that can exist all in all. The chemists were convinced that since experience up until then always confirmed that some new element did turn up, so why should it not be so in the future? The two great rivals continued their research and believed they had achieved success. Auer, for instance, reported that thulium can be separated into three, terbium into two further elements (Auer von Welsbach 1911). Urbain thought he found a further new element in his own lutetium and gave it the name celtium (Urbain 1911). All these were, of course, errors.

Carl Auer von Welsbach was born in Vienna in 1858. His father was director of the Imperial and Royal Court Printery. He visited various secondary schools in Vienna and started to study chemistry at the Vienna University with Professor Lieben. He continued and finished his university studies in Heidelberg under Bunsen and Kopp. Since, however, he never finished his doctoral dissertation on rare earth elements, he never took his doctor's degree. He returned to Vienna and began his career in Lieben's institute as an unpaid assistant. He still aimed at the doctorate: he studied the rare earth minerals he brought with him from Heidelberg and developed the separation method mentioned; he also continued his work leading to the invention of the Auer lamp. By that invention he became independent, started to work in a basement laboratory, then in the laboratory he set up in the house he bought in Vienna and subsequently in the laboratory of his factory. He became rich and his work was acknowledged with the baron title. From 1899 on he mainly lived in his south-Austrian castle near Rastenfeld and continued research in the laboratory he set up there. In addition to the inventions discussed he had several more, the most successful being the osmium-filament incandescent electric bulb. With less success he worked on a new battery and on colour photography. In the meantime he married and four children were born from this marriage. He hunted much, read less, not even chemical literature. In this respect he was similar to his master Bunsen. He bought Bunsen's library, but the major part of the books continued to remain uncut, just as Bunsen left them. Auer did not like to publish either, all in all only 16 of his papers appeared. He died in 1929. He suddenly felt unwell at a motorcar excursion, went to see a doctor, and after returning it is said that he went into his laboratory, burnt his papers, carefully covered his instruments, waved good-bye to them, went to bed and was dead by the morning (D'Ans 1931).

Henry Becquerel was born in Paris in 1852. Both his father and his grandfather were well-known scientists and university professors. Henry studied at the École Polytechnique and started his career there as an assistant. In 1891 he 'inherited' his father's chair in physics at the Conservatoire des Arts et Métiers, and in 1895 became a professor of the École Polytechnique too. He was a member of the French Academy of Science. His discovery in 1896 of uranium radiation was epoch-making, it was in fact the overture of the atomic age. For this discovery he won the Nobel Prize in Physics in 1903. The unit of radioactive radiation (1 disintegration/s), the becquerel, bears his name. He was successful in other fields of physics too. He dealt much with spectroscopy. He died in Le Croisis in 1908 (Ranc 1946).

Johann Friedrich Breithaupt was born in Freiberg in 1791. He studied at the Jena university and at the Mining Academy of Freiberg, where he became an assistant and, in 1826, professor of mineralogy. He retired in 1866 and died in 1873. He discovered 47 minerals. His major work is a three-volume Handbook on Mineralogy (*Vollständiges Handbuch der Mineralogie*, Dresden/Leipzig 1836–1847).

Eugene Demarçay was born in Paris in 1852. He studied at the École Polytechnique and started his career there as an assistant. Subsequently, he made a long journey through Africa and India.

After his return he lived on his inherited wealth and did research work in his private laboratory. He participated in the Curie couple's research by doing spectrometric measurements, he studied high-temperature reactions, and, in the field of organic chemistry, ethers and terpenes (Etard 1904).

Gerhard Krüss (1859–1895) studied in Munich and there became Bayer's assistant, and subsequently lecturer. He was occupied above all with photometry and spectral analysis. He was the author of the first monograph on photometry: *Kolorimetrie und quantitative Spektralanalyse* (Hamburg/Leipzig, 1891). He was the founder of the journal *Zeitschrift für anorganische Chemie* still appearing in our days.

Georges Urbain was born in Paris in 1872. His father was a university professor in chemistry. Georges studied at the École de Physique et de Chimie in Paris. He started research work in Pierre Curie's laboratory and subsequently worked as Charles Friedel's private assistant and earned his doctor's title with a dissertation dealing with rare earth elements. He became lecturer of chemistry at the Sorbonne in 1906, and professor of inorganic chemistry in 1908. In 1928, he took over as head of the Institute for General Chemistry. He was an eminently diligent researcher, the author of over one hundred papers and seven books on chemistry dealing with spectrochemistry, the chemistry of complex compounds, chemical energetics and atomic structure. His main field of research continued to be the rare earth elements; he asserted that during 15 years he performed more than two hundred thousand fractional crystallizations concerning rare earth elements. He loved music and played himself. He also wrote a book on music, called *Le tombeau d'Aristoxene. Essai sur la musique.* He was president on the International Atomic Weight Commission for some time. He died in Paris in 1938 (Job 1939).

5. Setting things in order and interpretation

In effect, from observing and experiencing the constant material transformations going on in the world, the assumption appeared obvious that the different materials consist of identical components and that some changes taking place in them are the causes of the transformations. This was the concept of all philosophical schools in antiquity, whether assuming one single primeval component, calling it water, fire or atom, or assuming a few such components like e.g. Aristotle did. The concept of the chemical element appeared with Boyle, however, he did not dismiss the idea that these elements may consist of common components, of the Aristotelian four if you like, but they are of no interest for the chemist, since chemical elements cannot be further decomposed by the methods of analytical chemistry. Boyle made no statement as to how many elements exist, nor did Lavoisier, who gave the exact definition of the chemical element. It was Dalton's atomic theory which excluded the possibility of the existence of the primeval element(s), of any sort of further divisibility. This theory says that every chemical element consists of its particular, independent and indivisible atoms differing in material quality from the atoms of all other elements. This is the reason why the properties of individual chemical elements differ. This last statement was – as a matter of fact – accepted generally since Boyle without any special reasoning, since it was this differentness on the basis of which new chemical elements could be discovered. A substance could be declared a new element on the basis of its properties differing from all other elements. The properties in question were usually perceivable, such as colour, state, melting point,

chemical reactions, etc. Dalton, however, introduced a new, more abstract characteristic: atomic weight. This should have been a more exact characteristic than all earlier ones, had not its determination encountered so many uncertainties. Atomic weight was determined by analysis, by finding the percentual composition of the compounds of the element in question. This part of the job was fairly simple, because it could be performed in the laboratory, with increasing accuracy as analytical methods of the age developed. However, to determine the atomic weight, it is necessary to know the atomic composition of the molecule, and this could only be assumed on the basis of analogies, no experimental method existed for determining it. Berzelius's genius is truly admirable, using the analytical methods at his disposal he was able to determine the atomic weights of 53 elements between 1807 and 1820 at a fairly acceptable level. We know his laboratory from the description of his pupil Wöhler who worked with him in 1823–1824.

'The laboratory consisted of two common rooms with the simplest possible equipment. There was no furnace, no exhaust hood, no running water, no gas pipe. In one of the rooms there were two common long pine-wood tables, one for Berzelius, one for me. On the walls there were some shelves with chemicals, in the middle of the room a glass-blowing table and a mercury tank. In the corner was a sink made of fayence and a wash tub under it, where Anna, Berzelius's cook, washed up our vessels each morning. In the other room we had the balances and a big cupboard with instruments. In the kitchen close by where Anna cooked there was a small furnace rarely used and a sand bath continually heated. There was also a small workshop with a lathe. Berzelius was usually cheerful, he talked much during work, he liked to tell jokes and liked to listen to jokes, except when he had one of his rather frequent headaches. Then he retired for days and did not come into the laboratory ...' (Wöhler 1875).

Berzelius's achievement under such conditions is outstanding. His results for atomic weights, at least the integers, are still correct, except where the number of atoms in the molecule that he assumed was incorrect, in such cases he arrived to half or double, two thirds or one and a half times the correct value. Two discoveries, made still in Berzelius's life time, helped to a certain extent, namely Mitscherlich's isomorphism law and the statement of Dulong and Petit that for metals the product of specific heat and atomic weight is a constant value (atomic heat law). Taking these statements into account Berzelius corrected his atomic weight values from time to time. In his textbook published in 1836, the atomic weights of two rare earth elements are listed: 46.01 for cerium and 32.31 for yttrium (Berzelius 1836). Since Berzelius considered the double hydrogen atom as unit, the above values shall be taken twice: 92.02 and 64.62. Berzelius obtained these values by assuming that the composition of the oxides is – analogously to earth alkali metal oxides – CeO and YO, respectively, i.e., to use an expression of a later period, he assumed that Ce and Y are bivalent. The researchers who in the following decades worked on atomic weights of rare earth elements also took them to be bivalent, as well as the rare earth elements discovered subsequently. Among those mentioned in this chapter, particularly Marignac and Brauner determined atomic weights with accuracies astonishingly good in their age.

During the century-long reign of Dalton's atomic theory some concepts involving primeval element hypotheses, common components of atoms always propped up. The growing group of rare earth elements was particularly puzzling for chemists, since their chemical properties were extremely similar, atomic weight determinations gave largely differing results for nominally one and the same element, by reason of the intermingling of the elements, by reason of working in most cases with mixtures that were separated into individual elements only later. In fact, it was the difference that appeared in the atomic weights of different samples that stirred the researchers to discover new rare earth elements. Can these elements be considered chemical elements at all – this is how many chemists put the question.

The human mind wishes to systematize things and phenomena. So it also wished to systematize chemical elements. A certain system was defined by chemical properties, by the chemical reactions to the compounds, which was the basis on which the qualitative wet analysis system for detecting elements developed. It was started perhaps with Bergman in the 18th century and improved in the early 19th century by Pfaff and Rose to achieve the form which up to the 20th century, to the age of instrumental analysis, was the standard method of analysis, described in Fresenius's book *Anleitung zur qualitativen chemischen Analyse* which first appeared in 1841 and later had many new editions and was translated into many languages (Szabadváry 1966, p. 121). The elements discovered later usually fitted into one of Fresenius's analytical groups and consequently were fitted into the next editions of the book. Rare earth elements, however, did not fit into this system. The concept of atomic weight opened up a new possibility for systematization: grouping the elements by increasing atomic weight appeared a numerical and hence more exact principle than their properties. The idea was not conceived in Lothar Meyer's and Mendeleev's mind without antecedents, systematization by atomic weight was taken up almost immediately after the concept of atomic weight was born. Its history from Döbereiner through Gladstone, Odling, Beguyer de Chancourtois to Newland, to mention only the most important predecessors, has been told many times (Szabadváry 1961). However, the scientists mentioned were unable to come to important conclusions through their attempts, by reason of the basic concept, since the atomic weights were uncertain. Not only numerically, due to experimental errors, but also on principle. Dalton took hydrogen as unity and related all other elements to it, Berzelius calculated either with the 2H unit or else with $O=100$ which he considered more reliable. Others took what later was called equivalent weight for atomic weight, and even in this there was a difference in many cases between the analytical and the electrochemical value. Elemental gases, with their two-atomic molecules were another source of confusion. Hence very many different value types were current, and this chaos began to make the sense of the concept of atomic weight itself questionable. No wonder that the different systems of elements based on such questionable values were not really reassuring. The French Academy of Science declared, regarding one such table, that it was pure figure mysticism. When Newland reported in the Royal Society that he observed a periodically recurring similarity in properties when elements are being put into the order of their atomic weights, somebody remarked that he should try to list the elements in alphabetic order, maybe he could detect some regularity in that case too.

It is well-known that it was Cannizzaro who finally, by deliberate thinking, cleared up things and defined equivalent weight, atomic weight and molecular weight unequivocally in his small book *Sunto di un corso di filosofia chimica* (1858) and proposed to accept these definitions at the congress of chemists held in Karlsruhe in 1860. Two young scientists also participated at this congress: Lothar Meyer from Breslau and Dmitry Mendeleev from St. Petersburgh. At the congress, as usual, there was much talk and debate over Cannizzaro's proposals. Some found them worthy, some did not, some accepted them, some did not. None the less finally the whole chemical world began to think in these categories. Meyer and Mendeleev were immediately under the influence of Cannizzaro's concept, as we know from their personal reminiscences. Mendeleev, for instance, wrote the following: 'I received a copy of the book and read in it on the long railway journey home. At home, I re-read it and was fascinated by the clarity with which the author interpreted the major points discussed. All of a sudden the scales fell from my eyes, my doubts disappeared and security took their place. If some years later I was able to contribute to some extent to order in these matters, it was due not insignificantly to Cannizzaro's book' (Danzer 1974).

Both Meyer and Mendeleev independently of one another started to group elements by their atomic weight which by now was consistently interpreted and by their periodically recurring properties. It is unnecessary for me to write about the table, which is by now taught in secondary school. Obviously the periodic table was not born in the form we know it today, both authors continuously changed and modified it. On this subject very much could be written, but we are here interested solely in the relationship of rare earth elements and the periodic table. Rare earth elements, in this field too, caused considerable confusion and problems.

Lothar Meyer solved the question very simply. He just took no notice of rare earth elements, they are not listed in his element table. He was not fully convinced of their being elements. In Mendeleev's first table which appeared in 1869 and was very different from what we know now as a periodic table, cerium, lanthanum and didymium were listed with the atomic weights of 92, 94 and 95, respectively, corresponding to bivalence at a unit O = 16, and also erbium and yttrium with atomic weights of 56 and 60, respectively, with interrogation marks. In this table no grouping of elements according to valence appears as yet (Mendeleev 1869). The table which appeared in 1871 is already in the usual form. In this year Mendeleev performed an important change – arbitrarily – with rare earth elements: he assumed that they were trivalent, and correspondingly recalculated their atomic weights, that is, instead of YO and LaO he calculated with Y_2O_3 and La_2O_3. He then listed yttrium with an atomic weight of 88, lanthanum with 137 and cerium with 138. He supported his assumption with specific heat measurements of cerium (Mendeleev 1871). The assumption proved true, Cleve confirmed it in the following years analytically, Hillebrand (in 1876) with specific-heat determinations for lanthanum and didymium (Hillebrand 1876). It was Hillebrand who in the previous year, using Bunsen's electrolytic method, obtained metallic cerium, lanthanum and didymium in satisfactory purity for the measurements (Hillebrand and Norton 1875). This was in fact the first actual proof for the reality of Mendeleev's periodical system, confirmed later in a striking manner by the discovery of some predicted elements such as

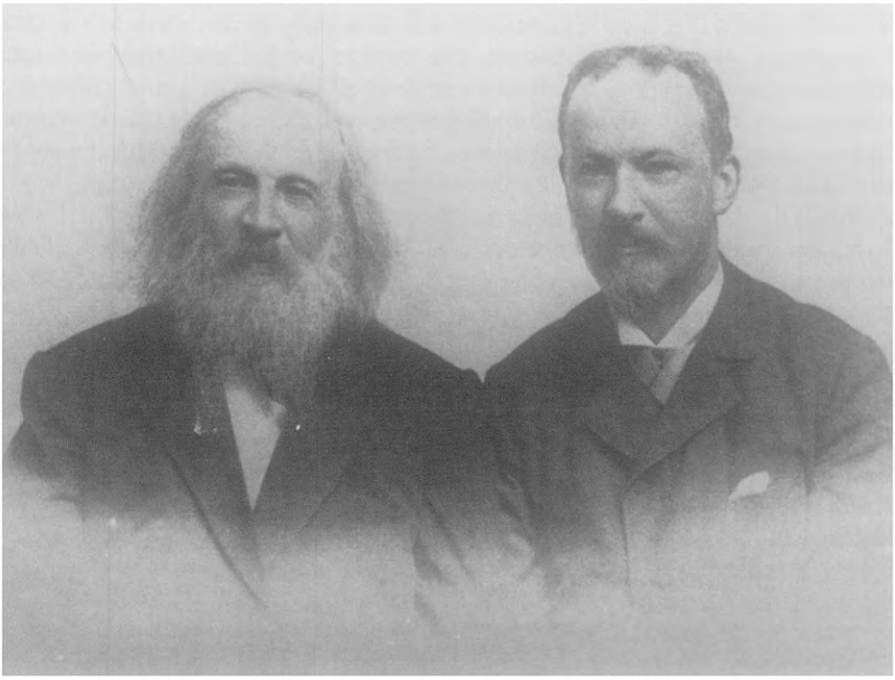

Fig. 11. Dmitry Ivanovich Mendeleev and Bohuslav Brauner.

gallium, scandium and germanium. From then on the table served as a sort of map where to look for as yet unknown elements. It proved useful in numerous cases, however, for rare earth elements it failed. As their number increased, there was simply no place to put them in the periodic table. They gave headaches to the author of the table and to others. Among these, Brauner was an outstanding figure, a personal close friend to Mendeleev and one of the first zealous backers of his table. His activity was concentrated above all on atomic wieght determinations, including more exact determinations of rare earth element values only calculated by Mendeleev. We have seen earlier that the anomalies in atomic weight determinations led Brauner to the assumption that didymium was not a homogeneous element, confirmed soon afterward by Auer. The results of the atomic weight determinations carried on for decades were: Ce, 140.22; La, 148.92; Pr, 140.9; Nd, 144.3; Sm, 150.4; i.e., the values still valid at present. He took great pains to place them in the periodical table. He attempted to complete Mendeleev's periods with two further periods, then gave up this idea. He also proposed some sort of interperiodical arrangement (Brauner 1902), similarly to Steele before him (Steele 1901). Finally his proposal that all rare earth elements with the exception of yttrium and scandium should be placed into a single square, the square of lanthanum, remained (Brauner 1899). Independently of him Retgers also made the same proposal (Retgers 1895). Brauner believed in the existence of some primeval element, all individual elements being forms differentiated and condensed in different degrees.

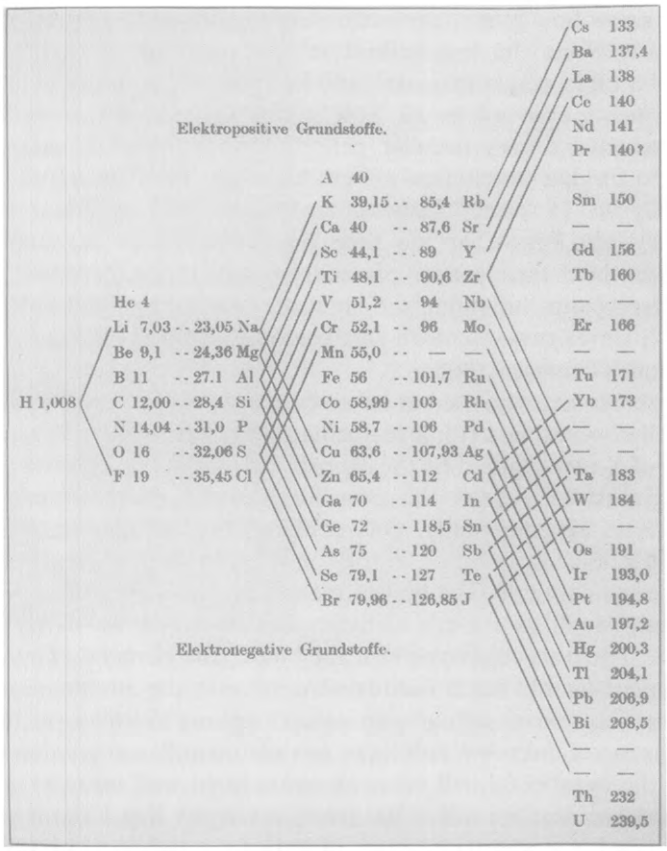

Fig. 12. The Periodic System of Julius Thomsen.

In rare earth elements the extent of differentiation is very small, this is the reason that they are so similar. Mendeleev who stiffly adhered to Dalton's concept did not agree with Brauner's theory, none the less the location of rare earth elements according to Brauner's proposal is still the most widespread solution of the problem, in most periodic tables lanthanum with the atomic number 57 is followed by hafnium with the atomic number 72, and the rare earth elements are listed separately somewhere at the bottom of the table.

At the time, of course, no atomic numbers existed as yet, they were introduced by Van den Broek in 1912, assuming that the nuclear charge of the individual elements and hence the number of electrons revolving around it is identical with the ordinal number occupied by the given element in the Mendeleev table (Van den Broek 1913). At the time, shortly after the discovery of radioactivity, atomic structure investigations were still at their very beginnings, statements now already based on experimental facts that the atoms are not indivisible, but consist – as so many earlier nature philosophic concepts maintained – of common components. It was thus

impossible to know how many rare earth elements are still to be expected into that common square. None the less, several scientists attempted to predict from the proportions of atomic weight increases, and fairly well as a matter of fact, how many rare earth elements exist all in all, how many are still unknown. Thomsen, for instance, constructed a very peculiar periodic system in 1895, very similar in its arrangement to the later periodical system based on Bohr's electron configuration table. He assigned 16 places between lanthanum and tantalum to rare earth elements. Ten were known at the time (not taking into account yttrium and scandium, which held their proper places from the start and caused no problem). Europium, dysprosium, holmium and lutetium were as yet unknown, at least to Thomsen. This leaves two unknown rare earth elements at the time, a surprisingly exact prediction! (Thomsen 1895).

Moseley, a researcher who died at an early age in World War I at the siege of the Dardanelles, discovered, in 1913, a mathematically expressible relationship between the frequency of X-rays emitted by the element serving as anticathode and its atomic number. This method yielded the possibility to determine atomic numbers of chemical elements experimentally. One could in this manner unequivocally state whether the substance in question is truly an element and if so, one could find its place in the periodical table. The first to make use of this possibility was Urbain: in 1914 he submitted all rare earth elements discovered in the latter times to the Moseley check. The tests confirmed that they were true elements. Thus, the range of rare earth elements would reach from lanthanum with the atomic number 57 to the atomic number 72, that is, actually 16 places. Among them the element with the number 61 was as yet unknown and there was no unequivocal opinion regarding the element with the number 72. All other elements fitted well into the system.

We have mentioned at the end of the previous chapter that Urbain announced the discovery of a further rare earth element in 1911, he called it celtium (Urbain 1911). This was the only one among the samples whose elemental nature was not confirmed by Moseley. It is difficult to convince a scientist of his error. Urbain did not believe Moseley in the celtium case, he considered it the last rare earth element with the atomic number 72. Further elucidation of the question was post poned by the War, and Moseley fell in its early stage. After the war, however, Urbain and Dauvillier studied the would-be celtium by X-ray spectrometry until they found some very pale lines that might putatively be considered proof of the existence of celtium and of its atomic number 72 (Urbain and Dauvillier 1922). However, the whose assumption proved to be incorrect, though Urbain still continued to defend celtium for a long time.

In the meantime, Bohr developed his electron shell theory applying the quantum theory. Bohr thereby interpreted the Mendeleev table theoretically: new periods in Mendeleev's system begin at the elements where the filling-up of a new electron shell begins and last until that electron shell is completed, explaining the periodicity of chemical properties, since chemical properties depend above all on the actual external electron shell.

Rare earth elements were a problem for Bohr too, which he could only solve by them making an exception. After lanthanum the filling of the external shell stops and

Fig. 13. George de Hevesy.

continues on a shell closer to the interior by two. This will then also explain the great chemical similarity of rare earth elements, their external electron shell being identical. The reason for this anomaly is explained by various quantum chemical and energetical theories, their discussion, however, is not the business of the science historian, on the one hand, because he is no specialist in quantum chemistry, and, on the other hand, because he does not fully believe in them. In nature order prevails, so why this apparent anomaly? Maybe rare earth elements will one day shake our present knowledge and conceptions. None the less, rare earth elements were direct proof of the correctness of Bohr's theory, since according to his electron configuration table, filling up of the N shell is complete at lutetium, atomic number 71, and atomic number 72 corresponds to the continuation of filling up the electron shell interrupted after lanthanum. Consequently the element 72 will not have the properties of rare earth elements, but rather those of the elements in the next column, one should therefore look for it in zirconium ores. At the time George de Hevesy – who made friends earlier with Bohr in Rutherford's institute in Manchester – worked in the Bohr institute. Before World War I, de Hevesy also worked with Moseley. Together with Dirk Coster, also working in Bohr's institute, they began to investigate Norwegian zirconium ores and detected a new element in it, first only by X-ray spectrometry in 1922 (Coster and de Hevesy 1923), which they named hafnium, from the Latin name of Copenhagen. Later de Hevesy succeeded to separate it chemically from zirconium based on the differing solubility of the fluorides and to obtain the pure element via reducing the fluoride by metallic sodium (de Hevesy 1925). Hafnium turned out to be unequivocally the element 72 and had no properties similar to rare earth elements. Thus Bohr was fully confirmed.

Hevesy's book *Die seltenen Erden vom Standpunkt des Atombaues* (which appeared in Leipzig in 1927) was the first monograph dealing in detail with rare earth elements based on general atomic structure. All elements from atomic number 57 to 71 are discussed in it. An element illinium (symbol Il) stands for atomic number 61, however, except its mention on the first page there is not a single word about it in the whole book. American researchers thought that they had discovered it, and named it after the state Illinois. At the time I was a student, this place in the periodic table was occupied by florentium as the discovery of Italian researchers who named it after Florence. However, neither discovery proved correct. Element 61 has not been discovered in nature, but in traces among the fission products of uranium by Marinsky and co-workers in 1947 (Marinsky 1947). It was named promethium after Prometheus who stole fire from the gods for man. It is an open question whether the fire which humanity procured by uranium fission will turn out a blessing or a curse.

Niels Bohr was born in Copenhagen in 1885 and died there in 1962. He studied physics at the university of his native town. He worked in Cambridge in Thomson's institute and, subsequently, in Manchester with Rutherford, where he became acquainted with the epoch-making phenomena of radioactivity and with Rutherford's atomic model conception. Bohr discovered its inadequacies and by uniting it with Planck's quantum theory he developed the Bohr model in 1913, and on its basis the electron configuration table of the elements. Bohr's atomic theory opened up a new age in the research of atomic structure. His achievements were recognized by the Nobel Prize in Physics in 1922. He continued to work on theoretical atomic research. The outbreak of World War II and Denmark's occupation by the Germans in 1940 found him in Copenhagen. When atomic bomb research started by both the Allies and the Germans, the Allies helped Bohr to escape from Denmark via Sweden. He went to the United States and served as a consultant in atomic bomb research. After the war he returned to his institute in Copenhagen and continued work there.

Bohuslav Brauner was born in Prague in 1855 and died there in 1935. He studied at the Technological University of Prague and made his doctorate at the Prague University. Meanwhile he also worked with Bunsen in Heidelberg and with Roscoe in Manchester. In 1882, he became an assistant at the Czech branch of the Charles University of Prague and became professor of inorganic chemistry in 1897. His scientific activities consisted almost wholly of checking and improving the accuracy of atomic weights (Druce 1944).

Stanislao Cannizzaro was born in Palermo (Sicily) in 1826. He started his studies as a student of medicine at the university of this native town and continued them in Pisa, where he changed over to chemistry. In 1847, he returned to Palermo and participated in the Sicilian revolution. After its fall he was condemned to death in 1849, but succeeded to flee in time to France. In Paris he worked in the Jardin des Plantes with Cahours. He was appointed professor to the university of Genoa in 1855. After the victory of Garibaldi's revolution in Sicily he again returned to Palermo and became professor of chemistry at its university. After the unification of Italy in 1871 he became professor at the university of Rome and simultaneously senator of the new kingdom. Besides the activities mentioned, he attained important results above all in organic chemistry. He died in 1910 in Rome (Tilden 1912).

Dirk Coster was born in Amsterdam in 1889. He studied at the technological university of Delft and took his doctor's degree at the university of Leyden. In 1922/23 he worked at Bohr's institute in Copenhagen. Returning to the Netherlands, he worked with Lorentz in the Teyler Laboratory in Haarlem. In 1924, he became professor of physics at the university of Groningen, where he continued to be active mainly in X-ray spectroscopy. He died in 1950 in Groningen.

George de Hevesy was born in Budapest in 1885. He studied in Budapest, in Berlin and in Freiburg. He started his career at the university of Zürich and worked subsequently as Haber's assistant in Karlsruhe. From there he went to the Rutherford institute in Manchester. It was there that he got acquainted with the novel field of radioactivity, to which he remained faithful in all his life. In 1912, Rutherford gave him the task to separate radium D, a lead isotope from natural lead. This work led him to the conclusion that isotopes cannot be separated by chemical methods. He utilized this recognition in 1913 in Vienna by developing – with Paneth – the isotope tracer method which was of great significance. During World War I and afterwards he worked in Hungary. With his novel method he discovered autodiffusion of metals. In 1920, he went to Copenhagen to work at Bohr's institute. In 1926, he was appointed professor of chemistry at the Freiburg university. It was here that he developed the isotope dilution method and X-ray fluorescence analysis. After Hitler came to power in Germany he returned to Copenhagen, his great discovery of that period was activation analysis (1936). After the Nazi occupation of Denmark he fled to Sweden and worked at the university of Stockholm; mainly biochemical applications of his methods were his concern. In 1943, he was awarded the Nobel Prize in Chemistry. He died in Freiburg in 1966 (Szabadváry 1972).

William Francis Hillebrand was born in Honolulu in 1853. He studied in Heidelberg. Between 1880 and 1908 he worked as a chemist at the US Geological Survey, between 1908 and 1925 he was chief chemist of the US Bureau of Standards. He died in Washington in 1925.

Dmitry Ivanovich Mendeleev was born in 1834 in the Sibirian town Tobolsk where his father was the director of the secondary school. He lost his father at an early age. He began his studies in 1850 at the Pedagogical Institute of St. Petersburgh and graduated as a secondary school teacher in chemistry. He began teaching in Simferopol and subsequently in Odessa. In 1856, he became lecturer at the university of St. Petersburgh. In 1859/60 he held a scholarship in Heidelberg, working in Bunsen's laboratory. He then continued as lecturer at the university of St. Petersburgh. In 1864, he was appointed professor of chemistry at the technological university of St. Petersburgh and later on, in 1867, professor of chemistry at the university of St. Petersburgh. In 1876, he became a member of the Russian Imperial Academy. In 1890, a student rebellion broke out at the university. Mendeleev disapproved of the attitude of the ministry and as a sign of protest, resigned from his professorship. In 1893, however, he accepted the post of president to the recently established Russian Bureau of Measures. He died in St. Petersburgh in 1907. His book *Osnovy Khimii* (Fundamentals of chemistry) had many Russian editions and was translated into numerous foreign languages. Besides developing the periodic system, he was active in physico-chemical and petrochemical research (Kedrov 1974).

Henry Growyn Jeffreys Moseley was born in 1887 in Weymouth (England). The three generations preceding him in the family were university professors, his early death prevented him following them. He studied in Oxford and started his career in Rutherford's laboratory in Manchester. His discovery gained him scientific prestige at an early age. At the outbreak of the first World War he was in Australia, but immediately returned to England and volunteered for the army. He fell in 1915 at Gallipoli, in the Dardanelles fights against the Turks.

Jörgen Julius Thomsen was born in 1826 in Copenhagen, he studied at the technological university of his native town and started to work at that institution, at the department of agricultural chemistry. After a study tour in Germany and France he became professor of physics at the Danish Military Academy. In 1866, he became professor of chemistry at the university of Copenhagen. He became famous above all by thermochemical activities: his book *Thermochemische Untersuchungen* (1882) is one of the fundamental works in that field. By means of the periodic system which he had developed, he predicted the existence of further noble gases after argon, this prediction was soon confirmed. In 1860, he became a member of the Danish Academy of Science. He was its president from 1888 until his death in 1909 in Copenhagen (Veibel 1976).

Abbreviations of earlier periodicals

Ann.: Abbreviation for a journal that has had various names: Annalen der Pharmazie in the period 1832–1839; Annalen der Chemie und Pharmazie 1840–1873; Liebigs Annalen der Chemie from 1874 onwards.
Arch. Phys. Nat.: Archives des Sciences Physiques et Naturelles (Geneva)
Crells Annal. Chem.: Chemische Annalen, ed. L. Crell (Helmstädt)
Gehlens J. Chemie: Journal für die Chemie und Physik, ed. by Gehlen (Berlin)
Jahresbericht: Jahresbericht über die Fortschritte der physischen Wissenschaften von J.J. Berzelius (Tübingen)
Pogg. Ann.: Annalen der Physik und Chemie, ed. J.C. Poggendorf.
Schweigers J.: Journal für Chemie und Physik, ed. by Schweiger (Nürnberg)
Svensk. Vetenskap. Akad. Hand.: Kongliga Svensk. Vetenskap Akademien Handlingar (Stockholm)

References

Ador, J., 1894, Bull. Soc. Chim. (Paris) **17**, 233.
Anonymus, 1816, Svensk. Vetenskap. Akad. Handl., p. 296.
Anonymus, 1824, Svensk. Vetenskap. Akad. Handl., p. 495.
Auer von Welsbach, C., 1883, Monatshefte für Chemie **4**, 63.
Auer von Welsbach, C., 1884, Monatshefte für Chemie **5**, 508.
Auer von Welsbach, C., 1885, Monatshefte für Chemie **6**, 477.
Auer von Welsbach, C., 1905, Wiener Akademischer Anzeiger **42**, 125.
Auer von Welsbach, C., 1907, Sitzungsber. Akad. Wiss. Wien 115, 737, 116, 1425; Monatshefte für Chemie **29**, 181.
Auer von Welsbach, C., 1911, Sitzungsber. Akad. Wiss. Wien **120**, 193; Monatshefte für Chemie **32**, 373; Z. Anorg. Allg. Chem. **71**, 439.
Bahr, J., and R.W. Bunsen, 1866, Ann. **131**, 1; J. für Prakt. Chem. **99**, 274.
Becquerel, H., 1887, C.R. Hebd. Séances Acad. Sci. **104**, 165.
Bergman, T., 1784, Svensk. Vetenskap. Akad. Handl., p. 121.
Berzelius, J.J., 1828, Jahresbericht **7**, 144.
Berzelius, J.J., 1836, in: Lehrbuch der Chemie, Vol. 6 (Arnold, Dresden/Leipzig) p. 104.
Berzelius, J.J., 1840, Jahresbericht **19**, 218.
Berzelius, J.J., 1844a, Jahresbericht **23**, 145.
Berzelius, J.J., 1844b, Jahresbericht **23**, 151.
Bettendorf, A., 1890, Ann. **256**, 159.
Bettendorf, A., 1891, Ann. **263**, 164.
Boklund, U., 1971, in: Dictionary of Scientific Biographies, Vol. 4 (Scribner's, New York) p. 343.
Brauner, B., 1882, Monatshefte für Chemie **3**, 1, 486.
Brauner, B., 1883, J. Chem. Soc. **43**, 278.
Brauner, B., 1899, in: Verhandlungen der Gesellschaft Deutscher Naturforscher und Ärzte, Vol. 2 (Vogel, Leipzig) p. 131.
Brauner, B., 1902, J. Russ. Obch. Fiz. Kim. **39**, 142.
Breithaupt, A., 1829, Schweigers J. **55**, 301.
Breithaupt, J.A., 1836–1847, Vollständiges Handbuch der Mineralogie (Arnold, Dresden/Leipzig).
Bunsen, R.W., 1853, Ann. **86**, 286.
Bunsen, R.W., 1875, Pogg. Ann. **155**, 230, 366.
Cannizarro, S., 1858, Sunto di un corso di filosofia chimica, Nuovo Cimento **7**, 321.
Cleve, P.T., 1879a, C.R. Hebd. Séances Acad. Sci. **89**, 419.
Cleve, P.T., 1879b, C.R. Hebd. Séances Acad. Sci. **89**, 521.
Cleve, P.T., 1879c, C.R. Hebd. Séances Acad. Sci. **89**, 708.
Cleve, P.T., 1882, C.R. Hebd. Séances Acad. Sci. **94**, 1528.
Cleve, P.T., 1885, Contributions to the Knowledge of Samarium.
Coster, D., and G. de Hevesy, 1923, Nature **111**, 182; Naturwissenschaften **11**, 133.
Cronstedt, A.F., 1751, Svensk. Vetenskap. Akad. Handl., p. 227.
Cuvier, G., 1833, Mém. Acad. Sci. (Paris) **12**, 39.
D'Ans, J., 1931, Berichte Dtsch. Chem. Ges. **64**, 59.
Danzer, K., 1974, Dmitri I. Mendelejew und Lothar Meyer (Teubner, Leipzig) p. 31.
de Hevesy, G., 1925, Chem. Reviews **2**, 1; Mat.-Fys. Medd. Dansk Vidensk. Selsk. **6**, 149.
de Hevesy, G., 1927, Die seltenen Erden vom Standpunkt des Atombaues (Springer, Berlin).
Delafontaine, M., 1864, Arch. Phys. Nat. **21**(2), 97; Ann. **134**, 99.
Delafontaine, M., 1865, Arch. Phys. Nat. **25**, 105; Bull. Soc. Chim. (Paris) **5**(2), 166.
Delafontaine, M., 1874, Arch. Phys. Nat. **51**, 48.
Delafontaine, M., 1877, Arch. Phys. Nat. **59**, 176.
Delafontaine, M., 1878a, Arch. Phys. Nat. **61**, 273.
Delafontaine, M., 1878b, C.R. Hebd. Séances

Acad. Sci. **87**, 559.
Delafontaine, M., 1878c, C.R. Hebd. Séances Acad. Sci. **87**, 634.
Delafontaine, M., 1878d, C.R. Hebd. Séances Acad. Sci. **87**, 933.
Delafontaine, M., 1880, C.R. Hebd. Séances Acad. Sci. **90**, 221; Arch. Phys. Nat. **3**(3), 246, 250.
Delafontaine, M., 1881, C.R. Hebd. Séances Acad. Sci. **93**, 63.
Demarçay, E., 1886, C.R. Hebd. Séances Acad. Sci. **102**, 1551.
Demarçay, E., 1893, C.R. Hebd. Séances Acad. Sci. **117**, 163.
Demarçay, E., 1896, C.R. Hebd. Séances Acad. Sci. **122**, 728.
Demarçay, E., 1901, C.R. Hebd. Séances Acad. Sci. **132**, 1484.
Druce, G., 1944, Two Czech Chemists, Bohuslav Brauner and Frantisek Wald (London).
Ekeberg, A.G., 1797, Svensk. Vetenskap. Akad. Handl., p. 156.
Ekeberg, A.G., 1799, Crells Ann. Chem. **II**, 63.
Etard, M.A., 1904, Bull. Soc. Chim. (Paris) **32**, 1.
Fresenius, C.R., 1841, Anleitung zur qualitativen chemischen Analyse, 1St Ed. (Vieweg, Braunschweig).
Gadolin, J., 1794, Svensk. Vetenskap. Akad. Handl., p. 137.
Gadolin, J., 1796, Crells Ann. Chem. **I**, 317.
Gadolin, J., 1798, Inleding till chemien (Åbo, Sweden).
Geijer, B.R., 1788, Crells Ann. Chem. **I**, 229.
Hillebrand, F.W., 1876, Pogg. Ann. **158**, 71.
Hillebrand, F.W., and F. Norton, 1875, Pogg. Ann. **155**, 633; **156**, 466.
Hisinger, W., and J.J. Berzelius, 1804, Afhandlingar i Fysik, Kemi och Mineralogi **1**, 158; Gehlens J. Chem. **2**, 308, 397.
Hitchcock, F.R.M., 1895, J. Am. Chem. Soc. **17**, 483, 520.
Hjelt, A., 1900, Aus Berzelius' und Magnus' Briefwechsel (Vieweg, Braunschweig) p. 60.
Job, P., 1939, Bull. Soc. Chim. (Paris) **6**, 745.
Kedrov, B.M., 1974, in: Dictionary of Scientific Biographies, Vol. 9 (Scribner's, New York) p. 286.
Klaproth, H.M., 1791, Crells Ann. Chem. **I**, 119.
Klaproth, H.M., 1801, Crells Ann. Chem. **I**, 307.
Klaproth, H.M., 1804, Gehlens J. Chem. **2**, 303.
Kopperl, S., 1974, in: Dictionary of Scientific Biographies, Vol. 9 (Scribner's, New York) p. 541.
Krüss, G., 1891, Kolorimetrie und quantitative Spektralanalyse (Voss, Hamburg/Leipzig).
Krüss, G., and L.F. Nilson, 1887, Ber. Dtsch. Chem. Ges. **17**, 2134.
Lecoq de Boisbaudran, P.E., 1874, Spectres lumineux (Dunod, Paris).
Lecoq de Boisbaudran, P.E., 1875, C.R. Hebd. Séances Acad. Sci. **81**, 493.
Lecoq de Boisbaudran, P.E., 1879a, C.R. Hebd. Séances Acad. Sci. **88**, 322.
Lecoq de Boisbaudran, P.E., 1879b, C.R. Hebd. Séances Acad. Sci. **89**, 212; Arch. Phys. Nat. **2**(3), 119.
Lecoq de Boisbaudran, P.E., 1879c, C.R. Hebd. Séances Acad. Sci. **89**, 516.
Lecoq de Boisbaudran, P.E., 1886, C.R. Hebd. Séances Acad. Sci. **102**, 1003, 1005.
Lecoq de Boisbaudran, P.E., 1892, C.R. Hebd. Séances Acad. Sci. **114**, 575.
Lecoq de Boisbaudran, P.E., 1893, C.R. Hebd. Séances Acad. Sci. **116**, 611, 674.
Mallet, J.W., 1877, Am. J. Sci. **14**(3), 397.
Marignac, J.C., 1848, Arch. Phys. Nat. **8**, 265.
Marignac, J.C., 1849, Arch. Phys. Nat. **11**. 21.
Marignac, J.C., 1853a, Ann. Chim. Phys. (Paris) **38**(3), 148.
Marignac, J.C., 1853b, Arch. Phys. Nat. **24**, 278.
Marignac, J.C., 1855, C.R. Hebd. Séances Acad. Sci. **42**, 288.
Marignac, J.C., 1878a, Arch. Phys. Nat. **61**, 283.
Marignac, J.C., 1878b, Arch. Phys. Nat. **64**, 87; C.R. Hebd. Séances Acad. Sci. **87**, 578.
Marignac, J.C., 1880, Arch. Phys. Nat. **3**(3), 413.
Marignac, J.C., 1886, C.R. Hebd. Séances Acad. Sci. **102**, 902.
Marinsky, J.A., L.E. Glendenin and C.D. Coryell, 1947, J. Am. Chem. Soc. **69**, 2781.
Mendeleev, D.I., 1869, J. Prakt. Chem. **106**, 251.
Mendeleev, D.I., 1871, Bull. de l'Académie des Sciences de St. Petersbourg **16**, 45; Ber. Dtsch. Chem. Ges. **4**, 348; Ann. Suppl. **8**, 133.
Mendeleev, D.I., 1891, Grundlagen der Chemie/ Osznovy Khimii (Rizker, St. Petersburg).
Meyer, L., 1870, Ann. **7**, 254.
Mosander, G.C., 1839, Pogg. Ann. **46**, 648; **47**, 207.
Mosander, G.C., 1842, Förhandlinger vid de Skandinaviska Naturforskarnes Tredje Nöte (Stockholm) p. 387.
Mosander, G.C., 1843, Pogg. Ann. **60**, 297, 311; Philos. Mag. **23**, 241.
Nilson, F.L., 1879, Ber. Dtsch. Chem. Ges. **12**, 551, 554; C.R. Hebd. Séances Acad. Sci. **88**, 642; **91**, 118.
Nilson, L.F., 1880, C.R. Hebd. Séances Acad. Sci. **91**, 56, 118.
Nilson, L.F., and O. Peterson, 1880, Ber. Dtsch. Chem. Ges. **13**, 1451.
Ojala, W., 1937, J. Chem. Ed. **14**, 161.
Popp, O., 1864, Ann. **131**, 197.
Ramsay, W., 1913, J. Chem. Soc. **103**, 742.
Ranc, A., 1946, Henri Becquerel et la Découverte de la Radioactivité (Paris).
Retgers, J.W., 1895, Z. Phys. Chem. **16**, 644.
Roscoe, H.E., 1882, J. Chem. Soc. **41**, 277.
Roscoe, H.E., and A.J. Schuster, 1882, J. Chem. Soc. **41**, 283.
Rose, G., 1833, Elemente der Krystallographie (Mittler, Berlin).
Rose, H., 1829, Handbuch der analytischen Chemie, 1St. Ed. (Mittler, Berlin).
Ruprecht, A., 1790, Crells Ann. Chem. **II**, 195, 291, 388.
Smith, L., 1878, C.R. Hebd. Séances Acad. Sci. **87**, 148.
Soret, J.L., 1878, Arch. Phys. Nat. **61**, 322; **63**, 89.
Soret, J.L., 1879, C.R. Hebd. Séances Acad. Sci. **89**, 521.

Soret, J.L., 1880, Arch. Phys. Nat. **4**(3), 261.
Steele, B.D., 1901, Chem. News **84**, 245.
Szabadváry, F., 1961, Az Elemek Nyomában (Gondolat, Budapest) p. 37.
Szabadváry, F., 1966, History of Analytical Chemistry (Pergamon Press, Oxford) p. 117.
Szabadváry, F., 1972, in: Dictionary of Scientific Biographies, Vol. 6 (Scribner's, New York) p. 365.
Thomsen, J., 1895, Z. Anorg. Chem. **8**, 77.
Thomson, J.J., 1882, Thermochemische Untersuchungen (Barth, Leipzig).
Thorpe, T.E., 1916, J. Chem. Soc. **109**, 395.
Tilden, W.A., 1912, J. Chem. Soc. **10**, 1677.
Urbain, G., 1907, C.R. Hebd. Séances Acad. Sci. **145**, 759.
Urbain, G., 1908, C.R. Hebd. Séances Acad. Sci. **146**, 406.
Urbain, G., 1911, C.R. Hebd. Séances Acad. Sci. **152**, 141.
Urbain, G., and P. Dauvillier, 1922, C.R. Hebd. Séances Acad. Sci. **174**, 1349.
Urbain, G., and H. Lacombe, 1903, C.R. Hebd. Séances Acad. Sci. **137**, 792.
Urbain, G., and H. Lacombe, 1904, C.R. Hebd. Séances Acad. Sci. **138**, 627.
Van den Broek, A., 1913, Phys. Z. **14**, 32; Nature **92**, 372, 476.
Vauquelin, L.N., 1801, Ann. Chim. (Paris) **36**, 43.
Vauquelin, L.N., 1805, Ann. Chim. (Paris) **54**, 28.
Veibel, S., 1976, in: Dictionary of Scientific Biographies, Vol. 13 (Scribner's, New York) p. 358.
Wallach, O., 1901, Briefwechsel zwischen J. Berzelius und F. Wöhler (Engelmann, Leipzig).
Wöhler, F., 1875, Ber. Dtsch. Chem. Ges. **8**, 838.
Young, C.A., 1872, Am. J. Sci. **4**(3), 353.

Handbook on the Physics and Chemistry of Rare Earths, Vol. 11
edited by K.A. Gschneidner, Jr. and L. Eyring

Chapter 74

ATOMIC THEORY AND OPTICAL SPECTROSCOPY

B.R. JUDD
Department of Physics and Astronomy, The Johns Hopkins University, Baltimore, Maryland 21218, USA

Contents

List of symbols and abbreviations[a]

$\boldsymbol{a}, \boldsymbol{a}^\dagger$	double tensors, of ranks $\frac{1}{2}$ and l with respect to s and l, that annihilate and create the $4l + 2$ electron states belonging to a given n and l
$a_\xi, a_\eta^\dagger$	components of $\boldsymbol{a}$ and $\boldsymbol{a}^\dagger$
A_{kq}	crystal-field parameter associated with Y_{kq}
A	label for spin-up electrons; class of configurations $4f^{N-1}C'$ ($C' \equiv 5d$, 5d6s, $5d^2$, $5d6s^2$, $5d^26s$)
B	label for spin-down electrons; class of configurations $4f^N6s^{N'}$ ($0 \leqslant N' \leqslant 2$)
c	crystal axis
cfp	coefficient of fractional parentage
C	configuration
CG	Clebsch–Gordan
$\boldsymbol{D}$	dipole moment of electron charges referred to nucleus as origin
D_k	numbers that renormalize the F^k to avoid fractions in tabulations of term energies for two-electron configurations
$\mathscr{D}_k$	irreducible representation of SO(3) with dimension $2k + 1$
$-e$	electronic charge
e_i	Two-electron operator (scalar with respect to $\boldsymbol{S}$ and $\boldsymbol{L}$) with well-defined U and W
E^i	strength of e_i for the Coulomb interaction between f electrons
$\boldsymbol{E}$	external electric field
$E(X)$	energy of term or level X
EL–SO	electrostatically correlated spin–orbit interaction
F	field-shift operator
FS	field shift
$F^k(a, b)$	Slater integral $e^2 \int\int R_a^2(1) R_b^2(2) (r_<^k / r_>^{k+1}) \mathrm{d}r_1 \mathrm{d}r_2$
g	Zeeman splitting factor of Landé
$g_\parallel, g_\perp$	Zeeman splitting factors associated with $\boldsymbol{H} \parallel c$ and $\boldsymbol{H} \perp c$ in a spin-Hamiltonian for which $S = \frac{1}{2}$
$g^k(a, b)$	SMS parameter
$G^k(a, b)$	exchange Slater integral $e^2 \int\int R_a(1) R_a(2) R_b(1) R_b(2) (r_<^k / r_>^{k+1}) \mathrm{d}r_1 \mathrm{d}r_2$
$\boldsymbol{H}$	external magnetic field
H_{so}	spin–orbit interaction
H_{soo}	spin–other-orbit interaction

H_{ss}	spin–spin interaction
HF	Hartree–Fock
I, II, III, ...	first, second, third, ... (spectra) for neutral, singly-ionized, doubly-ionized, ... atoms, respectively
$\boldsymbol{I}, I$	nuclear spin[b], associated quantum number
$\boldsymbol{j}, j$	total angular momentum[b] of a single electron, associated quantum number
$\boldsymbol{J}, J$	total angular momentum[b] of all the electrons in an atom, associated quantum number
K	quasi-spin rank
K_j	$(n_j l_j m_{sj} m_{lj})$, the jth quantum number quartet
$\boldsymbol{l}, l$	orbital angular momentum[b] of a single electron, azimuthal quantum number
$\boldsymbol{L}, L$	total orbital angular momentum[b] of all the electrons in an atom, associated quantum number
^{2S+1}L	spectroscopic term[c] with degeneracy $(2S+1)(2L+1)$
$m_l, m_s, M_L, \ldots$	eigenvalues of l_z, s_z, L_z, ... ('magnetic' quantum numbers)
MCQD	multi-channel quantum defect
$M^k(a, b)$	Marvin integral $\frac{1}{2}\beta^2 \iint R_a^2(1)\, R_b^2(2)(r_<^k / r_>^{k+3})\, dr_1\, dr_2$
n	principal quantum number
N	number of electrons in an atom
$\boldsymbol{p}_i$	momentum[b] of electron i
P_k	Legendre polynomial of rank k
$\boldsymbol{Q}, Q$	quasi-spin, associated quantum number; quadrupole moment
$\boldsymbol{r}_i, r_i$	radial vector from nucleus to electron i, its magnitude
$r_<, r_>$	lesser and greater of r_1 and r_2
r_{ij}	distance between electrons i and j
$R_a(i)/r_i$	radial eigenfunction for electron i in orbit defined by $a = n_a l_a$
R_{nl}	Sternheimer quadrupole correction factor for orbital nl
$\boldsymbol{s}, s$	spin angular momentum[b] for a single electron, associated quantum number $(=\frac{1}{2})$
$\boldsymbol{S}, S$	total spin angular momentum[b] for all the electrons in an atom, associated quantum number; fictitious spin appearing in the spin-Hamiltonian
SMS	specific mass shift
$SO_X(n)$	special orthogonal (rotation) group in n dimensions whose generators are (occasionally) distinguished by a label X
Sp(n)	symplectic group in n dimensions
t_i	three-electron operator (scalar with respect to $\boldsymbol{S}$ and $\boldsymbol{L}$) with well-defined U and W
T^i	strength of t_i
$\boldsymbol{T}^{(k)}$	spherical tensor[c] of rank k whose components $T_q^{(k)}$ transform identically to Y_{kq} under the operations of SO(3)
U	irreducible representation of G_2
U(n)	unitary group in n dimensions
$\boldsymbol{v}_i^{(k)}$	spherical tensor[d] of rank k with respect to $SO_L(3)$ for electron i
$\boldsymbol{V}^{(k)}$	sum of $\boldsymbol{v}_i^{(k)}$ for all electrons i
W	irreducible representation of SO(7)
WE	Wigner–Eckart
X_k, Y_k	generalized Trees parameters for mixed configurations
Y_{kq}	spherical harmonic
$z^{(k)}(ll')$	tensor of rank k that annihilates an electron l' and creates an electron l
Ze	nuclear charge
α	Trees parameter (coefficient of $\boldsymbol{L}^2$); operator equivalent factor; spin eigenfunction (for $m_s = \frac{1}{2}$); Euler angle
β, γ	Trees parameters generalized to higher rank; classificatory symbols; Euler angles
β	Bohr magneton; spin eigenfunction (for $m_s = -\frac{1}{2}$)
ζ_{nl}	spin–orbit coupling constant for nl electron
θ_i, ϕ_i	polar angles for electron i
Θ_L, Φ_L	polar angles for ligand L
κ	rank with respect to $\boldsymbol{S}$

λ	multiplet splitting parameter; unitary weight
$\boldsymbol{\mu}$	magnetic dipole moment of nucleus
μ	nuclear magnetic moment (in nuclear magnetons); crystal quantum number; quantum defect
$\zeta(r)$	functional coefficient of $\boldsymbol{s}\cdot\boldsymbol{l}$ in H_{so}, equal to $-\hbar^2(2em^2c^2r)^{-1}(\partial V/\partial r)$, where V is the central potential
ξ, η	components of a Kramers spinor; abbreviations for (m_s, m_l)
σ_k	screening factor for electric potential proportional to Y_{kq}
τ	classificatory symbol
χ	character; intermediate (virtual) state; linear combination of ligand orbitals
ψ	wavefunction; abbreviation for the term $\gamma^{2S+1}L$
Ω	Racah's two-electron operator for which $U = (22)$
Ω_k	Intensity parameter associated with tensor of rank k

[a]The list is not complete; nor are alternative meanings (separated by semicolons) all the possible ones. Symbols used briefly in a special context (nonce-symbols) are omitted unless their use is well established in the literature.

[b]Measured in units of $\hbar$ $(=h/2\pi)$, where h is Planck's constant.

[c]A term such as ^{5}D is read as 'quintet D' to distinguish it from 5d.

[d]Magnitude to be chosen at one's convenience.

1. Introduction

A good way to get some sense of the distance theoretical rare-earth spectroscopy has come in the last fifty years is to compare publications of the 1930's with one or two modern articles. In a recent analysis of the free-ion spectrum of Nd^+ (that is, of Nd II), Blaise et al. (1984) carried out a least-squares fit with 33 parameters for the energies of the levels of the two sets of configurations

$$4f^3 5d6s + 4f^3(^4I)5d^2 + 4f^4(^5I)6p \tag{1}$$

and

$$4f^3(^4I)5d6p + 4f^3(^4I)6s6p. \tag{2}$$

Respective mean errors of only 158 cm^{-1} and 144 cm^{-1} were obtained, and in the process of the analysis 126 new levels were found. This sophisticated treatment is a far cry from the example of La II $4f^2$ given by Condon and Shortley (1935) in their classic monograph. For that spectrum only four parameters were used to fit the seven LS terms of f^2. Even that represents a considerable advance in content over table 5.4 of White (1934), where the ground configurations of eleven lanthanide atoms (Pr, Nd, Pm, Sm, Eu, Tb, Dy, Ho, Er, Tm and Yb) are given incorrectly.

A comparison of crystal spectra is just as striking. Crosswhite and Newman (1984) have recently succeeded in establishing consistent lanthanide spin-correlated crystal-field (SCCF) parameters for the ions Gd^{3+} $4f^7$ and Ho^{3+} $4f^{10}$ substituted for La^{3+} in $LaCl_3$, thereby resolving a long-standing problem of the discrepancies in the crystal splittings of such levels as ^6I_J of Gd^{3+} and $^3K_8$ of Ho^{3+}. In contrast to this work, Van Vleck (1937), almost fifty years earlier, wrote about 'The Puzzle of Rare-Earth Spectra in Solids', in which the origin of spectral lines and the mystery of the

extra levels were discussed. Very little was known at that time beyond the fact that the ground configurations of the triply-ionized lanthanides are of the type $4f^N$. The tone of the article is one of educated speculation, as the reconciliation of apparently conflicting experimental data is worked out.

The two examples of modern work quoted above give us an idea of the general direction that theory and experiment have taken since the 1930's. Angular-momentum theory has had to be developed to cope with large quantum numbers (such as those appearing in $^3K_8$ of f^{10}) and with the problem of successively coupling the angular momenta of different parts of an atomic system. In (1), for example, the configuration $4f^35d6s$ requires the spin and orbital angular momenta of five electrons to be assembled in a way that satisfies the Pauli exclusion principle and also provides a basis for usefully labelling the states that appear from a matrix diagonalization. In another area, perturbation theory has had to be extended to allow for deviations from the central-field approximation, that is, the approximation that every electron of the lanthanide moves in a spherically symmetric potential produced by all the other charged particles in the system under study. This raises the whole issue of how to handle configuration interaction. The SCCF parameters mentioned above are one example of the many ways neighboring configurations make themselves felt. The first step in setting up an adequate procedure for representing the perturbing effects of such configurations dates from the early 1950's, when Trees (1951a,b; 1952) found that a term of the type $\alpha L(L + 1)$ could often materially improve the fit between the experimental and theoretical energies of the levels of a particular configuration under investigation. How best to allow for configuration interaction has grown in importance over the last thirty years to a point where it is now of major concern to many branches of spectroscopy, nuclear as well as atomic. It goes without saying that many of the later developments in the theory would have been impossible without the speed and efficiency of the modern computer. Details in a theoretical analysis of a spectrum can now be exposed and properly examined. Until the last decade or so it would have been quite impracticable to introduce the thirty or so parameters needed by Blaise et al. (1984) and by Crosswhite and Newman (1984) in their analyses described above.

What follows is an attempt to trace the history of optical lanthanide spectroscopy and the role it has played in the development of atomic theory. Two intertwining strands have to be described: free-ion spectroscopy and crystal spectroscopy. To keep the latter to manageable proportions no account is given of effects depending on more than a single lanthanide ion. There is also no detailed cataloguing of experimental or theoretical results; the aim throughout is to give priority to the development and assimilation of ideas. These are often presented in the form of examples rather than by formal mathematics; at the same time it is hoped that enough detail and background is provided to give the interested reader a sense of what the theory actually entails. Lie groups have proved to be of great value for the open shells of f electrons that characterize the lanthanides. They also present special problems to the writer, who must assume, if not a level of understanding, at least a willingness on the part of the reader to take angular-momentum vectors and their related rotations in ordinary three-dimensional space as a basis for plausible

extensions. Angular-momentum vectors generalize to spherical tensors of arbitrary rank, while the rotations become special cases of transformations in spaces of higher dimension, such as the seven-dimensional space spanned by the seven orbital functions of a single f electron. Before exploring these generalizations in detail we must step back to a time when atomic spectroscopy had just emerged from playing the principal role in the construction of quantum mechanics.

2. The situation in 1935

2.1. *Experiment*

By the early 1930's quantum mechanics had been applied to a wide variety of phenomena. The extent to which the energy levels of free atoms were known can be found by looking at the book of Bacher and Goudsmit (1932)*. Of all the lanthanide spectra, only Ce IV, La I, La II and La III make their appearance. For Ce IV and La III, the work of Gibbs and White (1929) and Badami (1931) is quoted in giving the energies of the levels of 6s, 6p and 6d relative to the doublet ^{2}D of 5d. The ground doublet ^{2}F of Ce IV 4f was not reported. Much more was known about La I and La II. The lowest levels of La I had been identified by Russell and Meggers (1932) as deriving from the close configurations $5d6s^2$ (the lower one) and $5d^26s$. Bacher and Goudsmit (1932) credit Meggers with providing them with other entries for their table concerning the odd configurations 5d6s6p and $5d^26p$, but a comparison with the modern tabulation of Martin et al. (1978) reveals a number of discrepancies. The level list for La II given by Bacher and Goudsmit on the basis of the work of Russell and Meggers (1932) contains over one hundred entries. Being a two-electron spectrum, it subsequently served as a natural starting point for analyses of the Coulomb interaction between electrons of the type 6s, 7s, 6p, 5d, 6d and 4f. Bacher and Goudsmit (1932) also cite the hyperfine-structure work on La I of White (1929b), who deduced (erroneously, as it turned out) a probable nuclear spin I of $\frac{5}{2}$ (instead of the correct value of $\frac{7}{2}$) for La^{139}.

Although the tables of Bacher and Goudsmit (1932) seem particularly modest for the rare-earth elements, the ground was being laid for further developments by the extensive line lists of King (1928, 1930, 1931, 1932, 1933, 1935). The closing of the lanthanide series was established by Meggers and Scribner (1930), who reported no evidence of f electrons playing any active part in the spectra of Lu I, Lu II or Lu III. As early as 1929, White (1929a) had measured the hyperfine structures of 173 lines of Pr II and was able to deduce a nuclear spin I of $\frac{5}{2}$ for Pr^{141} and that an unpaired s electron exists in a low configuration. An important step forward was made by Albertson (1934), who gave all the levels of Eu II $4f^7(^8S)6s$, 6p and 7s, as well as the ^{9}D levels of Eu II $4f^7(^8S)5d$. His discovery of a single 6s electron in the ground

*The well-worn copy in the library of The Johns Hopkins University contains the neatly pencilled mnemonic 'Solar physicists don't find giraffes hiding in kitchens' for the spectroscopic sequence s, p, d, f, g, h, i, k,...

configuration of Eu II enabled him to predict the ground terms of Eu I and Eu III to be $4f^7 6s^2\ {}^8S$ and $4f^7\ {}^8S$, respectively, a result for Eu I that was almost immediately confirmed by Russell and King (1934). Albertson's work provided the first contradiction of the widely accepted rule that the ground configurations of the neutral lanthanides were of the type $4f^N 5d6s^2$. Albertson (1935) also used the data of King (1935) to find all the levels of Sm I $4f^6 6s^2\ {}^7F$ and five levels of Gd I $4f^7({}^8S)5d6s^2\ {}^9D$.

In addition to confirming the ground state of Eu I as $4f^7 6s^2\ {}^8S$, Russell and King (1934) found the levels ${}^8P_{9/2}$, ${}^{10}P_{9/2}$ and ${}^{10}P_{7/2}$ of $4f^7({}^8S)6s6p$. The hyperfine structures of the transitions from these levels to the ground level ${}^8S_{7/2}$ were studied by Schüler and Schmidt (1935a), who were able to deduce that $I = \frac{5}{2}$ for both isotopes Eu^{151} and Eu^{153}, and that, for the ratio of the corresponding nuclear magnetic moments, $\mu_{151}/\mu_{153} = 2.2$. Deviations from the Landé interval rule in the hyperfine structures indicated that interaction terms of the type $A\boldsymbol{I}\cdot\boldsymbol{J}$ were inadequate, by themselves, to account for the experimental results. Schüler and Schmidt (1935a) concluded that both isotopes of europium possessed quadrupole moments. A little later they used the data of Meggers and Scribner (1930) on Lu II to deduce that Lu^{175} possessed a quadrupole moment and a nuclear spin I of $\frac{7}{2}$ (Schüler and Schmidt 1935b).

It was more difficult to make progress with the spectra of the lanthanide ions in crystals. In 1929, Freed and Spedding (1929) announced their intention of studying the sharp absorption lines of the hydrated chlorides, $RCl_3\cdot 6H_2O$. The spectral analysis of the gadolinium crystal yielded four low-lying levels at energies of 0, 37, 53 and $79\,cm^{-1}$ (Spedding 1931). The hydrated bromide gave a similar result. It was generally conceded that the ground level of Gd^{3+} was $4f^7\ {}^8S_{7/2}$, for which an optically negligible crystal splitting could be expected. Spedding (1931) was driven to speculate that levels of the Jj-coupled configuration $4f^6({}^7F_J)5d_{3/2}$ might be sufficiently near ${}^8S_{7/2}$ to contribute to the observed energy levels. A year later, Spedding and Bear (1932) gave the energies of six low-lying levels of $SmCl_3\cdot 6H_2O$ as 0, 145, 160, 204, 217 and $300\,cm^{-1}$. The anticipated ground level (${}^6H_{5/2}$ of $4f^5$) can provide at most three of them, since the ultimate two-fold Kramers degeneracy cannot be broken. The problem of too many observed energy levels was to bedevil crystal spectroscopy for several decades. For the hydrated chlorides, it seems as if inadequate experimental controls were mainly responsible for the misinterpretations. For example, the $79\,cm^{-1}$ spread between two of the four energy levels of $GdCl_3\cdot 6H_2O$ mentioned above is now known to correspond to the energy gap between the two outermost components of the excited level $4f^7\ {}^6I_{7/2}$ (Dieke and Leopold 1957). There is no need to invoke low-lying levels of $4f^6 5d$.

The analysis by Spedding (1933) of the Zeeman effect for $GdCl_3\cdot 6H_2O$ proved equally deceptive. Regularities in the Zeeman patterns led to the conclusion that the orbital moments of the active electrons played no part in the interaction with the external magnetic field, thereby leaving only the spins of the electrons to contribute to the Zeeman effect. This is true for the ground level ${}^8S_{7/2}$ but not for the excited levels. Experimental inadequacies again seem responsible for this erroneous conclusion. It led Spedding (1933) to speculate that the upper levels could be of the type

$4f^6 5x$, where the unknown excited electron $5x$ might have its orbital moment quenched in a similar way to a 3d electron in the transition-metal series. Bizarre though these arguments appear to us today, it is important to realize that the nature of the optical transitions was unknown in the 1930's. Whether the radiation was electric-dipole, magnetic-dipole, or electric-quadrupole was very much in question. This uncertainty made it impossible to use selection rules in a constructive way, and no quantum numbers could be assigned to the observed energy levels in the hydrated chlorides. Other work added little of use. The analysis of Spedding and Bear (1934) for $Sm_2(SO_4)_3 \cdot 8H_2O$ failed to solve the mystery of the extra levels. Work by other groups, such as that of Tomaschek (1932, 1933) and Tomaschek and Deutschbein (1933), was too purely descriptive to be of help. The difficulties facing crystal spectroscopists had one positive result, however: they attracted attention and heightened interest in the field.

2.2. *Theory*

In 1935 theory came in two forms: with group theory and without group theory. Every theorist was conscious of this dichotomy. It is probably impossible to recapture the partisan character of the early articles on atomic theory, though the passions that the methodology aroused are obvious enough. Slater (1929), in his fundamental article on the energies of spectroscopic terms, announced in the first sentence of his abstract that 'Atomic multiplets are treated by wave mechanics, without using group theory'. In the text he stressed the simplicity of the mathematics he proposed to use. Condon and Shortley (1935), in a famous passage in the introduction to their book on atomic spectra, stated, in regard to group theory, that they were 'able to get along without it'. They argued that the effort to understand group theory was an obstacle to the physicist anxious to apply quantum mechanics to atomic spectroscopy, though they conceded the power of group theory in the hands of a skilled practitioner. White (1934) made no mention of group theory at all in his introductory text. On the other hand, the development of atomic theory as presented in the books of Weyl (1931), Wigner (1931) and van der Waerden (1932) depends crucially on the theory of groups. Much is made of the homomorphism between the unitary group in two dimensions, U(2), and the special orthogonal group SO(3) corresponding to rotations in physical three-dimensional space. As long as the group theorists stayed with SO(3), the difference between their approach and that of the more physically inclined was merely a matter of language. The difficulties arose as soon as the group U(2) was used to derive actual formulas, for at that point the abstraction proved too much for the average physicist. One of the reasons for this was the cumbersome apparatus that had to be wheeled into place to derive what seemed to be quite obvious results: for example, that the acceptable quantum numbers J can be obtained from the compositional S and L by simply running in integral steps from $S + L$ down to $|S - L|$. To prove this, Weyl (1931, p. 190) appealed to a 'Clebsch–Gordan equation' previously derived for U(2) using monomials as basis functions for the two irreducible representations of dimensions $2S + 1$ and $2L + 1$. Physicists, however, had a much more potent image in the vector

model as described, for example, by White (1934). All they had to do was take two vectors with lengths S and L and find the lengths of the possible resultants, bearing in mind that these resultant lengths differed from one another by integers.

In order to appreciate the subsequent developments in the theory, we need to explore the relationships between the different theoretical approaches in more detail. This entails specifying the purely semantic differences and looking into the origin and working of U(2). We have also to describe the status of the theory with respect to rare-earth spectroscopy in 1935.

2.2.1. *Semantics*

Consider the basic commutation relations satisfied by the components J_x, J_y and J_z of an angular-momentum vector $\boldsymbol{J}$:

$$[J_x, J_y] = \mathrm{i}J_z, \qquad [J_y, J_z] = \mathrm{i}J_x, \qquad [J_z, J_x] = \mathrm{i}J_y. \tag{3}$$

To the physicist, the origin of these equations lies in such commutation relations as $[x, p_x] = \mathrm{i}$, where the momentum $\boldsymbol{p}$ of a particle is measured in units of $\hbar$. The construction of $\boldsymbol{l}$ from $\boldsymbol{r} \times \boldsymbol{p}$ leads to $[l_x, l_y] = \mathrm{i}l_z$ and its cyclic permutations, from which the general form of the commutation relations for the components of any angular-momentum vector (including spin) is hypothesized. To a group theorist, eqs. (3) specify the Lie algebra that underlies the group SO(3). Operations of the group are performed by $\exp(\mathrm{i}\theta_k J_k)$, where $k = x$, y or z. The angles of rotation, θ_k, are the *parameters* of the group: the operators J_k are the *generators*.

In the language of angular momentum theory, the equations

$$\boldsymbol{J}^2|J, M_J\rangle = J(J+1)|J, M_J\rangle, \tag{4}$$

$$J_z|J, M_J\rangle = M_J|J, M_J\rangle, \tag{5}$$

$$J_\pm|J, M_J\rangle = [J(J+1) - M_J(M_J \pm 1)]^{1/2}|J, M_J \pm 1\rangle, \tag{6}$$

where $J_\pm \equiv J_x \pm \mathrm{i}J_y$, specify the action of the components of an angular-momentum vector on kets defined by the pair of quantum numbers J and M_J (Condon and Shortley 1935). From the standpoint of group theory, eqs. (5) and (6) represent the action of a generator of SO(3) on a basis function for the irreducible representation $\mathscr{D}_J$ that possesses a dimension $2J + 1$. The operator $\boldsymbol{J}^2$ commutes with all the generators J_k and (apart from a possible constant factor) is Casimir's operator for SO(3). Group theorists visualize the kets and the shift operators $J_\pm$ in the following way. The basis functions $|J, M_J\rangle$ are represented by the $2J + 1$ points, $-J, -J+1, \ldots, J$, in a one-dimensional *weight* space. The action of $J_\pm$, as given by eq. (6), is to allow trips to be taken in the weight space, one step at a time.

A state of a rare-earth atom can be written as $|\gamma J M_J\rangle$, where γ denotes all the additional quantum numbers that are required to make the definition complete. In 1935, a mechanism was available for calculating the matrix elements of any operator H. The states $|\gamma J M_J\rangle$ had to be expressed as linear combinations of Slater determinants involving the quantum numbers $(n l m_s m_l)_j$ for each electron j. The required matrix elements thus became sums over integrals involving a pair of Slater determinants and H. The procedures and tables of Condon and Shortley (1935)

lightened this formidable task. If S and L were well-defined (that is, if Russell–Saunders coupling obtained), the state $|\gamma J M_J\rangle$ could first be expressed as a superposition of the states $|\gamma S M_S L M_L\rangle$ by writing

$$|\gamma J M_J\rangle = \sum_{M_S, M_L} (S M_S, L M_L | J M_J) |\gamma S M_S L M_L\rangle, \tag{7}$$

where the coefficients are the so-called Clebsch–Gordan (CG) coefficients. A general form for them had been given by Wigner (1931), and his result was quoted by Condon and Shortley (1935). They need not have done this: their own techniques were adequate to the task in hand had they but applied a few simple theorems from combinatorics (see, e.g., Griffith 1961, or Judd 1963). In the language of group theory, eq. (7) amounts to expressing a basis function for $\mathscr{D}_J$ of $SO_J(3)$ as a linear combination of bases for the Kronecker product $\mathscr{D}_S \times \mathscr{D}_L$ of the direct product $SO_S(3) \times SO_L(3)$. The notation being used here implies that the vector A forms the generators for the group $SO_A(3)$.

The next step involves expressing $|\gamma S M_S L M_L\rangle$ as a linear combination of the Slater determinants $\{K_1 K_2 \cdots K_N\}$, where $K_j \equiv (n l m_s m_l)_j$. Mathematically, this entails the construction of antisymmetric tensors from products of N spin-orbitals transforming as

$$(\mathscr{D}_{1/2} \times \mathscr{D}_{l_1}) \times (\mathscr{D}_{1/2} \times \mathscr{D}_{l_2}) \times \cdots \times (\mathscr{D}_{1/2} \times \mathscr{D}_{l_N}).$$

Weyl (1931, pp. 369–377) outlined how this can be done, but he limited his example to the classification of the terms of l^3 rather than giving an explicit calculation of their wavefunctions. From his general approach, however, it seems clear that he would have brought the group U(2) into play to do so. Condon and Shortley (1935, p. 226), on the other hand, proposed the method of Gray and Wills (1931), and they gave as an example the expansion of $|d^3\,{}^2D,\ M_S = \frac{1}{2},\ M_L = 2\rangle$. As written, this ket is ill-defined because there are two ^2D terms in d^3. The limited freedom in expanding the ket is removed by picking one state at random. This effectively defines a particular γ, say γ_a. The one remaining ^2D term can be found from the orthogonality constraint, thereby defining a second γ, say γ_b. The states $|^2D\gamma_a\rangle$ and $|^2D\gamma_b\rangle$ are now defined and available for use in calculating matrix elements. In 1935, no group-theoretical significance could be attached to γ_a and γ_b. Fortunately, terms like ^{2S+1}L occurring in most configurations of immediate interest could be separated by specifying a coupling scheme. For example, there are two ^2D terms in pds, but they can be formally separated by writing $|(pd)^3D, s, {}^2D\rangle$ or $|(pd)^1D, s, {}^2D\rangle$. This is not possible for configurations of equivalent electrons because it is not clear how the Pauli Exclusion Principle can be properly satisfied. It is apparent from table 1[7] of Condon and Shortley (1935, p. 208) that the frequent occurrence of like terms in the rare-earth configurations f^N was well known. The ad hoc procedure of Gray and Wills (1931) in fixing $\gamma_a, \gamma_b, \gamma_c, \ldots$, must have seemed highly unsatisfactory, to say the least.

2.2.2. *The unitary group U(2)*

The great appeal of U(2) over SO(3) lies in the fact that our basic equations (3)–

(6) remain valid if the following replacements are made:

$$J_+ \to -\eta\partial_\xi, \qquad J_- \to -\xi\partial_\eta, \qquad J_z \to -\tfrac{1}{2}\xi\partial_\xi + \tfrac{1}{2}\eta\partial_\eta, \tag{8}$$

$$|J, M\rangle \to (-1)^{J-M}\xi^{J-M}\eta^{J+M}[(J-M)!(J+M)!]^{-1/2}, \tag{9}$$

where $\partial_\xi \equiv \partial/\partial\xi$, etc. Thus the three components of $\boldsymbol{J}$ as well as the $2J+1$ states $|J, M_J\rangle$ can be represented by functions of just two quantities (ξ and η) and the corresponding differential operators (∂_ξ and ∂_η). We say that ξ and η form the components of a spinor. The connection between U(2) and SO(3) can be seen by writing the general unitary transformation in two dimensions for which the determinant is $+1$ as

$$\xi' = \xi e^{i(\alpha+\gamma)/2}\cos\tfrac{1}{2}\beta + \eta e^{-i(\alpha-\gamma)/2}\sin\tfrac{1}{2}\beta, \tag{10}$$

$$\eta' = -\xi e^{i(\alpha-\gamma)/2}\sin\tfrac{1}{2}\beta + \eta e^{-i(\alpha-\gamma)/2}\cos\tfrac{1}{2}\beta. \tag{11}$$

It is not difficult to show that the spinor $(-\partial_\eta, \partial_\xi)$ transforms in an identical way to (ξ, η). We can now use (8) to find how $\boldsymbol{J}$ transforms, and we get

$$\begin{aligned} J'_x = {} & J_x(\cos\alpha\cos\beta\cos\gamma - \sin\alpha\sin\gamma) \\ & + J_y(\sin\alpha\cos\beta\cos\gamma + \cos\alpha\sin\gamma) - J_z\sin\beta\cos\gamma, \end{aligned} \tag{12}$$

together with similar equations for J'_y and J'_z. These transformations correspond to a rotation in physical space through the Euler angles (α, β, γ). Thus an element of U(2), acting in the space of the spinor (ξ, η), induces a coordinate rotation in the laboratory space (x, y, z).

This approach impresses at once with its power. For example, we can immediately find how $|J, M_J\rangle$ behaves under a rotation characterized by (α, β, γ) by substituting the transformed spinor (ξ', η') into (9). The theory can be further developed by introducing an invariant formed from the two spinors (ξ, η) and (a, b). Under the transformations given by eqs. (10) and (11) we find

$$a'\eta' - b'\xi' = a\eta - b\xi,$$

and the combination $a\eta - b\xi$ is called a spinor invariant. The orbital states of an l electron can be represented by $(a\eta - b\xi)^{2l}$, since we have only to ask for the coefficient of $a^{l+m}b^{l-m}$ to produce the (unnormalized) state $\xi^{l-m}\eta^{l+m}$, which, according to (9), corresponds to $|l, m\rangle$. Spinor invariants are a key ingredient in what has become known as the symbolic method of Kramers (1930a, 1931). The method of using CG coefficients to couple angular momenta is replaced by the formation of the appropriate products of spinor invariants. Consider, for example, the two-electron configuration ll'. In addition to the spinor (ξ, η) for the orbital angular momentum $\boldsymbol{l}$ of the first electron, we need (μ, ν) for the second. We can form three spinor invariants, namely $(a\eta - b\xi)$, $(a\nu - b\mu)$ and $(\xi\nu - \eta\mu)$. The product Φ_L, given by

$$\Phi_L = (a\eta - b\xi)^{l+L-l'}(a\nu - b\mu)^{l'+L-l}(\xi\nu - \eta\mu)^{l+l'-L}, \tag{13}$$

is a sum of terms of the type

$$(a^{x+y}b^{2L-x-y})(\xi^{l+L-l'+z-x}\eta^{l+l'-L-z+x})(\mu^{2l'-y-z}\nu^{y+z}). \tag{14}$$

The powers of ξ and η add to $2l$, and the powers of μ and ν add to $2l'$: hence Φ_L is a linear combination of the orbital states of ll'. Since the powers of a and b add to $2L$, we know that the products $a^{x+y}b^{2L-x-y}$ transform under U(2) like the components of a state with angular-momentum quantum number L. But Φ_L is an invariant: hence the transformation properties of the part of Φ_L depending on ξ, η, μ and ν must also be characterized by L. That is, Φ_L is the orbital part of the wavefunction of ll' with total angular momentum L.

The representation of operators by spinors is a rather more delicate matter. By 1935 only one detailed application of Kramers's symbolic method to atomic spectroscopy appears to have been carried out: that of Wolfe (1932) to the atomic configuration *ls*. Some of the difficulties of the method are discussed below in section 5.1. For the moment we need only say that the abstract nature of the method did not prove appealing to most theoretical spectroscopists. No one in the 1930's or since, as far as the writer is aware, has used the functions

$$\xi^6, \quad \xi^5\eta, \quad \xi^4\eta^2, \quad \xi^3\eta^3, \quad \xi^2\eta^4, \quad \xi\eta^5 \quad \text{and} \quad \eta^6 \tag{15}$$

for the seven (unnormalized) orbital states of an f electron. Of course, the spinor whose two components α and β represent the spin-up and spin-down states of an electron are familiar to all. But students find these quantities difficult enough to come to grips with. Some wonder where α and β are located, unaware that a special space has been created for them. A mathematician might well be tempted to take the fourteen spin-orbitals of an f electron in the form $\xi^6\alpha$, $\xi^6\beta$, $\xi^5\eta\alpha, \ldots,$ $\eta^6\beta$. To a physicist, the loss of a mental image of a wavefunction, such as that provided by the spherical harmonics $Y_{3m}(\theta, \phi)$, is too high a price to pay for mathematical homogeneity.

2.2.3. *Application of the theory to lanthanide spectroscopy*

The attraction of the second spectrum of lanthanum for atomic spectroscopists has been mentioned in section 2.1. The analyses of the two-electron configurations 4f5d and $4f^2$ carried out by Condon and Shortley (1931) achieved great importance by being the only lanthanide spectrum described in detail in their subsequent monograph (Condon and Shortley 1935). The least-squares fits to the experimental data provided by Russell and Meggers (1932) yielded Slater parameters given (in cm^{-1}) by

$$F^2(4f, 5d) = 12075, \quad F^4(4f, 5d) = 11100,$$
$$G^1(4f, 5d) = 12500, \quad G^3(4f, 5d) = 9350, \quad G^5(4f, 5d) = 5750, \tag{16}$$

for La II 4f5d, and by

$$F^2(4f, 4f) = 21000, \quad F^4(4f, 4f) = 23500, \quad F^6(4f, 4f) = 1930 \tag{17}$$

for La II $4f^2$. It is highly interesting to compare these values with those of the modern analysis of Goldschmidt (1978). Taking the effects of the influence of 4f6s,

5d6p and 6s6p on 4f5d into account, she obtained

$$F^2(4f, 5d) = 15855 \pm 105, \qquad F^4(4f, 5d) = 12266 \pm 208,$$
$$G^1(4f, 5d) = 11025 \pm 35, \qquad G^3(4f, 5d) = 10080 \pm 157,$$
$$G^5(4f, 5d) = 6098 \pm 305, \tag{18}$$

for La II $4f5d + 4f6s + 5d6p + 6s6p$. A similar analysis for La II $5d^2 + 5d6s + 6s^2 + 4f6p + 4f^2 + 6p^2 + 6d6s$ yielded

$$F^2(4f, 4f) = 24043, \qquad F^4(4f, 4f) = 21964, \qquad F^6(4f, 4f) = 14668, \tag{19}$$

with mean errors of around 2%. It is evident that the numbers obtained by Condon and Shortley (1931, 1935) have stood the test of time pretty well, with one exception: $F^6(4f, 4f)$. This parameter is almost an order of magnitude too small in eqs. (17), a result which Goldschmidt (1978) attributes to $6p^2\ ^1D_2$ being mistaken for $4f^2\ ^1D_2$. A clue that something is amiss is the failure of the F^k of eqs. (17) to satisfy the requirement $F^2 > F^4 > F^6$, which follows from the very definition of the Slater integrals (see, e.g., Condon and Shortley 1935, p. 177). Goldschmidt's analysis confirms that the lowest term of 4f5d has ^1G as its principal component rather than ^3H. The latter would be expected from a naive application of Hund's rule. Since the lowest configuration of La II is $5d^2$, whose Hund term, ^3F, is indeed the lowest for that configuration, not much attention has been paid to the apparently anomalous situation for 4f5d in La II. The appearance of 4f5d as the ground configuration of Ce I and Ce III is much more striking (see sections 6.2 and 6.2.1).

The hyperfine structures of Eu I and Lu II reported by Schüler and Schmidt (1935a,b) were analyzed by Casimir in his 1936 prize essay for the Teyler's Foundation in Haarlem. The later reprint (Casimir 1963) has made this work more accessible. Racah (1931a,b) had worked out a method for using the electronic spin–orbit coupling constants (which could be easily deduced from experiment) together with some relativistic correction factors to find the hyperfine interaction strengths. The procedure was further elaborated by Breit and Wills (1933). Casimir (1963) was able to use this method to deduce actual numerical values for the magnetic-dipole and electric-quadrupole moments of the europium and lutetium isotopes. His results for the quadrupole moments provided the first quantitative figures for the non-spherical distribution of electric charge within the nucleus.

Nothing as striking as this occurred at that time in the interpretation of the spectra of rare-earth ions in crystals. The deceptively low value of F^6 given in eqs. (17) was to impede progress for several decades. No detailed analyses of crystal spectra had been attempted by 1935, though Bethe (1930) had examined in a qualitative way some Zeeman data of Becquerel (1929). Bethe (1929) had also set up a formal theory for the splittings of atomic levels produced by the crystal field, but no applications to rare-earth ions were possible.

3. Consolidation and compression

The methods described in section 2.2.1 for calculating the matrix elements of an

operator H involves expanding both bra and ket according to the symbolic scheme

$$|\gamma J M_J\rangle \rightarrow \sum |\gamma S M_S L M_L\rangle \rightarrow \sum \{K_1 K_2 \cdots K_N\}. \tag{20}$$

For ground levels of some lanthanide ions the sums in (20) can be reduced to a single term. Thus for Ho^{3+} $4f^{10}\,{}^5I_8$ we have

$$\begin{aligned} |4f^{10}\,{}^5I_8, M_J = 8\rangle &= |4f^{10}\,{}^5I, M_S = 2,\ M_L = 6\rangle \\ &= \{3^+ 2^+ 1^+ 0^+ -1^+ -2^+ -3^+ 3^- 2^- 1^-\}, \end{aligned}$$

where the numbers in the curly bracket give m_l values and the signs indicate $m_s = +\frac{1}{2}$ or $-\frac{1}{2}$. In this case the matrix element of H amounts to an integral over a product of two Slater determinants and H itself. On the other hand, the state $|4f^6\,{}^1P_1, M_J = 1\rangle$ of Eu^{3+} requires a sum over no fewer than 114 Slater determinants. If H were a two-electron operator like the Coulomb interaction it would be expressible as a sum over 15 operators of the type h_{ij}, where $1 \leqslant i < j \leqslant 6$ for the six-electron configuration f^6. To find the Coulomb energy of ^1P of f^6 we should have $114 \times 114 \times 15$ ($= 194940$) integrals to evaluate, each one of which is a linear combination of four terms involving F^0, F^2, F^4 and F^6. Hermiticity constraints and various selection rules would reduce the work, of course, but it is clear that much would still have to be done.

The reaction of the modern research worker to this kind of problem is to enlist the aid of the computer without further ado. It is often surprising to see to what extent the tedium of writing a computer program is preferred to bringing one's imagination into play. The situation is particularly piquant for atomic spectroscopy because all fundamental interactions between particles are known with high precision. If one merely wanted to calculate the energy levels of an atom one might well choose to use as an analog computer a second atom of precisely the same kind as the first. An important component of theoretical spectroscopy is the nature of the methods themselves. The opportunity for invention appeals to anyone with a taste for applied mathematics. In the 1930's, of course, there was no option but to try to simplify the theory. We now turn to some of these approaches to see how far problems specific to the rare earths could be reduced to manageable proportions.

3.1. *Diagonal sums*

Since the Coulomb interaction e^2/r_{ij} between electrons i and j commutes with $\boldsymbol{S}$ and $\boldsymbol{L}$, the energies of the terms ^{2S+1}L of an atomic configuration are independent of M_S and M_L. This was put to good use by Slater (1929), who recognized that a progressive calculation of the matrix elements of the total electronic Coulomb interaction, taken between a determinantal product state and its complex conjugate, could be made to yield the energies of the terms themselves. Consider, for example, the terms of f^3 with $M_S = \frac{3}{2}$. The one with maximum L is ^4I, for which the component with $M_L = 6$ is represented by the single Slater determinant $\{3^+ 2^+ 1^+\}$. The Coulomb energy is the sum of the Coulomb energies for $\{3^+ 2^+\}$, $\{3^+ 1^+\}$ and $\{2^+ 1^+\}$, which, from tables 1^6 and 2^6 of Condon and Shortley (1935, pp. 179, 180),

turns out to be given by

$$E(^4\mathrm{I}) = 3F_0 - 65F_2 - 141F_4 - 221F_6, \tag{21}$$

where $F_k = F^k/D_k$, with

$$D_0 = 1, \quad D_2 = 225, \quad D_4 = 1089, \quad D_6 = 7361.64 = 184041/25. \tag{22}$$

We now hold M_S at $\frac{3}{2}$ and step M_L down to 5. Only one determinant can be constructed, namely $\{3^+\,2^+\,0^+\}$. There is thus no ^{4}H term in f^3, and the sum of the Coulomb energies for $\{3^+\,2^+\}$, $\{3^+\,0^+\}$ and $\{2^+\,0^+\}$ gives eq. (21) again. Continuing, we step M_L down to 4. There are now two determinants, $\{3^+\,2^+\,-1^+\}$ and $\{3^+\,1^+\,0^+\}$. One linear combination of these corresponds to ^{4}I, the other, orthogonal to the first, corresponds to ^{4}G. The strength of the diagonal-sum method now appears. We do not need to know these linear combinations in detail. Instead, we simply use, for the energies E,

$$\begin{aligned} E(^4\mathrm{G}) + E(^4\mathrm{I}) &= E\{3^+\,2^+\,-1^+\} + E\{3^+\,1^+\,0^+\} \\ &= 6F_0 - 75F_2 - 216F_4 - 1443F_6. \end{aligned}$$

From (21) we can deduce that

$$E(^4\mathrm{G}) = 3F_0 - 10F_2 - 75F_4 - 1222F_6. \tag{23}$$

Continuing, we get

$$E(^4\mathrm{S}) = E(^4\mathrm{F}) = 3F_0 - 30F_2 - 99F_4 - 858F_6, \tag{24}$$

$$E(^4\mathrm{D}) = 3F_0 + 25F_2 - 33F_4 - 1859F_6. \tag{25}$$

This procedure can be repeated for $M_S = \frac{1}{2}$. However, the terms ^{2}D, ^{2}F, ^{2}G and ^{2}H all occur twice in f^3, and the method can only give the sums of the energies of like terms. In addition to this limitation, the method is quite long for terms of low S and L. Thus, for the ^{1}P term of f^6 mentioned in section 3, we would have to calculate the diagonal energies of not only the 114 determinantal product states appropriate to ^{1}P but also the several hundred determinants for which $(M_S, M_L) \equiv (0,1)$, $(0,2)$, $(1,1)$ and $(1,2)$ in order to be able to separate out $E(^1\mathrm{P})$ from the various diagonal sums. Such applications of the diagonal-sum method as appear in the literature are for much simpler configurations such as d^3s (see Bowman 1941, Catalan and Antunes 1936).

3.2. *Dirac–Van Vleck method*

The configuration *ls* comprises two terms, ^{1}L and ^{3}L. The energy separating them is proportional to the exchange integral $G^l(l,s)$. We can reproduce this energy separation by introducing an effective Hamiltonian of the type $xG^l(l,s)\mathbf{s}_1 \cdot \mathbf{s}_2$, where x is a suitably chosen constant. It turns out that $x = -2/(2l+1)$. The general approach, in which scalar products involving the spin and orbital angular momenta of the electrons are introduced to provide effective Hamiltonians, was developed by Van Vleck (1934) from a statement of Dirac (1929) relating $\mathbf{s}_1 \cdot \mathbf{s}_2$ to the permutation

operator for two electrons. It has been extended and described in great detail by Slater (1960).

We need not spend much time with the Dirac–Van Vleck method here. Its successes occur for very simple configurations such as p^3 and for configurations involving s electrons. For us the prime example of the latter is $f^N s$, which can be readily handled by alternative techniques. Although the method excited some attention in the 1930's, it is now little more than a curiosity. It had little impact on the development of atomic theory.

3.3. *Tensor analysis*

The application of angular-momentum theory to atomic spectroscopy is not limited to bringing eqs. (3)–(7) into play. In their book, Condon and Shortley (1935, ch. 3) developed the theory with particular attention to operators $\boldsymbol{T}$ that are vectors. They did this by specifying the commutation relations of $\boldsymbol{T}$ with respect to $\boldsymbol{J}$ rather than by stating the transformation properties of the components of $\boldsymbol{T}$ under rotations. They considered angular momenta $\boldsymbol{J}$ built from two parts ($\boldsymbol{S}$ and $\boldsymbol{L}$) and obtained formulas for the matrix elements of operators that behave as a vector with respect to one part (say $\boldsymbol{L}$) and a scalar with respect to the other ($\boldsymbol{S}$, in this case). These formulas involve proportionality constants that would be called reduced matrix elements today. Condon and Shortley systematized the methods that had come into current use but which were often only hinted at, if that, by many theorists. For example, Van Vleck (1932) gave the formula

$$\begin{aligned}&\langle S\,L\,J\,M|L_z|S\,L\,J+1\,M\rangle\\&\quad=-[(J+L+S+2)(S+L-J)(J+S+1-L)(J+L+1-S)\\&\qquad\times(J+M+1)(J-M+1)/4(J+1)^2(2J+1)(2J+3)]^{1/2}\end{aligned}\tag{26}$$

without proof, merely remarking that it 'can be shown' to be the above. It is by no means trivial to derive eq. (26), but we can easily retrace the steps leading to its final form by referring to the relevant parts of the analysis of Condon and Shortley [1935, section 9^3, eq. (9) and section 10^3, eq. (2b)].

Work of this kind was given in the language of group theory by Wigner (1931). For example, we can equally well obtain eq. (26) by using the techniques of his ch. XXIII. Why, then, did the analysis of Condon and Shortley make more of an impact than that of Wigner? An answer to this question can be sensed by using Wigner's book to actually derive eq. (26). The dependence of the matrix element on $\boldsymbol{M}$ is given by eq. (18) of ch. XXIII. The remaining part is set out in the first of the pair of equations labelled (19a); however, the factor $v_{NSL;N'SL}$ appearing there is not defined. Nor could it be, since the analysis is for a general vector operator $\boldsymbol{T}$ that commutes with $\boldsymbol{S}$, not just for $\boldsymbol{L}$. Two pages later, in deriving the Landé g factor, $v_{NSL;NSL}$ is given as $[L(L+1)]^{1/2}\hbar$ for $\boldsymbol{T}\equiv\boldsymbol{L}$, but the reader who is not totally secure in following the arguments leading to that result (in particular, the specialization $N'=N$) might wonder whether it is applicable to matrix elements off-diagonal with respect to J.

Although it provides more detail, the analysis of Condon and Shortley (1935, ch. 3) is not as far-reaching as that of Wigner (1931). In his chapter XXI, Wigner defined an irreducible tensor operator $\boldsymbol{T}$ of degree ω in terms of its transformation properties under rotations. In modern notation, a particular component ρ would be written as $T_\rho^{(\omega)}$, where $-\omega \leqslant \rho \leqslant \omega$. Condon and Shortley's analysis is limited to the special cases for which $\omega \leqslant 1$. The word *irreducible* makes it clear that, of the $2\omega + 1$ components of $\boldsymbol{T}^{(\omega)}$, no subset of n components, where $n < 2\omega + 1$, can be formed from the $T_\rho^{(\omega)}$ (perhaps by taking linear combinations of them) that transform among themselves under arbitrary rotations. Because of the formal nature of Wigner's definition, the full force of his results were not immediately recognized. The absence of examples was a contributing factor to the lack of appreciation. The casual reader would have been helped by a statement that the spherical harmonics $Y_{\omega\rho}$ are examples of the tensors $T_\rho^{(\omega)}$. It was left to Racah (1942b) to give an algebraic treatment for tensors similar to that of Condon and Shortley (1935, ch. 3) for vectors. Instead of their rotational properties, the operators $T_q^{(k)}$ (following Racah's use of roman letters rather than the greek of Wigner) were defined by their commutation relations with respect to $\boldsymbol{J}$:

$$[J_z, T_q^{(k)}] = qT_q^{(k)}, \tag{27}$$

$$[J_\pm, T_q^{(k)}] = [k(k+1) - q(q \pm 1)]^{1/2}\, T_{q\pm 1}^{(k)}. \tag{28}$$

The similarity of eqs. (27) and (28) to eqs. (5) and (6), respectively, is to be noticed. It indicates that the kets $|J, M_J\rangle$ transform under rotations in an identical way to that of the tensors $T_q^{(k)}$ for which $k = J$ and $q = M_J$.

Racah's motivation for extending the vector analysis to tensors was his need to cope with matrix elements of the Coulomb interaction in a more systematic way than that provided by Slater (1929). The definition of a Legendre polynomial P_k yields

$$r_{12}^{-1} = \sum_k (r_<^k / r_>^{k+1})\, P_k(\cos\omega_{12}), \tag{29}$$

where $r_<$ and $r_>$ are the lesser and greater of r_1 and r_2, the lengths of the vectors $\boldsymbol{r}_1$ and $\boldsymbol{r}_2$ that define the positions of the two electrons and that are separated by an angle ω_{12}. According to the addition theorem (see, e.g., Whittaker and Watson 1927, p. 326), $P_k(\cos\omega_{12})$ can be expressed as a sum over the products $Y_{kq}^*(\theta_1, \phi_1) Y_{kq}(\theta_2, \phi_2)$, so the problem of finding matrix elements of spherical harmonics arises in a direct way.

3.4. *The Wigner–Eckart theorem*

Although Condon and Shortley (1935, ch. 3) gave the dependence on M_J, q and M_J' of the matrix elements

$$\langle \gamma J M_J | T_q^{(k)} | \gamma' J' M_J' \rangle \tag{30}$$

for the special cases for which $k = 1$, they did not point out that it was the same as

that of the CG coefficients

$$(J\,M_J|k\,q, J'\,M'_J). \tag{31}$$

An explicit formula to that effect was given for arbitrary rank k by Wigner [1931, ch. XXI, eq. (19)]. He also recognized that his result had a deeper significance, merely remarking, however, that credit for a more general form should go to Eckart (1930). The proportionality of (30) to (31) would today be regarded as a statement of the Wigner–Eckart theorem for the group SO(3).

It took a little while for the full power of the WE theorem to be appreciated. In its most obvious applications, it allows any vector operator to be replaced by another provided a proportionality constant is included. For example, we can write $\boldsymbol{L}+2\boldsymbol{S}\equiv g\boldsymbol{J}$ since $\boldsymbol{L}$, $\boldsymbol{S}$ and $\boldsymbol{J}$ all satisfy similar commutation relations with respect to $\boldsymbol{J}$. The spin–orbit equivalence,

$$H_{so}=\sum_i \xi(r_i)\,\boldsymbol{s}_i\cdot\boldsymbol{l}_i=\lambda\boldsymbol{S}\cdot\boldsymbol{L}, \tag{32}$$

can be justified by examining the commutation relations of the two expressions for H_{so} with respect to $\boldsymbol{S}$, $\boldsymbol{L}$ and $\boldsymbol{J}$ separately. In other words, both forms of H_{so} given by (32) transform identically with respect to the generators of the three groups $SO_S(3)$, $SO_L(3)$ and $SO_J(3)$.

Racah (1942a) used the WE theorem to evaluate the matrix elements of $P_k(\cos\omega_{12})$ for a term L of the configuration $l_1 l_2$. Since there is no preferred direction in space, the result had to be independent of whatever component M_L of L was chosen. With some intricate manipulation, Racah (1942a) was able to obtain a symmetrical expression which he later related to the so-called Racah (1942b) coefficient $W(l_1 l_2 l_1 l_2; Lk)$. Similar work appears to have been done by Wigner, who constructed the 6–j symbol (a slightly more symmetrical quantity than the W function) in an unpublished manuscript of 1940 (see Wigner 1965). The introduction of these SO(3) invariants constituted an enormous psychological breakthrough. Although, at first, it was tedious to calculate them, advantage could be taken of their orthonormality relations to provide frequent checks. Nowadays we can use modern computing techniques to evaluate whatever 6–j symbols we need, as well as such higher extensions as 9–j or 12–j symbols. The stage was set in 1942 for the development of the modern quantum theory of angular momentum.

3.5. *Ll coupling*

One of the first uses that Racah (1942b) put his W function to was the calculation of the term energies of the lanthanide configuration f^3. The limitations of Slater's diagonal-sum method were mentioned in section 3.1. Racah neatly circumvented the problem of satisfying the Pauli exclusion principle by introducing 'spin-up' and 'spin-down' spaces. Two electrons are put in the first space (space A, say) and the remaining electron is put in the second (space B). Thus

$$M_{SA}=1, \qquad M_{SB}=-\tfrac{1}{2}, \qquad M_S=\tfrac{1}{2}. \tag{33}$$

In space A the allowed values of L (say L_A) are 1, 3 and 5. Given one of these numbers, the state $|L_A M_{LA}\rangle$ is automatically antisymmetric with respect to an interchange of the two electrons in space A. There is no need to impose the antisymmetrization for the interchange of either of these electrons with the one in space B because the m_s values are different. A state of f^3 can thus be written as $|(L_A f)LM_L\rangle$ with condition (33) understood. All calculations can be carried out in what we may term Ll coupling.

Consider, for example, the D terms of f^3. Our basis consists of $|(Pf)D\rangle$, $|(Ff)D\rangle$ and $|(Hf)D\rangle$. The roots of the 3×3 matrix of the Coulomb interaction yield the energies of ^4D and the two ^2D terms. We have already given $E(^4D)$ in eq. (25). Its extraction leaves us with a quadratic equation for $E(^2D)$, from which explicit expressions in terms of the Slater integrals can be obtained. Formulas for all the terms of f^3 were given by Racah [1942b, eqs. (98)].

Although this analysis broke new ground, its generalizations are limited. In the case of ^1P of f^6 mentioned in sections 3 and 3.1, we would be forced to put three electrons in space A and three in space B (since necessarily $M_S = 0$). Both L_A and L_B can run over the values 0, 2, 3, 4 and 6, these being the L values for $M_{SA} = \frac{3}{2}$ and $M_{SB} = -\frac{3}{2}$ (see section 3.1 for the terms of maximum multiplicity of f^3). There are thus eight possible coupled states of the type $|(L_A L_B)P\rangle$. The eight roots of the matrix of the Coulomb interaction yield the energies of ^5P, ^1P and the six ^3P terms. To find $E(^1P)$ we would have to perform auxiliary analyses for $M_S = 2$ (putting five electrons in A and one in B) and for $M_S = 1$ (putting four electrons in A and two in B) in order to extract the roots for the quintet and the triplets. Although this is a great improvement over the method of Slater determinants sketched in section 3.1, it leaves much to be desired.

Part of our sense of dissatisfaction comes from some unexpected simplifications in the f^3 analysis, which indicate – or at least strongly suggest – that some unknown structure in the analysis is being overlooked. For example, the energy spacings between terms of maximum multiplicity, which can be found very easily from eqs. (21)–(25), are all simple multiples of the single linear combination

$$5F_2 + 6F_4 - 91F_6. \tag{34}$$

Nothing in the analysis so far has prepared us for this amazing result. Again, the three energy separations between the two ^2D terms, between the two ^2G terms, and between the two ^2H terms [as given by Racah (1942b) in his eqs. (98)] are expressible through just two linear combinations of the F_k [one of which is (34)] rather than the three we might have expected. The solution of one problem has brought another to the fore.

3.6. *Coefficients of fractional parentage*

Shortly after his two 1942 papers, Racah (1943) presented a general method for coping with the Pauli exclusion principle when dealing with equivalent electrons. We imagine a term SL of l^N as being produced by coupling the Nth electron, l_N, to a state $\gamma' S' L'$ of the remaining $N - 1$ electrons. We write it as $|\gamma' S' L', l_N, SL\rangle$, where

the couplings $(S's)S$ and $(L'l)L$ are implied. It cannot be expected that such a state would be antisymmetric with respect to the interchange of the Nth electron with any of the other $N-1$; however, we can superpose a variety of such states with common SL to achieve a complete antisymmetry by writing

$$|l^N \psi\rangle = \sum_{\psi'} (\psi'|\}\psi)|l^{N-1}\psi', l_N, SL\rangle, \tag{35}$$

where $\psi' \equiv \gamma' S' L'$ and $\psi \equiv \gamma SL$. The weighting factors $(\psi'|\}\psi)$ are the celebrated coefficients of fractional parentage (cfp). The internal symbol $|\}$ is meant to stress that the tables of cfp are not necessarily square. It is a corruption of a special symbol chosen by Racah (1943) from an extended set of symbols once made available to authors of Physical Review articles (but long since discontinued).

The idea of fractional parentage stems from work of Bacher and Goudsmit (1934). These authors were interested in representing the many-particle effects of configuration interaction, in particular, the displacements of energy levels. For those purposes, only the squares of the cfp are required. The advantage of the formal expansion, given by (35), is that states of l^N are uniquely defined in terms of the states of l^{N-1}, the cfp, and, of course, the CG coefficients that are implicit in any coupled state. Terms like ^{2S+1}L can now be separated and defined by setting up tables of cfp.

In his 1943 paper, Racah limited his attention to the configurations p^N and d^N. No attempt was made to treat the lanthanide configurations f^N. Racah (1943) devised a method for separating like terms in d^N by means of the seniority number v, but he knew that it was inadequate for as simple a configuration as f^3. The two ^2D terms of d^3 can be separated by insisting that one of them contains no ^1S character in its parentage. Such a state, occurring first in a three-electron configuration, is said to have seniority 3 and we write ^2_3D. A similar device can be used to separate the two ^2F terms of f^3, but how do we cope with the pairs ^2D, ^2G and ^2H? We could, of course, insist that such a cfp as $(f^2\,{}^1D|\}f^3\,\gamma\,{}^2G)$ be zero to give meaning to γ. There are more options here than we need, so the next step would be to experiment with the choices available to see if some work better than others. Should we proceed along these lines, we would be immediately struck by all kinds of unexpected results. For example, if we pick one ^2H state by insisting that $(f^2\,{}^3H|\}f^3\,\gamma\,{}^2H)$ be zero, then the orthogonal state $|f^3\,\gamma'\,{}^2H\rangle$ possesses no component from the parent ^3F of f^2. Again, the exclusion of ^1S from the parentage of ^2F, which defines the state ^2_3F, also leads to the unexpected vanishing of $(f^2\,{}^3F|\}f^3\,{}^2_3F)$.

As soon as the cfp are used to calculate matrix elements, more and more surprises occur. For example, the two ^2H states defined above satisfy the remarkable relations

$$\langle f^3\,\gamma\,{}^2H|H_{so}|f^3\,\gamma\,{}^2H\rangle = \langle f^3\,\gamma\,{}^2H|H_{so}|f^3\,\gamma'\,{}^2H\rangle = 0, \tag{36}$$

where the spin–orbit interaction H_{so} is defined as in eq. (32). In addition to selection rules like (36), proportionalities abound. For example, the diagonal Coulomb matrix elements satisfy the equation

$$3[E(f^3\,\gamma\,{}^2H) - E(f^3\,{}^2P)] = E(f^2\,{}^3P) - E(f^2\,{}^3H),$$

both sides being equal to 14 times the linear combination given by (34). Some such results as these must have been known to Racah. They undoubtedly served to emphasize the need for a better understanding of the structure of the f shell.

4. The non-invariance groups of Racah

4.1. *Interim experimental developments*

The decade 1935–45 saw steady progress in the experimental spectroscopy of free rare-earth atoms and ions. Russell et al. (1937) were able to find almost all levels of the six configurations 4f5d, 4f6p, $5d^2$, 4f6s, 4f6d and 5d6s of Ce III, and, a little later, Harrison et al. (1941) used Zeeman data to help them identify low levels coming from 4f5d6s, $4f5d^2$, $4f^26s$ and $4f^25d$ of Ce II. For Pr II, Rosen et al. (1941) gave all the levels belonging to $4f^3(^4I)6s$ and $4f^3(^4I)5d\,^5L$, K. Levels from the analogous configurations $4f^4(^5I)6s$ and $4f^4(^5I)5d$ of Nd II were reported by Albertson et al. (1942). Somewhat earlier, Albertson (1936) had found 40 levels coming from $4f^6(^7F)6s$ and $4f^6(^7F)5d$ of Sm II, and he proposed a new scheme for the ground configurations of the neutral lanthanides, only two of which (Pr I $4f^25d$ and Tb I $4f^85d$) have subsequently proved to be the first excited configurations instead. Daring as he was to choose more ground configurations of the type $4f^N$, he did not go quite far enough. His proposal, although a step in the right direction, was in any case ignored by Meggers (1942) in his review of rare-earth spectroscopy. Albertson et al. (1940) found $4f^7(^8S)5d6s\,^{10}D$ and $4f^7(^8S)5d6p\,^{10}F$ of Gd II, though some levels of their ^8D and ^{10}D deriving from $4f^7(^8S)5d6s$ and $4f^7(^8S)5d6p$ are spurious. The earlier work of Albertson (1935) on Gd I was extended by Russell (1942), who found the undecets ^{11}P, ^{11}D and ^{11}F of $4f^7(^8S)6s5d6p$ as well as some nonets. Oddly, Russell (1942) refers to the 6p electron as 7p.

In contrast to that inconsequential lapse, an array of major misinterpretations afflicted the spectra of lanthanide ions in crystals. Ellis (1936) proposed identifications for the principal absorption bands of eight lanthanides, most of which are erroneous. Unaware of the severe perturbations in La II $4f^2$ from neighboring configurations and the misidentification of $^1D_2$ (see section 2.2.3), Bethe and Spedding (1937) simply scaled the term scheme of La II $4f^2$ and adjusted the spin–orbit coupling constant ζ ($=\langle\xi(r)\rangle$) to predict the levels of the conjugate configuration $4f^{12}$ of Tm^{3+} in $Tm_2(SO_4)_3\cdot 8H_2O$. The correspondence that they drew with experiment is almost wholly fallacious. We now know (Dieke 1968, or Hüfner 1978) that the levels identified as $^3F_4$, $^3F_3$, $^1D_2$ and $^1I_6$ are really $^3F_3$, $^3F_2$, $^1G_4$ and $^1D_2$, respectively. Only their supposition that part of the absorption band at 21 500 cm^{-1} should be $^1G_4$ is correct. A subsequent analysis of Pr^{3+} $4f^2$ by Spedding (1940), based on a similar connection to La II $4f^2$, is almost as bad. As in the case of Tm^{3+}, the calculated positions of $^1D_2$ and $^1G_4$ almost coincided, whereas, in reality, they are separated by about 7000 cm^{-1}. The actual $^1D_2$ level is misidentified as $^1I_6$. Other spectroscopists made equally mistaken analyses. Lang (1938) placed both $^1I_6$ and $^1G_4$ or Pr^{3+} $4f^2$ in a region now known to correspond to

$^1D_2$. Gobrecht (1938) gave a different analysis from that of Bethe and Spedding (1937) for Tm^{3+} $4f^{12}$, labelling the $^3P_2$ level $^1I_6$. Gobrecht's over-sized scaling of the theoretical scheme had the effect, however, of accidentally making a correct assignment for $^1D_2$. This level appeared unnaturally low in the analysis of Condon and Shortley (1935) for La II $4f^2$ owing to the misidentification discussed in section 2.2.3. Among the few articles of that period that can be read today without a sense of unease are those that are purely experimental, such as that of Ewald (1939) on the neodymium bands. By 1945, the puzzle of Van Vleck (1937) concerning rare-earth spectra in solids remained as baffling as ever.

4.2. *A precursor to Racah's analysis: Weyl's use of characters*

It is clear from the foregoing that, by the mid-1940's, no particular pressure to develop the theory for the general lanthanide configuration $4f^N$ was supplied by experiment. Racah's motivation to press ahead, and erect a totally new theoretical structure in his article of 1949, came from the challenge of the theoretical problem. Evidence for the need for some new approach, such as the unexpected simplifications mentioned in sections 3.5 and 3.6, was accumulating. The use of Kramers's symbolic method (see section 2.2.2) by Bijl (1945) to analyze the configuration $3d^9 4s5s$ of Cu I proved to be very unwieldy. It was Racah's genius to see a solution in the use of non-invariance (or non-symmetry) groups, that is, groups whose generators do not commute with the Hamiltonian.

Racah (1949) was not the first, however, to use non-invariance groups in atomic physics. Weyl (1931) had done so some twenty years earlier in one of the more arcane chapters of his book on groups and quantum mechanics. To get an idea of Weyl's method, we use it to derive the allowed quartets of f^3. The central idea is to use characters. For the irreducible representation $\mathscr{D}_l$ of SO(3), the character $\chi_l(\phi)$ corresponding to a rotation through an angle ϕ can be found by choosing the z-axis as the axis of rotation. Every single-electron orbital eigenfunction ψ_{lm} behaves like $Y_{lm}(\theta, \phi)$, so we have

$$\psi_{lm} \to e^{im\phi}\psi_{lm} \tag{37}$$

under the rotation in question. The character, being the trace of the transformation matrix, is given by

$$\chi_l(\phi) = e^{il\phi} + e^{i(l-1)\phi} + \cdots + e^{-il\phi}. \tag{38}$$

For $U(2l + 1)$, the unitary group corresponding to transformations among themselves of the $2l + 1$ eigenfunctions $\psi_{ll}, \psi_{ll-1}, \ldots, \psi_{l-l}$, the substitution given by (37) is replaced by

$$\psi_{lm} \to \exp(i\phi_m)\psi_{lm}. \tag{39}$$

We now have $2l + 1$ angles ϕ_m rather than just the one ϕ. If, for l^3, we pick $M_S = \frac{3}{2}$, all m_l values must be distinct. Thus the orbital parts of the three-electron eigenfunctions possess a character.

$$\sum \exp(i\phi_m + i\phi_{m'} + i\phi_{m''}), \tag{40}$$

where the sum is constrained by $l \geqslant m > m' > m'' \geqslant -l$. For $l = 3$ there are 35 terms in the sum. When the transformations of U(7) are limited to those of its subgroup SO(3), (39) becomes (37). That is, $\phi_m = m\phi$. Making this substitution in (40) gives

$$\varepsilon^6 + \varepsilon^5 + 2\varepsilon^4 + 3\varepsilon^3 + 4\varepsilon^2 + 4\varepsilon + 5 + 4\varepsilon^{-1} + 4\varepsilon^{-2} + 3\varepsilon^{-3} + 2\varepsilon^{-4} + \varepsilon^{-5} + \varepsilon^{-6}, \tag{41}$$

where $\varepsilon = e^{i\phi}$. From (38) we find that this sum is

$$\chi_6(\phi) + \chi_4(\phi) + \chi_3(\phi) + \chi_2(\phi) + \chi_0(\phi),$$

from which we deduce that the quartets of f^3 are I, G, F, D and S, in agreement with the analysis of section 3.1. Weyl's actual handling of this problem is rather more sophisticated than the simple presentation given here, and he was able to obtain a general solution for finding the quartets and doublets of l^3 for arbitrary l.

Racah (1949) examined the possibility that an intermediate group X might exist in the group–subgroup sequence

$$U(2l + 1) \supset X \supset SO(3). \tag{42}$$

The usefulness of a group X was never explored by Weyl. His preoccupation with arbitrary l seems to have distracted him from the enormously important special cases for which $l = 2$ and 3. Racah's realization that X can be chosen to be $SO(2l + 1)$ makes very little impression in the general case. For example, there are four ^2I terms in i^3, only one of which can be separated out and assigned a different irreducible representation of SO(13) from that for the other three. However, for d^3 the only ambiguity arises for the two ^2D terms, and the possibility of assigning them different irreducible representations of SO(5) solves a classic dilemma in an extraordinarily elegant way. What is more, *all* ambiguities in the d shell can be resolved with the choice $X \equiv SO(5)$, which turns out to provide an equivalent description to seniority for the states of the d shell (Racah 1949).

As we have already noticed (in section 3.6), the terms ^2D, ^2F, ^2G and ^2H each occur twice in f^3. Only the ^2F pair can be separated by using SO(7). By a remarkable accident, the exceptional group G_2 of Cartan (1894) exists as a subgroup of SO(7) and also contains as a subgroup the particular group SO(3) corresponding to rotations in physical space. Thus, for f electrons, the sequence

$$U(7) \supset SO(7) \supset G_2 \supset SO(3) \tag{43}$$

of groups and subgroups can be used to classify the states of f^N. Racah (1949) found that the terms ^2D, ^2G and ^2H of f^3 can be separated by assigning them irreducible representations of G_2. We can thus write a state of f^N as

$$|f^N W U \tau S L M_S M_L\rangle, \tag{44}$$

where W and U stand for irreducible representations of SO(7) and G_2, respectively. The additional classificatory symbol τ is needed to separate a few pairs of like terms when $5 \leqslant N \leqslant 9$. Racah's discovery of the usefulness of G_2 made the analysis of the f shell tractable.

4.3. *Racah's 1949 paper*

The problem that Racah (1949) solved by using non-invariance groups was the calculation of the energy matrices for the Coulomb interaction between f electrons. The idea is to replace the expansion

$$e^2 \sum_{i>j} (1/r_{ij}) = \sum_k F^k \sum_{i>j} P_k(\cos \omega_{ij}), \tag{45}$$

which follows from eq. (29), by

$$e^2 \sum_{i>j} (1/r_{ij}) = e_0 E^0 + e_1 E^1 + e_2 E^2 + e_3 E^3, \tag{46}$$

where the operators e_r are the components $T^{[WU]}_\rho$ of the generalized tensors $\boldsymbol{T}^{[WU]}$ corresponding to unique irreducible representations W and U of SO(7) and G_2, respectively. The E^r are linear combinations of the F^k. The advantage of using the tensors $\boldsymbol{T}^{[WU]}$ is that the Wigner–Eckart theorem can be applied to relate the matrix elements to CG coefficients for SO(7) and G_2. The only complication is that, in the evaluation of the matrix element

$$\langle \cdots W_1 U_1 \cdots | T^{[WU]}_\rho | \cdots W_2 U_2 \cdots \rangle, \tag{47}$$

the irreducible representations W_1 and U_1 sometimes occur more than once in the decompositions of their respective Kronecker products $W \times W_2$ and $U \times U_2$. The simple relationship for SO(3) between a matrix element and a CG coefficient, as exemplified by (30) and (31), no longer always holds: instead, a sum of CG coefficients appears. There are as many terms in the sum as the multiplicities of the Kronecker products demand. In spite of this complication, there is an enormous gain in efficiency, since the labels $W_1 U_1 W U W_2 U_2$ appearing in (47) may recur in various configurations f^N.

In order to put these ideas to use, Racah (1949) had to generalize the mathematics of SO(3) to SO(7) and G_2. Because of the great impact that this has had on many aspects of theoretical spectroscopy, it seems well worthwhile to describe his work in some detail.

4.3.1. *Two-electron matrix elements*

Powerful though the generalized Wigner–Eckart theorem is, we are no further forward in the calculation of the matrix elements of the e_r if the relevant CG coefficients are not known. No tables for the CG coefficients for SO(7) or G_2 were available in 1949; and even today we have only a very limited knowledge of them. One way to proceed is to invert the problem and calculate the matrix elements of the e_r by other means: we can then deduce sets of CG coefficients that may be used in the future when similar representations of SO(7) and G_2 appear. Equation (1) of Racah (1949) specifies the basic mechanism for calculating matrix elements step by step along the f shell. In a slightly different notation it runs

$$\langle \mathrm{f}^N \psi | e_r | \mathrm{f}^N \psi' \rangle = [N/(N-2)] \sum_{\psi_1 \psi_2} (\psi \{ |\psi_1\rangle \langle \psi_1 | e'_r | \psi_2 \rangle \langle \psi_2 | \} \psi'). \tag{48}$$

The states ψ_1 and ψ_2 belong to the parent configuration f^{N-1}. The operator e'_r acts on all pairs of electrons not involving the Nth electron. The ratio of the number of such pairs to all pairs is given by

$$^{N-1}C_2/{}^{N}C_2 = \tfrac{1}{2}(N-1)(N-2)/\tfrac{1}{2}N(N-1) = (N-2)/N,$$

which accounts for the square-bracketed factor in eq. (48). That equation relates the matrix elements for a configuration f^N to those for its predecessor f^{N-1}, and hence provides a means of advancing along the shell.

The obvious difficulty with this approach is that the cfp $(\psi\{|\psi_1)$ and $(\psi_2|\}\psi')$ have first to be worked out. Although we seem to have replaced one difficulty with another, the cfp are CG coefficients too: we have only to enlarge the group structure so that all the states of a particular configuration f^N form basis functions for a single irreducible representation $[\lambda]$ of some group containing SO(7) and G_2 as subgroups. The obvious choice is U(14), the unitary group acting in the space of all fourteen spin-orbitals. The cfp $(\psi\{|\psi_1)$ can now be visualized as the CG coefficient

$$([\lambda]\rho|[\lambda_1]\rho_1, [f]\rho_f), \tag{49}$$

where $[f]\rho_f$ are the labels defining a state of an f electron. Such labels are among the most elementary that we are likely to encounter. The CG coefficients in which they appear should therefore be among the easiest to calculate.

4.3.2. *Racah's lemma*

The correspondence between $(\psi\{|\psi_1)$ and (49) is not quite exact because the definition of the cfp given in eq. (35) involves states that are coupled in the spin and orbital spaces. It is more accurate to write

$$\begin{aligned}&(\psi\{|\psi_1)(S\,M_S|S_1\,M_{S1}, s\,m_s)(LM_L|L_1\,M_{L1}, f\,m_f)\\ &\quad = ([\lambda]\rho|[\lambda_1]\rho_1, [f]\rho_f).\end{aligned} \tag{50}$$

This connection reveals an important property of the generalized CG coefficients: they can be factorized. In section 3 of his paper, Racah (1949) proved this for a group G (with irreducible representations A) containing a subgroup H (with irreducible representations B possessing bases defined by labels b):

$$\begin{aligned}&(\alpha\,A\,\beta\,B\,b\,|\,A_1\,\beta_1\,B_1\,b_1, A_2\,\beta_2\,B_2\,b_2)\\ &\quad = \sum_{\gamma}(\gamma\,B\,b\,|\,B_1\,b_1, B_2\,b_2)(\alpha\,A\,\beta\,B\,|\,A_1\beta_1\,B_1 + A_2\,\beta_2\,B_2)_\gamma.\end{aligned} \tag{51}$$

The symbols α and γ are multiplicity labels that are required if A and B occur more than once in the respective decompositions of $A_1 \times A_2$ and $B_1 \times B_2$. The symbol β_i is a multiplicity label of a different kind: it is required when the reduction $G \to H$ yields more than one identical irreducible representation B_i in a given A_i. Like the proof of the Wigner–Eckart theorem, the derivation of (51) depends crucially on Schur's lemma. The second factor on the right-hand side of eq. (50), for want of a better expression, has become known over the years as an isoscalar factor, in analogy to the situation for SU(3) (Edmonds 1962).

For us the simple relation $G \supset H$ can be replaced by the very much richer scheme

$$\begin{aligned} U(14) &\supset SO_S(3) \times U(7) \supset SO_S(3) \times SO(7) \supset SO_S(3) \times G_2 \\ &\supset SO_S(3) \times SO_L(3) \supset SO_S(2) \times SO_L(2), \end{aligned} \tag{52}$$

which separates the spin space from the orbital space. The groups $SO_S(2)$ and $SO_L(2)$ are included for completeness, since they provide the labels M_S and M_L.

The factorization of the isoscalar factors and hence of the cfp, by itself, brings us no nearer to finding their numerical values. It is here that the detailed properties of the representations of G_2 and SO(7) play a role. Racah, of course, had to discover many of these properties for himself; today we can refer to the tables of Wybourne (1970) for much of what we need. Because of the variety of aids now at hand, it is quite difficult to get a sense of the problems that Racah faced. No tables of 3–j or 6–j symbols were available in 1949, though their algebraic forms were known, of course. It therefore seems worthwhile to show how some non-trivial isoscalar factors can be calculated by elementary techniques. We cannot know in detail how Racah built up his tables, but we can at least glimpse the kinds of methods available to him.

4.3.3. *Sample calculation of isoscalar factors using Slater determinants*

For our example, we pick G_2 and its subgroup $SO_L(3)$. The irreducible representations U of G_2 are defined by the coordinates $(u_1\, u_2)$ that specify the highest weight of the representation. They are the analogs of the maximum value L of M_L that is used to label the irreducible representation $\mathscr{D}_L$ of $SO_L(3)$ (see section 2.2.1). Racah needed to know the structure of Kronecker products of irreducible representations of G_2 as well as the decompositions of the representations into direct sums over the $\mathscr{D}_L$. It is likely that he pieced together the required formulas from general expressions for the dimensions of irreducible representations of G_2, such as those given by Weyl (1925) for an arbitrary Lie group. Today we simply turn to tables E-4 and E-3 of Wybourne (1970) to find

$$(10) \times (10) = (00) + (10) + (11) + (20),$$

and

$$(00) \to \mathscr{D}_0, \quad (10) \to \mathscr{D}_3, \quad (11) \to \mathscr{D}_1 + \mathscr{D}_5, \quad (20) \to \mathscr{D}_2 + \mathscr{D}_4 + \mathscr{D}_6. \tag{53}$$

Thus the terms of f^2 can be assigned G_2 labels as follows:

$$(00)^1S, \quad (11)^3P, \quad (20)^1D, \quad (10)^3F, \quad (20)^1G, \quad (11)^3H, \quad (20)^1I. \tag{54}$$

There are two ^2H states in f^3: one belongs to (11), the other to (21). Wybourne's table E-4 reveals that $(11) \times (10)$ does not contain (11) in its reduction: thus $(f^2\, {}^3H|\}f^3\, (11)^2H)$ is zero, and the symbols γ and γ' of section 3.6 can be given a precise meaning, namely, $\gamma \equiv (11)$ and $\gamma' \equiv (21)$. We can construct $|f^3\, (21)\, {}^2H\rangle$ by actually carrying out the coupling implied by $|f^2\, {}^2H,\ {}^2f,\ {}^2H\rangle$; but since there is no ^4H state in f^3 we can ignore the spin space and simply take $M_{S1} = +1$ for f^2 and

TABLE 1
Coefficients of Slater determinants in the expansion of states ^{2}H of f^3 for which $M_S = \frac{1}{2}$ and $M_L = 5$.

Determinant	States of f^3			
	$\|(21)^2\mathrm{H}\rangle$	$\|\mathrm{f}^2\,{}^1\mathrm{D},\mathrm{f},{}^2\mathrm{H}\rangle$	$\|\mathrm{f}^2\,{}^1\mathrm{G},\mathrm{f},{}^2\mathrm{H}\rangle$	$\|\mathrm{f}^2\,{}^1\mathrm{I},\mathrm{f},{}^2\mathrm{H}\rangle$
$\{3^+2^+0^-\}$	$(30/91)^{1/2}$	$-(5/21)^{1/2}$	$(240/1001)^{1/2}$	$(50/3003)^{1/2}$
$\{3^+1^+1^-\}$	$-(36/91)^{1/2}$	$(2/7)^{1/2}$	$-(288/1001)^{1/2}$	$-(20/1001)^{1/2}$
$\{2^+1^+2^-\}$	$(20/273)^{1/2}$	0	$(105/286)^{1/2}$	$-(243/1001)^{1/2}$
$\{3^+0^+2^-\}$	$(40/273)^{1/2}$	$-(5/21)^{1/2}$	$(15/4004)^{1/2}$	$37/(6006)^{1/2}$
$\{3^+-1^+3^-\}$	$-(5/273)^{1/2}$	$(5/42)^{1/2}$	$(135/2002)^{1/2}$	$-32/(3003)^{1/2}$
$\{2^+0^+3^-\}$	$-(10/273)^{1/2}$	0	$-(105/572)^{1/2}$	$(243/2002)^{1/2}$

$m_s = -\frac{1}{2}$ for f. Thus, for $M_S = \frac{1}{2}$ and $M_L = 5$, we get

$$|\mathrm{f}^3\,(21)^2\mathrm{H},\tfrac{1}{2},5\rangle = \sum_{M_{L1},m_l} (5\,M_{L1},3\,m_l|5\,5)|\mathrm{f}^2\,\mathrm{H},1,M_{L1};\mathrm{f},-\tfrac{1}{2},m_l\rangle$$
$$= \sum a_i\{m_l'^{+}\,m_l''^{+}\,m_l^{-}\}, \tag{55}$$

where the sum runs over the various Slater determinants for which $m_l' + m_l'' + m_l = 5$. The non-vanishing coefficients are given in table 1.

By a similar coupling process we can work out $|\mathrm{f}^2\,{}^1L,{}^2\mathrm{f},{}^2\mathrm{H}\rangle$ for $L = 2$, 4 and 6. The results are listed in table 1. As indicated in (54), the states ^{1}D, ^{1}G and ^{1}I of f^2 belong to (20) of G_2. Thus the overlaps

$$\langle \mathrm{f}^2\,(21)\,{}^2\mathrm{H}|\mathrm{f}^2\,{}^1L,{}^2\mathrm{f},{}^2\mathrm{H}\rangle \tag{56}$$

must be proportional to the isoscalar factors

$$((21)\mathrm{H}\,|\,(20)L + (10)\mathrm{f}). \tag{57}$$

The former can be easily found from table 1. They turn out to be

$$-(13/18)^{1/2},\quad (8/11)^{1/2},\quad (5/99)^{1/2}\quad \text{for}\quad L = 2,\ 4,\ 6,\ \text{respectively.}$$

These numbers can be normalized by multiplying them by $(2/3)^{1/2}$. In this way we find that the isoscalar factors (57) are given by

$$-(13/27)^{1/2},\quad (16/33)^{1/2},\quad (10/297)^{1/2}\quad \text{for}\quad L = 2,\ 4,\ 6,\ \text{respectively,} \tag{58}$$

The magnitudes agree with the original calculation of Racah (1949, table IVa), but the signs are reversed. This illustrates an extremely common problem in all branches of spectroscopy: establishing phase conventions. Every state ψ is associated with an arbitrary phase, and it is impossible to be sure that one's own choices coincide with those of others unless some specification is made. Fortunately, the tables of Racah (1949) for f^N do just that. To bring our results in coincidence with those of Racah we have only to replace our proportionality constant $(2/3)^{1/2}$ by $-(2/3)^{1/2}$.

4.3.4. *Reciprocity*

All kinds of isoscalar factors can be calculated with sufficient ingenuity. The proportionality factor $-(2/3)^{1/2}$ of section 4.3.3 is itself an isoscalar factor for

$U(14) \supset SO_S(3) \times U(7)$. Many more isoscalar factors can be calculated by generalizing that particular symmetry property of an SO(3) CG coefficient that interchanges a component $\mathscr{D}_S$ with a resultant $\mathscr{D}_J$:

$$(J\,M_J|S\,M_S,\,LM_L) = (-1)^{L+M_L}[(2J+1)/(2S+1)]^{1/2}(S\,-M_S|J\,-M_J,\,LM_L). \tag{59}$$

Edmonds (1957, eq. 3.5.15) has shown that this equation can be derived from the recursion relations satisfied by the CG coefficients. In seeking to generalize it, Racah (1949, section 5.1) used a result of Wigner (1931) for SO(3). The CG coefficients arise when triple products of the elements $\mathscr{D}^j_{mn}(\omega)$ of the rotation matrices are integrated over the Euler angles ω, suitably weighted. This procedure has the advantage that the three numbers of the type j that enter do so on a par. The disadvantage is that the result of the integration yields a product of a pair of CG coefficients rather than just one. In spite of this complication, Racah was able to extend the procedure and obtain analogs of eq. (59) for the isoscalar factors. For example, his eq. (49) runs

$$(U'\,\tau'\,L'|U\,\tau\,L + (10)\mathrm{f}) = (-1)^{L-L'}[(2L+1)D(U')/(2L'+1)D(U)]^{1/2}(U\,\tau\,L|U'\,\tau'\,L' + (10)\mathrm{f}), \tag{60}$$

where $D(U)$ is the dimension of the irreducible representation U of G_2. Equations such as this are very useful for finding new isoscalar factors from those already known.

4.3.5. *Calculation of the* e_r

A common difficulty in appreciating Racah's use of groups lies in the transformations themselves. It is not too hard to understand how the seven orbital wavefunctions ψ_{fm} (for $-3 \leqslant m \leqslant 3$) can be subjected to the unitary transformations of U(7), or how successive constraints on these transformations lead to the subgroups SO(7), G_2 and $SO_L(3)$; but to assign the group labels W and U to operators we need to know how the spherical harmonics $Y_{kq}(\theta_i, \phi_i)$ stand with respect to SO(7) and G_2. Substitutions of the type $(\theta_i, \phi_i) \rightarrow (\theta'_i, \phi'_i)$ merely yield transformations belonging to $SO_L(3)$. Some generalization is required.

We can take a step in that direction by first recalling (from section 3.3) that the Coulomb interaction between two electrons involves sums over products of the type $Y^*_{kq}(\theta_1, \phi_1)\, Y_{kq}(\theta_2, \phi_2)$. The ranks k match the labels of the Slater integrals F^k and are thus limited to 0, 2, 4, and 6 for f electrons. If, however, we consider the transformations among the 28 components of $\boldsymbol{Y}_0$, $\boldsymbol{Y}_2$, $\boldsymbol{Y}_4$, and $\boldsymbol{Y}_6$, we are led to U(28) and its subgroups. This generalization evidently goes too far.

The correct approach is to consider the operators that perform the transformations of the particular group under study. In analogy to $\exp(i\theta_k J_k)$ of section 2.2.1 for $SO_J(3)$, we introduce operators of the type $\exp(i\theta_{tp} V^{(t)}_p)$, where the tensors $\boldsymbol{V}^{(t)}$ are the generators of the group and the generalized angles θ_{tp} are its parameters. Since our Lie groups work on the single-electron orbitals ψ_{fm}, the generators are

operators that act on one electron at a time. That is,

$$V^{(t)} = \sum_{i=1}^{N} v_i^{(t)} \tag{61}$$

for f^N. For U(7), all possible values of t are called for: that is, $0 \leqslant t \leqslant 6$. As we proceed to the subgroups of U(7), operators are successively rejected from the set of operators. Just how this is done was not made explicit by Racah in his 1949 article, since he defined his Lie groups by specifying the algebraic forms that they left invariant. However, the paring away of the generators is remarkably simple: for SO(7) we have $t = 1$, 3 and 5; for G_2 we retain $t = 1$ and 5; while for $SO_L(3)$ we are left with $t = 1$, corresponding to the vector $V^{(1)}$ that is necessarily proportional to the orbital angular momentum $\boldsymbol{L}$. The crucial connection can now be made. It turns out that the commutators of the generators of SO(7) (or G_2) with the spherical harmonics Y_{2q}, Y_{4q} and Y_{6q}, suitably renormalized, produce residues that exactly match the results of acting with these generators on the components of the states ^1D, ^1G and ^1I of f^2 for which $M_L = q$. We have already assigned the G_2 label (20) to ^1D, ^1G and ^1I in section 4.3.3; it follows that the same label can be attached to the collection of 27 spherical harmonics Y_{2q}, Y_{4q} and Y_{6q}. Precisely similar methods allow us to also assign to these harmonics the SO(7) label (200), which exactly encompasses (20) of G_2.

The rest follows without too much trouble. The products of spherical harmonics arising from $P_2(\cos\omega_{ij})$, $P_4(\cos\omega_{ij})$ and $P_6(\cos\omega_{ij})$ must transform under the operations of SO(7) and G_2 like those parts of the Kronecker squares $(200)^2$ and $(20)^2$ that contain an $SO_L(3)$ scalar. From tables D-4, E-2 and E-3 of Wybourne (1970), we find that the acceptable irreducible representations are given by

$$WU \equiv (000)(00), \quad (400)(40), \quad (220)(22). \tag{62}$$

The linear combination of the $P_k(\cos\omega_{ij})$ corresponding to a particular WU entails the isoscalar factors $(WU0\,|\,(200)(20)k + (200)(20)k)$ as well as the renormalization factors for the Y_{kq}. Only one complication remains, and it is a very minor one. The constant $P_0(\cos\omega_{ij})$ is also present in the expansion of e^2/r_{ij} and this produces a second operator for which $WU \equiv (000)(00)$. The particular mixtures picked by Racah (1949) for e_0 and e_1 simplify the expressions for the energies of the terms of maximum multiplicity. Putting the pieces together, we can relate the parameters and operators of eqs. (45) and (46) by writing

$$\begin{aligned} E^0 &= F_0 - 10F_2 - 33F_4 - 286F_6, \\ E^1 &= \tfrac{1}{9}(70F_2 + 231F_4 + 2002F_6), \\ E^2 &= \tfrac{1}{9}(F_2 - 3F_4 + 7F_6), \\ E^3 &= \tfrac{1}{3}(5F_2 + 6F_4 - 91F_6) \end{aligned} \tag{63}$$

for the parameters and

$$\begin{aligned} e_1[(000)(00)] &= \Xi_0, \\ e_1[(000)(00)] &= \tfrac{1}{462}(594\Xi_0 + 11\Xi_2 + 6\Xi_4 + \Xi_6), \end{aligned}$$

$$e_2[(400)(40)] = \tfrac{1}{462}(1573\Xi_2 - 780\Xi_4 + 35\Xi_6),$$
$$e_3[(220)(22)] = \tfrac{1}{462}(121\Xi_2 + 24\Xi_4 - 7\Xi_6), \tag{64}$$

for the operators, where

$$\Xi_k = D_k \sum_{i>j} P_k(\cos \omega_{ij}), \tag{65}$$

the factors D_k being given by eqs. (22).

4.3.6. *Tabulation*

Equations (64) define the tensors $\boldsymbol{T}^{[WU]}$ whose properties are outlined in section 4.3. By means of eq. (48), augmented wherever possible by the generalized Wigner–Eckart theorem for G_2 and SO(7), Racah (1949) was able to completely solve the Coulomb problem for the f shell. His results are presented in a series of tables. Any matrix element we need can be found as a linear combination of the E^r (and hence of the F^k) by picking out the appropriate entries in the tables and putting the parts together.

As has already been mentioned, the groups G_2 and SO(7) are non-invariance groups, since their generators do not commute with the Coulomb interaction. To find the energies of the two ^{2}H terms of f^3, for example, the two-by-two matrix whose rows and columns are labelled by the two possibilities (11) and (21) for U must be constructed. Its diagonalization can be carried out once a choice is made for the E^r (or F^k), and the resulting eigenfunctions specify the two mixtures of (11) and (21) that correspond to the physical ^{2}H states.

The use of G_2 and SO(7) gives immediate explanations for many of the puzzles described in sections 3.5 and 3.6. In particular, the linear combination (34) appears as the coefficient of $\frac{1}{3}e_3$, and the difference between the energies of two terms ψ and ψ' will be a function of the parameter E^3 alone whenever

$$\langle\psi|e_r|\psi\rangle = \langle\psi'|e_r|\psi'\rangle \quad (r = 0, 1, 2). \tag{66}$$

This equation turns out to be frequently satisfied because e_0 and e_1 are scalars with respect to both G_2 and SO(7), while the selection rules for the operator e_2, which belongs to the unusual representations (400) of SO(7) and (40) of G_2, often preclude a contribution from that source.

It would be too great a digression to describe here the immensely rich structure of the tables of Racah (1949). Among the hundreds of entries only one error seems to have escaped his notice: the factor 73 in line K' of table VIb should be 72. Although the tables are sufficient for the evaluation of all the matrix elements of the Coulomb interaction in the f shell, many auxiliary tables, although necessarily calculated in part or in full by Racah, were not included by him in his article. Several tables of cfp are missing, and there are no tables of reduced matrix elements of tensor operators of the type $\boldsymbol{V}^{(t)}$ of eq. (61). It is clear, too, that in calculating the number of times irreducible representations W or U occur in the reduction of the Kronecker products $W' \times W''$ or $U' \times U''$, the tables given by Racah only represent part of his calculation. It was not until the late 1950's that work was started on making a more

extensive tabulation available. A succession of Raytheon Technical Memoranda by Nutter and Nielson culminated in the computer-generated tables of cfp and reduced matrix elements by Nielson and Koster (1963), who also provided a complete listing of all matrix elements of the Coulomb operators e_r. A further seven years were to elapse before Butler prepared the tables of branching rules and Kronecker products that are such a useful feature of the book by Wybourne (1970). Taken in conjunction with the tables of 3–j and 6–j symbols for SO(3) produced by Rotenberg et al. (1959), we have at our disposal today an array of numerical data that makes light of much of the algebra of f-shell calculations.

5. Crystal spectra

5.1. *The impact of Racah's 1949 article*

The ideas developed by Racah (1949) were so novel and intricate that it is not surprising that it took some time for them to be appreciated. Adding to the difficulty of assimilation was the terse style of the article itself, which made no concessions to the general reader. There were no examples of how to put to use the many tables or how to calculate the energy matrices for a particular configuration f^N. Racah realized, of course, that his methods need not be limited to atomic shell theory, and he suggested to Jahn that the group chain $U(5) \supset SO(5) \supset SO(3)$ could be useful in classifying the states of the nuclear d shell. The resulting article (Jahn 1950) is much easier to understand than Racah's. Reliance is placed on the calculus of the Young tableaux, and all the methods are illustrated by simple examples. Furthermore, Jahn's initial program was more limited than Racah's, and he could appeal to Racah's work for theorems that he needed. More remarkably, the short-range attractive force between d nucleons turned out to be represented by a term in the Hamiltonian that is scalar with respect to the generators of SO(5). Thus the irreducible representations of SO(5) play the role of good quantum numbers, and SO(5) is a true symmetry group of the Hamiltonian. Jahn and his colleagues exploited these properties in a series of articles (Jahn 1951, Jahn and van Wieringen 1951, Flowers 1952a,b, Elliott and Flowers 1955) that led eventually to SU(3) being used by Elliott (1958) to reconcile nuclear shell theory with the collective motions of the nucleons.

Racah took the opportunity to more fully explain his methods in a series of lectures given at the Institute for Advanced Study at Princeton in 1951. The mimeographed notes of Eugen Merzbacher and David Park circulated widely and were reproduced as a CERN report in 1961 before being included in a Springer Tract in Modern Physics (Racah 1965). Among the standard sources for background material we find the book by Eisenhart (1933), which evidently played an important part in helping Racah develop his ideas. In describing how to use the theory of Lie groups to construct the energy matrix, Racah (1965) chose an arbitrary two-particle interaction rather than a Coulomb potential. He was thus able to set his methods in the framework of nuclear shell theory, thereby supplementing the

work of Jahn (1950). It is sometimes wondered why Racah, with his background in atomic and nuclear physics, did not play a role in the application of Lie groups to particle theory. For one reason or another, the moment when he could have made a major impact on that field passed. A compilation by Gell-Mann and Ne'eman (1964) of the early articles on the symmetries of the strong interactions (the so-called eightfold way) scarcely mentions Racah's work. The style of their presentation – for example, the method they chose to distinguish the irreducible representations of SU(3) by the dimensions rather than the highest weights – shows that their achievements owe little to Racah. The overwhelming development of group-theoretical methods in particle physics has tended to obscure Racah's work; for example, in the introduction to his book on Lie groups, Gilmore (1974) assigns the date of the realization that non-symmetry (i.e., non-invariance) groups could be useful to around 1960, eleven years after Racah's 1949 article appeared. Another example of an oversight occurs in the chapter in the book by Hamermesh (1962) that describes applications of Lie groups to atomic and nuclear problems. Although reference is made to Racah's article, there is no recognition of the importance of non-invariance groups, and the generalized Wigner–Eckart theorem is not brought into play. States are classified by the irreducible representations of Lie groups and left at that. The reader is led to believe that Lie groups are useful in defining quantum states, but the computational advantages are not pointed out.

It took time, of course, for atomic spectroscopists to come to grips with Racah's approach. One of the most active theoretical groups in the early 1950's was that of Ufford at the University of Pennsylvania. The single volume 91 of the Physical Review for 1953 contains articles by Innes (1953), Reilly (1953) and Meshkov (1953) that apply Racah's methods to the electronic spin–spin interaction, to the matrix elements of the Coulomb interaction for f^4, and to fractional parentage coefficients for mixed configurations such as $(p + d)^N$, where $(p + d)$ denotes the 16 states provided by a p electron and a d electron. All acknowledge the guiding hand of Ufford. The reprintings in 1951, 1953, 1957 and 1959 of the book by Condon and Shortley (1935) scarcely helped the dissemination of Racah's methods. Nor did the book by Fano and Racah (1959). Admittedly, it contains one fascinating new idea: in appendices H and I a connection is made between projective geometry and angular-momentum theory, which is shown to be Desarguesian. However, the book was not accepted as a standard text by the spectroscopic community. The language and notation throughout are almost perversely at variance with the classic articles of Racah (1942b, 1943, 1949). Phase differences abound; in some instances pure imaginary factors appear where everything had been real before. The use of gothic characters, of $\overline{W}$, $\bar{V}$ and X coefficients, and the very title itself, which introduced the word – uncommon to spectroscopists – 'sets', together with the formidable qualifications 'irreducible' and 'tensorial', all conspired to make the book less attractive. The monograph of Edmonds (1957) had a greater impact, partly because of the wide range of examples that were provided. The only eccentricity was the use of boldface characters in the scalar proportionality factors (i.e., the reduced matrix elements) appearing in the Wigner–Eckart theorem.

The mid-1950's also saw a detailed description by Brinkman (1956) of the

symbolic method of Kramers (see section 2.2.2). The final chapter of the book describes the calculation of the Coulomb energies of the terms ^{2S+1}L of the atomic configuration $l_1 l_2$, and this makes it possible to assess the value of Kramers's approach. Instead of the Racah coefficient $W(l_1 l_2 l_1 l_2; Lk)$ (mentioned in section 3.4), a generalized hypergeometric function appears. Apart from additional factors, the two forms must be equivalent, of course. What has happened is that the Racah coefficient has been reconstructed ab ovo in Brinkman's analysis; and, in calculations involving more than one Racah coefficient, they would all be similarly reconstructed. The fatal difficulty with Kramers's method is that the building blocks – the spinor invariants – are too small and too many of them are required. The availability, later in the decade, of the tables of 6–j symbols prepared by Rotenberg et al. (1959) made it easy to apply Racah's methods to actual physical situations.

The decade ended with the publication of the two-volume work of Slater (1960) on atomic structure. A cautious treatment is given of tensor operators and fractional parentage. Expansions in determinantal product states are still resorted to, and there is no discussion of Racah's use of groups. A little later, the writer attempted to remedy that deficiency (Judd 1963). His prefatory assurance that the needs of the experimentalist were borne in mind was sourly commented on, in a private conversation, by Edlén. The recollection that the book of Condon and Shortley (1935) gave similar problems to Russell (its dedicatee), provided some solace.

5.2. *Interplay between theory and experiment*

In spite of various problems of identification of individual lines or bands, the general features of the spectra of the tripositive lanthanide ions in crystals were becoming clear by the early 1950's. The sharp absorption lines in the visible region were recognized as being produced by transitions within particular $4f^N$ configurations. The more diffuse lines associated with them were seen for what they are: transitions in which an odd vibrational mode of the lattice is excited at the same time as the parity-forbidden electronic transition within the 4f shell takes place. The occasional overlapping of these two kinds of lines could conceivably blur their distinctive features and lead to the extra levels mentioned in section 2.1. The onset of more intense absorption in the blue or beyond could be safely assigned to transitions of the type $4f \rightarrow 5d$, which are allowed by the Laporte parity-change rule. All of this was anticipated by Van Vleck (1937). It was Hellwege and Hellwege (1951) who finally established that the absorption band of Pr^{3+} in the yellow corresponds to the transition $^3H_4 \rightarrow {}^1D_2$ of $4f^2$, thus resolving a long-standing problem (see section 4.1). This work was carried out with crystals of the so-called double nitrates, $Pr_2M_3(NO_3)_{12}\cdot 24H_2O$, where M ≡ Mg or Zn. Almost as significant was the discovery by Hellwege and Kahle (1951a,b) that the absorption bands at 16900, 19020 and 21480 cm^{-1} in salts of Eu^{3+} correspond to, respectively, $^7F_1 \rightarrow {}^5D_0$, $^7F_0 \rightarrow {}^5D_1$ and $^7F_0 \rightarrow {}^5D_2$ of $4f^6$. The importance of these results lay in the information that they provided on the Slater integrals F^k (or, equivalently, on the Racah parameters E^k). The erroneous term scheme for La II $4f^2$, as reported by Condon and Shortley (1935), was now seen to be qualitatively different from that for

Pr^{3+} $4f^2$, indicating that some adjustment had to be made to the ratios F^4/F^2 and F^6/F^2. The latter had been thought to be extremely small (see section 2.2.3), but, through a misinterpretation of a decimal point for a multiplication symbol in the number 7361.64 of eqs. (22), which was printed, in the British convention, as 7361·64 in Condon and Shortley's book (but otherwise in their 1931 Physical Review article), the small value of F^6/F^2 appeared to be supported by calculations based on a physically realistic 4f wavefunction, such as that corresponding to a hydrogenic 4f orbital, for which the result $F_6/F_2 \simeq 2.5 \times 10^{-4}$ was given (Trefftz 1951). The eccentricities of British typography had also confused Laporte and Platt (1942) some years earlier. In their article on the degeneracies among terms deriving from configurations of equivalent electrons, they gave $D_6^{1/2}$ of eq. (22) correctly as $\frac{429}{5}$, but then stated that the figure of 7361.64 of Condon and Shortley was an error. Once D_6 is taken for what it actually is, the hydrogenic ratios become

$$F_4/F_2 = 41/297, \qquad F_6/F_2 = 175/11583 = 0.015. \tag{67}$$

These ratios (or values close to them) account for the position of $^1D_2$ in Pr^{3+} $4f^2$ rather well (Jørgensen 1955a, Judd 1955).*

Another significant step forward was the analysis of the absorption spectrum of $Nd(BrO_3)_3 \cdot 9H_2O$ by Satten (1953). The ion Nd^{3+} possesses the ground configuration $4f^3$, for which the terms of maximum multiplicity are separated by multiples of E^3 (see sections 3.1 and 3.5). The same parameter determines the separation of ^3P and ^3H in $4f^2$, so only a small adjustment for the effect of the increased nuclear charge is required to predict the positions of all the quartets of $4f^3$. This enabled Satten (1953) to identify the bands that had been earlier reported by Ewald (1939). Satten's discussion of the positions of the doublets was impeded by an error in converting the inequality $F^6/F^2 < 1$ (which follows from the definition of the Slater integrals) to $F_6/F_2 < 0.00306$ rather than the correct form $F_6/F_2 < 0.0306$. This mistake was not noticed because a small value of F_6/F_2 was consistent with current thinking in the early 1950's. An exchange of letters between Satten (1955) and Jørgensen (1955b) cleared the matter up.

By 1955, Jørgensen (1955c) had penetrated at least some of the mysteries of the article of Racah (1949) and had begun calculations on the low-lying terms of many $4f^N$ configurations. His analysis represents the first application of Racah's group-theoretical methods to ions in crystals. It is flawed only by the assumption that terms of low seniority could be ignored, which led to his finding it difficult to understand how ^5D of $4f^6$ could be as low in the energy scale as it appeared to be. An analysis based on determinantal product states circumvented that difficulty (Judd 1955). It also provided independent checks on Racah's approach, so that the piecing together of matrix elements from his tables could be carried out with a

*Condon and Shortley (1935) inserted the denominators D_k at only a few critical points in their tables 1^6 and 2^6. Their implicit presence elsewhere was not appreciated by Rao (1950), who was thereby misled so far as to claim that the calculation of Racah (1942b) of the term energies of f^3 was in error. See Racah (1952b).

greater degree of confidence. With such aids, and on the assumption of hydrogenic F_k ratios [as given in eq. (67)], Elliott et al. (1957) compiled a list of the energies of the terms of maximum and next-to-maximum multiplicity for all configurations $4f^N$. The spin–orbit splitting factors λ [defined in eq. (32)] for such terms were also calculated as multiples of ζ in the limit of Russell–Saunders coupling. The occurrence of unexpected simplifications [as exemplified by eqs. (36)] provoked McLellan (1960) to give a group-theoretical treatment of the spin–orbit interaction, H_{so}. The group labels for SO(7) and G_2 turn out to be (110) and (11), respectively, and the vanishing of the second matrix element in eqs. (36) is due to the absence of the identity representation (00) of G_2 in the decomposition of the triple Kronecker product $(11)\times(11)\times(21)$. Slightly more intricate arguments are needed to explain the vanishing of the first one (see section 11.2). Group theory helped considerably in understanding the unexpected simplifications; but it also exposed new ones. Mathematical puzzles of these kinds did not prevent the article of Elliott et al. (1957) from proving to be very useful in interpreting the absorption bands of many lanthanide ions. The situation in late 1964 can be assessed by referring to the monograph of Wybourne (1965a).

5.3. *Crystal-field splittings*

Paramagnetic resonance experiments were started in the mid-1940's and were well under way by 1950, particularly at Oxford. They provided an important stimulus to analyze the splittings in the levels $^{2S+1}L_J$ produced by the crystal lattice surrounding a lanthanide ion. In order to understand the magnetic properties of the low components (i.e., the sublevels) of a particular level, it was necessary to treat the crystal field as a perturbation. The most direct approach is to imagine the 4f electrons moving in an electric potential $V(\boldsymbol{r})$. The electron i contributes a term $-eV(\boldsymbol{r}_i)$ to the Hamiltonian, which can be expanded in a series of harmonic functions of the type $r_i^k Y_{kq}(\theta_i, \phi_i)$, each one of which is a solution to Laplace's equation $\nabla^2 V = 0$. This was the argument presented by Bleaney and Stevens (1953). It can be carried further: the coefficients A_{kq} of the harmonic functions depend on the distribution of electric charge in the crystal lattice, and a particular charge at $\boldsymbol{R}$ contributes a term to A_{kq} proportional to $R^{-k-1}Y^*_{kq}(\Theta, \Phi)$. Everything is thus reduced to electrostatics. However, we can evade the problem of calculating the A_{kq} by regarding them as parameters. This is feasible because only a few of them contribute when matrix elements of the type $\langle 4f|V(\boldsymbol{r})|4f\rangle$ are considered. Parity and angular-momentum constraints limit k to 0, 2, 4 and 6, and the number of possible components q can be minimized by a judicious choice of coordinate axes.

The harmonic functions are examples of the tensor operators $T^{(k)}_q$ of section 3.4. Their matrix elements, for a given J level, are thus proportional to the CG coefficients (31) with $J' = J$. Bethe (1929) had already found some algebraic expressions for some special cases for which $k = 2$ and 4. Stevens (1952) extended the analysis to $k = 6$ and showed how to determine the proportionality constants. Since the matrix elements of other tensors characterized by the same k and q must, by the Wigner–Eckart theorem, be proportional to the same set of CG coefficients, Stevens

found it possible to set up equivalences of the type

$$\sum_i (3z_i^2 - r_i^2) \equiv \alpha(3J_z^2 - J(J+1)), \tag{68}$$

where α is an operator equivalent factor. The importance of Stevens's paper was two-fold: it provided tables of values for such functions as $3M_J^2 - J(J+1)$, which occur when the equivalent operators are put to use; and it also showed how determinantal product states could be used to find the operator equivalent factors. Today, these factors would be called reduced matrix elements (and would be differently normalized). Although Stevens's article had considerable practical value, its main effect was psychological. It was no longer necessary to digest the details of the classical works on atomic theory: pencil and paper, and a knowledge of the action of shift operators [exemplified in eqs. (4–6)], were all that were needed to attack a problem. The goal might be far off and the route long and tedious but at least the direction to go in was clear. Trying to understand Racah's methods could be postponed with a moderately clear conscience.

In the mid-1950's crystals of the anhydrous trichlorides RCl_3 became available. The absorption spectra showed lines of unusual sharpness, particularly when the lanthanide ions were substituted in small quantities for La^{3+} in $LaCl_3$. The point symmetry at a lanthanide site is C_{3h}; that is, there exists a horizontal reflection plane and a three-fold axis of rotation perpendicular to it. The crystal field can be specified by just four parameters, provided our interest lies solely in matrix elements within the 4f shell. It was soon found that quite good agreement with the experimental work of Sayre et al. (1955) on praseodymium crystals could be obtained by adjusting the parameters and taking into account deviations from perfect Russell–Saunders coupling in $4f^2$ (Judd 1957a). Comparable results were found for other trichlorides and for several double nitrate crystals, where an approximate icosahedral symmetry (established later as coming from the packing of twelve O^{2-} ions around each lanthanide ion) was found (Judd 1957b). Two review articles of this period, that of Runciman (1958) and that of McClure (1959), convey the atmosphere of the time. They came too soon, however, to catalog the vast output of Dieke and his students at The Johns Hopkins University on the anhydrous trichlorides. Most of the sublevels of the lowest multiplets ^{2S+1}L of the lanthanides were found, as well as such excited multiplets as ^6P and ^6I of Gd^{3+} $4f^7$, ^5D of Eu^{3+} $4f^6$, and almost all the sublevels of Tm^{3+} $4f^{12}$. A great number of partial splittings were also established. In addition to work on the anhydrous trichlorides, considerable attention was also paid to the ethylsulphates, hydrated chlorides, double nitrates, bromates, sulphates and nitrates. A detailed summary is provided by the book of Dieke (1968), which was assembled by Crosswhite and Crosswhite from published and unpublished data of the Hopkins group and from an almost complete text written by Dieke himself shortly before his death in 1965.

5.4. *Selection rules*

The proper identification of the crystal-field components (the sublevels) of a J

level calls for a detailed knowledge of selection rules. Van Vleck (1937) argued that electric-dipole, magnetic-dipole and electric-quadrupole radiation might all be significant. In an experiment involving aqueous solutions of Eu^{3+} ions, Freed and Weissman (1941) used the different interference properties of electric-dipole and magnetic-dipole radiation to show that the fluorescence in the region of 6100 Å is electric-dipole while that near 5880 Å is magnetic-dipole. It was suspected (and is now known) that these two bands correspond to $^5D_0 \rightarrow {}^7F_2$ and $^5D_0 \rightarrow {}^7F_1$, respectively. A little later, Van Vleck's analysis was examined by Broer et al. (1945), who had begun a series of experiments on the absorption spectra of solutions of lanthanide ions. They concluded that Van Vleck had overestimated the importance of quadrupole radiation, while his calculation of the magnetic-dipole intensity, although giving a result in line with their own expectations, contained two omissions whose effects roughly cancelled. No major modifications to Van Vleck's calculation of the electric-dipole intensities were suggested by Broer et al. (1945). Their analysis contains an interesting error, however. They took their origin of coordinates at the equilibrium position of a lanthanide ion, which allowed them to omit terms of the type $r_i Y_{1q}(\theta_i, \phi_i)$ in the expansion of $-eV(\boldsymbol{r}_i)$. Such terms correspond to a constant electric field; were they present, the lanthanide would move. This would be inconsistent with its being at an equilibrium position. Thus harmonic terms for which $k = 3$ become the leading odd terms in the expansion of $-eV(\boldsymbol{r}_i)$; as such, they would be primarily responsible for mixing small amounts of excited configurations of the types $4f^{N-1}nd$, $4f^{N+1}n'd^{-1}$, or $4f^{N-1}ng$ into $4f^N$, thereby permitting electric-dipole transitions within the almost pure 4f shell to take place. That argument appears innocuous enough. But, for a lanthanide ion to be in equilibrium, there must be no electric field at its nucleus. In order to achieve that desirable state of affairs, each 4f wavefunction might have to possess admixtures of a d or a g character to build up the electric charge on one side of the atom and reduce it at the other. We should clearly retain any terms for which $k = 1$, should they be permitted by the site symmetry of the crystal, if we wish to take pure 4f eigenfunctions as our zeroth-order basis. However, we can begin with the terms for which $k = 3$ if our zeroth-order eigenfunctions are taken to be those superpositions of 4f with 5d, 5g, etc., that represent the effect of the constant electric field. A choice of this kind is a familiar feature of perturbation theory, since we have always to decide what is the zeroth-order Hamiltonian and what is the perturbation. This point seems to have escaped Broer et al. (1945), though it scarcely affected the semi-quantitative nature of their calculation. They recognized the important point that the presence of terms with high k in the expansion of $-eV(\boldsymbol{r}_i)$ leads to permissible electric-dipole transitions for which L and J change by large amounts. We can see that a transition $J \rightarrow J'$ is permitted (as far as the group $SO_J(3)$ is concerned) if the product

$$\mathscr{D}_{J'} \times \mathscr{D}_k \times \mathscr{D}_1 \times \mathscr{D}_J \tag{69}$$

contains $\mathscr{D}_0$. So ΔJ (and similarly ΔL) can be as large as 8, since the condition $k \leqslant 7$ holds for excitations of the type $f \rightarrow g$.

5.4.1. *Hellwege's analysis*

In a series of articles, Hellwege (1948, 1949, 1950) considered electric-dipole, magnetic-dipole and electric-quadrupole radiation in turn, and he worked out the selection rules for the various lanthanide site symmetries. The first step is to decide how to label the various sublevels of a given J level when it is split by the crystal-field perturbation, V_{CF}. The irreducible representations Γ_i of the point group G of the lanthanide site are, on the face of it, not very informative. Hellwege devised a crystal quantum number μ to describe the behaviour of an eigenfunction under rotations about a principal axis, c. To understand how it works, suppose the crystal goes into itself under a rotation C_n of $2\pi/n$ about c, which we take to be the z-axis of our coordinates. For V_{CF} to be invariant under C_n, it can only contain terms that transform like the spherical harmonics Y_{kq} for which $q = 0, \pm n, \pm 2n, \ldots$. This forces the eigenfunctions of a particular sublevel to be superpositions of M_J values differing by units of n. By writing the congruence $M_J \equiv \mu \pmod n$, each string of M_J values can be characterized by a number μ that specifies its transformation under C_n. Hellwege found that the existence of reflection planes or a center of inversion called for some elaboration of these ideas. He introduced the mirror quantum number S and the inversion quantum number I; and he found that it was sometimes necessary to replace μ by

$$\mu_I \equiv \mu \pm \tfrac{1}{2}np \pmod n, \tag{70}$$

where p is the parity of the configuration (i.e., the sum of all the azimuthal quantum numbers l of the electrons in the lanthanide ion). Hellwege's notation is not used much today. The reason for this is clear enough. In 1963, Koster et al. (1963) produced a complete listing of the irreducible representations Γ_i of the 32 point groups, including the associated double groups that are needed to accommodate the transformations of spinors. At a single stroke the symbols Γ_i were given a precise meaning, and the advantages of using μ, μ_I, S and I disappeared.

The appropriate perturbative terms to add to the Hamiltonian for electric-dipole and magnetic-dipole radiation are proportional to $\boldsymbol{E}\cdot\boldsymbol{D}$ and $\boldsymbol{H}\cdot(\boldsymbol{L}+2\boldsymbol{S})$, respectively, where $\boldsymbol{D}$ is the sum over all the electrons i of $\boldsymbol{r}_i$. The vectors $\boldsymbol{E}$ and $\boldsymbol{H}$ characterize the radiation field, whose direction of propagation, $\boldsymbol{k}$, makes no appearance in the dipolar perturbations. As for the quadrupolar term, we can take advantage of a very useful notational device introduced by Innes and Ufford (1958) whereby two tensors $\boldsymbol{T}^{(u)}$ and $\boldsymbol{U}^{(v)}$, when coupled to a resultant of rank w, are written as $(\boldsymbol{T}^{(u)}\boldsymbol{U}^{(v)})^{(w)}$. We get, for the term in question, an expression proportional to $(\boldsymbol{Ek})^{(2)}\cdot\boldsymbol{Q}^{(2)}$, where the quadrupole tensor $\boldsymbol{Q}^{(2)}$ is given by the sum over i of the coupled vectors $(\boldsymbol{r}_i\boldsymbol{r}_i)^{(2)}$. Group theory provides a straightforward procedure for determining the allowed transitions, or, more precisely, the ones that are not forbidden. A particular component of $\boldsymbol{D}$, $\boldsymbol{L}+2\boldsymbol{S}$ or $\boldsymbol{Q}^{(2)}$ appropriate to the physical situation under study is assigned a representation label Γ corresponding to the point group G of the site symmetry. A transition from a sublevel labelled Γ_i to one labelled Γ_j is not forbidden if Γ_j occurs in the decomposition of the Kronecker product $\Gamma \times \Gamma_i$. This principle was used by Hellwege (1948, 1949) to work out the selection rules for his special quantum numbers μ, μ_I, S and I.

For most of the crystals mentioned in section 5.3, the periodicity about the c-axis is greater than two-fold (i.e., $n > 2$). For such so-called uniaxial crystals it is not too difficult to distinguish different types of radiation. Three different spectra need to be compared: the axial (for which $\boldsymbol{k} \| \boldsymbol{c}$, and hence necessarily $\boldsymbol{E} \perp \boldsymbol{c}$ and $\boldsymbol{H} \perp \boldsymbol{c}$); the transverse π (for which $\boldsymbol{k} \perp \boldsymbol{c}$, $\boldsymbol{E} \| \boldsymbol{c}$, and hence necessarily $\boldsymbol{H} \perp \boldsymbol{c}$); and the transverse σ (for which $\boldsymbol{k} \perp \boldsymbol{c}$, $\boldsymbol{E} \perp \boldsymbol{c}$, and hence necessarily $\boldsymbol{H} \| \boldsymbol{c}$). As Runciman (1958) pointed out, a line coincident in both the axial and σ spectra is electric-dipole, while one coincident in both the axial and π spectra is magnetic-dipole or electric-quadrupole. The reader who attempts to verify these assertions soon discovers that the condition $n > 2$ is crucially important, since the components of $\boldsymbol{D}$, $\boldsymbol{L} + 2\boldsymbol{S}$ and $\boldsymbol{Q}^{(2)}$ for which $q = \pm 1$ must connect a particular lower sublevel to an upper one that is of a different type from that reached by the components for which $q = 0$. The identifications of $^1D_2$ of $4f^2$ and the levels of the ^5D multiplet of $4f^6$ referred to in section 5.2 were made by studying the polarizations of the various allowed transitions from sublevel to sublevel. The opportunity for several consistency checks made the J assignments very secure. It turned out that the transitions $^3H_4 \rightarrow {}^1D_2$ and $^7F_0 \rightarrow {}^5D_2$ are electric-dipole, while $^7F_1 \rightarrow {}^5D_0$ is magnetic-dipole. Deviations from perfect Russell–Saunders coupling are responsible for the apparent violations of the selection rule $\Delta S = 0$, which holds for $\boldsymbol{D}$, $\boldsymbol{L} + 2\boldsymbol{S}$ and $\boldsymbol{Q}^{(2)}$.

5.4.2. *Intensities*

Formulas for the line strengths for magnetic-dipole and electric-quadrupole radiation were included by Condon and Shortley (1935) in their classic text. Only minor modifications in the standard theory were necessary to allow for the presence of a lanthanide ion in a crystal. For electric-dipole radiation, on the other hand, the sequence of representations (69) has to be replaced by the product of matrix elements

$$\langle \psi'_{J'\mu'} | \sum_i r_i^k Y_{kq}(\theta_i, \phi_i) | \chi_{J''} \rangle \langle \chi_{J''} | \boldsymbol{E} \cdot \boldsymbol{D} | \psi_{J\mu} \rangle, \tag{71}$$

where ψ and ψ' denote terms of $4f^N$, and where $\chi_{J''}$ is a level of a configuration of opposite parity to $4f^N$, such as $4f^{N-1}5d$. In second-order perturbation theory the product given by (71) has to be divided by an appropriate energy denominator; it must also be combined with a similar expression in which the two operators are interchanged; the sums over all intermediate states $\chi_{J''}$ must be carried out; and further sums over k and q are required, each term in the sum being weighted by the appropriate crystal-field parameter A_{kq}. When the square modulus of the result is formed, we get an expression proportional to the intensity of the transition $\psi_{J\mu} \rightarrow \psi'_{J'\mu'}$.

Although Van Vleck could no doubt have formulated the above procedure in 1937, it became tractable only with the development of tensorial techniques. There remains, however, one difficulty. What should be taken for the energy denominators? If we include their dependence on J, J' and J'', we can only expect to be able to determine the relative intensities of the transitions $\psi_{J\mu} \rightarrow \psi'_{J'\mu'}$ for a given pair of levels, ψ_J and $\psi'_{J'}$. Ignoring the multiplet splittings, but treating the energies of the

terms ψ and ψ' on an individual basis, allows the intensities of the various J transitions to be related, but with a corresponding lack of accuracy. To relate all the transitions within a given $4f^N$ configuration, we must assume that the energy denominators are of the type $E(4f^N) - E(4f^{N-1}5d)$. That is, the relative energies of the configurations as a whole are entered in the calculation. When this is done, the effective operators producing the observed intensities turn out to be the components of sums of single-electron tensors $V^{(t)}$ acting solely within $4f^N$ [like those of eq. (61)] with ranks t given by 2, 4 and 6 (Ofelt 1962, Judd 1962). A useful result is thus obtained without having to resort to the ultimate step of assuming all excited configurations are degenerate. One of the several possible partial closures is enough.

The first test of the theory was made to the solution spectra of Hoogschagen and Gorter (1948) for $Nd^{3+}4f^3$ and $Er^{3+}4f^{11}$. This involved summing over the quantum numbers μ and μ', since the sublevel structure becomes blurred to at least some degree when the lanthanides are in solution. A remarkably good fit could be made to the experimental data with just three parameters, corresponding to $t = 2$, 4 and 6 (Judd 1962). The field soon developed a life of its own and is the subject of the review by Carnall (1979) in the third volume of this Handbook. Axe (1963) examined the fluorescence bands $^5D_0 \rightarrow {}^7F_4$ and $^5D_1 \rightarrow {}^7F_3$, $^7F_4$ in europium ethylsulphate and showed that the theory works equally well for the individual transitions of the type $\mu \rightarrow \mu'$. Two other bands, $^5D_0 \rightarrow {}^7F_1$ and $^5D_1 \rightarrow {}^7F_2$, were found to be almost completely magnetic-dipole in character. One interesting feature of Axe's analysis was that the limitations of the model forced him to conclude that the most important intermediate states $\chi_{J''}$ in the product (71) were those belonging to configurations of the type $4f^5 5g$, in which an f electron is excited to a g orbital. Axe (1963) introduced the parameters Ω_2, Ω_4 and Ω_6 to measure the relative importance of the three effective tensors $V^{(t)}$. They are the popular choice today.

5.4.3. *Vibronic lines*

The absorption lines to the blue of those corresponding to a particular electronic transition, and differing from them by the energies of vibrational quanta, were studied in detail for the double nitrate crystals by Hellwege (1939) and again by Hellwege and Hellwege (1952). These so-called vibronic lines were found to exhibit polarization phenomena, and the oscillations of the ion NO_3^- could be clearly discerned. A formal treatment of vibronic transitions was initiated by Satten (1957), who was puzzled by the frequent breakdown of the selection rules for electric-dipole radiation in his studies of neodymium bromate (Satten 1953). To understand how electric-dipole vibronic transitions can come about, consider a particular normal mode of the lanthanide complex, and suppose our states are written as $|\psi, n\rangle$, where ψ denotes as before a pure electronic state of $4f^N$, and n specifies the vibrational quantum number (or numbers, if the mode is degenerate). To connect $\langle\psi', 1|$ to $|\psi, 0\rangle$ by $\boldsymbol{E}\cdot\boldsymbol{D}$, we need an intermediate state $|\chi, 0\rangle$, where χ is an electronic state of a configuration of opposite parity to $4f^N$. The intensity of the corresponding line is proportional to the square modulus of

$$\langle\psi', 1| \sum_{i,L} (eq_L/r_{iL}) |\chi, 0\rangle \langle\chi, 0| \boldsymbol{E}\cdot\boldsymbol{D} |\psi, 0\rangle, \tag{72}$$

where $-e$ is the charge of electron i and $-q_L$ is the charge on ligand L. Satten (1957) used elementary techniques to expand r_{iL}^{-r} in powers of r_i and r_L, where $\boldsymbol{r}_L$ is the displacement of the ligand from its equilibrium position. He could have used the bipolar expansion of Carlson and Rushbrooke (1950), which expresses r_{iL}^{-1} as a sum over terms of the type

$$r_i^j r_L^k R_L^{-j-k} (\boldsymbol{Y}_j(\theta_i, \phi_i)\, \boldsymbol{Y}_k(\theta_L, \phi_L))^{(j+k)} \cdot \boldsymbol{Y}_{j+k}(\Theta_L, \Phi_L), \tag{73}$$

where the equilibrium position of ligand L is defined by the polar coordinates (R_L, Θ_L, Φ_L) relative to the lanthanide nucleus. In writing down (73), the compact notation of Innes and Ufford (1958) has again been used. The form of (73) is particularly useful for determining selection rules since the leading non-trivial term corresponds to $j = k = 1$. When combined with $\boldsymbol{E} \cdot \boldsymbol{D}$ and summed over i and L, we arrive at the selection rules

$$\Delta S = 0, \qquad \Delta n = 1, \qquad \Delta L \leqslant 2, \qquad \Delta J \leqslant 2, \tag{74}$$

in agreement with Broer et al. (1945).

It can happen, of course, that the state ψ' of $4f^N$ and the vibrational mode correspond to irreducible representations Γ_f and Γ_v of G for which $\Gamma_f \times \Gamma_v$ is reducible. In such a case the state $|\psi', 1\rangle$ can be expected to break up into components, and the intensity deriving from the linkage given by (72) is then distributed among them. In a series of papers, Satten (1958, 1959, 1964) worked out the selection rules for polarized spectra and developed methods to treat extended crystal systems, that is, systems where it is no longer appropriate to consider the complex of a lanthanide ion and its immediate surroundings as an isolated entity. The vibronic spectra of Pr^{3+} in $LaCl_3$ and $LaBr_3$ were first studied by Richman et al. (1963). Subsequent work by Cohen and Moos (1967) on other anhydrous trichlorides distinguished acoustic phonons from optical phonons. They also extended the work of Pollack and Satten (1962) and Satten (1964), and they derived electric-dipole selection rules for points of high symmetry of the Brillouin zone.

6. Racah's 1964 lectures at the Collège de France

Early in 1964, Racah visited Paris and gave a series of lectures at the Collège de France. After presenting some background material, he described the current status of the theory of configuration interaction (as it affects the energies of atomic levels) and the special problems facing the analysis and interpretation of the spectra of free lanthanide atoms and ions. Coming just a year before his death, the lectures probably represent his last thoughts on a subject – atomic spectroscopy – that had occupied his attention for most of his professional life. They were never published. It seems that they could serve as a framework for a description of the spectroscopy of the free lanthanides, not only from 1950 to 1964, but somewhat beyond that period. It is particularly illuminating to compare Racah's expectations and hopes to the reality of subsequent developments. The lectures conveyed a vivid impression of his enthusiasm for atomic spectroscopy, and they were an exciting occasion for all who

attended. Racah's entirely adequate French was colored by a variety of Italian and English pronunciations, but his meaning was never in doubt.

6.1. *Distant configurations*

6.1.1. *Two-electron excitations*

The importance of configuration interaction was recognized in the early 1930's. The Coulomb energies $E(^{2S+1}L)$ of the terms of a pure configuration p^2 obey the relation

$$[E(^1S) - E(^1D)]/[E(^1D) - E(^3P)] = \tfrac{3}{2}, \tag{75}$$

but the experimental value of the ratio for elements of the C I $2p^2$ isoelectronic sequence is more nearly equal to 1.14 (Condon and Shortley 1935). Evidently the terms are being perturbed by neighboring configurations. Over the years configuration interaction has been held responsible for many theoretical shortcomings. In his 1951 thesis, Trees reported that the mean errors of several iron-group spectra could be substantially reduced if the calculated energy of ^{2S+1}L were corrected by adding to it a term of the type $f(L)$, where $f(L)$ is an increasing function of L. Racah stated that he was concerned about the statistics and urged Trees not to pursue the matter. Trees went ahead anyway, and chose $\alpha L(L+1)$ for $f(L)$, thereby markedly improving the fits to the observed levels of Mn II $3d^54s$, Fe III $3d^54s$ and Fe III $3d^6$ (Trees 1951a,b). It did not take Trees (1952) and Racah (1952a) long to realize that a term of the type $\alpha \boldsymbol{L}^2$ in the Hamiltonian represents quite well the perturbative effects of distant configurations differing in two electrons from the configuration under study. In fact, if ^1S of d^2 is unknown, the four remaining terms of d^2 can be fitted exactly with an appropriate choice of F^0, F^2, F^4 and α. Terms of other configurations d^N containing appreciable components of ^1S of d^2 tend to be high and often unobserved. Looked at slightly differently, the parameters F^k are associated with the two-electron parts of the operators $(\boldsymbol{V}^{(k)})^2$, while $\boldsymbol{L}^2$ is proportional to $(\boldsymbol{V}^{(1)})^2$. Only $(\boldsymbol{V}^{(3)})^2$ is missing from the complete set for which $0 \leqslant k \leqslant 2l$, and although we could determine its strength from the position of ^1S of d^2, Racah preferred to include the fifth parameter by simply adding 5β to the expression for the energy of ^1S. By this device, a partial knowledge of the excited terms of a configuration leads to a large mean error in β alone.

These ideas can be readily extended to include the lanthanide configurations $4f^N$ or, for that matter, the general configuration l^N. Racah credited Bacher and Goudsmit (1934) for realizing that two-electron excitations *from* l^N can be represented by two-electron operators *within* l^N to second order in perturbation theory. To show how this can come about in detail, Racah introduced the single-electron tensor operators $z_i^{(k)}(ll')$ that convert a state of $l^N l'^M$ to one of $l^{N+1} l'^{M-1}$. As such, $z_i^{(k)}(ll')$ is identical to the tensor $\boldsymbol{u}_i^{(k)}(ll')$ that Elliott (1958) introduced in his studies of collective motion in the nuclear shell model. The excitation for which $M = 4l' + 2$ $(= \varepsilon$, say) is of particular interest to us since Trees and Jørgensen (1961) found that the effect of $3d^{N+2}3p^4$ on $3d^N3p^6$ provides an important source for α. The Coulomb interaction that excites two electrons from $l^N l'^{\varepsilon}$ to $l^{N+2} l'^{\varepsilon-2}$ is necessarily pro-

portional to a sum of terms of the type

$$\sum_{i>j} \mathbf{z}_i^{(k)}(ll')\cdot \mathbf{z}_j^{(k)}(ll'), \tag{76}$$

and so, in second-order perturbation theory, the effect of the excitation on the levels of $l^N l'^{\varepsilon}$ is reproduced by a sum (over various k and k') of the operators

$$\sum_{r>s}\sum_{i>j} (z_r^{(k')}(l'l)\cdot z_s^{(k')}(l'l))(z_i^{(k)}(ll')\cdot z_j^{(k)}(ll')). \tag{77}$$

An operator $z_p^{(k')}(l'l)$ can only de-excite an electron that has already been excited out of the closed shell. The constraints $r > s$ and $i > j$ thus limit the non-vanishing terms in (77) to those for which $r = i$ and $s = j$. This immediately converts (77) to an operator in which just the two indices i and j appear; moreover, the condition $i > j$ is maintained, and the effective operator (77) is a sum of true two-electron operators, which is the result that we want. This is the argument used in the article of Racah and Stein (1967, section IIA), submitted for publication a year after Racah's death.

The situation is more complicated if the l' shell is not completely filled, since we can no longer be sure that the electron that is excited (either i or j) is the same as the one de-excited (r or s). Racah touched on these difficulties and outlined the more formal treatment of the z tensors that needs to be set up. A crucial manipulation is the re-ordering of the various parts that go to form the products occurring in (77). We can, in fact, refer to eq. (4) of Elliott (1958) to evaluate such commutators as

$$\left[\sum_s \mathbf{z}_s^{(k')}(l'l), \sum_i \mathbf{z}_i^{(k)}(ll')\right], \tag{78}$$

which are expressible as sums over tensors of the type $\mathbf{z}_j^{(k'')}(ll)$ and $\mathbf{z}_j^{(k'')}(l'l')$. There seems little point in going into details here because the kinds of operations being studied are more efficiently carried out today by using the techniques of second quantization (Judd 1967a). In that approach, $\Sigma_i \mathbf{z}_i^{(k)}(ll')$ is replaced by $(\mathbf{a}_l^{\dagger}\,\mathbf{a}_{l'})^{(0k)}$. The tensor $\mathbf{a}_l^{\dagger}$ comprises the $4l + 2$ operators that create the states of an l electron; the tensor $\mathbf{a}_{l'}$ comprises the $4l' + 2$ operators (with some phase adjustments) that annihilate the states of an l' electron. Thus $\mathbf{a}_l^{\dagger}$ is a double tensor of rank $\frac{1}{2}$ in the spin space and rank l in the orbital space. The pair of ranks $(0k)$ labelling the coupled product indicate that the total spin rank is zero and that the total orbital rank is k. The advantage of working with annihilation and creation operators is that all electron indices (r, s, i and j) disappear from the analysis and all commutation relations can be worked out from the basic anticommutation relations for fermions.

6.1.2. *Single-electron excitations*

It is a remarkable fact that single-electron excitations lead to more complicated effective operators than do two-electron excitations. The analog of (77) is

$$\sum_{r\neq s}\sum_{i\neq j} (z_r^{(k')}(ll)\cdot z_s^{(k')}(l'l))(z_i^{(k)}(ll')\cdot z_j^{(k)}(ll)). \tag{79}$$

For excitations from the closed shell l'^{ε} we must have $s = i$, and (79) becomes a sum

over true three-electron operators (since $r \neq i \neq j \neq r$). The existence of effective three-electron operators had already been pointed out by Rajnak and Wybourne (1963). Their method was to actually evaluate the matrix elements of the exciting and de-exciting operators, form their product, and ask for the operator whose matrix elements within l^N could reproduce the product. A detailed reconciliation of the two approaches for a variety of interacting configurations can be found in the article of Racah and Stein (1967).

In his lectures, Racah showed that the use of the commutator (78) in simplifying (79) leads to z tensors for which the ranks k, k' and k'' are all even. He then stated that he expected that the four non-trivial possibilities (222), (224), (244) and (444) for $(kk'k'')$ in the d shell would lead to four three-electron operators and hence four new parameters. In that he was unduly pessimistic. In the summer of 1965, Feneuille (1966) showed that one linear combination of the four operators always had null matrix elements, while another possessed matrix elements proportional to a combination of those coming from the Coulomb interaction between the d electrons. A similar situation occurs for the lanthanides. At first sight we would expect single-particle excitations to require nine new operators, acting solely within the f shell, to reproduce the effect of the excitations, since, in this case, we have $(kk'k'') \equiv$ (222), (224), (244), (246), (266), (444), (446), (466) and (666), respectively. However, it turns out that one linear combination possesses vanishing matrix elements, while those of two others are proportional to those of the operators e_2 and $6e_0 - 7e_1$, respectively, where the e_i are defined in eqs. (64) (Judd 1966a). The remaining six operators, which are called t_i (with $i = 2$, 3, 4, 6, 7 and 8), are associated with six parameters T^i, just as the e_i are associated with the E^i. Each t_i, like each e_i, corresponds to a distinct pair of irreducible representations W and U of SO(7) and G_2. In fact, the analysis leading to the construction of the t_i employs the same group-theoretical arguments that Racah made use of in his 1949 article. It is now standard procedure to include the parameters T^i when fitting the terms of the configurations $4f^N$ (see Goldschmidt 1978). These six T^i, taken with the four E^i and the three Trees parameters α, β and γ, give 13 electrostatic parameters in all.

6.2. *Configuration ordering*

After describing the effects of configuration interaction in the d shell, Racah began a discussion of the status of the spectroscopy of free lanthanide ions. His opening statement was that we know very little; but he qualified that remark by pointing out that something was at least known about a few special cases, particularly some second spectra, and a certain amount of information on the fourth spectra could be gleaned from the work on crystals. The basic difficulty for a theorist is the fact that the 4f, 5d and 6s electrons all possess comparable energies. In the third spectra the levels of the configurations $4f^{N-1}5d$ and $4f^N$ compete for the ground level; in the second spectra the competition is between $4f^{N-1}5d6s$, $4f^{N-1}5d^2$ and $4f^N6s$: while for the first spectra (those of the neutral atom) we again have three low configurations to contend with, namely $4f^{N-1}5d6s^2$, $4f^{N-1}5d^26s$ and $4f^N6s^2$. Racah put the con-

figurations $4f^N$, $4f^N6s$ and $4f^N6s^2$ in class B, and the rest in class A. For a given N all the configurations in a single class possess the same parity.

Something of the difficulty facing spectroscopists in the mid-1960's can be appreciated when we ask for the ground levels of the cerium and praseodymium atoms and ions from the data available at that time. From the work of Harrison et al. (1941) it was known that low levels of Ce II existed of both types A and B. It was Racah (1955) who found the connection between the two systems and thus confirmed the opinion of Harrison and his co-workers that the lowest level of Ce II is of type A (principally $4f5d^2\,{}^4H_{7/2}$, in fact). On the other hand, the work of Rosen et al. (1941) indicated that the ground level of Pr II is $4f^36s\,{}^5I_4$, thus belonging to type B. Can we deduce anything about the lowest level of Ce I? We know that the ground level of the adjacent ion to Ce II, namely La II, belongs to $5d^2$ (see section 2.1). The addition of a 4f electron converts it into the ground configuration of Ce II. If, then, we add a 4f electron to the ground configuration of La I, that is, to $5d6s^2$, we might expect to obtain $4f5d6s^2$ as the ground configuration of Ce I. The validity of that argument was confirmed by Martin (1963), who found the lowest level to be $^1G_4$ (thus demonstrating an exception to Hund's rule). The bare recitation of this discovery does not do justice to the excitement of the time, when active experimental groups working with atomic beams of lanthanide atoms were thwarted from making an unambiguous determination of the ground level of cerium by the presence in their beams of other low-lying populated levels.

Our argument from lanthanum to cerium cannot be repeated for Pr II because the configurations do not match in the same way. However, we can confidently predict the lowest level of Pr III to belong to $4f^3$ because, if $4f^3$ were not lower than $4f^26s$, we would expect the ground configuration of Pr II to be $4f^26s^2$, which it is not. The work of Sugar (1963) confirmed $4f^3$ as the ground configuration of Pr III. At the time of his lectures, Racah was also aware of the Ce III analysis of Sugar (1965a), which established $4f^2$ as the ground configuration for Ce^{2+}. Thus the ground configurations of Pr III and Ce III are both of type B, in contrast to the second spectra, where the types are different. Racah asked whether any sense could be made of results such as these. In particular, can we make predictions for other lanthanides?

6.2.1. *The third spectra*

The basic idea developed by Racah in his lectures is to use our knowledge of what happens at both ends of the lanthanide series to interpolate towards the middle. We can allow for the widely differing energy spreads of the configurations $4f^N$ by choosing the centers of gravity E_{av} of the various compound configurations as the crucial energies to study across the series. In his lectures Racah began with the third spectra, for which he proposed the following formulas:

$$E_{av}(4f^{N-1}6p) - E_{av}(4f^{N-1}6s) = 36524 + 873(N - 8), \tag{80}$$

$$E_{av}(4f^{N-1}5d) - E_{av}(4f^{N-1}6s) = -3446 + 1459(N - 8) + 58[(N - 8)^2 - 33], \tag{81}$$

$$E_{av}(4f^{N-1}5d) - E_{av}(4f^N) = 23686 + 3660(N - 8) - 307[(N - 8)^2 - 33], \tag{82}$$

where the coefficients are in units of cm^{-1}. In addition to the data already mentioned for the early members of the lanthanide series, Racah could use the results of Meggers and Scribner (1930) for Lu III (for which $N = 15$), of Bryant (1965) for Yb III (for which $N = 14$), as well as the data of Callahan (1963) for Gd III $4f^7(^8S)5d$, 6s and 6p. It is impossible, today, to reconstruct the arguments that led Racah to choose the numerical coefficients in eqs. (80)–(82). Only three data points (Ce III, Pr III and Yb III) were available to establish eq. (82), since it was not until almost a decade later that Johansson and Litzén (1973) discovered the position of the ground term ^7F of $4f^8$ relative to ^9D of $4f^75d$ in Gd III. Not all the levels of $4f^3$ and $4f^25d$ were found by Sugar (1963), so Racah had to rely on the theoretical work of Trees (1964) to fix the relative positions of the centers of gravity of these configurations. The recognition today of the importance of configuration mixing gives us an additional problem to weigh. Should we find $E_{av}(C)$ for a configuration C by averaging over those levels whose principal components belong to C, or should we perform a diagonalization of the mixture $C + C' + C'' + \cdots$, and use as $E_{av}(C)$ the average of the entries appearing on that portion of the diagonal associated with C?

In spite of these difficulties, it is interesting to see how Racah's most vulnerable formula, eq. (82), which determines the lowest levels of the doubly ionized lanthanides, has stood the test of time. For $N = 1$ we get, from that equation,

$$E_{av}(\text{La III } 5d) - E_{av}(\text{La III } 4f) = -6846\ \text{cm}^{-1}.$$

This is in excellent accord with the value of -7090 found by Sugar and Kaufman (1965). Comparisons with other lanthanides are not so easy to make because the levels are only partially known. The best way to proceed appears to be to first pick an observed low-lying level (or entire multiplet) whose designation is as pure as possible. A theoretical expression is then worked out for its energy relative to the center of gravity of the configuration. The various Slater integrals $F_k(4f, 5d)$, $G_k(4f, 5d)$ or Racah parameters E^k (for the Coulomb interactions between the 4f electrons) that are needed can be found by linear interpolation between their values for Pr III $4f^3$, Er III $4f^{12}$, Pr III $4f^25d$ and Tm III $4f^{12}5d$, as given by Goldschmidt (1978, tables 1.27, 1.31 and 1.41), which yields

$$E^1(4f^N) = 5410 + 232(N - 8), \qquad E^2(4f^N) = 25.8 + 1.15(N - 8),$$
$$E^3(4f^N) = 520 + 22(N - 8); \tag{83}$$

$$E^1(4f^{N-1}5d) = 6078 + 229(N - 8), \qquad E^2(4f^{N-1}5d) = 28.6 + 1.17(N - 8),$$
$$E^3(4f^{N-1}5d) = 580 + 20(N - 8); \tag{84}$$

$$F_2(4f, 5d) = 188 + (N - 8), \qquad F_4(4f, 5d) = 20.4 - 0.2(N - 8),$$
$$G_1(4f, 5d) = 244 - 8(N - 8), \qquad G_3(4f, 5d) = 29 - 0.6(N - 8),$$
$$G_5(4f, 5d) = 3.9 - 0.1(N - 8). \tag{85}$$

Our occasional need for approximate spin–orbit coupling constants can be satisfied by using the data for Ce III 4f5d and Yb III $4f^{13}5d$ (Goldschmidt 1978, table 1.36) in

TABLE 2
Centers of gravity of $4f^{N-1}5d$ above $4f^N$ in the third spectra of the lanthanides.

State, X	$(E(X) - E_{av})$[a]		E_{exp}[b]	$E_{av}(4f^{N-1}5d) - E_{av}(4f^N)$	
				Calc.[c]	Racah[d]
La III $4f\,^2F$	0		8052	−7090	−6846
La III $5d\,^2D$	0		962		
Ce III $4f^2$	All states of $4f^2$ used		7632	963, 723[e]	805
Ce III 4f5d	All states of 4f5d used		8595		
Pr III $4f^3\,^4I$	$-\frac{27}{13}E^1 - 21E^3$	$= -17437$	2472	8069, 7762[e]	7842
Pr III $4f^25d\,^4K$	$-\frac{9}{13}E^1 - 9E^3 + 10F_2 - 4F_4 - 17G_1 - 18G_3 + 60G_5$	$= -11131$	16847		
Nd III $4f^4\,^5I$	$-\frac{54}{13}E^1 - 21E^3$	$= -27690$	2859	14289	14265
Nd III $4f^35d\,^5K$	$-\frac{27}{13}E^1 - 21E^3 - 4F_2 + 17F_4 - \frac{25}{2}G_1 - 20G_3 - 2G_5$	$= -25683$	19155		
Sm III $4f^6\,^7F$	$-\frac{135}{13}E^1$	$= -51362$	2504	22450	25269
Sm III $4f^55d\,^7H_2$	$-\frac{90}{13}E^1 - 9E^3 + \frac{35}{3}F_2 + 56F_4 - \frac{27}{2}G_1 - \frac{97}{3}G_3 - \frac{793}{3}G_5 - \frac{3}{10}\zeta_d - \frac{27}{10}\zeta_f$	$= -50032$	26284		
Eu III $4f^7\,^8S$	$-\frac{189}{13}E^1$	$= -75280$	0	29772	29850
Eu III $4f^65d\,^8H$	$-\frac{135}{13}E^1 - 10F_2 - 3F_4 - 12G_1 - 48G_3 - 54G_5$	$= -67332$	37720		
Gd III $4f^8\,^7F$	$-\frac{135}{13}E^1$	$= -56181$	4321	33706	33817
Gd III $4f^75d\,^9D$	$-\frac{189}{13}E^1 - \frac{21}{2}G_1 - 42G_3 - 231G_5$	$= -93046$	1162		
Tb III $4f^9\,^6H$	$-\frac{90}{13}E^1 - 9E^3$	$= -43938$	4057	34637	37170
Tb III $4f^85d\,^8G$	$-\frac{135}{13}E^1 - 15F_2 - 22F_4 - 9G_1 - 36G_3 - 198G_5$	$= -72674$	9958		
Er III $4f^{12}\,^3H$	$-\frac{9}{13}E^1 - 9E^3$	$= -9860$	5265	42763	43545
Er III $4f^{11}5d\,^5L_{10}$	$-\frac{27}{13}E^1 - 21E^3 - 4F_2 + 3F_4 - \frac{9}{2}G_1 - 18G_3 - 99G_5 + \zeta_d - 3\zeta_f$	$= -37418$	20470		
Tm III $4f^{13}\,^2F$	0		3760	43629	44442
Tm III $4f^{12}5d\,^4K_{17/2}$	$-\frac{9}{13}E^1 - 9E^3 - 10F_2 + 4F_4 - 3G_1 - 12G_3 - 66G_5 + \zeta_d - \frac{5}{2}\zeta_f$	$= -19831$	27558		
Yb III $4f^{14}\,^1S$	0		0	44646[e]	44725
Yb III $4f^{13}5d$	All states of $4f^{13}5d$ used		44643		

[a] The coefficients of F_k, G_k, ζ_f and ζ_d in the algebraic formulas can be found by using determinantal product states and adding $(N-1)$ $(\frac{3}{2}G_1 + 6G_3 + 33G_5)$ to center the splittings produced by the Coulomb interaction between the 4f and 5d electrons. The coefficients of E^1 for $4f^n$ and $4f^n5d$ are given by $-9n(n-1)/26$ for $0 \leqslant n \leqslant 7$ and by $-9(14-n)(13-n)/26$ for $7 \leqslant n \leqslant 14$, each of these quantities representing the average energy of the terms of maximum multiplicity relative to the average energy of the entire configuration $4f^n$. The coefficients of E^3 give the energies of the lowest terms relative to the first of these averages.

[b] The energies E_{exp} are given in cm^{-1} relative to the ground level.

[c] The calculated energy differences are constructed from the entries in the two preceding columns.

[d] From eq. (82)

[e] Used by Racah in his lectures to establish eq. (82).

the forms

$$\zeta_f(4f^{N-1}5d) = 1779 + 190(N-8), \qquad \zeta_d(4f^{N-1}5d) = 918 + 39(N-8), \tag{86}$$

which neglect a small quadratic term. By means of eqs. (83)–(86) we can deduce the positions of the centers of gravity of the configurations $4f^{N-1}5d$ and $4f^N$ from the experimentally known energies of a few (or even just one) low-lying level. The tabulation of energy levels given by Martin et al. (1978) proves extremely helpful here, since these compilers had access to unpublished material from many laboratories. In fact, the sheer size of table 2, where our results are collected, gives an indication of the considerable activity in rare-earth spectroscopy in the twelve or so years after 1964, the date when Racah only had Ce III, Pr III and Yb III to work with. Some of the spectroscopists at the National Bureau of Standards at Gaithersburg (Kaufman, Sugar and Martin) have already been mentioned. Other important groups that contributed to the experimental work on the third spectra were sited at The Johns Hopkins University (Becher, Bryant, Callahan and Dupont), the Zeeman Laboratorium, Amsterdam (Van Kleef, Meinders), the Laboratoire Aimé Cotton, Orsay (Blaise, Camus, Wyart), the Argonne National Laboratory (Crosswhite), and Lund (Johansson, Litzén). The reader is referred to the tables of Martin et al. (1978) for a detailed list of references.

As for table 2 itself, the first impression is that Racah's formula [our eq. (82)] works extremely well. We can see that the vagaries of the energies of the lowest levels of the configurations $4f^N$ and $4f^{N-1}5d$ conceal the smooth trend of the centers of gravity of the configurations. We can understand why $4f^7 5d\ ^9D$ of Gd III should lie lower than $4f^8\ ^7F$, thus presenting us with a ground level of type A (in contrast to all other entries in table 2 with the exception of La III). The enormous spread of $4f^7$ compared to other $4f^N$ configurations is at work here. Only the two spectra on either side of Gd III, namely Sm III and Tb III, lead to discrepancies larger than a few hundred cm^{-1}. It is likely that a failure in the linearity of eqs. (83) and (84) near the half-filled shell is at least partially responsible for this. Even so, the discrepancies are small compared to the spreads of the configurations $4f^6$, $4f^7$ and $4f^8$.

6.2.2. *The second spectra*

Racah began his discussion of the second spectra by regretting that the absence of relevant data precluded the construction of formulas of the type represented by eqs. (80)–(82). Instead, he suggested that it might be useful (and much more convenient) to compare differences in energy between the lowest levels of opposite parity (the so-called system differences) in the second and third spectra. He noted, for example, that we can write

$$\begin{aligned}
&E(4f^2\ ^3H_4) - E(4f5d\ ^1G_4) = 3277 && \text{(Ce III)},\\
&E(4f^2 6s, \tfrac{7}{2}) - E(4f5d6s, \tfrac{7}{2}) = -3854 && \text{(Ce II)},\\
&E(4f^{14}\ ^1S_0) - E(4f^{13}5d, 2) = 33386 && \text{(Yb III)},\\
&E(4f^{14}6s, \tfrac{1}{2}) - E(4f^{13}5d6s, \tfrac{5}{2}) = 26759 && \text{(Yb II)},
\end{aligned} \tag{87}$$

so that the differences of the system differences, which can be schematically written

as

$$\Delta(\mathrm{III, II}) = (\mathrm{A} - \mathrm{B})_{\mathrm{III}} - (\mathrm{A} - \mathrm{B})_{\mathrm{II}}, \tag{88}$$

evaluates to 7131 for cerium and to the very similar figure of 6627 for ytterbium. Racah suggested that Δ(III, II) might be approximately constant across the lanthanide series.

The rationale for the hypothesis of constant $\Delta(\mathrm{III, II})$ was not discussed by Racah, but it is evidently based on the idea that all interactions between the 4f electrons and between the 5d electron and the 4f electrons are cancelled by the differencing procedure. Apart from some smoothly varying terms representing configuration averages, the only remaining contributions to the energies correspond to interactions between the 6s electron on the one hand and, on the other, the 4f and 5d electrons. Should these too be smoothly varying, so should be $\Delta(\mathrm{III, II})$. This expectation was tested by Martin (1971, 1972) some six years after Racah's lectures, when more experimental data had become available. We can take advantage of the further advance in our knowledge, as represented by the tables of Martin et al. (1978), to make a detailed examination of Racah's hypothesis. This is done in table 3. The column headed Δ(III, II) exhibits not merely a smooth variation but a remarkable constancy, particularly in the light of the large variations in the numbers listed in the four preceding columns. However, it is not possible to make an unambiguous assessment of Racah's hypothesis. This is because the 6s and 5d electrons possess the same parity and, since their energies are comparable, appreciable mixing takes place. The $J = \frac{7}{2}$ level of 4f5d6s in eqs. (87), which was used by Racah to justify the relative constancy of Δ from Ce to Yb, is assigned to $4f5d^2$ by

TABLE 3

Differences of differences (in cm^{-1}) between the energies of low-lying levels of types A and B in the second and third spectra of the lanthanides.

R	N	$A_{III}(f^{N-1}d)$	$B_{III}(f^N)$	$A_{II}(f^{N-1}ds)$	$B_{II}(f^Ns)$	Δ(III, II)
La	1	0	7195	1895	14148	5058
Ce	2	3277	0	0[a] [2382][b]	3854	7131 [4749]
Pr	3	12847	0	5855[a] [7832][b,c]	0	6992 [5015]
Nd	4	15262	0	9229[a] [11310][b,c]	0	6033 [3952]
Sm	6	26284	0	21508[c]	0	4776
Eu	7	33856	0	30189[d]	0	3667
Gd	8	0	2381	0	7992	5611
Tb	9	8972	0	3235	0	5737
Er	12	16976	0	10667	0	6309
Tm	13	22897	0	16567	0	6330
Yb	14	33386	0	26759	0	6627

[a] Principal component listed by Martin et al. (1978) as $4f^{N-1}5d^2$

[b] Principal component listed by Martin et al. (1978) as $4f^{N-1}5d6s$

[c] Listed as tentative by Martin et al. (1978)

[d] This level is probably undershot by one for which $J = 1$ (so far unobserved). Martin (1971) uses the tentative number 29000 here, thus yielding $\Delta(\mathrm{III, II}) \simeq 4900$.

Martin et al. (1978). The adjustments that a correction entails are indicated by numbers in brackets in table 3. At the time of Racah's lectures, the position of the lowest level of type A of Pr II was unknown. From A − B for Pr III and the expectation that Δ should be about 7000 cm^{-1}, Racah predicted a low level of type A of Pr II about 5500 cm^{-1} above the ground level. This is in good agreement with the observed figure of 5855, which was not established until 1973. That this level belongs principally to $4f^2 5d^2$ (rather than $4f^2 5d6s$) does not diminish Racah's prediction. He was fully aware of the fact that both $4f^2 5d^2$ and $4f^2 5d6s$ must start quite close to the ground level.

In addition to studies of trends and interpolations, Racah outlined detailed work under way in Jerusalem for Gd II and Ce II. The extensive analysis of Russell (1950) for Gd II had established almost all the levels of $4f^7(^8S)(5d + 6s)^2$ and $4f^7(^8S)6p(5d + 6s)$, where 5d + 6s denotes the twelve states of a 5d and a 6s electron. All 71 levels of $4f^7(^8S)6p(5d + 6s)$ had been fit by Zeldes (1953) with 17 parameters, thereby obtaining a mean error of 338 cm^{-1}. By treating the 5d and 6s electrons together it was possible to allow for the interaction between the ^3P terms coming from 6s6p and 5d6p, which, if ignored, would lead to an anomalous value for $G_1(6p, 6s)$. Racah noted that Russell (1950) had reported the existence of 11 additional levels in the region of $4f^7(^8S)6p(5d + 6s)$, to which Racah added six more. In his lectures, he suggested that these 17 levels might belong to $4f^8(^7F)(5d + 6s)$, supporting his speculation by a preliminary calculation. We now know that these two configurations do indeed overlap.

Racah's description of the current work of his student, Goldschmidt, on Ce II gave many of his audience their first glimpse of what can be achieved by properly taking into account the interactions between several neighboring and overlapping configurations. Five odd configurations and seven even configurations were being investigated. Among the former, the three configurations that constitute $4f(5d + 6s)^2$ were treated as a group. Of the 122 possible levels, 80 were known and a good fit could be obtained. The two remaining odd configurations, $4f^3$ and $4f^2 6p$, were being considered together, but although 57 out of a total of 110 levels were known, those originating principally from $4f^2 6p$ were too sparse to allow a satisfactory analysis to be carried out. More spectacular was Racah's account of the simultaneous treatment of the seven configurations of even parity, namely,

$$4f^2 6s + 4f^2 5d + 4f5d6p + 4f6s6p + 5d^3 + 5d^2 6s + 5d6s^2,$$

where no fewer than 305 levels occur. Goldschmidt (1978), in the first volume of this Handbook series, has given a first-hand account of how successive fits can be used to find new levels and improve the parameters. Her article gives many details of the modern approach to fitting atomic energy levels, as well as providing a comprehensive survey of theoretical lanthanide spectroscopy to 1978. Of particular interest are the many diagrams showing the various kinds of coupling that can occur when the Coulomb and spin–orbit interactions of several inequivalent electrons compete in a single configuration. Reference has already been made in section 2.2.3 to her analyses of the configurations La II $(4f + 6p)(5d + 6s)$ and La II $(5d + 6s)^2 + (4f + 6p)^2 + 6s6d$. In these cases the numbers of parameters are com-

parable to the numbers of levels, so comparisons with other lanthanide spectra are essential to constrain the least-squares fitting procedure. The direction that this kind of work has taken was foreseen by Racah, and, indeed, it can be said to have grown naturally out of his own analysis of the two-electron spectrum of Th III (Racah 1950).

6.2.3. *The first spectra*

Racah left until last a discussion of the first spectra of the lanthanides. Before recounting the substance of Racah's lecture, it seems useful to recall the general situation in 1964. Very little had been firmly established. In his listing of the ground levels of the neutral lanthanides (running from lanthanum to ytterbium), Kuhn (1962, p. 320) set six of the ground levels and seven of the configurations in parentheses to indicate that they were uncertain. This corresponded closely to the tabulation of Klinkenberg (1947) and showed only a marginal improvement over the listing of Meggers (1942), where nine ground levels were not specified. In a carping review of Kuhn's book, Meggers (1962) stated that all of the parenthetical entries had been 'experimentally confirmed or corrected'. He did not allow for the crucial period that had elapsed after Kuhn had sent his manuscript to the printers. He also did not specify what he believed the ground levels to be. The ground level of Tb I was still uncertain in the present writer's mind at the time of the Zeeman Centennial Conference in Amsterdam in 1965, and it was not until a few years later that Klinkenberg and van Kleef (1970) determined that $4f^8\,(^7F)5d6s^2\,{}^8G_{13/2}$, the lowest level of $4f^8 5d6s^2$, lies a mere $286\,cm^{-1}$ above the lowest level of $4f^9 6s^2$, namely $^6H_{15/2}$. Meggers's confidence in knowing the lanthanide ground levels seemed odd in 1962. Perhaps, as the doyen of the experimental spectroscopists at the National Bureau of Standards, he felt a responsibility for taking a position in the matter, particularly since competing claims were being made by physicists working with atomic beams.

In his lectures, Racah proposed working again with the differences of the system differences, using the second spectra for reference points. The relevant quantity is $\Delta(II, I)$, defined in analogy to eq. (88). But Racah had much less to work with than before. Although $(A - B)_{II}$ for La II was known to be $-12\,253\,cm^{-1}$, the term ^2F of La I 4f was still unidentified. However, from the distribution of spectral lines Racah estimated $|(A - B)_I|$ to be greater than 17 500, and so, were it actually at that limit, we should get $\Delta(II, I) \simeq 5250$. The only other suitable data came from Eu. Racah took $(A - B)_{II} = 33\,780$ and $(A - B)_I = 27\,853$ to yield $\Delta(II, I) = 5927$, which was encouragingly close to 5250. He suggested that we might hope for some guidance in other spectra by using values of $\Delta(II, I)$ of around $5000\,cm^{-1}$.

We can see today that Racah was pushing the data beyond their limits. His figure of $-17\,500$ for $(A - B)_I$ in La I should be $-15\,197$ (Martin et al. 1978), so $\Delta(II, I)$ is actually 2944 for La. As for Eu II, the level at 33 780 is not the lowest level of $4f^6 5d6s$, the level $^9D_2$ lying 30 189 above ground (and used in the construction of table 3). The level of Eu I at 27 853 is $^8D_{5/2}$ and, to judge from Eu III, lies above at least some of the levels of ^8H, so far unobserved in Eu I. The problem of mixed configurations in table 3 would recur if any tabulation of $\Delta(II, I)$ were attempted.

However, with out present knowledge of the first and third spectra, which often differ only in $6s^2$, we can easily work out $\Delta(\mathrm{III,I})$. The numbers (in cm^{-1}) for La, Ce, Pr and Nd are 8002, 8040, 8415 and 8495, respectively; for Sm, 8208; for Gd and Tb, 8566 and 8686; and for Ho, Er, Tm and Yb they are 9654, 9799, 9777 and 10 197 respectively. These numbers fit rather well the provisional formula

$$\Delta(\mathrm{III,I}) = 7724 + 158N$$

of Martin (1971), which was proposed when the only available data were for $N = 2$, 6, 13 and 14.

In closing his lectures, Racah stressed the need for sound interpolative techniques. The use of large numbers of parameters is often mistakenly perceived as a weakness in the parametric approach, as if the parameters were meaningless quantities introduced in an arbitrary way to get a smaller mean error. The strength of the parametric approach is its success in predicting new levels and in correlating data originating in different atomic systems. If the parameters are associated with operators with well-defined tensorial ranks, or, more generally, with operators corresponding to sequences $\mathscr{S}$ of irreducible representations of Lie groups, the fitting of experimental data can be thought of as a kind of Fourier analysis. The experimental data are thereby converted to parameters that are more suitable for theoretical study. Although this point was appreciated for a long time, it is only recently that it has been explored in detail (Judd et al. 1982). Operators corresponding to different sequences $\mathscr{S}$ are orthogonal and their associated parameters are minimally correlated (Newman 1982). Applications to the lanthanides have so far been limited to Pr III $4f^3$ (Judd and Crosswhite 1984, Judd and Suskin 1984).

7. Ligand effects

7.1. *Crystal-field parameters*

Until the 1950's, it seemed perfectly adequate to imagine the effect of the crystal field on the 4f electrons of an embedded lanthanide ion to be purely electrostatic. Using the Thomas–Fermi model of an atom, Mayer (1941) had shown that, when $Z > 57$, the orbit of a 4f electron becomes trapped in a deep potential well only 0.2 Å from the nucleus (of charge Ze). The maximum of the radial part of the 4f wavefunction occurs at roughly 0.3 Å, and the 4f electrons play a minor role in the chemistry of the ion. Since the typical ligand distance R is roughly 2 Å, the expansion of the electrostatic crystal field in powers of (r/R) (described in section 5.3) should lead to coefficients A_{kq} that become rapidly less important as k increases. In their preliminary analysis of the paramagnetic resonance experiments on neodymium ethylsulphate, Elliott and Stevens (1951) had to use mixtures of doublets for which $M_J = \pm\frac{7}{2}$ and $\mp\frac{5}{2}$ to fit the Zeeman splitting factors $g_\parallel$ and $g_\perp$. The differences $\Delta M_J = \pm 6$ were forced on them by the site symmetry C_{3h} of Nd^{3+}. The parameters controlling such mixing are A_{66} and A_{6-6}, which, because of their large values of k, might be assumed to be small. Elliott and Stevens (1951) supposed that the

cylindrically symmetric part of the crystal field produced pure doublets $|\pm\frac{7}{2}\rangle$ and $|\pm\frac{5}{2}\rangle$ that were sufficiently close to each other to be substantially mixed when the rest of the crystal field was included. However, when they came to write up a comprehensive article on the ethylsulphate work (Elliott and Stevens 1953), their ideas had suffered a sea change. To get a consistent set of parameters for other lanthanide ions as well as for Nd^{3+}, it transpired that it was necessary to have large sixth-rank parameters A_{6q}. The situation was exaggerated for Nd^{3+} because the reduced matrix element of $V^{(6)}$ for the ground level $^4I_{9/2}$ of $4f^3$ is exceptionally large. The importance of the sixth-rank parameters was soon found to recur in other lanthanide crystals, such as the double nitrates and, to a lesser extent, the anhydrous trichlorides. A good summary of the data available in 1977 on the ethylsulphates and the trichlorides has been provided by Hüfner (1978, table 10). In passing, we note that his parameters A_{kq} are the coefficients of the unnormalized spherical harmonics used by Stevens (1952) and are hence slightly different from ours (see section 5.3).

The extent to which the sixth-rank parameters exceeded expectations could only be judged by carrying out an actual calculation. One of the earliest was that of Hutchison and Wong (1958) for the $LaCl_3$ lattice. Charges of $3e$ and $-e$ were placed at the La^{3+} and Cl^- sites, and allowance was made for the induced dipoles on the chlorine ions. In the 1950's it was none too easy to estimate $\langle r^k\rangle$ for the 4f electrons; however, a hydrogenic approximation led to values for the products $A_{kq}\langle r^k\rangle$ for Pr^{3+} that were too large by a factor of 25 for $k = 2$, and too small by a factor of 6 for $k = 6$. The results for a Thomas–Fermi wavefunction were not substantially different. Thus the combined discrepancy between the parameters for which $k = 2$ and those for which $k = 6$ amounted to roughly two orders of magnitude. Two qualitative arguments were brought to bear on the problem. Owing to the distribution of ligand electrons in a crystal, the tail of the 4f wavefunction must extend farther than it would for a free lanthanide ion, and only a small change of shape would account for the apparent increase of $\langle r^k\rangle$ for a high power of k like 6. The small value of $A_{20}\langle r^2\rangle$, on the other hand, was tentatively ascribed to the screening effect of the outer shells $5s^25p^6$ of the lanthanide ion. It was known that the 1s orbital of the hydrogen atom reduced an external electric potential Y_{kq} by the factor $1 - \sigma_k$ at the nucleus, where $\sigma_k = 2/k(k+1)$ (Judd 1959), and it might be presumed that the internal nature of the 4f electron and the plasticity of the 5s and 5p wavefunctions would give a value of σ_k approaching unity for small k.

In 1960, Ridley (1960) calculated values of $\langle r^k\rangle$ for Pr^{3+} and Tm^{3+} on the basis of a self-consistent field (without exchange), and a further improvement was made a little later by Freeman and Watson (1962) using a Hartree–Fock model of the lanthanide ion. These calculations reduced the discrepancy for $A_{20}\langle r^2\rangle$ somewhat but did little to improve matters overall. In fact, Burns (1962) used Ridley's wavefunctions to estimate $\sigma_2 \simeq 0.15$, thus throwing serious doubt on the screening hypothesis. Hutchings and Ray (1963) carried the calculation of Hutchison and Wong (1958) further by including the induced quadrupoles at the Cl^- sites in $PrCl_3$, and found that all parameters were substantially reduced, particularly A_{20}. Another step forward was taken by Ray (1963), who detected an error in the work of Burns

(1962) and obtained the larger value of 0.52 for σ_2. Subsequent calculations by Sengupta and Artman (1970), who found $\sigma_2 = 0.79$, $\sigma_4 = 0.14$ and $\sigma_6 = 0.11$ for Nd^{3+}, indicated that Ray's calculation probably underestimated the screening effect; but even with a value of 0.8 for σ_2 discrepancies of the order of a factor of 3 remained between the observed and calculated values of $A_{20}\langle r^2 \rangle$.

A contribution from a different direction was made by Jørgensen et al. (1963) with the provocative title 'Do the "ligand field" parameters in lanthanides represent weak covalent bonding?' These authors began by pointing out that the success of the parameterization scheme based on the $A_{kq}\langle r^k \rangle$ could be regarded as evidence for a crystal-field Hamiltonian involving operators that act on one electron at a time, and need not be regarded as justification for a theory based on electrostatics. This amounts to saying that each crystal-field parameter fixes the strength of the operator $(\boldsymbol{a}_f^\dagger \boldsymbol{a}_f)_{0q}^{(0k)}$ (in the notation of section 6.1.1), and that it is not necessary to consider terms of the type $(\boldsymbol{a}_f^\dagger \boldsymbol{a}_f^\dagger \boldsymbol{a}_f \boldsymbol{a}_f)_{0q}^{(0k)}$ or higher. From the point of view of the chemist who is alert to possible covalency, a single ligand on the z-axis interacts principally with the f orbital whose lobe points in the z-direction and exhibits cylindrical symmetry about the z-axis; that is, with the orbital for which $m_l = 0$. Such an interaction separates the state $|f, m_l = 0\rangle$ from the other six (corresponding to $m_l = \pm 1$, ± 2 and ± 3); and, when decomposed into operators of the type $(\boldsymbol{a}_f^\dagger \boldsymbol{a}_f)_{00}^{(0k)}$, immediately gives parameters $A_{k0}\langle r^k \rangle$ of comparable importance for $k = 2, 4$ and 6. A crystal can be built up in one's mind's eye by rotating ligands on the z-axis to their actual lattice sites. If ligand–ligand interactions can be neglected, as postulated in a formal way some years later by Newman (1971) in setting up his superposition model, this procedure can be used to assemble the crystal-field Hamiltonian from terms for which, initially, $q = 0$. Jørgensen et al. (1963) expressed their approach in a rather different way. The strength of what they refer to as σ antibonding for a ligand at $\boldsymbol{R}$ is assumed to be proportional to $|\psi_f(\boldsymbol{R})|^2$. The Coulomb interaction between the 4f electrons and the ligand charges is thus replaced by a δ-function interaction. In spite of what seems to be a model of wild eccentricity, they were able to give a reasonably good account of the relative values of the crystal-field parameters for the nine-fold co-ordinated ethylsulphates and trichlorides.

The article of Jørgensen et al. (1963) was an astonishing feu d'artifice but useless as a basis for correcting the electrostatic model. Any realistic approach must ultimately depend on the Coulomb interaction between the charged particles (the electrons and the nuclei) making up the crystal. A step in the right direction was taken by Ellis and Newman (1967), who orthogonalized a 4f wavefunction ψ_f of Pr^{3+} in $PrCl_3$ with respect to the linear combination χ of the 3s and 3p orbitals of the nine Cl^- neighbours by making replacements of the type

$$\psi_f \rightarrow (1 - S^2)^{-1/2}(\psi_f - S\chi), \tag{89}$$

where S is the overlap $\langle \psi_f | \chi \rangle$. This has the effect of extending the tail of the 4f wavefunction, and it was found that the calculated values of $A_{6q}\langle r^6 \rangle$ are increased over the electrostatic calculations of Hutchings and Ray (1963) by the large factor of 8.5. Bishton et al. (1967) extended this approach by also orthogonalizing the 5s and

5p orbitals of Pr^{3+} to the outer orbitals of the Cl^- ligands. The redistribution of electric charge that takes place is more easily tracked mathematically by rank-2 harmonics than by those of rank 6, with the result that $A_{20}\langle r^2\rangle$ is very substantially reduced and brought much closer to experiment. Raychaudhuri and Ray (1967) demonstrated that the purely electrostatic contributions to the crystal-field parameters are modified if the spatial extent of the spherical ligand ions is taken into account, and Ellis and Newman (1968) further refined the calculation by allowing for covalency, that is, charge transfer between the lanthanide ion and the surrounding ligands. They concluded that 'overlap and covalency contributions alone give nearly the correct relative magnitudes of all the crystal-field parameters', thus vindicating the conclusion of Jørgensen et al. (1963), if not their method. The review of Newman (1971) summarizes the situation at that time and gives more details than are provided here.

An extensive survey of crystal-field splittings as well as the fitted parameters (the $A_{kq}\langle r^k\rangle$ in our present notation) has been made for the tripositive lanthanides by Morrison and Leavitt (1982) in an earlier volume of this Handbook. Newman's current view of his ab initio work of some 20 years ago can be gauged from a recent article on the variability of overlap and attendant integrals on lanthanide–ligand distance (Newman and Ng 1986). The modifications brought about by modern computational techniques have been comparatively minor. This is also the impression given by the article of Garcia and Faucher (1985), where some twelve lanthanide or lanthanide-doped compounds are described. A flavor of the present philosophy of Jørgensen on the origin of the crystal-field parameters can be obtained from a recent publication (Jørgensen et al. 1986), where the importance of the contributions from the kinetic-energy operator (included, of course, by Newman in his work) is stressed.

All this is not to say, however, that the parameters A_{kq}, which are associated with the single-electron operators $(\boldsymbol{a}^\dagger \boldsymbol{a})^{(0k)}_{0q}$, are adequate to fit the observed splittings of the levels. This point is taken up in section 7.6.

7.1.1. *Crystal-field invariants*

The numerical values of the crystal-field parameters A_{kq} depend on the choice of coordinate axes. For C_{3h} symmetry, for example, the two terms $A_{66}Y_{66}$ and $A_{6-6}Y_{6-6}$ appear in the crystal-field Hamiltonian for a single 4f electron, but it is found that, in calculations of the splittings of the levels, the two sixth-rank parameters always appear in the combination $A_{66}A_{6-6}$. It is not difficult to see why that should be so. Under a rotation of the x and y axes by ϵ about c, the three-fold axis of symmetry, we have $\phi \to \phi + \epsilon$, and so $Y_{6\pm6} \to e^{\pm 6\epsilon} Y_{6\pm6}$. This is equivalent to making the substitutions $A_{6\pm6} \to e^{\mp 6\epsilon} A_{6\pm6}$ in the original Hamiltonian, and so the product $A_{66}A_{6-6}$ is an SO(2) invariant, since we have complete freedom in picking ϵ. The splittings of a level are physical quantities and cannot depend on ϵ: hence the sixth-rank parameters can only influence the splittings through the single quantity $A_{66}A_{6-6}$. Had we started with the more familiar form $A^6_6(Y_{66} + Y_{6-6})$, we would have concluded that the sign of the (necessarily) real parameter A^6_6 cannot be determined from the energies of the sublevels. In their analysis of the effect of

configuration interaction on the crystal splittings of Pr^{3+} $4f^2$ in $LaCl_3$: Pr^{3+}, Morrison et al. (1970a) considered an additional term of the type $iB_6^6(Y_{66} - Y_{6-6})$, but excluded it on the grounds that the local symmetry at a Pr^{3+} site approximates closely to D_{3h}. It was not necessary to use that argument, since the effect of including B_6^6 is equivalent to making the substitution $A_6^6 \rightarrow [(A_6^6)^2 + (B_6^6)^2]^{1/2}$ everywhere, the replacement being the new SO(2) invariant.

When rotations of the coordinate frame in the full three-dimensional space are considered, other invariants appear. If $A^{(k)}$ denotes the collection of parameters A_{kq}^* $(-k \leqslant q \leqslant k)$ the crystal field Hamiltonian for a single 4f electron can be written as $\Sigma_k r^k (A^{(k)} \cdot Y^{(k)})$. Although it may seem strange to construct a tensor out of numerical coefficients, there is nothing to prevent our doing so; after all, the point-charge model gives the A_{kq} directly in terms of the ligand coordinates (R_L, Θ_L, Φ_L), which necessarily change too when the coordinate frame is rotated. Viewed in this light, our approach makes it clear that other kinds of invariants can be constructed: all we have to do is ensure that the final rank in a multiply-coupled product of the tensors $A^{(k)}$ be zero. Kustov et al. (1980) pointed out that, for a given level ^{2S+1}L, the energies E_i of the sublevels relative to the center of gravity of the level are related to the invariants $A^{(k)} \cdot A^{(k)}$ by an expression of the form

$$\sum_i g_i E_i^2 = \sum_{k=2,4,6} h_k (A^{(k)} \cdot A^{(k)}),$$

where g_i is the degeneracy of sublevel i. The coefficients h_k depend on the level under consideration. Kustov et al. (1980) determined the three invariants $A^{(k)} \cdot A^{(k)}$ from the observed splittings of Nd^{3+} $4f^3$ ($^4F_{3/2}$, $^4I_{9/2}$, $^4I_{11/2}$), the process being repeated for 43 different crystals containing Nd^{3+}. Qualitative differences between garnets, scheelites, perovskites and fluorides were noted, and the method was extended to Eu^{3+} in NaBaZn silicate glass subjected to varying excitation wavelengths.

A more elaborate form of analysis was presented by Leavitt (1982), who found that corrections due to the J mixing of neighboring levels, if sufficiently small, could be taken into account by including the invariants of the type $(A^{(k')}A^{(k'')})^{(k)} \cdot A^{(k)}$ in the sum above. Yeung and Newman (1985) called attention to the difficulty of finding the crystal-field parameters A_{kq} for low-symmetry crystals, giving $Er^{3+}:LaF_3$ as a striking example of three widely varying sets of parameters extant in the literature. They showed that values of the $A^{(k)} \cdot A^{(k)}$ found from experiment, taken with a detailed knowledge of the crystal structure, could be used to derive the intrinsic parameters associated with the superposition model. In later work, they classified the quartic invariants

$$(A^{(k_1)}A^{(k_2)})^{(k)} \cdot (A^{(k_3)}A^{(k_4)})^{(k)},$$

pointing out that the most general f-electron lanthanide crystal field is described by 27 parameters, so some of the quartic invariants are not independent (Yeung and Newman 1986a). The quartic invariants have been used by Yeung and Newman (1986b) to test the consistency of the fits to 17 levels of Er^{3+} $4f^{11}$ in $YAlO_3$ under different constraints on the spin-correlated crystal-field parameters c_k (defined in section 7.6.1).

7.2. *Hypersensitive transitions*

The existence of many plausible sources for the contributions to the observed crystal-field parameters has an interesting parallel in the extraordinary sensitivity to the environment of certain lines in the absorption spectra of the lanthanides. These lines, the so-called hypersensitive transitions, satisfy the same selection rules as electric-quadrupole radiation: that is, $\Delta J \leqslant 2$. This condition was first noticed when the absorption spectra obtained by Hoogschagen and Gorter (1948) for different kinds of aqueous solutions were compared. In going from solutions of the chlorides to those of the nitrates, the lines ${}^4I_{15/2} \rightarrow {}^2H_{11/2}$ of Er^{3+} and ${}^4I_{9/2} \rightarrow {}^4G_{5/2}$ of Nd^{3+} show noticeable changes in their intensities relative to almost all other lines. Adding alcohol produces a marked enhancement of these two lines, as was demonstrated to the writer during a visit to Dr. C.K. Jørgensen at his laboratory in Cologny, Geneva, in 1963. All that was required was a test tube containing a solution of neodymium ions and a hand-held spectrograph. Other hypersensitive lines in the spectra of various lanthanides could be picked out without much difficulty. It was immediately recognized that this phenomenon, when cast in terms of the parameters Ω_k of section 5.4.2, exhibits itself by the variability of Ω_2. Why should that parameter be more sensitive to the environment of a lanthanide ion than the others?

A number of possible explanations were explored in an early article (Jørgensen and Judd 1964). The extension of the tail of the 4f wavefunction, as represented by the substitution given by (89), was quickly seen to be ineffective in enlarging $\langle r^2 \rangle$ to the point where pure quadrupole transitions could take place. Vibronic transitions were at first considered to be prime sources for the intensities in view of the identical selection rule $\Delta J \leqslant 2$ [see eq. (74)]. An order-of-magnitude calculation fell short by a factor of 10^3, however. Resort was finally made to a mechanism based on the inhomogeneity of the dielectric. The electromagnetic radiation field induces dipoles in the ligands surrounding a lanthanide ion, and the re-radiation that takes place must deviate markedly from a plane wave. This idea led to a value of Ω_2 that was too small by a factor of only 30. The discussion of these various sources was marred by an uncritical acceptance of the fallacious argument of Broer et al. (1945) (see section 5.4), which, when corrected, provides another possible source for Ω_2 in complexes whose symmetry permits harmonics of the type Y_{1q} in the crystal-field potential (Judd 1966b). Objections to this mechanism were later raised by Mason et al. (1975) on the grounds that it could not account for the hypersensitivity of Eu^{3+} doped into sites of D_{2d} or D_{3h} symmetry in metal oxide lattices (Blasse et al. 1966), nor for the more spectacular hypersensitivity of the transitions reported by Gruen et al. (1967) for the supposedly planar molecules of the lanthanide trihalides. However, there is some evidence that the structure of the latter are pyramidal (see Giricheva et al. 1967, Charkin and Dyatkina 1964); in which case the mechanism in question might well play a major role.

An apparently more promising mechanism, called dynamic coupling, was introduced by Mason et al. (1974, 1975). The idea is that the 4f electrons polarize the ligands, thus giving the entire complex of lanthanide ion and neighbors an extended dipole moment (should the site symmetry allow it) that has an enhanced interaction

with the radiation field. The polarizability of the ligands plays a central role in the dynamic-coupling mechanism, just as it did for the mechanism based on the inhomogeneity of the dielectric. With hindsight, it is perhaps not so surprising that the mathematics is identical for the two mechanisms, and indeed Newman (private communication) suspected as much all along. Thus one mechanism is just an alternative verbalization of the other (Judd 1979). Mason et al. (1975) did not encounter the discrepancy of the factor of 30 mentioned above because they used better structural information and polarization data. However, neither approach allowed for the screening by the outer shells of the lanthanide ions, which are able to follow the oscillatory variations of the vector $\boldsymbol{E}$ of the radiation field. The appropriate reduction factor for Ω_2 is $(1-\sigma_2)^2$; its omission vitiates the formula of Mason [1980, eq. (9)] as well as the reported good agreement between experiment and theory, such as that for the $^4I_{9/2} \rightarrow {}^4G_{5/2}$ transition of tris(1,3-diphenyl-1,3-propanedionato) aquoneodymium(III) described by Kirby and Palmer (1981). Another example is the detailed comparison of the dynamic-coupling and the electrostatic mechanisms that Richardson et al. (1981) made for Pr^{3+}, Eu^{3+}, Tb^{3+} and Ho^{3+} complexes of trigonal symmetry.

Mason (1985) has argued that a compensatory antiscreening exists as a result of an expanded 4f wavefunction, and this seems the most plausible way out of the difficulty. It is always possible, of course, that some crucial component in the theory has not been identified. Faced with a striking phenomenon, the theorist is always tempted to believe that a single key will unlock the mystery. In the case of the hypersensitivity it is more likely that various mechanisms combine or interfere to varying degrees under different experimental conditions. Such was the conclusion reached by Peacock (1975) after an examination of the status of the subject in the mid-1970's. It may still be valid today.

7.3. *Transitions between sublevels*

The intensity parameters Ω_k are appropriate for examining the coalesced transitions from level to level of the type $J \rightarrow J'$. The appearance of any fine structure (or, to use a more appropriate term, crystal fine structure) corresponding to transitions from sublevel to sublevel of the type $\mu \rightarrow \mu'$ makes it possible to extract more information about the nature of the transitions. All work in that area stems from the initial study of Axe (1963), which has been briefly mentioned in section 5.4.2. In order to appreciate the later developments, we need to recast the theory of section 5.4.2 in terms of tensor operators. We regard the even-rank tensors $\boldsymbol{V}^{(t)}$ as arising from the inner part of expression (71) when closure is used to remove the intermediate states $\chi_{J''}$ and when $\boldsymbol{Y}_k$ (for odd k) and $\boldsymbol{D}$ are coupled to rank t. In the electrostatic model the $\boldsymbol{Y}_k$ part is implicitly multiplied by $R^{-k-1}Y^*_{kq}(\Theta,\Phi)$ of section 5.3 for a ligand at $\boldsymbol{R}$; so the effective operator driving the transition is proportional to a sum over k and t of various terms of the type

$$R_L^{-k-1}(\boldsymbol{Y}_L^{(k)}\boldsymbol{V}^{(t)})^{(1)}\cdot\boldsymbol{E} \quad (k \text{ odd}, t \text{ even}), \tag{90}$$

where the spherical harmonics $Y_{kq}(\Theta,\Phi)$ have been subsumed into the tensor $\boldsymbol{Y}^{(k)}$.

The subscript L indicates the coordinates of a particular ligand L. The fact that (90) is an SO(3) scalar is predicated on its necessary invariance with respect to the orientation of our coordinate frame. It must also be invariant with respect to inversions and reflections.

For an actual crystal, expression (90) must also be summed over the ligands L after including their charges q_L. This has the effect of converting (90) to $(\boldsymbol{T}^{(k)}\boldsymbol{V}^{(t)})^{(1)}\cdot\boldsymbol{E}$, where $\boldsymbol{T}^{(k)}$ is an invariant with respect to the point group of the lanthanide site. In the electrostatic model, the relative weighting of $(\boldsymbol{T}^{(k)}\boldsymbol{V}^{(k+1)})^{(1)}$ and $(\boldsymbol{T}^{(k)}\boldsymbol{V}^{(k-1)})^{(1)}$ is determined by the relative importance of the virtual excitations $\mathrm{f}\rightarrow\mathrm{d}$, $\mathrm{d}\rightarrow\mathrm{f}$ and $\mathrm{f}\rightarrow\mathrm{g}$. Even without that constraint, it is clear that $(\boldsymbol{T}^{(k)}\boldsymbol{V}^{(t)})^{(1)}\cdot\boldsymbol{E}$ is not the most general scalar operator linear in $\boldsymbol{V}^{(t)}$ and $\boldsymbol{E}$. If we accept that t is even (a result of limiting perturbation theory to second order), there might very well exist tensors $\boldsymbol{T}^{(k)}$ that are scalar with respect to G but for which $k=t$. This possibility is excluded by the electrostatic model, of course. But other options are open to us. In a remarkable analysis of great generality, in which overlap and covalency were considered, Newman and Balasubramanian (1975) showed that the relative weighting of the two tensors $(\boldsymbol{T}^{(k)}\boldsymbol{V}^{(k\pm1)})^{(1)}$ could be relaxed, thereby clarifying the results of Becker (1971) for Ho^{3+} in YPO_4. More remarkably, they also showed that tensors $\boldsymbol{T}^{(k)}$ for which $k=t$ could occur. In the special case for which $G=C_{\infty v}$, however, they are excluded. This is the situation for a single ligand that exhibits cylindrical symmetry with respect to the axis linking it to the lanthanide ion. To see why this geometry gives no new terms, take the cylindrical symmetry axis to be the z-axis and xz the vertical reflection plane. Only the component $T_0^{(k)}$ appears, and this is necessarily invariant with respect to G. The effect of the reflection operator R on $\boldsymbol{E}$ is given by $E_x\rightarrow E_x$, $E_y\rightarrow -E_y$, and $E_z\rightarrow E_z$; that is, $E_{\pm}^{(1)}\rightarrow -E_{\mp}^{(1)}$ and $E_0^{(1)}\rightarrow E_0^{(1)}$. As it stands, there is no way of determining $RV_p^{(t)}R^{-1}$ unambiguously, since eq. (61) only specifies how $\boldsymbol{V}^{(t)}$ behaves with respect to rotations. However, we know that a component tensor $\boldsymbol{v}^{(t)}$ must ultimately be set between two f-electron wavefunctions, and the reflection properties of the latter can be found from the spherical harmonics Y_{3m}. The condition that $\langle \mathrm{f}m|v_p^{(t)}|\mathrm{f}m'\rangle$ not always vanish yields $RV_p^{(t)}R^{-1}=(-1)^pV_{-p}^{(t)}$. The relation

$$(k\,0,t\,p|1\,-p)=(-1)^{k+t+1}(k0,t\,-p|1\,p)$$

for the CG coefficients of SO(3) can be used to show

$$R(\boldsymbol{T}^{(k)}\boldsymbol{V}^{(t)})^{(1)}\cdot\boldsymbol{E}R^{-1}=(-1)^{k+t+1}(\boldsymbol{T}^{(k)}\boldsymbol{V}^{(t)})^{(1)}\cdot\boldsymbol{E}$$

for $C_{\infty v}$ symmetry. The invariance of the operator sandwiched between R and R^{-1} requires that $k\neq t$ for it to be nonzero. Although no actual crystal possesses $C_{\infty v}$ symmetry, the possibility of regarding a crystal as the superposition of isolated ligands, each one interacting solely with the central lanthanide ion in a cylindrically symmetrical way, is an extremely appealing approximation (Newman 1971). The fact that the new operators (those for which $k=t$) can only describe deviations from that model lessened the impact that the article of Newman and Balasubramanian (1975) had on crystal spectroscopy. An added reason is that they described their method in terms of local and non-local operators without making clear what the distinction was.

7.3.1. *Anisotropic ligands*

The theory of Newman and Balasubramanian (1975) languished in the literature until Kuroda et al. (1980) examined the intensities of the $\Delta M_J = \pm 1$ component of the $^7F_0 \rightarrow {}^5D_2$ transition in complexes of the type $[EuO_9]$ possessing D_3 symmetry. A more striking example is that of D_4 symmetry, which has been discussed by Reid and Richardson (1983a). If we adopt the mechanism of the inhomogeneous dielectric, each polarizability tensor $\boldsymbol{\alpha}^{(n)}$ for ligand L at $\boldsymbol{R}_L$ leads to the contribution $(\boldsymbol{\alpha}^{(n)}\boldsymbol{E}^{(1)})^{(1)}$ to the induced dipole moment produced by the electric field $\boldsymbol{E}$ of the radiation field. The potential at a 4f electron at $\boldsymbol{r}_j$ is given by

$$(\boldsymbol{\alpha}_L^{(n)}\boldsymbol{E}^{(1)})^{(1)}\cdot(\boldsymbol{r}_j - \boldsymbol{R}_L)/|\boldsymbol{r}_j - \boldsymbol{R}_L|^3,$$

for which the leading non-trivial term is proportional to

$$\langle r^2\rangle R_L^{-4}(\boldsymbol{\alpha}_L^{(n)}\boldsymbol{E}^{(1)})^{(1)}\cdot(\boldsymbol{V}^{(2)}\boldsymbol{Y}_L^{(3)})^{(1)},$$

when summed over the electrons j. A recoupling yields terms of the type

$$\langle r^2\rangle R_L^{-4}\{(\boldsymbol{\alpha}_L^{(n)}\boldsymbol{Y}_L^{(3)})^{(k)}\boldsymbol{V}^{(2)}\}^{(1)}\cdot\boldsymbol{E}. \tag{91}$$

For a ligand characterized only by a charge and an isotropic polarizability, we have $n = 0$ and so $k = 3$. In that case we recover a term of the type given by (90). But by allowing for anisotropic ligand polarizability we also admit nonzero values of n, and a resultant rank k of 2 is now possible. For a symmetric Cartesian tensor $\alpha_{\mu\nu}$ we must take $\boldsymbol{\alpha}_L^{(1)} = 0$, and we are thus left with $\boldsymbol{\alpha}_L^{(2)}$. Should $(\alpha_0^{(2)})_L$ be the only non-vanishing component of $\boldsymbol{\alpha}_L^{(2)}$, so that the ligand possesses cylindrical symmetry about the z-axis, and if, in addition, the ligand is itself situated on the z-axis, in which case $Y_{30}(\Theta_L, \Phi_L)$ is the only non-vanishing component of $\boldsymbol{Y}_L^{(3)}$, the coupled product $(\boldsymbol{\alpha}_L^{(2)}\boldsymbol{Y}_L^{(3)})^{(k)}$ vanishes for even k, since all CG coefficients $(20,30|kq)$ vanish when k is even. We thus recover again the result of Newman and Balasubramanian (1975) for $G \equiv C_{\infty v}$. In many cases, however, other components of $\boldsymbol{\alpha}_L^{(2)}$ exist and these allow non-vanishing terms of the type $k = t$ to appear. We thus obtain a concrete example of what Newman and Balasubramanian envisaged in general terms.

To see what effects the new operators (91) can produce, consider the transition $^7F_0 \rightarrow {}^5D_2$ of Eu^{3+} in D_4 symmetry. The crystal field splits $^5D_2$ into four components, one of which is the doublet characterized by $M_J = \pm 1$. The electrostatic model, as represented by (90), could give a transition if

$$\sum_L R_L^{-k-1}(\boldsymbol{Y}_L^{(k)}\boldsymbol{V}^{(2)})^{(1)} \quad (k = 1 \text{ or } 3) \tag{92}$$

were non-vanishing. For D_4 symmetry, and with suitably chosen axes, a single ligand at (Θ, Φ) implies the existence of seven others at $(\Theta, \Phi + \frac{1}{2}n\pi)$ and $(\pi - \Theta, -\Phi + \frac{1}{2}n\pi)$, where n is an integer. Taking all eight, we find

$$\sum_L Y_{kq}(\Theta_L, \Phi_L) = 0 \qquad (k = 1 \text{ or } 3),$$

so no transition from $^7F_0$ to the doublet of $^5D_2$ for which $M_J = \pm 1$ is possible. On

the other hand,

$$\sum_{\mathrm{L}} (\boldsymbol{\alpha}_{\mathrm{L}}^{(2)} \boldsymbol{Y}_{\mathrm{L}}^{(3)})_0^{(2)} \sim \sum_{\mathrm{L}} Y_{20}(\Theta_{\mathrm{L}}, \Phi_{\mathrm{L}}) \neq 0,$$

where we have used the fact that any tensor of rank two must transform like the spherical harmonics Y_{2q}. Thus a term in (91) of the type

$$(\boldsymbol{\alpha}_{\mathrm{L}}^{(2)} \boldsymbol{Y}_{\mathrm{L}}^{(3)})_0^{(2)} V_{\pm}^{(2)} E_{\mp}$$

has non-vanishing matrix elements (provided there is a large enough departure from perfect Russell–Saunders coupling to overcome the change in S), and a line should be seen in the σ spectrum. The D_3 case studied by Kuroda et al. (1980) is not so clear-cut as the example presented here, since there are terms in the crystal field that mix $|^5D_2, M_J = \pm 2\rangle$ into $|^5D_2, M_J = \mp 1\rangle$ when D_3 symmetry obtains. The effects of the anisotropic ligands are thus blended with those coming from a more mundane source. An extrication of these contributions and a detailed parameterization has been carried out by Dallara et al. (1984) for similar trigonal Eu^{3+} systems.

It is natural to wonder whether changes need to be made to the selection rules worked out by Hellwege (1948). It would be strange if the powerful group-theoretical arguments he developed required modification just because some of the atoms in the crystal were not perfectly isotropic. The resolution of the paradox lies in the actual transition that was chosen to be studied. We concealed the fact that the D_4 crystal field must mix a small amount of, say, $|^5D_4, M_J = \mp 3\rangle$ into $|^5D_2, M_J = \pm 1\rangle$. The operator $\Sigma_{\mathrm{L}} (\boldsymbol{Y}_{\mathrm{L}}^{(5)} \boldsymbol{V}^{(4)})_p^{(1)}$ can connect $^7F_0$ to the doublet $|^5D_4, M_J = \mp 3\rangle$ provided $\Sigma_{\mathrm{L}} Y_{54}(\Theta_{\mathrm{L}}, \Phi_{\mathrm{L}})$ does not vanish; and, indeed, for an arbitrary set of coordinates $(\Theta_{\mathrm{L}}, \Phi_{\mathrm{L}})$ consistent with D_4 symmetry it does not. Even in the electrostatic model, then, the transition from $^7F_0$ to $|^5D_2, M_J = \pm 1\rangle$ is allowed, albeit very feebly. The new operators (for which $k = t$) can produce large changes in intensity but they do not violate any selection rules.

In the process of working out the implications of expression (91), it was mentioned that terms of the type given by (90) could occur when we take isotropic ligands and set $n = 0$. Since their origin is different, the relative weighting of the two tensors $(\boldsymbol{Y}^{(k)} \boldsymbol{V}^{(k \pm 1)})^{(1)}$ as determined by the electrostatic model no longer obtains. Reid and Richardson (1983b, 1985a) used this property to disentangle the two mechanisms, and Reid et al. (1983) showed that in many cases the dynamic-coupling mechanism plays the dominant role. However, Poon and Newman (1984) have pointed out that the absence of any consideration of overlap and covalency in that kind of work still leaves something to be desired.

7.4. *Vibronic parameters*

It is only within the last few years that attempts have been made to set up a detailed theory for the intensities of vibronic transitions. To understand what is involved we can return to expression (72) and manipulate it in much the same way as we did the corresponding electronic linkage given by (71). This somewhat lengthy procedure can be circumvented by noticing that any operator producing an

electronic transition in virtue of ligands situated at $\boldsymbol{R}_L$ can be modified to produce a vibronic transition by the simple expedient of making the substitution $\boldsymbol{R}_L \to \boldsymbol{R}_L + \boldsymbol{d}_L$, where $\boldsymbol{d}_L$ is the displacement of ligand L from its equilibrium position $\boldsymbol{R}_L$. Methods for coping with the general problem of expressing the spherical harmonics $Y_{kq}(\Theta_L, \Phi_L)$ as sums over coupled products in which $\boldsymbol{d}_L$ appears have been given elsewhere (Judd 1975, ch. 5). In the present case we only require terms linear in $\boldsymbol{d}_L$ in order to produce a single-phonon transition. A further simplification is that $\boldsymbol{Y}_L^{(k)}$ in expression (90) is multiplied by R_L^{-k-1}, thus providing a product that satisfies Laplace's equation. Under these conditions it is straightforward to show that the substitution $\boldsymbol{R}_L \to \boldsymbol{R}_L + \boldsymbol{d}_L$ implies

$$R_L^{-k-1}\,\boldsymbol{Y}_L^{(k)} \to [(k+1)(2k+1)]^{1/2}\,R_L^{-k-2}\,(\boldsymbol{Y}_L^{(k+1)}\,\boldsymbol{d}_L^{(1)})^{(k)}, \tag{93}$$

so that expression (90) generates terms proportional to

$$R_L^{-k-2}((\boldsymbol{Y}_L^{(k+1)}\boldsymbol{d}_L^{(1)})^{(k)}\,\boldsymbol{V}^{(t)})^{(1)}\cdot\boldsymbol{E} \quad (k \text{ odd}, t \text{ even}). \tag{94}$$

Such terms are equivalent to those obtained by Satten et al. (1983) in their study of the excitations of the T_{1u} vibrational mode of the octahedral complex UCl_6^- at $260\,cm^{-1}$. They were aware that their approach would work in a similar way for lanthanide complexes; their choice of an actinide was partly determined by their familiarity with the UCl_6^- complex. Another important consideration was the high symmetry of the uranium site, which greatly reduces the number of intensity parameters required in the analysis. To assess the situation we note first that the possible pairs (k,t) in expression (94) are (1,2), (3,2), (3,4), (5,4), (5,6) and (7,6). The number of T_{1u} representations of O_h, that occur in the representations $\mathscr{D}_k^-$ of O(3) are 1, 1, 2 and 2 for $k = 1, 3, 5$ and 7, so we expect 9 parameters in all. Satten et al. (1983) reduced that number to 6 by carrying out a complete closure over all virtual electronic states, which has the effect of fixing the ratio of the two operators (94) for which $t = k \pm 1$. They were able to account quite well for the relative intensities of some 20 or so transitions of the type $A_{1g}(^3H_4) \to T_{1u}(^{2S+1}L_J)$, where $^{2S+1}L_J$ is a level of $5f^2$.

Satten et al. (1983) were not the first to attempt to fit vibronic lines, though their method is the easiest to describe. Some five years earlier, Faulkner and Richardson (1978a) had set up a vibronic-coupling model for the octahedral complex $EuCl_6^{3-}$ in $Cs_2NaEuCl_6$. In addition to the terms of the type (94) coming from the electrostatic model, they took into account contributions coming from the dynamic-coupling mechanism (or, equivalently, the mechanism based on an inhomogeneous dielectric). For us, we have only to make the substitution (93) in expression (91), thereby getting operators of the type

$$R_L^{-5}\{(\boldsymbol{\alpha}_L^{(n)}(\boldsymbol{Y}_L^{(4)}\,\boldsymbol{d}_L^{(1)})^{(3)})^{(k)}\,\boldsymbol{V}^{(2)}\}^{(1)}\cdot\boldsymbol{E}. \tag{95}$$

Faulkner and Richardson (1978a) assumed isotropic ligands, for which $n = 0$. Thus the rank k in expression (95) is limited to 3. After making various estimates of the charges, polarizabilities, and bond lengths, they were able to obtain reasonably good values for the relative intensities of the three vibronic lines

$$A_{1g}(^7F_0) \to E_g(^5D_2), \qquad A_{1g}(^7F_0) \to T_{2g}(^5D_2), \qquad T_{1g}(^7F_1) \to T_{1g}(^5D_1)$$

of $EuCl_6^{3-}$. In a companion study, they examined the magnetic-dipole and vibronically induced electric-dipole intensities of the $^5D_4 \rightarrow {}^7F_J$ transitions of Tb^{3+} in $Cs_2NaTbCl_6$, with generally satisfactory results. A more complete analysis of the vibronic fluorescence spectrum of $Cs_2NaEuCl_6$ was later carried out by Flint and Stewart-Darling (1981).

With fewer transitions to analyze, Faulkner and Richardson (1978a,b) did not attempt to fully parameterize their spectra. Their articles are thus different in style from that of Satten et al. (1983). In conjunction with various colleagues, they were nevertheless able to carry out similar analyses for other RCl_6^{3-} systems with considerable success (Faulkner et al. 1979, Morley et al. 1981, 1982a,b, Hasan and Richardson 1982). After the appearance of the article of Satten et al. (1983), Reid and Richardson (1984) decided to try to extend the parameterization of Satten et al. (1983) in a parallel way to the analysis of Newman and Balasubramanian (1975). A physical realization of this is provided by anisotropic ligands, which permit terms for which $n = 2$ in the operator given by (95). Ranks of 2 and 4 for k are now possible, and the number of parameters is increased from 9 to 11. However, the fit obtained by Reid and Richardson to Satten's UCl_6^- data was not improved when the two new operators were included, thus indicating that the superposition model (with $C_{\infty v}$ symmetry for individual U–Cl pairs) is adequate. One of the interesting results of the nine-parameter fit was the discovery that the relative signs of the parameters associated with the operators for which $t = k \pm 1$ could not be accounted for in the electrostatic model. Other mechanisms are evidently important.

Some impression of the continued interest in the energy levels of lanthanides at cubic sites can be gauged from the exchange of views between Tanner (1986) and Richardson (1986) concerning Tm^{3+} in the Cs_2NaYCl_6 system.

7.5. *External magnetic fields*

A large part of the theory of the effect of an external magnetic field on lanthanide ions in crystals was developed in the context of paramagnetic resonance (Bleaney and Stevens 1953). It is that field that bequeathed optical spectroscopists the spin Hamiltonian and its various elaborations. This is not to say that such devices have ever been taken much advantage of. After all, the perturbation Hamiltonian $\beta \boldsymbol{H} \cdot (\boldsymbol{L} + 2\boldsymbol{S})$, where β is the Bohr magneton and $\boldsymbol{H}$ the applied magnetic field, is particularly simple to evaluate, since the quantum number $\boldsymbol{S}$ and L are used in defining all lanthanide states.

A basic theorem was worked out by Kramers (1930b), who showed that any atomic system possessing N electrons and subject only to external fields of an electrostatic kind must exhibit at least a double degeneracy in its energy levels when N is odd. A crucial step in Kramers's proof involved taking complex conjugates. Today this would be done by invoking the time-reversal operator T. It has the advantage of immediately drawing a distinction between electric potentials, which are time-reversal invariant, and the operators $\boldsymbol{S}$ and $\boldsymbol{L}$ in the Zeeman Hamiltonian, for which

$$T\boldsymbol{L}T^{-1} = -\boldsymbol{L}, \qquad T\boldsymbol{S}T^{-1} = -\boldsymbol{S}. \tag{96}$$

These properties lead to the linear splittings of the doublets when the external magnetic field is applied.

It might be wondered how N can be considered an integer at all for an ion in a crystal, where inter-penetrating electronic orbitals are a commonplace. The answer is that the exact superposition of a multitude of doublets, each one being provided by an identical lanthanide ion for which N is odd, becomes smeared into a narrow band. Its width is usually small compared to βH, and so the effect on the optical spectrum is negligible.

The pair of eigenstates corresponding to a given doublet are often called Kramers conjugates. In an extensive tabulation of the number and kind of the various sublevels arising from a level J ($\leqslant 8$) in a crystal field, Prather (1961) listed the Kramers conjugates for all crystal point symmetries. Of course, certain site symmetries permit doublets when N is even, as we have already seen (in section 7.3.1) for the components of $4f^6\ {}^5D_2$ for which $M_J = \pm 1$ in D_3 symmetry. The action of T on an eigenstate must produce another eigenstate corresponding to the same energy when $\boldsymbol{H} = 0$; however, when N is even we have no guarantee that the two eigenstates are distinct. In the special case just mentioned, the two states $|M_J = \pm 1\rangle$ are indeed distinct, but $T|M_J = 0\rangle$ is equivalent (to within a phase factor) to $|M_J = 0\rangle$ itself.

7.5.1. *Transverse Zeeman effect for uniaxial crystals*

For many point symmetries at a lanthanide site, the effective Zeeman Hamiltonian for a doublet can be written as

$$g_{\parallel}\beta H_z S_z + g_{\perp}\beta(H_x S_x + H_y S_y), \tag{97}$$

where the components S_x, S_y and S_z of the fictitious spin $\boldsymbol{S}$ act in a space for which $S = \frac{1}{2}$, corresponding to the doublet in question. It is easy to confirm that for $\boldsymbol{H} \perp \boldsymbol{c}$ (where the crystal axis $\boldsymbol{c}$ is parallel to the z-axis), the splitting of the doublet is independent of the azimuthal angle ϕ defining the direction of $\boldsymbol{H}$ in the basal plane. But although the splittings of both the upper and lower doublets involved in an optical transition may be invariant with respect to rotations of the crystal about $\boldsymbol{c}$, the spectrum is not necessarily invariant too. Spedding et al. (1965) examined the variation of the absorption spectrum of erbium ethylsulphate when $\boldsymbol{c}$, $\boldsymbol{H}$ and $\boldsymbol{k}$ (the direction of the incident light) are mutually perpendicular. They found 60° periodicities in both the energies of the levels and the intensities. A theory, based on the mixing by the Zeeman Hamiltonian of neighboring sublevels, was developed by Murao et al. (1965). A subsequent article by Murao et al. (1967) introduced an antiunitary operator whose associated eigenvalues could be used to classify the C_{3h} doublets (appropriate for the ethylsulphates) according to two types, A and B. Syme et al. (1968) developed the theory further without, however, making it more accessible to the casual reader. The field of study was extended to systems possessing an even number of electrons by Spedding et al. (1968), who reported results for holmium ethylsulphate. Additional theoretical developments, still cast in terms of the properties of the antiunitary operator mentioned above, were described by Kambara et al. (1972, 1973). They showed that for sites of D_2 symmetry large variations in the intensities of transitions of the types $A \rightarrow A$ and $B \rightarrow B$ occur as the

crystal is rotated, while transitions of the types A → B and B → A usually show only small variations. A key element in their analysis is the classification of the states of the (split) doublet by the groups C'_{2h} and C''_{2h} whose symmetry axes are fixed in the crystal, make 90° with respect to each other, and coincide with $\boldsymbol{H}$ from time to time as the crystal is rotated. When that happens they become symmetry groups of the total Hamiltonian and their irreducible representations can be used to label the states. If the labels assigned to the upper and lower components of a particular doublet are reversed in passing from C'_{2h} to C''_{2h} the doublet is of type B: no reversal corresponds to type A.

The reversal or constancy of the C_{2h} labels of a doublet as the crystal is rotated has to be used in calculating the relevant transition probabilities. It is here that an added feature occurs: for the odd-parity part of the crystal-field Hamiltonian responsible for mixing states of opposite parity into the f shell itself possesses certain symmetry properties with respect to rotations about c, and these must be taken into account when the effective operator producing the transition is considered. It turns out that the transitions A → A and B → B exhibit the wide fluctuations in intensity as the crystal is rotated. The details of this analysis for D_{2d} symmetry have been described elsewhere (Judd and Runciman 1976). Similar results obtain for the other two tetragonal groups D_4 and C_{4v}, except that the striking alternations in intensity now occur for A → B and B → A. For hexagonal crystals, the variations in the intensities of the Zeeman components can only occur if the magnetic fields are strong enough to mix neighboring sublevels.

7.5.2. *Magnetic circular dichroism*

The differential absorption (or emission) of left- and right-circularly polarized light of a lanthanide crystal subjected to a magnetic field has not received the attention one might have expected. The reference list in the recent book by Piepho and Schatz (1983, p. 616) contains not a single article that refers specifically to a lanthanide spectrum. Part of the reason for this is the ease with which Zeeman data for the f → f transitions can be obtained from the pure electronic spectra. However, magnetic circular dichroism (MCD) possesses several advantages when the lines are broad, as is often the case for those with a vibronic origin.

The theory of Faraday rotation for lanthanide ions was developed by Shen (1964) and applied to several ions in CaF_2 by Shen and Bloembergen (1964). At the Zeeman Centennial meeting in Amsterdam in 1965, Margerie (1967) described his work on the ions Sm^{2+} in CaF_2, where the breadth of several lines originating from $4f^6\,{}^7F_0 \rightarrow 4f^5 5d$ was too great to permit their g values to be determined by conventional means. The host lattice CaF_2 was again used by Weakliem et al. (1970) for a more extensive survey of the MCD spectra of the divalent lanthanides. Entire bands were found to exhibit a common circular dichroism, which was attributed to a single dominant electronic state and a sequence of vibrational components possessing the same symmetry. The energy levels of $Eu^{2+}\,4f^6({}^7F)5d(e_g)$ were worked out as a function of the Coulomb exchange integrals $G_k(4f, 5d)$ by Weakliem (1972), who found that values given by roughly one half of the corresponding free-ion values were required to fit the data. Schwartz and Shatz (1973) chose the

host crystal Cs_2NaYCl_6 for their analysis of the $4f \rightarrow 5d$ transitions of Ce^{3+}. They found that the vibronic structure could be explained almost entirely in terms of progressions based on the breathing mode of the $CeCl_6$ complex. Schwartz (1975) turned his attention to transitions within the 4f shell by studying the MCD of the vibronic transitions associated with $^7F_1(T_{1g}) \rightarrow {}^5D_1(T_{1g})$ and $^7F_0(A_{1g}) + {}^7F_1(T_{1g}) \rightarrow {}^5D_2(T_{2g} + E)$ of $Cs_2NaEuCl_6$. The signs of the characteristic MCD parameters proved useful in distinguishing the t_{1u} and t_{2u} vibrations. Similar techniques were applied to $Cs_2NaPrCl_6$ (Schwartz 1976) and to the magnetic-dipole and vibronically induced electric-dipole transitions associated with $^7F_J \rightarrow {}^5D_4$ of Tb^{3+} $4f^8$ in $Cs_2NaTbCl_6$ (Schwartz et al. 1977). A curious feature of the latter is the absence of vibronic lines when ΔJ is odd (as with $^5D_4 \rightarrow {}^7F_3$ and $^7F_5$). The detailed intensity calculation by Faulkner and Richardson (1978b) referred to in section 7.4 accounted rather well for the relative intensities of the different kinds of transitions.

A certain amount of MCD work has been carried out for lanthanides in aqueous solution, from which a number of deductions can be made about the local site symmetry (Görller-Walrand and Godemont 1977a,b; Görller-Walrand et al. 1982).

7.6 *Correlation crystal fields*

Not long after the single-electron parameters A_{kq} were introduced to fit the crystal splittings of various J levels in the lanthanides, several attempts were made to see how far the residual discrepancies could be reduced by properly taking into account J mixing. The results were disheartening but not surprising. Margolis (1961) found that the major discrepancies in the fit to the sublevels of $^1D_2$ of Pr^{3+} in $PrCl_3$ could not be explained on the basis of a pure configuration $4f^2$. The 40 crystal-field sublevels he studied could be fitted to a standard deviation of $7\,cm^{-1}$, but that figure dropped to only $4\,cm^{-1}$ if the components of the $^1D_2$ level were excluded. Similar analyses by Eisenstein (1963a,b; 1964) yielded standard deviations of $4\,cm^{-1}$ for 72 sublevels of Er^{3+} in $ErCl_3$ and $0.9\,cm^{-1}$ for 31 sublevels of Nd^{3+} in $NdCl_3$. The latter is exceptionally good because Eisenstein only considered seven quartet levels for which the complete sublevel structures were known, thus excluding from consideration several problematic doublets.

Given the overriding constraint of limiting our basic eigenfunctions to those of the type $4f^N$, the only option open to us is to include n-electron crystal-field operators for which $n > 1$. The simplest of these correspond to $n = 2$. Bishton and Newman (1968) introduced two-electron terms of the type

$$A_{kk'}^{qq'} Y_{kq}(\theta_i, \phi_i) Y_{k'q'}(\theta_j, \phi_j) \tag{98}$$

into the crystal-field Hamiltonian. An equivalent formulation can be made with the operators

$$B_{kq}^{k_1 k_2}((\boldsymbol{a}^\dagger \boldsymbol{a}^\dagger)^{(\kappa k_1)}(\boldsymbol{a}\boldsymbol{a})^{(\kappa k_2)})_{0q}^{(0k)}. \tag{99}$$

It is clear that the hermiticity requirement must relate $B_{kq}^{k_2 k_1}$ to $B_{kq}^{k_1 k_2}$ (in fact,

$B^{k_1 k_1}_{k\bar{q}} = (-1)^q B^{k_1 k_2}_{kq}$). Bishton and Newman (1970) used time-reversal invariance (which is equivalent to the demand that the total Hamiltonian be real) to further constrain the parameters. Even so, there is an enormous increase in their number compared to the A_{kq}. For octahedral symmetry, the two standard single-electron parameters (for $k = 4$ and 6) are increased by 32 more. Sites with low point symmetries may require several hundred two-electron parameters $B^{k_1 k_2}_{kq}$ for a complete analysis. It is thus crucial to use physical arguments whenever possible to reduce their number. Bishton and Newman (1970) pointed out that k is necessarily even for $C_{\infty v}$ point symmetry, a result that can be quickly understood because any tensor $T^{(k)}_q$ for odd k would necessarily split the doublets $|\pm M_L\rangle$ that arise in cylindrical symmetry. Since the rotation of such a tensor preserves k, we can deduce that the superposition model, applied to any site symmetry G, limits the tensors (99) that we need consider to those for which k is even. The simplification that this argument affords is comparatively slight, however; for example, the 32 two-electron octahedral parameters are only reduced to 31 as the single octahedral scalar belonging to $k = 9$ drops out (Judd 1977a).

The approach via a general two-electron parameterization is not the only one we can take. As early as the mid-1960's, Rajnak and Wybourne (1964a) considered a number of perturbation mechanisms in which the inter-electronic Coulomb potential is introduced to mix other configurations into $4f^N$. Some mechanisms merely lead to overall changes in the A_{kq}, but there are others – such as $4f^N \longleftrightarrow 4f^{N-1}f'$ – for which the cross-terms of the single-electron crystal-field potential between f and f′ lead to effective two-electron operators. Since the Coulomb interaction commutes with $\boldsymbol{S}$ and $\boldsymbol{L}$, all sublevels and levels deriving from a single SL term can be treated by means of the familiar parameters A_{kq}, which are now term-dependent. This seemed to offer considerable scope for an enlarged parameterization. However, it is still severely restricted compared to the general treatment based on the operators given by (99); in particular, no tensors for which $k > 6$ occur. Such freedom as remains was found to be excessive by Rajnak and Krupke (1967), who carried out separate parameterizations of the ^{5}G and ^{5}I multiplets of Ho^{3+} $4f^{10}$ in $HoCl_3$ and discovered that they both led to virtually identical sets of parameters A_{kq}.

7.6.1 *Spin-correlated crystal fields*

The first efforts to construct a simplified parameterization relied on the very slight dependence of the radial wavefunction $R(r)$ of a 4f electron on the associated spin orientation m_s. There are strong attractive exchange forces between 4f electrons whose spins are similarly directed, and these forces should lead to less extended radial wavefunctions and hence to different A_{kq} for different 4f orbitals. Such variations in $R(r)$ are excluded, of course, from the central-field approximation on which all of shell theory is based; but it is not difficult to find a species of configuration interaction whose effects, in part, mimic the effects of the exchange forces. In fact, the mechanism f → f′ mentioned above preserves the f character of the orbitals and can only make itself felt through an equivalent variation in $R(r)$. In his efforts to account for the ground-level splitting of Gd^{3+} $4f^7$ $^8S_{7/2}$, Newman (1970)

introduced a spin-dependent operator of the type

$$\boldsymbol{S}\cdot\sum_i \boldsymbol{s}_i Y_{kq}(\theta_i, \phi_i), \tag{100}$$

arguing that the spin–orbit interaction, taken to second order, could produce such terms as corrections to spherical harmonics appearing in the standard crystal-field Hamiltonian. Put slightly differently, each Y_{kq} in this Hamiltonian can be corrected by making replacements of the type

$$Y_{kq}(\theta_i, \phi_i) \rightarrow Y_{kq}(\theta_i, \phi_i) + c_k \boldsymbol{S}\cdot\boldsymbol{s}_i Y_{kq}(\theta_i, \phi_i). \tag{101}$$

Substitution (101) appears to be the simplest way in which spin-dependent phenomena can be incorporated into the theory. The operator (100) commutes with $\boldsymbol{S}$ and is thus consistent with effects produced by such spin-independent interactions as the Coulomb and crystal-field terms in the Hamiltonian. Moreover, the effect of (101) turns out to be equivalent to adding to each reduced matrix element of $\boldsymbol{V}^{(t)}$ a part (proportional to c_t) that involves the reduced matrix element of the double tensor $\boldsymbol{V}^{(1t)}$, where $\boldsymbol{v}^{(1t)} = s\boldsymbol{v}^{(t)}$ (Judd 1977b). Such double tensors are straightforward to evaluate; furthermore the proportionality $\langle \boldsymbol{V}^{(t)} \rangle \equiv A\langle \boldsymbol{V}^{(1t)} \rangle$ holds for all terms of maximum multiplicity of a given configuration $4f^N$, so we can at once understand the consistent fit obtained for the ^5G and ^5I multiplets of Ho^{3+} (mentioned in section 7.6).

The signs of the parameters c_k are not so easily accounted for. If the exchange forces are to contract the orbitals whose common m_s value predominates, leading in turn to reduced parameters A_{kq} for those orbitals, then it transpires that we must have $c_k < 0$ ($k = 2, 4, 6$). Some of the evidence adduced to support negative values of the c_k has turned out to be less weighty and more ambiguous than was once thought (Judd 1977b). A further complication seemed to arise when it was realized that a positive value of c_6 would account for the remarkable drop in the magnitudes of the parameters A_{6q} in passing from $EuCl_3$ to $TbCl_3$ (Judd 1980). However, a positive c_6 was found to be produced by a charge-transfer mechanism of the type $Eu^{3+} + e^- \rightarrow Eu^{2+}$, as well as by the effects of covalency (Newman et al. 1982). In recent years, work on this topic has culminated in the analysis of Crosswhite and Newman (1984), which was referred to in section 1. Positive values of c_6 were found to give excellent fits for the crystal spectra of Gd^{3+} and Ho^{3+} in $LaCl_3$, and the especially troublesome deviations of the $^3K_8$ level of Ho^{3+} $4f^{10}$ were largely eliminated. This interpretation of the discrepancies left by the standard crystal-field theory has received support from the work of Reid and Richardson (1985b) on several crystals of the type Cs_2NaYCl_6, where Sm^{3+}, Dy^{3+} and Ho^{3+} were substituted for Y^{3+}. Their data sets are less extensive than those used by Crosswhite and Newman (1984); nevertheless, positive values of c_6 were obtained for all three systems, and the numerical values of around 0.1 are comparable to those obtained for the trichlorides.

Although the argument that led to a negative c_6 cannot be the dominant one, it was noticed by Siu and Newman (1983) that the variation of $R(r)$ as a result of exchange forces leads to slightly different matrix elements of the Coulomb in-

teraction. They showed that these effects could be accommodated by changes in the standard two-electron and three-electron parameters of section 6.1.2, but that, of the latter, only T^2 (and no other T^i) is involved. The reason for this is rather interesting. Of all the six t_i ($i = 2, 3, 4, 6, 7, 8$), only t_2 has group labels WU that are identical to those of a two-electron operator, namely e_3. The effective operators in $4f^2$ that reproduce the energy shifts coming from having two radial functions R_j (where $j = \frac{5}{2}$ or $\frac{7}{2}$) must necessarily be formed from operators of the type $(\boldsymbol{v}_i^{(\kappa k)}\boldsymbol{v}_j^{(\kappa' k')})^{(\kappa'' k'')0}$, where the spin ranks κ and κ' can be 0 or 1. These operators could be carried forward to $4f^3$; but it would clearly be preferable to represent their effects in $4f^3$ by increments to operators already present in the analysis wherever possible. The constraint that the symmetries represented by W and U be preserved limits the possible t_i to t_2 alone.

7.6.2. *Spin-correlated intensities*

Attempts to include correlation effects in the intensity theory of section 5.4.2 have been made by Jankowski and Smentek-Mielczarek (1979, 1981). The appearance of two-electron operators leads necessarily to a large increase in the number of parameters. In analogy to the substitution (101), Siu and Newman (1986) have replaced the even-rank tensor $\boldsymbol{V}^{(t)}$ appearing in eq. (90) according to the scheme

$$\boldsymbol{V}^{(t)} \rightarrow \boldsymbol{V}^{(t)} + d_t \sum_i \boldsymbol{S}\cdot\boldsymbol{s}_i\, \boldsymbol{v}_i^{(t)},$$

thereby introducing three new parameters (d_2, d_4 and d_6) into the theory. Some improvement in the fit to the solution data occurs, and the values of the d_t are reasonably stable (though unnervingly large in a few cases). It is probably too soon to judge how successful this approach will turn out to be in the long run.

7.7. *Spectra of divalent lanthanides*

The allowed transitions $4f^N \rightarrow 4f^{N-1}5d$ occur in the ultraviolet for ions of the type R^{3+}. The contraction in the energy scale that takes place when the effective nuclear charge is decreased in passing from R^{3+} to R^{2+} brings a number of transitions within the optical region of the spectrum. Unlike the narrow lines characteristic of the transitions $4f^N \rightarrow 4f^N$, broad bands are common. As has been mentioned in section 7.5.2, MCD analyses can be helpful here. An early survey of the absorption spectra of the divalent lanthanides in CaF_2 was that of McClure and Kiss (1963). Just how to produce the R^{2+} species is a problem in its own right, for which some ingenious solutions were found (see Kiss and Yocom 1964). The appreciable interaction of the 5d electron with the crystal lattice makes it impracticable to attempt calculations on systems other than those of octahedral symmetry. For these, a single-electron parameterization requires only one parameter (the one traditionally named Dq) for the d electron in addition to the two for the 4f electrons. The complexities of as elementary a system as Yb^{2+} $4f^{-1}5d$ in $SrCl_2$ is apparent in the work of Piper et al. (1967), where all transitions are of the type $A_{1g} \rightarrow T_{1u}$. Reasonably good agreement with experiment was obtained, though Piper et al. (1967) pointed out that setting the f-electron crystal-field parameters equal to zero

hardly affected the quality of the fit to the energies, for which discrepancies of around $500\,cm^{-1}$ were common.

Alig et al. (1969) interpreted the absorption spectrum of $CaF_2:Ce^{2+}$ in terms of transitions of the type $4f5d \rightarrow 4f^2$. That 4f5d lies lower than $4f^2$ tallies with the situation for the free ion Ce III (see section 6.2.2). The evolution of the ground state was described by Alig et al. (1969) in the following way. The e state of 5d is coupled to the combination $a_2 + t_1$ of 4f via the electrostatic interaction, thus neglecting, in the first instance, dt_2 and ft_2. The first-order spin–orbit interaction is then included, followed by a second-order contribution that mixes $^1T_2$ and $^3T_1$. The relative intensities of the transitions $4f5d \rightarrow 4f^2$ could be reproduced rather well, and Dq was estimated to be around $1700\,cm^{-1}$.

The europium chalcogenides (EuO, EuS, EuSe and EuTe) exhibit absorption bands corresponding to $4f^7(^8S) \rightarrow 4f^6(^7F)5d(t_{2g} + e_g)$ of Eu^{2+}. These crystals have been the subject of entire chapters in the present Handbook series (Wachter, 1979) and in the book of Hüfner (1978). Two broad peaks are observed, corresponding to an energy separation between t_{2g} and e_g running from 1.1 eV for EuO down to 0.6 eV for EuTe. Equating these figures to $10Dq$ gives a value for Dq of around $1000\,cm^{-1}$ or less. For Eu^{2+}:SrS, Eu^{2+}:KBr and EuF_2, the lower band (corresponding to $4f^7(^8S) \rightarrow 4f^6(^7F)5dt_{2g}$) exhibits a structure that is highly suggestive of the spin–orbit splitting of ^7F (see, e.g., Hüfner 1978, fig. 41). The detailed analysis of Weakliem (1972) (already referred to in section 7.5.2) indicated that the Coulomb interaction between the 5d electron and the $4f^6$ core, although substantially reduced compared to its strength for the free ion, is far too large to permit the energy levels of $5d(e_g + t_{2g})$ and $4f^6\,^7F_J$ to be simply superposed. The multiplet-like structure on the lower band must be fortuitous. Hernandez et al. (1980) studied the band shapes of the corresponding transitions for Eu^{2+} in NaCl, KCl, RbCl, KBr, RbBr and KI. They found that the experimental shapes of both the lower and upper bands could be accurately reproduced by a Hamiltonian in which the Slater integrals $F^k(4f, 5d)$ and $G^k(4f, 5d)$ are reduced from their free-ion values by factors of roughly 2, thus confirming Weakliem's analysis. However, reduction factors of that magnitude conflict with the earlier results of Piper et al. (1967) on Yb^{2+} and Alig et al. (1969) on Ce^{2+}, where free-ion Slater integrals were assumed. Presumably the positions (and intensities) of the lines for $4f^{14} \rightarrow 4f^{13}5d$ and $4f5d \rightarrow 4f^2$ are insensitive to the values of F^k and G^k.

8. Free-ion work since 1965

The deaths of both Racah and Dieke in 1965, immediately prior to the Zeeman Centennial Conference in Amsterdam, were severe blows to free-ion and crystal spectroscopy. The pall cast on the conference itself can well be imagined. But 1965 saw the continued development of two devices that have revolutionized optical spectroscopy: computers and lasers. The technical details of the working of either device have no place in a review article devoted to atomic theory, but this omission should not be interpreted as a lack of appreciation for their importance. The roles they have played are implicit in much of what follows.

8.1. *The fourth spectra*

In the late 1950's, Dieke made plans to obtain the fourth spectra of the lanthanides in his laboratory at The Johns Hopkins University. A major motivation was the light that such a study would throw on the crystal spectra of the tripositive ions. The only fourth spectrum that had been analyzed was that of Ce IV (Lang 1936), but its single-electron structure gave no information on the Coulomb interactions between pairs of electrons. A preliminary account of the project was provided by Dieke et al. (1961). In his 1960 Hopkins thesis, Sugar made tentative identifications of several Pr IV transition arrays, and he pursued the matter further after moving to the National Bureau of Standards. With a new experimental arrangement he was able to find all the levels of Pr IV $4f^2$ except $^1S_0$ (Sugar 1965b), a feat that provoked a similar article (including a claimed energy for $^1S_0$) from his former colleagues at Johns Hopkins (Crosswhite et al. 1965). The levels of 4f5d, 4f6s and 4f6p were also found (Sugar 1965c, Crosswhite et al. 1965).

Sugar (1965b) discovered that the energies of the levels of Pr IV $4f^2$ corresponded rather closely to the centers of gravity of the levels of Pr^{3+} in $LaCl_3$. The positions of the terms of $4f^2$ in the crystal are compressed by some 5% compared to the free ion, while the fine structures indicated that ζ_{4f} is reduced by less than half that amount. These results provided direct evidence of the expansion of the 4f wavefunction in the crystal. Instead of squeezing the wavefunction inwards, the ligands pressing on the lanthanide ion force the wavefunction outwards. Similar changes in the wavefunctions occur for all ions when placed in crystal lattices. The phenomenon was dubbed the *nephelauxetic* effect by Schäffer and Jørgensen (1958), who had the linguistic assistance of Kaj Barr of the University of Copenhagen. Part of the effect can be ascribed to the ligand electrons, which penetrate the orbits of the 4f electrons and thus screen the latter from the lanthanide nuclear charge. Covalency and orthogonalization mechanisms, such as that represented by the substitution given by (89), also play a role. A detailed discussion has been provided by Gerloch and Slade (1973) in the last chapter of their book on ligand-field parameters.

The success with Pr IV was not rapidly followed by comparable results for other fourth spectra. Sugar (1971) extended the energy levels for Pr IV to include nearly all those of 4f5f as well as portions of 4f6d, 4f7s and 5f6d. His fits yielded accurate eigenfunctions and various parameters. A major step forward was taken by Sugar and Kaufman (1972) by finding nearly all the levels of Lu IV $4f^{13}(5d + 6s + 6p + 6d + 7s)$. Their fits enabled a comparison to be made between the parameters at either end of the lanthanide series. They found $F^k(4f, 5d)$ to be almost unchanged but $G^k(4f, 5d)$ diminished (as Z increases) by 20%. The spin–orbit coupling constants ζ_{5d} and ζ_{6p} increase roughly linearly by factors of between 2 and 3. However, the main preoccupation of Sugar and Kaufman (1972) was with the system differences such as $(A - B)^R_{III}$ for $A \equiv 4f^{N-1}5d$ and $B \equiv 4f^N$ of a rare earth R. They found

$$(A - B)^R_{IV} - (A - B)^{R'}_{III} = 56932,\ 57894,\ 57046\,\mathrm{cm}^{-1}$$

for the isoelectronic pairs $(R, R') \equiv$ (Ce, La), (Pr, Ce) and (Lu, Yb), respectively, thus

demonstrating a remarkable similarity at the two ends of the lanthanide series. They also predicted values for Δ(IV, V), defined in analogy to eq. (86), on the basis of work that they had performed on Pr V (Kaufman and Sugar 1967).

A few years were to elapse before Spector and Sugar (1976) found the levels of Tb IV $4f^8\ ^7F$, as well as all levels of Tb IV deriving from $4f^7(^8S)5d$, 6s, 6p. The more extensive analysis of Yb IV by Sugar et al. (1978) yielded 77 levels of $4f^{12}5d$, 18 of $4f^{12}6s$, and 49 of $4f^{12}6p$ in addition to the two levels of $4f^{13}\ ^2F$ that were already known.

8.1.1. *Hartree–Fock results*

Epstein and Reader (1979) analyzed La IV and found all levels of $5p^6$, $5p^5(5d + 6s + 6d + 7s)$ as well as half those of $5p^54f$. Perhaps the most interesting feature of their paper was the comparison they made between the fitted parameters and those calculated on the basis of a Hartree–Fock (HF) model of the atom. The program of Froese-Fischer (1969a,b, 1972a,b; 1976) was used to evaluate such Slater integrals as F^k(5p, 4f), F^k(5p, 5d), F^k(5p, 6d), G^k(5p, 4f), etc., which were found to be generally larger (by amounts varying from a few percent to over 50%) than the fitted values. This property of the HF method had been previously noticed by Freeman and Watson (1962), who found that the HF integrals F^k(4f, 4f) for the free ions R^{3+} were 40% to 50% larger than the values obtained by fitting the experimental energies of the terms of $4f^N$. This effect is easy to understand qualitatively, since the Coulomb interaction between two electrons is necessarily attenuated by the reactive distortions of the intervening charge cloud. Morrison et al. (1970b) took Pr IV and examined how these distortions can be represented by the second-order perturbative effects of 27 bound configurations (such as $4s^{-2}4f^4$, $4s^{-1}4d^{-1}4f^4$, $5p^{-1}4f^3$, $5p^{-2}4f^36p$, etc.) and 8 single-electron excitations into the continuum (such as $4f \rightarrow kp$, $4d \rightarrow kg$, etc.). Substantial corrections to the HF values were obtained, but they only accounted for roughly half the discrepancy. By extending the approach to 32 bound configurations, 38 single-electron and 17 two-electron excitations into the continuum, as well as some third-order effects, Morrison and Rajnak (1971) were able to get good agreement with the Trees parameters α and β (see section 6.1.2), but large discrepancies for the Slater integrals remained. Third-order contributions to the latter were found to be comparable to second-order effects, indicating poor convergence of the perturbation process. Morrison and Rajnak (1971) were evidently dismayed enough to omit any direct comparison between the experimental and theoretical F^k. However, they were sufficiently confident of their calculations to interpret the poor agreement they found for the third Trees parameter γ as a faulty identification of Pr IV $4f^2\ ^1S_0$ by Crosswhite et al. (1965).

One of the principal conclusions of Morrison and Rajnak (1971) was that excitations involving a change in azimuthal quantum number (such as $4d \rightarrow g$) are extremely important. This result was confirmed by Balasubramanian et al. (1975), who found that h and k states both make appreciable contributions to the three-electron parameters T^i (of section 6.1.2) for Pr^{3+}. However, good agreement could only be obtained with experiment if the second-order contributions involving the 4p electron were screened by a factor of 0.69. This is not unreasonable when it is

recalled that the first-order calculation of the Slater integrals F^k have to be reduced by a very similar factor.

The fact that HF calculations, even when corrected up to third order in perturbation theory, lead to values of the Slater integrals that are often some 20% larger than the corresponding fitted parameters does not much diminish their usefulness. Wyart (1978) and Wyart and Bauche-Arnoult (1981) calculated the Slater integrals for the configurations $4f^N6p$ and $4f^N(5d + 6s)$ of a few second and third spectra of the lanthanides by the HF method, and they were able to fit the trends of the integrals across each of the series to general formulas of the type

$$P_k = A(P_k) + (N - 7)B(P_k) + (N - 7)^2C(P_k). \tag{102}$$

Such formulas proved extremely useful in the parametric fitting of the 143 levels of $4f^N(5d + 6s)$ that occur in Pr IV, Yb IV and Lu IV. Rather than treat each ion separately, constraints of the type given by (102) were applied and a generalized least-squares (GLS) fit to all 143 levels simultaneously was made. The coefficients $C(P_k)$ were sufficiently small to be taken equal to zero for F^k(4f, 5d) and G^k(4f, 5d), while each $C(F^k(4f, 4f))$ was set equal to the HF value. So successful was this approach that Wyart and Bauche-Arnoult (1981) were able to correct the level $(^3F_3, 5d_{5/2})_{11/2}$ of Yb IV $4f^{12}5d$ from the figure 106 557 cm^{-1} given by Sugar et al. (1978) to 106 444.41, which could be supported by five transitions. They also predicted the energies of the levels of the four lowest multiplets of Tm IV $4f^{11}5d$ in Jj coupling. The GLS fit can also be applied to the first, second and third spectra, as had first been done by Racah and his students in their work on the 3d transition series (see, e.g., Shadmi et al. 1969); but, as Wyart and Bauche-Arnoult (1981) pointed out, the method becomes particularly effective for higher stages of ionization, where the configurations tend to be more widely separated and less susceptible to the effects of configuration interaction.

8.2. *Magnetic interactions*

As fits to the crystal spectra became more detailed, a lack of balance in the theory appeared. The Coulomb interactions within the 4f shell and the effects of configuration interaction to second order can be taken into account by means of the four Slater integrals F^k(4f, 4f), the three Trees parameters α, β, γ, and the six three-electron parameters T^i. In contrast to these 13 electrostatic parameters, the spin–orbit interaction, until 1968, was represented by the single parameter ζ_{4f}. This scheme overlooks the terms that arise from the Breit interaction, which was developed on relativistic grounds to account for the fine structures of the multiplets ^3P of He I 1s*n*p (see Bethe and Salpeter 1957). In the non-relativisitc limit parts of the Breit interaction, such as the retardation of the Coulomb interaction and the magnetic interactions that exist between the electrons in virtue of their orbital motions, can be represented by adjustments to the electrostatic parameters. Two terms cannot be absorbed in that way: the spin–spin interaction H_{ss} and the spin–other-orbit interaction H_{soo}. Marvin (1947) showed that, for the configurations l^N,

the effect of H_{ss} and H_{soo} can be specified in terms of the l radial integrals M^k (where $k = 0, 2, \ldots, 2l - 2$). These so-called Marvin integrals are the analogs of the Slater integrals but are smaller by roughly the square of the fine-structure constant, that is, by $(1/137)^2$. Blume et al. (1964) used the HF method to calculate M^k for all configurations $4f^N$ occurring in R^{3+} ions, and it was seen that significant energy shifts in the levels of the order of up to $100\,cm^{-1}$ could be produced (Judd 1967b).

It is technically more difficult tó calculate the matrix elements of H_{soo} for pairs of inequivalent electrons. Jucys and Dagys (1960) extended the tables of Marvin (1947) to include the configurations fs, fp, fd (and f^2), but it soon became apparent to them that Marvin's handling of the radial integrals was in error. Because of the terse style adopted by Marvin, it is impossible to put one's finger on the actual fault. In the first volume of this Handbook series, Goldschmidt (1978, eqs. 1.117–124) has given the tensorial form of H_{soo} and defined the associated radial integrals $M^k(nl, n'l')$, $N^k(nl, n'l')$ and $K^{k\pm}(nl, n'l')$ that are required for a correct treatment. Jucys et al. (1961) listed the matrix elements of H_{soo} and H_{ss} for fs, fp, fd, as well as for other configurations not involving an f electron. A summary of the extensive work of the Lithuanian school led by Jucys can be found in the book by Jucys and Savukynas (1973).

8.2.1. *Group theory*

Within the f shell, the magnetic interactions H_{ss} and H_{soo} lend themselves to the same kind of analysis that Racah (1949) carried out for the Coulomb interaction (see section 4.3). Just as the latter can be described in tensorial terms by $\boldsymbol{T}^{(00)0}$, where the three superscripts specify ranks with respect to $\boldsymbol{S}$, $\boldsymbol{L}$ and $\boldsymbol{J}$, so H_{ss} and H_{soo} correspond to $\boldsymbol{T}^{(22)0}$ and $\boldsymbol{T}^{(11)0}$, respectively. The detailed structure of $\boldsymbol{T}^{(22)0}$ arises from terms of the type $(\boldsymbol{v}_i^{(1k)}\boldsymbol{v}_j^{(1k+2)})^{(22)0}$, where $k = 0$, 2 and 4 (Innes 1953). The four tensors $\boldsymbol{v}^{(10)}$, $\boldsymbol{v}^{(12)}$, $\boldsymbol{v}^{(14)}$ and $\boldsymbol{v}^{(16)}$, for any projection in the spin space, belong to the irreducible representations (000)(00) + (200)(20) of SO(7) and G_2, just as those of the type $\boldsymbol{v}^{(0k)}(k = 0, 2, 4, 6)$ do. However, as soon as we include tensors of non-zero spin rank in the analysis, the possible groups that we can usefully bring into play also increases. In analogy to eq. (61) we can write

$$\boldsymbol{V}^{(1t)} = \sum_{i=1}^{N} \boldsymbol{v}_i^{(1t)}. \tag{103}$$

The collection of tensors $\boldsymbol{V}^{(\kappa k)}$ for $\kappa + k$ odd close under commutation and form the generators of the symplectic group Sp(14). One way to see this result is to notice that there are no terms of f^2 for which $S + L$ is odd; so, when $\kappa + k$ is odd, the operator $\boldsymbol{V}^{(\kappa k)}$ yields zero when it acts on $|f^2\,{}^1S\rangle$. Thus ^1S is an invariant. Writing out its eigenfunction in full we get (ignoring normalization)

$$|{}^1S\rangle = \sum_m [\alpha(1)\psi_{lm}(1)\beta(2)\psi_{l-m}(2) - \beta(1)\psi_{l-m}(1)\alpha(2)\psi_{lm}(2)]. \tag{104}$$

The characteristic feature of symplectic groups is that they leave invariant antisymmetric bilinear forms [Weyl 1953, ch. VI, eq. (1.1)], a description that applies to the eigenfunction (104). We can regard Sp(14) as an alternative to $SO_S(3) \times U(7)$

in the sequence (52); that is, $U(14) \supset Sp(14) \supset SO_S(3) \times SO(7)$. The term ^1S belongs to the scalar representation $\langle 0 \cdots 0 \rangle$ of Sp(14); the other terms of f^2 form a basis for the 90-dimensional irreducible representation $\langle 110 \cdots 0 \rangle$ (see, e.g., Wybourne 1970). The collection of tensors $V^{(\kappa k)}$ for $\kappa + k$ odd, on the other hand, belong to $\langle 20 \cdots 0 \rangle$. These labels can be used to augment the description WU of Racah (1949).

Returning to the spin–spin interaction, we see that our tensors $(\boldsymbol{v}_i^{(1k)}\boldsymbol{v}_j^{(1\,k+2)})^{(22)}$ (for two electrons i and j) must belong to those representations $\langle \sigma \rangle$ occurring in the decomposition of $\langle 20 \cdots 0 \rangle \times \langle 20 \cdots 0 \rangle$ that, at the same time, contain the irreducible representation $\mathscr{D}_2 \times \mathscr{D}_2$ of $SO_S(3) \times SO_L(3)$. An additional constraint is that we need only consider representations $\langle \sigma \rangle$ occurring in $\langle 110 \cdots 0 \rangle^2$, corresponding to the non-vanishing of the symbolic matrix elements

$$\langle\langle 110 \cdots 0 \rangle | \langle \sigma \rangle | \langle 110 \cdots 0 \rangle\rangle$$

in f^2. The upshot of the analysis is that H_{ss} can be written as the sum of four operators z_i $(i = 1,2,3,4)$ for which $WU \equiv (200)(20)$, $(220)(20)$, $(220)(21)$ and $(220)(22)$; their strengths are determined by coefficients that are linear combinations of the three Marvin integrals M^0, M^2 and M^4 (Judd and Wadzinski 1967). Just as in the case for the Coulomb interaction, the group-theoretical labels provide many additional selection rules and proportionalities between blocks of matrix elements for different configurations $4f^N$. The group-theoretical method was used to calculate and check the matrix elements of H_{ss} for f^2 (Judd and Wadzinski 1967), f^3 (Crosswhite et al. 1968) and f^4 (Armstrong and Taylor 1969).

A similar analysis can be carried out for H_{soo}. The various contributions to $\boldsymbol{T}^{(11)0}$ require 7 operators z_i $(i = 5, 6, \ldots, 11)$; a 'combined' operator z_c that belongs to $\langle 110 \cdots 0 \rangle (110)(11)$ but for which the quasi-spin rank K (see section 11.1) is a mixture of 0, 1, and 2; and an operator z_{13} that possesses matrix elements within a given configuration $4f^N$ proportional to those of the ordinary spin–orbit interaction H_{so} given in eq. (32). The last can be dropped. The eight remaining, taken with the four from H_{ss}, were independently parameterized and used to fit the levels of Pr III $4f^3$ as well as those of Nd^{3+} $4f^3$ and Er^{3+} $4f^{11}$ in $LaCl_3$ (Crosswhite et al. 1968). Mean errors of the order of only $10\,cm^{-1}$ were obtained.

8.2.2. *Electrostatically correlated spin–orbit interaction (EL–SO)*

There is, of course, no prohibition against using elementary methods to evaluate the matrix elements of H_{ss} and H_{soo} in $4f^N$. In a flurry of activity in the late 1960's, Reilly (1968) calculated $\langle H_{ss} \rangle$ for f^3; Barnes et al. (1968) carried out a complementary analysis for H_{soo}, as well as extending the work (in unpublished form) to f^4; Malli and Saxena (1969) and Saxena and Malli (1969) presented some numerical work (based on HF calculations) for $\langle H_{ss} \rangle$ and $\langle H_{soo} \rangle$ for f^5 and (in other articles cited in the foregoing) other f^N; while Donlan (1969) reported his calculation of the matrix elements of $H_{ss} + H_{soo}$ (expressed as linear combinations of M^0, M^2 and M^4) for all configurations f^N. Donlan's two-electron coefficients of fractional parentage were used in the last calculation and published separately (Donlan 1970). Their definition is similar to that of the one-electron cfp of eq. (35) except that the parent

state is of the form $l^{N-2}\psi''$, and the added pair of electrons $(l_N l_{N-1})$ must be coupled to a state of l^2 before the final couplings to S and L are carried out.

Unfortunately, we cannot expect that the calculations of $\langle H_{ss} + H_{soo} \rangle$ will give good agreement with experiment upon substituting HF values for the M^k. Apart from various screening corrections similar to those discussed in section 8.1.1 for the Slater integrals, the coupling of different configurations by H_{so} and by the Coulomb interaction produces cross terms that have the same tensorial description $\boldsymbol{T}^{(11)0}$ as H_{soo}. This perturbative mechanism, which is now commonly called EL–SO (for electrostatically correlated spin–orbit interaction), was first discussed by Rajnak and Wybourne (1964b). In addition to the M^k, three more parameters, called variously P^k or Q^k (depending on the prefacing factor of the associated operator) are required. The operators z_i (and z_c) are sufficiently general to accommodate EL–SO, as was realized when the fits referred to in section 8.2.1 were carried out. Goldschmidt (1978) has given a detailed description of how the inclusion of EL–SO, H_{ss} and H_{soo} improves the fits (sometimes in a spectacular fashion) for Ce III ($4f^2 + 4f5d$), Pr IV ($4f^2 + 4f5d$) and Pr III, much of which dates back to her work of ten years earlier (Goldschmidt et al. 1968). The large number of magnetic parameters (particularly for configurations involving inequivalent electrons) calls for careful judgement on which parameters to fix (perhaps equal to their HF values) and which to leave free to vary. For the configurations 4f5d it turned out that EL–SO dominated H_{ss} and H_{soo}. Just as for the Slater integrals, it was found that the Marvin integrals fitted to experiment tend to be somewhat smaller than the corresponding HF values. A tabulation of the latter for the ground configurations of R I–XII is included in the Handbook of Atomic Data prepared by Fraga et al. (1976).

8.3. *Complex spectra*

In spite of the successes coming from the inclusion of the magnetic interactions in the Hamiltonian, much work continued – and still continues – to be done on lanthanide spectra in which these interactions are represented only by the spin–orbit parameters ζ_{nl}. The direction optical spectroscopy has taken is partly responsible for this state of affairs. There has been a natural desire to account for the level structures of configurations of ever-increasing complexity. This has meant that most attention has been given to evaluating the matrices of the standard Hamiltonian without attending to the comparatively small effects of the magnetic interactions and EL–SO. Indeed, there is little reason to do so until mean errors of less than $50\,cm^{-1}$ are approached. The matrix elements of H_{ss} are often very much smaller than that; and since, within a given LS multiplet, H_{soo} and EL–SO, having the same tensorial characteristics $\boldsymbol{T}^{(11)0}$ as H_{so}, possess matrix elements proportional to those of H_{so}, much of H_{soo} and EL–SO can often be absorbed by H_{so}. This was particularly true at a time when truncations of the configurations $4f^N$ were common. For example, Blaise et al. (1971b) diagonalized the matrices of $4f^4(^5I + {}^5F + {}^5S)5d6s$ for Nd I, but since their fit to experiment was limited to levels deriving from $4f^4(^5I)5d6s$, it was immaterial whether H_{soo} and EL–SO for the 4f electrons were included in the Hamiltonian or not. The same can be said for the

work of Eremin and Maryakhina (1969) on $4f^7(^8S)5d$ in Gd I and Eu II, as well as that of Meinders et al. (1972) on Tb III $4f^8(^7F)(5d + 6s + 6p)$, to name but a few of the many calculations of a similar type.

8.3.1. *Generalized Trees parameters*

The success of the Trees parameter α (and its extensions β and γ) for configurations of equivalent electrons prompted generalizations to cope with more complex situations. Sack (1956) suggested using the expression

$$\alpha L(L+1) + \beta S(S+1) + \alpha' L'(L'+1) \tag{105}$$

for configurations of the type $d^N p$, where L' refers to the core d^N. Since such corrections are intended to represent the electrostatic interactions with excited configurations, the appearance of the spin term $S(S+1)$ in (105) may seem somewhat odd. The Pauli exclusion principle is at work here. First-order Coulomb energies of the terms ^{2S+1}L (for a given L) depend on S, and there is no reason to expect second-order corrections not to do so too. The β term in (105) merely provides us with another scalar operator (namely $\boldsymbol{S}^2$) that possesses two-electron parts, as Wybourne (1965b) made clear. The equivalent operator $E_s(\boldsymbol{s}_f \cdot \boldsymbol{s}_d)$ was used by Goldschmidt (1968) in her analysis of Ce III 4f(5d + 6s) to halve the mean error, and this prompted Sugar (1969) to use E_s too in his analysis of Pr III $5d^2 4f$.

The correction (105) of Sack (1956) is not the most general. In their work on the configurations $4f^2 5d$, $4f^2 6p$ and $4f^2(6s + 5d)$ of Pr III, Feneuille and Pelletier-Allard (1968) extended Racah's analysis outlined in section 6.1.1. Without examining in detail the perturbing mechanism, they simply added to the effective Hamiltonian all possible scalar two-electron operators independent of the spin. For mixed configurations of the type $4f^N nl$, the two combinations

$$X_k(4f, nl)\boldsymbol{z}_i^{(k)}(ff) \cdot \boldsymbol{z}_j^{(k)}(ll), \tag{106}$$

$$Y_k(4f, nl)\boldsymbol{z}_i^{(k)}(fl) \cdot \boldsymbol{z}_j^{(k)}(lf) \tag{107}$$

are required, where the tensors $\boldsymbol{z}^{(k)}$, although similar to those in eq. (76), now act only within the states of the configuration under study. The parameter X_1 is associated with an operator proportional to $\boldsymbol{L}' \cdot \boldsymbol{l}$ (where $\boldsymbol{L}'$ is the angular momentum of the 4f electrons); its eigenvalues are $\frac{1}{2}L(L+1) - \frac{1}{2}L'(L'+1) - \frac{1}{2}l(l+1)$. The parameters X_k for k even, and Y_k for k odd, are absorbed by the Slater integrals F^k and G^k, respectively. Feneuille and Pelletier-Allard (1968) found that the fit obtained by Sugar (1963) for Pr III $4f^2 5d$ could be considerably improved with the help of X_1, Y_2 and Y_4, the mean error dropping from $182\,cm^{-1}$ to $89\,cm^{-1}$. However, little improvement occurred when X_k and Y_k were included in the fits for $4f^2 6p$ and $4f^2(6s + 5d)$. A complete set of X_k and Y_k obviates the need for a spin parameter E_s or β in expression (105). The use of such a set has been mainly confined to configurations of the type $4f^N 5d$. Two examples are $4f^8 5d$ of Tb I (Bauche-Arnoult et al. 1978) and $4f^{10} 5d$ of Ho I (Wyart and Camus 1978).

8.3.2. *Coupling schemes*

Competition between the various spin–orbit and Coulomb interactions in the

Hamiltonian typically leads to eigenfunctions that approximate more closely to one particular coupling scheme than to others. The configurations $4f^N$ are good examples of *LS* or Russell–Saunders coupling, since ζ_{4f} is much less than the integrals $F^k(4f, 4f)$. As soon as one or more inequivalent electrons are added to $4f^N$ the situation becomes more complex. Racah et al. (1966) used $J_I J_{II}$ coupling in their analysis of Eu I $4f^{12}6s6p$, the core $4f^{12}$ providing a total angular momentum J_I and the pair of electrons 6s6p the total angular momentum J_{II}. Lower-case letters are often used where the angular momentum of a single electron (or electron–hole) is involved. In his analysis of Tm I $4f^{13}5d6s + 4f^{12}6s^26p$, for example, Camus (1972a,b) found it appropriate to use $j_1 L_2$ coupling for $f^{13}ds$ and $J_1 j_2$ coupling for $f^{12}s^2p$. Camus and Sugar (1971) specified the states of $f^{12}ds$ and $f^{13}p$, which occurred in their analysis of Tm II $4f^{12}(5d + 6s)^2 + 4f^{13}6p$, in $J_1 J_2$ coupling.

Even two-electron systems can sometimes require quite intricate couplings. The orbit of the 5g electron of Ce III 4f5g lies far outside that of the 4f electron, with the result that the direct Slater integrals $F^k(4f, 5g)$, though small, are much larger than the exchange integrals $G^k(4f, 5g)$. The spin–orbit coupling constant ζ_{5g} is very small, so that the spin of the 5g electron plays very little role in determining energies. Consequently $\boldsymbol{j}$ for the 4f electron couples with $\boldsymbol{l}$ of the 5g electron to give a resultant $\boldsymbol{K}$, to which the spin $\boldsymbol{s}$ of the 5g electron is finally added to yield $\boldsymbol{J}$. The pairs of levels for which $J = K \pm \frac{1}{2}$ are close together, as can be seen from figure 1.3 of Goldschmidt (1978). In her language, this is an example of jK coupling: Sugar (1965a) called it Jl coupling. Other figures in Goldschmidt's article exemplify $J_1 j$ coupling (for Pr III $4f^26p$) and $J_1 L_2$ coupling (for Yb II $4f^{13}5d6s$).

In spite of elaborate coupling schemes, it has often proved possible to pick out well-behaved *LS* multiplets (that is, multiplets for which the Landé interval rule is not too seriously violated) from a morass of levels. The five low-lying multiplets ^4G, ^4H, $^4H'$, ^4I and ^4K of Pr III $4f^25d$ found by Sugar (1965a) are good examples of this. Two more are provided by the configurations $4f^7(^7F)5d$ of Eu I and Eu III (Smith and Wilson 1970, Sugar and Spector 1974). Such phenomena can be understood in terms of a theorem for a configuration

$$(n_1 l_1)^a (n_2 l_2)^b \cdots (n_j l_j)^k \quad (0 \leqslant a \leqslant 2l_1 + 1, \quad 0 \leqslant b \leqslant 2l_2 + 1, \ldots, \quad 0 \leqslant k \leqslant 2l_j + 1).$$

All matrix elements of H_{so} vanish between different *LS* multiplets of maximum S if $\zeta_{n_1 l_1} = \zeta_{n_2 l_2} = \cdots = \zeta_{n_j l_j}$ (Judd 1968). The condition $\zeta_{4f} = \zeta_{5d}$ is reasonably well fulfilled for the configurations $4f^N5d$ of many lanthanide ions near the beginning of the lanthanide series, and so multiplets of maximum multiplicity can overlap one another without interacting.

8.3.3. *Checking the energy matrices*

In the 1970's it became possible to diagonalize energy matrices of ever-increasing size. Interactions between neighboring or overlapping configurations could be handled by enlarging the matrices, allowance usually being made for slight differences between corresponding parameters. For example, Carlier et al. (1968), in their

analysis of Sm I $4f^6(^7F)6s6p + 4f^5(^6H + ^6F)5d6s^2$, relaxed the constraint $\zeta_{4f}(f^6sp) = \zeta_{4f}(f^5ds^2)$. Truncation of the states of the $4f^N$ core was still common at that time. An extension to the states of next-to-highest multiplicity was made by Blaise et al. (1971a) in their analysis of $4f^7(^8S + ^6P)(5d + 6s)(5d + 6s + 6p)$ and $4f^8(^7F + ^5D1 + ^5D2 + ^5D3)(5d + 6s)$ of Gd II, where the three terms ^5Di are given in the notation of Nielson and Koster (1963) for the three possible combinations W_iU_i of the irreducible representations of G_2 and SO(7). By 1976, Wyart (1976) was able to analyze Dy II $4f^{10}(5d + 6s)$ with a complete basis for the core $4f^{10}$, and an extension to other spectra of the type R II $4f^N(5d + 6s)$ was soon realized (Wyart 1978).

With the increase in size of the energy matrices came the greater opportunity for error. Methods for checking the matrix elements of the Coulomb interaction date back to Laporte and Platt (1942), who found that the energies of the terms of d^λ exhibited multiple degeneracies when the hypothetical (and unphysical) value of $\frac{5}{9}$ for $F^2(d, d)/F^4(d, d)$ was assumed. In this way they were able to correct some errors of Ostrofsky (1934) for d^4. It was later realized that the Laporte–Platt ratio for F^2/F^4 effectively eliminates the part of the Coulomb interaction belonging to the irreducible representation (22) of SO(5), leaving only an SO(5) scalar. For the f shell, we need to take $F_4/F_2 = \frac{6}{11}$ and $F_6/F_2 = \frac{1}{11}$ to force $E^2 = E^3 = 0$ in eqs. (63). Both e_0 and e_1 are scalars with respect to SO(7) and G_2, so W and U become good quantum numbers and many striking degeneracies occur when the energy matrices are diagonalized.

This approach needs some elaboration when more parameters than the four $F^k(4f, 4f)$ are involved. Operators of the Casimir type can be used here. To explain how the method works, we note first that a Casimir operator for a Lie group is a scalar (with respect to that group) formed from sums of products of the generators. Being scalar, it commutes with all the generators. The classic Casimir operators are quadratic products, such as $\boldsymbol{J}^2$ for $SO_J(3)$, which commutes with J_x, J_y and J_z. To get the Casimir operator for G_2 we have to add (with appropriate coefficients) the two products $\boldsymbol{V}^{(1)}\cdot\boldsymbol{V}^{(1)}$ and $\boldsymbol{V}^{(5)}\cdot\boldsymbol{V}^{(5)}$; for SO(7) we must also include $\boldsymbol{V}^{(3)}\cdot\boldsymbol{V}^{(3)}$; the three additional products $\boldsymbol{V}^{(2)}\cdot\boldsymbol{V}^{(2)}$, $\boldsymbol{V}^{(4)}\cdot\boldsymbol{V}^{(4)}$, and $\boldsymbol{V}^{(6)}\cdot\boldsymbol{V}^{(6)}$ are needed for SU(7). As can be seen from eq. (61), such products contain two-electron terms of the type $\boldsymbol{v}_i^{(k)}\cdot\boldsymbol{v}_j^{(k)}$, which normally occur in conjunction with such parameters as F^k (for k even) or α (for $k = 1$). If the two-electron operators that are scalar with respect to $SO_L(3)$ have been completely parameterized, we can evidently pick hypothetical values of the parameters that reproduce Casimir's operator for the group of our choice. The eigenvalues of Casimir's operator can be worked out in terms of the highest weights of the irreducible representations (see, e.g., Judd 1963, sections 5–9). Thus we can anticipate the results of diagonalizing the energy matrices and hence check the matrix elements themselves.

Roth (1971) extended these ideas to treat $(d + s)^Np$. He used the SU(3) model of Elliott (1958) to associate the p electron with the three-dimensional irreducible representation [1] of SU(3), while the combination d + s was associated with the six-dimensional representation [2] of the same group. Several parameters were missed in this procedure, and Roth (1972) developed what is essentially a more

elementary approach to cope with them. He introduced two new operators into the basic two-electron configuration (d + s)p and chose parameters that yielded zero eigenvalues except for a single ^{1}P term. For $N > 1$, the same set of parameters must produce zero eigenvalues for all terms not having that particular ^{1}P term as an ancestor. Bauche-Arnoult et al. (1978) used a similar device for checking the energies of the levels of Tb I $4f^8 5d$. They limited their attention to the 2492 levels for which $J < \frac{19}{2}$ (out of a total of 2725). By taking specific values for $E_{av}(f^N d)$, $F^2(4f, 5d)$, $F^4(4f, 5d)$, $G^k(4f, 5d)$ (where $k = 1, 3, 5$), α, α', $X_3(4f, 5d)$, $Y_2(4f, 5d)$, and $Y_4(4f, 5d)$, all the terms of 4f5d could be set equal to zero energy with the exception of ^{1}P. If the interactions between the 4f electrons of $4f^2 5d$ are neglected, all terms of that configuration not possessing ^{1}P as a parent must also have zero energies; and, as we proceed to larger N, the zeros percolate down the series to other terms. For example, the matrix of order 246 for the levels of $4f^8 5d$ for which $J = \frac{3}{2}$ was found by Bauche-Arnoult et al. (1978) to possess 156 zero eigenvalues for specified values of the parameters listed above, thereby checking all the numerical coefficients of the parameters in the expressions for the matrix elements.

Terms in the Hamiltonian that are sums of single-electron operators are easier to verify. For example, if all the electrostatic parameters are set equal to zero and only the spin–orbit parameters ζ_{nl} retained, the degeneracies characteristic of perfect *jj* coupling are obtained. Checks for hyperfine-structure calculations have been described by Bauche-Arnoult and Bauche (1968). The method can be extended to verify the energy matrices containing terms coming from the crystal-field Hamiltonian. The relation of the Laporte–Platt degeneracies to delta-function interactions has been explored (Judd and Lister 1984).

With the accuracy of the energy matrices assured, further advances in the analysis of complex lanthanide spectra could be carried out. The histories of the individual ions, complete up to a specified date (usually in 1976 or 1977), have been given by Martin et al. (1978). After 1978, many fits to lanthanide levels were carried out as a preliminary to other projects, such as the analysis of hyperfine structures or Rydberg series. This work is discussed in sections 8.4 and 8.5. Among articles in the classic vein that have not yet been mentioned are that of Wyart et al. (1976/7) on $4f^{11}$ and $4f^{10}(5d + 6s + 6p)$ of Ho III, and that of Kaufman and Sugar (1978) on Lu V $4f^{12}(5d + 6s + 6p)$. The Nd II analyses carried out by Blaise et al. (1984), which have been signposted in section 1, are other examples of that kind.

8.4. *Hyperfine structure*

For many years hyperfine structure was regarded primarily as a source of information on atomic nuclei. The work of Casimir (1963), referred to in section 2.2.3, falls into that category. The introduction of microwave techniques in the 1940's greatly increased the flow of nuclear data. Over the years the bald listing of nuclear moments and isotope shifts has had a declining appeal for nuclear physicists; at the same time the atomic calculations involved in finding these numbers have had an increased significance as our understanding of the many-electron atom has improved. Hyperfine structures now play a major role in the development of

theories of the atom, rather than (as one might have surmised) the nucleus. Such an attitude is fully apparent in the review articles of Lindgren and Rosén (1974a,b).

The Wigner–Eckart theorem is always applied to the nucleus to express its magnetic dipole $\boldsymbol{\mu}$ as $(\mu_N \beta_N / I)\boldsymbol{I}$, where β_N is the nuclear magneton ($= eh/2m_p c$, with m_p the mass of the proton), $\boldsymbol{I}$ is the total angular momentum (in units of h) of the nucleus (called its spin), I is the quantum number associated with $\boldsymbol{I}$, and μ_N is the nuclear moment, a dimensionless quantity. The most general Hermitian operator linear in $\boldsymbol{\mu}$ (and hence in $\boldsymbol{I}$), scalar overall (that is, commuting with $\boldsymbol{I} + \boldsymbol{J}$, the total angular momentum), and involving only those terms for which each electron i separately interacts with the nucleus, is

$$H_{\rm md} = \sum_i [a_i^{01} \boldsymbol{l}_i - a_i^{12}(8\pi)^{1/2}(\boldsymbol{s}_i \boldsymbol{Y}_i^{(2)})^{(1)} + a_i^{10} \boldsymbol{s}_i] \cdot \boldsymbol{I}. \tag{108}$$

When dealing with pure configurations, the suffixes i on the parameters $a_i^{\kappa k}$ can be replaced by the appropriate combinations $n_i l_i$. Until the importance of effective operators was realized, it was common to use the non-relativistic form of $H_{\rm md}$, which, for 4f electrons, corresponds to $a_{4f}^{10} = 0$ and

$$a_{4f}^{01} = a_{4f}^{12} = 2(\mu_N \beta \beta_N / I)\langle r^{-3} \rangle_{4f}. \tag{109}$$

In order, then, to find μ_N, the radial integral $\langle r^{-3} \rangle_{4f}$ had to be evaluated. Much effort has been expended in that direction.

By the mid-1960's it was recognized that this simple picture was not adequate. Sandars and Beck (1965) showed how relativistic effects of the type first described by Casimir (1963) could be accommodated by generalizing the non-relativistic Hamiltonian to the form given by (108). A rather profound mental adjustment was required: instead of setting the relativistic Hamiltonian between products of four-component Dirac eigenfunctions, they asked for the effective operator $H_{\rm md}$ that accomplishes the same result when set between non-relativistic states. The coefficients $a_{nl}^{\kappa k}$ now involve sums over integrals of the type $\int F_j G_{j'} r^{-2}\, dr$, where F_j and $G_{j'}$ are the two-component radial wavefunctions for a Dirac electron in a central field, and where $j, j' = l \pm \frac{1}{2}$. The equation $a_{nl}^{01} = a_{nl}^{12}$ is relaxed. At about the time when Sandars and Beck were developing their theory, Harvey (1965) discovered that $a_{2p}^{12}/a_{2p}^{01} = 1.13$ and 1.11 for ^{17}O I $2p^4\ ^3$P and ^{19}F I $2p^5\ ^2$P, respectively. Oxygen and fluorine are too light to exhibit significant relativistic effects, and it was soon realized that the deviation of a_{2p}^{12}/a_{2p}^{01} from 1 was produced by configuration interaction. An application of eq. (108) to a lanthanide spectrum, namely Eu I $4f^7(^8S)6s6p$, was made by Bordarier et al. (1965) on the basis of experimental work by Müller et al. (1965). Since the 4f electrons are coupled to ^{8}S, only a_{4f}^{10} is required for them. Good agreement with experiment was obtained using the calculated relativistic values for $a_{6p}^{\kappa k}$. The importance of treating the 6p electron relativistically was confirmed by Camus (1972b) in a detailed treatment of 27 levels of Tm I $4f^{13}6s6p + 4f^{12}5d6s^2$. In addition to $a_{6p}^{\kappa k}$, Camus found $a_{5d}^{\kappa k}$ and two sets of the parameters $a_{4f}^{\kappa k}$, one for $4f^{13}6s6p$, the other for $4f^{12}5d6s^2$. For the former, $a_{4f}^{01} : a_{4f}^{12} : a_{4f}^{10} :: -18.62 : -20.62 : 0.80$. These numbers are closely proportional to the relativistic HF results presented by Lindgren and Rosén (1974b, table 34). Expressed in terms of effective values of $\langle r^{-3} \rangle$, their results for Tm I $4f^{13}$ run $\langle r^{-3} \rangle_{01} : \langle r^{-3} \rangle_{12} : \langle r^{-3} \rangle_{10} :: 11.478 : 12.612 : -0.538$.

8.4.1. *Configuration interaction*

The striking correspondence between a_{4f}^{kk} and $\langle r^{-3}\rangle_{kk}$ does not mean that configuration interaction can be neglected. In an atomic-beam investigation of the ground multiplet ^{5}I of ^{143,145}Nd, Childs and Goodman (1972a) found $a_{4f}^{12}/a_{4f}^{01} = 0.973$ instead of the HF value of 1.061, indicating a deviation from the simple non-relativistic result in the opposite sense to the expected one. An examination of the effects of configuration interaction on hyperfine structures was undertaken by Bauche-Arnoult (1971, 1973). Some interactions, for example, those corresponding to the excitation of an electron in a closed shell to an empty shell, affect all the hyperfine structures of a valence shell in equal proportions. Core polarization, in which the orbits of the s electrons are radially distorted through their interaction with the open 4f shell, is an example of this. It can be represented by a contribution to a_{4f}^{10} in eq. (108). It is a curious fact that this contribution, which consists of a double sum over all occupied s states and over all unoccupied s states, almost exactly vanishes for neutral (that is, un-ionized) lanthanides; but the redistribution of s electrons among occupied and unoccupied orbits in the ions R^{2+} leads to a new double sum in which the almost exact cancellation of the positive and negative parts no longer occurs (Bordarier et al. 1965, Childs and Goodman 1972b). Equally interesting are those excitations of the type $(nl)^N \rightarrow (nl)^{N-1}n'l'$, which lead to effective hyperfine operators acting on two electrons at a time [and hence cannot be represented by H_{md} given in eq. (108)]. Different SL multiplets of a configuration $(nl)^N$ are now affected to different extents. Bauche-Arnoult (1971) expressed the correction factor associated with $\langle r^{-3}\rangle_{kk}$ by $(1 + \Delta_{kk})$, and found some remarkable patterns for the difference $\Delta_{01} - \Delta_{12}$ across the lanthanide series when $l' = l$. In particular, this quantity is the same for the Hund terms (the lowest of the configuration) coming from each member of the pairs (f, f^2), (f^5, f^6), (f^8, f^9) and (f^{12}, f^{13}).

Much of the above discussion can be paralleled for the nuclear quadrupole moment Q. The three parameters b_i^{11}, b_i^{13} and b_i^{02} are the analogues of the a_i^k; in the non-relativistic limit $b_i^{11} = b_i^{13} = 0$, and $\langle r^{-3}\rangle_{4f}$ reappears as the crucial radial integral. The difference $\Delta_{02} - \Delta_{12}$ possesses one value for configurations before the half-filled 4f shell and another value beyond it (Bauche-Arnoult 1971). However, the main interest in configuration interaction has centered on the so-called Sternheimer corrections, in which the plastic non-s closed shells of an atom screen (or enhance) the electrostatic interactions between the valence electrons and the nuclear quadrupole moment. The importance of this effect was recognized by Rabi. Sternheimer (1950) followed Teller's suggestion that he work out a quantitative theory, thereby embarking on an intellectual voyage of unimagined length. No account of the incidents incurred en route will be given here; a discussion of these has been outlined by Armstrong (1971) and, from a more general perspective, by Lindgren and Morrison (1982, chap. 14). We simply note here that the Sternheimer correction is usually expressed by a quantity R_{nl} that relates the experimentally observed and theoretical b_{nl}^{02} (in which, for the latter, the true Q is used) by the equation

$$(b_{nl}^{02})_{exp} = (1 - R_{nl})(b_{nl}^{02})_{theor}. \tag{110}$$

8.4.2. *Later developments*

Hyperfine-structure studies for the lanthanides were revitalized in the late 1970's by the introduction of two new techniques involving atomic beams: laser-induced fluorescence and laser–radio-frequency double resonance. Methods such as these enabled Childs et al. (1979) at the Argonne National Laboratory to find the hyperfine structures of several levels of Sm I $4f^6 6s6p$. Both the Argonne group and a group at Bonn turned their attention to ^{165}Ho I (Childs et al. 1983a, Burghardt et al. 1982). The principal motivation of the Argonne group was to test the conclusion of Wyart and Camus (1978) that substantially different Sternheimer factors were necessary for configurations of Ho I based on the two cores $4f^{10}$ and $4f^{11}$. Both the Argonne and Bonn groups found complete sets of the parameters a_{4f}^{kk} and b_{4f}^{kk}; differences in their figures can be ascribed to the different eigenfunctions they used for the levels ^4I_J of $4f^{11}$. The parameters agreed well with the optimized Hartree–Fock–Slater (OHFS) calculations of Lindgren and Rosén (1974b), and they were consistent with the results of Wyart and Camus (1978) for $4f^{11}$.

A similar experimental technique was used by Childs et al. (1983b) in their analysis of the hyperfine structures of ^3H_J and ^3F_J of ^{167}Er I $4f^{12}6s^2$. They were thwarted in their attempt to obtain extremely precise values of a_{4f}^{kk} and b_{4f}^{kk} by the difficulty in finding appropriate eigenfunctions for the levels. Such results as were obtained were found to agree well with the OHFS calculations of Lindgren and Rosén (1974b). The Argonne group extended their work to ^{159}Tb I $4f^9\,{}^6H_{11/2}$, ^{169}Tm I $4f^{13}\,{}^2F_{5/2}$, and ^{161,163}Dy I $4f^{10}\,{}^5I_{4,5,6}$ (Childs et al. 1984). Cheng and Childs (1985) used a multi-configuration Dirac–Fock (MCDF) program developed by Desclaux (1975) (but applied just to the states of the single configurations $4f^N$) to calculate hyperfine structures (as well as Landé g values) for the ground multiplets of most of the neutral lanthanides. Their ab initio results are generally in very good agreement with experiment; but, as Cheng and Childs themselves acknowledge, attention must now be directed to the residual discrepancies. The success of the relativistic theory, particularly for lanthanides in the second half of the series, has tended to obscure the relevance of the theory of Bauche-Arnoult (1971), which has been developed further to treat the term-dependent hyperfine parameters in the 3d shell (Johann et al. 1981).

Childs et al. (1986) have recently examined the hyperfine structures of several levels of $4f^{11}5d6s^2$ and one level of $4f^{12}6s6p$ belonging to ^{167}Er I. Satisfactory agreement with the MCHF calculations was obtained for the dipole parameters. Discrepancies for the quadrupole parameters were interpreted in terms of the Sternheimer correction factors of eq. (110). It was found that $R_{4f} = 0.22$ for $4f^{11}5d6s^2$, in good agreement with the figure of 0.23 for $4f^{12}6s^2$ found earlier (Cheng and Childs 1985), but at variance with the conclusion of Wyart and Camus (1978) for Ho I. The analysis of Childs et al. (1986) also yielded $R_{5d} = -0.18 \pm 0.05$ and $R_{6p} = -0.62 \pm 0.14$, thus confirming the anti-screening effects that had been expected for the 5d electron (Childs and Cheng 1984) and for the 6p electron too, though with a smaller $|R_{6p}|$ (Tanaka et al. 1983). The values of R_{nl} found by Childs et al. (1986) can scarcely be said to agree well with such calculations as are available.

Quoting from several articles and private communications of Sternheimer and his collaborators, Tanaka et al. (1983) gave the following theoretical estimates: $R_{4f} = 0.10 \pm 0.05$, $R_{5d} = -0.25 \pm 0.05$, $R_{6p} = -0.18 \pm 0.05$. The species of configuration interaction responsible for R_{nl} is evidently just as difficult to calculate accurately as that producing corrections to the Slater integrals.

8.4.3. *Isotope shifts*

The greater attention being paid to those aspects of hyperfine structure that have to do with atomic physics (rather than nuclear physics) is reflected in studies of isotope shifts. In 1970, Stacey (1971) could speak of using such studies to improve our knowledge of the distribution of charge within the nucleus, a prospect that he cast in terms of the major advances in the theory of nuclear structure that atomic spectroscopists have stimulated in the past. A few years later, Bauche and Champeau (1976), in their classic review of the field, showed how and why interest had moved towards electronic aspects. In the first place, the measurements of Striganov et al. (1962) on Sm I, which showed that relative isotope shifts are not constant, led to the realization that the specific mass shift (SMS) operator S, given by

$$S = \frac{1}{M} \sum_{i>j} \boldsymbol{p}_i \cdot \boldsymbol{p}_j, \tag{111}$$

was significant for nuclear masses M as large as those for the lanthanides (King 1963). The calculation of the matrix elements of S is an interesting problem in atomic physics, but there is absolutely no point in using isotope shifts to deduce values of M. In the second place, the distribution of nuclear charge makes itself felt by the electronic field-shift (FS) operator F, which, in the non-relativistic limit, is proportional to $\Sigma_i \delta(\boldsymbol{r}_i)$. Although the matrix elements of this operator are constant for a configuration – and thus rather uninteresting from an electronic standpoint – their appearance in second-order perturbation theory for a configuration such as $4f^N6s$ produces coefficients proportional to those of the Slater integrals $G^3(4f, 6s)$ that occur in the expressions for the term energies. As experimental techniques have improved it has become interesting to examine such extensions of the first-order theory.

The repetition of coefficients just mentioned is not limited to the FS operator. It was Stone (1959) who noticed that the tensorial structure of the term $\boldsymbol{p}_i \cdot \boldsymbol{p}_j$ occurring in the SMS operator is identical to that of $\boldsymbol{Y}_i^{(1)} \cdot \boldsymbol{Y}_j^{(1)}$. The latter appears in a configuration such as $4f^N5d$ in association with the Slater integrals $G^1(4f, 5d)$. The prefacing coefficients must reappear in a calculation of the matrix elements of S, given in eq. (111). To stress the correspondence, the new SMS parameter is written $g^1(4f, 5d)$. Because of the wide range of operators used in atomic shell theory it is perhaps not very surprising that matched parameters can be found as S and F are taken to second order of perturbation theory. The correspondence can be extended to several contributions to relativistic corrections, thereby introducing spin-dependent operators. The parameters analogous to ζ_{nl} are written z_{nl}.

In their review, Bauche and Champeau (1976) gave several examples drawn from

lanthanide spectra. The usefulness of z_{4f} was illustrated by the isotope shifts for $^{144-152}$Sm I $4f^6 6s^2\ ^7F$, an example drawn from the 1976 Paris thesis of Sallot. Lines from several transitions of Ce II (for isotope pairs 140–142, 138–140 and 136–140) were used to show how the so-called King plot could be used to separate the effects of FS from those of SMS. Bauche and Champeau (1976) also considered some lines of Sm I and Dy I (where the extent of configuration mixing for the levels involved was known) to show that the experimental SMS was roughly three-fifths of the HF value. Variable agreement with HF calculations was obtained by Wilson (1972) for the experimental FS for Sm I,II and Eu I,II. The comparison was made via what are known as screening ratios, which measure the ratios of differences of values of

$$\langle C|\sum_i \delta(\boldsymbol{r}_i)|C\rangle \tag{112}$$

for various configurations C. Coulthard (1973) used a relativistic HF program to recalculate (112). He found that substantial enhancements occurred (by factors of 3 or 4), and, although these enhancements largely disappeared when ratios were taken, there was a general improvement in the fit for Sm and Eu previously obtained by Wilson (1972).

Interest in the spectra of Sm I and Eu I has continued. Bauche et al. (1977) presented new isotope-shift measurements for $^{144-152}$Sm and interpreted the J dependence in the levels of $4f^6 6s^2\ ^7F_J$ in terms of a parameter $z_{4f} = 1.68 \pm 0.30$ mK, where $1\,\text{mK} = 10^{-3}\,\text{cm}^{-1}$. This value for z_{4f} corresponds well with the figure of 1.09 ± 0.22 obtained by Aufmuth (1978) for $^{162-164}$Dy II $4f^{10} 6s\ ^6I$. By taking several pairs of Sm isotopes, New et al. (1981) were able to deduce that the principal contribution to z_{4f} comes from the field-shift operator F taken to second order with the electronic Coulomb interaction. This result is consistent with the HF calculations reported by Aufmuth (1982) for the configurations $4f^N 6s$ in $^{142-144}$Nd II, $^{151-153}$Eu II and $^{162-164}$Dy II. The celebrated transitions $4f^7 6s^2 \leftrightarrow 4f^7 6s6p$ of Eu I were re-examined by means of laser absorption by Zaal et al. (1979), who were able to find improved isotope shifts for $^{151-153}$Eu. Griffith et al. (1981) interpreted some anomalies in Sm I as arising from the mutual perturbation of the two close levels at 19 174 and 19 192 cm^{-1}, a phenomenon for which Palmer and Stacey (1982) held F responsible. The parameter z_{5d} in Eu I $4f^7 5d6s\ ^{10}D$, ^8D was introduced by Pfeufer et al. (1982) and by Kronfeldt et al. (1982); a disconcerting sign difference has now been resolved (Kronfeldt et al. 1984), and there is good correspondence with the z_{5d} needed for $^{156-160}$Gd II $4f^7 5d6s\ ^{10}D$ (Kropp et al. 1985a). Parametric analyses of isotope shifts have continued with the work on Eu I $4f^7 6s6p$ and Eu I $4f^7 6s7s$ by Kropp et al. (1984, 1985b), who have been able to show that the ratio $g^3(4f,6s)/G^3(4f,6s)$ agrees with the HF value. Evidently the second-order corrections to g^3 and G^3 are roughly proportional to each other.

8.5. *Rydberg series*

Every configuration involving an electron nl has the potential for generating a

sequence of configurations in which n is replaced by $n+1$, $n+2$, $n+3$, etc. Levels in such a sequence that are matched in some way (usually by selecting a given core state and a given total angular momentum) are said to form a Rydberg series. The rich level structure of many low-lying configurations in the lanthanides almost always leads to a morass of overlapping Rydberg series. Progress has only been possible for cases where the low configurations are particularly simple. Garton and Wilson (1966) identified two Rydberg series of La I as corresponding to the transitions $6s^2 5d\,^2D_{3/2,5/2} \rightarrow 6s^2 np\,^2P_{3/2,1/2}$ ($n = 8, 9, \ldots, 23$) and were able to deduce an improved value for the ionization potential of La I. The relative isolation of ^8S in $4f^7$ made it possible for Smith and Tomkins (1976) to observe transitions of Eu I of the type $4f^7 6s^2\,^8S_{7/2} \rightarrow 4f^7 6snp\,^{2S+1}P_J$, where $J = \frac{5}{2}, \frac{7}{2}, \frac{9}{2}$, and $n \leqslant 62$. Camus and Tomkins (1969) reported the transitions $6s^2\,^1S_0 \rightarrow 6snp\,^{1,3}P_1$ ($n = 6, 7, \ldots, 48$) of Yb I, and showed that the smooth trend of the quantum defect μ_n ($= n - n^*$, where n^* is the effective principal quantum number) was broken by a perturbing level at 49 920 cm^{-1}. Laser excitation was used by Worden et al. (1978) to examine the Rydberg spectra of ten lanthanides and to determine ionization limits.

Summaries of the theoretical treatment of Rydberg series have been provided by Fano (1975) and Aymar (1984). Many of the ideas go back to the work of Seaton on multi-channel quantum-defect theory (MQDT) (see Saraph and Seaton 1971). The key element is that each nl electron, for large n, moves over most of its trajectory in a Coulomb potential. Thus the form of the wavefunction at large r is severely limited; in fact, it can be expressed as a linear combination of two basic forms, the relative strength of which fixes the quantum defect. The energies of the levels are given by $E = I - R/n^{*2}$, where R is the mass-corrected Rydberg constant and I an ionization limit. For a Rydberg series, the notion of a channel replaces that of a configuration. The angular momenta of the core and the outer electron are coupled in the usual way, but the radial integration is left in abeyance until channel mixing (the analog of configuration interaction) is considered.

In the late 1970's, the spectroscopy group at the Laboratoire Aimé Cotton (Orsay) returned to the Rydberg series of Yb I (Wyart and Camus 1979, Camus et al. 1980, Aymar et al. 1980, Barbier and Champeau 1980). The bound even-parity spectra (for which $J = 0$ and 2) and the bound odd-parity spectrum (for which $J = 1$) were analyzed with MQDT models involving up to six channels and four limits. The perturbations on the series $4f^{14}6sns\,^1S_0$ ($n \geqslant 7$) and $4f^{14}6snd\,^{1,3}D_2$ ($n \geqslant 8$) produced by the levels of $4f^{14}6p^2$ and $4f^{13}5d6s6p$ could be understood in a detailed way, as could the effect of the levels of $4f^{13}5d^26s$ on the series $4f^{14}6snp\,^{1,3}P_1$ ($n \geqslant 12$). Sixty levels for which $J = 0$ could be fit with an RMS deviation of 0.31 cm^{-1}; the corresponding deviations for 125 levels for which $J = 2$ and 14 levels for which $J = 1$ were 1.06 and 0.75 cm^{-1}, respectively. The parameters involved were the eigenquantum defects μ_α, the limits I_i for the series i, and the matrix elements $U_{i\alpha}$ describing the unitary transformation between the eigenchannels α and the so-called collision channels i. The details of this analysis are of considerable interest; however, they do not exhibit the spectral features of the lanthanides other than showing that the theory can accommodate the complications

that they give rise to. For that reason it does not seem appropriate to take space here to describe the theory at length.

The perturbers of the series $4f^{14}6snl$ of Yb I were found (or predicted) by Wyart and Camus (1979), who used the classic parametric approach to fit the levels of the two mixed configurations

$$4f^{14}(6s^2 + 5d^2 + 6p^2 + 5d6s + 6s6d + 6s7d + 6s8d + 6s9d + 6s10d + 6s7s + 6s8s + 6s9s) + 4f^{13}(6s^2 6p + 5d6s6p + 5d^2 6p),$$

and

$$4f^{14}(6s6p + 6s7p + 5d6p + 6s5f + 6s6f) + 4f^{13}(5d6s^2 + 5d^2 6s + 6s6p^2).$$

107 levels of the first configuration and 73 of the second (out of the respective totals 753 and 262) were fitted with deviations varying from a few cm^{-1} to just over $200\,cm^{-1}$. Wyart and Camus (1979) were also able to find some missing levels of Yb II $4f^{13}(5d^2 + 5d6p)$.

The hyperfine structures of ^{171,173}Yb I $4f^{14}6snd$ ($24 \leqslant n \leqslant 43$) were examined by Barbier and Champeau (1980). For these configurations, three terms in the Hamiltonian are of comparable importance: the electrostatic interactions between the 6s and nd electrons, the spin–orbit interaction H_{so} for the nd electron, and the hyperfine contact term at the nucleus for the 6s electron. The three parameters are $G^2(6s, nd)$, ζ_{nd} and a_s, respectively. As n becomes large the hyperfine parameter a_s dominates; for each isotope the configuration $4f^{14}6snd$ possesses a splitting that tends towards that for Yb II $4f^{14}6s$ as the trajectory of the nd electron becomes increasingly remote. Barbier and Champeau (1980) were also able to relate the isotope shifts for the Rydberg series to those of the resonance lines $4f^{14}6s \leftrightarrow 4f^{14}6p$ of Yb II.

Kotochigova et al. (1984) used the Hartree–Fock–Dirac method to calculate the energies of the levels of Eu I $4f^7(^8S)6snp$ ($6 \leqslant n \leqslant 17$) for which $J = 1$, and those of Yb I $4f^{14}6sn'p$ ($6 \leqslant n' \leqslant 11$) for which $J = \frac{7}{2}$. In general, the energies separating pairs of levels with a common n or a common n' are underestimated by roughly 20%, though the progression of the configurations to their respective ionization limits is given much more accurately. The underestimates of ζ_{np} and $\zeta_{n'p}$ indicate too great a radial extension to the p orbitals, a result that is consistent with the overestimate of the matrix elements of r (see section 8.7).

In order to help with the analysis of Rydberg series in Eu I, Wyart (1985) carried out a least-squares fit to the levels of

$$4f^7(^8S + {}^6P)(6s^2 + 5d6s + 5d^2 + 6s6d + 6s7d + 6p^2) + 4f^7(^8S)(6s7s + 6s8s + 6s9s + 6s10s)$$

by traditional means. 97 levels were fit with a mean error of $58\,cm^{-1}$. This work also has a relevance for three-step photo-ionization, such as that used to determine the isotope shifts of the short-lived pair $^{141-143}$Eu by Fedoseyev et al. (1984). Aymar et

al. (1984) used three-step laser spectroscopy to effect the transitions

$$4f^{14}6s^2\,{}^1S_0 \rightarrow 4f^{14}6s6p\,{}^3P_1$$
$$\rightarrow 4f^{14}6s7s\,{}^1S_0 \quad \text{or} \quad 4f^{14}6s7s\,{}^3S_1 \quad \text{or} \quad 4f^{13}({}^2F_{7/2})6s^26p_{3/2} \quad (J=2)$$
$$\rightarrow 4f^{14}6snp\,{}^1P_1, {}^3P_{0,1,2} \quad \text{or} \quad 4f^{14}6snf\,{}^1F_3, {}^3F_{2,3},$$

thereby reaching Rydberg series of odd parity and high n. The effects of perturbers coming from $4f^{13}5d^26s$ were studied. The revisions made in the earlier analyses for the $6snp$ series (Aymar et al. 1980) showed how delicate the choice of MQDT parameters can be. Aymar et al. (1984) concluded that the presence of perturbers near the ionization limit makes it essential to observe many Rydberg series to get a reliable value for the first ionization limit.

Two perturbing levels from $4f^{13}5d^26s$ were found by Blondel et al. (1983) to seriously affect the photo-ionization spectra of Yb I from the $6s7s\,{}^1S_0$ state in the presence of a static electric field. A more detailed description of this work has been provided by Blondel et al. (1985). Applying static electric fields to free lanthanide atoms is not currently used much. For a recent example of the classic Stark effect, the reader is referred to the measurements of Neureiter et al. (1986) on Sm I $(4f^66s6p + 4f^55d6s^2)^7F_1$.

8.6. *Spectra of highly ionized lanthanides*

The importance of astrophysical sources and plasma diagnostics to physicists has meant that there has always been considerable interest in the spectra of lanthanides from which many electrons have been stripped. Atomic species of that kind seldom show features that one associates with the lanthanides; indeed, the spectrum of Eu LXI, should it ever be studied, would bear on the two-electron problem. Such a possibility is not infinitely remote. In table 54 of his review article for the Handbuch der Physik, Edlén (1964) took the He I isoelectronic sequence only to Ne^{8+}; but, some 17 years later, Martin (1981) was working in a range that extended as far as Ar XVII. The functional dependence of the spectra on Z (the nuclear charge) is of prime interest here. In his extensive review of the spectra of highly ionized atoms reported during the period 1980–1983, Fawcett (1984) cited work on ten lanthanide ions (La XII through Ho XXII) like Pd I, ten ions (La XI through Ho XXI) like Ag I, two ions (Tm XLII and Yb XLIII) like Ni I, eight ions (La XXXI through Yb XLIV) like Co I, eight ions (La XXIX through Yb XLII) like Cu I, and two ions (Tm XL and Yb XLI) like Zn I. For the ions like Pd I, Sugar and Kaufman (1982) studied the trend of the resonance lines of the type $4d^95p^{3,1}P_1, {}^3D_1 \rightarrow 4d^{10}\,{}^1S_0$ and $4d^94f\,{}^3D_1, {}^1P_1 \rightarrow 4d^{10}\,{}^1S_0$. They found that there was a sharp increase in both the oscillator strengths and the Slater integrals at the onset of the contraction of the 4f orbit (that is, near Ba XI, where the binding energies of the 4f and 5p orbitals cross). To fit the energy levels, the HF values for the parameters had to be multiplied by the factors 0.90 for $F^2(4d,5p)$, 0.958 for $G^k(4d,5p)$, 0.75 for both $F^k(4d,4f)$ and $G^k(4d,4f)$, 0.85 for ζ_{4f}, 1.035 for ζ_{4d}, and 1.20 for ζ_{5p}. Similar scaling factors were found by Sugar and Kaufman (1980) for lanthanides in the Ag I sequence. As the

stages of ionization increase, the transitions move to the X-ray region, thus taking them out of the scope of the present review. For example, the 3d–4p, 3d–4f, 3p–4s, and 3p–4d transitions of Tm XLII and Yb XLIII are in the region 5–9 Å (Klapisch et al. 1980). The spin–orbit coupling constants ζ_{3d}, ζ_{4p}, ζ_{4d} and ζ_{4f} are very large and lead to *jj* coupling in such configurations as $3d^9 4p$, $3d^9 4f$, and $3p^5 4d$. For a detailed summary of work in the 1970's, the reader is referred to the works of Fawcett (1974, 1981).

8.7. *Intensities*

The great bulk of the spectra of the free lanthanides consists of lines that correspond to electric-dipole transitions. The contribution to the Hamiltonian is thus proportional to $\boldsymbol{E}\cdot\boldsymbol{r}_i$ for each electron i, and the whole problem turns on evaluating the matrix elements of $\Sigma_i \boldsymbol{r}_i$. Condon and Shortley (1935) listed the relative strengths of the lines of several transition arrays. The methods of Racah (1942b, 1943) can be readily applied to $\Sigma_i \boldsymbol{r}_i$. This operator possesses the tensorial characteristics of $\boldsymbol{T}^{(01)1}$ and thus leads to the selection rules ΔL, $\Delta J = 0, \pm 1$; $\Delta S = 0$. The details of working out the tensor algebra were described by Levinson and Nikitin (1965), who provided the transitions $4f^7(^8S)6p \rightarrow 4f^7(^8S)6s$ of Eu II and $4f^{13}6s6p \rightarrow 4f^{13}(6s^2 + 6s5d)$ of Yb II as examples.

A more complicated situation was considered by Camus (1970). He compared the data of Komarovskii and Penkin (1969) for 41 lines of Tm I with the results of a calculation based on transitions of the type $4f^{13}6s6p + 4f^{12}5d6s^2 \rightarrow 4f^{13}6s^2$. The radial integrals were evaluated by the HF method. With one overall scaling parameter, Camus (1970) was able to fit the observed line strengths to within 30% on the average. He also checked his working by comparing the lifetimes of twelve excited levels of Tm I with the figures obtained by Handrich et al. (1969) on the basis of the Hanle effect. Generally good agreement was found apart from a single level where a marked interference between the components belonging to $4f^{13}6s6p$ and $4f^{12}5d6s^2$ occurred.

Sugar (1972) used the calculated intensities for the transitions of the type $4d^{10}4f^N \rightarrow 4d^9 4f^{N+1}$ (which occur in the soft X-ray region) to confirm that the familiar term structure of the 4f-electron configurations appears in the metallic lanthanides. His results were consistent with the trivalent forms R^{3+} with the exceptions of Eu^{2+} and Yb^{2+}. The Slater integrals $G^1(4f,4d)$ and $F^2(4f,4d)$ had to be reduced from the corresponding HF values by roughly 33% and 25%, respectively, in order to get a reasonable fit to the experimental absorption curves.

Relative intensities can also be useful in confirming transitions in highly ionized species. Tech et al. (1984) examined the $4d^9$–$4d^8 5p$ transition array in La XIII (which occurs in the region 90–110 Å) and they were able to correlate 31 missing lines with low predicted intensities. The 25 known levels of La XIII $4d^8 5p$ were fit with nine adjustable parameters to an RMS error of $154\,cm^{-1}$. This is only 0.1% of the energy spread of the configuration.

Absolute line strengths are of considerable interest because a direct comparison can be made with the results of HF calculations. Dohnalik et al. (1979) measured the

oscillator strengths f of three lines of Er I $4f^{12}\,{}^3H_6(6s^2 \rightarrow 6s6p)$ with quoted errors of 25%, and found them roughly half as large as the corresponding HF values. Szynarowska and Papaj (1982) measured f for a single line of Gd I, thus scaling the 138 relative f values found by Penkin and Komarowsky (1973) for that spectrum. The latter authors were able to find the absolute values of f for the two lines $4f^{14}(6s^2 \rightarrow 6s6p\ {}^3P_1,\ {}^1P_1)$ of Yb I as 0.014 and 1.12, respectively (Komarovskii and Penkin 1969), which they compared to the figures 0.0167 ± 0.008 and 1.30 ± 0.06 obtained by Baumann and Wandel (1966) from the lifetimes derived by means of the zero-field crossing technique. A later measurement by Gustavsson et al. (1979) using the pulse modulations of a CW dye-laser beam yielded $f = 0.0159 \pm 0.005$ for the first of the two transitions, thus indicating that the figure of Komarovskii and Penkin (1969) may be somewhat too low. Similar discrepancies occur for Eu I (Gustavsson et al. 1979, Komarovskii et al. 1969). However, the differences between the experimental results are small compared to their deviations from the ab initio calculations. Loginov (1984) evaluated the radial transition integrals for Eu I $4f^7({}^8S)6s(5d \rightarrow 6p)$ using the Hartree–Fock–Dirac method and found them to be two to three times larger than those deduced directly from experiment. It is somewhat disconcerting, to say the least, that better results are obtained by the Coulomb approximation (Loginov 1984). That method is empirical by nature, being based on Heisenberg's form of the correspondence principle for non-relativistic matrix elements (Naccache 1972) and developed with considerable ingenuity by Picart et al. (1978) and Edmonds et al. (1979).

9. Non-linear spectroscopy

The intense electric field strengths $\boldsymbol{E}$ of laser beams have made it possible to greatly widen the scope of non-linear spectroscopy. This topic is characterized by the occurrence of more than one dipole operator of the type $\boldsymbol{E}\cdot\boldsymbol{D}$ connecting the initial and final states of a transition. The development of the theory can be traced back to the Göttingen thesis of Maria Mayer, which was summarized in an article she wrote while a Voluntary Assistant in Physics at The Johns Hopkins University (Göppert-Mayer 1931). Her method for describing two-photon phenomena was to take the perturbation $\boldsymbol{E}\cdot\boldsymbol{D}$ to second order, thus involving intermediate states χ in the perturbation process. Put crudely, we can imagine the first operator $\boldsymbol{E}\cdot\boldsymbol{D}$ as the agent that mixes $|\chi\rangle$ into the initial state $|\psi\rangle$, while the second connects the admixed part to the final state $|\psi'\rangle$. Since each operator $\boldsymbol{E}\cdot\boldsymbol{D}$ can only connect states of opposite parity, the parities of ψ and ψ' must be the same. Two applications of Mayer's work are of particular interest to us: two-photon absorption and Raman scattering.

9.1. *Two-photon absorption*

In 1961, Kaiser and Garrett (1961) illuminated $CaF_2{:}Eu^{2+}$ crystals with the red light of a ruby laser and observed fluorescence in the blue. The absence of any

energy levels below 22 000 cm^{-1} (other than the ground state $4f^7\,{}^8S_{7/2}$ of Eu^{2+} and some presumably irrelevant vibronic levels), taken with the dependence of the emitting intensity on E^4 (rather than E^2), made it clear that the fluorescence arose from a preliminary two-photon absorption followed by a cascading to the fluorescing level of $4f^6(^7F)5d$, whence the final transition to $4f^7\,{}^8S_{7/2}$ was made. Bayer and Schaak (1970) studied the anisotropy of this two-photon process, without, however, being able to provide a unique interpretation of their data. Several two-photon transitions for tripositive lanthanides in CaF_2 were reported by Apanasevich et al. (1973), who recognized that the two-photon process is similar in structure to that represented by expression (71) provided we set $k = 1$. Thus the effective transition operator is proportional to $(\boldsymbol{E}^{(1)}\boldsymbol{E}^{(1)})^{(2)}\cdot\boldsymbol{V}^{(2)}$. Another way of seeing this result is to note that $(\boldsymbol{EE})^{(0)}\cdot\boldsymbol{V}^{(0)}$ cannot produce a transition since $\boldsymbol{V}^{(0)}$ is a number, while $(\boldsymbol{EE})^{(1)}\cdot\boldsymbol{V}^{(1)}$ vanishes because $(\boldsymbol{EE})^{(1)}$, being the vector product of two identical commuting vectors, is zero. Any closure procedure that brings the two vectors $\boldsymbol{D}$ together to form an equivalent operator of the type $\boldsymbol{V}^{(t)}$ must thus lead us to $(\boldsymbol{EE})^{(2)}\cdot\boldsymbol{V}^{(2)}$.

Two-photon studies of Pr^{3+} in LaF_3 were made by Yen et al. (1981), who were able to populate the $^1D_2$ level and detect the two-photon transition $^1D_2 \rightarrow {}^1S_0$ of $4f^2$. However, the subject entered a new phase with the quantitative measurements of Dagenais et al. (1981) on $Gd^{3+}\,4f^7$ in LaF_3 at Harvard. With $\boldsymbol{E}$ parallel to the crystal axis $\boldsymbol{c}$, they found that the integrated intensities for the two-photon transitions $^8S_{7/2} \rightarrow {}^6P_{7/2}$, $^6P_{5/2}$, $^6P_{3/2}$ are in the proportions 320:5.4:1. Using the intermediate coupling wavefunctions of Carnall et al. (1977), they evaluated the reduced matrix elements of $\boldsymbol{V}^{(2)}$ and obtained the theoretical proportions 69:29:1. The difference between experiment and theory led them to conclude that $\langle 4f|r|5d\rangle$ must differ markedly for different J multiplets. It was soon found that a more plausible explanation existed (Judd and Pooler 1982): the vanishing of the diagonal matrix elements of $\boldsymbol{V}^{(2)}$ for the half-filled f shell depresses the contribution to the two-photon transition probability coming from the usual second-order mechanism to such an extent that third-order linkages of the type

$$\langle 4f^7\,{}^8S_{7/2}|\boldsymbol{E}\cdot\boldsymbol{D}|\chi\rangle\langle\chi|H_{so}|\chi'\rangle\langle\chi'|\boldsymbol{E}\cdot\boldsymbol{D}|4f^7\,{}^6P_J\rangle \tag{113}$$

must also be considered, where χ and χ' are both states of $4f^6 5d$. The most efficient way of evaluating the sums over χ and χ' is to use the method of second quantization. In the notation of sections 6.1.1, the operator product $(\boldsymbol{E}\cdot\boldsymbol{D})H_{so}(\boldsymbol{E}\cdot\boldsymbol{D})$, which results when closures over the angular parts of χ and χ' are performed, is expressed as

$$\boldsymbol{E}\cdot(\boldsymbol{a}_f^\dagger\boldsymbol{a}_d)^{(01)}\{\zeta_{5d}\sqrt{15}\,(\boldsymbol{a}_d^\dagger\boldsymbol{a}_d)^{(11)0}+\zeta_{4f}\sqrt{42}\,(\boldsymbol{a}_f^\dagger\boldsymbol{a}_f)^{(11)0}\}\boldsymbol{E}\cdot(\boldsymbol{a}_d^\dagger\boldsymbol{a}_f). \tag{114}$$

Since there is no 5d electron in the ground state ψ, we can transfer $\boldsymbol{a}_d$ to the right by means of the anticommutation relations for fermions until ultimately the equation $\boldsymbol{a}_d|\psi\rangle = 0$ can be employed. It turns out that expression (114) is proportional to

$$20(9\zeta_f+\zeta_d)E^2(\boldsymbol{a}_f^\dagger\boldsymbol{a}_f)^{(11)0}-\sqrt{3}\,(9\zeta_f-4\zeta_d)(\boldsymbol{E}^{(1)}\boldsymbol{E}^{(1)})^{(2)}\cdot(\boldsymbol{a}_f^\dagger\boldsymbol{a}_f)^{(11)2},$$

so that the characteristic second-rank tensor is preceded by a large term, scalar in $\boldsymbol{E}$, that can directly connect $^8S_{7/2}$ to $^6P_{7/2}$ and thus enhance the two-photon transition probability. This term disappears for circularly polarized light, since there is no way that $E_1^{(1)}E_1^{(1)}$ or $E_{-1}^{(1)}E_{-1}^{(1)}$ can produce a component $(\boldsymbol{E}^{(1)}\boldsymbol{E}^{(1)})_{+2}^{(t)}$ for which $t = 0$.

In order to account satisfactorily for two-photon transitions from $^8S_{7/2}$ to the ^6D and ^6I multiplets, a number of extensions to the theory must be made. A detailed account has been given by Downer and Bivas (1983) and by Downer et al. (1983). The crystal field for a 5d electron contains terms of the type $\boldsymbol{A}^{(04)}\cdot(\boldsymbol{a}_d^\dagger\boldsymbol{a}_d)^{(04)}$, where the various components A_{4q} of $\boldsymbol{A}^{(04)}$ are proportional to the crystal-field parameters of sections 5.3 and 7.1. The fourth-order product

$$\boldsymbol{E}\cdot(\boldsymbol{a}_f^\dagger\boldsymbol{a}_d)^{(01)}\boldsymbol{A}^{(04)}\cdot(\boldsymbol{a}_d^\dagger\boldsymbol{a}_d)^{(04)}(\boldsymbol{a}_d^\dagger\boldsymbol{a}_d)^{(11)0}\boldsymbol{E}\cdot(\boldsymbol{a}_f^\dagger\boldsymbol{a}_d)^{(01)}$$

yields terms of the type

$$((\boldsymbol{EE})^{(02)}\boldsymbol{A}^{(04)})^{(06)}\cdot(\boldsymbol{a}_f^\dagger\boldsymbol{a}_f)^{(16)6}, \tag{115}$$

which can directly link $^8S_{7/2}$ with ^6I_J. With the aid of such theoretical devices, Downer and his Harvard colleagues were able to give a remarkably complete description of the intensities and anisotropies of the two-photon transitions for Eu^{2+} in CaF_2 and SrF_2 as well as Gd^{3+} in LaF_3 crystals and in aqueous solution. From a theoretical point of view, the success of the multiple closure procedure was one of the most noteworthy results. The presence of varying energy denominators has often deterred the theorist from using the rigorous equation $\Sigma_\xi|\xi\rangle\langle\xi| = 1$ (which holds for a complete set of states ξ) to evaluate a sum such as $\Sigma_\xi|\xi\rangle E_\xi^{-1}\langle\xi|$. However, once it was recognized that the angular completeness holds for every configuration C, and that the energies appearing in the perturbation expansion are of the type E_C, the problem evaporated.

Two-photon spectroscopy should continue to develop in the years to come. Since the process conserves parity, the masking of the one-photon transitions $4f^N \rightarrow 4f^N$ by the much stronger transitions $4f^N \rightarrow 4f^{N-1}5d$ can be avoided, thereby allowing the higher levels of the configurations $4f^N$ to be detected. Examples of this have been given for Eu^{2+} $4f^7$ by Downer et al. (1983). The $^1S_0$ level of Pr^{3+} $4f^2$, which lies very close to the configuration 4f5d, has been found for Pr^{3+} in $LaCl_3$ by Rana et al. (1984), and the corresponding transition (namely $^3H_4 \rightarrow {}^1S_0$) has been reported for Pr^{3+} in LaF_3 by Cordero-Montalvo and Bloembergen (1984, 1985). The mediating operator is similar to that given by expression (115) except that the superscripted ranks for the coupled creation and annihilation operators are now (15)4 rather than (16)6. Further information on this system has been given by Bloembergen (1984).

9.2. *Raman scattering*

The theory of Raman scattering is virtually identical to that for two-photon absorption: the principal difference is that $\boldsymbol{E}_1\cdot\boldsymbol{D}$ for the incident wave need not be identical to $\boldsymbol{E}_2\cdot\boldsymbol{D}$ for the scattered wave. Thus $(\boldsymbol{E}_1\boldsymbol{E}_2)^{(1)}$ is not necessarily zero and terms involving $\boldsymbol{V}^{(1)}$ can appear in the effective Hamiltonian that drives the transition. Richman et al. (1963) observed the Raman spectrum of $LaCl_3$ and

observed three strong lines at 108, 186 and 211 cm^{-1}, the last exhibiting a shoulder at 217 cm^{-1}. These four active lines were confirmed by Hougen and Singh (1963, 1964), who assigned them the irreducible representations E_{2g}, $A_g + E_{1g}$, E_{2g} and E_{2g} of the group C_{6h}, corresponding to even-parity normal modes of the $LaCl_3$ crystal. Only one mode (of the type A_g) escaped detection. Hougen and Singh (1964) repeated their experiments for $PrCl_3$; in addition to a virtually unchanged vibrational pattern of lines, they observed some ten electronic transitions, which matched the known sublevel structure of $^3H_4$, $^3H_5$ and $^3F_2$ of $4f^2$ rather well. They obtained the selection rules for the electronic Raman effect by performing a complete closure over all intermediate states: that is, by directly coalescing the two vectors $\boldsymbol{D}^{(1)}$ in $(\boldsymbol{E}_1 \cdot \boldsymbol{D})(\boldsymbol{E}_2 \cdot \boldsymbol{D})$. Since $(\boldsymbol{D}^{(1)}\boldsymbol{D}^{(1)})^{(t)}$ is ineffective for $t = 0$ and vanishes for $t = 1$, we are left with a second-rank tensor proportional to $\boldsymbol{V}^{(2)}$. Thus Hougen and Singh (1964) found that, within the closure approximation, the selection rules should be identical to those for electric-quadrupole radiation. But although rough agreement was obtained for the polarizations of the lines, substantial discrepancies for the intensities were noted.

Axe (1964) showed that, by performing separate (partial) closures over the excitations $f \longleftrightarrow d$ and $f \rightarrow g$, contributions to the effective operator $\boldsymbol{V}^{(1)}$ emerge. Electronic Raman spectra of the type $^7F_0 \rightarrow {}^7F_J$ were observed by Koningstein (1966) for europium yttrium gallium garnet, and by Koningstein and Mortensen (1967) for Eu:YVO_4. A continuation of these experiments established the existence of an antisymmetric Raman scattering tensor (Koningstein and Mortensen 1968), which must owe its existence to $\boldsymbol{V}^{(1)}$. The polarization data necessary to obtain this result were taken further by Finkman et al. (1973) in their work on $NdAlO_3$. The measurements of Guha (1981) on $TmPO_4$ were re-evaluated by Becker et al. (1985) and extended to $ErPO_4$. By that time rather good crystal-field analyses had been made for these phosphates (Hayhurst et al. 1981, Becker et al. 1984), so that the eigenfunctions of the initial and final states of $4f^N$ were known. Finkman et al. (1973) had similar information at their disposal for their analysis of Nd^{3+} $4f^3\,{}^4I_J$. Since the proximity of the configurations $4f^{N-1}5d$ was well established, while the position of any configuration of the type $4f^{N-1}ng$ remained unknown, only those intermediate states χ belonging to $4f^{N-1}5d$ were considered. Both Finkman et al. (1973) and Becker et al. (1985) found that the calculated strength of the antisymmetric tensor turned out to be very much larger than their experiments suggested. Evidently the strength of $\boldsymbol{V}^{(1)}$ had been over-estimated.

To reduce it, the effects of the g electrons need to be considered. After all, we know from the total closure argument that a suitable weighting of the excitations $f \longleftrightarrow d$ and $f \rightarrow g$ can be found that eliminates $\boldsymbol{V}^{(1)}$ altogether. As was mentioned in section 5.4.2, Axe (1963) had found it necessary to include g electrons as intermediaries in his analysis of one-photon transitions within the configurations $4f^N$. Over the years, other were led to a similar conclusion (Krupke 1966, Hasunuma et al. 1984). Of course, the extended ng orbital of a free ion R^{3+} cannot exist untouched in a crystal, but, even with a strong perturbation, it is difficult to see how the crucial matrix element $\langle 4f|r|ng\rangle$ can be large enough. States in the continuum could increase the overlap between 4f and εg, but the energies ε labelling these g

states would have to be enormous. At first sight, it seems far from easy to account for the apparent importance of g electrons. As was discussed by Becker et al. (1985), the difficulty arises because the intermediate states χ are characterized by l. This quantum number is appropriate for SO(3) symmetries but not for a point symmetry such as D_{2d} (which obtains in the phosphates). The states χ that play an important role extend over the central lanthanide ion and the neighboring ligands, and there is no a priori reason why χ should possess more d character than g character. It does not seem appropriate to elaborate this point further because, even with a reduced strength of $V^{(1)}$, the intensities of the individual Raman lines do not agree well with theory. Several theoretically strong lines in $TmPO_4$ are completely missing. It can only be hoped that the situation will become clearer when data for other lanthanide ions in the same phosphate lattice become available. The experimental results of Williams et al. (1987) for Ce^{3+}:$LuPO_4$ should be of considerable help in that regard, since only one-electron configurations are involved.

10. Satellite lines

The spectra of lanthanide ions in crystals are frequently plagued – or favored, according to one's point of view – by lines other than those associated with the electronic and vibronic levels of a single lanthanide. Many of these satellite line are the result of crystal defects. For example, the Darmstadt group studied the complementary systems $Pr_2Mg_{3c}Zn_{3(1-c)}(NO_3)_{12}\cdot 24H_2O$ for which $c \simeq 0.01$ and 0.99 (Hellwege 1972, Heischmann et al. 1972). The presence of an exceptional Mg^{2+} or Zn^{2+} ion near a Pr^{3+} ion destroys the perfect C_{3v} point symmetry and lifts any degeneracy among the sublevels. Satellite structure is more striking in those cases where the standard theory predicts a single line. A good example is the transition $^5D_0 \rightarrow {}^7F_0$ in Eu^{3+}, which can occur (for non-centrosymmetric europium sites) when J mixing is considered. Caro et al. (1985) have reported the occurrence of at least four lines for Eu^{3+} in $GdNbO_4$ when an argon laser line (at 4658 Å) is used to excite the fluorescence. Crystal defects cannot be easily invoked here, and some interplay between electronic and vibronic levels is presumably at work.

10.1. *Hole-burning spectroscopy*

The transitions $^5D_0 \longleftrightarrow {}^7F_0$ of Eu^{3+} are interesting in another context. The two nuclei ^{151}Eu and ^{153}Eu both possess nuclear spins of $\frac{5}{2}$ and quadrupole moments for which $^{153}Q/{}^{151}Q \simeq 2.54$ (Krebs and Winkler 1960). The direct interaction of the protons of the nucleus with the crystal field can be found by making replacements of the type

$$A_{kq}r_i^k Y_{kq}(\theta_i, \phi_i) \rightarrow -A_{kq}r_j^k Y_{kq}(\theta_j, \phi_j)$$

in the crystal-field Hamiltonian, where (r_i, θ_i, ϕ_i) are the polar coordinates of an electron i, and (r_j, θ_j, ϕ_j) those of a proton j. In analogy to the equivalence given by (68), and with a suitable choice of coordinate axes, we can write the quadrupolar

part of the interaction as

$$\tfrac{1}{3}P[3I_z^2 - I(I+1) + \eta(I_x^2 - I_y^2)]. \tag{116}$$

Terms of this type might be expected to be revealed when the electronic splitting vanishes, as it does for levels for which $J = 0$. The parameter P, which is proportional to Q, would nevertheless be very difficult to detect were it not for Sternheimer anti-shielding factors of the order of 150 (Edmonds 1963). Macfarlane et al. (1980) detected the hyperfine splittings for the levels $^5D_0$ and $^7F_0$ of Eu^{3+} in EuP_5O_{14} by the so-called hole-burning technique. By this experimental procedure the populations of the hyperfine levels are redistributed, and the 'holes' and 'anti-holes' are detected by scanning the transition $^7F_0 \rightarrow {}^5D_0$ with an attenuated laser beam and monitoring changes in the fluorescence $^5D_0 \rightarrow {}^7F_J$. Subsequent experiments on $Eu^{3+}:YAlO_3$ determined the splittings induced in the nuclear doublets $|I, \pm M_I\rangle$ by an external magnetic field (Shelby and Macfarlane 1981). An analysis of these results confirmed the mixing (via the crystal-field and Zeeman Hamiltonians) that takes place between the comparatively closely spaced ^7F_J levels, in contrast to the situation for the extended ^5D multiplet.

This work set the stage for the astonishingly detailed experiments of Cone et al. (1984) on $EuVO_4$. Some 30 lines of the type $^7F_0 \rightarrow {}^5D_0$, extending over about $20\,cm^{-1}$, were observed in absorption. The D_{2d} site symmetry of Eu^{3+} in $EuVO_4$ precludes any transitions of the type $0 \rightarrow 0$, so each line must be due to a distinct defect or dislocation site in the crystal. The collection of 30 lines constitutes an array of satellites to a forbidden line. Cone et al. (1984) pointed out that there must be some 30-odd well defined ways, all chemically inequivalent, of disturbing the Eu^{3+} site symmetry in the vanadate structure. Hole-burning enabled the hyperfine structures of ten or so lines to be explored. For each line, only four parameters (and the known ratio of the quadrupole moments) were found to be required to give a good fit with experiment: these are P and η [appearing in expression (116)] for both $^7F_0$ and $^5D_0$. For perfect D_{2d} symmetry the x, y and z axes can be chosen so that $\eta = 0$. However, Cone et al. (1984) observed widely varying values of η, indicating that the principal axes associated with the various defects are differently oriented. Their measurements also revealed that, for a given line and a given isotope, it can well happen that $\eta(^5D_0) \neq \eta(^7F_0)$. This provides direct evidence of deviations from the ideal condition $J = 0$.

The fact that, for each line, a different set of axes has been set up complicates the analysis of the effect of an external magnetic field $\boldsymbol{H}$ on the nuclear moment $\boldsymbol{\mu}$. The direct term, $-\boldsymbol{\mu}\cdot\boldsymbol{H}$, needs to be multiplied by a factor to allow for cross terms involving the Zeeman Hamiltonian and the hyperfine interaction given by (108), as was recognized first by Elliott (1957). But as soon as $\boldsymbol{\mu}$ is replaced by $\boldsymbol{I}$ (times a factor), we arrive at combinations such as I_zH_z that can be easily evaluated in the basis $|I, M_I\rangle$ only if the coordinate frame defined by the principal axes is used. The required transformation of axes, which varies from line to line, has been described by Cone et al. (1984).

By such techniques the study of hyperfine structures has achieved a precision for crystal spectra comparable to that for the spectra for the free ions. Admittedly, the

line $^5D_0 \longleftrightarrow {}^7F_0$ is a very special case. But we have come a long way in the decade since Hüfner (1978) gave the work of Dieke and Crosswhite (1967) on Ho^{3+} in $LaCl_3$ as the sole example of optical hyperfine structure observed by direct spectroscopy in a lanthanide crystal.

11. Mathematical implications

One of the most remarkable features of the analysis of Racah (1949) for the Coulomb energies in the f shell is that the theory works much better and shows more simplifications than could possibly have been anticipated in 1949. As was explained in section 4.3.6, Racah's use of the Lie groups SO(7) and G_2 provides explanations for the vanishing of many matrix elements and for the proportionalities that some matrices bear to others; but it also goes beyond a straightforward application of the Wigner–Eckart theorem that such examples represent. The principal surprises are as follows:

(a) In the calculation of the matrix elements of the e_r of eqs. (64), multiplicity difficulties are much less of an encumbrance than might have been expected. For example, in working out

$$\langle f^N W U \tau S L | e_2 | f^N W' U' \tau' S L \rangle, \tag{117}$$

Racah needed to know how many times (40) (the G_2 label for e_2) occurs in the reduction of the Kronecker product $U \times U'$, since this determines the number of possible labels γ to be attached to the isoscalar factors

$$(U \tau L | (40) 0 + U' \tau' L)_\gamma \tag{118}$$

of eq. (51) when the generalized Wigner–Eckart theorem is used to evaluate the matrix element given by (117). But, although (40) occurs up to five times in the reduction of those products $U \times U'$ appearing in the f shell, Racah found that each set of isoscalar factors given by (118), for a given γ and various τ, τ' and L, is proportional to every other set; with, however, the sole exception of the set for which $U = U' = (21)$, where two labels γ_1 and γ_2 are required.

(b) The calculation of the matrix elements of e_3 is enormously simplified by introducing an operator Ω, given by $\frac{1}{2}L^2 - 12G(G_2)$, where $G(G_2)$ is Casimir's operator for G_2 (briefly mentioned in section 8.3.3). Racah brought Ω into play because its labels WU are the same as those for e_3, namely (220)(22), and because its eigenvalues can be immediately written down. It could thus be used to find a set of isoscalar factors $(U \tau L | (22) 0 + U' \tau' L)$ for a particular U and U', and hence define an initial γ. By what must have seemed like an astonishing piece of good luck, Racah discovered that the matrices of the combination $e_3 + \Omega$ (for a given U and U') are all proportional to one another. Thus no multiplicity labels are required at all for the operator $e_3 + \Omega$, although (22) occurs up to three times in the reduction of the relevant $U \times U'$.

(c) All matrices of $e_3 + \Omega$ vanish for states whose seniorities v (defined in section

3.6) are 6 or 7. Others (of specified U, U', v and S) are related by coefficients depending only on N and v.

(d) The following sum is valid:

$$\sum_{N=v}^{14-v} \langle \mathrm{f}^N v\, U\, S\, L | e_3 + \Omega | \mathrm{f}^N v\, U'\, S\, L \rangle = 0. \tag{119}$$

More unexpected simplifications were discovered when the matrix elements of other operators (like H_{so} or $V^{(t)}$) were evaluated. The casual reader who opens the book of tables compiled by Nielson and Koster (1963) might be surprised to find large numbers of null matrix elements. Most of these correspond to selection rules on W or U that come immediately from an application of the generalized Wigner–Eckart theorem, but the others constitute an unnervingly large residue. It was clear by the 1960's that they were the indicators of unrecognized group structure in the f shell.

11.1. *Quasi-spin*

Of the two ^{2}D terms in d^3, one possesses no ^{1}S character in its parentage (see section 3.6), and corresponds to a seniority v of 3. The other, for which $v = 1$, can be imagined as being produced by adding a ^{1}S term to ^{2}D of d^1. It can be written (in an unnormalized form) as $(\boldsymbol{a}^\dagger \boldsymbol{a}^\dagger)^{(00)} \boldsymbol{a}^\dagger |0\rangle$. The use of the fermion creation operators guarantees proper antisymmetry. The ^{2}D term of d^5 with seniority 1 can be constructed by a further application of $(\boldsymbol{a}^\dagger \boldsymbol{a}^\dagger)^{(00)}$; in fact, we can continue to d^7 and finally to d^9, thereby obtaining five ^{2}D terms for which $v = 1$ in all cases. We can return to ^{2}D of d^1 by means of $(\boldsymbol{aa})^{(00)}$. The commutator of $(\boldsymbol{a}^\dagger \boldsymbol{a}^\dagger)^{(00)}$ and $(\boldsymbol{aa})^{(00)}$ yields an operator proportional to $(\boldsymbol{a}^\dagger \boldsymbol{a})^{(00)} + (\boldsymbol{aa}^\dagger)^{(00)}$, and the collection of three operators closes under commutation. With suitable prefacing coefficients, the commutation relations can be made identical to those for the three components Q_+, Q_- and Q_z of an angular-momentum vector $\boldsymbol{Q}$, which is called the *quasi-spin*. An analogous operator was first constructed by Kerman (1961) for nuclear shell theory and elaborated by Flowers and Szpikowski (1964) and by Lawson and Macfarlane (1965). With the help of that work it was not difficult to extend the method to the atomic case (Judd 1967b).

The five ^{2}D terms of the d shell for which $v = 1$ constitute a quasi-spin quintet: that is, $Q = 2$. As we run from d to d^9, adding pairs of electrons coupled to ^{1}S, the eigenvalue M_Q of Q_z changes in integral steps from -2 to $+2$. For states of seniority v in l^N, we have, in general,

$$Q = \tfrac{1}{2}(2l + 1 - v), \qquad M_Q = -\tfrac{1}{2}(2l + 1 - N). \tag{120}$$

All properties of the seniority v can now be interpreted in terms of angular-momentum theory. The vector $\boldsymbol{Q}$ is scalar with respect to $\boldsymbol{S}$ and $\boldsymbol{L}$ as well as to the generators of G_2 and SO(7). Operators can be assigned quasi-spin ranks K; obviously $K = 1$ for $\boldsymbol{Q}$, while $K = 0$ for $\boldsymbol{S}$ and $\boldsymbol{L}$. However, $\boldsymbol{Q}$ does not commute with $V^{(t)}$ when t is even (and nonzero), and for these tensors it turns out that $K = 1$.

More to the point, a detailed analysis reveals that $K = 0$ for e_2 and $K = 2$ for $e_3 + \Omega$. This knowledge allows us to understand many of the puzzles listed under (a)–(d) in section 11 above. For example, the vanishing of $e_3 + \Omega$ for states for which $v = 6$ or 7 corresponds to the vanishing of a tensor of rank 2 when set between states for which $Q = \frac{1}{2}$ or 0. Again, we have only to apply the Wigner–Eckart theorem in quasi-spin space to the matrix elements appearing in eq. (119) to convert that equation to

$$\sum_{M_Q} (Q\, M_Q | 20,\, Q\, M_Q) = 0,$$

a result that is merely a statement of the orthogonality of CG coefficients of argument 2 to the corresponding ones of argument 0, all of which are equal to 1.

Once the idea of quasi-spin had been introduced, it did not take long for all kinds of properties to be put in perspective. For example, Racah's observation that every W occurs in the f shell with two pairs (S_1, v_1) and (S_2, v_2) turns out to correspond to a spin–quasi-spin pair (S_1, Q_1) and its companion (S_2, Q_2) for which $S_2 = Q_1$ and $Q_2 = S_1$. Other properties of the spin–quasi-spin interchange have recently been developed to explain, among other things, the inversion of the octets and sextets of f^7 compared to the terms of corresponding L in f^2 (Judd et al. 1986). Similar methods can be used to account for some of the properties of e_2 mentioned in section 11, note (a), above. However, not all of the unexpected simplifications listed in section 11 yield to this approach.

11.2. *Spin-up and spin-down spaces*

The idea of dividing the electrons of the f shell into two classes according to their spin orientation was mentioned in section 3.5 as being the method that Racah (1942b) used to calculate the term energies of f^3. We can go further and imagine that f electrons come in two kinds: those with their spins up (f_A), and those with their spin down (f_B). The configuration f^N is thus a collection of the configurations $f_A^r f_B^{N-r}$ for $r = 0, 1, \ldots, N$. The Pauli exclusion principle need only be imposed on the f_A electrons or on the f_B electrons separately; and we can introduce Lie groups such as G_{2A} for the f_A electrons or $SO_B(7)$ for the f_B electrons (Judd 1967b). Several options are available for coupling the spin-up and spin-down spaces. It was found that a coupling at the G_2 level was particularly useful in accounting for the reduction in the number of multiplicity labels γ of section 11, notes (a) and (b), (Judd and Armstrong 1969). Of course, our operators must also be given a classification in the A and B spaces, but this is usually not too difficult to do. For example, e_2 has non-vanishing matrix elements in f^2 only for the singlets, that is, for states for which $U \equiv (20)$ and $M_S = 0$. These belong to $f_A f_B$, which has a $G_{2A} \times G_{2B}$ structure of $(10) \times (10)$. For

$$\langle ((10) \times (10))(20) | (U_A \times U_B)(40) | ((10) \times (10))(20) \rangle \tag{121}$$

not to vanish, we must have $U_A \equiv U_B \equiv (20)$, as can be confirmed from the table of Kronecker products given by Wybourne (1970). So $e_2 \sim ((20)_A \times (20)_B)(40)$. The

operator e_3 is somewhat more complicated to treat: it needs the superposition of four products $(U_A \times U_B)(22)$.

As an example of the method, consider the two sets of matrix elements

$$C_L = \langle f^5\,{}^4(211)(30)L|e_2|f^5\,{}^4(211)(30)L\rangle \tag{122}$$

and

$$D_L = \langle f^5\,{}^2(221)(30)L|e_2|f^5\,{}^2(221)(30)L\rangle, \tag{123}$$

where L runs over the possibilities P, F, G, H, I, K and M. In spite of the fact that (30) × (30) contains (40) twice (Racah 1949, table V), thus implying the potential need for two symbols γ in the isoscalar factor (118), it turns out that $C_L = 4D_L$. Can we understand how an equation of this simplicity can come about? We first note that the possible representations U_A in f_A^N (or, equally, U_B in f_B^N) are (10) for $N = 1$, (10) + (11) for $N = 2$, and (00) + (10) + (20) for $N = 3$ or 4 (Racah 1949, table I). Picking $M_S = \frac{3}{2}$ (corresponding to $f_A^4 f_B$), eq. (122) becomes

$$C_L = \langle((20) \times (10))(30)L|((20) \times (20))(40)|((20) \times (10))(30)L\rangle. \tag{124}$$

We can equally well pick $M_S = \frac{1}{2}$, but first we have to make the expansion

$$|f^5\,{}^4(211)\,(30)\,(M_S = \tfrac{1}{2})L\rangle = a|((20) \times (11))(30)L\rangle + b|((20) \times (10))(30)L\rangle, \tag{125}$$

getting an equation of the form

$$C_L = a^2 E_L + 2abF_L + b^2 G_L, \tag{126}$$

where E_L, F_L and G_L are defined in a similar way to C_L in eq. (124). In fact, G_L has exactly the same structure as C_L except that (20) in the bra and ket refers to f_A^3 rather than f_A^4, while (10) refers to f_B^2 rather than f_B. The first corresponds to a hole–particle interchange in spin-up space, the second to passing from ^{2}F of f^1 to ^{3}F of f^2. For the operator e_2, which possesses the structure (20) × (20) corresponding to even-rank tensors in the A and B spaces, these two changes produce the factors -1 and $-\frac{1}{3}$ (Nielson and Koster 1963, p. 70). So $G_L = \frac{1}{3}C_L$. The orthogonal expansion to (125) gives $|f^5\,{}^2(221)(30)(M_S = \frac{1}{2})L\rangle$, so we have

$$D_L = b^2 E_L - 2abF_L + a^2 G_L. \tag{127}$$

Since e_2 is diagonal with respect to S, the cross term must vanish: that is,

$$ab(E_L - G_L) - (a^2 - b^2)F_L = 0. \tag{128}$$

Equations (126)–(128), together with $G_L = \frac{1}{3}C_L$, are enough to show that C_L, D_L, E_L and G_L are all proportional to one another. In particular, C_L is proportional to D_L, the result we want. For readers interested in following the argument in detail, the additional information $a = \pm\frac{1}{3}\sqrt{8}$ and $b = \pm\frac{1}{3}$ (from Donlan 1970, p. 54) may be useful.

The line of reasoning given above is a good example of how group theory can be used to establish connections across the entire f shell. The spin-up and spin-down spaces lead to a better understanding of the properties of the Coulomb interaction – an interaction which, in itself, makes no reference to the orientation of the spins of

the electrons. Because exchange and direct interactions are of comparable magnitude for 4f electrons, one would not expect the A and B spaces to have any direct application to experiment. Most remarkably, however, it turns out – for reasons that are still obscure today – that the three ^{5}D terms of $4f^6$ for which $M_S = 2$ are almost pure states of the type $|f_A^5(L_A)f_B, D\rangle$, where $L_A \equiv H$ (for the lowest ^{5}D term), $L_A \equiv F$ (for the middle ^{5}D term), and $L_A \equiv P$ (for the highest ^{5}D term). These results are important for understanding the multiplet splittings of the ^{5}D terms, since it turns out that ζ_f and λ of eq. (32) are related by

$$\lambda = \zeta_f[L_A(L_A + 1) - L_B(L_B + 1)]/2M_S L(L + 1). \tag{129}$$

So λ is large for the lowest ^{5}D term, very small for the middle one, and negative for the highest one. The large observed separations between $^5D_0$, $^5D_1$ and $^5D_2$ of Eu^{3+} $4f^6$ are thus a direct consequence of the purity of the lowest ^{5}D term in *Ll* coupling.

Equation (129) also provides an explanation for $\langle f^3\,{}^2(11)H|H_{so}|f^3\,{}^2(11)H\rangle$ being zero, a result presented as a curiosity in eq. (36) and mentioned again in section 5.2. For $f_A^2 f_B$, the representation (11) can only be formed from the product $(10)_A \times (10)_B$ of the representations of $G_{2A} \times G_{2B}$ (Wybourne 1970, table E-4). So $L_A = L_B = 3$, and $\lambda = 0$ from eq. (129). A similar argument can be used to explain $\lambda(f^3\,{}^2P) = 0$ and $\lambda(f^6\,{}^5P) = 0$, both of which would be tedious to account for otherwise.

11.3. *Group extensions*

The development of the theory of the spin-up and spin-down spaces did not end the search for new group structure in the f shell. It has been a theme of recurring interest to the writer for the last twenty years. A summary of the situation in 1969 was provided by Wybourne (1970), though he could not evade the difficulty anyone faces who writes about Lie groups for physicists: how to strike the right balance between giving rigorous mathematical proofs, which is tedious in the extreme, and describing the grand themes of the subject, which can only be achieved through examples if the pace is not to lag. The theorist is continually distracted by results that have aesthetic appeal but which, in all probability, very little utility. For example, the collection of 2^{14} states that make up the f shell can be regarded as the basis for a single irreducible representation of the unitary group $U(16\,384)$; but this striking piece of information does not get us very far.

The group SO(28), formed by taking for its generators all pairs of operators $a_\xi a_\eta$, $a_\mu^\dagger a_\nu$ and $a_\lambda^\dagger a_\tau^\dagger$ that act in the f shell, has fared better. All the states of f^N with even N form the basis for the most elementary spin representation $(\frac{1}{2}\frac{1}{2}\cdots\frac{1}{2})$ of SO(28); these with odd N correspond to the complementary representation $(\frac{1}{2}\frac{1}{2}\cdots\frac{1}{2}-\frac{1}{2})$. By forming the products of such representations we can deduce that all operators must contain parts belonging to irreducible representations of the type $(11\cdots10\cdots0)$ of SO(28) if their matrix elements are not to vanish, thereby restricting the simultaneous assignments of quasi-spin rank K and symplectic symmetry $\langle\sigma\rangle$ when the reduction $SO(28) \supset SO_Q(3) \times Sp(14)$ is considered (Judd 1966a). This proved to be of considerable help when the three-electron operators associated with the parameters T^i of section 6.1.2. were being studied.

11.3.1. *Quasi-particles*

It was discovered in 1969 that the spin-up and spin-down spaces, for either even or odd N, can both be factored into two similar parts (Armstrong and Judd 1970a,b). If, for example, we take N even, the states of f_A^N belong to the irreducible representations W of $SO_A(7)$ given by (000), (110), (111) and (100) for $N = 0, 2, 4$ and 6, respectively. Their L_A content is S for (000), P + F + H for (110) (the triplets of f^2), S + D + F + G + I for (111) (the quintets of f^4), and F for (100) (the septet of f^6). Had we taken odd N, the same W would have occurred but in the reverse order. Now, it can be shown that

$$(\tfrac{1}{2}\tfrac{1}{2}\tfrac{1}{2}) \times (\tfrac{1}{2}\tfrac{1}{2}\tfrac{1}{2}) = (000) + (100) + (110) + (111). \tag{130}$$

By taking suitable linear combinations of $a^\dagger_{m_s m_l}$ and $a_{m_s -m_l}$, and coupling pairs of these combinations to odd rank in orbital space, the generators of four new SO(7) groups can be constructed for which $SO_A(7) \supset SO_\lambda(7) \times SO_\mu(7)$ and $SO_B(7) \supset SO_\nu(7) \times SO_\xi(7)$. The two spinor representations $(\tfrac{1}{2}\tfrac{1}{2}\tfrac{1}{2})$ in eq. (130) belong to $SO_\lambda(7)$ and $SO_\mu(7)$. These groups conserve neither S nor N; and the basic operators, being linear combinations of both creation and annihilation operators, are said to refer to quasi-particles.

The significance of eq. (130) can be more readily appreciated if it is first noticed (or simply accepted, if the reader is not familiar with Lie algebras) that $(\tfrac{1}{2}\tfrac{1}{2}\tfrac{1}{2})$ comprises the eight points $(\pm\tfrac{1}{2}\ \pm\tfrac{1}{2}\ \pm\tfrac{1}{2})$ in the three-dimensional weight space of SO(7). Under the reduction $SO(7) \supset SO(3)$, we have $(\tfrac{1}{2}\tfrac{1}{2}\tfrac{1}{2}) \rightarrow s + f$. Thus the terms of maximum multiplicity in f^N (for either $N = 0, 2, 4, 6$ or $N = 1, 3, 5, 7$) possess L values that are identical to those provided by $(s + f)^2$. From this point of view, the ^4I term of f^3 (or, more precisely, its components for which $M_S = \frac{3}{2}$) can be regarded as being produced by coupling two f quasi-particles to a rank of 6. The $M_S = \frac{3}{2}$ component of the ^4S term of f^3, on the other hand, is a superposition of the S states produced by the quasi-particle configurations s^2 and f^2. These quasi-particles have no physical existence, of course, but they may be brought into play to simplify calculations. Several mysteries receive ready explanations: in particular, the puzzle of the invariance of the Racah coefficients $W(3333; 3k)$ with respect to even (nonzero) k can be understood (Armstrong and Judd 1970b, p. 42). However, electrons for which $l = 3$ are too simple to allow the power of the quasi-particle approach to show to its best advantage. Its chief strength is that it allows us to eliminate the undefined classificatory symbols of the type τ included in the state (44) for all electrons for which $l \leqslant 8$. The method has been extended to configurations of inequivalent electrons by Cunningham and Wybourne (1969), and to nuclear configurations of the type j^N by Elliott and Evans (1970). A detailed description of the quasi-particle method for atomic shells has been given by Condon and Odabasi (1980) in their updating of the classic text of Condon and Shortley (1935).

11.3.2. *Other groups*

The group structures that have been discussed so far do not exhaust all the possibilities. It has already been pointed out (in section 8.2.1) that U(14) of the chain (52) can have Sp(14) as a subgroup. This symplectic group is identical to the one

mentioned in section 11.3 as occurring in $SO_Q(3) \times Sp(14)$. If, however, the configurations $4f^N$ had approximated more closely to *jj* rather than to *LS* coupling, we would have needed to classify the states of the configurations $(\frac{5}{2})^{N-M}(\frac{7}{2})^M$, for which the direct product $Sp(6) \times Sp(8)$ of two symplectic groups is required (Flowers 1952b). This possibility was included by Gruber and Thomas (1975, 1980) as a link in one of the three main chains running from U(14) to $SO_J(3)$, the other two being the sequence given by (52) and the seniority chain that includes Sp(14). The analysis of Gruber and Thomas (1980) established that no other chains exist (for $l \leqslant 6$, at least). No statement of comparable generality can be made for the number and kind of chains leading from U(16 384) to $SO_J(3)$, however. It might be thought that, at this late date, there could be little expectation of finding any new group structure. In spite of several techniques – which would take us too far afield to describe here, there remain, nevertheless, some inexplicable zeros in the tables of matrix elements compiled by Nielson and Koster (1963). Similar puzzles occur in the tables of the two-electron double-vector operators needed to evaluate the spin–other-orbit and EL–SO interactions in f^4 and f^5 (Crosswhite and Judd 1970). The possibility that such zeros are truly accidental cannot be discounted, of course, but to say as much has more the character of an excuse than an explanation. One's uneasiness is compounded by the existence of a suggestive feature of the triple products of creation or annihilation operators (in any combination): if the orbital rank is zero then the G_2 label is also a scalar, namely (00). An example of this general rule is the ^4S term of f^3, which belongs to (00). Commutators of the triple products must also be G_2 scalars; and, although successive commutation produces multiple products of the $a_\xi^\dagger$ and a_η, the fact that these operators correspond to fermions tells us that the commutation process must ultimately close and hence provide us with the generators of a Lie algebra. If these generators simply put all the terms of a given U and L in a single irreducible representation of the corresponding Lie group, nothing much is gained; but the difficult problem of finding possible subgroups has not been tackled.

It should be remembered, of course, that Lie groups have an independent existence apart from their role in the theory of f electrons in the lanthanides. Some of the bizarre properties that turn up in the f shell might well derive from isoscalar factors that receive a ready explanation in another context. An example of this is provided by the vanishing of the spin–orbit interaction H_{so} when it is set between F and G states belonging to the irreducible representation (21) of G_2. In the f shell, (21) is merely a 64-dimensional representation of no special interest. However, for mixed configurations of p and h electrons, it fits exactly into the spinor representations $(\frac{1}{2}\frac{1}{2}\frac{1}{2}\frac{1}{2}\frac{1}{2}\frac{1}{2} \pm\frac{1}{2})$ of SO(14) with dimensions 2^6 (Judd 1970). These are the analogs of the spinor representations of eq. (130), and (21) describes the quasi-particle basis of the configurations $(p + h)^N$. The spinor representations $\mathscr{D}_{1/2}$ of SO(3) and $(\frac{1}{2}\frac{1}{2}\frac{1}{2}\frac{1}{2}\frac{1}{2})$ of SO(11) provide the quasi-particle bases for the p and h shells respectively; and their SO(3) structures, namely $\mathscr{D}_{1/2}$ and $\mathscr{D}_{5/2} + \mathscr{D}_{9/2} + \mathscr{D}_{15/2}$, when coupled, must yield the L structure of (21) of G_2, namely D + F + G + H + K + L. In this context, the F and G terms of (21) are associated with the different irreducible representations $\mathscr{D}_{5/2}$ and $\mathscr{D}_{9/2}$. It is this property,

which, when examined in detail, leads to the vanishing of the matrix elements $\langle(21)\mathrm{F}|T^{(1)}|(21)\mathrm{G}\rangle$, where $T^{(1)}$ is any vector operator in the orbital space that also belongs (like H_{so}) to the irreducible representation (11) of G_2 (see Judd 1970). Several components of H_{soo} (discussed in section 8.2.1) also belong to (11), and their matrix elements between (21)F and (21)G must also vanish for any f^N.

11.4. *Unitary calculus*

A major departure from Racah's approach to atomic shell theory was taken by Harter (1973), who asserted that the complexities of 'quantum bookkeeping' could be alleviated by replacing the group chain (43) by the sequence of unitary groups

$$\mathrm{U}(7) \supset \mathrm{U}(6) \supset \mathrm{U}(5) \supset \mathrm{U}(4) \supset \mathrm{U}(3) \supset \mathrm{U}(2) \supset \mathrm{U}(1). \tag{131}$$

Weyl (1931, p. 391) had shown that an irreducible representation $[\lambda_1, \lambda_2, \ldots, \lambda_n]$ of $\mathrm{U}(n)$ decomposes into a sum of the irreducible representations $[\lambda'_1, \lambda'_2, \ldots, \lambda'_{n-1}]$ of $\mathrm{U}(n-1)$ for which

$$\lambda_1 \geqslant \lambda'_1 \geqslant \lambda_2 \geqslant \lambda'_2 \geqslant \cdots \geqslant \lambda'_{n-1} \geqslant \lambda_n, \tag{132}$$

and that every such representation occurs exactly once. Thus, by giving the $\frac{1}{2}n(n+1)$ labels $\lambda_i, \lambda'_j, \ldots, \lambda''^{\cdots'}_1$, where $[\lambda''^{\cdots'}_1]$ denotes an irreducible representation of U(1), all multiplicity conditions associated with repeated representations can be avoided. Symbols such as τ of the ket (44) no longer appear. The possibility of using a chain of the type given by (131) to classify the states of a many-fermion system was known to Moshinsky (1968), among others (not to mention Weyl himself, in all probability).

The transformations of U(7) can be effected by means of the operators $E_{vv'}$, where

$$E_{vv'} = a^\dagger_{(1/2)m_l} a_{(1/2)m'_l} + a^\dagger_{-(1/2)m_l} a_{-(1/2)m'_l}. \tag{133}$$

The subscripts v and v' are related to m_l and m'_l by a simple code: Harter (1973) uses $v = 1, 2, \ldots, 7$ for $m_l = 3, 2, \ldots, -3$. The operators $E_{vv'}$ are scalar with respect to spin, and all 49 can be taken as the generators for the U(7) groups appearing at the heads of the chains (43) and (131). To get the generators of U(6) we merely take the collection of $E_{vv'}$ that limit v and v' to six possibilities rather than seven. To understand how the conditions (132) follow from $\mathrm{U}(n) \supset \mathrm{U}(n-1)$, consider the doublets of f^3. There are 112 various linear combinations of Slater determinants here. The simultaneous eigenvalues of the seven commuting operators E_{vv} define a weight (see sections 2.2.1 and 4.3.3 for analogs); the highest weight (found by regarding the eigenvalues of $E_{11}, E_{22}, \ldots, E_{77}$ as a seven-digit number) is $[210\cdots0]$, corresponding to the single Slater determinant $\{3^+ 3^- 2^+\}$. If, now, we strike out $v = 7$, no state for which $m_l = -3$ can be transformed to another; thus the six non-vanishing determinants $\{m_l^+ -3^+ -3^-\}$ (for $3 \geqslant m_l \geqslant -2$) are separated from the rest and form a basis for the irreducible representation $[10\cdots0]$ of U(6). Similarly, the 15 distinct non-vanishing determinants $\{m_l^+ m_l'^+ - 3^-\}$ (for $3 \geqslant m_l \geqslant m'_l \geqslant -2$) form a basis for $[110\cdots0]$. There are 36 non-vanishing determinants of the type $\{m_l^+ -3^+ m_l'^-\}$ for which $m'_l \neq -3$, just 30 of which produce a non-vanishing determinant when acted on with S_+. This set of 30 consists of 15 distinct de-

terminants of the form $\{m_l^+ - 3^+ m_l'^+\}$, all of which are the components of the quartets of f^3. We are left with 21 (that is, $36 - 15$) determinants (or linear combinations of them) for the doublets; the highest weight is $[20\cdots0]$, corresponding to the determinant $\{3^+ 3^- - 3^+\}$. Omitting the trailing zeros in the representations, we have

$$[21] \to [21] + [2] + [11] + [1] \tag{134}$$

for the reduction $U(7) \supset U(6)$. The representations of U(6) on the right-hand side of (134) are precisely the ones specified by Weyl's conditions given by (132). The dimension check on the reduction (134) is $112 = 70 + 21 + 15 + 6$, as can be verified with the help of tables A-5 and A-6 of Wybourne (1970).

From the above it is clear that the use of the chain of groups (131) in defining a state is very cumbersome. For example,

$$\{3^+ 3^- 0^+\} \equiv |[21][21][21][2][2][2][2]\rangle. \tag{135}$$

The arrangement of the seven highest weights appearing here can be altered to form an inverted pyramid, the so-called Gelfand state:

$$\begin{array}{ccccccccccccc}
2 & & 1 & & 0 & & 0 & & 0 & & 0 & & 0 \\
& 2 & & 1 & & 0 & & 0 & & 0 & & 0 & \\
& & 2 & & 1 & & 0 & & 0 & & 0 & & \\
& & & 2 & & 0 & & 0 & & 0 & & & \\
& & & & 2 & & 0 & & 0 & & & & \\
& & & & & 2 & & 0 & & & & & \\
& & & & & & 0 & & & & & &
\end{array}$$

Such a state exposes the conditions given by (132) but inflates rather than simplifies the ket on the right in eq. (135). Harter (1973) therefore used an equivalent description, in which the numbers v are located in the cells of standard Young tableaux: that is, N of the seven numbers v are arranged in successive rows, each row flush with a left-hand edge and not containing more cells than the row above it; the numbers in the cells increasing from left to right in every row and from top to bottom in every column. The connection of these remarkable objects to the permutation groups was investigated by Young at the turn of the century; the whole subject has been summarized by Rutherford (1948). In terms of tableaux, the state given by (135) is written $\begin{smallmatrix}1 & 1\\ 4 & \end{smallmatrix}$, the first column referring to the spin-up space, occupied by $v = 1$ and 4 (that is, $m_l = 3$ and 0), the second column to the spin-down space.

It might well be wondered at this point why the familiar Slater determinants cannot be used instead. By so doing we could avoid having to study the properties of the Young tableaux, a subject presented by Harter (1973) mainly in the form of rules whose origin lies buried in the arcane mathematics of the Young tableaux. Harter and Patterson (1976) made the valid point that S is a good quantum number in their scheme (since the $E_{vv'}$ are all spin scalars), whereas the general Slater determinant guarantees a specific M_S but not necessarily a particular S. The calculus of unitary groups exacts a high price for what seems to be a small gain.

An exploration of Harter's method was made by Drake and his collaborators at the University of Windsor. They clarified the calculation of matrix elements for the doublets of f^3 (Drake et al. 1975) and calculated the spin–orbit splitting factors for the sextets of f^5 (Drake et al. 1977). In the second calculation they were unlucky enough to choose a problem whose solution was independent of the coefficients of the single-column tableaux that they needed, this property being equivalent to the invariance of λ (the spin–orbit parameter) with respect to L for all terms of maximum multiplicity for any configuration (a result that follows at once when Slater determinants are used). Thus they obtained the correct value for the spin–orbit parameter for ^6P although their tableau coefficients are wrong. It would not be worth mentioning this inconsequential error except that it points to a problem latent in any new method: it takes time to develop a feel for the mathematics, and Harter's unconventional approach is obviously taking longer than most. Drake and Schlesinger (1977) derived closed-form expressions for the matrix elements of two-electron operators taken between tableau states, and various elaborations for handling mixed configurations (such as f^4p^2) were worked out (Kent and Schlesinger 1981, Schlesinger et al. 1982). Extensions of the unitary-group approach to the spin configurations σ^N have also been made (see, e.g., Kent et al. 1985). In spite of the work of the Windsor group, as well as other work of Harter and Patterson, the unitary calculus cannot yet be said to be competitive with the methods of Racah. The urge to simplify the quantum bookkeeping has been overtaken by events. Programs are readily available to calculate the matrices of operators within bases defined by the successive coupling of angular momenta, any ambiguities being resolved by the standard chain of groups, augmented when necessary by a few classificatory symbols like τ (Cowan 1981).

The unitary calculus should not be written off, however. Many quantum chemists are taking it very seriously indeed, their frequently stated aim being to achieve the greatest possible efficiency in computation. In the process of this work, an elaborate mathematical structure is being constructed. It would be too great a digression to describe the various theoretical developments here; the interested reader can get an idea of what has been happening from the papers of Paldus and Boyle (1980) and from the many references therein.

12. Concluding remarks

Surveying the history of the theory of optical lanthanide spectroscopy, we can discern several main features: the usefulness of Lie groups, following their introduction by Racah (1949); the relevance of the method of second quantization, as demonstrated by the use of annihilation and creation operators for electrons; and the inability of the Hartree–Fock method and its various elaborations to provide accurate values (say to within 1%) of such crucial quantities as the Slater integrals F^k (4f, 4f) and the Sternheimer correction factors R_{nl} for a free ion. The success of the formal mathematics is in striking contrast to the failure of the machinery of computation. This turn of events has happened over a period of time when

hesitations to develop the mathematics have been interspersed with assurances of the imminent arrival of a golden age of computation. The remark of Condon and Shortley (1935) that they could manage without group theory (mentioned in section 2.2), which seems so mistaken today, was gracefully put in the context of its time by Condon and Odabasi (1980, p. 307). They drew a parallel with the classic work of Jeans (1920) on electricity and magnetism, which made no use of vector analysis at a time when it would diminish rather than improve the accessibility of the text. Slater's reluctance to use Lie groups was matched by his feeling towards second quantization, which to him was 'a more complicated method of treating matters which could be more easily taken up without their use' (Slater 1968). It would have been interesting to see how he would have handled Downer's fourth-order analysis of two-photon absorption in Gd^{3+}, described in section 9.1.

The formal mathematics has some way to go. The two-electron operators needed to describe residual crystal-field effects have not yet been firmly established, and a complete Lie-group classification of the four-electron electrostatic operators for the f shell has still to be done. New multi-electron operators will undoubtedly be required for other purposes as the analysis is pushed to higher orders of perturbation theory. However, the shortcomings of the Hartree–Fock method seem the most in need of attention at the present time. They are also the ones that will probably get the least of it, since the problem of extending the Hartree–Fock method to the myriad configurations required to give good accuracy for atoms as heavy as the lanthanides is very hard indeed. The question of incentive has to be faced here. The need to know the quadrupole moments of the lanthanide nuclei is no longer a strong motivation for calculating the Sternheimer correction factors. As for the Slater integrals $F^k(4f, 4f)$, spectroscopists have learned how to adjust the Hartree–Fock values by empirical correction factors, so that the absence of precise numerical values is not an overwhelming hindrance. If accurate ab initio calculations for the lanthanides are to be done at all, they will probably come about as applications of techniques that have been worked out primarily for other purposes. The effects of parity non-conservation in heavy atoms can only be properly handled if accurate atomic wavefunctions are known, and this has stimulated interest in improving the methods for taking relativity and correlation into account. The papers presented at the Atomic Theory Workshop at the National Bureau of Standards in 1985 give a good indication of where current interest lies. Much of the discussion turned on heavy atoms that possess very few electrons; but the contribution of Dietz (1985) on the g-Hartree method broke new ground for many-electron atoms. Considerations of a field-theoretic nature lead to equations involving a parameter g which can be fixed either by appealing to some appropriate experimental result (thus weakening its ab initio character) or by demanding that the correlation energy (that is, the correction to the standard Hartree–Fock energy) to a specified order of perturbation theory be set equal to zero. Dietz (1985) concludes that 'the g-Hartree method has shown, we think, important advantages, sometimes even its superiority, over many of the current approaches for treating the inhomogeneous many-electron problem'. Whether this assessment is relevant to the lanthanides is unclear. At least it avoids the predictions of lightning-like speed and unparalleled accuracy that

those attending scientific conferences have patiently listened to for thirty years or more. No doubt we shall eventually be able to calculate much of what we want with a high degree of accuracy. That day has not yet arrived.

Note added in proof

By drawing a correspondence between nuclear states classified by isospin and atomic operators classified by quasi-spin, Leavitt (1987) has provided a complete group-theoretical listing for the f shell of orthogonal operators scalar with respect to S and L.

Acknowledgements

Parts of the manuscript were read by Drs. I.E. Hansen, W.C. Martin, D.J. Newman, M.F. Reid and J. Sugar, who are thanked for their comments.

References

Albertson, W.E., 1934, Phys. Rev. **45**, 499.
Albertson, W.E., 1935, Phys. Rev. **47**, 370.
Albertson, W.E., 1936, Astrophys. J. **84**, 26.
Albertson, W.E., H. Bruynes and R. Hanau, 1940, Phys. Rev. **57**, 292.
Albertson, W.E., G.R. Harrison and J.R. McNally, 1942, Phys. Rev. **61**, 167.
Alig, R.C., Z.J. Kiss, J.P. Brown and D.S. McClure, 1969, Phys. Rev. **186**, 276.
Apanasevich, P.A., R.I. Gintoft, V.S. Korolkov, A.G. Makhanek and G.A. Skripko, 1973, Phys. Status Solidi b **58**, 745.
Armstrong Jr, L., 1971, Theory of Hyperfine Structure of Free Atoms (Wiley–Interscience, New York).
Armstrong Jr, L., and B.R. Judd, 1970a, Proc. R. Soc. London Ser. A **315**, 27.
Armstrong Jr, L., and B.R. Judd, 1970b, Proc. R. Soc. London Ser. A **315**, 39.
Armstrong Jr, L., and L.H. Taylor, 1969, J. Chem. Phys. **51**, 3789.
Aufmuth, P., 1978, Z. Phys. A **286**, 235.
Aufmuth, P., 1982, J. Phys. B **15**, 3127.
Axe, J.D., 1963, J. Chem. Phys. **39**, 1154.
Axe, J.D., 1964, Phys. Rev. A **136**, 42.
Aymar, M., 1984, J. Opt. Soc. Am. B **1**, 239.
Aymar, M., A. Débarre and O. Robaux, 1980, J. Phys. B **13**, 1089.
Aymar, M., R.-J. Champeau, C. Delsart and O. Robaux, 1984, J. Phys. B **17**, 3645.
Bacher, R.F., and S. Goudsmit, 1932, Atomic Energy States (McGraw-Hill, New York).
Bacher, R.F., and S. Goudsmit, 1934, Phys. Rev. **46**, 948.
Badami, J.S., 1931, Proc. Phys. Soc. London **43**, 53.
Balasubramanian, G., M.M. Islam and D.J. Newman, 1975, J. Phys. B **8**, 2601.
Barbier, L., and R.-J. Champeau, 1980, J. Phys. (France) **41**, 947.
Barnes, J.A., B.L. Carroll and L.M. Flores, 1968, J. Chem. Phys. **49**, 5453.
Bauche, J., and R.-J. Champeau, 1976, Adv. At. Mol. Phys. **12**, 39.
Bauche, J., R.-J. Champeau and C. Sallot, 1977, J. Phys. B **10**, 2049.
Bauche-Arnoult, Cl., 1971, Proc. R. Soc. London Ser. A **322**, 361.
Bauche-Arnoult, Cl., 1973, J. Phys. (France) **34**, 301.
Bauche-Arnoult, Cl., and J. Bauche, 1968, J. Opt. Soc. Am. **58**, 704.
Bauche-Arnoult, Cl., J. Sinzelle and A. Bachelier, 1978, J. Opt. Soc. Am. **68**, 368.
Baumann, M., and G. Wandel, 1966, Phys. Lett. **22**, 283.
Bayer, E., and G. Schaak, 1970, Phys. Status Solidi **41**, 827.
Becker, P.C., T. Hayhurst, G. Shalimoff, J.G. Conway, N. Edelstein, L.A. Boatner and M.M. Abraham, 1984, J. Chem. Phys. **81**, 2872.
Becker, P.C., N. Edelstein, B.R. Judd, R.C. Leavitt and G.M.S. Lister, 1985, J. Phys. C **18**, L1063.
Becker, P.J., 1971, Phys. Status Solidi b **43**, 583.
Becquerel, J., 1929, Z. Phys. **58**, 205.
Bethe, H., 1929, Ann. Phys. (Leipzig) **3**, 133.
Bethe, H., 1930, Z. Phys. **60**, 218.

Bethe, H.A., and E.E. Salpeter, 1957, Quantum Mechanics of One- and Two-Electron Atoms (Academic Press, New York).
Bethe, H.A., and F.H. Spedding, 1937, Phys. Rev. **52**, 454.
Bijl, D., 1945, Physica **11**, 287.
Bishton, S.S., and D.J. Newman, 1968, Chem. Phys. Lett. **1**, 616.
Bishton, S.S., and D.J. Newman, 1970, J. Phys. C **3**, 1753.
Bishton, S.S., M.M. Ellis, D.J. Newman and J. Smith, 1967, J. Chem. Phys. **47**, 4133.
Blaise, J., Th.A.M. van Kleef and J.-F. Wyart, 1971a, J. Phys. (France) **32**, 617.
Blaise, J., J.-F. Wyart, R. Hoekstra and P.J.G. Kruiver, 1971b, J. Opt. Soc. Am. **61**, 1335.
Blaise, J., J.-F. Wyart, M.T. Djerad and Z. Ben Ahmed, 1984, Phys. Scr. **29**, 119.
Blasse, G., A. Brill and W.C. Nieuwpoort, 1966, J. Phys. Chem. Solids **27**, 1587.
Bleaney, B., and K.W.H. Stevens, 1953, Rep. Prog. Phys. **16**, 108.
Bloembergen, N., 1984, J. Lumin. **31/32**, 23.
Blondel, C., R.-J. Champeau and C. Delsart, 1983, Phys. Rev. A **27**, 583.
Blondel, C., R.-J. Champeau and C. Delsart, 1985, J. Phys. B **18**, 2403.
Blume, M., A.J. Freeman and R.E. Watson, 1964, Phys. Rev. **134**, A320.
Bordarier, Y., B.R. Judd and M. Klapisch, 1965, Proc. R. Soc. London Ser. A **289**, 97.
Bowman, D.S., 1941, Phys. Rev. **59**, 382.
Breit, G., and L.A. Wills, 1933, Phys. Rev. **44**, 470.
Brinkman, H.C., 1956, Applications of Spinor Invariants in Atomic Physics (North-Holland, Amsterdam).
Broer, L.J.F., C.J. Gorter and J. Hoogschagen, 1945, Physica **11**, 231.
Bryant, B.W., 1965, J. Opt. Soc. Am. **55**, 771.
Burghardt, B., S. Büttgenbach, N. Glaeser, R. Harzer, G. Meisel, B. Roski and F. Träber, 1982, Z. Phys. A **307**, 193.
Burns, G., 1962, Phys. Rev. **128**, 2121.
Butler, P.H., 1981, Point Group Symmetry Applications (Plenum, New York).
Callahan, W.R., 1963, J. Opt. Soc. Am. **53**, 695.
Camus, P., 1970, J. Phys. (France) **31**, 985.
Camus, P., 1972a, J. Phys. (France) **33**, 203.
Camus, P., 1972b, J. Phys. (France) **33**, 749.
Camus, P., and J. Sugar, 1971, Phys. Scr. **4**, 257.
Camus, P., and F.S. Tomkins, 1969, J. Phys. (France) **30**, 545.
Camus, P., and F.S. Tomkins, 1976, Philos. Trans. R. Soc. A **283**, 345.
Camus, P., A. Débarre and O. Robaux, 1980, J. Phys. B **13**, 1073.
Carlier, A., J. Blaise and M.-G. Schweighofer, 1968, J. Phys. (France) **29**, 729.
Carlson, B.C., and G.S. Rushbrooke, 1950, Proc. Cambridge Philos. Soc. **46**, 626.
Carnall, W.T., 1979, The Absorption and Fluorescence of Rare Earth Ions in Solution, in: Handbook on the Physics and Chemistry of Rare Earths, Vol. 3, eds K.A. Gschneidner Jr and L. Eyring (North-Holland, Amsterdam) ch. 24.
Carnall, W.T., H. Crosswhite and H.M. Crosswhite, 1977, Energy Level Structure and Transition Probabilities of the Trivalent Lanthanides in LaF_3 (Department of Physics Report, The Johns Hopkins University, Baltimore, MD).
Caro, P., O.K. Moune, E. Antic-Fidancev and M. Lemaitre-Blaise, 1985, J. Less-Common Met. **112**, 153.
Cartan, E., 1894, Sur la Structure des Groupes de Transformations Finis et Continus, Thesis (Nony, Paris) [Reprinted, 1952, in: Oeuvres Complètes, Vol. 1 (Gauthier-Villars, Paris).
Casimir, H.G.B., 1963, On the Interaction between Atomic Nuclei and Electrons (Freeman, San Francisco).
Catalan, M.A., and M.T. Antunes, 1936, Z. Phys. **102**, 432.
Charkin, O.P., and M.E. Dyatkina, 1964, Zh. Strukt. Khim. **5**, 921.
Cheng, K.T., and W.J. Childs, 1985, Phys. Rev. A **31**, 2775.
Childs, W.J., and K.T. Cheng, 1984, Phys. Rev. A **30**, 677.
Childs, W.J., and L.S. Goodman, 1972a, Phys. Rev. A **6**, 1772.
Childs, W.J., and L.S. Goodman, 1972b, Phys. Rev. A **6**, 2011.
Childs, W.J., O. Poulsen and L.S. Goodman, 1979, Phys. Rev. A **19**, 160.
Childs, W.J., D.R. Cok and L.S. Goodman, 1983a, J. Opt. Soc. Am. **73**, 151.
Childs, W.J., L.S. Goodman and V. Pfeufer, 1983b, Phys. Rev. A **28**, 3402.
Childs, W.J., H. Crosswhite, L.S. Goodman and V. Pfeufer, 1984, J. Opt. Soc. Am. B **1**, 22.
Childs, W.J., L.S. Goodman and K.T. Cheng, 1986, Phys. Rev. A **33**, 1469.
Cohen, E., and H.W. Moos, 1967, Phys. Rev. **161**, 258, 268.
Condon, E.U., and H. Odabasi, 1980, Atomic Structure (Cambridge University Press, Cambridge).
Condon, E.U., and G.H. Shortley, 1931, Phys. Rev. **37**, 1025.
Condon, E.U., and G.H. Shortley, 1935, The Theory of Atomic Spectra (Cambridge University Press, Cambridge).
Cone, R.L., R.T. Harley and M.J.M. Leask, 1984, J. Phys. C **17**, 3101.
Cordero-Montalvo, C.D., and N. Bloembergen, 1984, Phys. Rev. B **30**, 438.
Cordero-Montalvo, C.D., and N. Bloembergen, 1985, Phys. Rev. B **31**, 613.
Coulthard, M.A., 1973, J. Phys. B **6**, 23.
Cowan, R.D., 1981, The Theory of Atomic Structure and Spectra (University of California Press, Berkeley, CA).
Crosswhite, H., and B.R. Judd, 1970, Atomic Data **1**, 329.

Crosswhite, H., and D.J. Newman, 1984, J. Chem. Phys. **81**, 4959.
Crosswhite, H., H.M. Crosswhite and B.R. Judd, 1968, Phys. Rev. **174**, 89.
Crosswhite, H.M., G.H. Dieke and W.J. Carter, 1965, J. Chem. Phys. **43**, 2047.
Cunningham, M.J., and B.G. Wybourne, 1969, J. Math. Phys. **10**, 2149.
Dagenais, M., M. Downer, R. Neumann and N. Bloembergen, 1981, Phys. Rev. Lett. **46**, 561.
Dallara, J.J., M.F. Reid and F.S. Richardson, 1984, J. Chem. Phys. **88**, 3587.
Desclaux, J.P., 1975, Comput. Phys. Commun. **9**, 31.
Dieke, G.H., 1968, Spectra and Energy Levels of Rare Earth Ions in Crystals (Interscience, New York).
Dieke, G.H., and H.M. Crosswhite, 1967, Physica **33**, 212.
Dieke, G.H., and L. Leopold, 1957, J. Opt. Soc. Am. **47**, 944.
Dieke, G.H., H.M. Crosswhite and B. Dunn, 1961, J. Opt. Soc. Am. **51**, 820.
Dietz, K., 1985, On the Relativistic Theory of Inhomogeneous Many-Electron Systems, in: Atomic Theory Workshop on Relativistic and Q.E.D. Effects in Heavy Atoms, AIP Conf. Proc. No. 136, eds H.P. Kelly and Y.-K. Kim (American Institute of Physics, New York) p. 36.
Dirac, P.A.M., 1929, Proc. R. Soc. London Ser A **123**, 714.
Dohnalik, A., T. Dohnalik and M. Szynarowska, 1979, Phys. Scr. **20**, 39.
Donlan, V.L., 1969, Bull. Am. Phys. Soc. Ser. II **14**, 939.
Donlan, V.L., 1970, Tables of Two Particle Fractional Parentage Coefficients for the p^N, d^N and f^N Configurations, Technical Report AFML-TR-70-249 (Air Force Materials Laboratory, Wright-Patterson Air Force Base, Ohio).
Downer, M.C., and A. Bivas, 1983, Phys. Rev. B **28**, 3677.
Downer, M.C., C.D. Cordero-Montalvo and H. Crosswhite, 1983, Phys. Rev. B **28**, 4931.
Drake, G.W.F., and M. Schlesinger, 1977, Phys. Rev. A **15**, 1990.
Drake, J., G.W.F. Drake and M. Schlesinger, 1975, J. Phys. B **8**, 1009.
Drake, J., G.W.F. Drake and M. Schlesinger, 1977, Phys. Rev. A **15**, 807.
Eckart, C., 1930, Rev. Mod. Phys. **2**, 305.
Edlén, B., 1964, Atomic Spectra, in: Handbuch der Physik, Vol. 27, ed. S. Flügge (Springer, Berlin) p. 80.
Edmonds, A.R., 1957, Angular Momentum in Quantum Mechanics (Princeton University Press, Princeton, NJ).
Edmonds, A.R., 1962, Proc. R. Soc. London Ser. A **268**, 567.
Edmonds, A.R., J. Picart, N. Tran Minh and R. Pullen, 1979, J. Phys. B **12**, 2781.
Edmonds, D.T., 1963, Phys. Rev. Lett. **10** 129.
Eisenhart, L.P., 1933, Continuous Groups of Transformations (Princeton University Press, Princeton, NJ) [Reprinted, 1961 (Dover Publications, New York)].
Eisenstein, J.C., 1963a, J. Chem. Phys. **39**, 2128.
Eisenstein, J.C., 1963b, J. Chem. Phys. **39**, 2134.
Eisenstein, J.C., 1964, J. Chem. Phys. **40**, 2044.
Elliott, J.P., 1958, Proc. R. Soc. London Ser. A **245**, 128.
Elliott, J.P., and J.A. Evans, 1970, Phys. Lett. B **31**, 157.
Elliott, J.P., and B.H. Flowers, 1955, Proc. R. Soc. London Ser. A **229**, 536.
Elliott, J.P., B.R. Judd and W.A. Runciman, 1957, Proc. R. Soc. London Ser. A **240**, 509.
Elliott, R.J., 1957, Proc. Phys. Soc. London Sect. B **70**, 119.
Elliott, R.J., and K.W.H. Stevens, 1951, Proc. Phys. Soc. London Sect. A **64**, 205.
Elliott, R.J., and K.W.H. Stevens, 1953, Proc. R. Soc. London Ser. A **219**, 387.
Ellis, C.B., 1936, Phys. Rev. **49**, 875.
Ellis, M.M., and D.J. Newman, 1967, J. Chem. Phys. **47**, 1986.
Ellis, M.M., and D.J. Newman, 1968, J. Chem. Phys. **49**, 4037.
Epstein, G.L., and J. Reader, 1979, J. Opt. Soc. Am. **69**, 511.
Eremin, M.V., and O.I. Maryakhina, 1969, Opt. Spectrosc. **26**, 479.
Ewald, H., 1939, Ann. Phys. (Leipzig) **34**, 209.
Fano, U., 1975, J. Opt. Soc. Am. **65**, 979.
Fano, U., and G. Racah, 1959, Irreducible Tensorial Sets (Academic Press, New York).
Faulkner, T.R., and F.S. Richardson, 1978a, Mol. Phys. **35**, 1141.
Faulkner, T.R., and F.S. Richardson, 1978b, Mol. Phys. **36**, 193.
Faulkner, T.R., R.W. Schwartz and F.S. Richardson, 1979, Mol. Phys. **38**, 1767.
Fawcett, B.C., 1974, Adv. At. Mol. Phys. **10**, 223.
Fawcett, B.C., 1981, Phys. Scr. **24**, 663.
Fawcett, B.C., 1984, J. Opt. Soc. Am. B **1**, 195.
Fedoseyev, V.N., V.S. Lektokhov, V.I. Mishin, G.D. Alkhazov, A.E. Barzakh, V.P. Denisov, A.G. Dernyatin and V.S. Ivanov, 1984, Opt. Commun. **52**, 24.
Feneuille, S., 1966, C.R. Séances Acad. Sci. Paris Ser. B **262**, 23.
Feneuille, S., and N. Pelletier-Allard, 1968, Physica **40**, 347.
Finkman, E., E. Cohen and L.G. van Uitert, 1973, Phys. Rev. B **7**, 2899.
Flint, C.D., and F.L. Stewart-Darling, 1981, Mol. Phys. **44**, 61.
Flowers, B.H., 1952a, Proc. R. Soc. London Ser. A **210**, 497.
Flowers, B.H., 1952b, Proc. R. Soc. London Ser. A **212**, 248.
Flowers, B.H., and S. Szpikowski, 1964, Proc. Phys. Soc. London **84**, 193, 673.
Fraga, S., K.M.S. Saxena and J. Karwowski, 1976, Handbook of Atomic Data (Elsevier,

Amsterdam).
Freed, S., and F.H. Spedding, 1929, Nature **123**, 525.
Freed, S., and S.I. Weissman, 1941, Phys. Rev. **60**, 440.
Freeman, A.J., and R.E. Watson, 1962, Phys. Rev. **127**, 2058.
Froese-Fischer, C., 1969a, Comput. Phys. Commun. **1**, 151.
Froese-Fischer, C., 1969b, Comput. Phys. Commun. **4**, 107.
Froese-Fischer, C., 1972a, At. Data **4**, 301.
Froese-Fischer, C., 1972b, At. Data Nucl. Data Tables **12**, 87.
Froese-Fischer, C., 1976, The Hartree–Fock Method for Atoms (Wiley–Interscience, New York).
Garcia, D., and M. Faucher, 1985, J. Chem. Phys. **82**, 5554.
Garton, W.R.S., and M. Wilson, 1966, Astrophys. J. **145**, 333.
Gell-Mann, M., and Y. Ne'eman, 1964, The Eightfold Way (Benjamin, New York).
Gerloch, M., and R.C. Slade, 1973, Ligand-Field Parameters (Cambridge University Press, Cambridge).
Gibbs, R.C., and H.E. White, 1929, Phys. Rev. **33**, 157.
Gilmore, R., 1974, Lie Groups, Lie Algebras, and Some of Their Applications (Wiley–Interscience, New York).
Giricheva, N.I., E.Z. Zasorin, G.V. Girichev, K.S. Krasnov and V.P. Spiridonov, 1967, Zh. Strukt. Khim. **17**, 797.
Gobrecht, H., 1938, Ann. Phys. (Leipzig) **3**, 600.
Goldschmidt, Z.B., 1968, Theory of Rare-Earth Spectra, in: Spectroscopic and Group Theoretical Methods in Physics, eds F. Bloch, S.G. Cohen, A. de Shalit, S. Sambursky and I. Talmi (Wiley–Interscience, New York).
Goldschmidt, Z.B., 1978, Atomic Properties (Free Atom), in: Handbook on the Physics and Chemistry of Rare Earths, Vol. 1, eds K.A. Gschneidner Jr and L. Eyring (North-Holland, Amsterdam) ch. 1.
Goldschmidt, Z.B., A. Pasternak and Z.H. Goldschmidt, 1968, Phys. Lett. A **28**, 265.
Göppert-Mayer, M., 1931, Ann. Phys. (Leipzig) **9**, 273.
Görller-Walrand, C., and J. Godemont, 1977a, J. Chem. Phys. **66**, 48.
Görller-Walrand, C., and J. Godemont, 1977b, J. Chem. Phys. **67**, 3655.
Görller-Walrand, C., N. de Moitié-Neyt, Y. Beyens and J.C. Bünzli, 1982, J. Chem. Phys. **77**, 2261.
Gray, N.M., and L.A. Wills, 1931, Phys. Rev. **38**, 248.
Griffith, J.A.R., G.R. Isaak, R. New and M.P. Ralls, 1981, J. Phys. B **14**, 2769.
Griffith, J.S., 1961, The Theory of Transition-Metal Ions (Cambridge University Press, Cambridge).
Gruber, B., and M.S. Thomas, 1975, Semisimple Subalgebras of Semisimple Lie Algebras, in: Group Theory and Its Applications, Vol. III, ed. E.M. Loebl (Academic Press, New York).
Gruber, B., and M.S. Thomas, 1980, Kinam. Ser. A **2**, 133.
Gruen, D.M., C.W. DeKock and R.L. McBeth, 1967, Adv. Chem. Ser. **71**, 102.
Guha, S., 1981, Phys. Rev. B **23**, 6790.
Gustavsson, M., H. Lundberg, L. Nilsson and S. Svanberg, 1979, J. Opt. Soc. Am. **69**, 984.
Hamermesh, M., 1962, Group Theory and Its Application to Physical Problems (Addison-Wesley, Reading, MA).
Handrich, E., A. Steudel, R. Wallenstein and H. Walther, 1969, J. Phys. Colloq. (France) **30**, C1–18.
Harrison, G.R., W.E. Albertson and N.E. Hosford, 1941, J. Opt. Soc. Am. **31**, 439.
Harter, W.G., 1973, Phys. Rev. A **8**, 2819.
Harter, W.G., and C.W. Patterson, 1976, A Unitary Calculus for Electronic Orbitals, in: Lecture Notes in Physics, Vol. 49, eds J. Ehlers, K. Hepp, H.A. Weidenmüller and J. Zittartz (Springer, Berlin).
Harvey, J.S.M., 1965, Proc. R. Soc. London Ser. A **285**, 581.
Hasan, Z., and F.S. Richardson, 1982, Mol. Phys. **45**, 1299.
Hasunuma, M., K. Okada and Y. Kato, 1984, Bull. Chem. Soc. Jpn. **57**, 3036.
Hayhurst, T., G. Shalimoff, N. Edelstein, L.A. Boatner and M.M. Abraham, 1981, J. Chem. Phys. **74**, 5449.
Heischmann, H., K.H. Hellwege and S. Leutloff, 1972, Phys. Kondens. Mater. **15**, 10, 23.
Hellwege, K.H., 1939, Z. Phys. **113**, 192.
Hellwege, K.H., 1948, Ann. Phys. (Leipzig) **4**, 95, 127, 136, 143, 150.
Hellwege, K.H., 1949, Ann. Phys. (Leipzig) **4**, 357.
Hellwege, K.H., 1950, Z. Phys. **127**, 513; **128**, 172.
Hellwege, K.H., 1972, Phys. Kondens. Mater. **15**, 1.
Hellwege, K.H., and A.M. Hellwege, 1951, Z. Phys. **131**, 98.
Hellwege, K.H., and A.M. Hellwege, 1952, Z. Phys. **133**, 174.
Hellwege, K.H., and H.G. Kahle, 1951a, Z. Phys. **129**, 62.
Hellwege, K.H., and H.G. Kahle, 1951b, Z. Phys. **129**, 85.
Hernandez A., J., W.K. Cory and J. Rubio O., 1980, J. Chem. Phys. **72**, 198.
Hoogschagen, J., and C.J. Gorter, 1948, Physica **14**, 197.
Hougen, J.T., and S. Singh, 1963, Phys. Rev. Lett. **10**, 406.
Hougen, J.T., and S. Singh, 1964, Proc. R. Soc. London Ser. A **277**, 193.
Hüfner, S., 1978, Optical Spectra of Transparent Rare Earth Compounds (Academic Press, New York).
Hutchings, M.T., and D.K. Ray, 1963, Proc.

Phys. Soc. London **81**, 663.
Hutchison Jr, C.A., and E. Wong, 1958, J. Chem. Phys. **29**, 754.
Innes, F.R., 1953, Phys. Rev. **91**, 31.
Innes, F.R., and C.W. Ufford, 1958, Phys. Rev. **111**, 194.
Jahn, H.A., 1950, Proc. R. Soc. London Ser. A **201**, 516.
Jahn, H.A., 1951, Proc. R. Soc. London Ser. A **205**, 192.
Jahn, H.A., and H. van Wieringen, 1951, Proc. R. Soc. London Ser. A **209**, 502.
Jankowski, K., and L. Smentek-Mielczarek, 1979, Mol. Phys. **38**, 1445.
Jankowski, K., and L. Smentek-Mielczarek, 1981, Mol. Phys. **43**, 371.
Jeans, Sir J.H., 1920, The Mathematical Theory of Electricity and Magnetism (Cambridge University Press, Cambridge).
Johann, U., J. Dembczyński and W. Ertmer, 1981, Z. Phys. A **303**, 7.
Johansson, S., and U. Litzén, 1973, Phys. Scr. **8**, 43.
Jørgensen, C.K., 1955a, Acta Chem. Scand. **9**, 540.
Jørgensen, C.K., 1955b, J. Chem. Phys. **23**, 399.
Jørgensen, C.K., 1955c, Mat.-Fys. Medd. K. Dan. Vidensk. Selsk. **29**, 11.
Jørgensen, C.K., and B.R. Judd, 1964, Mol. Phys. **8**, 281.
Jørgensen, C.K., R. Pappalardo and H.-H. Schmidtke, 1963, J. Chem. Phys. **39**, 1422.
Jørgensen, C.K., M. Faucher and D. Garcia, 1986, Chem. Phys. Lett. **128**, 250.
Jucys, A.P., and R.S. Dagys, 1960, Trudy Akad. Nauk. Litovsk SSR, Ser. B **1**, 41.
Jucys, A.P., and A.J. Savukynas, 1973, Mathematical Foundations of the Atomic Theory (Mintis, Vilnius).
Jucys, A.P., R.S. Dagys, J. Vizbaraite and S.A. Zvironaite, 1961, Trudy Akad. Nauk. Litovsk SSR, Ser. B **3**, 53.
Judd, B.R., 1955, Proc. R. Soc. London Ser. A **228**, 120.
Judd, B.R., 1957a, Proc. R. Soc. London Ser. A **241**, 414.
Judd, B.R., 1957b, Proc. R. Soc. London Ser. A **241**, 122.
Judd, B.R., 1959, Proc. R. Soc. London Ser. A **251**, 134.
Judd, B.R., 1962, Phys. Rev. **127**, 750.
Judd, B.R., 1963, Operator Techniques in Atomic Spectroscopy (McGraw-Hill, New York).
Judd, B.R., 1966a, Phys. Rev. **141**, 4.
Judd, B.R., 1966b, J. Chem. Phys. **44**, 839.
Judd, B.R., 1967a, Second Quantization and Atomic Spectroscopy (The Johns Hopkins University, Baltimore, MD).
Judd, B.R., 1967b, Phys. Rev. **162**, 28.
Judd, B.R., 1968, J. Opt. Soc. Am. **58**, 1311.
Judd, B.R., 1970, J. Phys. Colloq. (France) **31**, C-4, 9.
Judd, B.R., 1975, Angular Momentum Theory for Diatomic Molecules (Academic Press, New York).
Judd, B.R., 1977a, J. Chem. Phys. **66**, 3163.
Judd, B.R., 1977b, Phys. Rev. Lett. **39**, 242.
Judd, B.R., 1979, J. Chem. Phys. **70**, 4830.
Judd, B.R., 1980, J. Phys. C **13**, 2695.
Judd, B.R., and L. Armstrong Jr, 1969, Proc. R. Soc. London Ser. A **309**, 185.
Judd, B.R., and H. Crosswhite, 1984, J. Opt. Soc. Am. B **1**, 255.
Judd, B.R., and I. Lindgren, 1961, Phys. Rev. **122**, 1802.
Judd, B.R., and G.M.S. Lister, 1984, J. Phys. B **17**, 3637.
Judd, B.R., and D.R. Pooler, 1982, J. Phys. C **15**, 591.
Judd, B.R., and W.A. Runciman, 1976, Proc. R. Soc. London Ser. A **352**, 91.
Judd, B.R., and M.A. Suskin, 1984, J. Opt. Soc. Am. B **1**, 261.
Judd, B.R., and H.T. Wadzinski, 1967, J. Math. Phys. **8**, 2125.
Judd, B.R., H.M. Crosswhite and H. Crosswhite, 1968, Phys. Rev. **169**, 130.
Judd, B.R., J.E. Hansen and A.J.J. Raassen, 1982, J. Phys. B **15**, 1457.
Judd, B.R., G.M.S. Lister and M.A. Suskin, 1986, J. Phys. B **19**, 1107.
Kaiser, W., and C.G.B. Garrett, 1961, Phys. Rev. Lett. **7**, 229.
Kambara, T., W.J. Haas, F.H. Spedding and R.H. Good Jr, 1972, J. Chem. Phys. **56**, 4475.
Kambara, T., W.J. Haas, F.H. Spedding and R.H. Good Jr, 1973, J. Chem. Phys. **58**, 672.
Kaufman, V., and J. Sugar, 1967, J. Res. Nat. Bur. Stand. A **71**, 583.
Kaufman, V., and J. Sugar, 1978, J. Res. Nat. Bur. Stand. **68**, 1529.
Kent, R.D., and M. Schlesinger, 1981, Phys. Rev. A **23**, 979.
Kent, R.D., M. Schlesinger and P.S. Ponnapalli, 1985, Phys. Rev. B **31**, 1264.
Kerman, A.K., 1961, Ann. Phys. (USA) **12**, 300.
King, A.S., 1928, Astrophys. J. **68**, 194.
King, A.S., 1930, Astrophys. J. **72**, 221.
King, A.S., 1931, Astrophys. J. **74**, 328.
King, A.S., 1932, Astrophys. J. **75**, 40.
King, A.S., 1933, Astrophys. J. **78**, 9.
King, A.S., 1935, Astrophys. J. **82**, 140.
King, W.H., 1963, J. Opt. Soc. Am. **53**, 638.
Kirby, A.F., and R.A. Palmer, 1981, Inorg. Chem. **20**, 1030.
Kiss, Z.J., and P.N. Yocom, 1964, J. Chem. Phys. **41**, 1511.
Klapisch, M., A. Bar-Shalom, P. Mandelbaum, J.L. Schwob, A. Zigler, H. Zmora and S. Jackel, 1980, Phys. Lett. A **79**, 67.
Klinkenberg, P.F.A., 1947, Physica **13**, 1.
Klinkenberg, P.F.A., and Th.A.M. van Kleef, 1970, Physica **50**, 625.
Komarovskii, V.A., and N.P. Penkin, 1969, Opt. & Spectrosc. **26**, 483.
Komarovskii, V.A., N.P. Penkin and L.N. Shaba-

nova, 1969, Opt. & Spectrosc. **25**, 81.
Koningstein, J.A., 1966, J. Opt. Soc. Am. **56**, 1405.
Koningstein, J.A., and O.S. Mortensen, 1967, Phys. Rev. Lett. **18**, 831.
Koningstein, J.A., and O.S. Mortensen, 1968, Nature **217**, 445.
Koster, G.F., J.O. Dimmock, R.G. Wheeler and H. Statz, 1963, Properties of the Thirty-Two Point Groups (M.I.T. Press, Cambridge, Massachusetts).
Kotochigova, S.A., V.G. Kuznetsov and I.I. Tupitsyn, 1984, Opt. & Spectrosc. **57**, 113.
Kramers, H.A., 1930a, Proc. K. Ned. Akad. Wet. **33**, 953.
Kramers, H.A., 1930b, Proc. K. Ned. Akad. Wet. **33**, 959.
Kramers, H.A., 1931, Proc. K. Ned. Akad. Wet. **34**, 965.
Krebs, K., and R. Winkler, 1960, Naturwissenschaften **21**, 490.
Kronfeldt, H.-D., J.-R. Kropp and R. Winkler, 1982, Physica C **112**, 138.
Kronfeldt, H.-D., J.-R. Kropp and R. Winkler, 1984, J. Opt. Soc. Am. B **1**, 293.
Kropp, J.-R., H.-D. Kronfeldt and R. Winkler, 1984, Physica C **124**, 105.
Kropp, J.-R., H.-D. Kronfeldt and R. Winkler, 1985a, Z. Phys. A **321**, 57.
Kropp, J.-R., H.-D. Kronfeldt and R. Winkler, 1985b, Z. Phys. A **321**, 365.
Krupke, W.F., 1966, Phys. Rev. **145**, 325.
Kuhn, H.G., 1962, Atomic Spectra (Longmans and Green, London).
Kuroda, R., S.F. Mason and C. Rosini, 1980, Chem. Phys. Lett. **70**, 11.
Kustov, E.F., T.K. Maketov, G. Steczko and A.K. Prgevudsky, 1980, Phys. Status Solidi a **60**, 225.
Lang, H., 1938, Ann. Phys. (Leipzig) **31**, 604.
Lang, R.J., 1936, Can. J. Res. Sect. A **14**, 127.
Laporte, O., and J.R. Platt, 1942, Phys. Rev. **61**, 305.
Lawson, R.D., and M.H. Macfarlane, 1965, Nucl. Phys. **66**, 80.
Leavitt, R.C., 1987, J. Phys. B **20**, 3171.
Leavitt, R.P., 1982, J. Chem. Phys. **77**, 1661.
Levinson, I.B., and A.A. Nikitin, 1965, Handbook for Theoretical Computation of Line Intensities in Atomic Spectra (Monson, Jerusalem).
Lindgren, I., and J. Morrison, 1982, Atomic Many-Body Theory (Springer, Berlin).
Lindgren, I., and A. Rosén, 1974a, Case Stud. At. Phys. **4**, 93.
Lindgren, I., and A. Rosén, 1974b, Case Stud. At. Phys. **4**, 197.
Loginov, A.V., 1984, Opt. & Spectrosc. **56**, 568.
Macfarlane, R.M., R.M. Shelby, A.Z. Genack and D.A. Weitz, 1980, Opt. Lett. **5**, 462.
Malli, G., and K.M.S. Saxena, 1969, Can. J. Phys. **47**, 2779.
Margerie, J., 1967, Physica **33**, 238.
Margolis, J.S., 1961, J. Chem. Phys. **35**, 1367.
Martin, W.C., 1963, J. Opt. Soc. Am. **53**, 1047.
Martin, W.C., 1971, J. Opt. Soc. Am. **61**, 1682.
Martin, W.C., 1972, Opt. Pura & Apl. **5**, 181.
Martin, W.C., 1981, Phys. Scr. **24**, 725.
Martin, W.C., R. Zalubas and L. Hagan, 1978, Atomic Energy Levels – The Rare-Earth Elements (U.S. Government Printing Office, Washington, DC).
Marvin, H.H., 1947, Phys. Rev. **71**, 102.
Mason, S.F., 1980, Struct. Bonding (Berlin) **39**, 43.
Mason, S.F., 1985, Lanthanide (III) Transition Probabilities, in: Rare Earths Spectroscopy, eds B. Jeżowska-Trzebiatowska, J. Legendziewicz and W. Stręk (World Scientific, Singapore).
Mason, S.F., R.D. Peacock and B. Stewart, 1974, Chem. Phys. Lett. **29**, 149.
Mason, S.F., R.D. Peacock and B. Stewart, 1975, Mol. Phys. **30**, 1829.
Mayer, M.G., 1941, Phys. Rev. **60**, 184.
McClure, D.S., 1959, Solid State Physics, Vol. 9, eds F. Seitz and D. Turnbull (Academic Press, New York) p. 399.
McClure, D.S., and Z. Kiss, 1963, J. Chem. Phys. **39**, 3251.
McLellan, A.G., 1960, Proc. Phys. Soc. London **76**, 419.
Meggers, W.F., 1942, Rev. Mod. Phys. **14**, 96.
Meggers, W.F., 1962, Physics Today **15**, no. 12, 64.
Meggers, W.F., and B.F. Scribner, 1930, J. Res. Nat. Bur. Stand. **5**, 73.
Meinders, E., Th.A.M. van Kleef and J.-F. Wyart, 1972, Physica **61**, 443.
Meshkov, S., 1953, Phys. Rev. **91**, 871.
Morley, J.P., T.R. Faulkner, F.S. Richardson and R.W. Schwartz, 1981, J. Chem. Phys. **75**, 539.
Morley, J.P., T.R. Faulkner and F.S. Richardson, 1982a, J. Chem. Phys. **77**, 1710.
Morley, J.P., T.R. Faulkner, F.S. Richardson and R.W. Schwartz, 1982b, J. Chem. Phys. **77**, 1734.
Morrison, C.A., and R.P. Leavitt, 1982, Spectroscopic Properties of Triply Ionized Lanthanides in Transparent Host Crystals, in: Handbook on the Physics and Chemistry of Rare Earths, Vol. 5, eds K.A. Gschneidner Jr and L. Eyring (North-Holland, Amsterdam) ch. 46.
Morrison, J.C., and K. Rajnak, 1971, Phys. Rev. A **4**, 536.
Morrison, J.C., P.R. Fields and W.T. Carnall, 1970a, Phys. Rev. B **2**, 3526.
Morrison, J.C., K. Rajnak and M. Wilson, 1970b, J. Phys. Colloq. (France) **31**, C-4, 167.
Mortensen, O.S., and J.A. Koningstein, 1968, J. Chem. Phys. **48**, 3971.
Moshinsky, M., 1968, Group Theory and the Many-Body Problem (Gordon and Breach, New York).
Müller, W., A. Steudel and H. Walther, 1965, Z. Phys. **183**, 303.
Murao, T., F.H. Spedding and R.H. Good, 1965, J. Chem. Phys. **42**, 993.

Murao, T., W.J. Haas, R.W.G. Syme, F.H. Spedding and R.H. Good, 1967, J. Chem. Phys. **47**, 1572.
Naccache, P.F., 1972, J. Phys. B **5**, 1308.
Neureiter, C., R.-H. Rinkleff and L. Windholz, 1986, J. Phys. B **19**, 2227.
New, R., J.A.R. Griffith, G.R. Isaak and M.P. Ralls, 1981, J. Phys. B **14**, L135.
Newman, D.J., 1970, Chem. Phys. Lett. **6**, 288.
Newman, D.J., 1971, Adv. Phys. **20**, 197.
Newman, D.J., 1982, Phys. Lett. A **92**, 167.
Newman, D.J., and G. Balasubramanian, 1975, J. Phys. C **8**, 37.
Newman, D.J., and B. Ng, 1986, J. Phys. C **19**, 389.
Newman, D.J., G.G. Siu and W.Y.P. Fung, 1982, J. Phys. C **15**, 3113.
Nielson, C.W., and G.F. Koster, 1963, Spectroscopic Coefficients for the p^n, d^n and f^n Configurations (M.I.T. Press, Cambridge, MA).
Ofelt, G.S., 1962, J. Chem. Phys. **37**, 511.
Ostrofsky, M., 1934, Phys. Rev. **46**, 604.
Paldus, J., and M.J. Boyle, 1980, Phys. Rev. A **22**, 2299, 2316.
Palmer, C.W.P., and D.N. Stacey, 1982, J. Phys. B **15**, 997.
Peacock, R.D., 1975, Struct. Bonding (Berlin) **22**, 83.
Penkin, N.P., and V.A. Komarowsky, 1973, Opt. & Spectrosc. **34**, 1.
Pfeufer, V., A. Reimche and A. Steudel, 1982, Z. Phys. A **308**, 185.
Picart, J., A.R. Edmonds and N. Tran Minh, 1978, J. Phys. B **11**, L651.
Piepho, S.B., and P.N. Schatz, 1983, Group Theory in Spectroscopy with Applications to Magnetic Circular Dichroism (Wiley–Interscience, New York).
Piper, T.S., J.P. Brown and D.S. McClure, 1967, J. Chem. Phys. **46**, 1353.
Pollack, S.A., and R.A. Satten, 1962, J. Chem. Phys. **36**, 804.
Poon, Y.M., and D.J. Newman, 1984, J. Phys. C **17**, 4319.
Prather, J.L., 1961, Atomic Energy Levels in Crystals, National Bureau of Standards Monograph No. 19 (U.S. Department of Commerce, Washington, DC).
Racah, G., 1931a, Nuovo Cimento **8**, 178.
Racah, G., 1931b, Z. Phys. **71**, 431.
Racah, G., 1942a, Phys. Rev. **62**, 186.
Racah, G., 1942b, Phys. Rev. **62**, 438.
Racah, G., 1943, Phys. Rev. **63**, 367.
Racah, G., 1949, Phys. Rev. **76**, 1352.
Racah, G., 1950, Physica **16**, 651.
Racah, G., 1952a, Phys. Rev. **85**, 381.
Racah, G., 1952b, Curr. Sci. **21**, 67.
Racah, G., 1955, Bull. Res. Coun. Isr. Sect. A **5**, 78.
Racah, G., 1965, Group Theory and Spectroscopy, in: Springer Tracts in Modern Physics, Vol. 37, ed. G. Höhler (Ergebnisse der Exakten Naturwissenschaften) (Springer, Berlin).
Racah, G., and J. Stein, 1967, Phys. Rev. **156**, 58.
Racah, G., Z.B. Goldschmidt and S. Toaff, 1966, J. Opt. Soc. Am. **56**, 407.
Rajnak, K., and W.F. Krupke, 1967, J. Chem. Phys. **46**, 3532.
Rajnak, K., and B.G. Wybourne, 1963, Phys. Rev. **132**, 280.
Rajnak, K., and B.G. Wybourne, 1964a, J. Chem. Phys. **41**, 565.
Rajnak, K., and B.G. Wybourne, 1964b, Phys. Rev. **134**, A596.
Rana, R.S., C.D. Cordero-Montalvo and N. Bloembergen, 1984, J. Chem. Phys. **81**, 2951.
Rao, V.R., 1950, Curr. Sci. **19**, 8.
Ray, D.K., 1963, Proc. Phys. Soc. London **82**, 47.
Raychaudhuri, A.K., and D.K. Ray, 1967, Proc. Phys. Soc. London **90**, 839.
Reid, M.F., and F.S. Richardson, 1983a, Chem. Phys. Lett. **95**, 501.
Reid, M.F., and F.S. Richardson, 1983b, J. Chem. Phys. **79**, 5735.
Reid, M.F., and F.S. Richardson, 1984, Mol. Phys. **51**, 1077.
Reid, M.F., and F.S. Richardson, 1985a, What do f–f Electric Dipole Intensity Parameters tell us about [the underlying] Mechanism?, in: Rare Earths Spectroscopy, eds B. Jeżowksa-Trzebiatowska, J. Legendziewicz and W. Strek (World Scientific, Singapore).
Reid, M.F., and F.S. Richardson, 1985b, J. Chem. Phys. **83**, 3831.
Reid, M.F., J.J. Dallara and F.S. Richardson, 1983, J. Chem. Phys. **79**, 5743.
Reilly, E., 1953, Phys. Rev. **91**, 876.
Reilly, E., 1968, Phys. Rev. **170**, 1.
Richardson, F.S., 1986, J. Chem. Phys. **85**, 2345.
Richardson, F.S., J.D. Saxe, S.A. Davis and T.R. Faulkner, 1981, Mol. Phys. **42**, 1401.
Richman, I., R.A. Satten and E.Y. Wong, 1963, J. Chem. Phys. **39**, 1833.
Ridley, E.C., 1960, Proc. Cambridge Philos. Soc. **56**, 41.
Rosen, N., G.R. Harrison and J.R. McNally, 1941, Phys. Rev. **60**, 722.
Rotenberg, M., R. Bivins, N. Metropolis and J.K. Wooten Jr, 1959, The 3-j and 6-j Symbols (M.I.T. Press, Cambridge, MA).
Roth, C., 1971, J. Res. Nat. Bur. Stand. B **75**, 31.
Roth, C., 1972, J. Res. Nat. Bur. Stand. B **76**, 61.
Runciman, W.A., 1958, Rep. Prog. Phys. **21**, 30.
Russell, H.N., 1942, Astrophys. J. **96**, 11.
Russell, H.N., 1950, J. Opt. Soc. Am. **40**, 550.
Russell, H.N., and A.S. King, 1934, Phys. Rev. **46**, 1023.
Russell, H.N., and W.F. Meggers, 1932, J. Res. Nat. Bur. Stand. **9**, 625.
Russell, H.N., R.B. King and R.J. Lang, 1937, Phys. Rev. **52**, 456.
Rutherford, D.E., 1948, Substitutional Analysis (Edinburgh University Press, Edinburgh).
Sack, N., 1956, Phys. Rev. **102**, 1302.
Sandars, P.G.H., and J. Beck, 1965, Proc. R. Soc. London Ser. A **289**, 97.

Saraph, H.E., and M.J. Seaton, 1971, Philos. Trans. R. Soc. **271**, 1.
Satten, R.A., 1953, J. Chem. Phys. **21**, 637.
Satten, R.A., 1955, J. Chem. Phys. **23**, 400.
Satten, R.A., 1957, J. Chem. Phys. **27**, 286.
Satten, R.A., 1958, J. Chem. Phys. **29**, 658.
Satten, R.A., 1959, J. Chem. Phys. **30**, 590.
Satten, R.A., 1964, J. Chem. Phys. **40**, 1200.
Satten, R.A., C.L. Schreiber and E.Y. Wong, 1983, J. Chem. Phys. **78**, 79.
Saxena, K.M.S., and G. Malli, 1969, Can. J. Phys. **47**, 2805.
Sayre, E.V., K.M. Sancier and S. Freed, 1955, J. Chem. Phys. **23**, 2060.
Schäffer, C.E., and C.K. Jørgensen, 1958, J. Inorg. Nucl. Chem. **8**, 143.
Schlesinger, M., R.D. Kent and G.W.F. Drake, 1982, Can. J. Phys. **60**, 357.
Schüler, H., and Th. Schmidt, 1935a, Z. Phys. **94**, 457.
Schüler, H., and Th. Schmidt, 1935b, Z. Phys. **95**, 265.
Schwartz, R.W., 1975, Mol. Phys. **30**, 81.
Schwartz, R.W., 1976, Mol. Phys. **31**, 1909.
Schwartz, R.W., and P.N. Schatz, 1973, Phys. Rev. B **8**, 3229.
Schwartz, R.W., H.G. Brittain, J.P. Riehl, W. Yeakel and F.S. Richardson, 1977, Mol. Phys. **34**, 361.
Sengupta, D., and J.O. Artman, 1970, Phys. Rev. B **1**, 2986.
Shadmi, Y., E. Caspi and J. Oreg, 1969, J. Res. Nat. Bur. Stand. A **73**, 173.
Shelby, R.M., and R.M. Macfarlane, 1981, Phys. Rev. Lett. **47**, 1172.
Shen, Y.R., 1964, Phys. Rev. A **133**, 511.
Shen, Y.R., and N. Bloembergen, 1964, Phys. Rev. A **133**, 515.
Siu, G.G., and D.J. Newman, 1983, J. Phys. C **16**, 7019.
Siu, G.G., and D.J. Newman, 1986, Lanth. Act. Res. **1**, 163.
Slater, J.C., 1929, Phys. Rev. **34**, 1293.
Slater, J.C., 1960, in: Quantum Theory of Atomic Structure, Vol. II (McGraw-Hill, New York) pp. 119-130.
Slater, J.C., 1968, Am. J. Phys. **36**, 69.
Smith, G., and F.S. Tomkins, 1976, Philos. Trans. R. Soc. A **283**, 345.
Smith, G., and M. Wilson, 1970, J. Opt. Soc. Am. **60**, 1527.
Spector, N., and J. Sugar, 1976, J. Opt. Soc. Am. **66**, 436.
Spedding, F.H., 1931, Phys. Rev. **37**, 777.
Spedding, F.H., 1933, J. Chem. Phys. **1**, 144.
Spedding, F.H., 1940, Phys. Rev. **58**, 255.
Spedding, F.H., and R.S. Bear, 1932, Phys. Rev. **42**, 58, 76.
Spedding, F.H., and R.S. Bear, 1934, Phys. Rev. **46**, 975.
Spedding, F.H., W.J. Haas, W.L. Sutherland and C.A. Eckroth, 1965, J. Chem. Phys. **42**, 981.
Spedding, F.H., M.T. Rothwell, W.J. Haas and W.L. Sutherland, 1968, J. Chem. Phys. **48**, 4843.
Stacey, D.N., 1971, Isotope Shifts and Nuclear Physics, in: Atomic Physics 2, eds G.K. Woodgate and P.G.H. Sandars (Plenum, New York) p. 105.
Sternheimer, R.M., 1950, Phys. Rev. **80**, 102.
Stevens, K.W.H., 1952, Proc. Phys. Soc. London Sect. A **65**, 209.
Stone, A.P., 1959, Proc. Phys. Soc. London Sect. A **74**, 424.
Striganov, A.R., V.A. Katulin and V.V. Eliseev, 1962, Opt. & Spectrosc. **12**, 91.
Sugar, J., 1963, J. Opt. Soc. Am. **53**, 831.
Sugar, J., 1965a, J. Opt. Soc. Am. **55**, 33.
Sugar, J., 1965b, Phys. Rev. Lett. **14**, 731.
Sugar, J., 1965c, J. Opt. Soc. Am. **55**, 1058.
Sugar, J., 1969, J. Res. Nat. Bur. Stand. Sect. A **73**, 333.
Sugar, J., 1971, J. Opt. Soc. Am. **61**, 727.
Sugar, J., 1972, Phys. Rev. B **5**, 1785.
Sugar, J., and V. Kaufman, 1965, J. Opt. Soc. Am. **55**, 1283.
Sugar, J., and V. Kaufman, 1972, J. Opt. Soc. Am. **62**, 562.
Sugar, J., and V. Kaufman, 1980, Phys. Rev. A **21**, 2096.
Sugar, J., and V. Kaufman, 1982, Phys. Scr. **26**, 419.
Sugar, J., and N. Spector, 1974, J. Opt. Soc. Am. **64**, 1484.
Sugar, J., V. Kaufman and N. Spector, 1978, J. Res. Nat. Bur. Stand. **83**, 233.
Syme, R.W.G., W.J. Haas, F.H. Spedding and R.H. Good, 1968, J. Chem. Phys. **48**, 2772.
Szynarowska, M., and R. Papaj, 1982, Phys. Scr. **25**, 485.
Tanaka, Y., R.M. Steffen, E.B. Shera, W. Reuter, M.V. Hoehn and J.D. Zumbro, 1983, Phys. Rev. Lett. **51**, 1633.
Tanner, P.A., 1986, J. Chem. Phys. **85**, 2344.
Tech, J.L., V. Kaufman and J. Sugar, 1984, J. Opt. Soc. Am. B **1**, 41.
Tomaschek, R., 1932, Nature **130**, 740.
Tomaschek, R., 1933, Phys. Z. **33**, 878.
Tomaschek, R., and O. Deutschbein, 1933, Phys. Z. **34**, 374.
Trees, R.E., 1951a, Phys. Rev. **83**, 756.
Trees, R.E., 1951b, Phys. Rev. **84**, 1089.
Trees, R.E., 1952, Phys. Rev. **85**, 382.
Trees, R.E., 1964, J. Opt. Soc. Am. **54**, 651.
Trees, R.E., and C.K. Jørgensen, 1961, Phys. Rev. **123**, 1278.
Trefftz, E., 1951, Z. Phys. **130**, 561.
Van der Waerden, B.L., 1932, Die Gruppentheoretische Methode in der Quantenmechanik (Springer, Berlin).
Van Vleck, J.H., 1932, The Theory of Electric and Magnetic Susceptibilities (Oxford University Press, Oxford).
Van Vleck, J.H., 1934, Phys. Rev. **45**, 415.
Van Vleck, J.H., 1937, J. Chem. Phys. **41**, 67.
Wachter, P., 1979, Europium Chalcogenides, in:

Handbook on the Physics and Chemistry of Rare Earths, Vol. 2, eds K.A. Gschneidner Jr and L. Eyring (North-Holland, Amsterdam) ch. 19.
Weakliem, H.A., 1972, Phys. Rev. B **6**, 2743.
Weakliem, H.A., C.H. Anderson and E.S. Sabisky, 1970, Phys. Rev. B **2**, 4354.
Weyl, H., 1925, Math. Z. **23**, 271; **24**, 328, 377.
Weyl, H., 1931, The Theory of Groups and Quantum Mechanics (Dover, New York) [English translantion by H.P. Robertson of Gruppentheorie und Quantenmechanik (Hirzel, Leipzig), 2nd edition].
Weyl, H., 1953, The Classical Groups (Princeton University Press, Princeton, NJ).
White, H.E., 1929a, Phys. Rev. **34**, 1404.
White, H.E., 1929b, Phys. Rev. **34**, 1397.
White, H.E., 1934, Introduction to Atomic Spectra (McGraw-Hill, New York).
Whittaker, E.T., and G.N. Watson, 1927, A Course of Modern Analysis (Cambridge University Press, Cambridge).
Wigner, E.P., 1931, Gruppentheorie und ihre Anwendung auf die Quantenmechanik der Atomspektren (Vieweg, Braunschweig).
Wigner, E.P., 1965, On the Matrices which Reduce the Kronecker Product of Representations of S.R. [Simply Reducible] Groups, in: Quantum Theory of Angular Momentum, eds L.C. Biedenharn and H. van Dam (Academic Press, New York) p. 87.
Williams, G.M., P.C. Becker, J.G. Conway, N. Edelstein, M.M. Abraham and L.A. Boatner, 1987, Electronic Raman Scattering in Ce^{3+}/$LuPo_4$, in: Rare Earths 1986, Vol. 1, eds H.B. Silber, L.R. Morss and L.E. Delong (Elsevier Sequoia S.A., Lausanne) p. 302.
Wilson, M., 1972, J. Phys. B **5**, 218.
Wolfe, H.C., 1932, Phys. Rev. **41**, 443.
Worden, E.F., R.W. Solarz, J.A. Paisner and J.G. Conway, 1978, J. Opt. Soc. Am. **68**, 52.
Wyart, J.-F., 1976, Physica C **83**, 361.
Wyart, J.-F., 1978, J. Opt. Soc. Am. **68**, 197.
Wyart, J.-F., 1985, Phys. Scr. **32**, 58.
Wyart, J.-F., and Cl. Bauche-Arnoult, 1981, Phys. Scr. **22**, 583.
Wyart, J.-F., and P. Camus, 1978, Physica C **93**, 227.
Wyart, J.-F., and P. Camus, 1979, Phys. Scr. **20**, 43.
Wyart, J.-F., H.M. Crosswhite and R. Hussain, 1976/7, Physica **85**, 386.
Wybourne, B.G., 1965a, Spectroscopic Properties of Rare Earths (Wiley–Interscience, New York).
Wybourne, B.G., 1965b, Phys. Rev. **137**, A364.
Wybourne, B.G., 1970, Symmetry Principles and Atomic Spectroscopy (Wiley–Interscience, New York).
Yen, W.M., C.G. Levey, S. Huang and S.T. Lai, 1981, J. Lumin. **24/25**, 659.
Yeung, Y.Y., and D.J. Newman, 1985, J. Chem. Phys. **82**, 3747.
Yeung, Y.Y., and D.J. Newman, 1986a, J. Chem. Phys. **84**, 4470.
Yeung, Y.Y., and D.J. Newman, 1986b, J. Phys. C **19**, 3877.
Zaal, G.J., W. Hogervorst, E.R. Eliel, K.A.H. van Leeuwen and J. Blok, 1979, Z. Phys A **290**, 339.
Zeldes, N., 1953, Phys. Rev. **90**, 413.

Handbook on the Physics and Chemistry of Rare Earths, Vol. 11
edited by K.A. Gschneidner, Jr. and L. Eyring

Chapter 75

INFLUENCE OF RARE EARTHS ON CHEMICAL UNDERSTANDING AND CLASSIFICATION

Christian K. JØRGENSEN
Section of Chemistry (Sciences II), University of Geneva, CH 1211 Geneva 4, Switzerland

Contents

Symbols

A	atomic weight in amu
A	integer close to atomic weight (of conventional nuclei)
A_*	parameter of interelectronic repulsion
a_0	cubic unit-cell parameter
D	spin-pairing energy parameter, eq. (6)
d-quark	
d_l	Rydberg defect, eq. (1)
E^o	standard oxidation potential
$-E_{corr}$	electronic correlation energy
E^1 and E^3	Racah parameters of interelectronic repulsion in f shell
$(E - A)$	parameter in spin-pairing treatment
F^2, F^4 and F^6	Slater–Condon–Shortley parameters of interelectronic repulsion
hv	photon energy
I	ionization energy
I'	charge-compensated I relative to vacuum
I^*	ionization energy relative to Fermi level
I_n	ionization energy of gaseous monatomic M^{+n-1}
J	quantum number of angular momentum in (approximate or perfect) spherical symmetry
j	J for single electron, or for relativistic orbital
K	Kossel number of electrons
k	Boltzmann constant
L	quantum number of orbital angular momentum
l	L for single electron or orbital in spherical symmetry
M	mass of species in amu
N	coordination number in compound or polyatomic ion
N	neutron number in nucleus
n	'principal' quantum number
$\mathcal{N}$	number of nuclei in polyatomic system
q	number of electrons in 4f shell
P	oscillator strength
$\mathcal{R}$	spin-pairing function in 4f shell, eq. (7)
S	quantum number of total spin
S_{max}	highest S value for l^q configuration
s-quark	
T	absolute temperature
U_t	Judd–Ofelt matrix element ($t = 2, 4$, or 6)
u-quark	
$U(r)$	central field in Schrödinger equation
x_{opt}	optical electronegativity, eq. (5)
Z	atomic number (nuclear charge in protonic units)
z	ionic charge; oxidation state
Z_s	screening constant for inner shells
Δ	sub-shell energy difference in octahedral d-shell
δ	one-sided half-width of absorption band or photo-electron signal
ζ_{4f} or ζ_{nl}	Landé parameter of spin–orbit coupling
Ψ	more-electron wave-function
Ω	ratio between average density in the Universe and the closure density
Ω_t	Judd–Ofelt parameter ($t = 2$, 4 or 6) of transition probability

1. The rare earths as containing chemical elements

At the present time, the rare earths, R, are the seventeen elements characterized by the positive charge of the nuclei, in the units $+e$ of the protonic charge, being either 21 (scandium), 39 (yttrium) or one of the integers Z in the interval 57 through 71 (these 15 elements having the generic name lanthanides). The discovery and the painstaking separations of these elements from mixtures extracted from their minerals took place so early, that they contributed to the doubts and the controversies about what constitutes an element for a chemist. Mary Elvira Weeks (1968) has provided an excellent description of the discovery of the first hundred elements, and, in this volume, Szabadváry has reviewed the history of the discovery and separation of the rare earths.

It does not really make too much sense to say that nine among our elements, carbon, sulfur and the seven classical metals, gold, silver, mercury, copper, iron, tin and lead were known 2000 years ago. The metals formed a very tightly knit category. With the exception of iron they were known to form alloys in nearly all proportions, and the mass of these alloys being precisely additive. This fact had important economic corollaries; before Marco Polo returned in 1295 to tell the Italians how the Chinese make banknotes, spaghetti, ..., the only technique available to governments to sustain inflation was to continue to make alloys with less Au or Ag. The seven metals got so strongly connected to the mobile planets in the geocentric system and to the names of the days of the week that any contemporary theoretician knew that any new discovery could not be of a metal, but of a semimetal. This name was by no means bad for the medieval elements arsenic, antimony and bismuth, but perhaps a little strained for zinc (shown to be present in Chinese brass, the same way as bronze was known in the Mediterranean civilization to need the addition of cassiterite SnO_2). The name 'metalloid' meaning similar to a metal later became synonymous with non-metal. Around 1730, cobalt and nickel joined the supernumerary metals, and the idea of only seven metals became a joke, to the extent that Klaproth named uranium (which he discovered 1789) after Uranus, known since 1781, and in 1803, cerium and palladium got their names from the recently discovered asteroids. Then the joke was forgotten, until neptunium was discovered in 1940.

Our concept of the elements was elaborated in the century between the proposals of Boyle and the system proposed by Lavoisier a few years before his execution (as tax collector) in 1794. The scientific effort was concentrated in this period on the study of gases. The invariance of mass was much more difficult to conceive of and to prove for gases, typically having specific densities hundreds of times lower than water, than it was for solids. That copper can increase its weight up to 25% by heating in air, and mercury up to 8%, was not a glaring argument for oxygen being taken up from the atmosphere; after all, phlogiston might have negative mass, as hinted by the behavior of hydrogen gas.

1.1. *The status of elements in 1794*

The rare earths were found the same year as Lavoisier had said his last words

about chemistry. He argued that there is a moderate number (of order 30) of distinct elements having invariant, additive mass that cannot be transmuted (the legendary alchemistic experiments had not been satisfactorily reproduced). Furthermore, there were a very low number of principles without weight, such as heat (in a calorimetric context, not degrading kinetic energy), light, and one (excess or deficit possible) or two electricities. Lavoisier certainly had experimental evidence on his side in this theory; the rest-masses are changed by less than one part per 10^9 (except recombination of two hydrogen atoms) just beyond reach of later analytical balances. The rest-mass is not increased by 10^{-10} when graphite is heated to its boiling-point, and deviations from electroneutrality could not be weighed. However much this system remained without observed counter-examples until 1896 (when the radioactivity of uranium was discovered) and 1897 (when the electrons moving in a Crookes tube, as in modern television, were shown to be a common constituent of matter with atomic weight 0.00055 at low speeds, and hence combining the chemically acceptable properties of phlogiston with the new idea of a principle having a small mass) it should not be swept under the rug that some mistakes were argued by Lavoisier. For example, he considered all acids to contain oxygen [meaning 'acid-former'; it is a pity that he did not give this name to the lightest element, calling $Z = 8$ hydrogen ('water-former') instead, since its nuclei provide 88% of the weight of H_2O]. Although he recognized that chlorides and fluorides contain two elements, hydrochloric and hydrofluoric acids must contain oxygen (being acids) and the former is still called muriatic acid in some old-fashioned drug-stores, corresponding to the element murium, of which free chlorine must be a higher oxide. It should be emphasized that the status of being an element is always provisional in the books by Lavoisier, a supposed 'element' may be shown to be a compound of two or more elements (as happened several times; UO_2 was considered as an element until Peligot made UCl_4 in 1841, as was VO also for a long time, because most vanadium and uranium compounds contain constitutional oxygen).

There is a general tendency in chemistry to go on using words, though the underlying theoretical concepts show a gradual or sudden change. An earth was at one time the residue obtained by calcination at high temperature. This word should not be confused with calx, the material to which addition of phlogiston would restore the free metal. The most typical earth was perhaps (more or less pure) silica, but at the time of Lavoisier this material was classified as silicic acid, and there was a tendency to stress the acidic character of hydroxides of newer elements, such as titanic, niobic, molybdic, tantalic and tungstic acids. Just before 1800, an earth had come to mean an oxide that cannot be reduced at red heat either by hydrogen or carbon, and is not classified as an acid like silica. Alumina was by far the most common earth, though Lavoisier introduced the concept of alkaline-earths, considering magnesia, lime, strontia and baryta as oxides of highly reactive metals, as was indeed confirmed by Davy in 1808. It may be noted that though Davy prepared metallic sodium and potassium in 1807 by electrolysis of molten NaOH and KOH, Lavoisier had a nagging suspicion that these alkalis contain nitrogen (like ammonia and amines) forming a tempting analogy to all acids containing oxygen. When Ekeberg suggested the name yttria (Ytter-Erde) for the oxide reported by Gadolin in

1794, it was not considered unlikely that it might be a mixture of several earths, as familiar from the difficulties of characterizing exactly two elements (Weeks 1968) in the couples cobalt and nickel, niobium and tantalum, molybdenum and tungsten, and even vanadium and chromium. With the exception of glucina (later called beryllia) characterized by Vauquelin in 1798, and thoria discovered by Berzelius in 1828, there have not really been any earths in the 19th century except alumina and the rare earths. The first bifurcation in this fascinating group was ceria, discovered in 1803 by a complicated simultaneous effort of Klaproth (who characterized urania in 1789) and of Berzelius and Hisinger.

1.2. *The six R of Mosander, and the Periodic Table*

The first distinctions between yttrium and cerium were based more on their occurrence in two different sets of rare minerals than by striking differences in chemical behavior. However, it soon became clear that cerium can be oxidized to a higher oxidation state forming a much less soluble hydroxide (like manganese and iron) and salts could be prepared from solution, which were generally colorless for the lower, and yellow to orange for the higher oxidation state. Berzelius remained convinced that the R were much more complicated, and persuaded his gifted collaborator Mosander to work on rare earths extracted from minerals found in Sweden and Norway (one country at that time). Until 1880, the major criterion for separating R was a gradual change of basicity (we say an increasing pH for precipitation of the hydroxide, going from smaller to larger ionic radii of R). Lanthanum the most basic (least insoluble) element, was characterized by Mosander in 1839; it forms colorless compounds, when pure. With great difficulty it could be separated from didymium, which is pink in aqueous solution, and which is also slightly less basic than cerium in the lower oxidation state. Contrary to cerium, didymium could not be oxidized in aqueous solution. However, evidence was obtained for the oxidation (with rather unpredictable stoichiometry) of calcined oxides to a brown chamois color, which were reversibly reduced by heating in hydrogen to a pale blue oxide. The name proposed, didymium (meaning 'twin' in Greek) turned out to be involuntarily ironic. Auer von Welsbach separated it, in 1885, into a smaller fraction, praseodymium, providing the brown color of calcined oxides in the higher oxidation state (and green salts in solution) and the major fraction, neodymium, forming pale raspberry-red to mauve salts and a sky-blue calcined oxide. It also became clear that yttrium forms colorless salts, but is accompanied by at least one element forming pink solutions and salts. In 1843, Mosander published the reasons for believing the existence of six R, the oxides of lanthanum, cerium, didymium, terbium, yttrium and erbium (in order of decreasing basicity). The three latter elements have their name derived from Ytterby, a small village situated on an island close to Stockholm, and known for a feldspar quarry with many unusual minerals. It may be noted that the names terbium and erbium were used in the opposite order (of what we do) in some early publications. Our terbium was essentially recognized for a brown color of mixed oxides (orange in the case of yttria) similar to that produced by didymia, and it turned out in the later

studies of Urbain that the element had only been detected in trace concentration by Mosander. The least basic R, erbium, forms solutions, salts and the oxide all colored like strawberry ice-cream. The idea of six R remained unchallenged from 1843 to 1878. This span is important, because during this time the Periodic Table took form, having as a major difficulty the existence of the five known lanthanides. We must realize that the periodic variation of chemical properties of (all) the elements as a function of their atomic weight, A, could only be recognized after the hypothesis of Avogadro was accepted (as was largely true after the international Congress of Chemistry in Karlsruhe in 1860). We have to understand how conceptually onerous this hypothesis was to the contemporary chemists. Not only the oligomeric nature of gaseous H_2, N_2, O_2, P_4, S_8, Cl_2,... (though monatomic Hg) but also the blatant exception from Boyle–Mariotte behavior of brown NO_2 and its loosely bound dimer (though the impact of this exception was attenuated when the deviations from Avogadro behavior of gaseous PCl_5 could be removed in a mass-action influence of small amounts of Cl_2 or PCl_3). The equivalent weights of quantitative analysis (e.g. the amount of an element combined with 35.45 g chlorine in a chloride) only become atomic weights after multiplication with the oxidation number z. It is true that the ratio between known equivalent weights 5:3 for phosphorus, arsenic and antimony suggest $z = 3$ and 5, but the corresponding ratio 2:1 for copper, tin and chromium is due to Cu(I), Cu(II), Sn(II), Sn(IV), Cr(III) and Cr(VI). Anyhow, there were no R compounds sufficiently volatile to apply Avogadro's theory (and UF_6 was made too late to help the corresponding problem of uranium).

We are not going here to review the 10 or 12 independent versions of the Periodic Table (Weeks 1968, Van Spronsen 1969, Rancke-Madsen 1984) but rather concentrate on the version of Mendeleev from 1869. The definition of the column number is the highest z of a given element. Exceptions were allowed for oxygen and fluorine (lack of elements with higher electronegativity, in modern terms), Br(VII) was quite enigmatic until Appelman prepared BrO_4^- in 1968, and only Ru(VIII) and Os(VIII) have $z = 8$. Knowing copper(II) and gold(III), Mendeleev preferred at first three *tetrades* (Fe, Co, Ni, Cu; Ru, Rh, Pd, Ag; Os, Ir, Pt, Au) and it may be regretted that he later yielded to the pressure for 8 columns (and $2 \cdot 8 = 18$) introducing triades. For our purpose, the main mechanism of the Periodic Table is to establish priorities for belonging to a given column. For instance, beryllium salts have a chemistry more similar to aluminum than to alkaline earths, but boron(III) is so well-established that Be(II) was kicked out in the second column. As seen on a commemorative Russian stamp from 1969, Mendeleev first put uranium (with $A = 119$) in column III between Al(III) and Tl(I), Tl(III), assuming U(II) and U(III) compounds, but when he became aware of indium (discovered 1863) he shifted uranium to the second column after thorium ($A = 232$) now forming U(IV) and U(VI). Although R(II) and R(III) remained a controversial question beyond 1880, yttrium with $A = 59$ (we keep no decimals here) and lanthanides from 93 to 112 assuming R(II) would spread havoc in the Periodic Table, and this is how R(III) was considered the lesser evil. Cerium has the legitimate place in column IV, didymium might be squeezed into V (cf. section 3.6) and, sofar as I know, Mendeleev never tried to accommodate any of the R discovered after 1878, although he probably

thought of them as a kind of king-size tetrade. There is a problem connected with the gap between $A = 139$ for lanthanum and $A = 181$ for tantalum. There is a smoothly increasing slope of A values within the known values below 238. Thus, the slope is $(19 - 7)/6 = 2$ for lithium to fluorine, $(35 - 23)/6 = 2$ for sodium to chlorine, $(80 - 39)/16 = 2.5$ for potassium to bromine, and $(127 - 85)/16 = 2.6$ for rubidium to iodine. A slightly more extreme interval is $(238 - 197)/13 = 3.1$ for gold to uranium. Under these circumstances, one would expect some 13 or 14 elements between lanthanum and tantalum, and we know there are 15. For Mendeleev, the most attractive solution was to suggest an undiscovered halogen with A close to 151, and an undiscovered alkali metal with A close to 156, which was not absolutely incompatible with the A values later determined for the six R reported by Mosander. But then, there must be some kind of tetrade behavior; we can hardly tolerate another alkali metal with A around 170. However, the question of one or two periods furtively crossing the Periodic Table between lanthanum and tantalum reduced itself into an absurdity 10 years after 1869.

1.3. *The boom 1878–1886, and suggestions by Crookes*

The beginning of this period is still marked by the relative basicity of the hydroxides being the most important parameter distinguishing the individual R. When applying a technique developed by Bunsen of partially decomposing the molten nitrates to basic nitrate solids, Marignac obtained in 1878 a colorless R *less* basic than erbium, calling it ytterbium (Jørgensen 1978a) as the fourth element named after that already famous Swedish village. Marignac obtained $A = 172.5$, half a unit below the present-day value. Seen in this context, it is surprising that Nilson in 1879 found an even less basic R, beyond Yb, but this time having $A = 45$ and being called scandium, representing an element with many properties predicted by Mendeleev by interpolation between aluminum and yttrium. In the same year, 1879, Cleve in Uppsala separated erbium into three elements: holmium, forming orange salts, the pink major erbium, and thulium, having pale green salts. Finally, Lecoq de Boisbaudran (who had discovered gallium in 1875, again thoroughly predicted by Mendeleev) separated samarium on the less basic side of neodymium.

One of the most difficult 'white spots on the map' was between $A = 150$ of samarium and (modern value) $A = 165$ of holmium. The major impurity was yttrium with A as low as 89, and a careful determination of the atomic weight was mainly an indicator of the yttrium content, of which 1.5 per cent was sufficient to decrease A by one unit. Marignac investigated this region by fractional recrystallization of potassium double sulfates (like Auer von Welsbach used ammonium and magnesium double nitrates to separate the lighter lanthanides) and in 1880 found gadolinium (Jørgensen 1980b) given $A = 157.25$, coinciding with the present value. It may be noted that Marignac gives the amount of oxide containing 16 g oxygen. Thus, he gives 128 g for erbia, in order to avoid the R(II) vs. R(III) dispute, which corresponds to $A = 168$. As the Greek name indicates, it was very difficulty to separate small amounts of dysprosium from yttrium; the element is considered to have been discovered by Lecoq de Boisbaudran in 1886. During the painstaking

recrystallization, terbium salts (remaining colorless) by calcination formed darker and darker brown oxides, ending with genuine, almost black 'Tb_4O_7' as reviewed by Urbain (1925). During the exhausting work in this area, many R turned up in literature, with full-fledged names like decipium, mosandrium and philippium, and others with Greek letters as symbols. It is clear that the atomic number Z, and spectroscopic measurements in general, later took over the jurisdiction of what constitutes an element, whereas the pragmatic definition used by Lavoisier is always open to surprises tomorrow.

The inventor of the Crookes tube (which permitted the characterization of the first elementary particle, the electron, in 1897 and indirectly the discovery of X-rays by Röntgen, and television) and discoverer of thallium in 1861 (by the same method of spectral lines in flame spectra as used by Bunsen and Kirchhoff in detecting rubidium and cesium), William Crookes, gave a lecture to the Royal Institution in London 1887 about the 'Genesis of the Elements' (Crookes 1888, 1895). Rather than a fixed and non-transmutable stock of elements, Crookes suggested that drastic conditions (exceedingly high temperatures, ...) allowed a primitive material 'protyle' primordially forming hydrogen (hence joining the suggestion of Prout in 1815) having (before 1895) an atomic weight 7 times lower than the next-lowest A, of lithium. Then a consecutive series of reactions took place, where the heavier elements were formed. Either because of slow reactions, or because of low yield, or simply by strongly endothermic character, the formation of elements did not go much beyond iron except for a very small proportion.

It should not be overlooked that this is close to the picture of recent astrophysics. After the Big Bang some 10^{10} years ago, a dew-point was passed after 10^{-5} s, where the temperature fell below 2 terakelvin (this unit 10^{12} K) and all (or nearly all) the quarks combined to form protons and neutrons (the latter being β-radioactive with a half-life of 11 minutes, if they are not absorbed by other nuclei before) (cf. Jørgensen 1982b, 1983c). During the next four minutes, 22% of the protons (including in their mass all the neutrons) formed α-particles, that is, ^{4}He nuclei. Much lower concentrations of some few times 10^{-5} had the time to undergo fusion to the rarer nuclei ^{2}D (deuterium) and ^{3}He, less than 10^{-9} to ^{7}Li, and all other isotopes were much rarer (Weinberg 1979, Trimble 1975). After about a million years, at a temperature of about a few thousand K, the free electrons combined with the monatomic positive ions and modified the optical properties strongly, and the Universe became much more transparent to ambient photons (and today, we readily receive light from a distance of 1000 million light years or 10^{22} km). The detailed mechanism of granulation to, first the 10^{12} observable galaxies, and then, on the average, 10^{11} stars in each galaxy, is not perfectly known, but it must have taken some 10^8 to 10^9 years. The very first stars (called population III) had nothing but the Weinberg mixture to start with, and their thermonuclear fusion produced more ^{4}He from ^{1}H, as is still the business of normal stars like our Sun. A few big III stars burned out rapidly and exploded as supernovae, producing carbon and higher Z values (lithium, beryllium and boron are exceedingly scarce in the Cosmos, because of rapid thermonuclear reactions). Population II and population III stars are quite similar, but population II stars contain small amounts of carbon, nitrogen and

oxygen. The large majority of actual stars (like our Sun) belong to population I and have scooped up a certain amount of heavier elements (mainly with Z between 6 and 28) from the earlier supernovae. Nevertheless, a star has to be several times the solar mass to do anything but transform a few percent more ^{1}H to ^{4}He. The heavy supernovae are dramatic happenings (Trimble 1975, 1982 and 1983) getting somewhat beyond the most stable nuclei (close to ^{56}Fe) which would be the equilibrium end product at temperatures below 10^{9} K (gigakelvin). The mechanism is consecutive capture of neutrons (expelled from various neon and magnesium isotopes by ^{4}He impact) where one makes a distinction (Trimble 1975) between s-(slow) processes of neutron capture (the time-scale of consecutive neutron capture being longer than that of β-radioactivity) which cannot proceed beyond ^{209}Bi (since all isotopes with A between 211 and 225 have so short half-lifes) and r-(rapid) processes moving through A values well above the β-stability line. We return in section 1.4 to the possibility of undetected, but conceivable, alternative production of very heavy elements.

In order to get some geochemical perspective into this discussion, we may consider the abundances in the solar photosphere (Trimble 1975) among which several may be uncertain by a factor of 2. One ton (10^{6} g) of such material contains 13 kg of C, N and O, the major elements in living beings (including the superabundant H), and about 600 g Ne, 40 g Na, 600 g Mg, 60 g Al, 900 g Si, 400 g S, 30 g Ar, 70 g Ca, 25 g Cr, 1000 g Fe and 150 g Ni. No more than 10 g of any other element is found, excepting H and He. Elements with Z from 37 to 92 are only represented by 0.4 g, and among those, the R by only 0.05 g.

The situation is quite different for the outer part of the crust of the Earth, where 1 ton contains 466 kg O, 277 kg Si, 81 kg Al, 50 kg Fe, ..., and 1.3 kg of elements with Z above 30 (zinc). Among those, 28 g yttrium and 120 g of the lanthanides. It is a well-known fact that rare earths are not particularly rare; the least abundant, thulium (0.2 g/t), may be compared with 0.005 g Au, 0.5 g Hg, 16 g Pb, 0.2 g Bi, 12 g Th and 4 g U per ton. This comparison between the solar photosphere and the Earth's crust is unfair at one point. It would require 340 t of solar material to supply (by a kind of non-volatile residue) 1 t of crust. During this 'distillation', nearly all H, He, C, N, Ne and Ar would be removed (the argon in the atmosphere is ^{40}Ar formed by the radioactivity of ^{40}K) and only a fifth of the oxygen would be retained. Nevertheless, it remains true that the mass ratio R/Si is 540 ppm in the crust, compared to 60 ppm in the solar material. This corresponds to an enhancement by a factor of nine even relative to so 'terrestrial' an element as silicon. This is a very fortunate advantage for inorganic chemists, who would have problems detecting elements beyond nickel in a population II star. It may be noted that the ratio between the mass of the Earth and the amount of solar material needed to 'boil down' to form it, is 10^{-3} as far as silicon goes, and only 0.01 in the case of rare earths.

There is no longer any doubt that the Sun was formed since less than half the time elapsed since the Big Bang, and that it is only marginally older than meteorite and lunar samples known to have ages up to 4600 million years. A careful analysis of various isotope abundances (Kuroda 1982, Rowe 1986) shows that the major part of the supernova material was imported into the solar system under formation in a

very short time interval, 0 to 30 million years. Hence, it is conceivable that the Earth received unusually large contributions of elements above $Z = 37$. The formation of the solar system may have been triggered by a not too distant supernova.

Crookes went on to suggest that a given element may have a variety of A values corresponding to almost the same chemical properties (as later found by mass spectra). He called these isotopes meta-elements, and suggested that the lanthanides correspond to a great number of meta-elements having an exceptionally great extent of chemical variation (much as we would say about deuterium and light hydrogen). Actually, Marignac attempted to separate manganese by fractional crystallization (Jørgensen and Kauffman 1988) but did not find any effect (also ^{55}Mn is the only stable isotope). The first stable isotopes recognized were ^{208}Pb isolated from thorium minerals, and ^{206}Pb from uranium minerals (in 1914, cf. Kauffman 1982) to be compared with 207.1 for the usual mixture.

In comparison with absorption spectra, the cathodoluminescence due to impact of rapid electrons is a much less reliable technique for evaluating the concentration of a given luminophore [this difficulty already occurs to a certain extent for photoluminescence (Reisfeld and Jørgensen 1977, 1987)] and it must be admitted today that the different emitters found by Crookes in solids containing R cannot be ascribed to meta-elements [cf. the sharp criticisms by Urbain (1925)]. On the other hand, the ideas of Crookes fit remarkably well the concept of isotopes and their step-wise formation under astrophysically extreme conditions.

1.4. *The tying up of loose ends 1901–1947*

Around the beginning of this century, twelve of our lanthanides had been well established (though not without a background noise of spurious R, including incognitum and victorium of Crookes) and it is remarkable that two of those still missing were found by autonomous chemical studies (it was not argued before 1913 that there were exactly three missing in 1900). The last, $Z = 61$, is only known in short-lived radioactive isotopes (half-life 18 years for ^{145}Pm, and 2.5 years for the fission product ^{147}Pm available in gram quantities). $Z = 61$ had turned up prematurely with the names florentium and illinium (Weeks 1968). The most surprising among the two latest R is europium. In 1890, Lecoq de Boisbaudran obtained fractions between Sm and Gd showing spectral lines from an electric spark that were not due to Sm and Gd, the main constituents. This is one example of how atomic spectra started to play a (not always unambiguous) role in identifying the elements, mainly from 1900 to 1910. Demarçay obtained relatively pure Eu_2O_3 in 1901. Although the first Eu(II) was obtained in 1911 by Urbain and Bourion, white $EuCl_2$ from heating anhydrous $EuCl_3$ in H_2, the ready reduction to Eu(II) did not happen to assist the discovery of the element. However, Demarçay made the clever modification of recrystallizing $Mg_3R_2(NO_3)_{12}, 24H_2O$ (extensively used by Auer von Welsbach) after adding some bismuth(III) which is easy to separate from R(III). In the order of solubility, Bi intercalates itself between Sm and Gd, allowing an efficient separation. Urbain (1909) studied the Eu(III) line spectrum of cathodoluminescence thoroughly. This allowed the major application of europium today, i.e.

the red color television 'phosphor' in $Eu_xY_{1-x}VO_4$ (Palilla et al. 1965, Brecher et al. 1967) and later in $Eu_xY_{2-x}O_2S$ (Sovers and Yoshioka 1969). Actually, the other R tend to become a by-product of the isolation of europium today, much as the lighter lanthanides were a by-product of the extraction of the (small) amounts of thorium(IV) from monazite for use in Auer mantles (Weeks 1968, Gutmann 1970, Jørgensen 1976a) with composition $Th_{0.99}Ce_{0.01}O_2$ in gas flames. The scarcity of europium is exacerbated by the shift of Eu(II) from R(III) to conventional calcium and strontium minerals (Haskin and Paster 1979).

Auer von Welsbach continued the search for R on the less basic side of erbia. Assisted by atomic spectra of arcs and sparks, he expressed the view that thulium contains three distinct elements. It took many years of work recrystallizing $Tm(OH_2)_9(BrO_3)_3$ by James before he could conclude, in 1911, that thulium is indeed a single element (Weeks 1968). The simpler atomic spectra of ytterbium brought more luck. In 1905, Auer von Welsbach concluded that the Yb of Marignac was a mixture of aldebaranium and a small amount of cassiopeium, the oxide of which was isolated in 1907 (another stellar name is denebium, a spurious element). Urbain also succeeded in 1907 to separate Yb into neo-ytterbium and lutetium, and after the war, IUPAC recommended calling the two elements ytterbium and lutetium, but without taking any position on priority. Urbain believed he had detected minute traces of a less basic R than lutetia, having $Z = 72$, but when Hevesy found hafnium in 1923 as a (several percent) constituent of zirconium minerals, in collaboration with the X-ray spectroscopist Coster and Niels Bohr, it became clear that Urbain's R is invariantly Hf(IV) and the name celtium was abandoned. It is as difficult to separate Zr and Hf as it is to separate Y and Dy (it was actually accomplished by recrystallization of double fluorides, such as K_2HfF_6) but later ion-exchange techniques were used. It is not certain that the ionic radius of Zr(IV) is smaller than that of Hf(IV). This is not really alarming, because Lu(III) is distinctly smaller than Y(III), though Ta(V) is marginally larger than Nb(V). The two last elements possessing at least one non-radioactive isotope to be discovered were hafnium and rhenium ($Z = 75$) in 1925. At this time, only two elements were lacking between $Z = 1$ and 83; technetium ($Z = 43$, now available in kg quantities with half-lifes in the 10^6 year range) and the lanthanide $Z = 61$, although the discoverers of rhenium, the Noddacks, argued for masurium (based on weak X-ray lines). There is nothing really enigmatic about the absence of stable isotopes exactly for $Z = 61$ and $Z = 43$, although the question is somewhat related to the nucleon shell model of Maria Goeppert-Mayer (cf. Jørgensen 1981a). If we define the quantum number A as the integer closest to the atomic weight on the ^{12}C scale, and another integer $N = (A - Z)$, there are actually eight ($N = 19$, 35, 39, 45, 61, 89, 115 and 123) lacking β-stable isotopes for A below 209. Another, $N = 21$ is represented by ^{40}K with a half-life of 1280 million years (and producing a substantial share of the geothermal heat). Only two elements, argon and cerium, have no stable isotope with odd A.

There are two reasons why this sub-section has '1947' in its title. One is that in that year promethium compounds prepared from fission products were fully described (Marinsky et al. 1947) although several radioactive nuclei had been reported

in tiny yields between 1938 and 1946, obtained by bombardment of neodymium with neutrons or deuterons. There is nothing deviant about the absorption spectra of the mauve to lilac salts, and the J-levels of the partly filled 4f shell have been identified (Carnall et al. 1976) as in the adjacent lanthanides. The other reason is the method published in 1947 for separating kilogram quantities of R(III) by ion-exchange on sulfonic (and other) resin columns (Spedding et al. 1947).

Before Rutherford firmly established the atomic nucleus in 1911, it could not be refuted that the Periodic Table and the evolutionary step-wise transmutation of elements proposed by Crookes was connected with relatively exterior properties of the atom (in particular because J.J. Thomson proposed the raisin-pudding model of electrons moving in a uniformly positive background, neutralizing the atom). Other related concepts were the sets of three similar elements of Döbereiner, developed by Julius Thomsen to addition of links of constant weight (like $CH_2 = 14$ amu in alkane chains) and 'basic' constituents like α-particles, tritons ('protofluorine') explaining the alternation ^{23}Na, ^{24}Mg, ^{27}Al, ^{28}Si, ^{31}P,... When hot stars (with continuous spectra indicating temperatures in the 12 000–30 000 K range, to be compared with 5800 K for the Sun) showed Fraunhofer lines of absorption, which could not be matched in the laboratory with emission lines of the highest-power sparks obtainable, it was not surprising that Rudorf (1900) suggested a break-down to proto-elements, usually M^+ and M^{+2} though the proto-hydrogen with half-numbered n in the Balmer formula is He^+, and asterium and a few 'unknown' elements probably are non-metallic M. When the Fraunhofer lines of other stars could be compared with the solar spectrum, the first hypothesis was that Sirius and other stars with surface temperature about twice that of the Sun contain predominantly hydrogen (and might be an earlier stage of the evolution suggested by Crookes) since the Balmer series provide by far the strongest lines. In stars with lower temperatures, the lines of metallic elements increase in number and intensity. In the solar spectrum, most of the intense lines are due to iron atoms, and others to Na, Mg, Ca, Ca^+, Ti, V, Cr, Mn, Co, Ni, Sr and Sr^+, though the five strongest Balmer lines of hydrogen still can be noted. The idea of a star consisting mainly of Fe changed in the 1920s to an essentially standard mixture of hydrogen, helium and elements from carbon to zinc showing entirely different spectra according to the photosphere temperature. Whereas most of the absorption lines originate from the groundstate of the monatomic entity, or at least from levels at most 1 eV from the groundstate, the Balmer series is due to absorption from the $n = 2$ states 10.2 eV above the groundstate of the hydrogen atom, and the factor $\exp[-(E_n - E_0)/kT]$ is 1.6×10^{-9} at 5900 K and 4×10^{-5} at double the temperature, $T = 11800$ K. Hence, the Fraunhofer lines of the Sun at a given moment originate in only 5 mg out of a ton material, assuming thermal equilibrium, whereas, 130 g is operative in Sirius. The situation is more extreme for helium having its first excited state at 19.8 eV with the result that you need a T almost twice as high as in Sirius to have as much helium contributing to the visible absorption spectrum, as is the case for hydrogen in this 'hydrogen' star. Hence, it is not surprising that 40 g sodium and 70 g calcium per ton solar photosphere give so much stronger Fraunhofer lines, as is well-known from a Bunsen or kitchen gas burner giving yellow flares with dust containing

sodium. The very large majority of stellar spectra are compatible with the idea of a roughly invariant proportion of differing elements (Trimble 1975). However, the rare earths have provided some glaring exceptions to this rule of standard composition.

In 1913, Baxandall discovered strong lines of Eu^+ in the star α^2-Canum Venaticorum. These strong lines are situated in the violet and near ultraviolet, similar to those of Ca^+, Sr^+ and Yb^+. This star of third magnitude has also the name Cor Caroli. An eighth magnitude star HD 101065 is even more striking (Przybylski 1966) by having comparable amounts of all the lanthanides, in a total concentration about 10 g/t (an enhancement by a factor 200 relative to normal stars) and slightly more of each lanthanide than of strontium, and about 30 times more than of calcium. Such anomalies are also known for other elements. The fifth magnitude star HR 8911 (κ-Piscium) was already known to contain much Eu and furthermore shown (Galeotti and Lovera 1974) to contain enormous amounts of osmium atoms and U^+, and probably also Ir and Pt^+, whereas, no Au, Hg, Pb and Bi were detected. Jacobs and Dworetsky (1982) found strong Bi^+ lines in HR 7775 (HD 193452) already known to contain a lot of gallium and mercury. The bismuth abundance is 10^6 times the solar value, and close to 2 kg/t, an abundance greater than that of iron in the Sun. For our purposes, the star HR 465 is fascinating. Cowley and Rice (1981) reviewed it when it seemed to return to the spectrum it had around 1958. Among other observations, there has been some discussion as to whether promethium (of which the longest-living isotope known has a half-life of 18 years) is present. Around 1979, there was progressive strengthening of M^+ lines of heavier lanthanides, in particular of dysprosium. This trend included gliding, in 1981, toward holmium and erbium. Such Z-increase might be due to β-activity, but there are not really any isotopes known which fit this time scale. At the same time, strong lines of U^+ increased, as well as lines of Th^+ and Th^{+2}. Careful wave-length determinations of the uranium lines indicate A well below ^{238}U. Among the wild ideas, one may get, is to suspect somebody able to direct a star to form specific elements. Trimble (1975) noted that some 5 to 10% of stars in a quite narrow interval of T close to 10000 K (called 'peculiar A type stars') have strong deviations from standard abundances, and that precise wave-length measurements suggest that nearly all the platinum and mercury in these stars occur in the form of the heaviest stable isotope, ^{198}Pt and ^{204}Hg. Taken at its face value, this situation suggests a high concentration of free neutrons. There are red giants of lower surface T (close to 3000 K) of S type (characterized by absorption bands of the diatomic molecule ZrO in place of TiO in the more frequent type M) showing atomic lines of technetium. An extreme case of an isotope anomaly is the star 3-Centauri (Wallerstein 1962) of which 7% of the mass is the rare helium isotope ^3He, but only 1% of ^4He. There are several hundred times more phosphorus, gallium and krypton than usual. The connection between the peculiar abundances and nuclear physics is discussed by Onishi (1979) and on a symposium (Maeder and Renzini 1984). One of the enigmatic sides is why some of such stars specialize in odd Z-values such as P, Mn and Y.

Though we have a clear-cut picture of all sixteen R, their minerals may still have some surprises in stock. Glashow (1980) pointed out that many direct observations

have allowed insight not provided by dedicated instrumental experimentation. Thus, in 1894, a whole percent of the unexpected element argon was found in the atmosphere; the radioactive isotopes extracted from uranium and thorium minerals provided all the data for nuclear physics until 1932; and the high-energy cosmic rays were worthy precursors of the huge accelerators. In many ways, chemists have a much more clear-cut view of the elements, now that it is established that the chemical behavior and atomic spectra are (almost) exclusively determined by the Z of the nucleus. But out of healthy curiosity, the chemist wants to keep aware of nuclei. The first model was A protons and $(A - Z)$ electrons confined in the small nucleus (almost invariant density $10^{14}\,g/cm^3$) surrounded by Z electrons in the neutral atom. Chemists were happy that the only two elementary particles (with positive rest-mass) also defined the two major kinds of chemical reactions, the exchange of protons being acid–base behavior (at least for Brønsted) and the exchange of electrons for redox processes. Though the kinetic energy of electrons in nuclei was enormous, according to quantum mechanics, their presence was suggested by their emission during β-radioactivity. However, pre-existence is not as obvious in quantum mechanics, as it is in obstetrics, and even before the neutron was discovered in 1932, the model of confined electrons broke down, because of the difference between Fermi–Dirac and Bose–Einstein statistics. Both electrons and protons (and all subsequently discovered baryons, such as the other 'nucleon' the neutron) are fermions. An odd number of fermions form a system which is itself a fermion, whereas for an even number of fermions the system formed is a boson. Molecular spectra of N_2^+ demonstrated that the ^{14}N nucleus is a boson, though $14 + 7$ fermions would constitute a fermion. Another problem was that β-radioactivity must consist in the emission of *two* fermions, since the boson or fermion character of the nucleus is not modified. As pointed out by Pauli in 1930, and elaborated by Fermi in 1934, there is another reason to assume the simultaneous emission of a neutral fermion, the neutrino, since the kinetic energy of the emitted electron assumes all values between zero and the maximum value allowed by energy (including rest-mass) conservation. Anyhow, after the neutron was characterized, the model changed to the non-negative integer $N = (A - Z)$ neutrons and Z protons in the nucleus, as reviewed by the writer (Jørgensen 1981a, 1982b).

Gell-Mann (1964) proposed that among the two kinds of hadrons (particles undergoing strong interactions, as in nuclei), the baryons (always fermions) consist of three quarks, and mesons (always bosons) consist of one quark and one anti-quark (related to each other like other pairs of a particle and its anti-particle, such as an electron and a positron). Today, there are five well-characterized quarks (and there are good reasons to assume that there are six), the u-(up) and c-(charm) quarks with the electric charge $+2e/3$, and the d-(down), s-(strange) and b-(beauty) quarks charged $-e/3$. Similar ideas were also proposed in a preprint the same year, 1964, by George Zweig. When the number of short-lived 'elementary' particles increased beyond 100 in 1976, the picture of quarks became more accepted, in part helped by the review by Feynman (1974) and by the evidence for 'partons' in protons undergoing collisions at extremely high kinetic energies. The 'constituents' of a proton are u^2d and of a neutron ud^2. In general, matter (we mean having positive

rest-mass) outside high-energy physics is constituted by u- and d-quarks and by electrons, if it subsists for more than a few microseconds. The third-lightest baryon, the neutral Λ with a half-life slightly below 2×10^{-10}s (in this time light moves 6 cm) has the quark configuration uds, and an atomic weight of 1.20 amu.

In a somewhat remote analogy with quantum electrodynamics (QED), a new quantum chromodynamics (QCD) has been elaborated. The gluons of this theory differ from photons, in a way rendering quarks absolutely confined. It may still be a legitimate question to ask (Jørgensen 1983c, 1984c) whether a very small proportion of matter have nuclei 'containing' a number of quarks not divisible by 3, such as the $3(Z + N)$ quarks in a normal nucleus $u^{2Z+N}d^{Z+2N}$ characterized by the quantum numbers Z and $N = (A - Z)$. It may very well be true that no high-energy collision is able to smash a conventional nucleus, though it is not excluded that a gravitational singularity, a 'black hole', may extract one or two quarks from a proton passing very close to it. However, it may be more likely that any system containing unsaturated quarks is a relict from the time about 10^{-5} s after the Big Bang when the primordial quark soup coagulated to baryons. The surviving abundance depends strongly on the excess atomic weight of the unsaturated system (Wagoner and Steigman 1979). If it is 20 amu (if it were smaller, it would probably already have been detected by high-energy physics) the order of magnitude expected is one system per 10^{20} amu (that is 6000 per gram). This happens to be the concentration reported by the group of Fairbank at the Stanford University in 10^{-4} g samples of niobium metallic spheres in several articles since 1977 (LaRue et al. 1981). Several other laboratories have reported negative results, but with lower limits in the 10^{-19}–10^{-21}/amu range in the convincing cases. There is no argument that the Fairbank species has Z close to 41, it may very well have a comparable chemistry with Z close to 73, 105, 143 or higher values and be a fission product of a nucleus with very high $Z \pm \frac{1}{3}$, of which the fission barrier is enhanced by the dependence of excess energy on Z (Jørgensen 1983c).

Systems with unsaturated quarks are expected to show quite different behavior from conventional nuclei (DeRújula et al. 1978, Jørgensen, 1978d, 1981a, 1982b, 1984b,c). Since the vacuum is a source of particles and the corresponding anti-particles, against an energy investment $(2A) \times 0.94$ GeV, it is likely that the least mass excess occurs for $(3A + 2)$ quarks with rather high A, and that such systems may grow spontaneously in vacuum until an optimized Z is reached. Another aspect is that such systems may surround themselves with x quarks and x anti-quarks provided by vacuum, or a cloud of x mesons, if one prefers. This is particularly true for $(3A+1)$ quarks tending to become $(3A + 3)$ nuclei bound to 2 anti-quarks. It is important to realize that the chemical properties of such systems are almost exclusively determined by the fractional charge, $(Z + \frac{1}{3})$ or $(Z + \frac{2}{3})$, the former value being achieved in any case of $(3A + 2)$ quarks and no anti-quarks. Any system with an overall negative Z in the presence of normal matter is expected to zoom down on the first positive nucleus encountered (likely to be ^{1}H or ^{4}He in Cosmos) and stay there, like a negative muon would do, if it were not radioactive.

Besides these general considerations on Z values of unsaturated quarks, there has recently been much discussion about matter containing a comparable amount of u-,

d- and *s*-quarks, which might also be the most appealing opportunity to find unsaturated quarks. Quite early, there were suggestions of nuclear matter of a density twice or thrice that of usual nuclei (Lee 1975) being metastable, or (what is a scary thought) more stable, but not particularly contagious. In spite of the *s*-quark adding about 0.25 amu to 'hyperons' replacing *d*- or *u*-quarks, the kinetic energy related to Pauli's exclusion principle makes it favorable to use three quark types ('flavors') at high density. It is not certain that the Λ dimerizes to neutral $u^2 d^2 s^2$, but it is likely that large A values would be as stable, or even more stable (Witten 1984, DeRújula and Glashow 1984, Farhi and Jaffe 1984) but protected by a small positive charge Z against contact with adjacent nuclei. This is not the argument of an ostrich; protons in solutions do not blow up the laboratory, in spite of their enormous affinity to nuclei with A above 6. The neutron-stars (best known as 'pulsars') with A close to 10^{57} are likely rather to consist of such almost neutral *uds*-matter, but we have very little idea of 'nuclearites' of macroscopic weight, but minute size (10^{15} g having a diameter 1 cm). It is clear that collisions with such objects are unpleasant (and hardly have occurred to the Earth since its crust solidified) but it is not excluded that a few elephant-weight 10^{10} g objects sometimes run through the planet. With a typical speed of 30 km/s, they are not easily braked. Anyhow, for our purpose, moderate nuclearites with A in the 10^4–10^{10} range may be much more tolerant to contain a number of quarks not divisible by 3. If they 'contain' $(A + \delta - \varepsilon)$ *u*-quarks, $(A + \varepsilon)$ *d*-quarks and $(A - \delta - 1)$ *s*-quarks, Z has the moderate value $(\delta - \varepsilon + \frac{1}{3})$. This Z value not only discourages contacts with other nuclei, it also prevents the system from falling down to the center of the Earth, if its mass is below some 10^{16} amu or 10^{-8} g. This can be qualitatively seen by comparison of electrical conductivities of K^+ and Cl^- in aqueous solution, where a gradient 10^{-9} V/cm (corresponding to the gravitational gradient $M \times 10^{-9}$ eV/cm for a species of M amu at the Earth's surface) transports the ion with a velocity a few times 10^{-13} cm/s. If the loosest bound electron is lost by staying 10^{-7} cm behind the atomic core, we can gain 10 eV (for the electron being ionized) by moving a mass $M = 10^{17}$ downward by 10 Å, but masses well below 10^{15} amu should not be auto-ionizing. Below 10^{10} amu, they should remain suspended in solution for quite some time. Species with an atomic-size electron cloud should concentrate in the oceanic sediments for quite a large range of M values. The situation is entirely different for neutral nuclear-sized M above 10^7 behaving like a rapid neutron, dropping some 20 cm between each collision (every 0.2 s) with an average vertical velocity of 10 m/s to be compared with the Brownian motion $v = 2700\, M^{-1/2}$ m/s being 1 cm/s for $M = 8 \times 10^8$. Such species are 1000 km below ground level after two weeks.

Madsen et al. (1986) give good reasons to expect nuclearites with A much below 10^{50} (which had sometimes been considered a critical limit for early evaporation) may have survived the first millisecond after the Big Bang. Alcock et al. (1986) suggest that an intense γ-ray pulse from a definite star (with period of rotation of 8 s) might be due to a 10^{21} g (1 m^3) chunk of *uds*-matter falling down on a star also consisting of this dense material. Since several million such chunks may be orbiting the *uds*-star, fragmentation by collisions may expel much smaller splinters adding to the stock of interstellar matter.

Before nuclearites came into the limelight, in early 1984, there were other plausible species X^- with high atomic weights, such as technicolor hadrons and weakly interacting massive particles (WIMP). For all practical purposes, the Z nucleus attached to such a X^- behaves as a superheavy isotope of the preceding element $(Z-1)$ (Cahn and Glashow 1981, Jørgensen 1981c). Under equal circumstances, it should be easier to find exotic adducts XZ, when Z has a high, and $(Z-1)$ as a low abundance. Thus, the apparent boron XC, scandium XTi, technetium XRu, promethium XSm, actinium XTh and protactinium XU isotopes might constitute detectable traces in the minor amounts of the conventional elements occurring. It may be noted (Kuroda 1982) that many uranium minerals contain up to 10^{-12} technetium, 10^{-17} promethium, and 10^{-11} plutonium (as ^{239}Pu) originating in spontaneous and neutron-induced fission, and subsequent neutron capture in uranium. Interestingly enough, 10^{-18} of ^{244}Pu (with a half-life of 83 million years) has been found (Hoffman et al. 1971) in the cerium mineral bastnäsite. Since 60 half-lifes, bringing the primordial concentration down by a factor 10^{-18}, is 5000 million years, this is again a striking argument for incorporation of very heavy elements in the Solar system within a narrow interval of time around 4700 million years ago. ^{244}Pu plays an important role for our understanding of the Early Solar system (Kuroda 1982, Rowe 1986) in particular via the heavier xenon isotopes being its fission product. For many reasons, it is a cheerful experience that several species have been detected down to levels in the 10^{-18} range.

Zweig (1978) pointed out that any geochemically available species with a charge $-\frac{4}{3}e$ would have great technological importance as catalysts for fusion of deuterium and/or tritium to helium, as recently investigated for muon-assisted fusion (Jones 1986). The exotic adducts XZ (Jørgensen 1981c, Cahn and Glashow 1981) may have assisted formation of heavy elements soon after the Big Bang, bypassing supernova explosions (and perhaps constituting the first elements with Z above 6 in population III stars). This precocious build-up is favored by the lithium isotope ^{8}BeX not being instantaneously α-radioactive like the bottle-neck ^{8}Be. Cahn and Glashow argue that the nuclear synthesis may proceed beyond ^{232}ThX, and that ^{244}PuX and ^{247}CmX may have α-half-lifes compatible with the geochemical time-scale.

Lackner and Zweig (1983) discussed the expected chemical properties of fractionally charged species, based on the idea of Mulliken electro-negativities. This description involves many problems (Jørgensen 1969) in particular as far as cations such as Na^+ and $N(CH_3)_4^+$ go. The writer (Jørgensen 1984b) developed an alternative discussion, again pointing out that the only important parameter for chemists is $(Z+\frac{1}{3})$ or $(Z+\frac{2}{3})$, in the following written as $Z.33$ or $Z.66$, for short, independently of whether there is a single nucleus or a negative and a (more) positive system orbiting at a very short average distance. The major chemical features of the 22 fractional charges from 0.33 to 10.66, and a few more typical examples, were predicted. For our purpose, an interesting excercise is the expected chemistry of fractionally charged species containing q electrons in the 4f shell. The results can be reliably obtained from the treatment discussed here in sections 3.5 and 3.6, and disagree entirely with a definite Mulliken electronegativity for each element. In the 'elements' 58.33 to 71.33, the standard oxidation potential E° of +2.33 aqua ions

should be 2.5 V higher than of R(II) aqua ions with the same q. Hence, the 2.33 aqua ions of $4f^7$ 63.33 should first be oxidized at $E^\circ \sim 2V$, but O_2 in alkaline solution might form $M(OH)_{3.33}$. The other 2.33 aqua ions have E° decreasing along the series $70.33 > 62.33 > 69.33$. On the other hand, all the other 4f group 2.33 aqua ions evolve H_2 forming 3.33 aqua ions (probably having a pK close to 4 like Al(III) aqua ions). 58.33 might be obtained in fluorite-type mixed oxides with $z = 4.33$, but is unlikely to form in solution. On the other hand, $z = 2.66$ should be relatively more invariant in $4f^2$ 58.66 to $4f^{14}$ 70.66. One expects it to be about as difficult to oxidize +2.66 aqua ions of 58.66 and $4f^8$ 64.66 as iron(II) aqua ions, but the +3.66 aqua ions are quite strong acids (pK close to 1) like uranium(IV). The formation of hydroxo complexes by 2.66 should be as weakly pronounced as that of magnesium(II), though 70.66 is marginally more acidic because of its smaller ionic radius. Since the chemistry of Y is so similar to Dy and Ho, it may be worthwhile to add that 38.33, 38.66 and 39.33 are expected to form closed-shell ions with $z = (Z - 36)$.

Fractionally charged 'nuclei' might have other origins, e.g., if some heavy quarks carry integral charge and can form a baryon with two common quarks. Such species are likely to be protected by a selection rule of the same kind as the 'baryon conservation rule' and may hence have very high mass without being short-lived. Like *uds*-nuclearites, the most likely range is 1000 to 10^5, from 1 to 100 TeV rest-mass in the notation of high-energy physicists.

It is one of the most prominent problems in nuclear physics to what extent a nucleus, characterized by the quantum numbers Z and N, allows percolation of quarks between constituent nucleons (Baym 1982, Comfort et al. 1985, Satz 1986). The description of a nucleus by the quark configuration $u^{2Z+N}d^{Z+2N}$ is quite comparable to a description of liquid or solidified noble gases by delocalized molecular orbitals, whereas an unsaturated system with a number of quarks not divisible by 3 is more like a 'free radical' with an observable density of uncompensated spin. At the moment, it can only be said that quarks in nuclei are less mobile than electrons, but that there is more contact between adjacent nucleons in a nucleus than there is between nuclei in a compound. If systems of unsaturated quarks have a high, but definite, rest-mass, the chemist has to give up the idea of roughly additive masses of 'constituents'. The ratio R between the binding energy and the rest-mass of the product is less than 10^{-9} for atoms in compounds and typically 0.008 for nucleons in nuclei, but must be well above 50 for quarks in a nucleon (Jørgensen 1982b). Even if the rest-mass of a strictly single quark diverges, the instantaneous pictures would involve a cluster of $(x + 1)$ quarks and x anti-quarks, probably with alternative, slightly differing x values. In this sense, quark hunters (Lackner and Zweig 1982) do not expect free quarks, but larger systems containing unsaturated quarks. Their geochemical fraction has been discussed (Jørgensen 1978d, 1981a, 1984b).

There is also at the moment vivid discussion about whether the Universe contains the proportion $\Omega = 0.02$ of stars etc., or a larger Ω, between 0.1 and 0.2, of non-radiant baryons (say, Jupiter masses without adjacent stars) or finally is exactly 1 or marginally above one. In the latter case, the Hubble expansion will reverse itself in

some 10^{11} years and allow a cyclic series of alternating Big Bang and 'Big Crunch'. However attractive the hypothesis of $\Omega = 1$ may be, it needs the introduction of 'dark matter' (Scherrer and Turner 1986, Fraser 1986, Turok 1986) to the extent of some 50 times the luminous materials in stars. Many candidates can be thought of, such as stable, weakly interacting particles (Scherrer and Turner 1986, Peebles 1986), black holes [this may seem to be living dangerously, but primordial black holes have Hawking-evaporated, if below 10^{15} g, and black holes in the 10^{20}–10^{40} g class do not produce frequent collisions (with an average density of 10^{-29} g/cm^3) though it can be argued that we do not observe all the high-energy photons expected from the collision with other matter]. Neutrinos seem now to be out, their rest-mass (if any) is now known to be below 10 eV (which make them inefficient as dark matter) as far as the electronic (β) generation goes. It is not absolutely excluded that neutrinos of the muonic (μ) or tauonic (τ) type, or of some, as yet undetected, generation, or for that matter, supersymmetric neutral fermions ('photinos') might have the appropriate rest-mass close to 40 eV. Nevertheless, the *uds*-nuclearites discussed above may actually be the better candidates for dark matter.

Before taking up, in sections 3, the relations between the Periodic Table and the atomic spectra of the rare earths, it may be worthwhile to cite a few, more classical reference works. Meyer (1905) made an excellent bibliography of R and thorium with 777 references. A unique source of informations is the Gmelin–Kraut (1928) handbook, giving explicit analysis of minerals and compounds, a good historical perspective, and a quite personalized treatment of literature up to 1928. Interesting books in English are the books of Spencer (1919) and of Levy (1924) followed by the book of Yost et al. (1947). The pre-Spedding techniques of separating R are treated carefully in these books, as well as in the review by Prandtl (1938) summarizing a life's experience. Though many other chapters in this, and other, volumes of the present Handbook treat metallic R, it may be added that Klemm and Bommer (1937) reported 13 metallic lanthanides (lacking $Z = 61$ and holmium) with special emphasis on the magnetic properties, and noting the high molar volume and other barium-like characteristics of europium and ytterbium. On the whole, there had not been a great effort on metallic R before 1950, because it had been argued (like Lavoisier did for the alkaline-earths) that it was evident that the oxides correspond to metallic elements, and it was not considered a requirement for discovering a lanthanide to have succeeded the difficult reduction to the metallic element.

2. The individualistic oxidation states differing from R(III)

Until recently, the majority of chemists considered R(III) to be, by far, the most frequent oxidation state, and almost entering the definition of R. This is less true today as the effort dedicated to solid-state chemistry is comparable to that devoted to solution chemistry. However, it is also true that acidic aqueous solutions with pH between -1 and 3, and having an oxidizing character between $E^\circ = 0$ and $+1$ V, using typical inorganic acids, exclusively allow detection of R(III) of all 17 R, and, actually, in less than 4 molar perchlorate or chloride, the aqua ions of yttrium and

the lanthanides (forming second-sphere ion-pairs without direct M–Cl contacts, and having no influence on the narrow absorption bands due to $4f^q$ J-levels for $q = 2$ to 13).

It was already shown by Berzelius and Hisinger that cerium readily forms a higher oxidation state at higher pH, and this tendency is the best publicized deviation from R(III), in part because of the use of cerium(IV) acidic solutions as oxidants and titrimetric reagents for potentiometry of reducing species. We have already mentioned that Eu(II) acquired importance for separating europium from other R, for instance precipitating $EuSO_4$ or keeping $Eu(OH)_2$ in alkaline solution (e.g., NH_3) (Yntema 1930, Yost et al. 1947) in analogy with the strontium compounds. Contrary to the d-groups and the 5f group, there are not identified many ligands particularly apt to increase or decrease the oxidation state commonly found in the aqua ions.

2.1. *Cerium(IV)*

As far as solid-state chemistry goes, the closed-shell cerium(IV) is not strikingly different from the slightly larger thorium(IV) or the somewhat smaller tin(IV), all three form the perovskite $BaMO_3$ with coordination number $N = 6$ for M(IV) and $N = 12$ for Ba(II). The octahedral $CeCl_6^{-2}$ is known both in the cubic crystal $[N(CH_3)_4]_2$ $CeCl_6$ and in acetonitrile solution (Ryan and Jørgensen 1966). The fluorite-type oxides CeO_2 and ThO_2 have cubical $N = 8$. On the other hand, the orange-red crystals $(NH_4)_2Ce(O_2NO)_6$ have $N = 12$ (icosahedron, whereas the cuboctahedron $N = 12$ occurs for Ba(II) in perovskites, and M in cubic close-packed metals). This variation between 6 and 12 is also typical for R(III) and very similar to thorium(IV).

As first pointed out by Goldschmidt, fluorite-type CeO_2 and ThO_2 have a great tendency to incorporate trivalent lanthanides Ln in $Ce_{1-x}Ln_x O_{2-0.5x}$ where x sometimes is larger than 0.5, corresponding to lower O/M ratio than in the pyrochlore $Er_2Ti_2O_7$ (Jørgensen 1979a). It is not known whether Ce(IV) or (the larger) Ln(III) has the greater tendency to accept $N = 7$ in these statistically disordered, defect crystals. The sub-stoichiometric CeO_{2-x} is dark blue for quite moderate x, to be compared with black Pr_6O_{11}, Pr_7O_{12} and dark-brown PrO_{2-x} (Eyring 1979). In alkaline suspension, the white precipitate $Ce(OH)_3$ oxidizes in air to a pale mauve $Ce(OH)_{3+x}$ because of Ce(III) → Ce(IV) electron transfer bands (Jørgensen 1970b) comparable to almost white $Fe(OH)_2$ oxidizing to very dark green $Fe(OH)_{2+x}$ before finishing as rusty $Fe(OH)_3$ of much less intense color. However, the intensity of the mixed-z coloration is much weaker in $Ce(OH)_{3+x}$ (presumably with longer Ce–Ce distances than in CeO_{2-x}).

It is not always realized that only five M(IV) aqua ions are known to occur in acidic solution, colorless thorium(IV) being the most reluctant to deprotonate, with a pK close to 4 like $Be(OH_2)_4^{+2}$ and $Al(OH_2)_6^{+3}$, whereas U(IV) and Pu(IV) aqua ions both have pK close to 1.5 (Kraus and Nelson 1950). Similar pK values are likely to occur for Np(IV) and Pa(IV) aqua ions. Vanadium(IV) forms the blue vanadyl ion without perceptible proton affinity in aqueous solution, which seems to

be $OV(OH_2)_4^{+2}$ (Zeltmann and Morgan 1971) though other vanadyl complexes have $N = 6$ such as neutral organic molecules bound *trans-* to oxygen in vanadyl bis (β-diketonates) or *cis*$[OV(OH_2)(C_2O_4)_2]^{-2}$. Though titanium(IV) seems to form a similar titanyl oxalate complex, it does not tell too much about the composition of titanium(IV) in strongly acidic solutions. The textbook ZrO^{+2} and BiO^+ are suspected of being $Zr_8(OH)_{16}^{+16}$ and $Bi_6(OH)_{12}^{+6}$ identified in crystal structures. The presence of 8 molecules of constitutional water per ZrO^{+2} cannot be detected by the classical methods of physical chemistry of aqueous solutions, and present the same problem as $Al_{13}(OH)_{32}^{+7}$ identified in Stockholm as a major deprotonation product of aluminum(III) aqua ions, which is likely to be $AlO_4Al_{12}(OH)_{24}(OH_2)_{12}^{+7}$ known from a crystal. The situation seems rather foggy for cerium(IV) in perchloric acid. Sherrill et al. (1943) determined two species, $CeOH^+$ deprotonating with pK = 0.2 to $Ce(OH)_2^{+2}$. In 0.6 molar H_3O^+ ClO_4^-, in which equal amounts of the two hydroxo complexes are present, $E°$ for cerium (III) aqua ions is +1.72 V. This study suggested that Ce_{aq}^{+4} is not a predominant species at any pH above −1 [this opinion is checked by the number of solvated protons consumed by oxidation of Ce(III)]. Sulfate in one molar sulfuric acid decreases $E°$ to +1.44 V, indicating an effective $K \sim 10^5$ for the strong sulfate complex (relative to about 20 for $CeSO_4^+$). However, Heidt and Smith (1948) provided arguments for dimers like $HOCeOCeOH^{+4}$ and $CeOCeOH^{+5}$ (which again may have the oxo bridge replaced by two OH^- groups).

The situation may be far more complicated. When 0.01 molar solutions of crystalline $(NH_4)_2Ce(NO_3)_6$ are prepared in 1–3 molar perchloric acid, they are originally yellow, but go less limpid with time. After a few hours, they look very much like orange juice. It is not unusual to see such a time evolution in iron(III) and chromium(III) solutions with a pH at 2 or 3, and, on the other hand, yellow rhodium(III) hydroxide is soluble in one equivalent of H_3O^+, forming an unknown polymer of $Rh(OH)_2(OH_2)_x^+$.

It may be worthwhile to compare these observations with the review by Wyrouboff and Verneuil (1906). These authors defended the idea that the common oxidation state of the lanthanides is M(II) (even for thorium, ascribed $A = 116$) and that the A of cerium equals 93 rather than 140 (implicitly assuming that the specific heat of metallic cerium is as bad an exception from the law of Dulong and Petit as metallic beryllium is, insinuating $A = 13$) and the higher oxidation state 2.666. what is not entirely ludicrous, when comparing with Fe_3O_4 and Pb_3O_4 containing Fe(II), Fe(III), Pb(II) and Pb(IV). Anyhow, the important point for us is the meta-oxide salts $Ce_8O_5(OH)_{20}X_2$ transcribed to our Ce(IV), where X can be chloride, nitrate or half a sulfate. An amber-yellow, translucent meta-oxide (dehydrated over KOH) is described as X = OH with composition $CeO_{0.625}(OH)_{2.75}$. The para-oxide salts are similar solids $Ce_{40}O_{69}(OH)_{18}X_4$ with one anion X per ten Ce(IV). At first glance, this reminds one of the micro-analysis of a portion of ham and eggs, but it is true that the dark-green hydrolysis products formed slowly from the tan-brown plutonium(IV) aqua ion (Kraus and Nelson 1950) are surprisingly similar to the monstrous salts of Wyrouboff.

It is not a sufficient reason for the complicated deprotonation of cerium(IV) and plutonium(IV) in solution to say that Ce(IV) is larger than Zr(IV) and Hf(IV), but

smaller than Th(IV). When asking for the criteria for aqua ions deprotonating to hydroxide complexes, and then, eventually to oxo complexes (Jørgensen 1963c, 1979a, 1983b, Jørgensen and Reisfeld 1982a) it is enhanced by increasing the pH from -1 to 15, by increasing the oxidation state z, and by decreasing the ionic radius. This is an excellent description for R(III) aqua ions. As a matter of fact, the intercalation of yttrium between dysprosium and holmium, as far as most chemical and crystallographic properties go (cf. section 4.3) is a corollary of this idea. However, among R(III), the oxidizing character of Eu is not much more pronounced than that of Gd, whereas we know from the d-groups clear-cut cases of strongly oxidizing aqua ions being more acidic than expected from their size. Thus, iron(III) is more acidic than aluminum(III); copper(II) more than the adjacent nickel(II) and zinc(II); palladium(II) and mercury(II) much more than the far smaller beryllium(II); or thallium(III) compared with aluminum(III); and the most extreme case of all, the acidity of both ammonia and aqua ligands bound to gold(III). It seems very likely that the strongly oxidizing character of cerium(IV) in solution enhances acidity in the same way.

Since about 40% of R in minerals of the lighter lanthanides (large ionic radii) is cerium, it early attracted interest to remove the large majority of cerium in a simple process. Bromate oxidizes Ce(III) to a precipitate in solutions buffered by the reactive, but only slightly soluble base calcium carbonate. Ethers can extract an orange cerium(IV) complex from nitric acid. Concentrates with minor amounts of other R can be recrystallized as $(NH_4)_2Ce(NO_3)_6$.

In solid oxides, the problem is rather the opposite of aqueous chemistry, it is very difficult to insure full reduction to Ce(III). Dark blue CeO_{2-x} needs quite drastic reducing conditions to form mustard-yellow Ce_2O_3. We now turn to this problem for the other R(IV).

2.2. *Praseodymium(IV), neodymium(IV), terbium(IV) and dysprosium(IV)*

The strong colors imparted to mixed oxides by didymia are due to Pr(IV) having strong electron transfer bands (Jørgensen 1970b). In one way, it is surprising how much the color differs in various types of oxides, and also how similar it is to the color provided by terbium(IV) in the same kind of oxide. Thus, C-type Y_2O_3 is colored orange by small amounts, and the fluorite CeO_2 is chamois brownish. Bjørn-Andersen (1933) found that less than 0.04% of Pr can be detected by the brownish-red tint, whereas pure CeO_2 is pale lemon-yellow (and not white, as stated by Wyrouboff and Verneuil (1906), saying it only went yellow when heated, as is true for ZnO). The situation is also striking in fluorite ThO_2 going purple with less than 0.1% Pr(IV) or Tb(IV). It can be seen from the lattice constants that the grey samples of disordered fluorite-type $Zr_{1-y}M_yO_{2-x}$ contain more M(III) than M(IV), whereas ThO_2 is likely to ensure complete conversion to M(IV) (Jørgensen and Rittershaus 1967). Hoefdraad (1975) studied the reflection spectra of Pr(IV) and Tb(IV) in many oxides of differing colors. Octahedral $N = 6$ structures in the perovskites $SrZrO_3$, $BaZrO_3$, $BaCeO_3$, $BaHfO_3$ and $BaThO_3$ are colored bright yellow by M(IV). The same coordination and same color is observed in K_2NiF_4-

type Sr_2ZrO_4, and Ba_2ZrO_4 ($N = 8$) gives orange to violet colors in (wave-number of the first absorption band is given in parentheses) zircon $ZrSiO_4$ (22 700), scheelite-type $ZrGeO_4$ (21 800), fluorite-type ThO_2 (19 000) and zircon-type $ThGeO_4$ (18 400). The variation of the first electron transfer band by more than 6000 cm^{-1} is surprising, when compared to complexes of d-groups with the four halides (Jørgensen 1969, 1970b) though it may be added that Eu(III), Yb(III), Sm(III) and Tm(III) (mentioned in order of increasing wave-number of the first electron transfer band) look 5200 to 6700 cm^{-1} more oxidizing in octahedral $LnBr_6^{-3}$ (Ryan and Jørgensen 1966) than in MBr^{+2} solvated by ethanol (Jørgensen 1962a). When comparing MI_6^{-3} (Ryan 1969) with other bromide and chloride complexes, iodide looks particularly reducing, possibly due to a non-bonding MO with four angular node-planes becoming I–I anti-bonding for short I–I contacts (Jørgensen 1971). Nevertheless, there remains the problem that the optical electronegativity (derived from electron transfer spectra) is not nearly as invariant for the oxide as for each of the four halides. This problem takes dramatic proportions in tetrahedral complexes of the chromate, molybdate and tungstate type (Müller et al. 1973) and in uranyl cations (Jørgensen and Reisfeld 1982b). The strong variation of the reducing character of oxide may be rationalized by the highly varying Madelung potential (Jørgensen 1969, Duffy 1977) where the gaseous O^{-2} spontaneously loses an electron, but is nearly as stabilized as fluoride with small cations of high z, such as Al_2O_3 and ZrO_2, as also seen from the electric polarizabities derived from the refractive index (Salzmann and Jørgensen 1968, Jørgensen 1975a). The chemical reducing character of oxide anions can be evaluated from oxides not being prepared of the large cations of $N(CH_3)_4^+$ type, and that (excluding humidity) Cs_2O is readily oxidized by O_2 to the orange superoxide $Cs^+O_2^-$, and BaO at moderate heating to the peroxide BaO_2. Complexes of ligands formed by two oxygen atoms are reviewed by Gubelmann and Williams (1983). It may be argued that the yellow perovskites containing Pr(IV) and Tb(IV) studied by Hoefdraad (1975) have the oxide ligands (bound co-linearly to two M(IV), with four M(II) on the two other Cartesian axes) strongly stabilized by the Madelung potential, which is less true for $ThGeO_4$ and ThO_2. Blasse (1976) pointed out that the first electron transfer band of europium(III) invariantly occurs (within 1000 cm^{-1}) at 42 000 cm^{-1} in mixed oxides having $N = 6$ for Eu(III), whereas the wave-numbers are spread between 36 000 and 48 000 cm^{-1} for $N = 8$ and from 30 500 to 40 500 cm^{-1} for $N = 12$. There is little doubt that the effect is partly connected with the longer internuclear distances concomitant with higher N.

Since oxidation states difficult to study in aqueous solutions, such as manganese(IV) and nickel(IV), form heteropoly-anions with molybdenum and tungsten (Pope 1983) one may hope that Pr(IV) might occur in solution in such complexes. The cerium(III) complex $CeW_{10}O_{36}^{-9}$ has $E^o = 1.1$ V, showing that cerium(IV) is more stabilized in this environment than by sulfate, but still not to any extreme extent. Actually, $Pr(PW_{11}O_{39})_2^{-10}$ is known. We return below to the related question of Tb(IV) in solution.

In most elements, F_2 is at least as effective as O_2 to provide high oxidation states z. However, there are exceptions (Jørgensen 1986a) where the corresponding fluoride

is not known, or much less stable than the oxo complexes, e.g. for Cr(VI), Mn(VII), Fe(VI), Ru(VIII), Xe(VIII), Os(VIII) and Np(VII). Praseodymium does not go so far, colorless double fluorides with alkali-metals $APrF_5$ and A_2PrF_6 and syncrystallized $Ce_{1-x}Pr_xF_4$ are indeed known.

At present, neodymium(IV) is best known in orange Cs_3NdF_7 of which Varga and Asprey (1968b) measured the J-levels of $4f^2$ in the visible, and the first broad electron transfer band at 26 000 cm^{-1} (Jørgensen 1967b).

Brauer and Kristen (1979) prepared the cubic perovskite $BaCe_{0.7}Nd_{0.3}O_3$ but could not get beyond $x = 0.18$ in $BaPr_{1-x}Nd_xO_3$ and $BaTh_{1-x}Nd_xO_3$ and not beyond $x = 0.04$ in $BaZr_{1-x}Nd_xO_3$. For comparison, it may be noted that $SrTiO_3$ can incorporate both iron(IV) and iron(V) (Blazey et al. 1983).

The close similarities between Pr(IV) and terbium(IV) in mixed oxides were already mentioned. In solutions of $SiW_{11}O_{39}^{-8}$ and $BW_{11}O_{39}^{-9}$, Saprykin, Spitsyn and Krot (cf. Pope 1983) found in 1976 that the unusual oxidation state americium(IV) could be obtained by oxidizing Am(III) with peroxodisulfate $O_3SOOSO_3^{-2}$ to $Am(SiW_{11}O_{39})_2^{-12}$ and $Am(BW_{11}O_{39})_2^{-14}$. Only in a narrow pH interval close to 7 was it possible to obtain a 30–50% yield of the terbium(IV) complexes of analogous composition.

Colorless TbF_4, K_2TbF_6 and Cs_3TbF_7 have been described. The best characterized dysprosium(IV) compound is Cs_3DyF_7 of which Varga and Asprey (1968a) measured the $4f^8$ narrow absorption bands, and the strong, broad electron transfer band at 25 000 cm^{-1}. Brauer and Kristen (1980) could not introduce Dy(IV) in the yellow $BaTbO_3$ and $SrTbO_3$ but detected 6 to 4 percent Dy(IV) in $BaCeO_3$ having from 10 to 50 percent of the cerium replaced by dysprosium. The remainder of Dy in these grey samples was in the form of another [Dy(III)] compound $Ba_3Dy_4O_9$.

It is not absolutely excluded that one might find a new ligand stabilizing Ln(IV). As is discussed in section 3.7, the chances are not as high as in the d-groups, where dithiocarbamates, such as $(C_2H_5)_2NCS_2^-$ (in spite of their reducing character and ability to dimerize to S–S bonded species after loss of an electron) are known to coexist with iron(IV), nickel(IV) and copper(III) (Willemse et al. 1976), the same oxidation states as known to form complexes with a bidentate phosphine (Warren and Bennett 1974). This tendency takes extreme proportions in iridium(V) of which the two best known complexes are IrF_6^- and IrL_2H_5 containing triphenylphosphine L, also forming the iridium(III) complex IrL_3H_3 and Vaska's complex of iridium(I) $IrL_2(CO)Cl$.

However, as pointed out (Ryan and Jørgensen 1966) in connection with deep purple $CeBr_6^{-2}$ existing for a short while in acetonitrile, it is absolutely excluded that any new Ln(IV) complexes are colorless. Thus, a colorless Eu(IV) reported in zeolites on the basis of internuclear distances is difficult to believe (Jørgensen 1978b). Spitsyn et al. (1985) have reported the mixture of comparable amounts of Cs_3TmF_6 and Cs_3TmF_7 on the basis of infrared spectra. It would be very interesting to know whether the latter component produced the dark blue or violet color expected from the agreement of electron transfer spectra with the refined spin-pairing energy theory (Jørgensen 1962a, 1979a, Nugent et al. 1973).

The regularities of photo-electron spectra discussed in section 3.6 makes it most

certain that any Ln(V), even the most plausible Pr(V) and Dy(V), cannot occur. The electron affinity of the 4f shell is so great that such species are expected to oxidize not only fluoride, but also argon and cesium(I) (Jørgensen 1986a). Prandtl had argued that Pr(V) might be formed in yttrium oxide, but Marsh (1946) showed that one can only get Pr(IV) in $Y_{2-x}Pr_xO_{3+0.5x}$. The tiny science-fiction opportunity for Pr(V) would be a species similar to the neptunyl complex NpO_2^+.

2.3. *Europium(II)*

The first decreased oxidation state of a rare earth was samarium(II) in 1906 followed by Eu(II) in white $EuCl_2$ obtained by Urbain and Bourion (1911). Jantsch et al. (1929) and Yntema (1930) realized the barium-like features, and precipitated white $EuSO_4$. On the whole, Eu(II) bound to oxygen is pale yellow, such as $EuCO_3$ and $EuSiO_3$, but the NaCl-type EuO is dark red, ferromagnetic below 69 K [and this Curie temperature can be increased by doping with La, Gd or Ho (Wachter, 1979)]. This compound was the second known ferromagnetic non-metallic material, the first being anhydrous $CrBr_3$ below 37 K. Besides slightly doped EuO, there exists a $CaFe_2O_4$-type Eu_3O_4 of which the black color is ascribed to electron transfer from Eu(II) to Eu(III) (Allen et al. 1973). This electron transfer between two distinct z of the same element is not essentially different from the black color of the perovskite $EuTiO_3$ with Eu(II) and Ti(IV) in the groundstate, but Eu(III) and Ti(III) in the excited state.

The luminescence of europium(II) is usually a broad band in the blue and violet, corresponding to a large Stokes shift from the absorption band in the ultraviolet due to the excited configuration $[54]4f^65d$. Such luminescence has been studied in a large number of crystals, in vitreous materials (Reisfeld and Jørgensen 1987) and in the cryptand complexes, e.g. of multidentate poly-ethers (Sabbatini et al. 1982, 1984, Adachi et al. 1983). If the Stokes threshold has sufficiently high energy, narrow-band emission may occur from the first excited J-level $^6P_{7/2}$ of $[54]4f^7$ close to 27 800 cm^{-1}, only marginally below 28 200 cm^{-1} in gaseous Eu^{+2} [$SrAlF_5$ and $BaAlF_5$ studied by Hoffman (1972); perovskite $BaLiF_3$ by Fouassier et al. (1977); and KY_3F_{10} by Joubert et al. (1981)]. There is a strong tendency toward $4f^7$ line emission for the high $N = 12$, going with exceptionally long internuclear distances Eu–F.

$EuLiH_3$ is a cubic perovskite (Messer and Levy 1965) with $N = 12$ for Eu(III) and $N = 6$ for both Li(I) and H(−I) having the cubic lattice parameter $a_0 = 3.796$ Å to be compared with 4.023 Å in $BaLiH_3$ and 3.833 Å in $SrLiH_3$. In these cases, as well as the NaCl-type LiH ($a_0 = 4.09$ Å) and LiD (4.065 Å) the Li–H internuclear distance is half the a_0, showing that the LiH bond shortens by 7%, going from LiH to $EuLiH_3$.

Metallic europium is soluble in liquid ammonia with the usual blue color due to a solvated electron in a cavity. It has the broad Eu(II) absorption band in the near ultraviolet. Evaporations of such M(II) 'phlogistonide' solutions allow crystallization of the bronze-colored metals $M(NH_3)_6$ for M = Ca, Sr, Ba, Eu and Yb, as well as $Li(NH_3)_4$ (Dye 1984).

2.4. *Ytterbium(II)*

Klemm and Schüth (1929) reduced anhydrous $YbCl_3$ in H_2 to almost colorless $YbCl_2$. The compound was shown to be diamagnetic, showing the closed-shell structure. It is not certain whether a pale green color of this, and other reduced ytterbium salts, is due to Yb_6Cl_{13} containing one Yb(III) per five Yb(II) (Haschke 1979). Ball and Yntema (1930) prepared white, insoluble $YbSO_4$ serving to separate Yb from the neighbor elements Er, Tm and Lu (Yost et al. 1947).

Today, E° is known for Eu(II) aqua ions, -0.35 V, and for Yb(II) aqua ions, -1.15 V. No feasible pressure of H_2 is able to render these species thermodynamically stable toward evolution of hydrogen, but fortunately, the kinetics can be quite slow, in particular for Eu(II) solutions kept in the dark. Butement (1948) was able to photograph the absorption spectra of such solutions, finding the first strong $4f \rightarrow 5d$ band at 31 200 cm^{-1} of Eu(II), 28 400 cm^{-1} of Yb(II) and at 17 900 cm^{-1} of the red, much stronger reducing samarium(II) aqua ion. Again there is some ambiguity as to whether ytterbium(II) aqua ions are colorless, or weakly greenish yellow.

A long series of crystalline sulfides containing Eu(II), Eu(III), Yb(II) and Yb(III) were prepared and reviewed by Flahaut (1979).

2.5. *The other R(II)*

The major condition for studying the more reducing R(II) is to have a surrounding material very difficult to reduce. One of the most suitable is CaF_2 [of which the mineral frequently is colored by Sm(II) and Eu(II) and fluorescent (Przibram 1937)] and the fluorite-type SrF_2 and BaF_2. We have in Sm(II) a situation of crossing of $[54]4f^6$ and the lowest $[54]4f^55d$ state, analogous to Eu(II) discussed above in section 2.3, for luminescence. The level $^5D_0$ of $4f^6$ is situated at 14 620 cm^{-1} in SrF_2, 14 450 in $LaCl_3$ and 14 440 cm^{-1} in $LaBr_3$, moving considerably more than $^5D_0$ of the iso-electronic Eu(III) (Reisfeld and Jørgensen 1977, Durville et al. 1983). In the three crystals mentioned, the Stokes threshold of the first broad transition to $[54]4f^55d$ is above $^5D_0$ level, whereas it is below this level (14 370 cm^{-1}) in CaF_2 with important consequences for the luminescence.

Loh (1966) found the $4f \rightarrow 5d$ transition in all M(III) from Ce to Lu (except M = Pm) in very low concentration in CaF_2, being transparent beyond 80 000 cm^{-1} (or 10 eV, or 125 nm) and found excellent agreement with the refined spin-pairing energy treatment, as discussed in sections 3.3 and 3.5. McClure and Kiss (1963) had previously obtained comparable results for M(II) from La(II) to Yb(II) in CaF_2 (again excepting M = Pm). However, there are various problems for M = La, Ce, Gd and Tb. Apparently, lanthanum is a system with one 5d electron (as corroborated by gaseous La^{+2} with this groundstate followed by 4f at 7195 cm^{-1} higher energy) and McClure and Kiss (1963) argued that cerium(II) in fluorite has 4f5d ground configuration, whereas gaseous Ce^{+2} has the first J-level of [54]4f5d situated at 3277 cm^{-1} above the ground state belonging to $[54]4f^2$. It should not be ignored that even the crystals which are the most difficult to reduce may contain F (Farb-zentren) color centers, as first known from 'blue rock-salt'

adjacent to radioactive minerals, and then systematically studied in alkali halides by Pohl and two following generations of solid-state physicists. The simplest F center has an electron occupying a vacant halide site, e^- replacing X^- and producing an excited state with additional node-plane for the electron. Drotning and Drickamer (1973) suggest that Tb(III) is in close contact with such a F center.

When it is realized that eleven gaseous lanthanide atoms really are 'barides' by having their groundstate belonging to the configuration $[54]4f^q6s^2$ with $q = (Z - 56)$, and not like lanthanum, cerium, gadolinium and lutetium atoms to $[54]4f^q5d6s^2$ with $q = (Z - 57)$, it is not too surprising that at least nine Ln(II) have no problems being recognized in fluorite crystals, i.e. Ln = Pr, Nd, Sm, Eu, Dy, Ho, Er, Tm and Yb, by electron-spin resonance, narrow-band $4f^q$ excited states showing $q = (Z - 56)$ and other physical properties (we are agnostic about Pm). The number of Ln(II) in undiluted stoichiometric compounds includes Nd(II) in dark-green $NdCl_2$ and deep purple NdI_2, a large number of Sm(II) and Eu(II) anhydrous compounds, crystalline TmX_2 for X = Cl, Br, I and a few Yb(II) compounds. Doubtful cases involve Dy(II) in black materials, whereas the LnI_2 simply are metallic for Ln = La, Ce, Pr and Gd, like all NaCl-type RS are with exception of Sm, Eu and Yb. This escape into the metallic state of stoichiometric compounds with apparent unusually low z occurs frequently also outside the rare earths, ThI_2 and ThS are both metallic. It may be added that only Sm(II), Yb(II) and Eu(II) aqua ions have E° above -2 V. In section 3.5 we return to the rationalization of these facts.

Recently, spectroscopic studies have permitted elucidation of the mechanism of incipient metallicity of small amounts of Ln(II) in fluorites. Pedrini et al. (1985) showed that $Eu_xCa_{1-x}F_2$ photo-conducts at wave-numbers some 4000 cm^{-1} higher than the first absorption band due to one 4f electron jumping up to the two approximately non-bonding 5d orbitals, but at an energy 12 000 cm^{-1} below the next strong absorption band due to a 4f electron being excited to the three equally strongly anti-bonding 5d-like orbitals. This anti-Franck–Condon behavior reminds one of the iodides of alkali metals photoconducting at a threshold after the first strong absorption band, which can be described (Jørgensen 1975b) approximately as $5p^6 \rightarrow 5p^56s$ like the first transitions in a xenon atom. McClure and Pedrini (1985) have compared the photo-ionization of various Ln(II) in CaF_2, SrF_2 and BaF_2. Kobayasi et al. (1980) carefully studied the Eu(II) luminescence in various calcium, strontium and barium fluorides and chlorides, and pointed out that laser activity is impeded by strong absorption belonging to the excited state. Sardar et al. (1982) found that the perovskite $RbMgF_3$ containing traces of Eu(II) emitted both sharp $4f^7$ lines at 360 nm (as one would expect for a fluoride having $N = 12$ at the rubidium site) and the broad band from $4f^65d$. When irradiated at room temperature with about 10^{16} electrons/cm^3 of kinetic energy 1.5 MeV, a new emission at 680 nm occurred, having a structured excitation spectrum between 450 and 550 nm. Recall that the fluorescence of fluorite shows many color centers (Przibram 1937) in X-ray irradiated samples.

Red-brown, highly reactive, anhydrous samarium(II) chloride was prepared by Matignon and Cazes (1906) by heating $SmCl_3$ in H_2. No solvent was found, in

which $SmCl_2$ could be dissolved without hydrogen evolution, forming yellow Sm(III). One of the major arguments calming down the motivation for trying to make Ln(II) was that no ligands were identified, stabilizing the lower z, as is well-known from 2, 2'-dipyridyl, phenanthroline, ..., stabilizing iron(II), çopper(I) and ruthenium(II), or, to a much more extreme extent, CO, isonitriles like CH_3NC, and PF_3 stabilizing zero and negative z values for many d-group elements (Jørgensen 1969). Actually, most ligands compatible with aqueous solutions, such as biological and synthetic aminopolycarboxylates, form somewhat stronger complexes with Eu(III) than with Eu(II) resulting in E° decreasing from -0.35 V for the aqua ions in direction of -1 V.

A rather fancy area of chemistry is the condensation of d-group atoms (from heated metal) transported in a great excess of argon and forming solid argon on a surface kept at 4 K by liquid helium (Ozin and Van der Voet 1973). Slater et al. (1971) condensed uranium atoms evaporated at 1950 K with 1 CO:300 Ar and measured infrared spectra of $U(CO)_6$ and all the five lower n in supposed $U(CO)_n$. These species decompose above 30 K. Slater et al. (1973) continued this study with neodymium and ytterbium, and found again evidence for all n up to six: $Nd(CO)_6$ with strong back-bonding, but inconclusive results for Yb. It still remains to obtain electronic spectra, or spin resonance, of such species. Whereas $W(CO)_6$ is a straightforward $5d^6$ system, the truth must be much more complicated for carbonyls of neodymium, as is further discussed in section 3.7. Quite unexpected species, such as green $Ti(CO)_6$ and orange $Ti(N_2)_6$ (Busby et al. 1977), $V(N_2)_6$ (Huber et al. 1976) and yellow $Cr(N_2)_n$ with n from 1 to 6 (de Vore 1976) have been characterized in cool matrices.

As a fascinating contrast may be mentioned the reaction of CO with metallic Ce, Sm, Eu, Gd, Tm and Yb kept at 800°C forming a NaCl-type Ln_2CO (Darnell 1978). With the exception of Eu and Yb providing unusually large a_0, these crystals seem to contain C(−IV) and O(−II) on the anion sites. As reviewed by Eyring (1979) most of the so-called RO were either crystallographically highly defective (like TiO) or contained quite substantial amounts of hydride, nitride or carbide. Leger et al. (1980) continue such work, and argue that they were able to prepare NaCl-type NdO and SmO under high pressures. The a_0 values 4.994 Å and 4.943 Å for these two materials are interpreted as metallic character, as in NdS. On the other hand, $a_0 = 4.877$ Å for YbO existing at 40 kbar rather suggests a non-metallic ytterbium(II) oxide.

In the following, more interest is concentrated on comparative treatment across the whole lanthanide series.

3. Spectroscopy and the Periodic Table

At the end of last century. the most urgent question to answer about the Periodic Table was how many lanthanides there are. An interesting attempt to answer this question was made by Julius Thomsen (1895a) describing a set of vertical series containing 1, 7, 7, 17, 17 and 31 elements, each series starting with an alkali-metal

and ending with a halogen. The relations between the second 7-series and the first 17-series admitted a 'double allegiance', all the elements Na to Cl being connected by diagonal lines both to the element with the same Mendeleev column number. K to Mn, and Cu to Br. The only connection between one 17- and two members of the 31-series was between zirconium with cerium on one hand, and the unknown element just before tantalum on the other. Julius Thomsen allotted the same number, 14, of places to the elements including lanthanum to ytterbium (and two empty places between Yb and Ta) as we do, but mentioned only 10 lanthanides, and not all the atomic weights in the order accepted today. It was speculated that the series $1 + 2 \times 3 + 2 \times 5 + 2 \times 7$ involving the three first odd prime numbers may produce the numbers 1, 7, 17 and 31 by being broken off.

Having heard about argon (discovered 1894), Thomsen (1895b) wrote a second paper about a conceivable group of chemically inert elements with $A = 4, 20, 36, 84, 132, 212$ and 292 without mentioning helium explicitly. This element has an emission line close to the two Fraunhofer lines of sodium. This line was detected first during a solar eclipse in the outermost layers of the surface, by Janssen on August 18, 1868, and afterwards by Lockyer, who was observing the solar edge in October 1868, naming the element helium. In view of the simple line spectrum, it was considered likely to be a metallic element, and it was a great surprise when Ramsay (1895a) found that a gas extracted from uranium minerals gives this emission spectrum. This observation was presented to the Royal Society in London on April 25, 1895, and it is not too likely that Thomsen knew of it, though a telegram from Ramsay had been read in the Academy of Sciences in Paris March 25 (Ramsay 1895b) and the second paper by Thomsen arrived at the Editor on May 1, 1895. When the other noble gases (having complicated line spectra, rather similar to argon) neon, krypton and xenon were discovered in the atmosphere by Ramsay and Travers in 1898, no doubt was left that the vertical series of Thomsen had 2, 8, 18 and 32 elements. Niels Bohr published the vertical version (with two sets of inner boxes) repeatedly, beginning 1922, and because of the novel theoretical background, it became known as the Thomsen–Bohr Periodic Table. There is a recent trend (Fernelius 1986) to make rectangular versions with 18 columns, and though this is certainly better than 8, it may seem a little tough to put 15 'meta-elements' on the position of lanthanum, and even much more so to let Ac, Th, Pa, U, Np, ..., share the same bed. The next attempt to find 'platonic' regularities in the Periodic Table was done by Rydberg in 1906, suggesting each series to contain twice the square numbers, 2, 8, 18, 32, 50, ..., of elements. This proposal had not a particularly good press for two reasons. First of all, Rydberg did not state clearly that, in his table, cesium to radon is 32 elements, with the corollary of 15 lanthanides, before in a Swedish journal in 1913 (cf. Rydberg 1914) a few months before Moseley derived Z-values from X-ray spectra; and secondly, Rydberg insisted that each double square number occurred exactly twice, providing $Z = 5$ for lithium, and $(Z + 2)$ for all the subsequent elements. $Z = 2$ was allotted to a hypothetical element nebulium, of which spectral lines are seen in very dilute interstellar gases (much like helium) and much later identified with extremely slow transitions in O^{+2} (and in the isoelectronic N^{+}). The following $Z = 3$ coronium was supposed to give many spectral lines

seen in the solar corona (first during total eclipses, and later with refined screening of the solar disc) now known to be due to Fe^{+13} (retaining half the electrons in the neutral atom) as far as the strong green line goes, but also Fe^{+z} ($z = 9$, 10, 12 and 14) and Ni^{+14}. The region of the corona emitting such lines has a temperature in the range 2–4 megakelvin (Chandrasekhar et al. 1984) quite unfamiliar to atomic spectroscopists. In recent years, such high z values awake interest related to high-power lasers and controlled thermonuclear fusion.

Moseley insisted in 1914 that $Z = 13$ for aluminum and $Z = 79$ for gold, an opinion later confirmed by nuclear physics. It must be added in all fairness to Rydberg that the 1s energy either is determined from an X-ray absorption edge with an uncertainty around 10 eV, or from the emission from one 2p electron jumping down in the 1s vacancy. The photon energy is here much more precise, but the 2p ionization energy is far less predictable and shows distinct irregularities, especially in the d-group elements, and even more so in the lanthanides (Coster 1923, Jørgensen 1973b, 1974a) as is discussed below in section 3.6. Anyhow, Condon and Shortley (1953) give $I(1s) = (Z - Z_s)^2$ Rydberg with the screening constant varying smoothly from 2.00 for neon to slightly higher values, going through a plateau $Z_s = 2.65$ between $Z = 45$ to 51, and then decreasing, being 0.15 for thorium and -0.07 for uranium. The latter rapid decrease of Z_s is due to relativistic effects.

It is important to mention the Rydberg formula from 1895, the ionization energy of a single external electron (Leucht-Elektron) outside a closed shell being given (with modern nomenclature; it has no sense to review the many earlier symbols for the quantum number l) as

$$I(nl) = (z + 1)^2 \text{ rydberg}/(n - d_l)^2. \tag{1}$$

For neutral atoms such as Li, Na, K, Rb and Cs, $z = 0$; for Be^+, Mg^+, Ca^+, Sr^+, Ba^+ and Ra^+, $z = 1, \ldots$. The Rydberg defect d_l is *almost* the same for different n values (in our nomenclature, a positive integer larger than the non-negative integer l) of a given monatomic species, and d_l tends to decrease strongly for increasing l. Thus, it is normally below 0.2 for $l = 2$, when Z is below 20, and normally below 0.05 for $l = 3$ of neutral atoms having Z below 56, but may be considerably higher for larger Z and achieve the values 0.31 for Ba^+, 1.40 for La^{+2}, 1.56 for Ce^{+3} and 1.56 for Pr^{+4} (Jørgensen 1976c) in a way showing a greater influence of z than of Z on the behavior of 4f electrons in gaseous ions. In all known cases, d_l almost vanishes for l above 3. A list of Rydberg defects of many elements from cesium to lutetium, having various z, has been compiled (Jørgensen 1976c and 1979a). Equation (1) reduces to the Balmer formula (from 1885) for systems containing only one electron, i.e. H, He^+, $Li^{+2}, \ldots$, with all the Rydberg defects vanishing and the ionization energy of a (ground or excited) state only dependent on n, but not on l. The success of eq. (1) induced many tables of atomic energy levels which give the position of the level relative to the ionized state, or more accurately, the groundstate of the ion with z one unit higher. This might have had practical advantages, e.g. the groundstate of the helium atom was not known nearly as precisely as the energy differences in the visible region, but since the large majority of monatomic entities have the opposite problem today, all recent tables follow the choice of the National

Bureau of Standards, and give energies relative to the groundstate of a given M^{+z} of which the ionization energy to the lowest state of M^{+z+1} is called I_{z+1} (and hence I_1 for the neutral atom, and I_0 if it has any electron affinity to form gaseous M^-). It should be noted that atomic spectroscopists speak about the first, second, third,.... spectrum of a given element, and hence speak about Ce I, Ce II, Ce III, Ce IV, Ce V,..., for Ce^0 (the neutral atom), Ce^+, Ce^{+2}, Ce^{+3}, Ce^{+4},..., one unit higher than the oxidation states of chemistry, which have to be written in parentheses, Ce(IV) being analogous to gaseous Ce V. There was an obvious interest in using eq. (1) for rationalizing observed energy levels, and the line spectra studied were mainly of elements having one, two or three external electrons, and not belonging to the transition groups. It should not be felt that eq. (1) is an absolutely exact formula; agreement is not always perfect when n is varied for a given l value. Modern atomic spectroscopy started with species such as the neon atom (Paschen 1919) showing some features of series spectra (many n values detected) and, at the same time, many more J-levels than in the simple systems treated by eq. (1). The Fraunhofer lines kept interest alive in Ti, V, Cr, Mn, Fe, Co, Ni spectra of neutral atoms, for which the uncertainty of I_1 remained above 10% for many years, in contrast to alkali-metal atoms with the first ionization energy known better than 10^{-5}, using eq. (1). Such spectra are colloquially called 'multiplet spectra' but in actual usage, a multiplet is a group of closely adjacent spectral lines, where the J-levels of closely similar energy are said to form an S,L-term in Russell–Saunders coupling. The first-order width of such a term can be described (Condon and Shortley 1953) by the Landé parameter of spin–orbit coupling, which is really a relativistic effect related to $(1/c)$ not vanishing. The effects of spin–orbit coupling can be quite pronounced for many atoms having Z above 33. They are comparatively much stronger for inner shells.

It is worthwhile to inquire about the relations between the one-electron wave-functions corresponding to the energy levels of the Rydberg formula, eq. (1), and to the huge $I(nlj)$ ionization energies (we add the quantum number $j = l \pm \frac{1}{2}$ because of the frequent very large effects of spin–orbit coupling) obtained from X-ray spectra (and later, photo-electron spectra) with the much more intricate problem of multitudinous J-levels and the 'electron configuration' of the more general case of several active electrons besides the closed shells. At this point, X-ray ionization has the fortunate aspect of 'one electron with opposite sign' lacking in an inner shell, and not being influenced by loosely bound electrons, even if present in partly filled shells (this is less strictly true in the lanthanides).

3.1. *Stoner and the stubborn facts*

It is difficult to avoid a blurred time parallax for events more than 60 years ago, though a year lasted as long a time as today. It must be emphasized that the year 1923 differs fantastically from 1924, as well as 1924 from 1925 for our purpose. We come back below to the relation between chemistry and atomic and X-ray spectra discussed by Kossel (1916) but we introduce here the Kossel number of electrons in a monatomic entity $K = (Z - z)$ (Jørgensen 1978c, 1986a). The atomic spectroscopists were familiar with the iso-electronic series (same K) having energy differences

increasing rather regularly with z. Already in 1922, Niels Bohr had adopted the idea of Rydberg that each series of elements in the Periodic Table terminating with a noble gas contains $2n^2$ elements, and he was looking for relations with the quantum numbers, we call n and l. It was obvious from X-ray spectra that the $2n^2$ electrons can be highly separated in energy for n at least 2, and as late as 1923, he suggested an asymptotic distribution of n groups of each 2n electrons. Thus, radon has four times 8 electrons with n = 4, but in xenon, there are only 6, 6, 6. 0 electrons (the last group being empty) and in krypton 4, 4, 0, 0. Consequently, a rather enigmatic rearrangement takes place in the transition groups, the ten electrons added in the neutral atoms from yttrium to cadmium winding up as the complement 2, 2, 6, 0 to this set. This can be clearly seen in the July 1923 issue of *Naturwissenschaften* (Coster 1923, Bohr 1923) commemorating the 10-year jubilee of the 1913 model of the hydrogen atom (based on celestial mechanics with quantum conditions; it can still be seen as elliptic orbits on letterheads of nuclear energy commissions). However the next year Stoner (1924) said that each *nl*-shell is able to accommodate at most $(4l + 2)$ electrons, being 2 s, 6 p, 10 d and 14 f, using the symbols from the English words for series in line spectra, i.e., sharp, principal, diffuse and fundamental (because Balmer-like with very small Rydberg defect). For reasons explained at length elsewhere (Jørgensen 1976b, 1978c, 1979b, 1983a) the most interesting series for chemists

$$\begin{aligned} &1s \ll 2s < 2p \ll 3s < 3p \ll 3d < 4s < 4p \ll 4d \\ &\quad < 5s < 5p \ll 4f < 5d < 6s < 6p \ll 5f < 6d \cdots \end{aligned} \tag{2}$$

is valid for all known M^{+2} (with five exceptions, M = La, Gd, Lu, Ac and Th), M^{+3}, M^{+4}, M^{+5} and M^{+6}. The double inequality signs indicate closed-shell systems $K = 2$, 10, 18, 36, 54, 86,..., iso-electronic with the noble gases. For sufficiently high z, exceptions occur for K above 46. Thus Kaufman and Sugar (1976) studied gaseous ions with $K = 67$. The groundstate of W^{+7} still follows eq. (2), but from Re^{+8} to Bi^{+16}, the ion is more stable with a full 4f shell, lacking one 5p electron. By the same token, Hartree–Fock calculations for Nd^{+z}, Gd^{+z} and Er^{+z} (Cowan 1973) have the groundstate predicted by series (2) up to $z = 6$, but transfer one or more 5p electrons to the 4f shell for $z = 7$, 8 and 9. This case of shell-crossing between 5p and 4f is also observed for the inner shells of iridium compounds (Jørgensen 1976b) and is one more case of asymptotic restoring the hydrogenic order of n-values for sufficiently high Z (Katriel and Jørgensen 1982).

The main reason that series (2) is more appealing to chemists (Jørgensen 1969, 1986a) is that non-metallic compounds of V(−I), Cr(0), Mn(I),..., contain the number of d-like electrons indicated by (2) without any need of invoking 4s electrons. From this point of view, the compounds are entirely different from gaseous V^-, Cr^0, Mn^+,.... Textbooks frequently indicate a series intended for gaseous atoms, having the 4s, 5s, 6s and 7s shells immediately following 3p, 4p, 5p and 6p, respectively. However, this series is known to have 20 exceptions in the groundstates of neutral atoms from hydrogen to einsteinium. The two major reasons why this series intended for gaseous atoms strongly bewilders chemists is that undue emphasis is made on irrelevant irregularities (such as the chromium, rhodium,

palladium,..., atoms) and that the lowest level of two different configurations, such as $[54]4f^96s^2$ and $[54]4f^85d6s^2$ are only separated by 285 cm^{-1} in the terbium atom, much less than 1% of the spreading of J-levels of each of the two configurations, and quite negligible for chemical purposes. The textbook series can be cut in slices finishing after helium and after each alkaline-earth atom: 1s; 2s; 2p3s; 3p4s; 3d4p4d; 4d5p6s; 4f5d6p7s;... and is then called the Madelung order (Katriel and Jørgensen 1982). Each slice has an invariant sum $(n + l)$ and starts with the lowest n compatible with the sum, and then increases n (or, if one prefers, begins with the highest l, which then decreases). It is hilarious that the 1906 idea of Rydberg is confirmed by the Madelung order without need for nebulium and coronium, but most chemists do not appreciate the series in the Periodic Table terminating with each alkaline-earth.

After 1922 there has always been a feeling among chemists that not only is the chemical behavior determined almost exclusively by Z, but also that the Periodic Table has been 'explained' by electron configurations (Fernelius 1986). But since Stoner (1924), we really have two versions of the Periodic Table, a chemical one and a spectroscopic one. Nowhere is the distinction as dramatic as between helium being a 'spectroscopic alkaline-earth' quite different from the following noble gases having their electron configuration ending with a full p shell. However, for practical purposes, the interesting distinctions between the chemical and the spectroscopic versions occur for the lanthanides and the transthorium elements. It is more inviting to perplexity to use the same word for two quite similar entities, than if they are as different as gallates being 3,4,5-trihydroxo-benzoates and gallates being anions formed by the amphoteric behavior of gallium. Since Stoner (1924) we have two versions of the Periodic Table, and one version does not 'explain' the other.

It is sometimes argued that J.D. Main Smith (Smith 1924, 1925) had the priority of proposing $(4l + 2)$ shells. It is true that his 1924-paper was both submitted and published four months before Stoner (1924), but as discussed elsewhere (Jørgensen 1987) Smith gives a mixture of extraneous chemical evidence and arguments based on X-ray spectra (cf. Stoner 1925) letting the $2n^2$ electrons (the n-groups separated below by semicolons) occupy the $(2n - 1)$ distinct groups for each n value in the order (2; 2, 2, 4; 2, 2, 4, 4, 6;...) corresponding to our nlj-relativistic orbitals with $(2j + 1)$ electrons. Since the ground term ^3P of the carbon atom is split by spin–orbit coupling by only 43 cm^{-1}, and the two yellow sodium lines by 17 cm^{-1}, these effects cannot be detected by the chemistry of light elements. What is more objectionable is the filling of four d-electron sites before six less stable, and six 4f electrons before the next eight. The proposal of Smith is not compatible with the approximate validity of Russell–Saunders coupling for external electrons, and would not be applicable before bismuth(I). Another interesting precursor is the work of Bury (1921).

Schrödinger did his work on wave-functions at the earliest in 1925, and published it at the beginning of 1926. As we shall discuss now, this gave a theory for electron configurations in more-electron systems, and introduced the angular functions, which are the true carriers of the quantum number l (Jørgensen 1971, 1980a, 1981d). The discussion is centered here on the aspects of greatest relevance to chemists and

transition-group spectroscopists, in particular those who work on the 4f and 5f groups. The innovating result of the many-electron wave-functions was something that was desperately lacking in 1923, and ensnared a few chemists in the euphoric pipe-dream of chemistry becoming a subject for numerical calculations in the bright future. Also, for the first time, one could meaningfully ask the question of whether chemistry can be shown to be a sub-division of physics.

3.2. *Monatomic entities*

The model of more-electron vector coupling expounded in the book by Hund (1927) was already taking shape around 1920. Technically, an energy level of a monatomic entity in spherical symmetry has the quantum number J (a non-negative integer for an even number of electrons K, and an odd positive integer divided by two for odd K) and (even or odd) parity. It is a very important selection rule in atomic spectra that electric-dipole transitions are only allowed between levels of opposite parity, and that the two levels J_1 and J_2 (at most one of them zero) at most differ by one unit (or do not differ). It is an additional approximation that the J-levels are bunched together in Russell–Saunders terms; and also that they belong to a definite electron configuration allotting from zero to $(4l + 2)$ electrons to each nl-shell. It is worthwhile to note that both approximations are on an equal footing, in the sense that a count of the number of levels having a given parity and a given J is correct in both models, independent of configuration intermixing or strong effects of spin–orbit coupling. In many lighter atoms, such as beryllium, the Russell–Saunders coupling with well-defined quantum numbers of total spin S and of the orbital angular momentum L (a non-negative integer; S has the same possible values as J, except for the restriction, of minor importance for K above 3, that S can at most be $\frac{1}{2}K$) is a much better approximation than electron configurations such as $1s^2 2s^2$, $1s^2 2p^2, \ldots$. When the J-level belongs to a definite electron configuration, its parity is the even or odd character of the sum of all the l values of the electrons.

Though many of the semi-classical ideas entering the concept of vector-coupling no longer are useful, it may be just to define the Hund coupling of two quantum numbers Q_1 and Q_2 as the manifold of resulting values of the quantum number Q

$$(Q_1 \oplus Q_2) = (Q_1 + Q_2) \quad \text{or} \quad (Q_1 + Q_2 - 1) \quad \text{or} \quad (Q_1 + Q_2 - 2) \quad \text{or} \quad \cdots \quad \text{or} \quad |Q_1 - Q_2|. \tag{3}$$

Hund coupling occurs for J_1 and J_2 of two different, partly filled nl-shells, giving a set of resultant J-values; and for the J values belonging to a term with $Q_1 = S$ and $Q_2 = L$. If two partly filled shells present different terms, one a given (S_1, L_1) term and the other a given (S_2, L_2) term, they contribute to the terms of the configuration containing the two partly filled shells the terms combining all the resulting $S = (S_1 \oplus S_2)$ with all the possible $L = (L_1 \oplus L_2)$. It can be shown by induction that the number of states (i.e. mutually orthogonal more-electron wave-functions Ψ) is conserved by these operations, each J-level involving $(2J + 1)$ states with the result that the number of states in a term is $(2S + 1)(2L + 1)$. This is one of the two

reasons why the factor $(2S + 1)$ for a term is called the multiplicity [the other is that $(2S + 1)$ differing J-values occur, if L is not smaller than S]. For chemists, it has the interest that colloquial names derived from the multiplicity are used:

$$\text{even } K\text{: singlet } (S = 0)\text{; triplet } (S = 1)\text{; quintet } (S = 2)\text{; septet } (S = 3); \ldots,$$
$$\text{odd } K\text{: doublet } (S = \tfrac{1}{2})\text{; quartet } (S = \tfrac{3}{2})\text{; sextet } (S = \tfrac{5}{2})\text{; octet } (S = \tfrac{7}{2}); \ldots, \quad (4)$$

which are applicable to a large number of compounds (Jørgensen 1969) whereas it is relatively rare to meet a well-defined L outside the 4f and 5f groups. A few J-levels are known of the gaseous gadolinium atom (Martin et al. 1978) having $S = 5$ belonging to configurations with three or four partly filled shells $[54]4f^7 5d^2 6s$ and $[54]4f^7 5d6s6p$. In many tables, levels with odd parity are italicized, or marked with a small circle, such as $^3P_2^o$. There is a well-established tradition for writing $(2S + 1)$ as a left-hand superscript, J as right-hand subscript (without J, the term is meant) and give $L = 0, 1, 2, \ldots, 12$, as one of the capital letters S, P, D, F, G, H, I, K, L, M, N, O, and Q.

Many operations have a neutral element, such as 0 for addition (because $x + 0 = x$ for any x) or 1 for multiplication. The neutral element of Hund coupling eq. (3) is $S = L = J = 0$ and even parity, the quantum numbers of a full shell. The great analogy between the spectroscopic and the chemical version of the Periodic Table is that the low-lying configurations, and the J values, are similar like the chemical behavior in the same column. Though the energy levels are not identical going from He, Be to Ra, and including the post-transitional Zn, Cd, Yb, Hg and No, there is a strong sense in which the excited configurations (ns) $(n'l')$ have exactly the same J-levels. The main-group iso-electronic series B^+, Al^+, Ga^+, In^+ and Tl^+, as well as C^{+2} to Pb^{+2} are also closely similar, though their excited levels are much higher than in the neutral atoms. On the other hand, Sc^+, Y^+, La^+, Lu^+ and Ac^+ show additional low-lying J-levels related to d electrons, whereas Ce^{+2} and Th^{+2} show effects of both d and f electrons (Jørgensen 1976c).

In one sense, the atomic spectra of the lanthanides started with the most difficult task, concentrating on Ln^0 and Ln^+ with many thousand spectral lines, and hundreds of J-levels of five or ten low-lying configurations (Goldschmidt 1978) as tabulated by Martin et al. (1978). The M^{+2} and higher ionic charges are relatively less crowded, though $[54]4f^q 5d$ still has 10 times more states than $[54]4f^q$ and almost ten times more J-levels. It is surprising that the J-levels of Ln(III) in condensed matter have been identified essentially by techniques of atomic spectra (Carnall et al. 1968, Reisfeld and Jørgensen 1977) in spite of the only data to compare with from gaseous ions are the twelve J-levels of $4f^2$ (the highest has not been located) in Pr^{+3} (Sugar 1965), the seven J-levels of the lowest term ^7F of $[54]4f^8$ of Tb^{+3} (Spector and Sugar 1976) and the only excited level of $[54]4f^{13}$ of Yb^{+3} situated at 10 214 cm^{-1} (Kaufman and Sugar 1976). We return in section 3.4. to the question of M(III) in condensed matter.

The most striking aspect of the monatomic entities (Jørgensen 1975b, 1976c) is that the energy difference between the lowest J-level of $[54]4f^{q-1}5d6s^2$ and the lowest J-level of $[54]4f^q 6s^2$ varies in the atom in a very characteristic way with q,

increasing along a curve from $q = 1$ to $q = 7$ having an almost horizontal plateau for $q = 3, 4$ and 5; and then repeating itself with approximately identical values for $q + 7$ and q. This variation takes place a tiny bit below M(II) in condensed matter, which again occurs some 8000 cm^{-1} below the distance between the lowest J-level of $[54]4f^{q-1}5d$ and of $[54]4f^q$ in gaseous M^{+2}. We return to the evidence for the refined spin-pairing energy theory derived from these facts in section 3.5. It is interesting to note that the height of this variation going from $q = 1$ to 7, or from 8 to 14, is approximately 40 000 cm^{-1} or 5 eV.

Another striking aspect of the gaseous lanthanide ions is the extent to which the configuration barycenter (i.e. average weighted by the number of states) energies is not at all a linear function of the occupation number of the shells. This situation is already known from the 3d group. The barycenter of [18]3d4s of Sc^+ (to which the groundstate belongs) is at 714 cm^{-1} to be compared with the unique state of $[18]4s^2$ 11 376 cm^{-1} above the groundstate, and the barycenter of $[18]3d^2$ close to 9200 cm^{-1}. In other words, there is not a clear-cut answer to the question whether 3d or 4s is the most stable in monatomic scandium. If it is argued that the 4s shell is filled with first priority, this is true for all the atoms from calcium to nickel, with the exception of chromium. On the other hand, when the scandium atom loses an electron, it is one 4s electron in Sc^+ and the last 4s in Sc^{+2}, leaving in both cases exactly one 3d electron, which is definitely the most stable, as far as the preference of ionization goes.

It is possible to relate the Rydberg equation (1) with the configuration barycenter energies of gaseous atoms and ions with two or more external electrons (Jørgensen 1973a, 1976c, 1978c) by defining a parameter $A_*(nl, n'l')$ as the difference of the barycenter energy observed for the two external electrons in the shells nl and $n'l'$ (actually, it may be the same shell) and the sum of the two Rydberg energies $I(nl) + I(n'l')$ taken with opposite sign in the corresponding monatomic entity with z one unit higher, containing only one external electron. It turns out that the A_* parameter is rather small, if at least one of the two shells has a large average radius, whereas $A_*(nd, nd)$ in the d shell is quite large, and for Z above 56, $A_*(5d, 4f)$ is even larger, but smaller than $A_*(4f, 4f)$. These A_* are closely related to the theory (from 1929) of Slater, ascribing term distances in a configuration with one or more partly filled shells to slightly differing interelectronic repulsion; this treatment was systematized by Condon and Shortley (1953) and, in the case of one partly filled f shell, streamlined by Racah (1949). To a rough approximation, A_* is about $\langle r^{-1} \rangle$ times 1 hartree = 2 rydberg = 27.21 eV for two different shells, and the average reciprocal distance from the nucleus $\langle r^{-1} \rangle$ is the smaller of the two values. For A_* between two electrons in the same shell, this expression is close to $0.7\langle r^{-1} \rangle$. As also seen in table 23.2 and eq. (23.18) of this Handbook (Jørgensen 1979a) and in the book by Jørgensen (1969), the A_* parametrization can readily be extended to three or more external electrons producing a parabolic function of shell occupation numbers for different z (or K) of the same element, in surprising close agreement with the observed configuration barycenter energies (Jørgensen 1973a).

For our purpose, the most important consequence of the large $A_*(4f, 4f)$ is that a given lanthanide does not want to have all its external electrons ($K - 54$) in the 4f

shell. It is almost certain that a cerium atom in the configuration [54]4f^4 would ionize spontaneously to Ce^+. The coefficient $\frac{1}{2}q(q-1)$ to the large $A_*(4f, 4f)$ necessitates a buffering pad to two 6s electrons in the gaseous state without adjacent neighbor atoms. The role of this padding is taken over by electronic density of ligating atoms in compounds, and ambient conduction electrons in metallic elements and alloys.

The *conditional oxidation state* (Jørgensen 1969) written, according to a suggestion by Professor Kai Arne Jensen, with Roman numerals in rectangular brackets, is determined by the number of electrons in the shell with distinctly the smallest radius, and still able to change its occupation number. Thus, Ln[II] have $q = (Z - 56)$ and Ln[III] $q = (Z - 57)$ electrons in the 4f shell. This concept can also be applied to monatomic entities, and it is striking that nearly all the J-levels of Ln^0 and Ln^+ (Martin et al. 1978) have the conditional oxidation state Ln[II] or Ln[III]. It is informative that the lowest level ^8S of [54]4f^7 occurs at 18 289 cm^{-1} above the groundstate (belonging to [54]4f^{6}6s) of Sm^+. The arguments in section 3.5 show that no other gaseous Ln^+ is so close to being Ln[I], and the influence of condensed matter is, in all cases, to stabilize the higher conditional oxidation state relative to the gaseous ion.

It has great importance for checking occurrence of lanthanides in stars that the atomic spectra of Ln^+ and Ln^{+2} are now so complete. The spectral analysis introduced by Bunsen and Kirchhoff in 1860 was a disproof of the positivistic attitude that we would never be able to determine the chemical composition of stars, but it is frequently simplified in text-books to 'the Fraunhofer lines are identified with spectral lines measured in the laboratory'. It is not true that all our elements have been detected, and neither that all Fraunhofer lines have been identified. At the end of last century, many rarer elements, such as rhodium, platinum and uranium, were identified based on coincidence with a few laboratory lines, and it needed clever circumspection by the astrophysicists to decide what the most intense lines were at a given temperature. A major difficulty is that nearly all laboratory lines are observed in emission, and nearly all stellar lines in absorption. It is very useful that Meggers et al. (1961) measured the arc line spectra of each of 70 elements (including sixteen R) as 1:1000 mole mixtures with very pure copper. For instance, 2422 lines (of those, 58 strong) are given of cerium; 1465 (35 strong) of neodymium; 525 (22 strong) of europium; 1197 (24 strong) of erbium; and 432 (15 strong) of ytterbium. Among the strong lines compiled, the large majority is due to Ln^+ and are hence spark lines in the old wording. Without falling into sensationalism, a lot of weaker Fraunhofer lines could easily be due to unknown elements, e.g. having Z above 100. For some time, less than half the elements were considered safely proven, and nearly all having Z below 41, in the solar spectrum. Trimble (1975) quotes 19 elements undetected up to uranium, including only three Ln (=Pm, Tb and Ho). On the other hand, the distribution of Fraunhofer lines is almost overall dense, in the sense that their number per nm is larger than their reciprocal half-width. This background of weak absorption lines probably has a very prosaic origin, in iron and adjacent elements.

In the excellent book on line spectra by Hund (1927) it is uncritically interpolated

between the ground configurations [54]5d6s^2 of La^0 and [54]4f^{14}5d6s^2 of Lu^0 that at least the large majority of the other lanthanide atoms have their groundstate belonging to [54]4f^{q}5d6s^2, with the argument of the prevailing trivalency. This is only the case for Ce^0 and Gd^0 and shows how difficult it was to conceive distinct chemical and spectroscopic versions of the Periodic Table. Von Hevesy (1927) wrote a book about the rare earths based on pre-Schrödinger opinions on atomic structure, but essentially accepting the $(4l + 2)$ electron shells of Stoner. This book contained a lot of interesting data on relative concentrations of R in minerals (mainly derived from X-ray spectra) but was still at a stage of essentially trivalency.

3.3. *4f → 5d and electron transfer spectra in condensed matter*

Seen from the point of view of an atomic spectroscopist, the only intense transitions occur between states of opposite parity (the rule of Laporte) and experiences in the 1920's, had shown that by far the strongest transitions are those, where one electron in the configuration changes its value of l exactly by one unit. Freed (1931) photographed absorption spectra of crystalline $[Ce(OH_2)_9](C_2H_5OSO_3)_3$ and the corresponding lanthanum salt, alone or in mixture with a little cerium. The six bands found with time (Heidt and Berestecki 1955, Jørgensen 1956a, Jørgensen and Brinen 1963, Okada et al. 1985) have found an assignment based on the angular overlap model (Reisfeld and Jørgensen 1987) that the ennea-aqua ion has the strongest band at 39 600 cm^{-1} followed by four somewhat weaker bands at 41 700, 45 100, 47 400 and 50 000 cm^{-1}, whereas the weak and temperature-dependent band at 33 800 cm^{-1} is due to the same kind of transition in an aqua ion having $N = 8$ and unknown symmetry, occurring in a concentration of about 4%. The latter band may be compared with the band of octahedral $CeCl_6^{-3}$ at 30 300 cm^{-1} in acetonitrile solution (Ryan and Jørgensen 1966) and was showing a shift toward lower energy compared to the levels of [54]5d found by Lang in 1936, $^2D_{3/2}$ at 49 737 and $^2D_{5/2}$ at 52 226 cm^{-1} above the groundstate $^2F_{5/2}$ of gaseous Ce^{+3}. Becauseof spin–orbit coupling, $^2F_{7/2}$ occurs at a 2253 cm^{-1} higher energy, and Kröger and Bakker (1941) suggested that the two emission bands separated by some 2000 cm^{-1} in the luminescence of many cerium(III) containing solids (Blasse and Bril 1967, Reisfeld and Jørgensen 1977, 1987) are indeed related to the ^2F splitting. The Stokes shift of the luminescence enhances the energy decrease already found in absorption of the lowest 5d-like state in Ce(III) compared to 49 737 cm^{-1} in Ce^{+3}.

The ultraviolet absorption bands of cerium(III) are about 100 times higher (and being broader, an oscillator strength some 1000 times larger) than the strongest internal transitions in the partly filled 4f shell of other Ln(III), and have sometimes been reported as unrecognized impurities in Pr(III) solutions. The very careful investigation of the absorption spectra of Ce(III) to Nd(III) and Sm(III) to Yb(III) aqua ions by Prandtl and Scheiner (1934) only indicates weak absorption growing up below 220 nm in the later Ln. This was not the conclusion of Stewart (1948) finding distinct, broad bands in this region of Pr(III), Eu(III) and Tb(III), but not

the other aqua ions. These measurements were continued up to 54 000 cm^{-1} (185 nm) by Jørgensen and Brinen (1963) finding a weak band of praseodymium(III) at 46 800 cm^{-1} and a 16 times stronger band at 52 900 cm^{-1}. In view of the recent work on Ce(III), the best diagnosis seems to be the former being the first band of the species having $N = 8$, and the latter belonging to $N = 9$. The first J-level of [54]4f5d occurs in Pr^{+3} at 61 171 cm^{-1}, again some 1 eV higher in the gaseous ion than in the ennea-aqua ion. We return below to the broad electron transfer band of europium(III) aqua ions at 53 200 cm^{-1}.

Terbium(III) aqua ions have a broad hilly feature around 38 000 cm^{-1} before a really strong band at 45 900 cm^{-1} (Stewart and Kato 1958). By the same token, octahedral $TbCl_6^{-3}$ has a band at 42 750 cm^{-1}, 50 times higher than a band at 36 800 cm^{-1} (Ryan and Jørgensen 1966). Comparison with Tb^{+3} studied by Spector and Sugar (1976) finding the five J-levels of ^9D of [54]$4f^7$5d between 51 404 and 54 882 cm^{-1} and the five J-levels of ^7D between 62 681 and 64 312 cm^{-1} suggests that the weak band of Tb(III) at lower energy represents the highly spin-forbidden transition from the $^7F_6$ groundstate to ^9D components, and the stronger band going to ^7D. The separation between $S = 4$ and $S = 3$ is about half as large in the chloro complex as in the gaseous ion. Lammers and Blasse (1986) studied the luminescence of terbium(III) in $CsCdBr_3$ finding a peak in the excitation spectrum at 34 500 cm^{-1}, the spin-forbidden character of a transition to ^9D perhaps being attenuated by the bromide neighbors.

Butement (1948) studied the absorption spectra of the (highly ephemeric) samarium(II), Eu(II) and Yb(II) aqua ions in solution. The red Sm(II) has the first strong transition to $4f^5$5d at 17 900 cm^{-1} followed by six similar bands at higher wave-numbers, and oscillator strengths P of order 0.001 to 0.01. Europium(II) aqua ions have two broad bands at 31 200 cm^{-1} ($P = 0.006$) and 40 300 cm^{-1} ($P = 0.03$), quite similar to ytterbium(II) at 28 400 cm^{-1} ($P = 0.005$) and 40 600 cm^{-1} ($P = 0.027$). For us, it is instructive to compare Sm^{+2}, having the first J-level of [54]$4f^5$5d at 26 283 cm^{-1}, with Eu^{+2} having its first J-level of [54]$4f^6$5d at 33 856 cm^{-1}, and finally with Yb^{+2} where [54]$4f^{13}$5d starts at 33 386 cm^{-1}. As also seen in table 1, there is a smaller shift from Ln^{+2} to Ln(II) than in the trivalent case. It is also interesting to note that Butement (1948) found four weak, but very narrow, bands superposed the intense $4f \rightarrow 5d$ transitions, in both Sm(II) at 21 790, 22 270, 22 650 and 26 450 cm^{-1} (which is likely to be ^5L and ^5H components) and in Eu(II) at 30 960, 31 200, 31 450 and 31 700 cm^{-1} (probably ^6I). The writer has remeasured the weak Eu(II) bands.

Though the strong colors of most iron(III), copper(II), iridium(IV) and platinum(IV) complexes are due to electron transfer (Jørgensen 1963a, 1967b, 1970b, 1971, Jørgensen and Reisfeld 1982b) they look unfamiliar to the atomic spectroscopist accustomed to scrutinize one atom at a time. Nevertheless, for the chemist, the electron transfer spectra are among the most informative, as far as reducing and oxidizing characteristics go (quantified with the concept of *optical electronegativity* x_{opt}) of the complexes, where one ligand (or a set of reducing ligands collectively) loses one electron to a central atom containing an empty or partly filled shell. Within a precision of typically 3000 cm^{-1} one can describe the wave-number of the

TABLE 1
Energy differences (in cm^{-1}) between the lowest level of a configuration with $(q-1)$ electrons in the 4f shell, and the lowest level for q, of gaseous atoms Ln^0 and gaseous Ln^{+2} (Martin et al. 1978), of Ln(II) in calcium fluoride (McClure and Kiss 1963) and Ln(II) aqua ions (Butement 1948).[a]

Ln	q	Ln^0 $([54]4f^{q-1}5d6s^2) - ([54]4f^q6s^2)$	Ln^{+2} $([54]4f^{q-1}5d) - ([54]4f^q)$	Ln(II) in $Ca_{1-x}Ln_xF_2$	Ln(II) aqua ions	Refined spin-pairing results
La	1	−15 197	− 7195	negative	–	X + 1300
Ce	2	− 4763	3277	negative	–	X + 12 500
Pr	3	4432	12 847	4000	–	X + 20 900
Nd	4	6764	15 262	7000	–	X + 21 600
Pm	5	[8000]	[17 100]	–	–	X + 22 200
Sm	6	18 076	26 283	15 000	17 900	X + 30 200
Eu	7	27 853	33 856	26 000	31 200	X + 40 300
Gd	8	−10 947	− 2381	negative	–	X + 800
Tb	9	285	8972	negative	–	X + 11 900
Dy	10	7561	[17 200]	10 400	–	X + 19 800
Ho	11	8379	18 033	11 100	–	X + 20 000
Er	12	7176	16 976	10 900	–	X + 20 000
Tm	13	13 120	22 897	17 000	–	X + 27 200
Yb	14	23 188	33 386	27 500	28 400	X + 37 200

[a]The zero-point X is added to the result $\mathscr{R}$ of the refined spin-energy treatment for $q \rightarrow (q-1)$. Values in rectangular brackets are estimated from this theory.

first strong electron transfer band $h\nu_{e.t.}$ by

$$h\nu_{e.t.} = [x_{opt}(X) - x_{uncorr}(M)] \times 30\,000\,cm^{-1}, \quad (5)$$

where x_{opt} has the Pauling values 3.9 (F), 3.0 (Cl), 2.8 (Br) and 2.5 (I) for the four halides X^-, 3.5 for H_2O, 3.2 for SO_4^{-2}, 2.6 for NCS^-,.... The symbol x_{uncorr} for M keeps the door open for correction for spin-pairing and/or electron transfer to highly anti-bonding d-like orbitals. The values derived from observed spectra illustrate that the electronegativity x varies strongly for M having low and high oxidation states, as has always been obvious for Cr(III) versus Cr(VI); Mn(II) versus Mn(VII), ..., but the electron transfer spectra allow a numerical parameter to be attached to the problem how much x increases along the series Os(III), Os(IV), Os(V) and Os(VI) in octahedral complexes.

There are several kinds of electron transfer spectra (Jørgensen 1970b). Organic molecules with low ionization energy (say, substituted naphthalene, anthracene,...) may produce strong colors in unreactive solvents in the presence of inorganic ($TiCl_4$, $OVCl_3$, WCl_6,...) or organic (tetracyano-ethylene) molecules with large electron affinity, the excited state involving a complete transfer of an electron. A fascinating case of this behavior is xenon mixed with the yellow-orange gas IrF_6 which by strong cooling condenses to a deep purple liquid or solid (Webb and Bernstein 1978) where the broad absorption band corresponds to a state Xe(I) and Ir(V), one of the six Xe 5p electrons having jumped to the 5d shell of iridium. This

spectroscopic behavior may be compared with the chemical reaction in a mixture of xenon and the red-brown gas PtF_6, where Bartlett found a yellow solid, in 1962, later to be shown to have the xenon(II) compound $XeF^+PtF_6^-$ as the main constituent. Other types of electron transfer are called 'inverted' because they only occur with conjugated organic ligands with low-lying empty orbitals, to which one d-like electron can be transferred from reducing systems titanium(III), chromium(0), iron(II), copper(I), ruthenium(II), iridium(III), ... Acetylacetonates show electron transfer in both directions (Jørgensen 1962b).

For our purpose, the two important types of electron transfer bands are the straightforward transfer from reducing ligands to oxidizing central atoms M to which eq. (5) is adapted, and the transfer of an electron from one M to another. In the latter case, we may have the 'mixed valency' of one element, such as transfer from Ti(III) to Ti(IV); Fe(II) to Fe(III); Cu(I) to Cu(II); Ce(III) to Ce(IV); Eu(II) to Eu(III); Au(I) to Au(III) (Robin and Day 1967, Allen et al. 1973). However, there is not a large conceptual difference from strong colors due to electron transfer between atoms of two metallic elements. Thus, the fox-red copper(II) or uranyl ferrocyanides have excited states Fe(III) combined with Cu(I) or U(V), whereas black (and not tomato-red) thallium(I) ferricyanide has Tl(II) and Fe(II) as the excited states. We do not usually consider silver(I) and thallium(I) as particularly reducing, but perhaps because of their lack of protecting aqua ligands, they produce striking colors with Ag(II) and Tl(II) excited states, such as deep red Ag_2CrO_4, blue $AgMnO_4$, blue Ag_2IrCl_6, dark green Tl_2IrCl_6 and black Tl_2OsBr_6 (Jørgensen 1961, 1963b). In one way, it is difficult to understand why these transitions are so intense, when considering the relatively long M–M′ internuclear distance, even in the anhydrous compounds.

Since cerium(IV) is a closed-shell system, the yellow or orange colors of most of its compounds can only be explained by electron transfer, like in chromate and permanganate (Müller et al. 1973) and actually, they have very broad, strong bands in the near ultraviolet. It is true that their constitution is not too well known with the exception of $CeCl_6^{-2}$ having a very strong band at 26 600 cm^{-1} (Ryan and Jørgensen 1966). The electron transfer bands at lower energy of mixed oxides containing praseodymium(IV) or terbium(IV), discussed above in section 2.2, only presented the problem that x_{opt} for oxide ligands in eq. (5) vary far more with the surroundings than for halide.

When it comes to electron transfer bands of trivalent lanthanides, the major difficulty was to find solutions transparent in the ultraviolet allowing the demonstration that the less oxidizing among the Ln(III) did not show the bands studied. The first choice was bromides (or perchlorates to which small amounts of Br^- were added) in nearly anhydrous ethanol (Jørgensen 1962a). Though the constitution of the absorbing species is not perfectly established, the major part must be solvated $LnBr^{+2}$, and the wave-number of the first electron transfer band in the order Eu(31 200), Yb(35 500), Sm(40 200) and Tm(44 500) varied exactly as expected. Chloride complexes formed under similar conditions show bands at 5500–6000 cm^{-1} higher energy. However, the first well-defined complexes were measured in acetonitrile, the octahedral $LnCl_6^{-3}$ and $LnBr_6^{-3}$ (Ryan and Jørgensen 1966) and

LnI_6^{-3} (Ryan 1969). It may also be added that the electron transfer band of europium(III) aqua ions at 53 200 cm^{-1} (Jørgensen and Brinen 1963) has not been found close to the expected position, 57 000 cm^{-1} in Yb(III), because even very thin layers of water are not transparent there. Another interesting extension is the electron transfer bands of Sm(III), Tm(III), Dy(III), Ho(III), Nd(III) and Er(III) found in crystalline $CaGa_2S_4$ (Garcia et al. 1985) supplementing previous studies of sulfides (reviewed by Reisfeld and Jørgensen 1987).

Table 23.3 in Volume 3 of this Handbook (Jørgensen 1979a) gives a set of electron transfer bands of trivalent lanthanides. For comparison with section 3.5, table 2 here compares the halide complexes LnX_6^{-3} adding to the wave-number of the first electron transfer band the quantity $\mathscr{R}$ defined in section 3.5. It is seen that each halide then has an almost invariant sum, of which the average value is 73 600 cm^{-1} for chloride, 65 500 cm^{-1} for bromide, and 55 100 cm^{-1} for iodide. If eq. (5) was perfectly adapted to this situation, the differences of 8100 cm^{-1} and 10 400 cm^{-1} between these three sums would have been 6000 and 9000 cm^{-1}, respectively.

It is noted that the same values of $\mathscr{R}$ agree with the removal of a 4f electron in table 1, treating 4f → 5d excitations, as the addition of one 4f electron in the excited state of an electron transfer band in table 2. This seemed at first an unbelievable coincidence, but has at least the heuristic value that varying the Ln(III), the inter-shell and the electron transfer bands move in exactly the opposite direction. There are few groups in the Periodic Table having such well-characterized inter-shell transitions as 4f→5d in Ln(II) and Ln(III), and 5f→6d in transthorium M(III) and M(IV) compounds. Seen from the point of view of an atomic spectroscopist, the weak band of $Fe(OH_2)_6^{+2}$ at 40 500 cm^{-1} is quite close to represent $3d^5 4s$ as the excited configuration, the bands of $Ag(OH_2)_4^{+}$ starting at 44 400 cm^{-1} (Texter et al. 1983) close to $4d^9 5s$; we have already mentioned $4p^5 5s$ of bromide and $5p^5 6s$ of iodide (Jørgensen 1969, 1975b) and a well-elaborated area of inter-shell transitions (Reisfeld and Jørgensen 1977, 1987) occurs for $K = 48$ indium(I), tin(II), antimony(III) and tellurium(IV), and for $K = 80$ thallium(I), lead(II) and bismuth(III), but with exception of weakly perturbed mercury atoms, it is an intricate question (Jørgensen 1971) to what extent $[78]6s^2 \rightarrow [78]6s6p$ from atomic spectra is a good analogy.

TABLE 2

Wave-number $h\nu_{e.t.}$ of first electron transfer band of octahedral samarium(III), europium(III), thulium(III) and ytterbium(III) hexahalide complexes (Ryan and Jørgensen 1966, Ryan 1969). The parameter $\mathscr{R}$ of the refined spin-pairing treatment (table 1, last column) is added to $h\nu_{e.t.}$ in the corrected values.

	Sm(III)		Eu(III)		Tm(III)		Yb(III)	
	$h\nu_{e.t.}$	Corrected	$h\nu_{e.t.}$	Corrected	$h\nu_{e.t.}$	Corrected	$h\nu_{e.t.}$	Corrected
$LnCl_6^{-3}$	43 100	73 300	33 200	73 500	–	–	36 700	73 900
$LnBr_6^{-3}$	35 000	65 200	24 500	64 800	38 600	65 800	29 200	66 400
LnI_6^{-3}	24 900	55 100	14 800	55 100	28 000	55 200	17 850	55 050

3.4. *Narrow absorption and luminescence bands in condensed matter*

It had been observed previously that the two rather ubiquitous yellow emission lines coincide with two of the more intense Fraunhofer lines, but when Bunsen and Kirchhoff in 1860 established spectral analysis, also by reproducing the sodium absorption lines in the laboratory, it became the general rule that all absorption lines correspond to some among the emission lines observed in flame and arc spectra. These are certainly absorbed and emitted by rather isolated atoms (though it is food for thought for recent experts in non-localized, holistic aspects of quantum mechanics that nice, narrow lines are emitted by electric discharges in a gas with an average distance of 100 Å, and a high collision rate, and that most spectral lines are not broadened dramatically by a higher pressure and an average distance of 30 Å). Bunsen and Kirchhoff believed that all incandescent solids and liquids only emit a continuous spectrum, and they went so far as to suspect that the solar photosphere surrounded a liquid (we could only think of boiling tungsten or rhenium) but it was soon realized that any opaque system in equilibrium at a given temperature T (even if it is a 10 000 km thick layer of gas) emits a standard continuous spectrum with the wave-number of the maximum proportional to T (cf. Jørgensen 1976a, Reisfeld and Jørgensen 1977).

Already Gladstone (1857) found that solutions and solids containing pink rare earths, such as didymium, have quite narrow absorption bands reminiscent of Fraunhofer lines. By the way, Newton did not use collimated light and a sufficiently narrow slit in his rainbow experiment with a prism, but the narrow lines in the solar spectrum were detected by the discoverer of palladium, Wollaston, though they were carefully studied by Fraunhofer after 1815. When Bunsen heard about Gladstone's results, he started wondering whether rare earths may have some properties of isolated atoms, and the first question was whether the narrow absorption bands might show up in emission at high T, and indeed, pink Er_2O_3 emits green light showing several rather narrow emission bands (Bahr 1865). This effect can be studied as candoluminescence (a better word might perhaps be thermoluminescence, but this word is reserved for the release of energy stored in a solid, supplied by radioactivity or cosmic rays, observed by heating the solid, e.g. fluorite crystals or archeologic artefacts) and if Auer mantles are made of rare earths from cautiously calcining cotton textile soaked in nitrate solutions, brilliant mauve light is observed from holmium, emerald-green from erbium and purple from thulium, all with colors incompatible with the continuous spectrum of an incandescent opaque object at any T, and indeed showing emission bands slightly wider than the absorption bands at room temperature (Jørgensen 1975c, 1976a; Jørgensen et al. 1981).

After 1865, narrow absorption bands played a role for evaluating the separation of two elements, as elaborated by Auer von Welsbach, and Soret (who was professor of physics at the University of Geneva, where Marignac was professor of chemistry and mineralogy) ascribed some absorption bands prominent in some erbium fractions to a new element. A few years after, these bands turned out to occur in holmium, separated by Cleve in 1879. There are minor chemical effects in sulfate complexes, mixed anion–hydroxo complexes, etc., on absorption spectra in solution,

and the method was somewhat discredited as an argument for new elements. The reflection spectra of solids containing a given Ln(III) are somewhat more variable than solutions, and became a study in their own right, especially with the nephelauxetic effect on Pr(III), Nd(III) and Sm(III) compounds studied by Ephraim and collaborators after 1926 (cf. Jørgensen 1956a) and a very comprehensive investigation by Boulanger (1952). The cathodoluminescence of solids containing small amounts of rare earths introduced by Crookes, the narrow-band red cathodoluminescence of europium(III) found by Urbain and forming the basis for red color television, were also strong evidence for a behavior closely similar to atomic spectral lines.

Something happened (Du Bois and Elias 1908) which was not an unmixed progress. Whereas the lanthanides had the monopoly since 1857 to show very narrow absorption and emission bands in condensed matter, it was now argued that the odd-numbered series (Reihe) having propensity for paramagnetic behavior also frequently showed narrow-band absorption and fluorescence. It is not easy to express this concept in modern wording, but the first series, including NO, NO_2 and O_2, presumably ends at neon, and the second, exclusively diamagnetic, at argon. Though only titanium to copper are cited by Du Bois and Elias, the third series probably goes on to krypton. The narrow-line emission of ruby (giving the fluorescence mentioned in the *Tales of 1001 Nights*) might, after all, be due to ^2G of $3d^3$ chromium(III). As members of the fourth series are mentioned Zr–Ag, but it may end at xenon. The fifth series is exemplified by trivalent Pr, Nd, Sm, Ho, Er and Tm, and their minerals. The writer does not know whether $Z = 72$ (18 units after Xe) is a honorary noble gas, but Ta–Au are cited as belonging to the sixth series. Uranium is given as only example of the seventh series. A recent reader may grumble that the way in which uranyl compounds are not strictly diamagnetic, is that they are temperature-independent paramagnetic ('high-frequency' second-order perturbation, as proposed by Van Vleck) but it is true that most uranium(IV) compounds are paramagnetic, and indeed have narrow absorption bands (Ephraim and Mezener 1933) as further discussed in section 3.8.

It is striking that narrow-band absorption and emission is restricted to systems with paramagnetic groundstate. The reason that straight-forward diamagnetic compounds do not show narrow bands, is that the absence of co-excited vibrations in them is conditioned by potential surfaces of the excited electronic state and the groundstate running parallel (with almost invariant distance) both with regard to the 'breathing mode' of stretching by a scale factor, and all the other normal modes of vibration in the $(3\mathcal{N} - 5)$-dimensional space of $\mathcal{N}$ nuclei (at least three) as is the general case for lanthanides. If the groundstate is diamagnetic, it usually has a molecular orbital configuration with all occupied orbitals full, and such a system has to change to another MO configuration (with concomitant differing equilibrium distances and angular stereochemistry) to show excited electronic states. Since it is a sufficient condition for being diamagnetic (or temperature-independent paramagnetic) to have a single state in the sense of Schrödinger at an energy many kT below the next states, we must allow neglect of 'sophisticated' diamagnetism, such as $5f^6$ americium(III) having the first excited J-level $^7F_1$ 2700 cm^{-1} above the groundstate $^7F_0$ (on the other hand, europium has a distance of only 300 cm^{-1} and only

becomes diamagnetic at quite low T); one of the nine states of $^3H_4$ of $5f^2$ UCl_6^{-2} and PuF_6 is sufficiently isolated, as well as one state of the $5d^4$ osmium(IV) complexes OsX_6^{-2}; strong antiferromagnetic coupling (Jørgensen 1971) may isolate one state, such as complexes of two Cr(III) with a linear bridge CrOCr (Glerup 1972) where the states with increasing $S = 0$, 1, 2 and 3 are spread over 2700 cm^{-1}. Another instance of unexpected diamagnetism is the gyromagnetic factor g 'accidentally' vanishing, as it happens for gaseous NO at low T. Anyhow, with the exception of NO, our examples of 'sophisticated' diamagnetism all have sharp absorption bands. It is interesting that one of the first papers applying 'ligand field' theory to compounds containing a partly filled 3d shell (Finkelstein and Van Vleck 1940) identify the narrow bands connecting the groundstate $^4A_2$ of chromium(III) with ^2E, $^2T_1$ and $^2T_2$ (symmetry types in the point-group O_h) but deplore that the predicted spin-allowed transitions to $^4T_2$ and $^4T_1$ are hidden by broad, intense bands. Tanabe and Sugano demonstrated in 1954 that these bands are simply the spin-allowed transitions, but as pointed out by Orgel (1955) they are broad because one electron jumps from three roughly non-bonding to a set of two strongly anti-bonding d-like orbitals providing much longer equilibrium internuclear distances, a phenomenon of great importance for ruby, alexandrite and other lasers containing Cr(III) (cf. Reisfeld and Jørgensen 1987).

Van Vleck (1932) demonstrated in all trivalent lanthanides (except Pm) magnetic behavior predicted by the Hund (1927) ground J-level of $4f^q$ with the exception of the varying Boltzmann population of $^7F_0$ and $^7F_1$ of europium(III) [and samarium(II)]. Until around 1952, this remained the strongest evidence for behavior imitating monatomic entities, and showing a quite moderate energy spreading of the $(2J + 1)$ states of the ground level. Indirectly, this also supported the existence of numerous higher-lying J-levels for $q = 2$ to 12, but did not by itself indicate definite assignments. As reviewed by Carnall (1979), the visible narrow-band luminescence was studied by Tomaschek and co-authors after 1932, mainly in solids containing $4f^5$ samarium(III), $4f^6$ samarium(II) and europium(III), $4f^8$ terbium(III) and $4f^9$ dysprosium(III), whereas the ultraviolet emission lines of $4f^7$ gadolinium(III) had been discovered by Urbain (1925). Specific materials, such as crystalline and vitreous, mixed fluorides allow a much larger number of lanthanides, including Pr(III), Nd(III), Ho(III), Er(III), Tm(III) and Yb(III) (which luminescence in the near infrared, also in many mixed oxides) to show line emission, and frequently cascading down between several J-levels, like known from monatomic entities (Reisfeld and Jørgensen 1987, Jørgensen 1986b).

One detail impeding early attempts to predict J-levels of $4f^2$ and $4f^{12}$ is that $[54]4f^2$ is a very highly excited configuration of La^+ (Martin et al. 1978) and the original assignment (Condon and Shortley 1953) was erroneous, needing a revision (Jørgensen 1955) of the early analysis (Bethe and Spedding 1937) of $4f^{12}$ thulium(III), and of the closely related $4f^2$ praseodymium(III). The pioneer work (Satten 1953) on $4f^3$ neodymium(III) had essentially the same problem, the quartet terms (separated by a single Racah parameter E^3) being well described, but the spin-forbidden transitions to doublet levels being predicted at energies roughly 25% too low.

The first comparison of the lower-lying J-levels across the trivalent lanthanides

was done by Gobrecht (1938) measuring absorption spectra in borax beads (molten $Na_2B_4O_7$) and hence avoiding interference with O–H overtone frequencies. The corner-stone of this study was the identification of the $10\,300\,cm^{-1}$ band of ytterbium(III), showing an unexpected high value of the Landé parameter of spin–orbit coupling, $\zeta_{4f} = 2950\,cm^{-1}$. This has the same order of magnitude in the lanthanides as in the 5p group from indium to xenon, though it remains valid that the strongest effects of spin–orbit coupling occur in the 6p elements from thallium to radon. The explicit value of the Landé parameter is known for one-electron monatomic entities (Condon and Shortley 1953) and is proportional to Z^4 and strongly decreasing with increasing (positive) l. The first-order width with Russell–Saunders coupling of a term with the S_{max} occurring in the groundstate, and L at least equal to S_{max} is $(L+\frac{1}{2})\zeta_{nl}$. Hence, a reliable estimate was available to Gobrecht of the distribution of near infrared absorption bands, assuming a smooth (more or less parabolic) increase of ζ_{4f} from $644\,cm^{-1}$ in gaseous Ce^{+3} to the 4.6 times larger value in Yb(III). Broer et al. (1945) compared the areas of absorption bands of aqua ions in solution, proportional to the oscillator strength P (called f by many authors). It turned out that most narrow absorption bands have a P between 10^{-7} and 10^{-5}, indeed very weak, as one would expect for Laporte-forbidden transitions inside a partly filled 4f shell. However, another striking difference from usual atomic spectra is that a large part, if not most, of the J-levels must have been detected in the readily accessible region before $30\,000\,cm^{-1}$. Broer et al. (1945) suggested a model of weak perturbations from odd-parity vibrations and influence from adjacent atoms, providing the liberal selection rule that J should not change by more than 6 units, but the distinction between spin-allowed and spin-forbidden transitions not being attenuated more than it already is by deviations from Russell–Saunders coupling (equally strong in gaseous Ln^{+3}). This model was independently elaborated by Judd (1962) and by Ofelt (1962). Recently, it has been reformulated by Schuurmans and Van Dijk (1984).

Once it was realized that there is an almost invariant ratio between the parameters of interelectronic repulsion in the f shell, both in the Slater–Condon–Shortley parametrization $F^2:F^4:F^6 \sim 1:0.75:0.5$, and in the treatment of Racah (1949) such as E^1 being 10 times larger than E^3, it was possible to construct a scheme of S,L-term energies, to which diagonal and non-diagonal effects of spin–orbit coupling can be added. Such a scheme was published by Elliott et al. (1957). At this time, it was clear that $q = 3$ to 11 show a little too many J-levels for one quietly relying on agreement with predicted energies. The last time this was done successfully, was probably by Wybourne (1960) for $4f^3$ Nd(III) and $4f^{11}$ erbium(III) each having 364 states distributed in 41 J-levels, able to form 17 S,L-terms.

In practice, two methods were supplementing the identification. One is to look for the maximum of $(2J + 1)$ sub-levels induced in a level by the 'ligand field' when q is even [for odd, q, at most $(J + \frac{1}{2})$ Kramers doublets can be formed]. This technique was mainly explored by Hellwege and collaborators in Darmstadt after 1948. The other technique is to rely on the Judd–Ofelt treatment, expressing the oscillator strength P of each band (it can also be applied to luminescent transitions) as a function of the sum $(\Omega_2 U_2 + \Omega_4 U_4 + \Omega_6 U_6)$ involving three matrix elements U_t

($t = 2,4,6$) to be evaluated once for all for a given Ln(III) with known energy levels, and three material parameters Ω_t characterizing each surrounding material for the lanthanide, and which are determined empirically from the absorption band P values. Fortunately, these parameters are overdetermined, because in practice, 5 to 10 transitions can be treated for q between 3 and 12. It is too lengthy to go into the details of the Judd–Ofelt treatment here (Peacock 1975, Reisfeld and Jørgensen 1977, 1987, Jørgensen and Reisfeld 1983a) but it should be emphasized that it allowed the identification of the large majority of J-levels below 30000 cm^{-1} because of the distinct U_t matrix elements (Carnall et al. 1968). Excepting Pm, there are only lacking below 25000 cm^{-1} two Nd, five Sm, one Dy and one Ho level, and among those, one transition in each of Sm, Dy and Ho is forbidden by the $\Delta J \neq 7$ selection rule of Broer et al. (1945). Giving the number of calculated J-levels above 25000 cm^{-1} and the number in parentheses identified by Carnall et al. (1968) for various Ln(III): 19 (11) Nd; 170 (21) Sm; 284 (26) Eu; 326 (19) Gd; 287 (16) Tb; 183 (15) Dy; 93 (24) Ho; 30 (17) Er; and 6 (5) for Tm. The J-levels below 42000 cm^{-1} are given in fig. 1.

One of the most prolific areas of publications about lanthanides, is 'ligand field' calculations. We should stress that the situation is quite different from d-group compounds. Here, the five d-like orbitals fall in various sets dependent on the point-group of the local symmetry. Thus, octahedral MX_6 chromophores have two strongly (and equally) anti-bonding orbitals; cubical MX_8 and cuboctahedral MX_{12} three; and quadratic MX_4 in practice only one strongly anti-bonding orbital, whereas the rest of the five orbitals are roughly non-bonding, or at the most, π-anti-bonding (Jørgensen 1969, 1971, 1975b, 1980a). This behavior was ascribed before 1956 to the (small) non-spherical part $V(x,y,z) - V(r)$ of the Madelung potential, but this is untenable, because most anions produce smaller 'ligand field' effects than neutral aqua and ammonia ligands. However, it cannot be denied that the spherical part of the Madelung potential $V(r)$ can be quite important for inorganic compounds (Jørgensen 1969, 1978c) as pointed out earlier by Van Arkel, and by Rabinowitch and Thilo (1930). The Russell–Saunders S,L-terms are disrupted by the energy differences, typically 1–5 eV (8000–40000 cm^{-1}), between the d-like orbitals, and only S remains as a reasonably good quantum number in typical compounds. For our purpose, it may be added that the 5d orbitals providing excited states of cerium(III) show energy differences more than half those met in rather covalent complexes of $5d^6$ iridium(III) and platinum(IV).

The situation is entirely different in the 4f group. The $(2J + 1)$ states of a given J-level keep closer together than 500 cm^{-1} in nearly all cases (Morrison and Leavitt 1982). The writer is only aware of one separation above 1000 cm^{-1}, i.e., the ground level $^6H_{15/2}$ of C-type Dy_2O_3 reported to be 1080 cm^{-1} (Henderson et al. 1967) which is a little bit surprising, when compared to 833 cm^{-1} in $Dy_xY_{2-x}O_3$ (Chang et al. 1982). The latter authors observe sub-levels of $^2F_{5/2}$ in Yb_2O_3 at 10219, 10640 and 11044 cm^{-1}, whereas the four Kramers doublets of $^2F_{7/2}$ are calculated to occur at 0, 491, 590 and 1036 cm^{-1}. Ytterbium oxide is a slightly unusual case, the Yb–Yb internuclear distance is only 3.50 Å (it is 3.88 Å in the metallic element) and the absorption spectrum (Schugar et al. 1975) shows weak lines in the green between

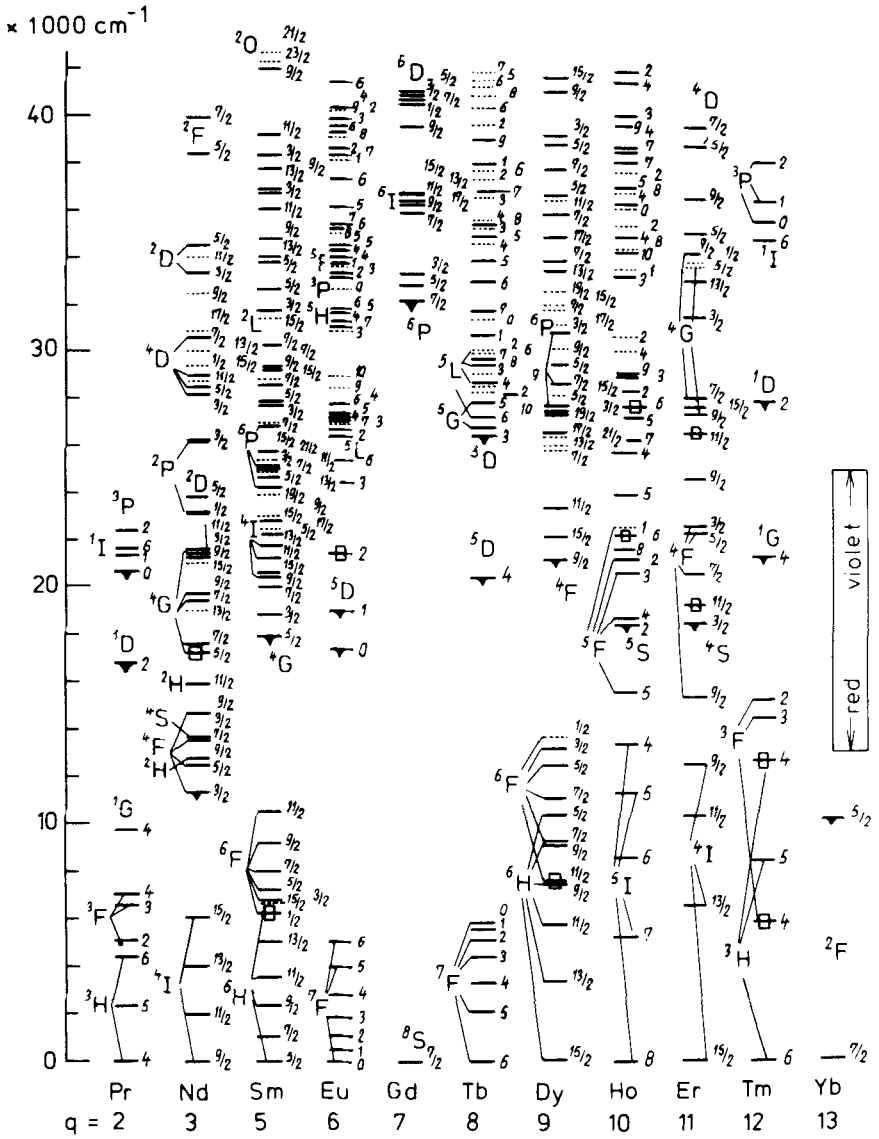

Fig. 1. Energy levels of trivalent lanthanides below 43000 cm^{-1} (5.3 eV) arranged according to the number q of 4f electrons. Excited levels known frequently to luminesce are indicated by a black triangle. The excited levels corresponding to hypersensitive transitions from the ground state are marked with a square. For each lanthanide, J is given to the right (in the notation of atomic spectroscopy, J is added to the Russell–Saunders terms as lower-right subscripts). When the quantum numbers S and L are reasonably well-defined, the terms are indicated to the left. It may be noted that the assignments $^3H_4$ and $^3F_4$ in thulium(III) previously were inverted; these two levels with $J = 4$ actually have above 60% of ^3H and ^3F character, respectively. Calculated J-levels are shown as dotted lines. They are taken from Carnall et al. (1968) who also contributed decisively to the identification of numerous observed levels, mainly by using the Judd–Ofelt parametrization of band intensities.

20490 and 21860 cm^{-1} due to one photon exciting two adjacent Yb(III) to their $^2F_{5/2}$ level. Such behavior is characteristic of strongly antiferromagnetic chromium(III) complexes (Glerup 1972; Glerup et al. 1983).

Anyhow, the splitting of a given J-level (normally well below 500 cm^{-1}) is somewhat smaller than the total energy separation of the seven 4f orbitals. One part of 'ligand field' theory is the general opinion that sub-level energy differences can be described exclusively as one-electron energy differences, multiplied by fractions between 0 and 7. However, not only are 4f one-electron energy differences described by the same *angular overlap* (AOM) (Jørgensen et al. 1963, Kuse and Jørgensen 1967, Linarès et al. 1977, Urland 1981, Garcia and Faucher 1983) as the d-group compounds (Schäffer and Jørgensen 1965, Schäffer 1982, Jørgensen 1971) but there is a growing argumentation (Jørgensen 1967a, Jørgensen et al. 1986) that the major part of the anti-bonding effect in both f- and d-group chromophores is connected with the kinetic energy operator of the Schrödinger equation applied to the polyatomic system (Jørgensen 1971). Correspondingly, the ratio between the angular overlap parameter and the square of the M–X overlap integral turns out (Faucher et al. 1986) to be somewhat above 100 eV for a large number of neodymium(III) and europium(III) cases on differing crystal sites, exactly as it is for several $3d^9$ copper(II) complexes (Smith 1978, Hitchman and Cassidy 1979). This huge ratio between angular overlap parameters and overlap integrals (cf. also Urland 1981) above 100 eV can hardly be connected with any quantity other than the angular part of the 3d kinetic energy of 175 eV for Hartree–Fock functions (kindly disclosed by Dr. R.E. Watson) of Fe^{+2}, 225 eV of Cu^+, and the 4f kinetic energy of 540 eV of Gd^{+3} (cf. Jørgensen 1975d) twelve times larger than $I_4 = 44$ eV of the gaseous ion, and 35 to 50 times larger than I(Gd 4f) determined from photo-electron spectra of solids (Jørgensen 1985a). It is true that 4f electrons are far less anti-bonding than 5d electrons, but it seems now established that the physical mechanism is the same in the two cases, the modified local contribution to the kinetic energy, as analyzed by Ruedenberg (1962) in the horribly complicated case of H_2. Like nostalgia, 'ligand field' theory is no longer what it used to be.

3.5. *The refined spin-pairing energy theory*

Hund (1927) gave rules for the quantum numbers of the groundstate of a monatomic entity containing one partly filled p, d or f shell. Assuming Russell–Saunders coupling, we make a distinction between the half-filled shell with $q = (2l + 1)$, the less than half-filled shell with q at most $2l$, and the more than half-filled shell with at least $2l + 2$ electrons. The highest possible value S_{max} of the total spin quantum number is $\frac{1}{2}q$ for shells at most half-filled, and $\frac{1}{2}(4l + 2 - q)$ for higher q. For the half-filled shell, there is only one term S_{max} having vanishing L (hence called ^{2l+2}S) with only one level according to Hund coupling, eq. (3), $J = S_{max}$. The groundstate belongs to the highest L value compatible with S_{max} (this is not normally the highest L value feasible for the configuration). For the q values $1; 2l; 2l + 2$ and $4l + 1$, there is only one term with S_{max} and it has $L = l$. The variation of L of the lowest term as a function of q is a parabola in each half-filled set

(looking like the arch in St. Louis). Thus, L is 3 for $q = 2, 3, 7$ and 8 in d shells, and L is 6 for $q = 3,4,10$ and 11 in f shells, symmetric around each quarter-filled shell (Jørgensen 1971). In the f shell, $L = 5$ for $q = 2,5,9$ and 12. When we consider the lowest term in Russell–Saunders coupling (which does not need to be a very good approximation for this purpose) the actual groundstate has $J = L - S_{max}$ before the half-filled shell is reached, and $J = L + S_{max}$ starting at $q = 2l + 1$. That means that the highest $J = 8$ is obtained for $q = 10$. Because of the dependence of the gyromagnetic factor g on J, S and L, it also means that dysprosium(III) and holmium(III) are more paramagnetic, have a higher number of Bohr magnetons, than gadolinium(III), though the latter element forms the metallic ferromagnetic lanthanide with the highest Curie temperature. The terms having the highest J value $S + L$ at lowest energy, followed by decreasing J values, are called 'inverted' in atomic spectroscopy. One should not extend the Hund rules beyond their legitimate domain of application, and in fig. 1, it is clearly seen that the order of Russell–Saunders terms for a given S is not generally arranged according to decreasing L, not even for S_{max}. However, there is a general trend for lower S values, on the whole, to correspond to higher energies.

In 1957, the writer found that the barycenters of all states of a given configuration [p^q, d^q, f^q, g^2 and g^9; the result was generalized to all l^q by Slater (1968)] having $S = S_0$ is situated $2DS_0$ below the barycenter of states having $S = S_0 - 1$, where D is a combination of parameters of interelectronic repulsion for a given l, but not depending explicitly on q (except via the change of numerical values of F^k from one z and/or q to another). This is equivalent to a spin-pairing stabilization $-D(S(S+1))$ and can then be expressed as a stabilization relative to the barycenter of l^q once the average $\langle S(S+1) \rangle$ for the whole configuration is known, namely

$$D\left\{\frac{3q(4l+2-q)}{16l+4} - S(S+1)\right\}, \tag{6}$$

which is identical for $(4l + 2 - q)$ and q electrons, in agreement with the rule of hole-equivalence found by Pauli. The most negative value of eq. (6) is obtained for the half-filled shell, $-Dl(l+1)(4l+2)/(4l+1)$ being $-\frac{168}{13}D$ for f shells. Further details of this treatment can be found in the books by Jørgensen (1969, 1971). It is trivial that if more terms differ in energy and have the same S_{max}, the Hund groundstate will be stabilized relative to the barycenter of all S_{max} states. This is the simple quantity $-\frac{9}{2}B$ for ^3F of d^2 and d^8 as well as for ^4F of d^3 and d^7. Racah (1949) gave the corresponding stabilizations $-9E^3$ of the ground terms ^3H of f^2 and f^{12}, and ^6H of f^5 and f^9; and $-21E^3$ for ^4I of f^3 and f^{11}, and ^5I of f^4 and f^{10}. It may be noted that $D = \frac{9}{8}E^1$ is roughly ten times larger than E^3. There is a general custom to put $D = 6500\,cm^{-1}$ in trivalent lanthanides, which is quite satisfactory, though this choice has been a little modeled by continuous divisions by 13 needed in the expressions. The 'refined spin-pairing treatment' adds a last contribution, the stabilization by spin–orbit coupling of the J groundstate relative to the barycenter of the lowest term. To the first order (Condon and Shortley 1953) the first half of the f shell has $-[(L+1)/2]\zeta_{4f}$ for this stabiliziation with $q < 7$, and the second half

$-\frac{1}{2}L\zeta_{4f}$. The numerical data are usually taken from observed spectra, the latter expression is almost 4500 cm^{-1} in $4f^{13}$ ytterbium(III).

On the whole, atomic spectroscopists were not particularly interested in comparing with the barycenter of an electron configuration, but rather considered the parametrizations of Slater (Condon and Shortley 1953) and Racah (1949) as applicable to the term energies relative to the lowest term. However, Catalán et al. (1954) compared configuration barycenters of configurations such as $[18]3d^q4s^2$, $[18]3d^{q+1}4s, \ldots$, in 3d group M^0 and M^+. This approach has a bearing on identifying excited levels of weak lines in the solar spectrum, and gave the first hints of parabolic variation of configuration barycenters, when varying $Z, z, K, q, \ldots$, and the more general occupation numbers in highly excited configurations of monatomic entities.

The writer got interested (Jørgensen 1956b) in the apparently wildly varying E^0 values for oxidizing M(II) to M(III) aqua ions of the 3d group across the series. One contribution was the 'ligand field' stabilization determined by the sub-shell energy difference Δ between strongly anti-bonding and roughly non-bonding d-like orbitals, which by itself was seen from absorption spectra to have values between 8000 and 18000 cm^{-1}. When the observed E° values were corrected for differences in 'ligand field' stabilization, a jump remained at the half-filled $3d^5$, amounting to 4 eV. It was also noted that D is about 7000 cm^{-1} for gaseous M^{+2}.

The situation in 4f compounds is simpler, by absence of significant 'ligand field' stabilized states, but it is indispensable to introduce the two additional contributions in the 'refined' treatment [the ordinary treatment being represented by eq. (6)] proportional to E^3 and to ζ_{4f}. This was done (Jørgensen 1962a) with the purpose of rationalizing the variation of electron transfer wave-numbers with q, where the M(III) groundstate is written $4f^{q-1}$ and the excited state $(MO)^{-1}4f^q$, where the absence of one electron in a filled set of orbitals is denoted by the exponent -1, as frequently done in X-ray spectra.

The lowest level of $4f^{q-1}5d$ relative to the lowest level of $4f^q$ can be treated with similar parameters, as shown in table 1 for gaseous M^{+2} and M(II) in fluorite and in aqueous solution. McClure and Kiss (1963) pointed out that a configuration such as $4f^{q-1}5d$ involving ten times more states than $4f^{q-1}$ has no evident reason in the Slater–Condon–Shortley parametrization to follow the refined spin-pairing treatment. It may be better in $M_xCa_{1-x}F_2$ than in M^{+2} because of the large separation above 12000 cm^{-1} between the 5d orbital energies. Nevertheless, it is also true that gaseous M^+ have the separation between the lowest J-levels of $[54]4f^{q-1}5d6s$ and of $[54]4f^q6s$ (Martin et al. 1978) approximately 4000 cm^{-1} below the distance in M^{+2} (for q up to 7) and 4000 cm^{-1} above the value for M^0 containing two 6s electrons. In the second half of the 4f group, this distance is about 6000 cm^{-1} smaller for M^+ than for M^{+2}, but only 3000 cm^{-1} larger for M^+ than for M^0 (Jørgensen 1975b). Such distances are called 'system differences' by Martin (1971).

In table 1, last column, the spin-pairing correction $\mathscr{R}$ is given in cm^{-1} already used in eq. (23.22) in Volume 3 of this Handbook, obtained by choosing the parameters $E - A = 3200\ cm^{-1}$, $D = 6500\ cm^{-1}$ and $E^3 = 500\ cm^{-1}$, using empirical ζ_{4f}. The first parameter indicates the stabilization of the 4f orbitals by increasing Z

by one unit, and keeping z constant by increasing q by one unit. It is written as a difference $E - A$ to remind one that the increased nuclear charge stabilizes the added 4f electron, but that the coefficient $\frac{1}{2}q(q-1)$ to $A_*(4f,4f)$ at the same time increases. We also give this function $\mathscr{R}$ in eV for q going from 1 to 14:

q	$\mathscr{R}$	q	$\mathscr{R}$	q	$\mathscr{R}$
1	0.16	6	3.74	11	2.48
2	1.55	7	5.00	12	2.48
3	2.59	8	·0.10	13	3.37
4	2.68	9	1.48	14	4.61
5	2.75	10	2.46		

(7)

showing a variation with an amplitude of almost 5 eV. This choice of $(E - A)$ gives marginally smaller $\mathscr{R}$ for $(q + 7)$ than for q 4f electrons. The most accessible comparison is the difference of $\mathscr{R}$ between 7 and 14 being

$$-7(E - A) + \tfrac{48}{13}D + 1900\,\mathrm{cm}^{-1}, \tag{8}$$

where $1900\,\mathrm{cm}^{-1}$ is the difference between the spin–orbit stabilization value of $4500\,\mathrm{cm}^{-1}$ of Yb(III) ($q = 14$) and $2600\,\mathrm{cm}^{-1}$ of Eu(III) ($q = 7$). In eq. (8), the first two contributions, $-23\,400\,\mathrm{cm}^{-1}$ and $+24\,000\,\mathrm{cm}^{-1}$, almost cancel. Using eq. (8), it was argued (Jørgensen 1980c) that $(E - A)$ seems to be marginally larger in relatively more covalent compounds. Thus, $(E - A) = 3200\,\mathrm{cm}^{-1}$ in MI_6^{-3} dissolved in acetonitrile; $2980\,\mathrm{cm}^{-1}$ for MBr_6^{-3} in acetonitrile and for MCl^{+2} in ethanol; and was suggested to be close to $2820\,\mathrm{cm}^{-1}$ in aqua ions and in fluorides. Actually, it is $2780\,\mathrm{cm}^{-1}$ if eq. (8) is applied to the E° standard oxidation potentials discussed below, but it is important to realize that E° refer to non-adiabatic reactions with strongly modified internuclear distances.

It may not be accidental that table 1 describing optical transitions from M(II) to M[III] states containing one 5d electron, and table 2 from M(III) groundstates to M[II] containing one 4f electron more, fit so well together. In a certain sense, it is the same type of reaction in opposite directions. When it comes to the ionization energies I_3 of gaseous Ln^{+2} and I_4 of Ln^{+3} (Sugar and Reader 1973) reproduced in table 23.1 of this Handbook (Jørgensen 1979a) the agreement is qualitatively good, but numerically less impressive. I_3 increases from 18.28 eV for La^{+2} (referring to [54]4f slightly above the groundstate belonging to [54]5d and having an ionization energy 19.18 eV) to 24.70 eV for Eu^{+2}, and then from 20.34 eV for Gd^{+2} to 25.03 eV for Yb^{+2}. If $\mathscr{R}$ of eq. (7) is subtracted from I_3, a smooth increase from 18.1 eV to 19.7 eV is observed in the first half of the shell, whereas $I_3 - \mathscr{R}$ oscillates weakly around 20.33 eV in the second half. By the same token, I_4 increases from 36.76 eV for Ce^{+3} to 44.01 eV for Gd^{+3}, and from 39.79 eV for Tb^{+3} to 45.19 eV for Lu^{3+}. The difference $I_4 - \mathscr{R}$ increases smoothly from 36.6 to 39.0 eV in the first half, and from 39.7 to 40.6 eV for Tb^{+3} to Lu^{+3}. It may be noted that eq. (8) has the opposite sign of the usual for Eu(II) and Yb(II), it is -0.33 eV comparing Eu^{+2} with Yb^{+2}, and -1.57 eV between Gd^{+3} and Lu^{+3}. This discrepancy cannot be removed by

changing $(E - A)$ to another value, the fundamental trouble is that the increase of I_3 (6.4 eV) and of I_4 (7.25 eV) in the first half of the 4f shell is larger than in the second half (4.7 and 5.4 eV). Of course, the atomic spectroscopist may ask the chemist why $E - A$ should be invariant across the lanthanides. There have actually been suggestions published that $E - A$ may decrease for higher Z having smaller average radii of the 4f shell, and hence 'A' increasing. It is rash to stretch a rationalization beyond its elasticity, and it may be that the earlier Ln are still contracting in a way slightly different from the truly inner 4f shell in the case of higher Z.

Nugent et al. (1973) applied the refined spin-energy treatment to study $E°$ of 4f and 5f group M(II) and M(III) aqua ions in weakly acidic solution. The least reducing Ln(II) not measured by Butement (1948) is thulium(II) predicted to have $E° = -2.3$ V. All the other Ln(II) should have $E°$ below -2.6 V. The values for Ln(III) aqua ions, Ce(III) 1.8 V, Pr(III) 3.4 V, and Tb(III) 3.3 V, have the weak point that the oxidized M(IV) is unlikely to occur as an aqua ion, even if it remains in solution as an oligomeric hydroxo complex. Nevertheless, the predicted $E°$ are useful for giving an idea of the difficulty of making a solid, anhydrous fluoride. Thus, the order of decreasing stability of Ln(IV) should be Ce, Tb, Pr, Nd, Pm, Dy, Sm, Tm, Er, Ho, Eu, Yb, Gd and Lu, which certainly is compatible with the data in section 2.2. Among the transthorium elements, the first M(II) aqua ion having $E°$ above -3.5 V (meaning instability toward disproportionation to the metallic element) is $5f^7$ americium(II) with $E° = -2.3$ V like Tm(II). Electron transfer spectra of $CfBr_6^{-3}$ and $EsBr_6^{-3}$ have helped establishing $E°$ for $5f^{10}$ californium(II) aqua ions to -1.6 V, and of $5f^{11}$ einsteinium(II) to -1.2 V. The values of $E°$ are -1.1 V for $5f^{12}$ fermium(II), -0.1 V for $5f^{13}$ mendelevium(II) and, quite surprising [but in agreement with the radium-like chemistry reported by Silva et al. (1974)] $E°$ is $+1.4$ V of the nobelium(II) aqua ion having an ionic radius between that of strontium and calcium. Hence, $K = 100$ like for lawrencium(III), undoubtedly the most important oxidation state of $Z = 103$.

Some of the nicest confirmations of the spin-pairing treatment come from the photo-electron spectra of solids, as discussed in the next sub-section. A related topic is the criterion for metallic and semiconducting solids choosing between Ln[III] and Ln[II], to which we return in section 4.5. However, it is worthwhile here to include the small, but perceptible, impact of spin-pairing energy on formation constants of complexes in solution (free energy changes relative to aqua ions). Jørgensen (1956b) suggested that there may be two reasons for $3d^5$ manganese(II) generally forming weaker complexes than adjacent M(II). One is the absence of 'ligand field' stabilization in the ^6S groundstate of Mn(II) having exactly one electron in each of the five d-like orbitals, regardless of local symmetry. The other is that the stabilization $-\frac{20}{3}D$ relative to the d^5 configuration barycenter might be diminished by a small nephelauxetic decrease of D [evaluated from absorption spectra (Jørgensen 1969)] relative to the aqua ion. Decreased formation constants of complexes of $4f^7$ gadolinium(III) and adjacent Ln(III) are indeed well-established (Fidelis and Mioduski 1981) and it is excluded that they are due to 'ligand field' stabilization. The stabilization of the groundstate ^8S relative to the $4f^7$ barycenter is $-\frac{168}{13}D$ according to eq. (6), of the order 10 eV, and less than a percent variation of this

energy difference can certainly have dramatic results. A closer analysis (Jørgensen 1970a, Nugent 1970) shows that the observed phenomena are more readily explained by a somewhat stronger variability of E^3, relative to the aqua ions, than the quite minute change of E^1, the major component of D. There remains a slightly enigmatic question: why is there a minor irregularity of the decreasing ionic radii of Ln(III) as a function of increasing Z, actually making Gd(III) slightly bigger than an interpolation between the neighbor elements. Some authors argue that the 4f shell contracts, allowing the more external 5p shell to expand.

This line of thought was elaborated by Vanquickenborne et al. (1986) comparing Hartree–Fock wave-functions [54] $4f^q$ for gaseous ions Ln^{+3} from Ln = Pr($q = 2$) to Tm($q = 12$) having flexible radial functions (for the 4f and for all the inner shells) being slightly different for each S value. This optimalization differs from the conventional SCS (Slater–Condon–Shortley) treatment (Condon and Shortley 1953) where all S,L-terms of a given configuration are assumed to have exactly the same radial functions as the lowest term. This novel flexibility is required by the virial theorem. All solutions of the Schrödinger equation with negative eigen-value E satisfy the relation that the total potential energy $V = 2E$ and the total (positive) kinetic energy $T = -E$. This, by the way, is the reason that atomic spectroscopists tend to use the unit 1 rydberg for E, half as large as the atomic unit 1 hartree for V. Since a monatomic entity with more than one electron has $V = Q + C$ where the nucleus–electron attraction $-Z\langle r^{-1}\rangle$ contributes a negative quantity (for each electron with average $\langle r^{-1}\rangle$ in reciprocal bohr units) to Q (Q is called L by many authors, but it is helpful to avoid confusion with the quantum number L of terms), and C is the sum of the $\frac{1}{2}K(K-1)$ contributions $\langle r_{12}^{-1}\rangle$ hartree/bohr for each distinct pair formed by the K electrons. The conventional SCS treatment predicts invariant T and Q (because of identical nl-radial functions) for higher terms of a given configuration, but at the same time a more positive C (and hence less negative V). This discrepancy from the virial theorem (demanding T of terms at higher E to decrease half as much as V increases) was analyzed by Katriel and Pauncz (1977), in particular for the iso-electronic series $K = 2$ and 6 as a function of increasing Z.

The Hartree–Fock results (Vanquickenborne et al. 1986) with flexible radial functions do not produce a striking variation of the radial functions for different S values belonging to a given [54]$4f^q$. Thus, the average distance $\langle r\rangle$ of the 4f electrons from the nucleus varies less than 2%, compared with the average for a given q. In the following, we concentrate on the four $S = \frac{1}{2}, \frac{3}{2}, \frac{5}{2}$ and (the groundstate) $\frac{7}{2}$ of Gd^{+3}. It turns out that $\langle r\rangle$ of 4f contracts with increasing S and is proportional to $[1 + kS(S+1)]$ with $k = -0.00116$. On the other hand, $\langle r\rangle$ of the filled 5p shell expands (perhaps explaining the slightly increased ionic radius of $4f^7$ systems) with $k = +0.00019$, and all the other inner shells with even smaller positive (or vanishing) values. However, when the spin-energy parameter D is evaluated according to eq. (6), a rather paradoxical redistribution of the seven components of Hartree–Fock E values occurs. Writing $E = T + Q + C$, the kinetic energy $T = T_c + T_f$, the nucleus–electron attraction $Q = Q_c + Q_f$, the interelectronic repulsion $C = C_{cc} + C_{cf} + C_{ff}$, where the subscript c refers to closed shells, and f to the partly filled 4f shell, it turns out (Vanquickenborne et al. 1986, Jørgensen 1988) that the contributions to the

calculated D value of 1.1 eV (for Gd^{+3}) are $+3.5D$ from T_c, $-4.5D$ from T_f (and hence $-D$ from the total T); $-7D$ from Q_c, $+13D$ from Q_f (and hence $+6D$ from Q); $+3.5D$ from C_{cc} (almost equal to the T_c contribution), nearly $-8D$ from C_{cf}, and only $+0.4D$ from C_{ff} with the counterintuitive result that the total contribution of interelectronic repulsion C is approximately -4 times the calculated D; and ten times larger than the SCS result, with opposite sign.

The three energy differences $3D$, $5D$ and $7D$ between consecutive S values of $[54]4f^7$ provide almost identical D values. Such behavior is also found in other Hartree–Fock results involving flexible radial functions. Thus the radial part T_{rad} (Jørgensen 1969, 1971) of the kinetic energy T_f is almost exactly 10% of the angular part T_{ang} (Vanquickenborne et al. 1986, and private communication). The huge $T_{ang} = 6\langle r^{-2} \rangle$ hartree/bohr^2 is 535.4 eV + (0.56 eV)$S(S+1)$.

The SCS treatment for 4f electrons was thoroughly analyzed by Racah (1949), introducing three ingeniously chosen parameters of interelectronic repulsion, one of which is $E^1 = \frac{8}{9}D$. This analysis is now being continued by Brorson and Schäffer (1987) for 3d electrons in both spherical and lower symmetries (i.e. compounds).

3.6. *X-ray and photo-electron spectra*

We have mentioned several times the important arguments derived from the X-ray spectra as the indicator, common for nearly all the Periodic Table, of the parameter Z that Mendeleev correctly suspected of subsisting behind the atomic weights as an earlier principle of sequential ordering. However, their behavior is by no means so simple as insinuated in textbooks. For two-digit Z values, the innermost shell 1s is in good shape. The Moseley expression in rydberg is $I(1s) = (Z - Z_s)^2$ where the screening constant Z_s goes from 2.0 in neon up to 2.65 at silver ($Z = 47$) and back to 2 at platinum ($Z = 78$). This mild variation of Z_s does not modify the slope $(dI/dZ) = (Z - Z_s)$ 27.2 eV strongly. When photo-electron spectra of lighter elements were also studied extensively (Jørgensen and Berthou 1972b), it turned out that $I(1s)$ between lithium and aluminum is only $Z(Z-1) \times 9.7$ eV with $(dI/dZ) = (2Z - 1) \times 9.7$ eV, only 71% of the hydrogenic value. This result can, of course, be described as a rapid increase of Z_s from 0.31 in helium to 2.0 in neon. Before reviewing much more worrying facts, it may be useful to summarize the ideas of X-ray spectroscopists. The almost identical Rydberg defect, eq. (1), of gaseous Ba^+ and Ra^+ (except that all values are increased by one unit, 6s, 6p, 5d and 4f in barium being replaced by 7s, 7p, 6d and 5f in radium) can be rationalized by almost perfect screening, the 32 electrons added in radium almost exactly compensating the increase of Z from 56 to 88. Such screening would ideally introduce $I(2p) = (Z - Z_s)^2 \times 3.4$ eV (the latter quantity being a quarter rydberg) and $I(3d) = (Z - Z_s)^2 \times 1.51$ eV (a-ninth of a rydberg) for inner shells, where the screening constant might be, say, 7 for 2p and 17 for 3d electrons of various elements. Unfortunately, this does not at all work, the 'constant' Z_s varies unexpectedly with Z, as we shall see, and tends also to be uncomfortably large. One way of escape is to invoke 'external screening'. In an electrostatic 'central field' $U(r)$ with the dielectric constant 1, charges outside the surface with r_0 have an effect on the potential at r_0

which is r_0/r times the effect they would have, if their distance from the nucleus were r_0 rather than r. The 1s orbital has an average radius close to the value for $K = 1$, i.e. 3 bohr/2Z, close to 0.011 Å for $Z = 70$, about 1% of the ionic radius of Yb(III). Under these circumstances, it is not surprising that the external screening contributes about 2 units to Z_s. The other 1s electron is supposed to screen roughly 0.3 as in helium.

Coster (1923) shows irregular variations of $I(nlj)$ for all the other shells, especially when closed-shell K values are passed, and during the intervals of Z belonging to d- and 4f-groups. These irregularities are usually plotted as I or $\sqrt{I}$ varying as a function of Z, the latter square-root varying locally 1% for each 2% variation of I. A much more instructive plot is the slope dI/dZ given for 2p between $Z = 10$ and 33; 3p between $Z = 17$ and 42; 3d between $Z = 28$ and 60; and finally 4d between $Z = 45$ and 60 (Jørgensen 1974a) and also for $3p_{3/2}$ and $3d_{5/2}$ between $Z = 39$ and 83, and for $4d_{5/2}$ between $Z = 47$ and 83 (Jørgensen 1973b). Among these slopes, 2p wiggles quite a lot, but remains below half the hydrogenic value $Z \times 6.8$ eV (a half rydberg) in the whole interval studied. The hydrogenic slope for $n = 3$ is $Z \times 3.02$ eV, but nevertheless, a line with half this constant $(Z - 15) \times 1.5$ eV lies above all the experimental points of dI/dZ (obtained as the difference of I from one element to the next) for 3p up to $Z = 79$ and for 3d up to $Z = 83$. This discrepancy becomes grotesque for the 4d slope. One can combine the points around $Z = 56$ and $Z = 80$–83 with a straight line increasing 0.6 eV per unit of Z, in spite of the hydrogenic slope being $Z \times 1.7$ eV. Nevertheless, this line overshoots the observed behavior in the transition-groups; the actual dI/dZ values are one third of the straight line in the lanthanides, and two-thirds between $Z = 71$ and 79. Said in other words, $I(4d_{5/2})$ increases from 67.5 eV in xenon atoms to 109 eV in lanthanum(III) compounds, and then slowly increases [as seen from photo-electron spectra (Jørgensen and Berthou 1972b)] to 203 eV in lutetium(III), on the average 6.7 eV per element. Rather than to restrict attention to an algebraic manipulation of slopes (and their slopes) it may be instructive to contemplate the actual $I(nlj)$ of truly inner shells obtained from X-ray spectra of the next to last lanthanide, ytterbium. Thus, $2p_{3/2}$ has $I = 8943$ eV or 657.6 rydberg. If the square-root of the latter number, 25.64, is multiplied by $n = 2$, one obtains 51.28, showing the screening constant to be 18.7. This is an unexpected high value of Z_s indicating a predominant role of external screening. This situation is more extreme in $3p_{3/2}$ having $I = 1950$ eV, and $3d_{5/2}$ with $I = 1528$ eV. The analogous numerical treatment indicates $Z_s = 34$ and 38 in these two cases, and $4p_{3/2}$ having $I = 344$ eV provides $Z_s = 50$. It may be added for comparison that $Z = 70$ and $K = 1$ in the non-relativistic Schrödinger equation has $I = 7407$ eV for $n = 3$, and $I = 4166$ eV for $n = 4$, approximately four and eight times the values observed in Yb.

These strong effects of external screening are well described by the Hartree–Fock model. In the Hartree approximation, the spherical average of the repulsion from the other $(K - 1)$ electrons is subtracted from the potential Z/r (in the atomic units of hartree/bohr) originating in the nucleus considered as a point, and the Schrödinger equation is solved for radial nl-functions in this central field $U(r)$. This needs an iterative process in order to obtain self-consistency between radial func-

tions and $U(r)$. The Hartree–Fock approximation includes a further refinement involving certain parameters of interelectronic repulsion, and in agreement with the variational principle, slightly lower eigen-values are obtained than in the earlier Hartree treatment. As discussed in section 4.8, the Hartree–Fock model has several problems in many-electron atoms (really for K above 3, already) and one is that the integrals of interelectronic repulsion derived from the radial functions for monatomic entities with a partly filled 3d shell tends to be $(z + 3)/(z + 2)$ times the Slater–Condon–Shortley parameters evaluated from atomic spectra (Jørgensen 1962c,d, 1969, 1976c) and further on, tend to be somewhat dependent on the S,L-term considered. These discrepancies are worse for Ln^{+3}, the F^k calculated for Hartree–Fock radial functions being about 1.3 times the parameters obtained from M(III) spectra, even allowing for a nephelauxetic decrease of 2–3%. It is convenient to talk about integrals of interelectronic repulsion, when calculated from radial functions. Anyhow, there are several good reasons to believe that Hartree–Fock functions for monatomic entities are quite accurate for the electronic density in our three-dimensional space, even for the individual shells.

Already in the observed X-ray spectra, as well as in the Hartree–Fock calculations the hydrogenic order of $I(nl)$ is respected, each group of the same n is separated from the adjacent $(n - 1)$ and $(n + 1)$, and arranged according to monotonically decreasing I for increasing l. There are some minor exceptions to this rule, somewhat related to eq. (2), when 4f crosses 5p close to $Z = 76$, and 4f crosses 5s at $Z = 83$, restoring n-ordering for higher Z (Jørgensen 1976b). There is little doubt that the full 5f shell is going to cross 6p somewhere above $Z = 104$.

Experimentally, it is very difficult to work with soft X-rays below 1000 eV (corresponding to 12 Å). This is one out of many reasons that photo-electron spectrometry has resolved many important (and in part unforeseen) problems for chemists. This technique, identifying the kinetic energy of an ejected electron with the difference between $h\nu$ of the mono-energetic photons bombarding the sample, and the ionization energy I to be measured, falls in two major branches. The study of gaseous samples (Turner et al. 1970, Rabalais 1977) was developed by Turner of the Imperial College of Science and Technology in London (later at the University of Oxford) since 1962, whereas work on solids originated at the the University of Uppsala, and was followed by work with commercial instruments available after 1970. The gaseous samples were, in the beginning, bombarded with 21.2 eV photons (the strongest ultraviolet emission line of the helium atom) and later also with 40.8 eV (3 rydberg, the $2p \rightarrow 1s$ line of He^+). The resolution obtained with gaseous molecules is excellent, showing a lot of vibrational structure, and even rotational structure in H_2. The main impact on chemists of this branch has been the acceptance of penultimate MO as experimentally accessible entities; previously, they had been a little suspected for being calculational artifacts with the (irrelevant) argument that a unitary transformation of an anti-symmetrized Slater determinant does not modify the wave-function (as discussed in section 4.8, many-electron Ψ are quite distinctly not exact anti-symmetrized determinants).

Photo-electron spectrometry of solids started (Hagström et al. 1964) as an

alternative to X-ray spectra at I values in the difficult range from 1000 to 2 eV. Photons used originate mainly in the $2p \rightarrow 1s$ transition in magnesium or aluminum anti-cathodes, providing 1253.6 or 1486.6 eV, respectively. In non-metallic samples, the resolution has difficulties getting better than 1 eV, and it is also difficult to get I reliably better than 0.3 eV. It does not seem (Jørgensen and Berthou 1972b, 1975a) that the somewhat mythological Fermi level of non-conducting samples is a satisfactory state of reference, and on the other hand, it seems that there exist realistic methods of obtaining charge-compensated I' values relative to vacuum, like for gaseous atoms and molecules, using for instance I(C 1s) = 290.0 eV for the one-sided Scotch Tape from the 3M company, of which the surface is $(CH_2)_x$ without any oxygen or other heavier atoms bound to carbon. Metallic samples show a I^* value relative to the Fermi level, which can be obtained more precisely (say, 0.1 eV) in fortunate cases.

Though chemical shifts of X-ray absorption edges of order 10 eV were known previously, the chemical effect on two differing shells, say I(1s) and I(2p) is normally so similar that X-ray emission lines usually shift less than 1 eV. Many chemical shifts up to 8 eV were found in photo-electron spectra of several elements, such as boron, carbon, nitrogen, sulfur, chlorine, chromium, selenium, bromine, palladium, iodine, ..., in 600 non-metallic compounds containing 77 elements (Jørgensen and Berthou 1972b). The original opinion had been that the important parameter determining the chemical shift is the oxidation state z, but this could soon be refuted. Most compounds of cobalt(II), thallium(I) and lead(II) have higher I values than almost all measured Co(III), Tl(III) and Pb(IV). Around 1974, it was believed that the two major factors are the fractional atomic charge (well below z) which can be estimated from the nephelauxetic effect in d-group compounds (Jørgensen 1969), and the Madelung potential agreeing qualitatively with the I' values of alkali-metal halides, though it was a little worrisome that the full Madelung potential predicted both M^+ and X^- to have I' 1 to 2 eV higher than observed. A closer investigation of the I(1s) of the neon atom opened the eyes to the large extent of intra-atomic relaxation effects, I typically being 0.8 times the square-root of I (in eV) predicted by Hartree–Fock functions lower than the predicted value (870.2 and 891.7 eV in neon), and interatomic relaxation effects (contributing to the chemical shift) of order 5 eV (Jørgensen 1974b). Since the change of interatomic relaxation energy can readily have the opposite effect of fractional charges and the Madelung potential, it became quite difficult to predict the chemical shift. That such contributions exist, is clear-cut in the gaseous mercury atom, where all the inner-shell $I(nlj)$ decrease by 3 eV by condensation to the metallic state. Even more strikingly, Perera et al. (1982) found that inner shells in gaseous alkaline-earth atoms have I about 10 eV higher than I^* of the metallic elements. After correcting for the work function of the metals, the decrease of I is found to be 4.6 eV for Mg 1s; 7.5 eV for Ca 2p; 5.5 eV for Sr 3d, and 5.2 eV for Ba 3d. This is an extreme case of a quite general effect of strong chemical polarizability (Jørgensen 1975a). Other interesting phenomena regarding inner shells include the regular linear variation of the inner-shell ionization energies ΔI (relative to the gaseous ion M^{+z}) in compounds of iso-electronic series of closed-

shell K values (Jørgensen 1978c) where the $\Delta I/z$ in eV turn out to be

K	$\Delta I/z$	K	$\Delta I/z$
2	$11.0 + 3.3z$	28	$10.0 + 1.0z$
10	$10.7 + 1.0z$	36	$7.8 + 0.8z$
18	$7.5 + 1.5z$	68	$7.7 + 0.9z$

(9)

which is the sense in which, for instance, chlorinet(−I), potassium(I), calcium(II), scandium(III),..., join the I(3p) of argon. By the way, gaseous ions with $K = 28$ (having the closed shell $n = 3$ from a hydrogenic point of view) such as Sm^{+34}, Gd^{+36} and Dy^{+38} have far-ultraviolet lines (Martin et al. 1978) playing an important role for the opacity of plasma, where one attempts to induce thermonuclear fusion. Klapisch et al. (1986) discussed $3d^9$–$3d^84f$ transitions in $K = 27$ systems such as Tm^{+42}, Yb^{+43} and Hf^{+45}; and $K = 31$ (Tm^{+38} to Re^{+44}); and $K = 32$ (Hf^{+40} to Re^{+43}).

Though inner shells provide interesting information for chemists, their main use of photo-electron spectra is the valence region with I below, say, 30 eV. Unfortunately, the signals induced by X-rays in this region tend to be quite weak (Jørgensen and Berthou 1972b, Berthou and Jørgensen 1975) though this presents a few advantages too. The 232 valence-shell electrons in hafnium(IV) mandelate, $Hf(C_6H_5CHOHCO_2)_4$, has a much weaker signal area than the 14 electrons in the Hf 4f shell. One of the great surprises was that the optical electronegativities x_{opt} introduced in eq. (5) for rationalizing electron transfer spectra have the following relations to halogen atoms and gaseous halide anions:

	F	Cl	Br	I	H
I_0 of X^-	3.40	3.61	3.36	3.06	0.75
I_1 of X^0	17.42	12.97	11.81	10.45	13.60
x_{opt}	3.9	3.0	2.8	2.5	3.2?
$3.7x_{opt}$	14.4	11.1	10.4	9.3	12?

(10)

with energies in eV. The constant 30 000 cm^{-1} of eq. (5) has been translated to 3.7 eV. It turns out that gaseous halide (and hydride) molecules have I of the loosest bound MO some 0–1 eV higher than $3.7x_{opt}$, whereas the loosest bound shell in halides (disregarding partly filled d- and f-shells) in solids has I some 1–2 eV lower than $3.7x_{opt}$ (which was not intended for this purpose). It is also interesting to compare $I = 12.6$ eV of the loosest bound MO of the gaseous H_2O molecule with $x_{opt} = 3.5$ multiplied by 3.7 eV, giving 12.9 eV. The large decrease of observed I values from gaseous molecules to (even non-metallic) solid compounds must be connected with a more pronounced interatomic relaxation in solids.

The result for filled MO in eq. (10) is closely related to an old dilemma in the quantum-chemical treatment of lanthanide compounds, which quite clearly (perhaps with the exception of R_2O_3) are not particularly covalent, and erbium(III) certainly

less covalent than thallium(III) with similar ionic radius. The usual thought about a heteronuclear bond MX is that it is pronounced covalent if the orbitals of M and X have comparable energy, i.e., they have closely similar diagonal elements of one-electron energy in the Hückel model. On the other hand, if the orbitals of M are loosely bound compared to X (such as F) the covalent bonding does not contribute much to a situation remaining essentially electrovalent. The photo-electron signals of the 4f electrons demolished this familiar picture (Jørgensen 1973b) and we have not fully recovered today. In $4f^7$ gadolinium(III) and $4f^{14}$ lutetium(III) compounds, it costs more energy to ionize a 4f electron than the loosest bound MO on the ligating atoms, and in $4f^6$ europium(III) and $4f^{13}$ ytterbium(III) fluoride and oxide, it costs almost the same energy. This should induce strong covalence, in blatant disagreement with the spectroscopic evidence from the partly filled 4f shell. The situation is different, but not easier to understand, in NaCl-type antimonides MSb of which fresh surfaces can be exposed to the X-rays by breaking the crystals inside the photo-electron spectrometer (Campagna et al. 1974, 1976). Table 23.4 of ch. 23 of this Handbook (Jørgensen 1979a) gives the lowest $I^*(4f)$ (as well as the higher I^* signals) for metallic Ln and for LnSb. In the antimonides, I^* increases from 3 eV for CeSb to 9.1 eV for GdSb, and then from 3.2 eV in TbSb to 5.5 eV in TmSb, a $4f^{12}$ system. The I values relative to vacuum should be 3 eV higher than I^*. In all the LnSb crystals, a Sb 5p signal can be detected at I^* close to 2.0 eV, hence lower than the first Ln 4f signal. In other words, the filled Sb 5p has lower ionization energy than the partly filled 4f shell. A comparable situation of anti-bonding orbitals in a partly filled 3d shell having higher I than their bonding counterpart has also been detected in certain iron(III) and copper(II) compounds (Jørgensen 1974a, 1975b).

The angular overlap model has its origin (Jørgensen et al. 1963) in the Wolfsberg–Helmholz model (Jørgensen 1962c, 1971) which is a Hückel treatment with specific assumptions. When in 1971 photo-electron spectra became available of many lanthanide compounds, the Wolfsberg–Helmholz model assuming anti-bonding effects proportional (with a factor close to 1) to $(H_M S_{MX})^2/(H_M - H_X)$ ran into three propositions, among which any two are incompatible with the third. It was established that solid chlorides have the order of magnitude 10 eV for $-H_X$, that electron transfer spectra of chloro complexes of lanthanide(III) start above 4 eV, Eu(III) being the lowest and Gd(III) extrapolated to 9 eV, and that $E^\circ + 4.5$ eV representing the non-adiabatic ionization energies of Ln(III) aqua ions is from 6.2 eV for Ce(III) up to 12.4 eV for Gd(III) (Nugent et al. 1973) and 4.1 eV for Eu(II) aqua ions. Though the very weak 'ligand field' effects on the 4f shell and the small overlap S_{MX} do not necessitate a very large denominator $(H_M - H_X)$, it is painful if it is below 5 eV (Garcia and Faucher 1983) and, as Zorbas says, it is the full catastrophe if the denominator is negative, as is difficult to avoid in LnSb. One way out of this dilemma is to adapt the opinion of Hubbard (Naegele et al. 1985) that the extent of covalent bonding in 4f and 5f group compounds is not determined by the I of the ligands, but by the electron affinity of the partly filled shell. As discussed below, $I^* = 8.0$ eV in metallic gadolinium gives a lower limit to this difference, and it actually must be close to 8 or 9 eV in Ln(III) compounds. But rather than

introducing this Hubbard parameter in the Wolfsberg–Helmholz model as the denominator $(H_M - H_X)$, it is probably advisable to accept that the 'ligand field' effects are directly connected with the local operator of kinetic energy in the Schrödinger equation, multiplying $(S_{MX})^2$ by an energy slightly above 100 eV (Jørgensen 1971, Jørgensen et al. 1986).

Whereas the compounds measured in Geneva were held at a pressure close to 10^{-6} Torr (Jørgensen and Berthou 1972b), it is necessary to measure metallic lanthanides below 10^{-10} Torr (Cox et al. 1973) though one advantage is that oxide formation can be detected by the O 1s signal, independently of the oxide being crystalline or amorphous. If all the J-levels of the ionized configuration $4f^{q-1}$ produced signals of comparable intensity, the values from $q = 3$ to 13 would have produced a broad feature, several eV wide. Fortunately, the intensities are strongly governed by numerical selection rules determined by coefficients of fractional parentage (cf. Goldschmidt 1978) and the spectra turn out to be quite instructive (Cox 1975, Jørgensen 1975b). One of the more attractive conclusions is that the nephelauxetic ratio has moderate values above 0.9 in Ln[IV] formed by ionization, smaller in the chemically oxidizing Tm[IV] than in Tb[IV]. As seen in table 23.4 of ch. 23 of this Handbook, the five signals of Tm[IV] are spread 5.5 eV in metallic thulium from $^4I_{15/2}$ to $^2L_{17/2}$ of $4f^{11}$, to be compared with 5.7 eV in TmSb and 5.2 eV in the absorption spectrum of erbium(III) aqua ions (Carnall et al. 1968) which have smaller parameters of inter-electronic repulsion by having $z = 3$ rather than 4. By the same token the six signals of metallic erbium, and of ErSb, are spread 4.6 eV from $^5I_8$ to $^3M_{10}$ of $4f^{10}$ Er[IV], to be compared with 4.3 eV in holmium(III) aqua ions. The most astonishing material is perhaps the NaCl-type thulium telluride containing comparable amounts of Tm[III] and Tm[II] in the ground state. When the Tm[II] on an instantaneous picture is ionized to Tm[III], the J-levels of $4f^{12}$ are spread 0.98 to 0.99 times the separations known from thulium(III) aqua ions, whereas the Tm[IV] obtained by ionizing Tm[III] present on the instantaneous picture of the ground state has a nephelauxetic ratio close to 0.90. This agrees with the Copenhagen principle of final states, i.e., the photo-ionization produces the eigen-state of the ionized system.

The influence of the conditional oxidation state in the sample can be seen in metallic europium having $I^* = 2.1$ eV for the ionization from ^8S of $4f^7$ to ^6F of $4f^6$ that is 5.9 eV below the iso-electronic gadolinium. Similar effects were observed early (Eastman and Kuznietz 1971) in semiconducting NaCl-type EuS having $I^*(4f) = 1.8$ eV (and hence, I close to 6 eV) and the isotypic metal GdS with $I^* = 8.9$ eV. Metallic ytterbium has $4f^{14}$ ionizing to $^2F_{7/2}$ of $4f^{13}$ with $I^* = 1.1$ eV and to the other J-level $^2F_{5/2}$ with $I^* = 2.4$ eV, to be compared with $I^* = 7.1$ and 8.6 eV in metallic lutetium. If the observed I^* values are corrected for spin-pairing effects by subtracting $\mathscr{R}$ of eq. (7), the difference is as low as 1.8 eV in metallic praseodymium, but in the later Ln it oscillates around 2.5 eV. The nine LnSb from PrSb to TmSb have the average $(I^* - \mathscr{R}) = 3.3$ eV. In both cases, the mean deviation is below 0.3 eV.

Between Pr and Gd, I^* increases by 4.7 eV, and between PrSb and GdSb by 4.5 eV, to be compared with $\mathscr{R}$ of eq. (7) increasing only by 3.45 eV. By the same

token, the I' of the oxides increase from 9 eV for Pr_2O_3 to 14.1 eV for Gd_2O_3, by some 5 eV, whereas the I' of fluorides increase from 10.7 eV for PrF_3 to 15.5 eV for GdF_3, again 4.8 eV. In the second half of the 4f shell, I' increases by 5.4 eV from 8.5 eV in Tb_2O_3 to 13.9 eV in Lu_2O_3, and it increases by 6.3 eV when going from 9.0 eV in TbF_3 to 15.3 eV in LuF_3. Besides a larger experimental uncertainty of I in the insulating oxides and fluorides in comparison with the metallic elements and LnSb, there is little doubt that the enhancement of the $\mathscr{R}$ variation in eq. (7), being only 4.5 eV, is partly connected with formation of ephemeric Ln[IV] during the ionization process. In this sense, the results are more similar to I_4 of gaseous M^{+3} increasing by 5.0 eV from Pr to Gd, and 5.4 eV from Tb to Lu.

Many volatile d-group organometallic molecules provide informative photo-electron spectra, but no 4f signal has been identified in such 4f group compounds (Green 1981). The vapors of $LnCl_3$ show distinct 4f signals, superposed on the MO signals of a complicated distribution (Lee et al. 1982). In the first half of the shell, $CeCl_3$ has a signal at 9.82 eV, $PrCl_3$ at 10.9 eV, and the following Ln a broader structure, which is centered around 16 eV in $GdCl_3$. An isolated signal due to the formation of ^8S of $4f^7$ is seen in $TbCl_3$ at 13 eV followed by signals due to sextet levels beginning at 17 eV. Like solid thulium(II) compounds, gaseous $YbCl_3$ has many signals between 15.5 and 21 eV due to $4f^{12}$ levels from $^3H_6$ to $^3P_2$. $LuCl_3$ has the first 4f signal at 17.39 eV and the $^2F_{5/2}$ signal at 18.68 eV, essentially the same separation as the 1.46 eV in gaseous Lu^{+3}. It is noted that $I - \mathscr{R}$ is about 20% larger for $q = 1$ to 7 than predicted by eq. (7), whereas this equation shows good agreement from $q = 8$ to $q = 14$. It may also be noted that the difference given in eq. (8) is still positive, 1.0 eV when comparing I^* of metallic europium with ytterbium, and 0.9 eV for gadolinium and lutetium, and for the I' values 0.2 eV for Gd_2O_3 and Lu_2O_3, as well as for GdF_3 and LuF_3. Comparison of gaseous $GdCl_3$ and $LuCl_3$ shows eq. (8) to be negative, close to -1.4 eV. One explanation might be that solid Lu(III) compounds have more effective interatomic relaxation than the vapor, but we cannot neglect that eq. (8) for gaseous Gd^{+3} and Lu^{+3}, comparing I_4 values, is less negative, -1.18 eV. At least, there is no doubt that gaseous $LuCl_3$ decreases I(4f) by 2 or 3 eV when solidifying, much like mercury. A study of the series of $LnBr_3$ and LnI_3 vapors (Ruscic et al. 1983) showed a rich material of sharp MO signals, but even using 40.8 eV photons for discrimination, the only 4f signals identified occur for $CeBr_3$ at 9.5 eV and of $LuBr_3$ at 16.8 eV and of LuI_3 at 16.15 eV (the second 4f signal in both cases looking a little shaky).

One of the most pertinent questions a rare earth chemist can ask a photo-electron expert is how difficult it is to reduce a given Ln(III) to Ln(II), or to oxidize it to Ln(IV). Europium(II) is known (Jørgensen and Berthou 1972b) to show $I' = 6.9$ eV in $EuSO_4$. Though the two quantities cannot be strictly compared, it is noted that E° for Eu(II) aqua ions, after adding 4.45 eV, is much smaller, 4.1 eV. $I^* = 1.8$ eV in EuS (Eastman and Kuznietz 1971) should correspond to I close to 6 eV. On the other hand, I' for Tb(IV) is 24.7 eV in TbO_2 (kindly provided by Professor G. Brauer) and 24.4 eV in 'Tb_4O_7' where the first signal of Tb(III) occurs at 8.5 eV. It was pointed out (Jørgensen 1973b) that correcting these I' values with the spin-pairing expression $\mathscr{R}$ gives an increase close to 8 eV from Ln(II) to Ln(III) and

about 9 eV from Ln(III) to Ln(IV), almost the same value as dI/dZ from $Z = 71$ (lutetium) to 79 (gold). There is also another argument for saying that the 4f shell does not acquire some absolute inner-shell character going beyond $Z = 71$. The spin–orbit splitting of ^2F constituting $4f^{13}$ is (in gaseous ions, in eV) Yb^{+2}, 1.27; Lu^{+3}, 1.46; Hf^{+4}, 1.67; Ta^{+5}, 1.90; and W^{+6}, 2.15 (Kaufman and Sugar 1976) and it is possible to continue the polynomial $[0.01\ (Z - 61)^2 + 0.46]$ eV all the way up to bismuth ($Z = 83$) obtaining excellent agreement with the separation of the two 4f signals (Jørgensen 1976b). The major conclusion (Jørgensen 1973b) is that the partly filled 4f shell does not induce a specific propensity for trivalency, but the small average radius of 4f orbitals provides a stronger difference between ionization energy and electron affinity, thus stabilizing a definite z, but it would not be easy to predict that it happens to be $+3$. The difference between $E°$ values for M(III) and M(II) aqua ions for the same q estimated from the refined spin-energy treatment (Nugent et al. 1973) is 5 V at the beginning of the 4f shell, and increases smoothly to 8 V for $q = 8$ and to 9.7 V at the end. The $E°$ difference is 4.3 V for $5f^3$ and 6 V for $5f^8$.

Coming back to terbium(IV), it may be noted that $I(4f)$ is almost 2 eV higher than for closed-shell hafnium(IV), providing an exceptionally large value of eq. (8). It is the highest possible ionization energy of a partly filled shell, unless we enter the 5g group (Jørgensen 1968).

Fadley and Shirley (1970) studied solid lutetium(III) fluoride, and found that the $4d_{5/2}$ and $4d_{3/2}$ signals with $I' = 203.1$ and 213.1 eV are unexpectedly wide, the one-sided half-width δ being 2.1 eV. They ascribed this width to Heisenberg's uncertainty principle, the corresponding half-life being 0.11 fs being due to a rapid rearrangement of $4d^94f^{14}$ to $4d^{10}4f^{13}$, or perhaps to an Auger process forming $4d^{10}4f^{12}$ and ejecting an electron with the excess kinetic energy. We found (Jørgensen and Berthou 1972b) that δ remains almost constant for higher Z, slightly increasing to 2.2 eV in bismuth(III) and 2.5 eV in thorium(IV) and uranyl compounds. Widths of photo-electron signals are not always due to a half-life of order 10^{-16} s, either radiative ('X-ray fluorescence') or Auger processes, but may also be due to co-excited vibrations (like in visible spectra); we found such cases in lithium, carbon, nitrogen, oxygen and fluorine 1s signals, where the excited state shortens the internuclear distances because of the positive charge left behind by the ejected photo-electron.

Whereas the two 4d signals of Lu(III) only show minor chemical shifts, such as $I' = 201.8$ and 211.8 eV for Lu_2O_3, the spectra of the earlier lanthanides are quite complicated. Ytterbium(III) compounds have four or more 4d signals in the region 189–214 eV (Jørgensen and Berthou 1972b, Jørgensen 1974b) probably related to the 140 states of $4d^94f^{13}$, but it cannot be excluded that they also involve satellite signals, as discussed below for lanthanum(III). Gadolinium(III) shows two well-behaved 4d signals close to 150 eV, separated by 5.3 eV, a reasonable value when interpolating between 2.6 eV for barium and 10.0 eV for lutetium.

Using 1486.6 eV photons, it is possible to detect Dy 3d signals in the strong background of inelastically scattered electrons, with $I' = 1300$ and 1339 eV. Again, Gd(III) behaves as expected, $I' = 1192$ and 1226 eV, as well as Eu(III) $I' = 1139.8$ and 1169.5 eV in the sulfate. $EuSO_4$ showed a second set of 3d signals at 1128.8 and 1158.6 eV, a chemical shift of 11 eV (cf. Fadley and Shirley 1970). Before discussing

the preceding lanthanides, starting with the closed-shell La(III), we may add evidence for a chemical shift from $I' = 1246.3$ eV of $3d_{5/2}$ in the Tb(III) component of TbO_2 to 1256.9 eV of the Tb(IV) component. Satellites of photo-electron signals is a quite complicated area (Jørgensen 1975d, 1976b) but most of them occur in paramagnetic compounds having positive S of their groundstate. Following the observation of a weak shoulder on the two La 3d signals of LaF_3 (Wertheim et al. 1972) a long series of La(III) compounds were shown (Jørgensen and Berthou 1972a) to have almost as strong satellites as the main signals (roughly at 841 and 858 eV) at 3.1 to 3.7 eV higher I (it is 4.4 eV in LaF_3). These studies were continued on cerium(III), praseodymium(III) and neodymium(III) compounds (Berthou et al. 1976) and the interpretation is still problematic today. There is little doubt of the origin of 'electron transfer' satellites in La(III). When an inner electron like 3d is removed from La(III), it acquires a central field $U(r)$ very similar to that produced by an additional proton on the nucleus, and hence, the ionized state is a little more oxidizing than cerium(IV). The electron transfer spectra of Ce(IV) complexes occur at 3–4 eV above the ground state, and a similar process makes $3d^94f(F\ 2p)^{-1}$ a fair description of the satellite signal. Baer and Schneider (1987) have recently analyzed the situation of 3d satellite signals in La(III) and Ce(IV) and come to the conclusion that a unified treatment may allow four signals all having comparable $4f^1$ and $4f^0$ squared amplitudes, justifying the suggestion of Professor Christiane Bonnelle (cf. Jørgensen 1975d) that the satellite may cross the main signal and get a lower I. This might also explain why it is easy to obtain photo-electron spectra of cerium(III) but that CeO_2 and other Ce(IV) compounds invariantly look as if they contain comparable amounts of Ce(III) with I(3d) and I(4d) some 16 and 13 eV below the genuine Ce(IV) signals. TbO_2 mentioned above may not necessarily contain a lot of Tb(III) impurities on the surface. A recent discussion of ionization of various shells of CeF_3 and CeF_4 (Kaindl et al. 1987) may be compared with the problem of NiO (Jørgensen et al. 1987).

Another part of the truth is that when a partly filled shell is present in the ground state, an ionized configuration such as $3d^94f^q$ contains a very large number of states, which are known not to be degenerate on the scale of resolution, 1 eV, of a photo-electron or X-ray spectrum. Spector et al. (1976) discussed the configurations $3d^94f^2$ for comparison with the photo-electron spectrum of metallic praseodymium, and $3d^94f^3$ relevant to neodymium. The 910 states of the former configuration distribute on 107 J-levels in spherical symmetry. Spin–orbit coupling is assumed to separate $3d_{5/2}$ and $3d_{3/2}$ to an extent of 17.5 eV, and this remains the dominant feature. With plausible parameters of interelectronic repulsion, the higher J-value corresponds to levels distributed between 931.19 and 939.32 eV, and between 949.34 and 956.79 eV, both intervals being some 8 eV wide. By the same token, the 3640 states of $3d^94f^3$ constitute 386 J-levels. Assuming a primary spin–orbit separation of 21.25 eV, the two intervals 979.06 to 991.49 and 1000.65 to 1012.51 eV are each approximately 12 eV wide. It is obvious that this tropical forest of levels cannot be compared with the observed photo-electron spectra, but fortunately the selection rules related to coefficients of fractional parentage (Cox 1975) can be approximated with a signal intensity distribution taking on a certain similarity with the spectra. It would be

very interesting to know whether the complicated structure of the 4d region of ytterbium(III) has this kind of origin.

It is useful to remember that 4d and 4f have Hartree–Fock radial functions with comparable average radii, rendering quite strong mixing of configurations such as $4d^8 4f^{q+2}$ with $4d^{10} 4f^q$ possible, and also explaining the highly decreased dI/dZ for 4d orbitals in the lanthanides discussed above. The main reason why I(4d) is some 110–180 eV higher than I(4f) from Ce to Yb, is that the angular part of the kinetic energy $3\langle r^{-2} \rangle$ hartree/bohr^2 for d electrons is half as large as it would be for f electrons with comparable radial extension. The paradoxical side of 4f electrons is that they occupy an inner shell, but that they occur in compounds, having I(4f) comparable to the valence-shell MO.

When discussing satellite signals (Jørgensen 1975d, 1976b), it is worthwhile to realize that the typical photo-electron spectrum of a solid does not present many signals half as strong as the mildly undulating background, and though this background is mainly due to inelastically scattered electrons it does not represent statistical noise in the sense that it does not become ten times weaker, relative to the signals, if the measurement is pursued 100 times longer. The background contains reproducible weak signals. It is naive to argue that the *nl*-signal intensities are proportional to the cross-section for the mono-energetic photons to ionize the *nl*-shell (Jørgensen and Berthou 1972b, Berthou and Jørgensen 1975). It is true that the 1s signal intensity is proportional to $(Z-1)^3$ from $Z = 3$ to 11, but all the other shells show a grossly irregular variation, leaving no doubt that Cr 2s, Sm 3d, Ba 3p, Hg 4s and all 4d of Z above 58 would have been at least ten times stronger, based on the cross-section argument. Hence, it looks as if 90% of the intensity sometimes goes in broad and distant satellites. We have to accept that the many-electron functions do not guarantee a simple picture of one-electron absence (Wendin 1981) and even xenon atoms can show very subtle deviations. Cadmium 4p signals are the broadest signals we measured (Jørgensen and Berthou 1972b) with $\delta = 5$ eV, whereas δ is down to 1.3 eV for Ba $4p_{3/2}$. Gelius (1974) found that the sharp Xe $4p_{3/2}$ peak at 145.5 eV is accompanied by nine satellites up to $I = 153.5$ eV, whereas the Xe $4p_{1/2}$ signal is only represented by a broad hill between 160 and 170 eV. It is argued to be a Coster–Kronig continuum with superposed satellites due to configuration interaction between the classificatory $[28]4s^2 4p^5 4d^{10} 5s^2 5p^6$ and the two-electron substituted $[28]4s^2 4p^6 4d^8 4f 5s^2 5p^6$ containing 630 states. Jørgensen and Berthou (1975b) measured salts of perxenate XeO_6^{-4} for comparison, and found I' of these xenon compounds 2.8 eV higher than of the atom. By the way, Auger electrons with definite kinetic energies can also be measured on a photo-electron spectrometer (and is the best technique for non-metallic samples) and they may occur even at low I^* such as 104 eV of Er_2O_3 and 46.6 eV of Tm_2O_3 using 1486.6 eV photons. They are quite prominent in perxenates. It also turned out that the $4p_{1/2}$ has been washed out to a hazy hill in iodides, cesium(I) and barium(II). As pointed out by Connerade (1983) and by Fuggle (1983), there are all kinds of unexpected photo-electron phenomena showing up at the onset of the lanthanides, connected with the strong stabilization of the 4f orbitals, and contracting their radial functions, when an electron is lacking in the 4d or more pronounced inner shells.

The criterion of detecting satellite signals is essentially that they are not much weaker than the main signal (and we already mentioned that some main signals are 500 times weaker than others) since a qualitative quantum-mechanical argument shows that there are hundreds of satellites (much like the weak Fraunhofer lines) and it is really surprising that no more lines are detected (perhaps due to the habit of measuring 20–30 eV intervals). The author believes that there are two major types of satellites, as far as goes high intensity. The electron transfer satellites are the strongest in diamagnetic lanthanum(III), but are also well-characterized in other diamagnetic compounds of titanium(IV), uranyl, etc. A common feature seems to be an empty shell with low average radius, such as 4f, 3d and 5f. The other type was proposed by Hamnett (1972) and is due to anti-bonding 3d electrons being present in the ground state, and one being promoted to a 4d-like orbital with one additional radial node (really the only way it has anything to do with 4d, which is not readily had in condensed matter containing 3d group elements) simultaneously with the removal of an inner electron, such as 2p. This scenario fits the high-spin manganese(II), iron(II), cobalt(II) and nickel(II), whereas no satellites are observed in diamagnetic compounds of iron(II), cobalt(III) and nickel(II) having no anti-bonding electrons, (Jørgensen 1975d, 1976b) and it really also fits copper(II). The latter case might look perfect for electron transfer satellites, but the satellite is the closest to the main Cu $2p_{3/2}$ signal in CuF_2 and the most distant, when the ligands are highly reducing. Further on, it is not easy to understand why cobalt(III), palladium(II) and platinum(IV) do not show electron transfer satellites, if Cu(II) does. It is distinctly the case that copper(I) shows no close (below 18 eV) satellites. This invites the impertinent question whether closed d shells ever are sufficiently involved to be anti-bonding. The question of the origin of many satellite signals is still unresolved, and it is not easy to explain why vanadium(V), chromium(VI), molybdenum(VI) and rhenium(VII) do not show electron transfer satellites. It may be a numerical question making them ten times too weak. At least, this area remains of great actuality for the electronic structure of lanthanide compounds and metallic materials.

Schools convince most students of the splendid isolation of inner shells, so it may be a traumatic experience to see chemical shifts in the 8 eV category, more than the dissociation energy of most chemical bonds. It should be remembered that $I(nlj)$ are one-shot ionization energies, leaving all the other electrons in the system. To first order (Jørgensen 1962c), such chemical shifts do not modify the total energy of the system, and hardly contribute to the free energy, though 10^{-4} times 1000 eV would certainly be perceptible. Finally, it may be added that $I(1s)$ of light gaseous atoms (Bisgaard et al. 1978) is 64.4 eV for lithium, 123.6 eV for beryllium, 200.8 eV for boron and 296.2 eV for carbon, in all cases some 6–7 eV *above* the values for typical compounds.

3.7. *Oxidation states, casting an eye on d-groups*

It may be worthwhile to define what the author (Jørgensen 1969, 1986a) calls an oxidation state of an atom (i.e. a Z nucleus surrounded by some electronic density)

in a compound. This expression should not be mistaken to denote 'oxidation number' though the two quantities may be identical (but it may also be that one of them is not defined; or that they differ). The compound should not be a metal (though it may then have a conditional oxidation state such as M[II] discussed in section 3.2) and it should not have direct M–M contacts (being 'catenated'). In practice, the author does not consider oxidation states viable, if they only occur in cooled matrices (like $U(CO)_6$ in section 2.5) or in diatomic molecules (perhaps with high dissociation energy to atoms) familiar in sun spots, stellar atmospheres below 5000 K, and in flame spectra and fire-works, such as BH, CN, MgH, SiO, CaCl, ScO, TiO, MnH, CuCl, SrBr, YO, ZrO, SnCl, BaF, LaO,..., or in molecular ions studied in mass spectra, such as HeH^+, $HeNe^+$, ArN^+, $ArCl^+$, $KrBr^+$, XeH^+, CH_5^+, $Xe(CN)_2^+$,.... The author is also reluctant to accept species in very low concentration in fluorite, zeolites, and similar solids, only characterized by their electron paramagnetic resonance, or by strong absorption bands not observed under more definite circumstances.

Now, the constructive definition: a non-metallic, non-catenated compound kept at a moderate temperature has its oxidation state $z = (Z - K)$ determined by the *Kossel number of electrons* K rationalizing the quantum numbers, in particular the total spin S, and the number of relatively adjacent states with given symmetry types, of the ground state and the lower-lying excited states (say, below 2–5 eV). This definition may seem slightly hopeless if the compound is diamagnetic, with only the ground state (and no excited states) in the interval chosen. However, the recognition of diamagnetic and colorless behavior is certainly better than no information at all, and combined with some chemical arguments, quite decisive for K. If both C and F have an oxidation state in CF_4, it can only be C(IV) and F(−I); or the less appealing C(−IV) and F(I). The choice of the former alternative, as well as O(II) and F(−I) in OF_2 but O(−II) and Cl(I) in Cl_2O is not as compelling as erbium(III), but is connected with general ideas of electronegativity x. The situation can be more equivocal for hydrogen having the choice between H(I) (the only case of $K = 0$) and H(−I). Reasons can be given (Jørgensen 1969) to fix H(I) only when bound to one of the nine elements F, Cl, Br, I, O, S, Se, Te and N. There are great advantages of assuming H(−I) in alkanes and in d-group compounds, in view of the substitution of hydride by halides without great modification, neither of stereochemistry nor physical properties.

The assignment of a Kossel number K to an atom in a compound does not involve ideas of nearly electrovalent bonding, and it does not deny the likelihood that the fractional atomic charge is well below z (but according to the nephelauxetic effect in partly filled d shells, probably above 1 in most compounds) and does not disagree with many iron(II) and cobalt(II) complexes having higher fractional charges of the central atom than iron(III) and cobalt(III) complexes of similar ligands. But admitting this situation is not reducing K to a sheer label for file cards; in the fortunate case where the 'ligand field' transitions in the partly filled 3d shell are clearly observed, the classification is immediate; and even if other strong absorption bands render this observation ambiguous or impossible, a determination of the magnetic susceptibility may allow the determination of S, values such as $\frac{5}{2}$ and

2 indicating Fe(III) and Fe(II), or again $S = \frac{1}{2}$ compatible with Fe(III) or diamagnetism ($S = 0$) Fe(II). In practice, nearly all ligands are 'innocent', allowing K to be found (Jørgensen 1969). A few diatomic ligands are not always innocent, such as NO^+, NO, NO^- or O_2, O_2^- and O_2^{-2}. It may be argued that this problem is related to the lowest empty orbitals of the ligand being comparable in energy to the d orbitals in the complex (Gubelmann and Williams 1983). Other categories of non-innocent ligands are conjugated systems, able to be collectively oxidized, like some sulfur-containing ligands of the maleonitrilodithiolate type, or collectively reduced, such as 2,2'-dipyridyl (Jørgensen 1969).

A recent list (Jørgensen 1986a) compiles 315 oxidation states of the 105 first elements arranged in 81 isoelectronic series. The twenty K values not yet observed are all outside the d- and f-groups, with a tiny doubt about $K = 77$ which may, or may not, have been observed in a few instances of gold (II) and one mercury (III) $5d^9$ case. It is surprising that less than 30 of these oxidation states have been found later than 1968. The eleven K values 2, 10, 18, 28, 36, 46, 54, 68, 78, 86 and 100 corresponding to closure of 1s, or a shell with positive l, correspond to a third, 105, among the 315 examples compiled. The characteristic of the closed-shell K values is that their isoelectronic series can be exceptionally long (being isoelectronic with a noble gas or not) with up to 13 members, such as $K = 10$ from C(−IV) to Cl(VII), $K = 28$ from Mn(−III) to Br(VII) and $K = 36$ from Ge(−IV) to Ru(VIII). The longest series not corresponding to closed shells have seven members, $K = 42$ from Nb(−I) to Ag(V) and $K = 74$ from Ta(−I) to Au(V) undoubtedly connected with the octahedral d^6 complexes being particularly stable. The $4f^{14}$ series $K = 68$ has also seven members, from Yb(II) to Os(VIII). The series isoelectronic with the xenon atom $K = 54$ is not much better off with 8 members from Sb(−III) to Ce(IV).

With the restrictions described above, the five Ln = Ce, Pr, Nd, Tb, Dy (and perhaps also Tm) are known as Ln(IV), and the six Ln = Nd, Sm, Eu, Dy, Tm and Yb as Ln(II). The highest z in the 3d group are V(V), Cr(VI), Mn(VII), Fe(VI), Co(V), Ni(IV) and Cu(IV), among which V, Cr are mainly known as oxo complexes, Fe and Co exclusively as oxo complexes, Ni as both, and Cu as a fluoro complex (Hoppe 1981). If there is a common z for the 3d group, like Ln(III), it is M(II) known from Sc to Zn, and V(II) to Zn(II) are all known as aqua ions. Perspectives may change with time; in the 4d group, the $4d^8$ almost quadratic palladium(II) aqua ion is the oldest known (Rasmussen and Jørgensen 1968, Jørgensen and Parthasarathy 1978) and the next example is $4d^6$ ruthenium(II) (both have $S = 0$) known in the Tutton salt $(NH_4)_2[Ru(OH_2)_6](SO_4)_2$ analogous to the iron(II) compound Mohr's salt (Joensen and Schäffer 1984; cf. also their earlier references). A slightly similar surprise is the crystal structure of $[M(OH_2)_6](ClO_4)_3$ (Glaser and Johansson 1981) prepared from strong perchloric acid (having low water activity) and containing octahedral ions of thallium, erbium, and even more surprisingly so, lanthanum.

The photo-electron spectra suggest that no Ln(V) can be prepared, since its electron affinity would be similar to the very high I(4f) observed for Ln(IV) oxides. On the other hand, Ln(I) with $q = (Z - 55)$ is almost excluded by the lowest such level in Ln^+ occurring 18 289 cm^{-1} above the ground state of Sm^+. This forms a

striking contrast to the d-groups, where many specific ligands, such as CO and even more so PF_3 (Nixon 1985), provide low, zero and negative z with $(Z - 18 - z)$ 3d-like electrons, in most cases an even number. From the way of defining oxidation states above, it is clear that one safe example is much more useful than ten dubious ones. The best $3d^4$ vanadium(I) case is colorless $HV(PF_3)_6$ with the coordination number $N = 7$ (showing that the 18-electron rule does not exclusively have exceptions). Previously, the textbook V(I) case was $C_5H_5V(CO)_4$. The author is afraid to have omitted a 316th oxidation state, titanium(0) probably occurring in the red (this is not by itself a good sign) molecules with $N = 7$ (Wreford et al. 1981) having two CO, one PF_3 and two bidentate diphosphine ligands.

An interesting case is the dark-colored solid $Eudip_4$ (Feistel and Mathai 1968) showing $S = \frac{5}{2}$ between 211 and 317 K. It is interpreted as an Eu[II] compound ($S = \frac{7}{2}$) antiferromagnetically coupled to a collectively reduced (Jørgensen 1969) set of ligands dip_4^{-2} having $S = 1$. This is supported by $S = 1$ of the $Yb[II]Ybdip_4$. The paramagnetism, 2.34 Bohr magnetons, of $Sr\ dip_4$ may be due to a mixture of 75% $S = 1$ and 25% $S = 0$. Metallic lithium can reduce colorless 2,2′-dipyridyl to deep purple dip^- and dark green dip^{-2} in unreactive solvents.

The enigmatic $Nd(CO)_6$ detected in solid argon at 10 K (Slater et al. 1973) mentioned in section 2.5 would hardly contain more than four 4f electrons, but might have two electrons in an extended Rydberg orbital of 6s type. Such situations are very rare in condensed matter, but the gaseous diatomic molecules TiO (ground state $S = 1$) and MnX ($S = 3$) with X = H or halides (Jørgensen 1964) are closely related to titanium 3d4s and manganese $3d^54s$ containing two partly filled shells. In contrast, the octahedral Mn(I) complexes $XMn(CO)_5$ are $3d^6$ with $S = 0$.

3.8. *4f characteristics, casting an eye on the 5f group*

As long as we only knew one f group, it was difficult to tell whether *all* the observed characteristics of the lanthanides (almost constant $z = 3$, weak acidity of aqua ions, ...) would occur also in the 5f group of Stoner. Since 1922, Niels Bohr let the second inner box in the Thomsen–Bohr table start somewhere after uranium, perhaps at $Z = 93$ or 94. The two only plausible arguments (seen in hindsight) for the 5f group beginning among the known elements were given by Ephraim and Mezener (1933) arguing that the narrow absorption bands of green uranium(IV) salts show $5f^2$ configuration like Pr(III) has $4f^2$; and by Goldschmidt, and later Zachariasen, arguing that the mineral thorianite ThO_2 is so apt to introduce not only Ce(IV) and Pr(IV) but also uranium(IV) that it is likely that the 5f group are thorides, Pa(V) and U(VI) playing the role of Ce(IV) as an early tendency to higher z. The former argument has been brilliantly vindicated by the twelve lowest J-levels of gaseous U^{+4} (Wyart et al. 1980) being compared with U(IV) absorption bands (Jørgensen 1982a) and both shown to indicate a strong deviation from Russell–Saunders coupling in $[Rn]5f^2$. By the way, the last J-level $^1S_0$ was found in 1955 by the author in the aqua ion at 40 800 cm^{-1} later confirmed by Cohen and Carnall (1960). We return below to the question of thorides, which has been less convincing, though all the elements from $Z = 90$ to 98 (californium) are known to form fluorite-

type MO_2. But first it is worthwhile to summarize the evidence from monatomic entities.

The gaseous atom of thorium has the lowest configuration $[Rn]6d^27s^2$ and is as good a homolog to zirconium $[Kr]4d^25s^2$ as lanthanum $[Xe]5d6s^2$ is to scandium $[Ar]3d4s^2$. By the way, the atomic spectrum is exceptionally rich in lines; the tables of Meggers et al. (1961) give 3276 lines, among which the 50 strongest all are due to Th^+ except two of Th^0. For comparison it may be noted that 1957 lines are given of uranium. Among the 42 strong lines, there are more U^+ than U^0 lines. Blaise and Radziemski (1976) have measured 92 000 spectral lines of the gaseous uranium atom. In 1946, the National Bureau of Standards published the ground state $^5L_6$ of U^0 as belonging to $[Rn]5f^36d7s^2$ (containing 3640 states). This was a considerable surprise to the chemists, who since 1870 considered uranium to be a reasonable homolog to molybdenum and tungsten, and hence expected $[Rn]6d^47s^2$, ignoring the distinct chemical and spectroscopic versions of the Periodic Table. When uranium was promoted to be a 5f element, it was also clear that some striking chemical differences occur between W and U, but after all, it was not worse than between tin and lead, or between antimony and bismuth. It has been noted (Jørgensen 1979b) that the Nd^0 ground state belongs to $[Xe]4f^46s^2$ in spite of Nd(II) being rare, and that the U^0 $[Rn]5f^36d7s^2$ does not suffice to make U(III) particularly frequent. In a way, it is a close shave: the Hund (1927) configuration $[Xe]4f^35d6s^2$ begins with $^5L_6$ at 6764 cm^{-1} above the ground state of the neodymium atom, whereas $^5I_4$ belonging to $[Rn]5f^46s^2$ occurs already at 7021 cm^{-1} above the ground state of gaseous uranium atoms. An interesting difference is (Blaise and Radziemski 1976) that $[Rn]5f^26d^27s^2$ begins with $^5L_6$ at 11503 cm^{-1} about the U^0 ground state, whereas Martin et al. (1978) do not mention any levels of $[Xe]4f^25d^26s^2$ of the neodymium atom.

It is evident from the neutral atoms reviewed that 5f electrons play as minor a role in thorium as 4f do in lanthanum, but that 5f electrons are at least as important in uranium as in cerium. One additional channel of information is the higher ionic charges (Jørgensen 1976c). Klinkenberg and Lang (1949) found the five lowest J-levels of Th^{+3} obviously belonging to $[Rn]$ $(nl)^1$ relative to the ground state, in cm^{-1}: $^2F_{5/2}$ 0; $^2F_{7/2}$ 4325; $^2D_{3/2}$ 9193; $^2D_{5/2}$ 14 486; and $^2S_{1/2}$ 23 130. This is indeed the same order as in Ce^{+3}, but the one-electron energy difference between 5d and 4f is 49 942 cm^{-1} in Ce^{+3}, five times the 6d–5f difference 9898 cm^{-1} in Th^{+3}. It is also noted that the effects of spin–orbit coupling are roughly twice as large in the latter case. The ion Th^{+2} with two external electrons was studied by Racah (1950) but minor details in the energy differences between configurations were revised by Litzén (1974). The ground state is now $^3H_4$ belonging to $[Rn]5f6d$ only 63 cm^{-1} below $^3F_2$ belonging to $[Rn]6d^2$. This is the closest next-lowest configuration in a monatomic entity known to the author. After the revision, $[Rn]5f^2$ starts with the Hund ground level $^3H_4$ at 15 148 cm^{-1} above the ground state. Again, this forms a small contrast to Ce^{+2} where the first level of $[Xe]4f5d$ occurs 3277 cm^{-1} above the ground state belonging to $[Xe]4f^2$.

It is interesting for the chemist whether oxidation states occur below colorless thorium(IV) and protactinium(V). Metallic ThI_2 and (NaCl-type) ThS are hardly relevant, accepting the definitions discussed above. A much more intriguing com-

pound is the dark translucent ThI_3 showing dichroitic olive green to violet color in a microscope using polarized light (Scaife and Wylie 1964). We do not know whether this iodide is an oligomeric array of the type Gd_2Cl_3 reviewed by Haschke (1979). If it is monomeric (without short Th–Th distances) we do not know whether it is $5f^1$ rather than $6d^1$. Much the same can be said about the deep violet $Th(C_5H_5)_3$. Many titanium and zirconium cyclopentadienides of decreased oxidation number are dimeric. Experience with cerium(III) compounds suggests that the 6d–5f energy difference 9193 cm^{-1} in gaseous Th^{+3} readily can go negative in a Th(III) compound, but the author is agnostic at this point.

There are no good monomeric, non-metallic Pa(III) cases known to the author. But protactinium(IV) is most definitely a $5f^1$ system. Fried and Hindman (1954) found three bands of the aqua ion at 36 300, 39 200 and 44 800 cm^{-1} strikingly similar to the strong bands of cerium(III) aqua ions at 39 600, 41 700 and 45 100 cm^{-1}. There is no doubt that they are $5f \rightarrow 6d$ excitations, and it is quite likely that both aqua ions have $N = 9$. The solutions of Pa(IV) in stronger hydrochloric acid behave rather similar to Ce(III), except that the yellow species having a strong band at 24 300 cm^{-1} in 12 molar HCl seems to be $PaCl_6^{-2}$ (Bagnall and Brown 1967) in contrast to pale green UCl_6^{-2} dissociating in this aqueous solvent. The near-infrared narrow bands due to the seven Kramers doublets of 5f have been identified in PaF_6^{-2}, $PaCl_6^{-2}$ and $PaBr_6^{-2}$, and their angular overlap parameters compared with those of UF_6^-, UCl_6^-, UBr_6^- and gaseous NpF_6 (Brown et al. 1974). We return to such problems in section 4.6.

The strong $5f \rightarrow 6d$ transitions of M(III) and M(IV) were reviewed by the author (Jørgensen 1969). It was already mentioned above that aqua ions of $5f^{12}$ mendelevium(III) are more readily reduced to $5f^{13}$ Md(II) than Eu(III) is reduced to Eu(II), and that $5f^{14}$ nobelium(II) aqua ions are exceedingly difficult to oxidize to No(III), in strong contrast to ytterbium(II). The other way round, the half-filled shell $5f^7$ americium(II) is known only from the intense transitions to $5f^6 6d$ of traces in fluorite, and from the black, non-metallic AmI_2. Nugent et al. (1973) predict from the refined spin-pairing energy treatment that Am(II) should have the same $E^o = -2.3$ V as predicted for thulium(II) aqua ions. From this point of view, Md(II) and Am(II) have almost exactly swapped their mutual chemical differences compared to their lanthanide homologs Tm(II) and Eu(II).

There is no need to reiterate that the closed-shell $K = 86$ isoelectronic series goes on Ac(III), Th(IV), Pa(V), U(VI) and Np(VII) whereas $K = 54$ stops abruptly at cerium(IV). At the same time as the spectroscopic properties in a clear and uncorrupted way indicate $5f^q$ ground configurations, it is also true that much of the chemistry takes on tendencies known from the d groups, and this is even true for the chemical shifts in photo-electron spectra (Jørgensen and Berthou 1972b, Naegele et al. 1985).

4. Lessons for general chemistry

The chemical and spectroscopic properties of rare earths represent one extreme, to which (loosely said) organic chemistry constitutes the opposite, with the multi-

farious trends of inorganic chemistry distributed between the two extremes, the d-groups being closer to the R, with the trans-thorium elements intervening. Nevertheless, some of the d-group aspects are almost exclusive, e.g. the formation of CO and PF_3 complexes of low z (Nixon 1985). There are major dividing lines in chemistry at $Z = 10$ (and in quantum chemistry as well) and at $Z = 20$. The most important axioms of trans-neon and of trans-calcium chemists find their clearest expression in the 4f and 5f groups.

The most fundamental difference is perhaps that low-Z chemists expect compounds to consist of molecules (including polyatomic cations and anions) and this is true for the majority of all compounds, because several millions of organic molecules have been characterized. It is still true that many biological or synthetic polymers are not strictly speaking molecules. It is also true that inorganic compounds in the gaseous phase at reasonable pressure and temperature (say, below 20 atm and 1000°C) in the absence of violent electric discharges consist indeed of molecules. But in the liquid state, and in vitreous and crystalline solids, this is not the case for the majority of compounds, in part because of the higher coordination numbers N achieved by anion bridging (Jørgensen 1983b, 1984d). Hence, it may not be possible to specify the number of inorganic compounds within a factor of 2. The same problem occurs with the few thousand minerals, if the student asks how many there exist.

Fortunately for us, the kinetics of slow reactions, rather than achieving thermodynamical equilibrium, renders the carbon chains of organic molecules stored for years, and some perennial to the extent that Calvin finds hydrocarbons of biological origin 3000 million years old. The next-strongest propensity to catenation is shown by sulfur. Some unreactive sulfur compounds may awake concern about adjacent positive fractional charges, as already exist in F_3CCF_3, but a more empirical comment by the inorganic generalist is that the molecule F_5SSF_5 despises the alternative of anion bridges used by crystalline niobium(V) chloride $Cl_4NbCl_2NbCl_4$ obtaining two octahedral $N = 6$ surroundings by sharing. Again, the quite unreactive dithionate $O_3SSO_3^{-2}$ might have preferred oxo bridges like pyrophosphate.

We return below to several gradual, but profound, changes from the one-digit Z elements to the lanthanides, but would like to write a qualitative series of average radii of the partly filled shell (as compared to the shortest internuclear distances)

$$(5g) < 4f < 5f < 3d < 4d < 5d < (2p)\cdots. \tag{11}$$

4.1. *Being stabilized by having high spin S*

This subject falls into two parts. A system containing an odd number of electrons cannot avoid having positive total spin quantum number S at least $\frac{1}{2}$, or otherwise $\frac{3}{2}$ or a higher odd integer divided by two. If a system has an even number of electrons, and then shows a positive integer 1, 2, ..., rather than (colloquially 'diamagnetic') $S = 0$, it is really a case of high spin. It is a source of complexes in an organic chemist that he is obliged to respire O_2 having a triplet ground state, followed by two excited singlet states contributing to the atmospheric absorption of 'terrestrial Fraunhofer

lines' in the red and near infrared, we seeing through 220 g oxygen/cm^2 in the direction of the zenith.

With exception of molecules like NO and ClO_2, most 'main-group' compounds with odd K and concomitant positive S either dimerize, usually by catenation, or otherwise disproportionate to adjacent K values, such As(IV), Sb(IV), Tl(II) and other favored kinetic intermediates. Nevertheless, the rule of Hund (1927) that the ground state of a monatomic entity containing one partly filled nl shell has a specified maximum value of S, is really quite general for MO configurations having $e = 2, 3$ or more orbitals of identical energy for group-theoretical reasons, or approximately the same energy (e.g. 4f orbitals) having a ground state with S at least 1, if the e orbitals contain at least two, and at most $(2e - 2)$ electrons. This is exactly the case for O_2 having two electrons in the π-antibonding orbitals (which are filled by four electrons in the peroxide anion and the isoelectronic F_2).

There is no reason to repeat that 4f group compounds behave like a Hund ground state. The situation is more interesting in the d-groups (Jørgensen 1969, 1971) where octahedral d^5 systems show ground states with $S = \frac{5}{2}$ or $\frac{1}{2}$. The former sextet ground state is closely related to ^6S in spherical symmetry, and has one electron in each of the three roughly non-bonding orbitals avoiding the ligating atoms X situated on the Cartesian axes going through the M nucleus by having angular functions proportional to xy, xz and yz. However, the sextet ground state also presents one electron in each of the two anti-bonding orbitals with angular functions proportional to $(x^2 - y^2)$ hitting four coplanar X nuclei, and to $(3z^2 - r^2)$, or $(2z^2 - x^2 - y^2)$ if one prefers. The very large majority of manganese(II), and the main part of iron(III) complexes, show this sextet ground state, and no tendency to dimerization, except for relatively weak cases of antiferromagnetic coupling. On the other hand, other d^5 systems, such as the vanadium(0) complex $V(CO)_6$, a few deeply violet manganese(II) complexes such $Mn(CNCH_3)_6^{+2}$ (obtained from the colorless Mn(I) isonitrile complexes with strong oxidants), the familiar tomato-red ferricyanide $Fe(CN)_6^{-3}$ and a strongly oxidizing cobalt(IV) fluoro complex CoF_6^{-2} as well as all known ruthenium(III), rhodium(IV), palladium(V), osmium(III), iridium(IV) and platinum(V) complexes, all have $S = \frac{1}{2}$, the lowest value for odd K. This behavior, more palatable to a main-group chemist, is connected with five electrons in the lower sub-shell (xy, xz, yz). The absence of two anti-bonding electrons present in the sextet cases, stabilizes the doublet groundstate by 2Δ, twice the sub-shell one-electron energy difference (once called $10\,Dq$ by 'ligand field' theorists). However, it is on the cost of the spin-pairing energy being less negative, to the first approximation $8D$ according to eq. (6). It is only the ratio between Δ and the parameters of interelectronic repulsion, in the simplified expression (Δ/D) being below or above 4, that decides whether the groundstate is high-spin (here $S = \frac{5}{2}$) or low-spin. Since cyanide has exceptionally large Δ (higher than nearly all ligands distributed between 0.8 and 1.3 times the value for aqua ions); since Δ under equal circumstances is 1.45 times larger in the 4d, and 1.8 times larger in the 5d group than in the 3d group; since D is about half as large in the 4d and 5d groups than in the 3d group; and since the nephelauxetic effect gives larger parameters in fluoro complexes than in cyanides, and since finally Δ increase with z from 2 upwards, there

is not a mysterious trend of covalent bonding providing low-spin, and electrovalent bonding high-spin compounds, in spite of Russell–Saunders coupling being a sufficiently good approximation that the choice between S values for all practical purposes is a black-or-white alternative. It should not be argued that fluoro complexes ipso facto are high-spin; the d^6 systems NiF_6^{-2}, RhF_6^{-3}, PdF_6^{-2}, AgF_6^-, PtF_6^{-2} and AuF_6^- are diamagnetic, in spite of CoF_6^{-3} having $S = 2$. There is a small second-order effect that low-spin ground states usually have shorter internuclear distances, increasing Δ slightly.

The situation is slightly more complicated in d^q systems strongly modifying their stereochemistry when changing to a lower S. In many ways, this situation is more similar to the main-groups. Thus, octahedral complexes of nickel(II) have $S = 1$, and the 45 states of $3d^8$ are distributed in cubic symmetry in a very characteristic way, 30 states forming four triplet energy levels, and the remaining 15 states seven singlet levels. The various kinds of diamagnetic Ni(II) such as quadratic $Ni(CN)_4^{-2}$; rectangular, insoluble dimethylglyoximate, or $Ni(S_2P(OC_2H_5)_2)_2$; and tetragonal pyramidal $Ni(CN)_5^{-3}$ are in quite rapid equilibrium, and form when their free energy is lower than the triplet constituents. The selectivity for definite stereochemical preference, such as d^6 octahedral and d^8 quadratic complexes, undoubtedly contribute to pronounced preference for even K at the end of the 4d and 5d groups, such as Pd(II), Pd(IV), Pt(II), Pt(IV), Au(III) and Au(V). Though it is not convincing to classify compounds in the main-groups as p^q systems, the quadratic bromine(III), iodine(III) and xenon(IV) complexes BrF_4^-, ICl_4^- and the planar dimer $Cl_2ICl_2ICl_2$ analogous to crystalline gold(III) chloride, and XeF_4 all invite description as $4p^2$ and $5p^2$ systems (Jørgensen 1971). They are diamagnetic, with two electrons in the p-orbital perpendicular on the molecular plane, to the compared to the d $(3z^2 - r^2)$ lone-pair perpendicular on the plane of quadratic d^8 systems.

Hence, specific requirements of stereochemistry may win, relatively to the monatomic propensity to have high S values. The middle of the arena is the 3d group; to the left in eq. (11), Hund wins, and to the right, only a few quartet groundstates are left in d^3 cases, and the rather curious low-spin but $S = 1$ of octahedral $4d^4$ and $5d^4$ complexes. The only triplet states for which the molecular symmetry cannot decrease, are cases like O_2. Most students do not realize that this is even more the case for spherical symmetry; not only nitrogen, but also phosphorus. arsenic and antimony atoms have quartet ground states. Another subtlety is antiferromagnetic coupling, which cannot be conceptually separated from weak chemical bonding at long internuclear distances (Jørgensen 1971). Whereas S is decreased by such effects, there exist also molecules going ferromagnetic in the sense of acquiring the maximum S at sufficient cooling, such as the trimer of nickel(II) acetylacetonate Ni_3aca_6 getting $S = 3$ at liquid helium. We mentioned in section 2.3 the translucent ferromagnetic crystals $CrBr_3$ and EuO.

4.2. *Showing J-levels of a partly filled 'inner' shell*

Not only the spin-pairing energy favorable to ground states having high S, but also the observation of distinct J values, are enhanced by having the partly filled shell

as close to the nucleus as possible. The ephemeric way of obtaining this goal is X-ray absorption by an inner shell. But even in the most perfect solid insulators, electrons are sufficiently mobile to invade the inner shell in very short time. The lanthanides, all M(III) and some M(IV) among 5f group elements, and a case of $6p^2$ bismuth(I) in molten mixed halides (Bjerrum et al. 1967) are the only partly filled shells with sufficiently unperturbed J-levels in condensed matter, which can be stored. It might be argued that mercury atoms in a series of environments, and alkali-metal atoms in cool matrices, also show J-levels weakly perturbed, but remember that most of these transitions are between ns and np orbitals with oscillator strengths P between 0.1 and 1.5, whereas internal transitions in the $4f^q$ configuration rarely have P above 10^{-5}, excepting hypersensitive pseudoquadrupolar transitions (Reisfeld and Jørgensen 1977, 1987) and in $5f^q$ rarely above 10^{-4}, the strongest absorption bands being observed in uranium(III) compounds in the $5f^3$ configuration.

The internuclear distances to which the average nl-shell radii are compared in eq. (11) are normally meant to be the ligating atoms; the Ln–O and Ln–F distances in crystals can be as low as 2.2 Å. The classical opinion for the individuality of $(2J + 1)$ states bunched together is the 'ligand field' treatment (Jørgensen et al. 1963, 1986, Morrison and Leavitt 1982) and it is clear that if the Ln–X distance had been down below 1.9 Å, the 4f one-electron energy differences would be above 3000 cm^{-1}, installing a situation reminiscent of tetrahedral cobalt(II) halide complexes. As further discussed in section 4.6 the $5f^2$ energy levels are not far from this point in $U(H_3BH)_4$. However, another way of reading eq. (11) is to look for Ln–Ln distances, which are down at the unusually low value 3.5 Å in Yb_2O_3 (Schugar et al. 1975). Contrary to qualitative arguments of beginning interaction between differing partly filled shells, the antiferromagnetism is quite negligible in this oxide, the Néel temperature is 3 K (Henry 1958), ten times lower than the Curie–Weiss T of Nd_2O_3.

A rather unexpected instance of detectable J-levels are the ground states of the metallic elements (Wallace et al. 1977) showing several properties indicating a 'ligand field' separation around 100 cm^{-1} (about a third of the splitting in aqua ions) being a particularly painful argument for the electrostatic model in such materials having the reciprocal dielectric constant zero. In Ln[III] metallic elements, the Ln–Ln internuclear distance varies from 3.74 Å in lanthanum to 3.43 Å in lutetium.

4.3. *Most R chemistry has passive f electrons*

We make a distinction between three kinds of involvement of f electrons in chemical bonding: *passive*, where they are just hidden in the closed shells only modifying the ionic radius; *dynamic*, where the possibility of changing the number of f electrons plays a perceptible role; and *delocalized*, where the chemistry is influenced by delocalization on a LCAO model, the f electrons being more or less anti-bonding, approaching the situation in 3d group compounds. We are not arguing that R compounds do not have partially covalent bonding, but on a LCAO basis it is connected with the empty 4d and 5s orbitals in yttrium, and the empty 5d and 6s

orbitals in lanthanides. Such covalent bonding is regrettably difficult to evaluate from spectroscopic measurements, and is similar to the partly covalent bonding in copper(I) and zinc(II) compounds, mainly effected by the 4s orbital (at lower energy in the Cu(I) case).

The historically important difficulties of separating yttrium from dysprosium and holmium are an impressive argument for the passive role of the $4f^9$ and $4f^{10}$ shells in Dy(III) and Ho(III). There are a few instances where yttrium has passed into the interval between holmium and erbium. Thus, the unit cell parameter a_0 in Å of C-type R_2O_3 is 10.6647 for Dy, 10.6065 for Ho, 10.6021 for Y and 10.5473 for Er, suggesting an effective 'Z' close to 67.1 for yttrium. It is not perfectly certain that this shift is due to more pronounced covalent bonding by yttrium 4d and 5s orbitals; compare the a_0 of cubic Ca_2RF_7 (Greis and Kieser 1981) which also can form a super-structure of fluorite with the mineral yttrofluorite $Ca_{1-x}R_xF_{2+x}$ (comparable to disordered UO_{2+x} forming the superstructure U_4O_9); they are actually 5.5445 Å for Dy, 5.5337 Å for Ho, 5.5291 Å for Y, 5.5235 Å for Er and 5.5128 Å for Tm, suggesting 'Z' = 67.45 for yttrium. Many complex formation constants (which, anyhow, are not always monotonic functions of Z) place yttrium between neodymium and samarium. Alzuhairi and Siekierski (1983) compared formation constants of $5f^6$ americium(III) complexes of several ligands with those of yttrium and lanthanides, and suggested increasing importance of covalent bonding along the series Y(III) < Ln(III) < Am(III). For the d-group chemist, it is striking how minor a role the optimum oxidizing character among Ln(III) in europium(III) seems to play for free energy differences and selectivity of ligands.

The smaller ionic radius of zinc(II) compared to calcium(II), and the highly different chemistry, was ascribed by Goldschmidt to 3d-group contraction accompanied with 'imperfect screening'. In a sense, the 10 additional charges on the zinc nucleus 'shine through' the 3d shell, and if the argument is pursued to its (probably absurd) conclusion, the comparable ionic radii of Sc(III) and Zn(II) indicate that, on the average, the $U(r)$ has an added contribution $1/r$ in zinc.

The smaller ionic radius of Lu(III) compared with La(III) should be due to a similar 'imperfect screening' of the 14 additional charges on the lutetium nucleus. However, there has been some argumentation that part of the lanthanide contraction originates in relativistic effect. It is beyond discussion that $I_1 = 10.44$ eV of the mercury atom is higher than 8.99 eV of cadmium because of relativistic stabilization of 6s, and that I_1 of Ra^0 and I_2 or Ra^+ are 1.4% higher than the corresponding values for barium, because the 7s orbital is more stabilized for $Z = 88$ than 6s for $Z = 56$. Chemists have argued that the striking stability of the isoelectronic series $K = 80$ in Au(−I), Tl(I), Pb(II), Bi(III) and Po(IV) has the same origin. Relativistic calculations (cf. Jørgensen 1971) leave no doubt that $Z = 120$ is the last alkaline earth with Z predicted by Rydberg, and that soon after, the 8s orbital transforms itself to an inner shell, in disagreement with the extrapolation of eq. (2) beyond the 5g shell filling between $K = 119$ and 136 in positive ions, and hopefully, in compounds. These relativistic modifications are important for the predicted palladium(II) type chemistry of $Z = 164$ (Penneman et al. 1971) by not behaving like the expected dwi-lead, but having a partly filled $7d^8$ shell in the compounds.

Bagus et al. (1975) compared various non-relativistic and relativistic calculations, and came to the Solomonic conclusion that about half of the lanthanide contraction is due to imperfect screening (on the Hartree–Fock level) and half to relativistic contraction. The lanthanide contraction provides a closer similarity between the chemistry of Y, Zr, Nb, Mo and Tc with Lu, Hf, Ta, W and Re than the 3d group contraction between Mg, Al, Si, P, S and Cl; and Zn, Ga, Ge, As, Se and Br. It is noted that the 4d group contraction is less efficient in decreasing ionic radii and modifies the chemistry of cadmium to xenon, and this is one argument (Penneman and Jørgensen 1976) why the 5f group contraction is expected to be less marked than the lanthanide contraction. It is probably that $Z \doteq 104$ to 109 achieve high oxidation states with the closed-shell $K = 100$ perhaps stretching from No(II) to 109(IX), though beginning around $Z = 106$, there should be a great variability in the z values, somewhat like ruthenium.

The chemical conclusion that the role of 4f electrons is predominantly passive, left the nice pastel colors of the 'Bunte Erden' as a superficial ornament, until the 'Sleeping Beauty' was woken up by the technological applications in the last 25 years, involving cathodoluminescence in color television, lasers, and much more.

4.4. *High coordination numbers N do not require N electron pairs*

In 1916, Lewis unified a lot of evidence about multiple bonds and lone pairs (especially in organic molecules) into what became known as the Lewis paradigm: each single bond is effected by one pair of electrons; double and triple bonds are effected by two or three electron pairs; in the well-behaved elements, the total number of chemically active electron pairs is 4, producing the definition of lone pairs, the number of electron pairs needed to bring the total number up to 4 (except hydrogen, where it is 1). Such lone pairs function as bases and are readily protonated, or react with anti-bases (Lewis acids) having great affinity for an additional pair of electrons, such as BF_3 and SO_3. Exactly like the Dalton opinion that all compounds consists of molecules, it must be admitted that the Lewis paradigm is valid for the large majority of one-digit Z values, by the simple context that it is valid for nearly all organic compounds. The inherent ideas of static electrons (like our nuclei) were entirely alien to atomic spectroscopy, but it must be added in all fairness that Lewis proposed the extensive system ten years before the Schrödinger equation, and eight years before Stoner brought l values to the attention of chemists. In the post-Schrödinger epoch, Pauling included the Lewis paradigm as a prerequisite for his hybridization treatment in 1931. In the meantime, crystal structures had also shown the Lewis paradigm to the superb in diamond and (the so-called adamantoid semi-conductors) Si, Ge, GaAs, grey Sn, InAs, InSb, CdTe, ...

However, a closer analysis (Jørgensen 1983b, 1984a, 1984d) shows that many exceptions occur to the Lewis paradigm. Already hydrogen has $N = 2$, not only in the strong symmetric hydrogen bonds like FHF^-, but also in hydride bridges like the chromium(0) complex $(OC)_5CrHCr(CO)_5^-$; and the NaCl-type alkali-metal hydrides as well as the perovskites $BaLiH_3$ and $EuLiH_3$ show $N = 6$. Carbon has frequently $N = 5$, as alkyl bridges in organo-beryllium and -aluminium molecules,

$N = 6$ in $Li_4(CH_3)_4$ not having bent hydride bridges like $H_2BH_2BH_2$ and $Zr(H_3BH)_4$ but carbon bound to three Li and three H, in the molecule $CRu_6(CO)_{17}$ in the middle of an octahedron, and $N = 8$ in the fluorite Be_2C with translucent amber-yellow color (and hence not a metal). The NaCl-type nitrides MN and oxides MO have the difficulty that there are not 12 valence-shell electrons available for 6 bonds. Some, like MgO and BaO, may be pretty electrovalent, but this is a difficult position to defend in NiO, CdO, LaN and LuN. Fluorite-type Li_2O has $N = 4$ for lithium(I) (which is unusually low) but $N = 8$ for oxide.

After this presentation of bad examples derived from one-digit Z cases, the trans-neon chemists may contemplate the isoelectronic series of $N = 6$ AlF_6^{-3}, SiF_6^{-2}, PF_6^-, SF_6 and ClF_6^+ which, like M(II) oxides, do not all seem perfectly electrovalent. One should refrain from equating formation of volatile molecules with covalency; as pointed out by Magnus, the neutral molecules MX_n of halides have $n = z$, whereas larger cations in NaF, MgF_2 and AlF_3 have $N = 6$, though their lower z necessitate halide bridges, impeding the volatility. There is no serious reason to believe that SiF_6^{-2} and PF_6^- are that much less covalent than gaseous SiF_4 and PF_5. It must be added in all fairness that N restricted to 4 is a relatively ancillary part of the Lewis paradigm; the more fundamental hypothesis is $2N$ electrons needed to form N bonds. It meant textbook writers running around, like Diogenes with his lantern, looking for the 12 electrons responsible for the covalent bonding in octahedral species. The major impetus given to MO theory after the rationalization of d-group spectra starting in 1952 derives from the capability, even in the LCAO version, to introduce three quite independent parameters of MO delocalization in the one, three and two orbitals having 0, 1 and 2 angular nodes (cones counting for two nodes) and hence being able to form covalent bonds with s, p and d orbitals of the central atom.

But much worse problems appear for N above 6. One of the bores is that the geometricians in Alexandria chose to name polyhedra after their number of surfaces (a cube being a regular hexahedron) whereas Alfred Werner and recent chemists are interested in N, the number of apexes. In particular rare earth chemists are pestered by elaborate descriptions of (frequently idealized) polyhedra looking like a carton of prunes trampled upon by an elephant, when they are only interested in the length of the N short internuclear distances (which are also given in the review by Sinha 1976). There is much recent evidence accumulated that yttrium(III) and the lanthanides rather indifferently assume all possible values of N from 6 (normally far removed from a regular octahedron) over 7, 8, 9, 10, 11 to the quite frequent $N = 12$, it being cuboctahedral or icosahedral (Jørgensen and Reisfeld 1982a). Many models assuming ligand–ligand repulsion and M–X attraction without explicit angular dependence reproduce this indifference for stereochemistry, as soon as N is above 6. Other cations with comparable behavior are thorium(IV) and calcium(II), of which $CaCO_3$ is most frequent in calcite-type with $N = 6$, but also exists as aragonite with $N = 9$, the normal type of $SrCO_3$ and $BaCO_3$. High, and indifferently dispersed, N values occur in molten germanium and molten metals, and also in liquid water, as far as oxygen–oxygen internuclear distances go.

One corollary of this variability is that it is very difficult to predict the local

symmetry of rare earths in glasses (Reisfeld and Jørgensen 1987, Jørgensen 1986b) whereas one can take 9:1 bets that nickel(II), and 99:1 bets that chromium(III) is octahedral in a given glass, though the situation is already much more debatable for manganese(II).

A closer analysis (Jørgensen 1983b, 1984d) shows that bonds never show very short internuclear distance. It is far more frequent for a bond to be 0.2 Å longer than usual, than it being 0.2 Å too short (such as the N–N distance in N_2 or the two short U–O distances in uranyl salts, both being very slowly reacting). Hence, it becomes a matter of judgement whether internuclear distances 15 to 30% longer than the other should be included in the number of bonds.

There is no need for further attempting a proof that two-digit Z values invariably need $2N$ electrons allocated to N bonds. The impressive paradigm had an end rather comparable to the other comprehensive paradigm, that of Lavoisier. It may still be true today that most acids contain oxygen, but it is no longer considered a constitutive definition of an acid.

4.5. *Some R chemistry is determined by dynamic f behavior*

A pure example of dynamic behavior is the reduction of a cerium(IV) solution with an europium(II) compound. For all practical purposes, the reactions oxidizing Ln(III) to Ln(IV) or reducing Ln(III) to Ln(II) are all instances of dynamic 4f behavior. Many of these reactions have been mentioned in the subsections concerning Ln(IV) and Ln(II).

A slightly different area is the criteria for a given solid containing Ln[III] or Ln[II]. In a paper about diatomic molecules containing one transition-group atom (Jørgensen 1964) and in a complementary paper (Hulliger 1968) it was suggested that the NaCl-type monosulfides MS are metallic if the lowest state of $4f^{q-1}5d$ of Ln(II) has lower energy than the lowest state (in situ) of $4f^q$, treating the numerical question with the refined spin-pairing energy theory. One way of describing this idea is that the conduction band of the metallic LnS is formed by the 5d orbitals, and that semiconducting LnS (with considerably larger unit cell parameter a_0) remain Ln(II) compounds, in the same sense as SrS and BaS contain M(II).

Johnson (1977) and the author (Jørgensen 1976c, 1979a) independently suggested that the tendency to change Ln[II] to Ln[III] increases with the Ln–Ln internuclear distance decreasing. The order of increasing M[III] propensity should then be

$$M^0(g) < MI_2 < MTe < MSe < MS < MB_6 < M(s) < MO, \tag{12}$$

where there is nothing paradoxical in the metallic NdO and SmO (Leger et al. 1980) having shorter Ln–Ln distances than in the metallic element. This is a fortiori the case in NaCl-type CsF with its Cs–Cs distance 4.25 Å much shorter than 5.31 Å in the metallic element. It is possible (Jørgensen 1985a) to use the spin-pairing function $\mathscr{R}$ of eq. (7) to express the order in eq. (12). A tiny discrepancy is that assigning the critical limit 1.5 eV to gaseous atoms Ln^0 should make the cerium atom $[Xe]4f^2$,

which it is not. The critical $\mathscr{R}$ for LnI_2 must be close to 2.5 eV though the borderline cases PrI_2 and DyI_2 are debatable. The limit for LnTe must be about 3.3 eV since TmTe contains comparable amounts of Tm[II] and Tm[III]. We can only say that the critical $\mathscr{R}$ for LnSe and LnS must be marginally higher, but certainly below 3.7 eV. LnB_6 (containing the large cations in the cavities with $N = 24$ between an interconnected network of B_6 octahedra) and the metallic elements must have the critical $\mathscr{R}$ not far from 4 eV, and LnO marginally below 4.6 eV. There are many high-density ytterbium alloys containing Yb[III], such as YbNi, $YbNi_2$, $YbNi_3$, $YbNi_5$, YbCu, YbRh, YbPd, YbIr, $YbIr_2$, $YbAu_2$ and $YbAu_3$, and a few Eu[III], such as $EuPd_3$ and $EuIr_2$ suggesting at face value a critical $\mathscr{R}$ above 5 eV. There are also a few alloys containing simultaneously Eu[II] and Eu[III], or Yb[II] and Yb[III]. High pressures tend to shift the critical $\mathscr{R}$ to higher energy, corresponding to Ln[II] transforming to Ln[III] with shorter Ln–Ln distances.

The changes described by eq. (12) are adiabatic, in the sense that all the internuclear distances are allowed to adjust. The prototype of such a situation is the standard oxidation potential E° relative to the standard hydrogen electrode at pH = 0 (1 molar H_3O^+ and 1 atm. H_2). There have been arguments for some time that the ionization energy relative to vacuum

$$\tfrac{1}{2}H_2(g) + H_2O(aq) = H_3O^+(aq) + e^-(\text{vacuum}) \tag{13}$$

is between 4.4 eV and 4.5 eV higher than E°, though the quantity may not be liable to a more precise definition (Rosseinsky 1965, Jørgensen 1975a, 1981b, Pearson 1986) but it seems now to be 4.42 ± 0.02 eV (Trasatti 1986). The analogous value is 4.6 eV in acetonitrile. It is noted that there is only an E° difference in aqueous solution, 1.2 eV, between being in equilibrium with 1 atm H_2 and with 0.2 atm O_2 (the amount of oxygen in atmospheric air) and hence, the relatively small variations of photo-electron I values (governed by the Franck–Condon principle of immobile nuclei, like optical transitions) by 1 or 2 eV (due to interatomic relaxation, and other effects) span this interval.

4.6. *Only higher oxidation states of trans-thorium elements involve f electrons significantly in covalent bonding*

We have all the desirable spectroscopic evidence needed that partly filled d shells participate in chemical bonding, to the extent of several eV. The small 'ligand field' parameters in Ln(III) show the opposite (Jørgensen et al. 1986): they are typically 20 times smaller than in 3d group ions such as Cr(III), Fe(III) and Co(III) (Jørgensen 1969). When it became clear that non-metallic compounds of transthorium elements contain a partly filled 5f shell, the first working hypothesis was that the early elements, such as uranium and neptunium, have rather strong 'ligand field' effects, perhaps a little weaker than in the 3d group, and that they attenuate with increasing Z, becoming quite small after americium. There are indeed such trends for certain properties; both the internal $5f^q$ and $5f^{q-1}6d$ transitions are some 10 to 30 times stronger in U(III) than in Nd(III) aqua ions (4f and 5d) and then decrease rapidly in intensity, becoming comparable in $5f^8$ berkelium(III) with the homologous

terbium(III) (Carnall et al. 1984). However, as far go 'ligand field' effects, the decisive parameter is not Z, but the oxidation state. The $5f^3$ J-levels of $U_xLa_{1-x}Cl_3$ are only split twice as much as the homologous $Nd_xLa_{1-x}Cl_3$ (Gruber et al., 1979, Crosswhite et al. 1980) and this trend continues among the M(III) at least up to berkelium(III), both in the chloride and in the aqua ion (Carnall et al. 1984). The situation is somewhat ambiguous in $5f^2$ uranium(IV), perhaps because of the same variability around 0.2 Å found in Ln–X distances (Jørgensen and Reisfeld 1982a), the sub-shell energy differences are 850 and 2600 cm^{-1} in salts of octahedral UCl_6^{-2} and comparable to $PaCl_6^{-2}$ (Brown et al. 1974, Satten et al. 1983) and some five times smaller than in $3d^3$ chromium(III). A striking characteristic of the octahedral uranium(IV) complex is that the electronic transitions are narrow lines (surrounded by co-excited vibrations of odd parity) having oscillator strengths P below 4×10^{-7}, whereas the broader bands of the uranium(IV) aqua ion (obviously lacking an inversion center) have P of order 10^{-4} (Jørgensen 1982a). The 'ligand field' parameters are ~ 3 times larger in UF_6^- and the sub-shell energy differences achieve values as high as 5600 and 17 500 cm^{-1} in gaseous NpF_6 (Brown et al. 1974). The situation is less clear in neptunyl and plutonyl ions, which have their electron transfer bands at slightly lower energy than the uranyl ion (Jørgensen and Reisfeld 1982b), but it seems that the linear sub-shell energy differences are comparable to NpF_6. The 5f group soon after runs out of oxidation states above M(IV): the last known are PuF_6 gas and AmO_2^{+2}.

One may then ask the question whether Ln(IV) have much larger 'ligand field' effects than Ln(III) compounds. It is difficult to find evidence; the $4f^2$ and $4f^8$ transitions of the orange Nd(IV) and Dy(IV)Cs_3LnF_7 may be a little broader than usual (Varga and Asprey 1968a,b) but it is not spectacular. A related question is the width of J-levels of Ln[IV] measured in photo-electron spectra of LnSb and metallic Ln. It is not absolutely incompatible with the signal widths (Jørgensen 1975b) that some J-levels are split to an extent of half an eV, but it may be much less.

Green (1981) has detected a sharp U $5f^2 \rightarrow 5f$ signal at 6.2 eV of the volatile $U(C_8H_8)_2$ having $N = 16$, and of one or two other organo-uranium compounds. The cyclo-octatetraenide 'uranocene' may like UCl_6^{-2} have 'ligand field' effects of the order of magnitude of the differences between the J-levels in the infrared and visible, but the importance of 5f bonding in this sandwich molecule does not seem to be nearly as pronounced as that of the 3d electrons in $Fe(C_5H_5)_2$ and $Co(C_5H_5)_2^+$. Solid uranium(IV) compounds also have sharp U 5f signals at low I (Jørgensen and Berthou 1972b, Naegele et al. 1985). As seen also from the chemical fact that most uranium(V) compounds readily disproportionate to U(IV) and U(VI), there are no very striking chemical shifts of I(5f) as z increases: at this point, the behavior is more like that of the 3d group compounds. Eller and Penneman (1987) reviewed mixed oxides (and also fluorides) of Np(VI), Np(VII), Pu(VI), Pu(VII), Am(IV), Cm(IV), Bk(IV) and Cf(IV) and compared them with Pr(IV) and Tb(IV).

We cannot know at present how Ln(V) would behave, if they kept several picoseconds. In a technical sense, they have been observed in the Auger signals of Er_2O_3 imitating $I^* = 104$ eV and of Tm_2O_3 with $I^* = 46.6$ eV, using 1486.6 eV

photons (Jørgensen and Berthou 1972b). It is almost certain that the corresponding kinetic energy of 1382 eV corresponds to an erbium $3d_{5/2}$ vacancy rearranging to $4f^9$ or Er[V], ejecting an Auger electron, and in the case of thulium, the same explanation may be given for the kinetic energy, 1440 eV, of the Auger electron leaving an ephemeric $4f^{10}$ configuration defining Tm[V].

An interesting aspect of photo-electron spectra of potassium(I) lacking one 3p (or, a fortiori, a 2p electron) is that the interatomic relaxation in compounds with pronounced chemical polarizability (Jørgensen 1975a) decreases the I values more than expected, and introduces variations in the opposite sense of the Madelung potential. One way of looking at this fact is to consider that K(I) lacking one electron in a closed shell, and hence technically being K[II], has a chemistry corresponding to a metal more noble than gold or platinum (Jørgensen 1975d).

Without speaking about species nearly as oxidizing, nor nearly as ephemeric as solids ionized in inner shells, it may be worthwhile to mention chemical behavior of excited J-levels of Ln(III) in aqueous solutions, and their reaction with anions such as bromide, nitrate, and deprotonation to hydroxo complexes at relatively low pH. Such studies have been performed mainly on $^5D_0$ and $^5D_1$ of europium(III) solutions, with $^5D_0$ 2.14 eV above the ground state $^7F_0$ (Marcantonatos and Deschaux 1981, Marcantonatos et al. 1981, 1984) and on $^6P_{7/2}$ of gadolinium, 4.0 eV above $^8S_{7/2}$ (Vuilleumier et al. 1982, Marcantonatos et al. 1982, 1986). The quite different chemical behavior of these excited states (living up to several milliseconds) may surprise R chemists, but Adamson (1983) pointed out that an excited electronic state, living for 10^{-7}s or more, may equilibrate its vibrational excitation with the thermal reservoir in condensed matter, and this 'thexi state' has its individual chemistry. Seen from the point of classical physical chemistry, the thexi state at an electronic energy E_1 is *at the same time more reducing* than the ground state (with the standard oxidation potential decreased from E° to $E^\circ - E_1$) and *more oxidizing* (with $E^\circ(r)$ applying to the ground state having received an electron changed to $E^\circ(r) + E_1$). This argument may seem more transparent in the photochemistry of the uranyl ion (Jørgensen and Reisfeld 1982b, 1983b) readily removing an electron from inorganic species, or abstracting hydrogen atoms from organic molecules. However, the argument does not depend on a definite MO vacancy, or an electron in a higher MO, for obtaining the oxidizing or reducing characteristics which, assuming equilibrium before the decay of the excited state, would be able to evolve at the same time H_2 and O_2 from most thexi states in aqueous solution. At this point, gadolinium(III) is somewhat special: its first excited state at 4.0 eV would only bring the predicted $E^\circ = +7.9$ V (Nugent et al. 1973) down to $+3.9$ V without any chemical consequences, and increasing $E^\circ(r)$, i.e. E° of Gd(II) aqua ions, from -3.9 V would just marginally allow evolution of H_2. Anyhow, the chemical differences found by Marcantonatos and collaborators are mainly stronger acidity (a decrease of pK close to 2.6, by about six units) and convincing evidence for decrease of N by two units (probably from 8 to 6) in the thexi state, showing a quite pronounced nephelauxetic effect in the line luminescence. It can hardly be imagined that the ionic radius of the thexi state decreases so much as to justify the decrease of N by two units, though it may have some relation with the enigmatic question why

the ionic radius of the Gd(III) ground state is slightly larger than interpolated from the surrounding Ln(III) (Fidelis and Mioduski 1981). However, as discussed in section 2.1 the general tendency of oxidizing aqua ions, such as iron(III), palladium(II) and thallium(III) being much more acidic than expected from their size, may be correlated with the behavior of the Gd(III) thexi state.

4.7. *Chemistry is the behavior of electrons pushing point-like nuclei with charge $+Ze$ to mutual distances representing (relative or absolute) minima of energy*

The very long title of this sub-section is really rather trivial. Since 1911 it has been admitted that if nuclei change, it is not chemistry, but nuclear physics. If chemistry can be explained, our only hope is to understand the detailed behavior of the electronic density around the nuclei. Nevertheless, the movies show the quantum chemist arriving at work, putting 16 gigabits in the computer, and pushing the red button with the nickel spatula (he inherited from his retired predecessor) after having fixed the nuclear positions according to X-ray or neutron diffraction of crystals, electron diffraction of gaseous molecules, or an educated guess.

There is a part of the truth in this idealized picture. For most cases, it is sufficient to limit oneself (by concentration on optical excitations and photo-electron ionization, obeying the principle of Franck and Condon; or by resignation) to scrutinize the electronic density determined by fixed nuclear positions. The really great success of quantum mechanics was the application to monatomic entities (but some restraining comments are made in section 4.8) where the nucleus is firmly put at the origin (unless below 10 amu, in which case perfectionists start worrying about the center of gravity shifted a trifle by the electrons).

Much has been written about the approximation of Born and Oppenheimer (cf. Jørgensen 1985b, Woolley 1986). In free space, any atom or molecule starts a continuum of translational states immediately at the ground state. The factorization in a translational and an electronic factor (and for systems containing more than one nucleus, also a rotational and a vibrational factor) is indeed an approximation, and is replaced in systems confined in a small volume (such as condensed matter) with a complicated, almost overall dense distribution of discrete states. The reason that one may send 1 eV photons for hundreds of km in optical fibres (cf. Reisfeld and Jørgensen 1987) is that the oscillator strength for transitions from the ground state is ultramicroscopic. Before weeping like Achilles seeing a tortoise, it may be wise to recognize five or ten almost impossible problems for the quantum chemist. Accepting the Born–Oppenheimer factorization of the total wave-function, the potential curve for two nuclei has one internuclear distance as variable, and can be plotted on two-dimensional paper. For a larger number $\mathcal{N}$ of nuclei, there are $(3\mathcal{N} - 6)$ independent distances, and the potential hypersurface as a function of these distances takes place in a $(3\mathcal{N} - 5)$ dimensional space, amounting to 22 dimensions for an ethanol molecule. It is familiar to the organic chemist that we give more or less systematic names to isomers representing different local minima of this potential hypersurface (on the other hand, optically active enantiomers can have the same set of distances and be situated on the same point of the surface). Thus, a box

containing a single C_6H_6 molecule also has relative minima representing isomers such as Dewar benzene and prismane, and a whole continuum representing three freely mobile acetylene molecules.

There is a long-standing tradition in luminescence to discuss only the 'breathing mode', a totally symmetric mode of vibration multiplying all the internuclear distances by the same scaling factor (quite close to 1). It may be slightly superficial to neglect the 14 other modes in octahedral MX_6. In organic textbooks, the reader appreciates the 'reaction coordinate' bringing a multinuclear system from one minimum of the potential hypersurface to another. As also suggested by the Arrhenius equation for activation energy, such a 'reaction path' is carefully optimized, avoiding the severely delaying effects of unnecessary energy increases. The only problem for the quantum chemist is that finding the optimal reaction path is like mountain hiking in mist; we can only recognize the best path when we have found it.

Getting beyond problems like NH_3 and HCl meeting in an otherwise empty box is plainly hopeless, if we really stick to what chemistry is: modifying the internuclear distances of the reactants. This is not to deny that most useful correlations can be obtained by clever chemists between properties of a series of related molecules or polyatomic ions, and approximate wave-functions of the series. Such an approach has to a great extent been the method of d group 'ligand field' treatment (Jørgensen 1969) simultaneously comparing differing ligands and central atoms. It is also obvious that accepting the principle of Franck and Condon alleviates a teraproblem to a megaproblem, and this is why spectroscopists feel happier than chemists.

Quantum chemistry in the strict sense is our best (and only) way to study species like CH_5^+ and the only neutral species HeLiH (Kaufman and Sachs 1969) and HeBeO (Koch et al. 1986) containing helium. Since gaseous MX^+ can only dissociate to M^+ and X^0 [or M^0 and X^+; Jørgensen (1971, ch. 35)], many cations, such as HeH^+, He_2^+, $HeNe^+$, $HePt^{+2}$, ..., are known from mass spectra, and HeO^+ from calculations. Most MX^{+2} have a repulsive potential curve for large internuclear distance, because they dissociate to M^+ and X^+. However, if I_2 of M is smaller than I_1 of X (24.59 eV in the case of helium) such asymptotic repulsion does not occur, and HeC^{+2} is calculated (Koch and Frenking 1986) to have a respectable dissociation energy above 0.7 eV, and several HeM^{+2} of order 1 eV. Hotokka et al. (1984) studied $HeTi^{+2}$ and the metastable minima of $HeAl^{+3}$ and HeV^{+3}. I_3 of M is smaller than I_1 of helium for Y, Zr, Hf and Th, and for nearly all the lanthanides (cf. Martin et al. 1978), again avoiding dissociation of HeM^{+3} to two cations. The exceptions are $HeEu^{+3}$ and $HeYb^{+3}$ dissociating to He^+ and R^{+2}. Unless the chemical bonding effects are well above 1 eV, providing an absolute potential minimum, the helium atoms are too reducing to be bound as ligands to the gaseous, oxidizing anti-bases Eu^{+3} and Yb^{+3}. Polyatomic helium-containing cations (Koch and Frenking 1986) are $HCCHe^+$ isoelectronic with acetylene, and $HeCHe^{+2}$ having a strongly bent (84°) ground state. The first triplet state has higher energy, but much shorter C–He internuclear distances, and may be compared with the ground state (having $S = 1$) of methylene HCH (Schaefer 1986, Wasserman and Schaefer 1986). This molecule might easily have been linear like OCO, but

calculations suggested that the equilibrium bond angle is close to 134° and recent experimental work confirmed the angle, and seems to be slightly more precise than the quantum calculation. Wasserman and Schaefer (1986) write: In the future we expect to find an increasing number of situations in which theory will be the preferred source of information for aspects of complex chemical systems. Quod felix faustumque sit.

4.8. *Is quantum chemistry feasible?*

There is a tendency to say that the truly chemical problems are at the dawn of the quantum treatment today, much like atomic spectra were sixty years ago. There is the faint shade of plausibility in this statement that in one definite sense, monatomic entities with at least $K = 10$ electrons are not in a much better shape than molecules with as many electrons. Section 3.2 was rather diplomatic and pussyfooted at one detail: the levels were characterized by the quantum number J and the (even or odd) parity. Then, the text went on telling that Russell–Saunders coupling combining J-levels to S,L-terms in agreement with the Hund coupling, eq. (3), might be a good approximation, and that could also be true for the comparable approximation of bunching the J-levels together in electron configurations, prescribing a definite number 0, 1, 2, ..., $(4l + 2)$ of electrons in each of the nl-shells introduced by Stoner in 1924. At first, this looks rather preposterous; atomic spectroscopists classify levels in configurations and there may sometimes be lacking levels not yet observed, but there is no convincing case of low-lying 'superfluous' levels not explained by a plausible configuration. Among atomic spectroscopists, the mixing of configurations was considered to be a faint correction, except for certain cases, where configurations of the same parity (even or odd number of electrons having odd l values) either overlap, or at the least, have a mutual distance of the same order as their width. It was admitted that the same operator of interelectronic repulsion having the diagonal element separating terms of the same configuration in the Slater–Condon–Shortley treatment, also has non-diagonal elements between terms with the same S, L and parity belonging to two different configurations. This line of thought was initiated by Ufford (1933) evaluating configuration intermixing of $[18]3d^{q-2}4s^2$, $[18]3d^{q-1}4s$ and $[18]3d^q$ and continued e.g. by Racah (1950) and Klinkenberg and Uylings (1986) of configurations involving 5f, 6d, 7s and 7p electrons in Th^{+2}. Condon and Shortley (1953) devoted one page to the mixing of ^1D in the $[10]3s3d$ and $[10]3p^2$ of the magnesium atom, and gave a slight hint that this may perhaps be a quite general phenomenon.

The wave-function for the ground state of the helium atom calculated by Hylleraas in 1930 was not a mixture of $1s^2$ with other configurations, but contained explicitly the distance between the two electrons. Around 1960, the Hylleraas and related functions were carefully transcribed to configuration intermixing (cf. Jørgensen 1962c,d, 1978c) and the tranquilizing conclusion was that the $1s^2$ Hartree function accounts for 99% of the squared amplitude of the ground state. It was also known that $1s^22s^2$ contributes only 90% of the ground state amplitude of the beryllium atom, but here a good excuse was available, since $1s^22p^2$ was known to contribute

8% of the remaining squared amplitude. It is still true that substitution in the ground configuration of two electrons into another shell with comparable average radius, such as 2s to 2p in nearly all elements, 3p to 3d for Z above 21, and 4d to 4f for Z above 58, is quite efficient. However, another substitution of two electrons takes place to an orbital in the continuum with positive one-electron energy, roughly the same average radius (once in the continuum, such orbitals can be tailor-made) and usually having one additional radial or angular node to keep orthogonal on the orbital in the Hartree–Fock model. Such substitutions were entirely elusive to atomic spectroscopists, but turned out to be dramatically important in atoms between carbon and argon.

Löwdin defines the *correlation energy* as the (negative) difference E_{corr} between the actual ground state energy (corrected for relativisitic effects, beginning as $-Z^4/2{\cdot}137^2$ rydberg, about 4 eV in the neon atom) and the optimized Hartree–Fock energy. For neon atoms, the correlation energy is -11 eV, about half of I_1 of the 2p shell, but for sodium atoms, and for all neutral atoms with higher Z, $-E_{corr}$ is larger than I_1. Gombas and Gaspar pointed out the empirical rule that the total binding energy of Z electrons to a Z nucleus for Z between 6 (carbon) and 90 (thorium) is $Z^{2.4}$ rydberg multiplied by a factor decreasing from 1.03 to 1.02 (around $Z = 28$) and then, for relativistic reasons, slowly increasing to 1.08 (non-relativistic case 0.996). Since m_0c^2 of one electron corresponds to $2{\cdot}137^2$ rydberg, this value is reached for $Z = 80$ (mercury). The many-electron system is rather feudal; as we already saw in section 3.2 the two 1s electrons contribute a large part of the total binding energy, and to a first approximation, this proportion is $2{\cdot}Z^{-0.4}$ or 41% for zinc and 35% for mercury. This also means that putting too much stress on the variational principle encourages finicking the 1s shell and neglecting the outer electrons, which may be acceptable for an X-ray expert, but not for a chemist. By the way, the closed-shell effects are rather negligible on the total binding energy, less than 0.1 percent in krypton and distinctly a few times 10^{-5} in radon. This forms a striking contrast to the binding energy of heavier nuclei with respect to Z protons and N neutrons, which is roughly proportional to $A = Z + N$ for most nuclei, within 10% for A above 12, but the Goeppert-Mayer shell effects for the quantum numbers Z or N (or both) 2, 8, 14, 20, 28, 50, 82 and 126 provide binding energies 1% higher than usual (Jørgensen 1981a).

It has become clear in recent years that $-E_{corr}$ in atoms with K above 10, and close to Z, is roughly proportional to the square root of the total binding energy, and actually close to $(0.7\text{ eV})Z^{1.2}$. This can be used for a crude, but quite interesting, estimate of the squared amplitude of the Hartree–Fock function in the actual wave-function for higher Z values. As long as this configuration intermixing does not virtually diverge, by increasing importance of 4, 6, 8,... electron substitutions, second-order perturbation theory applies to the two-electron substituted function with diagonal element of energy H_{kk} and the non-diagonal element H_{0k} with the conventional ground configuration having the diagonal energy element H_{00}. The difference $H_{kk} - H_{00}$ is also called $2I_k$. Then, the remaining squared amplitude of the conventional ground configuration in the lowest eigen-state is called $(1 - x_Z)$ since x_Z is the sum of the squared amplitude of the substituted configurations. The

second-order result is

$$-E_{\text{corr}} \sim \sum_k \frac{(H_{0k})^2}{(2I_k)}, \qquad x_Z \sim \sum_k \left(\frac{H_{0k}}{2I_k}\right)^2. \tag{14}$$

We now take a rather reprehensible step (which can only only be absolved by the need for an order of magnitude estimate) to identify the ratio (E_{corr}/x_Z) with an energy $2{\cdot}'I'$, where 'I' represents the average I_k weighted for this purpose. This provides rough estimates of the type

Z	$-E_{\text{corr}}$(eV)	x_Z	
2	1.1	(0.55 eV)/'I' ~ 0.009	if $2{\cdot}'I'$ ~ 120 eV,
10	11	(5 eV)/'I' ~ 0.08	if $2{\cdot}'I'$ ~ 140 eV,
30	38	(20 eV)/'I' ~ 0.3	if $2{\cdot}'I'$ ~ 120 eV,
60	90	(45 eV)/'I' ~ 0.6	if $2{\cdot}'I'$ ~ 150 eV,
80	133	(70 eV)/'I' ~ 0.7	if $2{\cdot}'I'$ ~ 200 eV.

(15)

These suggested values are not as arbitrary as they may look at first glance. It is expected in helium that the average parameter 'I' is relatively high since the substitution orbital is high up in the continuum, with kinetic energy close to $4{\cdot}I_1$ or 100 eV. There is no important contribution at lower energies. Most of the substitution in the neon atom takes place in the 2p shell, which is influenced mainly by orbitals $4I_1$ above 2p, or roughly $3I_1$ above the bottom of the continuum. As we go to higher Z, the 'I' increases because the inner shells with high $I(nl)$ contribute more to the substitutions. This is less true for neodymium having a rich stock of 4d orbitals able to acquire additional nodes at moderate cost, if for no other reason the multiple opportunities for replacing two 4d by two 4f electrons. This scenario is inverted for mercury, where both 4d and 4f shells are filled and have ionization energies close to 370 and 110 eV, respectively. It may of course be argued that the substitutions already diverge for $Z = 80$.

Several of the numbers in eq. (15) may readily be uncertain by a factor of two, but for our purpose, the most important feature is x_Z close to a half. This qualitative result pervades 'ligand field' calculations, and it is almost surprising that Hartree–Fock radial 4f functions only overestimate the parameters of interelectronic repulsion by 30–40%, and it is close to unbelievable that the relative distances of terms in Ln(III) are better described by Slater–Condon–Shortley–Racah parameters than d^q and p^q in monatomic entities.

Perhaps, one should not press the panic button; the numerous other configurations all have quite small squared amplitudes in $[54]4f^q$ (and probably, none is about 5%, though the seemingly distant $4d^84f^{q+2}$ may be more important). There is no discussion that $4f^q$ remains the preponderant configuration (Jørgensen 1969) in the sense of correctly classifying other low-lying configurations by substituting one or two of the 4f electrons with other nl electrons. Textbooks are reluctant to speak about a dielectric constant higher than 1 inside atoms, though it is normal to do it in adjacent condensed matter. It must certainly be admitted that

spectral lines of neutral atoms trapped in cool matrices such as solidified noble gases do not shift enormously, and the fact that they typically have wave-numbers 0.9 to 1.1 times the gaseous atoms prevents a rationalization by dielectric effects alone; the excited state is usually repelled by the neighbor atoms, connected with the local operator of kinetic energy. However, the smaller values of parameters than of integrals of interelectronic repulsion in partly filled shells suggest rather emphatically a dielectric decrease of the interelectronic repulsion. At this point, one should not expect the headline one morning that eq. (14) is divergent for the neptunium atom; the many small admixtures of configurations substituted in two *nl* values of the electrons in the conventional ground state have a close similarity to polarization orbitals introduced for explaining electric polarizability. The weird substituted configurations are there to provide interference cross-terms with the prevailing ground configuration, which are still 2% in the wave-function, if their squared amplitude is 10^{-4}.

Since we do not know any quantum operator involving more than two electrons at a time, it has been hoped that one might introduce a six-dimensional simplification (a second-order density matrix) rather than to disperse the wave-function in a useless way in $3K$ dimensions, plus the two-valued spin variable m_s, as is done implicitly in eq. (14). However, as far as the author understands, the hope now looks dimmer, because the variational principle (or an appropriate replacement for it) has not yet been found.

One may ask how Nature gets away with hiding eq. (14) and let a whole generation of atomic spectroscopists make their classifications, ignoring it. A few may even have torn out that page 366 of the book by Condon and Shortley. For a chemist, this is not really so surprising; the closed shells in the Periodic Table officiate as the neutral element of the Hund coupling, eq. (3). There is not a tremendous difference between the chemical similarity of yttrium and lanthanum; or between sulfur and selenium, and the similarity of the low-lying configurations of their monatomic entities. It is like two children playing; chemistry does not become less messy by being closer to physics today, but atoms with high K values (i.e. above 10) have given some nagging surprises to physicists.

The title question 'Is quantum chemistry feasible?' with special regard to R chemists and spectroscopists must be answered 'sorry, not today; perhaps next century' because the problem we have exposed for monatomic entities is necessarily a preliminary to further work on systems with additional nuclei. Chemistry at that level has the same relation to quantum mechanics as the weather forecast for next month, or rather the following, has to Newtonian mechanics. It is not conceptually excluded that it might be done, but how?

4.9. *We get more surprises from test-tubes than from computers*

The discovery of the rare earths in 1794 was a prototype of a surprise, it was not just one more metallic element, such as strontium and titanium. Many early observations are fascinating; Berzelius report that a very high concentration of didymium can be kept in solution in aqueous ammonia containing ammonium

tartrate (such solutions desiccate to transparent glasses soluble in weak ammonia). The suggestion of Matignon and Cazes (1906) of separating $SmCl_2$ from $NdCl_3$ and other $LnCl_3$ with anhydrous ethanol free of dissolved oxygen has a remarkable modern glamor; the first chemist knowing about the hygroscopic bromates $[Ln(OH_2)_9](BrO_3)_3$ and then precipitating the insoluble iodates $Ln(IO_3)_3$, or the inventor of the Auer mantle $Th_{0.99}Ce_{0.01}O_2$ (which might become important again in a hydrogen society, where gaseous H_2 may be produced in nuclear reactors situated in deserts without voters) must have had their day. The author is not familiar with permanent magnets, but would like to utter that $SmCo_5$ and $Nd_2Fe_{14}B$ have been found by serendipity. Like ferrocene $Fe(C_5H_5)_2$ nobody had expected the existence of co-volatility in $CsNdI_4$ and $NdCl_3(AlCl_3)_n$ nor that the most volatile R(III) compound is the cesium *salt* of yttrium tetrakis(hexafluoroacetylacetonate) (Lippard 1966) and among the tris(dipivaloylacetonates) the ytterbium(III) compound is more volatile than of the lighter Ln (Sicre et al. 1969).

There is a long-standing distinction between chemistry being inductive and physics deductive (Jørgensen 1979b). Perhaps due to the recent contact with physicists, the consumption and obsolescence of paradigms have taken unprecedented proportions in chemistry. Just after the war, Schrödinger quantum mechanics was only 20 years old, and it was not fully realized what impact it would have on (inorganic) chemistry. Today, it is 60 years old, and we have a much clearer picture of what it can do in actual practice, and what it cannot do.

Chemists have always liked models where one can make the calculations on the back of an envelope. This is how the Madelung energy of crystals combined with I_n of gaseous ions (Rabinowitch and Thilo 1930) became a healthy counterweight to the 1916 paradigm of Lewis. A late epigon of the Madelung model is the treatment (Jørgensen 1969) using differential ionization energies. Unfortunately, it does not work for the 4f group. A related question is that of hydration energies of cations and anions in water (Jørgensen 1975a, 1979a) showing unexpected regularities.

Molecular orbital calculations in the 4f and 5f groups run into the dilemma that if 'one-electron energies' mean I values, the calculations agreeing with photo-electron spectra provide almost coinciding ligand and 4f energies, inducing strong effects of delocalization and covalent bonding in disagreement with the absorption spectra, and in particular the weakly pronounced nephelauxetic effect. In the uranyl ion, six modern MO calculations disagree entirely about the order of the loosest bound orbitals (Jørgensen and Reisfeld 1982b, 1983b, DeKock et al. 1984) insinuating that at least five may not be entirely perfect. A minor problem in UO_2^{+2} (not present in UF_6) is the need for adding an external Madelung potential, but it seems to shift all the orbital energies by the same amount. Fortunately, photo-electron spectra of gaseous molecules are a valuable reference of comparison.

Although most preparative innovations in rare earths are not the direct result of numerical calculations, it should not be neglected that theory under less deductive forms play a very important role in rationalizing the chemical and spectroscopic observations. The major part of this (the more abstract side of the lanthanide research), is group-theoretical engineering having the same relations to group theory

as evaluation of real estate has to geometry since Euclid. We have to disregard that the point-group is abolished by a bird flying by the window, and forget many arguments as irrelevant as the distinction between irrational and rational numbers would be for the measurement of a length. It is a genuine surprise that J-levels persist in monatomic entities under conditions of moderate isolation, and to a quite good approximation in M(III) compounds in the 4f and 5f groups, and even, at least as far as the lowest J-level goes, in metallic lanthanides (Wallace et al. 1977) and in the photo-electron ionization producing Ln[IV] states (Jørgensen 1975b). The group-theoretical engineer (Schäffer and Jørgensen 1965, Jørgensen 1971) takes into account, if feasible, only the nearest neighbor atoms, and, when needed, idealize the local point-group like a mineralogist idealizes the chemical formula of a mineral. Many of the interactions important for chemistry (with the important exception of the spherically symmetric part of the Madelung potential) decrease exponentially with distance.

Theoretical considerations also play the role of rationalizing the observations in general ideas, not so much in a mnemotechnic sense (though the Periodic Table has some aspects of that too) as in an economy of 'botanical' efforts. When for instance the 4f group is the only group that has higher ionization energy half-filled than filled (one may ponder a moment what such a case in the 3d group would do to the chemistry of manganese and zinc) the refined spin-pairing treatment provided a consistent rationalization, combining this exceptional behavior with many other observations. The Judd–Ofelt parametrization is another concept originating in theoretical considerations, of widespread impact on the understanding of the 4f group.

The most surprising side is perhaps that atomic spectra to a great extent is in the same boat as the 4f group compounds. The persistence of J-levels in both cases (Jørgensen 1973b, 1976c, 1980a, 1981d, Reisfeld and Jørgensen 1977) is the more amazing, when it is realized how far both situations are from having well-defined configurations in the sense of Condon and Shortley. The numbers of states are invariant, compared to the conventional approximations, which is also astonishing in view of the inevitable continuum (Jørgensen 1985b) of coinciding states.

Acknowledgments

I am grateful to Professor Renata Reisfeld, the Hebrew University, Jerusalem for the opportunity (as an armchair commentator) of recalling the uncanny subject of luminescence, and for a most fruitful collaboration on the rare earths since 1974.

I am also grateful to Professor Sheldon L. Glashow, Harvard University, for many discussions on 'elementary' particles and astrophysics, and for his unique flair for posing the relevant questions about geochemical behavior of rare modifications of matter.

Finally, I am grateful to the late Professor Moise Haïssinsky; to Professor Kai Arne Jensen, University of Copenhagen; to Professor George B. Kauffman, California State University, Fresno; to Professor Edmond Rancke-Madsen, the

Royal Danish School of Educational Studies; and to Dr. Hans Toftlund, Odense University, for most informative and helpful discussions about the Periodic Table.

References

Adachi, G., K. Sorita, K. Kawata, K. Tomokiyo and J. Shiokawa, 1983, J. Less-Common Met. **93**, 81.

Adamson, A.W., 1983, J. Chem. Educ. **60**, 797.

Alcock, C., E. Farhi and A. Olinto, 1986, Phys. Rev. Lett. **57**, 2088.

Allen, G.C., M.B. Wood and J.M. Dyke, 1973, J. Inorg. Nucl. Chem. **35**, 2311.

Alzuhairi, T.J.M., and S. Siekierski, 1983, Radiochem. Radioanal. Lett. **57**, 301.

Baer, Y., and W.D. Schneider, 1987, This Handbook, Vol. 10, ch. 62.

Bagnall, K.W., and D. Brown, 1967, J. Chem. Soc. (A) p. 275.

Bagus, P.S., Y.S. Lee and K.S. Pitzer, 1975, Chem. Phys. Lett. **33**, 408.

Bahr, J.F., 1865, Liebig's Annalen **135**, 376.

Ball, R.W., and L.F. Yntema, 1930, J. Am. Chem. Soc. **52**, 4264.

Baym, G., 1982, Springer Tracts in Modern Physics **100**, 186.

Berthou, H., and C.K. Jørgensen, 1975, Anal. Chem. **47**, 482.

Berthou, H., C.K. Jørgensen and C. Bonnelle, 1976, Chem. Phys. Lett. **38**, 199.

Bethe, H., and F.H. Spedding, 1937, Phys. Rev. **52**, 454.

Bisgaard, P., R. Bruch, P. Dahl, B. Fastrup and M. Rødbro, 1978, Phys. Scr. **17**, 49.

Bjerrum, N.J., H.L. Davis and G.P. Smith, 1967, Inorg. Chem. **6**, 1603.

Bjørn-Andersen, H., 1933, Z. Anorg. Allg. Chem. **210**, 93.

Blaise, J., and L.J. Radziemski, 1976, J. Opt. Soc. Am. **66**, 644.

Blasse, G., 1976, Struct. Bonding **26**, 43.

Blasse, G., and A. Bril, 1967, J. Chem. Phys. **47**, 5139.

Blazey, K.W., M. Aguilar, J.G. Bednorz and K. Müller, 1983, Phys. Rev. B **27**, 5836.

Bohr, N., 1923, Naturwissenschaften **11**, 606.

Boulanger, F., 1952, Ann. Chim. (France) **7**, 732.

Brauer, G., and H. Kristen, 1979, Z. Anorg. Allg. Chem. **456**, 41.

Brauer, G., and H. Kristen, 1980, Z. Anorg. Allg. Chem. **462**, 35.

Brecher, H., H. Samelson, A. Lempicki, R. Riley and T. Peters, 1967, Phys. Rev. **155**, 178.

Broer, L.J.F., C.J. Gorter and J. Hoogschagen, 1945, Physica **11**, 231.

Brorson, M., and C.E. Schäffer, 1987, Inorg. Chem. in press.

Brown, D., B. Whittaker and N. Edelstein, 1974, Inorg. Chem. **13**, 1805.

Bury, C.R., 1921, J. Am. Chem. Soc. **43**, 1602.

Busby, R., W. Klotzbücher and G.A. Ozin, 1977, Inorg. Chem. **16**, 822.

Butement, F.D.S., 1948, Trans. Faraday Soc. **44**, 617.

Cahn, R.N., and S.L. Glashow, 1981, Science **213**, 607.

Campagna, M., E. Bucher, G.K. Wertheim, D.N.E. Buchanan and L.D. Longinotti, 1974, Phys. Rev. Lett. **32**, 885.

Campagna, M., G.K. Wertheim and E. Bucher, 1976, Struct. Bonding **30**, 99.

Carnall, W.T., 1979, This Handbook, Vol. 3, ch. 24.

Carnall, W.T., P.R. Fields and K. Rajnak, 1968, J. Chem. Phys. **49**, 4412, 4424, 4443, 4447, 4450.

Carnall, W.T., H. Crosswhite, H.M. Crosswhite and J.G. Conway, 1976, J. Chem. Phys. **64**, 3582.

Carnall, W.T., J.V. Beitz and H. Crosswhite, 1984, J. Chem. Phys. **80**, 2301.

Catalán, M.A., F. Röhrlich and A.G. Shenstone, 1954, Proc. R. Soc. London Ser. A **221**, 421.

Chandrasekhar, T., N.M. Ashok, J.N. Desai, J.M. Pasachoff and K.R. Sivaraman, 1984, Appl. Opt. **23**, 508.

Chang, N.C., J.B. Gruber, R.P. Leavitt and C.A. Morrison, 1982, J. Chem. Phys. **76**, 3877.

Cohen, D., and W.T. Carnall, 1960, J. Phys. Chem. **64**, 1933.

Comfort, J.R., W.R. Gibbs and B.G. Ritchie, 1985, AIP Conf. Proc. no. 133 (American Institute of Physics, New York).

Condon, E.U., and G.H. Shortley, 1953, Theory of Atomic Spectra, 2nd Ed. (University Press, Cambridge).

Connerade, J.P., 1983, J. Less-Common Met. **93**, 171.

Coster, D., 1923, Naturwissenschaften **11**, 567.

Cowan, R.D., 1973, Nucl. Instrum. & Methods **110**, 173.

Cowley, C.R., and J.B. Rice, 1981, Nature **294**, 636.

Cox, P.A., 1975, Struct. Bonding **24**, 59.

Cox, P.A., Y. Baer and C.K. Jørgensen, 1973, Chem. Phys. Lett. **22**, 433.

Crookes, W., 1888, J. Chem. Soc. **53**, 487.

Crookes, W., 1895, Die Genesis der Elemente, zweite deutsche Auflage von W. Preyer (Friedrich Vieweg, Braunschweig).

Crosswhite, H.M., H. Crosswhite, W.T. Carnall and A.P. Paszek, 1980, J. Chem. Phys. **72**, 5103.

Darnall, A.J., 1978, in: Rare Earths in Modern Science and Technology, eds G.J. McCarthy and J.J. Rhyne (Plenum, New York) p. 297.

De Vore, T.C., 1976, Inorg. Chem. **15**, 1316.

DeKock, R.L., E.J. Baerends, P.M. Boerrigter and J.G. Snijders, 1984, Chem. Phys. Lett. **105**, 308.
DeRújula, A., and S.L. Glashow, 1984, Nature **312**, 734.
DeRújula, A., R.C. Giles and R.L. Jaffe, 1978, Phys. Rev. D **17**, 285.
Drotning, W.D., and H.G. Drickamer, 1973, J. Chem. Phys. **59**, 3482.
DuBois, H., and G.J. Elias, 1908, Ann. Phys. (Germany) **27**, 233.
Duffy, J.A., 1977, Struct. Bonding **32**, 147.
Durville, F., G. Boulon, R. Reisfeld, H. Mack and C.K. Jørgensen, 1983, Chem. Phys. Lett. **102**, 393.
Dye, J.L., 1984, Progr. Inorg. Chem. **32**, 327.
Eastman, D.E., and M. Kuznietz, 1971, J. Appl. Phys. **42**, 1396.
Eller, P.G., and R.A. Penneman, 1987, J. Less-Common Met. **127**, 19.
Elliott, J.P., B.R. Judd and W.A. Runciman, 1957, Proc. R. Soc. London Ser. A **240**, 509.
Ephraim, F., and M. Mezener, 1933, Helv. Chim. Acta **16**, 1257.
Eyring, L., 1979, This Handbook, Vol. 3, ch. 27.
Fadley, C.S., and D.A. Shirley, 1970, Phys. Rev. A **2**, 1109.
Farhi, E., and R.L. Jaffe, 1984, Phys. Rev. D **30**, 2379.
Faucher, M., D. Garcia and C.K. Jørgensen, 1986, Chem. Phys. Lett. **129**, 387.
Feistel, G.R., and T.P. Mathai, 1968, J. Am. Chem. Soc. **90**, 2988.
Fernelius, W.C., 1986, J. Chem. Educ. **63**, 263.
Feynman, R.P., 1974, Science **183**, 601.
Fidelis, I.K., and T. Mioduski, 1981, Struct. Bonding **47**, 27.
Finkelstein, R., and J.H. Van Vleck, 1940, J. Chem. Phys. **8**, 790.
Flahaut, J., 1979, This Handbook, Vol. 4, ch. 31.
Fouassier, C., B. Latourette, J. Derouet and P. Hagenmuller, 1977, in: Colloque CNRS no. 255, ed. F. Gaume (CNRS, Paris) p. 83.
Fraser, G., 1986, CERN Courier **26**, no. 4 (May 1986) 29.
Freed, S., 1931, Phys. Rev. **38**, 2122.
Fried, S., and J.C. Hindman, 1954, J. Am. Chem. Soc. **76**, 4863.
Fuggle, J.C., 1983, J. Less-Common Met. **93**, 159.
Galeotti, P., and E. Lovera, 1974, Nature **249**, 130.
Garcia, A., R. Ibanez and C. Fouassier, 1985, in: Rare Earths Spectroscopy, eds B. Jeżowska-Trzebiatowska, J. Legendziewicz and W. Stręk (World Scientific, Singapore) p. 412.
Garcia, D., and M. Faucher, 1983, J. Less-Common Met. **93**, 119.
Gelius, U., 1974, J. Electron Spectr. & Relat. Phenom. **5**, 985.
Gell-Mann, M., 1964, Phys. Lett. **8**, 214.
Gladstone, J.H., 1857, J. Chem. Soc. **10**, 219.
Glaser, J., and G. Johansson, 1981, Acta Chem. Scand. A **35**, 639.
Glashow, S.L., 1980, Rev. Mod. Phys. **52**, 539.
Glerup, J., 1972, Acta Chem. Scand. **26**, 3775.
Glerup, J., D.J. Hodgson and E. Pedersen, 1983, Acta Chem. Scand. A **37**, 161.
Gmelin-Kraut, 1928, Handbuch der anorganischen Chemie, Band 6, Abteilung 1 and 2 (Winter, Heidelberg).
Gobrecht, H., 1938, Ann. Phys. (Germany) **31**, 600, 755.
Goldschmidt, Z.B., 1978, This Handbook, Vol. 1, ch. 1.
Green, J.C., 1981, Struct. Bonding **43**, 37.
Greis, O., and M. Kieser, 1981, Z. Anorg. Allg. Chem. **479**, 165.
Gruber, J.B., J.R. Morrey and D.G. Carter, 1979, J. Chem. Phys. **71**, 3982.
Gubelmann, M.H., and A.F. Williams, 1983, Struct. Bonding **55**, 1.
Gutmann, V., 1970, J. Chem. Educ. **47**, 209.
Hagström, S., C. Nordling and K. Siegbahn, 1964, Z. Phys. **178**, 439.
Hamnett, A., 1972, Discuss. Faraday Soc. **54**, 251.
Haschke, J.M., 1979, This Handbook, Vol. 4, ch. 32.
Haskin, L.A., and T.P. Paster, 1979, This Handbook, Vol. 3, ch. 21.
Heidt, L.J., and J. Berestecki, 1955, J. Am. Chem. Soc. **77**, 2049.
Heidt, L.J., and M.E. Smith, 1948, J. Am. Chem. Soc. **70**, 2476.
Henderson, J.R., M. Muramoto, T.M. Henderson and J.B. Gruber, 1967, J. Chem. Phys. **47**, 5097.
Henry, W.E., 1958, J. Appl. Phys. **29**, 524.
Hitchman, M.A., and P.J. Cassidy, 1979, Inorg. Chem. **18**, 1745.
Hoefdraad, H.E., 1975, J. Inorg. Nucl. Chem. **37**, 1917.
Hoffman, D.C., F.O. Lawrence, J.L. Mewherter and F.M. Rourke, 1971, Nature **234**, 132.
Hoffman, M.V., 1972, J. Electrochem. Soc. **119**, 905.
Hoppe, R., 1981, Angew. Chem **93**, 64; Int. Ed. **20**, 63.
Hotokka, M., T. Kindstedt, P. Pyykkö and B.O. Ross, 1984, Mol. Phys. **52**, 23.
Huber, H., T.A. Ford, W. Klotzbücher and G. Ozin, 1976, J. Am. Chem. Soc. **98**, 3176.
Hulliger, F., 1968, Helv. Phys. Acta **41**, 945.
Hund, F., 1927, Linienspektren und Periodisches System der Elemente (Julius Springer, Berlin).
Jacobs, J.M., and M.M. Dworetsky, 1982, Nature **299**, 535.
Jantsch, G., H. Alber and H. Grubitsch, 1929, Monatsheft für Chemie **53**, 305.
Joensen, F., and C.E. Schäffer, 1984, Acta Chem. Scand. A **38**, 819.
Johnson, D.A., 1977, Adv. Inorg. Chem. Radiochem. **20**, 1.
Jones, S.E., 1986, Nature **321**, 127.
Jørgensen, C.K., 1955, Acta Chem. Scand. **9**, 540.
Jørgensen, C.K., 1956a, Mat. Fys. Medd. Dan. Vidensk. Selsk. **30**, No. 22.
Jørgensen, C.K., 1956b, Acta Chem. Scand. **10**,

1505.
Jørgensen, C.K., 1961, Mol. Phys. **4**, 235.
Jørgensen, C.K., 1962a, Mol. Phys. **5**, 271.
Jørgensen, C.K., 1962b, Acta Chem. Scand. **16**, 2406.
Jørgensen, C.K., 1962c, Orbitals in Atoms and Molecules (Academic Press, London).
Jørgensen, C.K., 1962d, Solid State Phys. **13**, 375.
Jørgensen, C.K., 1963a, Adv. Chem. Phys. **5**, 33.
Jørgensen, C.K., 1963b, Acta Chem. Scand. **17**, 1034, 1043.
Jørgensen, C.K., 1963c, Inorganic Complexes (Academic Press, London).
Jørgensen, C.K., 1964, Mol. Phys. **7**, 417.
Jørgensen, C.K., 1967a, Chem. Phys. Lett. **1**, 11.
Jørgensen, C.K., 1967b, in: Halogen Chemistry, Vol. 1, ed. V. Gutmann (Academic Press, London) p. 265.
Jørgensen, C.K., 1968, Chem. Phys. Lett. **2**, 549.
Jørgensen, C.K., 1969, Oxidation Numbers and Oxidation States (Springer, Berlin).
Jørgensen, C.K., 1970a, J. Inorg. Nucl. Chem. **32**, 3127.
Jørgensen, C.K., 1970b, Progr. Inorg. Chem. **12**, 101.
Jørgensen, C.K., 1971, Modern Aspects of Ligand Field Theory (North-Holland, Amsterdam).
Jørgensen, C.K., 1973a, Angew. Chem. **85**, 1; Int. Ed. **12**, 12.
Jørgensen, C.K., 1973b, Struct. Bonding **13**, 199.
Jørgensen, C.K., 1974a, Chimia **28**, 6.
Jørgensen, C.K., 1974b, Adv. Quantum Chem. **8**, 137.
Jørgensen, C.K., 1975a, Top. Curr. Chem. **56**, 1.
Jørgensen, C.K., 1975b, Struct. Bonding **22**, 49.
Jørgensen, C.K., 1975c, Chem. Phys. Lett. **34**, 14.
Jørgensen, C.K., 1975d, Struct. Bonding **24**, 1.
Jørgensen, C.K., 1976a, Struct. Bonding **25**, 1.
Jørgensen, C.K., 1976b, Struct. Bonding **30**, 141.
Jørgensen, C.K., 1976c, Gmelins Handbuch der anorganischen Chemie, Seltenerd-Elemente, Vol. B1 (Springer, Berlin) p. 17.
Jørgensen, C.K., 1978a, Chimia **32**, 89.
Jørgensen, C.K., 1978b, J. Am. Chem. Soc. **100**, 5968.
Jørgensen, C.K., 1978c, Adv. Quantum Chem. **11**, 51.
Jørgensen, C.K., 1978d, Struct. Bonding **34**, 19.
Jørgensen, C.K., 1979a, This Handbook, Vol. 3, ch. 23.
Jørgensen, C.K., 1979b, J. Chim. Phys. (France) **76**, 630.
Jørgensen, C.K., 1980a, Isr. J. Chem. **19**, 174.
Jørgensen, C.K., 1980b, Chimia **34**, 381.
Jørgensen, C.K., 1980c, The Rare Earths in Modern Science and Technology, Vol. 2, eds G.J. McCarthy, J.J. Rhyne and H.B. Silber (Plenum Press, New York) p. 425.
Jørgensen, C.K., 1981a, Struct. Bonding **43**, 1.
Jørgensen, C.K., 1981b, Comments Inorg. Chem. **1**, 123.
Jørgensen, C.K., 1981c, Nature **292**, 41.
Jørgensen, C.K., 1981d, Int. Rev. Phys. Chem. **1**, 225.
Jørgensen, C.K., 1982a, Chem. Phys. Lett. **87**, 320.
Jørgensen, C.K., 1982b, Naturwissenschaften **69**, 420.
Jørgensen, C.K., 1983a, Radiochim. Acta **32**, 1.
Jørgensen, C.K., 1983b, Rev. Chim. Miner. (France) **20**, 533.
Jørgensen, C.K., 1983c, Nature **305**, 787.
Jørgensen, C.K., 1984a, Chimia **38**, 75.
Jørgensen, C.K., 1984b, Can Chemical Properties of Systems Containing Unsaturated Quarks be Deduced from Mulliken Electronegativities of Monatomic Species? (preprint, Geneva).
Jørgensen, C.K., 1984c, Naturwissenschaften **71**, 151, 418.
Jørgensen, C.K., 1984d, Top. Curr. Chem. **124**, 1.
Jørgensen, C.K., 1985a, J. Less-Common Met. **112**, 141.
Jørgensen, C.K., 1985b, J. Phys. Colloq. (France) **46**, C-7, 409.
Jørgensen, C.K., 1986a, Z. Anorg. Allg. Chem. **540**, 91.
Jørgensen, C.K., 1986b, Rev. Chim. Miner. (France) **23**, 614.
Jørgensen, C.K., 1987, Inorg. Chim. Acta **139**, 1.
Jørgensen, C.K., 1988, Chimia **42**, 21.
Jørgensen, C.K., and H. Berthou, 1972a, Chem. Phys. Lett. **13**, 186.
Jørgensen, C.K., and H. Berthou, 1972b, Mat. Fys. Medd. Dan. Vidensk. Selsk. **38**, No. 15.
Jørgensen, C.K., and H. Berthou, 1975a, Chem. Phys. Lett. **31**, 416.
Jørgensen, C.K., and H. Berthou, 1975b, Chem. Phys. Lett. **36**, 432.
Jørgensen, C.K., and J.S. Brinen, 1963, Mol. Phys. **6**, 629.
Jørgensen, C.K., and G.B. Kauffman, 1988, in preparation.
Jørgensen, C.K., and V. Parthasarathy, 1978, Acta Chem. Scand. A **32**, 957.
Jørgensen, C.K., and R. Reisfeld, 1982a, Top. Curr. Chem. **100**, 127.
Jørgensen, C.K., and R. Reisfeld, 1982b, Struct. Bonding **50**, 121.
Jørgensen, C.K., and R. Reisfeld, 1983a, J. Less-Common Met. **93**, 107.
Jørgensen, C.K., and R. Reisfeld, 1983b, J. Electrochem. Soc. **130**, 681.
Jørgensen, C.K., and E. Rittershaus, 1967, Mat. Fys. Medd. Dan. Vidensk. Selsk. **35**, No. 15.
Jørgensen, C.K., R. Pappalardo and H.H. Schmidtke, 1963, J. Chem. Phys. **39**, 1422.
Jørgensen, C.K., H. Bill and R. Reisfeld, 1981, J. Lumin. **24**, 91.
Jørgensen, C.K., M. Faucher and D. Garcia, 1986, Chem. Phys. Lett. **128**, 250.
Jørgensen, C.K., M. Lenglet and J. Arsène, 1987, Chem. Phys. Lett. **136**, 475.
Joubert, M.F., G. Boulon and F. Gaume, 1981, Chem. Phys. Lett. **80**, 367.
Judd, B.R., 1962, Phys. Rev. **127**, 750.
Kaindl, G., G.K. Wertheim, G. Schmiester and

E.V. Sampathkumuran, 1987, Phys. Rev. Lett. **58**, 606.
Katriel, J., and C.K. Jørgensen, 1982, Chem. Phys. Lett. **87**, 315.
Katriel, J., and R. Pauncz, 1977, Adv. Quantum Chem. **10**, 143.
Kauffman, G.B., 1982, J. Chem. Educ. **59**, 3, 119.
Kaufman, J.J., and L.M. Sachs, 1969, J. Chem. Phys. **51**, 2992.
Kaufman, V., and J. Sugar, 1976, J. Opt. Soc. Am. **66**, 439, 1019.
Klapisch, M., P. Mandelbaum, A. Zigler, C. Bauche-Arnoult and J. Bauche, 1986, Phys. Scr. **34**, 51.
Klemm, W., and H. Bommer, 1937, Z. Anorg. Allg. Chem. **231**, 138.
Klemm, W., and W. Schüth, 1929, Z. Anorg. Allg. Chem. **184**, 352.
Klinkenberg, P.F.A., and R.J. Lang, 1949, Physica **15**, 774.
Klinkenberg, P.F.A., and P.H.M. Uylings, 1986, Phys. Scr. **34**, 413.
Kobayasi, T., S. Mroczkowski, J.F. Owen and L.H. Brixner, 1980, J. Lumin. **21**, 247.
Koch, W., and G. Frenking, 1986, J.C.S. Chem. Comm. 1095.
Koch, W., J.R. Collins and G. Frenking, 1986, Chem. Phys. Lett. **132**, 330.
Kossel, W., 1916, Ann. Phys. (Germany) **49**, 229.
Kraus, K.A., and F. Nelson, 1950, J. Am. Chem. Soc. **72**, 3901.
Kröger, F.A., and J. Bakker, 1941, Physica **8**, 628.
Kuroda, P.K., 1982, The Origin of the Chemical Elements (Springer, Berlin).
Kuse, D., and C.K. Jørgensen, 1967, Chem. Phys. Lett. **1**, 314.
Lackner, K.S., and G. Zweig, 1982, AIP Conf. Proc. no. 93 (American Institute of Physics, New York) p. 1.
Lackner, K.S., and G. Zweig, 1983, Phys. Rev. D **28**, 1671.
Lammers, M.J.J., and G. Blasse, 1986, Chem. Phys. Lett. **126**, 405.
LaRue, G.S., J.D. Phillips and W.M. Fairbank, 1981, Phys. Rev. Lett. **46**, 967.
Lee, E.P.F., A.W. Potts and J.E. Bloor, 1982, Proc. R. Soc. London Ser. A **381**, 373.
Lee, T.D., 1975, Rev. Mod. Phys. **47**, 267.
Leger, J.M., N. Yacoubi and J. Loriers, 1980, Inorg. Chem. **19**, 2252.
Levy, S.J., 1924, The Rare Earths. Their Occurrence, Chemistry and Technology, 2nd Ed. (Arnold, London).
Linarès, C., A. Louat and M. Blanchard, 1977, Struct. Bonding **33**, 179.
Lippard, S.J., 1966, J. Am. Chem. Soc. **88**, 4300.
Litzén, U., 1974, Phys. Scr. **10**, 103.
Loh, E., 1966, Phys. Rev. **147**, 332.
Madsen, J., H. Heiselberg and K. Riisager, 1986, Phys. Rev. D **34**, 2947.
Maeder, A., and A. Renzini, 1984, Observational Tests of the Stellar Evolution Theory, IAU Symposium no. 105 (Reidel, Dordrecht).
Marcantonatos, M.D., and M. Deschaux, 1981, Chem. Phys. Lett. **80**, 327.
Marcantonatos, M.D., M. Deschaux and J.J. Vuilleumier, 1981, Chem. Phys. Lett. **82**, 36.
Marcantonatos, M.D., M. Deschaux and J.J. Vuilleumier, 1982, Chem. Phys. Lett. **91**, 149.
Marcantonatos, M.D., M. Deschaux and J.J. Vuilleumier, 1984, J. Chem. Soc. Faraday Trans. II **80**, 1569.
Marcantonatos, M.D., M. Deschaux, J.J. Vuilleumier, J.J. Combremont and J. Weber, 1986, J. Chem. Soc. Faraday Trans. II **82**, 609.
Marinsky, J.A., L.E. Glendenin and C.D. Coryell, 1947, J. Am. Chem. Soc. **69**, 2781.
Marsh, J.K., 1946, J. Chem. Soc., p. 15.
Martin, W.C., 1971, J. Opt. Soc. Am. **61**, 1682.
Martin, W.C., R. Zalubas and L. Hagan, 1978, Atomic Energy Levels, the Rare Earth Elements. NSRDS-NBS 60 (National Bureau of Standards, Washington, DC).
Matignon, C., and E. Cazes, 1906, C.R. Hebd. Séances Acad. Sci. **142**, 83; Ann. Chim. Phys. (France) **8**, 417.
McClure, D.S., and Z. Kiss, 1963, J. Chem. Phys. **39**, 3251.
McClure, D.S., and C. Pedrini, 1985, J. Phys. Colloq. (France) **46**, C-7, 397.
Meggers, W.F., C.H. Corliss and B.F. Scribner, 1961, Tables of Spectral-Line Intensities. NBS Monograph no. 32 (National Bureau of Standards, Washington, DC).
Messer, C.E., and I.S. Levy, 1965, Inorg. Chem. **4**, 543.
Meyer, R.J., 1905, Z. Anorg. Chem. **43**, 416.
Morrison, C.A., and R.P. Leavitt, 1982, This Handbook, Vol. 5, ch. 46.
Müller, A., E. Diemann and C.K. Jørgensen, 1973, Struct. Bonding **14**, 23.
Naegele, J.R., J. Ghijsen and L. Manes, 1985, Struct. Bonding **59**, 197.
Nixon, J.F., 1985, Adv. Inorg. Chem. Radiochem. **29**, 41.
Nugent, L.J., 1970, J. Inorg. Nucl. Chem. **32**, 4385.
Nugent, L.J., R.D. Baybarz, J.L. Burnett and J.L. Ryan, 1973, J. Phys. Chem. **77**, 1528.
Ofelt, G.S., 1962, J. Chem. Phys. **37**, 511.
Okada, K., Y. Kaizu, H. Kobayashi, K. Tanaka and F. Marumo, 1985, Mol. Phys. **54**, 1293.
Onishi, T., 1979, Nature **277**, 545.
Orgel, L.E., 1955, J. Chem. Phys. **23**, 1824.
Ozin, G.A., and A. Van der Voet, 1973, Acc. Chem. Res. **6**, 313.
Palilla, F.C., A.K. Levine and M. Rinkevics, 1965, J. Electrochem. Soc. **112**, 776.
Paschen, F., 1919, Ann. Phys. (Germany) **60**, 405.
Peacock, R.D., 1975, Struct. Bonding **22**, 83.
Pearson, R.G., 1986, J. Am. Chem. Soc. **108**, 6109.
Pedrini, C., F. Rogemond, F. Gaume and D.S. McClure, 1985, J. Less-Common Met. **112**, 103.
Peebles, P.J.E., 1986, Nature **321**, 27.
Penneman, R.A., and C.K. Jørgensen, 1976, in:

Heavy Element Properties, eds W. Müller and H. Blank (North-Holland, Amsterdam) p. 117.
Penneman, R.A., J.B. Mann and C.K. Jørgensen, 1971, Chem. Phys. Lett. **8**, 321.
Perera, J.S.H.Q., D.C. Frost, C.A. McDowell, C.S. Ewig, R.J. Key and M.S. Banna, 1982, J. Chem. Phys. **77**, 3308.
Pope, M.T., 1983, Heteropoly and Isopoly Oxometallates (Springer, Berlin).
Prandtl, W., 1938, Z. Anorg. Allg. Chem. **238**, 321.
Prandtl, W., and K. Scheiner, 1934, Z. Anorg. Allg. Chem. **220**, 107.
Przibram, K., 1937, Z. Phys. **107**, 709.
Przybylski, A., 1966, Nature **210**, 20.
Rabalais, J.W., 1977, Principles of Ultraviolet Photoelectron Spectroscopy (Wiley–Interscience, New York).
Rabinowitch, E., and E. Thilo, 1930, Periodisches System, Geschichte und Theorie (Enke, Stuttgart).
Racah, G., 1949, Phys. Rev. **76**, 1352.
Racah, G., 1950, Physica **16**, 651.
Ramsay, W., 1895a, Proc. R. Soc. London **58**, 65.
Ramsay, W., 1895b, C.R. Hebd. Séances Acad. Sci. **120**, 660.
Rancke-Madsen, E., 1984, Grundstoffernes Opdagelseshistorie (Gad, Copenhagen).
Rasmussen, L., and C.K. Jørgensen, 1968, Acta Chem. Scand. **22**, 2313.
Reisfeld, R., and C.K. Jørgensen, 1977, Lasers and Excited States of Rare Earths (Springer, Berlin).
Reisfeld, R., and C.K. Jørgensen, 1987, This Handbook, Vol. 9, ch. 58.
Robin, M.B., and P. Day, 1967, Adv. Inorg. Chem. Radiochem. **10**, 248.
Rosseinsky, D.R., 1965, Chem. Rev. **65**, 467.
Rowe, M.W., 1986, J. Chem. Educ. **63**, 300.
Rudorf, G., 1900, The Periodic Classification and the Problem of Chemical Evolution (Whittaker, London).
Ruedenberg, K., 1962, Rev. Mod. Phys. **34**, 326.
Ruscic, B., G.L. Goodman and J. Berkowitz, 1983, J. Chem. Phys. **78**, 5443.
Ryan, J.L., 1969, Inorg. Chem. **8**, 2053.
Ryan, J.L., and C.K. Jørgensen, 1966, J. Chem. Phys. **70**, 2845.
Rydberg, J.R., 1914, J. Chim. Phys. (France) **2**, 585.
Sabbatini, N., M. Ciano, S. Dellonte, A. Bonazzi and V. Balzani, 1982, Chem. Phys. Lett. **90**, 265.
Sabbatini, N., M. Ciano, S. Dellonte, A. Bonazzi, F. Bolleta and V. Balzani, 1984, J. Phys. Chem. **88**, 1534.
Salzmann, J.J., and C.K. Jørgensen, 1968, Helv. Chim. Acta **51**, 1276.
Sardar, D.K., W.A. Sibley and R. Alcala, 1982, J. Lumin. **27**, 401.
Satten, R.A., 1953, J. Chem. Phys. **21**, 637.
Satten, R.A., C.L. Schreiber and E.Y. Wong, 1983, J. Chem. Phys. **78**, 79.
Satz, H., 1986, Nature **324**, 116.
Scaife, D.E., and A.W. Wylie, 1964, J. Chem. Soc., p. 5450.
Schaefer, H.F., 1986, Science **231**, 1100.
Schäffer, C.E., 1982, Physica A **114**, 28.
Schäffer, C.E., and C.K. Jørgensen, 1965, Mol. Phys. **9**, 401.
Scherrer, R.J., and M.S. Turner, 1986, Phys. Rev. D **33**, 1585.
Schugar, H.J., E.I. Solomon, W.L. Cleveland and L. Goodman, 1975, J. Am. Chem. Soc. **97**, 6442.
Schuurmans, M.F.H., and J.M.F. Van Dijk, 1984, Physica B **123**, 131.
Sherill, M.S., C.B. King and R.C. Spooner, 1943, J. Am. Chem. Soc. **65**, 170.
Sicre, J.E., J.T. Dubois, K.J. Eisentraut and R.E. Sievers, 1969, J. Am. Chem. Soc. **91**, 3476.
Silva, R.J., W.J. McDowell, O.L. Keller and J.R. Tarrant, 1974, Inorg. Chem. **13**, 2233.
Sinha, S.P., 1976, Struct. Bonding **25**, 69.
Slater, J.C., 1968, Phys. Rev. **165**, 655.
Slater, J.L., R.K. Sheline, K.C. Lin and W. Weltner, 1971, J. Chem. Phys. **55**, 5129.
Slater, J.L., T.C. DeVore and V. Calder, 1973, Inorg. Chem. **12**, 1918.
Smith, D.W., 1978, Struct. Bonding **35**, 87.
Smith, J.D.M., 1924, Chemistry & Industry **43**, 323.
Smith, J.D.M., 1925, Chemistry & Industry **44**, 944.
Sovers, O.J., and T. Yoshioka, 1969, J. Chem. Phys. **51**, 5330.
Spector, N., and J. Sugar, 1976, J. Opt. Soc. Am. **66**, 436.
Spector, N., C. Bonnelle, G. Dufour, C.K. Jørgensen and H. Berthou, 1976, Chem. Phys. Lett. **41**, 199.
Spedding, F.H., E.I. Fulmer, T.A. Butler, E.M. Gladrow, M. Gobush, P.E. Porter, J.E. Powell and J.M. Wright, 1947, J. Am. Chem. Soc. **69**, 2812.
Spencer, J.F., 1919, The Metals of the Rare Earths (Longmans, Green & Co., London).
Spitsyn, V.I., V.G. Vokhmin and G. Ionova, 1985, Int. Rev. Phys. Chem. **4**, 57.
Stewart, D.C., 1948, Light Absorption ..., part I, AECD 2389 (Argonne, IL).
Stewart, D.C., and D. Kato, 1958, Anal. Chem. **30**, 164.
Stoner, E.C., 1924, Philos. Mag. **48**, 719.
Stoner, E.C., 1925, Philos. Mag. **49**, 1289.
Sugar, J., 1965, J. Opt. Soc. Am. **55**, 1058.
Sugar, J., and J. Reader, 1973, J. Chem. Phys. **59**, 2083.
Texter, J., J.J. Hastreiter and J.L. Hall, 1983, J. Phys. Chem. **87**, 4690.
Thomsen, J., 1895a, Z. Anorg. Chem. **9**, 190.
Thomsen, J., 1895b, Z. Anorg. Chem. **9**, 283.
Trasatti, S., 1986, Pure & Appl. Chem. **58**, 955.
Trimble, V., 1975, Rev. Mod. Phys. **47**, 877.
Trimble, V., 1982, Rev. Mod. Phys. **54**, 1183.
Trimble, V., 1983, Rev. Mod. Phys. **55**, 511.

Turner, D.W., C. Baker, A.D. Baker and C.R. Brundle, 1970, Molecular Photoelectron Spectroscopy (Wiley-Interscience, London).
Turok, N., 1986, Nature **322**, 111.
Ufford, C.W., 1933, Phys. Rev. **44**, 732.
Urbain, G., 1909, Ann. Chim. Phys. (France) **18**, 289.
Urbain, G., 1925, Chem. Rev. **1**, 143.
Urbain, G., and F. Bourion, 1911, C.R. Hebd. Séances Acad. Sci. **153**, 1155.
Urland, W., 1981, Chem. Phys. Lett. **83**, 116.
Van Spronsen, J.W., 1969, The Periodic System of Elements (Elsevier, Amsterdam).
Van Vleck, J.H., 1932, The Theory of Electric and Magnetic Susceptibilities (University Press, Oxford).
Vanquickenborne, L.G., K. Pierloot and C. Görller-Walrand, 1986, Inorg. Chim. Acta **120**, 209.
Varga, L.P., and L.B. Asprey, 1968a, J. Chem. Phys. **48**, 139.
Varga, L.P., and L.B. Asprey, 1968b, J. Chem. Phys. **49**, 4674.
von Hevesy, G., 1927, Die seltenen Erden vom Standpunkte des Atombaues (Julius Springer, Berlin).
Vuilleumier, J.J., M. Deschaux and M.D. Marcantonatos, 1982, Chem. Phys. Lett. **86**, 242.
Wachter, P., 1979, This Handbook, Vol. 2, ch. 19.
Wagoner, R.V., and G. Steigman, 1979, Phys. Rev. D **20**, 825.
Wallace, W.E., S.G. Sankar and V.U.S. Rao, 1977, Struct. Bonding **33**, 1.
Wallerstein, G., 1962, Phys. Rev. Lett. **9**, 143.
Warren, L.F., and M.A. Bennett, 1974, J. Am. Chem. Soc. **96**, 3340.
Wasserman, E., and H.F. Schaefer, 1986, Science **233**, 829.
Webb, J.D., and E.R. Bernstein, 1978, J. Am. Chem. Soc. **100**, 483.
Weeks, M.E., 1968, The Discovery of the Elements, 7th Ed. (J. Chem. Educ. Publishers, Easton, PA).
Weinberg, S., 1979, The First Three Minutes (Bantam Books, New York).
Wendin, G., 1981, Struct. Bonding **45**, 1.
Wertheim, G.K., R.L. Cohen, A. Rosencwaig and H.J. Guggenheim, 1972, in: Electron Spectroscopy, ed. D.A. Shirley (North-Holland, Amsterdam) p. 813.
Willemse, J., J.A. Cras, J.J. Steggerda and C.P. Keijzers, 1976, Struct. Bonding **28**, 83.
Witten, E., 1984, Phys. Rev. D **30**, 272.
Woolley, R.G., 1986, Chem. Phys. Lett. **125**, 207.
Wreford, S.S., M.B. Fischer, J.S. Lee, E.J. James and S.C. Nyburg, 1981, J. Chem. Soc. Chem. Comm. 458.
Wyart, F., V. Kaufman and J. Sugar, 1980, Phys. Scr. **22**, 389.
Wybourne, B.G., 1960, J. Chem. Phys. **32**, 639.
Wyrouboff, G., and A. Verneuil, 1906, Ann. Chim. Phys. (France) **9** 289.
Yntema, L.F., 1930, J. Am. Chem. Soc. **52**, 2782.
Yost, D.M., H. Russell and C.S. Garner, 1947, The Rare Earth Elements and their Compounds (Wiley, New York).
Zeltmann, A.H., and L.O. Morgan, 1971, Inorg. Chem. **10**, 2739.
Zweig, G., 1978, Science **201**, 973.

Handbook on the Physics and Chemistry of Rare Earths, Vol. 11
edited by K.A. Gschneidner, Jr. and L. Eyring

Chapter 76

HIGHLIGHTS FROM THE EXOTIC PHENOMENA OF LANTHANIDE MAGNETISM

James J. RHYNE
National Bureau of Standards, Gaithersburg, MD 20899, USA

Contents

Symbols*

A_l^m	crystal-field potentials
a, b, c	real-space lattice constants
$\tilde{B}_l^m$	single-ion magneto-elastic coupling coefficients
E	spin-wave excitation energy
g_J	Landé g-factor
$\tilde{H}_{cf}$	Hamiltonian for crystal-field interaction
$\tilde{H}_{ff}$	Hamiltonian for f–f exchange interaction
$\tilde{H}_{me}$	Hamiltonian for magneto-elastic interactions
$I_l(x)$	hyperbolic Bessel functions
J	total (spin plus orbital) angular momentum
$\tilde{J}(\boldsymbol{q})$	wave vector-dependent exchange interaction
$\tilde{J}(\boldsymbol{R})$	real-space exchange interaction
$\tilde{j}_{sf}(\boldsymbol{q})$	local 4f moment–conduction–electron exchange
$\boldsymbol{k}$	conduction-electron wave vector
L	orbital angular momentum
M	magnetization per unit volume
$\boldsymbol{Q}$	propagation vector of spin structure
Q	value of $\boldsymbol{Q}$ characterizing a stable spin state
$\boldsymbol{q}$	reduced reciprocal-space wave vector
$\boldsymbol{R}$	real-space position vector
$\langle r^l \rangle$	average over 4f wave functions
S	spin angular momentum
T	absolute temperature (K)
T_C	Curie ordering temperature (ferromagnetic)
T_N	Néel ordering temperature (antiferromagnetic)
T_K	Kondo temperature
V_l^m	crystal-field anisotropy constants
$Y_l^m(\boldsymbol{J})$	operator equivalent spherical harmonics
α^l	Stevens anisotropy coefficients
Δ	energy level splitting
ϵ^μ	hexagonally symmetric strains
μ_B	Bohr magneton
ρ	density of states
σ	magnetic moment per gram
τ	reciprocal lattice vector
χ	bulk magnetic susceptibility
$\chi(\boldsymbol{q})$	generalized conduction electron susceptibility

* Vector quantities are indicated by bold italic symbols.

In addition to the overall dedication of this volume to Prof. Frank H. Spedding whose pioneering work in this field is legend, this chapter is further dedicated to Prof. Sam Legvold and Dr. Wallace C. Koehler, both of whom passed away in the early months of 1986, and who in their parallel research careers provided the scientific community with much of the definitive insight underlying our knowledge of magnetism in the lanthanide metals.

1. Introduction

Possibly the most distinguishing feature of the rare earths, and the area in which they have provided the greatest challenges to condensed matter physics, is in the

understanding of the complex nature of the magnetism in these systems and its relationship to other observed physical phenomena such as transport properties and heat capacity anomalies. In this chapter we shall discuss some of the major milestones reached as theoretical and experimental investigations of the rare earths have proceeded intensely since about the early 1950s. This review is in no way intended to be comprehensive, and the reader is strongly urged to examine the many excellent review chapters and books available, such as found in other volumes in this series, in the works by Elliott (1972), Coqblin (1977), and in chapters by Legvold, Buschow, and Clark in the volume edited by Wohlfarth (1980), among others.

In the study of lanthanide magnetism, neutron scattering (both elastic and inelastic) has played a seminal role in elucidating the complex nature of the magnetic interactions, and thus much of the discussion here will focus on results obtained by these techniques and how they relate to those observed by more conventional bulk experimental tools.

2. Magnetic interactions

As is well known, the lanthanide metals (with the exception of Ce, Eu and Yb) offer possibly the best known examples of truly local-moment magnetic systems. The 4f wave functions responsible for the magnetism are well localized, the 4f electrons exhibit strong spin–orbit coupling, and the magnitude of the 0 K magnetic moment, in units of Bohr magnetons, is given by $g_J J$ where g_J is the Landé 'g' factor and J is the total angular momentum. The spin component alone is given by $S = (g_J - 1)J$.

The complexity of the magnetism in lanthanides then lies not in the intrinsic nature of the local moment but rather in the exchange coupling mechanisms that produce the long-range order of the 4f moments, and in the associated properties of anisotropy and magnetostriction which strongly perturb the magnetic ordering. The 4f magnetic electron wave functions do not in themselves have a significant direct overlap integral (except for Ce) and thus the magnetic phase coupling is via a polarization wave formed in the conduction-electron bands. This coupling is based on a suggestion by Zener (1951), and was initially calculated by Ruderman and Kittel (1954) for nuclear moments in a free-electron gas. Later Kasuya (1956) and Yosida (1957) provided the formalism describing the now well-known RKKY coupling between localized 4f electronic moments which may be written in the form

$$\tilde{H}_{\mathrm{ff}} = -\sum_{\boldsymbol{R}_{ij}} \tilde{\boldsymbol{J}}(\boldsymbol{R}_{ij}) \boldsymbol{J}_i \cdot \boldsymbol{J}_j, \tag{1}$$

where $\boldsymbol{J}_{i,j}$ is the total spin plus orbital angular momentum and $\tilde{J}(\boldsymbol{R}_{ij})$ is the effective exchange integral coupling 4f moments. The real-space $\tilde{J}(\boldsymbol{R}_{ij})$ can be written in terms of the Fourier transform of the wave vector dependent exchange $\tilde{J}(\boldsymbol{q})$, which can be directly obtained from neutron scattering experiments, as follows

$$\tilde{\boldsymbol{J}}(\boldsymbol{R}_l - \boldsymbol{R}_{l'}) = \sum_{\boldsymbol{q}} \tilde{\boldsymbol{J}}(\boldsymbol{q}) \mathrm{e}^{\mathrm{i}\boldsymbol{q}\cdot(\boldsymbol{R}_l - \boldsymbol{R}_{l'})}. \tag{2}$$

In turn $\tilde{J}(\boldsymbol{q})$ is described in terms of a bare s–f exchange function j_{sf} between conduction and 4f electrons and the generalized susceptibility χ_{sf} which represents the conduction electron response to the local exchange field and which is calculable from the band structure. The expression for $\tilde{J}(\boldsymbol{q})$ for N spins is then

$$\tilde{J}(\boldsymbol{q}) = 2N^{-1}(g_J - 1)^2 |\tilde{j}_{sf}(\boldsymbol{q})|^2 \chi(\boldsymbol{q}). \tag{3}$$

The resulting spin coupling of 4f magnetic moments involving a polarization wave in the conduction bands, or spin density wave as described by Overhauser (1960), is of a very long-range character. This is experimentally confirmed in dilute-alloy experiments which have shown the occurrence of long-range helimagnetic order in alloys approaching 1 atomic per cent, for example, neutron diffraction experiments on Y–1.5% Gd (Wenger et al. 1986), and in the phase coherence of magnetic order across Y layers of more than 20 Y atomic planes in Dy–Y multi-layer samples (Rhyne et al. 1987).

The lanthanides, particularly the light series, also show evidence of anisotropic exchange interactions (see sections 6.1 and 6.2) in which the exchange constant $J(\boldsymbol{R}_{ij})$ of eq. (1) depends on the spatial components of the total spin variables $\boldsymbol{J}_i, \boldsymbol{J}_j$. Dilute lanthanide alloys, for example in the noble metals, and specific intermetallic compounds, also show effects directly attributable to anisotropy in the basic 4f-conduction electron exchange interaction as discussed by Levy (1979). The interaction of the 4f and 5d electron charge clouds and the anisotropy associated with these charge distributions gives rise to additional terms in the Hamiltonian. For example, a term $\tilde{H}_1 = -A_1 \boldsymbol{l}_f \cdot \boldsymbol{l}_d$ describes an f and d electron orbital angular momentum interaction which gives rise to 'skew scattering' effects as seen in the anomalous Hall effect studies in Au and Ag with rare earth impurities by Fert and Friederich (1976) and by Fert et al. (1977). From their data it was determined that the orbital momentum term was about one order of magnitude smaller than the isotropic d–f exchange. Surprisingly, however, their magneto-transport studies also showed the effect of a d–f quadrupole–quadrupole moment interaction term which was of the same order of magnitude as the conduction-electron–local-moment exchange.

The form of the interaction of 4f moments in the lanthanides is further modified by both the crystal-field anisotropy and magnetostriction. The former is predominantly a single-ion interaction in the lanthanides and arises from the Coulomb coupling of the local spin moment (via the spin–orbit interaction) to the hexagonally symmetric charge cloud of the neighboring ions. Stevens (1952) was instrumental in providing the definitive description of this interaction via a series of operator equivalents of the spherical harmonics $Y_l^m(\boldsymbol{J}_i)$, which describe in effect the quadrupole, octapole, etc., moments of the 4f charge cloud, of the form

$$\tilde{H}_{cf} = \sum_{ilm} A_l^m \langle r^l \rangle \alpha^l Y_l^m(\boldsymbol{J}_i), \tag{4}$$

where the A_l^m contain the crystal-field potentials, $\langle r^l \rangle$ are the spatial averages over the 4f wave functions, and the α^l are the Stevens coefficients describing the relative

magnitudes of the l-pole moments of the 4f charge distributions for the various lanthanides. The sum over i spin components is taken with values of l and m appropriate to the site symmetry of the ion (for the hcp heavy lanthanides $l = 2$, 4 and 6 with $m = 0$ and $l = 6$ with $m = \pm 6$).

The strain derivatives of the exchange and crystal-field energies are the source of the magnetostriction in the lanthanides and this magneto-elastic interaction was originally formulated by Mason (1954) and recast in terms of hexagonally symmetric strains by Callen and Callen (1963, 1965) and Callen (1968) who also derived expressions for the temperature renormalization of the single-ion magnetostriction and anisotropy. The single-ion magnetostriction, which characterizes the crystal-field energy strain dependence and of itself contributes to the measured magnetic anisotropy, takes the generic form

$$\tilde{H}_{\text{me}} \approx -\tilde{B}_l^m Y_l^m(\boldsymbol{J})\,\epsilon^\mu, \tag{5}$$

where the $\tilde{B}$'s are the single-ion magneto-elastic coupling constants and the ϵ^μ are the hexagonally symmetric strain modes. The temperature dependence of the anisotropy and magnetostriction terms in the magnetic free energy is of the same general form and arises from the temperature dependence of the thermal averages of the functions $\langle Y_l^m(\boldsymbol{J})\rangle$,

$$\langle Y_l^0(\boldsymbol{J})\rangle_T / \langle Y_l^0(\boldsymbol{J})\rangle_0 = I_{l+1/2}(X)/I_{1/2}(X), \tag{6}$$

for $m = 0$, where X is the inverse of the Langevin function of the reduced magnetization and the $I_{l+1/2}(X)$ are hyperbolic Bessel functions (of the second kind).

The giant anisotropy and magnetostrictions found in the lanthanide elements (see McEwen 1978, Rhyne 1972) are also present in lanthanide compounds, particularly those with Fe and Co, in which the strong direct exchange interaction of the transition metal enhances the Curie temperature of the overall material and brings it into a realm useful for devices. Thus the lanthanides have made major impact on the technology of permanent magnets (e.g., $SmCo_5$ and $Nd_2Fe_{14}B$) and of magnetostrictive transducers (e.g., Terfenol, $Tb_{0.3}Dy_{0.7}Fe_{1.9}$). These materials as well as the remarkable nuclear magnetic cooling properties of $PrNi_5$ are discussed in ch. 78, sections 4.3.2–4.3.4.

3. Magnetic moments and spin structures

Initially, the magnetic properties of lanthanide metals were studied in polycrystalline samples due to the inability to produce single crystals by conventional means because of crystallographic phase transformations which occur below their melting points (e.g., the heavy metals transform from bcc to hcp on cooling). The polycrystal studies uncovered many apparent anomalies in the magnetization processes which could only be more fully revealed following the production of single crystals by a recrystallization (or strain-anneal) process applied to the heavy lanthanides by Nigh (1963), which resulted in highly perfect single crystals of a size sufficient for magnetization and neutron scattering studies.

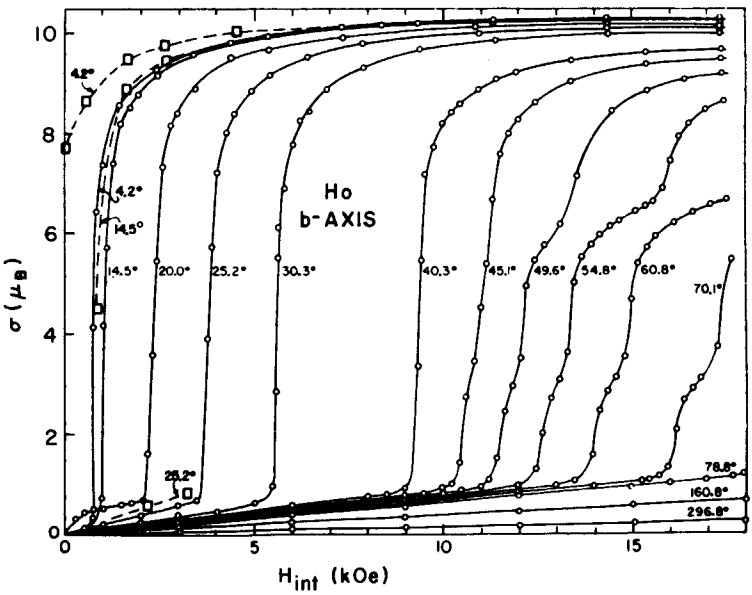

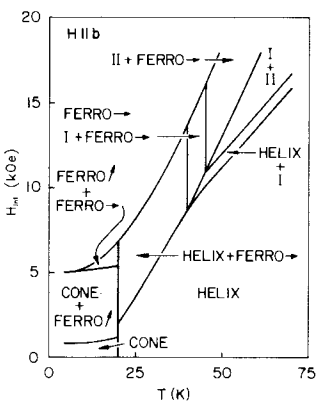

Fig. 1. Magnetic moment of Ho (in units of Bohr magnetons) measured along the b [10$\bar{1}$0] easy magnetic axis as a function of internal magnetic field. (After Strandburg et al. 1962.) The dashed curves were taken in decreasing field sequence. The critical fields correspond to transitions from the helical configuration to a ferromagnetic state. At the higher temperatures evidence was found for intermediate states which were identified from neutron diffraction as given in the phase diagram at the left. (After Koehler et al. 1967.)

3.1. *Single-crystal magnetization*

The initial revelation of the complex magnetic orderings in the lanthanides came from the parallel studies of magnetization by Prof. Sam Legvold and his students at Iowa State University and the landmark neutron diffraction studies of the magnetic spin orientations by Dr. Wallace C. Koehler and associates at the Oak Ridge National Laboratory. The magnetic data on the heavy lanthanides established the values for the $4f^{+++}$ free-ion magnetic moments and their temperature renormalization, as well as providing the initial evidence for a conduction-electron polarization moment amounting to several tenths of a Bohr magneton. In Gd, form factor

measurements by Moon and Koehler (1971), using isotopically enriched Gd to reduce the neutron absorption, showed that this conduction-electron spin density consists of a long-range oscillating diffuse contribution superimposed on the local part from the 4f spin moment. The wave vector ($\boldsymbol{q}$) dependence of the form factor, which represents the Fourier transform of the real-space local spin density, was found to be in good agreement with relativistic calculations of Freeman and Desclaux (1972).

In the heavy lanthanides (except for the nearly isotropic S-state ion Gd) the bulk magnetization data also revealed the effects of the enormous crystal-field anisotropy (order of 10^8 ergs/cm^3) between the basal plane and c-axis directions and established the alternating sequence of basal plane easy directions (i.e., $11\bar{2}0$ [a] for Dy and $10\bar{1}0$[b] for Tb, etc.) which was later to be understood in terms of the alternating sign of the $A_6^6\gamma\langle r^6\rangle Y_6^6(J)$ six-fold crystal-field anisotropy terms (Stevens 1952, factor γ). In addition, critical fields were found at which rapid increases in the moment to saturation occurred such as shown in fig. 1 for Ho at low temperature (Strandburg et al. 1962). These were later shown (see below) to be the result of a field-induced transformation from the intrinsic zero-field incommensurate helical magnetic order state to an aligned ferromagnetic state. At higher temperatures additional transition fields were found suggesting the formation of complex mixed periodic and ferromagnetic stable intermediate spin states as later revealed by neutron diffraction (Koehler et al. 1967) and illustrated in the form of a magnetic phase diagram in fig. 1.

3.2. *Neutron diffraction and the spin configurations revealed*

The insight provided by the neutron scattering was far reaching and provided the first definitive picture of the complicated spin structures of the lanthanides. These were described as 'a panoply of exotic spin configurations' by Koehler. Figure 2 illustrates schematically the stable spin structures of the heavy lanthanides, which consist of basal plane helical rotations of the moment layers in Dy, Tb, and Ho followed at low temperatures by a ferromagnetic phase. In Ho at low T a small ferromagnetic c-axis moment component is produced by the competition of opposite-sign second and fourth order axial anisotropy terms thus forming a flat cone with a 'bunching' effect in the basal plane helical moment component. For Er the axial anisotropy favors the c-axis, and the interplay of exchange and magnetostriction and anisotropy (see below) produces a spatial modulation of the c-axis moment component which is also found in Tm. All of these spin configurations, except for the ferromagnet Gd, have the common feature that the propagation vector $\boldsymbol{Q}$ describing the incommensurate structures is along the c-axis, independent of whether the spin ordering is in the basal plane or along the c-axis. The selection of basal plane or c-axis moment directions is controlled by the uniaxial anisotropy energy as are the variations of moment direction in Gd. (Although Gd is an S-state ion, it still has a weak anisotropy presumed to be of two-ion origin). The magnitude of the propagation vector is in general incommensurate with the lattice periodicity and has an initial (high-T) magnitude prescribed by Fermi surface effects as

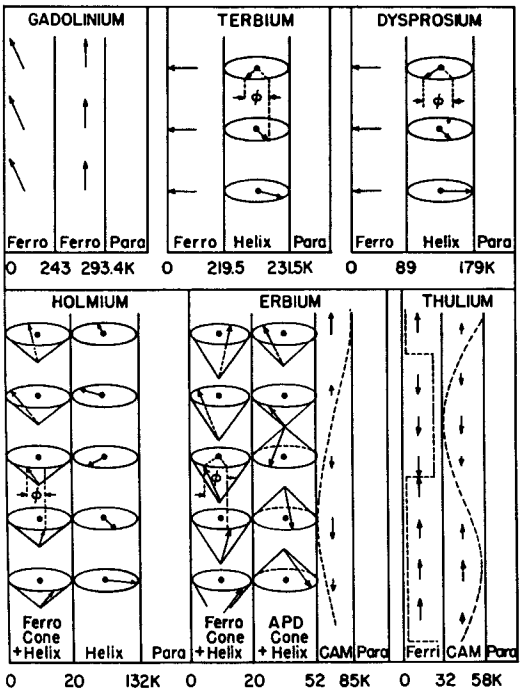

Fig. 2. Schematic description of the spin structures in the heavy rare earth metals. The initial high-T ordering, in all except the ferromagnet Gd, is to an incommensurate periodic spin order with propagation direction along the c-axis. CAM (c-axis modulation) is a structure in which the c-axis components of the moment are sinusoidally modulated which evolves into the APD (quasi anti-phase domain) in Er in which a gradual 'squaring-up' of the c-axis moment occurs with additional order appearing in the basal plane. The temperatures of the transitions are from magnetization and neutron diffraction data. (After Legvold 1980.)

described in the next section. The temperature dependence of the wave vectors for the periodic spin structures in Tm, Er, Ho, Tb, and Dy are shown in fig. 3 (top). Results are given in terms of the fractional c-axis reciprocal lattice parameter and in the number of unit cells required to complete a period. This illustrates the canonical seven layer (two layers/unit cell) repeat sequence observed at the initial ordering in Tm, Er, and dilute alloys with Y.

The temperatures given in fig. 2 are those at which the spin structures are observed to spontaneously transform (via a first-order phase transformation, except for Gd and the intermediate states in Er and Tm) from one periodic moment state to another, or from a periodic moment state to ferromagnetism. These transitions can also be induced at higher temperatures by the application of an external field above a critical value (see section 3.1). The origin of the spontaneous ferromagnetic transitions is discussed in section 5. By convention, the highest ordering temperature where a periodic moment configuration forms is designated T_N (Néel temperature), and T_C (Curie temperature) designates transitions to a ferromagnetic spin-aligned state.

Synchrotron radiation measurements in which the high brilliance of the source allows the observation of the extremely weak coupling of the photon to the 4f magnetic moments have also been used to study the incommensurate ordering in the lanthanide metals Ho and Er (Gibbs et al. 1985, 1986). In addition to the direct observation of the magnetic scattering, the incommensurate spin ordering in Er

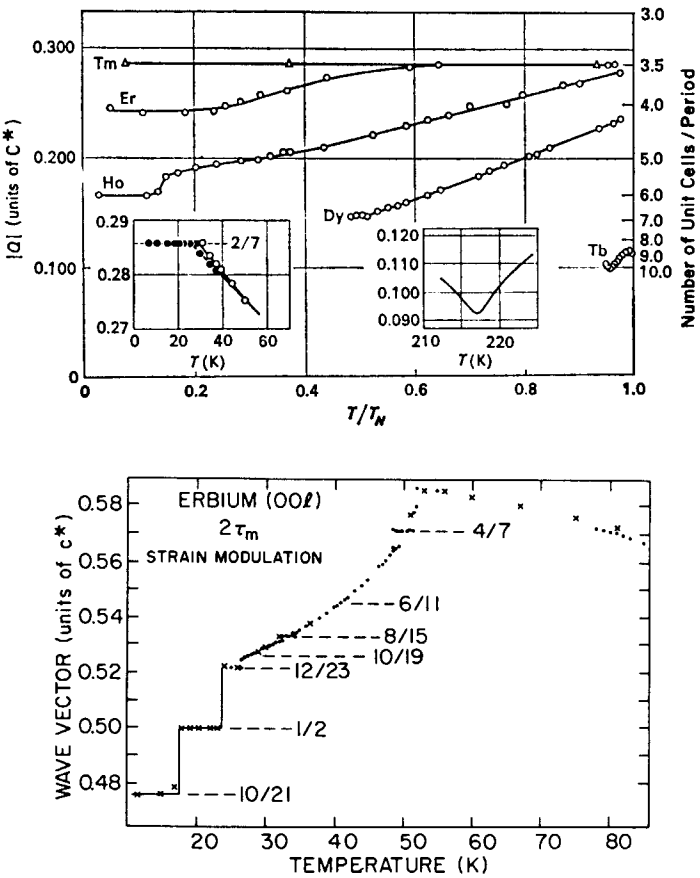

Fig. 3. (Top) Neutron diffraction determination of the propagation wave vector Q for the heavy rare earths as a function of reduced temperature T/T_N. The magnitude of the wave vector is given in units of the reciprocal c-axis parameter and in number of c-axis unit cell lengths per period. Data for Tm and Tb are shown with expanded temperature resolution in the left and right insets, respectively. (From Koehler 1972.) (Bottom) Wave vector in Er measured at more closely spaced temperature intervals showing 'lock-in' effects at specific values as measured using synchrotron radiation (values were obtained from the periodic strain modulation scattering and thus are given as twice the magnitude of the magnetic wave vector. Different data symbols reflect data from different spectrometers. (From Gibbs et al. 1987.)

gives rise to a periodic strain modulation which can be seen via the charge scattering at twice the magnetic wave vector ($2\tau_m$). Results shown in fig. 3 (bottom), confirmed the earlier neutron data (Habenschuss et al. 1974), and also gave additional information on the step-like progression of the magnetic ordering wave vector which was interpreted in terms of a 'spin-slip' model. A similar 'lock-in' to a wave vector $Q = \frac{2}{7}$ is observed in Tm at the 'ferrimagnetic' transition temperature [see fig. 3 (inset) and fig. 2]. The initial ordering in Er is into a state in which the c-axis moment component orders with a sinusoidally varying magnitude along the c-axis and the transverse components are disordered. At lower T, additional harmonics in

the neutron scattering (Habenschuss et al. 1974) signal a gradual squaring-up of the sinusoidal modulation toward a square-wave configuration (APD). Helical order of the basal plane components also appears below about 53 K, and the propagation wave vector enters into a series of step-like plateaus (see fig. 3). At about 20 K, the c-axis moment component becomes ferromagnetic resulting in the cone configuration.

The light lanthanides exhibit additional complex periodic ordering involving both hexagonal and cubic sites. Details of these structures can be found in the works by Koehler (1972), and Sinha (1978), and references therein. The structure of Nd is quite complex and involves incommensurate ordering on the hexagonal and cubic sites with different magntidues of the wave vectors (Johansson et al. 1970, McEwen et al. 1985). Pr (see also section 6.2) has a singlet ground state with exchange smaller than the threshold for ordering, and is thus intrinsically non-magnetic; however, in a series of elegant experiments, Bjerrum-Møller et al. (1982) established antiferromagnetic ordering at a temperature of about 50 mK, resulting from a hyperfine interaction between the 4f electrons and the nuclear spin as originally suggested by Murao (1971) and Jensen (1979). The ordering determined from neutron diffraction was observed to have significant critical-like or 'precursor' scattering extending up to several times the ordering temperature.

4. Band effects and the origin of complex orderings

4.1. *Band structure and the Fermi surface*

The origins of the oscillating moment spin structures, and in particular the fact that they show periods which, in general, are not commensurate with the lattice [see fig. 3 (top)], were initially not understood, nor was the absence of such structures in the ferromagnetic rare earth element Gd. The insight provided by calculations of the band structure and the form of the Fermi surface was crucial to this understanding. The initial calculation of the Fermi surface of Gd was done by Dimmock and Freeman (1964), and Watson et al. (1968). As shown in fig. 4 this complex hole surface, calculated for non-magnetic Gd by non-relativistic augmented plane-wave bands, shows many sections and large anisotropy which is reflected in the transport properties. The de Haas–van Alphen effect which measures the oscillations in the conduction-electron susceptibility provided the first experimental confirmation of some of the main features of the Fermi surface of Gd (Schirber et al. 1976, Young et al. 1973).

It was first shown by Keeton and Loucks (1968) using relativistic calculations that subtle differences in the Fermi surface between Gd and Dy could be responsible for the occurrence of incommensurate periodic ordering in the latter and likewise in the other lanthanides. These features, shown in fig. 5, consist of 'webbing' between the small arms in the AHL plane of the Fermi surface of Dy and yield parallel flat 'nesting' portions of the surface spaced by a $\boldsymbol{q}$-vector ($\boldsymbol{q} = 2\boldsymbol{k}_F$,) which correlated with the initial Q of the incommensurate order. The 'nesting' features also give rise to peaks in the generalized susceptibility [eq. (3)] at non-zero $\boldsymbol{q}$ as

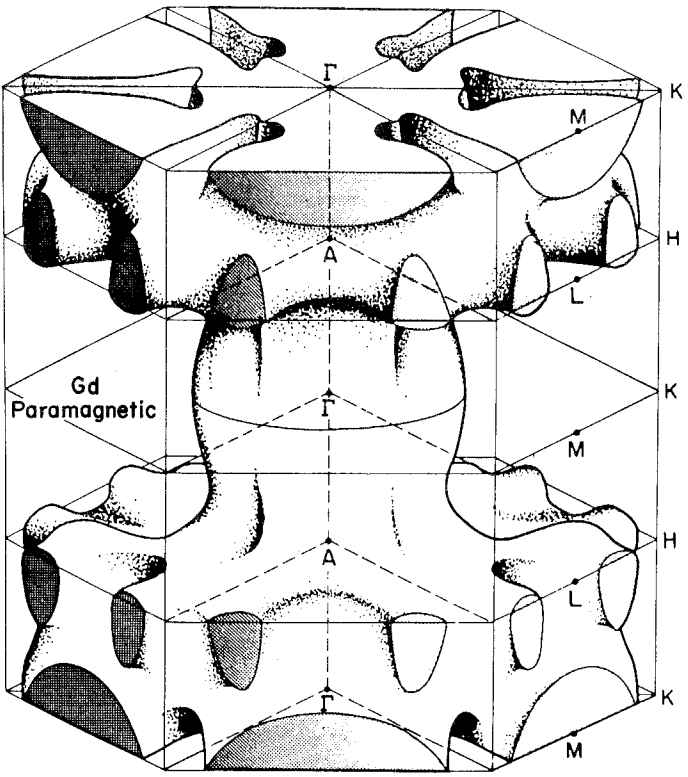

Fig. 4. Hole Fermi surface of Gd as calculated by Dimmock and Freeman (1964). Electron states outside the surface are filled. No 'webbing' is present between the arms in the *ALH* plane as compared to the elements exhibiting periodic magnetic structures (see fig. 5).

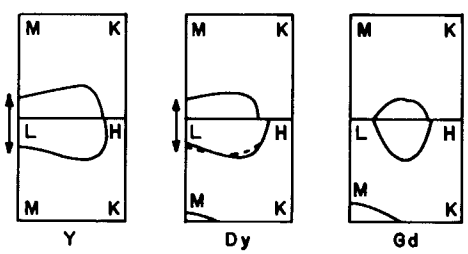

Fig. 5. Partial Fermi surface representation for Y, Dy, and Gd showing the development of 'webbing' between arms of the Fermi surface in the *L–H* direction which is associated with a peak in the generalized susceptibility $\chi(q)$ at non-zero Q and the conditions for periodic magnetic structures. (After Keeton and Loucks 1968.)

discussed below. The webbing is absent in Gd, but present in the surface of Y which is consistent with the occurrence of helimagnetic order in alloys of lanthanides with Y.

Additional sophistication in calculational procedures led to further refinements to the band structure of the rare earth metals as reviewed by Liu (1978). The improved detail gave better results for the calculated generalized susceptibility functions (see,

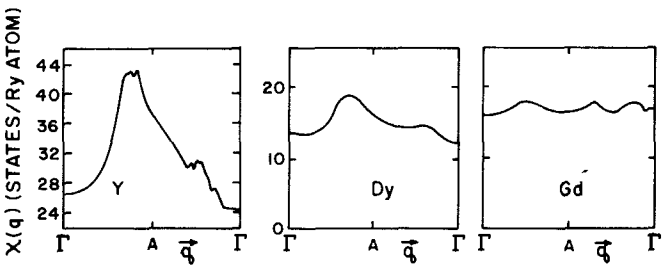

Fig. 6. Generalized susceptibility functions $\chi(\boldsymbol{q})$ for Y, Dy, and Gd showing the pronounced maxima in Dy and Y corresponding to the occurrence of incommensurate magnetic order. Alloys of Gd (see e.g., Wenger 1986) or other rare earths with Y show incommensurate order similar to Dy. The ripples in the Gd function are ascribed to matrix element instabilities. (After Liu et al. 1971.)

e.g. Liu et al. 1971), shown in fig. 6, which yielded a nearly flat (small ripples are not deemed significant) response for Gd corresponding to the ferromagnetic order, while for Dy and Y (and thus for Y alloys) the susceptibility shows pronounced peaks at Q's which agree well with the observed magnetic ordering wave vectors. Liu et al. point out that matrix element effects can be important in shifting the peak Q, for example in Tb.

4.2. *'Superzone' gaps and effects on transport properties*

The occurrence of peaks in the generalized susceptibility at finite $\boldsymbol{q}$ and the corresponding occurrence of incommensurate periodic magnetic ordering has provided a very fertile area for the study of the interaction of magnetism with the conduction bands and Fermi surface. In the case of a simple ferromagnet a rigid splitting of the spin-up and spin-down conduction bands occurs with magnitude proportional to the exchange. For the case of an incommensurate structure, new energy gaps are formed in the bands. These gaps arise from exchange matrix elements coupling Bloch states of wave vector $\boldsymbol{k}$ of spin down to those of wave vector $\boldsymbol{k} + \boldsymbol{Q} + \tau$ of spin up (in the planar helix case for example), where $|\boldsymbol{Q}| = Q$ is the characteristic wave vector of the helix and τ is a reciprocal lattice vector. Such 'superzone' gaps (Miwa 1963, Elliott and Wedgewood 1963) have the effect of actually destroying large portions of the Fermi surface parallel to the c-axis magnetic propagation vector direction of the periodic structures. This perturbation of the conduction electrons could be expected to have a dramatic effect on the resistivity, which is indeed the case, as shown in fig. 7 (Hegland et al. 1963) for the temperature dependence of the a and c axis resistivity in a single crystal of Tb. The dashed lines give the magnetic contribution to the resistivity after subtraction of the phonon contribution. Much of the sharp drop in resistivity at low T, which is isotropic in the ferromagnetic phase ($T < 218$K), arises from the suppression of 4f moment thermal fluctuations and the associated reduction in the spin disorder

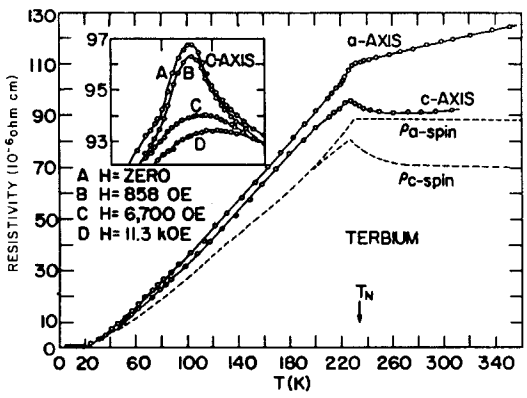

Fig. 7. Electrical resistivity (residual subtracted) versus temperature for the *a*- and *c*-axis of Tb. The dashed curves give the spin disorder component after subtraction of the phonon contribution from the total resistivity. The inset shows the anomalous rise in *c*-axis resistivity below T_N accompanying the opening of the superzone gaps in the Fermi surface. The peak is quenched by applied magnetic fields which destroy the helical order and thereby remove the superzone gaps. (After Hegland et al. 1963.)

scattering. However, in the helical range $218 < T < 230$ K (see inset of the figure) an anomalous *rise* in the *c*-axis resistivity occurs with decreasing temperature. This rise is a direct consequence of the opening of the superzone gaps and the destruction of segments of the Fermi surface in the *c*-direction. The *a*-axis resistivity is then relatively unchanged through this temperature region. The inset to the figure also shows the remarkable result that the superzone-induced peak is completely eliminated by the application of a basal plane magnetic field of approximately 10 kOe. The energy associated with this field is sufficient to destroy the helical spin configuration and to induce ferromagnetic order. As such the superzone gaps are eliminated and the resistivity returns to the lower values appropriate to a gapless Fermi surface.

The temperature dependence of the magnetic propagation vector (fig. 3) has been ascribed (Elliott and Wedgewood 1963) to the effects of the superzone gaps in modifying the stable Q. It is also suggested (Evenson and Liu 1969) that the magnetostriction may modify the wave vector.

5. Spontaneous transitions from periodic magnetic states to ferromagnetism

As compared to the strongly magnetic elements Fe, Co, and Ni, the lanthanides have provided an unusually rich area in which to study the effects of magnetostriction and crystal-field anisotropy on the magnetic interactions. This is a consequence of the exchange energy being smaller by a factor of five or more vis-a-vis the 3d transition metals [the highest ordering temperatures, T_N or T_C, range from 293 K (Gd) down to 58 K (Tm) in the heavy lanthanides and from 109 K for Sm to 13.7 K for Ce among the light lanthanides versus $T_C = 1044$ K for Fe and 1388 K for Co]. In addition, the crystal-field energies are much larger in the lanthanides (of the order of 20 K in Dy and Tb at $T = 0$ and still greater for the light lanthanides). Thus the anisotropy and the magnetostriction, which are of essentially equal magnitude, are

strong perturbations on the exchange in the heavy lanthanides and can dominate the magnetic behavior for the light lanthanides [e.g., Pr which does not order because of its $|J_z=0\rangle$ singlet ground state (Rainford 1972) but instead exhibits excitonic behavior as examined by Rainford and Houmann (1971) and Houmann et al. (1979)].

The spontaneous nature of the phase transitions from helical ordered states to ferromagnetism such as occur at 89 K in Dy and 220 K in Tb was initially a puzzle. Calculations by Cooper (1967, 1968) and by Evenson and Liu (1969) showed that the exchange favored the helical state over the ferromagnetic state by an energy of about 2.2 K/atom and that, except for external perturbations, the ferromagnetic state would not form spontaneously. The six-fold basal plane anisotropy energy was initially suggested as the symmetry breaking mechanism leading to the ferromagnetic state, but was found to contribute too small a free energy at the transition temperatures to be the driving force. (The six-fold anisotropy initially decreases as the 21st power of the order parameter!) Cooper (1967) first suggested that the transition was in fact driven by the magneto-elastic energy. He as well as Evenson and Liu (1969) showed that the γ-mode magnetostriction, which is an orthorhombic distortion of the hexagonal symmetry, is effectively constrained ('clamped') while the spins are in an helical arrangement, but is a freely allowed distortion in the ferromagnetic state. The γ-strain has the form

$$\epsilon^{\gamma} = \frac{\delta a}{a} - \frac{\delta b}{b}, \tag{7}$$

where a and b are the basal plane lattice constants. Evenson and Liu (1969) also calculated a partial clamping of the isotropic 'α' mode strains, but the corresponding magneto-elastic energy is small. The magneto-elastic energy associated with the γ-mode magnetostriction is large and increases as the temperature is reduced. The transition to ferromagnetism then spontaneously occurs when the 2.2 K/atom exchange energy difference favoring the helical state is exceeded by the gain in magnetostrictive energy on unclamping the γ-mode distortion, as allowed in the ferromagnetic state. This revelation that a magnetic phase change could be induced by single-ion magnetostriction was a significant landmark in lanthanide magnetism, which was later to be further tested and explored via experiments on Dy–Y multilayers (Erwin et al. 1987). These layered single crystals do not exhibit a transition to ferromagnetism at any temperature due to the physical clamping of the Dy strain by the non-magnetostrictive Y layers.

A feeling for the really giant energies associated with the magnetostriction can be obtained from the lattice parameter distortions at T_C in Dy found from the X-ray data of Darnell (1963a,b) shown in fig. 8 (left). The discontinuity corresponds to values of $\delta a/a = +0.2\%$, $\delta b/b = -0.5\%$, and $\delta c/c = +0.3\%$. The a and b values reflect the orthorhombic distortion, and the c discontinuity is from the exchange magnetostriction accompanying the destruction of the helical state, which is similar to the large distortion at the 20 K transition in Er shown in fig. 8 (right).

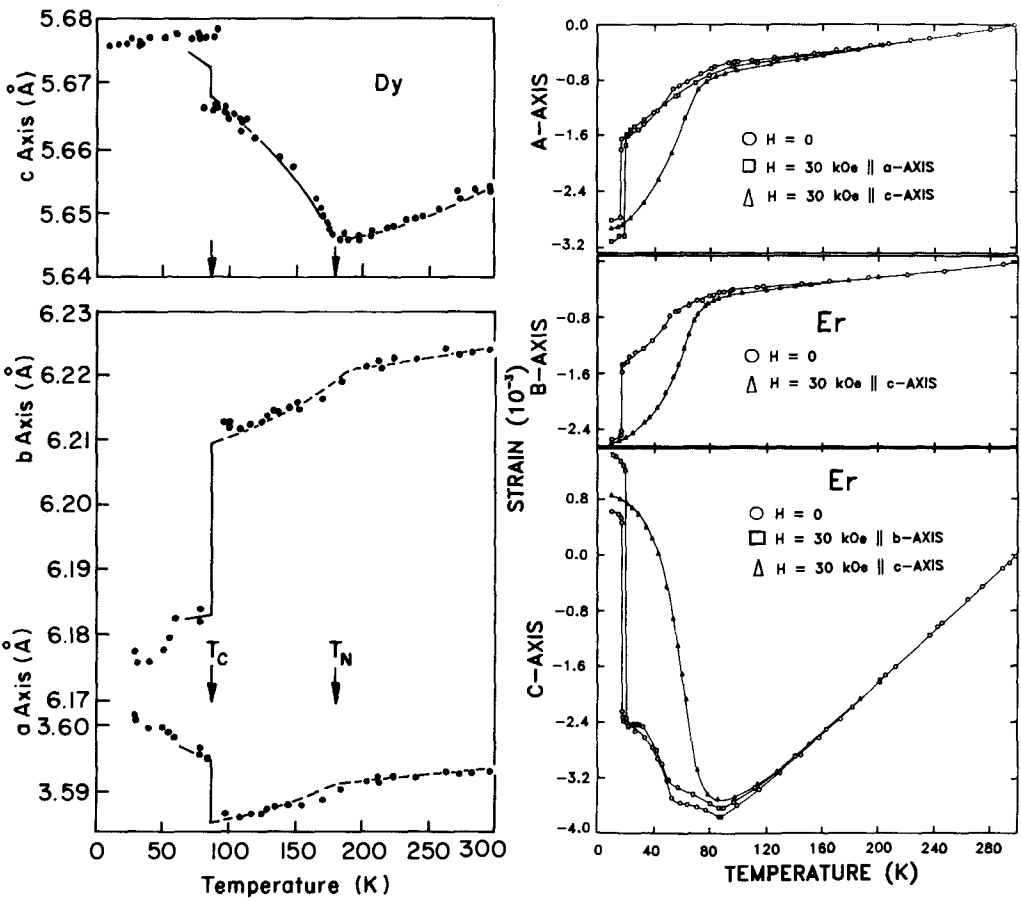

Fig. 8. (Left) Lattice parameters of Dy as a function of temperature from X-ray diffraction (Darnell 1963a,b). The large discontinuity at T_C reflects the magnetostrictively induced orthorhombic distortion of the unit cell (see text) which is the driving force for the helical to ferromagnetic transition. The solid lines are calculated from the theory of Evenson and Liu (1969). (Right) Temperature dependence of the *a*-, *b*- and *c*-axis fractional strain ($\Delta l/l$) in Er in zero field and in applied fields. The large discontinuity at 20 K reflects the exchange magnetostriction accompanying the transition from a modulated magnetic state to a conical ferromagnetic state. (After Rhyne and Legvold 1965.)

6. Magnetic excitations studied by inelastic neutron scattering

Perhaps the greatest insight into the microscopic mechanisms of the magnetism of the lanthanides has been obtained from studies of the spin excitations using neutron scattering. In these experiments the scattering of thermal neutrons from a magnetic specimen creates or annihilates an elementary magnetic excitation such as a spin wave or magnetic exciton, and the resulting energy gain or loss of the neutron, which is measured by the spectrometer, is a direct measure of the energy of the excitation. In a triple axis measurement, performed at constant $|\boldsymbol{q}| = q_0$ for example, this energy change can be correlated with the momentum or wave vector $\boldsymbol{q}$ of the excitation and thus a dispersion curve of energy E versus wave vector $\boldsymbol{q}$ is obtained. Model calculation fits to these spectra then provide values for the exchange and crystal-field parameters. In the case of the lanthanides, due to the relatively weak exchange interactions, the energies of the propagating spin wave modes are easily accessible to thermal neutrons as is also true of the crystal-field excitations which have been studied in many lanthanide alloys and compounds [see e.g., the review by Sinha (1978)].

6.1. *Spin waves in heavy lanthanides*

The first determination of the spin wave dispersion in a lanthanide metal was by Bjerrum-Møller and Houmann (1966) in Tb; followed by the extensive work of Bjerrum-Møller et al. (1970) on Tb and Tb–10% Ho; then for Gd by Koehler et al. (1970); and for Dy by Nicklow (1971) and Nicklow et al. (1971); all of which were studied in the ferromagnetic phase. The periodic moment regime of Ho was examined by Nicklow et al. (1971, 1969) and Stringfellow et al. (1970), and of Er by Nicklow et al. (1971) and Woods et al. (1967).

Figure 9 shows the magnon dispersion relations found for spin waves propagating along the three principal symmetry directions in the ferromagnetic phase of Tb at 4.2 K (Bjerrum-Møller and Houmann 1966, Nielsen et al. 1968, 1970a,b). The figure also shows certain of the phonon branches which are discussed in the original references. For the magnetic excitations, the dispersion of magnons propagating along the c-axis of a basal plane ferromagnet takes the form (Lindgard and Danielsen 1975),

$$E(\boldsymbol{q}) = \{[A(\boldsymbol{q}) + D(\boldsymbol{q})]\,[A(\boldsymbol{q}) - D(\boldsymbol{q})]\}^{1/2}, \tag{8}$$

where $\boldsymbol{q}$ is the wave vector of the spin excitation. The functions A and D can be written in terms of the Fourier transformed exchange constants, $\tilde{J}(\boldsymbol{q})$ and $\tilde{J}(\boldsymbol{q}=0)$, and the c-axis two-fold and basal plane six-fold anisotropy constants, V_2 and V_6^6 [renormalized terms from eq. (4)],

$$A(\boldsymbol{q}) + D(\boldsymbol{q}) = J[\tilde{J}(0) - \tilde{J}(\boldsymbol{q})] + 2J_1V_2 + 6J_5V_6^6, \tag{9}$$

and

$$A(\boldsymbol{q}) - D(\boldsymbol{q}) = J[\tilde{J}(0) - \tilde{J}(\boldsymbol{q})] + 36J_5V_6^6, \tag{10}$$

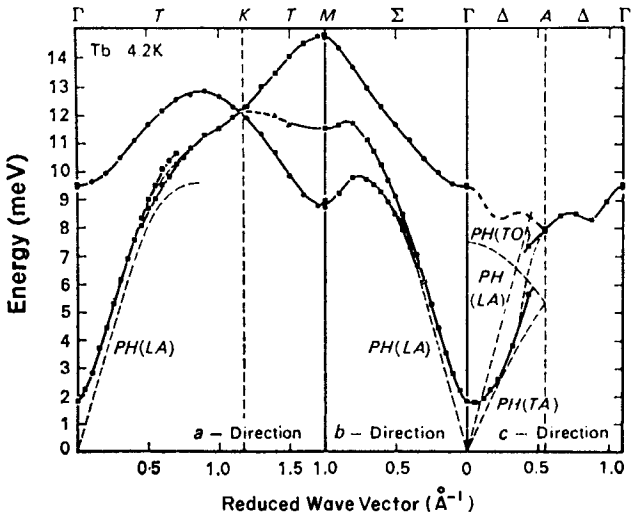

Fig. 9. Magnon dispersion for Tb in the ferromagnetic phase along the three principal axis directions. Symbols along the top of the diagram label the directions in the conventional notation shown in fig. 4. Dashed curves labelled *PH* are [longitudinal acoustic (LA), transverse acoustic (TA), and transverse optic (TO)] phonon branches which interact with the magnons. (After Mackintosh and Bjerrum-Møller 1972.)

where the total angular momentum function $J_n = (J - \frac{1}{2})(J - 1)\cdots(J - \frac{1}{2}n)$. The Fourier transform exchange $\tilde{J}(\boldsymbol{q})$ is related to the real-space exchange $\tilde{J}(\boldsymbol{R})$ as

$$\tilde{J}(\boldsymbol{q}) = N^{-1/2} \sum_i \tilde{J}(\boldsymbol{R}_i) e^{i\boldsymbol{q}\cdot\boldsymbol{R}_i}. \tag{11}$$

It can be seen from the experimental results of fig. 9 that the magnon energy does not go to zero for $\boldsymbol{q} = 0$, which is consistent with eq. (8) and the expressions for $A(\boldsymbol{q})$ and $D(\boldsymbol{q})$. Instead there is an energy gap Δ whose magnitude depends on the anisotropy constants and physically represents the fact that propagating spin wave modes can not be formed except at energies great enough to overcome the anisotropy. Extensive studies of the anisotropy gap in Tb–10%Ho by Nielsen et al. (1970b) showed that the gap energy demanded values of the anisotropy constants which were significantly larger than those measured by bulk methods. This discrepancy led Cooper (1968) to suggest that a significant contribution to the spin wave gap arises from the magnetostriction, and thus the effective six-fold basal plane anisotropy constant has the form

$$J_5 V_6^6 = J_5 \tilde{V}_6^6 - \tfrac{1}{4} c^\gamma \lambda^{\gamma,2} \lambda^{\gamma,4},$$

where $\lambda^{\gamma,2}$ and $\lambda^{\gamma,4}$ are second and fourth order magnetostriction coefficients and c^γ is an hexagonal elastic constant. In Tb at 0 K, the magneto-elastic part is larger that the convention crystal-field anisotropy term. This coupling of crystal-field and magnetostrictive anisotropy terms led to the discovery of the 'frozen lattice' behavior of the field dependence of the anisotropy gap. In an anisotropic

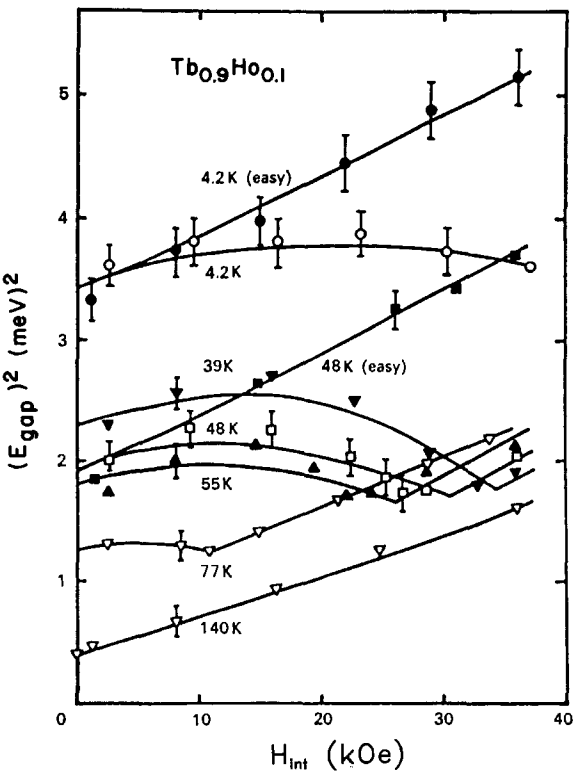

Fig. 10. Applied field dependence of the $q = 0$ magnon energy gap in Tb–10%Ho demonstrating the validity of the 'frozen-lattice strain' approximation as manifested by the minimum, but non-vanishing, of the gap energy at a field corresponding to the basal plane anisotropy field. Data taken with the field along the hard basal plane direction, except for the curves marked easy (axis) which show a linear increase of gap energy with field. The lines are theoretical curves. Different symbols are used to distinguish data taken at different temperatures. (After Nielsen et al. 1970b.)

ferromagnet if a field is applied along the easy direction, the gap energy increases linearly by the Zeeman splitting energy. For fields applied along the hard direction, an initial rise is followed by a cusp-like minimum at zero gap energy when the applied field rotates the magnetization into the hard direction and thus effectively cancels out the anisotropy field. At higher applied fields the cusp is followed by a linear increase in the gap energy. However, as originally discussed by Turov and Shavrov (1965) in the case when a significant part of the gap energy originates from magneto-elastic sources, the lattice may assume an average equilibrium strain rather than exhibiting local non-uniform strains in response to the dynamic fluctuations that accompany a spin wave. In this case the energy gap will not be driven to zero when the moment is forced along a hard direction, but will have a non-zero minimum. Definitive evidence for the validity of the frozen-lattice effect is shown in fig. 10 for the gap energy in Tb–10%Ho for magnetizations along the easy and hard basal plane directions (Nielsen et al. 1970b).

An expression similar to eqs. (8)–(10) has been derived for the dispersion in a helical structure (see Mackintosh and Bjerrum-Møller 1972) and predicts a linear dispersion in q at small q:

$$E(q) = J\{[\tilde{J}(Q) - \tfrac{1}{2}\tilde{J}(q+Q) - \tfrac{1}{2}\tilde{J}(q-Q)] \times [\tilde{J}(Q) - \tilde{J}(q) + 6V_2]\}^{1/2}. \qquad (12)$$

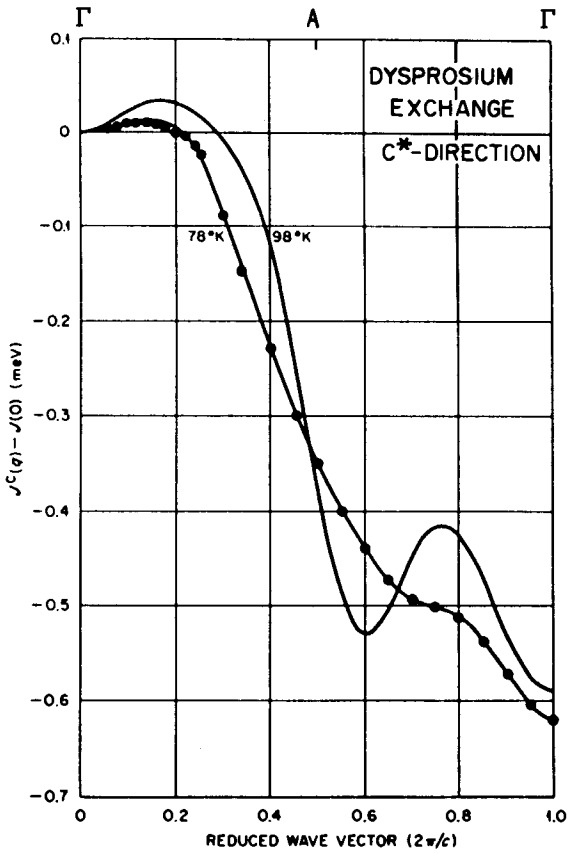

Fig. 11. Fourier transform exchange $J(q)$ for the c-axis direction in Dy in both ferromagnetic (78 K) and helical (98 K) temperature regions. The peak near $q = 0.2$ corresponds to the peak in the generalized susceptibility $\chi(q)$ and is a signature of the incommensurate helical 4f spin ordering occurring with the same wave vector. Note that the peak remains, even below T_C, consistent with a transition driven not by the exchange but by the magnetostriction. (After Nicklow 1971.)

Here Q is the characteristic wave vector of the incommensurate helical spin structure. Higher order anisotropy terms, in particular the six-fold anisotropy V_6^6, are assumed negligible at these temperatures. From the measured dispersion relationships (e.g., fig. 9 for Tb) and the anisotropy constants, one may then derive the q-dependence of the Fourier transform exchange functions which, as discussed above (section 2), are related to the generalized susceptibility. By this analogy a peak in $\chi(q)$ at finite q, which generates an incommensurate periodic magnetic structure, would also be expected to have a corresponding peak in $J(q)$ at a similar non-zero q. Such is in fact observed as shown in fig. 11 for the exchange functions in Dy at 98 K in the ferromagnetic phase, and at 78 K in the helical phase (Nicklow 1971). Both experimental results and the model fit for the exchange are indicated. The 98 K curve shows a pronounced maximum at a q corresponding to the helical turn angle for this temperature, as expected. The remarkable result is that a peak also appears in the 78 K curve at a slightly lower q in the ferromagnetic phase. This peak, also observed in $Ho_{0.9}Tb_{0.1}$ (Bjerrum-Møller et al. 1970), is ample indication that the exchange interaction continues to favor a helical periodic spin arrangement, and

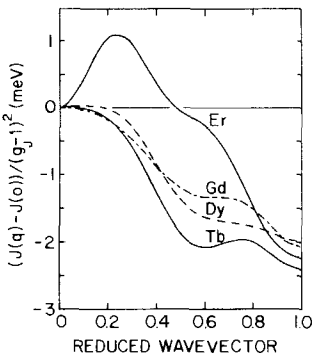

Fig. 12. Normalized exchange functions $[\tilde{J}(0) - \tilde{J}(q)]/(g_J - 1)^2$ in the c-direction for the ferromagnetic phases of Er, Tb, Dy and Gd. Apart from differences in the generalized susceptibility, exchange and wave functions these curves would be identical for all rare earths. (After Lindgard 1978.)

that it is the dominant influence of the magneto-elastic interaction which drives the overall spin system ferromagnetic.

Figure 12 shows the exchange functions in the ferromagnetic phase for Er, Gd, Tb and Dy, as determined from neutron scattering results. The division of the energy by $(g_J - 1)^2$ in the figure would make the curves identical if all elements had the same generalized susceptibility function and 4f wavefunctions, and if the coupling between ions were entirely of the RKKY type. The fact that differences exist, and in particular that the ions of largest orbital momentum $\boldsymbol{L}$ show the largest deviations, suggest an $\boldsymbol{L}$-dependent exchange coupling or a form of anisotropic exchange. Other indications of a substantial contribution from anisotropic exchange (or a $\boldsymbol{q}$-dependent anisotropy) were found in measurements of the spin waves in the conical phase of Er at 4 K (Nicklow et al. 1971) and in field-dependent measurements of the spin waves in Tb (Bjerrum-Møller et al. 1972). The light lanthanides (see next section) are the most clear cut manifestation of anisotropic exchange effects. Spin wave results in the c-axis modulated phase of Er by Nicklow and Wakabayashi (1982) also showed anomalous behavior. Constant energy scans with $\boldsymbol{q}$ along the c-axis showed only single excitation peaks centered at the satellite positions with increasing width as the energy increased. In contrast, scans with $\boldsymbol{q}$ perpendicular to the c-axis showed dispersive longitudinally polarized excitations emanating from the satellite positions.

6.2. *Excitations in light lanthanides*

The light lanthanides are in many ways far more complex than their heavy cousins, partly because of the more exotic crystal structures, and partly because the exchange interactions are significantly smaller relative to the crystal-field effects. The excitations in the case of weak exchange can be described as excitons, which are exchange-coupled combinations of the single-ion crystal-field states. These are quite different modes from spin waves and can exist in the paramagnetic state. An example of that is Pr in which both the hexagonal and cubic sites have singlet ground states as established by Rainford (1972), and as such the exchange must exceed a critical value before long-range ordering can occur. For isotropic Heisenberg

exchange the dispersion has the form (Cooper 1972)

$$E(\boldsymbol{q}) = \Delta^2 - 4\Delta\alpha^2\tilde{J}(\boldsymbol{q}), \tag{13}$$

where Δ is the splitting between the singlet ground state and the first excited state, and α is the dipolar matrix element for the transition. Thus only for exchange $|\tilde{J}(\boldsymbol{q})| > \Delta/4\alpha^2$ will the mode energy be driven soft and long-range order occur. In Pr, the splitting on the hexagonal sites as determined by Houmann et al. (1979) is $\Delta = 3.5$ meV and on the cubic sites the splitting is a much larger 8.4 meV. Figure 13 shows the resulting exciton dispersion at 6.4 K for the hexagonal sites. The pronounced minimum in the lowest mode for $q \approx 0.24\,\text{Å}^{-1}$ in the ΓM basal plane direction is indicative of a tendency towards softening and associated magnetic ordering. McEwen et al. (1978) examined the behavior of this mode under uniaxial stress and observed significant strain-induced softening as predicted by Jensen (1976); however, long-range ordered satellites appeared before the mode was driven completely to zero energy. The lifting of the degeneracy of the exciton modes along the c-direction (ΓA in fig. 13) provided clear evidence for the occurrence of anisotropic exchange terms in Pr of the form proposed by Jensen (1979).

Neodymium does exhibit spontaneous long-range order as shown by Moon et al. (1964) in which the moments on the hexagonal sites order in the basal plane parallel to the [10$\bar{1}$0] axis with a sinusoidal modulation. The cubic site moments also order in a modulated fashion but with a different modulation vector (McEwen et al. 1985). Excitations in Nd as studied by McEwen and Stirling (1982) showed the presence of both propagating excitations at low $\boldsymbol{q}$ and of excitonic states at energies above 6 meV. Constant-$\boldsymbol{q}$ measurements of the dispersive modes showed unusual width behavior, with those modes at the zone boundary having essentially resolution limited energy widths while those at other wave vectors had appreciable intrinsic width, suggesting a strong mixing of the mid-band excitations.

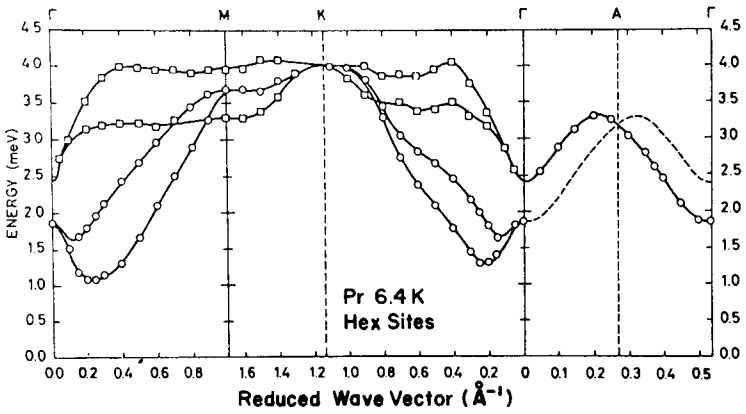

Fig. 13. Dispersion curves for magnons propagating in principal axis directions for the hexagonal (as distinct from cubic) sites of hcp Pr at 6.4 K. The circles and squares represent acoustic and optic modes, respectively. (After Houmann et al. 1979.)

7. Magnetism in lanthanide multi-layers

The development of molecular beam epitaxy (MBE) procedures for producing high-quality single-crystal layered structures of lanthanides (multi-layers) has recently provided the opportunity to study a variety of magnetic phenomena. Structures with alternate layers (typically 10–40 atomic planes per layer) of Gd and Y (Majkrzak et al. 1986) and of Dy and Y (Salamon et al. 1986, Rhyne et al. 1987) have been studied by neutron diffraction and magnetization techniques. Both systems showed the occurrence of long-range magnetic order in which spins in adjacent Gd or Dy layers are exchange-coupled across the magnetically 'dead' Y layer thus providing a unique confirmation of the long-range character of the indirect exchange interaction. In the Gd multi-layers, both ferromagnetic and antiferromagnetic couplings are found depending on the thickness of the intervening Y layer, suggesting a correspondence with the real-space oscillation of the exchange function as calculated by Yafet (1987). As shown in fig. 14 for a Dy–Y multi-layer, the observation of magnetic satellite peaks and bilayer harmonics confirms the formation of long-range helical ordering. Both the phase and chirality of the helix are preserved across the Y intervening layers (Erwin et al. 1987) in which

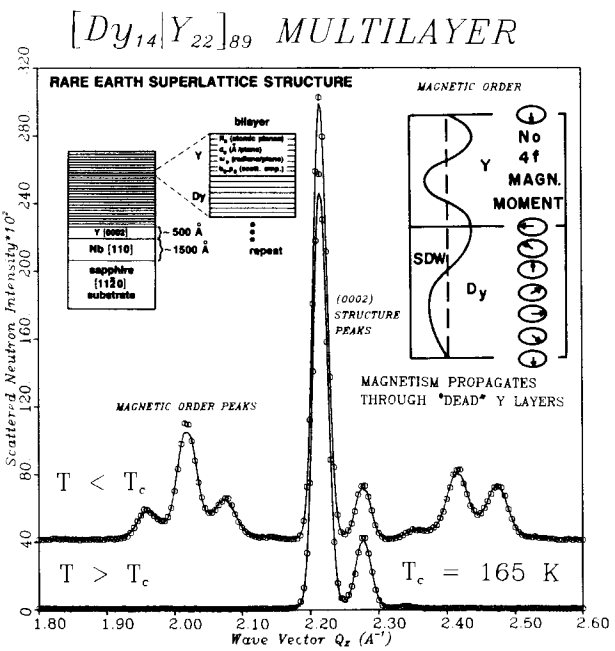

Fig. 14. Neutron diffraction scan along the reciprocal c-axis in a $[Dy_{14}|Y_{22}]_{89}$ multi-layer (89 layers with 16 planes of Dy and 20 planes of Y per layer). Above T_C, the principal features are the peak corresponding to the (0002) Bragg peak and the associated harmonic(s) arising from the bilayer chemical modulation period. Below T_C, the appearance of additional satellites signals the occurrence of long-range incommensurate (helical) magnetic ordering. The inset shows schematically the spin density waves of different wave length proposed for the magnetic coupling.

the phase lag is determined by the number of Y planes and a 'pseudo turn-angle' which is found to be 52° per plane in the Y, in close agreement with the calculated peak in the generalized susceptibility (see section 4.1). Neutron studies of a series of Dy–Y multi-layers with varying Y layer thicknesses have shown that the magnetic coherence length varies linearly with the reciprocal of the Y layer thickness.

8. Superconductivity and magnetism

Superconductivity is no stranger to the rare earths, in particular La and several of its compounds. Under pressure, Ce also becomes a superconductor as do Y, Lu (see Probst and Wittig 1978) and certain alloys; however, for those lanthanides in which well-defined local 4f moments are present, superconductivity is inhibited by the pair breaking associated with the spins. And yes, rare earths play a role, albeit not central, in what has been described as the condensed matter 'event' of the 1980s – the remarkable discovery of superconductivity above 90 K in YBaCuO (Wu et al. 1987, Cava et al. 1987). In this case the rare earth is electronically isolated from the superconducting electrons, and as a result the substitution of heavy lanthanides with large 4f spins for the yttrium (Fisk et al. 1987) has virtually no effect on the superconducting properties.

The intriguing question of the interaction of magnetism and superconductivity has been a subject of considerable interest for a number of years, in particular relating to the possible co-existence of these two phenomena which are normally mutually exclusive. Recently, a series of lanthanide compounds have been discovered [see the reviews by Fischer and Maple (1982) and Shelton (1982)] in which superconductivity does co-exist with long-range magnetism, but with a magnetism which shows an ordering which is antiferromagnetic or incommensurate with the lattice. As such the spatially averaged magnetization is zero, and thus the electromagnetic coupling to superconductivity is weak. The alloy system $(Ce_{1-x}R_x)Ru_2$ (Lynn et al. 1980) does show ferromagnetic correlations with coherence lengths in the range 10^2 Å which co-exist with the superconductivity, but true long-range order does not develop. A corollary phenomena to the co-existence problem is that of re-entrant superconductivity in which the zero-temperature ground state of the system is ferromagnetic with a low T_C, above which superconductivity appears and finally vanishes at a higher critical temperature T_{sc}. Examples of both the co-existent and re-entrant superconductivity and magnetism are found principally in two general classes of ternary lanthanide compounds – the Chevrel phases $RMo_6(S \text{ or } Se)_8$ (Chevrel et al. 1971) and the RRh_4B_4 compounds (Matthias et al. 1977). In the case of the Chevrel material $HoMo_6S_8$ (Lynn et al. 1983) and in $ErRh_4B_4$ (Sinha et al. 1982, Moncton et al. 1980) the tendency to ferromagnetism, which would couple strongly to the superconducting order parameter, results in a compromise ordered long-wavelength modulated state with a wavelength of about 200 Å which co-exists with the superconductivity in the range $0.7 < T < 0.732$ K. The wave vector of this modulated state is not temperature-dependent, and below ≈ 0.64 K the ferromagnetic interactions destroy the superconductivity and the modulated state. The other S_8 phases studied with Gd, Tb, Dy and Er are co-existence types as are the

RMo_6Se_8 materials with R = Gd, Ho, Tb, and Er. For example, the $HoMo_6Se_8$ (Lynn 1984) compound shows the development of a pure single-component sinusoidally modulated state with a strongly temperature-dependent wave vector derived from a coupling of the London penetration depth to the Ho magnetization density. The ordering is long range with the Ho developing the maximum moment allowed by the crystal-field mixing.

9. The novel properties of Ce and its alloys and compounds

9.1. *Band effects and intermediate valence*

Much of the excitement of lanthanide physics in the recent past has focussed on the anomalous properties of Ce and its alloys and compounds. Ce as an element begins the transition series of the lanthanide elements and itself possesses unique properties not seen in the remainder of the series. It exists in a number of allotropic structures – from above room temperature down to about 50 K it has the dhcp phase of β-cerium, which transforms gradually to a collapsed fcc phase of α-cerium at lower temperatures. Burgardt et al. (1976) artifically stabilized the β-phase to low temperature by a thermal cycling process, and showed that it orders antiferromagnetically at 12.5 K. A third phase, γ-cerium is fcc and non-magnetic, but it transforms to either the β-phase near 273 K or to the collapsed fcc phase of α-cerium at lower temperatures ($\approx$ 110 K). Many of the exotic properties of Ce relate to this α phase and to the γ–α phase transformation, at which point an approximately 15% volume change is observed, which originally evoked the idea of a valence change from 3^+ to 4^+ driven by a promotion of the single 4f electron to a 5d state. In the past twenty years ample experimental and theoretical evidence has been amassed to show that this simple promotional model is incorrect. The first definitive evidence was in the positron-annihilation studies of Gustafson and Mackintosh (1964) and Gustafson et al. (1969) in which they showed that the γ–α transition results in a valence change substantially less than one and that considerable 4f electron character is present in both phases. The promotional model evolved into the idea of a 4f band for α-cerium and the ideas of intermediate valence as discussed by Johansson (1974) and the band calculations of Skriver (1985). Lacking single crystals of α-cerium of sufficient size, Johanson et al. (1981) demonstrated the existence of itinerant 4f band electrons of large mass from de Haas–van Alphen measurements in $CeSn_3$ interpreted in light of the band calculations of Koelling (1982). Other evidence of the band character of α-Ce came from the photoemission studies of Wieliczka et al. (1984) and from the inverse photoemission (BIS) work by Wuilloud et al. (1983).

9.2. *Kondo lattices and heavy fermions*

In addition to the intermediate valence or valence-fluctuation effects seen in many Ce compounds, which arise from the proximity of the 4f level to the Fermi level,

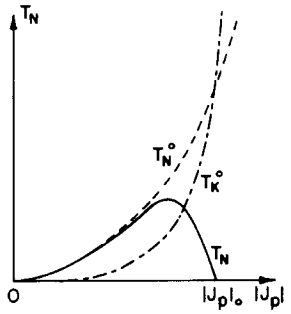

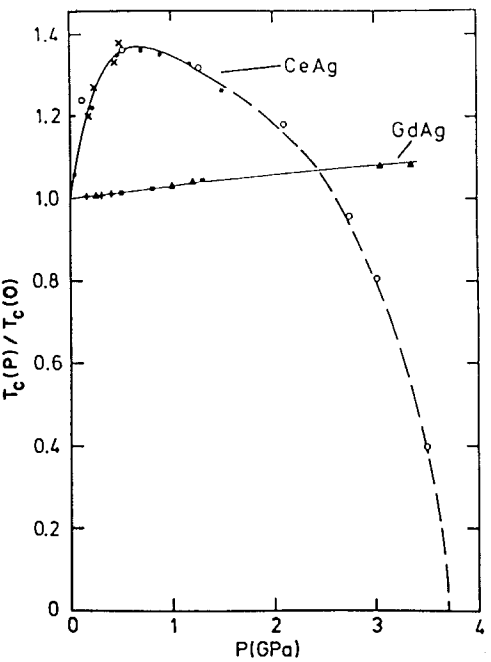

Fig. 15. (Left) Schematic representation of the competition between the Kondo Temperature T_K and the magnetic ordering temperature T_N, each in the absence of the other. Both are dependent on the magnitude of the exchange interaction and the density of states at the Fermi energy. The solid line represents the peaking of the magnetic ordering temperature that would be seen in a real material with these interactions (see text), and as actually observed in the pressure dependence of the Curie temperature of CeAg (right). (After Eiling and Schilling 1981.)

additional phenomena are found in materials exhibiting 'Kondo lattice' behavior. In this case the Ce ion is in the trivalent state with a 4f level well below E_F. However, a competition exists between the single-ion Kondo coupling present on each cerium atom and the indirect exchange (RKKY) interaction between different cerium atoms. One can define (Doniach 1977) a characteristic Kondo temperature T_K corresponding to the one-impurity (or extreme dilute limit) case and likewise a magnetic characteristic temperature T_N representing the ordering temperature if there were no local Kondo effect on a Ce atom. Both of these temperatures are dependent on the product $\tilde{J}\rho$, where $\tilde{J}$ is the exchange interaction and ρ is the density of states at the Fermi energy, but with different functional dependences [see fig. 15 (left)]. In a real system the ordering temperature resulting from the competition will exhibit a maximum and then go to zero at a limiting value of $|\tilde{J}\rho|_0$ (Doniach 1977) as is experimentally observed for the Curie temperature of CeAg by Eiling and Schilling (1981) shown in fig. 15 (right). In addition, if the magnitude of $|\tilde{J}\rho|$ is less than $|\tilde{J}\rho|_0$ then the low-temperature state will be magnetically ordered, or if $|\tilde{J}\rho|$ is greater than $|\tilde{J}\rho|_0$ the non-magnetic Kondo ground state will predominate. The first condition is found in $CeAl_2$, CeB_6, CeS, and CeTe, while the Kondo state is observed for $CeAl_3$ and $CeCu_2Si_2$, the latter two of which are also part of a new class of 'heavy fermion' superconductors (see below). In Kondo-lattice systems for $T > T_K$ (typically of the order of 1–10 K), well-defined crystal-field levels are observed which is another feature differentiating these materials from mixed valent compounds, and for $T \approx T_K$ the crystal-field doublets show characteristics of

independent spin $\frac{1}{2}$ Kondo impurities. Below T_K the loss of the magnetic ordered moment gives rise to large enhancements in both the susceptibility and in the electronic heat capacity term, for example in $CeAl_3$ (Andres et al. 1975) and in $CeCu_2Si_2$ (Steglich et al. 1979), a phenomena which has been termed 'heavy fermion' behavior. The giant electronic heat capacity coefficient (γ), which is enhanced by factors of hundreds to a thousand over normal values, is directly proportional to an effective electron mass and hence the basis of the term *heavy* fermion. Additional details of these systems and of systems undergoing large spin fluctuations are found in ch. 78, section 4.4.4.

10. Amorphous rare earth alloys

In the 1970s the techniques of rapid quenching (sputtering, melt-spinning, etc.) made possible the production of a variety of rare earth alloys in amorphous form, many of which have anomalous magnetic properties. A comprehensive review of amorphous rare earth alloys can be found in ch. 6 of the book by Moorjani and Coey (1984).

In an amorphous alloy the random atomic topology introduces fluctuations in both the magnetic exchange and anisotropy interactions, the latter coming from the random symmetry of the crystal field. These random magnetic interactions can be modelled as distributions in magnitude (exchange) or distributions in space (anisotropy) as follows

$$H = -\sum_{i,j} (\tilde{J}_0 + \Delta J_{ij}) \boldsymbol{J}_i \cdot \boldsymbol{J}_j - \sum_i D(\boldsymbol{n}_i \cdot \boldsymbol{J}_i)^2 \tag{14}$$

where $\tilde{J}_0$ is the average (ferromagnetic) exchange with distribution ΔJ_{ij}, D is an average crystal-field anisotropy constant, and $\boldsymbol{n}_i$ is a random-direction unit vector expressing the fluctuations in magnitude and direction of the local anisotropy field. The interactions in eq. (14) have a profound effect on the magnetic phase transition and the susceptibility. The random exchange generally has the effect of reducing the Curie temperature, or if the distribution is broad enough to encompass negative interactions, a spin-glass ground state may result as in amorphous YFe_2 (Forester et al. 1979). The effect of a finite random anisotropy, as calculated by Aharony and Pytte (1983), is to raise the lower marginal dimensionality of the system to four and thus no phase transition to ferromagnetic long-range order exists in three dimensions. This rather dramatic effect also precludes a divergence in the susceptibility at T_C which is found to depend on the ratio $\chi_{max} \propto (\tilde{J}_0/D)^4$ and thus will not reach the demagnetization limit for a random anisotropy system. This is shown in fig. 16 (left) for the AC susceptibility (Sellmyer and Nafis 1985) of a series of $Gd_{64}T_{20}Ga_{16}$ amorphous alloys, where T = Fe, Co, and Ni, which are characteristic of materials with large $\tilde{J}_0/D$ and thus show demagnetization limited susceptibility. In contrast, $Tb_{64}Co_{20}Ga_{16}$ and $Nd_{64}Co_{20}Ga_{16}$ (right) represent alloys with small $\tilde{J}_0/D \approx 0.2$ and show a very narrow susceptibility peak with magnitude considerably reduced from the demagnetization limit. A systematic study of the effect of varying the ratio

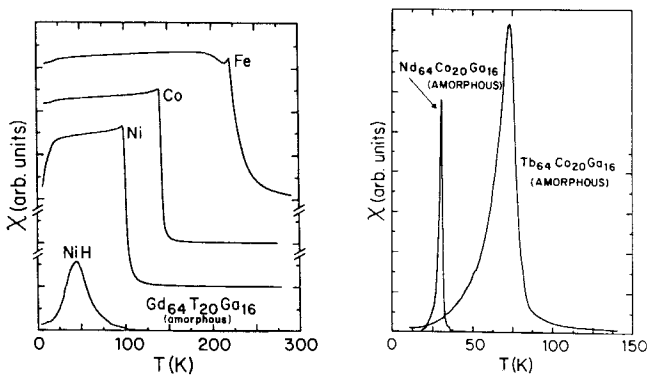

Fig. 16. (Left) AC susceptibility data for $Gd_{64}T_{20}Ga_{16}$ (T = Fe, Co, Ni) showing the demagnetization limited behavior (infinite intrinsic χ) for amorphous alloys with large values of $\tilde{J}_0/D$. The curve marked NiH is the susceptibility for the Ni compound after adding hydrogen and shows the behavior of a conventional spin glass for comparison. (Right) Susceptibility data for $Nd_{64}Co_{20}Ga_{16}$ and $Tb_{64}Co_{20}Ga_{16}$ showing the non-divergence of χ for random alloys with small values of $\tilde{J}_0/D$.

$\tilde{J}_0/D$ on the magnetization and the critical scaling exponents has been made by Dieny and Barbara (1985) and Filippi et al. (1985) using a series of amorphous alloys of $Dy_xGd_{1-x}Ni$ in which $\tilde{J}_0/D$ has been calculated to vary from ≈ 100 ($x = 0$) to ≈ 1.05 ($x = 1$).

The amorphous equivalents of the RFe compounds, in particular amorphous Tb_xFe_{1-x} have been studied by small-angle neutron scattering (SANS) (Rhyne 1985) in which the spin correlation length was determined as a function of composition from $x = 0.015$ to $x = 0.75$. This correlation length ξ is also proportional to $\xi \propto (\tilde{J}_0/D)^2$ (Chudnovsky et al. 1986) and is not divergent below T_C for a random anisotropy system. The results show the effect of the destruction of long-range order by the random anisotropy and the formation of correlated spin-glass-like clusters below T_C with values of the correlation length ξ in the 50–100 Å range at low temperature. Field-dependent measurements have shown an anisotropy in ξ and a field variation which again is consistent with the spin-cluster description of the magnetic state below T_C.

11. Summary

The study of the basic physics underlying the magnetism in the lanthanide metals, alloys, and compounds has been a subject of intense interest for several decades. During the 1960s and early 1970s much attention was focused on the heavy lanthanide metals, which led to an elucidation of the bulk magnetic moment and transport properties of the elements, as well as the definitive work on the spin structures from neutron diffraction. In addition the ground work was laid for an understanding of the fundamental exchange coupling, anisotropy, and magnetostric-

tion interactions of the 4f electrons and their interrelation. Simultaneously, the conduction-electron properties were revealed from band structure and Fermi-surface calculations, and the concept of the relationship between Fermi surface 'nesting', the generalized susceptibility properties, and the stable wave vectors of the incommensurate magnetic states was born.

Starting in the mid-1960s inelastic neutron scattering brought new insight to the fundamental magnetic excitations in the heavy lanthanides, the details of the exchange interaction, and the effect of crystal-field anisotropy and magnetostriction on the spin waves.

The light lanthanides received new emphasis in the 1970s with the availability of sizeable single crystals. These metals presented many more difficulties in understanding because of their complex crystal structure and the much weaker exchange relative to the crystal-field energies.

In what might be described as the contemporary era of rare earths, much emphasis has been placed on the use of lanthanides as local-moment impurities, for example in studies of the co-existence of superconductivity and magnetism and in spin-glass phenomena. Also the band-like characteristics of the 4f moment of Ce has been the cornerstone of an intense effort in understanding valence fluctuation effects, Kondo-lattice systems, and 'heavy fermion' superconductivity.

Throughout the period of accumulation of knowledge of the lanthanide elements, a vast literature was also developed on the bulk magnetic and transport properties of rare earth intermetallic compounds. This topic has been almost entirely omitted from this chapter, but details may be found in a number of comprehensive reviews including the book by Wallace (1973) and the chapter by Kirchmayr and Poldy (1979) in Volume 2 of this handbook.

Acknowledgements

The author would like to thank the many authors of past review articles who have assimilated much of the material from original works in a form easily accessible for summaries such as this. In addition I would like to thank personally my many collaborators on problems of lanthanide magnetism and amorphous materials. I express great appreciation especially to the late Dr. Wally Koehler and Prof. Sam Legvold for providing my introduction to the world of experiment in lanthanides, and to Prof. Alan Mackintosh and Prof. Sam Liu for providing the nucleus of understanding of the theory of lanthanide magnetism.

References

Aharony, A., and E. Pytte, 1983, Phys. Rev. B **27**, 5872.

Andres, K., J.E. Graebner and H.R. Ott, 1975, Phys. Rev. Lett. **35**, 1779.

Bjerrum-Møller, H., and J.C.G. Houmann, 1966, Phys. Rev. Lett. **16**, 737.

Bjerrum-Møller, H., and J.C.G. Houmann, 1966, Phys. Rev. Lett. **16**, 737.

Bjerrum-Møller, H., M. Nelsen and A.R. Mackintosh, 1970, in: Les Éléments des Terres Rares, Vol. II (CNRS, Paris) p. 277.

Bjerrum-Møller, H., J.C.G. Houmann, J. Jensen and A.R. Mackintosh, 1972, Neutron Inelastic Scattering (IAEA, Vienna) p. 603.

Bjerrum-Møller, H., J.Z. Jensen, M. Wulff, A.R. Mackintosh, O.D. McMasters and K.A. Gschneidner Jr, 1982, Phys. Rev. Lett. **49**, 482.

Burgardt, P., K.A. Gschneidner Jr, D.C. Kosken-

maki, D.K. Finnemore, J.O. Moorman, S. Legvold, C. Stassis and T.A. Vyrostek, 1976, Phys. Rev. B **14**, 2995.
Callen, E., 1968, J. Appl. Phys. **39**, 519.
Callen, E.R., and H.B. Callen, 1963, Phys. Rev. **129**, 578.
Callen, E.R., and H.B. Callen, 1965, Phys. Rev. **139**, A455.
Cava, R.J., B. Batlogg, R.B. van Dover, D.W. Murphy, S. Sunshine, T. Siegrist, J.P. Remeika, E.A. Rietman, S. Zuhurah and G.P. Espinosa, 1987, Phys. Rev. Lett. **58**, 1676.
Chevrel, R., M. Sergent and J. Prigent, 1971, J. Solid State Chem. **3**, 515.
Chudnovsky, E.M., W.M. Saslow and R.A. Serota, 1986, Phys. Rev. B **33**, 251.
Cooper, B.R., 1967, Phys. Rev. Lett. **19**, 900.
Cooper, B.R., 1968, Phys. Rev. **169**, 281.
Cooper, B.R., 1972, in: Magnetic Properties of the Rare Earth Metals, ed. R.J. Elliott (Plenum, London) ch. 2, p. 17.
Coqblin, B., 1977, The Electronic Structure of Rare Earth Metals and Alloys: the Magnetic Heavy Rare Earths (Academic Press, London).
Darnell, F.J., 1963, Phys. Rev. **130**, 1825; Phys. Rev. **132**, 1098.
Dieny, B., and B. Barbara, 1985, J. Phys. (France) **46**, 293.
Dimmock, J.O., and A.J. Freeman, 1964, J. Phys. Rev. Lett. **13**, 94.
Doniach, S., 1977, Physica B **91**, 231.
Eiling, A., and J.S. Schilling, 1981, Phys. Rev. Lett. **46**, 364.
Elliott, R.J., ed., 1972, Magnetic Properties of Rare Earth Metals (Plenum, London).
Elliott, R.J., and F.A. Wedgewood, 1963, Proc. Phys. Soc. (London) **81**, 846.
Erwin, R.W., J.J. Rhyne, M.B. Salamon, J. Borchers, S. Sinha, R. Du, J.E. Cunningham and C.P. Flynn, 1987, Phys. Rev. B **35**, 6808.
Evenson, W.E., and S.H. Liu, 1969, Phys. Rev. **178**, 783.
Fert, A., and A. Friederich, 1976, Phys. Rev. B **13**, 397.
Fert, A., R. Asomoza, D.H. Sanchez, D. Spanjaard and A. Friederich, 1977, Phys. Rev. B **16**, 5040.
Filippi, J., B. Dieny and B. Barbara, 1985, Solid State Commun. **53**, 523.
Fischer, Ø., and M.B. Maple, eds, 1982, Topics in Current Physics, Vols. 32 and 34 (Springer, Berlin).
Fisk, Z., J.D. Thompson, F. Zirngiebl, J.L. Smith and S.W. Cheong, 1987, to be published.
Forester, D.W., N.C. Koon, J.H. Schelleng and J.J. Rhyne, 1979, J. Appl. Phys. **50**, 7336.
Freeman, A.J., and J.P. Desclaux, 1972, Int. J. Magn. **3**, 311.
Gibbs, D., D.E. Moncton and K.L. D'Amico, 1985, J. Appl. Phys. **57**, 3619.
Gibbs, D., J. Bohr, J.D. Axe, D.E. Moncton and K.L. D'Amico, 1986, Phys. Rev. B **34**, 8182.
Gustafson, D.R., and A.R. Mackintosh, 1964, J. Phys. & Chem. Solids **25**, 389.
Gustafson, D.R., J.D. McNutt and L.O. Roellig, 1969, Phys. Rev. **183**, 435.
Habenschuss, M., C. Stassis, S.K. Sinha, H.W. Deckman and F.H. Spedding, 1974, Phys. Rev. B **10**, 1020.
Hegland, D.E., S. Legvold and F.H. Spedding, 1963, Phys. Rev. **131**, 158.
Houmann, J.G., B.D. Rainford, J. Jensen and A.R. Mackintosh, 1979, Phys. Rev. B **20**, 1105.
Jensen, J., 1976, J. Phys. C **9**, 111.
Jensen, J., 1979, J. Phys. (France) **40**, C5-1.
Johanson, W.R., G.W. Crabtree, A.S. Edelstein and O.D. McMasters, 1981, Phys. Rev. Lett. **46**, 504.
Johansson, B., 1974, Philos. Mag. **30**, 469.
Johansson, T., B. Lebech, M. Nielsen, H. Bjerrum-Møller and A.R. Mackintosh, 1970, Phys. Rev. Lett. **25**, 524.
Kasuya, T., 1956, Prog. Theor. Phys. **16**, 45.
Keeton, S.C., and T.L. Loucks, 1968, Phys. Rev. **168**, 672.
Kirchmayr, H.R., and C.A. Poldy, 1979, in: Handbook on the Physics and Chemistry of Rare Earths, Vol. 2, eds K.A. Gschneidner Jr and L. Eyring (North-Holland, Amsterdam) ch. 14, p. 55.
Koehler, W.C., 1972, in: Magnetic Properties of Rare Earth Metals, ed. R.J. Elliott (Plenum, London) ch. 3, p. 81.
Koehler, W.C., J.W. Cable, H.R. Child, M.K. Wilkinson and E.O. Wollan , 1967, Phys. Rev. **158**, 450.
Koehler, W.C., H.R. Child, R.M. Nicklow, H.G. Smith, R.M. Moon, J.W. Cable, 1970, Phys. Rev. Lett. **24**, 16.
Koelling, D.D., 1982, Solid State Commun. **43**, 247.
Legvold, S., 1980, in: Ferromagnetic Materials, ed. E.P. Wohlfarth (North-Holland, Amsterdam) ch. 3, p. 183.
Levy, P.M., 1979, J. Phys. (France) C **5**, 8.
Lindgard, P.A., 1978, Phys. Rev. B **17**, 2348.
Lindgard, P.A., and O. Danielsen, 1975, Phys. Rev. B **11**, 351.
Liu, S.H., 1978, in: Handbook on the Physics and Chemistry of Rare Earths, Vol. 1, eds K.A. Gschneidner Jr and L. Eyring (North-Holland, Amsterdam) ch. 3, p. 233.
Liu, S.H., R.P. Gupta and S.K. Sinha, 1971, Phys. Rev. B **4**, 1100.
Lynn, J.W., D.E. Moncton, L. Passell and W. Thomlinson, 1980, Phys. Rev. B **21**, 70.
Lynn, J.W., R. Pynn, J. Joffrin, J.L. Ragazzoni and R.N. Shelton, 1983, Phys. Rev. B **27**, 581.
Lynn, J.W., J.A. Gotaas, R.W. Erwin, R.A. Ferrell, J.K. Bhattacharjee, R.N. Shelton and P. Klavins, 1984, Phys. Rev. Lett. **52**, 133.
Mackintosh, A.R., and H. Bjerrum-Møller, 1972, in: Magnetic Properties of Rare Earth Metals, ed. R.J. Elliott (Plenum Publishing, London) ch. 5, p. 187.
Majkrzak, C.F., J.W. Cable, J. Kwo, M. Hong,

D.B. McWhan, Y. Yafet, J.V. Waszczak and C. Vettier, 1986, Phys. Rev. Lett. **56**, 2700.
Mason, W.P., 1954, Phys. Rev. **96**, 302.
Matthias, B.T., E. Corenzwit, J.M. Vandenberg and H.E. Barz, 1977, Proc. Nat. Acad. Sci. (USA) **74**, 1334.
McEwen, K.A., 1978, in: Handbook on the Physics and Chemistry of Rare Earths, Vol. 1, eds K.A. Gschneidner Jr and L. Eyring (North-Holland, Amsterdam) ch. 6, p. 411.
McEwen, K.A., and W.G. Stirling, 1982, J. Magn. & Magn. Mater. **30**, 99.
McEwen, K.A., W.G. Stirling and C. Vettier, 1978, Phys. Rev. Lett. **41**, 343.
McEwen, K.A., E.M. Forgan, H.B. Stanley, J. Bouillot and D. Fort, 1985, Physica B **130**, 360.
Miwa, H., 1963, Prog. Theor. Phys. **29**, 477.
Moncton, D.E., D.B McWhan, P.H. Schmidt, G. Shirane, W. Tomlinson, M.B. Maple, H.B. McKay, L.D. Woolf, Z. Fisk and D.C. Johnston, 1980, Phys. Rev. Lett. **45**, 2060.
Moon, R.M., and W.C. Koehler, 1971, Phys. Rev. Lett. **27**, 407.
Moon, R.M., J.W. Cable and W.C. Koehler, 1964, J. Appl. Phys. Suppl. **35**, 1041.
Moorjani, K., and J.M.D. Coey, 1984, Magnetic Glasses (Elsevier Science Publishers, Amsterdam).
Murao, T., 1971, J. Phys. Soc. Jpn. **31**, 683.
Nicklow, R.M., 1971, J. Appl. Phys. **42**, 1672.
Nicklow, R.M., and N. Wakabayashi, 1982, Phys. Rev. B **26**, 3994.
Nicklow, R.M., H.A. Mook, H.G. Smith, R.E. Reed and M.K. Wilkinson, 1969, J. Appl. Phys. **40**, 1452.
Nicklow, R.M., N. Wakabayashi, M.K. Wilkinson and R.E. Reed, 1971, Phys. Rev. Lett. **26**, 140.
Nielsen, M., H. Bjerrum-Møller and A.R. Mackintosh, 1968, J. Appl. Phys. **39**, 807.
Nielsen, M., H. Bjerrum-Møller and A.R. Mackintosh, 1970a, J. Appl. Phys. **41**, 1174.
Nielsen, M., H. Bjerrum-Møller, P.A. Lindgard and A.R. Mackintosh, 1970b, Phys. Rev. Lett. **25**, 1451.
Nigh, H.E., 1963, J. Appl. Phys. **34**, 3323.
Overhauser, A.W., 1960, J. Phys. & Chem. Solids **13**, 71.
Probst, C., and J. Wittig, 1978, in: Handbook on the Physics and Chemistry of Rare Earths, Vol. 1, eds K.A. Gschneidner Jr and L. Eyring (North-Holland, Amsterdam) ch. 10, p. 749.
Rainford, B.D., 1972, AIP Conf. Proc. **5**, 591.
Rainford, B.D., and J.G. Houmann, 1971, Phys. Rev. Lett. **26**, 1254.
Rhyne, J.J., 1972, in: Magnetic Properties of the Rare Earth Metals, ed. R.J. Elliott (Plenum, London) ch. 4, p. 129.
Rhyne, J.J., 1985, IEEE Trans. Mag. **MAG-21**, 1990.
Rhyne, J.J., and S. Legvold, 1965, Phys. Rev. **140**, 2143.
Rhyne, J.J., R.W. Erwin, J. Borchers, S. Sinha, M.B. Salamon, R. Du and C.P. Flynn, 1987, J. Appl. Phys. **61**, 4043.
Ruderman, M.A., and C. Kittel, 1954, Phys. Rev. **96**, 99.
Salamon, M.B., S. Sinha, J.J. Rhyne, J.E. Cunningham, R.W. Erwin, J. Borchers and C.P. Flynn, 1986, Phys. Rev. Lett. **56**, 259.
Schirber, J.E., F.A. Schmidt, B.N. Harmon and D.D. Koelling, 1976, Phys. Rev. Lett. **36**, 448.
Sellmyer, D.J., and S. Nafis, 1985, J. Appl. Phys. **57**, 3584.
Shelton, R.N., 1982, in: Superconductivity in d and f-band Metals, eds W. Buckel and W. Weber (Kernforschungszentrum Karlsruhe, Karlsruhe, FRG).
Sinha, S.K., 1978, in: Handbook on the Physics and Chemistry of Rare Earths, Vol. 1, eds K.A. Gschneidner Jr and L. Eyring (North-Holland, Amsterdam) ch. 7, p. 489.
Sinha, S.K., G.W. Crabtree, D.G. Hinks and H. Mook, 1982, Phys. Rev. Lett. **48**, 950.
Skriver, H.L., 1985, Phys. Rev. B **31**, 1909.
Steglich, F., J. Aarts, C.D. Bredl, W. Lieke, D. Meschede, W. Franz and H. Schafer, 1979, Phys. Rev. Lett. **43**, 1892.
Stevens, K.W.H., 1952, Proc. Phys. Soc. (London) A **65**, 209.
Strandburg, D.L., S. Legvold and F.H. Spedding, 1962, Phys. Rev. **27**, 2046.
Stringfellow, M.W., T.M. Holden, B.M. Powell and A.D.B. Woods, 1970, J. Phys. C **2**, S189.
Turov, E.A., and V. Shavrov, 1965, Fiz. Tverd. Tela **7**, 166.
Wallace, W.E., 1973, Rare Earth Intermetallics (Academic Press, New York).
Watson, R.E., A.J. Freeman and J.O. Dimmock, 1968, Phys. Rev. **167**, 497.
Wenger, L.E., G.W. Hunter, J.A. Mydosh, J.A. Gotaas and J.J. Rhyne, 1986, Phys. Rev. Lett. **56**, 1090.
Wieliczka, D., C.G. Olson and D.W. Lynch, 1984, Phys. Rev. B **29**, 3028.
Wohlfarth, E.P., ed., 1980, Ferromagnetic Materials (North-Holland, Amsterdam).
Woods, A.D.B., T.M. Holden and B.M. Powell, 1967, Phys. Rev. Lett. **19**, 908.
Wu, M.K., J.R. Ashbur, C.J. Torng, P.H. Hor, R.L. Meng, L. Gao, Z.J. Huang, Y.Q. Wang and C.W. Chu, 1987, Phys. Rev. Lett. **58**, 908.
Wuilloud, E., H.R. Moser, W.D. Schneider and Y. Baer, 1983, Phys. Rev. B **28**, 7354.
Yafet, Y., 1987, J. Appl. Phys. **61**, 4058.
Yosida, K., 1957, Phys. Rev. **106**, 893.
Young, R.C., R.G. Jordan and D.W. Jones, 1973, Phys. Rev. Lett. **31**, 1473.
Zener, C., 1951, Phys. Rev. **81**, 446.

Handbook on the Physics and Chemistry of Rare Earths, Vol. 11
edited by K.A. Gschneidner, Jr. and L. Eyring

Chapter 77

MAGNETIC RESONANCE SPECTROSCOPY AND HYPERFINE INTERACTIONS

B. BLEANEY
Clarendon Laboratory, Parks Road, Oxford OX1 3PU, UK

Contents

List of symbols

a_0	magnetic hyperfine frequency
A	magnetic hyperfine tensor
$A_x, A_y, A_z, A_\parallel, A_\perp,$	magnetic hyperfine tensor, principal values
A_J	magnetic hyperfine parameter, free ion
A_d, A_p, A_s	transferred magnetic hyperfine parameters
ADRF	adiabatic demagnetization in the rotating frame
B	magnetic field
$B_{20}, B_3, B_4, B_5, b_4, b_6$	crystal-field coefficients
B_c	critical field (Jahn–Teller effect)
B_{1g}, B_{2g}	elastic strain symmetry
$c_1, c_{11}, c_{22}, c_{66}$	elastic strains
c.e.	conduction electrons
c.p.	core polarization
CeETS, etc.	ethylsulphates of cerium, etc.
CMN, etc.	magnesium double nitrates of cerium, etc.
DNP	dynamic nuclear polarization
EMI	electric multi-pole interaction
ENDOR	electron–nuclear double resonance
EPR	electron paramagnetic resonance
EQQ	electric quadrupole–quadrupole interaction
EuIG, etc.	iron garnets of europium, etc.
g	electronic magnetic resonance tensor
$g_x, g_y, g_z, g_\parallel, g_\perp$	electronic magnetic resonance tensor, principal components
g_e	electronic magnetic resonance factor
$g^{(E)}$	electric electronic resonance tensor
g_I	nuclear magnetic Zeeman parameter
g_n	nuclear magnetic tensor
g_J	electronic magnetic parameter
$\boldsymbol{F}, \boldsymbol{I}, \boldsymbol{J}, \boldsymbol{L}, \boldsymbol{S}$	angular momenta vectors
J	exchange coupling energy
K_1, K_2	anisotropy energies
LMN	lanthanum magnesium nitrate
MCDA	magnetic circular dichroism absorption
MOR	magneto-optical rotation
NEQ	nuclear electric quadrupole
NMR	nuclear magnetic resonance
NQR	nuclear quadrupole resonance
P, P_1, P_2, P_3	nuclear electric quadrupole parameters
Q	nuclear electric quadrupole moment
$\langle r^2\rangle, \langle r^4\rangle, \langle r^6\rangle, \langle r^{-3}\rangle$	powers of electronic radii
T_1, T_b	spin relaxation times to lattice, bath
T_{ph}	phonon relaxation time to bath
T_C	Curie temperature
T_D	Jahn–Teller transition temperature
T_N	Néel temperature

V, V_{kq}	crystalline potential coefficients
VPE	virtual phonon exchange interaction
w	octupole frequency
YAG, YIG	yttrium aluminium/iron garnet
Z	Zeeman energy
$\gamma/2\pi$	nuclear magnetic resonance frequency in a field of 1 T
γ_∞	nuclear electric-quadrupole shielding coefficient
Γ	group-theory representation
Δ	energy difference
θ	angle, paramagnetic Curie temperature
λ	spin – orbit coupling energy
λ, μ	Jahn–Teller coefficients
μ_B	Bohr magneton
ν	frequency
σ_2	electronic electric quadrupole shielding coefficient
χ	susceptibility
ω	angular frequency

1. Hyperfine structure of atoms

1.1. *Nuclear spins and moments*

At the present time the values of the nuclear spins I are known for all the stable isotopes of the lanthanide 4f series, together with those of a number of radioactive isotopes. The nuclear magnetic moments have been determined with an accuracy of about 0.01 to 1%. In general, values of the nuclear electric quadrupole moments are less reliable, but an accuracy of 1% is claimed for values of Q from measurements by muonic and pionic hyperfine structure (Tanaka et al. 1983), in which problems of electronic shielding are avoided. A selected list is given in table 1, based on the compilation by Lederer and Shirley (1978), with some more recent results. This table includes all the stable isotopes, together with a small number of radioactive isotopes (data for some other radioactive isotopes can be found in the original table). These results have been obtained over the last 50 years, with increasing accuracy. A brief historical account of optical and magnetic resonance measurements is presented in the following sections.

1.2. *Optical measurements*

Before the advent of magnetic resonance spectroscopy, nuclear spins and moments were determined almost entirely by optical spectroscopy. When a hyperfine multiplet is observed with good resolution, the value of the nuclear spin I is obtained immediately from the multiplicity, provided that $I < J$. In practice, the resolution has proved to be adequate for the stable isotopes of odd Z, that are all odd-proton isotopes: ^{141}Pr, ^{159}Tb, ^{165}Ho and ^{169}Tm (each 100% abundant); ^{139}La, ^{175}Lu (abundances of 99.9% and 97.4% respectively). The only other stable odd-proton isotopes are ^{151}Eu and ^{153}Eu, with abundances of 47.9% and 52.2%.

TABLE 1

Selected best values of nuclear spins and moments from Table of Isotopes (Lederer and Shirley 1978) with some later data. In most cases the method identified applies only to measurements of magnetic moments (corrected for diamagnetic shielding). Values of the nuclear resonance frequency in MHz per tesla for the stable isotopes, uncorrected for diamagnetic shielding, are given in table 12.

	A	I	μ_I (nm)	Q (barns)	Method†
La	137(r)	$\frac{7}{2}$	+2.695(6)	+0.26(8)	O
	138	5	+3.7139(3)	+0.51(9)	NMR
	139	$\frac{7}{2}$	+2.7832(2)	+0.22(3)	NMR
Ce	141(r)	$\frac{7}{2}$	0.970(30)		EPR
Pr	141	$\frac{5}{2}$	+4.2754(5)	−0.0589(42)	OP
Nd	143	$\frac{7}{2}$	−1.065(5)	−0.484(20)	AB
			−1.088(61)		EPR
	145	$\frac{7}{2}$	−0.656(4)	−0.253(10)	AB
			−0.677(40)		ENDOR
Pm	147(r)	$\frac{7}{2}$	+2.63(10)	+0.67(18)	(Average)
Sm	147	$\frac{7}{2}$	−0.8148(7)	−0.18(3)	AB
			−0.8109(14)		ENDOR
	149	$\frac{7}{2}$	−0.6717(7)	+0.052(9)	AB
			−0.6692(11)		ENDOR
Eu	151	$\frac{5}{2}$	+3.4717(6)	+0.903*	AB
			+3.474(1)	1.12(7)	ENDOR
	153	$\frac{5}{2}$	+1.5330(6)	+2.412*	AB
			+1.534(2)	2.85(18)	ENDOR
Gd	155	$\frac{3}{2}$	−0.2591(5)	+1.30*	AB
			−0.2592(6)		ENDOR
	157	$\frac{3}{2}$	−0.3398(7)	+1.36*	AB
			−0.3396(12)		ENDOR
Tb	159	$\frac{3}{2}$	+2.014(4)	+1.432*	ENDOR
Dy	161	$\frac{5}{2}$	−0.4805(51)	+2.648*	AB
	163	$\frac{5}{2}$	+0.6726(35)	+2.57(17)	AB
Ho	165	$\frac{7}{2}$	+4.173(27)	+3.53*	AB
	166m(r)	7	+3.60(5)		NO
Er	167	$\frac{7}{2}$	−0.5665(24)	+3.565*	AB
Tm	169	$\frac{1}{2}$	−0.2316(15)		AB
	170(r)	1	0.2476(36)	0.576(9)	AB
Yb	171	$\frac{1}{2}$	+0.49367(1)		OP
	173	$\frac{5}{2}$	−0.67989(3)	+2.80(4)	OP
Lu	175	$\frac{7}{2}$	+2.23799(6)	+5.86(6)	AB
				3.46(6)	MH
	176	7	+3.139(22)	+8.0	AB

(r): Radioactive isotope.

*From Tanaka et al. (1983), claimed accuracy 1%.

†Method:

AB	Atomic beam magnetic resonance.	NMR	Nuclear magnetic resonance.
ENDOR	Electron-nuclear double resonance.	NO	Nuclear orientation.
EPR	Electron paramagnetic resonance.	O	Optical.
MH	Muon or pion hyperfine structure.	OP	Optical pumping

(Element 61, promethium, has no stable isotopes.) The elements of even Z (Ce, Nd, Sm, Gd, Dy, Er, Yb) are largely composed of even–even isotopes with $I = 0$, together with (apart from Ce) odd-neutron isotopes of 10 to 20% abundance. For these, optical spectroscopy has in general provided insufficient resolution for reliable determination even of the values of the nuclear spins.

On classical theory the orbital momentum $\boldsymbol{L}$ and the spin momentum $\boldsymbol{S}$ interact through the spin–orbit interaction $\lambda(\boldsymbol{L}\cdot\boldsymbol{S})$, and the total angular momentum $\boldsymbol{J}$ is a constant of the motion, with values of J from $|L - S|$ to $L + S$. The energy of level J in first order is given by

$$W_J = \tfrac{1}{2}\lambda[\,J(J+1) - L(L+1) - S(S+1)], \tag{1}$$

so that the energy separation between $J - 1$ and J is just λJ. The orbital momentum $\boldsymbol{L}$ is associated with a magnetic moment $\mu_B\boldsymbol{L}$, and the spin momentum $\boldsymbol{S}$ with $2\mu_B\boldsymbol{S}$; in a magnetic field $\boldsymbol{B}$ the Zeeman energy $Z = \mu_B\boldsymbol{B}\cdot(\boldsymbol{L} + 2\boldsymbol{S})$ is equivalent to $g_J\mu_B(\boldsymbol{B}\cdot\boldsymbol{J})$, where

$$g_J = \tfrac{3}{2} + [S(S+1) - L(L+1)]/2J(J+1). \tag{2}$$

There are a number of corrections to this formula, the most important arising from the interaction of the electron with the fluctuations of the radiation field. This has the effect of giving the spin a moment $g_S\mu_B S$, where $g_S = 2.00232$, so that the value of g_J becomes

$$g_J = \tfrac{1}{2}(g_S + 1) + [(g_S - 1)S(S+1) - L(L+1)]/2J(J+1). \tag{3}$$

In general we shall consider only the ground multiplets of the lanthanide atoms and trivalent ions. The configurations contain a number of closed atomic shells: 1s, 2s2p, 3s3p3d, 4s4p4d, 5s5p6s, only the partly filled 4f shell has non-zero values of L, S and J, apart from the following atoms: lanthanum, cerium, gadolinium and lutetium have one electron in the 5d shell. The configurations are listed in table 2, together with the values of L, S, and the value of J for the lowest level of the trivalent ions. For the light lanthanides the level with $|L - S|$ has the lowest energy, while that with $L + S$ is the ground state for the heavy lanthanides, because the sign of the spin–orbit interaction is positive in the first half of the shell and negative in the second half. Table 2 also lists the value of g_J for the lowest level J of the trivalent ion (Judd and Lindgren 1961).

If the atom has an isotope with a nuclear spin I, the hyperfine interaction $A_J(\boldsymbol{J}\cdot\boldsymbol{I})$ produces a manifold of states with quantum numbers F ranging from $|J - I|$ to $J + I$, and energy W_F given by

$$W_F = \tfrac{1}{2}A_J[F(F+1) - I(I+1) - J(J+1)]. \tag{4}$$

This gives a multiplet with a maximum of $2J$ or $2I$ levels, whichever is the smaller. The value of I is obtained immediately from the multiplicity in a state for which $J > I$.

The values of the nuclear magnetic moments are much more difficult to determine

TABLE 2

Values of n, the number of electrons in the 4f shell, for atoms and trivalent ions. For some atoms, one electron has lower energy in the 5d shell, as shown (the other 2 electrons fill the 6s shell). For the trivalent ions, the values of L, S and J are given, together with values of g_J [rounded values, based on those for the atom with the same configuration, from Judd and Lindgren (1961)]. Only the ground manifolds are included.

	Atom	Trivalent ion				
	n	n	L	S	J	g_J
La	0(+5d)	0	0	0	0	
Ce	1(+5d)	1	3	$\frac{1}{2}$	$\frac{5}{2}$	0.856
Pr	3	2	5	1	4	0.805
Nd	4	3	6	$\frac{3}{2}$	$\frac{9}{2}$	0.731
Pm	5	4	6	2	4	0.603
Sm	6	5	5	$\frac{5}{2}$	$\frac{5}{2}$	0.293
Eu	7	6	3	3	0	
Gd	7(+5d)	7	0	$\frac{7}{2}$	$\frac{7}{2}$	1.992
Tb	9	8	3	3	6	1.492
Dy	10	9	5	$\frac{5}{2}$	$\frac{15}{2}$	1.323
Ho	11	10	6	2	8	1.242
Er	12	11	6	$\frac{3}{2}$	$\frac{15}{2}$	1.195
Tm	13	12	5	1	6	1.164
Yb	14	13	3	$\frac{1}{2}$	6	1.141
Lu	14(+5d)	14	0	0	0	

precisely because they involve the measurement of the overall splitting of the multiplet. Even when the multiplet is reasonably well resolved, there is the further problem that the magnitude of A_J and hence of the splitting depends on both the nuclear moment and on $\langle r^{-3} \rangle$, the mean inverse cube of the distance of the electron from the nucleus. Calculation of a reliable value for the magnitude of $\langle r^{-3} \rangle$ has proved to be a long-standing difficulty. This is true also for electron paramagnetic resonance (EPR) measurements (see sections 2.3 and 10.1), although the much higher resolution has made it possible to determine unequivocally the nuclear spins of all the stable odd-neutron isotopes during the years 1950 to 1960.

For the majority of atoms in the periodic table, the most accurate values of the nuclear magnetic moments of the stable isotopes have been determined by nuclear magnetic resonance (NMR), using aqueous solutions of a suitable diamagnetic compound. A small 'diamagnetic correction', ranging from 0.78% for La to 1.22% for Lu, is needed for the local magnetic field set up by the precession of the electron moments in the closed shells. However, the entries in table 1 show that only for the two stable isotopes of lanthanum has this been the most accurate method used. The reason is that diamagnetic compounds do not exist as the ground state in any normal valency of the other lanthanides, apart from the last two, ytterbium and lutetium. The presence of electrons in the partly filled 4f shell sets up a hyperfine magnetic field at the nucleus of order 100 to 800 T, much greater than any external

field. The resulting hyperfine frequencies have been determined most accurately by magnetic resonance in atomic beams of free atoms (AB), or by EPR in solids. The magnetic moments themselves come from more complicated resonance methods, involving the measurement of the change in the resonance frequency associated with an external field. These methods are atomic beam triple resonance (section 1.4), or combined electron and nuclear resonance in which the latter is detected through its effect on the intensity of the EPR spectrum (ENDOR, see section 3).

1.3. *Atomic beam measurements*

The accuracy obtained by the use of beams of atoms, combined with magnetic resonance, is enormously greater than that available from optical experiments prior to the advent of the laser. [Measurements using laser hole-burning techniques on solids will be considered in section 9.3.] In a typical experiment (see fig. 1), a beam of atoms issuing from a hot source (an 'oven') traverses three regions of magnetic field before reaching a detector. In two of these regions, the A- and B-magnets, the fields are inhomogeneous, and exert transverse forces on the atoms through interaction with their electronic magnetic dipole moments. The field gradients have opposite directions in the two magnets, so that the transverse displacements are equal and opposite. Thus atoms continue to reach the detector, provided that they are in the same atomic sub-states in each magnet. Between the A- and B-fields there is a homogeneous magnetic field, the C-field, in which a wire loop is located. This is fed with RF current, producing an oscillatory magnetic field that induces transitions between the magnetic sub-states of the atom provided that the frequency is adjusted to resonance. Following such a transition, an atom follows a different trajectory in

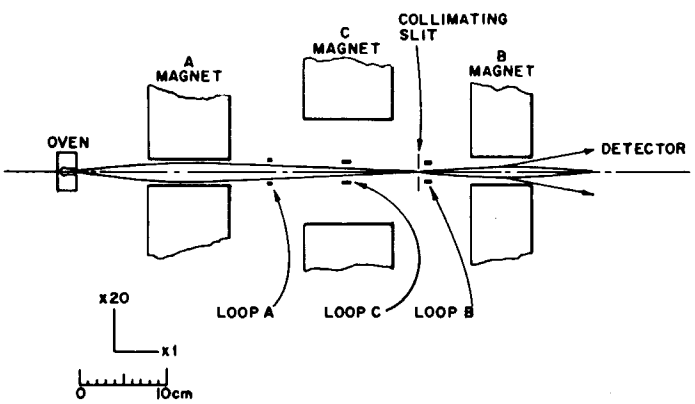

Fig. 1. Schematic diagram of a triple resonance atomic beam apparatus. Between source S (a hot oven) and detector D, magnets A and B produce inhomogeneous deflecting fields, and act as polarizer and analyzer; magnet C produces a homogeneous field in which magnetic resonance transitions occur at loops A, B and C. Resonance is detected by the deflection of atoms away from the detector D, if the gradients in magnets A and B are in opposite directions.

the B-field because it experiences a different transverse force. It is deflected away from the detector instead of back towards it, and the drop in the number of atoms reaching the detector therefore serves to detect resonance in the C-field. (This system is called 'flop-out'; an alternative arrangement, 'flop-in', allows atoms to reach the detector only if a transition has been induced in the C-field. 'Flop-in' gives a better signal/background ratio.)

The allowed transitions occur between successive electronic magnetic sub-states, at frequencies $h\nu = g_J \mu_B B$, so that precise measurements of the electronic g-factor g_J are obtained. If the nucleus has a spin, eq. (4) shows that measurements of transitions in which the quantum number F changes by unity determine the value of the magnetic hyperfine constant A_J, and that of the nuclear electric quadrupole coupling (see below). Purely nuclear transitions would change only the nuclear magnetic sub-states, and the alteration in the transverse force resulting therefrom is too small to produce appreciable changes in the path of the atoms. Nuclear g-factors cannot therefore be determined directly in such an apparatus. In general measurements are made only in the ground state of an atom, but for some lanthanides, such as samarium, low-lying excited states of the LS-multiplet have a finite population, sufficient for measurements to be made.

The accuracy of such measurements is determined by the uncertainty principle; if t is the time taken to traverse the length L of the C-field, then the linewidth $\delta\omega$ is given by $\delta\omega t \sim 1$. Greater accuracy is thus obtained by making L, and hence t, as large as possible. This is effective only if

(a) the field is accurately the same over the whole useable length of the magnet, and

(b) the RF field is uniform over the whole of this length.

To overcome this problem Ramsey (1949) introduced the method of two separate oscillatory field loops, through which the atomic beam passes at the beginning and end of the C-field. It is then only necessary for the *average* value of the C-field between the loops to be equal to the field at each of the loops, and its magnitude can be determined by proton NMR. An interference pattern is observed with resonances narrower by some 40% than with a single oscillatory field over the same length. [A classical analogy is with Michelson's two-slit stellar interferometer.]

As an example we consider the experiments of Pichanick and Woodgate (1961) in which the values of g_J were determined for the various states of the ground LS-multiplet of samarium. This has $L = S = 3$, and the values of J range from 0 to 6, the former being lowest. In fact the interval rule for the energy in eq. (1) is not obeyed exactly [see Albertson (1937) for measurements on samarium] because the spin–orbit interaction within the f^6 configuration admixes excited states ^5D, ^3F, ^5G with the same J. This has the further effect of slightly changing the values of g_J. From eq. (2), for $L = S$ the classical value of g_J should be just $\frac{3}{2}$ for all values of J, while from eq. (3) it becomes $\frac{1}{2}(g_S + 1) = 1.50116$. There are further effects from relativistic and diamagnetic corrections (Judd and Lindgren 1961). With these taken into account, the calculated values agree (within 0.00012 or better) with the measured values, ranging from 1.49840(5) for $J = 1$ to 1.49419(10) for $J = 6$. Later work by Robertson et al. (1968) and Childs and Goodman (1972) has extended both

the experiments and the calculations; their measured values of g_J agree with Pichanick and Woodgate to better than 0.00002, and their calculated values within 0.00003.

1.4. *Atomic beam – triple resonance*

In section 1.2 it was mentioned that conventional atomic beam methods did not permit a direct determination of the nuclear magnetic moment; the deflection of the atoms resulting from a change just in the orientation of the nuclear moment is too small. This difficulty was overcome by an ingenious improvement introduced by Woodgate and Sandars (1958) and independently by Brink and Nierenberg (1958). In the centre of the C-field magnet (see fig. 1), a third loop C produces an RF field of which the frequency is adjusted to induce resonance transitions in which the nuclear magnetic quantum number m_I changes by one unit. The atom is then no longer in the same quantum state as when it left loop A, so that on arriving at loop B this cannot induce the electronic resonance transition necessary to deflect it back to the detector. The effect of the steady magnetic field B on the nuclear magnetic frequency in loop C thus provides a direct determination of both the magnitude and sign of the nuclear magnetic moment. In practice the highest accuracy is obtained by working at a field stength where the presence of terms in B^2 make the resonance frequency field-independent in first order, thereby reducing the effects of field inhomogeneity. This has the further advantage that the ratio g_I/g_J is determined without needing to measure B.

This technique has been used to determine directly the nuclear magnetic moments of all the stable lanthanide isotopes, and comparison with the measured values of the magnetic hfs constant gives the parameter $\langle r^{-3}\rangle$. The high accuracy of such atomic beam measurements requires that the theory of hyperfine structure be refined by a relativistic treatment (Sandars and Beck 1965); although this was presented in terms of single-electron operators, it has been formulated in similar terms using the angular momenta $\boldsymbol{L}$ and $\boldsymbol{S}$ (Woodgate 1966). The magnetic hyperfine energy $A_J(\boldsymbol{J}\cdot\boldsymbol{I})$ can be represented as an interaction $-g_I\mu_B(\boldsymbol{I}\cdot\boldsymbol{B}_e)$, where $\boldsymbol{B}_e$ is the hyperfine magnetic field, to which there are three contributions:

(1) the magnetic field generated by the orbital motions of the electrons, given by

$$(\mu_0/4\pi)2\mu_B\boldsymbol{L}\langle r^{-3}\rangle_{orb}, \tag{5}$$

(2) the magnetic field set up by the electronic spin moments

$$-(\mu_0/4\pi)2\mu_B[\boldsymbol{S}-3\boldsymbol{r}(\boldsymbol{S}\cdot\boldsymbol{r})/r^2]\langle r^{-3}\rangle_{dip}, \tag{6}$$

(3) relativistic and 'core polarization' fields that can be written in terms of a third parameter $\langle r^{-3}\rangle_c$ as

$$(\mu_0/4\pi)2\mu_B\,\boldsymbol{S}\langle r^{-3}\rangle_c. \tag{7}$$

Parallel to these three parameters for the magnetic dipole interaction, there are also three for the electric quadrupole interaction, that we shall not discuss. We remark only that on previous theory the values of $\langle r^{-3}\rangle$ in eqs. (5), (6) should be equal; the

third would be ascribed to 'core polarization'. This produces a 'contact' term from a slight unbalancing of the magnetic fields of each pair of s-electrons, through exchange interaction with the partly filled 4f shell. The treatment of Sandars and Beck shows that there is also a relativistic contribution of the same form.

For an atom, the three magnetic contributions can only be determined separately by measurements of the hyperfine constants in states of at least three values of J, together with the nuclear magnetic moment. A prime example has been provided by studies of the samarium atom, already mentioned in the previous section. The nuclear magnetic moments of the two stable odd-neutron isotopes are given in table 1, and the hyperfine constants have been determined with high accuracy for all values of J from 1 to 6. The moments come from the classic work of Woodgate (1966), who also measured the hyperfine constants for $J = 1,2,3,4$. In addition to the simple hyperfine interaction terms $A_J(\boldsymbol{J}\cdot\boldsymbol{I})$, a number of corrections were needed, that have parallels in EPR. In Woodgate's nomenclature, these were:

(a) the field–field term, corresponding to a second-order electronic Zeeman energy (Van Vleck paramagnetism, see section 2);

(b) the field–dipole term, corresponding to the enhanced nuclear Zeeman energy (see section 8);

(c) the second-order hfs–hfs terms, of which the most important is the dipole–dipole term that has the form of a correction to the nuclear electric quadrupole interaction (cf. section 8.1).

Extension of the measurements up to $J = 6$ by Childs and Goodman (1972) has shown that the ratios of both the magnetic dipole and electric quadrupole interactions are independent of J, with ratios (147/149) equal to $+1.21305(2)$ and $-3.4601(6)$, respectively. The three magnetic hyperfine terms, eqs. (5), (6) and (7), and the three corresponding terms in the nuclear electric-quadrupole interaction were also determined. The two magnetic terms, eqs. (5), (6), differ only by 1.3%, while the third term eq. (7), is much smaller, by about a factor 0.03. It is close to the value calculated by Rosen (1969), showing that virtually all of this term is relativistic in origin, and not truly contact in nature, in agreement with the absence of any observable isotope anomaly. Similar measurements to those on samarium have been made by Childs and Goodman on a number of other lanthanide atoms; La, Nd, Tb, Dy, Er and Ho. A comprehensive list of values of g_J, A and B for various J-manifolds was given by Cheng and Childs (1985), together with theoretical calculations. Here we discuss only measurements on the europium atom, that differs in having a half-filled shell, $4f^7$.

In part the interest arises from the fact that the spectroscopic state $^8S_{7/2}$ is the same for the atom, $4f^76s^2$ as for the divalent ion, $4f^7$. The former has been studied by atomic beam triple resonance (Sandars and Woodgate 1960, Evans et al. 1965), and the latter by ENDOR (Baker and Williams 1962) in CaF_2, an environment with cubic symmetry. For a half-filled shell, with no orbital momentum and a spherical distribution of electron spin moment with zero density at the nucleus, both the magnetic dipole and electric quadrupole interactions should be zero. Experimentally, they are small compared with the values for other odd-proton lanthanide isotopes with comparable nuclear moments, for which the hyperfine

TABLE 3
Comparison of hyperfine data for the europium atom (triple atomic beam resonance) and for Eu^{2+} in CaF_2 (ENDOR).

	Eu atom	Eu^{2+} in CaF_2
g	1.9934(1)	1.9926(3)
^{151}A(total)	−20.0523(2)	−102.9069(13)
^{151}A(i.c.)	+7.70	+8
^{151}A(rel.)	(−28)	(−28)
^{151}A(c.p.)	(0)	(−83)
^{151}B	−0.7012(35)	−0.7855(52)
$^{151}(\gamma/2\pi)$	10.4860(18)	10.4927(28)
$^{151}A/^{153}A$	+2.26498	+2.25313
$^{151}B/^{153}B$	+0.393(3)	+0.387(4)
$^{151}\gamma/^{153}\gamma$	+2.26505	+2.2632(26)
Δ (%)	−0.003(20)	−0.53(2)

The values of A, B are in MHz; those of A are divided into contributions from intermediate coupling A(i.c.), relativistic A(rel.) and core polarization A(c.p.) effects. Values in parentheses are chosen to fit the measured A(total) assuming A(rel.) to be the same for atom and ion, and A(c.p.) = 0 for the atom. Δ is the hyperfine anomaly. The values of $\gamma/2\pi$ (MHz per tesla) differ slightly from those in table 12; the latter includes a correction of 1.009188 for diamagnetic shielding. The ratios of the values of B for the two isotopes agree with the more precise ratio 0.3900 (8) obtained by laser hole-burning experiments (see section 9.3).

frequencies range up to 6 GHz. There are two isotopes of mass 151 and 153, each with $I = \frac{5}{2}$, but with nuclear moments differing by a factor ~2.2. The results, summarized in table 3, show agreement (within experimental error) between the two sets of results for the nuclear magnetic moments, and the ratios of the electric quadrupole interaction constants B. For atom and ion, the values of g depart from the free-spin value by almost the same amount, resulting from a small admixture of the state $^6P_{7/2}$ through the spin–orbit interaction. For the atom this admixture gives small positive values for both the magnetic dipole and electric quadrupole hfs parameters, but relativistic effects produce contributions of negative sign. For the atom, the ratio of the values of A for the two isotopes agrees with the ratio of the nuclear magnetic moments. For the ion the ratio of the values of A is significantly different, showing the presence of a hyperfine anomaly; also, compared with the atom, the values of A are larger by a factor of about 5. The latter is mainly due to core polarization; this produces a small density of unpaired s-electron at the nucleus. The anomaly then arises from the fact that both the distribution of s-electron density and of nuclear magnetic moment are non-uniform over the nuclear volume. The size of the anomaly is close to that deduced by Bordarier et al. (1965) from the optical measurements of Müller et al. (1965). A list of hyperfine anomalies in the 4f group was given by Bleaney (1972a).

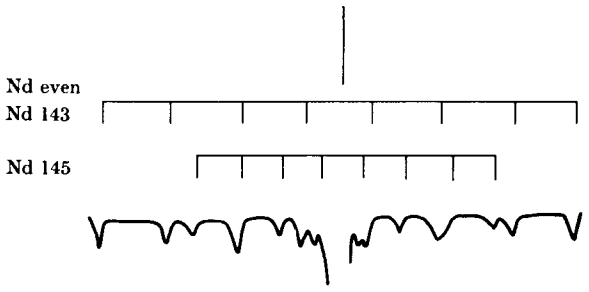

Fig. 2. Hyperfine structure of ^{143}Nd and ^{145}Nd at ca. 1% dilution in lanthanum ethylsulphate (Bleaney and Scovil 1950). Each isotope (relative abundances 12% and 8%) gives $(2I + 1) =$ lines, demonstrating that for each the nuclear spin $I = \frac{7}{2}$. From the overall widths of the structures, the ratio of the hyperfine splittings $(^{143}A/^{145}A) = 1.6087(10)$, in good agreement with the ratio 1.60860(36) for the atom from atomic beam measurements (Spalding 1963, Smith and Unsworth 1965).

2. Electron paramagnetic resonance (EPR) in insulating solids

2.1. *Introduction; first measurements*

The first electron paramagnetic resonance experiments on solids were carried out at Kazan in the USSR, by Zavoisky (1945). In Oxford an extended series of measurements on compounds of the 3d group at room temperature began in 1946, and was quickly extended to temperatures of 60–90 K and 10–20 K, and later to 1.5–4 K. In the 4f group the spectrum of a single crystal of neodymium ethylsulphate was observed in 1948 by Bleaney and Penrose (1948) and the first well-resolved lanthanide hyperfine structure (see fig. 2) was reported in a diluted crystal of this substance (Bleaney and Scovil 1950). Thereafter a systematic examination of dilute lanthanide ethylsulphates and double nitrates began in Oxford, and of the anhydrous trichlorides in Chicago by Hutchison. These have been described in some detail in Abragam and Bleaney (1970, 1986), and below we shall mainly consider other series of 4f compounds on which measurements have been made in the last two decades. However, the fact that almost the whole range of lanthanide ions, at sites of simple point symmetry C_{3h}, could be examined in the ethylsulphates was important in another way. In parallel with the experiments, the theory of the crystal-field interaction on the 4f ions was developed by Elliott and Stevens (1952, 1953), and later (for the double nitrates) by Judd (1957).

2.2. *Crystal-field theory*

In any dilute magnetic compound, the paramagnetic ion is surrounded by a matrix of diamagnetic ions that interact with the electrons on the central ion. The simplest representation of this interaction regards the ligand ions as giving rise to an electrostatic potential V, acting on the magnetic electrons. To calculate this potential, a 'point-charge' approximation may be used, in which each ligand ion is replaced by a point charge, but in many cases the neighbours consist of molecules

such as 'waters of crystallization'. The representation of these by point charges is clearly inadequate, and the position is further complicated by overlap and covalency effects, though these are much smaller for the 4f group than for the transition groups with d-electrons. The success of the electrostatic-potential method results from the fact that it permits numerical calculations. Though the magnitudes of the various terms in the potential V cannot be calculated accurately, they can be adjusted to give the best fit to the experimental results. Furthermore, the nature of the terms is dictated by the requirement that they must conform to the local symmetry of the complex in which the paramagnetic ion is embedded.

The potential V is a sum of terms V_{kq} that can be written as either algebraic functions or spherical harmonics. Simplification results from the fact that terms of odd degree have no matrix elements within a manifold of electrons with a given value of orbital quantum number, even if the ion is not at a centre of symmetry. In addition, for 4f electrons only terms up to the sixth degree are required. The electrostatic potential modifies the orbital motion, and each term can be replaced by an 'equivalent operator' involving the orbital quantum number of each electron. In LS-coupling these can be replaced by operators involving the total angular momentum $\boldsymbol{L}$ and its components; for the 4f group, where $\boldsymbol{L}$, $\boldsymbol{S}$ are coupled by the spin–orbit interaction to a resultant angular momentum $\boldsymbol{J}$, the equivalent operators involve $\boldsymbol{J}$ and its components J_x, J_y and J_z. These may be grouped in combinations corresponding to spherical harmonics, and are tabulated in the monograph by Abragam and Bleaney (1970) and elsewhere, together with their matrix elements for all values of J up to 8, the maximum that occurs in the ground states of the 4f ions.

Experimentally, the lanthanide ethylsulphates, typical formula $R(C_2H_5SO_4)_3 \cdot 9H_2O$, have a number of advantages. Single crystals can be grown from aqueous solution for all members of the lanthanide series; their crystal structure had been determined by Ketelaar (1937), and later by Fitzwater and Rundle (1959). At the R ion the point symmetry is C_{3h}, and close to D_{3h}. In another series, the anhydrous chlorides RCl_3 have space symmetry C6 3/m (Hutchison and Wong 1958), and point symmetry C_{3h} at the R site. In each case, for magnetic purposes there is only one R ion per unit cell, and this is true also of the double nitrates, with the formula type $R_2Mg_3(NO_3)_{12} \cdot 24H_2O$. For these it was conjectured by Judd (1957) that the crystal field closely resembled that appropriate to an icosahedron; later, an X-ray study by Zalkin et al. (1963) confirmed that the R ion is surrounded by twelve oxygen ions at the apices of a somewhat irregular icosahedron. For each of these series the crystal potential contains terms with $k,q = 2,0$; 4,0; 6,0 and 6,6, but in the double nitrates (symmetry D_{3v}) terms with 4,3 and 6,3 are also present.

For the ethylsulphates, with only four independent terms, the equivalent crystal-field operators were derived by Elliott and Stevens (1952) and used by them to interpret the magnetic resonance results (Elliott and Stevens 1953). Only minor modifications of the numerical coefficients of the terms V_{kq} were needed to give a reasonable fit for each member of the series. Some further interactions are required, however, for two cerium compounds. In the hexagonal crystal field of the ethylsulphate, the energy levels of the ground manifold $J = \frac{5}{2}$ are split into three

doublets, the lowest being $|\pm 5/2\rangle$, with $|\pm 1/2\rangle$ at 6.6(1) K and $|\pm 3/2\rangle$ at about 180 K (Cooke et al. 1955). Measurements of the heat capacity at liquid-helium temperatures (Meyer and Smith 1959) showed that the shape of the anomaly did not correspond exactly to a Schottky anomaly. At low temperatures the tail agreed with that calculated for an excited doublet at 6.6 K, but there was excess heat capacity at the maximum. Fletcher and Sheard (1971) were able to account for this by assuming that interactions with the phonons caused the splitting between the two lowest doublets to vary linearly with the lattice strain. This modifies both the Schottky anomaly and the heat capacity of the lattice; with a suitable choice of parameters, a good fit was obtained to the measurements of Meyer and Smith. Confirmation of this theory was obtained later by Taylor et al. (1977) from measurements of the electric susceptibility, which depends sensitively on the energy separation between the two doublets. These levels resemble those in $DyVO_4$, and the mean-field theory developed for the Jahn–Teller effect (see section 6.2) was shown to give the same variation of the splitting as that obtained by Fletcher and Sheard. The electric dipole moment of the cerium ion in this compound was found to be 4.8×10^{-31} C m.

Interaction with the phonons also affects the g-values of the doublets. For the lowest doublet, EPR gives the values 3.80 (parallel) and 0.22 (perpendicular), instead of the expected values of $5g_J = \frac{30}{7}$ and zero. This is attributed to a small crystal-field term of trigonal symmetry, dynamic rather than static in nature (Birgeneau 1967). This was the first clear-cut example of such dynamic effects, first discussed by Inoue (1963). Another is provided by Ce^{3+} in $LaCl_3$, where Bagguley and Vella-Colleiro (1969) measured the crystal-field energies and g-values for all three doublets of $J = \frac{5}{2}$ and all four of $J = \frac{7}{2}$. This was achieved by observing the near infra-red spectrum in the region ~ 21110–$23000\ \text{cm}^{-1}$, in pulsed magnetic fields up to 25 T. The ground doublet and the second excited doublet of $J = \frac{7}{2}$ were found to have g-values different from simple static crystal-field theory, but corrections for dynamic effects appear to be of the right size to account for the discrepancies.

As for the hexagonal symmetry just discussed, a particular advantage of high symmetry is that the number of independent terms in V is small. For cubic symmetry (see section 2.6) there are only two, and for tetragonal symmetry (section 2.5) there are five. The former, exemplified by R ions in CaF_2, is discussed in *Crystals with the Fluorite Structure*, edited by Hayes (1974). Crystals with the zircon structure, formulae RVO_4, RPO_4 and $RAsO_4$, together with the series $LiRF_4$, possess tetragonal symmetry, in most cases only for the heavier lanthanides. Results for the vanadates, the series most extensively studied, are discussed in section 2.5.

2.3. *Electron paramagnetic resonance (EPR)*

The primary effect of the crystal field on any manifold of levels of a 4f ion is to raise the $2J + 1$ degeneracy, giving a set of levels with an overall splitting of a few hundred wave-numbers. If the ion has an odd number of electrons, then by Kramers theorem a two-fold degeneracy must remain in each level, but for a non-Kramers ion there is no such restriction. All the degeneracy may be lifted by a field of low

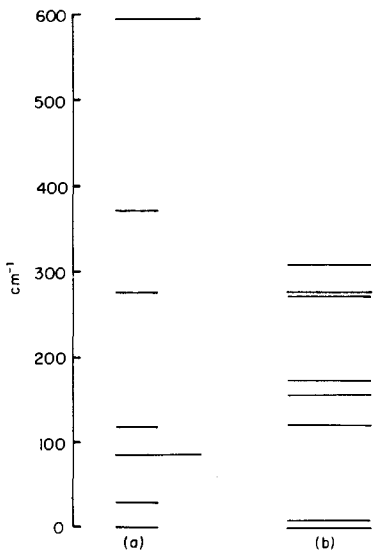

Fig. 3. (a) Energy levels of $PrVO_4$, calculated by Bleaney et al. (1978a), from enhanced NMR measurements (cf. section 8). The manifold $J = 4$ is split into 5 singlets (short lines) and 2 non-Kramers doublets (long lines). (b) Energy levels of $DyVO_4$. The $J = \frac{15}{2}$ manifold is split into 8 Kramers doublets. (From Ellis 1971.)

symmetry; but with higher symmetry, some degeneracy may remain. For example, in the presence of four-fold symmetry, the $2J + 1$ states split into a number of singlets and some doublets. This is illustrated in fig. 3a for the non-Kramers ion Pr^{3+}, $4f^2$, $J = 4$, in $PrVO_4$. The $2J + 1 = 9$ states are split into two doublets and five singlets. For the Kramers ion Dy^{3+}, $4f^9$, the ground state with $J = \frac{15}{2}$ is split into eight Kramers doublets (see fig. 3b). In general the separation between successive levels is so large ($\sim 10\,cm^{-1}$ or more), that EPR (typical frequencies $\sim 1\,cm^{-1}$ or less) can be observed only within each doublet. The behaviour of the resonance spectrum, usually highly anisotropic, can be described by a 'spin Hamiltonian' with relatively few parameters.

It is natural to treat a doublet as having 'effective spin' $S = \frac{1}{2}$, and introduce the effect of anisotropy by allowing g to become a 'tensor'. [The extent to which g is a true tensor is discussed in section 15.6 of the monograph by Abragam and Bleaney (1970)]. This gives an effective spin Hamiltonian

$$\mathcal{H} = \mu_B(\boldsymbol{S} \cdot \boldsymbol{g} \cdot \boldsymbol{B}). \tag{8}$$

The principal axes of the $\boldsymbol{g}$-tensor are dictated by the nature of the crystal field, and, when referred to the principal axes (x, y, z), the Hamiltonian can be written as

$$\mathcal{H} = \mu_B(g_x S_x B_x + g_y S_y B_y + g_z S_z B_z). \tag{9}$$

For a direction of B given by direction cosines (l, m, n) with respect to the axes (x, y, z), the energies of the two states are $W = \pm\frac{1}{2} g \mu_B B$, where

$$g^2 = [l^2 g_x^2 + m^2 g_y^2 + n^2 g_z^2]. \tag{10}$$

For axial symmetry about the z-axis, this reduces to

$$g^2 = [g_z^2 \cos^2\theta + g_{x,y}^2 \sin^2\theta], \tag{11}$$

where θ is the angle between B and the z-axis. A magnetic resonance transition occurs at a frequency ν given by

$$h\nu = g\mu_B B, \tag{12}$$

with maximum intensity when the RF magnetic field lies in a plane normal to the steady field B; the presence of anisotropy means that a particular direction in this plane may be the optimum.

Magnetic hyperfine interactions, given by $A_j(\boldsymbol{J}\cdot\boldsymbol{I})$ for a free ion, are represented for each doublet by terms such as

$$A_x S_x I_x + A_y S_y I_y + A_z S_z I_z. \tag{13}$$

On the assumption that only interactions within the ground manifold J need be included, the relation

$$A_x/g_x = A_y/g_y = A_z/g_z = A_j/g_j \tag{14}$$

should hold. Experimentally, departure from this relation shows that some admixture of the next J-manifold is present through effects of the crystal field. Such effects are largest for $4f^5$ Sm^{3+}, for which the first excited manifold with $J = \frac{7}{2}$ lies not much above $J = \frac{5}{2}$. An important result of the relation in eq. (14) is that fairly precise values of the magnetic hyperfine constant A_j for the free ion may be derived from EPR measurements, after allowing for admixtures of other J-manifolds (see Bleaney 1963, 1972a). Such values have proved useful for comparison with measurements of hyperfine interactions in the lanthanide metals.

Effects of the nuclear electric quadrupole (NEQ) interaction are smaller than those of the magnetic hfs; with axial symmetry they can be represented by a term

$$P[I_z^2 - \tfrac{1}{3}I(I+1)]. \tag{15}$$

For a Kramers doublet the strongly allowed transitions are those in which the nuclear magnetic quantum number does not change. The frequency at which the transition occurs is not altered by the presence of the term given by eq. (14), because the value of P is the same for each component of the doublet. However, in the presence of anisotropy, transitions in which the nuclear magnetic quantum number changes by ± 1 or ± 2 may be weakly allowed; if these are observable, they provide additional information from which the value of P may be derived.

As mentioned in section 1.2, the hyperfine structure is much better resolved in EPR than in optical spectra; the first example, the spectra of the two Nd isotopes of mass 143 and 145, is shown in fig. 2. Those of odd-neutron isotopes of other trivalent ions of Sm, Dy, Er and Yb followed soon afterwards, together with the odd-proton nuclei of Pr, Tb, Ho and Tm. Calculation of the nuclear moments from the hyperfine structure depended on estimates of the value of $\langle r^{-3}\rangle$; these have improved steadily through various modifications of the theory (see section 10.1). It was found also that the magnetic hyperfine constants of the $4f^7$ ions Eu^{2+}, Gd^{3+}, Tb^{4+}, though small, were not zero, as they should be for pure $^8S_{7/2}$ states (see section 3.1).

2.4. *Non-Kramers doublets and electric fields*

The earliest EPR experiments were carried out on ions of the 3d group, nearly all with Kramers degeneracy. The discovery of EPR for a non-Kramers doublet by Bleaney and Scovil (1952) occurred for a member of the 4f group, Pr^{3+} in lanthanum ethylsulphate (LaETS); it was unexpected, and required the addition of new terms to the spin Hamiltonian. Such doublets occur in a crystal field of axial symmetry, and have only one non-zero principal g-value, normally taken to lie along the z-axis. Transitions within the doublet should not be observable, since there are no off-diagonal magnetic matrix elements between the two states. However, the degeneracy is accidental, and the levels can be split by a distortion from axial symmetry. It is possible to represent the doublet by a spin Hamiltonian with effective spin $S = \frac{1}{2}$ with just the single term $g_z \mu_B S_z B_z$, together with $A_z S_z I_z$ if hyperfine structure is present. The effects of distortions are included by adding terms of the form $\Delta_x S_x + \Delta_y S_y$, where $\Delta_{x,y}$ are assumed to have random (usually Gaussian) distributions, with zero as the most probable value. Transitions are now allowed provided the RF magnetic field is along the z-axis, except that no transition is allowed for zero distortion; the line shape is therefore asymmetrical, with zero intensity at the point corresponding to eq. (12). Occasionally, such distortions are unnecessary; e.g., in a hexagonal crystal field, the six-fold terms produce matrix elements from $J_z = 0$ to the states with $J_z = +6$ and -6; these two states are thus indirectly admixed and the doublet is split. This situation occurs for the ground doublet of Tb^{3+} in LaETS (see Baker and Bleaney 1958). Transitions occur for an oscillatory magnetic field along the z-axis, with normal line shape.

It was pointed out independently by Williams (1967) and Culvahouse et al. (1967) that for a non-Kramers ion at a site lacking in full inversion symmetry, terms linear in an electric field may exist for a doublet state. Thus for C_{3h} symmetry (but not for C_{3v}) the system may have a permanent electric dipole moment, and its interaction with an electric field may be represented by additional terms of the form $g^{(E)}\mu_B(S_x E_x + S_y E_y)$. Transitions then occur with an RF electric field normal to the z-axis, even in the absence of a distortion from axial symmetry. As before, random distortions again produce an asymmetrical line shape, but with a maximum corresponding to the point for zero distortion, unlike the magnetic transitions referred to above. The asymmetry is present because in each case the distortions move the transitions to higher frequency at constant applied field, or to lower field at constant frequency. Such electric dipole moments also give rise to electric interactions between the ions (see section 5.6).

2.5. *The lanthanide vanadates*

The vanadates, together with the heavier phosphates and arsenates of the lanthanide ions, form one of the few examples of series with tetragonal symmetry both in the crystal and at the Ln ion. Of the considerable corpus of EPR measurements on the lanthanide ions, only those for the vanadates in the host lattice YVO_4 are included here. Table 4 gives the g-values and the magnetic hyperfine

TABLE 4

EPR data for the Kramers doublets in the lanthanide vanadates, measured at ~1% (or less) dilution in YVO_4. The g-values and the magnetic hyperfine constants A are given, the latter with errors where known. In general, the errors in the g-values are about 1 to 5 in the last figure.

Ion	g-values		Mass	I	A-values (MHz)	
	$g_\parallel$	$g_\perp$			$A_\parallel$	$A_\perp$
Nd	0.915	2.348	143	$\frac{7}{2}$	358(1)	777(3)
			145	$\frac{7}{2}$	223(1)	477(1)
Sm	0.506	0.344	147	$\frac{7}{2}$	258	550
			149	$\frac{7}{2}$	223	454
Dy	1.104	9.903	161	$\frac{5}{2}$	96(3)	855(15)
			163	$\frac{5}{2}$	130(1)	1173(3)
Er	3.544	7.085	167	$\frac{7}{2}$	368(1)	747(1)
Yb	6.08	0.85	171	$\frac{1}{2}$	4822	675(36)
			173	$\frac{5}{2}$	1329(10)	186(15)

parameters, both parallel and perpendicular to the tetragonal axis, for all the trivalent Kramers ions, measured by various authors at 4.2 K. The spectrum of the trivalent Gd ion has been observed, not only in YVO_4, but also in a number of other vanadates (see section 8.6). The Tm^{3+} ion, both in $TmVO_4$ and diluted in YVO_4, has a non-Kramers doublet as its ground state, with $g_z = 10.2$ and $A_z = (-)3.45$ GHz (Schwab and Hillmer 1975). The trivalent ions of Pr, Tb and Ho, and, of course, Eu, have singlet ground state ($HoVO_4$ is discussed in section 8).

2.6. *Lanthanide ions in cubic symmetry*

The EPR and other spectra have been observed for lanthanide ions on sites with cubic symmetry in a number of crystals such as MgO, CaO (six-fold coordination), and CaF_2, SrF_2, BaF_2, ThO_2 (eight-fold coordination). The manner in which a manifold of given J is split is readily found from group theory: for $J < 2$, no splitting; half-integral values of J give doublets (Γ_6 and Γ_7), and quartets (Γ_8); integral values give singlets (Γ_1 and Γ_2), doublets (Γ_3) and triplets (Γ_4 and Γ_5). When a given representation occurs only once, the wave-functions are uniquely determined from symmetry alone, but if they occur twice they depend on an additional parameter x (and are tabulated by Lea et al. 1962). For the Kramers doublets Γ_6, Γ_7 both the g-values and the magnetic hfs are isotropic, and the nuclear electric quadrupole coupling (NEQ) is zero. The Γ_8 quartets can be represented by a spin Hamiltonian with $S = \frac{3}{2}$, but the Zeeman and magnetic hfs are not isotropic, and an NEQ interaction may also be present; in each case two parameters are needed. The triplets Γ_4, Γ_5 can be represented using $S = 1$; the g-value and magnetic hyperfine parameters are each isotropic, but again two NEQ parameters are needed. The non-Kramers doublet Γ_3 has only a second-order Zeeman effect in small fields. Many of these features are special to the 4f and 5f groups because of their high values of J.

Work on the lanthanide ions in the cubic compounds listed above has been described in the monograph by Abragam and Bleaney (1970) and in *Crystals With The Fluorite Structure*, edited by Hayes (1974). However, mention should be made of the first investigation of a case of cubic symmetry to require an unusual spin Hamiltonian. This was the ground quartet Γ_8 of the Er^{3+} ion in MgO (Descamps and Merle d'Aubigné 1964), for which details of the theory (Ayant et al. 1962) are set out in the monograph by Abragam and Bleaney (1970). This quartet manifold has attracted considerable attention because it provides the opportunity of measuring several electronic transitions, and their variation in frequency with the direction of the applied magnetic field relative to the cubic axes. A drawback is that the line-widths are often increased by strain broadening, but Baker and Wood (1980) found that for $CaF_2:Nd^{3+}$ they can be reduced by the use of well annealed crystals. EPR measurements gave g-values accurate to 1 to 2 parts per 1000; however, exact agreement with theory could not be obtained, even with the inclusion of an orbital reduction factor and admixtures from states of excited J.

Another set of cubic compounds are the elpasolites which have the typical formula Cs_2NaRCl_6, in which the lanthanide ion is six-coordinated to the chlorine ions. EPR measurements on trivalent ions of Ce, Dy, Yb and Er in Cs_2NaYCl_6 (Schwartz and Hill 1974, O'Connor et al. 1977) have confirmed the presence of cubic symmetry, but for a number of other ions, and for some undiluted compounds, phase transitions have been observed at temperatures of 100 to 160 K. EPR measurements (Bleaney et al. 1982b) on the compounds with Pr^{3+}, Tb^{3+} and Tm^{3+}, indicate the presence at low temperatures of cubic symmetry with a small tetragonal distortion.

In this series, and the analogous fluorides, an unusual case is the occurrence of a Γ_3 doublet as the ground state. For the configuration $4f^{10}$, such a state, accompanied by low lying excited states, was first investigated for Dy^{2+} in CaF_2 by Kiss et al. (1965), and Mergerian et al. (1967). Later measurements on $Cs_2NaHoCl_6$ have shown that the lowest level of the Ho^{3+} ion, $J = 8$, split by the octahedral field, is also a Γ_3 doublet. Because of the large hyperfine structure of ^{165}Ho ($I = \frac{7}{2}$), there is a strong enhanced NMR spectrum (see section 8.4). Although the Γ_3 doublet is called 'non-magnetic', this is true only in small applied fields, and an unusual EPR spectrum is also observed (Bleaney et al. 1981a). This is anisotropic, but with overall cubic symmetry. The line-width is large, and no hyperfine structure is resolved; the experiments suggest that rapidly fluctuating strain fields are present. The EPR spectra of the trivalent ions of Gd, Dy, Er and Yb, present as impurities, are also observed, with cubic symmetry.

3. ENDOR

3.1. *The ENDOR technique*

ENDOR is an acronym for Electron–Nuclear Double Resonance, a technique introduced by Feher (1956). It makes possible the detection of a nuclear magnetic resonance (NMR) transition indirectly, through its effect on an EPR signal, thus

taking advantage of the much higher intensity associated with the latter. It requires a low temperature, such that the spin–lattice relaxation mechanism (see section 4) is relatively slow. This mechanism tends to maintain the populations of the two electronic states involved in a magnetic transition at their thermal equilibrium values, and it is necessary to increase the rate at which EPR transitions are induced until it competes with the spin–lattice relaxation rate sufficiently that thermal equilibrium is disturbed; that is, the EPR transition is partially 'saturated'. Under these conditions, application of power at a frequency appropriate to an NMR transition within one of the electronic levels removes some of the ions to another hyperfine level, thus altering the signal intensity in the EPR transition. Observation of this change provides a mechanism for detecting indirectly that a nuclear transition has occurred.

A good illustration of the ENDOR technique is provided by the measurements of Baker and Williams (1962) on the Eu^{2+} ion in CaF_2. This ion has the ground state $4f^7\,{}^8S_{7/2}$, similar to that of the Eu atom (see section 1.4); because of the cubic symmetry in CaF_2, the same hyperfine Hamiltonian can be used for atom and for ion. Observation of nuclear transitions by ENDOR measures both the magnetic dipole and electric quadrupole interactions, together with the nuclear Zeeman interaction. Thus the information obtained is similar to that from atomic beam triple resonance experiments on the atom; both are listed in table 3 (see section 1.4). The comparison is of additional interest because the two europium isotopes of mass 151 and 153, though each has the same nuclear spin $I = \frac{5}{2}$, possess different nuclear moments. The magnetic dipole moment is larger by a factor of 2.26 for isotope 151, but the nuclear quadrupole moment is smaller by a factor 0.39 (see table 3). Thus the distribution of nuclear magnetism and the shape of the nucleus are each quite different; the former is confirmed by the presence, for the ion, of a 'hyperfine anomaly'. For the atom, the relatively small magnetic hyperfine interaction is associated with intermediate coupling and relativistic effects; these produce no 'hyperfine anomaly': that is, the ratio of the magnetic hyperfine constants for the two isotopes is essentially the same as the ratio of the values of μ_I/I. The position is different for the ion, where the major contribution to the magnetic hyperfine constant is assigned to a 'core polarization' effect. Essentially, this arises from exchange interaction between the half-filled 4f shell and the s-electrons; this causes each pair of electrons in an s-shell to have slightly unequal energy, and hence a different radial distribution. Although this effect is very small, the fact that s-electrons have a finite density at the nucleus means that the unbalance contributes significantly to the magnetic hyperfine interaction. It also explores the distribution of nuclear magnetism, and thus the presence of some unpaired s-electron spin density at the nucleus gives rise to a hyperfine anomaly if the distribution of nuclear magnetism is different for different isotopes.

3.2. *Corrections to the nuclear interactions*

The divalent europium ion just discussed has a half-filled shell, and all excited states lie high in energy. Correction terms from matrix elements to these terms from

the ground state are negligible. The situation is very different for an ion such as Sm^{3+}, $4f^5\,{}^6H_{5/2}$. Not only is the separation between the ground manifold $J=\frac{5}{2}$ and $J=\frac{7}{2}$ of order $1000\,cm^{-1}$, but the crystal field splits the $J=\frac{5}{2}$ manifold into three Kramers doublets with separations only of order $50\,cm^{-1}$. Between such levels there are cross terms, both of the electronic Zeeman interaction and of the magnetic hyperfine interaction (Baker and Bleaney 1958). These are the same as those discussed in section 1.4, but are anisotropic (see also section 8.1). One is similar in nature to the nuclear Zeeman interaction, that thus becomes a tensor of the form $-\mu_n(\boldsymbol{B}\cdot\boldsymbol{g}_n\cdot\boldsymbol{I})$; there are also contributions to the magnetic hyperfine and electric quadrupole interactions. Corrections for these must be included in order to deduce the value of the true nuclear Zeeman interaction arising from the applied field, and of the true hyperfine interactions. This is possible only from measurements of the excited levels, and knowledge of their wave functions. ENDOR experiments on a compound of Sm^{3+} are presented as an example, since the results may be compared with those on the Sm atom already discussed in section 1.4.

Detailed ENDOR measurements have been made by Chan and Hutchison (1972) on $LaCl_3$ doped with samarium, enhanced in the two odd-neutron isotopes 147, 149 (both $I=\frac{7}{2}$). The energies of the two low-lying doublet levels of $J=\frac{5}{2}$, split by the crystal field, as well as the splitting of the $J=\frac{7}{2}$ manifold, have been determined by optical spectroscopy (Varsanyi and Dieke 1961, Magno and Dieke 1962). Also, the size of the J-mixing (Axe and Dieke 1962) was evaluated from these measurements. The ENDOR experiments determine the net hyperfine interactions in the lowest doublet, together with the effective nuclear Zeeman interaction, the tensor $-\mu_n(\boldsymbol{B}\cdot\boldsymbol{g}_n\cdot\boldsymbol{I})$. For the isotope 147, the values of g_n are found to be 0.2036 (parallel) and 0.5911 (perpendicular) to the unique crystal axis, while the true value is deduced to be 0.2296(5). This is somewhat more accurate than that obtained by atomic beam measurements (Woodgate 1966), but within the standard deviation of the latter. The correction in the perpendicular direction is different in sign from that of the parallel direction, and makes the measured value larger by a factor ~ 2.6 than the true value. Overall, the precision is a tribute to the accuracy both of the experiments and of the detailed work involved in evaluating the corrections.

Effects on the hyperfine constants are relatively smaller in magnitude. For the magnetic hfs, the correction in the parallel direction is only $\sim 0.1\%$, but zero for the perpendicular direction. The latter was therefore used to obtain the best ratio for the two isotopes 147/149 of the magnetic hyperfine constants. The result, 1.21337(3), is more accurate than the atomic beam result 1.2130(3), but the close agreement indicates that any hyperfine anomaly is very small, as would be expected from the fact that the magnetic hfs comes overwhelmingly from the 4f electrons. On this basis, the ratio of the magnetic hyperfine constants should be equal to that of the nuclear moments.

For the nuclear electric quadrupole interaction, the situation is rather different. Corrections similar to those just discussed, but arising from second-order terms involving the square of the magnetic hfs constants, change the value of P by about 2% for isotope 147, and 5% for 149. After these corrections, a ratio (147/149) of $-3.392(14)$ is derived, close to the atomic beam ratio of $-3.460(2)$. The negative

value shows that the two nuclei depart from spherical shape in opposite ways.

In the crystal, the true NEQ interaction contains two terms, one from the 4f electrons of the parent ion, the other from neighbouring ions in the lattice. The latter is related to the term V_{20} in the crystal field, but with a large antishielding factor $(1-\gamma_\infty)$, as first suggested by Sternheimer (1951). The electric field gradient of the 4f electrons also involves a shielding factor $(1-\sigma_2)$. The ratio of the two was deduced as $(1-\gamma_\infty)/(1-\sigma_2) = +255$, with individual values of $\gamma_\infty = -80$ and $\sigma_2 = +0.63$, respectively, in reasonable agreement with a range of theoretical estimates (see also section 10.3).

Finally, a value for $\langle r^{-3} \rangle$ was deduced from comparison of the nuclear moments and the magnetic hyperfine interaction. The result of 6.34(2) atomic units for Sm^{3+} in $LaCl_3$ is close to that for the atom.

3.3. *Transferred hyperfine interactions*

The technique of ENDOR was used by Feher (1956) in a series of comprehensive and elegant experiments on donors in silicon. The wave-function of the magnetic centre spreads out over many silicon atoms, and hyperfine interactions were measured with ^{29}Si nuclei ($I = \frac{1}{2}$) in an extended set of shells surrounding the centre. In contrast to the situation in a semiconductor, the f-electrons of a lanthanide ion in an insulating compound are highly localized near the nucleus. The interaction between these magnetic electrons and the nuclear moment of a neighbouring ion should thus be close to that between two point-dipoles. It was not until measurements were made on 4f-ions in fluoride lattices such as CaF_2, where the ^{19}F ions have large nuclear moments, that the existence of transferred hyperfine interactions was revealed by ENDOR measurements.

Many studies of such interactions have now been made, but this discussion is confined to two systems Eu^{2+} ($4f^7$) and Tm^{2+} ($4f^{13}$) in CaF_2. These ions replace Ca^{2+} ions at sites of cubic symmetry, and the bonds to the F-ions lie along the $\langle 111 \rangle$ crystal axes. Each transferred hyperfine interaction is symmetrical about this axis (taken as the parallel direction) with the form

$$A_\parallel S_z I_z + A_\perp (S_x I_x + S_y I_y). \tag{16}$$

This interaction can be resolved into an isotropic term A_s and a term A_p with the same form as a point-dipolar interaction:

$$A_\parallel = A_s + 2A_p; \qquad A_\perp = A_s - A_p. \tag{17}$$

The values of A_s, A_p for the nearest neighbour fluorine ions are given in table 5, together with A_d, the value calculated for a point-dipolar interaction. The latter is larger for the Tm ion (ground state a doublet with $g = 3.54$) than for Eu ($g = 2.00$) in the ratio of the g-values. For the non-dipolar parts of the interaction, a proper comparison requires correction for the fact that for Tm the effective spin $S = \frac{1}{2}$ for the ground doublet is not the true spin; both A_s and the non-dipolar part $(A_p - A_d)$ should be increased by a factor $\frac{7}{3}$. They are then each larger than for Eu, which is an

TABLE 5

ENDOR measurements of the transferred hyperfine interaction parameters A_s, A_p, A_d (all in MHz) for the nearest fluorine neighbours of two divalent lanthanide ions substituting for Ca^{2+} in CaF_2. The measurements on Eu^{2+} are by Baker and Hurrell (1963), and on Tm^{2+} by Bessent and Hayes (1965). Hyperfine constants for the two europium isotopes are given in table 3; for Tm^{2+} the ENDOR measurements of Bessent and Hayes give $g = (+)3.443(2)$, $A = (-)1101.376(4)$ MHz, for the single stable isotope of mass 169 ($I = \frac{1}{2}$).

		A_s	A_p	A_d
$4f^7$	Eu^{2+}	−2.23(1)	+ 4.01(1)	+5.7
$4f^{13}$	Tm^{2+}	2.584(10)	12.283(10)	+9.8

S-state ion. For fluorine ions at second nearest neighbour sites, the values of A_s are (within experimental error) zero, and A_p is close to A_d. For a review of other results for lanthanide ions in fluorite compounds, see Hayes (1974).

In contrast to these results, ENDOR has been used to determine the positions of protons in waters of crystallization, on the assumption that interaction with a nearby lanthanide ion is wholly dipolar. In single crystals of lanthanum nicotinate dihydrate, $[La(C_5H_4NCO_2)_3(H_2O)_2]_2$, doped with about 0.1% Nd, proton ENDOR spectra have been observed by Hutchison and McKay (1977). There are four protons about 0.3 nm from the Nd ion, whose distances (corrected for libration of the water molecules) are determined with a standard deviation of 0.0006 nm. Later experiments (Hutchinson and Orlowski 1980) on the same substance but with deuterons in the water of crystallization, give almost identical results, apart from a small isotope effect. Recent measurements (Field and Hutchison 1985), on the lanthanum compound with Gd instead of Nd, also give similar distances, but with rather less accuracy. Comparison with unpublished X-ray data of Glick at room temperature indicates bond length differences of order 0.004 nm.

4. Spin–lattice interactions

4.1. *Spin–lattice relaxation*

Spin–lattice relaxation is concerned with the following problem. In a solid the thermal reservoir consists of the natural vibrations of the constituent ions about their equilibrium positions, vibrations that increase in amplitude with temperature. The quantized lattice vibrations, Debye waves or phonons, travel with the velocity of sound. The paramagnetic system consists of ions carrying magnetic moments associated with electronic orbit and spin, and, more remotely, nuclei. Some mechanism of energy transfer must exist to establish thermal equilibrium between two such disparate systems.

This problem was first considered by Waller (1932), in terms of phonon

modulation of the dipole–dipole interactions. It rapidly became clear through experimental studies of oscillatory electronic susceptibilities, particularly by C.J. Gorter in the Netherlands, that only qualitative agreement existed with the general forms of Waller's predictions. For example, the relaxation time for a moderately concentrated paramagnetic compound of the 3d group, in a field of 1 T at 1 K, was predicted to be about 10^3 s, but the measured relaxation times are much shorter. Heitler and Teller (1936) suggested modulation of the crystalline electric field as a more powerful mechanism, and the theory was developed by Fierz (1938), Kronig (1939) and Van Vleck (1940).

Two processes were discussed by Waller. The first consists of a simple exchange of one quantum of energy between the phonon system and the magnetic system; it is known as the 'direct process'. The rate is proportional to the square of the quantum energy exchanged, and to the absolute temperature T, so long as the energy quantum $\ll kT$. The second process involves two phonons, such that the sum or difference (almost always the difference) of their energies is equal to the magnetic quantum (this satisfies the energy balance). This 'Raman process' is of higher order than the direct process, but it involves all the phonons rather than just the narrow band resonant with ('on speaking terms with') the magnetic system. It becomes the dominant process at higher temperatures, since it depends on the square of the energy density in the phonon system. The relaxation rate increases as T^7 in the region where $kT \ll$ the Debye energy, and then as T^2 when this inequality is reversed. Modulation of the crystalline electric field produces similar temperature dependences, except that for ions with Kramers degeneracy a magnetic field must be present to break the time-reversal properties of the spins (Van Vleck 1940). This 'Van Vleck cancellation' changes the temperature dependence of the Raman process to T^9.

The primary interaction of the crystalline electric field is with the electronic orbital motion, which is coupled with the electron spin through the spin–orbit interaction. In the lanthanide group relaxation rates to the lattice from the various levels into which the static crystalline electric field splits the J-manifold are sufficiently rapid that, except for ions with a half-filled shell, ^{8}S, magnetic resonance is unobservable except at temperatures of 20 K or lower. This was attributed to Raman processes until it was realized that, because of crystal-field splittings of order 20 to 100 K, excited levels well within the phonon spectrum were involved. A phonon of energy equal to the splitting Δ between the ground level and an excited crystal-field level can exchange a quantum with the magnetic system by a 'direct process', following which the excited state can get rid of its surplus energy by re-emission of a phonon. At low temperatures the rate for this process is simply determined by the chance of a thermal phonon of energy Δ being present, so that it follows the law

$$T_1^{-1} = A\Delta^3\{\exp - (\Delta/kT) - 1\}^{-1}, \tag{18}$$

a result first proposed by Orbach and verified experimentally for cerium magnesium nitrate by Finn et al. (1961). A similar mechanism was independently put forward by Manenkov and Prokhorov (1962).

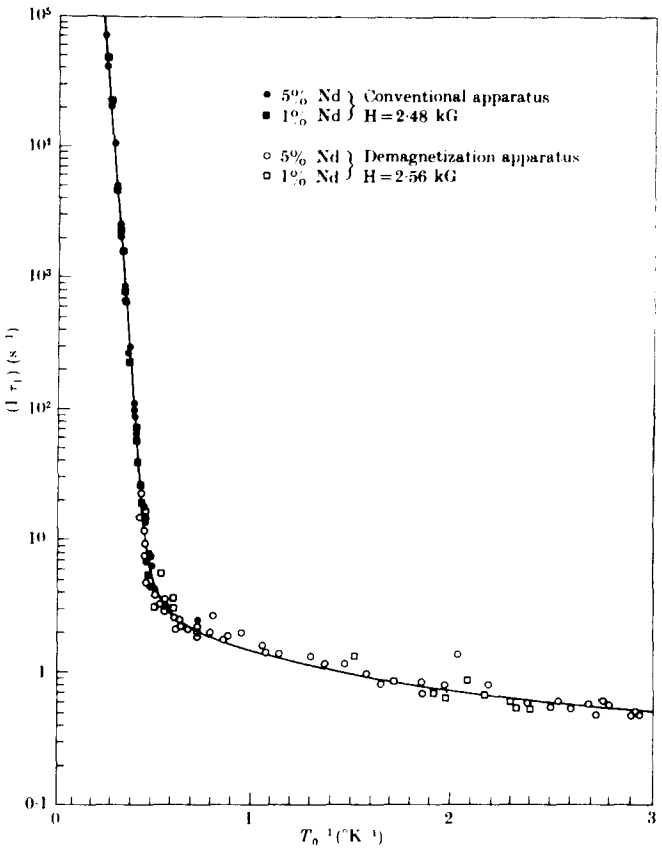

Fig. 4. Experimental results for the spin–lattice relaxation rate of Nd^{3+} ions in lanthanum magnesium nitrate (LaMN), magnetic field normal to c-axis. The data are fitted to a combination of an Orbach process, $6.3 \times 10^9 \exp(-47.6/T)$ and a direct process, $0.3 \coth(\hbar\omega/2kT)$. (After Ruby et al. 1962.)

A series of experiments was carried out by Jeffries and his colleagues at Berkeley in the following years in which spin–lattice rates were measured by observing recovery of the resonance signal after saturation in a number of dilute lanthanide compounds. These demonstrated the relative importance of the various processes, direct, Orbach and Raman, and gave quantitative results over a wide range of temperatures down to 0.3 K. At the lowest temperatures, where the magnetic quantum ($\hbar\omega$) is comparable with or greater than kT, the spin–lattice rate for the direct process varies as

$$T_1^{-1} = R(\hbar\omega)^n \coth(\hbar\omega/2kT), \tag{19}$$

where $n = 3$ for a non-Kramers ion and 5 for a Kramers ion. Experimental verification (Ruby et al. 1962) of this formula for neodymium ions in lanthanum magnesium nitrate is shown in fig. 4. At the higher temperatures the rate is dominated by an Orbach process.

The existence of yet another Raman process varying as T^5 for ions with a multiplet ground state was suggested by Orbach and Blume (1962), and verified by Chao-Yuan Huang (1965) for Eu^{2+} in CaF_2.

4.2. *Correlation with a spin–lattice Hamiltonian*

The dependence of spin–lattice relaxation rates on both frequency and temperature are accounted for satisfactorily by phenomenological theories, but attempts to estimate the *magnitudes* of the relaxation rates have in general proved to be much less satisfactory. One exception is a system studied in considerable detail, Tm^{2+} in CaF_2. For this ion the ground state left by the crystal field is an isotropic Γ_7 doublet, with (see table 5) $g = 3.443$, and a magnetic hyperfine constant $A = 1.10\,\text{GHz}$ for the single stable isotope ^{169}Tm ($I = \frac{1}{2}$). Because of the cubic symmetry, only four coupling constants are required in the orbit–lattice Hamiltonian to describe the interaction of the ground doublet with local strains. The four terms transform like the representations $\Gamma_1, \Gamma_3, \Gamma_4$ and Γ_5 of the cubic group, of which the first does not contribute to any relaxation mechanism. The same Hamiltonian, again without Γ_1, describes the effect of a local strain produced by the application of uniaxial stress. Experiments to measure the shift in the EPR line produced by such a stress were carried out by Baker and Van Ormondt (1974), who used the results to deduce spin–lattice relaxation rates. These were then compared with direct measurements of these rates (see also section 9.2) by Sabisky and Anderson (1970) and Abragam et al. (1972c). A special feature of this last paper is that it pointed out the importance of simple *rotations* of the local surroundings of the magnetic ion that had previously been neglected. These correspond to the representation Γ_4 referred to above, and have the unusual feature that the corresponding coefficient B_4 of the spin–lattice Hamiltonian is simply related to the g-value of the static spin Hamiltonian. As a result, only the parameters B_3, B_5 of Γ_3, Γ_5 remain to be determined, and they can be found from the results of uniaxial stress applied along the directions $\langle 100 \rangle$ and $\langle 111 \rangle$. For Tm^{2+} in CaF_2 the results give a value of B_4 some four times larger than B_3, while B_5 is only about one-tenth as large; for the same ion in SrF_2 all three values are much larger, with $B_4 \sim B_5$, and some 2.5 times larger than B_3. These results agree fairly well with those obtained by Abragam et al. (1972c) from observations of recovery, after a saturating pulse, of the EPR signal for the various hyperfine transitions and different directions of the applied magnetic field. Thus, for the first time, good quantitative agreement was obtained between spin–lattice relaxation rates and spin–lattice parameters measured in the static stress experiments. In further discussion, Baker and Van Ormondt conclude that a purely electrostatic model is inadequate to account for the orbit–lattice coupling, and that a model is required that includes both overlap of the wave-functions and covalency with the ligand ions.

Attempts have also been made (Baker and Currell 1976, Baker et al. 1977) to correlate measured spin–lattice relaxation rates with orbit–lattice parameters derived from EPR measurements on the systems $MgO:Er^{3+}$ and $CaF_2:Dy^{3+}$ under uniaxial stress. For these ions the ground states are Γ_8 quartets, for which a range of

parameters can be determined; in spite of the inclusion of a number of higher order effects, the agreement is less good than in the case of $CaF_2:Tm^{2+}$.

4.3. *The phonon 'bottle-neck' and 'phonon avalanche'*

A fundamental problem realised already by Van Vleck (1941) is that at low temperatures the heat capacity of the relatively few phonons 'on speaking terms' with the magnetic ions via the direct process is much smaller than that of the magnetic system, even in a magnetically dilute crystal. Even for a splitting of 30 GHz, typical of an ion with $g = 2$ in a field of 1 T, the number of resonant lattice modes is smaller by a factor of order 10^{-6} than the number of spins in an average crystal. If the spins are heated above the lattice temperature in the crystal, transfer of energy to the resonant phonons will quickly raise these to the temperature of the spin system, since each phonon must 'collide' with a spin on some 10^6 occasions for every time that a given spin collides with a phonon. Thus, in contrast to a diamagnetic crystal in which the mean free path of the phonons at liquid-helium temperatures is mainly determined by the size of the crystallites, in a paramagnetic crystal the mean free path is much smaller. The phenomenon is similar to the optical 'imprisonment of resonance radiation', and the phonons can only diffuse to the walls, greatly increasing the effective phonon–bath relaxation time. This phenomenon is known as the 'phonon bottle-neck', and the combined spin–phonon system must be treated as a strongly coupled system [see Jacobsen and Stevens (1963), Giordmaine and Nash (1965)].

In an approximate treatment, we can separate the problem into two regimes. Starting with a 'hot' magnetic system, energy is transferred to the resonant phonons with a time constant

$$T_1' = T_1/(1 + b), \tag{20}$$

where b is the ratio of the heat capacity of the spin system to that of the resonant phonons. If b is large, the temperature of the resonant phonons is quickly raised to that of the magnetic ions. The combined system then relaxes to the bath with a time constant T_b given by

$$T_b = T_1 + (1 + b)T_{ph}. \tag{21}$$

Here T_{ph} is the normal life-time of the phonons for heat transfer to the bath; it is increased by the factor $(1 + b)$, the ratio of the combined heat capacity of spins + phonons to that of the phonons alone. For large values of b the overall relaxation rate to the bath (the measured rate) should vary as $\coth^2(\hbar\omega/2kT)$, instead of the first power that occurs in eq. (19). An experimental confirmation of this result is shown in fig. 5; at the lowest temperatures the rate is found to be slower for the higher concentration of magnetic spins, because of the greater value of the parameter b.

In the experiments just described, the temperature of the spin system is initially increased by application of a short pulse of radiation at the resonance frequency, and the subsequent evolution of the population difference in the spin system is

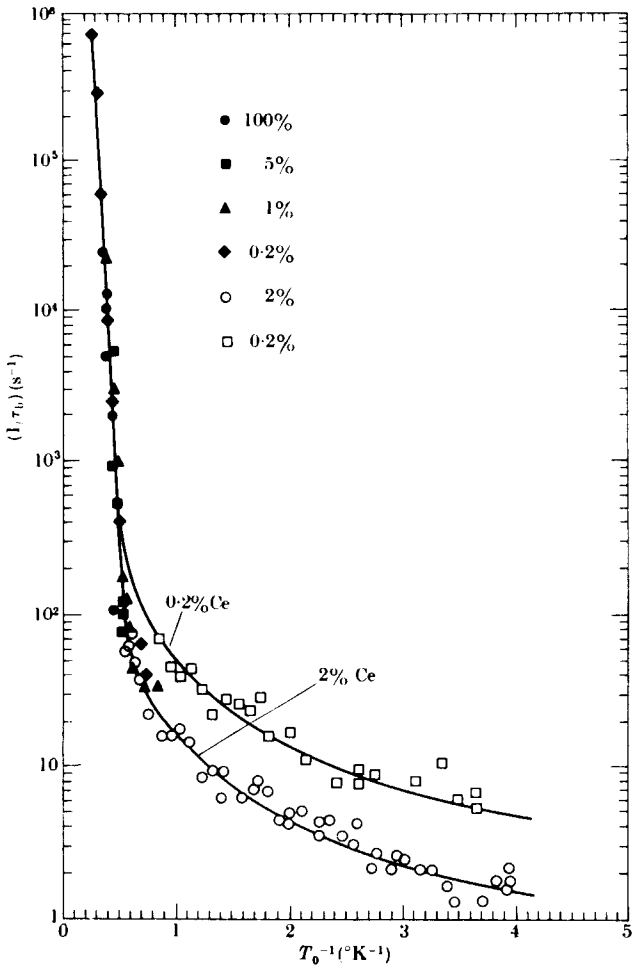

Fig. 5. The spin–bath relaxation rates for Ce^{3+} in LaMN, fitted to an Orbach process, $2.7 \times 10^9 \exp(-34/T)$, combined with R cotanh^2 $(\hbar\omega/2kT)$ at lower temperatures, where the lower rate for the higher concentration shows that it is limited by the phonon-bottleneck between spins and bath. (After Ruby et al. 1962.)

monitored by observing the resonance signal at a low applied power. It is possible to go further, and invert the populations of the two levels of the magnetic ions by application of adiabatic rapid passage or a 180° high-power pulse. The spin system is then at a 'negative temperature', and is hotter than if it were at an infinite temperature (equal population of the two magnetic levels). The phonon system has an infinite set of energy levels, for which the populations cannot be inverted to attain a 'negative temperature'. As a result, spontaneous emission of quanta from the spin system rapidly heats the resonant phonons, causing an increase in the phonon

energy density that stimulates the emission of further quanta from the spin system. The deluge rapidly becomes catastrophic, and is known as a 'phonon avalanche'.

The theory of the phenomenon has been analyzed by Brya and Wagner (1967), who also verified that experiments on single crystals of lanthanum magnesium nitrate containing ~0.2% cerium gave general confirmation of the theory. The spin resonance line at 11 GHz was inverted by adiabatic fast passage, and the resonance was then monitored at low power at a slightly different frequency. Below 2 K, the avalanche develops in a time of a few μs, and the general features of the decay curves follow predictions of the model without allowing a quantitative fit overall. Further investigations of this system were carried out by Mims and Taylor (1969, 1971) using electron spin-echo techniques at 9.1 GHz and 1.4 K to generate a signal proportional to the population difference in the spin system, following a 20 ns pulse of power 1 kW to invert the population. They found that for concentrations of cerium rising from 0.3 to 1.3% an avalanche occurred (though not at 2%), but the spectral diffusion time decreased from 130 to 1.6 μs. The avalanche life time of 7.7 to 9.5 μs was shorter than the phonon lifetime of 20(8) μs.

Optical methods have also been used (cf. section 9.2). Anderson and Sabisky (1968) generated a 'warm' band of phonons by continuous saturation of the thulium resonance at one end of a crystal of SrF_2 containing 0.02% Tm^{2+} at frequencies between 26 and 38 GHz. Diffusion of the warm phonons through the crystal was monitored at points 2 mm apart by measurements of the spin temperature, deduced from observations of the paramagnetic circular dichroism at 580 nm. The results were interpreted in terms of a phonon transmission coefficient into the helium bath ~4% at 1.3 K, and a mean free path determined by diffuse scattering from the crystal surfaces.

In such experiments information about the phonons is deduced by measurements on the spin system. With the advent of monochromatic laser sources, the technique of Brillouin scattering can be used to track phonons of definite momentum and polarization, together with the number of such phonons. Al'tshuler et al. (1971, 1972) used a helium–neon laser in experiments on cerium magnesium nitrate at 1.5 K. The resonance was saturated at 6.8 GHz, producing a phonon bottle-neck in which the effective temperature of the resonant phonons was raised to 150 K. The bandwidth was 270 MHz, of the same order as the unsaturated line width of the cerium resonance. Measurements of Brillouin scattering in $CaWO_4$ containing Nd^{3+} are described by Geschwind (1972).

5. Spin–spin interactions in insulators

5.1. *Dipolar and direct exchange interactions*

The well-known interactions between ions in insulators are the classical dipole–dipole interaction, which can be calculated exactly, and exchange interaction. The latter, in its direct form, depends on overlap of the wave functions of the two ions; it therefore falls off rapidly with distance, and is extremely difficult to calculate from

first principles. However, for ions in singlet orbital states, the form proposed by Heisenberg (1926), represented by $-J(\boldsymbol{S}\cdot\boldsymbol{S}')$, is generally assumed. For the lanthanide group, the europous ion, Eu^{2+}, has the half-filled shell $4f^7$, and its magnetic properties are close to 'spin-only'. The europium chalcogenides, with cubic symmetry, are the outstanding representatives of such simple interactions, and their properties are outlined in section 5.2.

For ions with other configurations, orbit and spin are coupled by the spin–orbit interaction, which in insulators is stronger than any inter-ionic interactions. The latter must therefore be projected onto the resultant angular momentum $\boldsymbol{J}$ for each ion, so that isotropic exchange interaction takes form $-J(\boldsymbol{J}\cdot\boldsymbol{J}')$, with a parameter equal to that for the $(\boldsymbol{S}\cdot\boldsymbol{S}')$ interaction multiplied by $(g_J-1)^2$. For the heavier members of the 4f group, this factor diminishes rapidly away from the half-filled shell, being only one-quarter as large for a pair of $4f^8$ ions ($g_J=\frac{3}{2}$) as for a pair of $4f^7$ ions. As a result, exchange interactions are in general much smaller than crystal-field splittings, and comparable with dipole–dipole interaction. For ions at sites of less than cubic symmetry, both exchange and dipolar interactions between the ground states of ions with large crystal-field splittings may be strongly anisotropic. A number of simple compounds that exemplify this are discussed in sections 5.3–5.5. Finally, after a brief outline of some properties of the garnets, a number of other types of interaction are discussed.

5.2. *The europium chalcogenides*

The discovery by Matthias et al. (1961) that EuO is a ferromagnet with transition temperature of 69 K, the first lanthanide oxide found to be ferromagnetic, set off a decade of extensive investigations of the europium chalcogenide series (also see ch. 78, section 4.3.5 of this volume). EuO, EuS, EuSe and EuTe have the simple fcc NaCl structure, in which each Eu-ion has 12 nearest Eu neighbours (nn) along $\langle 110\rangle$ directions at $a_0/\sqrt{2}$, and 6 next nearest Eu neighbours (nnn) along the $\langle 100\rangle$ four-fold axes at a_0. The values of the lattice constants a_0 in table 6 show a rapid increase in inter-ionic distance from EuO to EuTe. This table gives also the values of the transition temperatures to the magnetically ordered state, together with the

TABLE 6
Data for the europium chalcogenides (McGuire and Shafer 1964).

	a_0 (nm)	T_C/T_N	θ	Moment ($T=0$)
EuO	0.514	69(F)	76	6.80
EuS	0.596	16.5(F)	19	6.87
EuSe	0.619	7(F)	9	6.70
EuTe	0.660	7.8(AF)	−6	—

a_0 = constant of cubic unit cell.
T_C/T_N = Curie/Néel temperature (K).
θ = paramagnetic constant (K).
Saturation moment in Bohr magnetons.

'paramagnetic Curie temperature' θ (the Weiss constant) in the paramagnetic susceptibility. The last column lists the saturation moment per ion, in Bohr magnetons, extrapolated to 0 K. The saturation moments are close to the value of $7\mu_B$ appropriate to the Eu^{2+} ion, with its half-filled 4f shell, $S = \frac{7}{2}$, and spin-only magnetism ($g \sim 1.99$). For a series with simple cubic symmetry these properties suggest that the results should be amenable to exact theoretical treatments. McGuire and Shafer (1964) combined the formulae for the paramagnetic θ,

$$\theta = \tfrac{2}{3}S(S+1)(Z_1 J_1 + Z_2 J_2) = 126J_1 + 63J_2,$$

and the Curie temperature

$$T_C = \tfrac{2}{3}S(S+1)(-Z_2 J_2) = -63J_2,$$

to deduce that J_1, the simple isotropic exchange constant for interaction with the 12 nn, is positive (ferromagnetic), and decreases rapidly as the lattice constant increases. It probably arises from direct exchange, while J_2 is negative, and varies little between compounds. It was originally thought that EuSe also became a ferromagnet with $T_C = 8$ K, but the situation was later found to be considerably more complicated (see below).

Detailed and reliable measurements of the properties of this series had to await progress in the preparation of samples with good stoichiometry, and in some cases, single crystals with an accurate spherical shape. Only a brief outline of the most important magnetic properties can be included here.

The nuclear magnetic resonance (NMR) signal in EuO of the isotope ^{153}Eu ($I = \frac{5}{2}$), for which the frequency should be accurately proportional to the magnetic moment, was studied by Boyd (1967) from 2.09 to 4.17 K. The decrease with temperature in the resonance frequency from $\nu_0 = 138.7$ MHz for $T = 0$ agreed with a spin-wave calculation, and exchange constants $J_1/k = +0.759(3)$ K, $J_2/k = -0.097(4)$ K were deduced. The value of ν_0 is within 0.5% of that found by EPR for Eu^{2+} in SrO, which has almost the same lattice constant as EuO. The sensitivity of the exchange constant J_1 to the lattice parameter (see above) is confirmed by experiments of McWhan et al. (1966); under hydrostatic pressure, the volume of the unit cell of EuO decreased almost linearly, falling at 90 kilobar pressure to about 0.94 of its normal value, while the Curie temperature rose to over 120 K. At still higher pressures, Jayaraman (1972) found a sudden 4% drop in the volume at 300 kilobar, ascribed to the promotion of a 4f electron to a 5d level, with the onset of metallic conductivity; this was followed by another sharp decrease at about 400 kilobar to 0.72 of the initial volume, and transformation to a structure of the CsCl type.

In another series of experiments, Argyle et al. (1967) have compared the magneto-elastic component of the expansitivity, measured on a single crystal of EuO from 25 to 250 K, with the magnetic heat capacity above and below the Curie temperature, and find them accurately proportional to each other. They point out that this result is compatible with models proposed by Mattis and Schultz (1963), Pytte (1965), and Callen and Callen (1965). The temperature variation of the anisotropy constant K_1, determined by a static torque method by Miyata and Argyle (1967), is found to be in

good agreement with the single-ion theory of Wolf (1957), assuming a cubic crystal-field splitting within 10% of that measured by EPR for Eu^{2+} in BaO.

A similar result for the magnetic anisotropy of EuS had been found by van Molnar and Lawson (1965). More detailed results were obtained by Franzblau et al. (1967) from ferromagnetic resonance in strain-free highly polished spheres of less than 0.1 mm diameter. For a direction (l, m, n) of the magnetic moment, they found that the anisotropy energy could be represented by two terms of the form

$$K_1(l^2m^2 + m^2n^2 + n^2l^2), \qquad K_2(l^2m^2n^2),$$

with values of K_1, K_2 corresponding to crystal-field splittings of the $S = \frac{7}{2}$ manifold characterized by the constants (in units of $10^{-4}\,cm^{-1}$)

$$b_4 = +0.268(14), \qquad b_6 = -0.019(9).$$

In EuS, the NMR of both isotopes ^{151}Eu and ^{153}Eu (both $I = \frac{5}{2}$) was measured by Charap and Boyd (1964). As in EuO (see above) the frequency follows spin-wave theory, with values for ν_0 of 343.0 MHz and 151.6 MHz for the two isotopes (the ratio 2.262 is close to that for the europium ion in table 3). The most plausible values of the exchange constants,

$$J_1/k = +0.20(1)\,K, \qquad J_2/k = -0.08(2)\,K,$$

are close to those,

$$J_1/k = +0.172(19)\,K, \qquad J_2/k = -0.012(32)\,K,$$

deduced by Calloway and McCollum (1963) from the heat capacity between 1 and 4 K, again using spin-wave theory. Callen and Callen (1964) used a cluster model of pairs of interacting spins, with exchange interactions between nn and nnn, together with the values of J_1 and J_2 of Charap and Boyd, to deduce values of $T_C = 16.9\,K$, and $\theta = 17.5\,K$, both close to the experimental results in table 6. They also found a good fit to the magnetic heat capacity below T_C, but only about half the experimental value (Moruzzi and Teaney 1963) above the Curie temperature.

For EuSe, the values of J_1 and J_2 are both rather small, and there are several magnetic transitions. The value of $T_N = 5.8 \pm 1\,K$ (Pickart and Alperin 1968), was reduced to 4.55(2)K by heat capacity measurements (White and McCollum 1972), who also found small peaks at 1.7 and 2.8 K. In fields $<0.03\,T$, EuSe is an antiferromagnet with a long-wavelength structure, and zero overall magnetization; above this field it is antiferromagnetic, but with a ferromagnetic component of $2.2\,\mu_B$ per ion; at a higher critical field (again a function of temperature) of 0.1–0.3 T, it becomes ferromagnetic with the full moment of $7\mu_B$ per ion. An antiferromagnetic phase below 1.8 K, for $B < 0.5\,T$, was found by Griessen et al. (1971). The ferromagnetic phase above 0.2 T was also observed by McGuire et al. (1968); they suggested that the anisotropy is small, that the AF phase occurs because $J_2 > J_1$, but the value of θ is positive because there are 12 nn but only 6 nnn. Exchange coupling between planes is weak, and an applied magnetic field easily changes the magnetic structure. In high fields, ferromagnetic resonance (Everett and Jones 1971) has been used to determine the anisotropy constants K_1 and K_2; the results do not agree with the single-ion theory of Wolf, but this may be due to the presence of

small domains. A value of 4.6 K for T_N was found by Schwob and Vogt (1969), who also observed a metamagnetic transition to a ferrimagnetic structure below 2.5 K, strongly pressure-dependent, with a more complicated spin structure.

These authors give the value $T_N = 9.58(10)$ K for EuTe. A neutron diffraction study by Will et al. (1963) showed that the spins order in $\langle 111 \rangle$ planes, in a structure similar to that of MnO; values of $J_2/k = -0.12(1)$ K and $J_1/k = +0.025(25)$ K were deduced. This substance also becomes ferromagnetic in high fields (Busch et al. 1964). The resistivity of EuTe can vary over a wide range in different samples (Oliveira et al. 1971), resulting in changes in the magnetic properties.

5.3. *Compounds with tetragonal symmetry*

Several series of compounds with tetragonal symmetry have been studied, using single crystals grown from high-temperature flux and other methods. Co-operative behaviour at liquid-helium temperatures is shown by a number of compounds, and we consider first those with the formula $LiRF_4$, where R is one of the heavier lanthanides. The lanthanide ion is at a site of tetragonal symmetry (S_4), and the crystal-field splittings produce doublet ground states for the ions listed in table 7. The g-values have been measured by EPR for low concentrations ($\sim 1\%$) in diamagnetic $LiYF_4$, and the values for the undiluted compounds are little different. The trivalent ions of Tb and Ho are non-Kramers, and the ground doublet has a single g-value, along the tetragonal axis (the c-axis). With these large g-values, dipolar interactions outweigh the antiferromagnetic exchange interactions, and the two compounds order ferromagnetically at 2.874 and 1.527 K, respectively, with the moments along the c-axis. For the three Kramers ions Dy, Er and Yb, the value of g along the c-axis is smaller than that in the plane normal to this axis; the two former compounds order antiferromagnetically, with the Néel temperatures shown in table 7; dipolar interactions are slightly larger than exchange interactions, for which J/k is of order -0.2 to -0.3 (Beauvillain 1979). The moments lie in the plane normal to the c-axis, but the exact nature of the ordered arrangement has not been determined. A detailed study of these compounds has been made by Beauvillain (1979), whose

TABLE 7

Values of $g_{\|}$ and $g_{\perp}$ for lanthanide ions in $LiYF_4$, together with values of the Curie temperature T_C and the Néel temperature T_N for the undiluted compounds. (Based on Beauvillain 1979.) The Tm compound has a singlet ground state (see section 7.1)

	$g_{\|}$	$g_{\perp}$	T_C	T_N
Tb	17.75(10)	–	2.874	–
Dy	1.11	9.219	–	0.58
Ho	13.7	–	1.527	–
Er	3.137	8.105	–	0.38
Yb	1.331	3.917	–	–

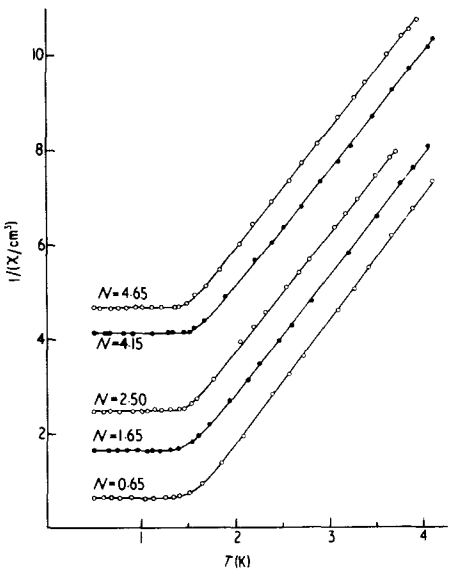

Fig. 6. Inverse χ^{-1} of the magnetic susceptibility χ of $LiHoF_4$ along the c-axis. The results for five different sample shapes show the variation with demagnetizing factor N; in each case χ^{-1} becomes constant below the Curie temperature $T_C = 1.53$ K. (Cooke et al. 1975).

thesis contains extensive references to earlier work. This includes measurements of susceptibility, heat capacity, and optical spectra; fluorine NMR; neutron diffraction. Two unusual measurements made use of far infra-red lasers for EPR at frequencies up to nearly 1000 GHz, in single crystals with spherical shape. The compounds $LiTbF_4$ and $LiHoF_4$ were found to have g-values along the c-axis of 17.8(1) and 14.1(2), respectively (Magarino et al. 1980, de Groot et al. 1971), both close to the values in table 7 measured by EPR for the diluted compounds. The value for the holmium compound agrees with an earlier result of 13.8(5) obtained from the optical spectrum (Battison et al. 1975b) with magnetic fields up to 2T, and is somewhat higher than 13.6(2), deduced from the magnetic moment by Cooke et al. (1975). The latter authors showed that below T_C the reciprocal of the susceptibility becomes a constant whose value depends on the demagnetizing factor of the sample, as shown in fig. 6.

A number of other compounds are rather similar in structure. The lanthanide vanadates, together with the phosphates and arsenates of the heavier lanthanides, have the tetragonal zircon-type structure, space group $14_1/amd$. Many of them order at liquid-helium temperatures, nearly all as antiferromagnets. The ordering temperatures are given in table 8. A number of these compounds show co-operative Jahn–Teller transitions (see section 6). Here we discuss mainly the vanadates, for which the g-values determined for the ground states of the vanadates diluted in YVO_4 are listed in table 4. They are presumably little different for the undiluted compounds.

The properties of $GdVO_4$ are well documented, starting with the magnetic and thermal measurements of Cashion et al. (1970). This compound forms an excellent example of a simple two sub-lattice antiferromagnet, the result of isotropic exchange, with the moments aligned along the c-axis, predominantly through dipolar

TABLE 8
Values of the antiferromagnetic ordering temperature (K) for the vanadates, phosphates and arsenates of the heavier lanthanides

Ion	RVO_4	RPO_4	$RAsO_4$
Gd	2.495(1)	<1	1.262
Tb		2.1	
Dy	3.066(2)	3.40	2.44
Ho	*S*	1.35	
Er	0.4(1)		
Tm	*J*	*S*	*J*
Yb	~0.15		~0.3

S = singlet ground state; *J* = doublet ground state, split by Jahn–Teller distortion. A number of other compounds undergo co-operative Jahn–Teller distortions (see section 6).

interaction. At 0.5 K, spin-flop occurs at a field of 1.08 T along the *c*-axis, followed by transitions to closed up spin configurations at 2.18 T along the *c*-axis, or 2.92 T normal to this axis. From these results a value was derived for the exchange constant of $J/k = -0.063$ K. This agrees with later Mössbauer measurements (Cook and Cashion 1979), that gave $J/k = -0.061(2)$ K for exchange interaction with the four nearest neighbour ions, and $-0.002(2)$ K for next nearest neighbours. These authors also determined the sub-lattice magnetization from the hyperfine splitting of the isotope ^{155}Gd; their results, together with another set derived from NMR of the ^{51}V nucleus (Bleaney et al. 1981c), are shown in fig. 7. Transitions in the antiferromagnetic state have also been studied by Metcalfe and Rosenberg (1972) using ultrasonics at 9 GHz.

$DyVO_4$ undergoes a co-operative Jahn–Teller transition (see section 6) at around

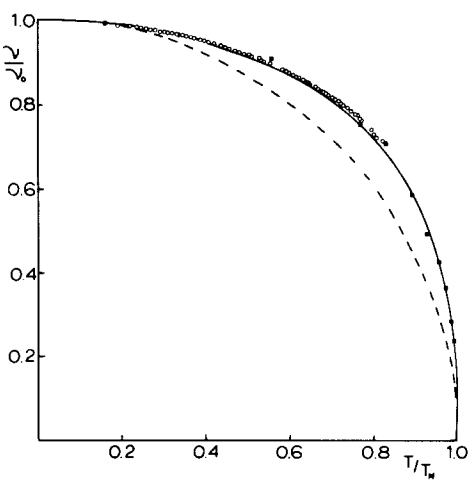

Fig. 7. Variation of the sub-lattice magnetization in the antiferromagnet $GdVO_4$ below $T_N = 2.4955(5)$K. ○ from NMR frequency of ^{51}V ($I = \frac{7}{2}$) (Bleaney et al. 1981c). ● Mössbauer data (Cook and Cashion 1979). --- Molecular field theory.

14 K, that reduces the tetragonal symmetry. The lowest doublet level becomes highly anisotropic, with principal g-values of 19, 0, 0.5 along the axes a,b,c. The direction of the high g-value may be along [100] or [010], and domains may exist in which the orthorhombic axes a, b are interchanged. As a result of the high magnetic anisotropy, the proportions of ions in the two orientations may be changed by the application of a magnetic field. The growth of energetically favourable domains was observed by viewing a single crystal between crossed polaroids in a magnetic field (Cooke et al. 1970). These authors found that the crystal could readily be converted to a single domain. In the antiferromagnetic state at 1.4 K, in a field of 4 T, optical absorption spectroscopy showed that the a- and b-axis interchanged as the crystal was rotated in a magnetic field. Magnetization measurements at 0.5 K showed that a field of 0.21 T, along the direction of spin alignment, produces a ferromagnetic state, for which the saturation magnetization corresponds to a g-value of 18.9(4).

Of the other vanadates, thermal resistivity measurements (Metcalfe and Rosenberg 1972) suggest that the erbium compound orders antiferromagnetically below 0.4(1) K, and Mössbauer results give $T_N \sim 0.15$ K (Hodges 1983) for $YbVO_4$. For this last compound the moments should order along the c-axis, mainly through the dipolar interactions. The Tm compound is discussed in section 6, and the Ho compound in sections 8.2 and 8.3.

The phosphates of Dy and Ho each have high g-values along the c-axis [19.4(4) and 16.0, respectively], and order antiferromagnetically with the moments along the c-axis. The values of T_N are 3.40 K (Colwell et al. 1969, Ellis et al. 1971) and 1.39 K (Cooke et al. 1973a). In high magnetic fields the optical spectrum of the former compound shows a pronounced quintet structure, from which values of the dipole and exchange interactions could be deduced (see also Wright et al. 1971). Of the other phosphates, $TbPO_4$ is more complicated. It has some four levels below ~ 20 K, and shows two specific heat maxima at 2.27 and 2.11 K (Hill et al. 1978); they suggest that the former corresponds to a Jahn–Teller transition, the latter to an antiferromagnetic transition.

In the magneto-electric effect, an applied electric field is found to induce a magnetization, and, conversely, an applied magnetic field induces an electric polarization. The first applications of this effect in lanthanide compounds were to the antiferromagnetic states of the phosphates of dysprosium (Rado 1969, 1970) and holmium (Cooke et al. 1973). These showed that the method can be used to determine the reduced sub-lattice magnetization, and that it corresponds to that calculated for a two sub-lattice Ising antiferromagnet. Close to T_N the magneto-electric coefficient (and hence also the reduced sub-lattice magnetization) varies as

$$(1 - T/T_N)^{\beta},$$

with $0.307 < \beta < 0.314$, in accordance with theory (Essam and Sykes 1963, Baker and Daunt 1967). For $GdVO_4$ the critical index was found to be 0.50(5) by Gorodetsky et al. (1973), but later measurements on a stress-free sample in a temperature region closer to the Néel temperature (within 2%) have also produced a critical exponent of 0.314 (England 1978). A general review of the basic theory of the magneto-electric effect for antiferromagnets is given by de Alcantara Bonfim and Gehring (1980).

5.4. *Compounds with trigonal/hexagonal symmetry*

Several series of compounds have been investigated in which the lanthanide ions occupy sites of C_{3h} symmetry. The development of crystal-field theory for the 4f group by Elliott and Stevens (1952, 1953) was based on EPR experiments on the ethylsulphates, for which single crystals of the whole series can be grown from aqueous solution. Later, single crystals of the anhydrous chlorides, RCl_3, were grown from the melt by C.A. Hutchinson Jr, and used for EPR experiments. The double nitrates form another series in which the lanthanide ions are at sites of C_{3v} symmetry; theory to accompany the EPR experiments was developed by Judd (1957). Magnetically dilute crystals were used, and the results are summarized in the monograph by Abragam and Bleaney (1970). In this section we discuss mainly the lanthanide hydroxides $R(OH)_3$, that have been investigated intensively by W.P. Wolf. The whole 4f series, and also the yttrium compound, form hexagonal prisms with space group $P6_3/m(C_{6h}^2)$, and the cation point symmetry is C_{3h}. Single crystals, grown by a hydrothermal process, are thin needles typically $10 \times 0.3 \times 0.3\,mm^3$ in dimensions.

The experimental measurements include susceptibility, magnetic moment, heat capacity (both calorimetric and AC magnetic methods) of the undiluted compounds, together with optical absorption and EPR on diluted crystals. The R ions form a close-packed hexagonal structure, in chains with two nn along the c-axis at $\pm c$, and six nnn on adjacent chains. A detailed study of $Gd(OH)_3$ was carried out by Skjeltorp et al. (1973). At liquid-helium temperatures the inverse of the susceptibility is represented by a series

$$T - \theta + B_2 T^{-1} + B_3 T^{-2}.$$

Along the c-axis the constants are

$$\theta = 0.02(10), \qquad B_2 = 2.05(10), \qquad B_3 = -0.59(10)$$

in units of degrees K, while perpendicular

$$\theta = -2.26(10), \qquad B_2 = 3.22(10), \qquad B_3 = -0.60(10).$$

The substance becomes an antiferromagnet at $T_N = 0.94(2)\,K$; the spins probably lie perpendicular to the c-axis. The values of the isotropic exchange constants are $J/k = +0.180(5)\,K$ for the nearest neighbours, and $-0.017 \pm 0.005\,K$ for the nnn. Exchange interactions with more distant ions are much smaller, zero within the experimental error. These values are consistent with EPR measurements of Cochrane et al. (1973) on Gd pairs in $Y(OH)_3$. Magnetic dipole interaction accounts for practically all the anisotropy. The behaviour of the hydroxide contrasts markedly with that of the structurally similar compound $GdCl_3$. This orders ferromagnetically at 2.2 K, with the spins along the c-axis (Wolf et al. 1962b), as the result of ferromagnetic exchange with the nearest neighbours.

A study of the properties of $Tb(OH)_3$ has been made (Catanese et al. 1973) using measurements similar to those on gadolinium hydroxide. In the hexagonal crystal field, the ground state of the Tb^{3+} ion is almost pure $J_z = \pm 6$, all other levels lying

above 150 K. The ground doublet has a g-value of 17.9 along the c-axis, and zero normal to this axis. Below $T_C = 3.72(1)$ K, the ferromagnetic state is an excellent example of an Ising system, with long thin domains containing moments along the c-axis. The ground doublet is split by 6.4(2) cm^{-1}, the result of combined dipolar and exchange interaction.

Two other hydroxides, those of dysprosium and holmium, also order ferromagnetically, with $T_C = 3.48(1)$ K and 2.54(1) K, respectively (Catanese and Meissner 1973). The interactions are again mainly dipolar and Ising in nature. The ground states are an almost pure $J_z = \pm\frac{15}{2}$ for Dy^{3+}, with g_c close to 20, and a non-Kramers doublet with $g_c = 15.3$ for Ho^{3+}. In each case the value of g normal to the c-axis is zero, and the presence of other low-lying crystal-field levels influences the properties above 4 K.

Measurements of the NMR of ^{165}Ho ($I = \frac{7}{2}$) in the ferromagnetic state of $Ho(OH)_3$ by Bunbury et al. (1985) have been fitted to a nuclear spin Hamiltonian

$$a_0 I_z + P I_z^2 + w I_z^3.$$

The magnetic interaction dominates, with $a_0 = 5013(1)$ MHz, and $P = 15.6(1)$ MHz, while the octupole term $w = 0.25(10)$ MHz is small. The measurements were made at 1.3 K, where the population of the upper component at 5.6(3) K of the ground doublet is 1.3%, but the hyperfine parameters are those of the ground state, not a thermal average.

In $Dy(OH)_3$ the ground doublet is a Kramers doublet, but with $g = 0$ normal to the c-axis. This occurs because the crystal field admixes only states differing by ± 3, so that $J_z = \pm\frac{15}{2}$ is admixed only with $\pm\frac{3}{2}$ and $\mp\frac{9}{2}$. Thus there are no matrix elements of J_x or J_y between the two states to give a finite g. A similar situation had previously been found in dysprosium ethylsulphate, for which $g_c = 10.8$. In this compound the arrangement of Dy ions is similar, but distances between them are almost exactly twice as large as in the hydroxide. Thus only magnetic dipole interactions are significant, and the ethylsulphate orders ferromagnetically at 0.13 K (Cooke et al. 1968), also with long thin domains parallel to the c-axis, and unusually abrupt domain walls. To obtain the low temperatures required for these experiments, a spherical single crystal of dysprosium ethysulphate, surrounded by powdered methylammonium chromium alum, was cooled by adiabatic demagnetization.

5.5. *The garnets*

For about a decade after the production in the laboratory of single crystals from high-temperature fluxes, the garnets were more intensely investigated than any other single series of magnetic insulating compounds, such as the ferrites. The garnets illustrate the large difference in magnitudes of the exchange interaction between pairs of 3d ions and pairs of 4f ions. Yttrium iron garnet (YIG) becomes ferrimagnetic below about 550 K, but dysprosium aluminium garnet (DAG) orders only at 2.49 K. In this section the properties are outlined of a few garnets chosen to illustrate facets of their magnetic behaviour as diverse as possible.

Garnet crystals are cubic, space group Ia3d (O_h^{10}), with chemical formula

$R_3X_5O_{12}$. Two formula units comprise 3 molecules R_2O_3, where R may be yttrium or a 4f ion, and 5 molecules X_2O_3, where X may be Fe, Al or Ga. The parameter of the cubic unit cell is about 1.24 nm; at the R-sites the point symmetry is C_2. The X-ions lie at sites of symmetry C_{3i} and S_4, in the proportions of 2:3. In YIG, ferric ions occupy these sites with the two moments antiparallel to the three, giving a ferrimagnetic structure with a net moment of $4.96\mu_B$ per formula unit $Y_3Fe_5O_{12}$.

Any of the heavier lanthanide ions may occupy the R-sites, but here we discuss only GdIG and YbIG. At low temperatures, the former compound should develop a moment of $7\mu_B$ on each Gd^{3+} ion, antiparallel to the net moment on the ferric ions, and giving overall a moment of $3 \times 7 - 5 = 16\mu_B$ per formula unit. The Gd ions are magnetized by the large exchange field of the ferric ions, with splittings between successive Gd levels rising to $28\,cm^{-1}$ at low temperatures. The exchange field changes little up to room temperature, and primarily the Gd moment declines as the thermal populations of the eight sub-levels of $S = \frac{7}{2}$ become more equal. The Gd moment remains larger than the net ferric moment almost up to room temperature; at 286 K there is a 'compensation point' above which the net moment is reversed. Similar compensation points are exhibited by the iron garnets with Tb, Dy, Ho and Er, but at progressively lower temperatures, because of the smaller moments on the R-sites (Pauthenet 1958).

Interpretation of bulk measurements of properties such as the net magnetization must allow for the presence of 6 magnetically equivalent sites for the 4f ions. The variation with temperature of the moments on these sites, except for GdIG, is further complicated by the presence of crystal-field splittings. In YbIG, for example, the ground manifold $J = \frac{7}{2}$ is split into four anisotropic Kramers doublets by the crystal field of C_2 symmetry, and each doublet is then split by the exchange field of the iron atoms. This was studied by optical absorption spectroscopy in a thin single crystal by Wickersheim and White (1960, 1962). They found that although the six sites of the Yb ions are formally magnetically equivalent, they are split by the exchange field of the ferric ions into two sets with different splittings, 17.1 and $31.7\,cm^{-1}$. The average of these is in excellent agreement with the mean splitting of $24.4\,cm^{-1}$ determined calorimetrically by Meyer and Harris (1960). By applying a magnetic field Wickersheim and White were able to determine the three principal components of the g-values and splittings of the ground doublet and of the lowest doublet in the excited manifold $J = \frac{5}{2}$ of the ^2F configuration. The splittings are not proportional to the g-values, particularly in the excited doublet, showing that the exchange interaction with the ferric ions is not completely isotropic [see the discussion in the article by Baker (1971), pp. 139, 140]. The exchange field acting on the Yb ions is of order 50 T. Using far infra-red spectroscopy, Sievers and Tinkham (1961) found a resonance at $14.1(2)\,cm^{-1}$, increasing in frequency at temperatures above about 15 K, and three lines near $25\,cm^{-1}$. A good fit to the temperature variation was obtained on including anisotropy in the exchange interaction.

The third example of a lanthanide garnet is provided by europium iron garnet, in which the ground state of the europic ion is $^7F_0$, with the first excited state $^7F_1$ at about 480 K. An exchange field has matrix elements between these two states,

producing a moment on each europium ion, opposed to the net ferric moment, and rising nearly to $5\mu_B$ below 200 K (Wolf and Van Vleck 1960). A Mössbauer measurement on the europium isotope of mass 151 shows that the effective field at the Eu nucleus rises to 60 T (Kienle 1964, Nowik and Ofer 1967). The latter fitted the hyperfine splitting at 0 K to the exchange field by including admixtures to both $J = 1$ and $J = 2$. (See also section 10.1.) Later work (Stachel et al. 1969) has shown that the Eu ions fall into two groups, with hyperfine fields at 0 K of 63 and 57 T, respectively, in good agreement with an independent result of Bauminger et al. (1969).

Finally, we refer to the aluminium and gallium garnets that order only through the interactions between the R-ions themselves. These ions, at sites of C_2 symmetry, are subject to crystal-field interactions that give rise to splittings of the J-manifolds, much larger than kT_N. When the ions are non-Kramers, and the ground state is a singlet, ordering occurs only below 1 K. [Examples are TbGaG and HoGaG, for which neutron diffraction experiments of Hamman and Ocio (1977) give antiferromagnetic transition temperatures 0.24 and 0.15 K, respectively.] For Kramers ions, the g-values of the resultant ground doublets are highly anisotropic (Wolf et al. 1962a). This is particularly true for dysprosium aluminium garnet (DAG), for which one component of the effective g-value is $g_z = 18.2$, the other two being close to zero (Ball et al. 1964). The first excited crystal field doublet lies at ~ 75 K, and its population may be neglected in studies of the antiferromagnetic state below $T_N = 2.49$ K. The six Ising-like Dy ions form three pairs, each with their g_z-axis along one of the four-fold cubic axes; in the AF state, the result mainly of dipolar interaction, this gives rise to six sub-lattices, a result that has been confirmed by neutron diffraction (see, e.g., Norvell et al. 1969). The development of the net magnetization in an applied field is complicated, even for a field along [111] in a spherical single crystal. This direction makes equal angles with the moments in the six sub-lattices, and in the AF state the system can be treated as one with two sub-lattices. An unusually detailed study of the phase diagram, using magnetic and thermal measurements, has been made by Landau et al. (1971) and Wolf et al. (1972). The interpretation is simplified by the fact that the heat capacity is virtually all magnetic. No spin-flop is observed, but a tri-critical point occurs at 1.66 K, when the internal field (corrected for demagnetizing effects) is 0.325 tesla. At this point the transition changes to first order, with a latent heat replacing the co-operative anomaly in the heat capacity. The effects of an external field along a [100] or a [110] axis are more complicated, and have been examined by Landau and Keen (1979). When a field is applied along a [100] axis, it interacts only with the pair of moments parallel to that axis; at 0 K a field close to 0.5 T reverses one moment of the pair, so that a net moment is developed, but the moments normal to the field direction remain almost unaffected.

In conclusion, it must be remarked that in this brief outline of work on the garnets a number of topics have necessarily been omitted. In particular, mention must be made of ferrimagnetic resonance, where the narrow lines of YIG are broadened and shifted by the inclusion of a small percentage of rare earth ions; see, e.g., Kittel (1959) and Van Vleck (1961, 1964).

5.6. *Other interactions*

The examples given above have been chosen to illustrate the rich variety of ordering phenomena that occur in rare earth insulating compounds, and are by no means exhaustive. In many cases magnetic dipole interaction plays the dominant role; in others, information about the exchange interaction can be deduced from the bulk properties, and from spectroscopy measurements. For ytterbium iron garnet (see section 5.5), optical spectroscopy has shown that the exchange interaction with the ferric ions must contain an anisotropic component, and other interactions. More detailed information may be obtained from magnetic resonance experiments on pairs of ions in semi-dilute compounds, and this has shown that other interactions, though small, also play a role. A general review has been given by Baker (1971).

For ions with unquenched orbital momentum, the exchange interaction of the form $(\boldsymbol{S}\cdot\boldsymbol{S}')$ must be projected onto the more complicated ground states, and this necessarily leads to anisotropy in the effective interaction. Two other types of anisotropic interactions have been proposed:

(a) electric multipole interaction (EMI), particularly quadrupole–quadrupole interaction (EQQ), arising from electrostatic interactions between the non-spherical distributions of electric charge on ions with orbital momentum;

(b) virtual phonon interaction (VPE), resulting from modulation of the electrostatic interactions by lattice vibrations. Again, this is significant only for ions with unquenched orbital momenta, sensitive to distortion of the surroundings produced by the phonons.

Evaluation of the evidence from EPR experiments concerning the importance of these interactions is complicated (see Baker 1971), and we mention only the main conclusions. The spectra of pairs of cerium ions and pairs of neodymium ions in the anhydrous halides (Birgeneau et al. 1968, Riley et al. 1970) show that superexchange, in the generalized form discussed by Levy (1964), provides a large contribution for both Ce and Nd pairs. EQQ plays a major role in interactions between the Ce pairs, also producing changes in the g-tensor from the values for single ions. In the ethylsulphates, particularly the cerium compound (Anderson et al. 1971), the VPE interaction is more important, partly because it is a longer range interaction.

The presence of electric dipole moments in non-Kramers ions has been pointed out in section 2.4. The possibility that interactions between them give rise to electric dipole ordering was demonstrated by Harrison et al. (1976) for $PrCl_3$. Measurements of the heat capacity and electric susceptibility confirmed that both one- and three-dimensional ordering occur below 1 K. A broad maximum in the heat capacity at $\sim$0.85 K is attributed to the former, and a sharp maximum at 0.4 K to the latter. The one-dimensional ordering is well described by a linear-chain model with XY-type interactions, that in sign and approximately in size agree with estimates of the electric dipole interaction between nearest neighbours. Measurements of the electric susceptibility show effects compatible with antiferroelectric ordering, and account for the fact that no anomaly in the magnetic susceptibility is observed at the transition at 0.4 K (Colwell et al. 1969). The one-dimensional XY-model with electric dipolar interaction has also been shown to

account for the properties of praseodymium ethylsulphate (PrETS) below 1 K by Folinsbee et al. (1977a). In praseodymium magnesium nitrate the electric dipole moment is smaller by a factor ~ 10 than in $PrCl_3$ or PrETS, and electric interactions are therefore negligible. The distribution of initial field splittings is in good agreement with a mechanism of random local electric fields set up by charged defects (Folinsbee et al. 1977b), rather than a Gaussian distribution.

6. The Jahn–Teller effect

6.1. *Introduction*

In a discussion of non-linear molecules with a low-lying electronic degeneracy (other than Kramers degeneracy), it was pointed out by Jahn and Teller (1937) that a distortion to a configuration of lower symmetry could produce a state of lower energy, and that the molecule should therefore be unstable to such a distortion. The first application of these ideas to magnetic solids was made by Van Vleck (1939). He estimated that the energies involved were of order $100\,cm^{-1}$ for compounds of 3d group ions, but only $0.01\,cm^{-1}$ for those of 4f ions. For the latter, the effect was therefore 'only of academic interest', and in hydrated compounds the ionic displacements involved would be less than the vibrational amplitudes of the water molecules through their zero-point energy. The discovery in the early 1970s of co-operative Jahn–Teller transitions in a number of lanthanide compounds with the zircon structure therefore came as a surprise. The transitions occur at temperatures from 2 to 30 K, instead of several hundred K for 3d compounds, so that studies could be made of many properties, not masked by thermal effects. Furthermore, magnetic fields and uniaxial stress may give changes in the energy levels comparable with the splittings induced by the phase transitions.

A phase transition at a temperature T_D, involving a distortion capable of producing a change of shape in the crystal, can be observed by X-rays. More important was the realization that an interaction involving the collective lattice vibrations and the elastic constants could be studied using ultrasonic techniques. There must be present a 'soft mode', associated with the fall to zero of the corresponding elastic constant. Measurements of the variation of this constant give direct information about the strength of the coupling of the electronic states to the elastic mode (the strain mode). Finally, a large amount of theoretical analysis was stimulated by the new experimental results, from which it turned out that the subject could be treated with surprising accuracy by molecular field theory. In this section we shall be concerned mainly with the experimental results; a review of these and of the theory has been given by Gehring and Gehring (1975).

6.2. *The co-operative Jahn–Teller effect*

As noted previously, the rare earth zircons are tetragonal, with space group $I4_1/amd$, and each of the two lanthanide ions in the unit cell, related by inversion

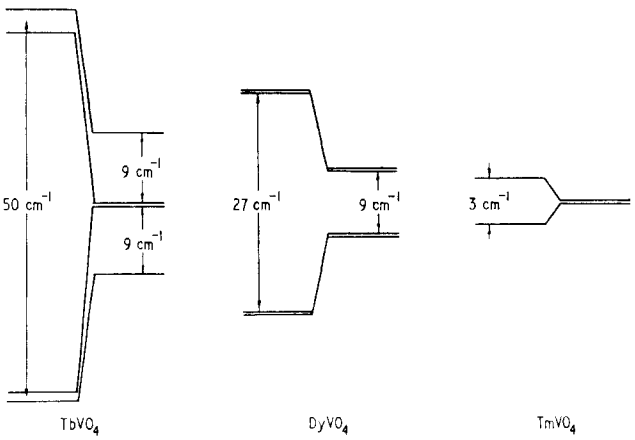

Fig. 8. Low lying energy levels of $TbVO_4$, $DyVO_4$ and $TmVO_4$, showing the effects of the Jahn–Teller distortions at T_D = 33, 14 and 2.156(5)K, respectively. In each case the levels above T_D are to the right, and those below T_D to the left. (Gehring and Gehring 1975.)

symmetry, occupy sites of tetragonal symmetry. The zircons comprise the phosphates, vanadates and arsenates, with general formula RXO_4, where X is P, V or As. The splittings produced by the tetragonal field may leave as ground state a singlet or a doublet. The degeneracy of a Kramers doublet cannot be lifted by a non-magnetic interaction, but the 'true' Jahn–Teller effect can split a non-Kramers doublet, such as the ground states of $TmVO_4$ and $TmAsO_4$. For the vanadates and arsenates of two other ions, Tb and Dy, the crystal field produces several low lying levels, with separations comparable with the Jahn–Teller energy; they are sufficiently close that a Jahn–Teller distortion can occur. This is known as the 'pseudo' Jahn–Teller effect, and it results in changes in the level separations. Such effects are illustrated in fig. 8. The distortions involve two different modes: the departure from tetragonal symmetry may result from a B_{1g} strain, in which the crystal a,b axes become unequal in length, but remain orthogonal; or a B_{2g} strain, a shear mode in which the angle between the two axes departs from 90°. These strains involve the elastic constants $c_1 = \frac{1}{2}(c_{11} - c_{22})$ and $c_2 = c_{66}$, respectively. For the zircon structure, the latter is much softer than the former, but a B_{1g} distortion may occur if it is more strongly coupled to the electronic states of the ion.

The temperatures at which a co-operative Jahn–Teller distortion occurs for compounds with the zircon structure are given in table 9. The effect was first discovered in $DyVO_4$, when it was found by optical spectroscopy (Cooke et al. 1970) that the separation between the two low-lying Kramers doublets was considerably larger at 4K than at 20K. A single crystal, cooled to 4.2K in zero magnetic field and viewed between crossed polaroids, showed domain-like regions that could be enlarged by the application of a magnetic field in the (001) plane. Absorption spectroscopy revealed the unusual Zeeman effect shown in fig. 9, fitted to $g_a = 19$, $g_b \sim 0$, $g_c \sim 0.5$. The cusp-like variation when the field makes an angle of

TABLE 9
Values of the co-operative Jahn–Teller distortion temperature T_D and the antiferromagnetic ordering temperature T_N for rare earth compounds with the zircon structure.

R	RPO_4		RVO_4		$RAsO_4$	
	T_D	T_N	T_D	T_N	T_D	T_N
Tb	2.27	2.11	33.0	~0.6	25.5	1.50
Dy	–	3.40	13.8	3.066	11.2	2.44
Tm	–	–	2.156	<0.0001	6.13	–

45° with the [100] and [010] axes results from an interchange of the *a*,*b* axes that keeps the direction of the large *g*-value nearest to that of the applied field. Far infrared spectroscopy showed that the separation of the two Kramers doublets had increased at 4.2 K to about 27 cm^{-1}, see fig. 8. Finally, heat capacity measurements (see also Cooke et al. 1971) showed a large co-operative anomaly at 14.00(5) K, attributed to the Jahn–Teller transition, followed by another at 3.066(2) K, arising from the antiferromagnetic transition (see section 5.3). The latter was observed independently by Becker et al. (1970).

In $DyVO_4$ the principal axes in the distorted phase are [100] and [010], showing that the effect arises from coupling to a B_{1g} phonon. Not only does the distortion increase the splitting between the two lowest doublets, it also admixes the wave functions so that their principal *g*-values become quite different. Above the transition they are presumably close to the EPR values listed in table 4, but below the transition one value for the lowest doublet increases from 9 to 19 (see above), while those for the excited doublet are reduced almost to zero. The preliminary theory of Elliott et al. (1971) was expanded to include strain couplings by Gehring et al. (1972), who calculated how the splitting should depend on uniaxial stress; the results were verified by optical spectroscopy (Gehring et al. 1972).

In $TbVO_4$ the lowest energy levels of the non-Kramers Tb^{3+} ion are a singlet,

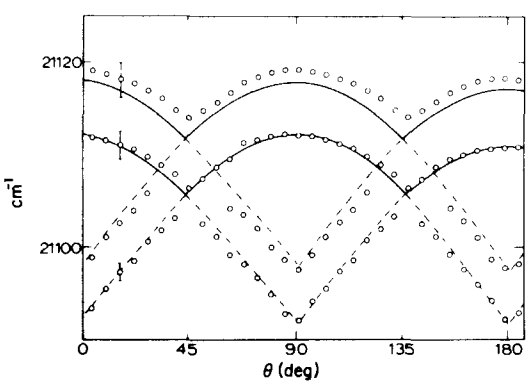

Fig. 9. Variation of Zeeman energy at $B = 4$ T and $T = 1.4$ K for $DyVO_4$ as the orientation of a magnetic field is varied in the (001) plane, from optical spectroscopy measurements. The full curves correspond to strong absorption, the broken curves to weak absorption. (Cooke et al. 1970.)

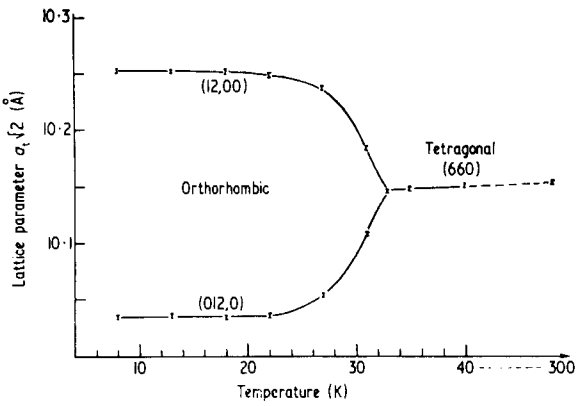

Fig. 10. Temperature variation of the lattice parameters of $TbVO_4$, measured by X-ray diffraction, showing the distortion below the Jahn–Teller transition temperature $T_D = 33$ K. (Will et al. 1972.)

doublet and singlet, but the overall separation is only $18\,cm^{-1}$. A co-operative Jahn–Teller distortion occurs at 33 K, changing the energy levels to two pairs of almost degenerate doublets with an overall separation of about $50\,cm^{-1}$ (Gehring et al. 1971), see fig. 8. A Raman study by Harley et al. (1971) shows that the E_g phonons are split by the distortion. Domains are formed with principal axes [110], [1$\bar{1}$0], but a magnetic field of a fraction of a tesla converts a crystal to a single domain, since the ground doublet has an effective g-value of 16.3 along one of these directions. The results obtained by Raman and Brillouin scattering, together with some ultrasonic measurements, were related to theory by Elliott et al. (1972), and Sandercock et al. (1972). An X-ray diffraction study by Will et al. (1972) shows a change in the lattice parameters for $TbVO_4$ (fig. 10) rising to over 2% as a result of the distortion. This is much larger than the corresponding measurement of 0.17% in $DyVO_4$ (Sayetat et al. 1971).

For $TmVO_4$ and $TmAsO_4$ the ground state in each case is a non-Kramers doublet that can be split by the 'true' Jahn–Teller effect. For the vanadate the co-operative transition occurs at $T_D = 2.156$ K; in this region the lattice heat capacity is negligible, and the co-operative anomaly dominates, as shown by the measurements of Cooke et al. (1972) in fig. 11. The distinctive triangular shape is a typical result for a molecular field model in which the splitting Δ of the doublet varies with temperature as

$$\Delta/\Delta_0 = \tanh(\Delta/2kT), \tag{22}$$

where the maximum splitting Δ_0 is related to the distortion temperature by $\Delta_0 = 2kT_D$. The non-Kramers doublet has a single g-value, $g_c = 10.2$, and below T_D the magnetic susceptibility becomes independent of temperature. Application of a magnetic field along the c-axis then produces a magnetic moment initially rising linearly at a rate independent of temperature, but departing from linear behavior at a field B_c related to the splitting Δ by $g_c\mu_B B_c = k\Delta$. Measurements of B_c showed that the temperature variation follows a Brillouin function for $S = \frac{1}{2}$, a result that was confirmed by optical spectroscopy (Becker et al. 1972). These authors also observed

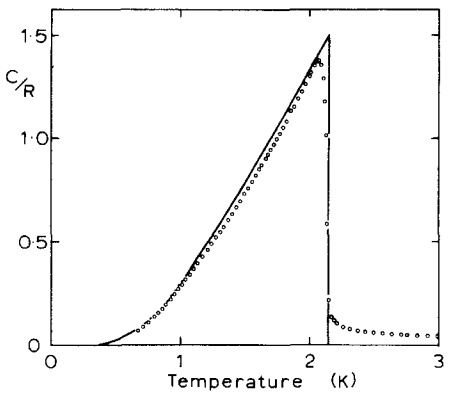

Fig. 11. Heat capacity of $TmVO_4$ from 0.6 to 3 K, excluding the lattice contribution. The anomaly at the Jahn–Teller transition at 2.156 K [experimental points (○)] is fitted to molecular-field theory (full curve). (Cooke et al. 1972.)

the presence of domains and showed that the principal axes of the distortion are [110], [1$\bar{1}$0], as in the case of $TbVO_4$.

6.3. *Radio-frequency acoustic and electromagnetic experiments*

The realization that co-operative Jahn–Teller systems should show large acoustic anomalies led to another type of investigation. In $DyVO_4$ Melcher and Scott (1972) measured the longitudinal acoustic velocity, and confirmed that the elastic constant $(c_{11} - c_{12})$ fell to zero at the distortion temperature T_D. They fitted their results

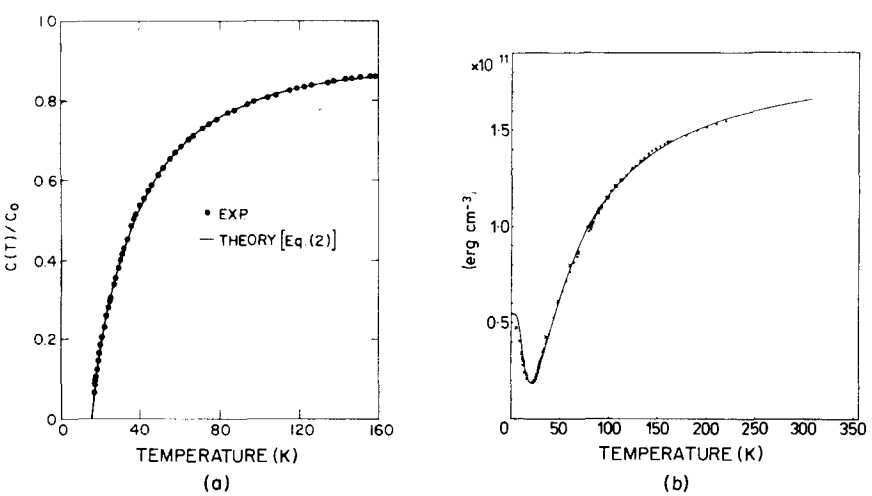

Fig. 12. Ultrasonic measurements of the elastic constants of (a) $DyVO_4$ (Melcher and Scott 1972); and (b) $TmPO_4$ (Harley and Manning 1978), with theoretical fits.

above this temperature (see fig. 12a) to a variation of the form

$$\frac{c}{c_0} = \frac{\Delta - (\lambda + \mu)\tanh(\Delta/kT)}{\Delta - \lambda\tanh(\Delta/kT)}, \tag{23}$$

a relation derived from mean-field theory. The value of c should go to zero when the numerator vanishes; i.e., when

$$\Delta/(\lambda + \mu) = \tanh(\Delta/kT),$$

a relation that is identical with that giving the value of T_D. It follows that unless $\Delta < (\lambda + \mu)$, the combined effect of the coupling coefficients λ (Jahn–Teller) and μ (strain) is not strong enough to cause a transition. Such a situation occurs in $TmPO_4$, where the ground state is a singlet, with a doublet at 29 cm^{-1}. The ultrasonic measurements of Harley and Manning (1978) show that c_{66} falls to a minimum (see fig. 12b), but then recovers as the thermal population of the Jahn–Teller active excited doublet declines to zero. Thus in this substance there is no co-operative transition, although the values of the constants λ and μ are similar to those found for $TbVO_4$.

Similar acoustic measurements were made in $TmVO_4$ by Melcher et al. (1973), who found that both the elastic constants c_{66} and $(c_{11} - c_{12})$ soften, indicating that there is coupling to B_{2g} and to B_{1g} strain modes. An anomaly in the temperature variation of c_{66} between 30 and 150 K shows that there is also a strong coupling of the B_{2g} mode to an excited electronic non-Kramers doublet at about 80 K. The coupling to the ground doublet is weaker by a factor of about 40, thus accounting for the rather low value of T_D. At this temperature the crystal becomes unstable to the B_{2g} strain, and $(c_{11} - c_{12})$ is constant below this temperature. A further investigation using acoustic waves of 9 GHz frequency was carried out by Page and Rosenberg (1977). This showed that the ratio λ/μ is close to the molecular field value of -3 for both B_{2g} and B_{1g} modes, but the coupling constants are about 10 times stronger for the former. The effects of a magnetic field along the c-axis on c_{66} were also measured at field strengths B close to the critical field B_c above which no distortion occurs. A log–log plot of c_{66} against $(B - B_c)/B_c$ gave a critical index of 1.00(2), again in agreement with mean-field theory.

In an NMR investigation of the ^{51}V spectrum in $TmVO_4$, Bleaney and Wells (1980) found that the frequency of oscillation of the RF circuit containing the crystal was a sensitive monitor of variations in the RF (adiabatic) magnetic susceptibility χ_s. Below T_D, where the ground doublet is split by the distortion, χ_s is independent of a field applied along the c-axis, until this reaches the critical field B_c at which the Jahn–Teller distortion is reduced to zero. At this field χ_s falls sharply, and the effect can be used to give a precise measurement of B_c. The results were fitted accurately to the relation $b = B_c/B_0 = \tanh(b/t)$, where $t = (T/T_D) = T/2.156$ is the reduced temperature. This is the result expected from mean-field theory. In the distorted state below T_D, the presence of domains with principal axes [110] and [1$\bar{1}$0] was confirmed by observation of two sets of anisotropic resonance curves (see fig. 13c), one set for ^{51}V ($I = \frac{7}{2}$) and the other for the enhanced NMR of ^{169}Tm ($I = \frac{1}{2}$).

Similar measurements, together with optical spectroscopic experiments, have been

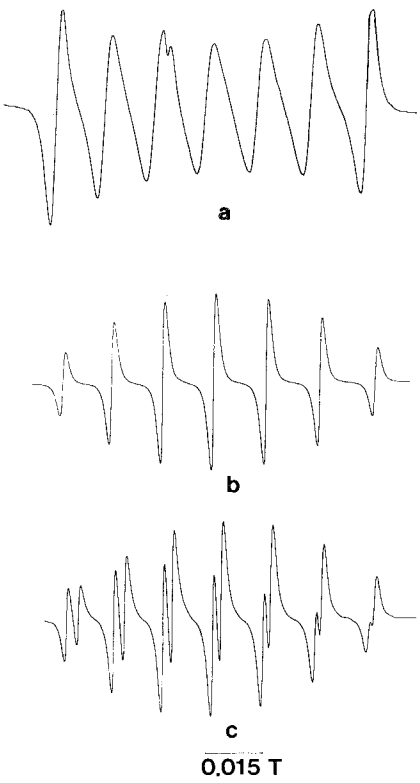

Fig. 13. NMR spectra of ^{51}V in $TmVO_4$, at a frequency of 8.8 MHz. (a) The spectrum at 4.2 K shows the anomalous intensity ratios, while (b) below T_D the normal ratios are observed. (c) shows the doubling of the spectrum at 1.5 K with B along [110] or [1$\bar{1}$0] the principal axes of the Jahn–Teller distortion. (Bleaney and Wells 1980.)

made by Bleaney et al. (1984) on $TmAsO_4$. The behavior is similar to that of $TmVO_4$, except that a singlet state lies only 13.8 cm^{-1} above the ground doublet, and the Jahn–Teller distortion temperature is higher, $T_D = 6.13(3)$K. The enhanced NMR spectrum of ^{169}Tm again confirms the presence of domains, and the principal values of the resonance frequency (in MHz per tesla) are, respectively, 706.5, 370(3) and 60(5) along [001], [110] and [110], extrapolated to 0 K. Along the c-axis the frequency rises by about 0.6% with temperature, because of matrix elements of the Jahn–Teller interaction to an excited doublet at about 140 K.

6.4. *Dynamic fluctuations and strains*

In the previous sections on the Jahn–Teller effect we have been concerned with uniform strains, the same at all lattice sites, at any rate within a domain. Such uniform strains are important below the distortion temperature T_D. Above T_D dynamic random strains are present, varying from site to site, for which the fluctuations slow down as the temperature is reduced. The presence of such effects has been revealed by observation of the EPR spectrum of Gd^{3+} in substances such as $TmVO_4$ and $TmAsO_4$ and is described in the review by Mehran and Stevens

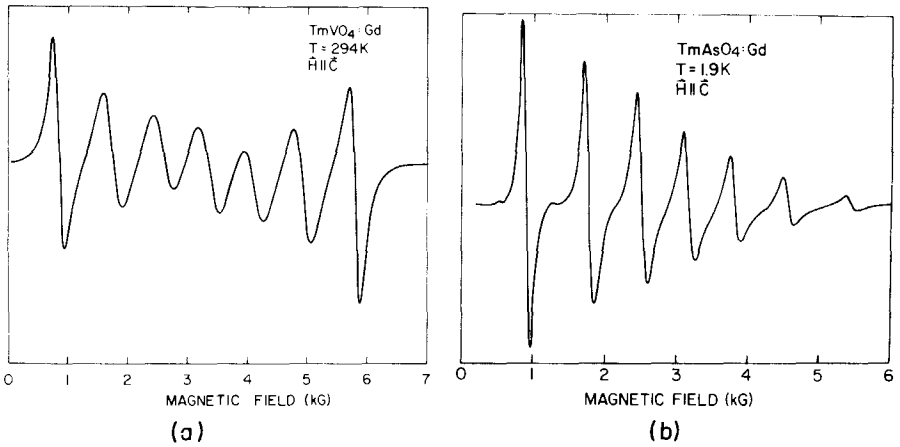

Fig. 14. Fine structure in the EPR spectra of Gd^{3+} in: (a) $TmVO_4$ at 294 K; and in (b) $TmAsO_4$ at 1.9 K. In each case the magnetic field is along the c-axis. (Mehran and Stevens 1982.)

(1982), which contains a full list of references. The Gd^{3+} ion, $4f^7$, is in an ^8S state, for which the spin–lattice relaxation time is sufficiently long that the EPR spectrum is observable up to and above room temperature. Although $TmVO_4$ is paramagnetic, at the higher temperatures the spin relaxation rates for the Tm^{3+} ions are so fast that spin–spin broadening is averaged out, an effect first observed in the EPR spectrum of Gd^{3+} in neodymium ethylsulphate by Bleaney et al. (1951). The spectrum of Gd^{3+} in $TmVO_4$ at room temperature (Mehran et al. 1976), with the magnetic field along the c-axis, is shown in fig. 14a. The line widths are 0.019(10) T, but increase rapidly below about 200 K, becoming twice as large at 100 K, below which temperature the spectrum broadens too much to be observable. The fluctuations produce rhombic distortions of the crystal field; these have the largest matrix elements for the Gd^{3+} levels that give rise to the central lines in the spectrum, so that these experience the greater broadening. A different effect is displayed in the spectrum (Mehran et al. 1977) of Gd^{3+} in $TmAsO_4$ below $T_D = 6.13$ K, and is shown in fig. 14b. The fine structure of the Gd^{3+} ion causes the spectrum to be spread over fields (along the c-axis) from 0.1 to 0.6 T. As the field increases, it counteracts the Jahn–Teller distortion (see section 6.3), and develops magnetic moments, proportional to the applied field, on the Tm sites. These moments produce broadening through spin–spin interaction, perhaps with some contribution from an inhomogeneous demagnetizing field. A similar effect has been observed in $TmVO_4$ diluted in YVO_4 by Mehran et al. (1982), who have also studied the variations in the gadolinium line widths in the temperature range up to about 50 K, for concentrations of 1, 5, 10 and 15%. They conclude that

(a) virtual-phonon exchange is present, increasing with concentration;
(b) its presence in such dilute systems shows that it is long-ranged; and
(c) it produces random strains that fluctuate more slowly at low temperatures.

Some other investigations using $4f^7$ ions as probes are summarized in section 8.6.

Anomalous intensity ratios, with the strongest lines on the outside, are displayed also by the NMR spectrum (Bleaney and Wells 1980) of ^{51}V ($I = \frac{7}{2}$) in $TmVO_4$ at 4.2 K, shown in fig. 13a, but the abnormal broadening disappears below T_D, as shown in fig. 13b. Here the applied field is normal to the c-axis, so that no large electronic moments are developed. The presence of domains is confirmed by the doubling of the spectrum in fig. 13c.

7. Magnetic cooling and nuclear orientation

7.1. *Magnetic cooling*

Before the production of the rare isotope ^3He in quantities sufficient for helium-3 cryostats and, later, the development of the dilution refrigerator, the only method of obtaining temperatures below 1 K was by means of adiabatic (isentropic) demagnetization. A paramagnetic salt is cooled to about 1.5 K, and magnetized in a field large enough to split successive levels of the paramagnetic ion by an amount $\gg kT$. The magnetic entropy, initially $R \ln (2J + 1)$, where $2J + 1$ is the multiplicity of the magnetic levels, is reduced almost to zero after the heat of magnetization has been carried away by the helium bath. The salt is then thermally isolated from the bath, and on demagnetization cools to the temperature at which the magnetic entropy, determined by the internal interactions, is equal to the initial entropy after magnetization. To obtain the lowest possible temperatures, the compounds used at first were gadolinium sulphate and ferric or chromium alum, in which the magnetic ions are well separated and the interactions between the ions are correspondingly reduced. Such interactions are generally smaller for ions of the 4f group than of the 3d group, and investigations by EPR of the lanthanide ethylsulphates and double nitrates suggested that many of them would be suitable for magnetic cooling. In particular, compounds of Ce^{3+} have the advantage that the stable isotopes of this ion have no nuclear moments, and the final temperatures reached are not restricted by hyperfine splittings. The most advantageous compound is cerium magnesium nitrate (CMN), formula $Ce_2Mg_3(NO_3)_{12} \cdot 24H_2O$, in which the nearest cerium neighbours of the Ce^{3+} ion are three at 0.856 nm and three at 0.859 nm. The crystal field at the Ce site has three-fold symmetry, and the $2J + 1 = 6$ levels of the ground state $^2F_{5/2}$ are split into three Kramers doublets, the lowest of which has g-values of 0.25(5) parallel and 1.84(2) perpendicular to the trigonal axis. All the magnetic ions are equivalent, and interactions between them are unusually small. The properties of this compound were explored by Cooke et al. (1953) above 1 K, and Daniels and Robinson (1953) below 1 K. Down to a few mK, the magnetic heat capacity follows the relation $CT^2/R = 7.5 \times 10^{-6}$, close to the value of 6.75×10^{-6} calculated for purely magnetic dipolar interactions. The susceptibility follows the Curie law quite accurately down to 6 mK, and the lowest temperature reached after demagnetization is 3 mK.

Another magnetically dilute compound of Ce^{3+} with axial symmetry is the

ethylsulphate, $Ce(C_2H_5SO_4)_3 \cdot 9H_2O$ (CeETS). In the hexagonal crystal field (see section 2.2), the ground state $J = \frac{5}{2}$ is split into three Kramers doublets, the lowest being $|\pm 5/2\rangle$, with g-values 3.80 (parallel) and 0.22 (perpendicular). Below 1 K the susceptibility is very anisotropic, being larger by a factor of about 300 parallel to the c-axis than perpendicular to it. Measurements on this compound at temperatures below 1 K, attained by adiabatic demagnetization, were made by Cooke et al. (1955) and extended by Johnson and Meyer (1959). In zero field the entropy drops sharply below 0.08 K, while the susceptibility parallel to the c-axis becomes almost constant at this point, rising slightly at the lowest temperatures (0.035 to 0.022 K). The interaction heat capacity is too large to arise from magnetic dipolar interaction, and is attributed to electric quadrupole–quadrupole coupling (Finkelstein and Mencher 1953), though a detailed fit raises problems with the signs of the parameters.

The large magnetic anisotropy of these compounds made possible a variety of novel experiments using single crystals. Application of a magnetic field perpendicular to the axis in CeETS produces little rise in temperature after demagnetization, and Cooke et al. (1955) made use of this to determine the superconducting transition curve of zinc metal [critical temperature 0.89(1) K]. Extrapolated to 0 K, the critical field is only 0.005(3) T, while that for lead is 0.080(2) T. In another ingenious experiment, Cooke et al. (1956) used a composite specimen, in which a single-crystal sphere of CMN was enclosed in a spherical shell of a paramagnetic powder, of various compounds including neodymium magnesium nitrate (NdMN). After demagnetization, temperatures of order 0.05 K were reached, and susceptibility measurements were made parallel and perpendicular to the c-axis of the CMN crystal. The CMN gives a negligible contribution (parallel) and a known contribution (perpendicular), that follows the Curie law down to the lowest temperatures reached. Since the susceptibiltiy of the powder in the outer shell is necessarily isotropic, that of the CMN can be separated from the total, and used to calculate the temperature. For NdMN it was thus shown that the susceptibility deviated from the Curie law by less than 2% down to 0.06 K.

7.2. *Nuclear orientation*

An important application of the large magnetic anisotropy of the hyperfine interaction in these compounds is to experiments in nuclear orientation, using the magnetic hyperfine method. At temperatures large compared with any hyperfine splittings each of the $2I + 1$ sub-states m_I of a nucleus of spin I have essentially the same population, and any radioactive emissions are isotropic in space. Nuclear orientation means that the sub-states no longer have equal populations, and that radio-active emissions become anisotropic. Application of a field of 5 T at 10 mK to the nucleus of a diamagnetic ion is required to produce substantial nuclear polarization (the 'brute force method'), but other methods make use of the hyperfine interaction in a paramagnetic ion. Such methods have the great advantage that the low temperatures are produced within the sample itself, thus avoiding the considerable problem of transfer of the heat of magnetization between two solid bodies at mK temperatures. Demagnetization to a small residual field produces some nuclear

polarization (Gorter 1948, Rose 1949), while demagnetization to zero field produces 'alignment' if anisotropy is present (Bleaney 1951). A simple illustration of the latter is provided by an electronic doublet with effective spin $S = \frac{1}{2}$, and an axial hyperfine interaction of the form $A_z S_z I_z$. The energy levels are $2I + 1$ doublets, each a pair of nuclear sub-states $\pm m_I$, with separations $\frac{1}{2}A_z$ between successive levels. At temperatures such that $kT \leqslant A_z$, nuclear 'quadrupolarization' is produced, in which levels with different values of $|m_I|$ are unequally populated. Application of a small magnetic field to split each doublet through the electronic Zeeman interaction, by amounts of order kT, produces nuclear 'polarization'.

For the lanthanide ions the hyperfine interaction is generally so large that temperatures of order 10–100 mK suffice to produce substantial nuclear orientation. Such temperatures can be reached by adiabatic demagnetization of the paramagnetic compound itself, particularly when the majority of the isotopes have no hyperfine interaction, or by incorporating the radioactive nuclei in another similar compound. In particular, CMN and the ethylsulphates of cerium and neodymium have been used. In the decade following the first successful orientation experiments on isotopes of the 3d group, similar experiments on a number of lanthanide isotopes, ranging from ^{139}Ce to ^{175}Yb, were carried out. Values of the nuclear spins and parity were established, the decay schemes were studied, and estimates of the nuclear moments were made. Many of the latter are rather imprecise, partly because not all details of the decay scheme were certain, partly because of uncertainty in the values of $\langle r^{-3} \rangle$. An example is given by the nuclear orientation of ^{175}Yb ($I = \frac{7}{2}$), where the original estimate of 0.15(2) n.m. for the nuclear moment, obtained from an experiment in YbETS, was increased to 0.277(15) n.m. following a later experiment (Spanjaard et al. 1972) in gold metal (allowance for the presence of a nuclear electric quadrupole interaction was then also included).

Much the most important nuclear orientation experiment involved the use of CMN to cool the radioactive isotope cobalt-60 ($I = 5$). This gave a direct experimental answer to the question of whether parity was conserved in weak nuclear interactions. This had generally been assumed, but Lee and Yang (1956) pointed out that there was little direct evidence, and suggested that it could be tested by observation of the angular distribution of β-particles from polarized nuclei, in particular, ^{60}Co. This isotope can be incorporated into CMN on a magnesium site, and cooled by adiabatic demagnetization. Then the small field needed to polarize the cobalt nuclei is applied along the c-axis, where the low value of g_z for the cerium ion means that the temperature is not significantly raised (Wu et al. 1957). In previous experiments γ-rays from the oriented nuclei were detected outside the cryostat, but because of their low penetrating power, β-rays must be detected inside and close to the surface of the radio-active crystal. An anthracene crystal was used, the scintillations being transmitted through a lucite light-pipe to a photomultiplier outside the vacuum chamber. A large asymmetry in the emission of β-particles, parallel and anti-parallel to the polarizing field, was observed. Its magnitude indicated that the principle of charge-conjugation must be violated, as well as that of parity-conservation. Later experiments on positron emitters show similar asymmetries, though of opposite sign, and β–γ angular correlation experiments with oriented nuclei were also carried out (see the review by Ambler 1960).

7.3. *Other cryogenic applications*

In nuclear orientation experiments, the problems with β-particles just outlined (section 7.2) were overcome by placing the detector within the cryostat, a method adopted also for the α-particles emitted from nuclei of the 5f group (Dabbs et al. 1958). It is much simpler to observe the emission of γ-rays since they penetrate the cryostat and the detectors can be outside; this is true also of neutrons. The capture of polarized neutrons has been studied, using samarium ethylsulphate (SmETS). In an experiment of Roberts et al. (1954) a single crystal of this substance, enhanced to almost 100% of the stable odd-neutron isotope ^{149}Sm ($I = \frac{7}{2}$), was cooled indirectly by thermal contact though metallic copper to ferric ammonium alum. After demagnetization an estimated temperature of 60–70 mK was reached, and a special magnet design produced a field of 1 T on the SmETS crystal, but less than 0.0001 T on the iron alum. A beam of neutrons from a reactor passes through the SmETS crystal to a magnetite single crystal that selects neutrons of energy 0.07 eV and given spin state before they reach a proportional neutron counter. The experiment showed that ^{149}Sm is more transparent to those neutrons whose spins are antiparallel to the samarium nuclear spins.

In a later and more sophisticated version of this experiment, a crystal of deuterated CMN is used in which about 6% of the Ce atoms are replaced by ^{149}Sm (Freeman and Williams 1978). This is cooled in a dilution refrigerator to 17(2) mK, and magnetic fields up to 0.5 T are applied along the c-axis of the crystal. In this direction the hyperfine interaction for Sm is large, giving a high degree of nuclear polarization, while the value of g for Ce is small, so that the crystal remains cold. Neutron polarizations of over 90% in the emergent beam are obtained for energies of 0.07–0.12 eV.

In a number of trivalent holmium compounds the crystal field of axial symmetry leaves as the ground state a non-Kramers doublet with a high value ($\sim$15) of g_z. Such a doublet has a large magnetic hyperfine splitting for the isotope ^{165}Ho ($I = \frac{7}{2}$), of order 1 K overall, and a useable degree of nuclear polarization can be obtained by applying a magnetic field along the c-axis at this temperature. Postma et al. (1962) used this to study the transmission of polarized monochromatic neutrons through deuterated HoETS and through holmium metal. Resonances at neutron energies of 3.92 and 12.8 eV were each found to correspond to spins $I + \frac{1}{2} = 4$ in the compound nucleus. In an earlier study, Postma et al. (1959) incorporated the radioactive isotope ^{166m}Ho in NdETS, obtaining almost complete nuclear orientation after demagnetization to a temperature of about 25 mK. Both the spatial anisotropy of emission of the γ-rays and their linear polarization were studied, and a spin of 6, 7 or 8 deduced for this nucleus in its isomeric state (the ground state has $I = 0$).

HoETS was also used by Abragam et al. (1976) to study the coherent precession of the neutron spin around the direction of the nuclear polarization. By analogy with the precession of a magnetic moment in a magnetic field, the nuclear polarization can be regarded as setting up a 'pseudo-magnetic field' resulting from a 'pseudo-magnetic moment' characteristic of the nuclear isotope and related to its scattering amplitude for neutrons. A single crystal of HoETS was cooled to about

30 mK in a dilution refrigerator, and magnetic fields applied both parallel and perpendicular to the c-axis. A value of $-0.74(8)$ (in units of Bohr magnetons) was obtained for the 'pseudo-magnetic moment' of ^{165}Ho, rather larger than an earlier value of $-0.59(6)$ obtained by Herpin and Meriel (1973). Two new relaxation mechanisms were invoked to describe the relaxation processes, one for the holmium nuclei with the applied magnetic field along the c-axis, the other for the protons with the field normal to this axis.

The experiment of Herpin and Meriel (1973) had the advantage of requiring neither a single crystal nor a polarized neutron beam, nor particularly low temperatures, because of the large hyperfine splitting of ^{165}Ho. A similar experiment, using the antiferromagnetic state of AgTb, was used to determine the pseudomagnetic nuclear moment of ^{159}Tb by Akopyan et al. (1975, 1976).

7.4. *Dynamic nuclear polarization*

In the technique of dynamic nuclear polarization (DNP), the nuclei of diamagnetic ions in a solid substance are polarized by irradiating a paramagnetic impurity with a strong oscillating field at a frequency equal to its electron resonance frequency plus or minus the nuclear resonance frequency. This produces transitions, forbidden except through the mixing effects of the dipolar interactions between the two sets of spins, in which simultaneous reversals occur of the electron and nuclear spins. Ideally, the system must be in a large magnetic field and at a low temperature, such that the electron spins are, in thermal equilibrium, completely polarized in the 'up' position, parallel to the applied field. Following a transition in which electron and nuclear spins are reversed, the former relaxes rapidly back to the 'up' position, but the nuclear spin does not, because of its long relaxation time. The process then repeats, the nuclear spins being continuously transferred to an 'up' state or a 'down' state. The former corresponds to nuclear polarization at a positive temperature, the latter to polarization at a 'negative temperature', since the moments are opposed to the applied field. The choice is effected by irradiating, respectively, at the difference or the sum of electron and nuclear frequencies.

DNP originated in a suggestion of Overhauser (1953) for polarization of nuclei in metals, modified and extended to other classes of coupled electron–nuclear systems by Abragam (1955), Jeffries (1957, 1960) and others (see Jeffries 1963a). A number of lanthanide compounds were used, such as LMN (lanthanum magnesium nitrate) with concentrations of Ce^{3+} down to 0.3%, or Nd^{3+}, that gave enhancement factors of 200 to 500 for the polarization of the protons. Another ingenious suggestion of Abragam (1963) and Jeffries (1963b) made use of the large magnetic anisotropy of lanthanide ions. A single crystal is rotated in a helium bath at 1.3 K, so that it is alternately magnetized when the direction of large g is parallel to the applied field, and then demagnetized when it is perpendicular. In the former direction the electron spins relax to the lattice and hence to the bath, allowing the heat of magnetization to escape. In the other direction, the electrons spins are cooled and weakly coupled to the bath, but strongly coupled to the nuclear spins, which are thereby cooled. This was demonstrated experimentally by Robinson (1963) using Ce^{3+} in LMN,

while later experiments used Yb^{3+} in yttrium ethylsulphate [see Abragam and Goldman (1982) for a fuller discussion].

Dynamic nuclear polarization has long been used for the production of polarized nuclear targets in particle physics (see again Abragam and Goldman 1982). It has also been the basis of a number of novel techniques in solid state physics. For example, the nuclear spins of ^{139}La ($I = \frac{7}{2}$) were polarized dynamically (Abragam and Chapellier 1964) in a single crystal of LMN doped with 1% Nd. The nuclear levels of the lanthanum ions are split by a nuclear electric quadrupole interaction, giving seven resolved NMR frequencies. By comparing the intensities of the signals of highest and lowest frequencies, the sign of the electric quadrupole splitting, previously unknown, was shown to be positive. The effective spin temperature of the lanthanum nuclei was deduced to be 1.2 mK, though the bath temperature remained at 1.5 K.

It was suggested by Abragam (1960) that the polarized nuclei could be demagnetized adiabatically, so that the polarized nuclear system is 'cooled' from mK temperatures to a much lower effective temperature of the order of 10 μK. Urbina and Jacquinot (1980) used the EPR of the electronic ground doublet of Tm^{2+} ($g = 3.45$, isotropic) as an impurity in CaF_2 as a 'pumping' mechanism at ~130 GHz in a field of 2.7 T at 0.7 K. This produced a polarization of 90% in the ^{19}F nuclei. The fluorine spins are then cooled to a temperature of about 5 μK by reducing the external field to ~0.005 T; in this process the thulium electron spins, relatively few in number, are cooled through cross-relaxation to the fluorine nuclei, since the spectral density of the Tm line width extends down to the resonance frequency of the fluorines (~0.2 MHz at 0.005 T). The cooling is demonstrated by observation of the thulium resonances within the low-field hyperfine triplet F = 1 ($S = \frac{1}{2}$; $I = \frac{1}{2}$). Only the lower of the two possible resonances is seen, because all the Tm nuclei are 'cooled' into the lowest level of this triplet. If instead the fluorine nuclei are polarized to a negative temperature, the Tm electron spins also reach a negative temperature, only the uppermost level of the Tm triplet being populated instead of the lowest. This is shown by

(a) only the upper Tm resonance is seen, and

(b) the EPR signal is reversed in sign.

In a further experiment, the thulium electron spin population was transferred from the lowest level of the triplet $F = 1$ to the singlet $F = 0$ some 1.1 GHz higher in energy. This was accomplished by applying an RF field of the correct frequency (1.214 GHz) to put this electronic transition on 'speaking terms' with the polarized fluorine nuclear spins.

In such a demagnetization of the polarized nuclear spins, their temperature is reduced by a factor of 10^3 to 10^4, insufficient to produce ordering within the nuclear system, that requires a temperature of order 0.1 μK or less. An ingenious alternative method, due to Abragam (1962), is to use adiabatic demagnetization in the rotating frame (ADRF). The nuclei are first dynamically polarized by pumping at the electron resonance frequency plus or minus the nuclear resonance frequency. After the oscillating pump field has been switched off, the applied field is changed slowly until the nuclear system is exactly at resonance, and the nuclear spins are polarized

in the rotating frame, normal to the steady magnetic field. Finally, the nuclear oscillating field is reduced to zero. There are several advantages of this method resulting from the presence of the high external field: electron spin–lattice relaxation times are very long (many days); NMR can be used as a probe with high sensitivity; the Hamiltonian for the dipolar interactions between the nuclei can be 'truncated', and varied with the direction of the applied field. Temperatures down to 0.1 μK in the nuclear spin system can be attained, both positive and negative. The ADRF can be carried out with more than one nuclear system, using different frequencies.

The first successful experiment (Chapellier et al. 1969, 1970) made use of a single crystal of CaF_2 doped with Tm^{2+} ions, and produced an antiferromagnetic arrangement of the ^{19}F nuclear spins, polarized parallel and anti-parallel to a [100] axis. Later, a ferromagnetic arrangement was attained with the external field along a [111] axis, verified by NMR of the rare isotope ^{43}Ca ($I = \frac{7}{2}$). In another tour de force, the presence of the antiferromagnetic state was observed by the Bragg scattering of a beam of polarized neutron spins from the fluorine nuclear spins (Abragam et al. 1972a). In the same year the precession of a beam of polarized neutron spins traversing the 'pseudo-magnetic field' of protons polarized dynamically in LMN doped with Nd^{3+} was observed, using an applied rotating magnetic field to produce a rotating 'pseudo-magnetic field' that flips the neutron spin (Abragam et al. 1972b). Such experiments have given values for the 'pseudo-magnetic nuclear moment' of the proton and of many other nuclear species (see Abragam and Goldman 1982).

8. Enhanced nuclear magnetism

8.1. *Introduction*

In an EPR experiment, the allowed electronic transitions are normally those for which the nuclear magnetic quantum number m_I does not change; the frequencies therefore yield no direct information on the size of the nuclear moments. Under some circumstances transitions in which m_I changes are partly allowed, and the resonant frequencies are then displaced by amounts proportional to the nuclear Zeeman energy. It was pointed out by Baker and Bleaney (1958) that, in addition to the direct interaction of the applied magnetic field with the nuclear magnetic moment, terms similar in form arise indirectly through cross-terms between the electronic Zeeman interaction and the magnetic hyperfine interaction. These are particularly important if there are low-lying excited crystal-field levels; if the magnetic ion is not at a site of cubic symmetry, the effective nuclear Zeeman interaction becomes anisotropic, and another term similar in form to a nuclear quadrupolar interaction may arise (provided $I \geqslant 1$) through quadratic effects of the magnetic hyperfine interaction. Such quantities are determined more directly and much more accurately by means of ENDOR, as illustrated by the measurements on the stable samarium isotopes of mass 147 and 149 in $(La,Sm)Cl_3$ by Chan and Hutchison (1972), described in section 3.2. For this system the electronic ground

state is a doublet, but similar terms arise also for an electronic singlet. They are directly related to the Van Vleck temperature-independent paramagnetism of such a singlet state.

A magnetic field with a component B_x along a principal magnetic axis x of an ion produces a quadratic energy change of the form

$$W = -\tfrac{1}{2}(g_J\mu_B)^2(a_xB_x^2), \tag{24}$$

together with similar terms

$$a_yB_y^2 + a_zB_z^2,$$

for the components B_y, B_z along the other principal axes. Here the parameter a_x represents a sum of terms $(2\alpha_x^2/X)$ where α_x is a matrix element of J_x from the ground singlet to an excited level of energy X. (Here we consider only levels within the ground manifold J.) The electronic magnetic moment m_x induced by the field B_x is

$$m_x = -\mathrm{d}W/\mathrm{d}B_x = a_x(g_J\mu_B)^2B_x. \tag{25}$$

If the nucleus has a spin I, the magnetic hyperfine interaction must be included in (24), so that it becomes

$$W = -\tfrac{1}{2}(a_x)(g_J\mu_BB_x + A_JI_x)^2. \tag{26}$$

This produces cross-terms that give the enhanced nuclear Zeeman interaction term $a_x(g_J\mu_BA_J)B_xI_x$, for which the coefficient can be written as

$$a_x(g_J\mu_BA_J) = \hbar(\gamma_x - \gamma_I). \tag{27}$$

Here $\gamma_x/2\pi$ is the resonance frequency in a field of 1 T along the x-axis, including the true nuclear term. An NMR measurement of this frequency can therefore be used to derive an indirect value for the Van Vleck paramagnetic moment, since

$$m_x/B_x = (g_J\mu_B/A_J)\hbar(\gamma_x - \gamma_I). \tag{28}$$

There are of course similar terms for the y,z axes, and in the absence of cubic symmetry, anisotropy arises because the values of α and X, and hence of the parameter a may be different for the various axes. An advantage of this method of measuring the Van Vleck moment, under conditions where inequivalent ions are present, is that the contribution from each type of ion can be found, where a measurement of the bulk susceptibility gives only the sum of all the individual contributions.

Finally, there is a quadrupole-like term from quadratic effects of the magnetic hyperfine interaction. These may be written as

$$P_xI_x^2 + P_yI_y^2 + P_zI_z^2, \tag{29}$$

where

$$P_x = -a_xA_J^2/2 = -(A_J/2g_J\mu_B)\hbar(\gamma_x - \gamma_I). \tag{30}$$

In cubic symmetry all three components of $\boldsymbol{P}$ are equal, and their sum becomes just

a constant $PI(I+1)$ that may be ignored. For axial symmetry the overall effect may be written as

$$P_2[I_z^2 - \tfrac{1}{3}I(I+1)] \tag{31}$$

with

$$P_2 = (A_J/2g_J\mu_B)\hbar(\gamma_\perp - \gamma_\parallel), \tag{32}$$

where the subscripts $\perp$ and $\parallel$ refer to directions perpendicular and parallel to the axis of symmetry. There are, of course, also terms P_1 and P_3 arising from the true electric quadrupole interactions resulting from the field gradients of the 4f electrons on the parent ion and the remainder of the lattice respectively.

It was pointed out by Al'tshuler (1966) that Van Vleck paramagnets with singlet ground states should show large increases in the effective nuclear magnetic moment that could be used in magnetic cooling; this idea has been exploited, particularly by Andres and Bucher (1968, 1971), using intermetallic lanthanide compounds of Pr and Tm (see section 4.4.3 of ch. 78, this volume). Such compounds are important because the conduction electrons provide a mechanism for heat transport, absent in insulators. NMR measurements of the enhanced nuclear Zeeman interaction have been made in a number of such intermetallic compounds with cubic symmetry by E.D. Jones; they are listed in the paper by Teplov (1977), who also summarizes results for a range of insulating compounds. Most of the latter have only low symmetry, and NMR results for compounds with axial symmetry are listed in table 10. The resonant frequencies are highly anisotropic, particularly when there are large matrix elements to a low lying level for one direction of the magnetic field, but not for the others ($TmVO_4$ is an extreme case). In many cases the NMR signal can be followed up to temperatures at which excited levels are populated, because the

TABLE 10
Enhanced NMR data for insulating compounds with axial symmetry. Values of $(\gamma/2\pi)$ in MHz T^{-1}, and P/h in MHz.

Compound	Isotope	I	$\gamma_z/2\pi$	$\gamma_{x,y}/2\pi$	P/h
$PrAlO_3$	141	$\frac{5}{2}$	94(6)	20.2(3)	(−)4.2(1)
$PrVO_4$	141	$\frac{5}{2}$	24.5	77.62	+3.35(3)
$HoVO_4$	165	$\frac{7}{2}$	15(5)	1526(3)	+25.9(3)
TmETS	169	$\frac{1}{2}$	5.6(4)	260.2(2)	
$LiTmF_4$	169	$\frac{1}{2}$	7.94(1)	245(1)	
$TmPO_4$	169	$\frac{1}{2}$	11.3	276	
$TmVO_4$	169	$\frac{1}{2}$	3450(10)*	94, 24	
$TmAsO_4$	169	$\frac{1}{2}$	706.5	370, 60	

TmETS = Thulium ethylsulphate has hexagonal symmetry. The other compounds have tetragonal symmetry, except $TmVO_4$ and $TmAsO_4$, that have doublet states split by Jahn–Teller distortions below 2.156 K and 6.1 K, respectively (see section 6). These lower the symmetry and the constants given are extrapolated to $T = 0$ K.
*Estimated value.

hyperfine field is motionally averaged by rapid relaxation between the electronic levels. The measured parameters are then thermal averages, and in $PrVO_4$ Bleaney et al. (1978a) were able to fit the results from 1 to 20 K by including parameters for both the first and second excited states. $PrAlO_3$ is unusual (Harley et al. 1973); it undergoes three separate phase transitions at $\sim$200 K, 150 K and 99(5) K, below which it becomes tetragonal, with the values listed in table 10.

8.2. *Enhanced nuclear magnetic resonance in $HoVO_4$*

High-resolution optical spectroscopy (Battison et al. 1975a) revealed that in $HoVO_4$ crystal-field splittings leave as the ground state a singlet, with a doublet at 21 cm^{-1}. These states are almost pure $|J_z\rangle = |0\rangle$ and $|\pm 1\rangle$, producing almost no magnetic moment along the c-axis, but a large moment normal to this axis because of matrix elements between the singlet and the doublet. The Zeeman effect for these levels confirmed the presence of high anisotropy, over 200:1 in the induced magnetic moment at liquid-helium temperatures.

The single stable isotope ^{165}Ho has $I = \frac{7}{2}$, and the natural nuclear resonant frequency is 9.0(1) MHz in a field of 1 T. However, the electronic moment produced by such a field induces an enormously greater field at the nucleus through hyperfine interaction, so that the resonant frequency is shifted upwards and becomes anisotropic. From NMR experiments at 500 MHz the constants in the effective nuclear spin Hamiltonian were found (Bleaney et al. 1978b) to have the values listed in table 10. Values of the parameters for a crystal of YVO_4 containing 2% Ho are almost identical. The contributions to the nuclear electric quadrupole interaction are estimated to be $P_1/h = -35$ MHz, $P_2/h = +35.3$ MHz; since these almost cancel, the measured value of 25.9 MHz implies a lattice contribution $P_3/h = \sim +25$ MHz. The NMR signals are strong, because the enhancement applies also to the RF field, provided this is in the (001) plane, but normal to the steady field. Essentially the RF field causes the induced electronic moment to oscillate in direction, producing a greatly enhanced RF field at the nucleus through the hyperfine interaction.

An alternative resonance method is to use longitudinal acoustic waves at about 1 GHz (Bleaney et al. 1983a). Measurements are made with a magnetic field in the (001) plane, and with acoustic waves propagated in this plane. The acoustic strains produce an effect in third order, involving both the applied magnetic field and the hyperfine interaction. Essentially the fluctuating acoustic strain modulates the direction of the electronic moment induced by the applied field; at the nucleus, through the magnetic hfs, this produces an oscillating magnetic field, giving rise to resonance transitions within the nuclear spin system. The acoustic waves are generated by a transducer of zinc oxide, grown directly onto a single crystal of $HoVO_4$ by sputtered epitaxial deposition. Pulses of order 100 ns duration are applied, the transducer alternately being switched from transmit to receive. Signals are observed corresponding both to transitions in which the nuclear magnetic quantum number changes by ± 1 or by ± 2, the latter being much weaker. Values of the acoustic absorption coefficient are given in table 11. The strong ± 1 transitions

TABLE 11

Acoustic attenuation for longitudinal waves in $HoVO_4$ (above) and the corresponding direct spin–lattice rates for longitudinal phonons (below). The frequency f is in GHz and ϕ = angle of magnetic field with [100] axis in the (001) plane.

Longitudinal waves in $HoVO_4$	
Along [100]	$5.7f^2T^{-1}\cos^2 2\phi + 950f^4T^{-1}\sin^2 2\phi$
Along [110]	$0.1f^2T^{-1}\sin^2 2\phi + 17f^4T^{-1}\cos^2 2\phi$
Direct spin–lattice rates for longitudinal phonons	
Along [100]	$1.9 \times 10^{-8}f^2T\cos^2 2\phi + 3.2 \times 10^{-6}f^4T\sin^2 2\phi$
Along [110]	$2 \times 10^{-10}f^2T\sin^2 2\phi + 9 \times 10^{-8}f^4T\cos^2 2\phi$

and the weaker ± 2 transitions have maxima and minima at different orientations of the magnetic field, 45° apart in the x–y plane. They are stronger by a factor ~ 100 for acoustic waves propagated along a [100] axis than for similar waves along a [110] axis.

As in magnetic resonance with electromagnetic waves, the intensity of absorption is proportional to the energy quantum $h\nu$ and the population difference $(h\nu/kT)$, giving in all cases a factor ν^2/kT. Thus the intensity of the ± 2 transitions, involving the square of the hyperfine interaction, increases with the second power of the frequency. The position is different for ± 1 transitions because of an additional frequency dependence; their acoustic matrix elements involve the magnetic field, and their intensity thus rises with the square of the magnetic field. This introduces a further factor proportional to ν^2, so that their intensity increases with the fourth power of the frequency. These frequency dependences have been confirmed in an experiment at liquid-helium temperatures where the frequency is varied from 800 to 1600 MHz, as shown in fig. 15. The measurements also verify that the absorption increases as T^{-1}.

The process of absorption of energy from an acoustic wave is the same as the 'direct process' by which thermal phonons induce transitions in the spin system, maintaining it in thermal equilibrium with the lattice. The rates for the direct process can therefore be calculated from the measurements, and are shown also in table 11. The differences in the spin–lattice relaxation rates for the two directions of phonon propagation correspond to those in the acoustic absorption. The results are in marked contrast to the measured overall relaxation rate, determined by observing recovery of the signal after saturation. In a low field (5 mT) the measured rate (Suzuki 1986) between 0.08 and 1.33 K is faster by a factor 10^{13} to 10^{15} than that calculated for the direct process for longitudinal waves. Transverse waves may give faster rates of relaxation, but the difference cannot account for the observed discrepancy. This has been ascribed to the presence of paramagnetic impurities, but the mechanism has only been identified by novel experiments of Jacquinot et al. (1986). These have been made on the enhanced holmium spin system, magnetized at a temperature of 50 mK in a field of 2 T, and then demagnetized to about 5 mK in a field of 50 mT. The results suggest that energy is transferred by spin–spin interaction

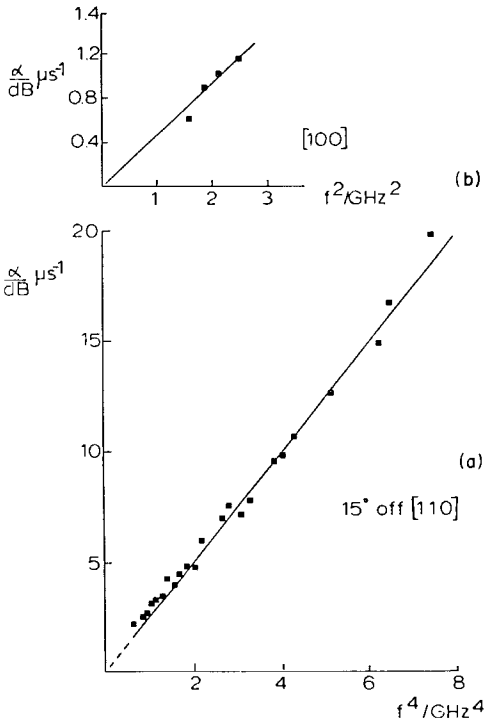

Fig. 15. Frequency dependences of the enhanced acoustic NMR in $HoVO_4$. The intensities of the strong $\delta m = 1$ transitions vary with the fourth power of the frequency, those of the $\delta m = 2$ transitions with the square of the frequency. (Briggs et al. 1984.)

to impurity ions with electronic moments such as dysprosium. These have a much higher resonance frequency, ~7 GHz, and are broadened, ~1.5 GHz, through interactions with the enhanced holmium moments. They 'talk' to a wide band of phonons, which then transmit energy rapidly from the impurity ions to the surrounding bath of dilute liquid helium-3 at 100 mK, the last barrier being the Kapitza resistance at the surface. It seems probable that a mechanism such as this could acount for the relaxation rates observed by Suzuki (at the lower field of 5 mT).

8.3. *$HoVO_4$: the enhanced nuclear ordered state*

Ordinarily the forces between nuclear moments are small, and the temperatures at which magnetic order should set in are correspondingly low. For example, in copper metal it is known from the work in Finland of Lounasmaa and his colleagues that the nuclei do not order until temperatures of about 0.01 μK. In holmium vanadate, however, we are dealing with 'nuclear lambs wearing electronic wolves' clothing', and the interactions are much larger. One result of this is that the resonance frequency depends on the shape of the sample, because of the large demagnetizing field set up by the Van Vleck paramagnetism. Comparison of NMR measurements on different shapes shows that the interactions between the enhanced nuclear moments are mainly dipolar in nature, and that exchange interaction is small. This

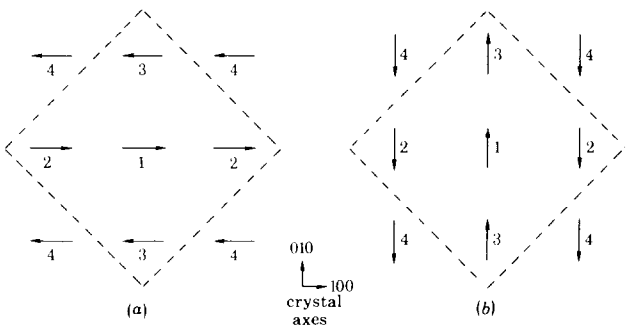

Fig. 16. Two alternative antiferromagnetic arrangements of the enhanced nuclear moments in $HoVO_4$. The largest interactions (almost wholly dipolar) are between the central ion and the four nearest neighbours within the diamond indicated by broken lines. (Bleaney 1980.)

made possible predictions about the nature of the ordered nuclear state, and the temperature below which it should occur (Bleaney 1980).

Because of the large anisotropy, the interactions are enhanced only when the nuclear moments lie in the (001) plane: it follows that in any ordered state the nuclear moments must be oriented in this plane. Each holmium ion has four equivalent holmium nearest neighbours, that lie close to this plane, and two equivalent ordered-spin systems are shown in fig. 16. In each case the 'end-on' positions are occupied by dipoles parallel to the central dipole, and the 'broadside-on' positions by anti-parallel dipoles. Thus the dipolar fields of all four neighbours add at the central site, but the exchange forces cancel, because they are the same for each of the four, two of which are parallel and two anti-parallel. Interactions with more distant dipoles are much smaller, and the arrangement shown gives the largest field at the centre, and hence the lowest energy. Each dipole in the lattice has the same arrangement of neighbours, so that translational symmetry is present, and the system corresponds to a simple two-sublattice antiferromagnet. For a moment of $1\,\mu_B$ on each site, the 'molecular field' in the ordered state is $B_I = 0.0734\text{T}$ at each site. The temperature at which an ordered state will develop is that at which the product of the nuclear susceptibility, expressed in units of μ_B/T, multiplied by this value of B_I, reaches unity. Allowing for the departure of the susceptibility from the Curie law at mK temperatures because of the nuclear electric quadrupole interaction, a value of $T_N = 4.8\,\text{mK}$ was predicted (Bleaney 1980), for the onset of anti-ferromagnetism

To check this experimentally, enhanced magnetic cooling is used. A single crystal, attached to the cold finger of a dilution refrigerator, is magnetized in a field of about 2 T at 35 mK. This removes practically all the nuclear entropy, since successive nuclear levels are split by nearly 100 mK. On demagnetization, a temperature of about 2 mK is reached; measurement of the RF susceptibility as the sample warms up shows that it passes through a maximum, confirming that an antiferromagnetic state has been reached at about the expected temperature (Suzuki et al. 1978).

To make further investigations, a nuclear orientation study was undertaken using

the long-lived (1200 years half-life) isomeric state of ^{166m}Ho ($I = 7$), produced by irradiating a crystal in a neutron pile. On magnetization at about 50 mK, a large anisotropy in the emission of six different γ-rays is observed, from which the nuclear moment of the radioactive isotope is deduced as (+) 3.60(6) n.m. (Allsop et al. 1980).

In fig. 16 the two equivalent ordered-spin arrangements in the ordered state, with the spins along the [100] and [010] axes, respectively, are not the only possible arrangements. There is also a whole range of 'puckered' configurations (Bleaney 1980), each of which has the same energy, that might be present as 'domains'. However, there is no anisotropy energy, and as soon as a small external magnetic field is applied, the spins should 'flop', and then turn towards the applied field to a 'ferromagnetic' arrangement with all the spins parallel. Such changes can be detected by detailed studies of the anisotropy of the γ-ray emission (Clark et al. 1987). The results indicate that initially most of the spins are pinned in the two mutually perpendicular orientations, but as soon as a small field is applied, half of the domains undergo spin flop, while the other half remain pinned; fields of 10–60 mT modify the numbers of each type of domain. These results are attributed to the presence of paramagnetic impurities, which also cause the lowest temperature attained after demagnetization to be 1.8 mK instead of 1.1 mK, as calculated.

Two further investigations of the ordered magnetic state have been made. Suzuki et al. (1984) have made a neutron study of the ordered state at Oak Ridge National Laboratory. The expected peak in the (100) Bragg diffraction peak was observed, confirming the presence of an AF ordered state, decaying to zero as the crystal warmed up. At Oxford, NMR of the ^{51}V nuclei ($I = \frac{7}{2}$) shows a magnetic splitting (Bleaney et al. 1987) of the nuclear electric quadrupole transition at 987 kHz; the magnitude agrees with that expected in the ordered state through the internal magnetic field set up by the enhanced nuclear moments of the ^{165}Ho spins. Finally, calculations were made by Bowden and Clark (1983) of the magnetic excitations in the ordered state.

8.4. *The $\Gamma_3(^2E)$ doublet*

In cubic symmetry the Γ_3 doublet is an unusual system with a quadratic electronic Zeeman effect, already mentioned in section 2.6. The effect is different for the two levels of this doublet, and anisotropic, though of course with cubic symmetry. The levels thus have displacements proportional to B^2, and are split except when $\boldsymbol{B}$ is along a [111] axis. These effects result from off-diagonal matrix elements between Γ_3 and the triplets Γ_4 and Γ_5. In the octahedral crystal field of $Cs_2NaHoCl_6$, a Γ_4 triplet lies at 10.1(2) cm^{-1} above the doublet, so that the quadratic Zeeman effect of the Ho^{3+} ion is unusually large. Enhanced NMR measurements have been made by Bleaney et al. (1981a). With $\boldsymbol{B}$ along a [111] axis, the resonant frequency for the nucleus ^{165}Ho ($I = \frac{7}{2}$) is 1980 MHz per tesla at the lowest temperature, but falls with increasing temperature, as shown in fig. 17, as the Γ_4 triplet becomes thermally populated. The NMR result confirms the susceptibility measurement of Hoehn and Karraker (1974), and corresponds to an induced electronic moment of 3.01(2)μ_B per tesla below about 2 K. For other directions of

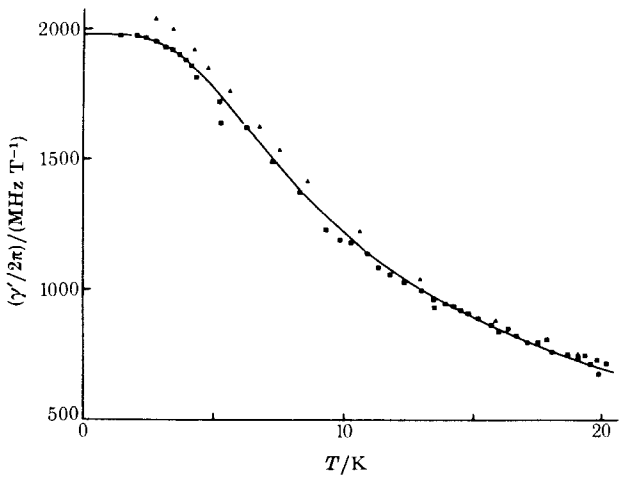

Fig. 17. Variation with temperature of the nuclear magnetic resonance frequency (MHz per tesla) of ^{165}Ho ($I = \frac{7}{2}$) in $Cs_2NaHoCl_6$ (Bleaney et al. 1981a). ▲ points deduced from susceptibility measurement of Hoehn and Karraker (1974).

magnetic field the doublet is split, and at 0.5 K the resonant frequency rises to even larger values because of the higher thermal population of the lower electronic level, with the larger induced moment. Such effects are largest for B along a [100] axis, where the quadratic Zeeman effect in the upper level is almost zero. Although such behaviour was predicted by Bleaney (1981), the agreement is only qualitative. The two levels have equal and opposite nuclear electric quadrupole interactions, that cancel through motional averaging at temperatures where the populations are equal. A quadrupole splitting of the NMR line should develop at low temperatures where the populations become unequal, but this is not observed. There are large motional effects in the system, as is apparent also in the EPR spectrum (see section 2.6). Similar enhancements in the NMR spectra of Tb^{3+} and Ho^{3+} in the analogous fluoride elpasolite compounds Rb_2NaTbF_6 and Rb_2NaHoF_6, were briefly reported by Tagirov et al. (1979); they indicate that these two lanthanide ions also have Γ_3 doublets as their ground states.

The theory of magnetic resonance and other effects for Γ_3 doublets is complicated, and further investigations have been made by Abragam and Bleaney (1982) and Bowden et al. (1985). The latter suggest that electronic quadrupole–quadrupole interactions may give rise to a quadrupolar ordered state at ~1 K, and that this may be the mechanism involved in transitions at about 400 mK in Cs_2NaHoF_6 found by Veenendaal and Brom (1982), and Veenendaal et al. (1983), and in $Cs_2NaHoCl_6$ by Bongers et al. (1983). In the latter compound, the large heat capacity anomaly seen by Suzuki et al. (1983) may also arise from such interactions. A transition to a nuclear ordered state occurs at ~1.5 mK (Suzuki et al. 1982, 1986).

8.5. *Thulium phosphate*

$TmPO_4$ is a tetragonal compound with a singlet ground state, and a first excited state (a doublet) at about $29\,cm^{-1}$; at helium temperatures it is a Van Vleck paramagnet and an enhanced nuclear magnet. Values of the principal resonance frequencies of the nucleus ^{169}Tm ($I = \frac{1}{2}$) are listed in table 10. The variation of these frequencies at higher temperature has been studied by Bleaney et al. (1983b), and correlated with a crystal-field calculation. An alternative crystal field, for which the wave functions of the ground singlet and first-excited singlet at about $70\,cm^{-1}$ are interchanged, is given by Hodges (1983). At higher field strengths the Van Vleck magnetization is no longer isotropic in the (001) plane, an effect attributed by Ioffe et al. (1983) to correlation of the Jahn–Teller distortions. Their results have been confirmed by NMR measurements at higher frequencies (Roinel et al. 1985). Along a [100] axis the frequency increases less rapidly than the applied field, but along a [110] axis the reverse is true.

Roinel et al. (1985) have made a detailed study of the relaxation rates for the enhanced ^{169}Tm ($I = \frac{1}{2}$) nuclear spins as a function of temperature from 0.05 up to 2 K, in fields up to 4 T perpendicular to the *c*-axis. The variation of the relaxation rate is rather complex; at 50–100 mK recovery is generally non-exponential. At fields below 0.5 T, relaxation is dominated by interactions with electronic impurities, but above 1 T effects are attributed to a bottle-neck between phonons and bath. It is concluded that the relaxation rate at low fields would be too short to allow study of a nuclear ordered state, produced by adiabatic demagnetization of the enhanced Tm nuclear spins.

An alternative technique is known as 'adiabatic demagnetization in the rotating frame', or ADRF (see section 7.4). This results in a cooling of the nuclear spins to temperatures sufficiently low that the nuclear system enters a co-operative phase, in which the nuclear spins are spatially ordered under the influence of their mutual interactions, though still precessing about the direction of the external magnetic field. The majority of such experiments have been carried out with the nuclei of diamagnetic ions, but one investigation has involved the enhanced nuclear moment of ^{169}Tm ($I = \frac{1}{2}$) in $TmPO_4$. In a field of 1 T, in this compound the enhanced values (Bleaney et al. 1983b) of the NMR frequency are 11.3 MHz (parallel to the *c*-axis) and 276 MHz (perpendicular) at liquid-helium temperatures (see table 10). The internuclear interactions vary as the square of these values, and the enhanced NMR line widths are anisotropic, being smallest when the field is accurately parallel to the *c*-axis. To produce dynamic nuclear polarization of the enhanced Tm nuclei, using the EPR line of Yb^{3+} present as an impurity for pumping, the alignment of the applied field needed to be along the *c*-axis within 2 minutes of arc (Abragam et al. 1984, Fermon et al. 1986). A positive advantage of the anisotropy is that polarization of the Tm nuclei occurs through interaction with the perpendicular components of their enhanced nuclear moments, and is therefore relatively rapid, a polarization of order 60% being obtained in 15 min.

On adiabatic demagnetization within the rotating frame, an ordered helical state

is obtained with transverse orientation of the Tm nuclei, since their interactions are largest in the (001) plane (cf. $HoVO_4$, section 8.3). An ordered state is attained only for positive temperatures, for which calculation indicates that an initial polarization of $\sim 20\%$ is needed, but not for population inversion (negative temperatures), for which 82% is required. The existence of the ordered state was demonstrated by observation of the NMR signal of the ^{31}P nuclei ($I = \frac{1}{2}$), using the transverse rotating Weiss field of the ordered Tm spins in conjunction with an externally applied RF field to produce resonant thermal mixing of the two spin systems (cf. Hartmann and Hahn 1962).

8.6. *The Gd^{3+} ion as a probe*

The lanthanide ions with a half-filled 4f shell, Eu^{2+} and Gd^{3+}, have long spin–lattice relaxation times and their EPR spectra can be observed up to and above room temperature. They have been used as probes to investigate a range of phenomena in Van Vleck paramagnets [see section 6.4 and the review by Mehran and Stevens (1982)]. In particular the seven EPR lines in the spectrum of the Gd^{3+} ion, $S = \frac{7}{2}$, are spread over a range of fields from 0 to ~ 0.8 T at 9 GHz because of the fine structure splitting. Unlike the Eu^{2+} ion, there is no complication from hyperfine structure because of the predominance of even–even isotopes. The phenomena observable include shifts in the g-value and line broadening as a function of temperature, giving clues to the nature of the interaction with the host lanthanide ions. In the Van Vleck paramagnet $TmPO_4$, the line widths of the Gd^{3+} spectra increase from some 0.005–0.007 T at 12 K, to 0.013–0.025 T at 100 K, and are still larger (~ 0.035 T) at 300 K. These widths and the increases with temperature are largest for the central lines in the spectrum, and smallest for the outer transitions, $\pm\frac{7}{2} \longleftrightarrow \pm\frac{5}{2}$. This is a valuable clue to their origin; they are interpreted as arising from random local distortions from tetragonal symmetry at the Tm^{3+} ion, present when the doublets at ~ 45 and 208 K are occupied. These are dynamic strains associated with the Jahn–Teller effect (Mehran et al. 1977); the lower doublet is shown to be strongly Jahn–Teller active by the acoustic measurements of Harley and Manning (1978), mentioned in section 6.3 (see fig. 12b). Similar but more dramatic effects (see section 6.4) are observed in $TmVO_4$ and $TmAsO_4$, where the ground state of the lanthanide ion in each case is a doublet, with a cooperative Jahn–Teller distorted phase at low temperatures (see section 6.3).

Another substance in which the interactions have been explored using the spectrum of the Gd^{3+} ion is $PrVO_4$. Here the energy levels of the Pr^{3+} ion are split by the tetragonal crystal field, giving singlets as the ground and first-excited state at 35 cm^{-1}, a doublet at 86 cm^{-1}, and another singlet at 127 cm^{-1} (Bleaney et al. 1978a). At helium temperatures the values of g for the Gd ion are increased by 0.002 (parallel) and 0.028 (perpendicular) above those for the same ion in YVO_4, while the line widths are larger by 0.001 T and 0.0028 T, for $\boldsymbol{B}$ along [001] and [110], respectively. These increases in width are greater than calculated from dipolar interaction, and are attributed to exchange interaction with the four nearest Pr ions. A detailed analysis is given by Mehran and Stevens (1982). At higher temperatures,

as other levels in $PrVO_4$ become occupied, the value of g for the Gd^{3+} decreases in the perpendicular plane, while in the parallel direction it increases slightly.

Similar measurements on Gd^{3+} in $EuVO_4$ and $EuAsO_4$ were used by Mehran et al. (1979) to study the various possible dynamical interactions between the Gd^{3+} and Eu^{3+} ions. The Eu^{3+} ion has a singlet ground state $J=0$, with an excited manifold $J=1$ at about $350\,cm^{-1}$. At the lowest temperatures the g-value for the Gd^{3+} ion is shifted down from its normal value of ~ 1.992 to 1.9814 in the vanadate and 1.9839 in the arsenate. These shifts result from the moment induced in the ground state of the europium ion by interaction with the Gd ion. At higher temperatures (measurements were made up to $\sim 570\,K$) the shift decreases, in accordance with theory, as $\coth(\Delta/2kT)$, where Δ is the energy of the level $(J, J_z) = (1,0)$ above the ground singlet $J=0$. The separations between the seven Gd lines also change, showing that the parameter B_{20} of the Stevens operator $B_{20}[3J_z^2 - J(J+1)]$ also decreases with temperature. More dramatic are the increases in line widths that occur as occupation of the Eu $J=1$ states rise with temperature: the increases are largest for the central transition $M = \frac{1}{2} \longleftrightarrow -\frac{1}{2}$, and smallest for the outermost transitions $M = \pm\frac{7}{2} \longleftrightarrow \pm\frac{5}{2}$. The changes are in excellent agreement with theory for dynamical magnetic or exchange interactions (predominately the latter), but not for fluctuating strains associated with the Jahn–Teller effect. In earlier EPR experiments [see Mehran and Stevens (1982)] the Eu^{2+} and Mn^{2+} ions were used as probes in the cubic samarium chalcogenides SmS, SmSe and SmTe. These compounds are semiconductors, and the value of g is increased above the free-spin value for Eu^{2+}, but decreased for Mn^{2+}. The shifts are most dramatic in SmS, where $g = 2.241(5)$ for Eu and is reduced to 1.05(1) for Mn.

9. Maser and laser experiments

9.1. *Solid state masers and lasers*

Following the successful operation of the ammonia gas molecule maser by Gordon et al. (1955), the use of a paramagnetic salt at low temperatures was proposed by Bloembergen (1956). The divalent nickel ion, $3d^8$, $S=1$, has three levels unequally spaced in the presence of a crystal field and a magnetic field. At liquid-helium temperatures the splitting is of order kT, and spin–lattice relaxation is sufficiently slow that paramagnetic transitions between the lowest and highest levels can be induced at a rate sufficient to make the population of the latter greater than that of the intermediate level. This 'population inversion' can be used to provide amplification at a microwave frequency, with a low noise background. The device is therefore used in applications such as radio-astronomy and satellite communication where the incoming background noise level also corresponds to a low temperature.

Lanthanide ions offer narrow EPR line widths, and the first successful device (Scovil et al. 1957) made use of three levels of the trivalent gadolinium ion, $^8S_{7/2}$, in lanthanum ethylsulphate. A 90 mg single crystal containing $\sim 0.5\%$ Gd, and $\sim 0.2\%$ Ce^{3+} to obtain suitable spin–lattice relaxation rates (Feher and Scovil 1957), was

placed in a resonator tuned to ~9 GHz and to 17.5 GHz. Transitions between the $|-\frac{5}{2}\rangle$ and $|-\frac{1}{2}\rangle$ levels of the gadolinium ion were induced at 17.5 GHz, and when this 'pump' power was raised above 100 mW, oscillation occurred at 9 GHz through population inversion between the $|-\frac{5}{2}\rangle$ and $|-\frac{3}{2}\rangle$ levels. Later versions to produce amplification rather than oscillation use a travelling 'slow-wave' structure. The active element is a 'ruby' crystal of Al_2O_3, containing Cr^{3+} ($3d^3$) ions, for which the ground state is a quartet ($S = \frac{3}{2}$) with a crystal-field splitting close to 11.5 GHz. Such a splitting combined with the Zeeman effect in a magnetic field at a suitable angle to the *c*-axis of the crystal is required to give allowed transitions at both 'pump' and 'signal' frequencies.

The possibility of maser action at optical frequencies was discussed by Schawlow and Townes (1958), and a pulsed ruby 'laser' was developed by Maiman (1960). The first optical laser action with a lanthanide ion was achieved using CaF_2 doped with 0.1% molar Sm^{2+} (Sorokin and Stevenson 1961). The divalent ions of Dy and Tm in CaF_2, and many trivalent 4f ions, in single crystal of $CaWO_4$, yttrium aluminium garnet (YAG) and in glass, have been found to produce laser output (see Geusic and Scovil 1964). Weak, narrow 4f–4f transitions give a laser output in the near infrared at ~1–2 μm wavelength, with relatively strong absorption bands that can be pumped in the visible region. High peak power outputs at 1.06 μm, ~50 MW in ns pulses, have been achieved in recent years from neodymium–YAG by special methods (see, e.g., Charlton and Ewart 1984).

9.2. *Optical radiation and magnetic resonance*

The variety of experiments involving optical radiation combined with magnetic resonance is so vast that only a brief outline of some techniques can be given here. Many of these experiments were carried out on ruby crystals, where the optical transitions associated with Cr^{3+} in Al_2O_3 are narrow, as for the 4f–4f transitions of many lanthanide ions. Here only experiments with the latter will be discussed.

The simplest type of experiment is the direct detection of magnetic resonance in excited states populated by optical 'pumping'. In an early example, an iodine-vapour–tungsten lamp was focussed onto a crystal of CaF_2, doped with Dy^{2+}, at 4.2 or 1.7 K (Sabisky and Anderson 1964). The low-lying triplet belonging to $^5I_8$ gives two resonance lines at 9.12 GHz, split through perturbations from the nearly Γ_3 doublet. Application of light produced a third resonance line of comparable intensity from a triplet state of the excited manifold $^5I_7$. For this line, the measured *g*-value of 4.69(2) overlaps the optical Zeeman value of 4.75(5), and the relaxation life-time is about 5 ms at 1.7 K. A similar optical pumping experiment (Sabisky and Anderson 1966) on Tm^{2+} in CaF_2 gave a resolved hyperfine structure [$A = 1160(6)$ MHz] from the isotope ^{169}Tm ($I = \frac{1}{2}$) in the Γ_7 doublet at 8966 cm^{-1} of the $^2F_{5/2}$ state. The value of $g = 1.453(2)$ is a little smaller than that calculated, (−)1.478; this reduction is larger than expected from measurements on the ground state. Similar results were obtained (Hayes and Smith 1971) for Tm^{2+} in SrF_2. An extensive discussion was given by Sabisky (1974).

Two photo-excited states of trivalent neodymium in $LaCl_3$ have been investigated

(Clarke and Hutchison 1971, Hessler and Hutchison 1973). The single crystals contained about 0.2% molar each of Nd^{3+} and U^{3+} ions; the latter ions have a strong, broad absorption band in the blue, and form efficient absorbing centres for optical pumping. Internal energy transfer then gives sufficient population of two excited states of the Nd^{3+} ions for EPR at 9 GHz and 24 GHz to be observed. These states are the crystal-field doublets of lowest energy belonging to $J = \frac{13}{2}$ and $J = \frac{15}{2}$, respectively, of the ^4I manifold. Hyperfine structure from each of the enriched odd isotopes of mass 143 and 145 was measured and compared with earlier ENDOR results for the ground state $J = \frac{9}{2}$. The relation $g_{\parallel}/g_{\perp} = A_{\parallel}/A_{\perp}$ is obeyed much more closely for the excited states than for the ground state, showing that admixtures from other J levels are much smaller.

In this system, greater pumping power was achieved by the use of an argon-ion laser, and Clemens and Hutchison (1983) were able to measure the EPR spectra at 24.5 GHz of pairs of neodymium ions. One remained in the ground state doublet of $J = \frac{9}{2}$, the other occupied a doublet (lifetime 18 ms) of the $J = \frac{15}{2}$ manifold. By making measurements in a whole plane of directions from the c-axis to the a-axis, they showed that axial symmetry was retained (nearest neighbours lie along the c-axis in $LaCl_3$), but there are small shifts in the g-values. As for pairs of ions both in the ground state doublet, the predominant interactions are magnetic dipole and superexchange, but comparison shows that the latter cannot arise from isotropic exchange between the real spins of the Heisenberg type. In another experiment with an argon-ion laser, Furrer and Hutchison (1983) made use of the fact that its wave number 19 429.67 cm^{-1} is only 1.26 cm^{-1} below that of an optical transition of the Nd^{3+} ion in $LaCl_3$, from the ground doublet of $^4I_{9/2}$ to a doublet of $^2G_{9/2}$. This transition can be tuned to exact resonance by application of a magnetic field. Application of power at 24.97 GHz to produce magnetic resonance in the ground state doublet then increases the population of the upper level of this doublet above its steady-state value at 1.3 K. Since optical pumping takes place from this upper level, the optical fluorescence signal is correspondingly increased. This was used as a detector for cross relaxation between the Nd^{3+} ions and Er^{3+} ions also present in the crystal, and it was found that this occurred when the neodymium Zeeman splitting was $\frac{1}{2}$, 1 or a multiple up to 4 of that of the erbium ions. This indicates that several ions are involved in the cross-relaxation process.

More sophisticated techniques, involving observation of light emitted from the magnetic ions in excited states [optical detection of magnetic resonance (ODMR)], have been reviewed by Geschwind (1972). Redistribution of population between magnetic sub-states, produced by magnetic resonance, produces an optical change that acts as a monitor of the EPR. Such techniques are extremely sensitive, making possible the observation of EPR of sparsely populated levels, not accessible by conventional methods. One method is to pump into a broad absorption band of higher energy, followed by radiationless decay to excited states, as in the experiments above, but to view the fluorescent output. Provided that thermalization has time to occur in the excited states, changes in population between the magnetic sub-states, caused by EPR, can be detected by observing the circular polarization of the fluorescent light. This method was used in a study of the Γ_8 quartet of the excited

state $4f^6 5d$ of Eu^{2+} in CaF_2, SrF_2 and BaF_2 by Chase (1970). Electric-dipole transitions from this state to the ground state $4f^7$ ($S = \frac{7}{2}$) give a sharp resonance line at 413 nm, with numerous weaker lines at higher energies and vibronic sidebands at lower energies. The splitting of the resonance line observed under applied stress and a magnetic field had previously confirmed that the excited state was a Γ_8 quartet. The ODMR experiments in CaF_2 gave a well-resolved hyperfine structure of the two isotopes of mass 151 and 153 (both with $I = \frac{5}{2}$) from a population of only 10^9 spins in the excited state. Dynamical Jahn–Teller effects in both the hfs and in the g-values were measured. The results were explained in terms of a large cubic crystal-field splitting of the 5d orbital, giving a lower ^2E state coupled by exchange interaction with the ^7F manifold of the $4f^6$ configuration.

Optical pumping using circularly polarized radiation has been used to produce inversion of the population of electron spins in the ground state of Tm^{2+} in CaF_2 by Anderson et al. (1966), and maser action at liquid-helium temperatures was demonstated by Duncan and Kiss (1963). Jeffries (1967) suggested that, by making use of the hyperfine splitting, enhancement of the nuclear polarization could also be achieved. Such an effect for Tm^{2+} in CaF_2 was demonstrated by Mollenauer et al. (1968). The enhanced polarization, both in the ground electronic doublet and in the nuclear system, was detected by observation of the differential absorption of right- and left-handed circularly polarized light of low intensity. Other effects observable with circularly polarized optical radiation are magnetic circular dichroic absorption (MCDA) and Faraday (magneto-optical) rotation (MOR), that arise respectively from the imaginary and real parts of the complex (optical) electric susceptibility. MCDA has been used by Sabisky and Anderson (1970) to measure the dependence on magnetic field and temperature of spin–lattice relaxation rates of Tm^{2+} in CaF_2, SrF_2 and BaF_2. Both direct and Raman processes were identified and measured, the former through the linear dependence on T and variation as the fourth power of the magnetic field, the latter through its variation as T^9. No resonance at a microwave frequency is involved, the fractional change in the optical circular dichroism being directly proportional to the difference in population of the Zeeman levels. Other results for these compounds have been discussed in section 4.2.

If the spin–lattice relaxation time is long compared with the lifetime of the excited state, there is insufficient time for thermalization to produce a population difference between the magnetic sub-states, but EPR may still be observed through selective feeding into these states. Effectively, the magnetization in the excited state retains some 'memory' of that in the ground state. For the cubic system CaF_2 with 0.05% Tm^{2+}, a detailed study of this effect for the doublet metastable level Γ_7 of $^2F_{5/2}$ was carried out by Anderson and Sabisky (1969). The existence of spin memory was demonstrated by saturating the ground doublet of $^2F_{7/2}$ with microwave radiation at 24 GHz; also, the degree of spin memory was strongly dependent on the wavelength (0.54–0.58 nm) of the unpolarized pumping light. It was found that optical cross-relaxation was a competing process, except at the lowest concentrations ($\sim 0.01\%$) of Tm^{2+}. The use of MCDA to monitor spin temperature, and of Brillouin scattering (using monochromatic radiation from an optical laser) to monitor phonon temperature, have been mentioned in discussion of the 'phonon avalanche' (section 4.3).

9.3. *Laser hole-burning experiments*

Although zero-phonon optical 4f–4f transitions have line widths $\sim 1\,\mathrm{cm}^{-1}$, the radiation from an optical laser has a much smaller width. If the lines are inhomogenously broadened, only a small 'spin packet' interacts with the laser radiation, and because of the high intensity of this radiation, 'optical pumping' takes place. An appreciable fraction of the ions in the ground-state spin packet is transferred to an excited state, and a 'hole' is burned in the ground state, with width much less than a MHz. This is small compared with hyperfine and nuclear Zeeman splittings. Application of an oscillatory magnetic field at a frequency corresponding to such a splitting transfers spins into the hole; provided this occurs at a rate comparable with that for the optical transitions, the optical pumping cycle is disturbed and the change may be used as a sensitive detector of the magnetic resonance. A tuneable laser is required, such as a CW dye laser, locked to a high-finesse reference cavity. In the last decade a number of NMR measurements have been made using such hole-burning techniques, of which two are described below.

The first is a determination of the nuclear magnetic moment of $^{141}\mathrm{Pr}$ ($I = \frac{5}{2}$), that differs from previous measurements in that it is made in an excited electronic state, and is also two orders of magnitude more precise. The substance used is CaF_2 doped with 0.01% Pr^{3+}. This ion replaces a Ca^{2+} ion, at a site where the symmetry is reduced from cubic to tetragonal (C_{4v}) symmetry through the presence of an adjacent F^- ion, that provides charge compensation, along a [001] axis in the vacant body-centred position. Since Pr^{3+} is a non-Kramers ion, the tetragonal crystal field splits all the levels into singlets or doublets. A dye laser is tuned to resonance (Macfarlane et al. 1982, 1984) at 594.097 nm with a transition from the lowest state, a doublet of $^3H_4$, to a singlet state, the lowest crystal-field component of $^1D_2$. Hole burning and optical pumping cause a reduction >95% in the fluorescent output. This output is measured with a phase-sensitive detector as the frequency of an RF square-wave modulated source is swept through resonance. The sample is at a temperature of 1.8 K, in a field of 2.21 T parallel to an [001] axis of the crystal. Transitions from the nuclear states $\pm\frac{3}{2}$ to $\pm\frac{1}{2}$ and $+\frac{1}{2}$ to $-\frac{1}{2}$ were observed, giving a nuclear electric quadrupole coupling constant $P/h = -0.44$ MHz for the $^1D_2$ state. Electronic contributions to the nuclear Zeeman splitting, of the type discussed in section 8 on enhanced nuclear magnetism, are zero. Only a small correction (+0.001 373) for intermediate coupling is required, and a value of 4.2754(5) nuclear magnetons (see table 1) is deduced, including a diamagnetic correction of +0.03536. In the second paper (Macfarlane et al. 1984) an enhanced value of 8.3 MHz per tesla for this level, perpendicular to the [001] axis, is measured, from which a pseudo-quadrupole contribution of +0.19 MHz is calculated, making the true EQQ interaction $P/h = -0.63$ MHz for $^1D_2$. For the ground doublet, $g_z = 3.89$, and the hyperfine constants are $A_z = 2.775(5)$ GHz, $P/h = +1.39$ MHz. Pseudo-quadrupole contributions to the latter are estimated to be $\sim +2$ MHz, and an enhanced nuclear Zeeman interaction of 16.5 MHz per tesla is measured, parallel to [001]. An interesting feature of this work is that the optical hole burning takes place through a mechanism (Burum et al. 1982) involving the coupling of the praseodymium ions to the neighbouring fluorines. This makes

possible NMR measurements on the neighbouring fluorine ions, with a line width ~ 5 kHz (HWHM). The resonance is shifted by interaction with the Pr ion, so that no spin flips occur with the bulk of the fluorines, but spin flips within this 'frozen core' provide the dominant mechanism for hole burning. The unshifted resonance from the 'bulk' fluorine ions was also observed, and used to measure the magnetic field within the crystal.

The second ion to be discussed here is Eu^{3+} ($4f^6$) for which $L = S = 3$. Atomic beam measurements on the Sm^{2+} atom, with the same configuration, have been discussed in sections 1.3 and 1.4. These, however relate to the levels with $J = 1$–6 of this manifold, while here we are concerned with the lowest level, $J = 0$. Since this is a singlet, with no magnetic hyperfine interaction, at first sight the nuclear moment could be determined by NMR. However, there are matrix elements of the hyperfine interaction and electronic Zeeman interaction, similar to those discussed in section 8 on enhanced nuclear magnetism, between $J = 0$ and the first excited level $J = 1$ at about 350 cm^{-1}. A major difference is that hfs matrix elements between manifolds J and $J = \pm 1$ are always negative, whereas they are positive for hfs matrix elements with a given J manifold. A consequence of this is that the pseudo-nuclear Zeeman interaction for $J = 0$ is of opposite sign to the true Zeeman interaction; the former is estimated by Elliott (1957) to be -0.89 times the latter. This 'anti-shielding' effect greatly reduces the net Zeeman interaction. Combined with long spin–lattice relaxation times and, in many compounds, quadrupole splittings of order 50 MHz, this has made it difficult to detect NMR directly of either of the two stable europium isotopes of mass 151 and 153, each with $I = \frac{5}{2}$. The values of the nuclear moments given in table 1 were obtained from radio-frequency measurements on the Eu atom and Eu^{2+} ion, each with configuration $4f^7$.

The Eu^{3+} ion has many optical transitions in the visible region. These have made it attractive for laser hole-burning experiments, for which the high sensitivity suggests that NMR could be detected indirectly. However, a crystal field of cubic symmetry does not allow either electric-dipole or magnetic-dipole transitions between the ground state $^7F_0$ and the excited state $^5D_0$. This is true also of $EuVO_4$, where the point symmetry at the R site is tetragonal (D_{2d}). Thus Cone et al. (1984) were able to observe hole-burning only with a range of quadrupole splittings, indicating that they arise from ions at sites where the local symmetry is reduced by the presence of a defect. Stronger optical transitions occur in compounds with lower symmetry, such as $YAlO_3$ with Eu^{3+} (Erickson and Sharma 1981, Shelby and Macfarlane 1981), and SrF_2, containing Sm^{2+} ions at perturbed cubic sites (Macfarlane and Meltzer 1985). Here we discuss only measurements on Eu^{3+} at 1% concentration in $LiYF_4$, made by Sharma and Erickson (1985).

In the tetragonal crystal $LiYF_4$ the point symmetry at the Eu site is S_4, and the optical transition is again forbidden and very weak, with a magnetic resonance signal of ~ 10 times the noise. Double resonances were observed in magnetic fields of 0, 0.01 and 0.0292 T with line widths (HWHM = half-width, half-maximum) ~ 0.002 of the frequency of resonance, indicating that the width arises from random crystal-field broadening. In zero field four NQR resonances were detected; two, at 13.110(4) and 26.146(8) MHz, are assigned to the transitions $\pm\frac{1}{2} \leftrightarrow \pm\frac{3}{2}$ and

$\pm\frac{3}{2} \longleftrightarrow \pm\frac{5}{2}$ for the isotope 151, and the other two, at 33.994(12) and 67.768(24) MHz, are assigned to the corresponding transitions for the isotope of mass 153. For each isotope the ratio of the two transition frequencies should be exactly 2 for axial symmetry; the measured ratios of 1.9944(9) and 1.9935(10) are attributed to a small departure from such symmetry.

In a magnetic field of 0.0292 T, splittings of the NQR lines for the isotope 151, that has the larger magnetic moment (see table 3), were resolved, both along the symmetry axis (the z-axis) and normal to it. The effective values of the magnetic splitting, in units of MHz per tesla, are found to be 4.08(4), parallel, and 0.64(4), perpendicular. From the value of g_I in table 3 the unshielded value should be 10.594(2) MHz per tesla, showing that admixtures of the $J = 1$ states produce large shielding effects. Normal to the c-axis the reduction by 94% approaches almost complete shielding.

The ratios of the quadrupole splitting for the two isotopes 151/153 are 0.3857(2), but a small correction for second-order effects of the magnetic hyperfine structure increases the ratio to 0.3900(8). This is slightly higher than the ratio of 0.3874(3) found by Erickson and Sharma (1981) from measurements on Eu^{3+} in $YAlO_3$, but bisects the two ratios of the quadrupole constants B listed in table 3.

10. Nuclear magnetic resonance

10.1. *Hyperfine interactions*

For the vast majority of stable nuclei the nuclear magnetic moments have been determined most accurately using nuclear magnetic resonance (NMR). This includes nuclei of the various transition groups with d-electrons, where compounds can be prepared with no unpaired electrons. For the 4f group only those ions with an empty shell (La^{3+}) or a full shell (Yb^{2+}, Lu^{3+}) have been measured in this way. The reason is that for all the other ions (except Eu^{3+}, discussed in section 9.3), the existence of unpaired electrons in the 4f-shell produces hyperfine fields at the nucleus of order 100–800 T. The presence of this large internal field makes it necessary to use the triple resonance atomic beam method (section 1.4) for atoms, or ENDOR (section 3) for ions in the solid state to measure the nuclear moments. With few exceptions, the values in table 1 have all been obtained by such methods, and the corresponding nuclear resonance frequencies for the stable isotopes are listed in table 12.

In paramagnetic salts the crystal field is the dominating interaction, partly or wholly lifting the $2J + 1$ degeneracy of each J-manifold with splittings of 10–300 cm^{-1}. When the lowest level is a degenerate doublet, the hyperfine interactions have been determined by EPR (section 2) or by ENDOR measurements (section 3). For the magnetic hyperfine interaction, the relation between the components of the tensors A and g within such an anistropic doublet is given by $A_x/g_x = A_y/g_y = A_z/g_z = A_J/g_J$ in an approximation (Elliott and Stevens 1953) that neglects admixtures of excited states from manifolds of different J. The corrections

TABLE 12

Values of the nuclear spin I and of the magnetic resonance frequency in MHz per tesla for the stable isotopes of the lanthanide ions. Based on the best values of the nuclear magnetic moments in table 1, without the correction for diamagnetic shielding, with rounded errors, calculated from the relation $\gamma/2\pi = 7.62253(2)\mu_I/I$.

Nucleus	Isotope	I	$(\gamma/2\pi)$ (MHz per tesla)
La	138	5	+6.6982(6)
	139	$\frac{7}{2}$	+6.0145(5)
Pr	141	$\frac{5}{2}$	+12.929(2)
Nd	143	$\frac{7}{2}$	−2.30(1)
	145	$\frac{7}{2}$	−1.42(1)
Sm	147	$\frac{7}{2}$	−1.759(2)
	149	$\frac{7}{2}$	−1.450(2)
Eu	151	$\frac{5}{2}$	+10.486(2)
	153	$\frac{5}{2}$	+4.630(2)
Gd	155	$\frac{3}{2}$	−1.304(2)
	157	$\frac{3}{2}$	−1.710(4)
Tb	159	$\frac{3}{2}$	+10.13(2)
Dy	161	$\frac{5}{2}$	−1.450(2)
	163	$\frac{5}{2}$	+2.030(1)
Ho	165	$\frac{7}{2}$	+8.99(6)
Er	167	$\frac{7}{2}$	−1.220(5)
Tm	169	$\frac{1}{2}$	−3.49(2)
Yb	171	$\frac{1}{2}$	+7.4382(2)
	173	$\frac{5}{2}$	−2.0488(1)
Lu	175	$\frac{7}{2}$	+4.8153(1)
	176	7	+3.377(24)

for such admixtures are fairly small, except for Pm^{3+} and Sm^{3+}, but even for the latter ion the values obtained for A_J from different compounds have a spread of only $\pm 2\%$ (Bleaney 1964). Before methods such as the triple resonance atomic beam technique produced direct measurements of nuclear moments, estimates of the latter were obtained from hyperfine structure measurements using empirical formulae for $\langle r^{-3} \rangle$, the mean inverse cube of the distance of the electrons from the nucleus. These were subject to considerable uncertainty [$\pm 25\%$ was allowed by Elliott and Stevens (1953)], and several efforts were made to improve them. These were either empirical (e.g., Bleaney 1955) or theoretical (Judd and Lindgren 1961, Lindgren 1962, Freeman and Watson 1962). Over the years further refinements have been introduced into the theory; for example, Freeman and

TABLE 13
Values of A_J/h, of JA_J/h and of P/h (all in MHz) for the stable isotopes of the trivalent ions.

Ion	J	Isotope	I	A_J/h (MHz)	JA_J/h (MHz)	P/h (MHz)
Pr	4	141	$\frac{5}{2}$	+1093(10)	+4372(40)	−2.6
Nd	$\frac{9}{2}$	143	$\frac{7}{2}$	−220.3(2)	−991.4(9)	−5.3
		145	$\frac{7}{2}$	−136.9(1)	−616.0(5)	−2.8
Sm	$\frac{5}{2}$	147	$\frac{7}{2}$	−240(3)	−600(8)	−4.8
		149	$\frac{7}{2}$	−194(3)	−485(8)	+1.4
Gd	$\frac{7}{2}$	155	$\frac{3}{2}$		(+42)	(−0.16)
		157	$\frac{3}{2}$		(+55)	(−0.17)
Tb	6	159	$\frac{3}{2}$	+530(5)	+3180(30)	+386
Dy	$\frac{15}{2}$	161	$\frac{5}{2}$	−109.5(22)	−821(16)	+219
		163	$\frac{5}{2}$	+152.4(30)	+1143(22)	+228
Ho	8	165	$\frac{7}{2}$	+812(1)	+6500(10)	+60
Er	$\frac{15}{2}$	167	$\frac{7}{2}$	−125.3(12)	−940(9)	−68
Tm	6	169	$\frac{1}{2}$	−393.5	−2333	–
Yb	$\frac{7}{2}$	171	$\frac{1}{2}$	+887.2(15)	+3105(5)	–
		173	$\frac{5}{2}$	−243.3(4)	−852(2)	−316

The values are based on relatively few data, and the errors are estimated, not statistical. The values of P/h (for the state $J_z = J$) are less reliable than these for the magnetic hyperfine interaction.

Desclaux (1979) have made relativistic Dirac–Fock calculations of the spin–orbit coupling, together with $\langle r^{-3} \rangle$, $\langle r^2 \rangle$, $\langle r^4 \rangle$, $\langle r^6 \rangle$ and other data for divalent and trivalent ions of the 4f group.

A list of 'best' values of A_J/h has been given by Bleaney (1964, 1972a); a slightly updated version is given in table 13. In part, the stimulus for this work was the realization that values deduced from EPR measurements on insulating compounds afforded a useful comparison with hyperfine interactions measured in lanthanide metals, alloys and intermetallic compounds. The hyperfine Hamiltonian can be written as

$$\mathcal{H} = ha_0 I_z + P[I_z^2 - \tfrac{1}{3}I(I+1)], \tag{33}$$

provided that the moment in the ordered state lies along a unique symmetry axis, such as the c-axis of a simple hexagonal structure. In other cases extra terms are required in the electric quadrupole interaction. If the ordered state at low temperatures is that with a value of $J_z = J$, then $a_0 = JA_J/h$, for which values are also listed in table 13. These include contributions to the magnetic hyperfine interaction from 'core polarization' (c.p.), but in electrically conducting materials there are further effects from the conduction electrons. For ions with a half-filled 4f shell, the net field varies considerably; e.g., in conducting compounds of Gd, from (−)35 T in GdN to +43 T in $GdFe_2$. In metallic Gd and Eu the core-polarization field (cf. section 1.4) is estimated to be −35 T, while that from conduction electrons (c.e.) contains two

comparable contributions of opposite sign. [References to early measurements are given in the paper by Bleaney (1972a)]. For other ions, the core-polarization field is assumed to be proportional to $S = (g_J - 1)J$, and is less than 10% of the whole. For example, from NMR measurements on ^{165}Ho in alloys with Gd, Tb and Dy, Mackenzie et al. (1974) have deduced a field of +12 T from c.e. polarized by the parent Ho ion, and $-8.3\langle S\rangle$ T from c.e. polarized by neighbouring ions, where $\langle S\rangle$ is the mean spin of the alloy. The c.p. contribution is estimated to be −20 T out of a total of 718(5) T for pure holmium metal [recalculated from the values of a_0 (table 14) and of $\gamma/2\pi$ (table 12)]. The overall situation was reviewed by Bleaney (1972a) and, more recently and comprehensively, by McCausland and Mackenzie (1980). The experimental data are obtained either from thermal methods (hyperfine heat capacity), or spectroscopic methods (Mössbauer, NMR). Of these, NMR is generally the most accurate, and a range of experimental values is listed in table 14. Except for the earlier members of the series, particularly Sm, for which admixtures from excited J-states are most important, these values lie within 3% of these of JA_J/h in table 13. A detailed exposition, including measurements on a range of intermetallic compounds, is given in the work of McCausland and Mackenzie (1980), where relaxation mechanisms in conducting materials are also discussed.

In europium metal and in a number of cubic chalcogenide compounds the europium ion is divalent, and NMR has been used to investigate the ordered state (see section 5.2). Measurements have also been made on a number of trivalent ions in ordered insulating compounds. The precision obtainable is illustrated by ^{165}Ho in the ferromagnet $Ho(OH)_3$, where the spectrum is centred on 5013(1) MHz, and a 'pseudo-octupolar' term wI_z^3 with $w = 0.25$ MHz is needed (see section 5.4) to fit the

TABLE 14

NMR values of a_0 and of P/h (both in MHz) for the stable isotopes of the trivalent ions in the pure metal, and in a dilute alloy in Gd metal. The values are based on the work of Bleaney (1972a), except those for Ho, which are taken from the work of Mackenzie et al. (1974).

Isotope		I	Pure metal		Dilute alloy	
			a_0	P/h	a_0	P/h
Nd	143	$\frac{7}{2}$			834(3)	2.3(5)
	145	$\frac{7}{2}$			519(3)	1.8(5)
Sm	147	$\frac{7}{2}$			624(3)	4.8(5)
	149	$\frac{7}{2}$			516(3)	2.5(5)
Tb	159	$\frac{3}{2}$	3120	337	3068(3)	351
Dy	161	$\frac{5}{2}$	830(3)	193(2)	817(3)	200(2)
	163	$\frac{5}{2}$	1162(3)	204(2)	1144(3)	211(2)
Ho	165	$\frac{7}{2}$	6444(10)	54(2)	6352(2)	57.3(5)
Er	167	$\frac{7}{2}$	913(3)	53(2)	896(3)	57(2)
Tm	169	$\frac{1}{2}$			2223(3)	–

experimental data (Bunbury et al. 1985). Enhanced NMR in singlet electronic states has been outlined in section 8; the Eu^{3+} ion differs (see section 9.3) in that it exhibits an 'anti-shielding' effect to applied magnetic fields, so that its effective NMR frequency is reduced. The situation is different for an exchange field, for this has no direct interaction with a nuclear magnetic moment, but it does have a matrix element between the ground state $J = 0$ and the excited state $J = 1$. As for a magnetic field, this produces a splitting of the nuclear levels through the hyperfine interaction. This may be large because exchange fields are generally greater in magnitude than any applied magnetic field, as is illustrated by the case of europium iron garnet (EuIG). Streever (1969) observed NMR in a polycrystalline powder of EuIG at 4.2 K, the resonances being ascribed to nuclei in domain walls. For ^{151}Eu, with the larger magnetic moment, resonance occurs at $a_0 = 740$ MHz, with an unresolved quadrupole splitting $2P/h \sim 5$ MHz between adjacent lines, while for ^{153}Eu $a_0 = 327$ MHz and $2P/h = 13$ MHz. Subsequently, Streever and Caplan (1971) detected NMR in a spherical single crystal of EuIG at 4.2 K in an applied field of 0.8 T. This is sufficient to saturate the magnetization in three principal directions, for which resonance frequencies of 680, 740 and 400 MHz were obtained. The theory is discussed including effects from both $J = 1$ and $J = 2$ states admixed by exchange interaction and the orthorhombic crystal field.

10.2. *Nuclear magnetic resonance of near-neighbour nuclei*

Dipolar and transferred hyperfine interactions between an R-ion and nuclei of neighbouring ions have mostly been determined by ENDOR (see section 3.2) in diamagnetic crystals doped with 0.1–1% of R-ions. An alternative is to use a direct NMR measurement with sensitive equipment (see Wolfe 1977). Nuclei with the highest resonance frequency are the easiest to measure, and for this reason ^{1}H and ^{19}F have mostly been observed. At temperatures below 4 K and at high magnetic fields, the electronic moment relaxes so slowly that it produces a shift in the resonance frequency of near neighbour (nn) nuclei proportional to the electronic magnetic moment on the R-ion. If this arises from a doublet, there are two possible moments, parallel and anti-parallel to the applied field (the latter with the lower thermal occupation), and two shifts are produced, identifiable by their different signal intensities. Wolfe and Markiewicz (1973) have applied this to ^{19}F nuclei, neighbours of Yb^{3+} in CaF_2, while King et al. (1972) observed the proton resonance from hydrated waters near to Yb^{3+} in yttrium ethylsulphate (YES). A detailed analysis of the latter experiments is given by Wolfe (1977), who concluded that, within experimental error, the shift for the nearest protons is wholly dipolar in character.

The opposite regime occurs at higher temperatures, where the shift is proportional to the time-averaged moment on the paramagnetic ion, and hence to the susceptibility. The averaging is effective only if the spin–spin or (more usually) the spin–lattice relaxation rates for the electronic moment on the R-ion are high compared with the NMR line width. In the cubic intermetallic compounds PrP, PrAs, TmP, TmAs and TmSb, the enhanced NMR of ^{141}Pr ($I = \frac{5}{2}$) and ^{169}Tm ($I = \frac{1}{2}$) could be

followed up to temperatures at which the enhancement falls to about half its maximum value, obtained when only the ground singlet state is occupied. NMR of ^{31}P ($I = \frac{1}{2}$) and ^{75}As ($I = \frac{3}{2}$) could be followed from 4 K to over 500 K with a shift proportional to the susceptibility of the 4f ions. A survey of results for these and other compounds is given by Jones (1969).

In insulating compounds the relaxation rates may become so slow that the NMR lines are broadened, and in extreme cases they may become undetectable. Apart from the simple fluorides RF_3, with orthorhombic symmetry, the series $LiRF_4$ with tetragonal S_4 symmetry has been studied by a variety of techniques (cf. section 5.3). Examples are neutron diffraction (Als-Nielsen et al. 1975); optical and magnetic measurements (Cooke et al. 1975, Battison et al. 1975b, Beauvillain et al. 1978); EPR up to 600 GHz (Magariño et al. 1980). NMR measurements at 295 K on single crystals with R = Tb, Dy, Ho and Er, were made by Hansen and Nevald (1977), and extended down to 1.3 K for the Tb and Ho compounds by Nevald and Hansen (1978) in fields up to 4 T. For the light nucleus ^7Li ($I = \frac{3}{2}$) the shift is dominated by dipolar interaction, but for ^{19}F ($I = \frac{1}{2}$) the dipolar and transferred hyperfine interactions are comparable in magnitude. In $LiHoF_4$, which becomes ferromagnetic below 1.53 K, signals could be followed down to the lowest temperature, but in $LiTbF_4$ ($T_C = 2.87$ K) signals disappeared at temperatures of order 10–60 K, presumably because of increasingly long relaxation times. In the crystal $LiTmF_4$, where the Tm^{3+} ion is an enhanced nuclear paramagnet, a detailed study of the NMR lines of ^{19}F at temperatures up to 25 K has revealed that the shift is not accurately proportional to the paramagnetic susceptibility of the Tm ion (Eremin et al. 1978). The deviation is ascribed to higher multi-pole moments on the Tm ion interacting with the nuclear moments on the fluorine ions.

In an NMR study at room temperature, Sato et al. (1980) have determined the co-ordinates of the hydrate protons in erbium ethylsulphate (ErETS) and erbium chloride, $ErCl_3 \cdot 6H_2O$. The paramagnetic shift was found to be point-dipolar within experimental error, and it was concluded that proton coordinates can be determined by this method with an accuracy of 0.005 nm.

The use of lanthanide ions in high resolution NMR of protons in liquids was initiated by Hinckley (1969), who showed how some paramagnetic lanthanide chelates could be used to induce stereo-specific chemical shifts. Spectral analysis was facilitated by reducing the complexity of the spectra without loss of spectral resolution, and by making use of the definite relationship between the magnitude of the shifts and the details of molecular geometry. Furthermore, lanthanide 'shift reagents' can be used both in aqueous solutions and in organic solvents. The shifts are considerably larger than the usual 'diamagnetic' chemical shift, and arise both from a 'contact' interaction, proportional to $\langle S_z \rangle$, the projection of the net electron spin moment on the applied magnetic field, and from dipolar interaction. Spatial averaging through rapid molecular motion means that the latter produces a shift only if the magnetic susceptibility of the R-ion is anisotropic. A concise theory (Bleaney 1972b) predicts how such shifts should vary along the 4f series, together with the temperature dependence. Although the magnetic properties of an isolated group may be very anisotropic, the short life-time ($\sim 10^{-13}$ s at room temperature)

of any given state means that a time averaged moment must be calculated, allowing for the Boltzmann factors in the population of such states. This results in a second order anisotropic susceptibility, varying as T^{-2} (for Eu^{3+}, with a singlet ground state, the temperature variation is more complex). For a given value of the geometrical factor $r^{-3}(3\cos^2\theta - 1)$, the shift varies through the R-series as $g_J^2 J(J+1)(2J-1)(2J+3)\langle J\|\alpha\|J\rangle$, where the last term is the Stevens factor for crystal-field interactions of the second degree, assumed to be constant through the series for a given complex. Much the largest effects arise from Tb^{3+} and Dy^{3+} ions. In a general review, Reuben and Elgavish (1979) conclude that this theory 'accounts satisfactorily for the dipolar shifts in lanthanide complexes'. Details of numerous applications of such shift reagents are given in this review and in a following article (Reuben 1979) covering systems of biological interest.

10.3. *Nuclear electric quadrupole resonance*

For nuclei with $I \geqslant 1$, an electric quadrupole interaction may be present, and magnetic resonance transitions can be observed at finite frequencies in the absence of an applied magnetic field. This is generally known as nuclear electric quadrupole (NEQ) resonance; for the Hamiltonian of eq. (33) the frequencies are multiples of $(2P/h)$. This technique was applied by Edmonds (1963) to measure the NEQ frequencies for the nucleus ^{139}La ($I = \frac{7}{2}$) in three compounds with axial symmetry. The values of P/h (in MHz) were 0.505(3), 0.493(3) and 0.574(3) for the ethylsulphate, the double nitrate and the anhydrous trichloride, respectively. Much larger frequencies are observed for some of the heavier lanthanides, partly because of their bigger nuclear electric quadrupole moments (see table 1). In the ethylsulphates the values are $P/h = -43(2)$, $-36(2)$ and 32.57(6) MHz for ^{159}Gd, ^{161}Dy and ^{175}Lu, the method used being respectively nuclear alignment, Mössbauer and NEQ spectrometry. The systematics for a wide range of R isotopes in the ethylsulphates were reviewed by Blok and Shirley (1966), who list references to the original publications. They extract values of the quadrupole shielding parameters, using the relation $P = -[3Q/I(2I-1)](1-\gamma_\infty)A_{20}$ together with values of $V_{20} = A_{20}(1-\sigma_2)\langle r^2\rangle_{4f}$ obtained from crystal-field splittings determined (mainly) from optical spectroscopy. Here the parameter γ_∞ is the shielding factor for the electric-field gradient at the nucleus introduced by Sternheimer (1950), and σ_2 is a corresponding term for that acting on the 4f electrons. From estimates or measured values of Q the ratio $(1-\gamma_\infty)/(1-\sigma_2)$ is derived, and Blok and Shirley found that for the heavier lanthanide ions $(1-\sigma_2) = 0.4(1)$, assuming $\gamma_\infty = -80$, based on values of Watson and Freeman (1964).

As a complementary investigation to the ENDOR determination of proton co-ordinates in lanthanum nicotinate dihydrate (see section 3.2), Davidson et al. (1981) have observed NEQ resonance of three inequivalent ^{14}N ($I = 1$) on pyridine sites and four hydrate ^{1}D ($I = 1$) nuclei at 77 K in this compound. They made use of a highly sensitive technique in which energy fed into the NEQ resonances in zero magnetic field is transferred internally to nearby protons, and then detected by proton NMR following rapid movement of the sample into a field of 1 T. The NEQ

resonance of ^{17}O ($I = \frac{5}{2}$) (Hsieh et al. 1972, Brosnan and Edmonds 1980) and ^{1}D (Edmonds and Mailer 1977, 1978) can easily be measured at their natural abundances of (respectively) 0.037% and 0.0156%. Single crystals are not required; high-resolution spectra are obtained from powdered solids and frozen solutions. For nuclei with $I = 1$, at sites of lower than axial symmetry, three resonances are observed from each site, and an aid to identification is provided by the requirement that the sum of two frequencies must be equal to the third. The structural information obtained by such NEQ resonance is compared by Davidson et al. with that from X-ray crystallography.

We conclude this survey by a brief reference to a relation between NEQ measurements and the well-known 'lanthanide contraction' – the steady decrease in ionic radius from 0.115 nm for La^{3+} to 0.093 nm for Lu^{3+} (values from Evans 1964). This results in corresponding changes in the lattice constants of a series of compounds. The vanadates, RUD_4 exhibit the tetragonal structure, space group $14_1/amd$ (D_{4h}^{14}) throughout the series from Pr^{3+} to Lu^{3+}. The NEQ splitting for the isotope ^{51}V ($I = \frac{7}{2}$) has been determined for all the vanadates except Pm^{3+} (that has no stable isotopes), and shown to vary smoothly (Bleaney et al. 1982a) with the ratio of the lattice constants of the unit cell c_0/a_0. A value of 0.67(2) is obtained for the product $Q(1 - \gamma_\infty)$ and, combined with $Q = -0.052(10)$ barns (Childs 1967), gives a value of $-12(3)$ for the Sternheimer shielding parameter γ_∞ of the isotope ^{51}V.

References

Abragam, A., 1955, Phys. Rev. **98**, 1729.

Abragam, A., 1960, C.R. Hebd. Séances Acad. Sci. **251**, 225.

Abragam, A., 1962, C.R. Hebd. Séances Acad. Sci. **254**, 1267.

Abragam, A., 1963, Cryogenics **3**, 42.

Abragam, A., and B. Bleaney, 1970, Electron Paramagnetic Resonance (Clarendon Press, Oxford); Corrected reprint, 1986 (Dover Publications Inc., New York).

Abragam, A., and B. Bleaney, 1982, Proc. R. Soc. London Ser. A **382**, 61.

Abragam, A., and M. Chapellier, 1964, Phys. Lett. **11**, 207.

Abragam, A., and M. Goldman, 1982, Nuclear Magnetism: Order and Disorder (Clarendon Press, Oxford).

Abragam, A., G.L. Bacchella, C. Long, P. Meriel, J. Piesvaux and M. Pinot, 1972a, Phys. Rev. Lett. **28**, 805.

Abragam, A., G.L. Bacchella, H. Glättli, P. Meriel, J. Piesvaux and M. Pinot, 1972b, C.R. Hebd. Séances Acad. Sci. B **274**, 423.

Abragam, A., J.F. Jacquinot, M. Chapellier and M. Goldman, 1972c, J. Phys. C **5**, 2629.

Abragam, A., G.L. Bacchella, H. Glättli, P. Meriel, J. Piesvaux and M. Pinot, 1976, Physica B **81**, 245.

Abragam, A., V. Bouffard, C. Fermon, G. Fournier, J.F. Gregg, J.-F. Jacquinot and Y. Roinel, 1984, C.R. Hebd. Séances Acad. Sci. **299**, 509.

Akopyan, G.G., V.P. Alfimenikov, L. Lason, O.N. Ovchinnikov and E.I. Shapiro, 1975, Zh. Eksp. & Teor. Fiz. **69**, 777.

Akopyan, G.G., V.P. Alfimenikov, L. Lason, O.N. Ovchinnikov and E.I. Shapiro, 1976, Sov. Phys.-JETP **42**, 397.

Albertson, W., 1937, Phys. Rev. **52**, 644.

Allsop, A.L., B. Bleaney, G.J. Bowden, N. Nambudripad, N.J. Stone and H. Suzuki, 1980, Proc. R. Soc. London Ser. A **372**, 19.

Als-Nielsen, J., L.M. Holmes, F. Krebs Larsen and H.J. Guggenheim, 1975, Phys. Rev. B **12**, 191.

Al'tshuler, S.A., 1966, JETP **3**, 112.

Al'tshuler, S.A., R.M. Valisev, B.I. Kochelaev and A.Kh. Khasanov, 1971, JETP-Lett. **13**, 382.

Al'tshuler, S.A., R.M. Valishev, B.I. Kochelaev and A.Kh. Khasanov, 1972, Sov. Phys.-JETP **35**, 337.

Ambler, E., 1960, Progr. Cryogenics **2**, 235.

Anderson, C.H., and E.S. Sabisky, 1968, Phys. Rev. Lett. **21**, 987.

Anderson, C.H., and E.S. Sabisky, 1969, Phys. Rev. **178**, 547.

Anderson, C.H., H.A. Weakliem and E.S. Sabisky, 1966, Phys. Rev. **143**, 223.

Anderson, R.J., J.M. Baker and R.J. Birgeneau, 1971, J. Phys. C **4**, 1618.

Andres, K., and E. Bucher, 1968, Phys. Rev. Lett. **21**, 1221.

Andres, K., and E. Bucher, 1971, J. Appl. Phys. **42**, 1522.
Argyle, B.E., N. Miyata and T.D. Schultz, 1967, Phys. Rev. **160**, 413.
Axe, J.D., and G.H. Dieke, 1962, J. Chem. Phys. **37**, 2364.
Ayant, Y., E. Beloritzky and J. Rosset, 1962, J. Phys. (France) **23**, 201.
Bagguley, D.M.S., and G. Vella-Colleiro, 1969, J. Phys. C **2**, 2310.
Baker, J.A., and D.S. Daunt, 1967, Phys. Rev. **155**, 545.
Baker, J.M., 1971, Rep. Prog. Phys. **34**, 109.
Baker, J.M., and B. Bleaney, 1958, Proc. R. Soc. London Ser. A **245**, 156.
Baker, J.M., and G. Currell, 1976, J. Phys. C 9, 3819.
Baker, J.M., and J.P. Hurrell, 1963, Proc. Phys. Soc. **82**, 742.
Baker, J.M., and D. van Ormondt, 1974, J. Phys. C **7**, 2060.
Baker, J.M., and E.I.B. Williams, 1962, Proc. R. Soc. London Ser. A **267**, 283.
Baker, J.M., and R.L. Wood, 1980, J. Phys. C **13**, 4751.
Baker, J.M., R. Buisson and J.-C. Vial, 1977, J. Phys. C **10**, 4407.
Ball, M., W.P. Wolf and K.A.G. Wyatt, 1964, Phys. Lett. **10**, 7.
Battison, J.E., A. Kasten, M.J.M. Leask and J.B. Lowry, 1975a, Phys. Lett. A **55**, 173.
Battison, J.E., A. Kasten, M.J.M. Leask, J.B. Lowry and B.M. Wanklyn, 1975b, J. Phys. C **8**, 4089.
Bauminger, E.R., I.R. Novik and S. Ofer, 1959, Phys. Lett. A **29**, 199.
Beauvillain, P., 1979, Thesis, Centre d'Orsay, Université Paris Sud.
Beauvillain, P., J.-P. Renard, I. Laursen and P.J. Walker, 1978, Phys. Rev. B **18**, 3360.
Becker, P.J., G. Dummer, H.G. Kahle, L. Klein, G. Muller-Vogt and H.C. Schopper, 1970, Phys. Lett. A **31**, 499.
Becker, P.J., M.J.M. Leask and R.N. Tyte, 1972, J. Phys. C **5**, 2027.
Bessent, R.G., and W. Hayes, 1965, Proc. R. Soc. London Ser. A **285**, 430.
Birgeneau, R.J., 1967, Phys. Rev. Lett. **19**, 160.
Birgeneau, R.J., M.T. Hutchings and R.N. Rogers, 1968, Phys. Rev. **175**, 1116.
Bleaney, B., 1951, Philos. Mag. **42**, 441.
Bleaney, B., 1955, Proc. Phys. Soc. A **68**, 937
Bleaney, B., 1963, J. Appl. Phys. **34**, 1024.
Bleaney, B., 1964, in: Quantum Electronics III, Vol. 1 (Columbia University Press, New York) p. 596.
Bleaney, B., 1972a, in: Magnetic Properties of Rare Earth Metals, ed. R.J. Elliott (Plenum Press, New York) ch. 8.
Bleaney, B., 1972b, J. Mag. Res. **8**, 91.
Bleaney, B., 1980, Proc. R. Soc. London Ser. A **370**, 313.
Bleaney, B., 1981, Proc. R. Soc. London Ser. A **376**, 217.
Bleaney, B., and R.P. Penrose, 1948, unpublished results.
Bleaney, B., and H.E.D. Scovil, 1950, Proc. Phys. Soc. A **63**, 1369.
Bleaney, B., and H.E.D. Scovil, 1952, Philos. Mag. **43**, 999.
Bleaney, B., and M.R. Wells, 1980, Proc. R. Soc. London Ser. A **370**, 131.
Bleaney, B., R.J. Elliott and H.E.D. Scovil, 1951, Proc. Phys. Soc. A **64**, 933.
Bleaney, B., R.T. Harley, J.F. Ryan, M.R. Wells and M.C.K. Wiltshire, 1978a, J. Phys. C **11**, 3059.
Bleaney, B., F.N.H. Robinson and M.R. Wells, 1978b, Proc. R. Soc. London Ser. A **362**, 179.
Bleaney, B., A.G. Stephen, P.J. Walker and M.R. Wells, 1981a, Proc. R. Soc. London Ser. A **376**, 235.
Bleaney, B., A.G. Stephen, Sung Ho Choh and M.R. Wells, 1981b, Proc. R. Soc. London Ser. A **376**, 253.
Bleaney, B., A.C. de Oliveira and M.R. Wells, 1981c, J. Phys. C **14**, L505.
Bleaney, B., J.F. Gregg, A.C. de Oliveira and M.R. Wells, 1982a, J. Phys. C **15**, 5293.
Bleaney, B., A.G. Stephen, P.J. Walker and M.R. Wells, 1982b, Proc. R. Soc. London Ser. A **381**, 1.
Bleaney, B., G.A.D. Briggs, J.F. Gregg, G.H. Swallow and J.M.R. Weaver, 1983a, Proc. R. Soc. London Ser. A **388**, 479.
Bleaney, B., J.H.T. Pasman and M.R. Wells, 1983b, Proc. R. Soc. London Ser. A **387**, 75.
Bleaney, B., J.F. Gregg, M.J.M. Leask and M.R. Wells, 1984, Proc. R. Soc. London Ser. A **394**, 69.
Bleaney, B., R.G. Clark, J.F. Gregg, Y. Roinel and N.J. Stone, 1987, J. Phys. C **20**, 3175.
Bloembergen, N., 1956, Phys. Rev. **104**, 1956.
Blok, J., and D.A. Shirley, 1966, Phys. Rev. **143**, 278.
Bonger, E., H.B. Brom, E.J. Veenendaal, W.J. Huiskamp and H.D. Amberger, 1983, Physica B **115**, 72.
Bordarier, Y., B.R. Judd and M. Klapisch, 1965, Proc. R. Soc. London Ser. A **289**, 81.
Bowden, G.J., and R.G. Clark, 1983, J. Phys. C **16**, 1089, 3305.
Bowden, G.J., R.J. Elliott and J. Oitmaa, 1985, Proc. R. Soc. London Ser. A **399**, 73.
Boyd, E.L., 1966, Phys. Rev. **145**, 174.
Briggs, G.A.D., J.F. Gregg and J.M.R. Weaver, 1984, private communication.
Brink, G.O., and W.A. Nierenberg, 1958, J. Phys. Rad. **19**, 816.
Brosnan, S.P.G., and D.T. Edmonds, 1980, J. Magn. Resonance **38**, 47.
Brya, W.J., and P.F. Wagner, 1967, Phys. Rev. **157**, 400.
Bunbury, D.St.J., C. Carboni and M.A.H. McCausland, 1985, J. Phys. C **18**, L1151.
Burum, D.P., R.M. Shelby and R.M. Macfarlane, 1982, Phys. Rev. B **25**, 3009.
Busch, B., P. Juno, P. Schob, O. Vogt and F. Hul-

liger, 1964, Phys. Lett. **9**, 7.
Callen, E.R., and H.B. Callen, 1965, Phys. Rev. **139**, A455.
Calloway, J., and D.C. McCollum, 1963, Phys. Rev. **130**, 1741.
Cashion, J.D., A.H. Cooke, L.A. Hoel, D.M. Martin and M.R. Wells, 1970, Colloques Internationaux du C.N.R.S., No. 180, Les Éléments des Terres Rares, Vol. II, page 417.
Catanese, C.A., and H.E. Meissner, 1973, Phys. Rev. B **8**, 2075.
Catanese, C.A., A.T. Skjeltorp, H.E. Meissner and W.P. Wolf, 1973, Phys. Rev. B **8**, 4223.
Chan, I.Y., and C.A. Hutchison Jr, 1972, Phys. Rev. B **5**, 3387.
Chapellier, M., M. Goldman, V. Hoang Chau and A. Abragam, 1969, C.R. Hebd. Séances Acad. Sci. **268**, 1539.
Chapellier, M., M. Goldman, V. Hoang Chau and A. Abragam, 1970, J. Appl. Phys. **41**, 849.
Charap, S.H., and E.L. Boyd, 1964, Phys. Rev. **133**, A811.
Charlton, A., and P. Ewart, 1984, Opt. Commun. **50**, 241.
Chase, L.L., 1970, Phys. Rev. B **2**, 2308.
Cheng, K.T., and W.J. Childs, 1985, Phys. Rev. A **31**, 2775.
Childs, W.J., 1967, Phys. Rev. **156**, 71.
Childs, W.J., and L.S. Goodman, 1972, Phys. Rev. A **6**, 1772, 2001.
Clark, R.G., A.L. Allsop, N.J. Stone and G.J. Bowden, 1987, J. Phys. C **20**, 797.
Clarke, R.H., and C.A. Hutchison Jr, 1971, Phys. Rev. Lett. **27**, 638.
Clemens, J.M., and C.A. Hutchison Jr, 1983, Phys. Rev. B **28**, 50.
Cochrane, R.W., C.Y. Wu and W.P. Wolf, 1973, Phys. Rev. B **8**, 4348.
Colwell, J.H., B. Mangum, D.D. Thornton, J.C. Wright and H.W. Moos, 1969a, Phys. Rev. Lett. **23**, 1245.
Colwell, J.H., B.W. Mangum and D.B. Utton, 1969b, Phys. Rev. **181**, 842.
Cone, R.L., R.T. Harley and M.J.M. Leask, 1984, J. Phys. C **17**, 3101.
Cook, D.C., and J.D. Cashion, 1979, J. Phys. C **12**, 605.
Cooke, A.H., H.J. Duffus and W.P. Wolf, 1953, Philos. Mag. **44**, 623.
Cooke, A.H., S. Whitley and W.P. Wolf, 1955, Proc. Phys. Soc. B **68**, 415.
Cooke, A.H., H. Meyer and W.P. Wolf, 1956, Proc. R. Soc. London Ser. A **233**, 536.
Cooke, A.H., D.T. Edmonds, C.B.P. Finn and W.P. Wolf, 1968, Proc. R. Soc. London Ser. A **306**, 313, 335.
Cooke, A.H., C.J. Ellis, K.A. Gehring, M.J.M. Leask, D.M. Martin, B.M. Wanklyn, M.R. Wells and R.L. White, 1970, Solid State Commun. **8**, 689.
Cooke, A.H., D.M. Martin and M.R. Wells, 1971, Solid State Commun. **9**, 519.
Cooke, A.H., S.J. Swithenby and M.R. Wells, 1972, Solid State Commun. **10**, 265.
Cooke, A.H., S.J. Swithenby and M.R. Wells, 1973, J. Phys. C **6**, 2209; Int. J. Magnetism **4**, 309.
Cooke, A.H., D.A. Jones, J.F.A. Silva and M.R. Wells, 1975, J. Phys. C **8**, 4083.
Culvahouse, J.W., D.P. Schinke and D.L. Foster, 1967, Phys. Rev. Lett. **18**, 117.
Dabbs, J.W.T., L.D. Roberts and G.W. Parker, 1958, Physica **24**, S69.
Daniels, J.M., and F.N.H. Robinson, 1953, Philos. Mag. **44**, 630.
Davidson, M.M., D.T. Edmonds and J.P.G. Mailer, 1981, J. Chem. Phys. **74**, 890.
de Alcantara Bonfim, O.F., and G.A. Gehring, 1980, Adv. Phys. **29**, 731.
de Groot, P., F. Leempoels, J. Witters, F. Herlach and I. Laursen, 1981, Solid State Commun. **37**, 681.
Descamps, D., and Y. Merle d'Aubigné, 1964, Phys. Lett. **8**, 5.
Duncan Jr, R.C., and Z.J. Kiss, 1963, Appl. Phys. Lett. **3**, 23.
Edmonds, D.T., 1963, Phys. Rev. Lett. **10**, 129.
Edmonds, D.T., and J.P.G. Mailer, 1977, J. Magn. Resonance **26**, 93.
Edmonds, D.T., and J.P.G. Mailer, 1978, J. Magn. Resonance **29**, 213.
Elliott, R.J., 1957, Proc. Phys. Soc. B **70**, 119.
Elliott, R.J., and K.W.H. Stevens, 1952, Proc. R. Soc. London Ser. A **215**, 437.
Elliott, R.J., and K.W.H. Stevens, 1953, Proc. R. Soc. London Ser. A **218**, 553; A **219**, 387.
Elliott, R.J., G.A. Gehring, A.P. Malozemoff, S.R.P. Smith, W. Staude and R.N. Tyte, 1971, J. Phys. C **4**, L179.
Elliott, R.J., R.T. Harley, W. Hayes and S.R.P. Smith, 1972, Proc. R. Soc. London Ser. A **328**, 217.
Ellis, C.J., M.J.M. Leask, D.M. Martin and M.R. Wells, 1971, J. Phys. C **4**, 2937.
England, N.J., 1978, Ph.D. Thesis, Oxford University.
Eremin, M.V., I.S. Konov and M.A. Teplov, 1978, Sov. Phys.-JETP **46**, 297.
Erickson, L.E., and K.K. Sharma, 1981, Phys. Rev. B **24**, 3697.
Essam, J.W., and M.F. Sykes, 1963, Physica **29**, 378.
Evans, L., P.G.H. Sandars and G.K. Woodgate, 1965, Proc. R. Soc. London Ser. A **289**, 114.
Evans, R.C., 1964, An Introduction to Crystal Chemistry (Cambridge University Press).
Everett, G.E., and R.C. Jones, 1971, Phys. Rev. B **4**, 1561.
Feher, G., 1956, Phys. Rev. **103**, 834.
Feher, G., and H.E.D. Scovil, 1957, Phys. Rev. **105**, 760.
Fermon, C., J.F. Gregg, J.-F. Jacquinot, Y. Roinel, V. Bouffard, G. Fournier and A. Abragam, 1986, J. Phys. (France) **47**, 1053.
Field, R.A., and C.A. Hutchison Jr, 1985, J. Chem. Phys. **82**, 1711.
Fierz, M., 1938, Physica **5**, 433.
Finkelstein, R., and A. Mencher, 1953, J. Chem.

Phys. **21**, 472.
Finn, C.B.P., R. Orbach and W.P. Wolf, 1961, Proc. Phys. Soc. **77**, 261.
Fitzwater, D.R., and R.E. Rundle, 1959, Z. Krystallogr. **73**, 116.
Fletcher, J.R., and F.W. Sheard, 1971, Solid State Commun. **9**, 1971.
Folinsbee, J.T., J.P. Harrison, D.B. McColl and D.R. Taylor, 1977a, J. Phys. C **10**, 743.
Folinsbee, J.T., J.P. Harrison and D.R. Taylor, 1977b, J. Phys. C **10**, 3411.
Franzblau, M.C., G.E. Everett and A.W. Lawson, 1967, Phys. Rev. **164**, 716.
Freeman, A.J., and J.P. Desclaux, 1979, J. Magn. & Magn. Mat. **12**, 11.
Freeman, A.J., and R.E. Watson, 1962, Phys. Rev. **127**, 2058.
Freeman, F.F., and W.G. Williams, 1978, J. Phys. E **11**, 459.
Furrer, R., and C.A. Hutchison Jr, 1983, Phys. Rev. B **27**, 5270.
Gehring, G.A., and K.A. Gehring, 1975, Rep. Prog. Phys. **38**, 1.
Gehring, G.A., A.P. Malozemoff, W. Staude and R.N. Tyte, 1972, J. Phys. Chem. Solids **33**, 1487, 1499.
Gehring, K.A., A.P. Malozemoff, W. Staude and R.N. Tyte, 1971, Solid State Commun. **9**, 511.
Geschwind, S., 1972, in: Electron Paramagnetic Resonance, ed. S. Geschwind (Plenum Press, New York) ch. 5.
Geusic, J.E., and H.E.D. Scovil, 1964, Rep. Prog. Phys. **27**, 241.
Giordmaine, J.A., and F.R. Nash, 1965, Phys. Rev. **138**, A1510.
Gordon, J.P., H.J. Zeiger and C.H. Townes, 1954, Phys. Rev. **95**, 282.
Gordon, J.P., H.J. Zeiger and C.H. Townes, 1955, Phys. Rev. **99**, 1264.
Gorodetsky, G., R.M. Hornreich and B.M. Wanklyn, 1973, Phys. Rev. B **8**, 2263.
Gorter, C.J., 1948, Physica **14**, 504.
Griessen, R., M. Landolt and H.R. Ott, 1971, Solid State Commun. **9**, 2219.
Hamman, J., and M. Ocio, 1977, Physica B+C **86-88**, 1153.
Hansen, P.E., and R. Nevald, 1977, Phys. Rev. B **16**, 146.
Harley, R.T., and D.I. Manning, 1978, J. Phys. C **11**, L633.
Harley, R.T., W. Hayes and S.R.P. Smith, 1971, Solid State Commun. **9**, 515.
Harley, R.T., W. Hayes, A.M. Perry and S.R.P. Smith, 1973, J. Phys. C **6**, 2382.
Harrison, J.P., J.P. Hessler and D.R. Taylor, 1976, Phys. Rev. B **14**, 2979.
Hartman, S.R., and E.L. Hahn, 1962, Phys. Rev. **128**, 2024.
Hayes, W., ed., 1974, Crystals with the Fluorite Structure (Clarendon Press, Oxford).
Hayes, W., and P.H.S. Smith, 1971, J. Phys. C **4**, 840.
Heisenberg, W., 1926, Z. Phys. **38**, 411.
Heitler, W., and E. Teller, 1936, Proc. R. Soc. London Ser. A **155**, 629.
Herpin, A., and P. Meriel, 1973, J. Phys. (France) **34**, 423.
Hessler, J.P., and C.A. Hutchison Jr, 1973, Phys. Rev. B **8**, 1822.
Hill, R.W., J. Cosier and S.P. Smith, 1978, Solid State Commun. **26**, 17.
Hinckley, C.C., 1969, J. Am. Chem. Soc. **91**, 5160.
Hodges, J.A., 1983, J. Phys. (France) **44**, 833.
Hoehn, M.V., and D.G. Karraker, 1974, J. Chem. Phys. **60**, 393.
Hsieh, Y., J.C. Koo and E.L. Hahn, 1972, Chem. Phys. Lett. **13**, 563.
Huang, Chao-Yuan, 1965, Phys. Rev. **139**, A241.
Hutchison Jr, C.A., and D.B. McKay, 1977, J. Chem. Phys. **66**, 3311.
Hutchison Jr, C.A., and T.E. Orlowski, 1980, J. Chem. Phys. **73**, 1.
Hutchison Jr, C.A., and E. Wong, 1958, J. Chem. Phys. **29**, 754.
Inoue, M., 1963, Phys. Rev. Lett. **11**, 196.
Ioffe, V.A., S.N. Andronenko, A.N. Bazhan, S.V. Kravchenko, C. Bazan, B.G. Vehkter and D.M. Kaplan, 1983, Sov. Phys.-JETP **84**, 707.
Jacobsen, E.H., and K.W.H. Stevens, 1963, Phys. Rev. **129**, 2036.
Jacquinot, J.-F., J.F. Gregg, Y. Roinel, C. Fermon and V. Bouffard, 1986, J. Low Temp. Phys. **64**, 115.
Jahn, H.A., and E. Teller, 1937, Proc. R. Soc. London Ser. A **161**, 220.
Jayaraman, A., 1972, Phys. Rev. Lett. **29**, 1674.
Jeffries, C.D., 1957, Phys. Rev. **106**, 164.
Jeffries, C.D., 1960, Phys. Rev. **117**, 1056.
Jeffries, C.D., 1963a, Dynamic Nuclear Orientation (Interscience, New York).
Jeffries, C.D., 1963b, Cryogenics **3**, 41.
Jeffries, C.D., 1967, Phys. Rev. Lett. **19**, 1221.
Johnson, C.E., and H. Meyer, 1959, Proc. R. Soc. London Ser. A **253**, 199.
Jones, E.D., 1969, Phys. Rev. **180**, 455.
Judd, B.R., 1957, Proc. R. Soc. London Ser. A **241**, 122, 414.
Judd, B.R., and I. Lindgren, 1961, Phys. Rev. **122**, 1802.
Ketelaar, J.A.A., 1937, Physica **4**, 619.
Kienle, P., 1964, Rev. Mod. Phys. **36**, 372.
King, A.R., J.P. Wolfe and R.L. Ballard, 1972, Phys. Rev. Lett. **28**, 1099.
Kiss, Z.J., C.H. Anderson and R. Orbach, 1965, Phys. Rev. A **137**, 1761.
Kittel, C., 1959, Phys. Rev. **115**, 1587.
Kronig, R. de L., 1939, Physica **6**, 33.
Landau, D.P., and B.E. Keen, 1979, Phys. Rev. B **19**, 4905.
Landau, D.P., B.E. Keen, B. Schneider and W.P. Wolf, 1971, Phys. Rev. B **3**, 2310.
Lea, K.R., M.J.M. Leask and W.P. Wolf, 1962, J. Phys. & Chem. Solids **23**, 1381.
Lederer, C.M., and V. Shirley, 1978, Table of Isotopes (Wiley, New York).
Lee, T.D., and C.N. Yang, 1956, Phys. Rev. **104**, 254.
Levy, P.M., 1964, Phys. Rev. A **135**, 155.

Lindgren, I., 1962, Nucl. Phys. **32**, 151.
Macfarlane, R.M., and R.S. Meltzer, 1985, Opt. Commun. **52**, 320.
Macfarlane, R.M., D.P. Burum and R.M. Shelby, 1982, Phys. Rev. Lett. **49**, 636.
Macfarlane, R.M., D.P. Burum and R.M. Shelby, 1984, Phys. Rev. B **29**, 2390.
MacKenzie, I.S., M.A.H. McCausland and A.R. Wagg, 1974, J. Phys. F **4**, 315.
Magariño, J., J. Tuchendler, P. Beauvillain and I. Laursen, 1980, Phys. Rev. B **21**, 18.
Magno, M.S., and G.H. Dieke, 1962, J. Chem. Phys. **37**, 2354.
Maiman, T.H., 1960, Nature **187**, 493.
Manenkov, A.A., and A.M. Prokhorov, 1962, Sov. Phys.-JETP **15**, 951.
Matthias, B.T., P.M. Bozorth and J.H. Van Vleck, 1961, Phys. Rev. Lett. **7**, 160.
Mattis, D.C., and T.D. Schultz, 1963, Phys. Rev. **129**, 175.
McCausland, M.A.H., and I.S. MacKenzie, 1980, Nuclear Magnetic Resonance in Rare Earth Metals (Taylor & Francis, London).
McGuire, T.R., and M.W. Shafer, 1964, J. Appl. Phys. **35**, 984.
McGuire, T.R., F. Holtzberg and R.J. Joenk, 1968, J. Phys. & Chem. Solids **29**, 410.
McWhan, D.B., P.C. Souers and G. Jura, 1966, Phys. Rev. **143**, 385.
Mehran, F., and K.W.H. Stevens, 1982, Phys. Rep. **85**, 124.
Mehran, F., K.W.H. Stevens and T.S. Plaskett, 1976, Phys. Rev. Lett. **37**, 1403.
Mehran, F., K.W.H. Stevens and T.S. Plaskett, 1977a, Solid State Commun. **22**, 143.
Mehran, F., T.S. Plasket and K.W.H. Stevens, 1977b, Phys. Rev. B **16**, 1.
Mehran, F., K.W.H. Stevens and T.S. Plaskett, 1979, Phys. Rev. B **20**, 1817.
Mehran, F., K.W.H. Stevens and T.S. Plaskett, 1982, Phys. Rev. B **25**, 1973.
Melcher, R.L., and B.A. Scott, 1972, Phys. Rev. Lett. **28**, 607.
Melcher, R.L., E. Pytte and B.A. Scott, 1973, Phys. Rev. Lett. **31**, 307.
Mergerian, D., I.H. Harrop, M.P. Stombler and K.C. Krikorian, 1967, Phys. Rev. **153**, 349.
Metcalfe, M.J., and H.M. Rosenberg, 1972, J. Phys. C **5**, 450, 459, 474.
Meyer, H., and A.B. Harris, 1960, J. Appl. Phys. **31**, S49.
Meyer, H., and P.L. Smith, 1959, J. Phys. & Chem. Solids **9**, 285.
Mims, W.B., and D.R. Taylor, 1969, Phys. Rev. Lett. **22**, 1430.
Mims, W.B., and D.R. Taylor, 1971, Phys. Rev. B **3**, 2103.
Miyata, N., and B.E. Argyle, 1967, Phys. Rev. **157**, 448.
Mollenauer, L.F., W.B. Grant and C.D. Jeffries, 1968, Phys. Rev. Lett. **20**, 1968.
Moruzzi, V.L., and D.T. Teaney, 1963, Solid State Commun. **1**, 127.
Müller, W., A. Steudel and H. Walther, 1965, Z. Phys. **183**, 303.
Nevald, R., and P.E. Hansen, 1978, Phys. Rev. B **18**, 4626.
Norvell, J.C., W.P. Wolf, L.M. Corliss, J.M. Hastings and R. Nathans, 1969, Phys. Rev. **186**, 557, 567.
Nowik, I., and S. Ofer, 1967, Phys. Rev. **153**, 409.
O'Connor, C.J., R.L. Carlin and R.W. Schwartz, 1977, J. Chem. Soc. Faraday Trans. II **73**, 361.
Oliveira Jr, N.F., S. Foner, Y. Shapira and T.B. Reed, 1971, J. Appl. Phys. **42**, 1783.
Orbach, R., and M. Blume, 1962, Phys. Rev. Lett. **8**, 478.
Overhauser, A., 1953, Phys. Rev. **92**, 411.
Page, J.H., and H.M. Rosenberg, 1977, J. Phys. C **10**, 1817.
Pauthenet, R., 1958, Ann. Chim. Phys. **3**, 424.
Pichanick, F.M.J., and G.K. Woodgate, 1961, Proc. R. Soc. London Ser. A **263**, 89.
Pickart, S.J., and H.A. Alperin, 1968, J. Phys. Chem. Solids **29**, 414.
Postma, H., A.R. Miedema and M.C. Eversdijk-Smulders, 1959, Physica **25**, 671.
Postma, H., H. Marshak, V.L. Sailor, F.J. Shore and C.A. Reynolds, 1962, Phys. Rev. **126**, 979.
Pytte, E., 1965, Ann. Phys. (New York) **32**, 377.
Rado, G.T., 1969, Phys. Rev. Lett. **23**, 644.
Rado, G.T., 1970, Solid State Commun. **8**, 1349.
Ramsey, N.F., 1949, Phys. Rev. **76**, 996.
Reuben, J., 1979, Handbook on the Physics and Chemistry of Rare Earths, Vol. 4, eds K.A. Gschneidner Jr and L. Eyring (North-Holland, Amsterdam) ch. 39, p. 515.
Reuben, J., and G.A. Elgavish, 1979, Handbook on the Physics and Chemistry of Rare Earths, Vol. 4, eds K.A. Gschneidner Jr and L. Eyring (North-Holland, Amsterdam) ch. 38, p. 483.
Riley, J.D., J.M. Baker and R.J. Birgeneau, 1970, Proc. R. Soc. London Ser. A **320**, 369.
Roberts, L.D., S. Bernstein, J.W.T. Dabbs and C.P. Stanford, 1954, Phys. Rev. **95**, 105.
Robertson, R.G.H., J.C. Waddington and R.G. Summers-Gill, 1968, Can. J. Phys. **46**, 2499.
Robinson, F.N.H., 1963, Phys. Lett. **4**, 180.
Roinel, Y., V. Bouffard, J.-F. Jacquinot, C. Fermon and G. Fournier, 1985, J. Phys. (France) **46**, 1699.
Rose, M.E., 1949, Phys. Rev. **75**, 213.
Rosen, A., 1969, J. Phys. (France) B **2**, 1257.
Ruby, R.H., H. Benoit and C.D. Jeffries, 1962, Phys. Rev. **127**, 51.
Sabisky, E.S., 1974, in: Crystals with the Fluorite Structure, ed. W. Hayes (Clarendon Press, Oxford) ch. 5.
Sabisky, E.S., and C.H. Anderson, 1964, Phys. Rev. Lett. **13**, 754.
Sabisky, E.S., and C.H. Anderson, 1966, Phys. Rev. **148**, 194.
Sabisky, E.S., and C.H. Anderson, 1970, Phys. Rev. B **1**, 2028.
Sandars, P.G.H., and J. Beck, 1965, Proc. R. Soc. London Ser. A **289**, 97.
Sandars, P.G.H., and B. Dodsworth, 1967, in: Hyperfine Interactions, eds A.J. Freeman and R.B.

Frankel (Academic Press, New York) p. 115.
Sandars, P.G.H., and G.K. Woodgate, 1960, Proc. R. Soc. London Ser. A **257**, 269.
Sandercock, J.R., S.B. Palmer, R.J. Elliott, W. Hayes, S.R.P. Smith and A.P. Young, 1972, J. Phys. C **21**, 3126.
Sato, S., A. Reuveni and B.R. McGarvey, 1980, J. Chem. Phys. **73**, 712.
Sayetat, F., J.X. Boucherle, M. Belakhovsky, A. Kallel, F. Tcheou and H. Fuess, 1971, Phys. Lett. A **34**, 361.
Schawlow, A.L., and C.H. Townes, 1958, Phys. Rev. **112**, 1940.
Schwab, F., and W. Hillmer, 1975, Phys. Status Solidi b **70**, 237.
Schwartz, R.W., and N.J. Hill, 1974, J. Chem. Soc. Faraday Trans. II **70**, 124.
Schwob, P., and O. Vogt, 1969, J. Appl. Phys. **40**, 1328.
Scovil, H.E.D., G. Feher and H. Seidel, 1957, Phys. Rev. **105**, 762.
Sharma, K.K., and L.E. Erickson, 1985, J. Phys. C **18**, 2935.
Shelby, R.M., and R.M. Macfarlane, 1981, Phys. Rev. Lett. **47**, 1172.
Sievers III, A.J., and M. Tinkham, 1961, Phys. Rev. **124**, 321.
Skjeltorp, A.T., C.A. Catanese, H.E. Meissner and W.P. Wolf, 1973, Phys. Rev. B **7**, 2062.
Smith, K.F., and P.J. Unsworth, 1965, Proc. Phys. Soc. **86**, 1249.
Sorokin, P.P., and M.J. Stevenson, 1961, IBM J. Res. & Dev. **5**, 557.
Spalding, I.J., 1963, Proc. Phys. Soc. **81**, 156.
Spanjaard, D., J.D. Marsh and N.J. Stone, 1973, J. Phys. F **3**, 1243.
Stachel, M., S. Hufner, G. Crecelius and D. Quitman, 1969, Phys. Rev. **186**, 355.
Sternheimer, R.M., 1950, Phys. Rev. **80**, 102.
Sternheimer, R.M., 1951, Phys. Rev. **84**, 244.
Streever, R.L., 1969, Phys. Lett. A **29**, 710.
Streever, R.L., and P.J. Caplan, 1971, Phys. Rev. B **3**, 2910.
Suzuki, H., 1986, private communication.
Suzuki, H., N. Nambudripad, B. Bleaney, A.L. Allsop, G.J. Bowden, I.A. Campbell and N.J. Stone, 1978, J. Phys. (France) **39**, C-6, 800.
Suzuki, H., M. Miyamoto, Y. Masuda and T. Ohtuska, 1982, J. Low Temp. Phys. **48**, 297.
Suzuki, H., Y. Masuda, M. Miyamoto, S. Sakatsume, P.J. Walker and T. Ohtsuka, 1983, J. Magn. & Magn. Mat. **31-4**, 741.
Suzuki, H., T. Ohtsuka, S. Kawarazaki, N. Kunitomi, A.M. Moon and R.M. Nicklow, 1984, Solid State Commun. **49**, 1157.
Suzuki, H., Y. Masuda, M. Miyamoto, S. Sakatsume, P.J. Walker and T. Ohtsuka, 1986, J. Low Temp. Phys. **62**, 497.
Tagirov, M.S., M.A. Teplov and L.D. Lidanova, 1979, Sov. Phys. Solid State **21**, 2016.
Tanaka, Y., R.M. Steffen, E.B. Shera, W. Reuter, M.V. Hoehn and J.D. Zumbro, 1983, Phys. Rev. Lett. **51**, 1633.
Taylor, D.R., D.B. McColl, J.P. Harrison, R.J. Elliott and L.L. Goncalves, 1977, J. Phys. C. **10**, L407.
Teplov, M.A., 1977, in: Crystal Field Effects in Metals and Alloys, ed. A. Furrer (Plenum Press, New York) p. 318.
Urbina, C., and J.F. Jacquinot, 1980, Physica B **100**, 333.
van Molnar, S., and A.W. Lawson, 1965, Phys. Rev. **139**, A1598.
Van Vleck, J.H., 1939, J. Chem. Phys. **7**, 62, 72.
Van Vleck, J.H., 1940, Phys. Rev. **57**, 426.
Van Vleck, J.H., 1941, Phys. Rev. **59**, 724, 730.
Van Vleck, J.H., 1961, Phys. Rev. **123**, 58.
Van Vleck, J.H., 1964, J. Appl. Phys. **35**, 882.
Varsanyi, F., and G.H. Dieke, 1961, J. Chem. Phys. **36**, 385.
Veenendaal, E.J., and H.B. Brom, 1982, Physica B **113**, 118.
Veenendaal, E.J., H.B. Brom and W.J. Huiskamp, 1983, Physica B **121**, 1.
Waller, I., 1932, Z. Phys. **79**, 370.
Watson, R.E., and A.J. Freeman, 1964, Phys. Rev. **135**, A1209.
White, H.W., and D.C. McCollum, 1972, J. Appl. Phys. **43**, 1225.
Wickersheim, K.A., and R.L. White, 1960, Phys. Rev. Lett. **4**, 123.
Wickersheim, K.A., and R.L. White, 1962, Phys. Rev. Lett. **8**, 483.
Will, G., S.J. Pickart, A.A. Alperin and R. Nathans, 1963, J. Phys. & Chem. Solids **24**, 1679.
Will, G., W. Schafer, C.F. Sampson and J.B. Forsyth, 1972, Phys. Lett. A **38**, 207.
Williams, F.I.B., 1967, Proc. Phys. Soc. **91**, 111.
Wolf, W.P., 1957, Phys. Rev. **108**, 1152.
Wolf, W.P., and J.H. Van Vleck, 1960, Phys. Rev. **118**, 1490.
Wolf, W.P., M. Ball, M.T. Hutchings, M.J.M. Leask and A.F.G. Wyatt, 1962a, J. Phys. Soc. Jpn. Suppl. B-1 **17**, 443.
Wolf, W.P., M.J.M. Leask, B. Mangum and A.F.J. Wyatt, 1962b, J. Phys. Soc. Jpn. Suppl. B **17**, 487.
Wolf, W.P., B. Scheider, D.P. Landau and B.E. Keen, 1972, Phys. Rev. B **5**, 4471.
Wolfe, J.P., 1977, Phys. Rev. B **16**, 128.
Wolfe, J.P., and R.S. Markiewicz, 1973, Phys. Rev. Lett. **30**, 1105.
Woodgate, G.K., 1966, Proc. R. Soc. London Ser. A **293**, 117.
Woodgate, G.K., and P.G.H. Sandars, 1958, J. Phys. (France) **19**, 819.
Wright, J.C., H.W. Moos, J.H. Colwell, B.W. Mangum and D.D. Thornton, 1971, Phys. Rev. B **3**, 843.
Wu, C.S., E. Ambler, R.W. Hayward, D.D. Hoppes and R.P. Hudson, 1957, Phys. Rev. **105**, 1413.
Zalkin, A., J.D. Forrester and D.H. Templeton, 1963, J. Chem. Phys. **39**, 2881.
Zavoisky, E., 1945, Fiz. Zh. **9**, 211, 245.

Handbook on the Physics and Chemistry of Rare Earths, Vol. 11
edited by K.A. Gschneidner, Jr. and L Eyring

Chapter 78

PHYSICAL METALLURGY

K.A. GSCHNEIDNER, Jr.
Ames Laboratory and Department of Materials Science and Engineering, Iowa State University, Ames IA 50011, USA*

and

A.H. DAANE
Department of Chemistry, LaGrange College, LaGrange, GA 30240, USA

Contents

* Operated for the US Department of Energy by Iowa State University under contract no. W-7405-ENG-82. This work was supported by the Office of Basic Energy Sciences.

1. Introduction

... a riddle wrapped in a mystery inside an enigma.
Sir Winston Churchill (October 1, 1939)

The words of Sir Winston Churchill which he had used to describe Russia, apply equally well to the rare earths. Prior to today we have probably unwrapped the 'riddle' and are working on the 'mystery' aspects of the rare earths, but we will inevitably be facing the 'enigma' for the foreseeable future. The excitement and challenge of our quest for knowledge and understanding draws us ever forward unlocking new doors, but a few steps later we find a new puzzle which we must solve to reach a new level of understanding. We plan to examine some of these 'riddles' or 'puzzles' of their time and how they were solved, thus increasing our level of understanding and appreciation of the delicately beautiful but mysterious world of rare earth materials science.

The historical origins of rare earth metallurgy date back 160 years with the preparation of cerium metal by Mosander (1827). But basically it was not until about 40 years ago that a rapid expansion of our knowledge of these metals occurred (see Gschneidner 1984). That is not to say that there were no important developments or discoveries before the late 1940's because there were several important ones, and they were just whetting our appetites in our quest for knowledge and understanding of this exotic group of metals. The more important pre-1950 events were the discovery:

(1) of ferromagnetism in gadolinium (Urbain et al. 1935);

(2) that the crystal structures were not identical for the entire lanthanide series of metals and that europium and ytterbium had anomalously small densities (or anomalously large atomic volumes) relative to the other lanthanide metals (Klemm and Bommer 1937); and

(3) of the existence of superconductivity in lanthanum (Mendelssohn and Daunt 1937).

The discovery of ferromagnetism in gadolinium at approximately room temperature, had a pronounced affect on science's then current understanding of magnetism since only iron, cobalt and nickel were known to be ferromagnetic. The existence of ferromagnetism in the lanthanide metals remained a puzzle until Kasuya (1956) and Yosida (1957) applied the Ruderman -Kittel (1954) indirect-interaction model (to explain the hyperfine interactions between nuclear moments on adjacent ions) to the exchange interaction between localized 4f electrons on neighboring ion sites. This interaction is now known as the RKKY interaction.

The discovery of superconductivity in lanthanum also aroused a great deal of interest among the scientific community – a superconductor and a ferromagnet in the same group of almost 'identical' metals. But with the development of the BCS theory of superconductivity (Bardeen et al. 1957) and the RKKY mechanism for explaining the magnetic behavior, this apparent difficulty was overcome. But at about the same time experimentalists presented the first evidence of the co-existence of ferromagnetism and superconductivity in one and the same material, $CeRu_2$–$GdRu_2$ (Matthias et al. 1958), which created a great deal of consternation when science thought such things were pretty well understood.

The existence of changes in the crystal structure, probably was not so earth-shaking since the R_2O_3 compounds were known to have three polymorphic forms in the lanthanide series. But the anomalous densities (or atomic volumes) for europium and ytterbium was an exciting development, since it showed that these two metals were divalent while the remaining lanthanide elements were trivalent. This discovery was one of the first examples verifying Hund's rule (that half-filled and completely filled shells are stable electronic states), which involved a solid-state property other than a magnetic or an optical property measurement.

Since the late 1940's, as mentioned by Gschneidner (1984), fourteen major scientific discoveries or advancements had occurred in the 'Age of Enlightenment', which covered the two decades from 1950 through 1969, and an additional ten discoveries in the 'Golden Age' (1970 to date). Many of these 24 events plus several from the Dark Ages (1787–1949) will be discussed in the various sections of this chapter under the appropriate topic (see table 1), with special emphasis being placed on how these impacted the whole of science and not just the rare earths themselves.

2. Preparation of the metallic form

There are two basic methods of preparing the rare earth metals – metallothermic reduction or the electrolytic reduction of a rare earth salt, usually a fluoride or chloride or sometimes the oxide. The latter method is limited to the light

TABLE 1
Major events in the field of metallurgy since the discovery of the rare earths in 1787. (After Gschneidner 1984.)

Years	Scientific discovery or technical advancement or special event	Section(s) in which further information is found
Dark Ages (1787–1949)		
1827	Preparation of the first rare earth metal (Ce)	2.1.1
1875	Electrolytic method used for the first time to prepare rare earth metals (La, Ce and didymium [1Pr–3Nd])	2.3
1908	First major metallurgical application of the rare earths: mischmetal–iron lighter flints	2.3.2.1
1911	First rare earth metal binary phase diagram study reported (Ce–Sn system)	4.1.1
1912	X-ray spectra confirms that only 15 lanthanides are to be expected plus the two closely related metals Sc and Y	–
1925	The term 'lanthanide contraction' was coined	5.1
1931	Preparation of 'reasonably pure' light lanthanides by electrolysis (bulk metals)	2.3
1935	Discovery of ferromagnetism in a rare earth metal (Gd)	3.3
1937	Preparation of 'reasonably pure' powder lanthanide metals (essentially all of them) and determination of their crystal structures (many for the first stime)	2.1.1; 3.2
1937	Discovery of superconductivity in a rare earth metal (La)	3.3
1947	First successful separations of adjacent lanthanides by ion exchange	–
1948	Beginning of the utilization of Ce (mischmetal) additions to produce nodular cast irons	–
Age of Enlightenment (1950–1969)		
1949–50	Beginning of valence fluctuations: discovery of a valence transformation in cerium ($\alpha \rightleftarrows \gamma$) at low temperature and at high pressure	3.2; 3.3.4
1951	Discovery of the high thermionic emissivity properties of LaB_6	4.4.1
1953	Development of the metallothermic reduction of R_2O_3 method for preparing the high vapor pressure metals (R ≡ Sm, Eu, Tm and Yb)	2.1.2
1953–54	Determination of the unique structure of Sm	3.2
1958	Discovery of a solid-state critical point (Ce)	3.7.2
1959	First issue of the Journal of the Less-Common Metals published; a major journal for reporting rare earth metallurgical research	–
1960	First Rare Earth Research Conference, held at Lake Arrowhead, CA, USA.	–
1961	Discovery of the unique beautifully complex magnetic structures of the heavy lanthanide metals	–
1962	Discovery of the existence of the Sm(δ)-phase in intra rare earth binary alloys	–
1963	Last rare earth element to be prepared in the metallic state: radioactive Pm	–
1966	Establishment of the Rare-earth Information Center at Iowa State University, Ames, IA, USA	–

TABLE 1 (continued).

Years	Scientific discovery or technical advancement or special event	Section(s) in which further information is found
Age of Enlightenment (1950–1969)		
1966	First successful application of solid-state electrolysis to purify a rare earth metal (Y)	2.2.3
1966	Discovery of the high-strength rare-earth–cobalt permanent magnets YCo_5	4.3.3
1967	Reporting of the superior permanent magnet properties of $SmCo_5$	4.3.3
1967	First direct Fermi surface measurements (de Haas–van Alphen) on a rare earth metal (Yb)	–
Golden Age (1970 to date [1984])		
1970	Discovery of the unique hydrogen absorption properties of the $LaNi_5$-family of materials	4.4.2
1970	Preparation of the first rare-earth-containing amorphous alloys	–
1970	Initial commercial realization of mischmetal additions to steels to achieve shape control of metal sulfide inclusions	–
1971	Discovery of giant magnetostrictions in RFe_2 phases	4.3.4
1976	Demonstration of a rare-earth-based magnetic heat pump	–
1976	Kondo scattering observed in a pure element (Ce)	3.3.4
1978	First volume of the Handbook on the Physics and Chemistry of Rare Earths published	–
1979	First Frank H. Spedding Prize awarded at the Fourteenth Rare Earth Research Conference, Fargo, ND, to W.E. Wallace	–
1980	Successful application of $PrNi_5$ in ultralow temperature refrigerators	4.4.3
1981	Discovery that spin fluctuations could be quenched in magnetic fields of less than 10 T ($LuCo_2$)	4.4.4
1981	Discovery of the high strength iron–rare-earth permanent magnets	4.3.3

lanthanides (La, Ce, Pr and Nd) and mischmetal (a mixture of the rare earth metals in the same proportions as in the naturally occurring ore) because of their low melting temperatures. In principle, the remaining rare earths could be reduced electrolytically, but at the high temperature required to operate the cell, which must be greater than the given rare earth metal's melting point, there is a horrendous materials compatibility problem vis-a-vis the electrodes and container. Electrolytic reduction at lower temperatures is possible but because of the dendritic nature of the deposit, recovery of the metal is difficult and the process is not practical. Commercial production of master alloys of a high melting rare earth metal with a non-rare earth metal, such as iron, cobalt, copper, has been accomplished by electrolysis using the non-rare earth metal as the cathode.

Thus the metallothermic method is basically our only choice for preparing 75% of the rare earth metals. Fortunately the basic method works quite well for all of the

rare earths, but there are significant variations in the processes that are used to prepare the individual metals. These variations are dictated primarily by the melting temperature and vapor pressure of the given rare earth metal.

For the above reasons we will discuss the metallothermic methods first, followed by purification processes and then the electrolytic reduction process. This section will close by reviewing the preparation of single crystals and intermetallic compounds.

2.1. *Metallothermic methods*

2.1.1. *Reduction of halides*

Following the discovery of the element cerium by Klaproth and also by Berzelius and Hisinger in 1803, the preparation of metallic cerium was reported by Mosander (1827) by the reduction of cerous chloride with potassium in a stream of hydrogen. Although this is described as the first preparation of cerium metal, it is quite likely that the product was a cerium-rich material that contained amounts of other rare earths, as separation and identification methods for these elements were just developing. Subsequent discovery of lanthanum and 'didymium' in these same source materials suggests the likelihood of this. It is interesting to note that potassium metal had been first prepared by Davey in 1807, and had been recognized as an appropriate reducing agent for other active metals. Considering the extremely hygroscopic nature of the chlorides it is surprising that these early workers were able to prepare and handle these salts in a manner that retained their characteristic nature in the reduction-preparation process without forming excessive amounts of the oxychlorides. A number of workers reported reductions of rare earth salts by sodium, cesium and other active metals, and without the general availability of argon or other protective gases or the attainability of high vacua for these processes, that a rare earth metal was obtained is surprising. All of these early preparations of rare earth metals resulted in powdered products as opposed to consolidated (melted) metals. In a number of cases the resulting rare earth metal powder was mixed with a halide slag such as sodium chloride, and the mixture was studied without separation, as a number of data could be obtained under such conditions. The most successful and complete approach to the preparation and study of the rare earth metals up until the 1940's was the work of Klemm and Bommer (1937). They reduced lanthanide chlorides with potassium in sealed glass tubes and were able to obtain X-ray diffraction patterns that allowed crystal structures and lattice constants to be reported for most of the lanthanides except promethium, samarium and holmium; data that were to stand until significantly larger amounts of purer rare earth materials were available after World War II. Of the 15 lanthanide metals, six (Eu, Tb, Dy, Tm, Yb and Lu) were prepared in the metallic form for the first time by Klemm and Bommer who were able to measure magnetic properties of some of their samples and confirm the magnetic uniqueness of some of the rare earth metals, particularly the heavy lanthanides, and allowed some correlation of their magnetic findings with electronic structures of the elements. Although Klemm and Bommer included samarium in their study, their data on this element, particularly its crystal

structure, did not suggest the unique nature of this metal that was reported later. The densities (and the atomic volumes) of the rare earth metals reported by Klemm and Bommer were generally consistent with later measurements.

The biggest surprise of their study was the discovery of the divalent character of metallic europium and ytterbium. Earlier studies of the light lanthanide (La, Ce, Pr and Nd) and erbium metals indicated that these lanthanides and yttrium were trivalent and so the expectation was that the remaining lanthanides should also be trivalent. Since divalent salts of europium and ytterbium were known in addition to the corresponding trivalent ones, the divalent nature was readily understood in terms of Hund's rules for stable half-filled and completely filled electronic levels (in these cases, $4f^7$ and $4f^{14}$, respectively).

The alkaline earth metals have generally proved to be much better reductants for the rare earth halides than the alkali metals. However, the availability of calcium and magnesium (less desirable) in a purity satisfactory for metallothermic reductions delayed until later the actual preparation of cerium metal using calcium as a reductant (Moldenhauer 1914, Karl 1934). However, impurities introduced in the process and an inability to eliminate residual calcium (1.7% iron and 12% calcium in the case of Karl's work) occasioned further work. Trombe and Mahn (1944) prepared metallic cerium, neodymium and gadolinium by the addition of the chlorides to a molten magnesium bath, followed by vacuum melting to eliminate the large amount of magnesium in the products. They reported an average of 1% magnesium remaining in their specimens.

Keller et al. (1945) described the preparation of large amounts of cerium metal by the reduction of cerous chloride with calcium. The reductions were on a several hundred grams scale in dolmitic oxide-lined steel bombs. Next a vacuum melting step in Ca–MgO crucibles was used to remove the excess calcium added to the reaction mixture to promote good yields. Because of the larger scale of these operations, oxide contamination, although certain because of reaction of the product metal with the containers, was not such as to prevent agglomeration of the metal.

As larger quantities of lanthanum, praseodymium and neodymium oxides became available, this same technique served well for the preparation of these metals (Spedding et al. 1952). However, when this same procedure was extended to the preparation of the higher melting gadolinium, frothing of the calcium chloride slag prevented collection of a consolidated product. Also, the refractory oxide containers suffered penetration and attack by the slag and the product metal. The substitution of gadolinium fluoride for the chloride avoided the frothing and agglomeration problem, and the use of tantalum metal containers for the reduction and vacuum melting operations provided a relatively inert crucible material (Daane and Spedding 1953) that promoted high yields of pure metal at the cost of a small tantalum impurity content, present as dendrites that separated out as the metal cooled down. Tantalum forms no intermetallic compounds with the rare earth metals and is only slightly soluble in the liquid metals. The rare earth metals in turn are not soluble in solid tantalum to a measurable degree, so tantalum has become a container of choice for rare earth metallurgical operations. Niobium, molybdenum

and tungsten are also resistant to attack by liquid rare earth metals, but for various reasons [embrittlement (tungsten) or increased solubility in the liquid rare earth metals (niobium and molybdenum) at high temperatures] do not serve as well as tantalum. In a study by Dennison et al. (1966a,b) it was shown that tungsten is more resistant to attack by the rare earth metals than is tantalum. But because of the embrittlement problem it is used only occasionally for some specialized situations.

The utilization of tantalum in the preparation of the rare earth metals was an extremely important step in improving the quality of these metals. The use of ceramic oxide crucibles puts an upper limit of about 95–98 at.% on the purity of the metal, depending on the rare earth metal in question. The use of tantalum immediately allowed the purity level to jump to 99 at.% or higher, especially reducing the oxygen content.

The reduction of the trifluoride with 10% excess calcium (beyond the stoichiometric amount) in tantalum containers has been the most used technique to prepare all of the rare earth metals except samarium, europium and ytterbium which are discussed below. Beaudry and Gschneidner (1978) and Gschneidner (1980a) have discussed more up-to-date refinements in this process that represent the best of current preparative methods for these metals. These include 'topping' the molten fluoride in a stream of hydrogen fluoride, and improved handling techniques for the calcium reductant and the reaction mixture. The charged tantalum crucible is heated in an inert atmosphere to 1450°C (the melting point of the calcium fluoride slag) or to the melting point of the rare earth metal, whichever is higher, and the reaction products are easily separated on cooling. The large difference in density between the slag (3.1 g/cm^3) and the lanthanide metals (6.2 to 9.8 g/cm^3) is a positive factor in the clean separation of these phases in the liquid state of the reduction process, contributing to the high yields (98%) that are achieved.

The 'topping' of the molten fluoride, which was suggested by Spedding and co-workers (Beaudry and Gschneidner 1978), was also a major step in improving the metal quality, since such fluorides contain less than 10 wt. ppm oxygen. Untopped fluorides will generally contain about 10 times this amount of oxygen, have a much higher surface to volume ratio and generally have higher silicon contents.

Moriarty (1968) discussed a relatively low temperature process for the preparation of some rare earth metals using lithium as the reductant for the trichlorides in sealed containers. This results in a metal sponge product that requires a melting step to achieve consolidated metal. The process, while successful in the laboratory where it was developed, has not been generally used elsewhere.

2.1.2. *The obstinate ones: Sm, Eu and Yb – reduction of the oxide*

When all of the rare earth oxides became available in large quantities via ion-exchange separation techniques, samarium was included in metal preparation studies. While there had been some earlier reports of samarium metal being prepared (Klemm and Bommer 1937, Trombe 1938), the absence of general descriptions of the properties of the metal suggested that it had not been obtained. In later studies, both the trichloride and the trifluoride (of samarium) were treated with calcium just as the other rare earth metals (Keller et al. 1945, Spedding et al.

1952, Daane and Spedding 1953), but in each case, only reduction to the $SmCl_2$ or SmF_2 state was achieved. The substitution of other alkaline earth and alkali metals for calcium served to no avail. Similar results were obtained for the less abundant europium and ytterbium.

The major breakthrough occurred in 1953 when the Ames Laboratory team (Daane et al. 1953) reported the preparation of samarium, europium and ytterbium in high purity and high yields by the reduction of their oxides with lanthanum metal in a vacuum. With the preparation of samarium metal, finally, 126 years after the first rare earth element was reduced to its metallic state, all of the *naturally* occurring rare earths were now available in their elemental state in sufficient quantity and purity to measure their physical and chemical properties. The success of this reaction is due to the low vapor pressure of lanthanum and the extremely high vapor pressures of samarium, europium and ytterbium (Daane 1951, 1961, Habermann and Daane 1961). It is interesting to note that this same technique has been the method of choice for the preparation of some transplutonium metals (Cunningham 1964).

In practice, the oxides should be relatively low-fired materials from the decomposition of the oxalates; low-fired to prevent crystal growth into a refractory condition. At the same time they should be fired to a sufficiently high temperature to degas the material, and they should be held in a protective atmosphere until used. The lanthanum should be in the form of turnings in order to present a large surface area in the reaction mixture, and should be kept in a protective atmosphere until used. The mixture is placed in an outgassed tantalum crucible and heated to the melting point of the lanthanum (920°C) in a high vacuum, with the product metal condensing on a tantalum surface in a cooler region of the furnace (Daane 1961, Beaudry and Gschneidner 1978).

2.2. *Purification processes*

2.2.1. *Vacuum casting*

As described above, the metallothermic reductions of rare earth halides with calcium involved a 10% excess amount of calcium. This insures complete reaction with a resulting high yield, generally over 99%. But it also results in some contamination of the product metal with calcium, present mostly as a condensate on the outside of the samples, but with some occluded material in the interior of the products. Since calcium is sufficiently more volatile than the rare earth metals a vacuum melting operation in tantalum crucibles reduces this impurity to a minimum level, generally less than a few ppm atomic and at the same time eliminates other trace volatiles such as fluorides and hydrogen (Gschneidner 1980a). The metals are held in the molten state in a vacuum for various times and temperatures dependent on the particular rare earth metal: the amount of metal, the melting point and vapor pressure of the metals being obvious factors. As mentioned above, this melting operation introduces some tantalum metal into the sample. For the light rare earth metals with lower melting points, a quiescent holding of the melt just above the melting point allows crystallizing of the tantalum from the resulting supersaturated

solution and a settling out of the heavier tantalum dendrites occurs. The higher melting heavy rare earth metals dissolve a larger amount of tantalum, but because of their generally higher vapor pressures, they may be purified by vacuum distillation/sublimation as discussed below.

2.2.2. *Distillation/sublimation*

The primary reason for distillation/sublimation as a purification process is to separate the non-volatile tantalum from the higher melting lanthanide metals gadolinium through erbium, plus lutetium, and scandium and yttrium. As explained earlier samarium, europium and ytterbium are prepared in a vacuum process that involves their distillation from the reaction mixture; they may be re-sublimed to achieve a higher purity.

The distillation process can be used to reduce the oxygen content if the metal is significantly contaminated as it is in many commercially available products. But there is a lower limit of about 0.01 to 0.1 at.% oxygen, at which point no further purification is possible because of the formation of an azeotropic mixture between RO and R.

The condenser temperature is quite critical. It should be high enough that agglomerating metal forms a fairly dense condensate with a small surface-to-volume ratio. In some of our initial distillation/sublimation experiments the condenser temperature was too low and the condensate consisted of a finely divided metal agglomerate in the shape of a cone with an extremely high surface-to-volume ratio, which spontaneously ignited into a spectacular brilliant white mass when it was removed from the vacuum system and brought into the air, glowing from 30 s up to a few minutes depending upon the size of the condensate.

In summaries of work by Beaudry and Gschneidner (1978) and Gschneidner (1980a), conditions for the distillation/sublimation of rare earth metals are given; batch sizes are 0.5–1 kg, vacua of 10^{-8}–10^{-9} Torr are maintained and transport rates of 1 to 4 grams per hour are achieved at temperatures that correspond to vapor pressures in the range of 10^{-2} to 10^{-1} Torr for the metal being purified.

Generally at this state, the rare earth metals are ~99.8 at.% pure with respect to all impurities in the periodic table. The major impurities are the non-metallic elements, especially H, N, C and O. But if one considers only the metallic elements then the purities are ~99.99 at.%, and just considering the other rare earth elements, the purities are >99.999 at.%. The point of this is that one must carefully define the basis for the number of nines cited. This is especially true for the rare earth metals, which Spedding has remarked – 'they are universal solvents for most of the periodic table', and because of their large atomic weights (especially the lanthanides) a few ppm by weight increases by a factor of ~10 for carbon, nitrogen and oxygen and ~150 for hydrogen when converted into ppm atomic.

2.2.3. *Electrotransport*

For further purification of the rare earth metals electrotransport [or solid-state electrolysis (SSE) as it is sometimes called] has been the most successful technique. But it has only been demonstrated on the low vapor pressure rare earth metals (Sc,

Y, La, Ce, Pr, Nd, Gd, Tb and Lu). Because of their efficient gettering behaviors, this method was not successfully applied until vacua of 10^{-9} Torr or better became available.

The success of this method depends on the rapid diffusion of the impurities in the rare earth metal in a strong electric field. Most of the non-metallic elements (carbon, nitrogen and oxygen) and the small 'interstitial-like' transition metals (iron, cobalt, nickel and copper) migrate from the cathode towards the anode, purifying the cathode portion of the rod. After 100 to 1000 hours a steady-state condition is built-up after which the forward diffusion from the cathode to the anode due to the electric field is equal to the backward diffusion due to the chemical concentration difference, and no further purification is realized.

The major limiting factor is the small size of the final high-purity product. Because of the large current densities, $\sim 200\,A/cm^2$, the rare earth metals are in the form of long thin rods (~ 3 mm in diameter $x \sim 150$ mm long) to allow the Joule heating to be dissipated by radiation. Of this long rod ~ 40 mm is usable as the high-purity sample.

The overall purities increase by ~ 0.5 at.% to > 99.9 with respect to all impurities after electrotransport purification with a 5- to 10-fold reduction in the above mentioned impurities. A similar 5- to 10-fold increase in the resistance ratio $\rho_{300}/\rho_{4.2}$ is observed. These changes are sufficient to allow de Haas–van Alphen measurements to be made on single crystals of Sc, Y, Pr, Gd, Tb and Lu (Young 1979, Gschneidner 1980a) and refinement of some of their physical properties which are sensitive to impurities (Tsang et al. 1985, Hill et al. 1987).

To prepare higher purity metals one must use the 'boot strap' method, whereby two rods of the given rare earth metal are first purified by SSE. Then the purest section of each is butt-welded together and this new rod is electrotransport purified for a second time. In this manner Carlson et al. (1975) and Carlson and Schmidt (1977) obtained high-purity yttrium and gadolinium with resistance ratios of 127 and 405, respectively, while Mattocks et al. (1977) prepared a 99.98% pure (with respect to the entire periodic table) neodymium with a resistance ratio of 120, which is extremely good since neodymium orders at 19.2 and 7.8 K and there is still a strong spin-disorder scattering contribution to the resistivity even at 1.2 K.

Details concerning this process have been summarized in several reviews (Jordan 1974, Beaudry and Gschneidner 1978, Gschneidner 1980a).

2.2.4. *Zoning*

The passage of a narrow molten zone along a solid rod has been successfully used to purify semiconductor materials and less reactive metals for over 25 years. Just as for the electrotransport purification method, zoning was unsuccessful until vacua of 10^{-9} Torr or better became standard practice in the laboratory. In this technique a molten zone is repeatedly passed in one direction, usually ~ 20 passes are required to reach steady-state conditions. Impurities which raise the melting point of the solvent are left behind during solidification as the liquid zone moves forward. Thus with continued passes these impurities are moved to the 'beginning' end of the rod. Those impurities which lower the melting point tend to remain in the molten zone

and thus move with the zone towards the 'end of zoning' end of the rod. As might be expected from the known phase diagrams, most of the metallic impurities and carbon move with the liquid zone and concentrate at the 'end' end, while hydrogen, nitrogen and carbon move against the molten zone direction and concentrate at the 'beginning' end of the rod (Jones et al. 1978, Fort et al. 1981).

Although many of the metallic impurities were lowered to extremely low levels the movement of carbon, nitrogen and oxygen was not nearly so effective, and thus the center portion of the zone-melted rod was on the average only slightly purer than the original metal especially with respect to the non-metals. The amount of metal available after a zoning run is 2 to 5 times more that from an electrotransport run, but the overall purity is less.

Fort et al. (1981) suggested that if the zoning method were used to reduce the major metallic impurities in the beginning half of the rod, and then use the 'end' half of this half (i.e. the portion of the rod from 0.25 to 0.5 from the beginning end) for electrotransport purification perhaps one could make the highest purity rare earths known. Recently they have succeeded in doing so for gadolinium (Fort et al. 1987) – reporting a 99.94 at.% pure (with respect to the entire periodic table) gadolinium sample with a resistance ratio of 730, which is also twice as large as the previous highest value. In the case of neodymium they were able to prepare the second highest purity material only exceeded by doubly electrotransport refined material reported on by Mattocks et al. (1977), see section 2.2.3.

Additional details may be found in the reviews by Beaudry and Gschneidner (1978), and Gschneidner (1980a), and the papers cited earlier in the section.

2.3. *Electrolytic methods*

Following Davey's preparation of potassium and sodium in 1807 by the electrolysis of a fused salt, other active metals were investigated with this technique. Lanthanum and cerium were prepared by Hillebrand and Norton (1875) and later on, these and the other light lanthanide metals by Muthmann and Weiss (1904), Hirsch (1911), Kremers and Stevens (1923), Trombe (1936) and Gray (1952). In recent years this method was refined and extended to a few of the heavy lanthanide and yttrium metals by the US Bureau of Mines group headed by Henrie and Morrice (see Morrice and Knickerbocker 1961, Beaudry and Gschneidner 1978, for more details).

By far the largest amounts of rare earth metals produced since the early 20th century is a mixture of the rare earth metals in their respective proportions as found in the natural occurring ore. This metallic form is known as 'mischmetal' and is prepared by electrolysis of the rare earth chloride mixture (Hirschhorn 1968).

The basic principle for preparing a metal is to reduce one of its salts by an electric current. Usually a second or third salt is added to the rare earth salt to lower the melting point, and to improve the liquidity and electrical conductivity. Two electrodes (a cathode and anode) are put into the molten salt and a current is passed through the bath to reduce the rare earth material. The rare earth metal (usually molten) is collected at the cathode and the anion is oxidized at the anode. The

voltage must be sufficient to reduce the salt. Current densities range from 3 to 12 A/cm^2. The second and third salt must be more stable than the rare earth compound and this generally limits the materials to salts of the alkali and alkaline earth metals.

The cell which holds the molten salt and metal can be made of a variety of materials, such as iron, graphite, fire brick, alumina, magnesia, molybdenum or tantalum. The cathode is usually molybdenum, tantalum or tungsten and sometimes iron, cobalt or nickel. The choice of the cell and cathode materials will depend on the product desired. Graphite is almost always the choice for the anode because it is relatively inert to the halide gases (F_2 or Cl_2) or oxygen liberated at this electrode.

2.3.1. *Electrolysis of the halide*

For the commercial production of the individual light lanthanides and mischmetal the chloride is used because it is cheap and molten at the temperature of electrolysis. Usually NaCl, KCl or $CaCl_2$ are used as the fluxing salts with the rare earth chloride. The hygroscopic nature of the rare earth chloride is one major drawback, but this has been solved successfully in the commercial production of these materials by vacuum drying just prior to electrolysis (Hirschchorn 1968, Beaudry and Gschneidner 1978). Additional comments and discussion concerning mischmetal are given below in section 2.3.2.

For preparing higher purity rare earth metals, the fluorides are used because they are not hygroscopic and hence easier to handle. But because of their high melting points ($\sim$400°C higher than the metals) a second salt is required to lower the temperature of the molten salt bath. Usually LiF, CaF_2 or BaF_2 are used as fluxing agents. In principle the metals prepared electrolytically should be as pure as those prepared by the metallothermic method, but this has not been demonstrated. The major impurities being lithium, carbon, oxygen, fluorine and molybdenum. As discussed by Beaudry and Gschneidner (1978) these could be lowered, but whether or not the carbon and oxygen levels could ever be reduced to the level found in the calcium-reduced material is still a major question.

2.3.2. *The emerging metallurgical industry*

2.3.2.1. *Pyrophoric cerium.* Cerium is one of the most pyrophoric metals known – when it is machined it gives off a shower of brilliant white sparks like a fireworks display. The pyrophoric nature of cerium was recognized by Carl Auer von Welsbach at the turn of the century when he patented a 70% mischmetal–30% iron alloy as a 'flintstone'. But it was not until 1908, when he developed a satisfactory fused-salt electrolytic process for producing sound ingots of mischmetal (similar to that described above) that his lighter flints could be utilized by the populus to light their incandescent gas mantles which he had also invented. In that year his Treibacher Chemische Werke produced 800kg of mischmetal–iron lighter flints and this marks the birth of the rare earth metallurgical industry (Greinacher 1981).

In recognition of Carl Auer von Welsbach's entrepreneurship and other important

contributions to the industrialization of Austria, he has been featured on two Austrian postage stamps (in 1936 and 1954) and on the 20 Schilling currency (see ch. 73, fig. 9). Before von Welsbach's inventions and developments into commercial utilization, basically there was no rare earth industry, and so he is truly its founder.

These flints are still in use today in cigarette lighters, industrial strikers, etc., and they are about the only rare earth 'chemical' which can be purchased in drug store and/or supermarket. Over the last 60 years several interesting anecdotes have surfaced. One is concerned with the efforts of the allied intelligence officers after World War II to investigate German efforts to achieve nuclear fission. The intelligence team, following a hot lead, ended up in the southern Austrian factory of the Treibacher Chemische Werke. The report issued by this team described in detail the production of mischmetal by electrolysis of a fused-salt bath containing mixed rare earth chlorides, with the end product being lighter flints (Singer et al. 1945). In addition to the cerium production they also manufactured radioactive materials, primarily radium and mesothorium.

Of more recent vintage is that these small lighter flints were involved in illicit international trade, especially in south central and south east Asia. The flints are purchased legally in North America and/or Europe and shipped to Middle Eastern countries for repackaging into smaller quantities. Because of import restrictions on this commodity, the flints command a premium price from the populace during the monsoon season when matches fail to ignite in the high humidities. Since the flints are small and easily hidden, sailors, black marketers, travelers, etc., can easily smuggle them into various countries.

In the early 1970's another major, but short-term application developed based on the pyrophoric nature of cerium/mischmetal. This use involved the manufacture of a mischmetal–magnesium alloy as a liner for artillery shells, which would burn with an intense heat upon impact. These shells were primarily intended for antitank warfare. Although the mischmetal production for these shell liners was high, it only lasted about 18 months.

2.3.2.2. *Alloying agents.* Over the years a variety of applications developed in the magnesium, aluminum, ductile iron, steel and zinc industries whereby the rare earths, in the form of mischmetal, were added as strengtheners, refiners, desulfurizers, etc. The amounts of rare earths added are generally a few percent in the case of magnesium and zinc, to a few tenths of a percent or less in the case of steels.

The use of mischmetal as alloying agents can vary significantly over a period time from euphoric highs, as a new rare earth application takes-off, to calamitous lows, when a competitive product or process pushes it out of the market place. The addition of mischmetal to steels in order to improve the tensile properties, especially the transverse rupture strength, is such an example. In the mid-1970's mischmetal additions were used to reduce the sulfur content and to control the shape morphology of the rare earth oxysulfide/sulfide inclusions in the steels. But by the early-1980's calcium almost exclusively replaced mischmetal because it was cheaper and primarily because calcium does not alloy (dissolve) in liquid iron, and thus an

inadvertent excess of calcium does not cause any subsequent problems in the mechanical working of the steel (excess rare earths do).

2.3.2.3. *Impact on samarium–cobalt permanent-magnet market.* In the production of mischmetal, the samarium metal does not reduce to the metallic state, but only to the divalent state, which remains in the fused-salt slag. Thus we have a natural process for separating the samarium out of the rare earth mixture at practically no cost. Before the development of the samarium–cobalt permanent magnets most companies discarded this source of samarium, except for one major producer who had the foresight to stockpile this slag, and even purchase it from other mischmetal producers for the day a samarium metal market developed. Their enterprising efforts paid-off handsomely in the 1970's with the maturity of these permanent magnets.

Since samarium comes as a by-product of mischmetal production, its cost is significantly less than it would be if the samarium were a product of the normal separation process of producing individual rare earths from basnasite or monazite. Thus there was an upper limit of the amount of samarium ($\sim$200 tons per year in 1980) available to make these permanent magnets at a reasonable price. With the fall-off of the mischmetal markets in the early 1980's, the amount of inexpensive samarium is significantly less today. Of course a lot more samarium could be made available, but at significantly higher costs if producers needed the material. With the advent of the new neodymium–iron–boron permanent magnets, the pressure on demand for more samarium has eased considerably and supply and demand are in fairly good balance.

2.3.3. *Reduction of the oxide*

The direct reduction of the oxide electrolytically in principle would be an economical way of producing the metal since it would by-pass the step to make the rare earth halide. Efforts in this regard have been successful for at least 80 years when Muthmann et al. (1907) demonstrated that cerium could be prepared from CeO_2 dissolved in CeF_3. A great deal of effort was spent in the 1960's to develop and refine the oxide reduction process for making the light lanthanide metals and mischmetal by the US Bureau of Mines (Henrie 1964, Beaudry and Gschneidner 1978). They were quite successful in preparing small batches of metals, <1 kg. Industry spent a considerable effort to scale up the Bureau of Mines process to a pilot plant level, but after several years this effort was abondoned. The main difficulties are the small solubility of the oxide in the fluoride flux, and the need to control the amount of oxide to tight tolerances due to this low solubility.

2.3.4. *Preparation of the high melting metals* ($>1100°C$)

The major difficulty preparing the high melting rare earth metals is that at the temperature required to operate the cell (greater than the rare earth metal's melting point) the materials which make up the cell and electrodes are attacked by the halide fluxes and rare earth metal or vice versa. Henrie and Morrice (1966) tried to overcome part of this problem by maintaining a large temperature gradient whereby the region near the electrodes was above the melting point of the rare earth metal

while the remainder of the cell was much cooler. However, the yields were low and the impurity levels, especially of oxygen and carbon, were high.

A study to prepare gadolinium by fused-salt electrolysis well below its melting point was carried out by Gschneidner and co-workers (Bratland and Gschneidner 1980a,b, also see references therein to earlier papers). Fairly pure gadolinium could be obtained, but the fluoride level was quite high, because the gadolinium formed as dendrites when reduced at the cathode, trapping fluoride between the dendrites as they branched and grew. Yields were low, and the cost of preparing gadolinium this way would be significantly higher than the metallothermic method (section 2.1.1).

A third possible solution for preparing high melting rare earths is to prepare a master alloy of the rare earth metal with a non-rare earth metal, which form a eutectic which melts below 1000°C. This has been successfully demonstrated by the US Bureau of Mines scientists using Mg, Al, Cr, Fe, Co and Ni as the cathode (Morrice et al. 1969, Beaudry and Gschneidner 1978). This is satisfactory if an alloy with these non-rare earth metals is the desired end product, but if a pure rare earth metal is required, then one must be able to easily remove the non-rare earth metal. Of the metals investigated magnesium, because of its high vapor pressure, would be the best choice, but as far as we are aware no one has attempted to do this.

2.4. *Single crystals*

The first crystal of a rare earth metal large enough to carry out physical property measurements (other than a single crystal X-ray structure determination) was grown approximately 30 years ago by Behrendt et al. (1957). Neodymium crystals about 3 mm on an edge were grown by the Bridgman technique. Since then most of the rare earth metals have been prepared as single crystals, by a variety of techniques, ranging in size from $\sim 1\,cm^3$ to $\sim 20\,cm^3$. The most common method used is the strain anneal or recrystallization method. It is fortuitous that the strain induced in a rare earth metal after it has been arc-melted on a water-cooled hearth is just sufficient to promote the growth of a single crystal when the sample is heated at the proper temperature for ~ 1 day. The proper temperature is generally a narrow 25–50°C window where the single crystal will rapidly grow from the strained polycrystal sample. Heat treating outside this window results in a sample which consists of several small grains or worse.

Other techniques used to grow the metals are vapor deposition, Czochralski, zone melting, crystallographic transformation and solid-state electrotransport. The most successful method of those mentioned is the zone-melting technique. The Bridgman technique is not recommended for growing crystals of the higher melting rare earths since the attack of the crucible material will lead to contamination of the rare earth material. More details concerning these methods can be found in the reviews by Beaudry and Gschneidner (1978) and Abell (1988).

With the tremendous scientific and technological interest in the magnetic behavior of rare earth intermetallic compounds a great deal of effort has gone into preparing single crystals of intermetallic phases. In this case the various zoning methods and the Bridgman technique seem to be the most popular ways of preparing such materials (see Abell 1988). Another method that has been reasonably

successful, but somewhat limited in which materials can be grown, is the growth of intermetallic single crystal compounds from a molten metal flux (Fisk and Remeika 1988).

In the past few years scientists have been able to grow the first coherent single-crystal R–R′ (where R and R′ are two different trivalent rare earths) superlattices using a molecular beam epitaxy technique (Kwo et al. 1985). One of the most interesting developments of this research is the discovery of the epitaxial growth of the (0001) of hcp rare earth metal on the (110) of niobium. In this arrangement there is a perfect crystalline match (within 1%) of four niobium atoms to every three rare earth atoms (Kwo et al. 1986). Research on the properties and behaviors of modulated superlattices consisting of alternating layers only a few atoms thick of rare earth materials appears to be one of the exciting areas of research of the late 1980's and early 1990's, also see chapter 76, section 7, in this volume.

2.5. *Intermetallic compounds*

The rare earth metals form compounds with approximately two-thirds of the non-rare earth elements in the periodic table. They do *not* form with the alkali (Li, Na, K, Rb and Cs) and alkaline earth metals (Ca, Sr and Ba) and the early transition elements (Ti, V and Cr and their congeners), nor do they form intermetallic compounds among themselves. The number of compounds in a given R–M system ranges from ~ 1 at Mn and its congeners to a maximum of ~ 7 at Co and Ni and their congeners, then slowly dropping off to ~ 2 compounds for the halides. Usually, but not always, the heavy lanthanides and yttrium form more compounds with M than do the light lanthanides.

Most compounds can be prepared by arc-melting and induction melting of the component metals, followed by an appropriate heat treatment. Induction melting should be carried out by levitation melting to avoid contamination from the crucible material. The choice of crucible material will vary depending upon the non-rare earth component(s) and the composition desired. Materials that have been used as crucibles include Ta, W, Mo, BN and, occasionally, refractory oxides.

For metals with high vapor pressures, the alloys are best prepared by melting in sealed tantalum or tungsten crucibles heated inductively or in a resistance furnace. Fortunately these high vapor pressure non-rare earth metals do not react with the crucible materials.

2.5.1. *Special techniques*

Compounds of the high vapor pressure non-metallic elements and the gaseous elements (X) can be prepared by direct combination of the gas with solid rare earth metals at fairly low temperatures. Many times the reactions do not go to completion because of the formation of an impervious RX coating which prevents or slows down the reaction. For the sulfides and selenides a few milligrams of I_2 helps break up this coating and the reaction goes to completion in the matter of a few hours, compared to weeks or months when no I_2 is present (Takeshita et al. 1982).

In order to prepare various compositions in the LaS_x solid-solution region (from

$x = 1.33$ to $x = 1.50$), Takeshita et al. (1985) reaction-sintered a mixture of powders of stoichiometric La_2S_3 and LaH_3 in a hot press. This pressure-assisted reaction sintering (PARS) method is quite effective in obtaining the desired composition with densities of 97% of theoretical. But because of the reactivity of LaH_3 it must be handled in glove boxes.

Splat cooling can also be used to prepare metastable phases and also thermodynamically stable phases which are difficult to prepare by other techniques. In this case the metastable amorphous metal alloy is slowly heated up to allow the appropriate crystalline phase to form.

2.5.2. *Influence of impurities*

Most of the rare earth metals used in preparing intermetallic compounds have been obtained from commercial sources. But as Gschneidner (1980a) pointed out these metals contain anywhere from 2 to 5 at.% impurities, mostly hydrogen, carbon and oxygen, and occasionally nitrogen and fluorine (or chlorine). A comparison of the properties and behaviors of intermetallic compounds prepared using 95–98 at.% pure commercial rare earth metals and those prepared using high-purity metals >99 at.% pure, shows that there are generally only slight differences. One wonders why fate has smiled so favorably on us, even though large quantities of hydrogen and oxygen (>10 at.%) are soluble in the rare earth metal at high temperatures. For hydrogen, in the alloying process most of the hydrogen will vaporize at the temperature used and thus is effectively removed from the intermetallic compound. Since the composition of most intermetallic compounds is governed by specific size relationships and valences of the components which make up the compound, the atom species which can occupy a given site in the structure are quite limited. This will tend to lead to the exclusion of these impurity atoms from the lattice sites of the desired intermetallic compound. The impurity atoms will be present as a second phase in the form of a rare earth non-metallic compound RX_y because the free energies of formation of the RX_y phases are among the most negative values known. In addition, since some of the rare earth metal is tied up with the non-metallic impurity atoms, the desired alloy will be richer in M than intended. For intermetallics which exist over a solid-solution range this may account for differences in reported physical property values for the same composition (Ikeda et al. 1982). But for line compounds, there is a good likelihood that some second phase of the next M-rich phase will also be present in the alloy (it could be appreciable if the next M-rich phase is only a few (<10) atomic percent away from the desired phase, such as in the R–Co and R–Ni systems).

Impurity atoms sometimes can stabilize a phase, which otherwise might not form. This has been established for R_3Al phases, where a small amount of carbon will stabilize the $AuCu_3$ type phase, but neither nitrogen nor oxygen would. Buschow and van Vucht (1967) found that only Ce_3Al and Pr_3Al will exist without the presence of carbon but the R_3Al phases of R = Nd, Sm, Gd, Tb, Dy, Ho and Er will only form if some carbon is present. In the impurity-stabilized $AuCu_3$ structure the carbon atoms occupy the open body-centered site, which is normally vacant, while the Au atoms occupy the corners and the Cu atoms the face-centered positions.

There may be other cases of compounds which only exist because they are impurity stabilized, but these have not been as well documented.

3. Physical property studies – similarities, non-similarities and surprises

As students, we all learn initially that the rare earths are 'all alike'. But as our knowledge increases we find – yes, they are similar, but yet they show many differences, and some have amazing differences. For example, their melting points vary by nearly a factor of two, which is much greater than what is observed in a normal group of elements in the periodic table, e.g., the IVA group titanium, zirconium and hafnium. An even larger difference is found in the vapor pressures of lanthanum and ytterbium at 1000°C, which differ by more than *one billion*. Keeping this in mind (they are similar, but yet different) we shall explore the physical properties of these elements in the next few subsections.

3.1. *4f orbitals*

The 4f orbitals are radially buried below the 5d and 6s orbitals and generally do not become involved in the chemical bonding to any great extent. Even so, there is considerable evidence that there is some hybridization between the 4f wave functions and the normal bonding electron (s, p and d) wave functions. In general the admixture of 4f character into the bonding states is less than 10% with most of the 4f character remaining in localized orbitals (see section 6). An important aspect is the shape and directional properties of the 4f orbitals since this can have some influence on the properties of the rare earth metals and their compounds, and these will be discussed at the appropriate time in various places in this chapter. The seven shapes for the hydrogenic 4f orbitals (Friedman et al. 1964, Becker 1964) are shown in figs. 1a–1g.

In the absence of internal and external applied fields all of these orbitals are degenerate and there is an equal probability of an electron being in any one of the seven orbitals. With interactions the actual charge density of the 4f electron(s) is a linear combination of these one-electron states. For Russell–Saunders coupling the charge density has been determined for all of the trivalent lanthanide ions in the absence of a crystal field by Sievers (1982) and the twelve possible shapes are shown in fig. 2a–2l. It should be noted that those for Eu^{3+}, Gd^{3+} and Lu^{3+} (as well as Eu^{2+} and Yb^{2+}) are perfectly spherical and are shown in fig. 2f. When the lanthanide ion or atom is placed into a real crystal the potential from the neighboring ions or atoms (which can be non-lanthanides or lanthanides) will have a great affect on the anisotropy of the 4f charge distribution, due to the symmetry of this crystal field. Thus it is impossible to state a priori what the exact shape of the 4f charge density will be until the crystal structure is specified. In cubic or axial crystal fields the anisotropy of the 4f charge densities has been calculated for some of the lanthanide ions by Schmitt (1986). Even larger anisotropies are expected in lower symmetries, and as we shall see this can have important effects on some of the

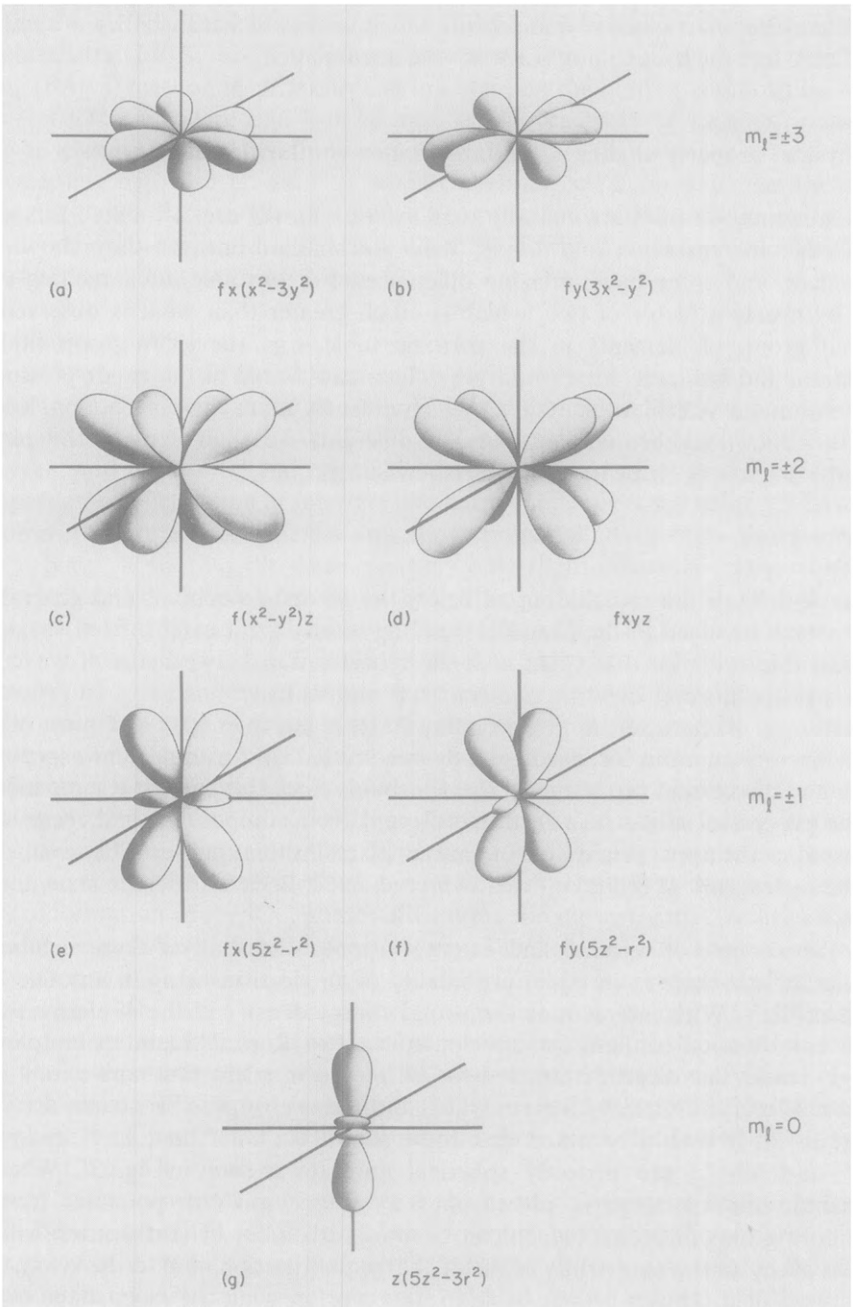

Fig. 1. The atomic orbitals of the hydrogenic wave functions of the 4f electrons in the absence of a crystal field. The wave functions for (a) and (b) have the maximum projection on the xy plane and correspond to the case for $m_l = \pm 3$; while those for (c) and (d), $m_l = \pm 2$, and (e) and (f), $m_l = \pm 1$, have successively smaller projections on the xy plane until the minimum is reached at (g) $m_l = 0$.

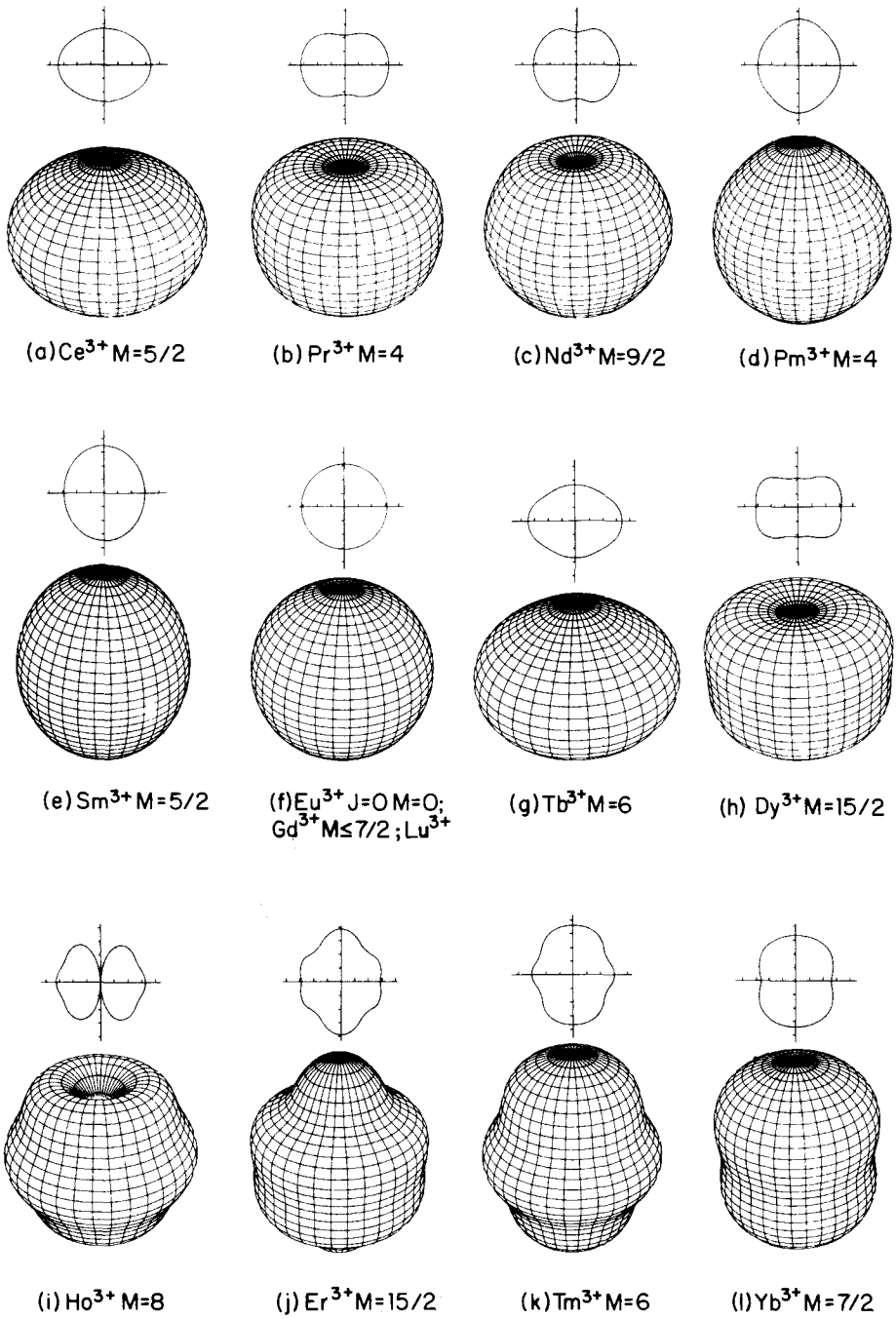

Fig. 2. The 4f charge densities in the fourteen trivalent lanthanide ions in the absence of a crystal field. After Sievers (1982) (by permission of Springer Verlag).

physical properties of the lanthanide metals and compounds (see sections 4.3.3, 4.3.4 and 6.2).

3.2. *Crystal structures*

Although the crystal structures of about half of the rare earth metals were well established by the mid- to late 1930's the work by Klemm and Bommer (1937) stands as a landmark paper because they determined the crystal structures and the lattice parameters of all the lanthanides, except holmium, samarium and radioactive promethium. In so doing they

(1) confirmed the existence of the lanthanide contraction in the metals (it had been established about ten years earlier in the oxides, see section 5.1),

(2) discovered the anomalous valences for cerium ($>3+$), europium ($2+$) and ytterbium ($2+$), and

(3) confirmed that the lanthanides crystallize in at least three different structures – fcc, bcc and hcp.

It was not until about 25 years later, however, that the final details became available concerning the room-temperature crystal structure sequence in the lanthanides.

Klemm and Bommer prepared the lanthanide metals in sealed glass capillaries containing lanthanide chlorides and potassium metal. After heating to achieve reaction, the mixture of the lanthanide metals and the slag was used for X-ray diffraction and magnetic susceptibility studies. After World War II with the availability of high-purity oxides and better techniques for preparing pure metals Spedding et al. (1956, 1958, 1961) reported detailed studies on the crystal structures of the rare earth metals, describing the double *c*-axis hexagonal (dhcp) form of lanthanum, praseodymium and neodymium (Spedding 1956) as well as the high-temperature bcc form of La, Ce, Pr, Nd, Sm, Gd and Yb (Spedding 1961). The unique crystal structure of samarium reported by Daane et al. (1954) is a complex stacking of close packed layers (ABABCBCAC) and it presents an interesting phenomenon with the double *c*-axis stacking of layers in the light lanthanide metals before samarium in the periodic table and the regular hexagonal stacking in the heavy lanthanide metals after samarium. The puzzle is compounded when the samarium structure was found in alloys formed between a light lanthanide metal and a heavy lanthanide/or yttrium metal (Spedding et al. 1962). An explanation for this layering sequence is presented in section 6.1. The crystal structure of promethium has been determined to be dhcp by Pallmer and Chikalla (1971).

The atomic volumes of the lanthanides, as calculated from their room-temperature lattice parameters, are shown in fig. 3. Basically this is the same plot as given by Klemm and Bommer where the lanthanide contraction is evident, and also the anomalous valence states for cerium (slightly greater than three) and europium and ytterbium (both divalent). Anomalies due to divalency are also evident in many of the physical properties and these will be duly noted throughout the chapter. The occurrence of divalency in europium and ytterbium is a striking confirmation of Hund's rule that half-filled (in the case of divalent europium with a $4f^7$ con-

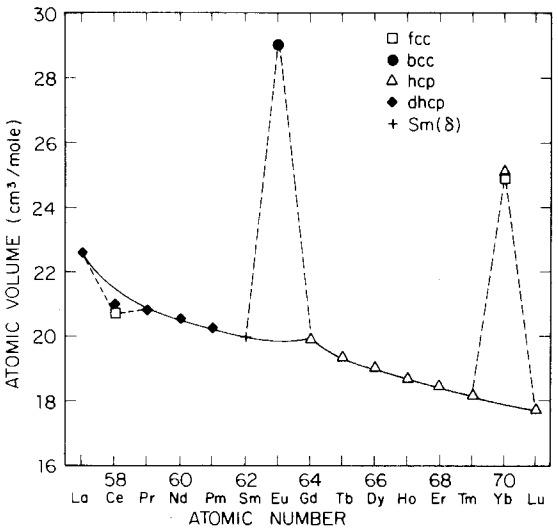

Fig. 3. The room-temperature atomic volumes of the lanthanide elements and their room-temperature crystal structures. For cerium and ytterbium their just below room-temperature structures and atomic volumes are also given (dhcp and hcp, respectively).

figuration) and completely filled (in the case of divalent ytterbium with a $4f^{14}$ configuration) shells are stable states. The negative deviation from the trivalent curve of cerium is due to its tendency to become tetravalent, also trying to obey Hund's rule by giving up a 4f electron to empty its 4f level. Furthermore, when the room-temperature fcc form of cerium (γ-Ce) is cooled down to ~ 110 K or compressed to ~ 0.8 GPa (8 kb) it undergoes a large volume contraction ($\sim 15\%$) becoming an even higher valent (but still somewhat less than four) polymorph of cerium (α-Ce) (see Koskenmaki and Gschneidner 1978).

The actual situation is more complicated than this simple explanation. The current thinking is that the localized 4f electron becomes a delocalized 4f electron (or at least partially so) giving rise to these volume anomalies and other unusual physical property changes at the $\gamma \rightarrow \alpha$ transformation.

The cusp at gadolinium and the up-swings at the beginning (lanthanum) and end (lutetium) are evident (this could also be seen on Klemm and Bommer's curve, but it was not discussed), and are thought to be due to crystal-field contractions in the lanthanides which do not have spherical 4f wave functions (Ce → Sm and Tb → Tm, see fig. 2) (see Beaudry and Gschneidner 1978). No such contractions due to crystal fields are expected for lanthanum since it has no 4f electrons, or for gadolinium since its half-filled shell is spherically symmetrical, or for lutetium since its 4f shell is completely full.

The high-temperature polymorphic form for most of the rare earth metals just before melting is the bcc structure. Four of the trivalent lanthanides (holmium, erbium, thulium and lutetium) are monomorphic and do not form a bcc structure before melting at atmospheric pressure (see fig. 4). However, the bcc phase can be formed in holmium and erbium by the application of pressure (< 1 GPa), see section 3.7.1. The existence of the bcc phase in the lanthanides has been correlated with the d occupation number, which decreases along the lanthanide series, but increases

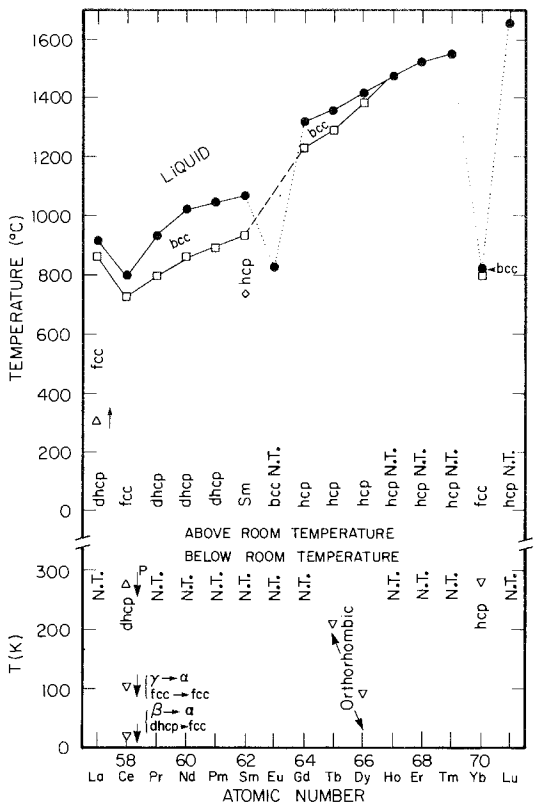

Fig. 4. The allotropy, transformation and melting temperature of the lanthanides. Note that room temperature is the baseline. Below room temperature the scale is in degrees Kelvin (K) and above room temperature it is in degrees Celsius (°C), because this is the common usage. N.T. means no transformation occurs in the temperature direction from room temperature. The low-temperature transformations (<400°C or <673 K) exhibit hysteresis and thus an arrow next to the transformation point indicates the direction in temperature which was used to measure the given point (usually away from room temperature). P means a partial transformation and that the transformation does not go to completion unless some unusual means are employed.

with increasing pressure (Gschneidner 1985a, Gschneidner and Calderwood 1986a). When the number of d-electrons per atom is either too large, >2.2, or too small, <1.6, the bcc phase does not exist in the lanthanide metals, while at 1.9 (neodymium) the bcc phase seems to be the most stable.

In addition to these bcc phases, lanthanum (β-La) and samarium (β-Sm) have intermediate high-temperature phases which exist between the room-temperature form and the bcc form. For lanthanum this phase has an fcc structure, while for samarium it is hcp (fig. 4).

Upon cooling below room temperature several more polymorphic phases (in addition to α-Ce mentioned above) form (see fig. 4): β-Ce with a dhcp structure, α'-Tb and α'-Dy both having an orthorhombic structure, and α-Yb with a hcp structure (Beaudry and Gschneidner 1978, Gschneidner and Calderwood 1986a). The α' phases of terbium and dysprosium are unusual because they form when the helical magnetic phase of these two metals transforms into the ferromagnetic phase. The magnetoelastic energy associated with the ferromagnetic alignment of the magnetic moments in the basal plane is sufficiently strong to overcome the normal electrostatic bonding between atoms to cause a distortion of the hcp lattice. The anisotropy of 4f wave functions (see section 3.1) is different in terbium and

dysprosium, such that in terbium there is an expansion in the *b*-direction (the normal to the prismatic face of the hcp unit cell) relative to the *a*-direction while in dysprosium there is a contraction along *b* relative to *a*. As one might surmise the easy magnetic directions are along the axis which has expanded, i.e. *b* in terbium and *a* in dysprosium (McEwen 1978).

In summary, the surprises in the crystal structures of the rare earth metals are:

(1) the formation of the dense α-Ce phase;

(2) the existence of the intermediate (between fcc and hcp) stacking arrangement of the dhcp phase (50% hcp/50% fcc) and the Sm or δ structure (66.7% hcp/33.3% fcc);

(3) the formation of the low-temperature orthorhombic phases upon ferromagnetic ordering; and

(4) the non-existence of the high-temperature bcc phase in the last four lanthanides.

3.3. *Magnetic and electrical behaviors*

In the mid- to late-1930's several major discoveries occurred, which indicated that the rare earth (or more specifically the lanthanide) metals were really an unusual group of elements. The existence of ferromagnetism at room temperature in gadolinium reported by Urbain et al. (1935) was the first major clue that some exciting things might be happening. Two years later we have the discovery of superconductivity in lanthanum (Mendelssohn and Daunt 1937) and the first extensive study of the magnetic properties of europium and the heavy lanthanides, in which Klemm and Bommer (1937) presented evidence of magnetic ordering in europium, terbium and dysprosium, and confirmed ferromagnetism in gadolinium. Their data also suggested that erbium and thulium will order below 100 K, the lowest temperature they were able to attain.

3.3.1. *Heavy lanthanides*

Low-temperature heat capacity, magnetic susceptibility and electrical resistivity measurements by the Ames group in the 1950's, led by Spedding and Legvold (Spedding et al. 1957a), on the heavy lanthanides with unpaired 4f electrons, other than gadolinium, showed several magnetic ordering temperatures, indicating that some rather unusual magnetic phenomena are occurring. The initial studies and also some preliminary neutron scattering measurements were made on polycrystalline samples. Since the neutron data were difficult to interpret, and since the polycrystalline magnetic susceptibility and resistivity studies were not very meaningful, it became apparent that single crystals of the metals were necessary if the magnetic behaviors of the heavy lanthanides were to be fully understood. The first single crystals of sufficient size to make physical property measurements were grown by the Ames group in the late-1950's (see section 2.4). By 1960, the crystals were sufficiently large for neutron scattering measurements, and Spedding then sent these crystals to Koehler who headed the Oak Ridge neutron scattering group. Shortly thereafter Koehler et al. (1961) found that the magnetic lanthanides formed some

unique, exotic and diverse magnetic structures. More details concerning this subject will be found in Rhyne's chapter (76) in this volume and an earlier review by Sinha (1978).

3.3.2. *Theory*

Our understanding of the magnetic phenomena in the pure metals was greatly aided by theorists, and extension of their models to intra rare earth alloys and intermetallic compounds not only helped in comprehending the magnetic behaviors of these materials, but also served as guides to the development of new magnetic rare earth materials such as the permanent magnets and magnetostrictive materials. There were two great thrust periods: the mid- to late-1950's and approximately ten years later. In the former period Kasuya (1956) and Yosida (1957) independently proposed that magnetic ordering in the lanthanide metals occurs because of indirect exchange between 4f electrons on neighboring ion sites via the conduction electrons. Since this theory was an extension of the Ruderman –Kittel (1954) indirect-exchange model used to explain the hyperfine interaction between nuclear moments on adjacent ion sites, this model is known as the RKKY indirect-exchange model. Another major theoretical paper was the one written by de Gennes (1958) in which he showed that the paramagnetic Curie constant (which is obtained from the Curie–Weiss behavior of the magnetic susceptibility above the highest ordering temperatures) of the lanthanide metals is proportional to $J(J+1)(g-1)^2$, which is now known as the de Gennes factor. Subsequently several other physical properties were shown to depend upon the de Gennes factor, e.g., the depression of the superconducting transition temperature of lanthanum doped with 1 at.% lanthanides (Suhl and Matthias 1959) and the magnetic contribution to the electrical resistivity (Legvold 1972). Later work also showed that the proportionality between the paramagnetic Curie constant and the de Gennes factor held for the lanthanide intermetallic compounds (Kirchmayr and Poldy 1979) and solid-solution alloys (Sinha 1978).

The second great theoretical thrust period took place in the mid- to late-1960's when scientists were able to explain semi-quantitatively how the various striking and diverse magnetic structures occurred in the heavy lanthanide metals (Sinha 1978). Starting with the RKKY interaction and introducing the anisotropy of the 4f wave functions due to crystal field (see section 3.1) and other contributions, theorists were able to describe the occurrence of the various magnetic structures as a function of Z (the atomic number of the lanthanide) and temperature.

3.3.3. *Light lanthanides*

The light lanthanides also exhibit some unusual electrical and magnetic properties. The superconductivity of lanthanum has already been mentioned. But when its behavior is compared to the superconductivity in scandium, yttrium and lutetium, we find lanthanum is unusual. The ordering temperature T_s and pressure dependence of T_s are both larger in lanthanum than in the other three superconductors (see section 3.7.3 and fig. 12a).

Also noteworthy is the fact that magnetic ordering in the dhcp and Sm structures

initially occurs in the crystallographic hexagonal layers and then at lower temperatures in the cubic layers (see section 3.2 for the description of these structures). The temperature differences in occurrence of ordering increases from ~1 K in β-Ce (dhcp) (Koskenmaki and Gschneider 1978) to ~10 K in dhcp α-Nd to ~100 K in α-Sm with the nine layer stacking arrangement (Sinha 1978). While these three lanthanides order magnetically, dhcp α-Pr does not if it is a pure single crystal due to its singlet ground state.* But by applying a small stress, either physically or by using a polycrystalline sample in which stress is introduced due to the anisotropic thermal expansion on cooling down, praseodymium will begin to order at ~25 K. Alloying with a few atomic percent of another lanthanide, such as neodymium, will also cause the praseodymium to order, even in a single-crystal specimen (Sinha 1978, Mackintosh and Bjerrum-Møller 1986).

3.3.4. *Cerium – the keystone element*

Probably the most remarkable element of the entire rare earth series (for that matter the whole periodic table), is cerium. From ~50 K to well above room temperature, it is in a non-magnetic Kondo state (the only such known pure element), but at low temperatures it orders antiferromagnetically (~13 K). This behavior has been observed in the dhcp β-Ce phase. The fcc γ-Ce phase is also in a non-magnetic Kondo state, but because it transforms to either β-Ce at ~0°C or to the collapsed fcc α-Ce at ~110 K we cannot say much about γ-Ce's low-temperature behavior. α-Ce at high pressures is a superconductor at ~30 mK, and when it transforms to α′ at ~4 GPa its T_s increases to ~1.8 K (see fig. 12b). The α/γ Ce transformation, in which Ce undergoes an ~15% volume change, has been of considerable interest for the last 35 years for both experimentalists and theorists in trying to understand the intermediate valence/valence fluctuation behavior in this system (see Koskenmaki and Gschneider 1978). If the rich and diverse behaviors observed in this one element (a Kondo lattice, anti-ferromagnet, superconductor and valence fluctuator) were completely understood, our knowledge of the remainder of the periodic table undoubtedly would be fully known at the same time – clearly cerium is the cornerstone of our house of knowledge of the periodic table.

3.4. *Thermal properties*

3.4.1. *Allotropic transformation temperatures*

The allotropy was discussed above, in the crystal structure section, 3.2. The polymorphic forms and the various transformation temperatures of the lanthanide metals are summarized in fig. 4. The behavior of scandium and yttrium are similar to those of the middle-heavy lanthanides having a room-temperature hcp phase and a high-temperature bcc form.

For most of the polymorphic transformation temperatures there does not appear

*By this statement we mean that α-Pr does not order magnetically via the normal RKKY mechanism which governs the other lanthanides. α-Pr does order, however, at 40 mK via a hyperfine interaction between the 4f electrons and the nuclei (Bjerrum-Møller et al. 1982).

to be any systematic relationships in the lanthanide series, except for the close-packed to bcc transformation at high temperature. This is partially true and partially false. The $\alpha \rightleftarrows \beta$ transformation in lanthanum and samarium, and the $\beta \rightleftarrows \gamma$ transformation in cerium are part of the systematic trends in the crystal structure sequence in the trivalent lanthanides (Gschneidner 1985a,b, Gschneidner and Calderwood 1986a), see also section 6.1. The $\alpha \rightleftarrows \gamma$ transformation in cerium and $\alpha' \rightleftarrows \alpha$ phase transformations in terbium and dysprosium, as noted earlier in section 3.2, depend upon the 4f electrons.

The high-temperature transformation to the bcc phase follows a systematic trend, i.e. the transformation temperature increases with increasing atomic number. But the trend is not just that simple, a closer look reveals that the temperature range for the existence of the bcc phase is a maximum at neodymium/promethium (158/152°C) and it decreases toward either end of the lanthanide series. This is consistent with the d electron count being most favourable at neodymium for the maximum stability of the bcc phase (see section 3.2).

3.4.2. *Melting points*

Early values given for the melting points of the rare earth metals were generally estimates obtained from indirect observations, such as the temperature at which powdered metals 'welded' together, or the temperature at which a loaded indenter sank into a heated specimen, or temperatures obtained by extrapolation into the heavy lanthanide metal region from measured values of the melting points of light lanthanide metals. These were reasonable attempts to provide the best values at the time but suffered from misinterpretations. For instance, the melting point of neodymium was once reported as 840°C, the temperature at which a loaded indenter suddenly sank into a heated specimen of the metal. This temperature corresponds to the hcp $\rightleftarrows$ bcc transformation for neodymium, with the soft cubic form of the metal allowing for this misinterpretation of a melting point.

Metal purity also had an effect on the reported values, especially for metals prepared before World War II. One of the early reports for the melting point of lanthanum gave a value of 805°C which is more than 110°C below the currently accepted value of 918°C. Work on the La–C phase diagram by Spedding et al. (1959) offers a reasonable explanation for this low value. These authors found that the La–C eutectic melts at 806°C, and since most of the early light lanthanide metals were prepared by electrolysis using graphite electrodes it is quite likely that their metal was contaminated by carbon. About 0.5 wt.% C would be sufficient for some of the metal (or better yet, alloy) to melt at 806°C.

In the 1950's when large amounts (>100 g) of pure rare earth metals became available, thermal analysis provided the true melting points (see fig. 4). These measurements also showed the presence or absence of the high-temperature close-packed $\rightleftarrows$ bcc transitions in these metals (see section 3.4.1).

Wheelwright's (1969) preparation of promethium metal and attempts to measure the melting point of the metal by conventional thermal analysis are interesting to read. The internal heating of the metal from radioactive decay of the ^{147}Pm (2.64 year half life) to ^{147}Sm is large enough to defeat normal thermal analysis measure-

ments, and the less direct observations of the temperature of flow of metal in a hole in a 53-gram ingot of the metal gave a best estimate of 1168°C for the melting point. However, this figure must be viewed in the context of a complicating factor: during the time of metal preparation and measurement, the samarium content grew so that the sample was actually a 2.5% samarium alloy by the time measurements were made! Since the daughter samarium is generated in a metallurgically septic atmosphere it is reasonable to assume a completely homogeneous alloy is the product. This alone, however, can not explain this high value, since the accepted melting temperature of promethium is 1042°C, and that of samarium is 1074°C. The high value is probably due to the formation of an oxide film on the Pm–2.5 at.% Sm alloy which did not allow the flow of the melt into the hole until the temperature exceeded the melting point by ~120°C.

The approximate two-fold variation in the melting points from lanthanum to lutetium is indeed unusual for a group of similar 'nearly identical' elements. The ΔT_m is ~750°C for the metals (lanthanum versus lutetium) ignoring the lower melting cerium. This compares to ΔT_m values of 150 or 300°C for ionic-like compound series, such as the oxides or halides. The melting points for the early light lanthanides are low (slightly higher than those of the alkaline earth metals) relative to the rest of the periodic table, while those for the late heavy lanthanides (slightly higher than those of scandium and yttrium) are about what one would expect on going from the alkali to the alkaline earth to the tetravalent titanium, zirconium, hafnium metals (see fig. 5). The anomalous low melting temperatures are thought to be due to 4f-conduction electron (5d6s) hybridization, which decreases along the lanthanide series, except for cerium where it is the largest (Gschneidner 1971). The greater the amount of hybridization the lower the melting point. In compound series such as the R_2O_3 the 4f electrons are not expected to be as highly hybridized as in the metals since the valence electrons of the R atom are transferred to the oxygen atom to form this ionic compound. This lack of hybridization is evident in ΔT_m which is 150°C for the R_2O_3 series of compounds. Further discussion on how 4f hybridization influences the melting process is deferred to section 6.2.

The anomalously low melting points of the divalent europium and ytterbium is quite evident in fig. 4, and when these values are compared to those of the alkaline earth metals (fig. 5) it is seen that they are close to each other, ~800°C. This again supports the claim of the divalent nature of these two elements.

3.4.3. *Vapor pressures and boiling points*

Specific studies of the vapor pressures of rare earth metals were not carried out until the late 1940's. However, various earlier manipulations of rare earth metals, including vacuum melting of cerium and lanthanum gave a clear indication that these metals had relatively low vapor pressures, compared to the alkaline earth metals for instance. The first concerted study of the vapor pressure of a rare earth metal was that of Ahmann (1950) who used a radioactive tracer modification of the Knudsen technique to show that cerium had a vapor pressure of 10^{-2} Torr at 1735°C. Daane (1951) measured the vapor pressures of lanthanum using a direct weight loss Knudsen technique to show that lanthanum has a vapor pressure of

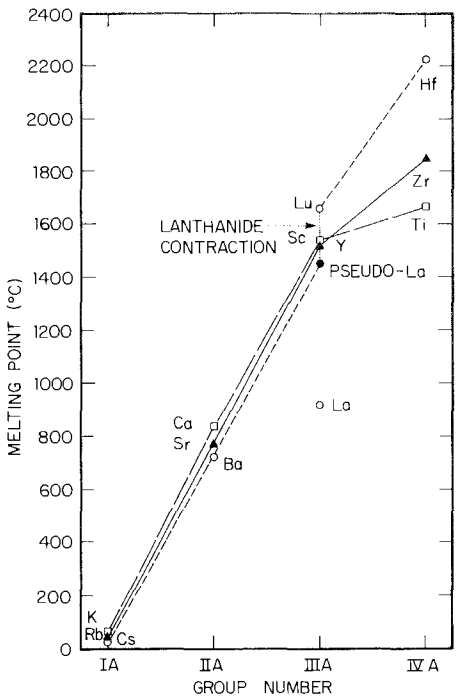

Fig. 5. The melting points of the group I A through group IV A elements (after Gschneidner 1971). The point labelled 'La' is the experimentally observed melting point for lanthanum. The observed melting points for the trivalent lanthanides are not shown for clarity but lie between the lanthanum and lutetium points, except for cerium which lies below that of lanthanum (see fig. 4). The point labeled 'pseudo-La' is the expected melting point of lanthanum (estimated from the periodic trends of the melting points) if there were no 4f hybridization involved in the bonding. The dotted line labeled 'lanthanide contraction' gives the expected range of melting points of the trivalent lanthanides between lanthanum and lutetium due to the lanthanide contraction in the absence of 4f hybridization.

10^{-2} Torr at 1750°C. In the same study praseodymium was shown to have a vapor pressure of 10^{-2} Torr at 1420°C, indicating it was significantly more volatile than lanthanum or cerium. Other vapor pressure studies on rare earth metals by the Ames Laboratory, Iowa State University group, include work by Hanak on europium (Spedding et al. 1958), Barton on thulium (Spedding et al. 1957b) and Wakefield (1957) on holmium, but the most extensive study of the vapor pressures of the rare earth metals was that of Habermann and Daane (1961) who reported data for all of the rare earth metals except promethium. Other studies have been reported by various scientists from other laboratories, but none have been as extensive as the Habermann and Daane work. The available vapor pressure data up to about 1970 was critically evaluated by Hultgren et al. (1973) and these are considered to be accepted values. The derived heats of sublimation at 298 K and the boiling points are shown in fig. 6.

The anomalous variation of the heats of sublimation (ΔH_s) and boiling points (T_b) as a function of the atomic number was immediately recognized by Habermann and Daane (1961) in their extensive study of the vapor pressure of all of the rare earth metals. The nearly parallel variation of these two quantities follows from Trouton's rule, which states that

$$\Delta S_v = \frac{\Delta H_v}{T_b} \simeq 25.5 \text{ e.u.},$$

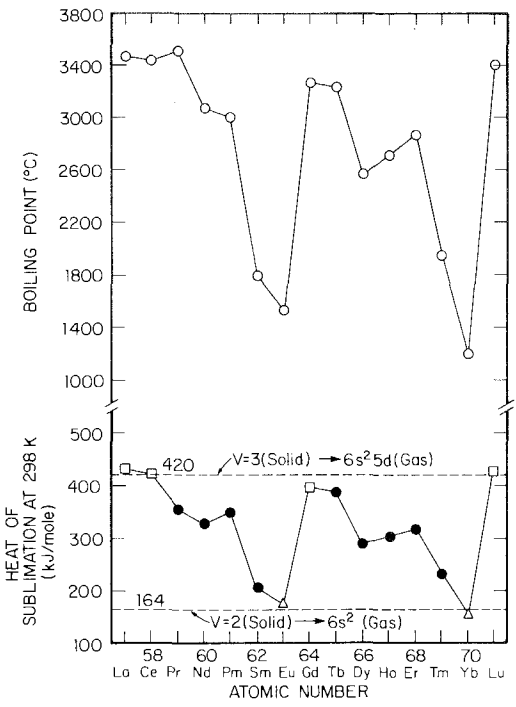

Fig. 6. The boiling points and heats of sublimation at 25°C of the lanthanide metals as a function of the atomic number. (After Beaudry and Gschneidner 1978.) The values of promethium were estimated (Beaudry and G schneidner 1978). The open squares for the heats of sublimation are for the trivalent solid metals (with $4f^n$ configuration), which vaporize to a gas with the $4f^n5d6s^2$ configuration; the open triangles are for the divalent solid metals (with a $4f^{n+1}$ configuration) which vaporize to a gas with the $4f^{n+1}6s^2$ configuration; and the solid circles are for trivalent solid metals ($4f^n$) vaporizing to a gas with a $4f^{n+1}6s^2$ state.

and since $\Delta H_v \propto \Delta H_s$. They suggest that the vapor pressures, heats of vaporization (sublimation) and electronic structures of these metals correlate well with the concept of enhanced cohesive strength when d electrons are present in the metallic state. In the case of europium and ytterbium, their divalent, alkaline earth-like nature in the metallic state finds no d electrons present, and a weaker bonding and higher vapor pressure (lower heats of sublimation and lower boiling points) are evident. Furthermore, they noted that the corresponding values for samarium and thulium lie between those of the two divalent metals (europium and ytterbium) and the other 'traditional' heavy lanthanides (dysprosium, holmium and erbium). Today, however, we recognize that not only is the electronic configuration of the solid phase important, but also that of the final phase – the gaseous atom (Gschneidner 1971, Beaudry and Gschneidner 1978). Examination of fig. 6 reveals that ~420 kJ/mol are required to sublime a trivalent lanthanide metal (with a 4f configuration) to a gaseous atom with a $5d6s^24f^n$ configuration, i.e. lanthanum, cerium, gadolinium and lutetium. Only ~165 kJ/mole, however, are required for a divalent lanthanide (with a $4f^{n+1}$) configuration to sublime to a $6s^24f^{n+1}$ gaseous atom, i.e. europium and ytterbium. The remaining trivalent lanthanides undergo an electronic transition on sublimation to a $6s^24f^{n+1}$ ground state, and in so doing the de-excitation energy on going from a $(5d6s)^34f^n$ configuration to the $6s4f^{n+1}$ state lowers the sublimation energy as shown in fig. 6 to a value between 420 and 165 kJ/mole. In general, the de-

excitation energy increases as we approach the half-filled and completely filled 4f levels, again another important verification of Hund's rules.

Johansson and Mårtensson (1987) have presented an interesting and different approach. Since most of the gaseous lanthanides (the ground state) are divalent (except La, Ce, Gd and Lu) and since the cohesive energies of the metallic divalent and trivalent states are $\sim$170 and $\sim$420 kJ/mole, respectively, these lanthanides gain an additional binding energy of $\sim$250 kJ/mole by condensing into the trivalent metallic state. But this gain of additional binding energy comes at the expense of exciting a 4f electron to the 5d level. From atomic spectroscopic levels it is clear that this promotion energy is larger than the gain of binding energy only for europium (333 kJ/mole) and ytterbium (277 kJ/mole) and this is why these two elements are divalent in their condensed metallic state and the remaining lanthanides are trivalent.

It is important to note that when one makes thermodynamic cycle calculations which involve the gaseous lanthanide atoms the 'saw-tooth'-like variation of the heat of sublimation observed in fig. 6 will also be found in the calculated thermodynamic heat or energy quantity, for example the dissociation energies of the gaseous molecules R_2, RAu, RO, RC_2, etc. (Cater 1978).

3.5. *Chemical properties*

3.5.1. *Oxidation*

As anyone who has worked with the pure trivalent rare earth metals, especially the light lanthanides, knows these metals readily react with air. As one might expect the rate of oxidation will depend on several variables, and these are quickly summarized here. The rate of oxidation is higher

(1) the higher the impurity level (of most common impurities),
(2) the higher the relative humidity,
(3) the higher the temperature, and
(4) the lower the atomic number of the lanthanide.

The four points will be amplified upon below.

The presence of impurities such as carbon, iron, calcium and many of the p-group elements, such as zinc, gallium and germanium, and their congeners, will greatly increase the rate of oxidation. This was quite evident in the late 1950's and early 1960's; as we prepared purer and purer metals, it became easier to handle them because the rate of oxidation had slowed down considerably. The presence of iron, of course, is quite important in one major application – cerium lighter flints. The oxidation behavior of the p-group elements is interesting, in that the rate of oxidation increases as one goes down the periodic table in a given group, i.e. the sixth period metals (Hg, Tl, Pb) are generally more reactive than the corresponding fifth period congener metals (Cd, In, Sn) which are more reactive than the corresponding fourth period metals (Zn, Ga, Ge).

The rate of oxidation of lanthanum increases more than a factor of ten by increasing the relative humidity from 1% (80 mg/dm^2 day) to 75% (950 mg/dm^2 day). Similarly an increase in the temperature greatly accelerates the oxidation.

Again for lanthanum the rate of oxidation (in mg/dm^2 day) increases from 80 at 35°C to 510 at 95°C to 3200 at 400°C to 13000 at 600°C (Love and Kleber 1960).

The rate of oxidation varies considerably from one rare earth to another, with the heavy lanthanides, yttrium and scandium being much more stable than the light lanthanides. For example, the rates of oxidation (in mg/dm^2 day) at 95°C in a 75% relative humidity atmosphere are: 21000 for lanthanum, 5500 for praseodymium, 2000 for neodymium, 100 for samarium and 0 to 35 for the trivalent lanthanides gadolinum through lutetium, and scandium and yttrium (Love and Kleber 1960). This variation in oxidation rate is in part due to variation in the oxide product formed: the light lanthanides lanthanum through neodymium form the hexagonal A-form R_2O_3 structure, the middle lanthanides samarium through gadolinium form the monoclinic β-form R_2O_3 phase, while the remaining rare earths form the cubic C-form R_2O_3 modification. Furthermore, the A-form R_2O_3 phase reacts with water vapor in the air to form an oxyhydroxide, which causes the white coating to spall, exposing the fresh metal surface allowing the oxidation to proceed. But for the heavies which have the C-type structure oxides, this modification forms a tight coherent substoichiometric gray black colored oxide coating, i.e. R_2O_{3-x}, with x varying from 0.01 to 0.03 depending on R (Miller and Daane 1965), which prevents further oxidation, similar to the behavior of aluminum.

The driving force for this chemical reactivity is the high free energy of formation of the oxides – among the highest known of all the elements in the periodic table, see fig. 7. Only CaO has a ΔG_f which is slightly larger (more negative) than most of the rare earth oxides, while MgO and BeO have free energies which are slightly smaller (less negative) than those of the trivalent R_2O_3 phases.

This chemical reactivity is responsible for some uses of the rare earth metals, such

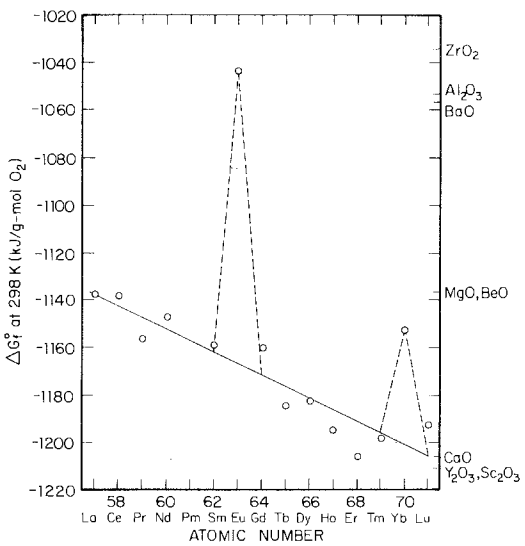

Fig. 7. The free energy of formation at 298 K of the R_2O_3 phases for the lanthanides as a function of atomic number. The free energies of formation of some other stable oxides, including Sc_2O_3 and Y_2O_3, are indicated on the right edge of the figure.

as getters in vacuum tubes (much more important before the advent of semiconductor technology than today), lighter flints, incendiary devices and getters in metals and alloys. Lighter flints are a 50–75% mischmetal–iron alloy which ignites when sharply struck. It is the pyrophoric nature of cerium which accounts for the sparking of the flint. The incendiary devices also rely on the pyrophoricity of cerium, but in this case the alloy is composed of mischmetal and magnesium, see section 2.3.2.1. When the rare earths, usually in the form of mischmetal, are added to a commercial alloy, such as a steel or superalloy, the rare earths react with the residual oxygen, sulfur and other 'tramp' elements to form compounds which segregate to the surface or grain boundaries and clean the steel, etc.

3.5.2. *Reactivity with other elements*

The rare earth metals will react much more slowly with nitrogen than with oxygen under any of the conditions described above. Usually high temperatures are required to observe any appreciable reaction. Furthermore, the formation of RN on the surface greatly reduces any further nitridation.

The metals will easily hydride at modestly elevated temperatures (400–600°C). Usually there is an incubation period before the reaction proceeds, but once the metal has been hydrided, it can be rehydrided almost instantaneously as long as the activated surface has not been exposed to air. Unless special care is taken, when the metal is hydrided up to and beyond RH_2 in hydrogen content, the solid material fragments. Since hydrogen is easily removed this process can be used to make metal powders, which can be used as an intermediate step to prepare other compounds. If one wishes to make metal powders, one must, however, make a compromise – one can get fine separated powders containing some hydrogen, or if hydrogen cannot be tolerated one will get a sintered mass of powders because of the high temperatures required to drive off the last remaining hydrogen molecules.

The rare earth metals will react exothermically with sulfur, selenium, phosphorus, etc. If heated up to the appropriate temperature the reaction will take off and could seriously damage the crucible, furnace, vacuum enclosures, etc. However, at low temperatures some of the rare earths will hardly react, e.g., the heavy lanthanides with sulfur. In the case of sulfur and selenium a small amount of iodine ($\sim$100 mg per 20 g metal sample) will catalyze the reaction, such that the sample is completely sulfidized in 24 hours, whereas without the iodine even after months the reaction is incomplete (Takeshita et al. 1982).

3.5.3. *Reaction with acids and bases*

The rare earth metals, except europium, react slowly or not at all with water. But as the pH is lowered by the addition of most mineral acids the reaction proceeds quite rapidly giving off H_2. The reactivity is proportional to the acid concentration within limits. The metals also react with the common organic acids, but generally at a slower rate than with the mineral acids at the same concentration.

The one exception is hydrofluoric acid where the formation of a RF_3 coating prevents further reaction. Even in a 1:1 mixture of HF and HNO_3 the rare earth metals do not react. As a matter of fact, it is possible to dissolve tantalum metal in

this mixture leaving behind the rare earth metal which, however, has a fluoride coating.

The metals react only slowly with strong bases, i.e. NaOH, and essentially not at all with weak bases such as NH_4OH. The formation of the insoluble rare earth hydroxide on the metal surface is undoubtedly responsible for this lack of reactivity. Unfortunately little is known about this reaction.

The dissolution of samarium metal in acid, particularly, HCl, is interesting. In the initial reaction of the metal the solution has a deep red wine color, due to the formation of the Sm^{2+} ion and within a few minutes the color slowly fades due to the oxidation of Sm^{2+} by the oxygen in the air to form the light yellow colored Sm^{3+} ion in solution. In about the ten minutes it takes for this change to occur the color changes from a red burgundy to a rosé to a Rhine wine color. A similar behavior is observed on dissolving ytterbium, but in this case a green color is formed first which bleaches to a colorless solution. This color change can be speeded up by blowing air through a straw into the green solution – the electronic configuration is so touchy that just a breath of air will change it.

3.5.4. *Metallography and surface passivation*

There are several metallographic chemical polishing techniques. The recommended approach is to electropolish the metal in a 6% perchloric acid dissolved in absolute methanol at dry-ice temperatures (Beaudry and Gschneidner 1978). The advantage of this technique is that the metal has a shiny silvery color and a passivated surface (see below). This electropolishing procedure is also used to clean the metal surface after mechanical fabrication and/or heat treating operations. The major disadvantage when cleaning or polishing cerium and ytterbium is the formation of their low-temperature phases (β-Ce and α-Yb) at the dry-ice temperature. If it is important that the room-temperature forms are maintained then chemically polishing or cleaning with Roman's solution is recommended. Roman's solution is a complex solution of organic and mineral acids and is used at room temperature (Beaudry and Gschneidner 1978). Roman's solution can be used for the other rare earth metals in place of the perchloric acid/methanol electropolishing technique, but the latter is our first choice.

As noted above, electropolishing with perchloric acid will passivate the surface. The reason for this passivation effect was not known for many years, but it was clear it worked. Auger analysis of unetched and electropolished gadolinium samples revealed a surface layer which has an appreciable fraction of chlorine in it (along with oxygen) in the electropolished sample, while the unetched sample contained only oxygen (Bevolo et al. 1980). It is thought that the formation of an oxychloride layer on the surface is responsible for the passivation of the metal surface.

3.5.5. *Anomalies*

We now turn our attention to europium and ytterbium, since most of the above discussion was concentrated on the trivalent rare earth metals. Europium metal is the most reactive rare earth metal with respect to handling in air. Within minutes after exposure to moist air a yellow film of $Eu(OH)_2 \cdot H_2O$ develops on the surface

(Spedding et al. 1958). Europium should always be handled in inert atmospheres. Furthermore, there is no satisfactory method for chemically or electrolytically preparing an europium surface for metallographic examination.

Ytterbium, on the other hand, is quite inert to air and can be handled like the heavy trivalent lanthanides and yttrium and scandium. Ytterbium can be electropolished using the perchloric–methanol method at dry-ice temperatures, but some hcp α-Yb will be present. If an ytterbium sample free of α-Yb is needed both a room-temperature chemical etchant and an electropolishing method have been developed (see Beaudry and Gschneidner 1978).

There is another major anomaly with respect to europium and ytterbium, and that is observed in the free energies and heats of formation of compounds in which europium and ytterbium are trivalent. This is best seen in fig. 7 where the free energy of formation of the oxides of europium and ytterbium are anomalously small (less negative) than those of the other trivalent lanthanides. This may seem to suggest that the values for europium and ytterbium are in error, but as first pointed out by Gschneidner (1969b), one needs to consider the standard states of the element being oxidized to form the R_2O_3 phase. Both europium and ytterbium are divalent in their standard state, while the other rare earths are trivalent and thus when the metals react with oxygen the divalent metals must promote the extra 4f electron to the valence or outer electron level in order to form the trivalent oxide R_2O_3. This promotion energy as given by Gschneidner (1969b) is 96 kJ/g at. Eu and 38 kJ/g at. Yb. Subsequent re-analyses by others have led to the refined values of 88 and 46 kJ/g at. R, respectively (Johansson and Mårtensson 1987).

3.6. *Elastic and mechanical properties*

3.6.1. *Elastic behavior*

As soon as reasonably pure metals became available in large quantities elastic properties were measured first on polycrystalline materials and later on single crystals. The compressibility of polycrystalline materials was measured by Bridgman (Harvard University) in the late 1940's and early 1950's, but it was not until the late 1950's that the other elastic properties [Young's (or elastic) and shear moduli and Poisson's ratio] were measured by Smith and co-workers (Iowa State University) and Love (Research Chemicals, Phoenix) (see Gschneidner 1961). With the availability of single crystals in the early 1960's of sufficient size to measure the c_{ij} values (see section 2.4) scientists began to measure these properties (primarily Smith and co-workers at Iowa State University and Palmer and associates at the University of Hull), (see Scott 1978). In general, the elastic properties increase with increasing purity. The best values for the lanthanide metals are plotted in fig. 8 as a function of the atomic number (Scott 1978). The anomalies are clearly evident at cerium (premonition of the $\gamma \rightarrow \alpha$ transformation) and europium and ytterbium (divalency). Furthermore, there is a general increase in these elastic moduli as a function of increasing atomic number until a maximum is reached at thulium. As expected the single-crystal c_{ij} values exhibit the same trend as observed in fig. 8 for the bulk elastic constants (Scott 1978).

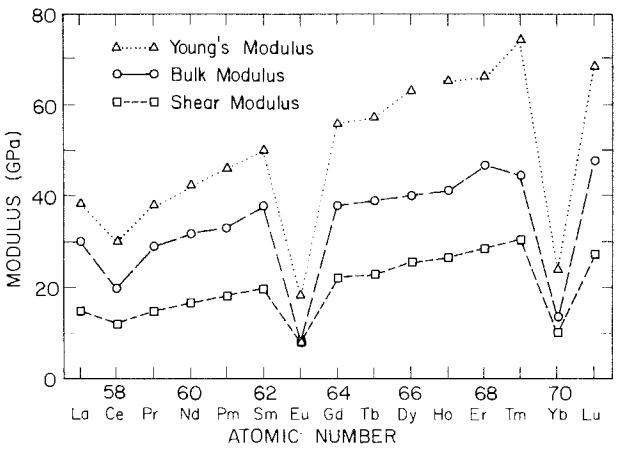

Fig. 8. The bulk elastic constants of the lanthanide metals (after Scott 1978). The values for promethium are estimated.

The behavior of some of the elastic constants of the magnetic lanthanides have been measured in magnetic fields. In general, the onset of magnetic transitions are quite observable in the elastic properties, see fig. 9. In the case of terbium the application of a magnetic field is quite evident, since a modest field will destroy the antiferromagnetic state by causing the spins to flip and align ferromagnetically. A large change in both the c_{11} and c_{33} elastic constants near the ordering temperatures is seen in fig. 9 when a field of 2.5 T (25 kOe) is applied (Palmer et al. 1974). An extremely large change is seen in c_{11} below the Curie temperature. This is apparently related to the crystallographic distortion in the basal plane (i.e. the formation of the orthorhombic α'-Tb, see section 3.2) due to ferromagnetic ordering

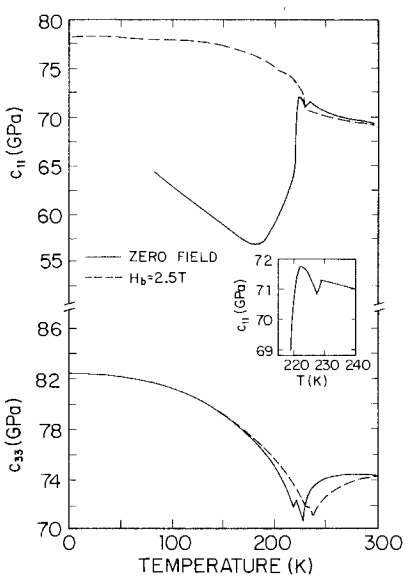

Fig. 9. The temperature dependence of the single-crystal elastic constants c_{11} and c_{33} of terbium at zero magnetic field, and in an applied field along the easy axis. The inset shows the details of c_{11} at the Néel and Curie temperatures. (After Palmer et al. 1974.)

at zero field, but in the applied field such a distortion presumably does not occur and a more typical temperature dependence is observed (dashed line in fig. 9 for c_{11}).

More details concerning the elastic behavior of the rare earth metals can be found in the extensive review by Scott (1978).

3.6.2. *Mechanical properties*

The early work (in the 1950's) on the mechanical properties of the rare earth metals was carried out by B. Love (Research Chemicals, Phoenix), C.R. Simmons and co-workers (General Electric, Cincinnati) and E.M. Savitskii and co-workers (A.A. Baikova Institute of Metallurgy, Moscow) (see Scott, 1978). Since these early studies were carried out on fairly impure metals, probably of the order of 95 at.% pure with the interstitial elements as the major impurities, the hardness, yield strength and ultimate strength are two to ten times larger than the values obtained more recently by Scott and co-workers (Scott 1978) on much purer metals, ~99 at.% pure. As might be expected the elongation and reduction in area values for the older measurements are two to ten times smaller than those obtained more recently.

In general, the hardness and strength values for the lanthanides appear to have the same periodic trend as observed for the elastic moduli shown in fig. 8. Although the experimental scatter of the data is quite large, cerium, europium and ytterbium definitely have anomalous low values for the same reason as discussed above for the elastic constants (section 3.6.1), and the increase from the light lanthanides to the heavy lanthanides seems to occur. The mechanical properties of the trivalent rare earth metals are similar to those of aluminum at the low range of the reported lanthanide values and fall between those of aluminum and titanium for the upper range of values. Most of the rare earths do not neck down, or only slightly if they do, before fracture and thus the ultimate tensile strength and fracture strength are nearly the same. A detailed review of the mechanical behavior of the rare earths has been described by Scott (1978) and further details can be sought there.

3.7. *High-pressure studies*

Most of the high-pressure studies have involved the determination of the phase boundaries as a function of pressure and temperature using volumetric, electrical resistivity and X-ray techniques. As a result of these studies a few new allotropic phases have been discovered. Other studies include the superconducting behavior of these elements, some magnetic property measurements, and the valence fluctuation behavior of cerium. And as a result of these investigations several surprises were found, which are noted below.

3.7.1. *Crystal structure sequence and P–T diagrams*

In the mid-1960's the Bell Laboratory group led by Jayaraman and McWhan studied the high-pressure polymorphism of the lanthanides, and much to everyone's surprise they found that the high-pressure phase in gadolinium and terbium has the

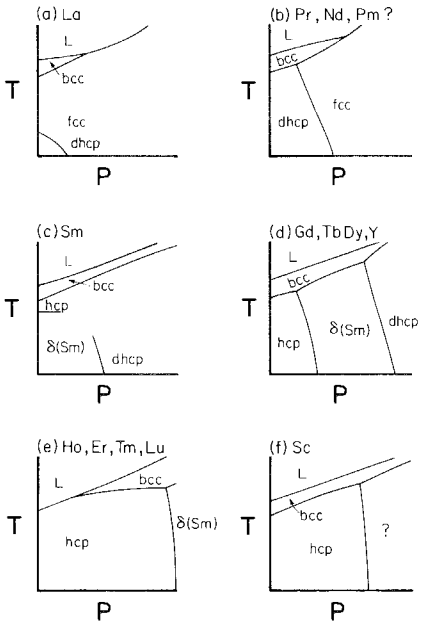

Fig. 10. The pressure–temperature diagrams (schematic representation) of the trivalent rare earth metals.

samarium-type structure, and that samarium has the dhcp structure, see fig. 10. Shortly thereafter they and other scientists found that the dhcp metals (lanthanum, praseodymium and neodymium) became fcc at high pressure, fig. 10 (Jayaraman 1978, Gschneidner 1985b). From these studies it was evident that the normal crystal structure sequence at atmospheric pressure (fcc→dhcp→Sm-type→hcp) is reversed by application of pressure. This unexpected behavior led to a number of papers attempting to explain this sequence of structure and its pressure dependence (see Langley 1982, and references cited therein). This is considered further in section 6.1.

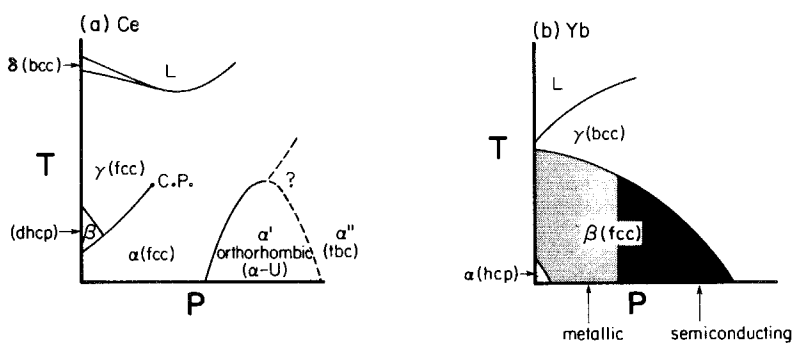

Fig. 11. The pressure-temperature diagrams (schematic representation) of (a) cerium and (b) ytterbium. In the cerium diagram (a) the letters 'C.P.' means critical point, and 'tbc' means tetragonal body-centered.

A schematic representation of the pressure–temperature diagrams for all of the rare earth metals, except europium, is shown in figs. 10 and 11. The europium diagram is not shown because europium is monomorphic at all conditions studied so far. However, its melting behavior shows a maximum at ~3 GPa and 990°C (Jayaraman 1978). For the 14 trivalent rare earths, the pressure–temperature relationships can be represented by six different behaviors as shown in fig. 10. In addition to the unusual close-packed crystal structure sequence behavior at high pressure, it is evident that pressure tends to favor the bcc phase – this is most evident in the sequence of P–T diagrams from lanthanum (a) to praseodymium, neodymium (b) to samarium (c). Also the development of the bcc phase in the holmium, erbium, thulium, lutetium diagram (e) at high pressures gives further support to this. The existence of this bcc phase and its dependence on the d-occupation numbers has been discussed earlier in section 3.2. For scandium a high-pressure transformation has been observed at 17 GPa, but its structure is not known (Wittig et al. 1979). If this high-pressure form should have the δ(Sm) structure then the scandium P–T diagram (fig. 10f), would presumably be the same as that for gadolinium, terbium, dysprosium and yttrium (d).

Recent studies show that at pressures greater than 6 GPa a new high-pressure phase develops in the fcc region at room temperature for lanthanum and praseodymium. Two different structures have been proposed for this phase – a 'distorted fcc' and a triple hexagonal close-packed (thcp) structure (Gschneidner 1985a, Gschneidner and Calderwood 1986a). See also the recent comments of Gerward et al. (1986) and Sikka and Vijayakumar (1986) concerning these high-pressure phases. Also noteworthy is the recent discovery by Grosshans et al. (1983) of the formation of the α-U structure in praseodymium at ~19 GPa. This structure has been known to exist in cerium (α'-Ce) for many years (Koskenmaki and Gschneidner 1978), see fig. 11 and section 3.7.2. The existence of the α-U structure in praseodymium has been suggested as evidence for some delocalization of 4f electrons and subsequent 4f hybridization with the outer valence electrons to give rise to this structure (Grosshans et al. 1983).

The field of ultrahigh pressures is still a young one and there are many new structures to be found; this new knowledge will probably cause us to modify some of our ideas on the electronic structure and bonding of materials.

3.7.2. *The eccentric ones: cerium and ytterbium*

Cerium as we had noted previously exhibited some anomalous behaviors (sections 3.3.4 and 3.4.1), and thus one might expect its high-pressure properties to be different. A quick glance at fig. 11 reveals that we will not be disappointed. The existence of a critical point (a point where the two phases in co-existence are indistinguishable) in the solid state at 2.5 GPa and 695 K (422°C) is unique – the only one known to exist between two solids. This critical point arises from the 4f valence fluctuation behavior in the fcc phases of α- and γ-Ce. As the critical point is approached with increasing temperature and pressure the properties of the two phases become more and more alike – the valence in γ increases from 3.06 to 3.26 at the critical point while that of α decreases from 3.67 to 3.26, and the volume of

transformation at atmospheric pressure ($\sim 17\%$) decreases to zero at the critical point (Koskenmaki and Gschneidner 1978).

The negative sloping liquidus line at low pressures, unique among the rare earth metals, is also an obvious anomaly. Not obvious from a P–T diagram is the fact that in cerium, one has an element which is both an antiferromagnet (β-Ce) and a superconductor at high pressures, see fig. 12b (α-, α'- and α''-Ce). Cerium is indeed a fascinating element.

Ytterbium, off hand, with its filled 4f level and two conduction electrons might not be expected to have abnormal properties. But it too has at least one unique property among the rare earth elements. As indicated by the shading in fig. 11b at ~ 2 GPa β-Yb becomes a semiconductor due to the opening of a gap between the filled 6s level with two conduction electrons and the empty 5d band. When the pressure reaches ~ 4 GPa at room temperature the fcc β-Yb transforms to the bcc γ-Yb phase, and the material once more becomes a metallic conductor. The resistivity of β-Yb at room temperature and atmospheric pressure, which is about 27 $\mu\Omega$, rises slowly by about one order of magnitude with increasing pressure up to the $\beta \rightarrow \gamma$ transformation, at which time the resistivity suddenly drops by more than one order of magnitude, such that the resistivity of γ-Yb at 4 GPa is less than that a ambient condition (β-Yb) (see Jayaraman 1978).

3.7.3. *Superconductivity*

Of the seventeen rare earth metals only lanthanum is superconducting at atmospheric pressure. Lanthanum is one of the better elemental superconductors – its 6.1 K transformation (β-La, fcc) is only exceeded by those of lead (7.2 K) and niobium (9.2 K), and its thermodynamic critical field, $H_c(0) = 1600$ Oe is second to that of niobium's 1980 Oe. When the pressure dependence of the superconducting transition temperatures is taken into account lanthanum has the highest known elemental transition temperature, ~ 13 K, see fig. 12a.

The dhcp α-La is also superconducting below 5.04 K. In a recent study Herchenroeder et al. (1985) speculated that if metastable bcc γ-La could be retained it would become a superconductor at 8.0 ± 0.1 K. These outstanding superconducting properties of elemental lanthanum suggest that lanthanum-based superconducting materials may someday be as important in superconducting technology as niobium-based materials, which today dominate this field. Although a number of lanthanum containing alloys and compounds have excellent superconducting properties, none are able to match the properties of the best niobium-containing materials. But there are still a large number of lanthanum–non-metallic element ternary phases which have not been studied and offer much promise for a material which would be competitive with Nb_3Sn and related phases.

As this manuscript was being written we received numerous prepublished reports that present evidence for rare earth containing superconductors with transition temperatures [*where the resistance goes to zero* ($\rho = 0$)] of 30 to 90 K. The breakthrough came in late 1986 when Bednorz and Müller (1986) (who were awarded the 1987 Nobel Prize in Physics) reported evidence for superconductivity at ~ 30 K in a $(La,Ba)_2CuO_{4-y}$ compound. The highest superconducting temperature ($\rho = 0$) re-

ported for a lanthanum copper oxide, is 38 K for the La–Sr–Cu–O phase which has the K_2NiF_4 structure (Tarascon et al. 1987). In early 1987 a second break-through occurred when Chu announced at a news conference that a new oxide superconductor with transition temperature that started near 100 K had been discovered. The initial details were first published by Wu et al. (1987). This new phase subsequently was found to have a distorted perovskite structure of the formula $YBa_2Cu_3O_{9-x}$, and $\rho = 0$ superconducting transition temperatures of 65 K for Lu–Ba–Cu–O (Moodenbaugh et al. 1987) and 94 K for Y–Ba–Cu–O (Chu et al. 1988). The substitution of the magnetic lanthanides, which do not have higher oxidation states, for yttrium (Hor et al. 1987) has little if any effect on the superconducting transition temperature. This suggests that the major role played by the trivalent rare earth ion is the stabilization of the structure and that it has a negligible role in the superconducting process per se. Cerium, praseodymium and terbium, which have higher oxidations states, apparently do not form this phase. Other scientists have made claims of evidence of superconductivity in a mixture of oxide phases with ordering temperatures as high as 240K, but these have not yet been verified by others. Although these compounds have high critical fields, the critical currents are low and the current carrying capacity needs to be improved if major utilization of these materials is to be realized.

The interest and excitement these high-temperature superconductors have generated are enormous and unfathomable – by May 1, 1987 over one hundred papers had appeared in print primarily in the *Japanese Journal of Applied Physics* (84 papers alone in the April issue) and in *Physical Review B*. The developments in this rapidly growing field have been recorded by various science writers from major trade journals and general science journals (Caplin 1987, Dagani 1987, Dickman 1987, Khurana 1987, Maddox 1987, Miura 1987, Pease 1987, Robinson 1987, Swinbanks 1987).

The application of pressure is known to cause materials, which are not superconducting at ambient pressures, to become superconductors, and the non-4f rare earth elements are members of this group of elements, see fig. 12. The pressure dependences for lanthanum (both α- and β-La), lutetium, scandium and yttrium are shown in fig. 12a and those for the high-pressure allotropes of cerium in fig. 12b. The large difference in the T_c values of lanthanum and the other three rare earths is thought to be due to the presence of low lying 4f levels which are slightly occupied and hybridized with the other conduction electrons in the 6s and 5d bands (also see sections 3.4.2 concerning the effect of 4f hybridization and the low melting points of the light lanthanides and section 6.1). The pressure dependence of T_c of lanthanum has been discussed in terms of phonon softening and band structure effects (Probst and Wittig 1978); however, the decrease in spin fluctuations as a function of increasing pressure in lanthanum may also be an important contribution, especially since lanthanum has a large λ_{spin} (spin fluctuation enhancement factor) of 1.05 (Tsang et al. 1985).

The increase in T_c of lutetium, scandium and yttrium is probably due to the quenching or partial quenching of λ_{spin} of these three metals [0.6, 1.6 and 0.4, respectively, at one atmosphere (Tsang et al. 1985)] as a function of increasing

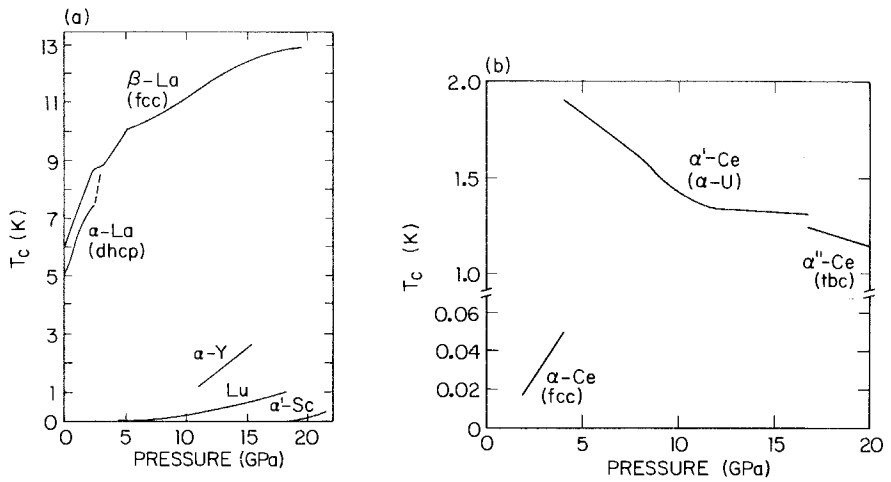

Fig. 12. The pressure dependences of the superconductivity transition temperatures of several rare earth elements: (a) lanthanum, lutetium, scandium and yttrium (after Wittig et al. 1979); and (b) cerium (after Probst and Wittig 1978).

pressure. One notes that the pressure dependences of T_c of lanthanum and yttrium are nearly the same and are significantly steeper than those of lutetium and scandium, which are about the same. Sheng Jiang and Zhang Liyuan (1985) proposed on the basis of band-structure calculations that in yttrium at these high pressures there is some hybridization of the 4f wave functions, which are high lying levels at ambient pressures, with the 5s4d conduction electrons and this accounts for the observed behavior. No 4f hybridization would be expected in either lutetium, since all of the 4f levels are filled, or scandium, since the 4f levels are extremely high lying levels, probably near or above the first ionization potential.

The critical pressure, P_c, at which superconductivity begins (i.e. $T_c = 0\,\mathrm{K}$), is consistent with the λ_{spin} values for these three metals. That is, the P_c of lutetium and yttrium are about the same, but significantly lower than that of scandium (fig. 12a), and λ_{spin} for yttrium and lutetium are nearly the same and about 3 to 4 times lower than λ_{spin} for scandium. This supports the above analysis that the absence of superconductivity in lutetium, scandium and yttrium is due to spin fluctuations in these metals.

The story of the discovery of superconductivity in scandium is an interesting one and it came about as a result of discussions between J. Wittig (Kernforschungsanlage Jülich) and K.A. Gschneidner Jr (Ames Laboratory, Iowa State University) at the 12th Rare Earth Research Conference in Vail, CO, July 18–22, 1976. Wittig in his presentation on superconductivity of the rare earths at high pressure stated that no one had succeeded in finding superconductivity in scandium at any pressure and temperatures down to the tens of millikelvins range. Gschneidner pointed out that most scandium metal prepared in the world contained anywhere from 25 to more than 100 ppm atomic of iron, and suggested that this iron

impurity level prevented superconductivity from occurring since Kondo scattering is observed in scandium containing $\geqslant$25 ppm atomic iron. Gschneidner offered to supply some scandium, which contained less than 10 ppm atomic iron, if Wittig would check for superconductivity at high pressures and low temperature. Gschneidner and F.A. Schmidt succeeded in preparing this high-purity scandium by electrotransport purification (see section 2.2.3) and C. Probst and Wittig carried out the T_c measurements in a diamond anvil high-pressure apparatus. The results of this synergistic collaboration are seen in fig. 12a (Wittig et al. 1979). This is an illustrative example of the importance of high-purity materials to determine the intrinsic behavior of materials, which in turn anchors our basic knowledge and understanding of materials.

4. Alloys

The information on rare earth alloys is vast and nearly incomprehensible, and yet we estimated that perhaps only one half of the possible *binary* alloy systems with the rare earth metals have been studied in any detail at all. And if one considers in addition all possible ternary and higher component alloys our present day knowledge of rare earth alloys is minuscule. To give the reader an idea of the vastness of our knowledge it would take one person working full time twelve years to compile, critically evaluate and write up his/her evaluation of *all* of the known crystallographic and phase relationship data of the rare earth binary alloys. If one were to do the same with the thermodynamic, magnetic and electrical, and miscellaneous property data of these same alloys one would need another 12 person years to complete this aspect.

Thus this vast, but yet quite incomplete, body of knowledge, presents us with a problem as how to describe what has occurred in this area of rare earth research, development and application. Our descriptions will be brief and hopefully touch on the more important and interesting scientific and technological aspects and materials, at least from our limited view. The history of rare earth alloys starts just after the turn of the century with the development of a commercial alloy – mischmetal – in lighter flints by von Welsbach in 1908 – and the publication of the first rare earth binary phase diagram by Vogel in 1911 (see Gschneidner 1984). Only a few phase diagrams per year (generally <5) were studied in the next fifty years, but then a rapid expansion of information occurred in the 1960's with more than 25 phase diagrams per year being reported by 1965. The number of diagrams appearing in the literature is still continuing to grow today.

4.1. *Phase relationships*

4.1.1. *Early work*

R. Vogel in Germany and G. Canneri in Italy were the principal early pioneers in determining phase diagrams of the rare earth metals. Vogel primarily concentrated on cerium systems – the first studied was the Ce–Sn system (Vogel 1911) – and

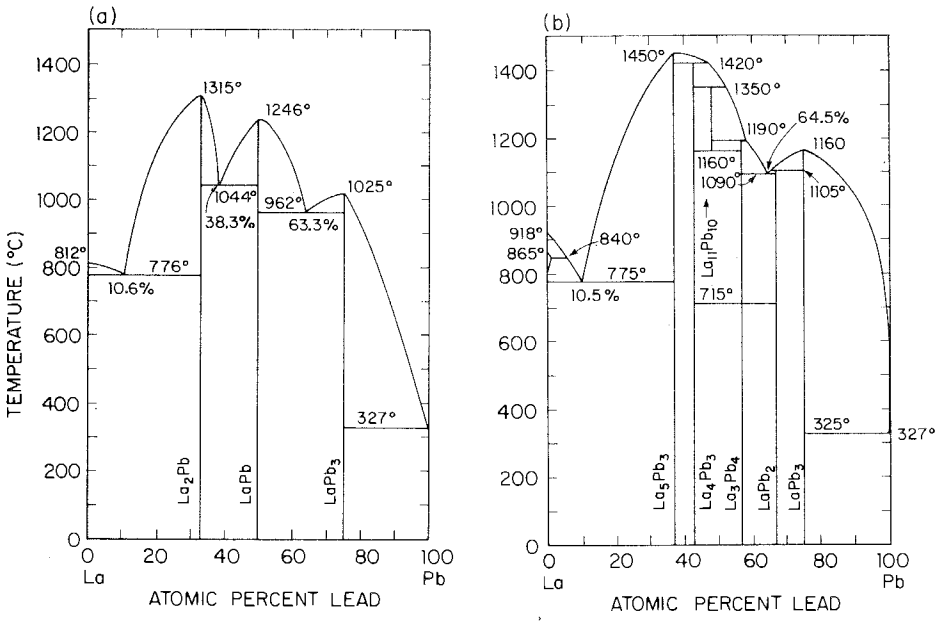

Fig. 13. The lanthanum–lead system. (a) The evaluated diagram presented by Hansen (1958) based on the original work of Canneri (1931), the X-ray study of Rossi (1933) and the re-investigation of the lead-rich side by Vogel and Heumann (1943). (b) The diagram reported by McMasters et al. (1968).

Canneri devoted most of his efforts to lanthanum diagrams – the first studied were the lanthanum systems with Mg, Cu, Ag, Sn, Au, Tl and Pb (Canneri 1931). These and other scientists did a remarkable job determining the phase relationships of light lathanide metals, primarily lanthanum, cerium and praseodymium, especially when one considers the low purity of the starting lanthanides; the lack of reasonably good vacuum and inert atmosphere facilities; poor quality of refractory crucibles and thermocouple protection tubes; the unavailability of modern thermal analysis and X-ray equipment; and the high reactivity of the rare earth metals. Consequently, in spite of their valiant efforts, generally, major portions of the reported phase diagrams are not correct. This is readily seen in fig. 13, where we present the La–Pb phase diagram (fig. 13a) as evaluated by Hansen (1958) based on the early researches of the 1930's and 1940's, and the most recent version of this diagram (fig. 13b) as reported by McMasters et al. (1968). It is immediately obvious that a number of intermediate phases were not observed in the early work, that two of the three observed intermetallic compounds do not have the correct composition, and that most of the melting points of three compounds, and that of the 'pure' lanthanum are 100°C lower than those given in the latest study. The low melting points for the 'La_2Pb' and 'LaPb' compounds may be due to the fact that, as reported by Canneri, the lanthanum-rich alloys reacted with the crucible and thermocouple protection tube at temperatures above 1000°C, but high impurity

contents (see below) could also account for all or part of this disparity in melting temperatures. On the other hand, there is agreement at the lanthanum-rich end with respect to the eutectic temperature and composition, and at the lead-rich end with respect to the composition of the lead-rich compound $LaPb_3$.

The low lanthanum melting point given by Canneri (see fig. 13a) is close to the 806°C eutectic temperature reported for the La-rich La–C alloys (Spedding et al. 1959). And since much of the early lanthanide metals were prepared electrolytically using graphite anodes and cathodes, it is likely that Canneri (1931) actually was using a La–C alloy as his 'pure' lanthanum in these binary phase diagram studies. If this is so then the 'binary' system shown in fig. 13a really represents the phase relationships along a line from the La–C alloy composition to pure Pb, i.e. a cut in ternary La–Pb–C system from ~20 at.% C–La (the eutectic composition in the La–C system) to pure Pb.

In conclusion it is best to consider the pre-1950 binary phase diagrams as being wrong unless proven correct by more recent studies. But in the event of the paucity of new results and the immediate need for phase relationship data, the rare earth-poor side can be considered more likely to be correct than wrong, while the rare earth-rich side of the diagram should be disregarded (no information is better than erroneous data).

4.1.2. *Solid solutions*

Extensive solid-solution formation in the binary rare earth alloy systems is summarized in fig. 14. If the solid solubility at any temperature in any polymorphic form is $\geqslant$5 at.% of either R (a *trivalent* rare earth metal) in M (a non-rare earth metal) or M in R, the solid solubility is considered to be extensive, and limited when it is $<$5 at.%. Since both europium and ytterbium are divalent in their elemental

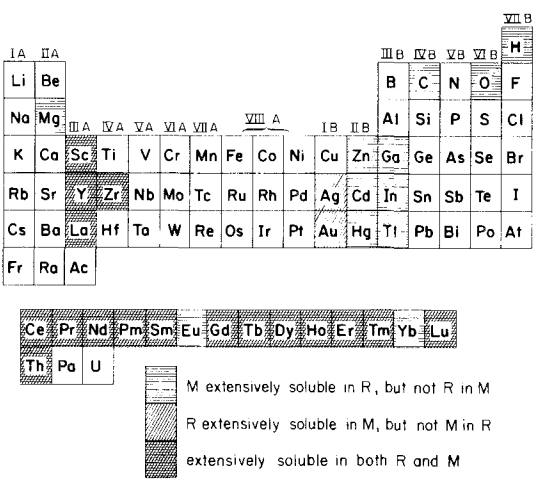

Fig. 14. Solution formation by the trivalent rare earth metals. Extensive solid solutions means that 5 at.% or more of R in M or M in R is found in most of the R–M (or R–R′) systems when M (or R′) is shaded, where R′ is a second rare earth element in an intra rare earth binary alloy system. For M = Ga there is some evidence that gallium dissolves extensively in the high-temperature bcc form of the rare earth metals.

states they are included in M and excluded from R. In the case of intra rare earth binary alloys the second rare earth metal is designated by R′.

Examination of fig. 14 reveals as expected that R–R′ alloys form extensive solid solutions and in general they are completely miscible with one another, in at least one common polymorphic form. These systems have recently been discussed in detail by Gschneidner (1985b) and the reader is referred to this paper for further details, and also to section 5.4.

The R–Zr and R–Th systems also form extensive solid solutions at both ends of the phase diagrams. In the case of thorium the alloys are completely miscible if the rare earth metal has either a fcc or bcc (or both) polymorphic form(s). For the R–Zr systems only the Sc–Zr system exhibits complete miscibility; the light lanthanides and yttrium form limited solid solutions at both ends of the diagram; and the heavy lanthanides form extensive solid solutions at both ends. Generally the rare earths are more soluble in zirconium than vice versa, and the solid solubility is greater in the bcc phase than in the close-packed phase (Gschneidner 1980b). The variation in the solid solubility in the R–Zr series of alloys is considered to be a classic textbook example of how the solid solubility increases as one proceeds along the lanthanide series from lanthanum to lutetium and continuing on to the smaller size scandium (Gschneidner 1980b). In this sequence of elements the size difference relative to zirconium and electronegativity difference, in parentheses, vary from 17.2% (0.22) from lanthanum to 12.4% (0.18) at gadolinium to 8.3% (0.12) at lutetium to 2.4% (0.06) at scandium.

The solid solubility of a number of the non-rare earth metals (including europium and ytterbium in this group) are more extensive in the trivalent rare earths than vice versa, see fig. 14. This group includes the small size divalent metals (M = Mg, Zn, Cd and Hg), the interstitial elements (M = H, C and O), the two divalent barides (M = Eu and Yb), and the trivalent group III B metals (In and Tl, and probably Ga). Except for carbon, M is more soluble in the bcc phase than in the close-packed lower temperature polymorph. Indeed it is possible to retain the bcc phase at room temperature by modest quenching techniques in the R–Mg (Miller and Daane 1964, Herchenroeder et al. 1985) and R–Cd (Herchenroeder et al. 1985) alloys.

The solid solubility behavior of the divalent barides (europium and ytterbium = M) are interesting in that 5 to 20 at.% of M is soluble in R, but little or no solubility of R in M is found. Since the alkaline earth metals (M) appear to be insoluble in R (and also R in M), it appears that the tendency of these two bivalent metals (Eu and Yb) to form a trivalent state in the trivalent R matrix accounts for this extensive solubility. But in the europium or ytterbium divalent matrix the trivalent rare earth metals are essentially insoluble because of their smaller size and different electronic (trivalent) nature.

There are only two known sets of R–M systems where R is extensively soluble in M and the M solubility in R is limited, these are the R–Ag and R–Au systems. For these systems the light lanthanides are only slightly soluble in silver or gold, but the heavies exhibit extensive solubilities in these two solvents. This extensive solubility is anomalous and is not expected from the theory of alloy phase formation because of

the large size disparity and the large electronegativity difference (Gschneidner 1980b).

Extensive studies by Gschneidner and his co-workers of these rare earth binary alloys have led to a much better understanding of the formation of solid-solution alloys between any two elements in the periodic table and the various factors which influence their formation (see Gschneidner 1980b,c). They have shown that the first-order effects are the electronic structures of the two components, their sizes and electronegativities. Of these the first is the foremost while the size difference is also important provided the electronic structures are compatible, and the third factor, the electronegativity, does not seem to be important and generally can be neglected. They also found that second-order effects can affect the extent of solid solution when the energetics of the two first-order parameters are such that the given binary system lies at extensive/limited borderline. These second-order parameters are: electron transfer, lattice rigidity and the composition of the compound nearest the solvent. These studies have led to a new predictive model for solid-solution formation which is superior to the three Hume–Rothery rules and the Darken–Gurry method (Gschneidner 1980b,c).

The anomalous solid solubility of magnesium in the lanthanides and the higher solubility of the corresponding rare earths in gold than in silver, showed that the lattice rigidity, as measured by the Debye temperature (θ_D), may be the deciding factor whether extensive or limited solutions are found in some cases. That is, the more rigid the lattice (a high θ_D material) the smaller the solubility and conversely a less rigid lattice will be able to dissolve more of a solute. The experimental verification of this logical postulate could not have been made without the use of the rare earth metals. Furthermore, with this new knowledge it was possible to explain one of the oldest riddles known to metallurgist – why copper and silver form two terminal solid solutions with an intermediate eutectic (because of silver's high $\theta_D = 228$ K) and copper and gold form a completely miscible solid solution (gold's $\theta_D = 165$ K), when the other physical properties of these two metals (silver and gold) are essentially identical.

4.1.3. *Liquid immiscibility*

The rare earth metals form immiscible liquids with the alkali, alkaline earth, the group V A metals (V, Nb and Ta), the barides (Eu and Yb) and uranium, see fig. 15. For the group VI A metals, chromium and molybdenum, only the light lanthanides with low vapor pressures form immiscible liquids, while the heavy lanthanides (the lanthanides with high vapor pressures), scandium and yttrium form simple eutectics. In the case of manganese only lanthanum and cerium are known to form immiscible liquids, and no intermetallic phases, while the remaining rare earths are known to form one or two or three intermetallic compounds with manganese, and presumably no immiscible liquids. This is why the chromium, molybdenum and mangenese boxes are partially shaded.

In view of the divalent nature of europium and ytterbium and similarities to alkaline earth metals, it is not surprising that these two barides form immiscible liquids with the trivalent rare earth metals. Although our information is limited it

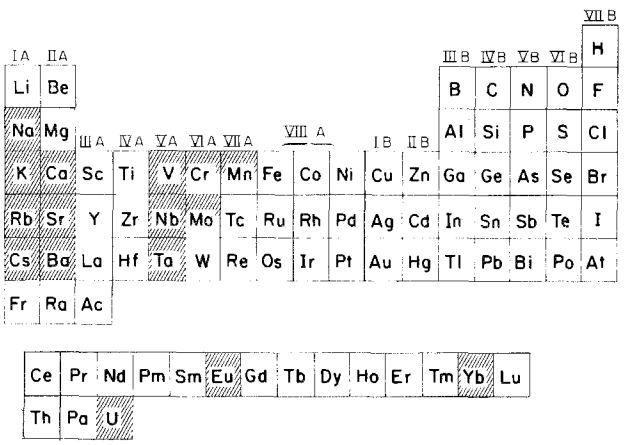

Fig. 15. Liquid immiscibility formation by the trivalent rare earth metals in the R–M systems. The shaded boxes indicate the M metal partners which form immiscible liquids with R.

appears that the width of the miscibility gap is larger in the Eu–R systems than in the corresponding Yb–R system. Furthermore, the miscibility gap width becomes increasingly larger with increasing atomic number of R for a series of R–Yb alloys. These behaviors can be correlated with the size difference of the two components in a given binary alloy – the larger the size disparity the wider the region of immiscibility.

The formation of immiscible liquids in these R–M systems is consistent with Mott's theory of immiscible phase formation (Mott 1957).

4.1.4. *Compound formation*

As seen in fig. 16 the rare earth metals form compounds with all of the elements to the right of chromium and its congeners except for the rare gases, which are not shown but lie to the right of the group VII B elements. Hydrogen is included in group VII B, since it acts as an anion with the strongly electropositive rare earth elements. The block for astatine (At) is not shaded because there is no information on the formation of R–At compounds, but considering its position in the periodic table at least one RAt_x compound is expected to form. Except for beryllium and magnesium no intermetallic phases are formed with the elements to the left of manganese and its congeners.

Compound formation is known for all R, except near the group VI A–VII A boundary. The exceptions are the La–Mn, Ce–Mn and La–Fe systems for which no intermetallic compounds have been reported to exist. The number of RM_x compounds in a given R–M system varies with M and also with R. As a function of the group position in the periodic table the maximum number of reported compounds in a R–M system varies from one to three at the manganese group to a maximum of six to eight at cobalt and nickel groups and then slowly decreases to one to three for the halides. The number of compounds for a given M varies with R, the light

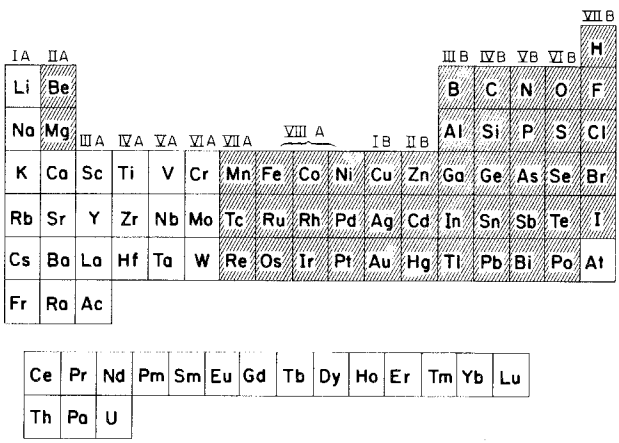

Fig. 16. Compound formation by the trivalent rare earth metals in the R–M systems. The shaded boxes indicate that at least one RM_x compound is formed by R and M.

lanthanides generally form fewer compounds than the heavy lanthanides and yttrium. Thus, we estimate that over 3000 binary compounds are formed by the rare earth metals with the other elements in the periodic table.

The melting points of the intermetallic compounds vary in a uniform way across the block of compound formers on the right-hand side of fig. 16. From the VII A (Mn, Tc, Re) through the II B groups (Zn, Cd, Hg) the melting of the compounds is comparable to those of the component metals and rarely exceed the melting point of the highest melting pure metal, and if so by less than 100°C. This suggests that the bonding in these compounds is predominately metallic in nature.

From the III B (B, Al, Ga, In, Tl) through VI B (O, S, Se, Te, Po) the melting points for at least one or two or even three of the compounds are much higher (several hundreds to more than one thousand °C) than that of the highest melting component element (generally the rare earth element). Boron and carbon, of course,

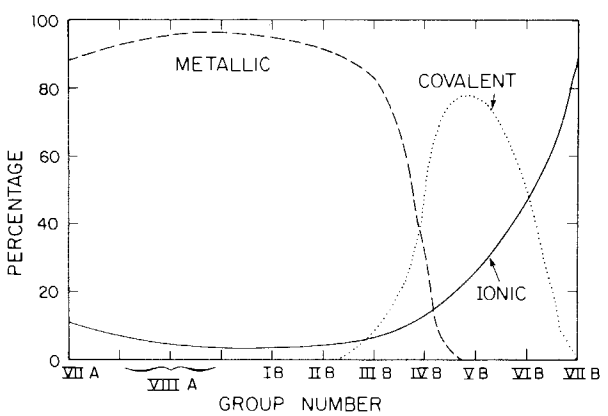

Fig. 17. The bonding character in binary rare earth compounds formed with the elements from the VII A (Mn, Tc, Rh) group to the VII B (halides) group of the periodic table.

are exceptions because of their elemental high melting points, but never-the-less many of the rare earth borides and carbides are high melting compounds. The melting temperature reaches a maximum at the group V B elements (N and congeners). This suggests that there is an increase in both the covalent and ionic bonding in the compounds formed starting at approximately the III B–IV B groups with a corresponding rapid drop in the metallic bonding. The amount of covalent bonding rises rapidly and dominates for compounds formed by the group V B elements ($\sim 80\%$ covalent) and then drops rapidly towards the end of the series, see fig. 17. Covalent bonding probably accounts for about 50% of the bonding in the group IV B and VI B element compounds. The ionic bonding across this portion of the periodic table rises more slowly and finally dominates in the compounds formed by the VII B elements.

4.2. *Crystal chemistry*

With over 3000 binary rare earth compounds some efforts have been made to:

(1) classify the various compound stoichiometries and crystal structures that have been found, and

(2) make and discuss correlations, systemations and interrelationships.

Some of the important reviews include those by Gschneidner (1961), Kripyakevich et al. (1963), McMasters and Gschneidner (1964), Iandelli and Palenzona (1979), and Gschneidner (1980b), and the reader is referred to these for further details.

One of the most important and useful tools is the existence–crystal-structure diagram which summarizes the known crystallographic data and the existence/non-existence of compounds at all possible compositions in the R–M binary systems for a given M. A typical example is shown in fig. 18. Basically this diagram represents 15 binary R–Al phase diagrams, including both the divalent and trivalent lanthanides. The Iandelli–Palenzona (1979) version includes scandium and yttrium in addition to 14 of the 15 lanthanides (promethium is left out since it is a radioactive element and essentially no phase diagram information is known) and thus represents 16 binary diagrams.

Several things are immediately obvious in such a diagram – the anomalous behavior of the divalent europium and ytterbium (in fig. 18 ytterbium does not appear to be anomalous but in most such diagrams it is) and the similarities and the differences in the trivalent lanthanides. The similarities are the existence of the RAl_2 and RAl_3 phases for all trivalent lanthanides and the same crystal structure for the RAl_2 compounds. The differences are many more: the incomplete compound series of the R_3Al, R_2Al, RAl, and R_3Al_{11} compositions and the crystal structure changes in the RAl and RAl_3 stoichiometries. Unfortunately there is no way to represent melting and transformation temperatures on such a two-dimensional diagram and a three-dimensional one would be difficult to construct and utilize with any reasonable precision. An extensive set of existence–crystal-structure diagrams can be found in the review by Iandelli and Palenzona (1979). They have presented 30 such diagrams for the M elements from group VII A (Mn, Tc, Re) through the group

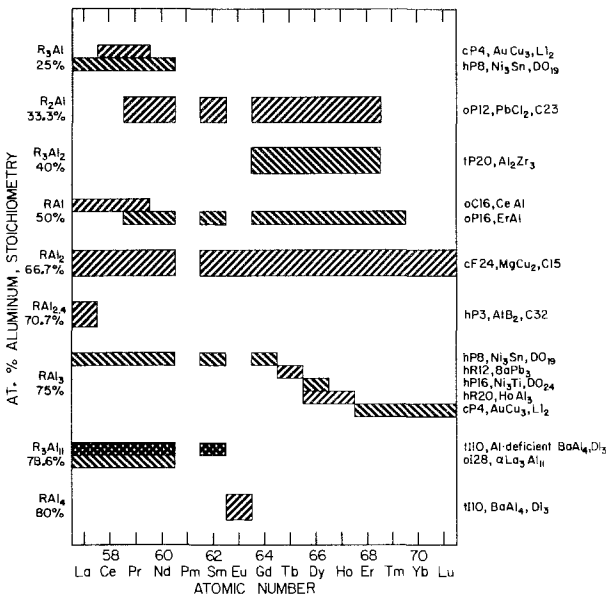

Fig. 18. The existence–crystal-structure diagram for the R–Al alloys. (After Gschneidner and Calderwood 1983a).

IV B (C, Si, Ge, Sn, Pb), with the exception of carbon, plus those for magnesium, antimony and bismuth. In addition to these, other such diagrams are available for carbon (Gschneidner and Calderwood 1986c) and arsenic (Gschneidner and Calderwood 1986b). More up to date existence–crystal-structure diagrams that have been published since the Iandelli–Palenzona review are available for aluminum (see fig. 18), silver (Gschneidner and Calderwood 1983b, 1986d) and gold (Gschneidner and Calderwood 1986d).

Of the more than 3000 compounds many occur at the same composition and, in turn, many of these have the same crystal structure. The largest number of compounds at the various compositions (with the percentage of the total number of compounds given in parenthesis) are: RM_2 (20), RM (17), RM_3 (12), R_5M_3 (7), RM_5 (5) and R_2M_{17} (5). Thus these six compositions account for two-thirds while the RM_2 and RM compositions account for $\sim 40\%$ of the known R–M compounds (Iandelli and Palenzona 1979). In table 2 we have listed the most important crystal structures which form at the six most common stoichiometries found in rare earth binary compounds. Details, especially crystallographic data can be found in the reviews by Buschow (1977, 1979), Gschneidner (1961), McMasters and Gschneidner (1964) and Iandelli and Palenzona (1979).

4.3. *Magnetic properties*

The second most common property measured on rare earth compounds, after the crystal structure, is their magnetic behaviors as a function of temperature. But with over 3000 compounds a wide variety of behaviors can be expected. An attempt to

TABLE 2
Summary of the most important crystal structures at the six most common compositions, and the corresponding M element which form the given structure with at least some of the rare earth metals.

Composition R:M	Structure type	M-partner
5:3	1. Mn_5Si_3	Rh, Pt, Ga, In, Tl, Si, Ge, Sn, Pb, Sb, Bi
	2. Cr_5B_3	Same as for Mn_5Si_3
	3. W_5Si_3	Same as for Mn_5Si_3
1:1	1. CaCl	Mg, Ru, Rh, Ir, Pd, Cu, Ag, Au, Zn, Cd, Hg, In, Tl
	2. NaCl	N, P, As, Sb, Bi, S, Se, Te, Po
	3. CrB	Rh, Ni, Pd, Pt, Au, Ga, Si, Ge
	4. FeB	Ni, Pt, Cu, Au, Si, Ge
1:2	1. $MgCu_2$	Mg, Mn, Fe, Ru, Os, Co, Rh, Ir, Ni, Pt, Al
	2. $MgZn_2$	Mg, Mn, Tc, Re, Ru, Os
	3. $CeCu_2$	Cu, Ag, Au, Zn
	4. $CeCd_2$	Cd, Hg
	5. AlB_2	B, Ga
	6. $MoSi_2$	Ag, Au
1:3	1. $AuCu_3$	Rh, Pd, Pt, In, Sn, Tl, Pb, Al
	2. $PuNi_3$	Fe, Co, Ir, Ni
	3. $SnNi_3$	Cd, Hg, Al
1:5	$CeCu_5$	Co, Rh, Ni, Pt, Cu, Zn
2:17	1. Th_2Ni_{17}	Mg, Fe, Co, Ni, Zn
	2. Th_2Zn_{17}	Fe, Co, Zn

classify the magnetic behaviors has been carried out by Kirchmayr and Poldy (1979). We will follow their classification scheme and highlight some of the important aspects in this field – the details can be found in their extensive review.

In addition to the Kirchmayr–Poldy review, additional information concerning the magnetic behaviors of rare earth compounds are found in the reviews by Buschow (1977, 1979), Nesbitt and Wernick (1973), Taylor and Darby (1972) and Wallace (1973). The review by Nesbitt and Wernick is exclusively on rare-earth–cobalt permanent magnets, while the others generally cover a wide range of compounds.

But before we proceed we should briefly discuss a few background items. The de Gennes factor has been discussed in section 3.3.2 and will not be described here. The RKKY indirect-exchange model is important and may account for some of the behaviors in rare earth compounds. In this model neighboring localized 4f electrons communicate with each other via the conduction electrons, especially the s electrons. At a sufficiently low temperature the 4f electron on one ion core polarizes a conduction electron, which as it travels through the lattice, in turn polarizes the 4f electron on a neighboring ion. The conduction electron, however, as it travels away from the original 4f electron can spin flip and thus, depending on the distance the second 4f electron is from the first it may be polarized by the conduction electron

with its spin (moment) parallel (if close) or antiparallel (if further away) to the original 4f electron. This then leads to ferromagnetism and to antiferromagnetism depending on the 4f–4f separation. A more quantitative description is given in section 2 of the chapter by Rhyne (chapter 76, this volume).

Another important interaction is that between that of a localized 4f and a 3d electron in intermetallic compounds formed between the magnetic 3d elements (Mn, Fe, Co and Ni) and the magnetic lanthanides. In the early magnetic property measurements of these compounds (the 1960's) it was immediately noted that the magnetic moments were quite low in the heavy lanthanides and large in the light lanthanides. This was rather unexpected since the magnetic moments of the light lanthanide metals are less than those of the heavies. This can be explained in the following way: the 3d magnetic moments which depend upon the S quantum number (since the orbital quantum number, L, is quenched) are coupled parallel to one another; the R magnetic moments which depend upon the J quantum number ($J = L \pm S$) are also coupled parallel to the other R moments; and since the spins of the 3d atom and the R atom always couple antiparallel to each other, the total magnetic moment depends upon the coupling (additivity) of J (of R) and S (of the 3d atom). The direction of J relative to S (of R) will be given by the sign between L and S. This is illustrated in fig. 19, where it is seen that because of the minus sign J (of R) and S (of the 3d atom) are parallel in the light lanthanides, and in the heavies the J (of R) and S (of the 3d atom) are antiparallel because J (of R) and S (of R) are parallel (plus sign). This coupling arrangement leads to the large magnetic moments in R–3d compounds formed by the light lanthanides and reduced magnetic moments in the compounds involving the heavy lanthanides. This coupling has a pronounced

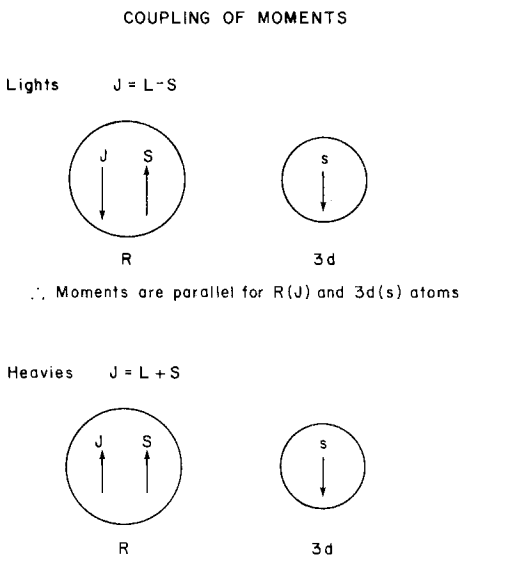

Fig. 19. Schematic representation of the coupling of magnetic moments of the lanthanide (R) and 3d metal (M) atoms in RM intermetallic compounds.

effect on the utilization of lanthanide compounds in commercial applications based on their magnetic behaviors (see section 4.3.3).

4.3.1. *R–nonmagnetic-metal compounds*

In these compounds the M atom has a zero magnetic moment and includes all of the atoms shaded in fig. 16 except Mn, Fe, Co and Ni which are discussed in the next section. In these compounds only the R–R interactions account for the observed magnetic properties: the absolute value of the Curie–Weiss paramagnetic constant, θ_p, is proportional to the de Gennes factor; the Néel, T_N, and Curie, T_C, ordering temperatures are roughly proportional to the de Gennes factor; and the effective magnetic moment, p_{eff}, is proportional to $g[J(J+1)]^{1/2}$, where g is the gyromagnetic ratio and J is the J quantum number.

In the RM CsCl-type compounds, when M is a monovalent metal (Cu, Ag, Au) the compounds order antiferromagnetically, while for divalent M (Mg, Zn, Cd, Hg) the compounds generally order ferromagnetically (cerium is more than likely to be an exception since most cerium compounds order antiferromagnetically). In RRh compounds for R = Gd, Tb and Dy the compounds order ferromagnetically and for R = Ho, Er, and Tm they order antiferromagnetically. This is probably a result of a critical RKKY distance falling between the Dy–Dy and Ho–Ho separations in these compounds.

For the RM_2 Laves phases ($MgCu_2$ and $MgZn_2$ type structures) all compounds are ferromagnetic except $CeAl_2$ which is antiferromagnetic. In this case M = Al, Ru, Os, Rh, Ir, Ni and Pt, and in the RNi_2 compounds nickel has a zero moment, i.e. a filled 3d band. The RM_3 compounds, with the $AuCu_3$ type structure, are found to be antiferromagnetic, where M = Al, Pd, In, Sn and Pb.

4.3.2. *R–3d-magnetic-metal compounds*

In these compounds, M (= Mn, Fe, Co and Ni) has a magnetic moment and the

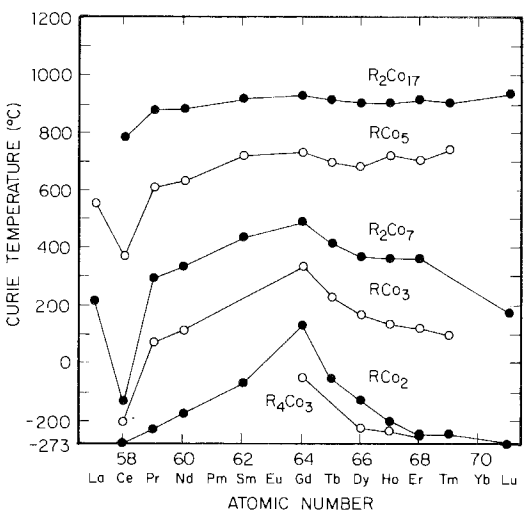

Fig. 20. Curie temperatures of some RCo_x intermetallic compounds. (After Strnat and Ray 1971.)

magnetic behavior is a little more complicated because in addition to the indirect R–R interactions, which are weak, we have 3d–3d interactions which are strong as a result of direct overlap of the 3d wave functions. There are also the R–3d interactions which have an intermediate strength. The effect of these interactions is quite evident in the variation of the Curie temperature versus the cobalt content, see fig. 20. At low cobalt concentrations (R_4Co_3 and RCo_2) the Curie temperature scales with the de Gennes factor and varies by $\sim$400°C from $GdCo_2$ to $LuCo_2$, and the R–R interactions are still quite important. But as the cobalt concentration increases the difference in the Curie temperature between Gd and Lu for the various compounds decreases to $\sim$200°C for R_2Co_7 and vanishes for RCo_5 and R_2Co_{17} compositions.

As noted earlier (section 4.3) because the coupling between the Co and R changes from the lights to the heavies, this has a pronounced effect on the saturation moments. This is quite evident for the RCo_5 compounds for which the saturation moments are: 7.1 for $LaCo_5$; 9.0 – $PrCo_5$; 9.1 – $NdCo_5$; 7.2 – $SmCo_5$; 2.6 – $GdCo_5$; 1.7 – $TbCo_{5.1}$; 3.2 – $DyCo_{5.2}$; 4.6 – $HoCo_{5.5}$; and 5.6 – $ErCo_6$. These low saturation moments in the heavy lanthanide compounds account for the fact that these materials are not used for permanent magnet materials, see next section.

4.3.3. *Permanent magnet materials*

Although the magnetic properties of the R–3d-metal compounds were studied by a number of research groups in the late 1950's and early 1960's (Gschneidner 1961, Kirchmayr and Poldy 1979) nothing unusual was found with respect to their potential as permanent magnet materials. It was not until 1966 that Strnat and Hoffer (1966) pointed out that YCo_5 has an extremely large uniaxial magnetocrystalline anisotropy and a theoretical energy product heretofore unheard of and thus it might make an excellent permanent magnet (see also Becker 1970, Kirchmayr and Poldy 1979). Once Strnat had announced his finding the race was on to see which particular light lanthanide RCo_5 compounds would be the best permanent magnet. And in 1967 several groups, including Strnat and co-workers, showed that $SmCo_5$ was the best. Because of his initial discovery, dedicated research efforts, technical accomplishments and activities promoting $SmCo_5$–Sm_2Co_{17} and related materials, Prof. Karl Strnat is considered the father of Sm–Co permanent magnets.

Although theoretically the magnetic moments for the $NdCo_5$ and $PrCo_5$ are $\sim$25% larger than that of $SmCo_5$, $NdCo_5$ is an extremely poor material for a permanent magnet because it essentially does not have an axial anisotropy. It is the anisotropy of the 4f wave functions (section 3.1) in the given crystal field (hexagonal for RCo_5 and R_2Co_{17}), which locks-in the 3d spins and prevents them from rotating in an applied field in the case of Sm–Co magnets. However, in the case of Nd–Co magnets, the anisotropy is such that 3d moments are essentially free to rotate in an applied field and thus $NdCo_5$ and Nd_2Co_{17} are useless as permanent magnetic materials. As we will see below, just the opposite occurs for the tetragonal $R_2Fe_{14}B$ permanent magnet materials.

Although Sm–Co permanent magnet properties are excellent and were far superior to any material known at the time, extensive utilization of these materials in the

industrial magnet market (beyond 1000 tons per year) did not appear to be feasible from an economic view point for two reasons:

(1) Relatively inexpensive samarium depends upon the mischmetal production and the production of other separated light lanthanides from the monazite and bastnasite ores for other products. In the preparation of mischmetal samarium is naturally concentrated in the slag because it is only reduced to the divalent state during electrolysis while the other rare earths are reduced to metal at the cathode. The samarium is cheaply recovered from the slag. In the early 1980's when mischmetal production peaked, the total amount of samarium available from both the mischmetal production and as a by-product for other separated rare earths was about 400 tons per year. The production of samarium could be increased but it would be much more expensive since it would have to be separated from the ores for itself and bear the burden of the separation costs since the other lanthanides would be surplus materials.

(2) The more important reason, is that most of the cobalt comes from politically unstable or unreliable countries and the supply could dry-up over night causing the price to skyrocket. That indeed did happen in the late 1970's when the price of cobalt increased from \$5 to \$25 per pound in a matter of weeks.

Because of these two factors magnet manufacturers and users alike looked for other possible compounds or alloys which did not have these economic drawbacks. Given this scientific background and economic realities one is limited to iron-rich alloys containing a light lanthanide metal: iron because it is cheap and is available in most politically stable free world countries, and has good magnetic properties; iron-rich because the magnetic ordering temperature needs to be $>150°C$; a light lanthanide because of the additivity of magnetic moments as discussed above.

The first major break-through came when Croat (1981) observed large room-temperature coercivities in amorphous Nd–Fe alloys. About three months later Koon and Das (1981) noted that boron additions to an amorphous La–Tb–Fe alloy improved the magnetic properties. Armed with this knowledge several researchers found that an iron-rich alloy containing $\sim$85 at.% Fe, 10 at.% Nd and 1 at.% B had excellent permanent magnetic properties equal to or better than the best Sm–Co magnets. Indeed, three groups of investigators presented results on Nd–Fe–B alloys at the 29th Annual Conference on Magnetism and Magnetic Materials (November 1983) and their papers were published in the Conference Proceedings (Croat et al. 1984, Sagawa et al. 1984, Sellmyer et al. 1984). By mid-1986 (Capellen et al. 1986) over 275 papers had been published on $Nd_2Fe_{14}B$ permanent magnets.

In the case of $Nd_2Fe_{14}B$, which has a tetragonal structure, the anisotropy of the 4f wave functions in the tetragonal crystal field gives rise to the large anisotropy required to make this material a good permanent magnet. The samarium counterpart has poor magnetic properties required for a good permanent magnet. In this case this is an economic advantage since neodymium is more abundant and is cheaper to produce and does not depend so much on other processes to make it available in almost unlimited quantities. Within about three years since the initial discovery, the best experimental energy product (a measure of the permanent magnet's magnetic power) of a Nd–Fe–B magnet is $\sim$50% higher than the best

value achieved for a Sm–Co material after ~15 years of studies. The major problem with Nd–Fe–B material is its low Curie temperature which limits its usefulness to temperatures below ~100°C. The Sm–Co magnets, however, will serve well in a high-temperature environment since Curie temperatures are in the 700 to 900°C range, see fig. 20. For more information on these permanent magnet materials (both Sm–Co and Nd–Fe–B) the readers is referred to the recent review by Buschow (1986).

4.3.4. *Magnetostrictive terfenol*

Early studies (in the mid-1960's) on the magnetic properties of the pure lanthanide metals revealed that some of them exhibited large magnetostrictions at low temperatures (see Clark 1979). Several scientists logically reasoned that if some heavy lanthanides could be alloyed with the magnetic 3d metals, they might find a compound which possesses this large magnetostriction and which orders magnetically well above room temperature. Within about five years A.E. Clark and H.S. Belson (Naval Ordnance Laboratory) announced at the 1971 Magnetism and Magnetic Materials Conference that $TbFe_2$ exhibited magnetically induced strains at room temperature which were larger by a factor of ten, than that of any known material (Clark and Belson 1972). This was confirmed almost simultaneously by Koon and co-workers (Koon et al. 1971).

Realizing the great potential for materials with giant magnetostrictions in sonar devices, micropositioners, fluid control valves, etc., work was carried out on developing the optimum properties of these $TbFe_2$-based materials at the Naval Ordnance Laboratory by Clark and co-workers. Shortly thereafter Clark began working with O.D. McMasters of the Ames Laboratory, Iowa State University, to grow single crystals and directionally orientated polycrystalline materials (McMasters et al. 1986). The materials were called 'terfenol' after terbium–iron (Fe) and the initials of the Naval Ordnance Laboratory.

As work progressed they found that dysprosium additions to the $TbFe_2$ compound would allow one to use lower magnetic fields to produce the strain with some degradation in the total strain achieved. The optimum composition chosen was $Tb_{0.3}Dy_{0.7}Fe_{1.9}$ and is now known as 'terfenol-D'.

The magnetostriction, λ_s, is defined as $\lambda_s = \frac{2}{3}(\lambda_{\parallel} - \lambda_{\perp})$, where $(\lambda_{\parallel} - \lambda_{\perp})$ is the fractional length change when the applied field is rotated from perpendicular to parallel in the measurement direction. In the RFe_2 series of compounds, which have the cubic Laves phase structure, λ_s can vary from large positive values, as for $TbFe_2$ (1753×10^{-6}), to large negative values, as for $SmFe_2$ (-1560×10^{-6}). For RFe_2, with R = Dy, Er and Tm, the λ_s are considerably smaller, but positive for $DyFe_2$ and negative for $ErFe_2$ and $TmFe_2$. These large magnetostrictions and their signs are due to the anisotropy of 4f wave functions and their interaction with the cubic crystal field in RFe_2 compounds. One can readily see that the differences in the shapes of the 4f charge densities, which resemble oblated spheroids for terbium and dysprosium and prolated spheroids for samarium, erbium and thulium (fig. 2), would account for the observed signs in these magnetostrictive materials.

More details concerning these RFe_2 and other magneostrictive materials can be found in the reviews by Clark (1979) and by Belov et al. (1983).

4.3.5. *Discovery of ferromagnetic semiconducting EuO*

EuO was the first ferromagnetic semiconductor found in the compounds of the lanthanide elements. There are several surprises associated with this unusual material. One of these is how can EuO be ferromagnetic ($T_c = 77\,K$) without any conduction electrons, i.e. the RKKY exchange mechanism cannot account for this ferromagnetism. The current model is based on a cation–cation superexchange mechanism in which a 4f electron of one europium ion is transferred to 5d state of a next nearest (nn) europium ion, which then polarizes the 4f spin of the nn europium ion via an intra atomic f–d exchange (Wachter 1979).

The most interesting aspect of this material is its discovery, which resulted from some measurements on the superconducting and magnetic property studies of the RIr_2 compounds by Bozorth et al. (1959). Based on X-ray studies these authors reported that most of the RIr_2 compounds crystallized in the cubic Laves phase structure, and that europium was trivalent in $EuIr_2$. They also reported that $EuIr_2$ had a Curie temperature of 70 K, just slightly less than that of $GdIr_2$ (88 K). But in a private conversation J.H. van Vleck (the 1977 Nobel prize winner) pointed out to the authors that if europium were trivalent, then $J = 0$ and the magnetic moment should be quite small, and it would seem to be incongruous for $EuIr_2$ to have such a high magnetic ordering temperature and essentially a zero moment, especially when compared to the 88 K ordering temperature of $GdIr_2$ where gadolinium has $J = \frac{7}{2}$ and an effective magnetic moment of $7.9\,\mu_B$. The only reasonable explanation was the presence of a magnetic impurity and oxygen appeared to be the most likely contaminant because of the ease with which europium oxidizes (see section 3.5.5). Since the magnetic behavior of Eu_2O_3 was known and could not account for this high ordering temperature, Matthias et al. (1961) thought it might be EuO, which had been prepared for the first time by Eick et al. (1956). They (Matthias et al. 1961) prepared EuO by reacting Eu and Eu_2O_3 at 1220°C, and found that EuO orders at 77 K. More recent studies show that $T_c = 69.3\,K$ (Wachter 1979).

This discovery logically led to the finding of ferromagnetic ordering in EuS (16.6 K) and EuSe (4.6 K) and antiferromagnetic ordering in EuTe (9.6 K) (Wachter 1979). Although the low ordering temperatures for these four europium monochalcogenides, which have the simple NaCl type structure, preclude significant commercial applications at present, they are ideal model systems for magnetic, magneto-optical and electrical studies of magnetic semiconductors. Additional information on these materials may be found in section 5.2 of the chapter by Bleaney (ch. 77, this volume).

4.4. *Other remarkable intermetallic compounds*

As noted earlier there are over 3000 binary rare earth intermetallic compounds, many of which exhibit interesting behaviors, but there are only a few, in addition to those noted earlier, which exhibit sufficiently unusual properties to be mentioned here. Undoubtedly in the eyes of many of the readers there will be compounds with which they are familiar and which they believe deserve mention here. Indeed the reader may be correct but in the authors' limited views and experience the following have had the greater impact on us.

4.4.1. *LaB_6 – electron emitter*

LaB_6, which has a CsCl-like structure composed of B_6 clusters and La atoms as the two components, was found by Lafferty (1951) of the General Electric Company to have superior thermionic properties. This compound has an extremely high melting point (>2500°C) and low vapor pressure, and these combined with its low work function and excellent thermionic emission current make LaB_6 a better electron emitter than tungsten. The thermionic emission can be improved by using single crystals oriented in ⟨111⟩ direction (Verhoeven et al. 1976). Although more expensive than tungsten, LaB_6 is used in electron guns of electron microscopes where high intensities are highly desirable if not essential.

4.4.2. *$LaNi_5$ – hydrogen absorber*

Zijlstra and Westendorp (1969) of the Philips Research Laboratories, Eindhoven, The Netherlands, were the first to note that the RM_5 (R = rare earth, M = iron, cobalt or nickel) phases readily absorb reasonable amounts of hydrogen at room temperature, in particular $SmCo_5$ absorbed 2.5 moles. Their co-workers, Van Vucht et al. (1970), were the first to report on the excellent hydrogen absorption properties of $LaNi_5$.

$LaNi_5$ readily absorbs H_2 at room temperature to form the compound $LaNi_5H_6$. The number of hydrogen atoms per cubic centimeter in $LaNi_5H_6$ is larger than that of liquid hydrogen. Other advantages of the $LaNi_5$-based materials is that the hydrogen atoms are extremely mobile and that there is a large heat of reaction associated with hydrogen absorption/desorption processes. Furthermore, since the desorption of hydrogen is almost reversible, i.e. a small hysteresis loop, this material and related alloys are being used commercially as a hydrogen storage medium, for hydrogen purification, as hydrogen getters, as heat pumps and as energy storage systems.

$LaNi_5$ has the hexagonal $CaCu_5$-type structure and various transition metal atoms (notably Al, Co, Cu and Pt) can be substituted for Ni and the rare earth and Th atoms can be substituted for La in this compound. This flexibility allows one to vary the hydrogen absorption/desorption properties for the various commercial application and for basic research studies to understand this class of materials. More details can be found in the review by Buschow (1984).

4.4.3. *$PrNi_5$ – low-temperature record setter*

$PrNi_5$, which has the same structure as $LaNi_5$, is one of many praseodymium compounds which do not order magnetically, or if they do, only do so in the micro-kelvin range, because praseodymium has a singlet ground state. But because there is a large magnetic entropy associated with the $4f^2$ configuration (18.3 J/mol Pr) Andres (1978) of the Bell Laboratories pointed out that these praseodymium compounds would be good candidates for obtaining extremely low temperatures by nuclear magnetic cooling.

Based on Andres ideas and results, Pobell and co-workers of the Institut für Festkörperforschung, Kernforschunsanlage Jülich, designed a two-stage nuclear hyperfine adiabatic demagnetization refrigerator, hopefully to set a record for

attaining the *lowest working temperature at which useful experiments could be performed on materials, other than on the refrigerant itself* (Mueller et al. 1980). The system was designed to be cooled down in various stages by the normal refrigerants, liquid N_2 to reach 77 K, and liquid helium to reach 4 K. Then a dilution refrigerator cooled the system to 25 mK (0.025 K), at which point the two-stage adiabatic demagnetization unit would take over. The first-stage refrigerator composed of 60 rods of $PrNi_5$ (4.2 moles) cooled the system down to $\sim$5 mK when the 6 T magnetic field around the $PrNi_5$ was slowly removed, and then the demagnetization of the second-stage copper allowed the system to reach a world's record 38 μK (0.000038 K) for a working temperature* (Pobell 1982). This record was, however, short lived as the Japanese group headed by Ishimoto of the Institute for Solid State Physics, University of Tokyo, reached 27 μK in early 1983 using essentially the same set-up, except they used more $PrNi_5$ (11 moles) in their refrigerator (Ishimoto et al. 1984). Today there are at least 35 laboratories throughout the world using $PrNi_5$ as a refrigerant, although most systems are not as big as the Jülich and Tokyo machines. Most of the $PrNi_5$ used in these refrigerators was prepared by B.J. Beaudry and co-workers at the Materials Preparation Center of the Ames Laboratory, Iowa State University.

4.4.4. *Heavy fermions and spin fluctuators*

In the early 1970's two groups measured the heat capacity of $CeAl_3$ and it was evident that the heat capacity of this compound might have a large electronic contribution (van Maaren et al. 1971, Mahoney et al. 1974). But because of extra peaks in the heat capacity due to other $CeAl_x$ compounds which order magnetically and the fact that their low-temperature limit was $\sim$1.5 K, it was difficult to conclude definitely that the electronic specific heat constant, γ, was an unusually large number. Measurements down to 15 mK by Andres et al. (1975) on $CeAl_3$ showed that $\gamma = 1620$ mJ/mol K^2, an enormously large value (2700 times larger than that of copper). Although the full impact of the discovery was not appreciated at the time, this paper is considered the start of the 'heavy fermion' field. The discovery of superconductivity in a material which also has a large γ, specifically $CeCu_2Si_2$, spurred a tremendous amount of interest (Steglich et al. 1979). Since then several other heavy fermions have been found: superconducting UBe_{13} and UPt_3; non-magnetic, non-superconducting $CeCu_6$; and magnetic $NpBe_{13}$, U_2Zn_{17} and UCd_{11} (see the reviews by Ott 1984, Steglich et al. 1984, Stewart 1984, Steglich 1985).

The term 'heavy fermion' was coined by Steglich, since the quasi-particle is a fermion (i.e. obeys Fermi statistics) and its mass is extremely large, several hundreds to thousand times larger than that of a free electron. This mass is measured by the electronic specific heat constant, since $\gamma/\gamma_0 = m^*/m$ where γ_0 is the unenhanced electronic specific heat constant as calculated from the band structure and m is the free-electron mass and m^* is the effective mass of the electron. Since γ_0 is of the order

* Others have reached lower temperatures but in these cases the experimental observations were made on the refrigerant itself, see, e.g., Huiki and Loponen (1982) who reached temperatures of the order of 50–100 nK [$(50–100) \times 10^{-9}$ K].

of one, m^* will be extremely large, since $\gamma \simeq 1000\,\text{mJ/mole K}^2$. Such large m^* values means that the f electron in cerium and uranium is strongly correlated with conduction electrons in these compounds, and these interactions led to a wide variety of behaviors – magnetic, superconducting and neither. In addition there are many more cerium and uranium compounds with smaller γ's (in the low hundreds), and still more with γ's less than $50\,\text{mJ/mole K}^2$, and yet no one has presented a uniform picture or explanation for these materials. Once we understand these materials, we will have made a significant contribution to our knowledge of the electron properties of metallic materials – not just the lanthanides and actinides but also the whole periodic table.

Also of recent vintage are studies on closely related materials which are known as spin fluctuators – materials which are just about to order magnetically. The term spin fluctuators comes about since magnetic electrons want to line up (magnetic order) and may do so in small parts of the material (~ 100 nearest neighbors) for just a brief period of time before they become random once more. This process is continued throughout the solid, with spins aligning and then unaligning, i.e. they fluctuate. In this fluctuation process, especially below 20 K, the physical properties, in particular the heat capacity, magnetic susceptibility and electric resistivity, have unusual temperature dependences, much different from that of normal materials. Prior to 1980 theory held that magnetic fields of $\sim 100\,\text{T}$ (1000 kOe) would be necessary to have much effect on spin fluctuations, however, Ikeda and Gschneidner (1980) were the first to show unequivocally in a study of $LuCo_2$, that spin fluctuations could be quenched (destroyed) by applying fields of 10 T or less. Since then, they and their co-workers and others have shown that spin fluctuations can be quenched in a number of different materials – lanthanide, actinide and transition metal alloys and compounds (see the review by Gschneidner and Dhar 1984). The various types of observed behaviors have been categorized into six groups, primarily based on the magnetic field dependence of the low temperature heat capacities.

Closely related to the heavy fermions and spin fluctuators are the valence fluctuation/intermediate valence materials. The origin of this phenomenon starts with cerium and its $\alpha \rightleftarrows \gamma$ transformation (see sections 3.3.4 and 3.7.2). Today it involves many cerium materials and also compounds of samarium, europium, thulium and ytterbium. Because of the breadth of the subject matter and space limitations in this chapter we refer the reader to the following reviews: Jayaraman (1979), Lawrence et al. (1981), de Châtel (1982), Coqblin (1982), Nowik (1983), Brandt and Moshchalkov (1984), Varma (1985) and Stassis (1986).

4.4.5. *Superconducting alloys*

There are many rare earth superconducting alloys involving the non-magnetic rare earths (Sc, Y, La and Lu). However, because of space limitations, we will limit our discussion to those superconductors which also order magnetically, and thus contain the magnetic lanthanides. Generally these compounds are ternary compounds in which there is a competition between superconductivity and long-range magnetic order. This competition results in either 're-entrant' superconductivity as the material orders ferromagnetically or the 'co-existence' of superconductivity and

antiferromagnetism. In the former case, the sample is in the ferromagnetic state at 0 K (i.e. its ground state) and upon warming it becomes superconducting when the temperature reaches the Curie temperature, i.e. the sample is 're-entering' the superconducting state, and it remains in this state until the sample is warmed up to the superconducting transition temperature, at which point the sample becomes normal. In the second case, just as the word means – superconductivity and antiferromagnetism co-exist in the same sample – the material is indeed superconducting and the magnetic moments on the magnetic lanthanide ions exhibit long-range order.

As noted in the introduction (section 1) at one time these two phenomena were thought to be mutually exclusive but as science has evolved we see that this is not the case. However, the two phenomena are competitive and generally only one or the other prevails. In the ternary superconductors which exhibit either 're-entrance' or 'co-existence', the superconductivity is carried by conduction electrons of a transition metal ion and the magnetism is due to the 4f electrons of the magnetic lanthanide ion. But if there is long-range magnetic order one would expect the conduction electrons to be involved if the RKKY mechanism is responsible for this magnetism. Therein lies the interesting and exciting physics, and why there is a great deal of activity involving these materials.

There are a number of materials which have been studied but the two favorite ternary superconductors are the so called 'Chevrel' phases, named after R. Chevrel (Université de Rennes, France) who first prepared the MMo_6S_8 or MMo_6Se_8 compounds (Chevrel et al. 1971), and the RRh_4B_4 compounds. In the Chevrel phases, M can be any number of metals including the rare earth metals, and in the latter compound R represents the rare earths and thorium. In both instances Matthias and his co-workers were the first to report the existence of superconductivity in the Chevrel phases (Matthias et al. 1972) and in RRh_4B_4 (Matthias et al. 1977).

In the Chevrel phases only $HoMo_6S_8$ is a re-entrant type superconductor, while the RMo_6S_8 phases, with R = Gd, Tb, Dy and Er, and the RMo_6Se_8 phases, with R = Gd, Tb and Er, are co-existing type materials. The rest of the RMo_6S_8 and RMo_6Se_8 phases are normal superconductors, except for the europium compounds, which are neither superconductors nor magnetic, and $CeMo_6S_8$ and $CeMo_6Se_8$ which are an antiferromagnet and a ferromagnet, respectively.

For the RRh_4B_4 phases, only $ErRh_4B_4$ is a re-entrant type and only $SmRh_4B_4$ is a co-existent type superconductor. The $NdRh_4B_4$ and $TmRh_4B_4$ exhibit both superconductivity and some type of magnetism which has not been clearly established. Several of the rare earth metals do not form this phase, these include R = Sc, La, Ce, Pr, Eu and Yb. Of the remaining six, two are superconductors, R = Y and Lu, and four are ferromagnets, R = Gd, Tb, Dy and Ho.

Thus we see a wide diversity of behaviors in these compounds and studies on such materials will enable us to better understand the natures of superconductivity and magnetism and the competition between them. More details can be found in the two-volume series by Maple and Fischer (1982), and the reviews by Fischer (1978) and Shelton (1982).

In addition to the interesting superconductivity/magnetism behavior, the $LaMo_6Se_8$ compound has some outstanding superconducting properties. Its superconducting transition temperature is a respectable 11 K, but its upper critical field at 0 K is an outstanding −55T, one of the highest known. If one could fabricate this compound into wires one could build a superconducting solenoid with a workable field of ~25T, a factor of two better than the best available solenoids built today using Nb_3Sn.

5. Systematics

The regular and systematic variation of the physical and chemical properties of the lanthanides was recognized as soon as scientists had enough information about a property for most of the lanthanide elements (see next section). Since then scientists have used systematics and deviations thereof to understand the lanthanide elements. An example of this was discussed earlier in section 3.2 where the atomic volume of the trivalent lanthanide metals decreases in a smooth manner and the two anomalies at europium and ytterbium are associated with their divalent character and that at cerium with intermediate (between three and four) valence behavior (see fig. 3). The use of systematics is a powerful tool for understanding the nature of the rare earth elements (it is sometimes important to include yttrium and scandium in such analyses, see, e.g., section 6.3); for evaluating the reliability of published data; and for predicting or estimating data which is unknown. But as noted by Gschneidner and Calderwood (1983a) systematics must be applied cautiously and carefully because incorrect conclusions can be drawn or erroneous values can be estimated.

The use of systematics in other fields of science involving the rare earths/lanthanides can be found in the NATO conference proceedings edited by Sinha (1983).

5.1. *Goldschmidt's lanthanide contraction*

The first application of systematics was made in the mid-1920's by V.M. Goldschmidt when the lattice parameters of the C-form (cubic) of the R_2O_3 compounds became available. In compiling the ionic radii of the elements Goldschmidt et al. (1925) noted that radii of the lanthanide elements decreased in a regular and smooth fashion from lanthanum to lutetium. Since both europium and ytterbium are trivalent in the R_2O_3 phase, their radii are in line with those of the other trivalent lanthanides. Goldschmidt coined the words 'lanthanide contraction' to describe this systematic decrease in ionic radii. He realized that this contraction is due to the fact that the 4f electrons do not effectively screen the outer electrons from the increased nuclear charge as an additional 4f electron is added as one proceeds from one element to the next in increasing atomic number along this series. The importance of this observation was recognized by the Nobel laureate G. von Hevesy and given prominence in his classical book on the atomic structure of the rare earths (von Hevesy 1927).

Today the lanthanide contraction is still one of the most important tools available to the scientist in applying systematics to the behavior of lanthanide materials. Deviations from the lanthanide contraction established for a given compound series gives a measure of anomalous valences for cerium, samarium, europiun, thulium and ytterbium (see section 3.2) which are important in evaluating the nature of these elements in valence fluctuation, heavy fermion, and spin fluctuation behaviors (see section 4.4.4).

In the case of compounds, especially non-cubic materials, McMasters et al. (1971) suggested the use of an effective radius which is defined as:

$$r_{\text{eff}} = (V/n)^{-1/3},$$

where V is the unit cell volume and n is the total number of atoms in the unit cell. This gets around the problem of which lattice constant one should use for the non-cubic cell to establish the absence or presence of deviations from the lanthanide contraction. There are other advantages of using r_{eff} versus Z (the atomic number) plots for all the compounds formed between R and a given M, and these are discussed by the authors.

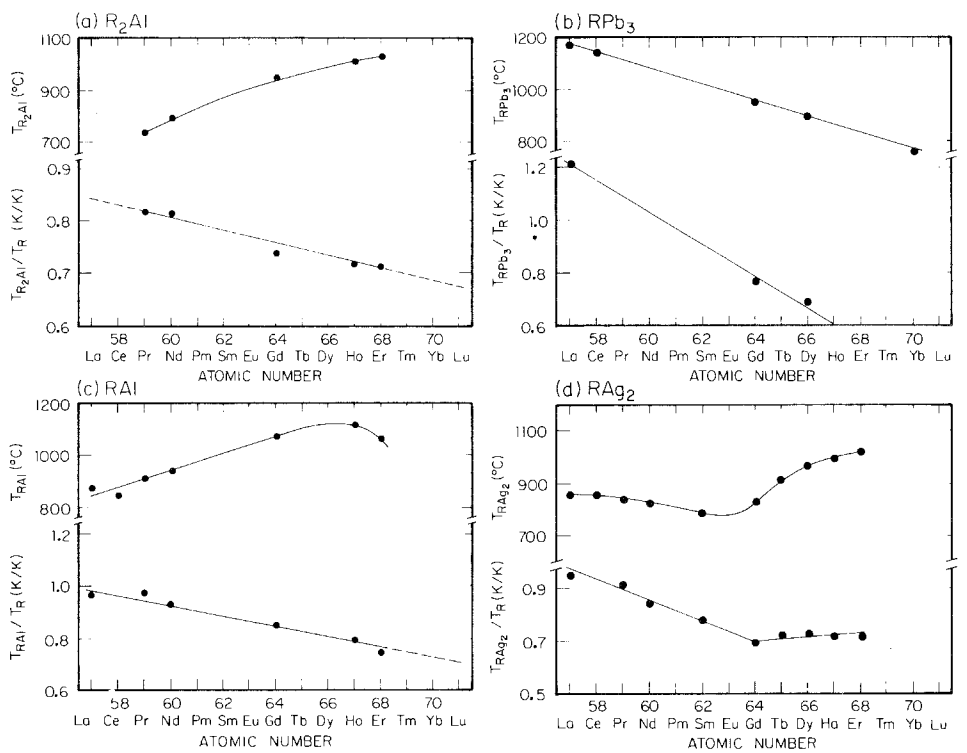

Fig. 21. Melting point and reduced melting points for the four possible melting behaviors: (a) melting point increases; (b) melting point decreases; (c) maximum in melting points; and (d) minimum in melting points.

5.2. *Melting behavior*

It has long been recognized that the melting behavior of a compound series of the trivalent lanthanides does not necessarily follow the approximate linear increase observed in the trivalent metals (see fig. 4). Indeed four different behaviors have been noted (Gschneidner 1969a) as shown in fig. 21. But when one plots the reduced absolute melting points (the melting point of the compound in K divided by the melting point of the pure metal in K) many times one obtains a straight line, as is shown in fig. 21. This may be helpful when estimating melting points for lanthanide compounds by extrapolation, especially if the melting behaviors are not linear functions of the atomic number, see, e.g., fig. 21c. As shown in fig. 21d, however, the reduced melting temperature versus the atomic number in the case of a melting minima has two linear segments. This seems to be more prevalent in the case of melting minima; in addition to the RAg_2 series (fig. 21d) both the RCl_3 and RBr_3 compound series show similar behaviors. Again we note that one must be careful in using such plots for estimating data.

For estimating melting points by interpolation the normal melting point versus atomic number plot serves just as well and saves one the step of calculating the reduced melting temperatures and plotting them.

5.3. *Lattice parameter, free energy (heat) of formation and melting-point correlation*

All lanthanide compound series exhibit the lanthanide contraction when one considers the molar volume of the compound. But in four of the compound series which have the tetragonal $ThCr_2Si_2$-type structure the c lattice parameter actually expands, but a decreases sufficiently such that the unit-cell volume shows the normal lanthanide contraction (Gschneidner 1986). These compound series are: RM_2Si_2, with M = Cu, Ag and Au, and RCu_2Ge_2. Although this 'lanthanide expansion' was originally observed over 15 years ago, no one has proposed an explanation.

When one compares the lanthanide contraction in a compound series with that of the metals, three different behaviors are possible; the lanthanide contraction in the compound series relative to that in the metals is: (1) more severe, (2) less severe and (3) the same. Gschneidner (1969a) argued that since the volume of formation of the compound from the elemental constituents, ΔV_f, is proportional to the free energy (heat) of formation, ΔG_f, then in the first case ΔG_f should become more negative, indicating more stability in the compound series as the atomic number of the lanthanide increases, and this is what is observed in the R_2O_3 and RH_2 phases (Gschneidner 1969a) and also the R_2C_3 series of compounds. For the second case the converse is expected and this has been verified in the RMg, RCd and RCl_3 phases (Gschneidner 1969a), and RAl, RAl_2, RAl_3, R_5Bi_3, R_4Bi_3 and RBi compound series. In the last (third) case ΔG_f is expected to remain constant for a compound series and this is the situation for the RAs compounds.

Gschneidner et al. (1973) used this technique along with some limited experimental data to predict the free energies of formation at 1100 K, and heat of formation at 298 K of the rare earth oxysulfides. Recently, Akila et al. (1987) measured the free energies of formation of eleven lanthanide oxysulfides and they noted that there was

good to excellent agreement between the experimental and the theoretical values.

In the melting process, at least for the normal metallic elements, melting occurs when about one bond out of twelve is broken and if this correlation holds for compounds then one might expect the melting trends in a compounds series to be related to relative lanthanide contraction. This correlation was found to hold for 15 of 17 different compound series (Gschneidner 1969a). More recently we have examined 14 additional systems and find that only eight of these obey the correlation, and that two of the original 15 systems found to hold as reported by Gschneidner (1969a) in the light of new data do not. This makes a total of 21 compound series out of 31 that follow this correlation, suggesting that the lattice-parameter–melting-point interrelationship is not as good as originally thought.

5.4. *Generalized phase diagram*

The occurrence of the various crystal structures in the pure metals across the lanthanide series, in their intra rare earth alloys and at high pressures (see sections 3.2 and 3.7.1) has generated a great deal of interest in the systematics that are involved [for most of the earlier references see Langley (1982)]. Johansson and Rosengren (1975) showed that the high-pressure transformations for the various polymorphic forms are systematically related, and they showed this in a sort of three-dimensional projection in which the temperature and pressure axes are shifted for each lanthanide. More recently, a single generalized phase diagram was proposed to represent 91 individual intra trivalent rare earth metal binary phase diagrams (78 intra lanthanide and 13 yttrium–lanthanide diagrams) at atmospheric pressure (Gschneidner 1985b). A method was proposed to enable anyone to calculate unknown binary diagrams. Furthermore, it was shown that there are only 13 different types of intra rare earth binary alloy phase diagrams (exclusive of scandium and the divalent europium and ytterbium). This generalized one-atmosphere binary phase diagram was extended to higher pressures (Gschneidner 1985a). Three isopiestic sections at 1, 2 and 4 GPa were presented in addition to the atmospheric section. These four generalized diagrams and the eight isothermal sections given by Gschneidner and Calderwood (1986a) should enable scientists to determine the phase relationships in the 91 individual binary alloy systems at high pressures up to 4 GPa. The 25°C isothermal section of the generalized phase diagram up to 24 GPa presented by Gschneidner (1985a) and Gschneidner and Calderwood (1986a) has recently been extended up to 50 GPa by Benedict et al. (1986) based on new high-pressure results.

In connection with these generalized phase diagrams as a function of pressure, the phase boundary of the bcc phase is clearly established and follows systematics as has been discussed earlier in section 3.2.

5.5. *Dual valency nature of europium and ytterbium*

One of the best known and understood anomalies in the lanthanide series is the divalent character of europium and ytterbium metals which, as noted earlier, is quite

evident in figs. 3, 4, 6 and 8. In compounds, however, both divalent and trivalent as well as intermediate valence forms are known for these two elements. Since the standard state of these two metals (the pure metallic element at 25°C [298 K] and one atmosphere pressure) is the divalent state, compounds in which europium and ytterbium are divalent may be easily formed. But in order to form compounds in which these elements are trivalent, the extra 4f electron must be promoted to the valence level. As noted earlier (section 3.5.5) this promotion energy is 88 and 46 kJ/g at. R for europium and ytterbium, respectively. Thus the free energy of formation of a compound containing these trivalent elements must be greater than these promotion energies. For intermediate valence states, the promotion energies are proportional to the fractional valence.

It is immediately obvious that ytterbium should form more compounds in which it is trivalent than in the case of europium, and that is what is observed (Gschneidner 1969b). As one might expect from the electronegativities of the elements in the periodic table and the way the bonding changes with the M element partner in a RM_x compound (fig. 17), there is a relationship between the M element's position in the periodic table and the valence state of europium and ytterbium in the various compounds. This has been discussed by Gschneidner (1969b) and Iandelli and Palenzona (1979).

In addition to using the lattice parameter(s) of the RM_x compound to estimate the valence state of europium and ytterbium one can use magnetic susceptibility data (Gschneidner 1969b, Wohlleben 1981) and L_{III} absorption edges, XPS and UPS (Wohlleben 1981) to distinguish between the $4f^n$ and $4f^{n+1}$ configurations and intermediate valences. For europium one can also use Mössbauer isomer shift data (Brix et al. 1964, Clifford 1967, van Steenwijk and Buschow 1977, de Vries et al. 1984).

The valence state of europium is important in some technological applications. For example, as a trivalent ion it emits a red light when used as a phosphor and a blue light when it is divalent. Also, the formation of trivalent europium compounds is quite critical for its application as a control rod or neutron absorber (McMasters and Gschneidner 1964). Europium has a high neutron cross-section and as it captures neutrons its eventual decay product is always a gadolinium atom. Thus if europium were divalent in such a material, each atom would undergo $\sim 30\%$ volume contraction when it formed gadolinium, and within a short time the control rod would probably not meet engineering standards and thus be unacceptable for nuclear applications. If europium, however, were trivalent there would only be a 1% volume contraction during the absorption of neutrons, and these materials would be acceptable. Thus there are only a limited number of compounds that could serve as useful europium control rod or neutron absorber materials.

5.6. *Contributions to alloy theory*

The systematic variation of the size and electronegativity and a constant valence of the lanthanide elements and also yttrium, make these groups of elements a useful research tool for probing the chemical and alloying natures of materials, and solving

some problems, whereby this newly gained knowledge transcends the rare earth group and adds understanding to the entire field.

The anomalous high solid solubility of holmium in gold reported by Wunderlin et al. (1963, 1965) led Gschneidner and co-workers to study the solid solubilities of the rare earths in gold and silver. These studies along with a study of the solid solubility of magnesium in the rare earth metals and of the crystal chemistry of the rare earth–gold and –silver intermetallic compounds, revealed that lattice rigidity, compound stoichiometry and electron transfer are important parameters which govern the formation of solid solutions (Gschneidner 1980b,c). In time a new theory evolved for predicting the formation of solid solutions which improved the reliability from $\sim 60\%$ to $\sim 85\%$.

Another contribution involved the measurement of the high-temperature heat contents of the rare earth metals. An analysis of the data revealed that the entropy of transformation, ΔS_{tr}, for the close packed to bcc transformation in the rare earth metals depended upon the number of valence electrons (Dennison et al. 1966c), i.e. $\Delta S_{tr} \simeq 0.2$ e.u. per valence electron. Extension of these observations to the remainder of the periodic table indicated that the entropy of transformation of metals which posses two or more of the common metallic structures and the entropy of fusion depend upon both the crystalline structure of the phases involved and the number of valence electrons (Gschneidner 1975). These results were then used to predict the entropies of fusion for 16 metals, including two lanthanide metals – promethium and lutetium – and the entropies of transformation of 5 metals including promethium, for which no reliable experimental values existed.

Analyses of the systematics involved in various properties, such as the crystal structure sequence and melting points of the metals have led several authors to conclude that 4f electrons are involved in the bonding of the metals via hybridization with the 5d and 6s valence electrons. This extension of systematics leads naturally into the topic of the next section.

6. 4f hybridization and bonding

About 25 years ago it was rare that any scientist would speak about 4f electrons being involved in bonding, since 'everyone' knew that the 4f electrons were localized in the ion core and were well shielded by the $5p^6$ and $5s^2$ electrons, especially in the case of the lanthanide metals. However, a few scientists led by Matthias and Gschneidner believed that some of the properties of the lanthanide elements were sufficiently anomalous with respect to the rest of the periodic table that just the $(5d6s)^3$ valence electrons could not account for these behaviors. Slowly the evidence built up, such that today virtually everyone believes that there is some hybridization of the 4f electrons with the outer 5d and 6s electrons, especially in the light lanthanides (see, e.g., Freeman et al. 1987). The work on intermediate valence cerium and more recently the heavy-fermion studies (see section 4.4.4) convinced even the most conservative scientists that 4f electrons must be involved. Reference to the early papers on this subject can be found in the article by Gschneidner (1971).

Below we will describe briefly the major early contributions which pointed the way to our present state of knowledge (sections 6.1 and 6.2). In addition to these two topics, more recent supporting information is found in the pressure dependence of the superconducting temperatures (section 3.7.3) and the solid solubilities of Sc, Y and Lu relative to those of lanthanides which have unpaired 4f electrons (section 6.3).

6.1. *Crystal-structure sequence*

The existence of a sequence of close-packed structures in which the fcc to hcp stacking percentage changes from 100% fcc to 50% fcc–50% hcp to 33% fcc–67% hcp to 100% hcp as one proceeds along the lanthanide series (section 3.2) may not seem so unusual that one needs to invoke 4f hybridization. True enough, but when this information is combined with the facts that (1) intra lanthanide alloys between a light and a heavy always yield this same sequence of structures (see section 5.4 on the generalized phase diagram), and (2) application of pressure reverses this sequence (see section 3.7.1) most of the explanations proposed for one or two of these facts failed to explain the other two or the third. In the late 1960's Gschneidner and Valletta (1968) and later Langley (1982) proposed that 4f hybridization could account for the observed structures both at atmospheric pressure and also under pressure, while Hodges (1967) and more recently Skriver (1983) suggested that variation in the number of d electrons would account for the observed behaviors. High-pressure studies by Grosshans et al. (1982), which showed that hcp yttrium transformed successively to the Sm-type to the dhcp and finally the fcc structure, would appear to rule out the need for 4f hybridization to explain the observed crystal structures. But by application of systematics, Gschneidner (1985a) pointed out that the corresponding phase transformations in the elements which have no unpaired 4f electrons (yttrium and lutetium) transform at pressure ~ 7 GPa higher than those elements which have unpaired 4f electrons. He concluded that relative s/d occupancy may play a major role in governing the crystal-structure sequence but 4f hybridization cannot be ignored and also plays a role.

6.2. *Melting points*

As noted earlier (section 3.4.2) the melting points for the light lanthanides are much too low relative to the rest of the periodic table, and also the change in the melting temperature from lanthanum to lutetium is much too large relative to that observed in a compound series with normal bonding. Matthias et al. (1967) recognized these anomalies and proposed that the low melting temperature of the lights were due to 'some f character in the hybridized wave functions describing the band structure for the valence electrons'. This work on the melting points was expanded upon and extended to include the heats of sublimation in the analysis (Gschneidner 1971). Gschneidner suggested the low melting points arose because of the low mobility of the 4f electron allowing one bond in twelve to break which is sufficient to permit melting, even though the 4f contribution to the bonding is

expected to increase the bond strength. Kmetko and Hill (1976) on the other hand proposed that the angular dependence of the 4f wave functions (see fig. 1) accounts for the low melting points because they do not have the appropriate directionality to form good bonds in the bcc structure, and that in the liquid state the 4f electrons bond better than in the bcc phase. But in the metallic state the conduction/bonding electrons are mobile and move throughout the 'sea' of conduction electrons between the ion cores, so that the bonds are continually being broken and reformed between neighboring ions, i.e. there are resonating bonds between the atoms. Thus the truth of the matter is that both the mobility and the anisotropy of the 4f electrons contribute and account for the anomalous melting behaviors.

6.3. *Solid-solution behavior*

As noted in the previous sections the evidence for 4f hybridization and involvement in the bonding of the lanthanide elements is strong. If this is the case, then surely there should be other evidence for this in alloys and compounds, but it may be difficult to demonstrate clearly that the observed behavior is indeed due to 4f hybridization with the bonding electrons.

One such a situation is the room-temperature solid solubility of hydrogen in Sc (Azarkh and Funin 1965), Y, Gd, Er, Tm and Lu (Beaudry and Spedding 1975), which are plotted in fig. 22 as a function of the metallic radius. It is immediately seen that the amount of hydrogen dissolved in the rare earth elements with no unpaired 4f electrons is enormously higher than in those lanthanides with unpaired electrons. If the 4f electrons were *truly localized* and *not involved in the chemical bonding* one

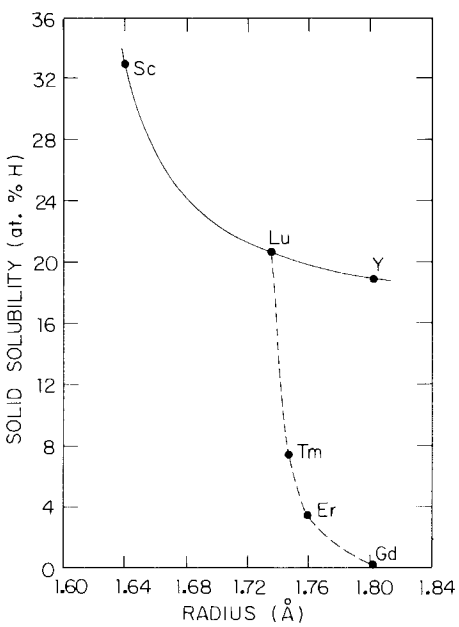

Fig. 22. The room-temperature solid solubility of hydrogen in the rare earth metals as a function of the rare earth radius. The solubility in the light lanthanides (not shown) is less than that in gadolinium.

would expect all of the solid solubilities to fall on (or close to) a smooth curve from scandium to gadolinium, yttrium (which have essentially the same size), but clearly this is not the situation here. Furthermore, any other type of correlation of the hydrogen solubility with a physical property of the rare earth metal (such as the electronegativity, melting point, Debye temperature) will lead to a similar separation of the non-4f rare earths from the 4f containing ones as shown in fig. 22. Thus by default we come to the conclusion that 4f hybridization with the valence electrons leads to a much reduced hydrogen solubility, and the larger the amount of hybridization the smaller the solubility.

This application of systematics to the solubility of hydrogen in the rare earth metals actually turns out to be the strongest case that we have to support our claim that 4f electrons are involved in the chemical bonding.

Acknowledgements

The authors are indebted to B.J. Beaudry, M.A. Damento, B.N. Harmon and R.N. Shelton (Ames Laboratory, Iowa State University) for their comments and constructive criticism of parts of this paper. We also acknowledge the assistance of J. Capellen (Rare-earth Information Center) and R.O. Elliott (Los Alamos National Laboratory) for helping us find some of the papers referred to in this review.

References

Abell, J.S., 1988, in: Handbook on the Physics and Chemistry of Rare Earths, Vol. 12, eds K.A. Gschneidner Jr and L. Eyring (North-Holland, Amsterdam) to be published.

Ahmann, D.H., 1950, ISC-68, U.S. Atomic Energy Commission Report (National Technical Information Service, Springfield, VA).

Akila, R., K.T. Jacob and A.K. Shukla, 1987, Metall. Trans. B **18**, 163.

Andres, K., 1978, Cryogenics **18**, 473.

Andres, K., J.E. Graebner and H.R. Ott, 1975, Phys. Rev. Lett. **35**, 1779.

Azarkh, Z.M., and V.N. Funin, 1965, Kristallografiya **10**, 29 [Sov. Phys.-Cryst. **10**, 21].

Bardeen, J., L.N. Cooper and J.R. Schrieffer, 1957, Phys. Rev. **108**, 1175.

Beaudry, B.J., and K.A. Gschneidner Jr, 1978, in: Handbook on the Physics and Chemistry of Rare Earths, Vol. 1, eds K.A. Gschneidner Jr and L. Eyring (North-Holland, Amsterdam) p. 173.

Beaudry, B.J., and F.H. Spedding, 1975, Metall. Trans. B **6**, 419.

Becker, C., 1964, J. Chem. Educ. **41**, 358.

Becker, J.J., 1970, Sci. Am. **223**(6), 92.

Bednorz, J.G., and K.A. Müller, 1986, Z. Phys. B **64**, 189.

Behrendt, D.R., S. Legvold and F.H. Spedding, 1957, Phys. Rev. **106**, 723.

Belov, K.P., G.I. Kataev, R.Z. Levitin, S.A. Nikitin and V.I. Sokolov, 1983, Usp. Fiz. Nauk **140**, 271 [Sov. Phys.-Usp. **26**, 518].

Benedict, U., W.A. Grosshans and W.B. Holzapfel, 1986, Physica B **144**, 14.

Bevolo, A.J., B.J. Beaudry and K.A. Gschneidner Jr, 1980, J. Electrochem. Soc. **127**, 2556.

Bjerrum-Møller, H., J.Z. Jensen, M. Wulff, A.R. Mackintosh, O.D. McMasters and K.A. Gschneidner Jr, 1982, Phys. Rev. Lett. **49**, 482.

Bozorth, R.M., B.T. Matthias, H. Suhl, E. Corenzwit and D.D. Davis, 1959, Phys. Rev. **115**, 1595.

Brandt, N.B., and V.V. Moshchalkov, 1984, Adv. Phys. **33**, 373.

Bratland, D., and K.A. Gschneidner Jr, 1980a, Electrochim. Acta **25**, 145.

Bratland, D., and K.A. Gschneidner Jr, 1980b, Acta Chem. Scand. A **34**, 683.

Brix, P., S. Hüfner, P. Kienle and D. Quitmann, 1964, Phys. Lett. **13**, 140.

Buschow, K.H.J., 1977, Rep. Prog. Phys. **40**, 1179.

Buschow, K.H.J., 1979, Rep. Prog. Phys. **42**, 1373.

Buschow, K.H.J., 1984, in: Handbook on the Physics and Chemistry of Rare Earths, Vol. 6, eds K.A. Gschneidner Jr and L. Eyring (North-Holland, Amsterdam) p. 1.

Buschow, K.H.J., 1986, Mater. Sci. Rep. **1**, 1.
Buschow, K.H.J., and J.H.H. van Vucht, 1967, Philips Res. Rep. **22**, 233.
Canneri, G., 1931, Met. Ital. **23**, 803.
Capellen, J., K.A. Menzel and K.A. Gschneidner Jr, 1986, Source Book on Neodymium–Iron–Boron Permanent Magnets, IS-RIC-9 (Rare-earth Information Center, Iowa State University, Ames, IA).
Caplin, D., 1987, Nature **326**, 827.
Carlson, O.N., and F.A. Schmidt, 1977, J. Less-Common Met. **53**, 73.
Carlson, O.N., F.A. Schmidt and D.T. Peterson, 1975, J. Less-Common Met. **39**, 277.
Cater, E.D., 1978, J. Chem. Educ. **55**, 697.
Chevrel, R., M. Sergent and J. Prigent, 1971, J. Solid State Chem. **3**, 515.
Chu, C.W., P.H. Hor, R.L. Meng, L. Gao, Z.J. Huang, Y.Q. Wang, J. Bechtold, D. Campbell, M.K. Wu, J. Ashburn and C.Y. Huang, 1988, Phys. Rev. Lett., to be published.
Clark, A.E., 1979, in: Handbook on the Physics and Chemistry of Rare Earths, Vol. 2, eds K.A. Gschneidner Jr and L. Eyring (North-Holland, Amsterdam) p. 231.
Clark, A.E., and H.S. Belson, 1972, AIP Conference Proceedings No. 5 (American Institute of Physics, New York) p. 1498.
Clifford, A.F., 1967, Adv. Chem. Ser. **68**, 113.
Coqblin, B., 1982, J. Magn. & Magn. Mater.**29**, 1.
Croat, J.J., 1981, J. Appl. Phys. Lett. **39**, 357.
Croat, J.J., J.F. Herbst, R.W. Lee and F.E. Pinkerton, 1984, J. Appl. Phys. **55**, 2078.
Cunningham, B.B., 1964, Ann. Rev. Nucl. Sci. **14**, 323.
Daane, A.H., 1951, AECD-3209, U.S. Atomic Energy Commission Report (National Technical Information Service, Springfield, VA).
Daane, A.H., 1961, in: The Rare Earths, eds F.H. Spedding and A.H. Daane (Wiley, New York) p. 102.
Daane, A.H., and F.H. Spedding, 1953, J. Electrochem. Soc. **100**, 442.
Daane, A.H., D.H. Dennison and F.H. Spedding, 1953, J. Am. Chem. Soc. **75**, 2272.
Daane, A.H., R.E. Rundle, H.G. Smith and F.H. Spedding, 1954, Acta Crystallogr. **7**, 532.
Dagani, R., 1987, Chem. Eng. News **65**(5), 29 (Feb. 2) and (19), 7 (May 11).
de Châtel, P.F., 1982, Physica B **109-110**, 1849.
de Gennes, P.G., 1958, C.R. Hebd. Séances Acad. Sci. **247**, 1836.
de Vries, J.W.C., R.C. Thiel and K.H.J. Buschow, 1984, Physica B **124**, 291.
Dennison, D.H., M.J. Tschetter and K.A. Gschneidner Jr, 1966a, J. Less-Common Met. **10**, 108.
Dennison, D.H., M.J. Tschetter and K.A. Gschneidner Jr, 1966b, J. Less-Common Met. **11**, 423.
Dennison, D.H., K.A. Gschneidner Jr and A.H. Daane, 1966c, J. Chem. Phys. **44**, 4273.
Dickman, S., 1987, Nature **236**, 432.
Eick, H.A., N.C. Baenziger and L. Eyring, 1956, J. Am. Chem. Soc. **78**, 5147.
Fischer, Ø., 1978, Appl. Phys. **16**, 1.
Fisk, Z., and J.P. Remeika, 1988, in: Handbook on the Physics and Chemistry of Rare Earths, Vol. 12, eds K.A. Gschneidner Jr and L. Eyring (North-Holland, Amsterdam) to be published.
Fort, D., D.W. Jones, B.J. Beaudry and K.A. Gschneidner Jr, 1981, J. Less-Common Met. **81**, 273.
Fort, D., B.J. Beaudry and K.A. Gschneidner Jr, 1987, J. Less-Common Met. **134**, 27.
Freeman, A.J., B.I. Min and M. Norman, 1987, in: Handbook on the Physics and Chemistry of Rare Earths, Vol. 10, eds K.A. Gschneidner Jr, L. Eyring and S. Hüfner (North-Holland, Amsterdam) p. 165.
Friedman Jr, H.G., G.R. Choppin and D.G. Feuerbacher, 1964, J. Chem. Educ. **41**, 354.
Gerward, L., J.S. Olsen and U. Benedict, 1986, Physica B **144**, 72.
Goldschmidt, V.M., T. Barth and G. Lunde, 1925, Skr. Nor. Vidensk.-Akad. Oslo. I **1925**(7), 1.
Gray, P.M.J., 1952, Trans. Inst. Mining Met. **61**, 141.
Greinacher, E., 1981, in: Industrial Applications of Rare Earth Metals, ACS Symposium Series, No. 164, ed. K.A. Gschneidner Jr (American Chemical Society, Washington, DC) p. 3.
Grosshans, W.A., Y.K. Vohra and W.B. Holzapfel, 1982, J. Magn. & Magn. Mater. **29**, 282.
Grosshans, W.A., Y.K. Vohra and W.B. Holzapfel, 1983, J. Phys. F **13**, L147.
Gschneidner Jr, K.A., 1961, Rare Earth Alloys (Van Nostrand, Princeton, NJ).
Gschneidner Jr, K.A., 1969a, J. Less-Common Met. **17**, 1.
Gschneidner Jr, K.A., 1969b, J. Less-Common Met. **17**, 13.
Gschneidner Jr, K.A., 1971, J. Less-Common Met. **25**, 405.
Gschneidner Jr, K.A., 1975, J. Less-Common Met. **43**. 179.
Gschneidner Jr, K.A., 1980a, in: Science and Technology of Rare Earth Materials, eds E.C. Subbarao and W.E. Wallace (Academic Press, New York) p. 25.
Gschneidner Jr, K.A., 1980b, in: Science and Technology of Rare Earth Materials, eds E.C. Subbarao and W.E. Wallace (Academic Press, New York) p. 51.
Gschneidner Jr, K.A., 1980c, in: Theory of Alloys Phase Formation, ed. L.H. Bennett (The Metallurgical Society, Warrendale, PA) p. 1.
Gschneidner Jr, K.A., 1984, J. Less-Common Met. **100**, 1.
Gschneidner Jr, K.A., 1985a, J. Less-Common Met. **110**, 1.
Gschneidner Jr, K.A., 1985b, J. Less-Common Met. **114**, 29.
Gschneidner Jr, K.A., 1986, in: Noble Metal Alloys, eds T.B. Massalski, W.B. Pearson, L.H. Bennett and Y.A. Chang (The Metallurgical

Society, Warrendale, PA) p. 325.
Gschneidner Jr, K.A., and F.W. Calderwood, 1983a, Bull. Alloy Phase Diagrams **4**, 129.
Gschneidner Jr, K.A., and F.W. Calderwood, 1983b, Bull. Alloy Phase Diagrams **4**, 364.
Gschneidner Jr, K.A., and F.W. Calderwood, 1986a, in: Handbook on the Physics and Chemistry of Rare Earths, Vol. 8, eds K.A. Gschneidner Jr and L. Eyring (North-Holland, Amsterdam) p. 1.
Gschneidner Jr, K.A., and F.W. Calderwood, 1986b, Bull. Alloy Phase Diagrams **7**, 274.
Gschneidner Jr, K.A., and F.W. Calderwood, 1986c, Bull. Alloy Phase Diagrams **7**, 421.
Gschneidner Jr, K.A., and F.W. Calderwood, 1986d, in: Noble Metal Alloys, eds T.B. Massalski, W.B. Pearson, L.H. Bennett and Y.A. Chang (The Metallurgical Society, Warrendale, PA) p. 335.
Gschneidner Jr, K.A., and S.K. Dhar, 1984, in: Magnetic Excitations and Fluctuations, eds S.W. Lovesey, U. Balucani, F. Borsa and V. Tognetti (Springer, Berlin) p. 177.
Gschneidner Jr, K.A., and R.M. Valletta, 1968, Acta Metall. **16**, 477.
Gschneidner Jr, K.A., N. Kippenhan and O.D. McMasters, 1973, Thermochemistry of the Rare Earths, IS-RIC-6 (Rare-earth Information Center, Iowa State University, Ames, IA).
Habermann, C.E., and A.H. Daane, 1961, J. Chem. Phys. **41**, 2818.
Hansen, M., 1958, Constitution of Binary Alloys (McGraw-Hill, New York).
Henrie, T., 1964, J. Met. **16**, 978.
Henrie, T., and E. Morrice, 1966, J. Met. **18**, 1207.
Herchenroeder, J.W., P. Manfrinetti and K.A. Gschneidner Jr, 1985, Physica B **135**, 445.
Hill, R.W., S.J. Collocott, K.A. Gschneidner Jr and F.A. Schmidt, 1987, J. Phys. F **17**, 1867.
Hillebrand, W.F., and T.H. Norton, 1875, Ann. Phys. (Leipzig) (formely Pogg. Ann.) **156**, 466.
Hirsch, A., 1911, J. Ind. Eng. Chem. **3**, 880.
Hirschhorn, I.S., 1968, J. Met. **20**, 19.
Hodges, C.H., 1967, Acta Metall. **15**, 1787.
Hor, P.H., R.L. Meng, Y.Q. Wang, L. Gao, Z.J. Huang, J. Bechtold, K. Forster and C.W. Chu, 1987, Phys. Rev. Lett. **58**, 1891.
Huiki, M.T., and M.T. Loponen, 1982, Phys. Rev. Lett. **49**, 1288.
Hultgren, R., P.D. Desai, D.T. Hawkins, M. Gleiser, K.K. Kelley and D.D. Wagman, 1973, Selected Values of the Thermodynamic Properties of the Elements (American Society for Metals, Metals Park, OH).
Iandelli, A., and A. Palenzona, 1979, in: Handbook on the Physics and Chemistry of Rare Earths, Vol. 2, eds K.A. Gschneidner Jr and L. Eyring (North-Holland, Amsterdam) p. 1.
Ikeda, K., and K.A. Gschneidner Jr, 1980, Phys. Rev. Lett. **45**, 1341.
Ikeda, K., K.A. Gschneidner Jr, B.J. Beaudry and U. Atzmony, 1982, Phys. Rev. B **25**, 4604.
Ishimoto, H., N. Nishida, T. Furubayashi, M. Shinohara, Y. Takano, Y. Miura and K. Ono, 1984, J. Low Temp. Phys. **55**, 17.
Jayaraman, A., 1978, in: Handbook on the Physics and Chemistry of Rare Earths, Vol. 1, eds K.A. Gschneidner Jr and L. Eyring (North-Holland, Amsterdam) p. 707.
Jayaraman, A., 1979, in: Handbook on the Physics and Chemistry of Rare Earths, Vol. 2, eds K.A. Gschneidner Jr and L. Eyring (North-Holland, Amsterdam) p. 575.
Johansson, B., and N. Mårtensson, 1987, in: Handbook on the Physics and Chemistry of Rare Earths, Vol. 10, eds K.A. Gschneidner Jr, L. Eyring and S. Hüfner (North-Holland, Amsterdam) p. 361.
Johansson, B., and A. Rosengren, 1975, Phys. Rev. B **11**, 2836.
Jones, D.W., D. Fort and D.A. Hukin, 1978, in: The Rare Earths in Modern Science and Technology, Vol. 1, eds G.J. McCarthy and J.J. Rhyne (Plenum, New York) p. 309.
Jordan, R.B., 1974, Contemp. Phys. **15**, 375.
Karl, A., 1934, Bull. Soc. Chim. **1**, 871.
Kasuya, T., 1956, Progr. Theor. Phys. **16**, 45.
Keller, W.H., R.P. Ericson and C. Hach 1945, TID-5212, paper 5, U.S. Atomic Energy Commission Report (National Technical Information Service, Springfield, VA).
Khurana, A., 1987, Phys. Today **40**(4) 17.
Kirchmayr, H.R., and C.A. Poldy, 1979, in: Handbook on the Physics and Chemistry of Rare Earths, Vol. 2, eds K.A. Gschneidner Jr and L. Eyring (North-Holland, Amsterdam) p. 55.
Klemm, W., and H. Bommer, 1937, Z. Anorg. Allg. Chem. **231**, 138.
Kmetko, E.A., and H.H. Hill, 1976, J. Phys. F **6**, 1025.
Koehler, W.C., E.O. Wollan, M.K. Wilkinson and J.W. Cable, 1961, in: Rare Earth Research, ed. E.V. Kleber (Macmillan, New York) p. 149.
Koon, N.C., and B.N. Das, 1981, J. Appl. Phys. Lett. **39**, 840.
Koon, N.C., A.I. Schindler and F.L. Carter, 1971, Phys. Lett. A **37**, 413.
Koskenmaki, D.C., and K.A. Gschneidner Jr, 1978, in: Handbook on the Physics and Chemistry of Rare Earths, Vol. 1, eds K.A. Gschneidner Jr and L. Eyring (North-Holland, Amsterdam) p. 337.
Kremers, H.C., and R.G. Stevens, 1923, J. Am. Chem. Soc. **45**, 614.
Kripyakevich, P.I., E.I. Gladyshevskii, O.S. Zarechnyuk, V.I. Evdokimenko, I.I. Zalutskii and D.P. Frankevich, 1963, Kristallografiya **8**, 596 [Sov. Phys.-Cryst. **8**, 477].
Kwo, J., E.M. Gyorgy, D.B. McWhan, M. Hong, F.J. DiSalvo, C. Vettier and J.E. Bower, 1985, Phys. Rev. Lett. **55**, 1402.
Kwo, J., M. Hong and S. Nakahara, 1986, Appl. Phys. Lett. **49**, 319.
Lafferty, J.M., 1951, J. Appl. Phys. **22**, 299.
Langley, R.H., 1982, Phys. Status Solidi b **111**,

501.
Lawrence, J.M., P.S. Riseborough and R.D. Parks, 1981, Rep. Prog. Phys. **44**, 1.
Legvold, S., 1972, in: Magnetic Properties of Rare Earth Metals, ed. R.J. Elliott (Academic Press, New York) p. 335.
Love, B., and E.V. Kleber, 1960, Mater. Design Eng. **52**(5), 134.
Mackintosh, A.R., and H. Bjerrum-Møller, 1986, J. Less-Common Met. **126**, 1 (4th F.H. Spedding Award).
Maddox, J., 1987, Nature **326**, 439.
Mahoney, J.V., V.U.S. Rao, W.E. Wallace, R.S. Craig and N.G. Nereson, 1974, Phys. Rev. B **9**, 154.
Maple, M.B., and Ø. Fischer, eds, 1982, Superconductivity in Ternary Compounds I, and Superconductivity in Ternary Compounds II (Springer, Berlin).
Matthias, B.T., H. Suhl and E. Corenzwit, 1958, Phys. Rev. Lett. **1**, 449.
Matthias, B.T., R.M. Bozorth and J.H. van Vleck, 1961, Phys. Rev. Lett. **7**, 160.
Matthias, B.T., W.H. Zachariasen, G.W. Webb and J.J. Engelhardt, 1967, Phys. Rev. Lett. **18**, 781.
Matthias, B.T., M. Marezio, E. Corenzwit, A.S. Cooper and H.E. Barz, 1972, Science **175**, 1465.
Matthias, B.T., E. Corenzwit, J.M. Vandenberg and H.E. Barz, 1977, Proc. Nat. Acad. Sci. (USA) **74**, 1334.
Mattocks, P.G., C.M. Muirhead, D.W. Jones, B.J. Beaudry and K.A. Gschneidner Jr, 1977, J. Less- Common Met. **53**, 253.
McEwen, K.A., 1978, in: Handbook on the Physics and Chemistry of Rare Earths, Vol. 1, eds K.A. Gschneidner Jr and L. Eyring (North-Holland, Amsterdam) p. 411.
McMasters, O.D., and K.A. Gschneidner Jr, 1964, Nucl. Met. **10**, 93.
McMasters, O.D., S.D. Soderquist and K.A. Gschneidner Jr, 1968, Trans. Quarterly ASM **61**, 435.
McMasters, O.D., K.A. Gschneidner Jr, G. Bruzzone and A. Palenzona, 1971, J. Less-Common Met. **25**, 135.
McMasters, O.D., J.D. Verhoeven and E.D. Gibson, 1986, J. Magn. & Magn. Mater. **54-57**, 849.
Mendelssohn, K., and J.G. Daunt, 1937, Nature **139**, 473.
Miller, A.E., and A.H. Daane, 1964, Trans. Met. Soc. AIME **230**, 568.
Miller, A.E., and A.H. Daane, 1965, J. Inorg. Nucl. Chem. **27**, 1955.
Miura, N., 1987, Nature **326**, 638.
Moldenhauer, M., 1914, Chem. Ztg. **38**, 147.
Moodenbaugh, A.R., M. Suenaga, T. Asano, R.N. Shelton, H.C. Ku, R.W. McCallum and P. Klavins, 1987, Phys. Rev. Lett. **58**, 1885.
Moriarty Jr, J.L., 1968, J. Met. **20**, 41.
Morrice, E., and R.G. Knickerbocker, 1961, in: The Rare Earths, eds F.H. Spedding and A.H. Daane (Wiley, New York) p. 126.
Morrice, E., E.S. Shedd, M.M. Wong and T.A. Henrie, 1969, J. Met. **21**(1) 34.
Mosander, C.G., 1827, Ann. Phys. (Leipzig) (formerly Pogg. Ann.) **11**, 406.
Mott, B.W., 1957, Philos. Mag. **2**, 259.
Mueller, R.M., Chr. Buchal, H.R. Folle, M. Kubota and F. Pobell, 1980, Cryogenics **20**, 395.
Muthmann, W., and L. Weiss, 1904, Justus Liebigs Ann. Chem. **331**, 1.
Muthmann, W., L. Weiss and J. Scheidemandel, 1907, Justus Liebigs Ann. Chem. **335**, 116.
Nesbitt, E.A., and J.H. Wernick, 1973, Rare Earth Permanent Magnets (Academic Press, New York).
Nowik, I., 1983, Hyperfine Interactions **13**, 89.
Ott, H.R., 1984, Physica B **126**, 100.
Pallmer, P.G., and T.D. Chikalla, 1971, J. Less-Common Met. **24**, 233.
Palmer, S.B., E.W. Lee and M.N. Islam, 1974, Proc. R. Soc. London Ser. A **338**, 341.
Pease, R., 1987, Nature **326**, 433.
Pobell, F., 1982, Physica B **109-110**, 1485.
Probst, C., and J. Wittig, 1978, in: Handbook on the Physics and Chemistry of Rare Earths, Vol. 1, eds K.A. Gschneidner Jr and L. Eyring (North-Holland, Amsterdam) p. 749.
Robinson, A.L., 1987, Science **235**, 531, 1137, 1571; Science **236**, 28.
Rossi, A., 1933, Atti Accad. Naz. Lincei Rend., Cl. Sci. Fis. Mat. & Nat. **17**, 839.
Ruderman ., M.A., and C. Kittel, 1954, Phys. Rev. **96**, 99.
Sagawa, M., S. Fujimura, M. Togawa, H. Yamamoto and Y. Matsuura, 1984, J. Appl. Phys. **55**, 2083.
Schmitt, D., 1986, J. Phys. (Paris) **47**, 677.
Scott, T.E., 1978, in: Handbook on the Physics and Chemistry of Rare Earths, Vol. 1, eds K.A. Gschneidner Jr and L. Eyring (North-Holland, Amsterdam) p. 591.
Sellmyer, D.J., A. Ahmed, G. Muench and G. Hadjipanayis, 1984, J. Appl. Phys. **55**, 2088.
Shelton, R.N., 1982, in: Superconductivity in d- and f-Band Metals, eds W. Buckel and W. Weber (Kernforschungszentrum Karlsruhe, Karlsruhe, FRG) p. 123.
Sheng, Jiang, and Zhang Liyuan, 1985, Acta Phys. Temp. Humilis Sin. **7**(3), 169 [1986, Chin. Phys. **6**, 694].
Sievers, J., 1982, Z. Phys. B **45**, 289.
Sikka, S.K., and V. Vijayakumar, 1986, Physica B **144**, 23.
Singer, R., H.E. Airey, L.C. Grimmett, H.R. Leech and R. Bennett, 1945, British Intelligence Objectives Sub-Committee, Final Report, 400 Item 21 (H.M. Stationary Office, London) 105 pp.
Sinha, S.K., 1978, in: Handbook on the Physics and Chemistry of Rare Earths, Vol. 1, eds K.A. Gschneidner Jr and L. Eyring (North-Holland, Amsterdam) p. 489.
Sinha, S.P., ed., 1983, Systematics and Properties of the Lanthanides (Reidel, Dordrecht).

Skriver, H.L., 1983, in: Systematics and Properties of the Lanthanides, ed. S.P. Sinha (Reidel, Dordrecht) p. 213.
Spedding, F.H., H.A. Wilhelm, W.H. Keller, D.H. Ahmann, A.H. Daane, C.C. Hach and R.P. Ericson, 1952, Ind. & Eng. Chem. **44**, 553.
Spedding, F.H., A.H. Daane and K.W. Herrmann, 1956, Acta Crystallogr. **9**, 599.
Spedding, F.H., S. Legvold, A.H. Daane and L.D. Jennings, 1957a, in: Progress in Low Temperature Physics, Vol. 2, ed. C.J. Gorter (North-Holland, Amsterdam) p. 368.
Spedding, F.H., R.G. Barton and A.H. Daane, 1957b, J. Am. Chem. Soc. **79**, 5160.
Spedding, F.H., J.J. Hanak and A.H. Daane, 1958, Trans AIME **212**, 379.
Spedding, F.H., K.A. Gschneidner Jr and A.H. Daane, 1959, Trans. AIME **215**, 192.
Spedding, F.H., J.J. Hanak and A.H. Daane, 1961, J. Less-Common Met. **3**, 110.
Spedding, F.H., R.M. Valletta and A.H. Daane, 1962, Trans Quarterly ASM **55**, 483.
Stassis, C., 1986, Physica B **137**, 61.
Steglich, F., 1985, in: Theory of Heavy Fermions and Valence Fluctuations, eds T. Kasuya and T. Saso (Springer, Berlin) p. 23.
Steglich, F., J. Aarts, C.D. Bredl, W. Lieke, D. Meschede, W. Franz and J. Schäfer, 1979, Phys. Rev. Lett. **43**, 1892.
Steglich, F., C.D. Bredl, W. Lieke, U. Rauchschwalbe and G. Sparn, 1984, Physica B **126**, 82.
Stewart, G.R., 1984, Rev. Mod. Phys. **56**, 755.
Strnat, K., and G.I. Hoffer, 1966, AFML-TR-65-446, U.S. Air Force Report (National Technical Information Service, Springfield, VA).
Strnat, K.J., and A.E. Ray, 1971, AFML-TR-71-36, U.S. Air Force Report (National Technical Information Service, Springfield, VA).
Suhl, H., and B.T. Matthias, 1959, Phys. Rev. **114**, 977.
Swinbanks, D., 1987, Nature **326**, 432, 630.
Takeshita, T., B.J. Beaudry and K.A. Gschneidner Jr, 1982, in: The Rare Earths in Modern Science and Technology, Vol. 3, eds G.J. McCarthy, H.B. Silber and J.J. Rhyne (Plenum, New York) p. 255.
Takeshita, T., K.A. Gschneidner Jr and B.J. Beaudry, 1985, J. Appl. Phys. **57**, 4633.
Tarascon, J.M., L.H. Greene, W.R. McKinnon, G.W. Hull, T.H. Geballe, 1987, Science **235**, 1373.
Taylor, K.N.R., and M.I. Darby, 1972, Physics of Rare Earth Solids (Chapman and Hall, London).
Trombe, F., 1936, Ann. Chim. (France) **6**, 349.
Trombe, F., 1938, Tech. Mod. **30**, 855.
Trombe, F., and F. Mahn, 1944, Ann. Chim. (France) **19**, 345.
Tsang, T.-W.E., K.A. Gschneidner Jr, F.A. Schmidt and D.K. Thome, 1985, Phys. Rev. B **31**, 235.
Urbain, G., P. Weiss and. F. Trombe, 1935, C.R. Hebd. Séances Acad. Sci. **200**, 2132.
van Maaren, M.H., K.H.J. Buschow and H.J. van Daal, 1971, Solid State Commun. **9**, 1981.
van Steenwijk, F.J., and K.H.J. Buschow, 1977, Physica B **85**, 327.
van Vucht, J.H.N., F.A. Kuijpers and H.C.A.M. Bruning, 1970, Philips. Res. Rep. **25**, 133.
Varma, C.M., 1985, Comments Solid State Phys. **11**, 221.
Verhoeven, J.D., E.D. Gibson and M.A. Noack, 1976, J. Appl. Phys. **47**, 5105.
Vogel, R., 1911, Z. Anorg. Allg. Chem. **72**, 319.
Vogel, R., and T. Heumann, 1943, Z. Metallkd. **35**, 29.
von Hevesy, G., 1927, Die Seltenen Erden von Standpunkte des Atombaues (Julius Springer, Berlin) p. 22.
Wachter, P., 1979, in: Handbook on the Physics and Chemistry of Rare Earths, Vol. 2, eds K.A. Gschneidner Jr and L. Eyring (North-Holland, Amsterdam) p. 507.
Wakefield, G.F., 1957, Ph.D. Thesis (Iowa State University, Ames, IA).
Wallace, W.E., 1973, Rare Earth Intermetallics (Academic Press, New York).
Wheelwright, E.J., 1969, J. Phys. Chem. **73**, 2867.
Wittig, J., C. Probst, F.A. Schmidt and K.A. Gschneidner Jr, 1979, Phys. Rev. Lett. **42**, 469.
Wohlleben, D.K., 1981, in: Valence Fluctuations in Solids, eds L.M. Falicov, W. Hanke and M.B. Maple (North-Holland, Amsterdam) p. 1.
Wu, M.K., J.R. Ashburn, C.J. Torng, P.H. Hor, R.L. Meng, L. Gao, Z.J. Huang, Y.Q. Wang and C.W. Chu, 1987, Phys. Rev. Lett. **58**, 908.
Wunderlin, W., B.J. Beaudry and A.H. Daane, 1963, Trans. Met. Soc. AIME **227**, 1302.
Wunderlin, W., B.J. Beaudry and A.H. Daane, 1965, Trans. Met. Soc. AIME **233**, 436.
Yosida, K., 1957, Phys. Rev. **106**, 893.
Young, R.C., 1979, J. Phys. Colloq. (France) **40**, C5-71.
Zijlstra, H., and F.F. Westendorp, 1969, Solid State Commun. **7**, 857.

Handbook on the Physics and Chemistry of Rare Earths, Vol. 11
edited by K.A. Gschneidner, Jr. and L. Eyring

Chapter 79

THE SIGNIFICANCE OF THE RARE EARTHS IN GEOCHEMISTRY AND COSMOCHEMISTRY

Stuart Ross TAYLOR and Scott M. McLENNAN*
Research School of Earth Sciences, Australian National University, Canberra, Australia

Contents

* Present address: Department of Earth and Space Sciences, State University of New York at Stony Brook, Stony Brook, NY, USA 11794-2100.

1. The unique nature of the lanthanides

The geochemical and cosmochemical uses of the rare earths, and of the lanthanides in particular, depend on the presence of a large number of elements which are distinguished by rather subtle variations in properties. Probably the most significant is that under normal conditions of temperature and pressure in the earth, they are trivalent, except for Eu under reducing conditions, and Ce under oxidising conditions. There is a regular decrease in ionic radii from La^{3+} to Lu^{3+}, constituting the well-known lanthanide contraction (table 1). In most cases they are found in eight-fold coordination sites in mineral lattices. Among geochemical systems, the only abundant and common cations of comparable size are Ca^{2+} and Na^{+}. Accordingly, there are also charge balance difficulties restricting the entry of the lanthanides into the cation lattice sites of most common rock-forming minerals (fig. 1). In this chapter, we will deal principally with the lanthanides, with occasional reference to Sc and Y.

Their remarkable properties mean that the lanthanides, as trace elements, are sensitive indexes of crystal–liquid equilibria in typical geological systems, whose mineralogy is dominated by major elements such as Si, Al, Fe, Mg, Ca, Na and K. Under reducing conditions, as in the terrestrial mantle or in the moon, Eu is reduced from the trivalent to the divalent state. This leads to an increase in ionic radius of

TABLE 1
Ionic radii for geochemically important species of the rare earths. (Data are from Shannon 1976.)

Ion	Ionic radius (Å)	
	CN6	CN8
Sc^{3+}	0.745	0.870
Y^{3+}	0.900	1.109
La^{3+}	1.032	1.160
Ce^{3+}	1.101	1.143
Ce^{4+}	0.87	0.97
Pr^{3+}	0.99	1.126
Nd^{3+}	0.983	1.109
Sm^{3+}	0.958	1.079
Eu^{3+}	0.947	1.066
Eu^{2+}	1.17	1.25
Gd^{3+}	0.938	1.053
Tb^{3+}	0.923	1.040
Dy^{3+}	0.912	1.027
Ho^{3+}	0.901	1.015
Er^{3+}	0.890	1.004
Tm^{3+}	0.880	0.994
Yb^{3+}	0.868	0.985
Lu^{3+}	0.861	0.977

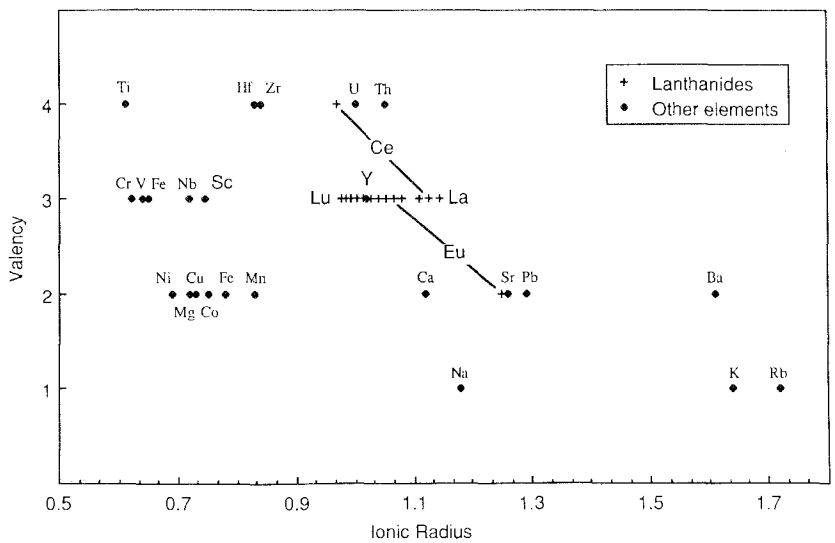

Fig. 1. The relationship between valency and radius for the rare earth elements (in larger font) and a number of other geochemically important species. Note the relative isolation of the trivalent lanthanides and yttrium from most common cations, which accounts for much of their geochemical behaviour. Sc^{3+} on the other hand lies close to many other common trivalent cations and enters major rock-forming mineral phases. The increase in radius of divalent Eu brings it close to Sr^{2+}, whose geochemical behaviour it mimics. Note the decrease in the radius of Ce^{4+} relative to Ce^{3+} which brings it close both in size and valency to U and Th. (Data are from tables 1 and 2.)

17% (Shannon 1976), thus making Eu^{2+} indistinguishable in size and valency from Sr^{2+}. This effect leads to a totally distinctive geochemical behaviour for Eu compared to the other lanthanides, and induces spectacular enrichments and depletions of that element, relative to the abundances of the other lanthanides.

Under oxidising conditions, notably associated with deposition of iron hydroxides in the oceans, cerium is oxidised to Ce^{4+}, with a consequent reduction in radius of 15% (Shannon 1976). This results in the precipitation of cerium hydroxides and phosphates in manganese nodules and a consequent dramatic depletion of Ce, compared to the other lanthanides, in seawater. This property has been used, for example, to estimate paleoredox conditions in ancient oceans.

The lanthanides are notably insoluble under conditions existing at the surface of the earth and relatively immobile under most metamorphic conditions. They have extremely short residence times in sea water, less than the mixing time of the oceans, which is about 1000 years. Accordingly, this property is of use in tracing oceanic mixing history.

The immobile nature of the lanthanides is one of the properties responsible for their extensive use in igneous petrology. Many elements are mobile and readily redistributed under conditions of low-temperature alteration, but the relative immobility of the lanthanides makes them of particular use in investigating, for example, Archean volcanic rocks, which may have suffered profound alteration. This property

also means that the lanthanides preserve their relative abundance patterns during erosion and transportion, so that the lanthanide patterns of terrigenous sedimentary rocks bears genetic information concerning their provenance.

Another major property which leads to cosmochemical fractionation of the rare earths is that although they are refractory elements, they display significant variations in relative volatility. Sc, Y and Er are super-refractory elements, while Eu and Yb are notably more volatile than the remaining elements. This wide range in volatility is responsible for separation of the rare earths in high-temperature processes either in the early solar nebula, or in pre-solar events. Temperatures within planets are not extreme enough to cause such fractionations on the basis of volatility.

The rare earth elements are trace constituents in most geochemical and cosmochemical environments. Only rarely are they individually present at more than a few parts per million, as in the products of extreme fractionation processes such as pegmatites. Rare earth minerals were first discovered 200 years ago in such deposits, in the pegmatite at Ytterby, near Stockholm, in 1787, by Lieut. C.A. Arrhenius; this was the material that Gadolin analysed in 1794. Because of their low abundances in rocks, the potential use of the rare earths in geochemistry was handicapped for many years by the absence of sensitive and convenient analytical methods, capable of routine determination at parts per million levels. Except for Sc, Y and La, the rare earths are not readily determined by optical emission spectroscopy, which was the principal analytical technique employed in geochemistry up to about 1960 (Ahrens and Taylor 1961). There was also a general belief that fractionation of the rare earths by natural processes was unlikely, except under extreme conditions, such as the formation of individual rare earth minerals in pegmatites, as the following quotation shows.

"The rare earth elements have chemical properties so similar that any major separation of these elements from each other seems to be improbable in any kind of cosmochemical process. ... Furthermore, it seems improbable that even on the surface of the earth these elements have been separated from one another by a large factor, except in certain types of minerals .... The analyses of meteorites carried out by Ida Noddack (1935) lead to values considerably different from those given by Minami (1935) for terrestrial sediments.... It seems difficult to believe that a fractionation of that order of magnitude could have occurred during the formation of the earth, and it seems more probable that one of the series of analytical data is considerably in error." (Suess and Urey 1956, p. 67).

Our modern understanding of their geochemical behaviour dates from about 1960, following the introduction of sensitive and accurate radiochemical neutron activation procedures. Some of the earliest work validated the distinctive patterns of both the sediments and the meteorites (although the absolute levels measured were much lower than the earlier estimates). This led to the realisation among geochemists that the lanthanides were indeed widely fractionated under common geological conditions of temperature and pressure, and so opened up broad perspectives for research.

In the following sections, we discuss many of these developments, to illustrate the

TABLE 2
Ionic radii for Eu^{2+}, Ce^{4+} and other geochemically important species.

Ion	Ionic radius (Å)	CN	Ion	Ionic radius (Å)	CN
Cs^+	1.88	12	Nb^{3+}	0.72	6
Rb^+	1.72	12	Nb^{5+}	0.64	6
K^+	1.64	12	Cr^{3+}	0.62	6
Ba^{2+}	1.61	12	V^{3+}	0.64	6
Pb^{2+}	1.29	8	Fe^{3+}	0.65	6
Sr^{2+}	1.26	8	Sc^{3+}	0.745	6
Eu^{2+}	1.25	8	Ti^{4+}	0.61	6
Na^+	1.18	8	Ni^{2+}	0.69	6
Ca^{2+}	1.12	8	Co^{2+}	0.75	6
Th^{4+}	1.05	8	Cu^{2+}	0.73	6
U^{4+}	1.00	8	Fe^{2+}	0.78	6
Ce^{4+}	0.97	8	Mn^{2+}	0.83	6
Zr^{4+}	0.84	8	Mg^{2+}	0.72	6
Hf^{4+}	0.83	8			

level of understanding of many fundamental questions in the earth sciences which has been gained from the study of the rare earth elements.

Yttrium, for which the trivalent ion is intermediate in size between Ho and Dy (another consequence of the lanthanide contraction), commonly follows the geochemical behaviour of those elements and is usually enriched or depleted to the same degree. Accordingly, it is generally considered by geochemists to be a close associate of the lanthanides and is usually both determined and discussed with them. Scandium, on the other hand, is much smaller (Sc^{3+} = 0.75 Å). This element, which is rarely present in rocks at more than 40 ppm, has a completely contrasting geochemical behaviour, typically entering six-fold coordination sites in early crystallising minerals. It is closer in geochemical behaviour to elements such as Cr, V, Ni or Co (table 2). Geochemists rarely consider it together with the lanthanides, or Y, preferring to group it with those trace elements listed above, which occupy six-fold coordination (CN) sites typically replacing the major elements Fe and Mg. For these reasons, it is discussed only incidentally in this review.

In geochemistry and cosmochemistry, elemental properties such as ionic radius frequently override the more traditional behaviour expected by chemists on the basis of valency. This is because liquid–crystal equilibrium at high temperatures and pressures controls mineral compositions. In gas–solid reactions in the solar nebula, relative volatility also becomes a significant parameter. In meteorites and planets, the distribution of elements is governed, at least initially, by their ability to enter metallic phases dominated by iron, sulfide phases dominated by FeS, or silicate phases. In table 3, the geochemical subdivision into volatile and refractory elements is given, along with the conventional geochemical usage of lithophile, chalcophile and siderophile elements. The lanthanides are prime examples of lithophile elements, entering silicate phases, in preference either to sulfide or metallic phases, during crystallisation of melts.

TABLE 3
Geochemical classification of elements.

(A) Based on relative volatility

Refractory	Al	Ba	Be	Ca	Hf	Ir	Mo
	Nb	Os	Pt	REE	Re	Rh	Ru
	Sc	Sr	Ta	Ti	U	V	W
	Y	Zr					
Moderately refractory	Cr	Li	Mg	Si			
Volatile (1300–600 K)	Ag	Cs	Cu	F	Ga	Ge	K
	Mn	Na	Rb	S	Sb	Se	Sn
	Te	Zn					
Very volatile (<600 K)	B	Bi	C	Cd	Cl	Hg	I
	In	Pb	Rare gases	Tl	Br		

(B) Based on preference for silicate (lithophile), sulfide (chalcophile) or metal (siderophile) phases

Li	Be						Lithophile: Na					B	C		O	F
							Chalcophile: **Zn**									
Na	Mg						Siderophile: **Fe**					Al	Si	P	S	Cl
K	Ca	Sc	Ti	V	Cr	Mn	**Fe**	**Co**	**Ni**	**Cu**	**Zn**	**Ga**	**Ge**	**As**	**Se**	Br
Rb	Sr	Y	Zr	Nb	**Mo**	—	**Ru**	**Rh**	**Pd**	**Ag**	**Cd**	**In**	**Sn**	**Sb**	**Te**	I
Cs	Ba	La–Lu	Hf	Ta	**W**	**Re**	**Os**	**Ir**	**Pt**	**Au**	**Hg**	**Tl**	**Pb**	**Bi**		
			Th		U											

In the past few years, a number of review articles and books dealing with lanthanide geochemistry have appeared (e.g. Haskin and Paster 1979, Hanson 1980 and Henderson 1984). It is not our intention merely to duplicate this material, and the reader is referred to these publications, in particular the text book edited by Henderson (1984) which contains 13 chapters on various aspects of rare earth element geochemistry, to complement this review.

Our major purpose is to demonstrate how the rare earths, and the lanthanides in particular, have provided unique insights into geochemistry and cosmochemistry. Many of the examples which we will use will be drawn from those aspects which have received rather less attention in previous reviews. These include the use of the rare earths to elucidate both the evolution of the moon and the composition and evolution of the continental crust of the earth. We will, however, attempt to provide some comment on all areas of geochemistry and cosmochemistry where lanthanides have added significantly to our understanding.

This review is concerned principally with the use of the rare earth elements as tracers of geological processes. We do not discuss, except in passing, the great advances which have resulted from the use in geochemistry and cosmochemistry of the radioactive decay of ^{147}Sm to ^{143}Nd and ^{176}Lu to ^{176}Hf. These topics each

require chapter length treatment in their own right. Recent reviews of Sm–Nd isotopic systematics have been given by O'Nions et al. (1979), DePaolo (1981a) and by Hawkesworth and van Calsteren (1984), while the Lu–Hf system has been reviewed by Patchett et al. (1981) and by Patchett (1983).

Some of the lanthanide nuclides have extremely large capture cross sections for thermal neutrons. These include ^{150}Sm, ^{156}Gd and ^{158}Gd. This property has been used to monitor the flux of low-energy thermal neutrons produced by cosmic ray bombardment on the lunar surface. Other work has been carried out on meteorites. Such studies are not reviewed here, but details may be found in work by Burnett and Woolum (1977).

2. Lanthanide abundance patterns and normalising factors

A principal difficulty in handling and comparing data for the lanthanides has been the so-called 'odd–even' effect, in which the even-numbered lanthanides are more abundant than those with odd atomic numbers. Thus, ^{57}La is almost always less abundant than ^{58}Ce, a consequence of the inherent stability of even-numbered nuclides compared to those of odd mass number (the well-known Oddo–Harkins effect). These variations are shown in fig. 2.

Various normalising procedures have been adopted to overcome the complexity induced by the Oddo–Harkins effect in comparing data. These have included plotting odd- and even-numbered elements separately, normalising to La, or Yb, and so on. All these methods are of historical interest only, and the Coryell–Masuda (Masuda, 1962, Coryell et al. 1963) method of normalising the lanthanide data is now universally used. This method consists of forming a ratio of one lanthanide pattern to another, commonly a chondritic abundance pattern (fig. 2). This procedure has several advantages:

(a) it removes the odd–even effect, producing smoother patterns;

(b) it enables comparisons between different patterns (normalised to the same base);

(c) it clearly displays relative degrees of enrichment or depletion, and the contrasting behaviour of neighbouring elements.

Normalised abundances are plotted either against ionic radius or against atomic number of the lanthanides. In principle, plots based on ionic radius should produce the smoothest curves. In practice, plots using atomic number as the x-axis are almost universally used, mainly for historical reasons, but also to avoid the complexity introduced by variations in radius due to changes in valency.

The commonest normalising patterns employed are those generally referred to as 'chondritic'. This practice has arisen on account of the general uniform abundances observed in 'chondritic' meteorites, a feature recognised from the earliest days of geochemical investigations of lanthanides. Subsequent work showed that there are in fact minor variations among differing classes of chondritic meteorites (Evensen et al. 1978). The particular rationale for the use of chondritic abundance patterns is of course that they represent our best estimate of primitive solar nebula abundances, as

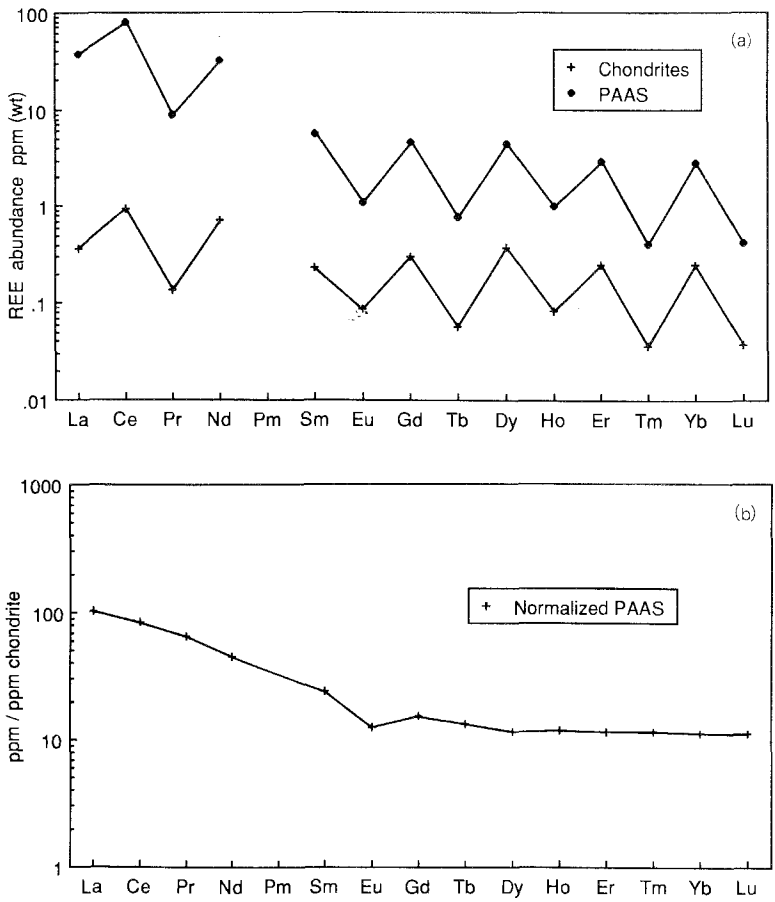

Fig. 2. (a) Raw lanthanide abundance data for Australian shales and CI chondritic meteorites, showing the inherently higher concentrations of even-numbered elements (the Oddo–Harkins effect, due to the greater stability of even-numbered nuclides). (b) The lanthanide pattern resulting from normalising the Australian shale abundance data to the CI chondritic values. This normalisation illustrates both the relative abundance and fractionation of the lanthanides compared to values typical of the primordial solar nebula. (Data are from table 4.)

discussed in section 4.1. There has been no agreed set of values used by all workers, with many laboratories using an unspecified 'chondritic' normalisation, usually traceable back to the values published by Haskin et al. (1966a) for ordinary (H and L) chondrites. In practice, this is not a major difficulty, since the various sets of chondrite values used for normalisation have similar inter-element ratios for the lanthanides. This results in parallel patterns for the same sample, but the patterns may be displaced up to 15–20%.

The best estimate of primordial lanthanide abundances, as discussed in section 4.1, is given by those in the primitive CI class of carbonaceous chondrites. When normalised to an element such as Si, they closely match the abundances in the sun.

TABLE 4
Rare earth element abundances [in ppm (wt)] in chondritic meteorites and average post-Archean shale (PAAS) used for normalising.

Element	Chondrites[a]	PAAS[b]
La	0.367	38
Ce	0.957	80
Pr	0.137	8.9
Nd	0.711	32
Sm	0.231	5.6
Eu	0.087	1.1
Gd	0.306	4.7
Tb	0.058	0.77
Dy	0.381	4.4
Ho	0.0851	1.0
Er	0.249	2.9
Tm	0.0356	0.41
Yb	0.248	2.8
Lu	0.0381	0.43
Total	3.89	183
La/Yb	1.48	13.6
La_N/Yb_N	1.00	9.17
Eu/Eu*	1.00	0.66
Y	2.25	27
Sc	8.64	16

[a]From Evensen et al. (1978); volatile free: original data X 1.50.
[b]From Nance and Taylor (1976); except Sc: from Taylor and McLennan (1985).

CI meteorites contain about one-third water and other volatile elements. For these reasons, we use 'volatile-free' lanthanide abundances for normalisation. Such values are similar to those in H and L ordinary chondrites, used by many workers previously. Accordingly, the use of 'volatile-free' CI lanthanide abundances for normalisation does not introduce a substantial variation from previous practices, but has a much better cosmochemical justification. The values selected are given in table 4. Since there is no apparent relative fractionation of the lanthanides during planetary accretion processes, these abundances are generally taken to be simply related to bulk earth compositions. Accordingly, their use as normalising abundances for terrestrial samples provides a measure of the degree of fractionation from the primitive terrestrial abundance patterns.

The second common lanthanide abundance pattern which is uniform and which has widespread geochemical significance, is that observed in most post-Archean sedimentary rocks such as shales. This pattern, as discussed later, is generally taken to represent that of the upper continental crust exposed to weathering and erosion, so that it forms a suitable base for comparison of terrestrial surface processes affecting the lanthanides. Two different sets of shale abundances have been used for normalisation. The first is the North American Shale Composite (NASC, Haskin et

al. 1968, Gromet et al. 1984) which is a composite sample of 40 Paleozoic shales mainly from North America. The other is the Post-Archean Australian Average Shale (PAAS, Nance and Taylor 1976) which is an average of 23 shales of post-Archean age. Both patterns are similar but we prefer in principle to use PAAS rather than NASC, because of the potential for inclusion of aberrant material in composite samples. Values for PAAS are listed in table 4.

Other patterns useful for normalisation include those of a bulk rock composition as a base for comparing the lanthanide patterns in its constituent minerals. Examples of all these usages will be found in this chapter.

Geochemists frequently divide the lanthanides into two groups, the so-called light lanthanides (La–Sm) and the heavy lanthanides (Gd–Lu), commonly referred to by the symbols LREE and HREE. This usage reflects the fact that an inflection in lanthanide patterns often appears at about Eu, due to the effect of the increasing ionic radius (for trivalent ions) of the 'lighter' elements. A more rational convention would be to refer to large and small lanthanides, reflecting the basic cause of the division, but usage of 'LREE' and 'HREE' is deeply entrenched in the geochemical literature.

Because europium is commonly fractionated from the other lanthanides, the relative enrichment or depletion (commonly referred to as positive and negative Eu anomalies, respectively) has been quantified as the term Eu/Eu*. Eu* is the theoretical value for no anomaly (i.e. a smooth lanthanide pattern between Sm and Gd) and is calculated on that assumption. Thus:

$$Eu/Eu^* = Eu_N/(Sm_N \cdot Gd_N)^{0.5}$$

where the subscript N indicates chondrite-normalised values. A geometrical mean is used because chondrite-normalised abundances are plotted on a logarithmic scale. An analogous notation may be used to specify cerium enrichments and depletions. Although it is common to find that Eu* has been estimated by using the simple arithmetic mean of $(Sm_N + Gd_N)/2$, this is incorrect and can lead to serious errors for very steep chondrite-normalised lanthanide patterns.

3. International standard samples

Methods for the determination of the rare earths in geological samples are not dealt with here. They have been discussed in previous chapters in this Series (Boynton 1979, Schuhmann and Philpotts 1979, Taylor 1979), and in other places (Henderson and Pankhurst 1984), and demand chapter length treatment in their own right. The question of calibration of analytical techniques has generally not been addressed directly, and is worth commenting upon.

The concept of circulating, to participating laboratories, standard samples to enable their composition to be unequivocally established, goes back for trace element geochemistry to the distribution of the standard granite G-1 and diabase W-1. The results from this exercise (Fairbairn 1951) showed so much scatter of data that a major effort was instituted in an attempt to improve both the precision and

TABLE 5
REE content [in ppm (wt)] in USGS standard rock sample BCR-1 (Columbia River Basalt).

Element	BCR-1 [a]
La	24.2
Ce	53.7
Pr	6.50
Nd	28.5
Sm	6.70
Eu	1.95
Gd	6.55
Tb	1.08
Dy	6.39
Ho	1.33
Er	3.70
Tm	0.51
Yb	3.48
Lu	0.55
Total	145
La/Yb	6.95
La_N/Yb_N	4.70
Eu/Eu*	0.90
Y	34
Sc	33

[a]From Taylor and Gorton (1977), except Y: from Taylor and McLennan (1985), and Sc: from Abbey (1983).

accuracy of trace element determinations. The general solution adopted has been to provide more and more 'standard samples' so that now about 170 are in circulation. This proliferation has to a large extent defeated the good intentions of the analytical community, since truly reliable values exist for only a few elements in a handful of these standard samples.

A peak in accurate trace element analysis appears to have been reached in the early 1970's. There are three reasons for this. Firstly, the number of standard samples in circulation was small, with attention directed upon the six United States Geological Survey (USGS) standards (peridotite PCC-1, dunite DTS-1, basalt BCR-1, andesite AGV-1, granodiorite GSP-1 and granite G-2) which supplemented G-1 and W-1. Secondly, many new methods of analysis were being introduced, so that careful interlaboratory calibration was important to demonstrate the reliability of the new techniques. Thirdly, the arrival of the lunar samples placed a premium on high quality analyses of this unique material, access to the samples being denied to laboratories whose data were shown to be in error. The situation since that time has deteriorated, and the quality of many published trace element determinations appears to be little better than in the 1960's.

Although many analyses of the plethora of standard samples have appeared, and a

whole subculture, with its own journal, has arisen, few samples have achieved the desirable status of being unquestionably correct despite this large effort. We demonstrate that highly accurate data are in fact obtainable by reference to the USGS standard basalt BCR-1. In table 5, we give our best estimate of the 'true' lanthanide abundances in that sample (Taylor and Gorton 1977). This estimate was obtained in the following manner. Ten sets of values for the REE by high precision analytical methods (mainly isotope dilution from participants in the lunar program) were averaged. The overall reproducibility among the laboratories was about $\pm 3\%$. Regrettably, such a level of agreement is reached only rarely in interlaboratory checks. These data were plotted against the ionic radii for the trivalent REE ions (eight-fold coordination) from Shannon (1976). The assumption was made that the REE (except Eu) should fall on a smooth curve, and the average values adjusted accordingly to fit (this correction fell within the precision limits of 3%). Interpolated data were calculated for mono-isotopic elements where there were few data.

The resulting set of values for BCR-1 are presented as the closest approach to the 'true' values. There appears to be little systematic bias due to sample heterogeneity, although this explanation has been frequently invoked to explain analytical aberrations. This approach contrasts with the usual method of averaging all the data irrespective of analytical method, or the established reliability of the analyst, and regarding the average as the true value. Substantial bias can be introduced by the application of such statistical techniques without regard to these less readily quantifiable factors.

4. The early solar system

4.1. *The solar nebula*

The solar system began to form about 4.55 Ae ago from a rotating disk of dust and gas (the solar nebula) which had sepatated from a larger molecular cloud a little earlier. The original composition of this disk can be obtained from two sources. The first of these are the spectral data from the sun. Rare earth abundances may be obtained both from photospheric absorption lines and coronal emission lines. These data are given in table 6 as atomic abundances relative to $Si = 10^6$ atoms (Aller 1987) and give the composition of the outer layers of the sun.

The second source of information about the early solar nebula comes from the primitive meteorites, which provide ages of 4.55 Ae. Although many classes of meteorites show elemental fractionations, the Type 1 carbonaceous chondrites (or CI, where I = Ivuna, the type example of this class of meteorites) have a composition (excluding the 'volatile' elements by which are meant in this context: H, C, N, O and the rare gases) which is close to that of the relative abundances, normalised to Si, derived from the solar spectra. Lanthanide data are given in table 6. A comparison of the solar and meteoritic data is plotted in fig. 3 which shows the close correspondence between the two sets. This similarity is one of the pieces of evidence that we are dealing with the overall composition of the original solar

TABLE 6
Comparison of elemental abundances in the solar atmosphere and in CI meteorites. (Atomic abundances relative to Si = 10^6 atoms.)

Element	Solar atmosphere[a]	CI chondrites[b]
Sc	2.8	34.5
Y	4.0	4.33
La	0.30	0.46
Ce	0.79	1.2
Pr	0.12	0.18
Nd	0.38	0.85
Sm	0.14	0.27
Eu	0.11	0.099
Gd	0.30	0.34
Tb	–	0.060
Dy	0.26	0.40
Ho	–	0.089
Er	0.13	0.26
Tm	0.041	0.039
Yb	0.18	0.25
Lu	0.13	0.038

[a]Data for solar atmosphere from Aller (1987).
[b]Data for CI chondrites from Evensen et al. (1978), except for Sc and Y from Schmitt (1964).

nebula, since the CI meteorites are most probably derived from the asteroid belt, located far from the sun, between Mars and Jupiter.

The second piece of evidence is derived from the observation that the isotopic abundances in CI chondrites are a smooth function of mass number (fig. 4) (Suess and Urey 1956). If the CI abundances were fractionated from those originally present in the primitive solar nebula, it seems unlikely that such a relationship would either result from the fractionation process itself or be preserved by it (Anders and Ebihara 1982).

Accordingly, we take the CI abundances as representative of the original solar nebula. It is this feature which makes them useful for normalising other lanthanide abundances. By such a calculation, we obtain information on the amount of fractionation relative to the abundances in the primordial solar nebula.

4.2. *Heterogeneity in the solar nebula*

Although the CI and solar data indicate broad homogeneity in the solar nebula, there is considerable evidence for local heterogeneity. The principal information for this comes from the observed spread of the oxygen isotopes among various meteorite classes (Clayton et al. 1985). The main evidence obtained from the lanthanides comes from inclusions present in the Allende and Murchison meteorites. These data provide evidence for high-temperature evaporation and condensation, although the precise sites of these events remain to be identified.

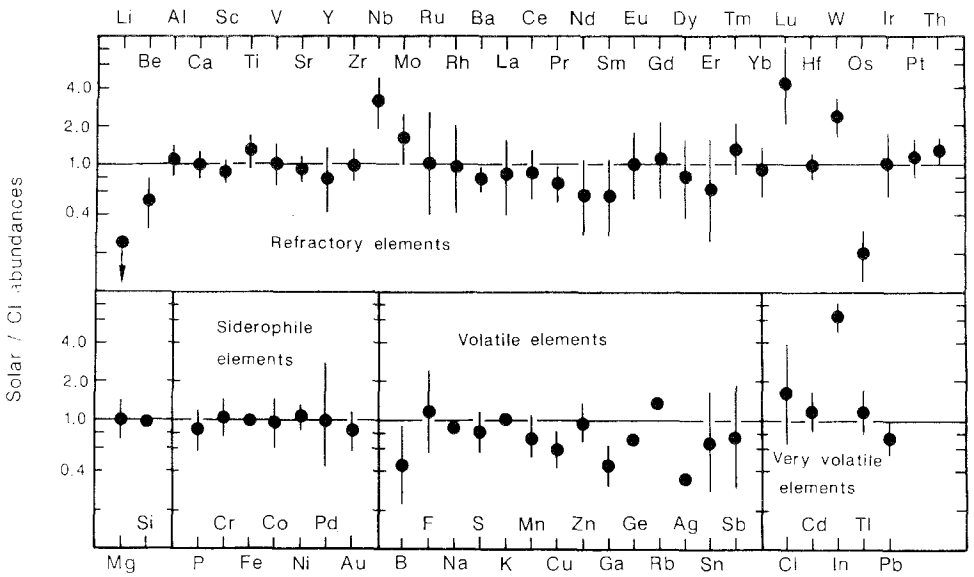

Fig. 3. Comparison between the abundances in the solar photosphere and those in the CI carbonaceous chondrites. Apart from Li, which is consumed in nuclear reactions in the sun, there is little significant difference in the two data sets. Uncertainties in the solar data for Nb, Lu, W, Os, Ga, Ag, and In are probably responsible for discrepancies for these elements. This diagram forms the basis for the assumption that the CI carbonaceous chondrites provides us with a sample of the primordial solar nebula, excluding the gaseous elements. [Data are from Anders and Ebihara (1982), and from table 6.]

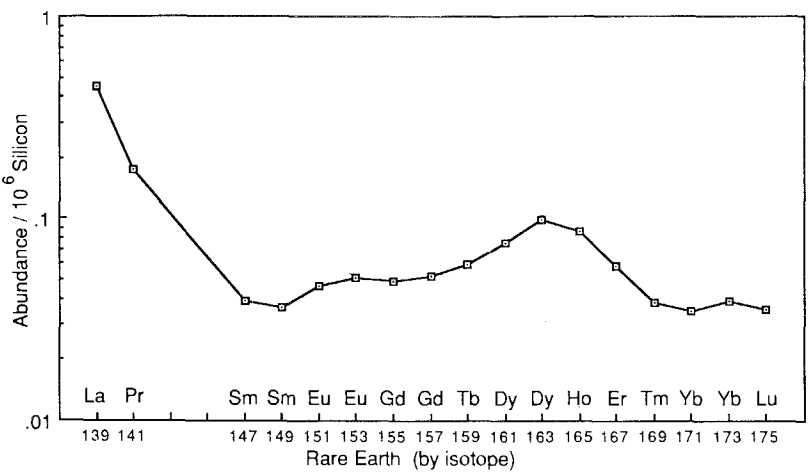

Fig. 4. The smooth curve through the odd-numbered isotopes of the lanthanides which was used by Suess (1947) and by Suess and Urey (1956) as evidence that the meteoritic abundance data were reflecting nucleosynthetic processes. Anders and Ebihara (1982) give an updated discussion. The slight spike at Eu is not due to analytical uncertainty. They suggest that this peak may be due to a spike of Eu enriched material, added to CI meteorites, or due to depletion of Sm from the decay of ^{147}Sm.

TABLE 7
Calculated 50% oxide condensation temperatures for ideal solid solution in perovskite (for three different total pressures) for lanthanides and other refractory elements. (Data are from Kornacki and Fegley 1986).

Oxide	Condensation temperature (K)		
	10^{-3} bar	10^{-6} bar	10^{-9} bar
ZrO_2	1786	1594	1437
HfO_2	1753	1577	1434
Sc_2O_3	1724	1524	1366
Y_2O_3	1692	1499	1346
Lu_2O_3	1676	1463	1302
Er_2O_3	1676	1463	1303
ThO_2	1676	1463	1296
Ho_2O_3	1676	1463	1296
Tb_2O_3	1676	1463	1296
Tm_2O_3	1676	1463	1296
Dy_2O_3	1675	1463	1296
Gd_2O_3	1674	1462	1296
UO_2	1663	1437	1253
Pu_2O_3	1654	1445	1280
Nd_2O_3	1640	1430	1260
Pr_2O_3	1636	1420	1254
Sm_2O_3	1633	1433	1275
La_2O_3	1621	1410	1247
Ta_2O_5	1614	1418	1265
NbO_2	1609	1362	1190
Yb_2O_3	1549	1392	1263
V_2O_3	1542	1308	1122
Ce_2O_3	1532	1286	1109
Eu_2O_3	1398	1232	1104
SrO	1275	1116	992
BaO	1227	1052	919

As was noted earlier, the lanthanides, although refractory, display significant differences in volatility. Table 7 gives a list of condensation temperatures from the work by Kornacki and Fegley (1986) which illustrates this difference and also their relation to other refractory elements. The abundance patterns of the lanthanides in the calcium–aluminum (CAI) refractory inclusions from the Allende and Murchison meteorites further demonstrate this phenomena. In the simplest cases (Groups I and III) only the more volatile lanthanides Eu and Yb are depleted or enriched. The most spectacular examples are provided by the so-called Group II lanthanide abundance patterns (fig. 5). In these, both the most refractory lanthanides (Er, Lu and Ho) as well as super-refractory elements such as Zr, Hf, Th, Sc and Y, and the most volatile species (Eu and Yb) are depleted. The curious resulting pattern is that due to the relative enrichment of the lanthanides of intermediate volatility. No similar patterns have ever been observed in terrestrial or lunar samples or in bulk meteorites: the temperatures required for such fractionation are not reached in intra-

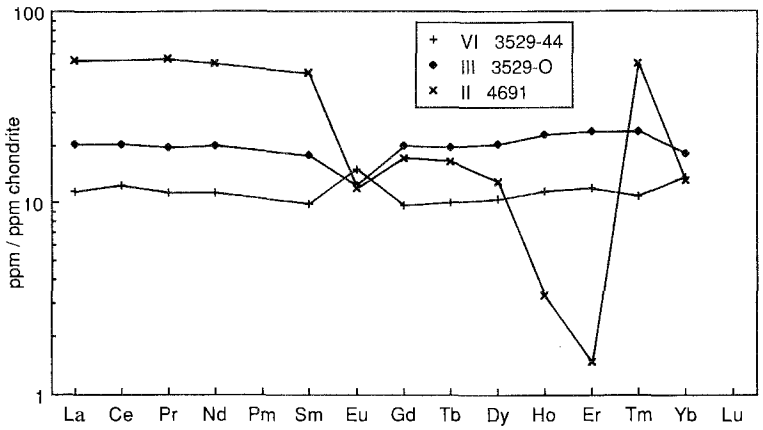

Fig. 5. Lanthanide patterns for white inclusions from the Allende meteorite. Data from Mason and Taylor (1982) for Groups II, III and VI are shown. Groups III and VI respectively show depletion and enrichment of volatile Eu and Yb. Group II patterns are depleted in both super-refractory and volatile species.

planetary environments. These refractory inclusions retain the evidence of high-temperature processes within the early nebula, or in precursor events, perhaps connected with supernovae.

A principal conclusion is that the preservation of these lanthanide abundance patterns argues against homogenisation of the solar nebula. The complexity of the patterns also argues against simple monotonic cooling of an original hot solar nebula. Although such models have been popular among some students of meteorites (see discussion in the work by Wasson 1985), there is little support among astrophysicists for an initially hot ($\sim$2000 K) nebula (see discussion in the work by Black and Matthews 1985).

Further examples of lanthanide patterns showing the effects of volatility are found in the highly refractory mineral hibonite ($CaAl_{12}O_{19}$). A veritable zoo of patterns is found in individual hibonite grains from the Murchison meteorite (fig. 6). Patterns representing Groups I, II and III are all present and clearly indicate multiple stages of evaporation and recondensation.

In summary, the principal contributions of the REE to our understanding of the early solar nebula are the following:

(a) The smooth abundance patterns for the odd-numbered isotopes of the lanthanides in Type 1 carbonaceous chondrites, and in chondrites generally, are evidence that the lanthanides have not been subjected to serious cosmochemical fractionation effects on a nebula-wide scale. This, coupled with the similarity between the solar photospheric lanthanide abundances and those in the chondritic meteorites, enables us to use the well-determined abundances in the CI meteorites as representative of the abundance patterns in the primordial solar nebula of the lanthanides.

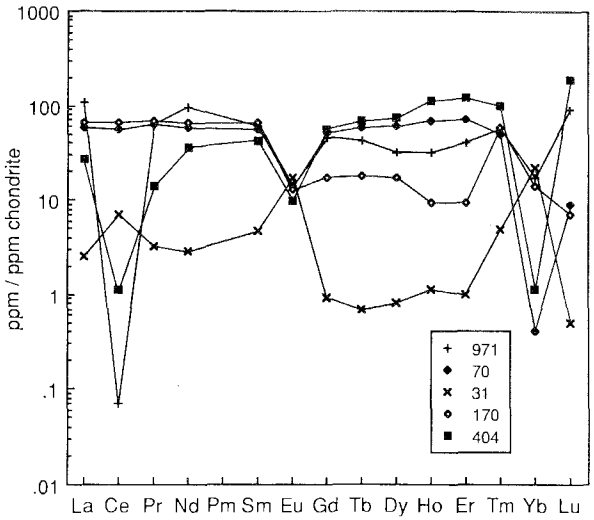

Fig. 6. A wide variety of lanthanide patterns for individual hibonite ($CaAl_{12}O_{19}$) grains from the Murchison meteorite, which reflect multiple episodes of evaporation and condensation. [Data are from Crozaz and Zinner (1986) and from Zinner and Crozaz (1986).]

(b) The second major conclusion is that the lanthanide patterns in inclusions in the Allende meteorite and in hibonite grains in the Murchison meteorite provide evidence of multiple evaporation and condensation events in the early nebula, or in pre-solar events, and contain the important information that the nebula was not homogenised following these events. This observation is difficult to reconcile with the hypotheses which form the planets through condensation from an initially hot ($\sim$2000 K) nebula, and favors their accretion from planetesimals formed under lower temperature conditions (Wetherill 1987).

4.3. *Meteorites*

The latest review of meteorite classifications and properties is given by Wasson (1985). A simplified classification scheme is given in table 8. Bulk lanthanide abundances in chondritic meteorites do not indicate any major cosmochemical fractionation during their formation. Lanthanide patterns in chondrites are relatively uniform, and bulk compositions show no dependence on volatility. No Eu or Yb anomalies are apparent. This information indicates that extreme temperatures were not experienced during their formation. Loss of more volatile elements was common among the H, L, LL, C2, and C3 classes, whereas E chondrites, with fully reduced Fe, have their full complement of volatile elements.

Most meteorites are derived from the asteroid belt, although a few of the fractionated members come from Mars (SNC types) and from the moon. The asteroid belt shows gradations in composition with the percentage of C-type asteroids (low albedo, identified most probably with primitive CI carbonaceous meteorites) increasing outwards, possibly consistent with decreasing temperature conditions with increasing distance from the sun.

As noted earlier, the lanthanide elements and yttrium, within the principal groups

TABLE 8
Classification of meteorites. (Adapted from Mason 1962, and Wasson 1985.)

Class	Clan	Group
Chondrites	Refractory-rich	CV
	Minichondrule	CO
		CM
	Volatile-rich	CI
	Ordinary	LL
		L
		H
	Enstatite	EL
		EH
Differentiated meteorites (achondrites and stony-irons)		Eucrites
		Howardites
		Diogenites
		Mesosiderites
		Pallasites
		Aubrites
		Ureilites
Irons*		Hexahedrites
		Octahedrites
		Ni-rich ataxites

*13 groups are separated on the basis of Ni, Ga, Ge and Ir contents.

of meteorites (E, H, L, LL), show little fractionation and constitute evidence for a general uniformity of composition for the refractory elements in the solar nebula. These same meteorites display large variations among metal/silicate ratios and in the amounts of volatile elements, but processes involving reduction of FeO to metallic Fe, and loss of volatile elements such as Bi and Tl, have not affected the relative abundances of the lanthanides.

Among the fractionated meteorites, such as the eucrites, the lanthanides show some variation. These meteorites, the basaltic achondrites, are basalts, originating as lavas on small asteroidal bodies (Basaltic Volcanism Study Project 1981, p. 214). The eucrites form one important class. Since the asteroid 4 Vesta, 555km in diameter, has a basaltic-like surface from spectral reflectance data, it is a prime candidate for the source of such meteorites, although considerable dynamical problems remain (Gehrels 1979).

Figure 7 shows typical lanthanide patterns for the eucrites (see table 8). These display flat patterns parallel to those of chondrites, but with variable europium anomalies. Such patterns provide much useful genetic information as discussed below. Based on this and other petrological evidence, the eucrites are basalts, derived, in a manner analogous to terrestrial lavas, by partial melting at depth in a

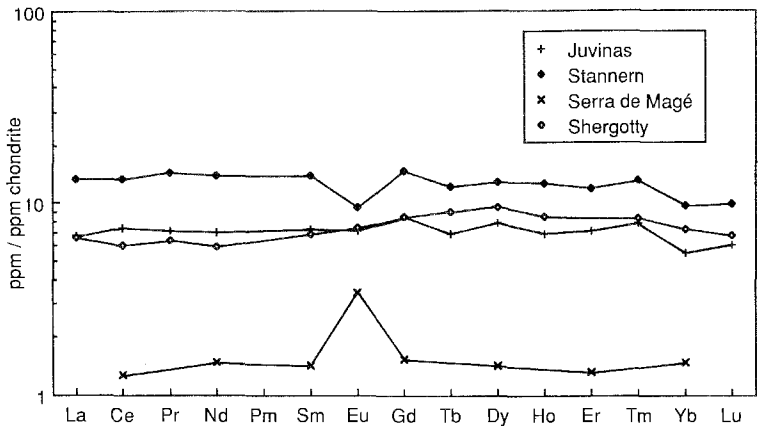

Fig. 7. Fractionation patterns of lanthanides, due to crystal–liquid effects, in the eucrite class of meteorites (data are from table 9). The Eu enrichments and depletions relative to the other lanthanides are due to the preferential entry of Eu^{2+} into plagioclase feldspar. Otherwise there is little relative fractionation of the other lanthanides from the CI pattern.

planetary body, albeit a small one. The eucrites fall into three main groups:

(a) The main trend exemplified by Juvinas and Sioux County, with flat lanthanide abundance patterns about 10 times chondritic. These can be derived by about 10–15% partial melting from a source with chondritic abundances of the lanthanides.

(b) Stannern, with a strong depletion in Eu, can be derived by about 4% partial melting from a similar source (containing minerals olivine, pigeonite and plagioclase). The depletion of Eu occurs because in this case some plagioclase feldspar remains in the source. This mineral retains Eu^{2+}, which, like Sr^{2+}, preferentially enters the plagioclase structure ($CaAl_2Si_2O_8$), replacing Ca^{2+}.

(c) The third group of eucrites, such as Moore County or Serra de Magé, which shows a strong enrichment in Eu, and otherwise low lanthanide abundances, are so-called 'cumulates', formed from an already melted lava by separation and accumulation of pyroxene and plagioclase crystals. The accumulation of the plagioclase crystals, preferentially enriched in Eu, accounts for the enrichment of the bulk meteorite in that element. These examples are described in some detail to show the usefulness of the lanthanides in deciphering the history of igneous rocks, derived by partial melting from more primitive sources and undergoing varying degrees of crystallisation and separation of phases.

Another more exotic class of meteorites are the SNC meteorites (named after the Shergotty, Nakhla and Chassingny classes of meteorite) (McSween 1985). They contain evidence, principally from the similarity of their rare gas compositions to that measured by the Viking missions, that they are derived from Mars. They are among the youngest meteorites with crystallisation ages of about 360 million years (Jagoutz 1987) differing in this respect from most meteorites which formed at about 4.55 Ae.

TABLE 9
Rare earth element abundances [in ppm (wt)] in differentiated meteorites.

Element	Juvinas[a]	Stannern[a]	Serra de Magé[b]	Shergotty[c]
La	2.5	4.9	—	2.44
Ce	7.2	12.9	1.22	5.8
Pr	0.98	2.0	—	0.88
Nd	5.0	10.0	1.06	4.2
Sm	1.7	3.2	0.33	1.60
Eu	0.62	0.83	0.30	0.65
Gd	2.6	4.5	0.47	2.6
Tb	0.40	0.71	—	0.52
Dy	3.0	4.9	0.55	3.65
Ho	0.59	1.07	—	0.73
Er	1.8	3.0	0.33	—
Tm	0.28	0.47	—	0.30
Yb	1.37	2.4	0.37	1.80
Lu	0.23	0.38	—	0.26
Total	28	51	—	26
La/Yb	1.83	2.0	—	1.36
La_N/Yb_N	1.23	1.38	—	0.92
Eu/Eu*	0.90	0.67	2.32	0.97
Y	17	28	—	—
Sc	29	32	—	55

[a]From Haskin et al. (1966a,b).
[b]From Schnetzler and Philpotts (1969).
[c]From Laul et al. (1986).

The lanthanide abundance pattern for Shergotty (table 9, fig. 7) is unique among meteorites and indicates a complex prehistory in the Martian mantle from which they appear to have been derived, as basalts, by partial melting. The enriched pattern of the heavy lanthanides (Gd–Lu) resembles that of pyroxenes (the parent rocks appear to have been pyroxene cumulates). It provides no evidence that garnet was a residual phase in the source from which these basalts were derived, for, if so, the reciprocal pattern would be displayed. Leaching experiments show that most of the lanthanides are contained in accessory phases (whitlockite and apatite) rather than in the major mineral phases.

A final question which may be considered in the general context of the cosmological significance of meteorites is whether any of the present population can be considered to comprise the building blocks of the terrestrial planets. The answer to this interesting question is that none of the current population of meteorites have appropriate compositions. All are ruled out on the basis of rare gas data, oxygen isotopes, K/U and K/La ratios and so on (Kerridge 1988). Accordingly, they must be regarded, except for the Martian and lunar examples, as providing us with samples from the asteroid belt. The population of planetesimals which accreted to form the earth and the other terrestrial planets differed in important respects from

those now being derived from the asteroid belt, particularly in the ratios of volatile to refractory elements. The lanthanides, however, were present in both in the same relative abundances.

An extensive review of the lanthanides in meteorites is given by Boynton (1984), which should be consulted for further details.

5. Lunar geochemistry

The rare earth elements, and the lanthanides in particular, have been of decisive importance in elucidating the evolution of the moon. They provide an example *par excellence* of the insights which can be gained from their behaviour in a natural environment, and for this reason an extended treatment is given.

It was fortunate that the return of the first lunar samples in 1969 took place following ten years of development and refinement of analytical techniques for the determination of the rare earths. Accordingly, from the outset of lunar studies accurate and reliable values at the parts per million level were available and the progress of the investigations was not hampered, as has commonly been the case in trace element studies, by data of questionable and uncertain quality. General reviews may be found in works by Taylor (1975, 1982).

The first lunar samples were returned from the smooth basaltic plains of Mare Tranquillitatis. One of the initial observations on the geochemical nature of these basaltic lavas was that they were characterised by a depletion in Eu relative to the other lanthanides. These patterns (figs. 8 and 9) also showed a depletion in the light lanthanide elements (La–Nd) relative to chondritic abundances. The basaltic lunar samples were recognised as being derived, like terrestrial basaltic lavas, from deep within the moon by partial melting of the lunar mantle. Depths of origin between 100–400 km were inferred from the experimental petrology data (the depths are still

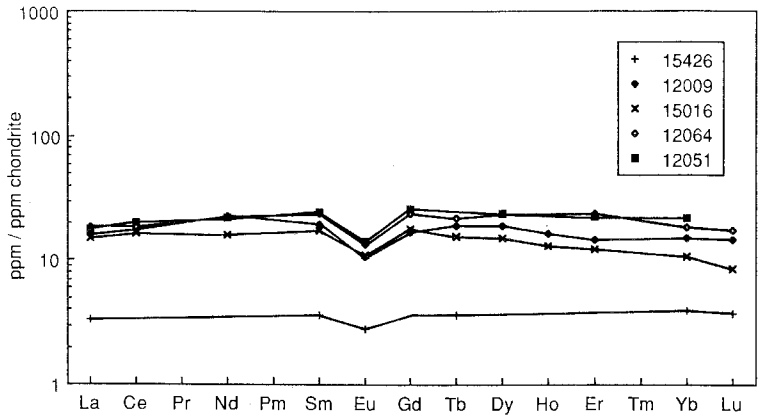

Fig. 8. Typical lanthanide patterns for low-Ti lunar basalts showing the ubiquitous depletion in Eu and slight depletion in the light lanthanides. (Data are from table 10.)

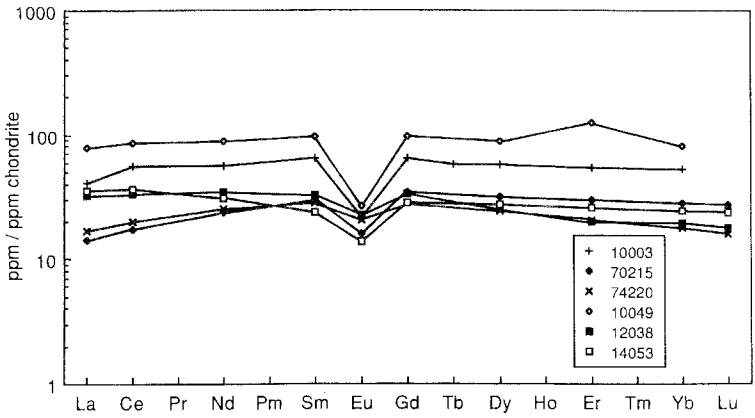

Fig. 9. Lanthanide abundance patterns for high-Ti, high-K and high-Al lunar basalts, again showing the general depletion in Eu, which reflects the pattern in the source regions at depths of 150–400 km within the moon. (Data are from table 11.)

not well-constrained, despite many years of effort by different investigators). It was thus realised that the lunar basalts conveyed some information about the composition of the lunar interior, but the discovery of the Eu depletion was eventually to invalidate those investigations of experimental petrology which assumed that the lunar basalts were derived from a primitive lunar interior.

Among the many hypotheses advanced to account for the distinctive lanthanide patterns (soon shown from succeeding missions to comprise a ubiquitous signature of lunar basalts), two schools of thought can be distinguished. The first held that the source regions had essentially chondritic abundances of the lanthanides, and that the depletion of Eu was due either to retention of Eu in mineral phases during partial melting, or to the removal of phases such as plagioclase, in which the Eu was concentrated during crystallisation of the melt. The second school proposed that the depletion of Eu was an inherent feature of the source regions deep within the moon. Before discussing the resolution of this controversy, which was both elegant and simple and led to major insights into lunar evolution, it is necessary to discuss in some detail the features of the lanthanide patterns both in the lunar mare basalts, and in the plagioclase-rich highland samples, returned from subsequent missions.

5.1. *The mare basalts*

The lanthanide patterns, normalised to the chondritic abundances, are shown in figs. 8 and 9 and the data are listed in tables 10 and 11. Several interesting features emerge. The most informative is the depletion in europium which is discussed in the next section. Secondly, the abundance patterns are broadly parallel to one another, but with some differences in detail. The generally parallel nature of the total patterns (excluding Eu) over more than an order of magnitude is attributed to two causes.

TABLE 10
Rare earth element abundances [in ppm (wt)] in low-Ti lunar mare basalts. (Adapted from Taylor 1982.)

Element	Green glass 15426	Apollo 12 olivine 12009	Apollo 15 olivine 15016	Apollo 12 pigeonite 12064	Apollo 12 ilmenite 12051
La	1.20	6.1	5.58	6.76	6.53
Ce	—	16.8	15.6	17.5	19.2
Nd	—	16	11.4	16	15.4
Sm	0.83	4.53	4.05	5.51	5.68
Eu	0.24	0.94	0.97	1.16	1.23
Gd	—	5.2	5.4	7.2	7.89
Tb	0.21	1.11	0.9	1.27	—
Dy	—	7.13	5.74	9.03	9.05
Ho	—	1.4	1.1	—	—
Er	—	3.6	3.1	6.0	5.57
Yb	0.97	3.74	2.62	4.59	5.46
Lu	0.14	0.55	0.32	0.67	—
La/Yb	1.24	1.63	2.13	1.47	1.20
Eu/Eu*	0.76	0.59	0.63	0.56	0.56
Y	7.2	34	21	41	48
Sc	38	46	39	63	58

Firstly, the lunar patterns are consistent with only a limited amount of fractional crystallisation during cooling, for otherwise the patterns would not remain relatively parallel. Secondly, small amounts of partial melting produce strong enrichment of lanthanides in the melt, since the accessory phases containing them are among the

TABLE 11
Rare earth element abundances [in ppm (wt)] in high-Ti, high-K and Al lunar mare basalts. (Adapted from Taylor 1982.)

Element	Apollo 11 low-K 10003	Apollo 17 B 70215	Orange glass 74220	Apollo 11 10049	Apollo 12 12038	Apollo 14 14053
La	15.2	5.22	6.25	28.8	11.8	13.0
Ce	53	16.5	19.0	83	31.6	34.5
Nd	40	16.7	17.8	63	24.6	21.9
Sm	14.8	6.69	6.53	22.3	7.6	5.56
Eu	1.85	1.37	1.80	2.29	1.97	1.21
Gd	19.5	10.4	8.52	29.3	10.1	8.59
Tb	3.3	—	—	—	—	—
Dy	21.9	12.2	9.40	33.4	9.7	10.5
Er	13.6	7.4	5.10	30.9	5.0	6.51
Yb	13.2	7.0	4.43	20.1	4.8	6.0
Lu	1.0	1.03	0.61	—	0.69	0.90
La/Yb	1.17	0.74	1.41	1.43	2.46	2.2
Eu/Eu*	0.33	0.50	0.74	0.27	0.68	0.49
Y	112	—	—	—	80	55
Sc	78	86	—	81	50	55

first components to enter the melt. Increasing the degree of partial melting dilutes the total lanthanide content through the addition of lanthanide-poor phases.

5.2. *The europium anomaly*

Although many geochemical and geophysical problems have been posed by the study of the lunar rocks, the europium anomaly exhibited by nearly all the lunar lanthanide patterns in mare basalts has probably produced the most controversy, conflicting explanations and interpretations of the geochemical, mineralogical and experimental petrological results.

Several hypotheses have been advanced to account for the depletion in europium observed in the mare basalts. These are discussed in order of increasing probability:

(a) The moon as a whole is depleted in Eu (Nguyen Long Den and Yokoyama 1970). Was Eu lost selectively from the moon, at or before accretion, as was H_2O and the most volatile elements such as Pb, Bi and Tl? Among the lanthanides, Yb is of comparable volatility to Eu but there is no sign of Yb depletion relative to neighbouring Tm and Lu in any of the lunar lanthanide patterns. Accordingly, we may conclude that the lanthanide patterns for the whole moon are not seriously divergent from those in chondritic meteorites.

(b) Eu was volatilised from lava lakes during the filling of the mare basins (O'Hara and Biggar 1970). The objections noted above about the equally volatile nature of Eu and Yb are valid, no relative depletion of the latter element being noted. There is no evidence that more volatile elements (e.g. Rb, from Rb–Sr isotopic systematics) are depleted by such mechanisms. Lava lakes of course freeze over very rapidly, even on the earth, and a very thin chilled crust (of millimeter thickness) is sufficient to prevent volatile loss.

(c) Plagioclase feldspar, incorporating Eu, is removed by near-surface fractionation from the crystallising melt (Gast 1970, Gast and Hubbard 1970). Eu is concentrated in plagioclase feldspar in the main lunar rock-forming minerals and depleted in pyroxenes and ilmenite. From these observations, many workers concluded that plagioclase separation had occurred, thus depleting the residual liquid in Eu. The total rock samples show Eu depletions by factors of 2–3 relative to neighbouring lanthanides (Sm–Gd). To account for this depletion by crystallisation and removal of plagioclase, 60–90% of plagioclase removal is necessary. However, most of the chemical and mineralogical data are consistent with rapid chilling and crystallization, without wholesale separation of plagioclase. The Apollo-12 basalts show some evidence of near-surface crystal fractionation, but this involved mainly removal of olivine, which has little effect either in Eu or the total lanthanide patterns except to selectively remove the heavy lanthanides (Gd–Lu). The evidence from experimental petrology indicated that plagioclase was not a liquidus phase (except in the relatively uncommon aluminous mare basalts) and so could not be responsible for depleting the total rock compositions in Eu. The textural evidence indicates that plagioclase is a late, rather than an early, phase to crystallise in mare basalts. The possibility of massive separation of plagioclase, just prior to or early in the course of eruption of the mare basalts, is remote and has not been widely accepted as an explanation of the Eu depletion.

(d) Eu is selectively retained in plagioclase in the lunar interior during the partial melting event which produced the mare basalts. The experimental evidence shows that plagioclase is not a stable phase at the depth of formation of the lavas (200–300 km) (Green 1972) thus ruling out this explanation.

(e) Eu is selectively retained in accessory minerals in the lunar interior during partial melting. This model proposes that the trivalent REE were mainly contained in accessory phases, such as the phosphate mineral whitlockite, in the lunar interior. During the partial melting process that produced the mare basalts, such accessory minerals preferentially enter the melt. Eu is then selectively retained in the lunar interior in major mineral phases, such as pyroxene (Graham and Ringwood 1972). However, most lunar pyroxenes are depleted rather than enriched in Eu, as demanded by the hypothesis. Several other objections to this model have been advanced (Schnetzler and Philpotts 1971). The abundance of phosphorus is only about 500–1000 ppm in mare basalts. If all this is partitioned into the melt, then, for 5 percent partial melting, the source region contains only 25–50 ppm P. This is too low a concentration to allow a phosphate mineral to exist as a separate phase. Well-developed correlations are noted between, for example, Ba and the trivalent REE. Ba does not enter phosphate lattice sites, so that the correlation becomes fortuitous leading Schnetzler and Philpotts (1971) to reject the phosphate fusion model. Modifications to this model were proposed which involved the distribution of the REE among refactory phases, resulting from condensation in the solar nebula. Thus the trivalent REE would enter minerals such as perovskite, while Eu enters melilite. Although these proposals avoided the difficulties with pyroxene it is difficult to see how these phases might survive the well-documented melting of most of the moon following accretion.

(f) Eu was concentrated in the highlands and depleted in the mare basalt source regions by early melting and differentiation. Many of the difficulties associated with single-stage models for the Eu anomaly disappear when multistage explanations are considered. Thus, the debate whether or not plagioclase is a liquidus phase becomes irrelevant for the europium problem if Eu has already been mostly removed from the source regions of mare lavas. The question of single-stage versus multistage origins for the Eu anomaly has wider implications. Single-stage models derive the mare basalts from the pristine lunar mantle, whereas multistage models derive them from already melted and fractionated (i.e. no longer primitive) material. In this context, even the most primitive mare basalts such as the Apollo-15 green glass (15426) bear an unmistakable signature of depletion in Eu (fig. 8), so that they come not from primitive, but from fractionated sources which have undergone prior removal of plagioclase. Before considering the further implications of this model, it is necessary to enquire into the distribution of the lanthanides in the lunar highlands.

5.3. *The lunar highlands*

These comprise the white areas of the moon as seen from the earth. They form a chemically distinct crust on the moon, varying in thickness from 60 km on the near-side, to over 100 km on the far-side. They are heavily cratered, their mineralogy is

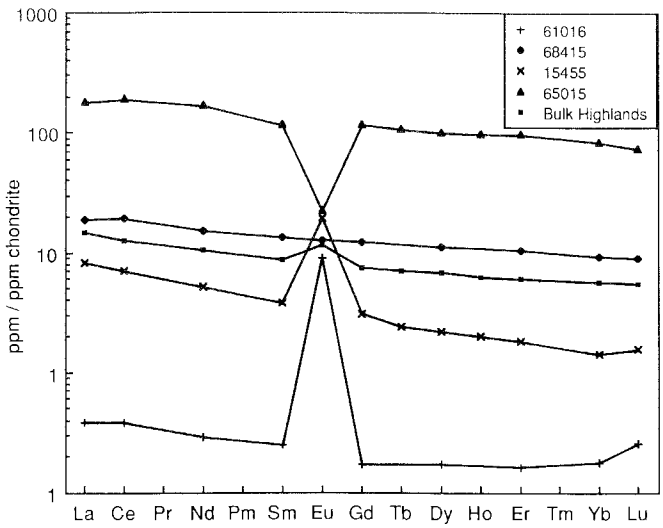

Fig. 10. The wide variety of lanthanide abundance patterns observed in lunar highlands samples ranging from extreme enrichment in Eu in feldspathic rocks (anorthosites, 61016, 15455) to massive depletion of Eu in KREEP (65015), which represents the final residual liquid from the crystallisation of the magma ocean. Sample 68415 is a granulitic breccia close in composition to that of the average highland crust. (Data are from table 12).

dominated by Ca-rich plagioclase feldspar (typically An_{95-97}) and they formed shortly after accretion of the moon, at about 4.4 Ae. The lanthanide abundance patterns for the feldspar or anorthosite component is shown in fig. 10. The striking features are the rather low abundance of the elements, but with a massive enrichment in Eu. Data are given in table 12. Such patterns are typical of Ca feldspars which Eu^{2+} preferentially enters as a trace constituent, along with Sr^{2+}, in the Ca^{2+} lattice site. The other lanthanide elements, present as trivalent ions, have much greater difficulty in entering the Ca sites. The larger cations (La–Sm) are accommodated rather more readily than the smaller (Gd–Lu), a simple consequence of their more appropriate ionic size for the available lattice sites.

The lunar highlands are not, of course, comprised of pure Ca feldspar. The bulk composition of the highlands and the lanthanide abundances of the various components are given in table 12. Three major components may be distinguished. These are the anorthosites, the Mg-rich suite, and the component labelled as KREEP, or Fra Mauro basalt. All these components have distinctive lanthanide patterns. A compilation of the patterns for the various components making up the highland crust is shown in fig. 10. The most interesting feature which emerges is that despite great variations in abundance of the lanthanides, the patterns, except for the Eu anomalies, remain relatively parallel. This suggests that the crust is dominated by only a few components, that the various patterns are mainly a result of mixing, and that intra-crustal melting, which would perturb these patterns, must be minimal.

TABLE 12
Rare earth element abundances [in ppm (wt)] in lunar highland rocks. (Adapted from Taylor 1982.)

Element	Anorthosites		Gabbroic anorthosite	Anorthositic gabbros		Norite	KREEP		Bulk highlands composition
	15415	61016	68415	15455	60335	78235	14310	65015	
La	0.12	0.14	6.8	3.0	20.0	—	56	66	5.3
Ce	0.33	0.37	18.3	6.7	52	9.2	144	185	12
Nd	0.18	0.21	10.9	3.73	32	5.4	87	120	7.4
Sm	0.046	0.058	3.09	0.88	9.1	1.49	24	27	2.0
Eu	0.81	0.77	1.11	1.67	1.28	1.03	2.15	1.97	1.0
Gd	0.05	0.054	3.78	0.95	10.6	—	28	36	2.3
Tb	—	—	—	0.14	1.9	—	5.1	6.3	0.41
Dy	0.044	0.065	4.18	0.84	11.5	2.26	33	38	2.6
Ho	—	—	—	0.17	2.5	—	6.5	8.3	0.53
Er	0.019	0.040	2.57	0.46	6.77	1.47	20	24	1.51
Yb	—	0.045	2.29	0.36	6.23	1.64	18	21	1.4
Lu	—	0.01	0.34	0.06	0.68	0.24	2.5	2.8	0.21
La/Yb	3.4	3.1	3.0	3.0	3.2	—	3.1	3.1	3.8
Eu/Eu*	51.6	45.2	0.99	5.58	0.40	1.97	0.25	0.19	1.4
Y	—	—	22	4.8	57	—	175	174	13.4
Sc	—	0.5	8.2	—	8.5	4.6	20	17	10

5.4. *Evolution of the moon: the rare earth element contribution*

The evidence discussed above has been a major contributor to our understanding of lunar evolution (e.g. Taylor 1982). During accretion of the moon at least the outer half, or perhaps all, became molten. Whether this was due to rapid accretion, or whether it was an intrinsic feature of lunar formation remains uncertain. However, the current hypothesis which best explains lunar origin (a giant impact with the earth of a Mars-sized body, with most of the protolunar material being derived from the impacting body in a high-temperature state) calls for a largely molten moon initially. The bone-dry composition of the moon (no water has been identified even at ppb levels) is a consequence of its high-temperature origin. The moon is also strongly depleted in volatile elements such as Bi, Tl, K, etc. This is well shown on a K/La diagram (see fig. 11), which illustrates the strong depletion of volatile K relative to refractory La. As the moon cools and crystallises, olivine and orthopyroxene crystals sink, slightly depleting the residual liquid in heavy lanthanides (Gd–Lu). As plagioclase feldspar crystallises, two things happen. The melt is depleted in Eu and the plagioclase crystals rise to the surface of the moon. This occurs because plagioclase is slightly less dense than the anhydrous melt (the mineral sinks in silicate melts with more than 0.1% H_2O; for this reason a feldspar-rich crust would not form on an initially molten earth).

The end result is the formation of a thick plagioclase-rich crust, floating over the magma ocean. As crystallisation of the interior proceeds, a zoned series of minerals

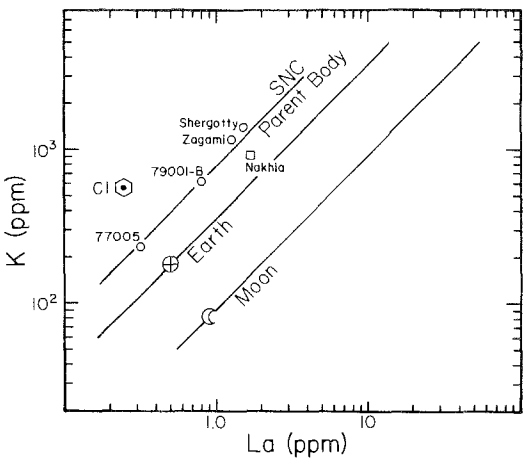

Fig. 11. Fractionation between the refractory lanthanide element La and the volatile element K, for CI meteorites, the earth, the moon and the SNC meteorites (probably derived from Mars). Note that Mars has a higher volatile element content than the earth. Both K and La are incompatible elements in igneous fractionation processes and so tend to preserve bulk planetary ratios. (From Taylor 1987a,b.)

develop, crystallising from a melt which has been strongly depleted in Eu. The major phases are olivine and pyroxenes, which form the lunar mantle at depths of 100–400 km. It is from these regions that the basaltic lavas were derived later by partial melting.

When crystallisation is about 98% complete, the final residual melt is strongly enriched in those trace elements which have difficulty in entering the major mineral phases. These elements include Y and the lanthanides. Sc, in contrast, was incorporated into early crystallising pyroxenes. The final 2% or so residual fluid from the magma ocean crystallisation percolated upward into the plagioclase-rich highland crust, with which it was intimately mixed by a continuing massive meteoritic bombardment. This component is generally referred to as KREEP, an acronym from the elements typically concentrated in it. It is characterised by extremely high abundances of the lanthanides, except for a massive depletion in Eu (fig. 10), which was removed from the melt by the previous crystallisation of the plagioclase feldspar, now residing in the lunar highlands. The degree of concentration of the lanthanides by large-scale fractional crystallisation processes is illustrated by the La content of 700 times chondritic in lunar sample 15405, 85, which accordingly has been termed 'super-KREEP'. Final crystallisation of this KREEP liquid occurred at about 4.35 Ae. This model accounts satisfactorily for many features of the lanthanide distribution in the moon. The most important observation is of the complementary nature of the lanthanide patterns in the highland crust and in the mare basalts (section 4.1), which provides the basic information that the moon melted and differentiated on a lunar-wide scale (fig. 12). This model has been buttressed by information from the Sm–Nd isotopic systematics. KREEP samples from widely separated regions of the moon have very uniform Sm–Nd isotopic ratios, consistent with derivation from a single, uniform source. The mare basalts, which were erupted typically several hundred million years after the final solidification of the magma ocean, have a multistage isotopic history with the source regions crystallising by about 4.4 Ae. In addition to the Eu depletion, two other features of the mare basalt

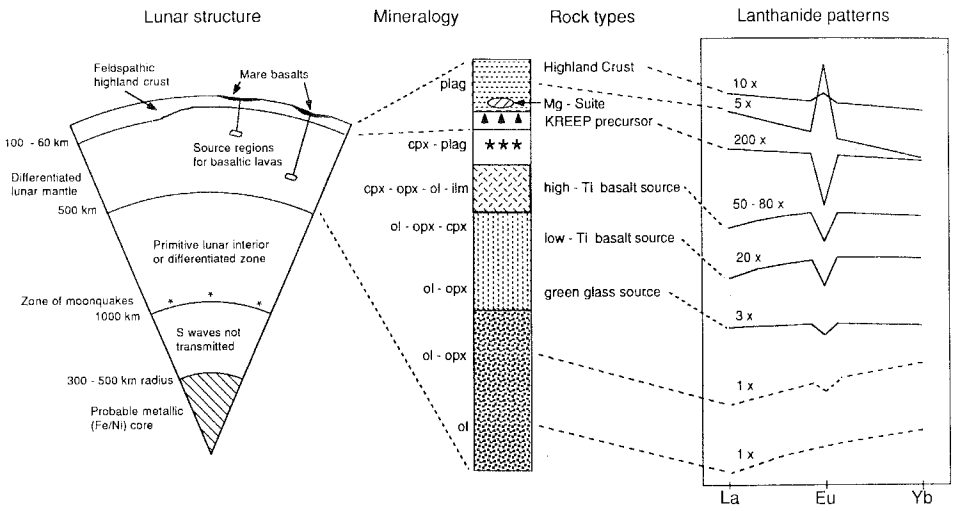

Fig. 12. Simplified internal structure of the moon, showing the mineralogically zoned source regions from which the mare basalts were derived, the feldspar-rich crust, and KREEP. Lanthanide abundance patterns for these various regions are depicted on the right with the approximate concentrations relative to average chondrites indicated. The lunar interior is undoubtedly more complex both vertically and laterally than depicted.

lanthanide abundance patterns are explicable from the magma ocean model. The general depletion of the light lanthanides (La–Nd) is due to their prior extraction into the highland crust. The tendency for the heavy lanthanides (Gd–Lu) to be depleted in the mare basalts, and also in the highland samples (figs. 8–10) is due to an initial removal of these elements in early crystallising olivine and orthopyroxene phases (now buried deep within the moon), which preferentially accommodate these elements relative to the lighter La–Nd.

The evolution of the moon, as outlined here, remains as an outstanding example of the value of the rare earth elements, and the lanthanides in particular, in resolving such questions.

5.5. *The origin of the moon*

The moon is a very unusual object in the solar system:

(a) The orbit of the moon about the earth is neither in the equatorial plane of the earth, nor in the plane of the ecliptic, but is inclined at 5.1° to the latter.

(b) Relative to the earth, the moon has the largest mass of any satellite–planet system (1/81.3), except for the Pluto–Charon pair.

(c) The earth–moon system is unmatched among the inner or terrestrial planets. Neither Venus, close in size to the earth, nor Mercury have moons, while Phobos and Deimos, the two moons of Mars, are probably tiny captured asteroids, with primitive compositions.

(d) The angular momentum of the earth–moon system is anomalously high compared to that of Venus, Mercury or Mars.

(e) The moon has an unusual composition. It is bone-dry, depleted in elements (e.g. Tl, Bi, K) which are volatile below about 1000 K, is enriched in refractory elements such as the rare earths, Al and U, and has a low density attributable to a low bulk iron content, relative to the terrestrial planets. The lanthanide content of the whole moon is assumed to be parallel to those in the CI meteorites. Based partly on the strong concentration of the lanthanides in the highland crust, but depending mainly on assessments of the abundances of the other refractory elements such as Al and U, the overall abundance of the rare earths in the bulk moon is about 2.5 times the CI levels. The moon is thus a very fractionated object in comparison with our understanding of the composition of the primordial solar nebula.

Thus, in several respects, the moon and the earth–moon system appear to be unique among the inner or terrestrial planets, while the moon appears to have a distinct composition among either planets or satellites in the solar system.

The rare earth elements contribute some constraints to the problem of the origin of the moon. Thus, although the material now in the moon has been subjected to high temperatures, causing massive loss of volatile elements as shown by low K/La ratios (fig. 11), the presence of normal abundances of the more volatile lanthanides, Eu and Yb, in bulk moon compositions places upper limits on the temperatures involved. This means that those elements which condense above about 1100 K have been retained in their CI proportions. As noted earlier, the refractory elements in general are enriched in the moon. Although many hypotheses have been advanced, the only current explanation which satisfies the presently available constraints including the criteria listed above is that a massive (0.1–0.2 earth-mass: i.e. Mars-sized or larger) object struct the earth, about 4.4–4.5 Ae ago. The mantle of this impacting body was partly vaporised and spun out to condense and form the moon (Hartmann et al. 1986, Taylor 1987a,b).

6. Planetary compositions

In this section, we discuss the question of the bulk planetary abundances of the rare earth elements. Central to the problem of planetary abundance determinations is the assumption that the composition of the original solar nebula, for the non-gaseous elements, is given by the composition of the CI meteorites. It is accordingly of interest to see what evidence is available from the planets, and how it relates to the primordial nebula values. In the previous section, we have seen that although the moon is enriched in the lanthanides relative to those in the primordial solar nebula by about 2.5 times, the pattern is probably parallel to that of CI. The evidence for an apparent depletion in the heavy lanthanides is readily explicable as a consequence of early lunar magma ocean crystallisation of phases such as olivine and orthopyroxene, which selectively accept Gd–Lu.

The rare earth elements are refractory elements, sharing this property with Al, Ti, U, Sr, Zr, Hf, Ba and others. These elements form a coherent group not readily

fractionated from one another in the solar nebula, except by extreme cosmochemical processes such as those responsible for the formation of the exotic lanthanide patterns of the Allende meteorite CAI inclusions. Accordingly, if data for one element of the group are available, estimates of the others may be obtained by assuming that they are present in CI ratios. This procedure is perhaps responsible for the comment that geochemists can produce abundance estimates for the whole periodic table on the basis of one measurement.

6.1. *Rare earth element abundances in the bulk earth*

The overall abundance of the rare earths in the earth is an important parameter both in geochemistry and cosmochemistry. Various estimates, based on the abundances in xenoliths, comprising direct samples of the upper mantle coupled with information from basaltic lavas derived as partial melts from the same source, indicate abundance levels about 1–2 times CI chondritic abundances. There is no good evidence that the bulk earth pattern is other than parallel to the CI abundances. No evidence exists, for example, of Eu or Yb anomalies suggesting any depletion of these relatively volatile elements (although more volatile elements such as K, Rb, Bi, Tl, etc., are depleted in the earth relative to CI abundances). Table 13 lists an estimate of values for the rare earths in the primitive (i.e. existing just after the accretion of the earth and separation of mantle and core) mantle (Taylor and McLennan 1985, table 11.3). Present-day upper mantle abundances are of course depleted in those elements which have been concentrated in the continental crust (this is shown by the depletion of light lanthanides in the voluminous lavas erupted at mid-ocean ridges). Although the crust comprises only about 0.5% of the volume of the earth, it contains about 16% of the La content of the bulk earth. In contrast only 3.4% of the Yb is so concentrated. Being smaller, it is more compatible with the major element lattice sites in mantle minerals (see, e.g., fig. 1).

Accordingly, it is difficult to find undepleted or primitive mantle samples, in regions from which accessible material is available. This remains as a principal

TABLE 13
REE content [in ppm (wt)] in the earth's primitive mantle (present-day mantle plus crust).

La	0.551	Tm	0.054
Ce	1.436	Yb	0.372
Pr	0.206	Lu	0.057
Nd	1.067		
Sm	0.347	Total	5.84
Eu	0.131	La/Yb	1.48
Gd	0.459	La_N/Yb_N	1.00
Tb	0.087	Eu/Eu*	1.00
Dy	0.572	Y	3.4
Ho	0.128	Sc	13
Er	0.374		

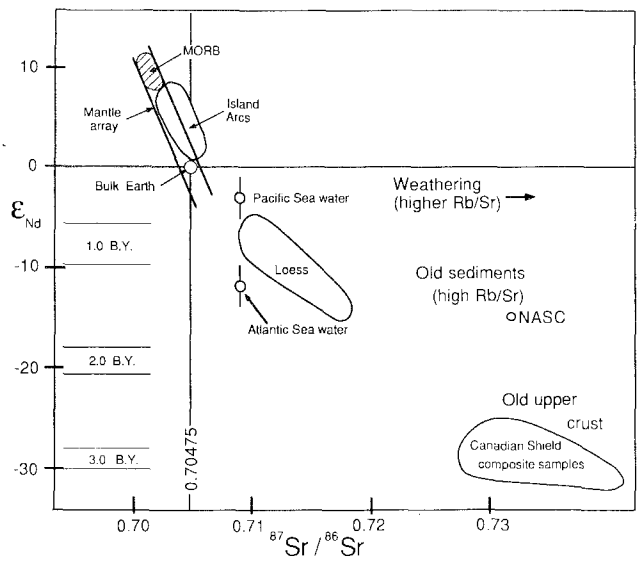

Fig. 13. The relationship between Nd and Sr isotopic systematics for terrestrial samples. Nd-model ages are indicated on the left. The mantle array is a field defined by mantle-derived igneous rocks, mainly mid-ocean ridge basalts (MORB) and ocean island basalts (OIB). Many island-arc volcanic rocks are found in a field with slightly elevated Sr and possibly slightly lower Nd isotopic composition, relative to the mantle array. This, along with other isotopic and geochemical evidence, has been used to suggest a small (<1–2%) sediment component in the source. Rocks from the upper continental crust tend to have very low Nd and high Sr isotopic composition, a reflection of their long residence in a low Sm/Nd and high Rb/Sr reservoir. Loess samples tend to fall on the mantle–crust trend, whereas typical sedimentary rocks (such as the North American Shale Composite, NASC) generally have much higher Sr isotopic composition, a reflection of the unweathered character of the loess source (Taylor et al. 1983). The very short residence time of Nd in seawater (see section 8) allows for significant differences in Nd isotopic composition in different ocean masses, making this a potential tool for research in paleo-oceanography. This contrasts with the case of Sr which has a relatively long residence time, resulting in uniform Sr isotopic composition among the ocean masses.

difficulty in all attempts to establish bulk mantle compositions, or to decide on the present-day distribution of various mantle reservoirs. Although the mantle is heterogeneous, maintaining distinct reservoirs over periods of 1–2 Ae, unambiguous evidence concerning the location and extent of such reservoirs, and whether the mantle is zoned either horizontally or vertically, continues to elude geochemists.

Sm–Nd isotopic systematics are compatible with CI chondritic meteorite ratios for the bulk earth. Use of this assumption is a valuable asset in establishing other geochemical abundances. Since both Sm and Nd are relatively refractory, it is a reasonable assumption to take their bulk earth ratios as chondritic. When Nd isotopic ratios are plotted against Sr isotopic ratios (fig. 13), the points from mantle derived samples fall along a narrow zone, the so-called mantle array. The intersection of this zone with the Sm/Nd chondritic ratio provides an estimate of the bulk terrestrial Rb/Sr ratio (=0.03). Since Sr is refractory, the Sr/lanthanide ratios

may be assumed to be the same as in CI chondritic meteorites. This leads to the conclusion that Rb is depleted in the bulk earth, similar to the depletion of K inferred from K/La or K/U ratios. In such a manner, a self-consistent abundance table can be constructed for many elements. It is notable that the CI chondritic Rb/Sr ratio is 0.29, about one order of magnitude higher than the bulk terrestrial ratio, indicating the extent of the depletion of volatile elements in the bulk earth. Since such elements cannot be lost from a planet of earth-size because of gravitational attraction, this depletion must have been a property of the accreting planetesimals.

6.2. *Lanthanide abundances in Mars and Venus*

The data base for Mars consists of the Viking Lander major element data, and that for the SNC meteorites (McSween 1985), which are interpreted as basic igneous rocks from, or near to, the planetary surface from which they were excavated and accelerated to escape velocities by meteorite impact. Information on the radiogenic elements K and U are commonly available from gamma-ray measurements. Since U is refractory, it serves as an analogue for the rare earths, so that, for example, K/U ratios provide the same information as K/La ratios. The SNC meteorites have K/U ratios somewhat higher than terrestrial values, but much lower than CI values (fig. 14). A crucial point is that since these elements are not readily separated from one another in intra-planetary processes, they tend to retain their bulk planetary values. They show that Mars is depleted in volatile elements relative to primitive nebula values although not to the same extent as is the earth. If we assume that the lanthanides have not undergone any internal fractionation, so that the Sm/Nd ratio is 'chondritic', we can then estimate the Rb/Sr ratio of Mars, assuming that the Sm–Nd and Rb–Sr isotopic systems have the same relationship as on the earth (Jagoutz 1987). This is shown in fig. 15, which indicates that the mantle $^{87}Sr/^{86}Sr$ ratio on Mars (0.721) is higher than on the earth (0.704). This indicates that a higher proportion of radiogenic Rb is present, and that the Rb/Sr ratio is about 0.11,

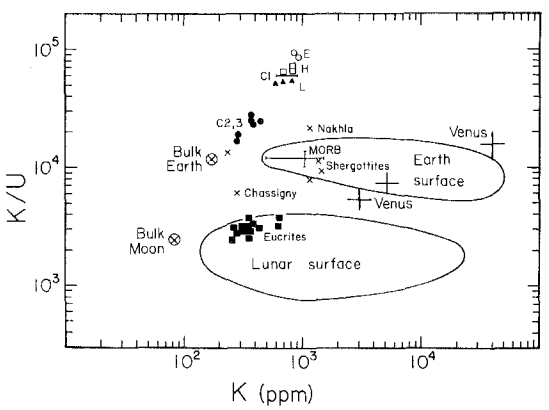

Fig. 14. Uranium is refractory like the rare earths, so that K/U ratios are an analogue for K/La ratios (fig. 11). K and U data are available for a wide variety of solar system material, since both elements are readily determined by gamma-ray spectroscopy. Both are incompatible in igneous processes and so tend to preserve their bulk planetary ratios during differentiation. This diagram illustrates that substantial volatile element depletion was widespread in the inner solar nebula, so that similar variations to K/U in volatile element/rare earth ratios are to be expected. (From Taylor 1987a.)

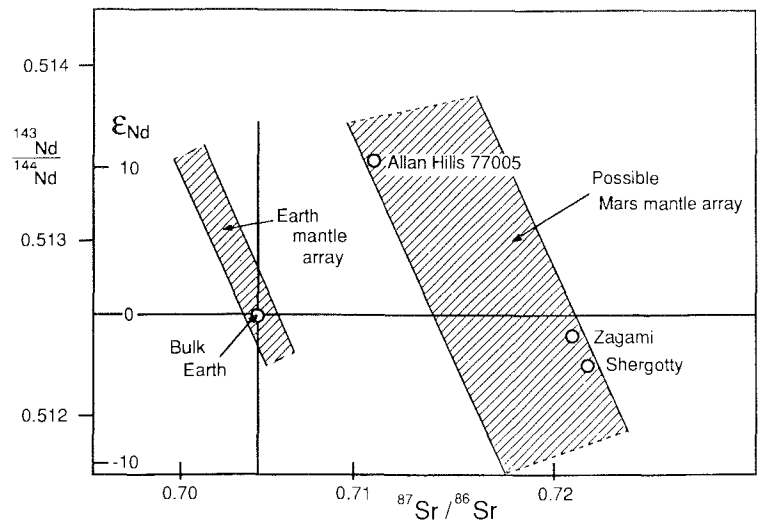

Fig. 15. Nd–Sr isotope diagram showing the position of the SNC meteorite data relative to mantle derived samples for the earth. If the SNC meteorites come from Mars, then that planet has a higher content of the volatile element Rb relative to refractory Sr than the earth, by a factor of about two. Similar conclusions may be drawn from the K/La (fig. 11) and K/U (fig. 14) diagrams.

compared to 0.03 for the earth and to 0.30 for the primitive nebula. Sr is a refractory element like the rare earths, whose absolute abundance level on Mars is likely to be in the range 1–2 times chondritic.

The surface of Venus has K/U ratios of the same order as those of terrestrial surface rocks (Surkov 1981), so that it also is depleted in volatile elements relative to primitive nebula values. This relative depletion of the more volatile elements thus appears to have been a widespread feature of the inner solar nebula rather than being a feature unique to the earth. Accordingly, a widespread loss of volatile elements occurred in the inner solar system prior to the accretion of the terrestrial planets (Taylor 1987a). No information is yet available for the rare earth elements on Venus, but on the basis of the discussion above, they are probably similar to the terrestrial abundance levels.

Data for other planets and satellies are not yet available. It is expected that the Martian satellite, Phobos, due to be visited in 1988 by USSR spacecraft, will have a primitive CI type composition.

7. Terrestrial igneous and metamorphic geochemistry

A vast body of literature now exists on the use of the rare earth elements (principally the lanthanides) in terrestrial ingenous geochemistry. Much of this is summarised in work by Haskin (1979), Haskin and Paster (1979), Hanson (1980), Moller and Muecke (1984) and by Henderson (1984). Frey (1979) has reviewed all of

the important literature up till 1978. Exhaustive accounts of the use of distribution coefficients abound in the petrological literature, and there are extensive discussions of modelling of source regions, parent magmas and igneous fractionation in almost all papers dealing with the lanthanides in igneous rocks (e.g. Arth and Hanson 1975, Langmuir et al. 1977, Nicholls et al. 1980, Cameron and Hanson 1982, Gromet and Silver 1987). A principal reason for their usefulness in this context is their relative insensitivity to alteration by secondary processes. In this review, we concentrate on examples where the distribution of the lanthanide elements has increased our fundamental understanding of geological processes, or placed new constraints on general models.

7.1. *The question of lanthanide mobility*

Our understanding of the origin and evolution of igneous rocks has made much progress through quantitative studies of trace element partitioning in crystal–liquid equilibria. Although particular attention has been paid to the lanthanide elements, they are not in principle the most sensitive index elements for such processes. For example, the alkali elements K, Rb, and Cs are very sensitive indicators of igneous fractionation processes. A major reason for the use of and interest in the lanthanides is the general perception that these elements are particularly immobile during secondary alteration and metamorphism of igneous rocks, so that they preserve the evidence of their genesis. Under similar conditions, many elements, notably the alkali and alkaline earth elements, can be readily mobilised, so that their distribution no longer records the early history of the rock. Accordingly, the question of their relative mobility is central to the use of the lanthanide elements in igneous geochemistry.

There is a substantial, and for the most part, confused literature on this crucial topic. Much of the confusion appears to stem from the following causes:

(a) a lack of detailed knowledge, or appreciation of the mineralogical controls on lanthanide mobility;

(b) a lack of understanding of the significance of glass phases, and

(c) a dearth of relevant experimental studies. A good introduction may be found in the work by Humphris (1984).

Lanthanide element mobility appears to be most closely associated with hydrothermal processes. The most critical factors are high fluid/rock ratios, sufficient duration of metamorphism and appropriate metamorphic grade. Hydrothermal alteration in igneous rock systems is most common in submarine volcanic rocks because of the readily available heat sources, the presence of easily altered glass phases and fine-grained mineral phases, and the ubiquitous presence of water. For these reasons, investigations of lanthanide mobility in geological environments have concentrated on such rocks, although studies have also been carried out in continental areas where appropriate conditions have existed (e.g. Martin et al. 1978, Alderton et al. 1980).

Lanthanide mobility has been suggested to occur during the low-temperature metamorphic conditions such as spilitization and submarine weathering of basalts

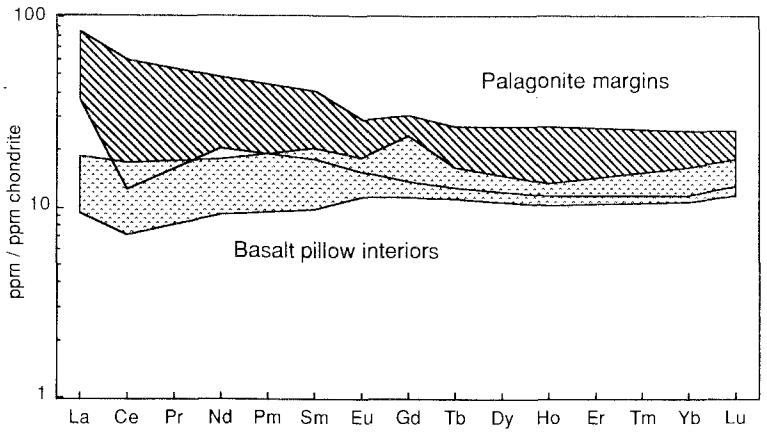

Fig. 16. Fields of lanthanide element patterns for co-existing unaltered basalt pillow interiors and altered palagonite margins from the Atlantic ridge (data are from Ludden and Thompson 1979). The enrichment of light lanthanides in the altered margins has been used as evidence for lanthanide mobility under hydrothermal conditions.

(Hellman and Henderson 1977, Floyd 1977), palagonitization of basalt glass (see fig. 16) (Frey et al. 1974, Ludden and Thompson 1978, 1979, Staudigel et al. 1979, Staudigel and Hart 1983) and zeolitization (Menzies et al. 1977, Humphris et al. 1978). Mobility has also been suggested to occur in low-grade metamorphic conditions in the zeolite facies (Wood et al. 1976). In these studies it was generally argued that the lanthanides moved as a group, but were not internally fractionated from one another (e.g. Staudigel et al. 1979, Staudigel and Hart 1983), or that the light lanthanides (La–Sm) were preferentially mobilised, resulting in their enrichment or depletion relative to the heavy lanthanides (Gd–Lu) (e.g. Ludden and Thompson 1978, 1979). Where no fractionation effects were evident, the cause is usually attributed to low fluid/rock ratios or to short duration of the metamorphic conditions (e.g. Menzies et al. 1977; see also Humphris 1984).

Most of the experimental work on hydrothermal alteration of rocks has been carried out at somewhat higher temperatures, corresponding to the greenschist metamorphic facies, mainly for kinetic reasons. Thus, Menzies et al. (1979) investigated the problem at temperatures of 150–300°C, 500 bar pressure, and with water/rock ratios ranging from 10–125, while Hajash (1984) worked in the range 500–600°C, at 800–1000 bar, with water/rock ratios in the range 1–3. No evidence of any mobility of the lanthanides was found in these studies even when the basaltic rock was totally altered to clay minerals (fig. 17). This behaviour is also found in natural rock systems altered under analogous conditions. One explanation is that chlorite, forming under these metamorphic conditions, incorporates any lanthanides released from other mineral phases, thus ensuring their immobility in the bulk rock (Humphris 1984).

How do these results affect the use of lanthanide elements as tracers of igneous processes? Hydrothermal alteration is associated with obvious mineralogical

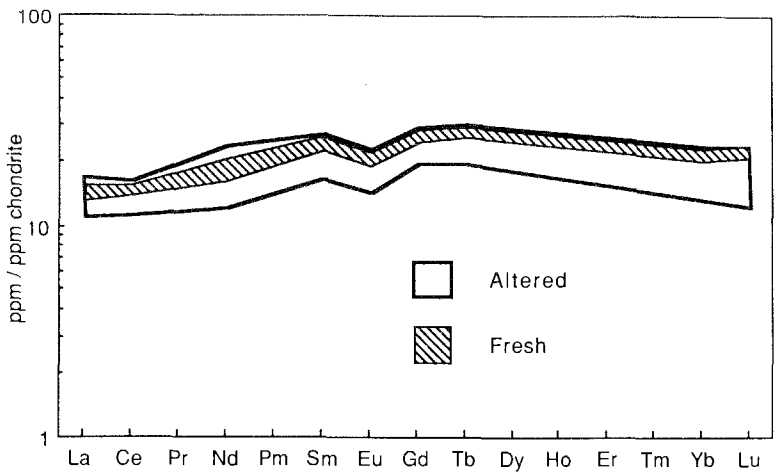

Fig. 17. Fields of lanthanide element patterns for basalt altered under experimental conditions (150–300°C, 500 bar) and the unaltered precursor (data are from Menzies et al. 1979). There is no evidence for mobility at such metamorphic conditions which probably correspond to greenschist facies (chlorite grade).

changes (e.g. palagonitization, zeolitization) and it is easy to avoid such material in young rocks. In older rocks, subsequent higher grades of metamorphism may obscure the effects of low-temperature alteration, and a detailed examination for chemical or mineralogical evidence of such processes should be carried out.

Notwithstanding the discussion above, it should be emphasised that the lanthanides are among the least mobile of elements under geological conditions, and remain as the single, most useful group of elements for the quantitative modelling of igneous processes.

7.2. *Regional metamorphism*

Although metamorphism associated with very abundant volatile contents and high fluid/rock ratios may produce some REE mobility, the lanthanides are relatively immobile during most regional metamorphic processes up to at least amphibolite grade (see review by Muecke et al. 1979). Studies of the distribution of the lanthanides in metamorphic rocks have failed to reveal changes in the patterns attributable to metamorphism, except under the special conditions of very high fluid (water or CO_2) conditions (e.g. Frey 1969, Green et al. 1969, 1972, Cullers et al. 1974, Wendlandt and Harrison 1979, Dostal and Strong 1983). Even under granulite facies conditions the lanthanides are immobile (Green et al. 1972, Hamilton et al. 1979, Weaver 1980), except where partial melting occurs. The lanthanides thus generally retain the pattern of the parent rock, making them particularly useful geochemical indicators. For example, in a study of meta-sediments in Archean high-grade terrains, Taylor et al. (1986) were able to establish that some sediments

TABLE 14
REE content [in ppm (wt)] of high-grade metasedimentary rocks[a] from the Archean Limpopo Belt and Kapuskasing Structural Province. (From Taylor et al. 1986.)

Element	Limpopo		Kapuskasing	
	LP-4	LP-20	KSZ 12	KSZ 13
La	34.6	24.6	59.1	19.1
Ce	65.0	50.6	113	40.0
Pr	6.85	4.92	11.6	4.37
Nd	26.3	20.5	40.8	17.2
Sm	5.99	3.99	6.20	2.76
Eu	1.23	1.07	1.39	1.07
Gd	5.51	3.15	3.38	1.68
Tb	0.92	0.42	0.50	0.29
Dy	5.73	2.32	2.68	1.72
Ho	1.14	0.42	0.48	0.35
Er	3.38	1.21	1.33	0.92
Yb	3.01	1.26	1.28	0.89
Total	160	115	242	91
La/Yb	11.5	19.5	46.2	20.8
La_N/Yb_N	7.77	13.2	31.2	14.0
Eu/Eu*	0.65	0.95	0.93	1.52
Y	29	15.7	9.4	12.2
Sc	32	12	—	—

[a]Description:
LP-4: quartz–garnet–cordierite–biotite–sillimanite metasedimentary gneiss; $K_2O/Na_2O = 4.9$.
LP-20: quartz–plagioclase–biotite–garnet metasedimentary gneiss; $K_2O/Na_2O = 0.99$.
KSZ 12, KSZ 13: quartz–plagioclase–biotite melted paragneiss from same outcrop representing partial melt and restite, respectively.

represented metamorphosed greenstone belts, while others were derived from small cratonic areas, forerunners of the present major continental crustal massifs (table 14) (see below, section 10.3) (fig. 18).

7.3. *Rock-forming minerals and distribution coefficients*

Data for typical lanthanide abundances in major rock-forming minerals are given in table 15 and fig. 19. Two of the most important aspects of the use of the lanthanides depends on the selective uptake of Eu by plagioclase, and of the heavy lanthanides (Gd–Lu) by garnet. Since any plagioclase fractionation will cause an Eu anomaly, this is a sensitive control of the primitive nature of the rock. Since garnet is stable only under high pressures, signatures of heavy lanthanide depletion provide evidence of depths of origin or segregation of igneous rocks.

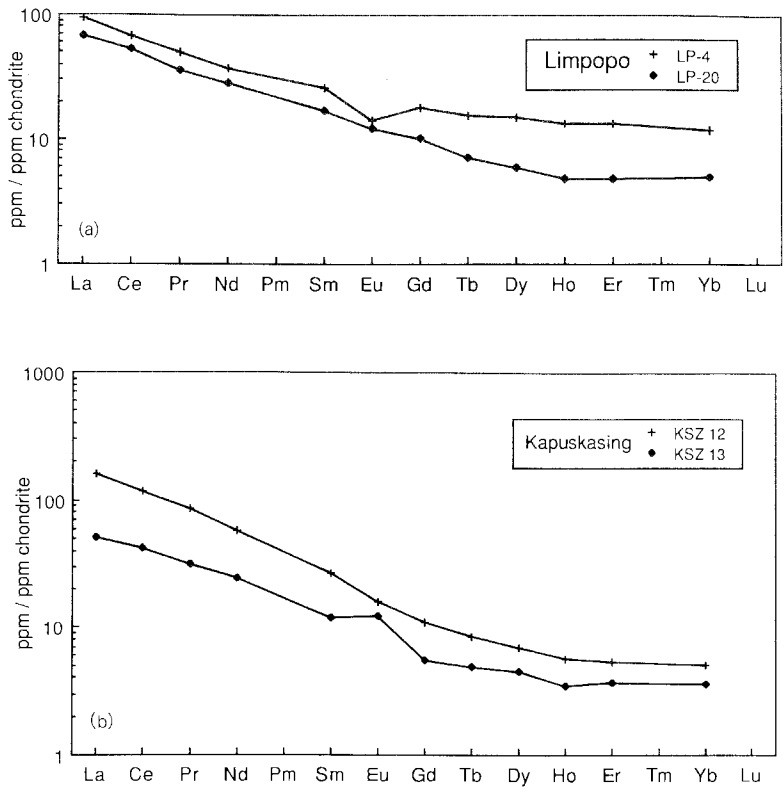

Fig. 18. Lanthanide element patterns for high-grade metasedimentary rocks. (a) The Limpopo samples from southern Africa preserve the lanthanide patterns of their sedimentary precursors. LP-20 represents a typical greenstone belt pattern, while LP-4 was derived from a source with a significant component of K-rich granite. (b) The Kapuskasing samples from Canada provide an example of partial melting, representing melt (KZ 12) and residue (KZ13), respectively. Eu has been selectively retained in the residue. (Data are from table 14.)

Following the development of more precise analytical methods for the lanthanides about 20 years ago, a quantitative approach to modelling trace element distribution during crystal-liquid equilibria was developed (see Haskin 1984 and DePaolo 1981b for relevant equations). The distribution coefficient, K_d, is a measure of the partitioning behaviour of an element between a crystal and a co-existing melt:

$$K_d = \frac{\text{concentration in mineral}}{\text{concentration in liquid}}.$$

Similarly, a bulk rock solid–liquid distribution coefficient, D, for the sum of all minerals in a rock may be defined as

$$D = \sum^{n} x_i \cdot K_{di} = \frac{\text{concentration in solid}}{\text{concentration in liquid}},$$

TABLE 15
REE contents [in ppm (wt)] of common rock-forming minerals.

Element	(1)	(2)	(3)	(4)	(5)	(6)	(7)	(8)	(9)
La	–	–	–	–	–	–	–	86.0	–
Ce	0.569	5.94	0.442	22.5	1.36	0.264	2.20	127.3	20.0
Nd	0.365	7.23	0.645	27.5	0.252	0.0796	1.03	–	15.0
Sm	0.090	3.3	0.347	8.67	0.0200	0.0112	0.221	20.9	15.1
Eu	0.024	0.554	0.064	1.375	0.155	0.0821	0.0377	1.14	1.42
Gd	0.084	–	–	9.74	–	–	0.213	–	53.6
Tb	–	–	–	–	–	–	–	2.73	–
Dy	0.079	6.75	1.35	8.29	0.00552	0.0060	0.170	–	122
Er	0.046	4.04	1.40	4.18	0.00308	0.0029	0.0913	–	77.9
Yb	–	–	2.10	3.18	0.00301	0.0033	0.0792	14.48	70.3
Lu	0.0094	–	0.414	–	–	–	–	2.12	10.1

(1) Olivine basalt (Schnetzler and Philpotts 1970).
(2) Clinopyroxene, andesite (Schnetzler and Philpotts 1970).
(3) Orthopyroxene, andesite (Schnetzler and Philpotts 1970).
(4) Hornblende, granodiorite (Gromet and Silver 1983).
(5) Plagioclase, granodiorite (Gromet and Silver 1983).
(6) Alkali feldspar, granodiorite (Gromet and Silver 1983).
(7) Biotite, granodiorite (Gromet and Silver 1983).
(8) Muscovite, granodiorite (Arniaud 1984).
(9) Garnet, dacite (Schnetzler and Philpotts 1970).

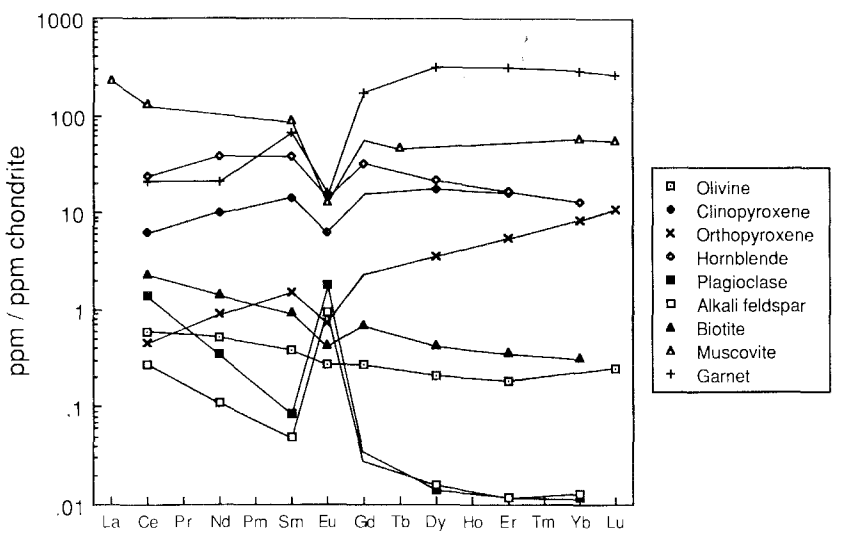

Fig. 19. Lanthanide patterns for common rock-forming minerals from igneous rocks. (Data are from table 15.)

where x is the mass fraction of mineral i. Yttrium and the lanthanides are representatives of the group of incompatible elements where $K_d < 1$ for most, but not all, mineral–melt equilibria, and thus they tend to be concentrated in the melt relative to the crystal phases. Scandium, on the other hand, readily enters such early crystallising phases as pyroxene, and so is depleted in the melt as crystallisation proceeds. The levels of incompatibility for the lanthanides vary greatly for different minerals and different melt compositions and this characteristic makes them a useful group of elements for quantitative modelling.

Two minerals illustrate this feature particularly well. Feldspars, notably Ca-rich plagioclase, among the common rock-forming minerals strongly concentrate Eu^{2+}, resulting in significant depletion of that element both in the liquid and in other minerals crystallising from it. Thus melting or crystallisation involving plagioclase as a separate phase commonly results in enrichment or depletion of Eu relative to the other lanthanides. Experimental studies indicate that plagioclase is a stable phase only at low pressures (< 10 kbar ≈ 40 km) within the earth (e.g. Wyllie 1977). The presence of Eu anomalies in bulk rock lanthanide patterns is thus usually indicative of intra-crustal processes. The presence of feldspar in itself is not sufficient to produce an Eu anomaly; separation of the mineral is required. Thus island-arc andesites typically have plagioclase as a major phenocryst phase, but only rarely do they show either depletion or enrichment of Eu unless physical separation of the mineral from the bulk rock had occurred.

Garnet has a unique lanthanide abundance pattern among the common rock-forming minerals, concentrating the heavy lanthanides (Gd–Lu). Melts which have been in equilibrium with this mineral thus possess complementary patterns steeply enriched in the light lanthanides (La–Sm), and depleted in the heavy lanthanides (Gd–Lu). These patterns usually indicate that they have been derived from the mantle, where eclogite is stable, rather than from the crust.

Quantitative modelling has been less successfully applied to rocks of more felsic composition, such as granodiorites, dacites, granites and rhyolites. This is principally due to the ubiquitous presence in these evolved rocks of minor mineral phases, such as sphene, allanite, apatite and zircon, whose lanthanide contents may account for a substantial fraction of the total rock budget. Thus Gromet and Silver (1983) found that sphene and allanite, in a granodiorite from the Peninsular Ranges, California, contained 80–95% of the lanthanide content of the total rock. Distribution coefficients are not well known for these phases and the abundances of these trace minerals are difficult to determine accurately.

Two features are worth commenting upon with regard to the use of distribution coefficients. The first is their strong dependence on bulk chemical composition. This is particularly well shown in figs. 20 and 21. Figure 20 shows a plot of the distribution coefficients for clinopyroxenes in various volcanic rocks ranging in composition from basalt to rhyolite. The K_d values for La change from basalt ($< 50\%$ SiO_2) to rhyolite ($> 74\%$ SiO_2) by a factor of nearly 300! The values for Eu change over this range by an order of magnitude, from those recording a very slight depletion to those recording a massive depletion relative to the other lanthanides. A similar situation is observed for the distribution coefficients for plagioclase (fig. 21),

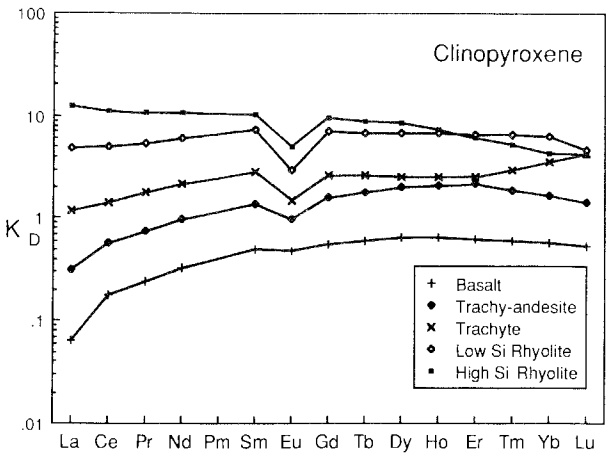

Fig. 20. Lanthanide mineral/melt distribution coefficient values for clinopyroxenes from volcanic rocks, showing the extreme dependence on the composition of the bulk rock. For example, the values for La extend over three orders of magnitude. (Data by courtesy of Dr. A. Ewart, University of Queensland, Australia.)

although in this case the variation is not so simply related to variation in silica content. Europium K_d values, in this case reflecting enrichment rather than depletion, change by a factor of 26 for the particular compositions considered! For both minerals, there are significant differences in K_d changes in major element chemistry. In addition to the changes due to bulk chemistry, further complexities are introduced by the varying effects of pressure, temperature, and H_2O activity as Irving (1978) has emphasised. Because of these many variables which may cause changes in K_d values of an order of magnitude, it seems essential that they should be determined for each specific modelling exercise. An excellent example of such an application is the study by Mahood and Hildreth (1983). Like many new applications in subjects dealing with complex natural phenomena, the introduction of

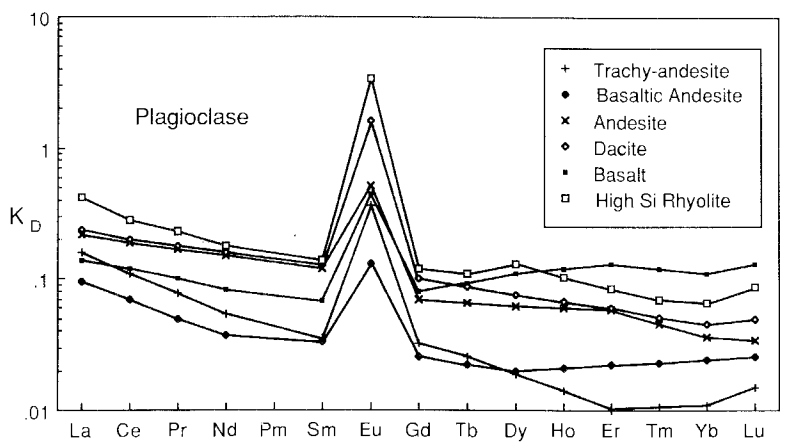

Fig. 21. Lanthanide mineral/melt distribution coefficient values for plagioclase from volcanic rocks, also showing wide variations related to the composition of the bulk rock. (Data by courtesy of Dr. A. Ewart, University of Queensland, Australia.)

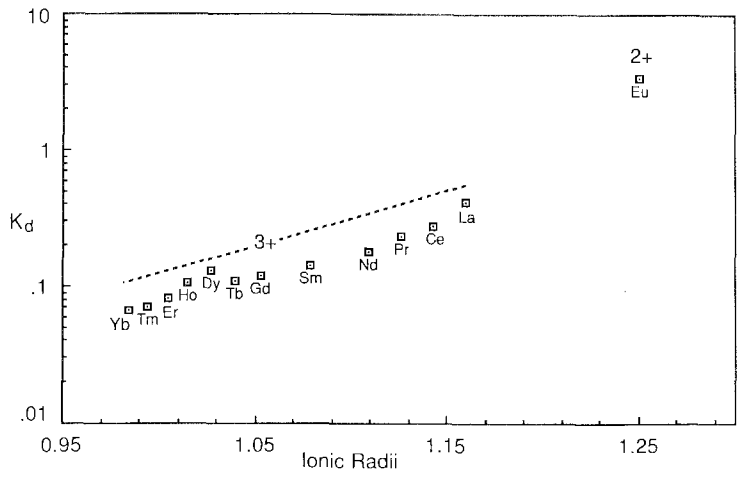

Fig. 22. The regular variation of mineral/melt distribution coefficients for plagioclase with ionic radius, showing the effect of lattice size and valency. Eu^{2+} enters the Ca^{2+} ($r = 1.12$ Å) site more readily than the trivalent lanthanides, the largest (La) of which have preference over the smaller (Yb).

distribution coefficients was regarded as a panacea with the potential of placing trace element geochemistry on a fully quantitative basis. The wide variety of temperature, pressure and compositional factors which cause variations in distribution coefficients of orders of magnitude have in practice restricted their application to specific modelling of individual rock suites.

The second point of interest is the relationship between ionic radius and distribution coefficients (Onuma et al. 1968, Jensen 1973, Philpotts 1978). This is demonstrated in fig. 22 for plagioclase which shows the regular variation in K_d with ionic radius, and the dramatic effect due to the presence of europium as the divalent ion.

7.4. *Igneous rocks*

The subtle variations in ionic radius among the trivalent lanthanides, coupled with the variable oxidation state of Eu have made these elements of unique interest to students of terrestrial igneous rocks. A wide variety of patterns, which are in general quite distinctive for differing rock types, are found. In all these cases, there is a clear separation between the geochemical behaviour of Sc, which typically enters early crystallising pyroxene phases, and that of yttrium and the lanthanides. The discussion in the rest of this section concentrates on the latter.

Very low lanthanide abundances are found in ultrabasic rocks of mantle origin (table 16) (see the extensive review by Frey 1984). Such rocks are particularly valuable because they represent relatively high degrees of partial melting and so provide good estimates of the lanthanide content of their mantle sources. The outstanding feature of this class is their remarkable heterogeneity, especially for the

TABLE 16
REE analyses [data in ppm (wt)] of ultramafic rocks, mid-ocean ridge basalts and oceanic intraplate basalts.

Element	(1)	(2)	(3)	(4)	(5)	(6)	(7)	(8)	(9)
La	0.04	0.045	0.18	0.51	2.32	1.47	8.75	38.0	11.0
Ce	–	0.27	0.69	1.70	5.80	5.22	23.0	85	27.0
Pr	–	–	0.11	0.31	0.75	0.89	–	–	3.10
Nd	0.21	–	–	–	3.83	4.44	–	–	13.8
Sm	0.09	0.193	0.27	0.54	1.22	1.68	4.98	11.8	3.56
Eu	0.033	0.083	0.10	0.20	0.49	0.64	1.67	3.5	0.15
Gd	0.13	–	0.38	0.69	1.97	2.52	–	–	3.97
Tb	0.025	–	0.075	0.12	0.41	0.49	0.84	1.49	0.67
Dy	0.16	–	0.54	0.77	2.78	3.38	–	–	4.19
Ho	–	–	0.12	0.17	0.70	0.81	–	–	0.97
Er	0.10	–	0.37	0.44	2.15	2.37	–	–	2.74
Tm	–	–	–	–	0.36	–	–	–	0.34
Yb	0.095	0.31	0.37	0.47	2.20	2.33	2.08	3.08	2.51
Lu	–	0.054	0.056	0.071	0.35	–	0.32	0.42	–
Total	–	–	3.3	6.1	25.3	27	–	–	75
La/Yb	0.42	0.15	0.49	1.09	1.05	0.63	4.2	12.3	4.4
La_N/Yb_N	0.26	0.10	0.33	0.73	0.71	0.43	2.8	8.3	3.0
Eu/Eu*	0.90	–	0.95	1.00	0.97	0.98	–	–	0.94
Y	0.90	–	–	–	24	21.8	23	39	24
Sc	49	13.8	14.7	16.9	34	–	30.6	23.2	–

(1) Olivine websterite 051, New Guinea (Jaques et al. 1983).
(2) Spinel lherzolite, UM2, New Mexico, USA (Basaltic Volcanism Study Project 1981).
(3) Spinel lherzolite, Ka168, Austria (Jagoutz 1979).
(4) Spinel lherzolite, Sc-1, New Mexico, USA (Jagoutz 1979).
(5) MORB glass, 527-1-1, Famous Area, North Atlantic (Langmuir et al. 1977).
(6) MORB basalt, Site 105, North Atlantic (Ayuso et al. 1976).
(7) OIB tholeiite, Mauna Lao HAW 8 (Basaltic Volcanism Study Project 1981).
(8) OIB alkali basalt HAW 20 Kohala, Hawaii (Basaltic Volcanism Study Project).
(9) Karoo basalt, Lesotho JP 58, South Africa (Erlank 1984).

light lanthanides, the La abundances varying by a factor of $> 10^4$ (Frey 1984). This indicates a considerable degree of trace element variability in the upper mantle, as is also indicated for isotopic studies.

Igneous rocks from the oceanic crust fall into two major classes. These are respectively the Mid-Ocean Ridge Basalts (MORB), which form the upper part of the oceanic crust and accordingly are the most voluminous igneous rocks erupted at the surface of the earth, and the Oceanic Island Basalts (OIB), which in contrast are erupted from point sources termed 'hot spots' (tables 16 and 17). These two classes of basalt have distinctive lanthanide patterns (fig. 23) (see extensive review by Saunders 1984). Much diversity in composition exists, but there is a tendency for MORB to have lanthanide patterns characterised by flat heavy lanthanides and depleted light lanthanides. In contrast, typical OIB have strong light lanthanide enrichment. The MORB patterns show no sign that garnet was a residual phase in

TABLE 17
REE analyses [data in ppm (wt)] of intraplate volcanic rocks, and island-arc rocks.

Element	(1)	(2)	(3)	(4)	(5)	(6)	(7)	(8)	(9)
La	29.3	61.7	78.5	39.4	5.2	15.3	19.4	35.1	30.9
Ce	62.5	137	160	83.8	14.6	34.8	40.9	68.0	58.9
Pr	7.3	15.1	17.8	10.0	2.0	4.0	4.9	7.9	8.4
Nd	30.4	58.0	66.0	41.1	9.2	17.4	19.4	33.8	28.8
Sm	6.5	12.0	12.0	8.1	2.4	4.0	3.5	7.3	5.0
Eu	2.0	3.8	1.5	2.6	0.86	1.3	1.0	2.0	0.97
Gd	5.5	10.5	9.0	6.4	2.7	3.8	3.3	6.4	3.7
Tb	0.9	1.6	1.4	1.0	0.48	0.66	0.53	0.99	0.68
Dy	4.8	8.6	8.4	5.7	3.0	3.9	3.3	5.9	4.0
Ho	1.0	1.7	1.7	1.1	0.69	0.87	0.73	1.4	0.86
Er	2.5	4.0	4.8	2.7	2.1	2.5	2.2	4.0	2.5
Tm	0.3	0.5	–	0.3	–	–	–	–	–
Yb	1.9	3.4	4.45	2.1	2.0	2.5	2.1	3.8	2.4
Total	155	318	367	205	46	92	102	178	148
La/Yb	15.4	18.1	17.6	18.8	2.5	6.0	9.1	9.1	12.9
La_N/Yb_N	10.4	12.3	11.9	12.7	1.8	4.1	6.2	6.2	8.7
Eu/Eu*	1.0	1.04	0.44	1.1	1.03	1.0	0.90	0.89	0.69
Y	21	50	39	25	24	27	28	36	39
Sc	–	–	–	–	42	24	16	16	12

(1) Basalt, T-80, Akaroa, New Zealand (Price and Taylor 1980).
(2) Mugearite T-102, Akaroa, New Zealand (Price and Taylor 1980).
(3) Trachyte T-123, Akaroa, New Zealand (Price and Taylor 1980).
(4) Hawaiite T-101, Akaroa, New Zealand(Price and Taylor 1980).
(5) Island-arc basalt, Indonesia (Whitford et al. 1979).
(6) Island-arc basaltic andesite, Indonesia (Whitford et al. 1979).
(7) Island-arc andesite, Indonesia (Whitford et al. 1979).
(8) Island-arc high-K andesite, Indonesia (Whitford et al. 1979).
(9) Island-arc dacite, Indonesia (Whitford et al. 1979).

their source regions, and accordingly are postulated to be derived from shallow depths in the mantle. In contrast, the OIB, with heavy depleted/light enriched patterns, come from greater depths in the mantle, bearing the signature of equilibration with garnet as a residual phase in the zone of partial melting. It has long been argued that the very distinctive lanthanide patterns of MORB and OIB demand separate source regions, and accordingly indicate that the mantle is heterogeneous with respect to the lanthanides (e.g. Schilling 1975). Such information has been crucial in formulating models involving large-scale chemical layering in the mantle and for models involving mantle metasomatism.

The observed heterogeneity in many samples has led to the concept of widespread mantle metasomatism, for which there is some evidence in veins in mantle xenoliths which are rich in clinopyroxene, various hydrous phases and light lanthanides (e.g. Frey and Green 1974). Such views have become common in an attempt to resolve the paradox created by the evidence from Sm–Nd isotopes that the source for OIB

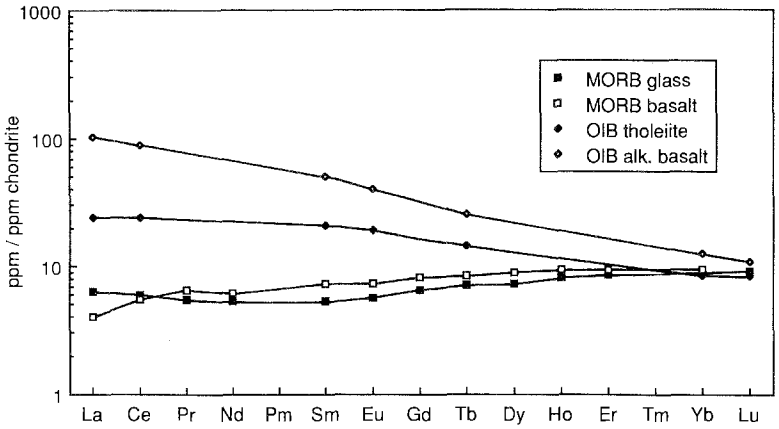

Fig. 23. Lanthanide abundance patterns for Mid-Ocean Ridge Basalts (MORB) and Ocean-Island Basalts (OIB) (data are from table 16). Note the depletion in the light lanthanides (La–Sm) in MORB derived from a depleted mantle source, and the enrichment of light lanthanides in OIB. Nd isotopic evidence indicates that the source of both these rock types was characterized by long term depletion of Nd relative to Sm, indicating the observed light lanthanide enrichment in OIB is a recent event.

is generally depleted in light lanthanides, having an Sm–Nd ratio higher than that of the bulk earth or CI chondritic values. Since OIB are enriched in the light lanthanides, with low Sm/Nd ratios, the solution has been to invoke late metasomatism to enrich a source that has been depleted for most of earth history. More recently, the contradictory isotopic and trace element evidence for the origin of OIB has been explained by a model in which OIB are derived from remelting, in the lower mantle, of ancient subducted lithosphere (Chase 1981, Hofmann and White 1982). In these rocks, as in most mantle derived species, there is an absence of Eu

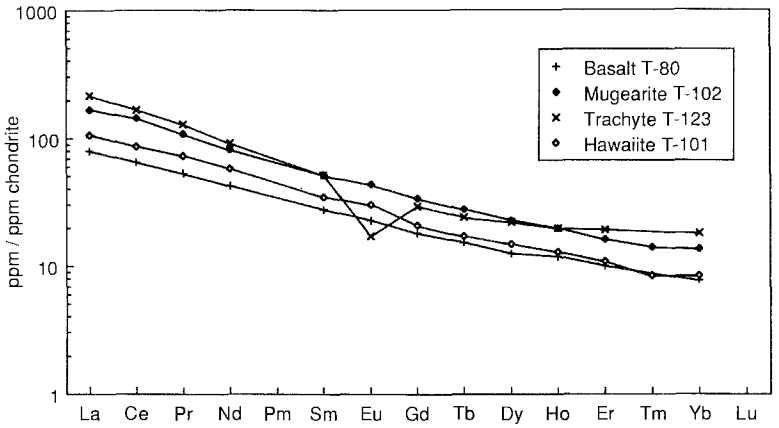

Fig. 24. Lanthanide patterns for a typical fractionated suite of volcanic rocks from an intra-plate basaltic volcano, Akaroa, New Zealand. (Data are from table 17.)

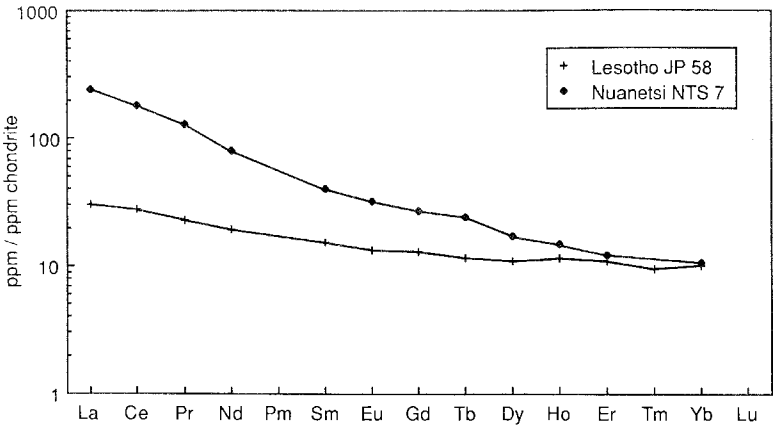

Fig. 25. Variations in lanthanide patterns between the southern (Lesotho) and northern (Nuanetsi) sectors of the Karoo plateau basalt province, probably reflecting major changes in mantle chemistry. There is no change in crustal thickness or composition across this boundary. [Data are from Erlank (1984) and from table 16.]

anomalies, except locally due to plagioclase fractionation. The implication of this is that plagioclase is not a stable residual phase in the source regions from which these basalts are derived.

An example of differentiation within a typical intraplate volcano is given by the sequence basalt–hawaiite–mugearite–trachyte at Akaroa, Banks Peninsula, New Zealand (table 17, fig. 24). Although erupted through a continental plate, the sequence is similar to that observed in many oceanic settings. Cullers and Graf (1984a,b) have given a general review of the behaviour of the lanthanides in basaltic rocks erupted in continental settings. The most important volumetric species of mantle derived rocks erupted through the continental crust are the plateau basalts (table 16). They display evidence of crustal contamination, but when studied on a broad enough scale, provide insight into regional differences in the mantle. A recent study by Erlank (1984) of the widespread Karoo igneous province (whose present eroded outcrop amounts to over 140 000 km^2) shows a distinct difference in lanthanide patterns (and for many other trace elements) on a regional scale (fig. 25). These compositional differences cannot be related to differing degrees of partial melting or to the operation of fractional crystallisation. Crustal contamination is likewise shown to be minor, since the chemistry of the lavas appears unrelated to crustal provinces. The basic change in the chemistry of the lavas of the northern and southern provinces appear to be due to changes in the composition of the underlying mantle.

Island-arc rocks (table 17) display notable uniformity in their lanthanide patterns (fig. 26), typically forming a smooth curve from La about 50 times chondritic to Yb at about 10 (see reviews by Gill 1981, Basaltic Volcanism Study Project 1981, Pearce 1982, White and Patchett 1984). Eu depletion or enrichment is uncommon and usually associated with local enrichment or depletion in plagioclase. Although this

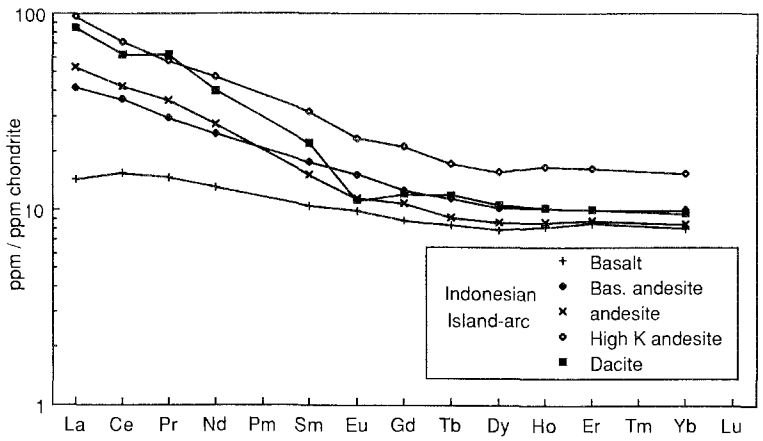

Fig. 26. Variation in the lanthanide abundances of a typical suite of island-arc volcanic rocks, erupted above a subduction zone [data are from the Sunda arc, Indonesia (Whitford et al. 1979) and from table 17]. Note the absence of Eu anomalies except in the most fractionated rocks (dacites).

mineral is a ubiquitous phenocryst phase in the calc-alkaline lavas typical of the subduction-zone environment, little separation of this mineral has occurred during crystallisation of the melt. Neither could the source regions have contained residual plagioclase, for a depletion in Eu would result in the melt. Those rocks have occasioned a great deal of interest since they represent a voluminous addition of silica-rich ($\sim$60% SiO_2) material from mantle sources. Their close spatial relationship with the down-going slab of oceanic crust, and the uniformity of their lanthanide patterns and isotopic systematics, point to a uniform petrogenetic process, at odds with many current models which involve mixing of various components: more diversity in composition should result than is apparent. The rather flat lanthanide patterns in andesites and related rocks is generally used to argue against derivation of these rocks by melting of the down-going slab of basaltic oceanic crust (e.g. Gill 1981). At the depths ($\sim$140 km) where melting occurs the down-going sea-floor basalt should be transformed to quartz eclogite (thus containing garnet), so that melts derived from it should be depleted in heavy lanthanides (Gd–Lu). However, Brophy and March (1986) have argued that final equilibration of melts from the slab occurs at much shallower depths, within the plagioclase stability field, so that the tell-tale garnet signature will be absent. This observation, if correct, will force a major re-evaluation of current petrogenetic models for the genesis of this important group of rocks, and will reintroduce the subducting slab as a major factor in the genesis of island-arc rocks. It illustrates a general principle that all factors involved in the melting, ascent and fractionation of igneous rocks have to be taken into account when using quantitative trace element modelling.

In the section on continental growth, the assessment is made that island-arc and related orogenic-zone igneous rocks are responsible for present day addition of

TABLE 18
REE analyses [data in ppm(wt)] of anorthosites, tonalites, trondhjemites, granites and rhyolites.

Element	(1)	(2)	(3)	(4)	(5)	(6)	(7)	(8)	(9)
La	0.87	—	30.9	—	59	103	30.8	69	24.2
Ce	1.78	7.81	58.5	14.7	123	234	75	153	50.2
Pr	—	—	—	—	—	—	9.9	16.3	6.0
Nd	0.72	3.42	24.7	4.7	—	—	41	66.7	26.0
Sm	0.19	0.53	4.60	0.73	7.2	22	10.9	14.0	6.4
Eu	0.37	0.75	1.18	0.49	0.84	1.5	0.31	1.97	0.14
Gd	—	0.43	3.93	0.76	—	—	12.3	13.0	5.4
Tb	0.033	—	—	—	0.73	3.8	2.35	2.28	1.0
Dy	—	0.31	3.84	0.30	—	—	15.8	14.0	6.0
Ho	—	—	—	—	—	—	3.49	2.82	1.1
Er	—	0.15	2.30	0.16	—	—	10.3	7.96	2.9
Tm	—	—	—	—	—	—	—	—	0.4
Yb	0.09	0.14	2.29	0.17	2.0	13	9.1	7.34	2.8
Lu	0.014	0.022	0.36	0.03	0.33	2.3	—	—	—
Total	—	—	133	—	—	—	224	371	133
La/Yb	9.7	—	13.5	—	29.5	7.9	3.4	9.4	8.6
La_N/Yb_N	6.5	—	9.1	—	20	5.4	2.3	6.3	5.8
Eu/Eu*	—	4.8	0.85	2.0	0.52	0.21	0.08	0.45	0.07
Y	—	—	23	9	—	—	86	71	29

(1) Archean anorthosite, Ontario, Canada (Ashwal et al. 1983).
(2) Proterozoic anorthosite, Labrador, Canada (Simmons and Hanson 1978).
(3) Tonalite 3824, Pilbara, Western Australia (Jahn et al. 1981).
(4) Trondhjemite UK12, Finland (Arth et al. 1978).
(5) Average late-Archean K-granite (Condie, 1981).
(6) Mid-Proterozoic K granite, New Mexico USA (Condie 1978).
(7) Granite, G4-161, Temora, New South Wales, Australia (Research School of Earth Sciences).
(8) Granite, G4-62, Temora, New South Wales, Australia (Research School of Earth Sciences).
(9) Rhyolite, T96, Banks Peninsula, New Zealand (Price and Taylor 1980).

material to the continents from the mantle, and that this process has operated from some time in the Proterozoic. Nevertheless, such additions comprise probably less than twenty-five percent of the present mass of continental material, most of which was derived from the mantle in the late Archean before 2500 million years by different tectonic processes (see section 11).

Somewhat related to these rocks are the tonalites and trondhjemites (table 18), which dominated Archean environments in the way that andesites and other island-arc rocks dominate igneous activity along subduction zones. Their lanthanide patterns contrast strongly with those of andesites (e.g. Arth and Hanson 1975, Arth et al. 1978, O'Nions and Pankhurst 1978, Jahn et al. 1981, Jahn and Zhang 1984; see also numerous papers in a book edited by Barker 1979). The patterns are steep, strongly enriched in La–Sm and depleted in Gd–Lu. Typically there is no europium anomaly, although some trondhjemites (fig. 27) are enriched in Eu, due to plagioclase enrichment. The steep lanthanide patterns reflect equilibration with a garnet-

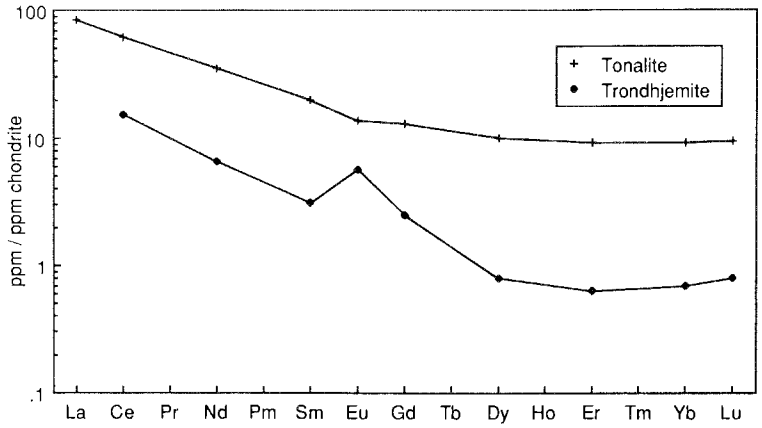

Fig. 27. Lanthanide abundance patterns for typical Na-rich plutonic rocks (tonalites and trondhjemites) The enrichment of Eu in the trondhjemite is a not uncommon feature of the more differentiated types. (Data are from table 18.)

bearing residue (which has the complementary pattern, see fig. 19). This implies derivation from mantle depths where garnet is a stable phase. They cannot be derived from primary melting of mantle peridotite, but must form by a two-stage process. The current model derives them by partial melting of basalts, which are derived as initial primary melts from the mantle. As the basalts sink back into the mantle, they form eclogitic (garnet-bearing) rocks. The tonalities and trondhjemites were derived from these by melting at depths below about 40 km, where garnet is a stable phase for such compositions. Thus they are derived by two stages from the primitive mantle composition. Their importance lies in their abundance in terrains of Archean age, compared to younger terrains. Models for the growth of the continental crust consider such rocks and their volcanic equivalents, to be the dominant silica-rich component in the Archean crust. If this is correct, they may be responsible for the production of the major portion of the continental crust.

The major igneous components of the upper continental crust are 'granitic' rocks of various types, ranging, for the plutonic species, from granodiorite to adamellite, with voluminous volcanic equivalents of rhyolites and ignimbrites (see reviews by Hanson 1978, McCarthy and Kable 1978, Cullers and Graf 1984a,b) (table 18). A large amount of experimental work has established a dominant origin by melting within the continental crust at depths of 15–30 km (see review by Wyllie 1977). Scandium is usually present at low levels, being retained in minerals such as pyroxene during the melting process. Their lanthanide patterns have marked features in common (fig. 28). Generally, the lanthanides are enriched strongly, except for Eu, which almost always displays a marked depletion. The high concentration of the lanthanides in granitic rocks, due to their concentration as 'incompatible' elements during crystal fractionation leads to the formation of phases enriched in the lanthanides or even to independent rare earth mineral phases (e.g. Hildreth 1979,

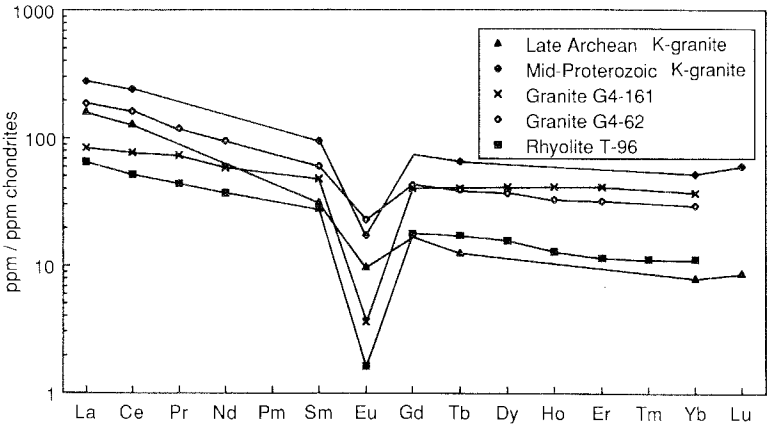

Fig. 28. Typical lanthanide abundance patterns for K-rich granites and rhyolites (data are from table 18). Note the development of extreme depletion in Eu in the more highly fractionated granites.

Mahood and Hildreth 1983, Gromet and Silver 1983). Their presence as minor constituents makes model calculations based on the major mineral phases of little significance. Some of the deepest Eu anomalies (Eu/Eu* <0.01) occur in the more fractionated members. This depletion in Eu is principally a consequence of melting in source regions where plagioclase feldspar is a stable residual phase. Eu is retained in residual plagioclase, within the middle or lower crust, while the upper crust is dominated by a lanthanide pattern with a characteristic Eu depletion (Eu/Eu* $= 0.65$) inherited from the events leading to the formation of granite. The lanthanides, however, are not particularly sensitive indicators of subtle variations in source chemistry. Their patterns do not, for example, distinguish between the I and S granites (e.g. Shaw and Flood 1981) which can be separated on the basis of mineralogical and isotopic parameters (e.g. Chappell and White 1983).

Extreme enrichment of the lanthanides occurs during crystallisation of the silica-rich igneous rocks, due to their exclusion from the lattice sites of the common rock-forming minerals. The final residual melts from these magmas crystallise as pegmatites. These are small pod-shaped bodies (typically <100 m in length) of coarse grain size. They contain high concentrations of incompatible elements, including the lanthanides which may form a wide variety of independent minerals, in which individual lanthanide elements may be the major constituents (Clark 1984).

A more enigmatic rock type is anorthosite (table 18). The existence of batholitic masses of this plagioclase-rich crustal rock, mainly of Proterozoic age, have continued to frustrate the attempts of petrologists to provide a satisfactory explanation. Their lanthanide patterns (fig. 29) show a characteristic enrichment in Eu (e.g. Simmons and Hanson 1978, Ashwal and Seifert 1980). They are derived either from highly aluminous magmas of mantle deviation (Morse 1982, Ashwal 1982) or from melting of aluminous lower crustal rocks (Taylor et al. 1984).

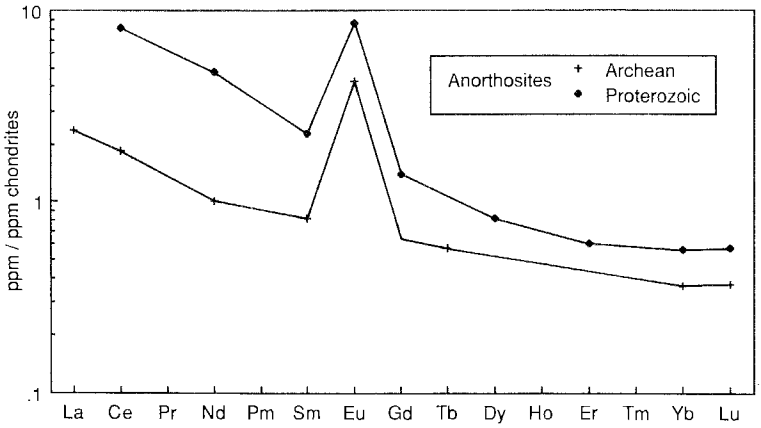

Fig. 29. Lanthanide abundance patterns for anorthosites showing enrichment in Eu in these plagioclase-rich plutonic rocks. (Data are from table 18.)

7.5 *Lanthanide characteristics of ore deposits*

Economic sources of the rare earth elements are usually in pegmatites, or concentrated as resistant minerals in beach sands (e.g. monazite). Reviews of these sources are given by Neary and Highley (1984).

In this section, the major interest is in relating the characteristics of lanthanide abundances to the occurrence of economic deposits of other elements. Major interest in this topic occurred when it was realised that hydrothermal processes, responsible for many ore deposits, were selectively mobilising lanthanide elements (e.g. Taylor and Fryer 1982). Thus the 'black smokers' at mid-ocean ridges produce fluids enriched in the light lanthanides (La–Sm) containing a dramatic enrichment in Eu indicating that a breakdown of plagioclase is involved (Michard et al 1983, Michard and Albarede 1986). In contrast, hydrothermal solutions of crustal origin are depleted in Eu relative to chondrites, and in some cases, relative to upper crustal patterns (Michard and Albarede 1986) (fig. 30). Such large differences in the behaviour of Eu indicate significant differences of temperature and oxygen fugacity (i.e. the Eu/Eu* ratio) in the hydrothermal solutions (Sverjensky 1984). Data from lanthanide distributions in such occurrences thus provide evidence, not only for the origin of the metal deposit, but also fundamental evidence of geological processes.

Such studies by Graf (1977) showed that Eu enriched in chemical sediments including the ore body, in the New Brunswick, Canada, massive sulfide deposits. This enrichment was ascribed to water–rock interaction. Bence and Taylor (1985) have shown that such Eu enrichment is characteristic of many massive sulfide deposits (fig. 31), and occurs in deposits in which copper, lead and zinc sulfides are precipitating near active 'black smokers' at mid-ocean ridges sites. The enrichment in Eu appears to be due to reduction and mobilisation of rocks with hydrothermal fluids (Sverjensky 1984). Whitford et al. (1987) have found evidence for extensive

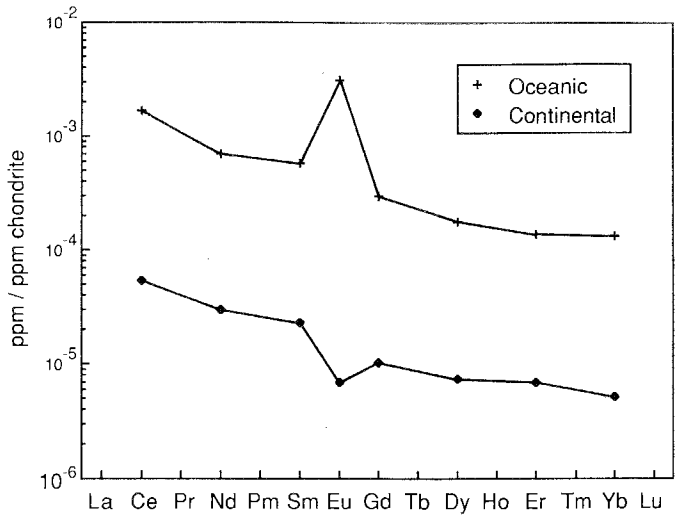

Fig. 30. Selected lanthanide patterns for hydrothermal solutions from oceanic and continental environments (data are from Michard and Albarede 1986). Oceanic hydrothermal solutions tend to have much higher abundances and are strongly enriched in Eu, suggesting that plagioclase is being preferentially attacked by the hydrothermal solutions. The negative Eu anomaly in the continental hydrothermal solution is quite variable, commonly being even more pronounced. This pattern is probably reflecting the average upper crustal rocks which are being affected by such solutions.

depletion of Eu in altered volcanic rocks associated with base metal ore deposits in Tasmania.

Leaching of light lanthanides (La–Sm) and of Eu by such hydrothermal alteration may produce flat chondrite-normalised patterns with large depletions of Eu, which resemble those produced by extreme crystal fractionation of silica-rich igneous rocks. Accordingly, the possibility of confusing these two similar patterns, developed by separate processes, exists. Bence and Taylor (1985), Strong (1984) and Whitford et al. (1987) all suggest caution in attempting to use lanthanide patterns to distinguish between mineralised and barren sequences of igneous rocks for these reasons (cf. Campbell et al. 1981, 1984).

Kerrich and Fryer (1979) also used the fractionation of the lanthanides to constrain the origin of Archean hydrothermal gold deposits in the Canadian Shield. Strong enrichment in Eu occurred in stratiform carbonate beds and in quartz veins, indicative of hydrothermal processes under reducing conditions on the sea floor. The widespread occurrence of such deposits in rocks of Archean age has led to the suggestion that oceanic chemistry in that epoch was dominated by inputs from volcanic sources, rather than by inputs from continental crustal sources, as is presently the case (Fryer et al. 1979).

The lanthanides have also contributed to our understanding of the formation of uranium deposits found at major unconformities in the Precambrian. Thus McLennan and Taylor (1979, 1980) discovered extreme fractionation of the lan-

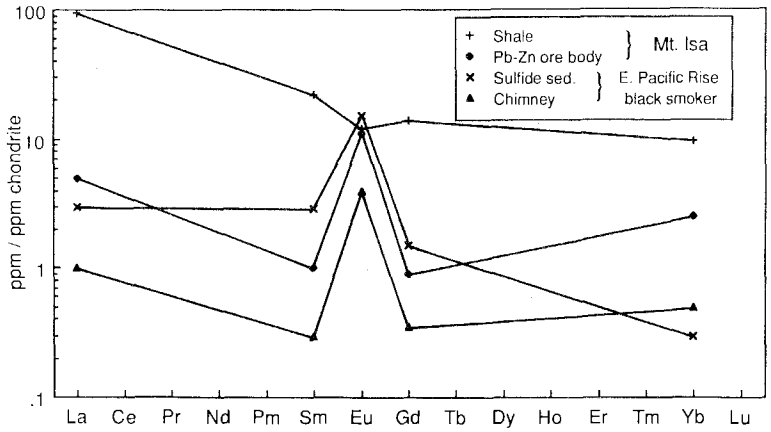

Fig. 31. Strong enrichment in Eu in strata-bound massive Pb–Zn ore deposits at Mt. Isa, compared to normal shales. The enrichment is related to hydrothermal activity during ore-body formation. Similar enrichment in Eu, shown in the two lower patterns, is observed in sulfides being precipitated at submarine 'black smokers' at a mid-ocean ridge crest. [Data by courtesy of Mt. Isa Mines, Dr. A.E. Bence, Exxon Production Company, Houston, TX, USA, and from Bence (1983).]

thanides associated with uranium mineralisation in the Early-Proterozoic Pine Creek geosyncline of Northern Australia. The mineralised zones were depleted in light lanthanides and enriched in heavy lanthanides (Gd–Lu) relative to the country rock (fig. 32), with the degree of enrichment correlated with the abundance of uranium (see also Fryer and Taylor 1984). Since uranium is transported as a carbonate complex in these environments (Langmuir 1978) the lanthanides are

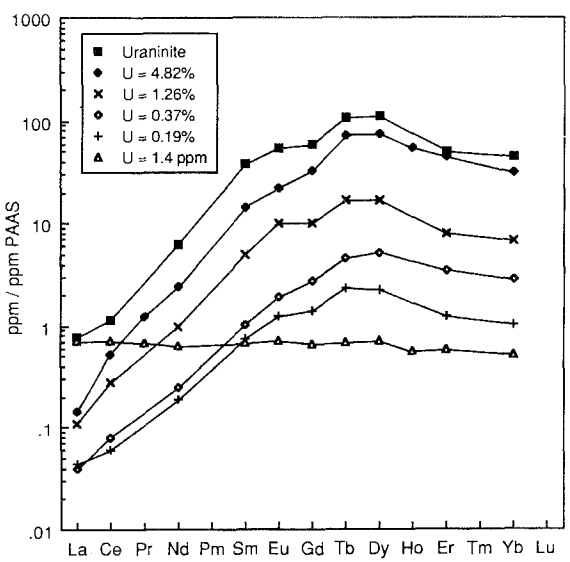

Fig. 32. PAAS-normalized lanthanide patterns for early Proterozoic uranium deposits from the Pine Creek Geosyncline, Australia (data are from McLennan and Taylor 1979). Compared to the unmineralized host sedimentary rock, these deposits are extremely enriched in heavy lanthanides and depleted in light lanthanides. The abundances and amount of fractionation is related to the U content, suggesting the lanthanide mobility and U mineralization are directly related, thus helping to constrain the origin of the deposit. The fractionation of Sm and Nd during ore-formation allows dating by the Sm–Nd method.

TABLE 19
Lanthanide content (parts per trillion) of seawater and river water.

Element	Atlantic Ocean[a]		N.W. Pacific Ocean[b]		Garonne and Dordogne Rivers[c]
	100 m	2500 m	surface	2500 m	
La	1.81	4.08	1.2	6.5	47.5
Ce	2.35	3.68	1.4	1.3	79.0
Pr	—	—	—	—	7.3
Nd	1.85	3.61	0.74	4.3	37.9
Sm	0.401	0.714	0.15	0.80	7.8
Eu	0.0979	0.136	0.050	0.21	1.48
Gd	0.536	1.13	0.25	1.3	8.5
Tb	—	—	—	—	1.24
Dy	0.777	0.991	0.33	1.6	—
Ho	—	—	—	—	1.44
Er	0.681	0.851	0.28	1.6	4.2
Tm	—	—	—	—	0.61
Yb	0.614	0.829	0.19	1.4	3.64
Lu	—	—	—	—	0.64
Total	13	16	5	19	202
La/Yb	8.31	4.92	6.32	4.64	13.0
La_N/Yb_N	5.61	3.33	4.27	3.14	8.82
Eu/Eu*	0.65	0.46	0.79	0.63	0.56

[a]Elderfield and Greaves (1982).
[b]Klinkhammer et al. (1983).
[c]Martin et al. (1976).

probably transported in a similar form, probably as $REE(CO_3)_3$ (Kosterin 1959, Naumov 1959). The observed fractionation correlates with the complexing potential of the lanthanides. The strong relative depletion of the light lanthanides includes major changes to the Sm/Nd ratio, so that the timing of such events is potentially recorded by the Sm–Nd isotopic systematics (e.g. Fryer and Taylor 1984, Maas et al. 1986).

8. Marine geochemistry

8.1 *Natural waters*

Lanthanide abundances in natural waters are extremely low (table 19, fig. 33). This observation is well illustrated by Haskin et al. (1966b), who calculated that the entire mass of lanthanides in the oceans is equivalent to that in about a 0.2 mm thickness of sediment of the same areal extent. The lanthanide patterns of normal ocean waters are significantly enriched in the heavy lanthanides relative to the light lanthanides, when compared to terrigenous sedimentary rocks. Ocean waters are relatively depleted in Ce; a reflection of preferential incorporation of this element in

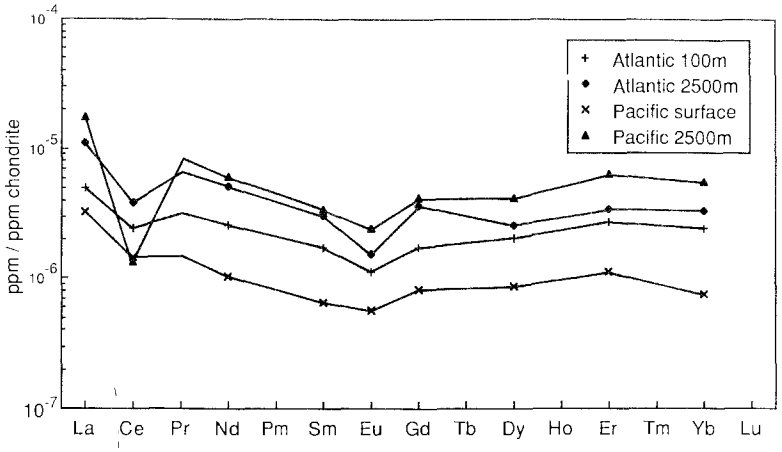

Fig. 33. Lanthanide abundance patterns for selected seawater samples (data are from table 19). With the exception of some surface waters, seawater is typically depleted in Ce. Relative to the upper continental crust, seawater is also typically enriched in heavy lanthanides, although considerable variability exists, related both to depth and location.

manganese nodules (which will be discussed in section 8.2). River waters have higher lanthanide abundances than oceanic waters and show very different characteristics (Martin et al. 1976). The patterns are similar to that typical of shales, although the abundance levels are much lower (fig. 34).

There is a considerable variability in lanthanide patterns in sea water, both regionally and with depth (Elderfield and Greaves 1982, De Baar et al. 1983, 1985a). With the exception of a thin surface zone which may be dominated by aeolian input, there is a general increase of light lanthanides with depth. Total lanthanides are higher in surface waters of the Atlantic Ocean, but lower in deep waters, compared with those of the Pacific (De Baar et al. 1985a).

The sources of the lanthanides in sea water have occasioned much debate. Three

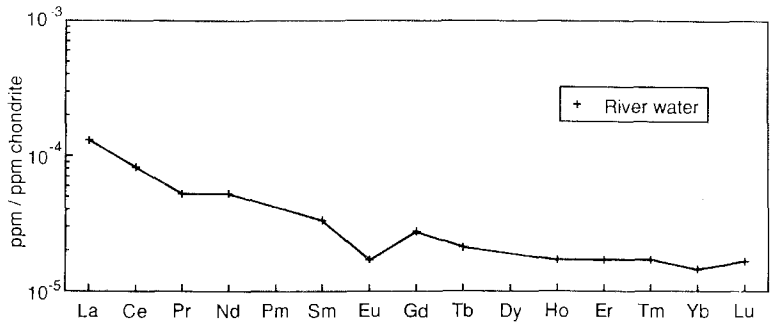

Fig. 34. Lanthanide abundance pattern for river water (data are from table 19). Note the higher abundances and lack of Ce anomaly, compared to seawater (fig. 33). In general, the pattern is nearly parallel to that of the upper continental crust.

sources are recognised (Elderfield and Greaves 1982): (1) a surface source dominated by aeolian input, with lanthanide patterns similar to those of the upper continental crust, (2) a riverine source with similar characteristics, and (3) a bottom source. This last source results from the recycling of lanthanides from marine sediments during diagenesis.

The removal of lanthanides from sea water appears to be dominated by adsorption onto settling particles. Evidence for this process in surface waters is well established and is thought to be responsible for the fractionation of light and heavy lanthanides, but the suggestion of scavenging in deep waters is less securely based. If equilibrium conditions are obtained, for example between sea water and calcium carbonate, some substitution of lanthanides in crystal-lattice sites might be expected. Further evidence for the removal of lanthanides in deep waters is supported by the study from the Pacific Ocean by Klinkhammer et al. (1983). Strong depletion of the light lanthanides, compared with deep Atlantic waters, was observed, consistent with scavenging by iron and manganese oxides derived from hydrothermal activity on the sea floor.

The residence times of the lanthanides in sea water are less than the mixing time of the oceans (about 1000 years). This accounts for the great variability of the patterns. Residence times, calculated both with respect to input and output by Elderfield and Greaves (1982) are given in table 20; it should be realised that these values are model-dependent. Few other elements have such short residence times; combined with their overall geochemical coherence, this makes the lanthanides uniquely suited to paleo-oceanography studies (e.g. Wright-Clark et al. 1984, Wang

TABLE 20
Residence times (in years) of lanthanides in seawater.
(From Elderfield and Greaves 1982.)

Element	(1)	(2)
La	690	240
Ce	400	110
Pr	(640)[a]	(360)
Nd	620	450
Sm	600	220
Eu	460	470
Gd	720	300
Tb	(760)	(320)
Dy	810	340
Ho	(890)	(380)
Er	980	420
Tm	(980)	(420)
Yb	970	410
Lu	(970)	(410)

(1) Relative to sediment output.
(2) Relative to aeolian and river input (probably minimum values).
[a]Values in parentheses are interpolated values.

et al. 1986, Piepgras and Wasserburg 1980, Piepgras et al. 1979, Hooker et al. 1981).

Nd isotopes have been of particular use, the most important observation being that different oceanic masses have distinct signatures, indicative of a varying component of mantle derivation (e.g. Piepgras et al. 1979, Piepgras and Wasserburg 1980, Stordal and Wasserburg 1986). Since marine authigenic phases record the Nd isotopic signature of their coexisting sea water, they may be used to study the composition of ancient oceans (e.g. Hooker et al. 1981, Miller and O'Nions 1985, Staudigel et al. 1985, Palmer and Elderfield 1985). Thus Hooker et al. (1981) established the Nd isotopic composition of the ancient Iapetus ocean in Ordovician times by this means.

Reports continue to appear alleging anomalous behaviour in sea water of lanthanide elements other than Ce and Eu (e.g. Roaldset and Rosenqvist 1971, Masuda and Ikeuchi 1979, De Baar et al. 1985b). The latter authors argue for Gd and Tb anomalies, which they relate to the decrease in ionisation potential associated with the half-filled 4f electron shell. For four reasons, we remain unconvinced of the reality of the anomalies:

(a) The reported Gd anomalies are based on analyses by neutron activation techniques. Gd is one of the most difficult elements to determine in this manner, and confirmation by other methods or laboratories is needed [see point (c)].

(b) The anomalies appear on shale-normalised patterns, but the normalising values used are old (Haskin and Haskin 1966, Balashov et al. 1964). If modern values are substituted (e.g. PAAS, Taylor and McLennan 1985, NASC, Gromet et al. 1984), the magnitude of the anomalies decreases, and some essentially disappear.

(c) Sea water analyses using precise isotope dilution techniques (e.g. Elderfield and Greaves 1982) fail to show consistent significant anomalies, such as those reported by the analytical technique of neutron activation.

(d) There is a well-documented fractionation of heavy from light lanthanides in sea water and inflections in the lanthanide patterns may give rise to apparent anomalies.

8.2 *Marine phases*

Manganese nodules

An interesting aspect of REE geochemistry is the behaviour of Ce in the marine environment. The abundance of Ce is high relative to that of the other lanthanides in most manganese nodules (e.g. Goldberg et al. 1963, Piper 1974, Addy 1979, Elderfield et al. 1981) (table 21, fig. 35) and this anomaly is thought to be the cause of Ce depletion seen in seawater (see preceeding section). The preferential incorporation of Ce into manganese nodules is generally considered to be due to oxidation of Ce:

$$Ce^{3+} + 4OH^- = Ce(OH)_4 + e^-.$$

For typical marine pH's (about 8), Eh values of about 0.15–0.45 V would probably be required (see review of Addy 1979). This suggests that Ce anomalies should only be found in nodules formed in quite oxidised sediments, an observation substantiated by the limited body of data (Addy 1979).

TABLE 21
Lanthanide content [in ppm(wt)] of selected manganese nodules and other marine phases.

Element	(1)	(2)	(3)	(4)	(5)	(6)	(7)	(8)	(9)
La	95.5	161	12.8	35.3	56	167	5.85	3.8	5.67
Ce	313	1098	4.73	22.8	102	54.7	7.19	5.5	2.98
Pr	—	—	—	—	15	—	—	—	—
Nd	135	189	10.5	46.7	57	169	5.86	3.5	6.96
Sm	32.7	40.6	2.38	9.30	11	21.8	1.3	0.65	1.569
Eu	8.02	9.03	0.574	2.22	2.8	4.7	0.30	0.15	0.395
Gd	31.9	42.3	—	—	15	—	1.4	—	1.864
Tb	—	—	0.305	1.40	2.1	3.5	—	0.11	—
Dy	30.2	40.1	—	—	12	—	1.3	—	1.835
Ho	—	—	—	—	3.3	—	—	—	—
Er	15.7	23.5	—	—	9.0	—	0.75	—	1.157
Tm	—	—	—	—	1.1	—	—	—	—
Yb	14.3	21.6	3.60	4.67	6.7	9.5	0.61	0.28	1.059
Lu	—	—	0.675	0.667	1.2	1.89	—	0.042	0.1893
Total	—	—	—	—	294	—	—	—	24
La/Yb	6.7	7.5	3.6	7.6	8.4	17.6	9.6	13.6	5.35
La_N/Yb_N	4.5	5.0	2.4	5.1	5.7	11.9	6.5	9.2	3.6
Eu/Eu*	0.76	0.67	—	—	0.67	—	0.68	—	0.71

(1) WAH 24F6, Pacific Mn-nodule (todokokite) in siliceous ooze (Elderfield et al. 1981).
(2) AMPH 85 PG, Pacific Mn-nodule (S–MnO_2) in ridge flank sediment (Elderfield et al. 1981).
(3) A-32, East Pacific Rise ridge crest sediment ($Al_2O_3 = 0.264\%$) (Piper and Graf 1974).
(4) A-14, East Pacific Rise flank sediment ($Al_2O_3 = 1.15\%$) (Piper and Graf 1974).
(5) Phosphorite from Magdalena Bay (100 m) (Goldberg et al. 1963).
(6) MP-36P Phillipsite (0–8 cm depth) (Piper 1974).
(7) Average non-detrital foraminifera (Atlantic Ocean) (Palmer 1985).
(8) Biogenic $CaCO_3$ (Spirn 1965).
(9) 7-66-3, Oligocene radiolarian ooze (Shimizu and Masuda 1977).

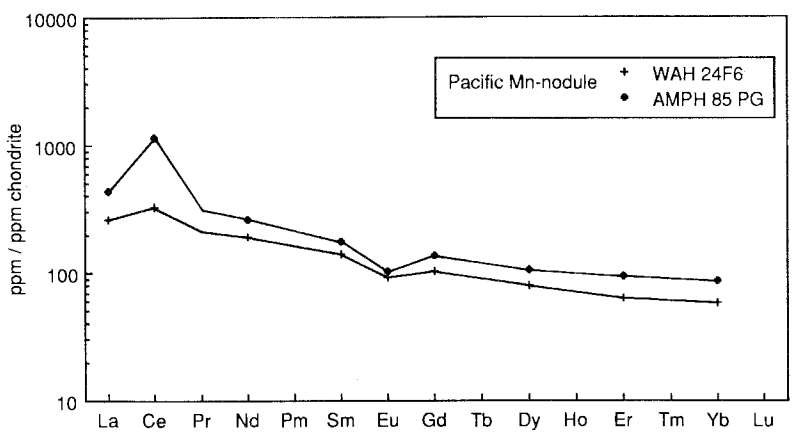

Fig. 35. Lanthanide patterns for selected manganese nodules (data are from table 21). Note the enrichment in Ce. This enrichment is the major cause of the depletion of cerium in seawater.

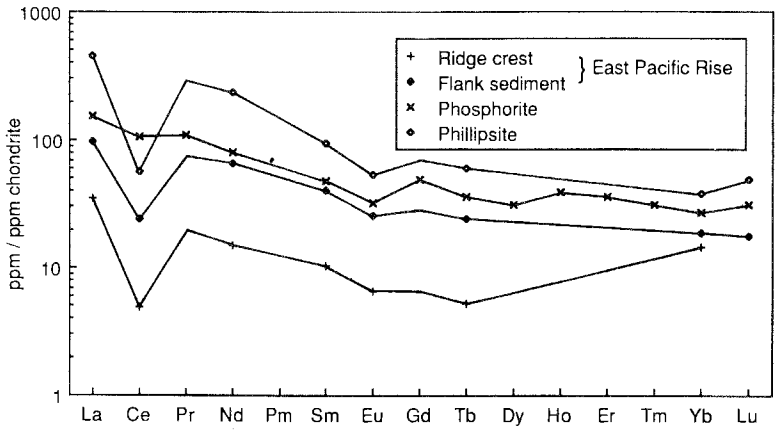

Fig. 36. Lanthanide abundance patterns of selected marine sediments. Most phases which have precipitated from seawater show the characteristic depletion in Ce. (Data are from table 21.)

The total trivalent lanthanide content of Mn nodules shows an inverse correlation with that of the associated sediment. In contrast, Ce anomalies (Ce/Ce*) are positively correlated (nodules are enriched and sediments depleted in Ce) (Elderfield et al. 1981). These workers suggest diagenetic transfer of trivalent lanthanides from the sediments into the nodules, with the rates of diagenetic reactions being related to sedimentation rate. Although Nd isotopic data indicate a seawater origin for Nd in Mn nodules, the associated sediment has virtually identical $^{143}Nd/^{144}Nd$ ratios, so that early diagenetic transfer of Nd from the sediment is not ruled out by this observation.

A direct origin from seawater for cerium in both Mn nodules and associated sediment is inferred by Elderfield et al. (1981) and by Elderfield and Greaves (1981) from the negative correlation between cerium anomalies and Mn/Fe ratios in the nodules. Inter-element relationships and leaching experiments point to the presence of lanthanides in two major phases, one Fe-rich and the other P-rich. The surfaces of these phases are thought to be the sites for the diagenetic reactions.

Other marine phases

The lanthanide content of most authigenic phases (table 21) tends to reflect the pattern of seawater (table 19, fig. 36). The abundances in deep-sea chert and siliceous microfossils (fig. 37; Shimizu and Masuda 1977) are highly variable (by over a factor of 10). The abundance levels are related to the degree of diagenesis (Shimizu and Masuda 1977) and indicate the inability of REE to enter such phases. A major problem in assessing the data is the prevalence of terrigenous debris. Non-clay phases generally have very low lanthanide concentrations and any incorporation of other material will swamp the indigenous lanthanide abundances. Thus Fleet (1984) noted a correlation between Al content and lanthanide concentrations in calcareous oozes, including that most of the lanthanides were in phases other than carbonate.

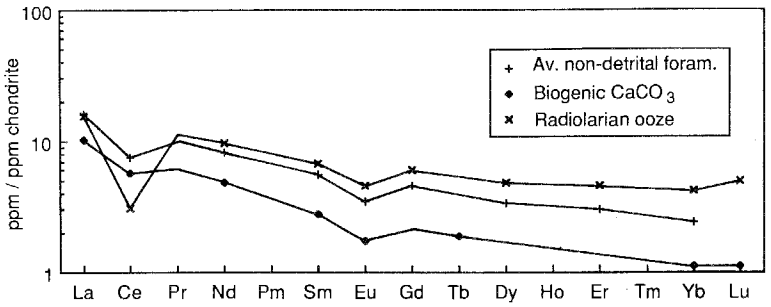

Fig. 37. Lanthanide patterns for radiolarian chert sample and biogenic marine carbonates. Note the negative Ce-anomalies, particularly in the chert samples. (Data are from table 21.)

Evidence from lanthanide abundances identified the source of metalliferous sediments deposited at mid-ocean ridges. They possessed a significant depletion in Ce, pointing clearly to a seawater source for the lanthanides present in the hydrothermal solutions (Piper and Graf 1974, Fleet 1984).

The fact that the lanthanides in marine phases reflect quite closely their pattern in seawater (but not the absolute abundances) produces a possible method of examining secular variations of lanthanide patterns in seawater. This aspect has not been investigated in any detail, with the exception of some studies of lanthanide patterns in apatite (Wright-Clark et al. 1984) and in iron formations (see section 8.4).

8.3. *Sedimentary carbonates and evaporites*

Rather low concentrations of lanthanides also occur in sedimentary carbonate rocks and minerals (Haskin et al. 1966b, Jarvis et al. 1975, Palmer 1985) with typical totals in marine calcite of about 15 ppm or less (Jarvis et al. 1975, Parekh et al. 1977). Most studies dealing with carbonate minerals have relied on acid leaching. Some caution is warranted since even weak acids can strongly leach minerals other than carbonates (Parekh et al. 1977, McLennan et al. 1979a). This can result in overestimating total lanthanide concentrations and perhaps affect the shape of the pattern. In general, carbonate patterns are similar to those of associated terrigenous sedimentary rocks. In marine carbonates, a distinct Ce depletion is common, reflecting the Ce anomaly in seawater.

Lanthanide distributions in evaporites have not been studied in any great detail. Some incomplete average analyses of evaporites from Russia were reported by Ronov et al. (1974). These data were characterized by very low concentrations with total lanthanide abundances being less than about 10–15 ppm.

8.4. *Iron formations*

Lanthanide abundances in these chemically precipitated sediments have the potential to reflect seawater composition at the time of deposition. Fryer (1977a)

TABLE 22
REE content [in ppm (wt)] of selected oxide facies iron formations and other iron-rich sediments.

Element	(1)	(2)	(3)	(4)
La	1.82	4.21	3.96	66.7
Ce	2.01	6.86	7.64	21.7
Pr	—	—	1.12	15.5
Nd	1.09	3.60	4.1	59.0
Sm	0.274	0.708	1.20	14.3
Eu	0.303	0.242	0.29	3.60
Gd	—	—	1.37	15.1
Dy	—	—	1.10	13.4
Ho	0.124	0.170	—	—
Er	—	—	0.55	6.76
Yb	0.289	0.374	—	3.92
Lu	0.0486	0.044	—	—
Total	—	—	22	222
La/Yb	6.3	11.3	—	17.0
La_N/Yb_N	4.3	7.6	—	11.5
Eu/Eu*	—	—	0.69	0.75
Y	—	—	5.77	59.9
Sc	—	0.320	—	—

(1) Archean oxide-facies iron formation, Temagami, Canada (Fryer 1977a, Analysis 22).
(2) Early Proterozoic oxide-facies iron formation, Sokomon Iron Formation (Fryer 1977b, analysis 16).
(3) Late Proterozoic oxide-facies iron formation, Rapitan Group, Canada (Fryer 1977a, analysis 6).
(4) Cyprus Ochres (Cretaceous) (Fryer 1977a).

noted significant difference in Eu content of early Precambrian and younger iron formations (table 22, fig. 38). He attributed this to changes in seawater composition related to increased amounts of free oxygen in younger oceans. Graf (1978), however, pointed out that changing oxidation states was an untenable explanation for differing Eu anomalies since Paleozoic volcanogenic iron formations from New Brunswick also commonly display positive Eu anomalies (Graf 1977, 1978). Kerrich and Fryer (1979) similarly noted strongly enriched Eu in Archean hydrothermal veins in the Dome Mine, Abitibi greenstone belt. This led to a reinterpretation of iron formation data (Fryer et al. 1979, Fryer 1983), relating Eu enrichment in Archean iron formations to much more vigorous hydrothermal activity. Such an interpretation is also consistent with more recent studies of the action of hydrothermal fluids in mid-ocean ridge environments (see section 7.5), which may also display extreme enrichment of Eu.

Figure 38 shows lanthanide abundance patterns for iron formations and for young iron-rich sediments from Cyprus. These patterns are normalised to the average contemporaneous sediment, reflecting the terrigenous sources of seawater lanthanides [PAAS is used for Post-Archean iron formations; average Archean shale

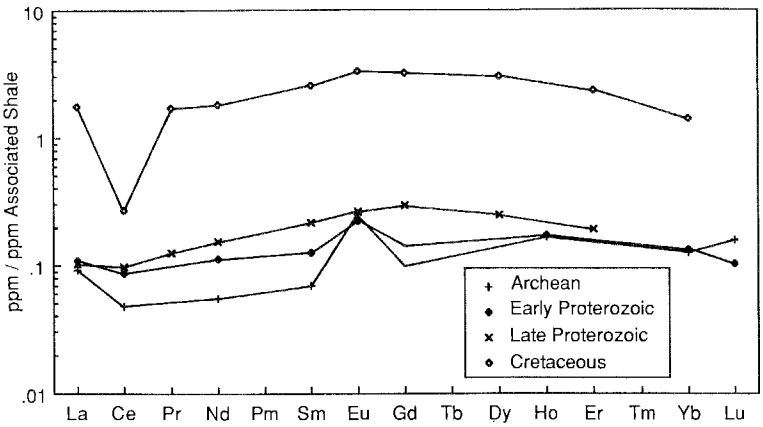

Fig. 38. Lanthanide abundance patterns for selected iron formations and iron-rich sedimentary rocks. Data are normalized to average shale values of the same period, Archean iron formation being normalized to average Archean shale (McLennan and Taylor 1984) and the others normalized to PAAS. In detail, iron formations exhibit considerable variability in lanthanide patterns. These samples illustrate the general feature of Eu enrichment, relative to contemporaneous upper continental crust, for Archean and early Proterozoic iron formations. The younger examples display no such Eu enrichment. This feature has been used to suggest that early Precambrian seawater was dominated by a hydrothermal signature, enriched in Eu (see fig. 30). (Data are from table 22.)

from McLennan and Taylor (1984) for the Archean examples]. In general, Archean and early Proterozoic examples show enrichment in Eu compared to contemporaneous sediments, whereas younger deposits have zero or negative Eu anomalies, unless they are closely associated, as in the case of the New Brunswick deposits, with hydrothermal activity (Graf 1977). The inference can be drawn that Archean and early Proterozoic oceans were dominated by hydrothermal activity. Younger iron formations reflect the decline of hydrothermal activity (associated with a declining global heat flux in post-Archean time) and the dominating influence of upper crustal signatures in ocean water chemistry. When iron formations are studied in detail, much complexity is found in lanthanide abundance patterns. For example, in a study of the Sokoman iron formation (Fryer 1977b) much variability was found both between and within silicate–carbonate and oxide facies. This resulted both from lanthanide mobility during diagenesis and to variable terrigenous components.

9. Sedimentary processes and lanthanide distribution

The other major example of a relatively uniform lanthanide abundance pattern, in addition to that observed in chondritic meteorites, is found in most terrigenous sedimentary rocks, notably shales (table 23). This pattern (fig. 39) is characterised by light-lanthanide enrichment, a pronounced depletion in Eu ($Eu/Eu^* = 0.66$) and for the heavy lanthanides, abundances parallel to, and about ten times those of

TABLE 23
REE content [in ppm(wt)] of shale composites and averages and average loess

Element	PAAS[a]	NASC[b]	ES[c]	Loess[d]
La	38	32	41.1	35.4
Ce	80	73	81.3	78.6
Pr	8.9	7.9	10.4	8.46
Nd	32	33	40.1	33.9
Sm	5.6	5.7	7.3	6.38
Eu	1.1	1.24	1.52	1.18
Gd	4.7	5.2	6.03	4.61
Tb	0.77	0.85	1.05	0.81
Dy	4.4	5.8	—	4.82
Ho	1.0	1.04	1.20	1.01
Er	2.9	3.4	3.55	2.85
Tm	0.40	0.50	0.56	—
Yb	2.8	3.1	3.29	2.71
Lu	0.43	0.48	0.58	—
Total REE	183	173	204	181
La/Yb	13.6	10.3	12.5	13.1
La_N/Yb_N	9.17	6.98	8.44	8.83
Eu/Eu*	0.66	0.70	0.70	0.66
Y	27	27	—	25
Sc	16	14.9	—	8.4

[a]Post-Archean average Australian shale; average of 23 post-Archean shales from Australia (Nance and Taylor 1976, Taylor and McLennan 1985).
[b]North American shale composite; composite of 40 North American shales (Haskin et al. 1968, Gromet et al. 1984).
[c]European shale composite; composite of numerous European shales (Haskin and Haskin 1966).
[d]Estimate of average carbonate-free loess (Taylor et al. 1983).

chondritic meteorites. This was the abundance pattern that Minami (1935) detected in European shales. Similar patterns are observed in sediments from other continents (fig. 39). Thus patterns for European, North American and Australian shales are indistinguishable. Similar patterns are observed back in time for about 2.0 Ae, toward the base of the Proterozoic. The igneous rocks, from which the continental crust was formed, have diverse patterns in contrast to the more uniform patterns observed in the sedimentary rocks (see section 7). The general interpretation of this observation is that the processes of weathering, erosion, transportation and deposition typically produce a thorough mixing of the differing lanthanide patterns in upper crustal rocks, and so provide geochemists with an overall average of the upper crust exposed to weathering. This useful observation simplifies the problems of studying the composition and geochemical evolution of the continental crust by resolving many of the problems in sampling that complex body. Central to this use of the lanthanides is their relative insolubility in natural waters under surface or near surface conditions of temperature and pressure. Before continuing this discussion, we address several related questions.

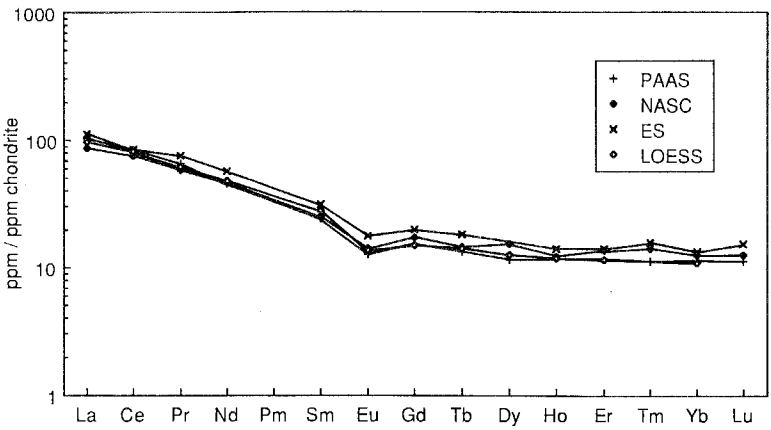

Fig. 39. The uniform lanthanide abundance patterns observed in terrigenous sedimentary rocks from widely separated geographical regions (PAAS, Australia; ES, Europe; NASC, North America and the wind-derived sediment, loess). This illustrates the general uniformity in the composition of the upper continental crust. (Data are from table 23.)

9.1. *Weathering*

Weathering is a dominant process governing the major element composition of sedimentary rocks (Nesbitt and Young 1984). Many trace elements may also be affected, but few studies have systematically examined the influence of weathering on lanthanide distribution. A major area of difficulty is in interpreting changes in absolute abundances, because of the significant volume changes which occur in the development of a weathering profile. As is the case with questions of lanthanide mobility the most vital question is whether significant fractionation occurs among the lanthanides during the weathering process.

Incomplete analyses or data of uncertain quality make much early work difficult to assess. The best documented study is that by Nesbitt (1979) who studied a weathering profile of the Torrongo granodiorite in southeastern Australia. Progressive enrichments (relative to Ti) up to twice the parent rock values were noted during moderate stages of weathering, with selective enrichment of the heavy lanthanides. Residual clays (mainly kaolinite and illite), preserved in cracks, displayed a complementary pattern (fig. 40). Nesbitt (1979) considered that the lanthanides were mobilised in response to pH changes in the soil and in ground waters. Fractionation of the lanthanides within the weathering profile was attributed to mineralogical changes. The complementary patterns in weathered and residual material indicated that there was no overall loss of lanthanides from the profile. Thus although the lanthanides may be mobilised during weathering, and may be fractionated, these effects appear to be confined within the weathering profile. The observed uniformity of lanthanide patterns in sedimentary rocks thus becomes explicable since reasonably efficient physical mixing of the profile during erosion and sedimentation will result in quantitative transfer and homogenisation of the lanthanides from parent rock to sediment.

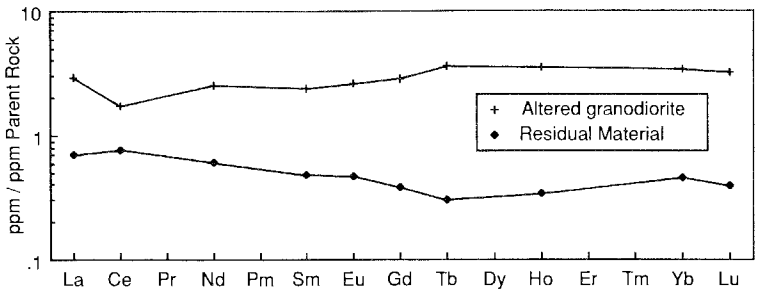

Fig. 40. Lanthanide patterns for weathered material from a granodiorite (Nesbitt 1979). Data normalized to the unweathered parent rock. Note the complementary pattern between the residual material found in fractures and the most altered granodiorite. Mixing of these patterns in a ratio of about 3:1 results in a pattern indistinguishable from the parent rock. This suggests that although some mobility of lanthanides occurs within the weathering profile, there is no significant loss or gain of lanthanides in the overall weathering profile.

9.2. *Sedimentary transport*

Variations both or grain size and mineral density result in separation of minerals and rock fragments during aqueous and aeolian transport of sedimentary material. Such transport may affect lanthanide abundance patterns in the resulting sedimentary rock because of the widely variable patterns in the constituent minerals. The two most important effects are

(a) Concentration of quartz in sands results in dilution of total lanthanide abundances, since quartz has extremely low lanthanide contents.

(b) Physical separation of heavy minerals, especially zircon, results in enrichment of the heavy lanthanides in sands.

9.3. *Diagenesis and metamorphism*

Only one detailed study has systematically examined the effects of diagenesis on lanthanide distributions. Chaudhuri and Cullers (1979) analysed Miocene/Pliocene sediments from a deep well (1.8–4.8 km depth) in the Gulf Coast of Louisiana, which was sampled through the illite/montmorillonite mixed layer of illite transition. Such variability as was seen in absolute lanthanide abundances and in La/Yb ratios was correlated to changes in provenance rather than to diagenetic factors.

Effects due to metamorphism are discussed in section 7.2. Although greenschist-to-amphibolite-facies metamorphism of regional extent commonly affects sedimentary rocks, no perceptible mobility of the lanthanides occurs.

9.4. *Location of lanthanide elements in sediments*

Quartz, feldspars, clay minerals and assorted rock fragments are the volumetrically most important constituents. Lanthanide contents for the major

TABLE 24
Lanthanide content [in ppm (wt)] of various grain size fractions in unconsolidated sediment.[a] (From Cullers et al. 1979.)

Element	Whole rock	Sand	Sand; less heavy minerals	Silt	Silt; less heavy minerals	Fraction < 2 μm	Weighted sum of fractions
La	7.3	4.4	3.0	31.5	22.6	27.8	8.05
Ce	15	9.2	6.3	73.1	48	61.6	17.7
Sm	1.53	0.98	0.45	7.48	4.31	4.62	1.78
Eu	0.29	0.17	0.077	1.42	0.78	0.08	0.32
Tb	0.25	0.20	0.05	1.19	0.59	0.61	0.32
Yb	1.50	1.25	0.31	4.5	2.22	2.2	1.62
Lu	0.23	0.20	0.052	0.84	0.36	0.40	0.27
Total REE	40	25	14	178	115	135	—
La/Yb	4.87	3.52	9.68	7.00	10.2	12.6	—
La_N/Yb_N	3.29	2.38	6.54	4.73	6.88	8.54	—
Eu/Eu*	0.58	0.50	0.60	0.59	0.59	0.57	—
Wt% of rock		86.0		10.2		3.8	

[a]Sample: Okaloosa shale Elkgaii (late Paleozoic).

rock forming minerals are given in table 15 and fig. 19. Quartz contains virtually no lanthanides, the amounts reported being principally contained in inclusions in that mineral. The most notable feature of the lanthanide distribution in feldspars is the extreme enrichment in Eu, due to substitution of Eu^{2+} for Sr^{2+} (in Ca^{2+} lattice sites). Clay minerals in sedimentary rocks result from the breakdown of feldspar glass, and the more labile igneous minerals, and are individually difficult to separate.

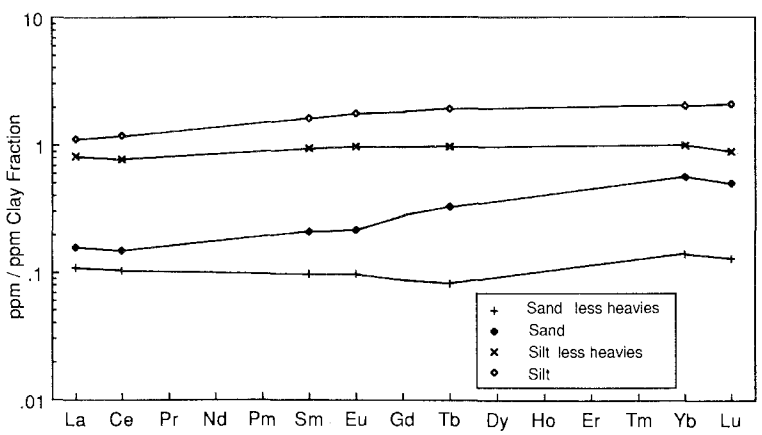

Fig. 41. Lanthanide patterns for various grain size fractions of an unconsolidated sediment. Data normalized to the <2 μm fraction, the closest approximation to a shale derived from the same source. (Data are from table 24.)

TABLE 25
Lanthanide content [(in ppm (wt)] of some common accessory minerals.

Element	(1)	(2)	(3)	(4)	(5)	(6)	(7)	(8)
La	—	—	—	119,000	—	—	—	10.3
Ce	42.3	20.0	509	195,000	66,560	152	3305	13.7
Pr	—	—	—	32,100	—	—	—	—
Nd	14.9	15.0	302	98,000	16,060	58.2	2680	—
Sm	5.40	15.1	52.9	24,500	1,260	9.45	655	1.86
Eu	1.27	1.42	15.2	635	133.3	3.38	165	0.11
Gd	17.4	53.6	—	14,700	460	8.15	564	—
Tb	—	—	—	1,960	—	—	—	0.16
Dy	56.9	122	31.7	7,710	118.4	5.67	470	—
Ho	—	—	—	1,400	—	—	—	—
Er	116	77.9	17.1	—	28.5	2.69	237	—
Yb	253	70.3	13.9	540	17.4	2.10	207	0.59
Lu	—	10.1	—	—	—	—	—	0.10

(1) Zircon, granodiorite (Gromet and Silver 1983).
(2) Garnet, dacite (Schnetzler and Philpotts 1970).
(3) Apatite, granodiorite (Gromet and Silver 1983).
(4) Monazite, granite (Lee and Bastron 1967).
(5) Allanite, granodiorite (Gromet and Silver 1983).
(6) Epidote, granodiorite (Gromet and Silver 1983).
(7) Sphene, granodiorite (Gromet and Silver 1983).
(8) Tourmaline, granite (Arniaud 1984).

Lanthanide abundances in various grain size fractions (and in accessory heavy minerals) were examined by Cullers et al. (1979) in an attempt to address this problem. They concluded that

(a) The bulk of the lanthanide elements reside in the fine-grained (clay and silt) fraction, but that there is no correlation with specific clay moneralogy. This is perhaps not too surprising, since most clay minerals are disordered, with irregularities in composition, mixed layering and misfits between tetrahedral and octahedral sheets which all provide ample opportunities for accomodating the trivalent lanthanide ions.

(b) Although the silt fraction has lower abundances, they do not differ from the lanthanide patterns in finer fractions (down to <1 μm).

(c) Sands have significantly lower total abundances and lower La/Yb ratios than finer-grained fractions.

(d) Significant enrichment of the heavy lanthanides due to the presence of heavy minerals may occur in silt and sand fractions.

(e) Eu anomalies are similar in all size fractions.

A particularly good example of these effects is illustrated in table 24 and fig. 41.

The potential of heavy minerals to distort lanthanide patterns in sedimentary rocks is well recognised (see table 25 and fig. 42 for some typical lanthanide abundances and patterns in common heavy, or accessory minerals). An example from Archean metaquartzites from the Western Gneiss Terrain, Australia is instructive (Taylor et al. 1986). Enrichments of light lanthanides were observed in

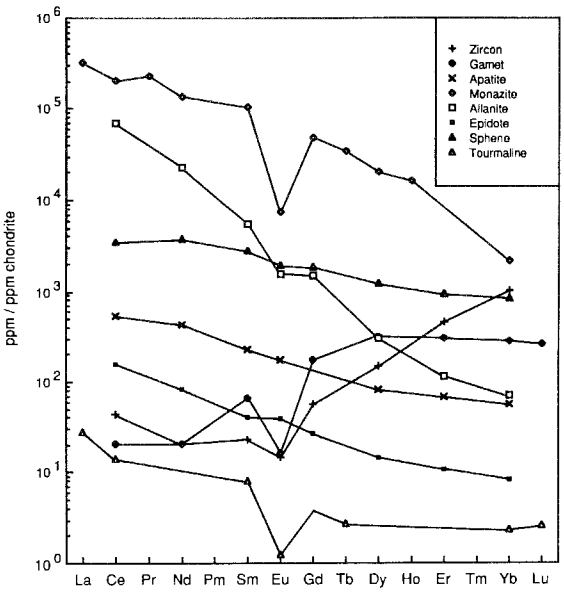

Fig. 42. Lanthanide abundance patterns for accessory minerals. Note in particular the high abundances are light lanthanide enrichment of monazite and allanite, and the extreme heavy lanthanide enrichment of zircon. (Data are from table 24.)

samples with the highest contents of SiO_2 (fig. 43). This unusual behaviour was due to the presence of monazite. Microprobe analyses indicated that only 0.1–0.3% of the mineral was sufficient to account for the enrichment. However, it should be noted that these minerals are only rarely concentrated in amounts sufficient to cause perceptible effects on the lathanide patterns of sedimentary rocks. This may be shown by considering the resistant mineral zircon, typically enriched in heavy lanthanides. The bulk rock patterns are only affected when zircon constitutes more

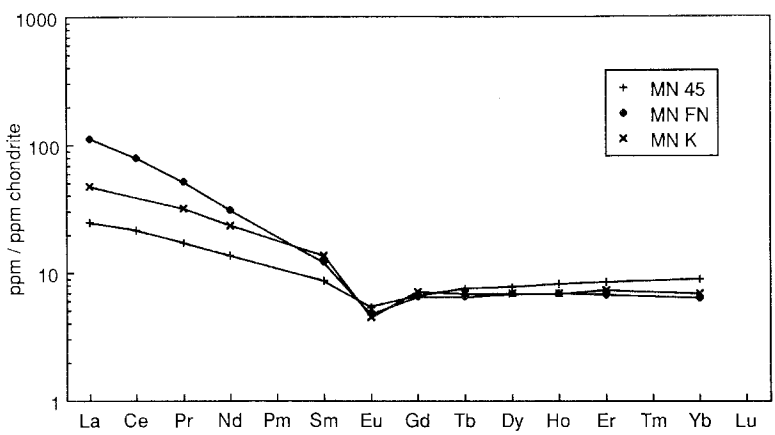

Fig. 43. Enrichment of light lanthanides in Archean quartz-rich sedimentary rocks (MN, FN and MNK) from Western Australia, due to high abundance of monazite. The other sample (MN45) has much lower silica content and does not exhibit any enrichment in light lanthanides. (Data are from Taylor et al. 1986.)

than about 0.06% (or Zr abundances exceed about 300 ppm), since every 100 ppm of Zr as zircon adds only abour 0.25 times chondritic levels of Yb (typical bulk rock patterns are about 10 times chondritic for that element).

10. Terrigenous sedimentary rocks

Goldschmidt (1938) was the first to suggest that the homogenizing effects of sedimentary processes should result in nearly constant lanthanide distributions in sedimentary rocks and that the pattern should reflect upper continental crust abundances. Although findings by e.g. Ronov et al. (1974), Cullers et al. (1975, 1979), Dypvik and Brunfelt (1976) and Bhatia (1985) have shown significant variability in some sedimentary environments, the original prediction of Goldschmidt has proven remarkably accurate. This is especially the case for fine-grained terrigenous sedimentary rocks (i.e. shales). The remarkable similarity of their lanthanide patterns adds a great deal of support to the idea that the composition of shales reflects the composition of the exposed crust.

Taylor and McLennan (1981) suggested that while lanthanide patterns in fine-grained sedimentary rocks were parallel to upper crustal abundances, they probably overestimated the absolute abundances by about 20%. Mass balance calculations involving averages of the various sedimentary rock types (shales, sandstones, carbonates, evaporites) substantiate this adjustment (Taylor and McLennan 1985).

Haskin and Gehl (1962) were the first to notice unusual lanthanide patterns for Precambrian sedimentary rocks. Haskin et al. (1968) confirmed a relative enrichment of Eu in Precambrian sedimentary rocks compared to the North American Shale Composite (NASC) sample. More detailed studies by Wildeman and Haskin (1973) and by Wildeman and Condie (1973) confirmed Eu enrichment and lower total lanthanides for Precambrian sedimentary rocks. Most of the samples for these latter studies came from Archean terrains. These differences in lanthanide patterns between Archean and post-Archean terrigenous sediments have become a crucial observation for models of the evolution of the continental crust.

The Eu depletion in post-Arcean sedimentary rocks can be taken as strong evidence for an intracrustal origin for much of the upper crust. No common volcanic rock derived directly from the mantle (i.e. primitive) exhibits negative Eu anomalies (e.g. Bence et al. 1980, Basaltic Volcanism Study Project 1981). Thus the most likely mechanism for producing Eu depletion is partial melting where feldspar is a residual phase. Since Ca-plagioclase is not stable below about 40 km ($\sim$10 kbar pressure), Eu anomalies are probably produced by shallow melting processes within the crust (or very shallow mantle).

10.1. *Post-Archean sedimentary rocks*

The most remarkable feature of the lanthanide abundance patterns in post-Archean sedimentary rocks is their uniformity. Figure 44 shows patterns for

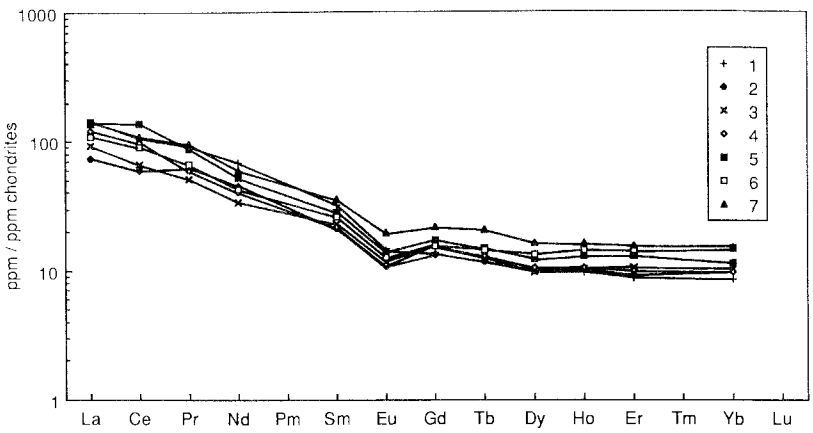

Fig. 44. Lanthanide abundance patterns in Australian shales ranging in geological age from mid-Proterozoic to Triassic. There is no change in the relative abundance patterns over a period of about 1.5 billion years. (See table 26 for sample details.)

TABLE 26
REE content [in ppm(wt)] of selected Australian shales of post-Archean age.

Element	(1)	(2)	(3)	(4)	(5)	(6)	(7)
La	51.0	27	34	44	52	40	50
Ce	103	57	63	94	132	86	104
Pr	12.8	8.8	7.0	8.1	12	9.1	13
Nd	48	32	24	29	37	30	43
Sm	7.39	4.9	5.3	5.0	6.5	6.0	8.2
Eu	1.23	0.94	1.0	0.95	1.2	1.1	1.7
Gd	4.19	4.0	4.8	4.7	5.2	4.7	6.7
Tb	0.68	0.68	0.71	0.74	0.84	0.82	1.2
Dy	3.80	3.8	3.7	4.0	4.6	5.0	6.2
Ho	0.83	0.86	0.87	0.89	1.1	1.2	1.4
Er	2.15	2.3	2.6	2.5	3.2	3.6	3.8
Yb	2.10	2.4	2.5	2.4	2.8	3.6	3.7
Total REE	238	145	149	196	258	192	242
La_N/Yb_N	16.4	7.6	9.2	12.4	12.6	7.5	9.2
Eu/Eu*	0.67	0.65	0.61	0.60	0.63	0.63	0.70
Y	30	18	20	34	36	29	38
Sc	17	13	19	20	15	19	21

(1) 46436, Earaheedy Gp., Nabberu Basin (*c*: 1.7 Ae) (McLennan 1981).
(2) M15, Mount Isa Gp, (*c*: 1.7 Ae) (Nance and Taylor 1976).
(3) A010, Pertatataka Fm., Amadeus Basin (*c*: 0.85 Ae) (Nance and Taylor 1976).
(4) SC8, State Circle shale (Silurian) (Nance and Taylor 1976).
(5) PL6, Laurel Fm., Canning Basin (Carboniferous) (Nance and Taylor 1976).
(6) PL1, Poole Sst., Canning Basin (Permian) (Nance and Taylor 1976).
(7) PW5, Kockatea shale, Perth Basin (Triassic) (Nance and Taylor 1976).

Australian shales dating back to the mid-Proterozoic (data are from table 26). These patterns, which are representative of the data base for the Australian average shale (PAAS), are similar to those of composite shale samples from Europe (ES) and North America (NASC). All these patterns are characterised by light-lanthanide enrichment and relatively flat heavy lanthanides (at about 10 times chondritic), and a rather uniform depletion in Eu ($Eu/Eu^* = 0.65$). This uniformity both within and between continents is interpreted to represent the lanthanide abundances in the upper continental crust exposed to weathering.

The lanthanide patterns for many modern sediments are similar to that of the post-Archean shales. The chemical composition of suspended particulate matter in some of the world's major rivers was examined by Martin and Meybeck (1979) (table 27, fig. 45). The patterns are very similar to PAAS although slightly enriched in total lanthanides (about 1.1–1.4 times). The cause of the enrichment is probably related to grain size.

Coarser-grained sedimentary rocks such as arkoses typically have lanthanide patterns which are parallel to those of shales. Chondrite-normalised plots are given in fig. 46 (table 28). The patterns of these sandstones tend to have lower total abundances than shales, although, like shales, the values are quite variable. A number of authors have noted the lower abundances in coarser-grained sedimentary rocks as compared to shales (Haskin et al. 1966b, Nance and Taylor 1976, Culler et al. 1979). On the other hand, the overall shape of the patterns (Eu/Eu^*, La_N/Yb_N, etc.) is generally similar for such sandstones and shales.

The lanthanide abundances in quartz-rich sedimentary rocks (quartzites, orthoquartzites, etc.) are typically very low (table 28, fig. 46). The shape of the pattern, however, is similar to that of typical shales. As discussed above, the role of heavy minerals is more important when sizeable clay fractions are absent (Cullers et al. 1979, Taylor et al. 1986, see also below). The most common effect is to cause enrichment of the heavy lanthanides (Gd–Lu).

TABLE 27
REE content [in ppm (wt)] of particulate matter from selected rivers. (From Martin and Meybeck 1979.)

Element	Amazon	Ganges	Garonne	Mekong
La	48	42	44	48
Ce	112	98	93	93
Nd	—	48	36	47
Sm	9.7	9.7	6.2	5.4
Eu	1.8	1.2	1.1	1.5
Gd	—	—	6.1	5.3
Tb	—	0.7	0.9	0.9
Yb	3.7	3.2	2.8	3.2
Lu	0.6	0.51	0.42	0.58
La/Yb	13.0	13.1	15.7	15.0
La_N/Yb_N	8.77	8.87	10.6	10.1
Eu/Eu^*	0.57	0.51	0.54	0.85
Sc	18	11.5	—	19.5

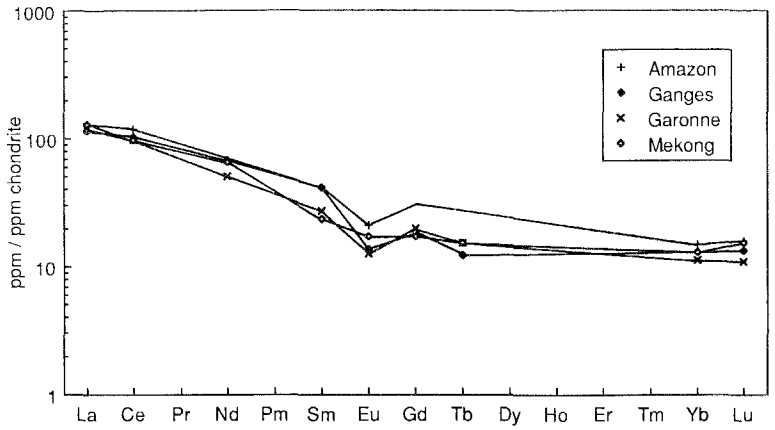

Fig. 45. Lanthanide abundance patterns in particulate matter from rivers. Most samples have a pattern similar to PAAS. (Data are from table 27.)

The origin of the marked depletion of Eu typical of chondrite-normalised lanthanide patterns in terrigenous sedimentary rocks is not due to surficial processes of oxidation or reduction. Neither, however, is it due to mantle processes, since igneous rocks of mantle derivation rarely display Eu anomalies. Eu is present as the trivalent ion in sediments and the depletion in Eu is the signature of an earlier igneous event, when Eu was divalent under reducing conditions. The generally accepted explanation is that intra-crustal melting, which produced K-rich granites and granodiorites which now dominate the upper crust, left Eu in residual plagioclase phases in the lower crust. Thus the presently observed depletion records a major event of crustal evolution.

Such post-Archean patterns are typically not observed in the Archean (see section 10.3). McLennan et al. (1979b) studied early Proterozoic (about 2.5–2.2 billion years old) sedimentary rocks from the Huronian sequence of Canada. They found a

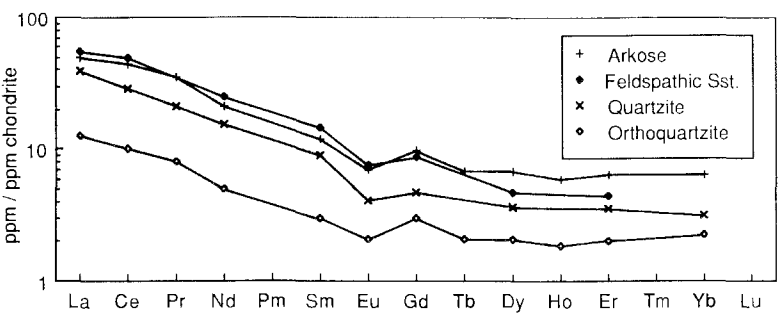

Fig. 46. Lanthanide abundance patterns for arkoses and quartzites. Note the overall lower abundances but similar patterns to typical shales. Quartzites, with very low abundances and high heavy-mineral concentrations, can exhibit some heavy lanthanide enrichment. (Data are from table 28.)

TABLE 28
REE content [in ppm (wt)] of selected feldspathic sandstones and quartzites.

Element	(1)	(2)	(3)	(4)
La	18	20	14.4	4.7
Ce	42	47	27.8	9.7
Pr	4.8	–	2.91	1.1
Nd	15	18	11.0	3.6
Sm	2.8	3.4	2.12	0.70
Eu	0.61	0.67	0.36	0.18
Gd	3.0	2.7	1.44	0.93
Tb	0.40	–	–	0.12
Dy	2.6	1.8	1.38	0.80
Ho	0.51	–	–	0.16
Er	1.6	1.1	0.88	0.50
Yb	1.6	–	0.78	0.56
Total	93	–	64	23
La/Yb	11.3	–	18.5	8.39
La_N/Yb_N	7.60	–	12.5	5.67
Eu/Eu*	0.64	0.68	0.63	0.68
Y	13	–	2.57	3.5

(1) Triassic arkose, Perth Basin, Australia (Nance and Taylor 1976).
(2) Early Proterozoic feldspathic sandstone, Serpent Formation, Canada (McLennan et al. 1979a).
(3) Late Archean quartzite, Witwatersrand Supergroup, South Africa (95.0% SiO_2) (McLennan et al. 1983).
(4) Permian orthoquartzite (PL4), Canning Basin, Australia (96.7% SiO_2) (Nance and Taylor 1976).

progressive change through the succession from Archean-like lanthanide patterns at the base to typical post-Archean patterns at the top. This was interpreted to reflect an episodic change in upper crustal composition, related to a massive emplacement of K-rich granitic rocks, depleted in Eu, toward the close of the Archean. Similar abrupt changes in the lanthanide patterns in terrigenous sedimentary rocks are observed over time intervals from 3.3 to 2.5 Ae in South Africa (Taylor et al. 1983) and in Western Australia (Taylor and McLennan 1985). Thus the changes in upper crustal composition occurred at differing times in different regions, and mark the development of fully stabilised continental crust.

10.2. *Plate tectonic controls on lanthanide patterns in sedimentary rocks*

The ability of plate tectonic theory to explain many geological features is once again illustrated by the chemical and petrographic composition of terrigenous sedimentary rocks (e.g. Dickinson and Suczek 1979, Maynard et al. 1982). Much of the variability observed in these rocks occurs in greywacke–turbidite sequences deposited at continental margins and can be understood in relation to plate tectonics. Such sequences and depositional environments represent the closest

TABLE 29
REE content [in ppm (wt)] of selected Phanerozoic greywackes.

Element	Magmatic arc				Recycled orogen		Continental block	
	Undissected		Dissected					
	M277	M285	P40136	MK64	MK84	MK86	P39803	MK97
La	10	6.8	35.5	25	39	35	35.8	43
Ce	18	15	80.7	53	82	75	69.1	83
Pr	2.2	2.0	–	5.8	9.7	9	–	12
Nd	10	8.2	–	22	37	35	45	42
Sm	2.8	2.2	5.33	4.5	7.3	6.2	8.09	7.1
Eu	0.97	1.1	1.11	0.9	1.2	0.99	1.31	1.0
Gd	3.4	2.6	–	3.5	5.6	3.8	–	5.6
Tb	0.52	0.39	0.65	0.6	0.95	0.64	0.64	0.88
Dy	3.1	2.7	–	3.6	5.5	4.4	–	4.7
Ho	0.79	0.59	–	0.8	1.2	0.94	–	1.0
Er	2.2	1.9	–	2.2	3.6	2.8	–	2.9
Yb	2.3	1.8	1.62	2.0	3.2	2.8	2.85	2.9
Lu	–	–	0.34	–	–	–	0.48	–
Total REE	56	45	176	124	196	177	186	207
La_N/Yb_N	2.94	2.55	14.8	8.45	8.24	8.45	8.49	10.0
Eu/Eu*	0.96	1.41	0.70	0.69	0.57	0.62	0.63	0.48
Y	19	15	–	22	32	27	–	32
Sc	37	25	16.3	25	8	10	10	10

M277, M285, Baldwin Formation (Devonian), Australia (Nance and Taylor 1977, Taylor and McLennan 1985).
P40136, Robertson Bay Group (late-Proterozoic–Cambrian), Antarctica (Nathan 1976).
MK64, Hill End Suite (Silurian–Devonian), Australia (Bhatia 1985, Bhatia and Crook 1986).
MK84, MK86, Hodgkinson Suite (Devonian) Australia (Bhatia 1985, Bhatia and Crook 1986).
P39803, Greenland Group (Ordovician), New Zealand (Nathan 1976).
MK97, Bendigo Suite (Ordovician), Australia (Bhatia 1985, Bhatia and Crook 1986).

modern analogue to conditions under which most Archean terrigenous sediments were deposited. This has led to some superficial and unrealistic comparisons and interpretations and is discussed at length here for these reasons.

Dickinson and Suczek (1979) divided sandstones (including greywacke–turbidite sequences) into three basic provenance types. These are magnatic arcs (ranging from volcanogenic to dissected), recycled orogens (e.g. foreland basins) and continental blocks (e.g. passive margins). Some representative analyses from these environments are given in table 29 and shown on figs. 47 and 48. Only greywackes from undissected magmatic arcs are totally devoid of a signature of depletion in Eu (Eu/Eu* = 1). Greywackes from other environments have lanthanide patterns which range from those indistinguishable from PAAS (Eu/Eu* = 0.66) to some mixture of these two end-member patterns (Nathan 1976, Bhatia 1985). These variations are the result of the addition of differing amounts of an arc-derived component to an

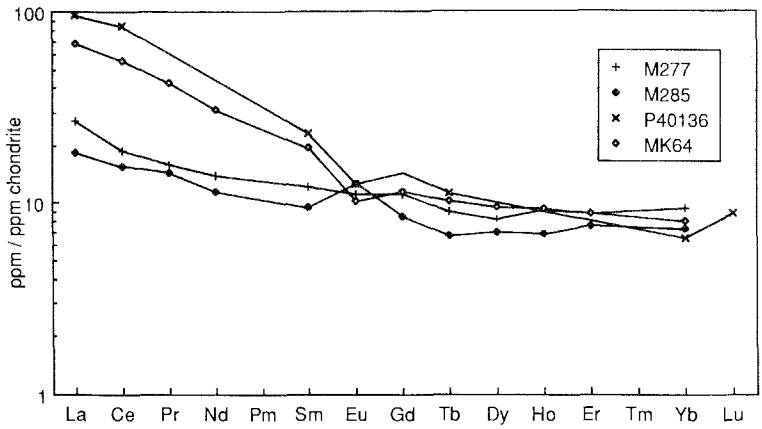

Fig. 47. Lanthanide abundance patterns for Phanerozoic greywackes from magmatic arcs. Samples from undissected (immature) arcs (M277, M285) have only slight light lanthanide enrichment and lack negative Eu anomalies, thus showing a superficial resemblance to some Archean sedimentary rocks from greenstone belts (see figs. 49 and 50). Examples of dissected magmatic arcs (P40136, MK64) have patterns more similar to PAAS with a substantial depletion in Eu. (Data are from table 29.)

upper crustal lanthanide pattern. In contrast to post-Archean greywackes, Archean turbidites are not depleted in Eu, although they mostly would be classified as being derived from dissected magmatic arcs or recycled orogens (McLennan 1984).

Present-day examples of turbidites deposited at continental margins (McLennan et al. 1985) generally confirm these ideas, but recognise the existence of Eu depletion even in a number of fore-arc basins, indicating that a component of fractionated upper crustal material is being deposited there. Thus in present-day examples, Eu

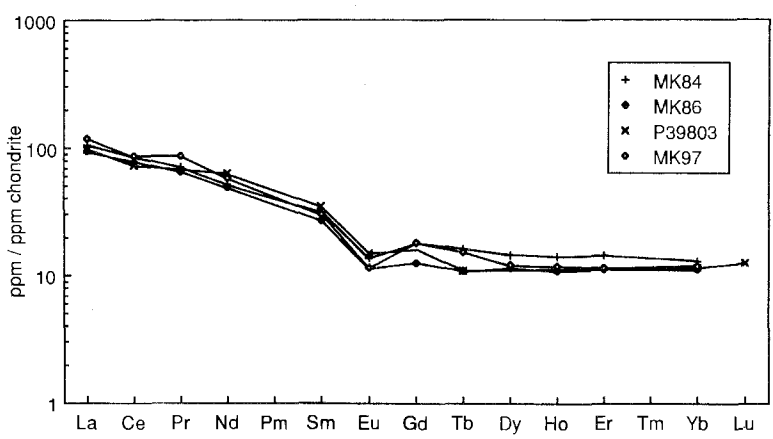

Fig. 48. Lanthanide abundance patterns for Phanerozoic greywackes from recycled orogen (MK84, MK86) and continental block (P39803, MK97) provenances. These varieties of greywackes exhibit distinct negative Eu anomalies. (Data are from table 29.)

depletion in turbidite sands is nearly ubiquitous and is entirely missing only in fore-arc basins in a wholly oceanic environment.

The use of such lanthanide patterns to distinguish between ancient tectonic environments of sandstone deposition (e.g. Bhatia 1985) is seductive but premature for the following reasons:

(a) The present data based for lanthanide patterns in greywackes is small,

(b) A thorough investigation of modern environments is needed before extrapolation into the past is warranted. An example of the hazards is the transport of sediment across tectonic boundaries. Thus samples from the trough in front of the Lesser Antilles island arc, which might be expected to show an andesitic pattern with no Eu depletion, have typical post-Archean patterns with strong depletion in Eu (White et al. 1985). These sediments are in part being derived by lateral transport from the South American continental shield (a trailing-edge setting), a result confirmed by Nd isotopic data.

(c) The experience of using the elemental signatures of igneous rocks to discriminate between differing tectonic settings (e.g. Pearce and Cann 1973) has shown that much caution is needed, and that unequivocal indicators are unlikely.

10.3. *Archean sedimentary rocks*

The distribution and significance of the lanthanide patterns in Archean sedimentary rocks has been extensively reviewed by McLennan and Taylor (1984) and by Taylor and McLennan (1985). These dealt chiefly with the relatively well-preserved low-grade sediments of the ubiquitous greenstone belts. Turbidites are the most abundant type of sediment in greenstone belts. Early work noted both the absence of Eu anomalies and the general resemblance to the lanthanide patterns of island-arc volcanic rocks such as andesites (e.g. Wildeman and Haskin 1973, Wildeman and Condie 1973, Jakes and Taylor 1974, Nance and Taylor 1977, Bavinton and Taylor 1980). It was soon realised that the lanthanide patterns on their own could not distinguish between a source from the sediments from island-arc volcanics or from a mixture of the ubiquitous bimodal suite of basaltic and felsic igneous rocks (tonalites, trondhjemites, dacites) which characterise many Archean terrains (see section 7.4).

Subsequent work demonstrated the extreme variability of lanthanide patterns in these sediments (e.g. Jenner et al. 1981, McLennan and Taylor 1983, McLennan et al. 1983, 1984, Ujike 1984). Although most have intermediate patterns (fig. 49), both very steep and flat patterns are locally abundant (fig. 50), and support, along with other geochemical data, derivation of these sediments from the Archean 'bimodal igneous suite', which dominates the Archean upper crust (table 30).

The distinction between the lanthanide patterns of Archean and post-Archean sediments, as discussed in the next section, is a crucial piece of evidence for models of crustal evolution. Some workers (e.g. Gibbs et al. 1986) have argued that this distinction is largely a reflection of differing tectonic settings, without age significance, and that post-Archean greywackes are identical to those of Archean age. However, as discussed above, the former display the signatures of Eu depletion

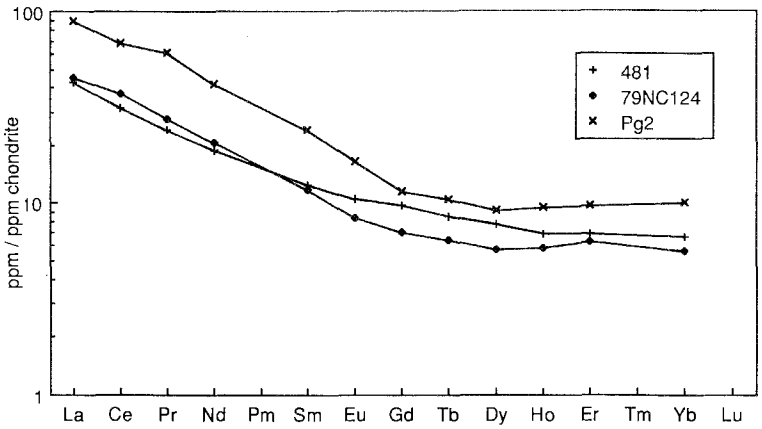

Fig. 49. Typical lanthanide patterns for Archean sedimentary rocks from greenstone belts showing light lanthanide enrichment and lack of Eu anomalies. Such a pattern can be explained by derivation of the greywackes either from andesitic sources or from a bimodal basic–felsic igneous source. Several lines of evidence indicate that the latter model is most likely. (Data are from table 30.)

(although not always as large as in PAAS) in all tectonic environments except fore-arc basins of oceanic island arcs. Moreover, geological and petrographic evidence suggest tectonic settings such as back-arc, continental arc, trailing edge and foreland basins for many Archean greywackes, particularly those for which lanthanide abundances have been determined. Further, the overall evidence for derivation from the 'bimodal suite' rather than from 'andesites' makes the supposed analogy with modern arc environments superficial (see discussion by McLennan and Taylor 1984).

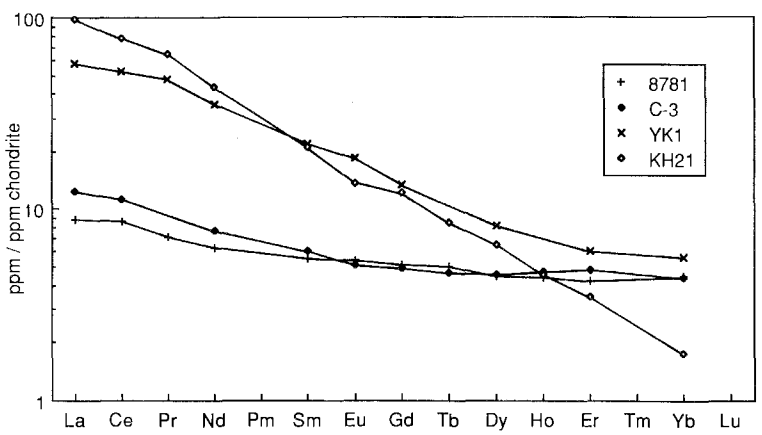

Fig. 50. Both steep (KH21, YK1) and flatter (C-3, 8781) lanthanide abundance patterns are observed in Archean sedimentary rocks, and reflect derivation from felsic and basic igneous rocks, and lend weight to the suggestion that a bimodal mixing model best explains the provenance of Archean sedimentary rocks in greenstone belts. (Data are from table 30.)

TABLE 30
REE content [in ppm (wt)] in selected fine-grained sedimentary rocks from Archean greenstone belts

Element	(1)	(2)	(3)	(4)	(5)	(6)	(7)
La	3.23	4.6	15.5	16.7	32.5	21	36
Ce	8.28	10.9	29.9	35.7	65.7	50	75
Pr	0.98	–	3.33	3.77	8.33	6.5	8.9
Nd	4.46	5.5	13.4	14.7	29.9	25	31
Sm	1.26	1.39	2.87	2.73	5.62	5.1	4.9
Eu	0.47	0.44	0.92	0.73	1.43	1.6	1.2
Gd	1.55	1.5	2.97	2.14	3.51	4.1	3.7
Tb	0.29	0.27	0.49	0.37	0.61	–	0.49
Dy	1.71	1.73	2.93	2.18	3.52	3.1	2.5
Ho	0.37	0.40	0.59	0.50	0.81	–	0.39
Er	1.06	1.2	1.71	1.57	2.41	1.5	0.87
Yb	1.10	1.09	1.66	1.38	2.51	1.4	0.44
Total	25	31	77	83	158	121	162
La/Yb	2.94	4.22	9.34	12.1	12.9	15.0	81.8
La_N/Yb_N	1.98	2.85	6.31	8.18	8.75	10.1	55.3
Eu/Eu*	1.03	0.93	0.96	0.92	0.98	1.07	0.86
Y	7.35	–	19.1	21	29	20	11
Sc	–	28	–	15	–	–	22

(1) 8781, Kambalda, Yilgarn Block, Australia (Bavinton and Taylor 1980).
(2) C-3, Fig Tree Group, Barberton, South Africa (Condie et al. 1970, Wildeman and Condie 1973).
(3) 481, Kambalda, Yilgarn Block, Australia (Bavinton and Taylor 1980).
(4) 79NC124, Moodies Group, Barberton, South Africa (McLennan and Taylor 1983).
(5) Pg2, Gorge Creek Group, Pilbara Block, Australia (McLennan et al. 1983).
(6) YK1, Yellowknife Supergroup, Slave Province, Canada (Jenner et al. 1981).
(7) KH21, Kalgoorlie, Yilgarn Block, Australia (Nance and Taylor 1977, Taylor and McLennan 1985).

Significant advances in our understanding of the sedimentary sequences preserved in high-grade metamorphic terrains have occurred more recently (Taylor et al. 1986). Studies of such terrains from Greenland (Boak et al. 1982, Dymek et al. 1983, McLennan et al. 1984), India (Naqvi et al. 1983), Montana–Wyoming (Mueller et al. 1982, Gibbs et al. 1986), Canadian Shield (Sawyer 1986, Taylor et al. 1986), Western Gneiss Terrain, Australia and Limpopo Belt, South Africa (Taylor et al. 1986) have indicated that these regions commonly represent a tectonic environment distinct from that of the greenstone belts. Typical lanthanide patterns in fig. 18 (see also fig. 43) show that they fall into two groups (see table 14 for data). One group [e.g. Kapuskasing (Taylor et al. 1986) and Quetico Belt, Canada (Sawyer 1986)] has patterns indistinguishable from those of Archean greenstone belt sediments and are simply highly metamorphosed equivalents. A second group [Montana–Wyoming (Gibbs et al. 1986), Western Gneiss Terrain (Taylor et al. 1986)] is indistinguishable from typical post-Archean patterns, and represents deposition on a stable shelf environment, most probably occurring on small stable mini-cratons (see Taylor et al. 1986 for discussion).

In India, Greenland and the Limpopo Belt, both groups of patterns are found, demonstrating, as is the case for many Archean sediments, the relative importance of local provenance. In such regions, small areas of stable crust (mini-cratons) must exist in close association (<100 km) with greenstone belts, but neither area is contributing significant amounts of erosional debris to the other. The relative proportions of these Archean mini-cratons and greenstone belts is complicated by the tendency of the greenstone-belt environments to destruction by erosion and recycling (Veizer 1984, Veizer and Jansen 1985), so that the high-grade belts are preferentially preserved. They probably represented about 10 percent of the Archean crust (Taylor et al. 1986).

10.4. *Loess*

About ten percent of the land surface of the earth is covered with loess of Pleistocene age. The blanketing deposits may in places exceed 100 m in thickness, and have been the cause of much debate, puzzling geologists as perceptive as Lyell (Taylor et al. 1983). The aeolian origin of loess was originally proposed by von Richthofen (1882) and this hypothesis has survived. The origin of loess by aeolian transport from glacial outwash deposits, particularly during cold dry climatic regimes, appears well established. The uniformity of grain size in loess is presumably due to wind transport, while the angularity of the grains attests to a glacial, rather than a desert origin. Glacial erosion grinds up rocks, a task carried out less efficiently by geochemists. This combination of widespread production of silt-sized rock flour, and its transport by wind over tens to hundreds of kilometres thus provides geochemists with a natural sampling of comparatively unweathered material from the exposed crust.

The lanthanide patterns for loesses from widely scattered localities (North America, Europe, China) show very uniform abundances (Taylor et al. 1983), with Eu depletions essentially equivalent to those observed in clastic sedimentary rocks (table 31, fig. 51). The lanthanide data for the New Zealand loesses show slightly lower Eu depletion, reflecting their derivation from greywackes. The uniformity of the lanthanide patterns for the widely scattered loess deposits and their similarity to PAAS, ES and NASC indicates that loess is providing the same information on the composition of the upper crust as that provided by clastic sediments. In addition to providing the information that upper crustal abundances are uniform on a world-wide scale, the loess data provide another significant piece of information concerning crustal evolution.

The loess ages for the Nd model cover a wide range, indicating that their source rocks were derived from the mantle over periods ranging from about 500 million years to about 1500 million years (Taylor et al. 1983). Nevertheless, their lanthanide abundance patterns are uniform. Accordingly, the processes producing the upper crustal composition, which is being sampled during the formation of loess, have remained the same well back into the Proterozoic. This conclusion reinforces the previous evidence for uniformity of crustal composition back to early Proterozoic times.

TABLE 31
Rare earth element composition [data in ppm (wt)] of loesses. (Adapted from Taylor et al. 1983.)

Element	(1)	(2)	(3)	(4)	(5)
La	35.2	38.5	34.0	33.1	30
Ce	72.0	84.9	77.0	74.1	64
Pr	8.74	9.14	7.14	8.08	7.1
Nd	32.9	35.2	31.7	36.0	26
Sm	5.86	6.66	5.89	6.78	4.5
Eu	1.16	1.28	0.95	1.14	0.88
Gd	4.14	4.98	4.00	4.52	3.8
Tb	0.68	0.92	0.63	0.88	0.64
Dy	3.78	5.48	3.49	5.34	3.5
Ho	0.82	1.19	0.77	1.05	0.80
Er	2.24	3.24	2.12	3.07	2.3
Yb	2.13	2.85	2.17	3.15	2.2
Total	170	194	170	177	146
Eu/Eu*	0.72	0.68	0.60	0.63	0.66
La_N/Yb_N	11.2	9.1	10.6	7.09	9.3
Y	21	26	22	–	22
Sc	7.6	11.9	5.7	–	11.0

(1) Banks Peninsula 5, New Zealand.
(2) Nanking, China.
(3) Kansas A, USA.
(4) Iowa, USA.
(5) Average upper crust (Taylor and McLennan 1985).

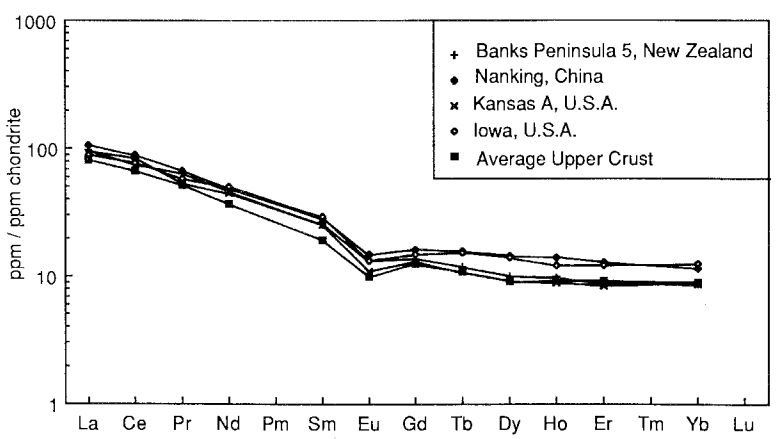

Fig. 51. The lanthanide abundance patterns for the aeolian sediment, loess, from China, New Zealand and USA are parallel to that of average upper crust so reflecting the composition of the upper continental crustal material. (Data are from table 31.)

11. Composition and evolution of the continental crust

The continental crust, although it comprises only about 0.5% of the volume of the earth, nevertheless contains substantial concentrations of elements such as K, La and U, which are concentrated in residual melts during igneous fractionation processes. Accordingly the crust is a major geochemical reservoir and its overall composition is important for geochemical models of the bulk earth. However, the problem of sampling the diverse and heterogeneous continental crust is formidable. Major compositional changes occur, sometimes on a scale of meters, as even the most cursory glance at a geological map will testify. Thus it is a herculean task to set up an appropriate sampling procedure to provide a reliable average. Nature, however, has carried out its own overall sampling of the crust through the processes of erosion and sedimentation. In this context, the rare earths possess the desirable property of being relatively insoluble and so have short residence times in water. They are thus transferred quantitatively during erosion and sedimentation from the parent rocks into clastic sediments. Although the heterogeneous source rocks of the crust contribute diverse lanthanide patterns, the very uniform patterns observed in terrigenous sediments testifies to the efficient mixing which occurs during their production. For these reasons, rare earth abundances, and lanthanide abundances in particular, in sedimentary rocks have helped to resolve the sampling problems and have provided crucial information about the composition and evolution of the continental crust. The entire topic has been recently reviewed in depth by Taylor and McLennan (1985) and only a brief overview is presented here.

Lanthanide abundances for the present upper continental crust are given in table 32 and are derived from the sedimentary rock data. Lanthanide abundances for the Archean upper crust can also be estimated from the Archean sedimentary rock data, although such estimates are less securely based, on account of the inherently greater variability in lanthanide patterns found in most Archean examples. The most recent estimate from Taylor and McLennan (1985) is also given in table 32.

It is important to realise that the sedimentary rock data provide information on that portion of the crust exposed to weathering and erosion. Evidence from heat flow data shows that the upper crust (about 10 km thick) is strongly enriched in the heat-producing elements (K, U, and Th) and thus is not representative of the entire 40 km or so of the continental crust. Early models of crustal composition (e.g. Taylor 1967, 1977) assumed that the bulk crust was equivalent in composition to that of average island-arc volcanic rocks, the so-called 'andesite' model. Although island-arc volcanism is now the principal mechanism by which material is extraced from the mantle and accreted to the continental crust, such a process has probably been operating only for the past two billion years and is responsible for only about twenty-five percent of the crust. The major growth of the continental crust appears to have occurred episodically, mostly in the late Archean. A likely mechanism was by igneous activity of the bimodal basaltic–felsic type common in Archean terrains, rather than by the 'andesitic' activity typical of present island arcs. The overall crustal bulk composition is thus calculated from a 75/25 mixture of the Archean bimodal and the andesitic compositions and by allowing for other constraints, such

TABLE 32
Crustal abundances [in ppm (wt)] of the REE. (After Taylor and McLennan 1985.)

Element	Post-Archean				Archean	
	Upper crust	Total crust	Andesite crust	Lower crust	Upper crust	Total crust
La	30	16	19	11	20	15
Ce	64	33	38	23	42	31
Pr	7.1	3.9	4.3	2.8	4.9	3.7
Nd	26	16	16	12.7	20	16
Sm	4.5	3.5	3.7	3.17	4.0	3.4
Eu	0.88	1.1	1.1	1.17	1.2	1.1
Gd	3.8	3.3	3.6	3.13	3.4	3.2
Tb	0.64	0.60	0.64	0.59	0.57	0.59
Dy	3.5	3.7	3.7	3.6	3.4	3.6
Ho	0.80	0.78	0.82	0.77	0.74	0.77
Er	2.3	2.2	2.3	2.2	2.1	2.2
Tm	0.33	0.32	0.32	0.32	0.30	0.32
Yb	2.2	2.2	2.2	2.2	2.0	2.2
Lu	0.32	0.30	0.30	0.29	0.31	0.33
Total	146	87	96	67	105	83
La/Yb	13.6	7.27	8.64	5.00	10.0	6.82
La_N/Yb_N	9.21	4.91	5.84	3.38	6.76	4.61
Eu/Eu*	0.65	0.99	0.92	1.14	0.99	1.02
Y	22	20	22	19	18	19
Sc	11	30	30	36	14	30

as the heat flow data. By subtracting the composition of the upper crust, a model-dependent composition for the lower crust can be established (table 32, fig. 52). A complete discussion of this model and various other alternatives is given by Taylor and McLennan (1985). The Archean crustal pattern is shown in fig. 53.

The change in lanthanide abundance patterns between Archean and post-Archean terrigenous sedimentary rocks has provided a major clue to the overall evolution of the continental crust. Any crust existing before 3.8 Ae was probably destroyed by the

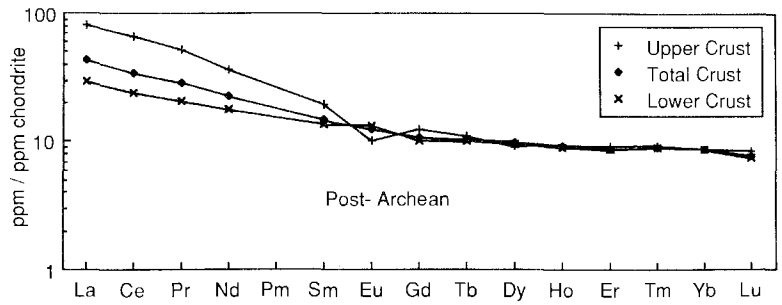

Fig. 52. Lanthanide abundance patterns for the post-Archean upper, lower and bulk crusts (data from table 32). The upper crust is depleted in Eu, and the lower crust enriched in Eu relative to the bulk crust.

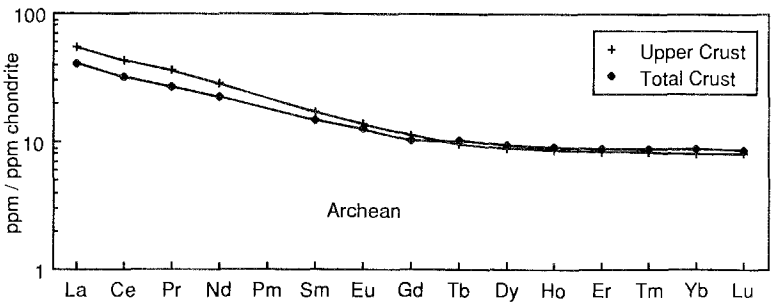

Fig. 53. Lanthanide abundance patterns for the Archean upper and bulk crusts. In contrast to the post-Archean upper crust, there is no depletion in Eu, suggesting that K-rich granites were only a minor component in the Archean upper crust, compared with their later dominance. (Data are from table 32.)

ongoing meteoritic bombardment which was endemic throughout the solar system down to about 3.9 or 3.8 Ae. Major basin-forming (>300 km diameter) events only ceased on the moon at that time. In the interval between about 4.4 and 3.8 Ae, at least 200 such major collisions occurred on the earth, totally destroying any pre-existing crust.

Two major hypotheses have been advanced to explain the evolution of the continental crust. The first proposes that the present mass of the crust formed very early in earth history, and has been recycled through the mantle in steadily decreasing fashion such that new additions are balanced by losses resulting in a steady-state system. The second proposes that the crust grew throughout geological time, with variations from a steady rate to growth in major episodic pulses. The lanthanide abundances shed considerable light on these problems. As noted above, there is a major dichotomy in the sedimentary record at about the boundary between Archean and Proterozoic (~2500 million years) and this has been correlated with a major pulse of crustal growth during the late Archean.

Archean clastic sedimentary rocks are typified by a variety of patterns (figs. 49 and 50) which only very rarely display Eu depletion. They are interpreted as being derived from mixtures of the two dominant igneous lithologies in the Archean: basalts and Na-rich igneous rocks such as tonalites and trondhjemites. Rarely, lanthanide patterns with Eu depletion are observed but appear to be restricted to cratonic sediments preserved in some high-grade metamorphic terrains. These are interpreted as being derived from mini-cratons (Taylor et al. 1986), forerunners of the massive cratonic development in the late Archean. Over a somewhat extended period of about 3.2–2.6 Ae (with the exact age differing for individual cratonic regions) a massive increase in growth of the continental crust occurred, as best documented by the Nd isotopic evidence (e.g. McCulloch and Wasserburg 1978). Closely following this event, massive intracrustal melting produced an upper crust dominated by K-rich granodiorites and granites. These typically have negative Eu anomalies. This change is reflected in the lanthanide patterns observed in the terrigenous sediments. Archean-type patterns are swamped, and the upper crust assumed its present composition.

Models which recycle the crust through the mantle encounter various difficulties. Some of the constraints are provided by the lanthanide data. For example, continental crustal sediments have a characteristic depletion in Eu (Eu/Eu* = 0.65). If this material is carried down subduction zones into the mantle, no sign of this appears in igneous rocks derived from these regions. Typically Eu/Eu* in mantle-derived igneous rocks is unity. Various other geochemical and isotopic constraints limit the amount of subducted sediments to a few percent. The lanthanide evidence is consistent with episodic growth of continental material from the mantle throughout geological time.

The application of Nd-model ages as a means of estimating crustal-formation ages is now well established (McCulloch and Wasserburg 1978, DePaolo 1981c). Major chemical fractionation of Sm and Nd occurs during extraction of material from the mantle and incorporation into the continental crust. Further fractionation of Sm and Nd also is expected during intracrustal melting events but this is comparatively minor and generally follows crust formation within 100–200 million years. For sediments, the Nd-model ages provide unique information. They give the time of formation of the sources of the sediments rather than the age of deposition. (This depends on the assumption that Sm and Nd are not fractionated during sedimentation or diagenesis over the past 3800 million years).

The Nd-model ages of sediments also provide some information regarding possible changes in upper crustal composition during the post-Archean. In fig. 54, it is apparent that the Nd-model ages of post-Archean sediments cover a wide range from about 2.5 to 1.0 Ae. These dates effectively represent the average age of the upper crust which contributed to these sediments. Thus, the constancy of lanthanide distributions in post-Archean sediments represent a wide range of provenance age. Accordingly, any additions to the upper crust during the post-Archean could not have differed significantly in composition to the upper crust itself.

The growth and evolution of the continental crust has proceeded in an episodic fashion throughout geological time (e.g. Moorbath 1977), with a major burst of

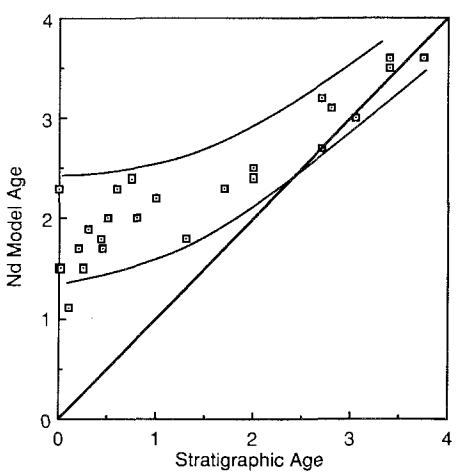

Fig. 54. The relation between stratigraphic age and Nd-model ages for sediments. Nd-model ages become progressively greater than stratigraphic age as the sedimentary sequences become younger. This trend is the result of sedimentary and crustal recycling. The wide range in model ages for a given stratigraphic age is due to differing crustal formation ages and variable recycling rates. (Adapted from Taylor and McLennan 1985.)

growth at the transition between the Archean and the Proterozoic. These evolutionary changes in crustal composition occur over hundreds of millions to billions of years. Changes on these time scales are reflected especially well by the lanthanide patterns in terrigenous sedimentary rocks.

12. Tektites

Tektites are small glassy objects produced by splashing of melted terrestrial country rock during large meteorite impacts (e.g. Taylor 1973). Before the receipt of the lunar samples, it was the scientific consensus that tektites were melted and splashed material formed during large cometary or meteorite impact events. Whether the impact took place on the earth or the moon was the topic of a long-standing scientific debate, which raged with particular intensity during the decade prior to the lunar landings. These impact events have been large-scale for the tektites have been sprayed over immense distances. The strewn field for the south-east Asian and Australian tektites covers about four percent of the earth's surface.

Four separate tektite-strewn fields are known: bediasites (North America, 34 million years); moldavites (Czechoslovakia, 14 million years); Ivory Coast (1.3 million years); and southeast Asian and Australian fields (0.7 million years). No normal geological processes (e.g. volcanic action) are capable of explaining this distribution. Neither do these small objects come from deep space, for they record no evidence of any exposure to cosmic radiation. These facts have restricted their origin to the earth or the moon. The chemistry of tektites reflects that of the parent material, and losses during formation appear to be restricted to elements and compounds more volatile than cesium. Terrestrial impact glasses provide small-scale analogues of tektite-forming events and indicate that only the most volatile components are lost during fusion. The present composition of tektites can accordingly be used to infer the composition of the parent material.

Among the many chemical and isotopic parameters which have been used to study tektites, the lanthanide elements have been among the most useful (Taylor 1973, Taylor and McLennan 1979). The lanthanide patterns (table 33, fig. 55) observed in tektites and in bottle-green microtektites are identical to those of terrestrial sedimentary rocks. This fact constitutes strong evidence for a parental terrestrial sedimentary rock, and mineralogical studies likewise indicate that the parent material of tektites was 'a well-sorted, silt-size sedimentary material'. In contrast, fig. 56 shows a comparison between lunar and tektite lanthanide patterns, illustrating their totally distinctive character. The lanthanides are useful in this context, because of their refractory nature. Accordingly, the signature of the parent material survives through the high temperature melting events which produced tektites.

This feature is particularly well demonstrated in the case of the small bottle-green microtektites. The major element chemistry of the bottle-green microtektites is enigmatic, not resembling that of any common terrestrial or extraterrestrial sample. However, they possess sedimentary-type lanthanide patterns (Frey 1977). Perhaps the bottle-green microtektites may represent a refractory residue following severe heating of the source material. Some of the compositions could represent material

TABLE 33
Rare earth element abundances [ppm (wt)] in tektites and impact glasses. (Data from Taylor and McLennan 1979).

Element	(1)	(2)	(3)	(4)	(5)	(6)	(7)
La	19.7	35.8	36.2	36.5	37.4	36.5	34.8
Ce	44.2	73.2	74.8	73.1	76.3	72.3	73.8
Pr	4.53	8.59	8.76	8.80	8.62	9.0	9.39
Nd	18.7	31.7	34.5	33.2	33.6	35.8	34.7
Sm	3.78	5.70	6.74	6.60	6.20	7.30	7.25
Eu	0.80	1.05	1.28	1.22	1.15	1.37	1.36
Gd	3.46	5.40	5.92	5.24	5.99	6.33	6.40
Tb	0.60	0.73	0.88	0.85	0.81	1.06	1.10
Dy	3.45	4.29	5.44	5.58	5.00	6.03	6.35
Ho	0.67	0.85	1.12	1.03	1.01	1.30	1.48
Er	1.89	2.41	3.32	2.91	2.97	3.75	4.36
Yb	1.90	2.35	3.01	2.90	2.76	2.50	3.92
Total	105	174	184	180	184	187	187
Eu/Eu*	0.68	0.59	0.63	0.64	0.58	0.62	0.62
La/Yb	10.8	15	12	13	13.6	10	8.9
La_N/Yb_N	6.9	10.9	7.9	8.3	8.9	6.9	5.9
Y	17.5	24	28	29	26	32	40
Sc	8.8	8.0	11.5	10.5	10	11	11

(1) Irghizite 2, 1-21.
(2) Javanite 6, 29.
(3) Philippinite 9, 30.
(4) Indochinite 10, 102.
(5) Australite 11, 365.
(6) Henbury impact glass 8.
(7) Henbury subgreywacke 16 (parent material of 6).

condensed from a vapor phase. During these extreme conditions, few element signatures characteristic of the source rock will survive. However, the lanthanides are notably refractory and could be expected to preserve the evidence of their parental material.

The lanthanide abundance patterns provide unequivocal evidence of a terrestrial sedimentary parent material for tektites. This conclusion is reinforced by the Sm–Nd isotopic systematics (Shaw and Wasserburg 1982) which demonstrate an origin for the various tektite groups from terrestrial crustal source material. Many other isotopic and chemical (e.g. a negative correlation between SiO_2 and K_2O) parameters reinforce this conclusion and all the evidence points unequivocally to an origin for tektites by meteoritic, cometary or asteroidal impact on terrestrial sedimentary rocks.

Epilogue: Europium as a universal tracer in geochemistry and cosmochemistry

In many respects, the distribution of europium serves as an epitome of the usefulness of the lanthanides in geochemistry and cosmochemistry. By its en-

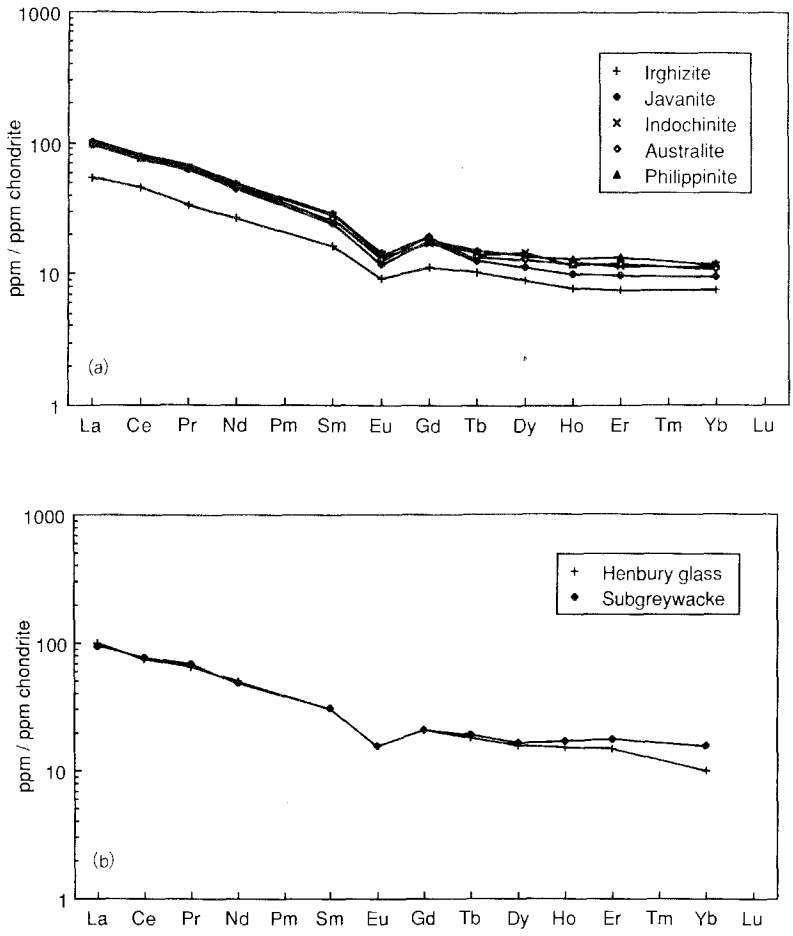

Fig. 55. (a) Lanthanide abundance patterns for tektites. Note that they parallel those of common sedimentary rocks and the upper crustal pattern consistent with derivation from such material. (Data are from table 33.) (b) Lanthanide abundance patterns for glass derived by melting of subgreywacke by meterorite impact at Henbury, Australia. No significant change in relative or absolute abundances has occurred during the melting process.

richment or depletion relative to neighbouring elements, one might trace much of the history of processes in the solar system and in the earth. It records the existence of a diverse series of events in meteorites. These include high-temperature evaporation and condensation in the early solar nebula, which separated Eu relative to the other lanthanides on account of its volatility. In the basaltic meteorites, it records the details of feldspar fractionation occurring in basaltic lavas on small planetesimals prior to the accretion of the earth.

The depletion of Eu in lunar basalts and its enrichment in highland feldspars was a major key to our understanding that much of the moon had been melted, and that

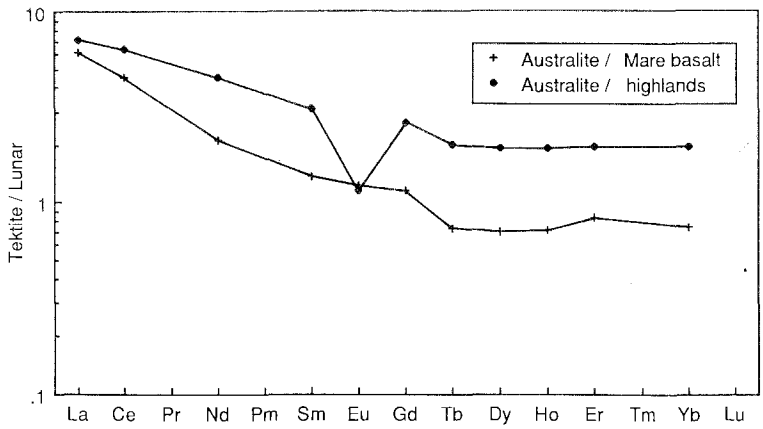

Fig. 56. Tektite lanthanide patterns normalised to those for typical lunar samples, illustrating their wide differences (data are from tables 10–12 and 33). Many such discrepancies between lunar and tektite chemical and isotopic data effectively rule out the moon as a possible source for the objects.

a feldspathic crust had formed very early in lunar history; processes not known on the earth, and perhaps unique in the solar system. In retrospect, it appears as one of the most significant of all lunar observations.

The uniform lanthanide pattern observed in crustal sediments on the earth, with its regular depletion in Eu, provides not only a key to the problem of sampling the continental crust, but also provides a crucial piece of evidence about crustal evolution. Eu is trivalent at the earth's surface, so that the observed depletion in upper crustal rocks recalls a previous history of the element as a divalent ion under more reducing conditions. It thus provides evidence that the upper crust of the earth resulted from production of granitic melts deep within the crust leading to retention of Eu in the deep crust, with a corresponding depletion at the present surface.

Acknowledgements

Many of the analytical data presented in this paper have originated in our laboratory. We thank the following colleagues for collaborative work: Pat Oswald-Sealy, Annette Capp, Maureen Kaye, Mike Shelley, Roberta Rudnick, Weldon Nance, David Whitford, Brian Mason, Mike Gorton, Mike Perfit, Andrew Duncan, Tony Ewart, Richard Wormald, Dick Price, Richard Arculus, Angelo Peccerillo, Ted Bence, Arthur Day, Mukul Bhatia, Lynton Jaques, Ian Smith, Ian Wilson and Warrington Cameron. We thank Mike Shelley who made a major contribution by producing the figures and Melissa Stevenson for typing assistance. Tony Ewart supplied figs. 20 and 21. We thank Ted Bence, Exxon Production Research (formerly at Exxon Mineral Company), Neil Williams and Mt. Isa Mines for permission to present the data plotted in fig. 31.

References

Abbey, S., 1983, Studies in 'standard samples' of silicate rocks and minerals 1969–1982, Geol. Surv. Can. Paper 83-15.

Addy, S.K., 1979, Geochim. & Cosmochim. Acta **43**, 1105.

Ahrens, L.H., and S.R. Taylor, 1961, Spectrochemical Analysis (Addison-Wesley, Reading, MA).

Alderton, D.H.M., J.A. Pearce and P.J. Potts, 1980, Earth & Planet. Sci. Lett. **49**, 149.

Aller, L.H., 1987, in: Spectroscopy and Astrophysical Plasmas, eds A. Dalgarno and D. Layzer (Cambridge University Press, Cambridge).

Anders, E., and M. Ebihara, 1982, Geochim. & Cosmochim. Acta **46**, 2363.

Arniaud, D., 1984, Chem. Geol. **45**, 263.

Arth, J.G., and G.N. Hanson, 1975, Geochim. & Cosmochim. Acta **39**, 325.

Arth, J.G., F. Barker, Z.E. Peterman and I. Friedman, 1978, J. Petrol. **19**, 289.

Ashwal, L.D., 1982, Proterozoic Anothosite Massifs: A Review, LPI Tech. Rep. 82-01 (Lunar Planetery Institute, Houston, TX) p. 40.

Ashwal, L.D., and K.E. Seifert, 1980, Geol. Soc. Am. Bull. Part II **91**, 659.

Ashwal, L.D., D.A. Morrison, W.C. Phinney and J. Wood, 1983, Contrib. Miner. Petrol. **82**, 259.

Ayuso, R.A., A.E. Bence and S.R. Taylor, 1976, J. Geophys. Res. **81**, 4305.

Balashov, Yu.A., A.B. Ronov, A.A. Migdisov and N.V. Turanskaya, 1964, Geochem. Int. **5**, 951.

Barker, F., ed., 1979, Trondhjemites, Dacites and Related Rocks (Elsevier, Amsterdam) 659 pages.

Basaltic Volcanism Study Project, 1981, Basaltic Volcanism in the Terrestrial Planets (Pergamon, New York) 1286 pages.

Bavinton, O.A., and S.R. Taylor, 1980, Geochim. & Cosmochim. Acta **44**, 639.

Bence, A.E., 1983, Fourth Int. Symp. Water–Rock Interaction, (International Association of Geochemistry and Cosmochemistry, Misasa, Japan).

Bence, A.E., and B.E. Taylor, 1985, Econ. Geol. **80**, 2164.

Bence, A.E., T.L. Grove and J.J. Papike, 1980, Precambrian Res. **10**, 249.

Bhatia, M.R., 1985, Sediment. Geol. **45**, 97.

Bhatia, M.R., and K.A.W. Crook, 1986, Contrib. Mineral. Petrol **92**, 181.

Black, D.C., and M.S. Matthews, 1985, Protostars and Planets II, eds D.C. Black and M.S. Matthews (University of Arizona Press, AZ).

Boak, J.L., R.F. Dymek and L.P. Gromet, 1982, Lunar Planet. Sci. XIII (Lunar and Planetary Institute, Houston, TX) pp. 51, 52.

Boynton, W.V., 1979, Neutron activation analysis, in: Handbook on the Physics and Chemistry of Rare Earths, Vol. 4, eds K.A. Gschneidner Jr and L. Eyring (North-Holland, Amsterdam) pp. 457–470.

Boynton, W.V., 1984, Cosmochemistry of the Rare Earth Elements: Meteorite Studies, in: Rare Earth Element Geochemistry, ed. P. Henderson (Elsevier, Amsterdam) pp. 63–114.

Boynton, W.V., 1985, in: Protostars and Planets II, eds D.C. Black and M.S. Matthews (University of Arizona Press, AZ) pp. 772–787.

Brophy, J.G., and B.D. Marsh, 1986, J. Petrol. **27**, 763.

Burnett, D.S., and D.S. Woolum, 1977, Phys. & Chem. Earth **10**, 76.

Cameron, K.L., and G.N. Hanson, 1982, Geochim. & Cosmochim. Acta **46**, 1489.

Campbell, I.H., J.M. Franklin, M.P. Gorton, T.R. Hart and S.D. Scott, 1981, Econ. Geol. **76**, 2248.

Campbell, I.H., C.M. Lesher, P. Coad, J.M. Franklin, M.P. Gorton and P.C. Thurston, 1984, Chem. Geol. **45**, 181.

Chappell, B.W., and A.J.R. White, 1983, Geol. Soc. Am. Mem. **159**, 21.

Chase, C.G., 1981, Earth & Planet. Sci. Lett. **52**, 277.

Chaudhuri, S., and R.L. Cullers, 1979, Chem. Geol. **24**, 327.

Clark, A.M., 1984, Mineralogy of the Rare Earth Elements, in: Rare Earth Element Geochemistry, ed. P. Henderson (Elsevier, Amsterdam) pp. 33–61.

Clayton, R.N., T.K. Mayeda and C.A. Molini-Velsko, 1985, in: Protostars and Planets II, eds D.C. Black and M.S. Matthews (University of Arizona Press, AZ) 755 pages.

Condie, K.C., 1978, Chem. Geol. **21**, 131.

Condie, K.C., 1981, Spec. Pub. Geol. Soc. Austr. **7**, 469.

Condie, K.C., J.E. Macke and T.O. Reimer, 1970, Geol. Soc. Am. Bull. **81**, 2759.

Coryell, C.D., J.W. Chase and J.W. Winchester, 1963, J. Geophys. Res. **68**, 559.

Crozaz, G., and E. Zinner, 1985, Earth & Planet. Sci. Lett. **73**, 41.

Crozaz, G., and E. Zinner, 1986, Scanning Electron Microscopy **2**, 369.

Cullers, R.L., and J.L. Graf, 1984a, Rare Earth Elements in Igneous Rocks of the Continental Crust: Predominantly Basic and Ultrabasic Rocks, in: Rare Earth Element Geochemistry, ed. P. Henderson (Elsevier, Amsterdam) pp. 237–274.

Cullers, R.L., and J.L. Graf, 1984b, Rare Earth Elements in Igneous Rocks of the Continental Crust: Intermediate and Silicic Rocks – Ore Petrogenesis, in: Rare Earth Element Geochemistry, ed. P. Henderson (Elsevier, Amsterdam) pp. 275–316.

Cullers, R.L., L.-T. Yeh, S. Chaudhuri and C.V. Guidotti, 1974, Geochim. & Cosmochim. Acta **38**, 389.

Cullers, R.L., S. Chaudhuri, B. Arnold, M. Lee and C.W. Wolf Jr, 1975, Geochim. & Cosmochim. Acta **39**, 1691.
Cullers, R.L., S. Chaudhuri, N. Kilbane and R. Koch, 1979, Geochim. & Cosmochim. Acta **43**, 1285.
De Baar, H.J.W., M.P. Bacon and P.G. Brewer, 1983, Nature **301**, 324.
De Baar, H.J.W., M.P. Bacon, P.G. Brewer and K.W. Bruland, 1985a, Geochim. & Cosmochim. Acta **49**, 1943.
De Baar, H.J.W., P.G. Brewer and M.P. Bacon, 1985b, Geochim. & Cosmochim. Acta **49**, 1961.
DePaolo, D.J., 1981a, EOS **62**, 137.
DePaolo, D.J., 1981b, Earth & Planet. Sci. Lett. **53**, 189.
DePaolo, D.J., 1981c, Nature **291**, 193.
Dickinson, W.R., and C.A. Suczek, 1979, Am. Assoc. Pet. Geol. Bull. **63**, 2164.
Dostal, J., and D.F. Strong, 1983, Can. J. Earth Sci. **20**, 431.
Dymek, R.F., R. Weed and L.P. Gromet, 1983, Rapp. Gronlands Geol. Unders. **112**, 53.
Dypvik, H., and A.O. Brunfelt, 1976, Sedimentology **23**, 363.
Elderfield, H., and M.J. Greaves, 1981, Earth & Planet. Sci. Lett. **55**, 163.
Elderfield, H., and M.J. Greaves, 1982, Nature **296**, 214.
Elderfield, H., C.J. Hawkesworth, M.J. Greaves and S.E. Calvert, 1981, Geochim. & Cosmochim. Acta **45**, 513.
Erlank, A.J., ed., 1984, Petrogenesis of the Volcanic Rocks of the Karoo Province, Geol. Soc. (South Africa), Spec. Pub. **13**.
Evensen, N.M., P.J. Hamilton and R.K. O'Nions, 1978, Geochim. & Cosmochim. Acta **42**, 1199.
Fairbairn, H.W., 1951, A co-operative investigation of precision and accuracy on chemical, spectrochemical and model analysis of silicate rocks, U.S. Geol. Surv. Bull. **980**, 71.
Fleet, A.J., 1984, Aqueous and Sedimentary Geochemistry of the Rare Earth Elements, in: Rare Earth Element Geochemistry, ed. P. Henderson (Elsevier, Amsterdam) pp. 343–373.
Floyd, P.A., 1977, Nature **269**, 134.
Frey, F.A., 1969, Geochim. & Cosmochim. Acta **33**, 1429.
Frey, F.A., 1977, Earth & Planet. Sci. Lett. **35**, 43.
Frey, F.A., 1979, Rev. Geophys. Space Phys. **17**, 803.
Frey, F.A., 1984, Rare Earth Element Abundances in Upper Mantle Rocks, in: Rare Earth Element Geochemistry, ed. P. Henderson (Elsevier, Amsterdam) pp. 153–203.
Frey, F.A., and D.H. Green, 1974, Geochim. & Cosmochim. Acta **38**, 1023.
Frey, F.A., W.B. Bryan and G. Thompson, 1974, J. Geophys. Res. **79**, 5507.
Fryer, B.J., 1977a, Geochim. & Cosmochim. Acta **41**, 361.
Fryer, B.J., 1977b, Can. J. Earth Sci. **14**, 1598.
Fryer, B.J., 1983, REE in iron-formations, in: Iron-formation, Facts and Problems, eds A.F. Trendall and R.C. Morris (Elsevier, Amsterdam) 345 pages.
Fryer, B.J., and R.P. Taylor, 1984, Geology **12**, 479.
Fryer, B.J., W.S. Fyfe and R. Kerrich, 1979, Chem. Geol. **24**, 25.
Gast, P.W., 1970, Proc. Lunar Sci. Conf. **1**, 1143.
Gast, P.W., and N.J. Hubbard, 1970, Earth & Planet. Sci. Lett. **10**, 94.
Gehrels, T., ed., 1979, Asteroids (University of Arizona Press, AZ) 1181 pages.
Gibbs, A.K., C.W. Montgomery, P.A. O'Day and E.A. Erslev, 1986, Geochim. & Cosmochim. Acta **50**, 2125.
Gill, J.B., 1981, Orogenic Andesites and Plate Tectonics (Springer, Berlin) 390 pages.
Goldberg, E.D., M. Koide, R.A. Schmitt and R.H. Smith, 1963, J. Geophys. Res. **68**, 4209.
Goldschmidt, V.M., 1938, Skr. Nor. Videns.-Akad. **1**, 1.
Graf Jr, J.L., 1977, Econ. Geol. **72**, 527.
Graf Jr, J.L., 1978, Geochim. & Cosmochim. Acta **42**, 1845.
Graham, A.L., and A.E. Ringwood, 1972, Earth & Planet. Sci. Lett. **13**, 105.
Green, D.H., 1971, Proc. Lunar Sci. Conf. **2**, 617.
Green, T.H., A.O. Brunfelt and K.S. Heier, 1969, Earth & Planet. Sci. Lett. **7**, 93.
Green, T.H., A.O. Brunfelt and K.S. Heier, 1972, Geochim. & Cosmochim. Acta **36**, 241.
Gromet, L.P., and L.T. Silver, 1983, Geochim. & Cosmochim. Acta **47**, 925.
Gromet, L.P., and L.T. Silver, 1987, J. Petrol. **28**, 75.
Gromet, L.P., R.F. Dymek, L.A. Haskin and R.L. Korotev, 1984, Geochim. & Cosmochim. Acta **48**, 2469.
Hajash Jr, A., 1984, Contrib. Miner. Petrol. **85**, 409.
Hamilton, P.J., N.M. Evensen, R.K. O'Nions and J. Tarney, 1979, Nature **277**, 25.
Hanson, G.N., 1978, Earth & Planet. Sci. Lett. **38**, 26.
Hanson, G.N., 1980, Ann. Rev. Earth & Planet. Sci. **8**, 371.
Hartmann, W.K., R.J. Phillips and G.J. Taylor, eds, 1986, Origin of the Moon (Lunar Planetary Institute, Houston, TX) 781 pages.
Haskin, L.A., 1979, Phys. & Chem. Earth **11**, 175.
Haskin, L.A., 1984, Petrogenetic Modelling – Use of Rare Earth Elements, in: Rare Earth Element Geochemistry, ed. P. Henderson (Elsevier, Amsterdam) pp. 115–152.
Haskin, L.A., and M.A. Gehl, 1962, J. Geophys. Res. **67**, 2537.
Haskin, L.A., and T.P. Paster, 1979, Geochemistry and Mineralogy of the Rare Earths, in: Handbook on the Physics and Chemistry of Rare Earths, Vol. 3, eds K.A. Gschneidner Jr and L. Eyring (North-Holland, Amsterdam) pp. 1–80.
Haskin, L.A., F.A. Frey, R.A. Schmitt and R.H. Smith, 1966a, Phys. & Chem. Earth **7**, 167.
Haskin, L.A., T.R. Wildeman, F.A. Frey, K.A.

Collins, C.R. Keedy and M.A. Haskin, 1966b, J. Geophys. Res. **71**, 6091.
Haskin, L.A., M.A. Haskin, F.A. Frey and T.R. Wildeman, 1968, Relative and Absolute Terrestrial Abundances of the Rare Earths, in: Origin and Distribution of the Elements, ed. L.H. Ahrens (Pergamon, New York) pp. 889–912.
Haskin, M.A., and L.A. Haskin, 1966, Science **154**, 507.
Hawkesworth, C.J., and P.W.C. van Calsteren, 1984, Radiogenic Isotopes – Some Geological Applications, in: Rare Earth Element Geochemistry, ed. P. Henderson (Elsevier, Amsterdam) pp. 376–421.
Hellman, P.L., and P. Henderson, 1977, Nature **267**, 40.
Henderson, P., ed., 1984, Rare Earth Element Geochemistry (Elsevier, Amsterdam) 510 pages.
Henderson, P., and R.J. Pankhurst, 1984, Analytical Chemistry, in: Rare Earth Element Geochemistry, ed. P. Henderson (Elsevier, Amsterdam) pp. 467–499.
Hildreth, W., 1979, Geol. Soc. Am. Spec. Paper **180**, 43.
Hofmann, A.W., and W.M. White, 1982, Earth & Planet. Sci. Lett. **57**, 421.
Hooker, P.J., P.J. Hamilton and R.K. O'Nions, 1981, Earth & Planet. Sci. Lett. **56**, 180.
Humphris, S.E., 1984, The Mobility of the Rare Earth Elements in the Crust, in: Rare Earth Element Geochemistry, ed. P. Henderson (Elsevier, Amsterdam) pp. 317–342.
Humphris, S.E., M.A. Morrison and R.N. Thompson, 1978, Chem. Geol. **23**, 125.
Irving, A.J., 1978, Geochim. & Cosmochim. Acta **42**, 743.
Jagoutz, E., 1979, Proc. Lunar Planet. Sci. Conf. **10**, 2031.
Jagoutz, E., 1986, Lunar Planet. Sci. XVII, 385.
Jagoutz, E., 1987, private communication.
Jahn, B.-M., and Z.-Q. Zhang, 1984, Radiometric ages (Rb–Sr, Sm–Nd, U–Pb) and REE Geochemistry of Archaean Granulite Gneisses from Eastern Heibei Province, China, in: Archaean Geochemistry, eds A. Kroner, G.N. Hanson and A.M. Goodwin (Springer, Berlin) pp. 204–234.
Jahn, B.-M., A.Y. Glikson, J.J. Peucat and A.H. Hickman, 1981, Geochim. & Cosmochim. Acta **45**, 1633.
Jakes, P., and S.R. Taylor, 1974, Geochim. & Cosmochim. Acta **38**, 739.
Jaques, A.L., B.W. Chappell and S.R. Taylor, 1983, Contrib. Miner. Petrol. **82**, 154.
Jarvis, J.C., T.R. Wildeman and N.G. Banks, 1975, Chem. Geol. **16**, 27.
Jenner, G.A., B.J. Fryer and S.M. McLennan, 1981, Geochim. & Cosmochim. Acta **45**, 1111.
Jensen, B.B., 1973, Geochim. & Cosmochim. Acta **37**, 2227.
Kerrich, R., and B.J. Fryer, 1979, Can. J. Earth Sci. **16**, 440.
Kerridge, J.F., 1988, Meteorites and the Early Solar System (University of Arizona Press, AZ) in press.
Klinkhammer, G., H. Elderfield and A. Hudson, 1983, Nature **305**, 185.
Kornacki, A.S., and B. Fegley, 1986, Earth & Planet. Sci. Lett. **79**, 217.
Kosterin, A.V., 1959, Geochemistry 1959, p. 381.
Langmuir, C.H., J.F. Bender, A.E. Bence, G.N. Hanson and S.R. Taylor, 1977, Earth & Planet. Sci. Lett. **36**, 133.
Langmuir, D., 1978, Geochim. & Cosmochim. Acta **42**, 547.
Laul, J.C., M.R. Smith, H. Wanke, E. Jagoutz, G. Dreibus, H. Palme, B. Spettel, A. Burghele, M.E. Lipschutz and R.M. Verkouteren, 1986, Geochim. & Cosmochim. Acta **50**, 909.
Lee, D.E., and H. Bastron, 1967, Geochim. & Cosmochim. Acta **31**, 339.
Ludden, J.N., and G. Thompson, 1978, Nature **274**, 147.
Ludden, J.N., and G. Thompson, 1979, Earth & Planet. Sci. Lett. **43**, 85.
Maas, R., M.T. McCulloch, I.H. Campbell and P.R. Coad, 1986, Geology **14**, 585.
Mahood, G., and W. Hildreth, 1983, Geochim. & Cosmochim. Acta **47**, 11.
Martin, J.-M., and M. Meybeck, 1979, Marine Chem. **7**, 173.
Martin, J.-M., O. Hogdahl and J.C. Philippot, 1976, J. Geophys. Res. **81**, 3119.
Martin, R.F., J.E. Whitley and A.R. Woolley, 1978, Contrib. Miner. Petrol. **66**, 69.
Mason, B., 1962, Meteorites (Wiley, New York) 274 pages.
Mason, B., and S.R. Taylor, 1982, Smithson. Contrib. Earth Sci. **25**, 1.
Masuda, A., 1962, J. Earth Sci. (Nagoya University) **10**, 173.
Masuda, A., and Y. Ikeuchi, 1979, Geochem. J. **13**, 19.
Maynard, J.B., R. Valloni and H.-S. Yu, 1982, Composition of Modern Deep-Sea Sands from Arc-related Basins, in: Trench and Fore-arc Sedimentation, ed. J.K. Leggett (Geological Society of London, London) pp. 551–561.
McCarthy, T.S., and E.J.D. Kable, 1978, Chem. Geol. **22**, 21.
McCulloch, M.T., and G.J. Wasserburg, 1978, Science **200**, 1003.
McLennan, S.M., 1981, Ph.D. Thesis (Australian National University, Canberra).
McLennan, S.M., 1984, J. Sed. Petrol. **54**, 889.
McLennan, S.M., and S.R. Taylor, 1979, Nature **282**, 247.
McLennan, S.M., and S.R. Taylor, 1980, Rare Earth Elements in Sedimentary Rocks, Granites and Uranium Deposits of the Pine Creek Geosyncline, in: Uranium in the Pine Creek Geosyncline, eds J. Ferguson and A.B. Goleby (IAEA, Vienna) pp. 175–190.
McLennan, S.M., and S.R. Taylor, 1983, Precambrian Res. **22**, 93.
McLennan, S.M., and S.R. Taylor, 1984, Archaean Sedimentary Rocks and their Relation

to the Composition of the Archaean Continental Crust, in: Archaean Geochemistry, eds A. Kroner, G.N. Hanson and A.M. Goodwin (Springer, Berlin) pp. 47–72.
McLennan, S.M., B.J. Fryer and G.M. Young, 1979a, Can. J. Earth Sci. **16**, 230.
McLennan, S.M., B.J. Fryer and G.M. Young, 1979b, Geochim. & Cosmochim. Acta **43**, 375.
McLennan, S.M., S.R. Taylor and K.A. Eriksson, 1983, Geochim. & Cosmochim. Acta **47**, 1211.
McLennan, S.M., S.R. Taylor and V.R. McGregor, 1984, Geochim. & Cosmochim. Acta **48**, 1.
McLennan, S.M., M.T. McCulloch, S.R. Taylor and J.B. Maynard, 1985, EOS **66**, 1136.
McSween, H.Y., 1985, Rev. Geophys. **23**, 391.
Menzies, M., D. Blanchard and J. Jacobs, 1977, Earth & Planet. Sci. Lett. **37**, 203.
Menzies, M., W. Seyfried Jr and D. Blanchard, 1979, Nature **282**, 398.
Michard, A., and F. Albarede, 1986, Chem. Geol. **55**, 51.
Michard, A., F. Albarede, G. Michard, J.F. Minster and J.L. Charlou, 1983, Nature **303**, 795.
Miller, R.G., and R.K. O'Nions, 1985, Nature **314**, 325.
Minami, E., 1935, Nach. Gess. Wiss. Goettingen, 2, Math.-Physik K.L. IV, **1**, 155.
Moller, P., and G.K. Muecke, 1984, Contrib. Miner. Petrol. **87**, 242.
Moorbath, S., 1977, Philos. Trans. R. Soc. A. **288**, 401.
Morse, S.A., 1982, Am. Miner. **67**, 1087.
Muecke, G.K., C. Pride and P. Sarker, 1979, Phys. & Chem. Earth **11**, 449.
Mueller, P.A., J.L. Wooden and D.R. Bowes, 1982, Rev. Bras. Geosci. **12**, 216.
Nance, W.B., and S.R. Taylor, 1976, Geochim. & Cosmochim. Acta **40**, 1539.
Nance, W.B., and S.R. Taylor, 1977, Geochim. & Cosmochim. Acta **41**, 225.
Naqvi, S.M., K.C. Condie and P. Allen, 1983, Precambrian Research **22**, 125.
Nathan, S., 1976, N.Z. J. Geol. Geophys. **19**, 683.
Naumov, G.B., 1959, Geochemistry **5**, 1959.
Neary, C.R., and D.E. Highley, 1984, The Economic Importance of the Rare Earth Elements, in: Rare Earth Element Geochemistry, ed. P. Henderson (Elsevier, Amsterdam) pp. 423–466.
Nesbitt, H.W., 1979, Nature **279**, 206.
Nesbitt, H.W., and G.M. Young, 1984, Geochim. & Cosmochim. Acta **48**, 1523.
Nguyen Long Den, and Y. Yokoyama, 1970, Meteotitics **5**, 214.
Nicholls, I.A., D.J. Whitford, K.L. Harris and S.R. Taylor, 1980, Chem. Geol. **30**, 177.
Noddack, I., 1935, Z. Anorg. Allg. Chem. **225**, 337.
O'Hara, M.J., and G.M. Biggar, 1970, Geol. Soc. Am. Abstr. **2**, 639.
O'Nions, R.K., and R.J. Pankhurst, 1978, Earth & Planet. Sci. Lett. **38**, 211.
O'Nions, R.K., S.R. Carter, N.M. Evensen and P.J. Hamilton, 1979, Ann. Rev. Earth & Planet. Sci. **7**, 11.
Onuma, N., H. Higuchi, H. Wakita and H. Nagasawa, 1968, Earth & Planet. Sci. Lett. **5**, 47.
Palmer, M.R., 1985, Earth & Planet. Sci. Lett. **73**, 285.
Palmer, M.R., and H. Elderfield, 1985, Earth & Planet. Sci. Lett. **73**, 299.
Parekh, P.P., P. Moller, P. Dulski and W.M. Bausch, 1977, Earth & Planet. Sci. Lett. **34**, 39.
Patchett, P.J., 1983, Geochim. & Cosmochim. Acta **47**, 81.
Patchett, P.J., O. Kouvo, C.E. Hedge and M. Tatsumoto, 1981, Contrib. Miner. Petrol. **78**, 279.
Pearce, J.A., 1982, Trace Element Characteristics of Lavas from Destructive Plate Boundaries, in: Andesites, ed. R.S. Thorpe (Wiley, New York) pp. 525–548.
Pearce, J.A., and J.R. Cann, 1973, Earth & Planet. Sci. Lett. **19**, 290.
Philpotts, J.A., 1978, Geochim. & Cosmochim. Acta **42**, 909.
Piepgras, D.J., and G.J. Wasserburg, 1980, Earth & Planet. Sci. Lett. **50**, 128.
Piepgras, D.J., G.J. Wasserburg and E.J. Dasch, 1979, Earth & Planet. Sci. Lett. **45**, 223.
Piper, D.Z., 1974, Geochim. & Cosmochim. Acta **38**, 1007.
Piper, D.Z., and P.A. Graf, 1974, Marine Geol. **17**, 287.
Price, R.C., and S.R. Taylor, 1980, Contrib. Miner. Petrol. **72**, 1.
Reed, S.J.B., 1986, Miner. Mag. **50**, 3.
Roaldset, E., and I.Th. Rosenqvist, 1971, Nature Phys. Sci. **231**, 153.
Ronov, A.B., Yu.A. Balashov, Yu.P. Girin, R.Kh. Bratishko and G.A. Kazakov, 1974, Sedimentology **21**, 171.
Saunders, A.D., 1984, The Rare Earth Element Characteristics of Igneous Rocks from the Ocean Basins, in: Rare Earth Element Geochemistry, ed. P. Henderson (Elsevier, Amsterdam) pp. 205–236.
Sawyer, E.W., 1986, Chem. Geol. **55**, 77.
Schilling, J.-G., 1975, J. Geophys. Res. **80**, 1459.
Schmitt, R.A., 1964, Geochim. & Cosmochim. Acta **28**, 67.
Schnetzler, C.C., and J.A. Philpotts, 1969, in: Meterorite Research, ed. P. Millman (Reidel, Dordrecht) p. 207.
Schnetzler, C.C., and J.A. Philpotts, 1970, Geochim. & Cosmochim. Acta **34**, 331.
Schnetzler, C.C., and J.A. Philpotts, 1971, Proc. Lunar Sci. Conf. **2**, 1011.
Schuhmann, S., and J.A. Philpotts, 1979, Mass-spectrometric Stable-Isotope-Dilution Analysis for Lanthanides in Geochemical Materials, in: Handbook on the Physics and Chemistry of Rare Earths, Vol. 4, eds K.A. Gschneidner Jr and L. Eyring (North-Holland, Amsterdam) pp. 471–481.
Shannon, R.D., 1976, Acta Crystallogr. **32**, 751.
Shaw, H.F., and G.J. Wasserburg, 1982, Earth & Planet. Sci. Lett. **60**, 155.
Shaw, S.E., and R.H. Flood, 1981, J. Geophys. Res. **86**, 10530.

Shimizu, H., and A. Masuda, 1977, Nature **266**, 346.
Simmons, E.C., and G.N. Hanson, 1978, Contrib. Miner. Petrol. **66**, 119.
Spirn, R.V., 1965, unpublished Ph.D. Thesis (M.I.T. Cambridge, MA); quoted in: Piper (1974).
Staudigel, H., and S.R. Hart, 1983, Geochim. & Cosmochim. Acta **47**, 337.
Staudigel, H., F.A. Frey and S.R. Hart, 1979, Init. Rep. Deep Sea Drilling Proj. 51,52,53, Vol. 2, p. 1137.
Staudigel, H., P. Doyle and A. Zindler, 1985, Earth & Planet. Sci. Lett. **76**, 45.
Stordal, M.C., and G.J. Wasserburg, 1986, Earth & Planet. Sci. Lett. **77**, 259.
Strong, D.F., 1984, Can. J. Earth Sci. **21**, 775.
Suess, H.E., 1947, Z. Naturforsch. A **2**, 311.
Suess, H.E., and H.C. Urey, 1956, Rev. Mod. Phys. **28**, 53.
Surkov, Y.A., 1981, Proc. Lunar Planet. Sci. Conf. **12**, 1377.
Sverjensky, D.A., 1984, Earth & Planet. Sci. Lett. **67**, 70.
Taylor, R.P., and B.J. Fryer, 1982, Rare Earth Element Geochemistry as an Aid to Interpreting Hydrothermal Ore Deposits, in: Metallization Associated with Acid Magmatism, ed. A.M. Evans (Wiley, New York) pp. 357–365.
Taylor, S.R., 1967, Tectonophys. **4**, 17.
Taylor, S.R., 1973, Earth-Sci. Rev. **9**, 101.
Taylor, S.R., 1975, Lunar Science – A Post-Apollo View (Pergamon, New York) 372 pages.
Taylor, S.R., 1977, Am. Geophys. Union. Maurice Ewing Ser. I, 325.
Taylor, S.R., 1979, Trace Element Analysis of Rare Earth Element by Spark Source Mass Spectrometry, in: Handbook on the Physics and Chemistry of Rare Earths, Vol. 4, eds K.A. Gschneidner Jr and L. Eyring (North-Holland, Amsterdam) pp. 359–376.
Taylor, S.R., 1982, Planetary Science: A Lunar Perspective (Lunar Planetary Institute, Houston, TX) 481 pages.
Taylor, S.R., 1987a, Geochim. & Cosmochim. Acta **51**, 1297.
Taylor, S.R., 1987b, Amer. Sci. **75**, 468.
Taylor, S.R., and M.P. Gorton, 1977, Geochim. & Cosmochim. Acta **41**, 1375.
Taylor, S.R., and S.M. McLennan, 1979, Geochim. & Cosmochim. Acta **43**, 1551.
Taylor, S.R., and S.M. McLennan, 1981, Philos. Trans. R. Soc. London Ser. A **301**, 381.
Taylor, S.R., and S.M. McLennan, 1985, The Continental Crust: Its Composition and Evolution (Blackwell, Oxford) 312 pages.
Taylor, S.R., S.M. McLennan and M.T. McCulloch, 1983, Geochim. & Cosmochim. Acta **47**, 1897.
Taylor, S.R., I.H. Campbell, M.T. McCulloch and S.M. McLennan, 1984, Nature **311**, 372.
Taylor, S.R., R.L. Rudnick, S.M. McLennan and K.A. Eriksson, 1986, Geochim. & Cosmochim. Acta **50**, 2267.
Ujike, O., 1984, Can. J. Earth Sci. **21**, 727.
Veizer, J., 1984, Proc. 27th Int. Geol. Congr. **11**, 325.
Veizer, J., and S.L. Jansen, 1985, J. Geol. **93**, 625.
von Richthofen, F., 1882, Geol. Mag. **9**, 293.
Wang, Y.L., Y.-G. Liu and R.A. Schmitt, 1986, Geochim. & Cosmochim. Acta **50**, 1337.
Wasson, J.T., 1985, Meteorities: Their Record of Solar System History (Freeman, New York).
Weaver, B.L., 1980, Contrib. Miner. Petrol. **71**, 271.
Wendlandt, R.F., and W.J. Harrison, 1979, Contrib. Miner. Petrol. **69**, 409.
Wetherill, G.W., 1987, Philos. Trans. R. Soc. A **323**, 323.
White, W.M., and J. Patchett, 1984, Earth & Planet. Sci. Lett. **67**, 167.
White, W.M., B. Dupre and P. Vidal, 1985, Geochim. & Cosmochim. Acta **49**, 1875.
Whitford, D.J., I.A. Nicholls and S.R. Taylor, 1979, Contrib. Miner. Petrol. **70**, 341.
Whitford, D.J., M.J. Korsch, P.M. Porritt and S.J. Graven, 1987, Chem. Geol. (in press).
Wildeman, T.R., and K.C. Condie, 1973, Geochim. & Cosmochim. Acta **37**, 439.
Wildeman, T.R., and L.A. Haskin, 1973, Geochim. & Cosmochim. Acta **37**, 419.
Wood, D.A., I.L. Gibson and R.N. Thompson, 1976, Contrib. Miner. Petrol. **55**, 241.
Wright-Clark, J., R.S. Seymour and H.F. Shaw, 1984, REE and Nd Isotopes in Conodont Apatite: Variations with Geological Age and Depositional Environment, in: Conodont Biofacies and Provincialism, ed. D.L. Clark, Geol. Soc. Amer. Spec. Paper **196**, 325–340.
Wyllie, P.J., 1977, Tectonophys. **43**, 41.
Zinner, E., and G. Crozaz, 1986, Int. J. Mass Spectrom. & Ion Process. **69**, 17.

ERRATA

Vol. 3, ch. 27, Eyring

1. Page 385, line 13: Volume II instead of "Volume I".

Vol. 4, ch. 31, Flahaut

1. Page 9, table 31.1, a "δ" is missing from the middle line (from top to bottom), which runs from Dy to Tm.

Vol. 5, ch. 43, Netzer and Bertel

1. Page 283, line 10: activity instead of "acrivity".

Vol. 5, ch. 45, Greis and Haschke

1. Page 426, table 20, first column, sixth entry: $KTmF_4$ instead of "$KtmF_4$".

Vol. 7, ch. 51, Rogl

1. Page 193, fig. 47: replace the figure shown with the one given below:

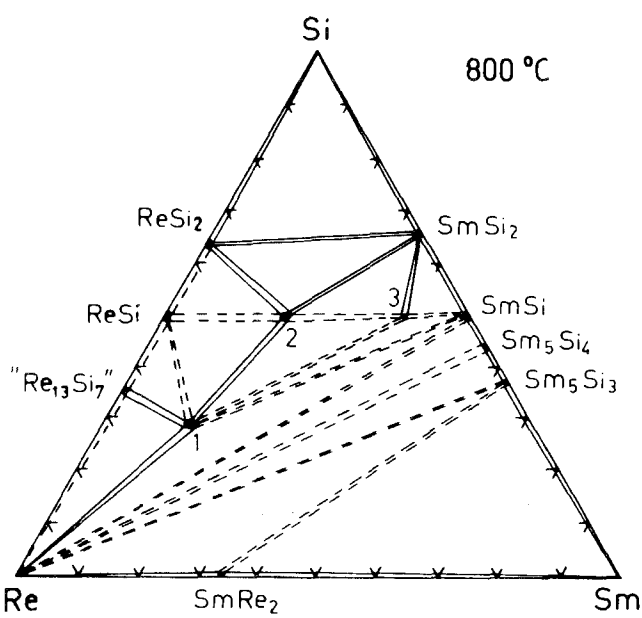

Vol. 7, ch. 53, Schumann and Genthe

1. Page 528, table 29, second column, first entry: yellow instead of "yelow".

Vol. 8, ch. 54, Gschneidner and Calderwood

1. Page 149, last line: the correct year in the reference is 1974.

Vol. 8, ch. 56, Leskelä and Niinistö

1. Page 247, table 6, first column, eighth entry: $R(HCO_3)_3 \cdot 5H_2O$ instead of "$R(HCO_3) \cdot 5H_2O$".
2. Page 278, table 14, second column, seventh line: La $\cdots$ Nd instead of "Na $\cdots$ Nd".

SUBJECT INDEX